

# Some recent works on diagnosis and treatment of gastric cancer

ZHANG Xue-Yong

**Subject headings** stomach neoplasms/diagnosis; stomach neoplasms/therapy; antibody, monoclonal; gene therapy

Aiming at earlier diagnosis and better result of treatment of gastric cancer, we endeavored to do some laboratory and clinical studies in recent years. The following is a brief sketch of these works.

## PREPARATION AND USES OF MONOCLONAL ANTIBODIES

By means of cell fusion technic we established several hybridoma cell lines capable of producing antigastric cancer monoclonal antibodies<sup>[1]</sup>. These antibodies were named MG series among which MGa-7, MGa-9, MGa-11 and MGb-2 were used more widely<sup>[2]</sup>. The corresponding antigens of these antibodies were different from the known cancer related antigens such as CEA, AFP, X-hap ten, Tn antigen, etc. Their chemical nature was proved to be lipoprotein, glycoprotein, or glycolipid. Immunoelectron microscopy demonstrated that these antigens were chiefly distributed on the cell membranes and/or in the cytoplasm of the gastric cancer cells, being especially abundant in the microvilli, the fossate surface of the cell membrane, the coarse endoplasmic reticulum and the microcysts.

### Diagnostic uses

**Immunohistological and cytological diagnosis** Owing to the high specificity of these McAbs, they were used to determine the source of some metastatic tumors by immunohistological examination when ordinary histological staining gave ambiguous results<sup>[3]</sup>.

Dysplasia of gastric mucosa is quite common in atrophic gastritis. Its outcome is highly variable. It may remain stationary, regress or undergo

malignant degeneration after a certain period. Hence it is deemed as a precancerous lesion, causing anxiety to the patients and their relatives and leading to repeated gastroscopy with increased economical burden and physical sufferings. So far there has been no reliable method to predict the relative risk of malignant degeneration. We found that immunohistochemical staining of the gastric mucosa with MGa-7 may serve as an important parameter for judging the relative risk of malignant degeneration. In 156 patients with dysplasia of gastric mucosa, 84 gave positive reaction and 72 gave negative reaction. Patients of each group were followed up for 2 - 4 years by repeated gastroscopies. Among the positive reactors, gastric cancer was detected in 17 cases, 7 of which were in the early stage. Among the 72 negative reactors, no one developed gastric cancer.

**Serological diagnosis** Detection of the MG series McAb corresponding antigens (MG-Ags) in blood either by ELISA<sup>[4]</sup> or by radioimmunoassay gave positive result in 58.7% to 72.8% of gastric cancer patients<sup>[5]</sup>. A follow-up study in a group of patients undergoing gastrectomy showed that after the excision of the tumor, MG-Ags in serum decreased in titre or became undetectable, while in those with unresectable gastric cancer or metastasis to remote sites, the serum titre did not change significantly. Hence it could serve as a preliminary test in the diagnosis for gastric cancer and could be used for the surveillance of relapse after excision and for the appraisal of treatment efficacy. Owing to the simplicity and low cost of these serological tests, they were used as a screening measure in the mass survey for gastric cancer, many symptomless cases being discovered and properly treated.

More recently a new method for determination of serum MG-Ags was established through the construction of mAb-pXJ19 chimera<sup>[6]</sup>. The mAb possesses specific affinity for gastric cancer related antigen, the pXJ19 is a recombinant template DNA and can be amplified by a pair of designed primers. This method was much more sensitive for detection of gastric cancer related antigen, yielding positive reaction in 85.2% of gastric cancer patients.

Department of Gastroenterology, Xijing Hospital, Fourth Military Medical University, Xi'an 710038, Shaanxi Province, China

**Correspondence to:** ZHANG Xue-Yong, Department of Gastroenterology, Xijing Hospital, Fourth Military Medical University, 15 Changle West Road, Xi'an 710033, Shaanxi Province, China

Tel. +86-29-3374576

Received 1999-01-04

### **Targeting therapy**

**Immunoconjugates** Since MG series monoclonal antibodies possess specific affinity to gastric cancer tissue, they may carry anticancer agents to the targeted tumor cells. Various immunoconjugates were produced by linking these McAbs ricin, ricin A chain, methotrexate, daunorubicin, adriamycin, epirubicin, mitomycin C, bleomycin, cisplatin and radioactive iodine<sup>[7]</sup>. After conjugation, both the immunological affinity of the antibodies for the tumor cells and the pharmacological activity of the cytotoxic agents were well preserved. These immunoconjugates exhibited selective cytotoxicity to gastric cancer cells. In vitro studies demonstrated that they could inhibit the growth rate of cancer cells. In vivo experiments showed that they could inhibit the growth of transplanted gastric cancer in nude mice much more effectively than unconjugated McAb or anticancer agents<sup>[8]</sup>. In order to demonstrate the process of internalization of these immunoconjugates, we carried out observations by double dynamic electron microscopy labeling technic, using streptavidin-gold and sheep antimouse IgG gold probes<sup>[9]</sup>. It was found that the main entry fashion of the conjugates was through non-coated microinvagination, followed by coated pits and interiorization of microvilli. Intracellularly, the endocytosed conjugates were transported from tubovesicular structures to multivesicular bodies and finally to lysosomes, where they were degraded. In the presence of verapamil, they stayed longer in tubovesicular structures, therefore, increased amount of them would remain in the cytosol. Thus cytotoxic effect could be augmented.

**Immunoliposomes** Immunoliposomes are spherical capsules with double-layered phospholipid coats, 40 nm - 120 nm in diameter, incorporating with antigastric cancer monoclonal antibodies. It could entrap a large number (6000 - 10000) of molecules of anticancer agents. By virtue of the specific affinity of the mAb to the gastric cancer related antigen, the immunoliposomes carrying the anti-tumor agents could be concentrated in the tumor cells manifesting a selective cytotoxic effect on the gastric cancer cells.

**Boron neutron capture therapy** Boron neutron capture therapy (BNCT) is based on the nuclear reaction ( $^{10}\text{B}_5 + {}^1_0\text{n}_0 \rightarrow {}^7\text{Li}_3 + {}^4\text{He}_2$ ), yielding lithium atom and alpha particles with high LET when  $^{10}\text{B}$  is irradiated with thermal neutron<sup>[10]</sup>. The essential factors for a successful BNCT are a large number of  $^{10}\text{B}$  atoms concentrated in tumor cell and an adequate fluence rate of thermal neutrons. We

prepared immunoliposomes, 40nm in diameter, conjugated with mAb MGb-2 and entrapping a  $^{10}\text{B}$  rich compound  $(\text{Et-}_4\text{N})_2\text{-}^{10}\text{B}_{10}\text{H}_{10}$ . There were  $1.4 \times 10^4$  atoms of  $^{10}\text{B}$  encapsulated and 20 molecules of MGb-2 incorporated per liposome. The immunoliposomes showed specific affinity to the gastric cancer cells and could deliver sufficient amount of  $^{10}\text{B}$  to them. Thus when irradiated with thermal neutrons, the gastric cancer cells were selectively killed.

### **EXPERIMENTAL GENE THERAPY**

The development of malignant tumors is believed to be related with the overactivation of the oncogenes and the inactivation of the tumor suppressor genes. So it is a logical approach to treat malignant tumors by inhibiting the oncogenes. The oncogenes related with gastric cancer include *c-myc*, *ras*, *c-erbB-2*, *K-sam*, *hst*, *n-myc*, *met*, *p53* (mutant form), etc. and telomerase, cyclin D1, PCNA, etc. are also oncogenic for gastric cancer. In recent years we used experimental gene therapy in the following ways.

#### ***Gene transfection of specific ribozyme of c-erb B2***

It was found that the amplification and overexpression of c-erb B2 bear a close relationship with the occurrence, development and metastasis of malignant tumors. A specific ribozyme RZ1 for c-erb B2 mRNA, which can be splitted and inactivated by it, was constructed and transplanted into the gastric cancer cell line SGC 7901. The transfected cell line SGC/RZ1 manifested remarkable changes in growth rate, cell cycle, morphology and tumorigenicity. In comparison with the original SGC-7901 cells, the growth rate was inhibited by 55%. Under flow cytometry, there was a 44% decrease of cells in S phase. Electron microscopy demonstrated vacuole degeneration, karyopyknosis and apoptosis in many cells. In nude mice, the transplanted SGC/RZ1 cells showed a delayed tumor-formation time. The size of the tumor was much smaller than that of the control.

#### ***Transfection of antisense RNA of PCNA***

Proliferating cell nuclear antigen (PCNA) is a cofactor for DNA polymerase, playing a very important role in the replication of DNA, proliferation of cells and regulation of cell cycle. Inhibition of PCNA expression would bring about changes of malignant behavior of tumor cells. To testify this, we transfected antisense RNA of PCNA into SGC-7901 cells. The transfected cells manifested retardation of growth rate,

degeneration, necrosis and apoptosis. The tumorigenic power in nude mice was inhibited.

#### ***Transfection of wild type p53 gene***

Wild type *p53* (*wtp53*) gene is a tumor suppressor gene. When *wtp53* cDNA was transplanted into SGC-7901 cells, the transfected cells (SGC7901/*wtp53*) manifested decreased growth rate and prolonged doubling time. Transmission electron microscopy revealed shrinkage of the cells and characteristic morphological features of apoptosis. By flow cytometry, the percentage of cells in G1 phase increased while that in S phase decreased in comparison with the parental SGC 7901 cells.

#### ***Transfection of herpes simplex virus thymidine kinase (HSV-TK) gene***

HSV-TK can turn the nontoxic ganciclovir (GCV) into phosphorylated GCV, which is a potent inhibitor of DNA synthesis. When HSV-TK-mRNA was transfected into gastric cancer cells and the transfected cells were exposed to GCV in the culture medium, they were killed in a dose-dependent fashion.

#### ***Transfection of cyclin D1 antisense RNA***

Cyclin D1 gene, located on the chromosome 11q13 region, has been found in many cancers, including gastric cancer, and is regarded to be related to carcinogenesis. To testify the effect of inhibiting cyclin D1 in gastric cancer cell, cyclin D1 antisense RNA was first constructed and then was transfected into SGC-7901 cells. The transfected cells displayed a much longer doubling time, an increased percentage of cells in G1-G0 phase, and marked inhibition of tumorigenicity in nude mice.

#### ***Transfection of telomerase antisense RNA***

Recent studies indicated that the activation of telomerase is a very important factor for the uncontrolled proliferation of tumor cells. We found that telomerase was detected in 84.2% of 38 cases of gastric cancer, and only 5.2% of normal gastric mucosa. After SGC-7901 cell was transfected with human telomerase anti-sense RNA, its growth rate slowed down in culture. Morphological changes of necrosis and apoptosis occurred, and oncogenic property was reduced.

The above-mentioned preliminary experiments indicate that gene therapy might be a promising approach to the treatment of gastric cancer.

#### **REFERENCES**

- 1 Fan DM, Zhang XY, Chen XT, Mu ZX, Hu JL, Qiao TD, Chen BJ. Establishment of four monoclonal antibodies to a poorly differentiated gastric cancer cell line MKN-46-9 and immunohistochemical study on their corresponding antigens. *Med J Chin PLA*, 1988;13:12-15
- 2 Zhang XY, Li S, Fan DM. Use of MG series monoclonal antibodies in the diagnosis and experimental therapy of gastric cancer. *Chin Med Sci J*, 1991; 6:56-59
- 3 Wang WL, Fan DM, Zhu MH, Zhang XY, Yang WM, Hu JL. Immunohistochemical study on related antigen of gastric carcinoma defined by monoclonal antibody MG7 of gastric carcinoma. *Chin J Digestion*, 1988;8:127-129
- 4 Zhang JR, Zhang XY, Shao J, Chen XT. Establishment and application of immunofluorescence using monoclonal antibody in diagnosis of gastric cancer. *J Med Coll PLA*, 1992;7:27-30
- 5 Li G, Zhang XY, Chen XT, Mu ZX, Hu JL, Chen M. Level of a panel of tumor associated antigens MG Ags in sera of patients with gastric cancer and its value in diagnosis. *Med J Chin PLA*, 1990;15:1-3
- 6 Ren J, Fan DM, Zhou SJ, Zhang XY, Yang AG, Li MF, Chen Z. Establishment of immuno PCR technique for the detection of tumor associated antigen MG 7-Ag on the gastric cancer cell line. *Chin J Oncol*, 1994;16: 247-249
- 7 Li S, Zhang XY, Chen XT, Zhang SY, Chen LJ, Ni YH, Zhan JL. Specific targeting of mitomycin C to tumors with the use of antigastric cancer monoclonal antibodies. *Natl Med J China*, 1990;70:363-366
- 8 Li S, Zhang XY, Zhang SY, Chen XT, Chen LJ, Shu YH. Preparation of anti-gastric cancer monoclonal antibody MGb 2 mitomycin C conjugate with improved antitumor activity. *Bioconjugate Biochem*, 1990;2:245-250
- 9 Wang FA, Zhang XY, Fan DM, Li S, Ding J. Internalization of monoclonal antibody immunconjugates against gastric cancer. *Chin J Digestion*, 1994;14:189-192
- 10 Xu L, Zhang XY, Fan DM, Chen XT, Lu YS, Ding HX. Boron neutron capture therapy of human gastric cancer by boron containing immunoliposomes under thermal neutron irradiation. *Natl Med J China*, 1991;71:568-571

Edited by MA Jing-Yun

Original Articles

# Relationship between DNA ploidy, expression of ki-67 antigen and gastric cancer metastasis \*

XU Lei, ZHANG Su-Min, WANG Yan-Ping, ZHAO Feng-Kai, WU Dong-Ying and XIN Yan

**Subject headings** Ki-67 antigen; neoplasms metastasis; immunocytochemistry; DNA ploidy; stomach neoplasms/pathology

## Abstract

**AIM** To evaluate the relationship between the expression of Ki-67 antigen and the pathobiological behaviours of gastric cancers especially their distant metastases.

**METHODS** Fifty-six specimens of gastric cancer routinely fixed in formalin and embedded in paraffin (FFEP) were studied by immunohistochemical method.

**RESULTS** Expression of Ki-67 antigen was significantly related to the distant metastases to liver, ovary and adrenal gland ( $P < 0.01$ ), but not related to the histological type, growth pattern, depth of invasion, histological differentiation and the metastases to local lymph nodes ( $P > 0.05$ ). Furthermore, the Ki-67 antigen expression was significantly related to the DNA aneuploidy pattern, which is closely related to poor prognosis ( $P < 0.05$ ).

**CONCLUSION** Overexpression of Ki-67 can be used as an objective marker of the proliferative activity for predicting prognosis of gastric cancer and metastatic potential to distant organs.

## INTRODUCTION

Ki-67 is a mouse monoclonal antibody which recognizes a nuclear antigen expressed in all phases of the cell cycle except G<sub>0</sub> and early G<sub>1</sub><sup>[1]</sup>. And Ki-67 immunoreactivity can thus be used as biomarker for cell proliferation. Another method to measure cell proliferation is flow cytometry. In our study, we detected 56 gastric cancer tissue specimens immunohistochemically by PcAb-Ki-67 (Dako, A047) and compared with DNA ploidy pattern in order to evaluate the relationship between the proliferative activity of gastric cancer cell and pathobiological behavior of gastric cancer, especially the relationship with the distant organ metastases.

## MATERIALS AND METHODS

### Materials

Fifty-six specimens of gastric cancer were collected from Cancer Institute of China Medical University. Among these 56 cases, no metastasis was found in 7 cases, 12 were accompanied with liver, 4 with ovarian, 1 with adrenal and 47 with lymph node metastasis. Tissue blocks from primary and metastatic tumours were chosen from each case.

### Methods

PcAb to human Ki-67 antigen (A047) was used in this study to identify the proliferative activity of gastric cancer cell. The dilution for Ki-67 was 1:100. Sections were immunostained using the avidin-biotin-peroxidase complex method and pressure cooking was used to unmask Ki-67 antigen<sup>[2]</sup>.

### Evaluation of immunostaining

Four semi-quantitative classes were used for grading: negative(-), no positive cells; weak positive (+), positive cells < 10%; moderately positive (++) , the positive cells between 10%-50%; strong positive (+++), the positive cells > 50%.

DNA ploidy was measured by flow cytometry, the detailed procedures and the standard of evaluation followed the method reported previously<sup>[3]</sup>.

## RESULTS

Expression of the Ki-67 antigen was not related to WHO's classification and Lauren's classification ( $P < 0.05$ ). It was not related to the depth of local invasion of gastric cancer ( $P > 0.05$ ), growth pattern

Cancer Institute, China Medical University, Shenyang 110001, China  
XU Lei, female, born on 1970-09-04 in Shenyang City, Liaoning Province, graduated from China Medical University in 1993, doctor and research assistant, majoring gastrointestinal pathology, having 2 papers published.

\*Project Supported by the National Natural Science Foundation of China, No.39370772.

**Correspondence to:** Dr. XU Lei, Cancer institute, China Medical University, 155 Nanjing Beijie, Shenyang 110001, Liaoning Province, China

Tel. +86-24-3863731 Ext. 6351

Received 1998-09-15

( $P > 0.05$ ) and local lymph nodes metastasis ( $P > 0.05$ ). But the expression of Ki-67 was significantly related to the distant organ metastases ( $P < 0.005$ , Table 1) and also related to DNA aneuploidy pattern (Table 2).

**Table 1 Relationship between expression of Ki-67 antigen and metastasis of gastric cancer**

Metastasis (Mets)	n	Expression of Ki-67 antigen	
		+ + + (%)	+ + + (%)
Non-Mets	7	3(42.9)	4(57.1)
LN Mets	32	23(71.9)	9(28.1)
Distant organ Mets	17	3(17.6)	14(82.4) <sup>b</sup>
Total	56	29(51.8)	27(48.2)

<sup>b</sup> $P < 0.01$ , vs LN (lymph node).

**Table 2 Relationship between expression of Ki-67 antigen and DNA ploidy**

DNA ploidy	n	Expression of Ki-67 antigen	
		+ + + (%)	+ + + (%)
Di(Tetra)ploid	35	22(62.9)	13(37.1)
Aneuploid	21	7(33.3)	14(66.7) <sup>a</sup>

<sup>a</sup> $P < 0.05$ .

## DISCUSSION

Proliferative activity of cancer cells was closely related to the biological behavior of carcinoma, especially the invasion, metastasis and prognosis. In this study, the results showed that Ki-67 could be used as a marker to measure the proliferative activity of

gastric cancer cells and predict the potential of metastasis to distant organs of gastric cancer. The method was simple and quick. The detection of Ki-67 antigen could be used as a useful marker to foretell the high risk of the metastases to distant organs and predict the prognosis of gastric cancer.

DNA aneuploidy was one of the markers of malignant tumour cells. Xin, *et al* had reported that aneuploidy DNA pattern may be related to the development of distant organ metastases, especially through the blood vascular system<sup>[4]</sup>. The results of this study showed that DNA aneuploidy was related to the expression of Ki-67, the latter was also closely related to the distant metastases ( $P < 0.01$ ). These suggested that the expression of Ki-67 and aneuploidy DNA pattern are two objective markers which may be valuable in predicting high potential of metastases to the distant organs, and the combined detection of these two markers could be a more useful method for predicting metastases to the distant organs and prognosis.

## REFERENCES

- 1 Getdes J, Lemke H, Baisch H. Cell cycle analysis of a cell proliferation associated human nuclear antigen defined by the monoclonal antibody Ki-67. *J Immunol*, 1994;133:1710
- 2 Norton AJ, Jourdan S, Yeomans P. Brief high temperature heat denaturation (pressure cooking): a simple and effective method of antigen retrieval for routinely processed tissues. *J Pathol*, 1994;173:371
- 3 Hedley DW, Fridlannder ML, Taylor IW. Method for analysis of cellular DNA content of paraffin embedded pathological material using flow cytometry. *J Histochem Cytochem*, 1993;31:1333
- 4 Xin Y, Zhao FK, Wu DY. DNA ploidy, expression of p53 protein and the metastases of gastric cancer. In: Nishi M, Sugano H, Takahashi, eds. Gastric cancer. Italy: Monduzzi Editore International Proceedings Division, 1995:735

Edited by MA Jing-Yun

# ***In situ* detection of tumor infiltrating lymphocytes expressing perforin and fas ligand genes in human HCC \***

QIAN Qi-Jun, XUE Hui-Bin, QU Zeng-Qiang, FANG Shi-Gang, CAO Hui-Fang and WU Meng-Chao

**Subject headings** carcinoma, hepatocellular; lymphocytes; fas ligand genes; perforin; *in situ* hybridization; liver neoplasms

## **Abstract**

**AIM** To investigate the expression of perforin and fas-ligand (fas-L) of tumor infiltrating lymphocytes (TILs) in human hepatocellular carcinoma (HCC).

**METHODS** By *in situ* hybridization and immunohistochemistry, the perforin and fas-L gene expression of TILs was studied in 20 HCC cases.

**RESULTS** Positive expression of perforin and fas-L genes was detected in 16 HCC cases. One patient had expression of perforin and fas-L genes in the majority of TILs and survived 1.5 years after tumor resection without HCC relapse. This seems that the presence of a large number of activated T cells might be beneficial for the antitumor immunity. In other cases, less than 10% of TILs were able to express perforin and fas-L genes.

**CONCLUSION** Although there were a number of T cells in HCC, only few of them were immunoreactive and able to kill tumor cells. It seems important to promote further proliferation of these activated T cells *in vitro* or *in vivo*.

## **INTRODUCTION**

Cytotoxic T lymphocytes (CTLs) play a major role in killing tumor cells. Two pathways have been described by which a cytotoxic cell may induce lysis of its target<sup>[1,2]</sup>. The first pathway is called perforin pathway. T cell receptors (TCRs) of CTLs binding with MHC antigens on the tumor cells induce the release of granules filled with perforins and granzymes, and perforins then attack the target cell surface, followed by granzymes entering into the cell and killing it. The second is fas-L pathway. Fas-L from activated T cell binds with Fas antigen on the tumor cell surface, directly causing cell apoptosis. Although we applied TILs to treat tumor several years ago<sup>[3]</sup>, this is the first domestic report studying whether activated T cells around the tumor express the two killing genes, perforin gene and fas-L gene. We studied the expression of perforin and fas-L genes of TILs in the HCC specimens using *in situ* hybridization and immunohistochemistry to find out whether there are T cells with killing activities in HCC tissues.

## **MATERIALS AND METHODS**

### **Materials**

Specimens were obtained from 20 HCC patients (16 men and 4 women; ranging in age from 25 to 64 years with a mean of 47 years) who underwent tumor resection from January to June, 1994 in our hospital. Among these patients, 17 were associated with liver cirrhosis. The control specimens were from the normal liver tissues of 3 patients with hepatic angioma. The normal liver tissues and HCC tissues were quickly frozen in liquid nitrogen within half an hour after removed from the bodies of the patients, and stored at -70°C. The specimens cut from the margin between tumor and paratumor areas were embedded with O. C. T, fixed with 40mL/L-paraformaldehyde, gradually dehydrated with ethanol, and then stored at -70°C. Human fas-L cDNA was kindly presented as a gift by Dr. Nagata of Japanese Bioscience Institute, and human perforin cDNA by Dr. Kevin Y.T. Thia of Australia Austin Institute. Rabbit-anti-human fas-L polyclonal antibodies were purchased from Santa Cruz Biotech Company of USA. Rat-anti-human

Tumor Immunology and Gene Therapy Center, Eastern Institute of Hepatobiliary Surgery, Shanghai 200438, China

Dr. QIAN Qi-Jun, male, born on 1964-09-18 in Shaoxing City, Zhejiang Province, graduated from the First Military Medical University in 1987, now Associate Professor of tumor immunology, majoring in hepatic tumor immunology, having 19 papers published.

\*Project supported by the Key National Natural Science Foundation of China, No.39730440 and the National Natural Science Foundation of China, No.39500082.

**Correspondence to:** Dr. QIAN Qi-Jun, Tumor Immunology and Gene Therapy Center, Eastern Institute of Hepatobiliary Surgery, Shanghai 200438, China

Tel. +86-21-65564166 Ext. 75430

Received 1998-11-09

perforin monoclonal antibody was donated by Dr. Eckhard. R. Padack of the Medical Academy of Miami University, USA. Digoxin labeling and detection kit was purchased from Boehringer Mannheim Company of Germany. The immunohistochemistry kit of streptavidin-biotin amplification system was a product of WAK Company of Germany.

### Methods

#### HE staining

**In situ hybridization** Probe labeling proceeded according to the method of random primer labeling presented by the digoxin labeling kit of Boehringer Mannheim Company. In situ hybridization was performed following a previously published protocol<sup>[3]</sup>. The concentration of the probe was  $1 \times 10^3 \mu\text{g/L}$  and cells with blue granules under microscope were regarded as positive.

**Immunohistochemistry** The specimens were processed according to the ABC method, and visualized with DAB. Cells with brown granules under microscope were regarded as positive.

### RESULTS

#### HE staining and immunohistochemistry

A few lymphocytes with negative perforin and fas-L expression were seen in the 3 normal liver tissues, while in the 19 HCC specimens, there was a various number of TILs, most in the mesenchyma of the tumor and a few in the parenchyma. Furthermore, in another HCC case (No.14) which had not-experienced relapse for 1.5 years after tumor resection, there were a large number of TILs with positive expression of perforin and fas-L not only in the mesenchyma of the tumor, but also extensively in the parenchyma of the liver (Figures 1-3). TILs of 15 patients had positive perforin and fas-L expression with a positive rate below 10%. In the other four cases, although there was a various number of TILs infiltrating in the tumor mesenchyma, no TILs expressed perforin and fas-L. There was no relationship between the number of TILs in the liver tissue and the positive rate of perforin and fas-L expression.

#### In situ hybridization

There were no perforin and fas-L positive-hybridization signals in the 3 normal liver specimens. In HCC specimens, perforin and fas-L expression of TILs showed strong positivity in one case (No.14), mild positivity in 15 cases and negativity in 4 cases, indicating that perforin and fas-L expression in transcriptive level was parallel to that in protein level in HCC.

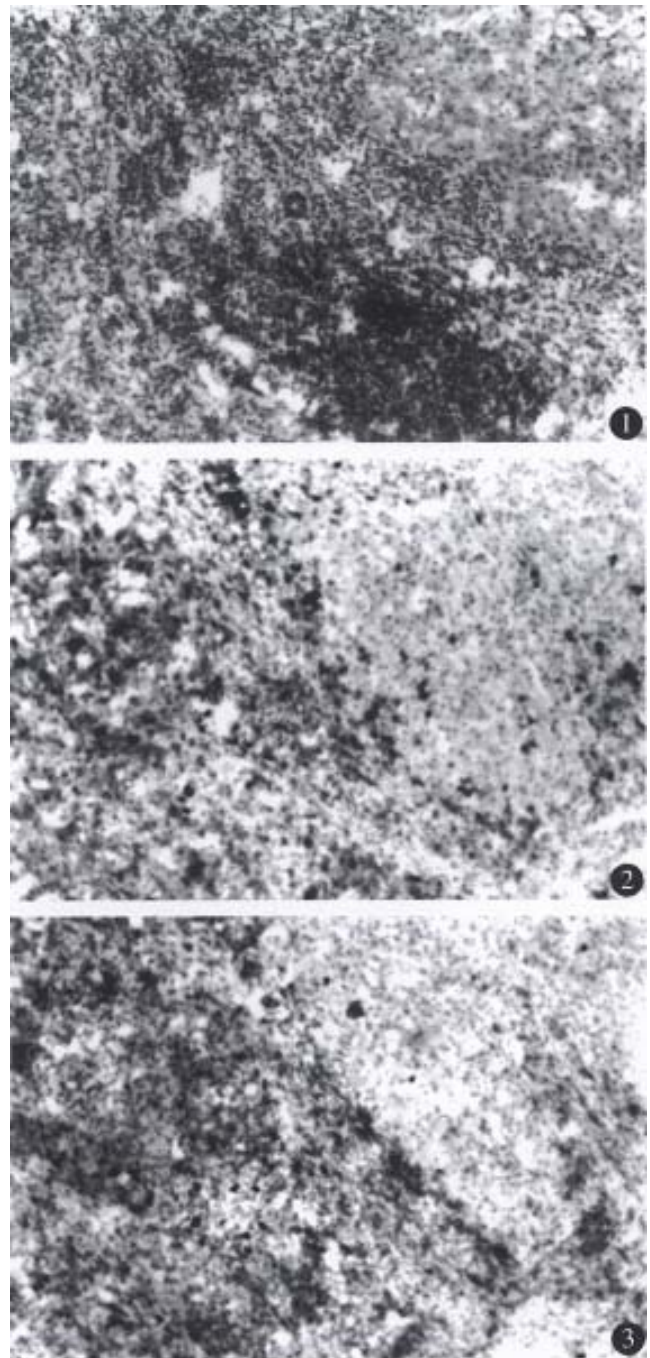


**Figure 1** Most infiltrating TILs in the mesenchyma of the tumor, few in the parenchyma. HE $\times 100$

**Figure 2** Strong positive signals of perforin in the TILs of hepatoma tissue. ABC $\times 100$

**Figure 3** Strong positive signals of fas-L in the TILs of hepatoma tissues. ABC $\times 100$

### DISCUSSION

TILs, a heterogeneous group of lymphocytes consisting largely of T lymphocytes, are located mainly in the tumor mesenchyma. As early as 1907, TILs were found in tumor tissues and the phenomenon that lymphocytes infiltrated in tumor tissues was supposed to be the result of the resistance of the

host to the tumor. Later, it was found that the greater the number of TILs in the tumor tissue, the better outcome the patient would get<sup>[4]</sup>.

Early studies on TILs focused on their phenotypes. Recent investigations showed that T lymphocytes killed the tumor cells mainly under the perforin and fas-L pathways. Perforin and fas-L expression in TILs of tumor tissues is directly related to the killing activity of TILs in tumor tissues. In 1994, Leger-Ravet *et al*<sup>[5]</sup> found perforin and granzyme B expression in TILs in 10 follicular lymphoma cases. Of all 20 HCC cases we studied, TILs expressed perforin and fas-L in varying degrees in 16 patients, and negatively in 4. This indicates that cytotoxic T lymphocytes existed in most of the HCC patients. Furthermore, in one case there was a large number of TILs expressing fas-L and perforin in both the mesenchyma and the parenchyma of the tumor tissues. This patient did not sustain relapse within the 1.5 year follow-up period. This implies that large quantities of T lymphocytes with killing activities existing in the tumor tissues are beneficial for the prognosis of HCC patients. Except the case

presented above, TILs expressing perforin or fas-L in the other 19 cases of HCC were below 10%, showing that most of the TILs were in an immunosuppressive state. The mechanism of this phenomenon might be ① the HCC could not activate T lymphocytes due to its deficient expression of the second signal B7; ② T lymphocytes expressing high levels of fas and fas-L resulted in self-apoptosis<sup>[6,7]</sup>. Therefore, amplification of the T lymphocytes with killing activities *in vivo* or *in vitro* may improve the therapeutic effect for the patients with tumors.

## REFERENCES

- 1 Kagi D, Vignaux F, Ledermann B. Fas and perforin pathways as major mechanisms of T cell mediated cytotoxicity. *Science*,1994;265:528-530
- 2 Lowin B, Hahne M, Mattmann C. Cytolytic T-cell cytotoxicity is mediated through perforin and Fas lytic pathways. *Nature*,1994;370:650-652
- 3 Guo YJ, Wu MC, Kong XT. Immuno-response in primary hepatocellular carcinoma and paratumor tissues. *Chin J Exp Sur*,1987;4:545-547
- 4 Lipponen PK, Eskelinen MJ, Jakkhiainen K. Tumor infiltrating lymphocytes as an independent prognostic factor in transitional cell bladder cancer. *Eur J Cancer*,1992;29:69-75
- 5 Leger-Ravet M, Devergne O, Peuchamaur M. In situ-detection of activated cytotoxic cells in follicular lymphomas. *Am J Pathol*,1994;144:492-499
- 6 Dhein J, Walczak H, Baumber C. Autocrine T-cell suicide mediated by APO-1/(Fas/CD95). *Nature*,1995;373:438-441
- 7 Alderson MR, Tough TW, Davis-Smith T. Fas ligand mediates activation induced cell death in human T lymphocytes. *J Exp Med*,1995;181:71-77

Edited by MA Jing-Yun

# Expression and significance of proapoptotic gene *Bax* in gastric carcinoma \*

LIU Hai-Feng, LIU Wei-Wen, FANG Dian-Chun and MEN Rong-Pu

**Subject headings** stomach neoplasms/ pathology; *Bax* gene; gene expression; immunohistochemistry

## Abstract

**AIM** To study the expression of proapoptotic gene *Bax* in human gastric carcinoma and its significance.

**METHODS** Using immunohistochemistry methods, the *Bax* protein expression in 57 specimens of gastric carcinoma and its relationship with clinical status and pathomorphological parameters were observed.

**RESULTS** Thirty-three (57.9%) cases were positive for *Bax* protein staining which was mainly located in the cytoplasm of tumor cells. The rate of *Bax* protein expression was not correlated with the tumor size, lymph node metastasis, depth of invasion, clinical stages of tumors and age and sex of patients ( $P < 0.05$ ), but strongly associated with the morphological type and differentiation degree of tumors. It was significantly higher in intestinal type and well or moderately differentiated gastric carcinoma than in diffuse type and poorly differentiated gastric carcinoma ( $P < 0.05$  and  $P < 0.01$ ).

**CONCLUSION** The proapoptotic gene *Bax* is differently expressed in most of gastric carcinoma and may take part in the modulation of apoptosis in gastric carcinoma. The expression of *Bax* might be associated with the occurrence of intestinal type gastric carcinoma and the differentiation of gastric carcinoma.

## INTRODUCTION

Recent investigations have demonstrated that apoptosis plays a significant role in the pathogenesis of tumors<sup>[1,2]</sup>. Emphasis has been laid on the mechanisms that regulate apoptosis pathways. Bcl-2 associated X protein (*Bax*), which has extensive amino acid homology with Bcl-2, can form heterodimers with Bcl-2 *in vivo*. Overexpressed *Bax* can counter the death repressor activity of Bcl-2, and accelerate apoptotic cell death<sup>[3]</sup>. To determine whether proapoptotic gene *Bax* plays a role in the regulation of apoptosis in gastric carcinoma, an immunohistochemical study of *Bax* protein expression in gastric carcinoma and its relation to clinical status, pathomorphological parameters were carried out.

## MATERIALS AND METHODS

### *Histological specimens*

Fifty-seven cases of surgically resected gastric carcinomas (male 39, female 16; mean age 58.6 years) were collected from the files of the Department of Pathology of our hospital. All blocks were fixed in 10% formalin and embedded in paraffin. Serial sections were cut from each block in 4 $\mu$ m, stained with hematoxylin and eosin and confirmed pathologically.

### *Immunohistochemical methods*

Immunohistochemical staining for *Bax* protein was performed using SP technique with the following procedure: ① slides were deparaffinized in xylene for 10 minutes each and then were hydrated in decreasing concentrations of ethanol and rinsed in phosphate-buffered saline. Endogenous peroxidase was blocked by 30 mL/L H<sub>2</sub>O<sub>2</sub> in methanol for 5 minutes, and then incubated for 10 minutes at room temperature in normal goat serum (1:20). ② Slides were incubated with a 1:50 dilution of the primary rabbit antihuman *Bax* polyclonal antibody (Santa Cruz, USA) for 30 minutes at 37°C. A biotin-streptavidin detection system was employed with diaminobenzidine as the chromogen. ③ Slides were washed twice with phosphate-buffered saline and incubated with the linking reagent (biotinylated anti-immunoglobulin) for 10 minutes at 37°C. After rinsing in phosphate-buffered saline, the slides were incubated with the peroxidase-conjugated streptavidin

Department of Gastroenterology, Southwest Hospital, Third Military Medical University, Chongqing 400038, China

Dr. LIU Hai-Feng, physician in chief, having 18 papers published.

\*Key project of the 9th 5-year plan for Medicine and Health of Army, No.96Z047.

**Correspondence to:** Dr. LIU Hai-Feng, Department of Gastroenterology, Southwest Hospital, Third Military Medical University, Chongqing 400038, China

Tel. +86-23-65317511 Ext. 73094

Received 1998-10-08

label for 10 minutes at 37°C, and incubated with diaminobenzidine and H<sub>2</sub>O<sub>2</sub> for 10 minutes in the dark, the sections were then counterstained with hematoxylin. With each batch of test samples, a positive control consisting of a tissue section from tonsil was evaluated. In addition, a negative control was prepared for each sample using an irrelevant antibody of the same isotype as the primary antibody.

The immunostaining of Bax protein was visually classified into negative and positive groups by observing 1000 tumor cells in the areas of the sections: no staining present in any of tumor cells or less than 10% tumor cells with staining (-); more than 10% tumor cells with positive staining. The classification was done by two senior pathologists who did not know the clinicopathological data.

### Statistics

Analysis of data was accomplished using Chi-square test. *P* values less than 0.05 were considered to be statistically significant.

## RESULTS

### Expression of Bax protein in gastric carcinoma

Thirty-three (57.89%) of the fifty-seven gastric carcinomas showed immunoreactivity for Bax protein in gastric carcinoma cells. The Bax protein immunoreactivity appeared brown or dark brown, which was mainly located in the cytoplasm (Figure 1), and a few specimens simultaneously expressed Bax protein in the cell nuclear of tumor cells. Some of the mature lymphocytes infiltrating in the stroma of gastric carcinomas also had Bax protein expression.

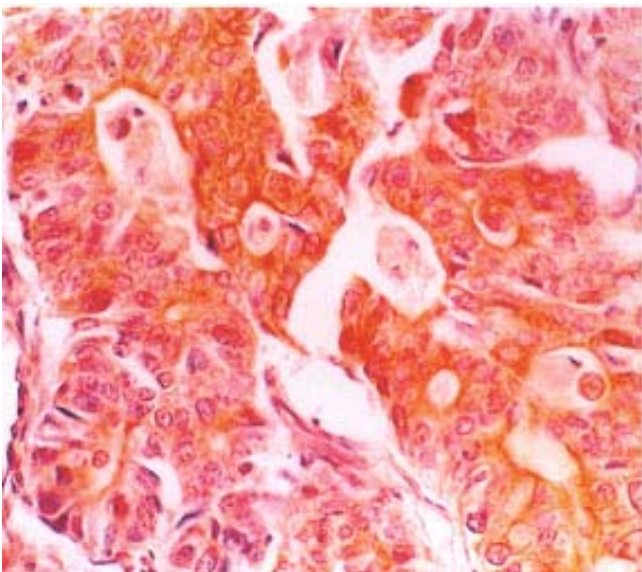


**Figure 1** Bax immunoreactivity was detected in cytoplasm of gastric carcinoma cells. SP×200

### Correlation between Bax protein expression and clinicopathological parameters of gastric carcinomas

Correlation between Bax protein expression and clinical pathological data of gastric carcinoma is illustrated in Table 1. The rate of Bax protein expression was not correlated with patient age, sex, tumor size, lymph node metastasis, depth of invasion and clinical stages (*P*>0.05). The immunoreactivity of Bax was significantly associated with morphologic phenotype and grades of differentiation of gastric carcinoma. 20 (73.3%) of 30 gastric carcinomas of intestinal morphologic phenotype were immunoreactive versus 11 (40.7%) of 27 diffuse gastric carcinomas (*P*<0.05). 17 (81.0%) of 21 well and moderately differentiated gastric carcinomas were immunoreactive versus 10 (38.5%) of 26 poorly differentiated gastric carcinomas (*P*<0.01).

**Table 1** Correlation between Bax protein expression and clinicopathological parameters of gastric carcinomas

Parameters	<i>n</i>	Bax protein expression		Positive rate (%)
		-	+	
Age (year)				
≤59	39	22	17	56.41
≥60	18	11	7	61.11
Sex				
M	39	24	15	61.54
F	18	9	9	50.00
Type				
Intestinal	30	22	8	73.33 <sup>a</sup>
Diffuse	27	11	16	40.74
Grade of differentiation				
Well/moderate	21	17	4	80.95 <sup>b</sup>
Poor	26	10	16	38.46
Mucoid	10	6	4	60.00
Tumor size				
<5cm	35	21	14	60.00
≥5cm	22	12	10	54.55
Lymph-node metastasis				
Negative	23	13	10	56.52
Positive	34	20	14	58.82
Serosal invasion				
Absent	27	14	13	51.85
Present	30	19	11	56.67
Clinical stages				
I and II	34	20	14	58.82
III and IV	23	13	10	56.52

<sup>a</sup>*P* < 0.05,  $\chi^2 = 6.193$ , vs diffuse-type gastric carcinoma, <sup>b</sup>*P* < 0.01,  $\chi^2 = 8.580$ , vs poorly differentiated gastric carcinoma.

## DISCUSSION

Apoptosis is a highly regulated form of programmed cell death defined by distinct morphological and biochemical features. Apoptosis plays a major role in development, embryogenesis, regulation of the immune system, and carcinogenesis, as well as in the

maintenance of tissue homeostasis. Various protein molecules or oncogenes and suppressor genes are involved in the process of apoptosis, including *p53*, *myc*, *ras*, *Bcl-2*, *Bax* and the Fas/Fas ligand system<sup>[4]</sup>. In recent studies, *Bax* protein expression has been identified in various human malignant tissues, including the prostate, colon, breast, testis and ovary<sup>[5-8]</sup>. But, little is known about *Bax* protein expression and its relationship with the biological behavior of human gastric carcinoma.

In this study, we found that the positive rate of *Bax* protein staining in gastric carcinoma was 57.9%. The proapoptotic gene *Bax* can express to various degrees in most kinds of the gastric carcinoma and may take part in the regulation of apoptosis of gastric carcinoma. Our findings concerning the relationship between *Bax* protein expression and the pathological characteristics of gastric carcinoma showed that *Bax* expression was associated with morphologic phenotype and grades of differentiation of gastric carcinomas. The difference in the *Bax* protein expression in the intestinal and diffuse types demonstrated that aberrant *Bax* protein expression was preferentially associated with development of intestinal type gastric carcinoma, indicating once more the different biologic mechanisms involved in the development of these two histologic subtypes. The difference in the *Bax* protein expres-

sion between poorly differentiated and well/moderately-differentiated gastric carcinomas demonstrated that aberrant *Bax* protein expression was associated with differentiation or growth speed of gastric carcinomas. There was no significant relationship between *Bax* protein expression and tumor size, lymph node metastasis, serosal invasion or clinical stages. Therefore, *Bax* protein expression might play an important role in the early development and phenotypic differentiation of gastric carcinomas, but not in tumor progression.

## REFERENCES

- 1 Que FG, Gores GJ. Cell death by apoptosis: basic concepts and disease relevance for the gastroenterologist. *Gastroenterology*, 1996;110:1238-1243
- 2 Solary E, Dubrez L, Eymin B. The role of apoptosis in the pathogenesis and treatment of diseases. *Eur Respir J*, 1996;9:1293-1305
- 3 Oltvai ZN, Milliman CL, Korsmeyer SJ. *Bcl-2* heterodimerizes *in vivo* with a conserved homolog, *Bax*, that accelerates programmed cell death. *Cell*, 1993; 74:609-621
- 4 Hale AJ, Smith CA, Sutherland LC, Stoneman VEA, Longthorne VL, Culhane AC. Apoptosis: molecular regulation of cell death. *Eur J Biochem*, 1996;236: 1-26
- 5 Krajewski S, Blomqvist C, Franssila K, Krajewska M, Wasenius VM, Niskanen E. Reduced expression of proapoptotic gene *Bax* is associated with poor response rates to combination chemotherapy and adenocarcinoma. *Cancer Res*, 1995;55:4471-4478
- 6 Krajewska M, Moss SF, Krajewski S, Song K, Holt PR, Reed JC. Elevated expression of *Bcl-x* and reduced *Bak* in primary colorectal adenocarcinomas. *Cancer Res*, 1996;58:2422-2427
- 7 Chresta CM, Masters JRW, Hickman JA. Hypersensitivity of human testicular tumors to etoposide-induced apoptosis is associated with functional *p53* and a high *Bax*: *Bcl-2* ratio. *Cancer Res*, 1996;56:1834-1841
- 8 Krajewska M, Krajewski S, Epstein JI, Reed JC, Franssila K. Immunohistochemical analysis of *Bcl-2*, *Bax*, *Bcl-x* and *mcl-1* expression in prostate cancers. *Am J Pathol*, 1996;148:1567-1576

Edited by MA Jing-Yun

# Antisense to cyclin D1 reverses the transformed phenotype of human gastric cancer cells \*

CHEN Bing<sup>1</sup>, ZHANG Xue-Yong<sup>2</sup>, ZHANG Yu-Jing<sup>3</sup>, ZHOU Ping<sup>3</sup>, GU Yan<sup>4</sup> and FAN Dai-Ming<sup>2</sup>

**Subject headings** stomach neoplasms; cyclin D1; RNA, antisense; gene therapy

## Abstract

**AIM** To further investigate the effect of cyclin D1 on the biologic behavior of cancer cells and its potential role in gene therapy of tumor.

**METHODS** A cyclin D1 subcloning plasmid termed BKSD1 was constructed by subcloning the human cyclin D1 cDNA into Bluescript-KS, a plasmid vector with a pair of T7 and T3-promoters, with recombinant DNA technology of molecular biology. So, it is easy to generate digoxigenin (DIG)-labeled RNA probes of antisense and sense to cyclin D1 using RKSD1 as a template vector. PDORD1AS, an eukaryotic expression vector containing the full-length human cyclin D1 cDNA in its antisense orientation cloned into the retroviral vector pDOR-neo, was successfully constructed with BKSD1 to change restriction sites. A gastric cancer cell line, SGC7901/VCR, was transfected with pDORD1AS by Lipofect Amine-mediated introduction and a subline termed SGC7901/VCRD1AS, which had stable overexpression of antisense RNA to cyclin D1, was obtained by selection in G418. The subline, control subline transfected pDOR-neo and SGC7901/VCR were evaluated by methods of immunohistochemistry, flow cytometry, molecular hybridization, morphology and cell biology.

**RESULTS** Compared with control cell lines, SGC7901/VCRD1AS had a reduced expression of cyclin D1 (inhibition rate was about 36%), in-

creased cell size and cytoplasm to nucleus ratio, increased doubling time (42.2 h to 26.8 h and 26.4 h), decreased saturation density ( $18.9 \times 10^4$  to  $4.8 \times 10^5$  and  $4.8 \times 10^5$ ), increased percentage of cells in the G1/G0 phase (80.9%-64.6% and 63.8%), reacquired serum dependence, and a loss of tumorigenicity in nude mice (0/4 to 4/4 and 4/4).

**CONCLUSION** Stable overexpression of antisense RNA to cyclin D1 can reverse the transformed phenotype of human gastric cancer cells and may provide an approach of gene therapy for gastric cancer.

## INTRODUCTION

Studies on the functions of cellular proto-oncogenes and tumor suppressor genes indicate that most of these genes mediate signal transduction pathways that play a critical role in cell proliferation and differentiation as well as cell cycle control<sup>[1]</sup>. This has led to the realization that cycle regulatory proteins can also be directly involved in oncogenesis. Critical transitions in the eukaryotic cell cycle are regulated by the sequential activation of a series of cyclins and cyclin-dependent kinases (CDKs)<sup>[2]</sup>. Since the major regulatory events leading to mammalian cell proliferation and differentiation occur in the G1 phase of the cell cycle<sup>[3]</sup>, the deregulated expression of G1 phase cyclins or their related CDKs might cause loss of cell cycle control, thus enhancing oncogenesis. Cyclin D1 has been strongly implicated in controlling the G1 phase of the cell cycle. So, cyclin D1 gene is regarded as one of the best oncogene candidates<sup>[4]</sup>. Indeed, rearrangement, amplification, and overexpression of the cyclin D1 gene, which is located on the human chromosome 11q13 region, have been found in several types of human cancer<sup>[5]</sup>. Overexpression of cyclin D1 in rat fibroblasts enhanced their growth and tumorigenicity and cyclin D1 collaborated with an activated *ras* oncogene<sup>[6]</sup> or a defective adenovirus E1A oncogene<sup>[7]</sup> to increase the transformation of primary rodent fibroblast. The present study was undertaken to obtain more direct evidence that cyclin D1 plays a critical role in establishing and maintaining the transformed phenotype of these tumor cells. To this end,

<sup>1</sup>Department of Gastroenterology, Southwest Hospital, Third Military Medical University, Chongqing 400038, China

<sup>2</sup>Institute of Digestive Diseases, Xijing Hospital, Fourth Military Medical University, Xian 710033, China

<sup>3</sup>Columbia-Presbyterian Cancer Center, Columbia University, New York 10032, USA

<sup>4</sup>Department of Gastroenterology, Jiuxianqiao Hospital, Beijing 100016, China

CHEN Bing, male, born on 1960-11-27 in Nanjing City, China, associate professor of internal medicine, Ph.D. & MD in gastroenterology, post doctor of Third Military Medical University, China, having 24 papers published.

\*Supported by the National Outstanding Youth Science Foundation of China, No.3952520.

**Correspondence to:** Dr CHEN Bing, Department of Gastroenterology, Southwest Hospital, Third Military Medical University, Chongqing 400038, China.

Tel. +86-23-68754259

E-mail.bingchen@cq.col.com.cn

Received 1998-07-30

an antisense cyclin D1 cDNA was stably expressed in human gastric cancer cell line SGC7901/VCR that kept high expression of cyclin D1. This led to decreased levels of the endogenous cyclin D1 protein, marked inhibition of cell proliferation, and loss of tumorigenicity. These findings provide direct evidence that the cyclin D1 gene plays an essential role in the increased proliferation and oncogenesis of the gastric cells.

## MATERIALS AND METHODS

### Cell culture

The human cell lines used in the study, SGC7901/VCR gastric cancer cell line<sup>[8]</sup>, T24 bladder carcinoma cell line and K562 leukemia cell line, were obtained from Digestive Diseases Institute and Stomatology Biology Center of the Fourth Military Medical University, Xi'an, China. Cells were maintained in RPMI 1640 medium plus 100mL/L fetal calf serum (FCS). The medium for the cell lines containing the *neo* resistant gene was supplemented with G418.

### Construction of antisense cyclin D1 expression plasmids

The RKSD1 that contains the 1.1kb-human cyclin D1 cDNA in *Hind* III site is a present of Columbia-Presbyterian Cancer Center. A cyclin D1 subcloning plasmid termed BKSD1 was constructed by subcloning the human cyclin D1 cDNA into a subcloning vector Bluescript KS with recombinant DNA technology of molecular biology. pDORD1AS, an eukaryotic expression vector containing the 1.1 kb human cyclin D1 cDNA in its antisense orientation cloned into the retroviral vector pDOR-*neo*, was successfully constructed by the method as described before<sup>[9]</sup>.

### Lipofectamine mediated transduction

The pDORD1AS and vector control pDOR-*neo* plasmids were transfected into SGC7901/VCR gastric cancer cells using standard lipofectamine transfection procedure. A stable expression of cyclin D1 antisense RNA subline termed SGC7901/VCRD1AS was obtained by selection in G418.

### Immunohistochemistry

Exponentially proliferating cells grown on glass slides were subjected to immunohistochemical staining by using a monoclonal antibody DSC-6 against cyclin D1. T24 and K562 cell lines were used as positive and negative controls of cyclin D1 overexpression, respectively<sup>[6,10]</sup>.

### In situ hybridization

Using BKSD1 containing a pair of promoters for T7 and T3 RNA polymerase as a template vector, DIG-labeled, antisense and sense RNA probes of cyclin D1 was made by *in vitro* transcription of DNA. Ex-

ponentially proliferating cells grown on glass slides were subjected to *in situ* hybridization by a standard nonradioactive *in situ* hybridization procedure. Control cell lines included T24, K562, SGC7901/VCR and SGC7901/VCRneo which is a pDOR-*neo* transfected subline of SGC7901/VCR.

### Flow cytometric analysis

Cells were cultured in complete medium. When they were exponentially dividing, the cells were collected and analyzed for the cell cycle distribution (PI dyeing) and the expression level of cyclin D1 (immunofluorescence) by flow cytometry. All experiments were repeated three times.

### Doubling times and saturation density

Cells were plated in triplicate at a density of  $2.5 \times 10^4$  per well in 24-well plates in 1mL of RPMI 1640 plus-100mL/L-FCS. The number of cells per well was counted every day for 10 days. The doubling times and saturation densities of each cell line were calculated.

### Assessment of serum dependence

The growth rates of the two control cell lines and SGC7901/VCRD1AS cell line were measured at different concentrations of FCS. All cells were seeded initially of  $2.5 \times 10^4$  cells/well. Growth of each of the three cell lines was determined at three different serum concentrations (10%, 2.5% and 0.5%).

### Soft agar assay

Growth in 3g/L-Noble agar was assayed. In brief, cells were suspended in RPMI1640 plus 200mL/L-FCS containing 3g/L-agar and plated in triplicate in 24-well plates. After 2 weeks of growth, the cells were counted by microscopy. All experiments were repeated two times and similar results were obtained.

### Tumorigenicity assays

Cells of  $5 \times 10^5$  were injected subcutaneously into multiple sites in athymic (nude) mice. The animals were monitored for tumor formation every week and sacrificed one month later.

## RESULTS

### Expression of antisense RNA of cyclin D1 in SGC7901/VCR cells

We introduced an antisense cyclin D1 cDNA sequence into the SGC7901 cell line, whose cyclin D1 gene was overexpressed. Following G418 selection, the drug resistant (*neo*+) cell SGC7901/VCRD1AS was randomly collected from the cultures infected with the pDORD1AS construct. As controls, *neo*+ clone SGC7901/VCRneo was selected from SGC7901/VCR culture infected with pDOR-*neo* vector lacking the antisense cyclin D1 cDNA sequence.

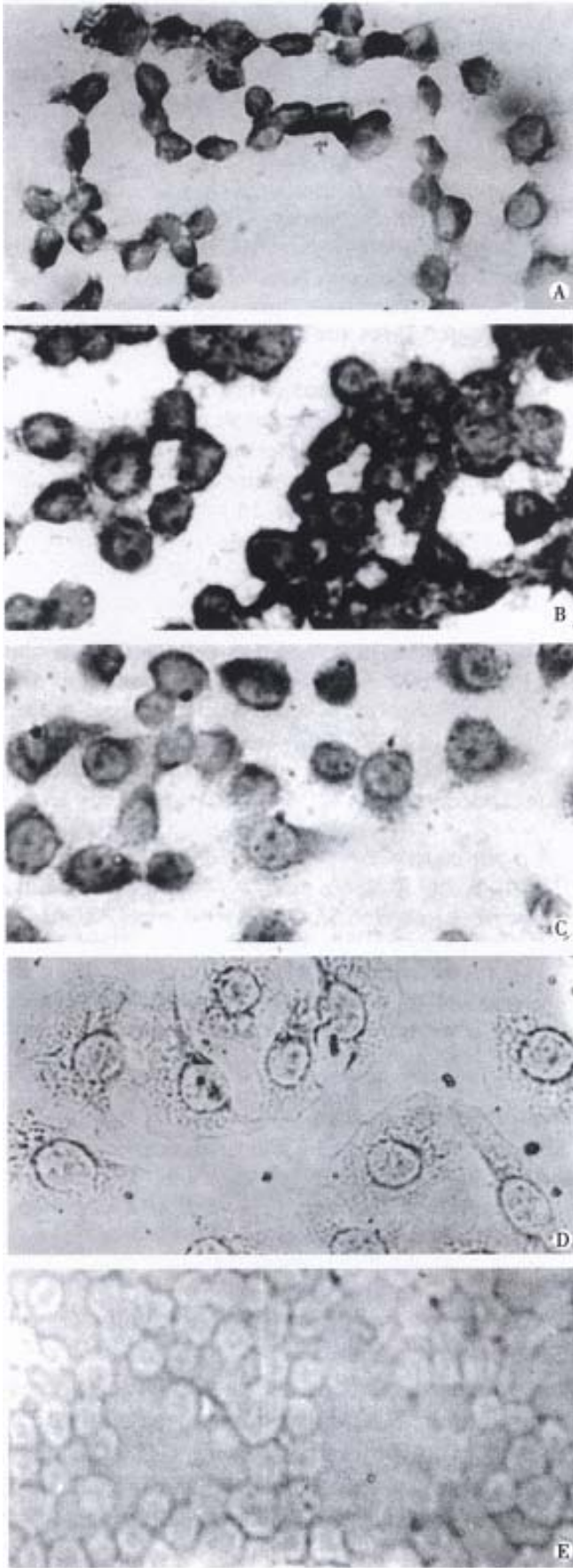


**Figure1** The result of *in situ* hybridization of cyclin D1 mRNA. A T24; B. SGC7901/ VCR; C. SGC7901/ VCRneo; D. SGC7901/VCRD1AS; E. K562

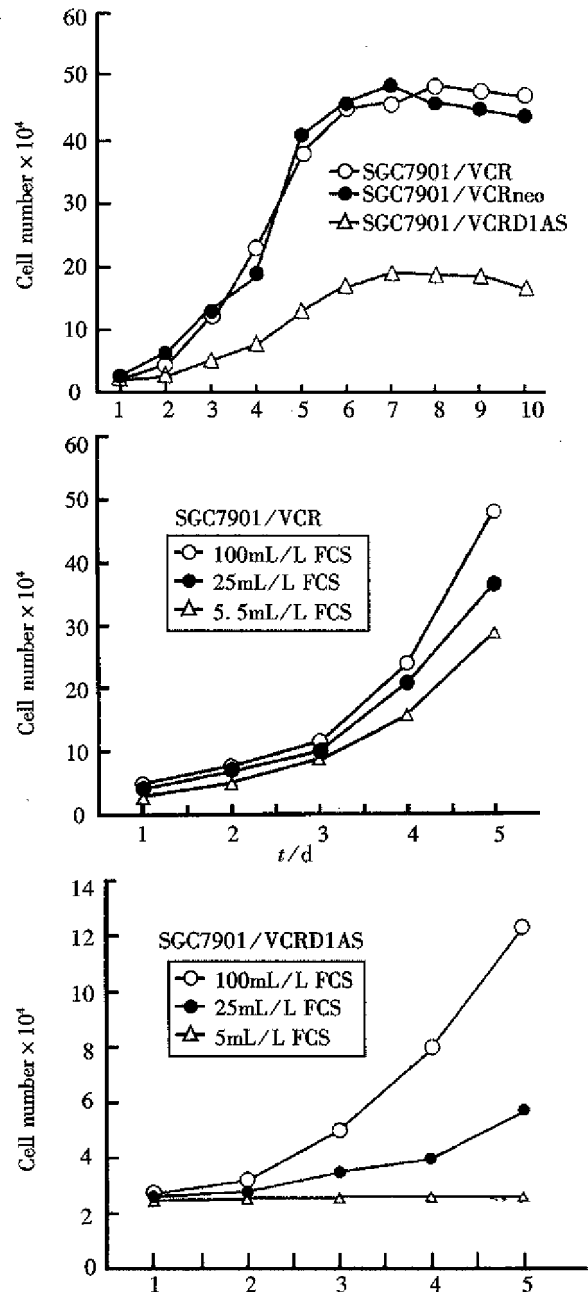


**Figure2** Growth curve of SGC7901/VCRD1AS and control cell lines.

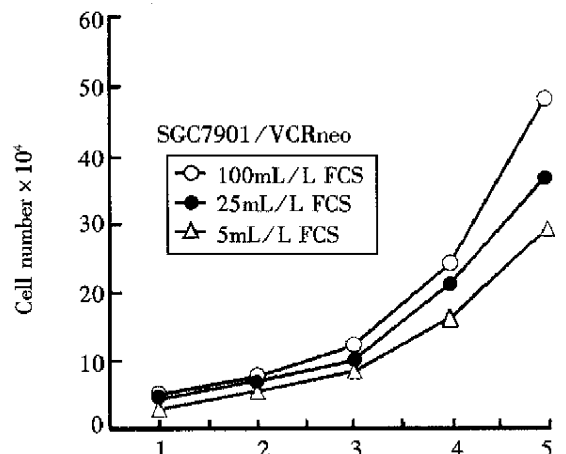


**Figure3** Serum dependence of SGC7901/VCRD1AS and control cell lines.

It turned out by immunohistochemistry, flow cytometry and *in situ* hybridization that the expression levels of cyclin D1 protein and mRNA were much lower ( $P < 0.01$ , inhibition rate of cyclin D1 protein expression level by flow cytometry assay was 36%) in SGC7901/VCRD1AS than in SGC7901/VCR and SGC7901/VCR neo control cells.

### Characterization of morphology, growth properties and cell cycle progression of antisense cyclin D1 expressing cells

The observation results of morphology. The SGC7901/VCR and SGC7901/VCR neo control cells displayed a loss of contact inhibition and formed dense foci when they grew to a high saturation density. The SGC7901/VCRD1AS cells grew at monolayer and low cell density, manifested an increased cytoplasm to nucleus ratio, and were much flatter and larger in cell size than the control cells (Figure 1).

The analysis of cell biology. As Figures 2, 3 and Table 1 show, compared with control cells, the SGC7901/VCRD1AS cells displayed a much longer doubling time ( $P < 0.01$ ), an increased percentage of cells in the G1/G0 phase, required serum dependence to some extent, a much lower saturation density ( $P < 0.01$ ), and a marked inhibition on tumorigenicity in nude mice and soft agar cloning efficiency ( $P < 0.01$ ).

**Table 1 Growth properties and tumorigenicity of SGC7901/VCRD1AS and control cell lines**

Cell line	SGC7901/VCR	SGC7901/VCRneo	SGC7901/VCRD1AS
Doubling time (h)	26.8	26.4	42.2
Saturation density ( $\times 10^5$ )	4.8	4.8	1.9
Cell cycle distribution (%)			
G1/G0	64.6	63.8	80.9
S	25.9	27.8	13.0
G2-M	9.4	8.3	6.1
Colony forming efficiency (%)	5.47	5.50	0.03
Tumor formation in nude mice	4/4	4/4	0/4

### DISCUSSION

In previous studies, the anti-cyclin D1 antibodies or cyclin D1 antisense plasmids were microinjected into fibroblast<sup>[10]</sup> or B-cell lymphoma cell lines<sup>[11]</sup> during

the G1 interval. The cells were prevented from entering the S phase. These results indicated that cyclin D1 is required for cells to undergo the G1-S transition. However, because of the transient nature of these microinjection studies, they did not address the role of cyclin D1 overexpression in continuously dividing cells, in growth control and tumorigenesis. Overexpression of cyclin D1 in fibroblasts shortened the G1 phase<sup>[6]</sup>. In our study, stable overexpression of antisense RNA to cyclin D1 can inhibit the cell growth and reverse the transformed phenotype of gastric cancer cells besides a marked decrease in the mRNA and protein level of cyclin D1. For example, a much longer doubling time and increased percentage of G1/G0 cells reveal G1 phase arrest, a much lower saturation density and reacquired serum dependence announce restored adjustability by exogenous signals, a monolayer growth feature in low density and increased cytoplasm to nucleus ratio manifest reacquired anchorage dependent and somewhat epithelial feature. Our present studies provide the evidence that inhibition of the expression of cyclin D1 in tumor cells that overexpress this gene can reverse their transformed phenotype. It is of clinical significance because large numbers of human tumors display overexpression of cyclin D1. Our findings may provide a potential approach of gene therapy for gastric cancer<sup>[12]</sup>.

### REFERENCES

- 1 Oliff A, Gills JB, Cormick FM. New molecular targets for cancer therapy. *Sci Am*, 1996;275:110-112
- 2 Sherr CJ. G1 phase progression: cycling on cue. *Cell*, 1994;79:551-555
- 3 Weinberg RA. How cancer arises. *Sci Am*, 1996;275:32-34
- 4 Resnitzky D, Reed SI. Different roles for cyclin D1 and E in regulation of the G1-S transition. *Mol Cell Biol*, 1995;15:3463-3469
- 5 Sherr CJ. Cancer cell cycle. *Science*, 1996;274:1672-1677
- 6 Jiang W, Kahn SM, Zhou P, Zhang YJ, Cacace A, Infante SD. Overexpression of cyclin D1 in rat fibroblasts causes abnormalities in growth control, cell cycle progression and gene expression. *Oncogene*, 1993;8:3447-3457
- 7 Hunter T. Cyclins and cancer. *Cell*, 1991;66:1071-1074
- 8 Cai XI, Fan DM, Zhang XY. Establishment and phenotype of MDR human gastric cancer cell lines. *Chin Clin Tumor*, 1995;21(Suppl):67-72
- 9 Chen B, Zhang XY, Wang CJ, Hui HX, Jing M, Fan DM. Construction and appraisal of eukaryotic expression vector antisense to cyclin D1. *J Cell Mol Immunol*, 1997;13:45-46
- 10 Kurzrock R, Ku S, Talpa Z. Abnormalities in the PRAD1 (CYCLIN D1/BCL-1) oncogene are frequent in cervical and vulva squamous cell carcinoma cell lines. *Cancer*, 1995;75:584-590
- 11 Lukas J, Pngano Mi Staskova Z, Draetta G, Bartek J. Cyclin D1 protein oscillates and is essential for cell cycle progression in human tumor cell lines. *Oncogene*, 1994;9:707-718
- 12 Xu CT, Pan BR. Current status of gene therapy in gastroenterology. *WJG*, 1998;4:85-88

# Effect of cell fusion on metastatic ability of mouse hepatocarcinoma cell lines \*

JI Yan<sup>1</sup>, LING Mao-Ying<sup>1</sup>, LI Ying<sup>1</sup> and XIE Hong<sup>2</sup>

**Subject headings** carcinoma, hepatocellular; cell lines; cell fusion; neoplasm metastasis; lymphatic metastasis

## Abstract

**AIM** To study the effect of cell fusion on metastatic ability of mouse hepatocarcinoma cells and the factors involved in the process of metastasis.

**METHODS** By the method of successively increasing the concentrations, cell fusion and limit dilution, 8-Ag resistant cells were selected, and HGPRT-Hca-P cells and eight cloned hybridoma cells were obtained. To observe their metastatic ability, they were inoculated into mice foodtaps and the drainage lymph nodes were examined under microscope.

**RESULTS** The end concentration of 8-Ag which was used to select HGPRT deficient Hca-P cells was 30mg/L. All the cells selected died in HAT culture medium in one week. Fused cells appeared approximately 9 days later. They were round, transparent and a little larger than their parental cells. Eight clones of hybridoma cells were obtained and named as PSH1-PSH8. The metastatic rate of HGPRT-Hca-P cells and PSH7 cells was 28.6% and 71.4% respectively, the difference being significant ( $P < 0.05$ ). The metastatic rate of other clones was no more than 20% and there was no significant difference from HGPRT-Hca-P cells ( $P > 0.05$ ).

**CONCLUSION** In normal mice splenic lymphocytes, there are some factors that could inhibit tumor metastasis, however, there are some other factors accelerating tumor cells to metastasize. The establishment of PSH7 provides an experimental model which could be used to study the factors involved in metastasis.

## INTRODUCTION

It was known during the 1970s that the malignancy of hybridoma cells decreased when tumor cells were fused with normal cells and the malignant phenotype was suppressed obviously or diminished. But since 1980, in many laboratories, the increased invasive and metastatic abilities of hybridoma cells have been found when tumor cells were fused with lymphocytes or macrophages which had ambulant ability<sup>[1-5]</sup>. These results implied that there were some factors that could increase the metastatic ability of tumor cells and raised a hypothesis that tumor cells used the ambulant mechanism of normal cells<sup>[6]</sup>. In this study, cell fusion was used to study the factors involved in the process of metastasis.

## MATERIALS AND METHODS

### Animals

A total of 615 inbred mice were provided by the Department of Pathology of Dalian Medical University.

### Tumor cell lines

Mouse hepatocarcinoma cell lines Hca-P(P) with low lymphatic metastatic ability were established and stored as described previously<sup>[7]</sup>.

### Hypoxanthine-guanine phosphoribosyltransferase deficient (HGPRT-) cells

In order to select HGPRT- cells, P cells were converted into 8-Ag resistant by growing in successively increased concentration of 8-Ag as described previously<sup>[8]</sup>. The initial concentration was 3mg/L. If alive tumor cells had the dominant position, the concentration was increased successively, from 3 mg/L to 6 mg/L, 10 mg/L, 15 mg/L, 20 mg/L, 25 mg/L, and 30 mg/L. To test the sensitivity of selected cells to HAT, 8-Ag resistant cells which had been cloned by limit dilution method were inoculated into HAT culture medium. A week later, Trypan blue repelling test was used to judge the vitality of cells and the 100% dead cells which kept alive in normal culture medium were proliferated. The cells were taken as parental cells in fusion. To measure their metastatic ability, HGPRT-Hca-P cells were inoculated into foodtaps of 615 mice<sup>[7]</sup>. The animals were sacrificed 28 days later, and original tumor, the ipsilateral popliteal, inguinal and axillary lymph nodes were removed, fixed in 10% formalin, made into paraffin section, stained with HE

<sup>1</sup>Department of Pathology, Dalian Medical University, Dalian 116027, Liaoning Province, China

<sup>2</sup>Cell Biology Institute of the Chinese Academy of Sciences, Shanghai, China

LING Mao-Ying, female, born on 1934-08-03 in Yibin city, Sichuan Province, graduated from Guiyang Medical College in 1956, Professor of Pathology, majoring in studies on experimental tumor metastasis and its relative mechanism, having more than 30 papers published.

\*Project supported by the National Natural Science Foundation of China, No.39470776

Correspondence to: Professor LING Mao-Ying, Department of Pathology, Dalian Medical University, Dalian 116027, Liaoning, China  
Tel. +86-411-4691802 Ext. 277

Email. ly8853@pub.dl.inpta.net.cn

Received 1998-08-04

and observed under microscopy.

### Fusion

Spleen lymphocytes of normal mice were prepared routinely. HGPRT<sup>-</sup>-Hca-P cells and normal spleen lymphocytes were taken as parental cells of fusion. Solution of fusion was 50% PEG-4000. The average cell numbers of each well in 96 well plate used for fusion were  $3 \times 10^5$  and the ratio of lymphocytes to tumor cells was 8:1. While fused cells appeared, they were suspended in 2×HAT culture medium, then were cultured at 37°C in a humidified atmosphere (950 mL/L air, 50 mL/L CO<sub>2</sub>). The medium was changed every three days and two weeks later it was substituted by normal medium. Subsequently, the obtained hybridoma cells were cloned by limit dilution method. To measure the metastatic ability of hybridoma cells, Hca-P cells and HGPRT<sup>-</sup>-Hca-P cells were inoculated into foodtaps of 615 mice respectively as described above.

### RESULTS

The end concentration of 8-Ag which was used to select HGPRT deficient Hca-P cells was 30mg/L. All of the cells proliferated after being cloned died in HAT culture medium within one week, suggesting that they were HGPRT<sup>-</sup> cells.

Fused cells appeared approximately 9 days later. They were round, transparent and were a little larger than their parental cells. Eight clones of hybridoma cells were obtained by using limit dilution method and were named PSH1-PSH8. It was shown by the histological examination that the metastatic ability of PSH7 increased but the rest decreased. The metastatic ability of PSH7 was significantly higher than that of HGPRT<sup>-</sup>-Hca-P cells, but there was no significant difference between HGPRT<sup>-</sup>-Hca-P and Hca-P which were not treated with 8-Ag ( $P < 0.05$ , Table 1). Because the sample size was small, exact probabilities in 2×2 table of Chi-square test was used to analyze the data.

**Table 1** Metastatic rate of cells

Cells	Number of experimental animals	Number of metastatic animals	Metastatic rate (%)	<i>P</i>
HGPRT <sup>-</sup> -Hca-P	14	4	28.6	0.24>0.05
Hca-P	16	3	18.8	
PSH1	8	1	12.5	
PSH2	8	0	0	
PSH3	8	1	12.5	
PSH4	10	2	20	
PSH5	8	0	0	
PSH6	10	1	20	
PSH7	14	10	71.4	0.027<0.05
PSH8	8	0	0	

### DISCUSSION

The method of successively increasing concentration was often used to select resistant cells. In this study, it was used to select 8-Ag resistant Hca-P cells. The critical concentration was 30 mg/L under which most cells died. As the concentration was increased, the survived and proliferated cells were 8-Ag resistant cells. These cells could be transplanted into normal culture medium. In order to prevent HGPRT<sup>-</sup> cells from turning into HGPRT<sup>+</sup> cells, it was necessary to treat them with 8-Ag now and then or always keep them growing in culture medium containing 8-Ag.

Cell fusion has been extensively used in the study of phenotypic expression and regulation of malignant cells. It has been known that the metastatic ability of hybridoma cells could decrease or increase while certain normal cells were fused with nonmetastatic or low metastatic cells. In those experiments, the metastatic ability of hybridoma cells increased only when the parental cells were ambulant cells, such as lymphocytes or macrophages and the hybridoma cells obtained certain characters.

Both Hca-F and Hca-P cells isolated from mouse hepatocarcinoma cells had different metastatic ability only to lymph nodes but not to other organs. Because the metastatic rate of P cell was 18.8% and metastatic phenotype was stable, it is of great advantage to study the changes and related mechanism of metastatic ability of hybridoma cells which were obtained from the fusion of Hca-P and spleen cells of mice.

The metastatic rate of HGPRT<sup>-</sup>-Hca-P cells was still lower than 30% and there was no significant difference from that of Hca-P cells. The metastatic ability of most hybridoma cells kept stable or decreased, in contrast, that of PSH7 increased up to 71.4%, being significantly different from that of HGPRT<sup>-</sup>-Hca-P cells. Because hybridoma cells had the nature of their parental cells, it is important to study the factors which affect tumor metastatic ability by cell fusion. Hca-P as one of the parental cells had the character of stable metastatic ability to lymph nodes. Therefore no matter how the metastatic ability changed, it was caused by lymphocytes. The metastatic ability of seven hybridoma cell lines decreased, while only one increased. These results suggested that the lowering trend was dominant, which was probably due to tumor suppressive gene existing in normal cells, furthermore, there were some other factors that could enhance tumor metastatic ability.

There were many similar aspects between metastasis of tumor cells and ambulence of lymphocytes. Both of them could enter circulation by passing endothelia of vessels, proliferate in drainage lymph nodes, and enter peripheral tissue by immi-

gration. Furthermore, organ preference of tumor metastasis was similar to the homing of lymphocytes. The relationship between homing receptor and tumor metastasis was discovered recently<sup>[9]</sup>. Here comes the question: do the hybridoma cells with increased metastatic ability use some special mechanism of lymphocytes or macrophages, such as ambulant mechanism and homing receptor. It is suspected that probably tumor cells metastasize to special organs by means of some structures like homing receptor and a certain mechanism like the homing of lymphocytes. The results of our study show that there must be something existing in spleen lymphocytes that accelerates tumor cells to metastasize. The establishment of PSH7 has provided an experimental model which could be used to study the factors involved in metastasis.

## REFERENCES

- 1 Baetselier PD, Gorelik E, Eshhar Z, Ron Y, Katzav S, Felgman M. Metastatic properties conferred on non metastatic tumor by hybridization of spleen B-lymphocyte with plasmacytoma cells. *J Natl Cancer Inst*,1982;67:1079
- 2 Hays EF, Weinroth SE, Macleod CL, Kitada S. Tumorigenicity of T-lymphoma/ T-lymphoma hybrids and T-lymphoma/normal cell hybrids. *Int J Cancer*,1986;38:597
- 3 Larizza L, Schirmacher V, Pfluger E. Acquisition of high metastasis capability after *in vivo* fusion of a non-metastasis tumor line with a bone marrow-derived macrophage. *J Exp Med*, 1984;160:1579
- 4 Roos E, La Riviere, Collard JG, Stuart MJ. Invasiveness of T-cell hybridomas *in vitro* and their metastatic potential *in vivo*. *Cancer Res*,1995;45:6238
- 5 Larizza L, Schirmacher V, Graf L. Suggestive evidence that the highly metastatic variant Esb of the T cell lymphoma Eb is derived from spontaneous fusion with a host macrophage. *Int J Cancer*,1984;34:699
- 6 Peter H, Margot Z, Steven T, Helmut P. CD44 splice variant: metastasis meet lymphocyte. *Immunol Today*,1993;14:395
- 7 Ling MY, Wang MH, Guo LL, Wang B. Study on the character of Hca/16A3-F and Hca/A2-P cell lines of mouse hepatocarcinoma cells with lymphatic metastatic ability. *Natl Med J China*,1995;75:170
- 8 Zheng E. Technique of tissue culture. 2nd ed. *Beijing: People's Health Pubing House*, 1993
- 9 Roos E. Adhesion molecules in lymphoma metastasis. *Cancer Metastasis Rev*, 1991;10:33

Edited by MA Jing-Yun

# Effect of HCV infection on expression of several cancer-associated gene products in HCC \*

YANG Jian-Min, WANG Rong-Quan, BU Bao-Guo, ZHOU Zi-Cheng, FANG Dian-Chun and LUO Yuan-Hui

**Subject headings** carcinoma; hepatocellular/etiology; hepatitis C-like viruses/pathogenicity; oncogenes/genetics; genes, suppressor; tumor/genetics; immunohistochemistry/methods

## Abstract

**AIM** To study hepatocarcinogenesis of hepatitis C virus (HCV).

**METHODS** Expression of HCV antigens (CP10, NS3 and NS5) and several cancer-associated gene products (ras p21, c-myc, c-erbB-2, mutated p53 and p16 protein) in the tissues of hepatocellular carcinoma (HCC,  $n = 46$ ) and its surrounding liver tissue were studied by the ABC (avidin-biotin complex) immunohistochemical method. The effect of HCV infection on expression of those gene products in HCC was analyzed by comparing HCV antigen-positive group with HCV antigen negative group.

**RESULTS** Positive immunostaining with one, two or three HCV antigens was found in 20 (43.5%) cases, with either of two or three HCV antigens in 16 (34.8%) cases, and with three HCV antigens in 9 (19.6%) cases. Deletion rate of p16 protein expression in HCC with positive HCV antigen (80%, 16/20) was significantly higher than that in HCC with negative HCV antigen. Where as no significant difference of the other gene product expression was observed between the two groups.

**CONCLUSION** HCV appears related to about one-third of cases of HCC in Chongqing, the southwest of China, and it may be involved in hepatocarcinogenesis by inhibiting the function of p16 gene, which acts as a negative regulator of cell cycle.

Department of Gastroenterology, Southwest Hospital, Third Military Medical University, Chongqing 400038, China

YANG Jian-Min, male, born on 1956-06-21 in Linhai, Zhejiang Province, graduated from Third Military Medical University in 1983, earned doctor degree in 1993, now associate professor and tutor of postgraduates, mainly engaged in the basic and clinical research on hepatocellular carcinoma, as first and second or third author having 30 and 20 papers published, co-edited 3 monographs, which were awarded both the 2nd and 3rd Class prizes for scientific and technological progress of the PLA.

Tel. +86-23-68754124(O), 68754270(H)

\*Supported by the PLA Eighth 5-year Scientific Research Fund for Youths.

Correspondence to: Prof YANG Jian-Min.

Received 1998-09-17

## INTRODUCTION

Our previous studies by seroepidemiological, molecular epidemiological and immunopathological methods have revealed that hepatitis C virus (HCV) infection is closely linked to development of hepatocellular carcinoma (HCC) and HCV may be the second important factor in association with HCC-etiology in Chongqing, the southwest of China<sup>[1-5]</sup>. But the molecular mechanisms involved in hepatocarcinogenesis of HCV remain poorly understood. Up to now, many authors believe that HCV can not directly change the structure of the host genes like hepatitis B virus by integration because HCV is a RNA virus. Therefore, the effect of HCV on factors of controlling cell growth and development is an important field in the hepatocarcinogenesis studies. In this study, expression of several oncogene and tumor suppressor gene products in HCV-associated and non-HCV-associated HCC was investigated, so as to identify if HCV infection can affect expression of these gene products.

## MATERIALS AND METHODS

### Specimens

HCC specimens of 46 cases were randomly selected from partial hepatectomy in 1994 in this hospital. Of them, 38 cases contained pericancerous liver tissues. All specimens were fixed in 100mL/L-formalin, embedded in paraffin and sequentially sectioned with a thickness of 5  $\mu$ m.

### Reagents

Mouse monoclonal antibodies (mAb) to HCV NS3 and NS5 were kindly provided by Professor TAO Qi-Min (The Institute of Hepatology, Beijing Medical University). Mouse mAb against HCV CP10 was kindly presented by Professor LI Meng-Dong (Department of Infectious Diseases, the Southwest Hospital). Mouse mAbs to human ras p21, C-myc, C-erbB-2 and mutated p53 protein were purchased from Fuzhou Maxim Biotechnical Company. Mouse mAb to human p16 protein was purchased from Beijing Zhongshan Biotechnical Company. Avidin-biotin complex (ABC) kits were purchased from Fuzhou Maxim Biotechnical Company and Vector company.

### Immunostaining

Immunostaining of HCV antigens CP10, NS3, NS5 and cancer-associated gene products ras p21, c-myc,

c-erbB-2, mutated p53 and p16 proteins was performed by the ABC method in each case. The procedures of ABC staining were taken according to the manufacturer's recommendations as previously described<sup>[5]</sup>. The color was developed with diaminobenzidine and hematoxylin. Positive and negative controls were simultaneously used to ensure specificity and reliability of the staining.

## RESULTS

### Expression of HCV antigens

In the 46 cases of HCC, positive HCV antigen was found in 20 (43.5%) cases, of which 4 cases with one positive HCV antigen, 7 cases with two positive HCV antigens, and 9 cases with three positive HCV antigens. The positive staining of HCV antigen CP10, NS3 and NS5 in the cancer tissues was observed in 10 (21.7%), 10 (21.7%) and 7 (15.2%) cases, respectively, while in its pericancerous liver tissues in 14 (36.8%), 13 (34.2%) and 12 (31.6%) cases. Although the expression rates were higher in the pericancerous tissues than in the cancer tissues, no statistical significance was obtained ( $P > 0.05$ ) (Table 1). The immunostaining of each HCV antigen was mainly seen in HCC and hepatocyte cytoplasm, seldom in the cell membranes, none in the nuclei. The positive-staining cells were distributed mostly in scattered or focalized patterns, seldom in diffused pattern.

**Table 1 Expression of HCV antigens in HCC tissue and its surrounding liver tissue (% positive rate)**

HCV antigens	Cancer	Non-cancer
CP10	21.7(10/46)	36.8(14/38)
NS3	21.7(10/46)	34.2(13/38)
NS5	15.2(7/46)	31.6(12/38)

### The effect of HCV infection on expression of the gene products

On the one hand, positive rates of ras p21 and mutated p53 in HCC (58.7%, 27/46; 28.3%, 13/46) were significantly higher than in the pericancerous tissues (34.2%, 13/38; 7.9%, 3/38,  $P < 0.05$ ), whereas the positive rate of p16 in HCC (41.3%, 19/46) was significantly lower than in the pericancerous tissues (63.2%, 24/38,  $P < 0.05$ ). But the expression rates of c-myc and c-erbB-2 did not show significant difference between the cancer and pericancerous groups ( $P > 0.05$ ). On the other hand, it attracted our attention that the positive rate of P16 protein in HCV antigen-positive HCC (20%, 4/20) significantly lower than in HCV antigen-negative HCC (57.7%, 15/26,  $P < 0.025$ ),

even though the expression rates of ras p21, C-myc, C-erbB-2 and mutated p53 showed no significant difference between HCV-associated and non HCV-associated HCC (Table 2).

**Table 2 Relationship of HCV antigens with expression of cancer-associated gene products(CAGP) (n, positive cases)**

HCV antigens	n	CAGP expression				
		p21	C-myc	C-erbB-2	p53	p16
Positive	20	11	11	9	5	4
Negative	26	15	20	13	8	15

## DISCUSSION

In the previous studies, we found that HCV RNA could be detected in 36.6% (34/93) serum samples of patients with primary hepatic carcinoma and 37.5% (21/56) cases of HCC tissues<sup>[1,3]</sup>. In this study, using three McAbs to different HCV antigens and immunohistochemical ABC method, we found that the positive immunostaining with either one, two or three HCV antigens was found in 20 (43.5%) cases, with either two or three HCV antigens in 16 (34.8%) cases and with three HCV antigens in 9 (19.6%) cases among the 46 cases of HCC. The present data are consistent with our previous studies and further indicate that about one-third of HCC seems to be related to HCV infection in Chongqing, the southwest of China. Up to now, a lot of affirmative evidences in seroepidemiology, molecular epidemiology and immunopathology have been obtained concerning the association of HCV infection with HCC development in this area.

Recent studies have shown that the molecular mechanisms of hepatocarcinogenesis are involved in oncogene activation and anti-oncogene inactivation like many other tumors. The role of ras, c-myc, c-erbB-2, p53 and p16 gene in the development and progression of HCC have been noted by many workers. To understand the potential hepatocarcinogenesis of HCV, we studied the expression of these gene products in HCV-associated and non-HCV associated HCC tissues. The results showed that the expression of ras p21, c-myc, c-erbB-2 and mutated p53 was not significantly different between HCV antigen-positive and HCV antigen-negative groups, but the deletion rate of p16 protein expression in HCV antigen-positive HCC (80%, 16/20) was significantly higher than in HCV antigen-negative HCC (42.3%, 11/26,  $P < 0.025$ ). It implicates that the molecular mechanisms involved in HCV hepatocarcinogenesis seems to be connected with the repression of p16 gene function.

The p16 gene is a new negative regulator of cell

cycle and tumor suppressor gene found recently, which is located in chromosome 9p21 with 8.5kb long and encoding for a nucleus phosphoprotein with 16kD-P16 protein. P16 protein can bind to cycle-dependent kinase 4 (CDK4), preventing their interaction with cyclin D and thereby preventing cell cycle progression from G1 to S phase. Many authors proposed that when p16 gene function is repressed, the activity of cyclin D/CDK4 complex will increase because of the CDK4 being free from the inhibition of P16 protein, thereafter cell proliferation will be out of control and tumor may develop at last<sup>[6,7]</sup>. Recently, Ray *et al* reported that HCV core protein can act as an effector in the promotion of cell growth by repression transcription of the another negative regulator of cell cycle and inhibitor of cyclin D/CDK4 complex p21 (WAF1/Cip1/Sid1) gene through unknown cellular factors<sup>[8]</sup>. Therefore, the role of p16 gene in molecular mechanisms of HCV hepatocarcinogenesis deserves further studies.

**ACKNOWLEDGEMENT** We thank Professor TAO Qi-Min for kindly providing the HCV, NS3, NS5, mAbs and Professor LI Meng-Dong for kindly providing the HCV CP10 mAb.

## REFERENCES

- 1 Yang JM, Liu WW, Jin HY. Relationship of hepatitis C virus infection with primary hepatic carcinoma: an investigation of serum HCV RNA in different population groups. *J Med Coll PLA*, 1993;8:109-113
- 2 Yang JM, Liu WW, Jin HY. Study on the replicative intermediate of hepatitis C virus in the tissues of hepatocellular carcinoma. *Chin J Dig*, 1994;14:210-212
- 3 Yang JM, Liu WW, Jin HY. Detection of hepatitis C virus RNA in formalin-fixed, paraffin embedded liver tissues from patients with hepatocellular carcinoma and liver cirrhosis. *Chin J Cancer*, 1994;13:299-301
- 4 Yang JM, Liu WW, Luo YH. Genotypic investigation of hepatitis C virus in patients with primary hepatic carcinoma, liver cirrhosis and hepatitis. *Chin J Infect Dis*, 1995;13:1-3
- 5 Wang RQ, Zhou ZC, Yang JM, Fang DC. Immunohistochemical study of hepatitis C virus NS5 antigen in the tissues of hepatocellular carcinoma and its surroundings. *Natl J Med China*, 1996;76:623
- 6 Foulkes WD, Flanders TY, Pollock PM, Hayward NK. The CDKN2A (p16) gene and human cancer. *Mol Med*, 1997;3:5-20
- 7 Biden K, Young J, Buttenshaw R, Searle J, Cooksley G, Xu DB, Leggett B. Frequency of mutation and deletion of the tumor suppressor gene CDKN2A (MTS1/p16) in hepatocellular carcinoma from an Australian population. *Hepatology*, 1997;25:593-597
- 8 Ray RB, Steele R, Meyer K, Ray R. Hepatitis C virus core protein represses p21WAF1/Cip1/Sid1 promoter activity. *Gene*, 1998;208:331-336

Edited by MA Jing-Yun

# Experimental research on phospholipids variation of halothane on liver mitochondria

SUI Bo<sup>1</sup>, ZHANG Guang-Ming<sup>2</sup>, YU Wei-Feng<sup>3</sup>, WANG Xue-Min<sup>4</sup>, MA Yong-De<sup>1</sup> and LIU Shu-Xiao<sup>5</sup>

**Subject headings** halothane; sevoflurane; liver mitochondria; HPLC; hepatotoxicity

## Abstract

**AIM** To study the pathogenesis of hepatotoxicity of halothane.

**METHODS** The effect of different concentration of halothane and sevoflurane on mitochondrial membrane phospholipids composition of rat liver were analyzed using high performance liquid chromatography (HPLC) technology.

**RESULTS** Halothane at low concentration could degrade mitochondrial membrane major phospholipids and increase lysophosphatidylcholine.

**CONCLUSION** The pathogenesis of halothane hepatotoxicity was the phospholipids variation on liver mitochondria.

## INTRODUCTION

The effect of traditionally inhalational anesthetic halothane and new drug sevoflurane on mitochondrial membrane is reported below in an attempt to study the pathogenesis of halothane hepatotoxicity.

## MATERIALS AND METHODS

### *Preparation of liver mitochondria and pretreatment of specimen*

According to modified Estabrook's velocity gradient method<sup>[1]</sup>, the mitochondria of male rat weighing 150g-200g was separated. Seventy mmol sucrose and 220mmol bovine serum albumin were used as isolation medium. Albumin was assayed by biuret reaction. The mitochondria concentration was adjusted to 10g/L-30g/L. Phospholipids except for ganglioside and acetal phospholipid were extracted using improved Higgins' method<sup>[2]</sup>. The mitochondrial suspension was mixed well with the extraction solvent (1:10, V/V), and stood for 15min. The albumin was removed by centrifugation. CaCl<sub>2</sub> 0.05mL/L was added to the supernatant, and stood for centrifugation (3000 r/min). The lower layer was evaporated to dryness under nitrogen at 40°C - 50°C. After added with diluent accurately to the residue, the solution was sealed to protect from light and stored at -20°C for HPLC analysis. The whole procedure was carried out at 4°C in the air-tight ice-bath.

### *Preparation of solvent*

The standard control phospholipids of phosphatidylethanolamine (PE), phosphatidylinositol (PI), phosphatidylserine (PS), phosphatidylcholine (PC), cardiolipin (CL), sphingomyelin (SPH) and lysophosphatidylcholine (LPC) were purchased from Sigma Co.

Extracting solution: chloroform:methanol:hydrochloric acid (2:1:0.01, V/V/V).

Moving phase: n-hexane:isopropanol:ethanol:potassium dihydrogen phosphate (25 mmol/L):glacial acetic acid (370 : 485 : 100 : 562 : 0.1 V/V/V/V). The solution was evenly mixed and stood overnight for separating phosphoric acid crystal. After ultrafiltration and deoxygenation the supernatant was used as moving phase.

Standard solution: the standard control phospholipids were dissolved in the mixture of n-hexane:isopropanol (6 : 8, V/V). The concentration was 2g/L.

<sup>1</sup>Department of Anesthesia, General Hospital of Jinan Commanding Area, Jinan 250031, Shandong Province, China

<sup>2</sup>School of Pharmacy, the Second Military Medical University, Shanghai 200433

<sup>3</sup>Department of Anesthesia, East Liver Surgical Hospital, the Second Military Medical University, Shanghai 200433

<sup>4</sup>Department of Biochemistry, Basic Section, the Second Military Medical University, Shanghai 200433

<sup>5</sup>Department of Anesthesia, Changhai Hospital, the Second Military Medical University, Shanghai 200433

Dr. SUI Bo, male, born in 1958 in Shandong Province, graduated from the Second Military Medical University as a postgraduate in 1995, now an attending aesthetist, East Hepatobiliary Surgery Hospital, the Second Military Medical University, Shanghai 200433, having 12 papers published.

\*Project supported by the National Natural Science Foundation of China, No.94300126.

**Correspondence to:** Dr. SUI Bo, Department of Anesthesia, General Hospital of Jinan Commanding Area, Jinan 250031, China

Tel. +86-531-5946536

Received 1998-08-27

### HPLC analytical method

ISUZULC-6A liquid chromatograph, ISUZU Shim-Pack CLC-SIC column (6 mm × 15 cm), Guar PAKTM prepared column were used. The detection was performed at 206nm. After reaction of low concentration and high concentration of halothane or sevoflurane with mitochondrial membrane phospholipids, 10ml reaction solution was taken out for repeated injection<sup>[3]</sup>. Each sample was repeated for 8 times, and linear velocity (mm/min) was recorded. Qualitative analysis was made by identification of the retention time with standard control samples. The eluting sequence referred to Patton sequence<sup>[4]</sup>. Quantitative analysis was made by calculating the peak area and the relative content of phospholipids was expressed by the ratio between peak area and albumin.

## RESULTS

### Qualitative analysis

By comparing the HPLC chromatograph peak of phospholipids affected by halothane at low and high concentration with that of the normal liver mitochondria phospholipids, it could be seen that the main phospholipid peak decreased to some degree and LPC peak increased, especially when at high concentration. Sevoflurane at low concentration had no influence on phospholipid peak, but at high concentration it could decrease the main phospholipid peak and increase the LPC peak. However, the effect was not so obvious as that caused by halothane.

### Quantitative analysis

The change of liver mitochondrial phospholipids caused by halothane and sevoflurane is shown in Table 1. Halothane at both high and low concentration could decrease the main liver mitochondrial phospholipids and increase LPC significantly. The

change of phospholipids had no significant difference between sevoflurane at low concentration and the control while at high concentration the difference was marked. At high concentration, the change of phospholipids in liver mitochondria caused by halothane was much more obvious than that caused by sevoflurane.

### Time-phase change

The effect on the liver mitochondrial phospholipid principle started and went up rapidly as soon as halothane contacted with mitochondria and reached the peak at 4h. At low concentration it could recover to the level of the control group at 6h-8h while at high concentration it could not even within 24h. In each phase there had no significant difference between low concentration of sevoflurane and the control. At high concentration the effect caused by sevoflurane reached the peak at 4h and recovered to the control level at 8 h - 12 h. The time-phase change on LPC by halothane and sevoflurane at high concentration is demonstrated in Figure 1.

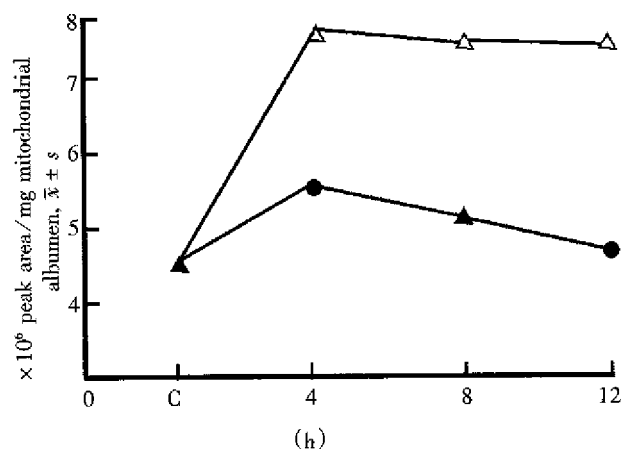


**Figure 1** The time phase change on LPC affected by halothane and sevoflurane in high concentration.

**Table 1** The variation of phospholipid in liver mitochondrial membrane affected by halothane and sevoflurane (phospholipid unit:  $\times 10^9$  peak area/g mitochondrial albumin  $\bar{x} \pm s$ )

Group	PE	PI	PS	CL	PC	SPH	LPC
Control	1.48±0.26	1.16±0.19	0.84±0.09	1.02±0.11	2.93±0.28	3.98±0.59	4.54±0.42
At low concentration							
Sevoflurane	1.37±0.19 (-7.62%)	1.08±0.09 (-7.12%)	0.78±0.07 (-6.93%)	0.95±0.11 (-6.55%)	2.72±0.17 (-7.19%)	3.76±0.33 (-5.52%)	4.89±0.33 (+7.81%)
Halothane	1.19±0.12 (19.60%) <sup>a,b</sup>	0.96±0.06 (-17.24%) <sup>a,b</sup>	0.70±0.80 (-16.94%) <sup>a,b</sup>	0.85±0.16 (-16.25%)	2.50±0.26 (-14.38%) <sup>a,b</sup>	3.37±0.29 (15.43%) <sup>a,b</sup>	5.90±0.12 (+30.1%) <sup>a,b</sup>
At high concentration							
Sevoflurane	1.30±0.12 <sup>a</sup> (11.89%)	1.02±0.04 <sup>a</sup> (12.02%)	0.63±0.04 <sup>a</sup> (-11.26%)	0.89±0.70 <sup>a</sup> (-12.55%)	0.64±0.16 <sup>a</sup> (-10.36%)	3.57±0.22 <sup>a</sup> (-10.40%)	5.69±0.32 <sup>c</sup> (+25.35%)
Halothane	1.06±0.09 <sup>c</sup> (-28.38%) <sup>b</sup>	0.81±0.07 <sup>c</sup> (-2.41%) <sup>b</sup>	0.78±0.09 <sup>c</sup> (-25.24%) <sup>b</sup>	0.75±0.09 <sup>c</sup> (-26.59%) <sup>b</sup>	2.09±0.16 <sup>c</sup> (-28.67%) <sup>b</sup>	2.95±0.24 <sup>c</sup> (-26.61%) <sup>b</sup>	7.81±0.67 <sup>c</sup> (+41.87%) <sup>b</sup>

<sup>a</sup>P<0.05, <sup>c</sup>P<0.01 vs control; <sup>b</sup>P<0.05 vs sevoflurane.

## DISCUSSION

This study indicated that halothane at low concentration could degrade mitochondrial membrane major phospholipids and increase LPC, at high concentration it could damage mitochondrial membrane irreversibly. Although sevoflurane had action on mitochondria, the effect was reversible. Probably due to its molecular structure halothane soluble in liver mitochondria easily and destroy phospholipids obviously. Halothane had the similar result in the study on the inhalational anesthetic effect on liver mitochondrial fluidity<sup>[5]</sup>.

Phospholipase A (PLA1, PLA2) is universal in liver membrane. Characterized by intramembranous mode of action, PLA2 has a high activity in mitochondria and the highest catalytic speed toward PE (twice that of PC, ten times of CL). PLA2 could be excited by Ca equilibration of liver cell caused by poison *in vivo* and *in vitro*. The phospholipid structure variation greatly influences biomembrane function and physical property including membrane conugase and receptor kinetics<sup>[6]</sup>. Some other studies showed that lipid variation such as mitochondrial phospholipids degradation and lipid peroxidation is an important original cause of liver cell damage. Destruction of the integration of mitochondria is the result of mutual function of the above-mentioned

two mechanisms while degradation of membrane phospholipid caused by activation of mitochondria probably plays a more important role in the early damage of overall function of liver cells<sup>[7]</sup>.

Besides hypoxia and low volume of blood flow the study also showed that mitochondrial phospholipids variation in the unorganized test is the main factor of halothane hepatotoxicity. Inhibition of PLA<sub>2</sub> activity and antilipid peroxidation may be the important measure of antihalothane hepatotoxicity<sup>[8]</sup>.

## REFERENCES

- 1 Estabrook IH. Oxidative and phosphorylation. Methods in enzymology. Vol 10. New York: Academic Press Inc. 1997;45:10003-10012
- 2 Higgins JA. Separation analysis of membrane lipid components, In: Findlay JBC, ed: Biological membrane: a practical approach. Washington DC: IRC Press, 1987:103-107
- 3 Yu WF, Liao MY. Effect of sevoflurane, anflurane, isoflurane and halothane on mice isolated liver mitochondrial respiration function. *Chin J Anesthesiol*, 1986;16:121-123
- 4 Patton G, Fasulo J, Robins S. Separation of phospholipids and individual molecular species of phospholipids by high performance liquid chromatography. *J Lipid Res*, 1982;23:190-194
- 5 Sui B, Yu WF, Liao MY. The effect of inhalational anesthetic on fluxion property of liver mitochondria. *Chin J Anesthesiol*, 1995;15:561-562
- 6 Liu MS, Karg GF. Activation of phospholipase A1 and A2 in heart, liver and blood during endotoxin shock. *J Surgical Res*, 1988;45:472-477
- 7 Yeagle PL. Lipid regulation of cell membrane structure and function. *FASEB J*, 1989;3:1833-1838
- 8 Yu WF, Wang JY, Liu SY. The hepatotoxicity of halothane and sevoflurane on primary culture mice liver cell. *Chin J Anesthesiol*, 1993;13:243-246

Edited by MA Jing-Yun

# Multifactorial analysis of recurrence of cholecystolithiasis in Shanghai area

CHEN Pei, WANG Bing-Sheng and HE Lian-Qi

**Subject headings** cholecystolithiasis/ therapy; recurrence; follow-up studies

## Abstract

**AIM** To explore the risk factors of gallbladder stone recurrence.

**METHODS** A multifactorial analysis was made for 1058 patients in Shanghai area whose gallbladder stones disappeared after different kinds of nonsurgical therapy, including oral litholytic therapy, extracorporeal shock wave lithotripsy and percutaneous choledocholithotripsy. Serum level of insulin and total bile acid were determined in 122 patients.

**RESULTS** After 1-8.8 years of follow-up, the recurrence rate of gallbladder stone was 11.6%, 22.4%, 29.5%, 36.4%, 39.3% and 39.7% respectively within 1, 2, 3, 4, 5 and over 5 years. The risk factors for the recurrence are: primary multiple gallstones ( $P<0.05$ ); family history of cholecystolithiasis ( $P<0.05$ ); greasy food intake ( $P<0.01$ ); low mean value of serum insulin ( $P<0.01$ ); and high mean value of total bile acid ( $P<0.01$ ).

**CONCLUSION** The recurrence of cholecystolithiasis is related to overintake of high fat and high cholesterol food, and might also be related to low level of serum insulin.

## INTRODUCTION

With the clinical application of different kinds of nonsurgical therapy, such as oral dissolution of gallstone (ODG), extracorporeal shock wave lithotripsy (ESWL), percutaneous transhepatic gallbladder catheterization (PTGC) and contact dissolution, and percutaneous choledocholithotripsy (PCCL), the recurrence and anti-recurrence of cholecystolithiasis come as a problem now. The clinical value of these methods mostly depends on the recurrence rate of this disease. Discovery of the risk factors of the recurrence of cholecystolithiasis, and interference procedures make it possible to lower the recurrence rate of gallstone. A multifactorial analysis of the recurrence of cholecystolithiasis in Shanghai area was carried out by the Shanghai Gallstone Research Coordination Group.

## MATERIALS AND METHODS

### Research subjects

A total of 1058 patients whose gallbladder stones had disappeared after different kinds of non-surgical therapy in Shanghai area entered this study, including 454 cases after ESWL, 594 cases after PCCL and 10 cases after ODG.

### Collection of follow-up materials

**Formulation of follow-up table** Let patients mark the items in the table and put the database into computer. The table includes sex, age of gallstone incipient occurrence, height, weight, diet hobby, symptom and medical treatment, related diseases (such as diabetes mellitus, coronary heart disease, liver disease), family history of gallstone, size and number of gallstone, recurrence and recurrence time of cholecystolithiasis.

**Examination of patients** One hundred and twenty-two patients were randomly selected from gallstone patients. Stone recurrence was found in 48 patients and non recurrence in 74. Venous blood of 5ml was drawn before breakfast in the morning. After standing still for half an hour, serum was sealed after centrifugation. Serum insulin level was determined with Coat-Acount insulin kit, and serum total bile acid (TBA) level by Ausbile Auto kit at the same time. Ultrasound examination was performed to evaluate the condition of gallbladder (length, width, height, stones), the degree of the liver lipid infiltration and the condition of the common bile duct (CBD), about 1 hour after greasy food. Ultra-

Department of General Surgery, Zhongshan Hospital, Shanghai Medical University, Shanghai 200032, China

Dr. CHEN Pei, male, born on 1970-08-04 in Shanghai, now a doctoral student in Shanghai Medical University, majoring in biliary tract surgery, working in the Department of General Surgery, Zhongshan Hospital, Shanghai 200032, China.

\*Supported by the scientific research fund of Shanghai Committee of Science and Technology.

**Correspondence to:** Professor WANG Bing-Sheng, Department of General Surgery, Zhongshan Hospital, Shanghai Medical University, Shanghai 200032, China

Tel. +86-21-64041990 Ext. 2912, 2302

Received 1998-10-04

som ography was repeated to reveal the width, length and height of the constricted gallbladder. With the formula  $V = (3.1416 \times L \times H \times W) / 6$ , the volume of gallbladder when starve or after diet, and the contraction ratio of the gallbladder volume were calculated.

### Statistical method

① There were 792 pieces of subjective materials and 122 objective materials when database was set up. ② The follow-up rate, recurrence rate and loss to follow-up rate of patients after ESWL, PCCL and ODG were calculated. ③ To find out the statistical difference between the recurrence and non-recurrence groups (Table 1). ④ To find out the statistical difference between the multiple and solitary stones groups (Table 2). ⑤ With the help from Epidemiology Teaching and Research group of Shanghai Medical University, the Epi-info Version 5.01a software was used to process the data.

**Table 1** Difference between recurrence and non-recurrence groups

	Odds ratio	M-H Chi square	P value
Incipient stone	1.52	6.43	<0.05
Sex proportion	0.91	0.31	0.58
Diet hobby	0.66	6.02	<0.05
Related disease	0.85	0.87	0.35
Clinical symptom	12.51	190.97	<0.01
Medical treatment	1.70	9.03	<0.01
Family history	1.55	4.54	<0.05
Mean thickness of gallbladder wall	1.95	2.75	0.10
Adipose infiltration of liver	1.01	0.00	0.98
	Recurrence	Non-recurrence	F test P value
Mean age	43.85±11.3	43.15±11.9	0.534 0.528
Mean weight/height	0.387±0.05	0.380±0.05	2.701 0.097
Mean contraction ratio of gallbladder	0.500±0.264	0.522±0.277	0.196 0.663
Mean value of serum insulin	0.611±0.320	0.753±0.261	7.289 <0.01
Mean value of serum TBA	5.963±1.883	5.00±1.955	7.545 <0.01

**Table 2** Difference between multiple stones and solitary stone groups

	Odds ratio	M-H Chi square	P value
Recurrence	1.52	6.43	<0.05
Sex proportion	1.08	0.21	0.65
Diet hobby	1.26	2.10	0.15
Related disease	0.95	0.09	0.76
Medical treatment	1.42	4.35	<0.05
Clinical symptom	1.21	1.38	0.24
Family history	1.08	0.13	0.72
Mean thickness of \gallbladder wall	0.55	2.15	0.14
Adipose infiltration of liver	0.91	0.05	0.83
	Multiple stones	Solitary stone	F test P value
Mean age	45.52±12.02	43.98±11.47	2.438 0.115
Mean weight/height	0.382±0.048	0.383±0.052	0.108 0.742
Mean contraction ratio of gallbladder	0.538±0.251	0.50±0.28	0.528 0.524
Mean value of serum insulin*	0.586±0.331	0.739±0.266	7.526 <0.01
Mean value of serum TBA	5.590±1.788	5.349±2.063	0.391 0.540

\*Because of abnormal distribution of the value of serum insulin, all data were changed into log value.

## RESULTS

### Total follow-up rate and stone recurrence rate

From January 1988 to October 1995, there were 1058 patients whose gallbladder stones had disappeared after different kinds of non-surgical therapy. Seven hundred and ninety-two patients were followed up for 1-8.8 years with a rate of 74.8%. The stone recurrence rate was 11.6%, 22.4%, 29.5%, 36.4%, 39.3% and 39.7% respectively within 1, 2, 3, 4, 5 and over 5 years. The total recurrence rate was 30.8%.

### Follow-up rate and recurrence rate after EWSL

Among 454 patients treated with ESWL, 413 patients are followed up, with a rate of 91.0%. There were 285 cases with non-recurrence and 128 with recurrence (17 were treated surgically, the others received conservative treatment). Forty-one patients were lost to follow-up. The recurrence rate of gallstone was 11.9%, 20.2%, 34.8%, 35.7%, 37.2% respectively within 1, 2, 4, 5 and over 5 years. The total recurrence rate was 31.0%.

### Follow-up and stone recurrence rate after PCCL

Among 594 patients treated with PCCL, 370 were followed up, the follow-up rate being 62.3%. There were 262 cases with non-recurrence and 108 with recurrence. Seven of them were treated surgically, the others received consecutive treatment, and 224 patients were lost to follow-up. The recurrence rate of gallstone was 8.8%, 22.4%, 29.5%, 36.7%, 47.4% respectively within 1, 2, 3, 4 and 5 years. The total recurrence rate was 29.9%.

### Follow-up and stone recurrence rate after ODG

Nine of 10 patients treated with ODG were followed up. The stone recurrence occurred in 8 patients. One case was lost to follow-up. Average follow-up length was 5 years and 4 months. The stone recurrence rate was 88.9%.

## DISCUSSION

### Recurrence rate of gallbladder stone

According to the literature, the recurrence rate of cholecystolithiasis is about 7%-11.8% after ODG, ESWL, PTGC and PCCL treatment<sup>[1-3]</sup>. In this study, the 1-year stone recurrence rate was 8.8%-11.9%, similar to the literature. It has been reported that the stone recurrence rate increases by about 10% each year, and by the fifth year it reaches 50%. After 5 years, a plateau with no further recurrence is usually seen<sup>[4]</sup>. The recurrence rates after ESWL, PCCL and ODG in the fifth year were 35.7%, 47.7% and 88.9% in this study. The lower gallstone recurrence rate after ESWL was probably related to strict selection of cases and higher ratio of solitary stone. More research should be done about

the relatively high recurrence rate of gallstone, otherwise the non-surgical therapy of gallbladder stone will lose their clinical application value.

#### **Risk factors for recurrence of gallstone**

The occurrence and the recurrence of the gallbladder stone probably have similar physiopathologic mechanism. It is related to many factors such as sex, age, weight index, diet hobby, labor strength, endocrine and metabolism, the size, number and character of the gallstone. In our study, no difference exists between recurrence and non-recurrence groups on such items as sex, average age, average weight/height, thickness of gallbladder wall, average ratio of gallbladder constriction, average degree of liver lipid infiltration and related diseases (diabetes, coronary heart disease, etc). Some items have significant difference between the two groups. The following in the recurrence group were significantly different from the non-recurrence groups: more clinical symptoms, more patients receiving medical treatment, low mean value of serum insulin and high mean value of serum TBA. The group with multiple gallstones, family history of gallstone and intake of greasy food has a higher recurrence rate. All of these differences are statistically significant ( $P < 0.05$ ).

Multiple gallstones seem to recur more often than solitary stone probably because ① most of solitary stones are cholesterol calculus, and lithotripsy and litholysis are effective treatment. The proportion of combined calculus is quite higher in multiple stones. The insoluble bile sludge after lithotripsy and dissolution might become the nucleus of the recurrence stone. ② Solitary stone is easier to be hit during the lithotripsy. The treatment takes less time and the broken stones are easier to be removed. There were less fine stones left and less injury to the gallbladder, while results were different for multiple stones.

Patients with family histories of gallstone had higher recurrence rates probably because of similar component and hobby of the diet, and hereditary factors.

Most literature reports that the serum insulin level in patients with gallstone is high<sup>[5]</sup>. The mechanism might be that insulin activates the cholesterol

synthesis reductase of liver, causing the increase of cholesterol synthesis and accelerating gallstone formation. Some authors have found no statistical difference in serum insulin level between diabetes patients with or without gallstone. In our cases, the mean serum insulin level in stone recurrence and multiple stone groups is significantly lower than in non-recurrence and solitary stone groups. When insulin is deficient, most glucose produced by glyconeogenesis was consumed, and the amount of pyruvate used to synthesize acetyl coenzyme A decreased. Most of acetyl coenzyme A is derived from lipose. A great quantity of acetyl coenzyme A provides the material for cholesterol synthesis. At the mean time, the deficiency of insulin reduces the capability of cholesterol utilization of liver, resulting in the hypercholesterolemia. This abnormal metabolism of lipid is often related to the formation of gallstone.

It has been proven that food is closely related to gallbladder stone. Epidemiological investigation also indicated that the high morbidity of cholecystolithiasis is correlated with the intake of low fiber and refined food in some developed countries. With the changing of the food components and reduction of the labor intensity, the morbidity of cholecystolithiasis is rising progressively.

Content and hobby of diet, over intake and low consumption of high fat and cholesterol food, relative deficiency of serum insulin, abnormal metabolism of glucose and lipose, liver disease and dysfunction of gallbladder might be all related to the formation of gallstone. Effective propaganda and education, reasonable diet structure, constant physical exercise and a certain amount of labor might help control the occurrence and recurrence of cholecystolithiasis.

#### **REFERENCES**

- 1 Schoenfeld LJ. Oral dissolution of gallstones. *Am J Surg*, 1993;165:427-430
- 2 Sackmann M, Niller H, Klueppelberg U, Von Ritter C, Pauletzki J, Holl J. Gallstone recurrence after shock-wave therapy. *Gastroenterology*, 1994;106:225-230
- 3 Mc Dermott VG, Arger P, Cope C. Gallstone recurrence and gallbladder function following percutaneous cholecystolithotomy. *J Vasc Interv Radiol*, 1994;5:437-438
- 4 O'Donnell LDJ, Heaton KW. Recurrence and re-recurrence of gallstones after medical dissolution: a long term follow-up. *Gut*, 1988;29:655-658
- 5 Han TQ, Zhang SD, Chen S, Yi F, Shi RT, Jiang ZH. A case control study on risk factors of cholelithiasis. *Chin J Experiment Surg*, 1995;12:99-100

# Consequence alimentary reconstruction in nutritional status after total gastrectomy for gastric cancer \*

WU Yin-Ai<sup>1</sup>, LU Bin<sup>1</sup>, LIU Jun<sup>1</sup>, LI Jiang<sup>1</sup>, CHEN Jiang-Rong<sup>2</sup> and HU Shi-Xiong<sup>1</sup>

**Subject headings** stomach neoplasms; gastrectomy; nutritional status; nutrition disorders; esophagitis

## Abstract

**AIM** To investigate the effect of gastroenteric reconstruction on the nutritional status of patients with gastric cancer after total gastrectomy.

**METHODS** From 1989-1994, nutritional status was studied in 24 patients, including 12 patients with the gastric reservoir and pyloric sphincter reconstruction (GRPS), 7 with Braun's esophago-jejunostomy (EJ) and 5 with Lawrance's Roux-en-Y reconstruction (RY). The ability of these patients to ingest and absorb the amount of nutrients was examined and compared, and metabolic balance test was performed to compare the efficiency of those patients to accumulate and use the absorbed nutrients.

**RESULTS** In the controlled hospital situation, the amount of food ingested by all the patients was greater than that required for maintenance of ideal body weight. In direct contrast, food intake in most patients with EJ or RY reconstruction significantly decreased when the patients returned home and that in EJ patients it was the lowest. The overgrowth of anaerobic bacteria was found in the jejunum in the patients with EJ and RY, due mainly to food stasis in the duodenum or in the Roux limb, caused by the operative procedure itself. In patients with GRPS, because of restoring of the alimentary continuity accord-

ing to the normal digestive physiologic characters, all the nutritional parameters could fall in the normal range.

**CONCLUSION** The most common mechanism responsible for postoperative malnutrition was inadequate food intake. Having solved the problem of alkaline reflux esophagitis, it is imperative to preserve the duodenal food passage to reduce malabsorption and other complications after total gastrectomy.

## INTRODUCTION

To investigate the nutritional consequences of gastroenteric reconstruction in patients with gastric cancer after total gastrectomy, nutritional status was studied among patients undergoing the gastric reservoir and pyloric sphincter reconstruction (GRPS), Braun's esophago-jejunostomy (EJ) and Lawrance's Roux-en-Y reconstruction (RY) from 1989 to 1994, and the metabolic balance test was performed to compare the patients' efficiency to accumulate and use the absorbed nutrients.

## MATERIALS AND METHODS

### Subjects

All the patients studied were free from malignant recurrence or metastasis confirmed by CT for more than 6 months after the study. They were divided into 3 groups: (I) those with GRPS (12 patients, 9 men and 3 women, mean age, 47 years, range, 32-61 years); (II) those with EJ (7 patients, 5 men and 2 women, mean age, 51 years, range 42-60 years); and (III) those with RY (5 patients, 3 men and 2 women, mean age, 48 years, range 35-57 years).

### Methods

Each patient stayed in hospital for 18 days which were divided into 4 periods.

**The smorgasbord period** From 1-3 days, according to "the Table of the Nutrition amount Supplied in Meals per Day" (published in "Food Elements Table" by the China Nutrition Research Institute in

<sup>1</sup>Department of General Surgery, the 157th Center Hospital of PLA, Guangzhou 510510, Guangdong Province, China

<sup>2</sup>The Second Affiliated Hospital of First Military Medical University, Guangzhou 510524, Guangdong Province, China

Dr. WU Yin-Ai, male, born on 1962-12-09 in Shanrao City, Jiangxi Province, graduated from First Military Medical University in 1989, now working as a chief doctor and director of surgery, having 26 papers published as the first author, and editor in chief for "Anal Reconstruction" and "Surgical Treatment of Proctological Cancer"

\*Supported by the Science and Education Development Foundation for Medicine of Guangdong Provincial Health Department, No.9626.

Correspondence to: Dr. WU Yin-Ai, Department of General Surgery, the 157th Center Hospital of PLA, Guangzhou 510510, China

Tel. +86-20-87783158, Fax. +86-20-87706157

Received 1998-10-04

1997), the standard diet was supplied to patients based on each one's dietary habits, and total caloric intake and the proportion of calories from protein, fat and carbohydrate were recorded accurately and calculated.

**The equilibration period** From 4 - 6 days, all patients were supplied the balance diet of 80g protein, and 100g fat, except the fat amount for those with steatorrhea reduced to 50g in the last 3 days.

**The metabolic balance period** From 6-12 days, the intake-output balance test period consisted of two consecutive 3-day periods, stool and 24h urine samples were collected for fat, nitrogen, Na<sup>+</sup>, K<sup>+</sup>, Cl<sup>-</sup>, P<sup>2+</sup>, Ca<sup>2+</sup> and Mg<sup>2+</sup> analyses.

**The special tests period** From 13-18 days, the Schilling test, D-xylose absorption test, glucose tolerance test and barium small intestinal transit time were made respectively. On the day of admission, while no treatment applied, serum specimens were drawn for various biochemistry examinations, and gastroscopy was performed to examine the esophagus carefully to discover if reflux esophagitis occurred. On the morning of the fourth day, via the guidance of fluoroscopy, a sterile tube was inserted through nose to jejunum to collect jejunal aspirate for culture and identification of anaerobes under sterile and anaerobic conditions. The aspirate was cultured and the anaerobic organisms were further classified according to procedures stipulated by "Bergey's Manual of Determination Bacteriology".

**Follow-up** Upon leaving the hospital, the patients were given the format designed according to "Nutritional Manual for Hospitalized Patients"<sup>[1]</sup>, and food intake was recorded accurately for 7 consecutive days at home environment for analysis later.

**Statistical analysis** The results were expressed as  $\bar{x} \pm s$ , and statistical analyses were made using Student's *t* test.

## RESULTS

### *Clinical data*

**Body weight** The average preoperative body weight of 3 groups all reached their ideal body weight (IBW). On the day of admission, group I patients achieved IBW, groups II and III weighted 10% and 20% less than their IBW respectively. The individual body weight of group I patients exceeded more than 5% - 10% of their pre-operative weight with one exception, in group III only 2 patients achieved their pre-operative weight, the others weighed 5%

- 15% less than their pre-operative weight, in group II all the patients weighted 10% - 20% less than their pre-operative weight.

**Dietary history** In the controlled hospital situation, the average caloric intake by all the patients reached or exceeded the Recommended Dietary Allowance (RDA). After returning to the home environment, the average daily caloric intake in group I was 100% of the RDA for the maintenance of IBW, and 75% in group II and 85% in group III, the largest decrease was noted in one patient of group II, only 63% of the RDA.

### *Absorption studies*

**Glucose tolerance and D-xylose absorption tests** Early hyperglycemia (> 11.01 mmol/L at 30min) and delayed hypoglycemia (< 3.92 mmol/L) were found by glucose tolerance test in 7 patients of group III and 4 patients of group II. Low D-xylose value in urine specimen was lowered in 2 patients of group II and 1 patient of group III.

**Fecal nitrogen examination** The nitrogen intake-output balance tests showed that the average value for fecal nitrogen in group I was less than 0.14mmol/d, and more than 0.14mmol/d in 4 patients of group II and 3 patients of group III, the most serious nitrogen wasting was noted in the azotorrhea patients of group II, whose average value was more than 0.16mmol/d. The loss rate for fecal nitrogen was 18.5% ± 3.2% in 4 patients of group II, and 17.4% ± 4.1% in 3 patients of group III. Low values of serum albumin were noted in 3 patients of group II and 2 patients of group III whose fecal nitrogen exceeded 0.15mmol/d.

**Fecal fat examination** Steatorrhea occurred in 6 patients of group II and 4 patients of group III. In those patients, the fecal fat loss rates averaged 16.1% ± 4.5% in 6 of group II and 17.5% ± 3.8% in 4 of group III. When the fat intake was reduced to 50g, the steatorrhea condition showed no alleviation. Fecal fat excretion of group I was less than 6g/d, while that in steatorrhea patients of group II and group III was more than 6g/d (range 8g/d - 21g/d). Serum carotene was low in steatorrhea patients (< 0.711 mmol/L), and serum cholesterol was low (< 2.84mmol/L) in 5 of group II steatorrhea patients and 3 of group III. Low values of serum albumin, serum carotene, serum cholesterol and D-xylose occurred only in the patients suffering from malabsorption of fat or protein.

**Caloric loss** In the patients with malabsorption of

protein and fat, the caloric loss was 351KJ on a standard diet due to fat and protein malabsorption. The highest caloric loss of 1966KJ occurred in one patient of group II.

**Water soluble vitamins** Normal serum values of Na, K, Cl, Mg, Ca, alkaline phosphatase, and prothrombin time, hemorrhagic phenomena and tetany and osteomalacia were not noted, all these serve as indirect evidence of adequate levels of vitamins D and K. Shelling test showed declined B12 absorption in all the patients.

**Gastroscopic examination and small intestinal transit time** Gastroscopic evidence of reflux esophagitis was noted in 7 patients of group II, and none in groups I and III. Barium small bowel transit time in group I was  $3.2 \text{ h} \pm 1.22 \text{ h}$  (normal time  $3.4 \text{ h} \pm 2.3 \text{ h}$ ). There was no significant difference, while there were significant differences between  $1.6 \text{ h} \pm 1.2 \text{ h}$  of group II, and  $2.3 \text{ h} \pm 1.3 \text{ h}$  of group III and the normal time.

**Bacterial culture** Anaerobes presented in the jejunal aspirate of one patient in group I, its count being  $10^7/\text{L}$ . Anaerobes were also found in the jejunal aspirate of 6 patients in group II and 4 patients in group III. Those were identified mainly as lactobacilli, yeasts, bacteroides, veillonella and clostrida.

**Balance studies** In the controlled hospital period, the data collected from the intake-output tests and repeated tests of serum samples showed that each element of N, P, Cl,  $\text{Ca}^{2+}$ ,  $\text{Mg}^{2+}$ ,  $\text{Na}^+$ , and  $\text{K}^+$  was in positive average daily balance, and there were no significant differences among the 3 groups.

## DISCUSSION

Protein, fat, carbohydrate, vitamins and minerals are the 5 major food elements required for proper nutrition. So it is important to ingest and absorb these 5 elements to keep good nutritional state of the post-operative patients.

### *Effect of reconstruction on body weight*

The major clinical manifestation of malnutrition is weight loss. Previous studies reported that the average postoperative weight loss was 24% as compared with preoperative one and only one-third patients achieved IBW<sup>[2]</sup>. Some studies indicated that a major contributing factor to weight loss and failure to gain weight was inadequate caloric intake of food<sup>[3]</sup>. The most serious complication leading to such state was alkaline reflux esophagitis<sup>[4]</sup>. The

most serious clinical symptoms caused by reflux esophagitis were found in group II patients in this study, and caloric intake was the lowest among the three groups after returning to home environment. In group III patients, although the Roux-en-Y reconstruction has solved the problem of esophagitis, the Roux-en-Y syndrome occurring in most post-operative patients also affects normal intake of food. Caloric loss is another factor contributing to malnutrition in groups II and III patients suffering from malabsorption of fat and protein.

### *Effect of reconstruction on digestion and absorption*

Besides adequate intake of the 5 food elements, good digestion and absorption are important as well. The duodenum plays an important role in the process of food digestion and absorption, and in controlling chyme emptying through a mechanism of immediate brake<sup>[5]</sup>, being the main site of cholecystokinin and gastric secretion stimulated by food after total gastrectomy. When the duodenum passage of digested food was excluded, secretion of bile and pancreatic enzymes could not coordinate and synchronize with emptying of chyme, therefore proper mixing of them could not precede within the time necessary for physiologic digestion. Without emulsification and specific hydrolysis of pancreatic peptidase and lipase, and without adequate biological re-action of conjugated bile salts, malabsorption of fat and protein would occur, and azotorrhea and steatorrhea ensued. In II and group III patients whose reconstruction excluded the passage of food through the duodenum, the barium small intestinal transit time was faster than that of normal control group, the glucose tolerance tests were abnormal in 7 patients of group II and 4 patients of group III, 6 patients of group II and 4 patients of group III experienced steatorrhea, and azotorrhea occurred in 4 and 3 patients of the two groups respectively. Because malabsorption of fat would result in malabsorption of some fat-soluble vitamins, the serum carotene level was low in those patients with steatorrhea. In group I patients, those parameters mentioned above could fall within normal biological range due to the maintenance of duodenal passage of food.

### *Effect of reconstruction on bacterial overgrowth*

The results of this study showed that anaerobes were cultured out of the jejunal aspirate in one patient of group I, 6 of group II and 4 of group III. Six hours after barium examination, barium residue was found in the jejunal loop and Roux limb in the corresponding patients of groups II and III respectively, imply-

ing that the ingested food would stay in the segment of reconstruction for rather a long time after intake of food stuff by those patients. The residual food would be an ideal place for microorganism overgrowth without sterilization of gastric acid after total gastric resection. Based on the results of this study, there is direct correlation between the reconstruction and bacterial overgrowth in the small bowels. Anaerobes proliferating in the small intestine, especially bacteroides, are able to change the structures of bile salts, to reduce water-soluble fat absorption impaired with inadequate concentration of conjugated bile salts. Anaerobes are also able to diversify ingested protein nitrogen to urea by deamination, resulting in impaired protein absorption. Meanwhile, bacterial consumption and toxins produced by bacterial metabolism would aggravate B12 deficiency of the postoperative patients.

#### ***Effect of reconstruction on nutritional balance and dietary habits.***

Patients in the controlled period of hospitalization, the food caloric intake by groups II and III could exceed RDA. The results of balance studies showed that all these patients could maintain positive balance of N, P and electrolytes. It was observed in this study that the abnormal nutritional status was mainly caused by gastrointestinal continuity altered by reconstruction after total gastrectomy for gastric

cancer, inducing abnormal changes of gastrointestinal dynamics and digestive environment, but the reconstruction exerted little influence on the absorption capacity of the small intestine, and the nutritional status could be improved by strict control. But in the home environment, especially for those with financial difficulties, it would not be easy, thus leading to malnutrition. However, the patients of group I could achieve normal nutritional state in daily life without any dietary control. Therefore, for maintenance of good nutritional status of postoperative patients, it is imperative to preserve the duodenal food passage, on the basis of having solved the problem of alkaline reflux esophagitis.

---

**ACKNOWLEDGMENTS:** We would like to thank Dr. ZHANG Ya-Li for his helpful discussion, and Professor SHEN Wei for the English verification of this manuscript.

#### **REFERENCES**

- 1 Huang JZ, Yang PY, Xu YH. Nutritional manual for hospitalized patients. Beijing: Publishing House of Ministry of Light Industry, 1987:11-35
- 2 Kelly WD, MacLean LD, Perry JF, Wangenstein OH. A study of patients following total and near-total gastrectomy. *Surgery*, 1954;35:964-982
- 3 Bradley EL, Isaacs J, Hersh T, Dadidson ED, Millikan W. Nutritional consequences of total gastrectomy. *Ann Surg*, 1975;182:415-429
- 4 Morrow D, Passaro ER. Alkaline reflux esophagitis after total gastrectomy. *Am J Surg*, 1976;132:287-291
- 5 Satish SCR, Charles LU, Konard SD. Duodenum as an immediate brake to gastric outflow: a videofluoroscopic and manometric assessment. *Gastroenterology*, 1996;110:740-747

Edited by MA Jing-Yun

# Detection of serum TNF- $\alpha$ , IFN- $\gamma$ , IL-6 and IL-8 in patients with hepatitis B \*

WANG Jing-Yan, WANG Xue-Lian and LIU Pei

**Subject headings** hepatitis B; TNF- $\alpha$ ; IFN- $\gamma$ ; IL-6; IL-8

## Abstract

**AIM** To assess the possible roles of cytokines (TNF- $\alpha$ , IFN- $\gamma$ , IL-6 and IL-8) in liver damage of hepatitis B.

**METHODS** The serum TNF- $\alpha$ , IFN- $\gamma$ , IL-6 and IL-8 were detected by ELISA in 66 patients with hepatitis B and 20 healthy blood donors.

**RESULTS** TNF- $\alpha$  and IL-6 in all types of clinical hepatitis B were significantly higher than those in healthy blood donors ( $P < 0.05$ ); meanwhile the levels of TNF- $\alpha$ , IFN- $\gamma$ , IL-6 and IL-8 in the patients with fulminant hepatitis B were much higher than those in the patients with acute hepatitis B ( $P < 0.05$ ); the level of TNF- $\alpha$  was positively correlated with the levels of IFN- $\gamma$ , IL-6 and IL-8 in all types of hepatitis B ( $r_{\text{IFN}} = 0.24$ ,  $r_{\text{IL-6}} = 0.35$ ,  $r_{\text{IL-8}} = 0.44$ ) and the TNF- $\alpha$ , IFN- $\gamma$ , IL-6 and IL-8 were positively correlated with serum bilirubin ( $P < 0.05$ ). Dynamic changes of these cytokines were observed in the course of acute and fulminant hepatitis. The level of IFN- $\gamma$  peaked in the initial period of acute hepatitis and early stage of hepatic coma in fulminant hepatitis; TNF- $\alpha$ , IL-6 and IL-8 increased with exacerbation, and reached a peak when the liver damage was most serious, then decreased when patient conditions were improved.

**CONCLUSION** The increased cytokines were related to the inflammation of liver cells and multiple factors may play certain roles in liver damage.

## INTRODUCTION

Since Muto<sup>[1]</sup> reported that TNF- $\alpha$  and IL-1 were related to fulminant hepatitis, the studies on the relationship between cytokines and liver damage have been paid more and more attention especially in recent years. Most scholars now agree that TNF and IFN are related to liver damage, so are IL-6 and IL-8. We detected the serum TNF- $\alpha$ , IFN- $\gamma$ , IL-6 and IL-8 in the patients with different clinical types of hepatitis B by ELISA for assessing the relationship between the cytokines and the liver damage.

## MATERIALS AND METHODS

### Samples

A total of 66 patients with HBV infection and 20 healthy blood donors were studied. They were admitted to this college between 1993 and 1997. The patients (48 men and 18 women) ranged in age from 21 to 56 years. There were 22 cases of acute hepatitis (AH), 25 cases of chronic hepatitis (CH) and 19 cases of fulminant hepatitis (FH). The serological markers of HAV, HCV, HEV, CMV and EBV were negative, and HBsAg and other markers of HBV were positive in all the patients.

### Healthy blood donors

Healthy blood donors, aged from 25 to 43 years, included 16 men and 4 women. They had no serological markers of HAV-HEV, CMV, EBV infection and liver functions were normal.

### Detection of cytokines

The kits of the four cytokines were produced by the Genzyme Company, U. S. A. No. 1 9970214. The four cytokines were detected by ELISA according to the manufacturer's instructions. The first antibody was biotin-labelled and the second one was connected with horse radish peroxidase.

## RESULTS

The serum TNF- $\alpha$ , IFN- $\gamma$ , IL-6 and IL-8 in patients with different types of hepatitis B are shown in Table 1.

Department of Infectious Diseases, The Second Clinical College, China Medical University, Shenyang 110003, China

Dr. WANG Jing-Yan, female, born on 1963-11-20 in Kaiyuan city, Liaoning Province, graduated from China Medical University as a postgraduate in 1992, now associate professor of infectious diseases, majoring in hepatitis, having 15 papers published.

\*Project supported by the National Natural Science Foundation of China, No.3920117.

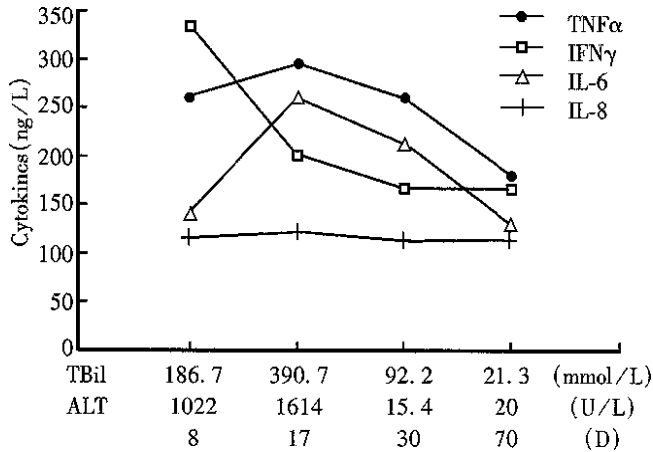
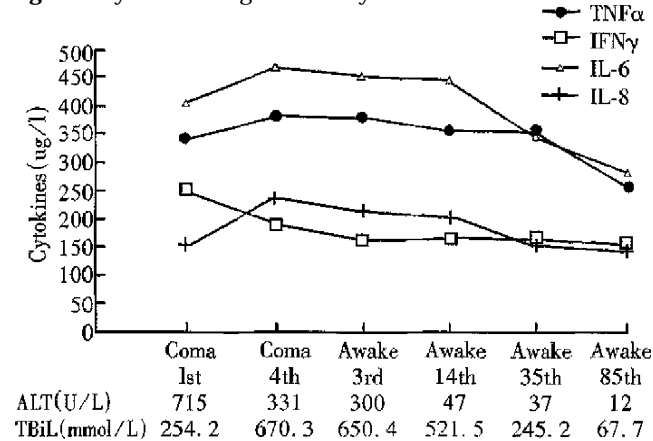
**Correspondence to:** Dr. WANG Jing-Yan, Department of Infectious Diseases, The Second Clinical College, China Medical University, No.36 Shanhaio Street, Heping District, Shenyang 110003, China  
Tel. +86-24-23893501 Ext. 926, Fax. +86-24-23892617

Received 1998-11-09

**Table 1** TNF- $\alpha$ , TNF- $\alpha$ , IL-6 and IL-8 in various types of hepatitis B

	<i>n</i>	TNF- $\alpha$	IFN- $\gamma$	IL-6	IL-8
FH	19	359.0 $\pm$ 17.2 <sup>ab</sup>	234.7 $\pm$ 16.5 <sup>ab</sup>	347.5 $\pm$ 31.3 <sup>ab</sup>	181.1 $\pm$ 19.6 <sup>ad</sup>
AH	22	220.6 $\pm$ 8.9 <sup>c</sup>	174.9 $\pm$ 12.0	285.8 $\pm$ 16.5 <sup>c</sup>	118.4 $\pm$ 5.1
CH	25	322.1 $\pm$ 13.0 <sup>c</sup>	200.0 $\pm$ 15.7 <sup>c</sup>	329.5 $\pm$ 25.2 <sup>c</sup>	133.1 $\pm$ 6.7 <sup>c</sup>
CI	20	146.7 $\pm$ 9.4	165.0 $\pm$ 7.7	231.1 $\pm$ 16.4	110.2 $\pm$ 2.9

CI: healthy blood donor. <sup>a</sup> $P$ <0.01, vs CI; <sup>c</sup> $P$ <0.05, vs CI; <sup>b</sup> $P$ <0.01, vs AH; <sup>d</sup> $P$ <0.05, vs AH.

**Figure 1** Dynamic changes of four cytokines in the course of AH.**Figure 2** Dynamic changes of four cytokines in the course of FH.

The TNF- $\alpha$  and IL-6 in various clinical types of hepatitis B were significantly higher than those in healthy blood donors ( $P$ <0.05). Except acute hepatitis B, the levels of IFN- $\gamma$  and IL-8 were obviously higher in other types than those in healthy blood donors. The levels of four cytokines of patients with FH were much higher than those of patients with AH ( $P$ <0.05).

#### Correlation between TNF- $\alpha$ and IFN- $\gamma$ , IL-6 and IL-8

The correlations between TNF- $\alpha$  and IFN- $\gamma$ , IL-6 and IL-8 in HBV infections were analyzed. The results suggested that TNF- $\alpha$  and the other cytokines were positively correlated ( $r_{\text{IFN}} = 0.24$ ,  $r_{\text{IL-6}} = 0.35$ ,  $r_{\text{IL-8}} = 0.44$ ).

#### Correlation between serum bilirubin and four cytokines

The correlation between serum bilirubin and four cytokines was analyzed in HBV infections. The re-

sults suggested that bilirubin was positively related to the levels of four cytokines ( $P$ <0.05).

#### Dynamic changes of four cytokines in AH and FH

The dynamic changes of four cytokines in the course of AH and FH are shown in Figures 1, 2. At the early stage of AH, IFN- $\alpha$  peaked and decreased rapidly. TNF- $\alpha$  and IL-6 increased with exacerbation, reached a highest level when jaundice became most severe, and then decreased gradually. IL-8 level did not change during the course.

On the first day of hepatic encephalopathy of FH, IFN- $\gamma$  reached a peak, then decreased rapidly. TNF- $\alpha$ , IL-6 and IL-8 increased when condition of the patients worsened. They reached the highest level during the peak of jaundice, then decreased gradually, and maintained abnormal for a long time.

#### DISCUSSION

Since it was reported that TNF and IL-1 in supernatant of cultured monocytes of peripheral blood in patients with FH were obviously higher than those with AH, the studies on cytokines related to liver damage advanced rapidly. Pei Liu<sup>[2]</sup> proved that TNF could cause liver necrosis in corynebacterium sensitized animals and the necrosis could be blocked by anti-TNF monoclonal antibody<sup>[3]</sup>. At present, the studies of hepatitis focused on the roles of cytokines in cell-mediated injury of tissues. Ferluga *et al*<sup>[4]</sup> reported that the liver injury of animal model induced by corynebacterium-endotoxin could be caused by the soluble factors produced by monocytes gathering at the hepatic lobules. Luca<sup>[5]</sup> proved that activation of CTL induced by IFN- $\gamma$  resulted in CTL-mediated hepatocytic injury in the study of HBV transgenic mouse. IL-6 may induce the activation, differentiation and maturation of NK cells<sup>[6]</sup> and expression of monocytic IL-8 gene<sup>[7]</sup>. The IL-8 may cause degranulation of neutrophil granulocyte, leading to DIC within the liver<sup>[8]</sup>.

The serum levels of TNF- $\alpha$ , IFN- $\gamma$ , IL-6 and IL-8 in patients with HBV infection were higher than those in healthy blood donors. The difference was obvious between the levels of cytokines in FH and those in AH. TNF- $\alpha$  and IFN- $\gamma$ , IL-6 and IL-8 were positively correlated in various types of hepatitis B. The bilirubin was also positively related to the four cytokines. In the course of AH and FH, IFN- $\gamma$  peaked in the early stage of AH and the 1st day of hepatic coma of FH. TNF- $\alpha$ , IL-6 and IL-8 in-

creased with exacerbation of condition of the patients with AH and FH except for IL-8 in AH. These suggested that the four cytokines were related to liver injury.

The roles of cytokines in the liver damage are complex. They affect each other to form a cytokine network, in which IFN- $\gamma$  may be the chief cytokine and induce the immune cells to release other cytokines and improve cytotoxic activities mediated by immune cells.

#### REFERENCES

- 1 Muto Y. Enhanced tumor necrosis factor and interleukin-1 in fulminant hepatitis failure. *Lancet*, 1988;2:72
- 2 Pei L. Tumor necrosis factor and interleukin-1 in an experimental model of massive liver cell necrosis/fatal hepatitis in mice. *Gastroenterol Jpn*, 1990;25:339
- 3 Pei L. The protective effects of Anti mouse TNF monoclonal antibody in experimental massive hepatic cell necrosis model. *Chin J Digestion*, 1994;14:150
- 4 Ferluga J, Allison AC. Role of mononuclear infiltrating cells in pathogenesis of hepatitis. *Lancet*, 1978;2:610
- 5 Luca GGK. Cytotoxic T lymphocytes inhibit hepatitis B virus gene expression by a noncytolytic mechanism in transgenic mice. *Proc Natl Acad Sci USA*, 1994;91:3764
- 6 Kimitaka K. Detection by in situ hybridization and phenotypic characterization of cells expressing IL-6 mRNA in human stimulated blood. *J Immunology*, 1990;144:1317
- 7 Matsushima K. Molecular cloning of a human monocyte-derived neutrophil chemotactic (MDNCF) and the induction of MDMCF mRNA by interleukin-1 and tumor necrosis factor. *J Exp Med*, 1988;167:1883
- 8 Larsen CG. Production of interleukin-8 by human dermal fibroblasts and keratinocytes in response to interleukin-1 or tumor necrosis factor. *Immunology*, 1989;68:31

Edited by MA Jing-Yun

# Gastroesophageal reflux disease is uncommon in Asia: evidence and possible explanations

HO Khek-Yu

**Subject headings** gastroesophageal reflux; esophagitis; Barrett's esophagus; hiatus hernia; *Helicobacter pylori*; gastric acid

## DEFINITIONS

Gastroesophageal reflux that predisposes an individual to the risk of physical complications, or produces symptoms leading to significantly impaired quality of life, is termed gastroesophageal reflux disease (GERD)<sup>[1]</sup>. Clinically, GERD encompasses a broad spectrum of separate, though related conditions that are sometimes conveniently grouped under two broad categories: endoscopic esophagitis and endoscopy negative reflux disease. Endoscopic esophagitis is considered to be present when there is endoscopically visible breakage of the mucosa<sup>[2]</sup>, regardless of whether the patient has symptoms. The term "endoscopic negative reflux disease" refers to GERD that is not associated with Barrett's esophagus or esophageal mucosal breaks. It includes such conditions as esophageal mucosal acid sensitivity, which is symptomatic reflux induced by acid reflux and proven by objective means; abnormal esophageal acid exposure, which is excessive acid reflux confirmed by objective measures; and reflux-type symptoms (heartburn and/or acid regurgitation) that clearly dominate the patient's complaints<sup>[3]</sup>. Barrett's esophagus is the eponym applied to the columnar epithelium-lined lower esophagus that is acquired as a consequence of chronic gastroesophageal reflux<sup>[4]</sup>. Hiatus hernia, on the other hand, has been defined as a displacement of the gastric mucosa 1.5cm or more above the diaphragmatic hiatus<sup>[5]</sup>.

## EVIDENCE FOR A LOW PREVALENCE OF GERD IN ASIA

### *Prevalence of reflux-type symptoms in general population*

Until recently, there has been no systematic study on the prevalence of reflux type symptoms in the general population of Asia. A cross-sectional survey of a race-stratified sample of adults in a Singaporean town provides some of the first evidences, that re-

flux-type symptoms are uncommon in the East<sup>[6]</sup>. Of 696 persons evaluated, only 2% had heartburn and/or acid regurgitation for more than once a month. This prevalence is much lower than those (29%-44%) of Western populations<sup>[7,8]</sup>.

### *Prevalence of GERD in pregnant women*

The individuals with the highest prevalence of heartburn are often said to be pregnant women. A prospective study, using a reliable questionnaire, on a consecutive series of pregnant women in Singapore, provides the second piece of evidence that reflux-type symptoms are uncommon among Asians<sup>[9]</sup>. Of the 35 pregnant women evaluated, 23% had heartburn some time during their pregnancy. This percentage is lower than those (48% - 96%) reported previously in the West<sup>[10,11]</sup>.

### *Frequency of GERD in outpatient clinics*

In a large clinical series from Singapore, Kang *et al* from Singapore noted a 2% frequency of GERD among 2141 consecutive patients investigated<sup>[12]</sup>. The diagnosis of GERD was established on the basis of an abnormal endoscopy, a positive acid perfusion test and/or an abnormal 24-hour pH monitoring. The frequency was lower as compared with a similar series from the West<sup>[13]</sup>.

### *Prevalence of endoscopic esophagitis*

Very few epidemiological data on reflux esophagitis in Asians are available in the literature. However, Chang *et al* found 5% with reflux esophagitis<sup>[14]</sup> in an endoscopic series of 2044 patients who underwent self-paid medical check-ups. Esophagitis, when present, was often mild. The prevalence of endoscopic esophagitis among symptomatic subjects has not been well studied and the available data are conflicting. In a study from Taiwan, a 15% prevalence of erosive esophagitis was found in 455 consecutive patients evaluated for various upper gastrointestinal tract symptoms<sup>[15]</sup>. Most of the patients presented with mild esophagitis. The expected high frequency of erosive esophagitis is not supported by other endoscopic series from Asia. Erosive esophagitis was uncommon in both indigenous Fijians and Indians, being detected in only 2% of a total of 693 endoscopic examinations<sup>[16]</sup>. This contrasts with the higher prevalence (11%) of reflux esophagitis noted by the same author among New Zealanders<sup>[17]</sup>. Esophagitis is likewise uncommon in Japan; a prevalence rate of 3% was recorded among 240 consecutive outpatients with dyspepsia<sup>[18]</sup>. Our own retro-

Department of Medicine, National University of Singapore, Singapore

**Correspondence to:** Dr HO Khek-Yu, MBBS (Syd Hons 1) FRACP FAMS, Department of Medicine, National University Hospital, Lower Kent Ridge Road, Singapore 119074  
Tel. +65-7724353, Fax. +65-7794112

Email. mdchoky@nus.edu.sg

Received 1998-12-30

spective series from Singapore showed that of 11943 patients undergoing diagnostic upper endoscopy for various complaints, 4% had esophagitis<sup>[19]</sup>. This frequency was lower than those reported from Western centers<sup>[20,21]</sup>. Thus, with the exception of the Taiwanese series, the proportion of patients with endoscopic esophagitis in Asian series appears lower than that in reports from Western countries. The severity of esophagitis also appears mild, unlike that in Western populations<sup>[20,21]</sup>.

#### **Prevalence of hiatus hernia**

Hiatus hernia, as seen on barium studies, appears rare in the Far East with a < 1% prevalence<sup>[22]</sup>. Recent endoscopic series from Asia confirm this impression. Chang *et al* from Taiwan found hiatus hernia in 2% of patients endoscoped as part of an annual medical examination<sup>[14]</sup>. In another Taiwanese study in patients endoscoped for gastrointestinal complaints, hiatus hernia was found in 7% of the cases<sup>[15]</sup>. In our retrospective series from Singapore, the proportion of hiatus hernia among patients seen for gastrointestinal complaints was 3%<sup>[19]</sup>. Thus, the available data show that the prevalence of hiatus hernia is lower than that in Western series (17%-22%)<sup>[20,21]</sup>.

#### **Prevalence of GERD complications**

The prevalence of Barrett's esophagus varies, depending on the population being studied. In a series from Taiwan, 2% of patients endoscoped for a variety of upper gastrointestinal symptoms were found to have Barrett's esophagus<sup>[15]</sup>. When evaluating only those with erosive esophagitis, this rate increased to 14%. The corresponding figures from the West are 4%-20%<sup>[23,24]</sup> and 36%, respectively<sup>[23]</sup>. Reports from a Taiwanese center, and our own center showed a frequency of benign (presumably reflux-related) esophageal stricture of only 0.4% and 0.2% respectively, among patients endoscoped for various gastrointestinal indications<sup>[16,19]</sup>. These frequencies are lower in comparison with those in reports from the West<sup>[25]</sup>.

#### **POSSIBLE REASONS FOR THE LOW FREQUENCY OF GERD IN THE EAST**

The pathogenesis of reflux esophagitis can be considered in terms of excessive acid load overwhelming mucosal defense. The degree of acid load is in turn determined by the anti-reflux barrier of the gastroesophageal junction<sup>[26]</sup>, the quantity of acid refluxed<sup>[27]</sup>, and the ability of the esophagus to clear any refluxate back into the stomach<sup>[28]</sup>. The latter depends on the integrity of peristaltic function<sup>[29]</sup> and the neutralizing ability of swallowed saliva<sup>[28]</sup>. More recently, an inverse relationship between *Helicobacter pylori* (*H. pylori*) and GERD has been suggested<sup>[30]</sup>. By examining the potential pathogenetic factors, it is hoped that the lower frequency

of GERD in the East than in the West could be explained.

#### **Anti-reflux barrier**

An increase in intra-abdominal and intragastric pressure overcomes the gastroesophageal pressure gradient maintained by the lower esophageal sphincter (LES). Such an increase may occur through obesity<sup>[31]</sup> and delayed gastric emptying by fatty meals<sup>[32]</sup>. Alcohol, smoking and fat can lower the LES pressure and esophageal peristalsis, thus favoring the occurrence of gastroesophageal reflux<sup>[33-35]</sup>. A large hiatus hernia traps gastric contents in its pouch above the diaphragm. This leads to free retrograde flow of acid into the esophagus.

Increased body mass index and presence of hiatus hernia were found to be the most important factors associated with the occurrence of esophagitis in a recent study from Taiwan<sup>[14]</sup>. The authors suggested that the lower prevalence of hiatus hernia and smaller body mass index in the Chinese population might account for the lower prevalence of reflux esophagitis in Taiwan. The low prevalence of hiatus hernia in the East has previously been attributed to the consumption of high residue diets in the developing world<sup>[22]</sup>. Another report from Taiwan found erosive esophagitis to be associated with smoking, and alcohol consumption<sup>[15]</sup>. The authors suggested that the recent increase in smoking, alcohol use, and fat consumption among Taiwanese were contributed to the observed rise in the prevalence of GERD in Taiwan.

#### **Gastric acid output**

Since acid secretion correlates with body surface area, Asians in general are characterized by a smaller parietal cell mass and a lower acid output as compared with Caucasians<sup>[36]</sup>. Except for the striking example of Zollinger-Ellison syndrome, however, the association between the amount of acid output and the occurrence or severity of reflux disease has remained unproven<sup>[37]</sup>.

#### **Acid clearance**

While evaluating the consecutive Singaporean patients who underwent esophageal manometry, we found that poor esophageal clearance was more common among those with esophagitis than among those without. The results were identical to Western studies<sup>[38]</sup>. It is possible that this clearance mechanism has an inherited basis, and is more efficient in Asians than in Caucasians. Data to support this is, however, lacking.

#### **Mucosal defence**

Presently, there is no risk factor known to disrupt tissue resistance, except for nonsteroidal anti-inflammatory drugs<sup>[39]</sup>. Such drugs cannot be an important factor underlying the geographical variation in the prevalence of GERD, because they are con-

sumed by Asians no more than by Westerners. However, it is possible that inborn differences in tissue resistance, due to yet unrecognized factors, may account for some of the geographical differences.

### *H. pylori* infection

There is circumstantial evidence to suggest that *H. pylori* infection is relatively protective for the occurrence of GERD<sup>[30]</sup>. It has been suggested that Hong Kong Chinese are protected against reflux esophagitis by their high prevalence of *H. pylori* associated gastritis<sup>[40]</sup>. Such gastritis, when becoming chronic, can lead to gastric atrophy and hypochlorhydria, thereby reducing the likelihood of GERD. If this hypothesis is correct, the effects of *H. pylori* induced gastritis may be an important factor determining the lower prevalence of reflux esophagitis in this part of the world, in which *H. pylori* infection is especially common. No data, however, exists to support this hypothesis.

### Genetic factors

It is unlikely that the lower frequency of GERD in Asian populations can be explained simply by the known extrinsic risk factors, such as obesity, smoking habits, and alcohol consumption, being less frequent in Asians as compared with Caucasians. It is likely that genetic factors are involved. If that was the case, the mechanisms through which they confer protection against GERD are poorly understood. It may be that LES function is truly more competent in Asians compared with Westerners. Alternatively, the esophageal mucosa in Asians is inherently more acid resistant. Differences in gastric acid output and esophageal clearance ability between Asian and Western patients are further possibilities. Comparative studies into these parameters in Eastern and Western populations may shed more light on this question, and may lead to formulation of appropriate therapeutic strategies.

In summary, most reports from Asia have suggested that GERD is an uncommon condition in this part of the world. The reasons for the lower frequency compared with the West are not known, and further studies are required.

### REFERENCES

- 1 Dent J, Brun J, Fredrick AM, Fennerty MB, Janssens J, Kahrilas PJ. An evidence based appraisal of reflux disease management: the Genval workshop report. In press
- 2 Armstrong D, Bennett JR, Blum AL, Dent J, de Dombal FT, Galmiche JP. The endoscopic assessment of esophagitis: a progress report on observer agreement. *Gastroenterology*, 1996;111:85-92
- 3 Klausner AG, Schindlbeck NE, Muller-Lissner SA. Symptoms in gastro-oesophageal reflux disease. *Lancet*, 1990;335:205-208
- 4 Cameron AJ. Epidemiology of columnar-lined esophagus and adenocarcinoma. *Gastroenterol Clin North Am*, 1997;26:487-494
- 5 Pridie RB. Incidence and coincidence of hiatus hernia. *Gut*, 1966;7:188-189
- 6 Ho KY, Kang JY, Seow A. Prevalence of gastrointestinal symptoms in a multi-racial Asian population, with particular reference to reflux-type symptoms. *Am J Gastroenterol*, 1998;93:1816-1822

- 7 Locke GR, Talley NJ, Fett SL, Zinsmeister AR, Melton LJ 111. Prevalence and clinical spectrum of gastroesophageal reflux: A population-based study in Olmsted County, Minnesota. *Gastroenterology*, 1997;112:1448-1456
- 8 Drossman DA, Li Z, Andruzzi E, Temple RD, Talley NJ, Thompson WG. US. household survey of functional gastrointestinal disorders. *Dig Dis Sci*, 1993;38:1569-1580
- 9 Ho KY, Kang JY, Viegas OAC. Symptomatic gastro-oesophageal reflux in pregnancy: A prospective study among Singaporean women. *J Gastroenterol Hepatol*, 1998;13:1020-1026
- 10 Nagler R, Spiro HM. Heartburn in late pregnancy. *Am J Dig Dis*, 1962;7:648-655
- 11 Bainbridge ET, Temple JG, Nicholas SP, Newton JR, Boriah V. Symptomatic gastro-oesophageal reflux in pregnancy: A comparative study of white Europeans and Asians in Birmingham. *Br J Clin Pract*, 1983;37:53-57
- 12 Kang JY, Yap I, Gwee KA. The pattern of functional and organic disorders in an Asian gastroenterological clinic. *J Gastroenterol Hepatol*, 1994;9:124-127
- 13 Harvey RF, Salih SY, Read AE. Organic and functional disorders in 2000 gastroenterology outpatients. *Lancet*, 1983;i:632-634
- 14 Chang CS, Poon SK, Lien HC, Chen GH. The incidence of reflux esophagitis among the Chinese. *Am J Gastroenterol*, 1997;92:668-671
- 15 Yeh C, Hsu CT, Ho AS, Sampliner RE, Fass R. Erosive esophagitis and Barrett's Esophagus in Taiwan: A higher frequency than expected. *Dig Dis Sci*, 1997;42:702-706
- 16 Scobie BA, Beg F, Oldmeadows M. Peptic diseases compared endoscopically in indigenous Fijians and Indians. *NZ Med J*, 1987;100:683-684
- 17 Scobie BA. Endoscopy in peptic diseases and bleeding: a community survey of 1635 patients. *NZ Med J*, 1988;101:78-80
- 18 Inoue M, Sekiguchi T, Harasawa S, Miwa T, Miyoshi A. Dyspepsia and dyspepsia subgroups in Japan: Symptom profiles and experience with cisapride. *Scand J Gastroenterol*, 1993;28(Suppl 195):36-39
- 19 Kang JY, Tay HH, Yap I, Guan R, Lim KP, Math MV. Low frequency of endoscopic esophagitis in Asian patients. *J Clin Gastroenterol*, 1993;16:70-73
- 20 Berstad A, Weberg R, Fryshov Larson I, Hoel B, Hauer Jensen M. Relationship of hiatus hernia to reflux esophagitis. A prospective study of coincidence, using endoscopy. *Scand J Gastroenterol*, 1986;21:55-58
- 21 Wright RA, Hurwitz AL. Relationship of hiatal hernia to endoscopically proved reflux esophagitis. *Dig Dis Sci*, 1979;24:311-313
- 22 Burkitt DP, James PA. Low<sup>2</sup>residue diets and hiatus hernia. *Lancet*, 1993;2:128-130
- 23 Winters C Jr, Spurling TJ, Chobanian SJ, Curtis DJ, Esposito RL, Hacker JF. Barrett's esophagus: A prevalent, occult complication of gastroesophageal reflux disease. *Gastroenterology*, 1987;92:118-124
- 24 Mann NS, Tsai MF, Nair PK. Barrett's esophagus in patients with symptomatic reflux esophagitis. *Am J Gastroenterol*, 1989;84:1494-1496
- 25 Sonnenberg A. Epidemiologie und Spontanverlauf der Refluxkrankheit. In Blum AL, Siewert JR, eds. Refluxtherapie. Gastroesophageale refluxkrankheit: konservative und operative therapie. Berlin: Springer Verlag, 1981:85-106
- 26 Dodds WJ, Dent J, Hogan WJ. Mechanisms of gastroesophageal reflux in patients with reflux esophagitis. *N Eng J Med*, 1982;307:1547-1552
- 27 Boesby S. Relationship between gastro-oesophageal acid reflux, basal gastro-oesophageal sphincter pressure, and gastric acid secretion. *Scand J Gastroenterol*, 1977;12:547-551
- 28 Helm JF, Dodds WJ, Pele LR, Hogan WJ, Teeter BC. Effect of esophageal emptying and saliva on clearance of acid from the esophagus. *N Eng J Med*, 1984;310:284-288
- 29 Kahrilas PJ, Dodds WJ, Hogan WJ. Effect of peristaltic dysfunction on esophageal volume clearance. *Gastroenterology*, 1988;94:74-80
- 30 Labenz J, Blum AL, Bayerdorffer E, Meining A, Stolte M, Borsch G. Curing *Helicobacter pylori* infection in patients with duodenal ulcer may provoke reflux esophagitis. *Gastroenterology*, 1997;10:1442-1447
- 31 Stene-Larsen G, Weberg R, Froyshov Larsen I, Bjortuft O, Hoel B, Berstad A. Relationship of overweight to hiatus hernia and reflux oesophagitis. *Scand J Gastroenterol*, 1988;23:427-432
- 32 McCallum RW, Berkowitz DM, Lerner E. Gastric emptying in patients with gastroesophageal reflux. *Gastroenterology*, 1981;80:285-291
- 33 Hogan WJ, de Andrade SRV, Winship DH. Ethanol-induced human esophageal motor dysfunction. *J Appl Physiol*, 1972;32:755-760
- 34 Dennish GW, Castell DO. Inhibitory effect of smoking on the lower oesophageal sphincter. *N Eng J Med*, 1971;284:1136-1137
- 35 Nebel OT, Castell DO. Inhibition of the lower oesophageal sphincter by fat-A mechanism for fatty food intolerance. *Gut*, 1973;14:270-274
- 36 Fung WP, Tye CY. Pentagastrin<sup>2</sup>stimulated gastric acid secretion in Chinese. *Am J Gastroenterol*, 1972;58:233-241
- 37 Miller LS, Vinayek R, Frucht H, Gardner JD, Jensen RT, Maton PN. Reflux esophagitis in patients with Zollinger Ellison syndrome. *Gastroenterology*, 1990;98:341-346
- 38 Ho KY, Kang JY. Reflux esophagitis patients in Singapore have motor and acid exposure abnormalities similar to patients in the Western hemisphere. *Am J Gastroenterol*. In press
- 39 Lanas A, Hirschowitz BI. Significant role of aspirin use in patients with esophagitis. *J Clin Gastroenterol*, 1991;13:622-627
- 40 Wu JCY, Go MYY, Chan WB, Choi CL, Chan FKL, Sung J. Prevalence and distribution of *H. pylori* in gastro-oesophageal reflux disease: a study in Chinese. *Gastroenterology*, 114(4):A1364

# Protective effects of polydatin against CCl<sub>4</sub>-induced injury to primarily cultured rat hepatocytes\*

HUANG Zhao-Sheng, WANG Zong-Wei, LIU Ming-Ping, ZHONG Shi-Qing, LI Qiao Mei and RONG Xiang-Lu

**Subject headings** polydatin; injury, hepatocyte; CCl<sub>4</sub>

## Abstract

**AIM** To investigate the protective effects of polydatin (PD) against injury to primarily cultured rat hepatocytes induced by CCl<sub>4</sub>.

**METHODS** Rat hepatocytes were separated by methods of liver infusion in vivo and cultured medium ( $7.5 \times 10^5$  cells/mL). Two mL or 0.2mL was added into 24-well or 96-well plates respectively. Twenty-four hours after cell preculture, PD at concentrations of  $10^{-7}$  mol/L- $10^{-4}$  mol/L was added into each plate. At the same time injury to hepatocytes was induced by adding 10mmol/L-CCl<sub>4</sub>. Then, 0.1mL or 1mL-culture solution was removed from the 96-well or 24-well plates at 6h, 12h, 24h and 48h after CCl<sub>4</sub> intoxication respectively for the determination of GPT, GSH and MDA. At 48h, the survivability of rat hepatocytes was assayed by the MTT colormetric method.

**RESULTS** After CCl<sub>4</sub> challenge, the release of GPT and the formation of MDA in rat hepatocytes markedly increased and maintained at a high level in 48h, whereas PD with different concentrations could markedly inhibit this elevation with  $10^{-5}$ mol/L PD having the strongest effects and inhibiting rate was over 50%. PD could also improve the decreased content of GSH caused by CCl<sub>4</sub> in accordance with the doses used. CCl<sub>4</sub> evidently decreased the hepatocyte survivability from  $91.0\% \pm 7.9\%$  to  $35.4\% \pm 3.8\%$ . On the other hand, PD at  $10^{-7}$ mol/L- $10^{-4}$ mol/L could re-

verse this change and improve the cell survival rates to  $56.1\% \pm 5.2\%$ ,  $65.8\% \pm 5.0\%$ ,  $88.7\% \pm 6.8\%$  and  $75.2\% \pm 7.3\%$ , respectively.

**CONCLUSION** PD at  $10^{-7}$  mol/L- $10^{-4}$  mol/L could protect primarily cultured rat hepatocytes against CCl<sub>4</sub> induced injury.

## INTRODUCTION

*Polygonum cuspidatum* Sieb. et Zucc. (Polygonaceae) is a traditional Chinese herbal drug, with bitter taste and cold nature. It mainly acts upon the liver, gallbladder and lung meridians. It is well known that *P. cuspidatum* has various activities such as promoting blood circulation, relieving swelling and pain, eliminating phlegm, alleviating cough, clearing away heat, and removing dampness and toxin. The drug has been widely used for cardiovascular and liver diseases. Its active compounds mainly consist of free anthraquinones which include emodin, physcion and chrysophanol. Another important compound is resveratrol<sup>[1]</sup>.

Polydatin (PD), 3, 4', 5-trihydroxystibene-3- $\beta$ -mono-D-glucoside, also named piceid, is the glycoside of resveratrol<sup>[1]</sup>. Some previous studies demonstrated that PD could lower the level of blood lipid, inhibit the platelet aggregation, dilate blood vessels, protect cardiocytes, reduce cerebral ischemic damage and inhibit lipid peroxidation<sup>[2-6]</sup>. However, the effects of PD on hepatocytes and its mechanisms have not been reported up to date. In this paper we report the details of protective effects of polydatin against injury to primarily cultured rat hepatocytes induced by CCl<sub>4</sub>.

## MATERIALS AND METHODS

### Materials

Collagenase (type IV), 3-[4,5-dimethylthiazol-2-yl]-2, 5-diphenyltetrazolium bromide (MTT), dexamethasone, N-2-hydroxyethyl-piperazine-N'-2'-ethane sulfonic acid (HEPES), insulin, penicillin and streptomycin were purchased from Sigma Chemical Corp (St. Louis, USA). RPMI 1640 was

Guangzhou University of Traditional Chinese Medicine (TCM), College of Pharmacy, Guangzhou 510407, China

HUANG Zhao-Sheng, male, born on 1953-09-02 in Jiayang City, Guangdong Province, graduated from Guangzhou University of TCM as a postgraduate in 1984, master of TCM pharmacy, now associate professor and director of the college, having more than 20 papers and 6 books published.

\*Supported by the Bureau of TCM Administration of Guangdong Province, No.96033.

**Correspondence to:** HUANG Zhao-Sheng, College of Pharmacy, Guangzhou University of TCM, 12 Jichang Road, Guangzhou 510407, Guangdong Province, China

Tel. +86-20-86591233 Ext. 2425

Received 1998-03-08

a product of Gibco Life Technologies INC (Grand Island, NY). Fetal calf serum was obtained from Institute of Hemopathy, Chinese Academy of Medical Sciences (Tianjin). PD (Purity>90%), which was isolated from the root and rhizome of *P. cuspidatum*<sup>[7]</sup>, provided by the Department of Chemistry, the First Military Medical University.

### Animals

Wistar rats, male, 6 weeks old, weighing 160 g-180 g, were used for hepatocyte isolation. They were provided by Laboratory Animal Center, Guangzhou University of TCM.

### Isolation and culture of rat hepatocytes

Rats were anesthetized with sodium pentobarbital (50 mg/kg, i.p.). Then the liver parenchymal cells of rat were isolated by the collagenase perfusion method following the procedure of Seglen and Kojima<sup>[8,9]</sup>. Simply, the portal vein of rat liver was exposed and cannulated with a teflon catheter. The liver was perfused with Ca<sup>2+</sup> free solution containing NaCl 142, KCl 6.7, HEPES 10, NaOH 5.5 (mmol/L), pH 7.4, at 37°C, with a flow rate of 40 mL/min. Twelve minutes later, recirculation started with collagenase solution composed of NaCl 67, KCl 6-7, CaCl<sub>2</sub>·2H<sub>2</sub>O 5, HEPES 100, NaOH 66, collagenase 0.2 g/L, pH 7.6. Isolated cells were cultured in RPMI 1640 containing 100mL/L-fetal calf serum, 10mmol/L-HEPES, 100kU/L-penicillin and streptomycin, 10mmol/L insulin and 10mmol/L-dexamethasone. The content of hepatocytes was adjusted to 7.5 × 10<sup>8</sup> cells/L with the above medium. Cultured medium 2mL and 0.2mL were added into 24-well and 96-well plates respectively. The cells were incubated for 4h at 37°C under 50mL/L CO<sub>2</sub> in air. Non-adherent hepatocytes were eliminated by replacing the medium, and adherent hepatocytes continued to be incubated, and the medium was changed every 24 h.

### CCl<sub>4</sub>-induced hepatocytes injury

After pre-culture for 24 h, the hepatocytes were exposed to fresh medium containing 10mmol/L-CCl<sub>4</sub> and various concentrations of PD. At 6, 12, 24 and 48 h after CCl<sub>4</sub> intoxication, 0.1 mL and 1 mL culture solution were removed from 96-well and 24-well plates respectively for determination.

### Measurement of glutamic pyruvic transaminase (GPT)

The kits of GPT analysis, provided by the Shanghai Institute of Biological Products of Ministry of Health, were used to measure the activity of GPT in 0.1 mL- culture medium.

### Determination of reduced glutathione (GSH) and malondialdehyde (MDA)

Utilizing the kits of GSH analysis and the kits of MDA analysis, all purchased from Nanjing Jiancheng Bio-engineering Institute, the content of GSH in 1mL culture medium and the level of MDA in 0.1mL culture medium were re measured.

### Cell survivability assay

The survivability of rat hepatocytes was assayed by the MTT colorimetric method<sup>[10]</sup>. At 48h after CCl<sub>4</sub> challenge, 20 μL/well- MTT stock solution (5 g/L) was added into each well of 96-well plates. The cells were continuously incubated for another 4 h before 0.1 mL/well dimethyl sulfoxide was added to all wells and mixed thoroughly to dissolve the brown-black crystals. The plates were read on microplate reader, using a test wavelength of 570 nm with a reference wavelength of 655 nm.

### Statistical analysis

The results were expressed as  $\bar{x} \pm s$  and significant difference was assessed by Student's *t* test.

## RESULTS

### Effects of PD on GPT activity in culture medium

The concentration of GPT in culture medium significantly increased after CCl<sub>4</sub> challenge, and maintained at a high level in 8 h (Table 1). Furthermore, a progressively elevated trend existed with time-dependence. PD could significantly inhibit the level of GPT in accordance with the doses used. Especially, PD 10 μmol/L had the strongest effects and the inhibiting rate was over 50%.

**Table 1** Effect of PD on GPT activity in culture medium

Group c/(mol/L)	GPT(U)			
	6 h	12 h	24 h	48 h
Normal	13.5±2.5 <sup>b</sup>	13.8±3.1 <sup>b</sup>	13.7±5.6 <sup>b</sup>	14.1±3.3 <sup>b</sup>
Control	72.3±14.1	79.7±10.3	85.4±9.2	88.3±19.6
PD 10 <sup>-7</sup>	60.3±17.1 <sup>a</sup>	62.0±15.6 <sup>a</sup>	68.8±17.5 <sup>a</sup>	71.4±20.5 <sup>a</sup>
PD 10 <sup>-6</sup>	55.0±10.3 <sup>a</sup>	58.3±16.7 <sup>a</sup>	64.1±13.6 <sup>a</sup>	69.1±19.2 <sup>a</sup>
PD 10 <sup>-5</sup>	30.6±10.6 <sup>b</sup>	38.3±5.5 <sup>b</sup>	42.5±7.0 <sup>b</sup>	45.0±7.6 <sup>b</sup>
PD 10 <sup>-4</sup>	42.1±7.8 <sup>a</sup>	47.5±9.8 <sup>a</sup>	56.8±11.3 <sup>a</sup>	59.2±10.7 <sup>a</sup>

<sup>a</sup>P<0.05, <sup>b</sup>P<0.01, vs CCl<sub>4</sub>-treated control group.

### Effects of PD on GSH content in culture medium (Table 2).

The content of GSH in culture medium decreased obviously as compared with that in normal hepatocytes after 6 h incubation with CCl<sub>4</sub> (Table 2). On the other hand, PD of various concentrations could

improve GSH in a dose-dependence manner, and 10  $\mu\text{mol/L}$  PD showed a most significant activity.

**Table 2** Effects of PD on GSH content in culture supernatant ( $\bar{x} \pm s$ ,  $n = 8$ )

Group c/(mol/L)	GSH (ng/L) after CCl <sub>4</sub> challenge			
	6 h	12 h	24 h	48 h
Normal	9.8±0.8 <sup>b</sup>	10.1±0.8 <sup>b</sup>	10.4±0.7 <sup>b</sup>	10.6±1.2 <sup>b</sup>
Control	4.2±0.6	4.1±0.7	4.1±0.3	3.8±0.6
PD 10 <sup>-7</sup>	5.0±0.3	5.4±0.5	5.6±0.9	6.1±1.0 <sup>a</sup>
PD 10 <sup>-6</sup>	5.3±0.8	5.6±0.9	6.4±0.6 <sup>a</sup>	6.8±1.1 <sup>a</sup>
PD 10 <sup>-5</sup>	8.4±1.2 <sup>b</sup>	5.9±1.3 <sup>a</sup>	7.7±0.8 <sup>a</sup>	9.0±1.2 <sup>b</sup>
PD 10 <sup>-4</sup>	6.7±0.4 <sup>a</sup>	6.1±1.0 <sup>a</sup>	6.8±0.7 <sup>a</sup>	7.6±0.9 <sup>a</sup>

<sup>a</sup> $P < 0.05$ , <sup>b</sup> $P < 0.01$ , vs CCl<sub>4</sub> treated control group.

### Effects of PD on MDA formation in rat hepatocytes

CCl<sub>4</sub> challenge obviously elevated the MDA formation in rat hepatocytes, with a marked rise in time-dependence manner, whereas MDA formation of rat hepatocytes decreased significantly at various concentrations of PD as compared with that in CCl<sub>4</sub> control group, and it reached minimum value at 10<sup>-5</sup> mol/L and slightly elevated when PD concentration was up to 10<sup>-4</sup>-mol/L (Table 3).

**Table 3** Effects of PD on MDA formation in rat hepatocytes ( $\bar{x} \pm s$ ,  $n = 8$ )

Group c/(mol/L)	GSH (ng/L) after CCl <sub>4</sub> challenge			
	6 h	12 h	24 h	48 h
Normal	4.0±0.4 <sup>b</sup>	4.5±0.6 <sup>b</sup>	4.8±0.4 <sup>b</sup>	4.6±0.7 <sup>b</sup>
Control	15.5±1.8	16.0±2.7	17.5±2.1	19.0±2.4
PD 10 <sup>-7</sup>	13.1±2.0	13.8±3.3	13.0±4.3 <sup>a</sup>	14.5±1.8 <sup>a</sup>
PD 10 <sup>-6</sup>	11.4±1.7 <sup>a</sup>	12.0±1.8 <sup>a</sup>	12.1±3.1 <sup>a</sup>	12.5±2.0 <sup>a</sup>
PD 10 <sup>-5</sup>	6.5±1.2 <sup>b</sup>	6.7±1.2 <sup>b</sup>	7.5±2.3 <sup>b</sup>	8.2±2.7 <sup>b</sup>
PD 10 <sup>-4</sup>	8.7±3.5 <sup>b</sup>	8.9±2.8 <sup>b</sup>	9.8±2.6 <sup>b</sup>	10.3±3.0 <sup>b</sup>

<sup>a</sup> $P < 0.05$ , <sup>b</sup> $P < 0.01$ , vs CCl<sub>4</sub> treated control group.

### Effects of PD on cell survivability in primary culture rat hepatocytes

The results of MTT assay showed that normal hepatocytes had high level of cell viability (91.0% ± 7.9%) and CCl<sub>4</sub> induced marked decrease of hepatocytes survivability (35.4% ± 3.8%,  $P < 0.01$  vs normal group), whereas the level of cell survivability could be significantly enhanced by PD at the concentrations of 10<sup>-7</sup> mol/L - 10<sup>-4</sup> mol/L to 56.1% ± 5.2% ( $P < 0.05$ , vs CCl<sub>4</sub>-treated control group), 65.8% ± 5.0% ( $P < 0.05$ ), 88.7% ± 6.8% ( $P < 0.001$ ) and 75.2% ± 7.3% ( $P < 0.01$ ) respectively. It reached a maximum value at 10<sup>-5</sup> mol/L and slightly declined when the concentration of PD was up to 10<sup>-4</sup> mol/L (Figure 1).

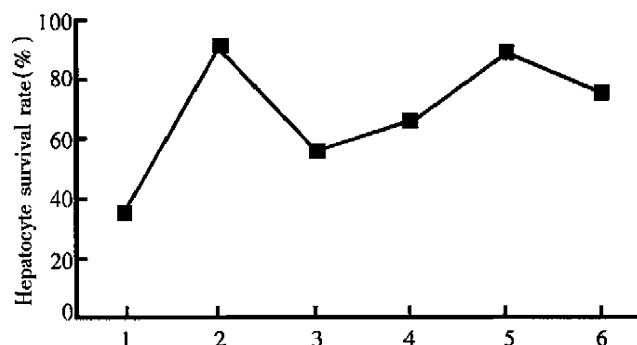


**Figure 1** Effects of PD on cell survivability in primary culture rat hepatocytes.

1. CCl<sub>4</sub>-treated control group; 2. normal hepatocytes; 3. PD 10<sup>-7</sup> mol/L; 4. PD 10<sup>-6</sup> mol/L; 5. PD 10<sup>-5</sup> mol/L; 6. PD 10<sup>-4</sup> mol/L.

### DISCUSSION

*P. cuspidatum* has been used to treat some chronic liver diseases such as hepatitis and hepatocirrhosis. We have been trying to search for hepatoprotective compounds of *P. cuspidatum*. Our previous *in vitro* studies showed that emodin, another active compound, had a hepatoprotective effect<sup>[11]</sup>. The present *in vitro* study also indicated that PD had a protective effect against CCl<sub>4</sub> induced injury to primarily cultured rat hepatocytes. Since the extraction and isolation of PD are relatively simple and have a high content of 1.23% in the root of *P. cuspidatum*<sup>[7]</sup>, we may take these advantages to further study its mechanisms of hepatoprotective effect and develop a new drug from it.

CCl<sub>4</sub> is a well-known example of a chemical that produces free radical-mediated liver injury. It generates CCl<sub>4</sub> by the activation of liver cytochrome P-450, initiating lipid peroxidation of bio-membranes<sup>[12]</sup>. In the present experiment, it was found that CCl<sub>4</sub> induced both the increase of GPT in supernatant and the elevation of MDA in rat hepatocytes. However, administration of 10<sup>-7</sup> mol/L - 10<sup>-4</sup> mol/L PD could partly reduce GPT and MDA. Therefore, there may be two possible mechanisms contributing to the hepatoprotective actions of PD. One is that PD inhibits further production of lipid peroxidation in rat hepatocytes, and the other is that it inhibits the destructive action of lipid peroxidation on liver cells.

GSH is an important endogenous anti-oxidant substance. The decrease of GSH content may be due to increased GSH consumption as it participates in the detoxification system for the metabolism of CCl<sub>4</sub>, and results in an enhanced susceptibility of hepatocytes to CCl<sub>4</sub> toxicity<sup>[13]</sup>. Our results showed that CCl<sub>4</sub> obviously decreased GSH content in the

hepatocytes, but PD could partly reverse it. This suggested that the nature of PD protecting-SH compounds (such as GSH) from CCl<sub>4</sub> injury may be the third mechanism of its hepatoprotection.

It is interesting that PD of 10<sup>-5</sup> mol/L was more effective than that of 10<sup>-4</sup> mol/L, at the same time, the hepatoprotective action of PD was in dose dependence at concentrations of 10<sup>-7</sup> mol/L - 10<sup>-5</sup> mol/L. Its mechanisms of action need to be further studied.

## REFERENCES

- 1 Ouyang CG. Chemical compounds in Polygonum cuspidatum. *Chin Trad Herbal Drugs*, 1987;18:44-45
- 2 Zhang PW, Yun CL, Wang YZ, Luo SF, Sun LS, Li RS. Influence of 3,4,5-trihydroxy-stibene-3-β-mono-D-glucoside on vascular endothelial epoprostenol and platelet aggregation. *Acta Pharmacol Sin*, 1995;16:265-268
- 3 Zhang PW, Shan CW, Zhang J, Yu CL. Effects of polydatin on human hemodynamics and cholesterol. *J Med Coll PLA*, 1995;15:47-48
- 4 Wang YZ, Luo SF, Zhang PW, Luo SF, Fang FZ, Pang JJ. Reducing effect of polydatin on arterial thrombosis induced by vascular endothelial injury. *Acta Pharmacol Sin*, 1995;16:159-162
- 5 Abbert WN, ZX mo. Protective effects of polydatin, an active compound from polygonum cuspidatum, on cerebral ischemic damage in rats. *Chin Pharmacol Bull*, 1996;12:126-129
- 6 Jin WJ, Chen SY, Qian ZX, Shi XH. Effects of polydatin IV on inhibiting respiratory burst of PMNS and scavenging oxygen free radicals. *Chin Pharmacol Bull*, 1993;9:355-357
- 7 Wang D, Tang Y. Quantitative determination of polydatin in Polygonum cuspidatum. *Chin Trad Herbal Drugs*, 1987;18:16-18
- 8 Seglen PO. Preparation of isolated rat liver cell. *Methods Cell Biol*, 1976;13:29-83
- 9 Koji H, Rena K, Purusotam B, Shigetoshi K, Tsunco N. Preventive effect of lithospermate B from Salvia miltiorhiza on experimental hepatitis induced by CCl<sub>4</sub> or D-Gal/LPS. *Planta Med*, 1997;63:22-26
- 10 Zheng YT, Ben KL. Use of MTT assay for the determination of cell viability and proliferation. *J Immuno (CHN)*, 1992;8:266-269
- 11 Huang ZS, Wang ZW, Zhong SQ. Protective effects of emodin on CCl<sub>4</sub>-induced injury of primary cultured rat hepatocytes. *Chin J Integr Med*, 1998 (in press)
- 12 Tribble DL, Aw TY, Jones DP. The pathophysiological significance of lipid peroxidation in oxidative cell injury. *Hepatology*, 1987;7:377-386
- 13 Zhu B, Liu GT. Cytotoxic effect of hydrogen peroxide on primary cultured rat hepatocytes and its mechanisms. *Chin J Pharm Toxicol*, 1996;10:260-266

Edited by MA Jing-Yun

# Effect of HCV NS<sub>3</sub> protein on p53 protein expression in hep atocarcinogenesis \*

FENG De-Yun, CHEN Rui-Xue, PENG Yong, ZHENG Hui and YAN Ya-Hui

**Subject headings** liver neoplasms; oncogenes; hepatitis virus; p53 protein

## Abstract

**AIM** To investigate hepatocarcinogenesis by detecting the effect of HCV NS<sub>3</sub> protein on p53 protein expression in hepatocellular carcinoma (HCC) and pericarcinomatous liver tissue (PCLT).

**METHODS** The expression of HCV NS<sub>3</sub> and p53 protein was detected with immunohistochemical technique (SP method) in specimens of HCC and PCLT from 47 patients with negative HBV.

**RESULTS** The positive rate of HCV NS<sub>3</sub> protein was lower in HCC (62%) than in PCLT (83%) ( $P < 0.025$ ). The better differentiation of cancer cells, the stronger expression of HCV NS<sub>3</sub> protein ( $P < 0.025$ ). The positive rate of p53 protein in HCC (81%) was higher than in PCLT (47%) ( $P < 0.025$ ). The worse differentiation of cancer cells, the stronger expression of p53 protein ( $P < 0.05$ ). The p53 protein expression was not correlated with the HCV NS<sub>3</sub> protein expression in HCC ( $P > 0.5$ ), whereas their expression was closely related to PCLT ( $P < 0.01$ ), and the expression rate of p53 protein in the cases of positive HCV NS<sub>3</sub> protein was higher than that in the cases of negative HCV NS-3 protein.

**CONCLUSION** HCV NS<sub>3</sub> protein may exert its hepatocarcinogenic effect in early stage on host cells by endogenous pathway which may bring about mutation of p53 gene and transformation of hepatocytes.

## INTRODUCTION

Hepatocellular carcinoma (HCC) is one of the most common human cancers in the world. Recently, the HCV infection was found to be an etiological factor to HCC. HCV is a RNA virus bearing no reverse transcriptase activity. Therefore, in stead of "promoter insertion", or "insertion mutagenesis", the HCV NS<sub>3</sub> expression of HCV gene may play an essential role in transformation of hepatocytes<sup>[1]</sup>. p53 gene, an oncogene, has been intensively investigated recently. Mutation of this gene was found to be related to HCC in a variety of studies. In order to understand the relationship among p53 protein, HCV NS<sub>3</sub> protein and HCC, we studied the effect of HCV NS<sub>3</sub> protein on expression of p53 protein in HCC and pericarcinomatous liver tissue (PCLT).

## MATERIALS AND METHODS

### Tissue samples

HCC and PCLT were obtained by surgical resection from 47 patients in Xiangya Hospital and the Second Affiliated Hospital of Hunan Medical University, China. Forty patients were males and 7 females. Their age ranged 33 to 67 years (mean, 52 years), and all patients were negative for HBsAg serological marks. The tissues were fixed in 10% formalin and embedded in paraffin.

### Reagents

Anti-HCV NS<sub>3</sub> protein MAb was purchased from GIB Comp. (Beijing, China), anti-p53 protein MAb and SP detection kit from Maixing Comp. (Fuzhou, China).

### Immunohistochemistry

Five  $\mu$ m tissue sections were deparaffinized and washed in 0.05mol/L PBS, handled with 20g/L H<sub>2</sub>O<sub>2</sub> and treated with microwave. According to SP method, the tissues were detected with immunohistochemical technique. HCV RNA(+) biopsy liver tissues and breast cancer tissues were used as positive control of HCV NS<sub>3</sub> protein and p53 protein respectively. PBS was used as substitutes of Mabs for negative control groups.

### Histological assessment

Semi-quantity analysis was performed as Formonitz<sup>[2]</sup> described.

Department of Pathology, Hunan Medical University, Changsha, 410078, Hunan Province, China

Dr. FENG De-Yun, male, born in 1964 in Hunan Province, graduated from Hunan Medical University in 1991, Master Degree of Pathology.

\*Project supported by the Health Ministry Science Foundation of China, No.94-120

**Correspondence to:** Dr. FENG De-Yun, Department of Pathology, Hunan Medical University, Changsha, 410078, Hunan Province, China

Received 1998-09-10

### Statistical analysis

The difference between each group was analyzed by Chi-square test.

## RESULTS

### Expression and distribution of HCV NS<sub>3</sub> protein in HCC and PCLT

Among 47 cases, the positive rate of HCV NS<sub>3</sub> protein in HCC was 62% (29/47), and the positive cells were clustered or diffused in HCC. The positive signal was localized in cytoplasm. The expression strength of HCV NS<sub>3</sub> protein in HCC was related to the degree of carcinoma cell differentiation ( $P < 0.05$ ). The better differentiation of cancer cells, the stronger expression of HCV NS<sub>3</sub> protein ( $P < 0.05$ ). The positive rate (83%) and the expression strength of HCV NS<sub>3</sub> protein in HCC were higher than those in PCLT. The distribution of positive cells in PCLT appeared large patchy or diffused.

### Expression and distribution of p53 protein in HCC and PCLT

Of the 47 cases, the positive rate of p53 protein in HCC was 81% (38/47), and the positive cells appeared focal or patchy in HCC. The positive signal was in the nuclei. The expression strength of p53 protein in HCC was correlated with the degree of carcinomatous cell differentiation ( $P < 0.05$ ). The worse differentiation of cancer cells, the stronger expression of p53 protein ( $P < 0.05$ ). The positive rate (47%) and the expression strength of p53 protein in HCC were lower than those in PCLT. The positive cells in PCLT was scattering in distribution.

**Table 1** The expression strength of HCV NS protein and p53 protein in HCC and PCLT

	HCV NS <sub>3</sub> protein					Positive rate(%)	p53 protein					Positive rate(%)
	-	+	++	+++	n		-	+	++	+++	n	
<b>HCC</b>												
I	8	2	0	3	3	6/8	4	2	2	0	4/8	4/8
II	10	2	1	2	5	8/10	2	3	4	1	8/10	8/10
III	18	8	3	6	1	56	2	0	6	10	89	89
IV	11	6	3	2	0	46	1	1	3	6	91	91
<b>PCLT</b>												
Normal	3	2	1	0	0	1/3	3	0	0	0	0	0
Hepatitis	23	4	2	5	12	83	13	8	2	0	44	44
Cirrhosis	21	2	2	6	11	91	9	7	5	0	57	57

### Relationship between p53 protein expression and HCV NS<sub>3</sub> protein

In HCC, the expression rate of p53 protein in 29 cases of positive HCV NS<sub>3</sub> protein was 83% (24/29), and in 18 cases of negative HCV NS<sub>3</sub> protein was 78% (14/18), the difference between the former and the latter being not significant ( $P > 0.1$ ).

In PCLT, the expression rate of p53 protein in 39 cases of positive HCV NS<sub>3</sub> protein was 54% (21/39), and in 8 cases of negative HCV NS<sub>3</sub> protein was only 13% (1/8), the difference between the former and the latter being significant ( $P < 0.05$ ).

## DISCUSSION

Chronic infection with HCV is strongly associated with the development of HCC. HCV causes HCC by expressing protein, especially HCV NS<sub>3</sub> protein<sup>[1,3]</sup>. Nevertheless, the exact molecular mechanism remains quite unknown. Our results showed that the positive rate and expression strength of HCV NS<sub>3</sub> protein in PCLT were higher than those in HCC, and the expression strength of HCV NS<sub>3</sub> protein in HCC was related to the degree of carcinoma cell differentiation. The better differentiation of cancer cells, the stronger expression of HCV NS<sub>3</sub> protein. It is indicated that the cellular internal environment for HCV replication is disturbed with cancer growth. HCV may be eliminated at the final stage of hepato cytes transformation because the virus without reverse transcriptase is unable to integrate into the host hepatocytes genome. On the other hand, the positive rate and expression strength of p53 protein in PCLT were lower than those in HCC. The expression strength of p53 protein in HCC was related to the degree of carcinoma cell differentiation. The worse differentiation of cancer cells, the stronger expression of p53 protein. It is suggested that p53 protein may play a role in the morphological change and the differentiated degree of cancer cells in HCC, thus detecting p53 protein expression is of benefit to HCC prognosis.

Effect of HCV NS<sub>3</sub> protein on mutation of p53 gene was not confirmed, although HCV infection may result in mutation of p53 gene<sup>[4]</sup>. This study revealed that there was no relationship between p53 protein and HCV NS<sub>3</sub> protein in HCC. In PCLT, p53 protein expression was positive in 21 of 39 cases of positive HCV NS<sub>3</sub> protein while only one case of p53 protein expression in 8 cases of negative HCV NS<sub>3</sub> protein was positive. HCV NS<sub>3</sub> protein may exert its hepatocarcinogenic effect in early stage on host cells by endogenous pathway which may bring about mutation of p53 gene and transformation of hepatocytes.

## REFERENCES

- Hino, Kajino K. Hepatitis virus-related hepatocarcinogenesis. *Intervirology*, 1994;37:133-135
- Fromowitz FB, Viola WV, Chao S. ras p21 expression in the progression of breast cancer. *Hum Pathol*, 1987;18:1268-1275
- Sakamuro D, Furukawa T, Takefami T. Hepatitis C virus nonstructural protein NS<sub>3</sub> transforms NIH3T3 cells. *J Virol*, 1995;69:3893-3896
- Teramoto T, Satonaka K, Kitazawa S. p53 gene abnormalities are closely related to hepatoviral infections and occur at a late stage of hepatocarcinogenesis. *Cancer Res*, 1994;54:231-235

# Expression of Cx genes in liver and stomach of different embryonic stages \*

ZHANG Jian-Xiang<sup>1</sup>, SHEN Shou-Rong<sup>2</sup>, ZHANG Xiao-Hui<sup>1</sup> and CHEN Xiang<sup>3</sup>

**Subject headings** liver/embryology; liver/cytology; stomach/embryology; stomach/cytology; Cx genes; gene expression

## Abstract

**AIM** To explore the relationship between the rules of Cx gene expression and cellular differentiation in organs of different embryonic stages.

**METHODS** A series of Cx gene serving as molecular probes and the Northern blot hybridization were employed to study the Cx gene expression.

**RESULTS** Cx31, Cx31.1, Cx46 did not express while other Cx genes expressed in the embryonic liver and stomach. The Cx gene expression in the liver and stomach showed different state at different embryonic stages. The Cx gene expression had organic diversity. The expression of Cx26 gene was overlapping in the above organs. Cx43 did not express in the human liver after birth, but it expressed in the embryonic stage.

**CONCLUSION** The expression state of Cx genes is concordant with cellular differentiation. It might be a key candidate gene to regulate some differentional events associated with cellular differentiation, proliferation, and morphogenesis in the early embryo.

## INTRODUCTION

Cellular connexin genes are a multigene family consisting of more than 10 members<sup>[1-4]</sup> which encode the gap junctional channel assembled protein, connexin (Cx). The latter is the key composite of gap junctional intercellular communication (GJIC). The expression of Cx genes determines the formation, pattern, amount and the degradation of GJIC channel. The specific connexin proteins transcribed and translated by different members of Cx gene family contribute to the diversity of gap junctional channel within different tissue cells or the same type of cells but in different functional states, leading to the differences in patterns and structures of gap junction. The members of connexin gene are related to the type and size of communication channel and communication ways of gap junction<sup>[5]</sup>. Gap junction is present in the early stage of embryonic development. The morphological study has verified that gap junction is detected within morula and blastocyst, and dense GJICs appear in cells of embryonic ectoderm at 20 h - 30 h of developing chicks<sup>[5]</sup>. In order to investigate the relationship between the expression law of Cx genes and cellular differentiation in the liver and stomach during embryonic development, the Cx gene expression state was studied using Cx26, Cx31, Cx31.1, Cx32, Cx37, Cx40, Cx43 and Cx46 as molecular probes and the Northern blot hybridization.

## MATERIALS AND METHODS

### Materials

The liver and stomach derived from the fetals of mothers receiving natural abortion with conceptional age of 5 weeks, 2, 3, 4 and 5 months. The tissues or organs were stored in fluid nitrogen.

### Methods

**Preparation of plasmids containing Cx cDNA** A small amount of bacteria containing 8 kinds of pCx plasmids and inner control pGAPDH plasmid was recovered. An inoculum of bacteria was streaked on an agar plate and incubated overnight at 37°C. The next day single bacterial colonies were picked for amplification; plasmids were extracted with alkaline lysis procedure and digested and identified with appropriate restrictive endonuclease. The termini were then isolated by electrophoresis in 10g/L agarose gel and retrieved and purified with Glass Max kit (Table 1).

<sup>1</sup>Department of Histology and Embryology, Hunan Medical University, Changsha 410078, China

<sup>2</sup>Department of Internal Medicine, Xiangya Hospital, Hunan Medical University, Changsha 410078, China

<sup>3</sup>The First People's Hospital of Zhaoqing City, Guangdong Province  
Dr. ZHANG Jian-Xiang, male, born on November 29, 1951 in Changsha City, Hunan Province, graduated from Hunan Medical University with a master degree in histology and embryology, now a professor, having 18 papers published.

\*Project supported by the National Natural Science Foundation of China, No.39670344.

**Correspondence to:** Dr. ZHANG Jian-Xiang, Department of Histology and Embryology Hunan Medical University, 88 Xiangya Road, Changsha 410078, China

Tel. +86-731-4471979 Ext.2880, Fax. +86-731-4471979

Received 1998-11-19

**Table 1 A list of plasmids containing Cx cDNA**

Plasmids	Vectors	Restriction enzymes	Inserts (kb)	Species
pCx26	pSG5	<i>Bam</i> H I	0.68	human
pCx31.1	SP63T	<i>Bgl</i> II	0.85	mouse
pCx32	pGEM3	<i>Eco</i> R I	1.5	rat
pCx33	SP64T	<i>Bgl</i> II	0.9	rat
pCx37	SP64T	<i>Hind</i> III/ <i>Xba</i> I	1.25	mouse
pCx40	pGEM4z	<i>Eco</i> R I/ <i>Xba</i> I	1.1	mouse
pCx43	pSG5	<i>Bam</i> H I	1.11	human
pCx46	BSK+	<i>Eco</i> R I	1.6	human
pGAPDH		<i>Eco</i> R I/ <i>Hind</i> III	0.6	human

**Table 2 Expression of Cx genes in different organs at different fetal ages**

Connexin genes	2 month		3 month		4 month		5 month	
	Liver	Stomach	Liver	Stomach	Liver	Stomach	Liver	Stomach
Cx26	++	+	+++	+	++	+	+	+
Cx31	-	-	-	-	-	-	-	-
Cx31.1	-	-	-	-	-	-	-	-
Cx32	+++	-	+++	+	+++	++	+++	+++
Cx37	-	++	-	+++	-	-	-	++
Cx40	-	+	-	++	-	-	-	+++
Cx43	++	-	+++	-	++	++	+	++
Cx46	-	-	-	-	-	-	-	-

+++ : high, ++ : moderate, + : low, - : no or weak

### Preparation and purification of total RNA

Total RNA was extracted by acid guanidinium-phenol chloroform procedure from the liver and stomach in different stages of embryo respectively.

### Northern blot

Total RNA (20 µg in each well) was separated by electrophoresis through formaldehyde denaturing gels and transferred onto nylon membranes by capillary transfer for 24 h in 20 × SSC. The RNA was cross-linked to the membranes by exposure to UV light.

### Northern hybridization between Cx gene probes and RNA

Connexin-specific cDNA probes were random-prime labeled with [ $\alpha$ -<sup>32</sup>P] dCTP. The membranes were prehybridized at 42°C for 4h in Northern hybridization solution (500 g/L-formamide, 5 × SSPE, 5 × Denhardt's reagent, 1 g/L-SDS solution and 100 mg/L salmon sperm DNA) and then hybridized with the labeled probe for 16 h - 24 h in the same solution.

### Autoradiograph (ARG)

The membranes were washed twice at 37°C in

2×SSC/ (1 g/L)-SDS for 40 min and three times at 65°C in 0.1 × SSC/ (1 g/L) SDS for 1 h. Exposure of X-ray film to the blots was conducted at -70°C with intensifying screens. To remove probes from the membranes, the membranes were immersed in 1 g/L-SDS solution in rotating platform from boiling to RT. The process was repeated. Then the membranes were rehybridized with GAPDH probe.

### RESULTS

Cx31, Cx31.1 and Cx46 did not express while other Cx genes expressed in the liver and stomach of embryonic stage. The expression of Cx genes showed different states in the liver and stomach at different embryonic stages. The expression of Cx genes was of organic diversity, e. g., the expression of Cx32 in the liver and Cx37 in the stomach. The Cx gene expression was overlapping in the above organs, and Cx26 presented different states of expression. Cx32 gene had high expression from the 5th week to the 5th month in the liver and the 4th to 5th month in the stomach. Cx43 did not express in human liver after birth, but it expressed in the fetal stage. Cx37 gene in the stomach of fetals highly expressed from the 3rd month to the 5th month (Table 2).

## DISCUSSION

Cx genes showed different expression states, e.g., Cx26, Cx32, Cx43 in the liver, and Cx26, Cx32, Cx37 and Cx43 in the stomach. The diversity of expression indicated that the various gap junctional channels between different cells or the same cells in different functional state was due to the expression of different members of Cx gene family<sup>[6]</sup>.

Cx26 gene in the fetal liver had weak expression in the 5th week, and high expression in the 3rd month, which lowered gradually during the 4th to 5th month. The expression and nonexpression of Cx26 gene are believed to be relevant to morphogenesis of hepatic lobule, central vein and portal area. There was no structure of hepatic lobule, central vein and portal area in the liver in the 5th week of embryo. The structures formed gradually during the 2nd month, and hepatic lobule was recognized in the 3rd month. Cx26 was in its high expression state during this stage. The structure of portal area became clear in the 4th month. Up to this stage, the Cx26 expression gradually reduced when the basal morphological structure of liver was established. The Cx26 gene expression was overlapping in the stomach, which might be related to the morphogenesis of stomach. It is suggested that the Cx26 expression plays an important role in the morphogenesis and structural building of the liver and stomach during embryogenesis.

The expression state of Cx genes is conformed to the cellular differentiation. It may be related to its own differentiation and proliferation of liver cells. This is compatible with Zeng's report in which the cells of primeval region will acquire further differentiative capacity, which is closely related to a high level of expression of Cx genes among the same cells<sup>[7]</sup>. Cx32 gene expression in the stomach is related to development of gastric gland, it was low during gastric gland bud stage in the 3rd month, and increased gradually during the developing stage of primordial gastric gland in the 4th month, and reached a peak in the 5th month when the gastric gland grew completely.

Eghbali<sup>[8]</sup> transfected cDNA of whole length Cx32 gene into the hepatocellular cancer lacking Cx32, and found mRNA expression level, and gap junction were increased markedly, and ion coupling and metabolite coupling reappeared in the tests of dye transfer and electric current of intercellular communication, meanwhile the growth rate of car-

cinoma cells transfected with Cx32 decreased rapidly, and cellular structure of neoplastic cells differentiated towards normal cells. It is indicated that the expression of Cx32 gene plays a significant role in the cellular differentiation.

Cx43 does not express in the human liver after birth<sup>[9]</sup>, but it expresses in the fetal stage. It may be related to hematopoietic function of the liver during the fetal stage. Hematopoietic stem cells migrate to liver from yolk sac at early embryonic stage; at this time, Cx43 expression is low and turns high when the weight of hematopoietic tissues amounts to 30%-40% of the liver by the 3rd to 4th month of embryonic development. With the formation of the spleen, thymus and bone marrow, most of the hematopoietic stem cells in the liver migrate to the above organs, and the Cx43 gene expression lowers distinctly in the 5th month of the fetal liver, indicating the lowered hematopoietic function of the liver. It may be related to the smooth muscle development in stomach<sup>[4]</sup>.

Wang SQ<sup>[10]</sup> held that gap junction appeared in the early embryonic stage made it possible the intercellular transfer of substances which regulated cellular differentiation, morphological formation and growth control. For example, in archigastrula and neurula, gap junctions made notochord-induced ectoderm develop into neural tubes. During embryonic development, the expression state of Cx genes is basically concordant with the formation and degradation of gap junctional communication channel. It is suggested that Connexin gene may be a key candidate gene to regulate some differentiative events associated with cellular differentiation, proliferation and morphogenesis and organ development.

## REFERENCES

- 1 Beyer EC, Paul DL, Goodenough DA. Connexin family of gap junction protein. *J Membr Biol*, 1990;116:187-194
- 2 Nalin MK, Nordin BG. The gap junction communication channel. *Cell*, 1996;84:381-388
- 3 Daniel AG. Connexins, Connexons, and Intercellular. *Annu Rev Biochem*, 1996;65:475-520
- 4 Zhang ZQ, Liu ZX. Connexins family, cellular gap junctional communication and tumor suppression. *Progr Physiol Sci*, 1994;25:121-125
- 5 Cheng LZ. Histology. 2nd Ed. Beijing: People's Public Health Press, 1994: 188-192
- 6 Willecke K, HenneMann H, Dahl E. The diversity of Connexin genes encoding gap junctional protein. *Eur J Cell Biol*, 1991;56:1-7
- 7 Zeng MB. Determination, differentiation and intercellular communication. *Chin J Cell Biol*, 1994;16:97-100
- 8 Eghball B, Kessler JA, Reid LM. Involvement of gap junctions in tumorigenesis: transfection of tumor with connexin 32 cDNA retards growth *in vivo*. *Proc Natl Acad Sci USA*, 1991;88:10701-10705
- 9 Wilgenbus KK, Kirkpatrick CJ, Knueche LR. Expression of Cx26, Cx32, Cx43 gap junction proteins in normal and neoplastic human tissues. *Int J Cancer*, 1992;51:522-529
- 10 Wang SQ. Gap junction and development. *Chin J Cell Biol*, 1988;10:20-24

# Expression of IL 1 $\beta$ converting enzyme in 5-FU induced apoptosis in esophageal carcinoma cells

DENG Li-Ying<sup>1</sup>, ZHANG Yun-Han<sup>2</sup>, XU Ping<sup>2</sup>, YANG Su-Min<sup>1</sup> and YUAN Xue-Bin<sup>1</sup>

**Subject headings** esophageal carcinoma; cell line; apoptosis; 5-fluorouracil; interleukin 1 $\beta$ -converting enzyme

## Abstract

**AIM** To study the role of interleukin 1 $\beta$ -converting enzyme (ICE) in antitumor drug-induced apoptosis in tumor cells.

**METHODS** Morphological changes in human esophageal carcinoma Eca-109 cells after treated with 5-fluorouracil (5-FU) were observed under light and electron microscope. Expression of ICE in the tumor cells exposed to 5-FU was examined by the immunocytochemical method.

**RESULTS** The cells treated with 5-FU displayed disappearance of nucleoli, chromatin gathering under nuclear envelope, karyorrhexis, budding and the formation of apoptotic bodies. The expression of ICE was negative in control cells, and 5-FU could induce the ICE expression in Eca-109 cells undergoing apoptosis. The number and the staining intensity of positive cells increased with the extension of action time.

**CONCLUSION** 5-FU may induce apoptosis in human esophageal carcinoma Eca-109 cells; ICE gene may be involved in the regulation of 5-FU-induced apoptosis; and ICE protein may mediate apoptosis induced by 5-FU.

## INTRODUCTION

Apoptosis is an important physiological form of cell death. It is strictly controlled by genes. It has been shown in experiments that external and internal signals of cells may start the process of apoptosis, e. g., anticancer drugs<sup>[1]</sup>. The genes involved in apoptosis include the family of *bcl-2*, *p53*, *c-myc* and so on. Recent studies showed that interleukin-1 $\beta$ -converting enzyme (ICE) gene was a mammalian homologue of the *C. elegans* cell death gene *ced-3*<sup>[2]</sup> and that overexpression of ICE gene could induce apoptosis in Rat-1 fibroblast<sup>[3]</sup>. Thus, the expression of ICE protein in human esophageal carcinoma Eca-109 cells treated with 5-fluorouracil (5-FU) was examined to investigate the role of ICE in anticancer drug induced apoptosis.

## MATERIALS AND METHODS

### Tumor cell culture

Human esophageal carcinoma Eca-109 cells were cultured in RPMI 1640 (Gibco) medium supplemented with 10% heat-inactivated new-born calf serum 100U/mL penicilin, and 100 $\mu$ g/mL streptomycin, and kept in a controlled atmosphere (5% CO<sub>2</sub>) incubator at 37°C.

### Drug treatment

Exponentially growing cells were seeded in plates for 24 h and treated with 5-FU (10, 50 and 100mg/L) for 48 h, 72 h and 96 h, respectively. The cells not treated with the drug served as control cells.

### Preparation of specimens for light and electron microscopy

The tumor cells of experimental and control groups were collected, made into smears and fixed. Some smears were HE stained and observed for morphological features under light microscope. some smears were stained by the immunocytochemical method in order to examine the expression of ICE protein. The cells were fixed in 25 g/L-glutaraldehyde for 1h at room temperature, and postfixed for 1 h in 10g/L osmium tetroxide, and dehydrated through gradient ethanol, stained and observed under electron microscopy (EM) (Hitachi 600A model).

### Immunocytochemical staining

Rabbit anti-human ICE (p20) monoclonal antibody

<sup>1</sup>Department of Pathology, Changzhi Medical College, Changzhi 046000, Shanxi Province, China

<sup>2</sup>Department of Pathology, Henan Medical University, Henan Key Laboratory for Tumor Pathology, Zhengzhou 450052, Henan Province, China

Correspondence to: DENG Li-Ying, Department of Pathology, Changzhi Medical College, Changzhi 046000, Shanxi Province, China

Received 1998-09-23

(Santa Cruze) was used at 1:100. The immunocytochemical staining was performed using the LSAB (Dako) method. The enzyme was developed with DAB in conjunction with hydrogen peroxide. A negative control for non-specific Ig binding was employed in which the first antibody was substituted with PBS. Results were judged from the number of positive cells, i.e., (-) was positive cells <25%; (+): positive cells 25% - 50%; (++): positive cells 51%-70%; and (+++): positive cells >70%.

## RESULTS

### *Morphological changes*

Most of the floating cells were presented with nuclear fragmentation, nuclear disappearance, budding and the formation of apoptotic bodies. Many cells detached with trypsin-EDTA from the plates showed that chromatin was gathered under the nuclear membrane in mass or ring-shape with the disappearance of nucleoli. Under EM, these changes were observed more apparently. In addition, some of the tumor cells displayed budding with several circular or semicircular protrusive vesicles, some of which were detached from the main body (Figure 1). Apoptotic cells were not easily observed in the group of low concentration (10 mg/L), and they increased with higher concentration (>50 mg/L) and longer action time (>48 h).

### *ICE protein expression*

ICE protein was expressed negatively in control tumor cells, but positively in the tumor cells treated with 5-FU. The number of positive cells increased with the 5-FU exposure-time (Table 1).

**Table 1** ICE expression in Eca-109 cells treated with 5-FU

Doses (mg/L)	Degrees of ICE expression		
	48 h	72 h	96 h
0	-	-	-
50	+	++	+++
100	++	++	•+++

Although individual control cells were sometimes stained brown, they were small in number and positive granules existed only near the cellular membrane. Brown granules in the cells treated with 5-FU were distributed all over the cytoplasm and cellular membrane. Most of apoptotic cells expressed ICE protein, however, a few cells with obvious features of apoptosis did not express ICE. In addition, some cells without features of apoptosis expressed ICE protein (Figure 2).

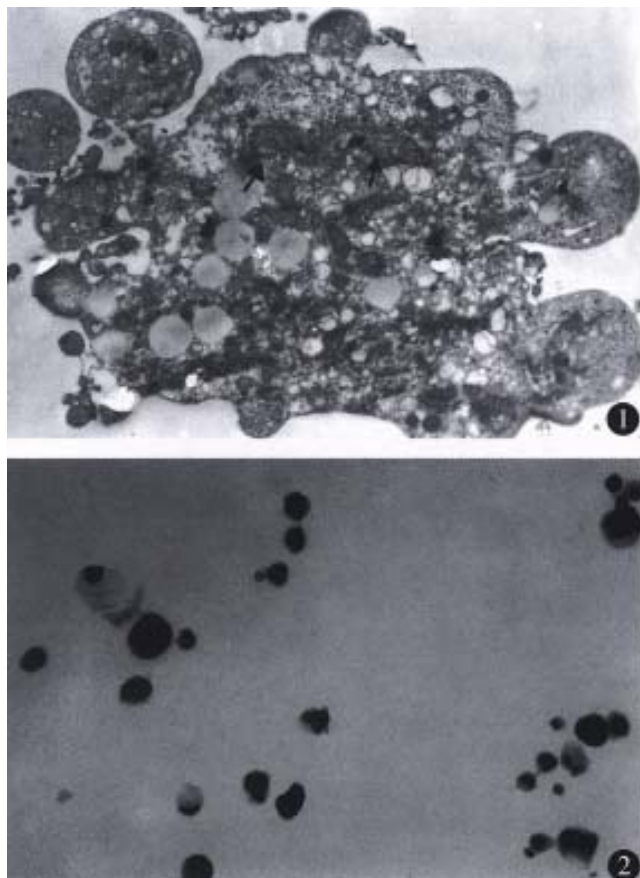


**Figure 1** An apoptotic cell with feature of budding. Nuclear fragments were shown by arrows.  $\times 6000$

**Figure 2** ICE protein expression in esophageal carcinoma cells after exposure to 5-FU. LSAB  $\times 400$

## DISCUSSION

5-FU may induce apoptosis in human esophageal carcinoma Eca-109 cells. 5-FU is one of the commonly used antitumor drugs. One of the principal mechanisms of action of 5-FU is inhibition of the enzyme thymidylate synthase (TS) and affecting DNA synthase. In recent years, it has been shown that 5-FU may induce apoptosis in fibroblast and acute leukaemic T-lymphocytes<sup>[4,5]</sup>. The present study indicated that 5-FU may induce apoptosis in human esophageal carcinoma Eca-109 cells. Chromatin gathering under nuclear, the disappearance of nucleoli and the formation of ring-shaped nucleus may be the early changes of apoptosis. Apoptotic cells became visible late at 24h and apparent by 48h. It may be related to the characteristic action of time-dependence.

ICE may mediate apoptosis induced by 5-FU. Ced-3 is known as one of the essential genes for cells to undergo apoptosis in *C. elegans*. ICE gene, a homologue of the ced-3, was recently identified as inducer of apoptosis in Rat-1 fibroblasts<sup>[3]</sup>. Kondo *et*

al reported that cisplatin increased the mRNA expression of ICE and induced apoptosis in malignant glioma cells<sup>[6]</sup>. In our study 5-FU increased the expression of ICE protein in Eca-109 cells undergoing apoptosis, suggesting that ICE protein may play a role in apoptosis induced by 5-FU. The expression of ICE protein was also detectable in some cells without features of apoptosis. From the phenomenon that the expression of ICE protein appeared at the early stage of apoptosis even before development of apoptosis, we inferred that ICE protein may be involved in the development of apoptosis. The induction of ICE does not necessarily trigger cell death, but the manifestation of cells which were seriously injured. If the injury can not be repaired, ICE may activate its downstream target molecules such as apopain, one member of the ICE family, and in the end, target proteins necessary for the existence of cells are cleaved and apoptosis becomes irreversible. The reason why negative expression of ICE protein was observed in some cells with typical features of apoptosis is not clear. The antibody used in this study was specific to ICEp20 subunit. There is no cross-reaction between ICEp20 and

ICEp10 subunits. Other member(s) of ICE family may be also involved in apoptosis. It is known that at least six members of the ICE family are expressed in mammalian cells. However, whether ICE acts directly or through its action product interleukin-1 $\beta$  is not fully understood. The recent studies found that ICE may directly cleave actin which makes up cytoskeleton and that alteration in actin was implicated in the formation of plasma membrane budding and disintegration of cells<sup>[7]</sup>.

## REFERENCES

- 1 Barry MA, Behnke CA, Eastman A. Activation of programmed cell death (apoptosis) by cisplatin, other anticancer drugs, toxins and hyperthermia. *Biochem Pharmacol*, 1990;40:2353
- 2 Yuan J, Shaham S, Ledoux S. The *C. elegans* cell death gene *ced-3* encodes a protein similar to mammalian interleukin-1 $\beta$ -converting enzyme. *Cell*, 1993;75:641
- 3 Miura M, Zhu H, Rotello R. Induction of apoptosis in fibroblasts by IL-1 $\beta$ -converting enzyme, a mammalian homolog of the *C. elegans* cell death gene *ced-3*. *Cell*, 1993;75:653
- 4 Lowe SW, Rulley HE, Jacks T. p53 dependent apoptosis modulates the cytotoxicity of anticancer agents. *Cell*, 1993;74:957
- 5 Huschtscha LI, Bartier WA, Anderson CE. Characteristics of cancer cell death after exposure to cytotoxic drugs *in vitro*. *Br J Cancer*, 1996;73:54
- 6 Kondo S, Barna BP, Morimura T. Interleukin-1 $\beta$ -converting enzyme mediates cisplatin induced apoptosis in malignant glioma cells. *Cancer Res*, 1995;55:6166
- 7 Kayalar CT, Ord T, Pia Testa M. Cleavage of actin by interleukin-1 $\beta$ -converting enzyme to reverse DNase I inhibition. *Proc Natl Acad Sci USA*, 1996;93:2234

Edited by MA Jing-Yun

# Congenital expression of *mdr-1* gene in tissues of carcinoma and its relation with pathomorphology and prognosis

ZHANG Li-Jian<sup>1</sup>, CHEN Ke-Neng<sup>1</sup>, XU Guang-Wei<sup>1</sup>, XING Hai-Ping<sup>2</sup> and SHI Xiao Tian<sup>2</sup>

**Subject headings** neoplasm; multidrug resistance; gene expression/ *mdr-1* gene; surgery; esophageal neoplasms

## Abstract

**AIM** To detect the congenital expression patterns of *mdr-1* gene in commonly encountered malignant tumors in clinic, and the relationship between the expression of *mdr-1* gene and the prognostic morphology in esophageal carcinomas.

**METHODS** A total of 151 resected samples of malignant tumors without preoperative treatment were taken from Anyang City Tumor Hospital. The congenital expression of their *mdr-1* gene was detected with reverse transcriptase on polymerase chain reaction (RT-PCR) and was compared with each other. The positive incidence of *mdr-1* gene in 46 samples of esophageal carcinoma was compared with their differentiated grades, TNM stages and macroscopic types, and the precautions and advantages of RT-PCR were evaluated.

**RESULTS** All the 151 samples were confirmed to be malignant histopathologically, including cancers of stomach and gastric cardia ( $n = 51$ ), esophagus ( $n = 46$ ), colorectum ( $n = 16$ ), breast ( $n = 15$ ), thyroid ( $n = 10$ ), lung ( $n = 9$ ) and uterine cervix ( $n = 24$ ). The positive expression rate of their *mdr-1* gene was 33.3%, 37%, 31.3%, 13.2%, 40%, 55%, and 0% respectively. All the 46 samples of esophageal carcinoma were pathologically confirmed to be squamous cell carcinoma. The total expression rate of their *mdr-1* gene was 37% (17/46), 35% (6/17), 40% (8/

20), and 33% (3/9) for differentiation grade I, II and III respectively. The expression rate of TNM classification was 33% (6/18), 40% (5/12) and 37% (6/16) in stage IIa, IIb and III. The expression rate was 33% (3/9) in ulcerous type, 37% (3/8) in constrictive types, 33% (5/15) in fungoid types, and 40% (6/14) in medullary types. No statistically significant difference was found.

**CONCLUSION** Compared with other methods, RT-PCR is more simple, reliable and accurate in detecting *mdr-1* gene expression in tissues of tumor. The overexpression of *mdr-1* gene in these neoplasms suggested that cases should be handled differently for chemotherapy with rational use of drugs. Excision is the chief treatment for carcinoma of esophagus. The expression of *mdr-1* gene in tissues of esophageal cancer is correlated with the parameters of tumor molecular biology which are independent of histopathological morphology.

## INTRODUCTION

Multidrug resistance (MDR) of malignant tumor cell has aroused widespread interest. It has been shown that MDR is present in many malignant tumors. One of its molecular bases is *mdr-1* gene amplification and its expression product. Failure of chemotherapy was chiefly due to drug resistance of tumor cells<sup>[1-9]</sup>. It is very important to detect MDR in choosing reasonable treatment, especially in using effective chemotherapeutic drugs for a specific patient. Others<sup>[10]</sup> believe that *mdr-1* gene expression in cancer tissue is a malignant biological indicator for neoplasms. Few research reports have been found in the literature on *mdr-1* gene expression in tissues of esophageal carcinoma, and on its relation with the morphological parameters of esophageal carcinoma. For these reasons, a primary study was made.

## MATERIALS AND METHODS

### *Specimens and clinical data*

One hundred and fifty-one specimens were taken

<sup>1</sup>Department of Thoracic Surgery, the School of Oncology, Beijing Medical University, Beijing 100036, China

<sup>2</sup>Anyang Cancer Hospital, Anyang 455000, Henan Province, China  
Dr. CHEN Ke-Neng, male, born on 1963-04-30 in Lanzhou City, Gansu Province, graduated from Hubei Medical University, now associate professor and Ph. D., engaged in thoracic surgery, especially esophageal cancer, having 60 papers published.

\*Supported by a grant from Science and Technology Committee of Henan Province, No.971200101.

Correspondence to: CHEN Ke-Neng, Thoracic Department, the School of Oncology, Beijing Medical University, No.52 Fucheng Road, Beijing 100036, China

Received 1998-11-09

from the Surgical Department of Anyang City Tumor Hospital, Henan Province soon after they were excised. Of the 151 cases, 78 were male and 73 female. They were aged from 21 to 80 years, averaging 52.1. All the cases were confirmed to be malignant tumors without preoperative treatment. Of them, 51 were cancers of stomach and gastric cardia, 46 cancers of esophagus, 16 cancers of colorectum, 15 cancers of breast, 10 cancers of thyroid, 9 cancers of lung and 4 cancers of uterine cervix. The 46 patients of esophageal carcinoma were all permanent residents of Anyang citizenship, 26 male and 20 female. The site of cancer was found in the upper, middle and lower thoracic segment in 8, 30, and 8 cases respectively according to 1987 UICC criteria. Eighteen cases were in stage IIa, 12 in stage IIb, and 16 in stage III according to TNM classification. All the cases were squamous cell carcinomas. Of them, 17 were in grade I, 20 in grade II, and 9 in grade III according to SUN Shao-Qian's grading system for squamous cell carcinoma. Nine were found to be ulcerous type, 6 constrictive type, 15 fungoid type, and 16 medullary type according to WU Ying-Kai's gross pathological typing method.

#### Main instrument and reagents

Reverse Transcription Polymerase Chain Reaction (RT-PCR) Reagent Kit was supplied by Beijing Jinghai Biological Engineering Company. Bio-RAD Gene Cycler™ (Gene Amplifier) was made in Japan. LG15-w high-speed centrifuge was made by Beijing Medical Centrifuge Factory. SA-U94.11 ultraviolet transilluminator was made by Shanghai Zhongya Biological Institute.

#### The sequences of *mdr-1* gene primers

5'ACCCATCATTGCAATAGCAG3'  
5'TGTTCAAACCTTCTGCTCCTG3'

#### The sequences of inner control $\beta_2$ -microglobulin gene primers

5'ATGGCTCGCTCGGTGACCCTAC3'  
5'TCATGATGCTTGATCACATGTCTCG3'

#### METHODS

##### Methods for determining *mdr-1* gene expression

Methods for determining *mdr-1* gene expression<sup>[1]</sup> was used with minor modifications. Major steps were extraction of total tumor RNA by guanidine isothiocyanate, synthesis and amplification of complementary DNA (cDNA) to *mdr-1* gene by RT-PCR. The products were separated by electrophoresis on agarose gel containing EB. DNA bands were made visible by transillumination with ultraviolet.

##### Assessment criteria

Only one 300bp band was found in the negative re-

sults. Inner control band and *mdr-1* gene 170 bp band were found in the positive results. Gene expression was calculated on a concentration scanner by the relative yield of the *mdr-1* gene to the  $\beta_2$  inner control gene. Its formula is expressed as:

$$\text{Mdr-1 expression ratio} = \frac{\text{mdr-1 band absorption}}{\text{Inner control band absorption}}$$

The ratio < 0.1 means negative expression, > 0.4 high expression, 0.1 - 0.4 moderate expression. The observed parameters included *mdr-1* gene expression positively in macro- and micro-scopic morphology of the specimens, and comparison *mdr-1* expression in various groups.

#### Statistical analysis

Chi-square test was used, and *P* value less than 0.05 stands for statistical significance.

#### RESULTS

The expression of *mdr-1* gene in the studied samples was over 30%, except that in cancer of uterine cervix and breast (Table 1).

The total expression rate of *mdr-1* gene was 37% (17/46) in the 46 cases of esophageal carcinoma with no relation to the morphological parameters of the tumor. It was an independent molecular biological characteristic of the tumor (Tables 2-4).

**Table 1** *mdr-1* gene expression in 151 specimens (%)

Site of tumors	<i>n</i>	H	M	L/N	H&M
Esophagus	46	10.9	26.1	63.0	37.0
Gastric cardia	35	17.1	11.9	71.0	29.0
Stomach	16	25.0	12.5	72.5	27.5
Colorectum	16	18.8	12.5	68.7	31.3
Lung	9	22.0	33.0	45.0	55.0
Breast	15	6.6	6.6	86.8	13.2
Thyroid	10	20.0	20.0	60.0	40.0
Uterine cervix	4	0.0	0.0	100.0	0.0
Total	151	15.2	18.6	66.2	33.8

H: high expression, M: middle expression, L(N): lower/no expression

**Table 2** *mdr-1* gene expression in TNM stages of esophageal carcinoma

TNM stage	<i>n</i>	No. of positive cases	Positive rate (%)
IIa	18	6	33
IIb	12	5	40
III	16	6	37

*P*>0.05, among the three stages.

**Table 3** *mdr-1* gene expression in SUN Shao-Qian's grading system of squamous cell carcinoma of esophagus (*n* = 17)

Grade	No. of positive cases	Positive rate (%)
II	6	35
II	8	40
III	3	33

*P*>0.05, among the three grades.

**Table 4** *mdr-1* gene expression in WU Ying-Kai's macroscopical typing system of esophageal carcinoma

Types	<i>n</i>	No. of positive cases	Positive rate (%)
Ulcerative	9	3	33
Constrictive	8	3	37
Fungoid	15	5	33
Medullary	14	6	40

$P > 0.05$ , among the four types.

## DISCUSSION

It is believed that *mdr-1* gene is one of the normal sequences of human genome. Nevertheless, its expression and expressive level are decided by different cell type and environmental factors. The *mdr-1* gene expression can be investigated with several molecular methods including evaluation of protein expression and mRNA. Protein may be detected by Western blot analysis and immunohistochemical techniques. Immunohistochemical staining is commonly used, but it is not suitable for quantitative determination of protein due to its complicacy and influence of experimental conditions. Since all organisms store their genetic information in nucleic acid, methods of direct detection of *mdr-1* at mRNA level have advantages of high efficiency, sensitivity, and specificity. Traditional methods for mRNA such as  $S_1$  nuclease test, RNA slot blots, RNA protection assays, *in situ* hybridization and Northern blot analysis are greatly limited due to their overlaborate procedure and poor sensitivity. RT-PCR was used in present study. After cDNA of *mdr-1* gene was synthesized according to the transcribed mRNA of *mdr-1*, it was detected by PCR *in vitro*. Compared with other gene measurements, RT-PCR is one of the most sensitive, specific, reproducible, effective, simple, and time-saving methods<sup>[2]</sup>. We believe that the prospects of its application in clinic are quite broad.

One of the mechanisms of drug resistance to cancer cells is called MDR which is known as the resistance to lipophilic drugs such as daunorubicin, adriamycin, vincristin, and colchicin. It is very unfavourable to chemotherapy, because once tumor cells develop resistance to one of the these drugs, they will develop resistance to all lipophilic drugs<sup>[5-7]</sup>. How to evaluate multidrug-resistant tumor cells is a problem demanding prompt solution. Recently, there were several papers on the mechanism, evaluation and reversion of MDR<sup>[5-8]</sup>. Most of them focused on *mdr-1* and its products, p-170<sup>[2-6]</sup>. p-170 (P-gp) was considered as an ATP-dependent drug molecular pump, which would lead to failure of chemotherapy as a result of drugs being pumped out from cells. This fact has been proved in

many researches of diseases such as leukocytopenia, breast cancer and melanoma. These researches were of no significance in clinical practice because they were usually focused on a certain kind of tumors and their results were obtained from malignant cell line with different methods. In the present study, the expression of *mdr-1* gene in commonly encountered malignant tumors was synchronically studied by the same technicians with same instruments, experimental methods and reagents. The results showed that all the detected neoplasms except cervical carcinoma, expressed *mdr-1* gene in different degrees (Table 1). Breast cancer also had a low expression of *mdr-1*. The positive number of *mdr-1* gene in the other tumor tissues was more than 1/3 except that in breast and cervical cancers. This kind of expression was congenital because these tumors had not received chemotherapy when they were detected. It indicated tumor carried *mdr-1* gene and its product-Pgp from the development of tumor. Clinicians should pay great attention to the mechanisms of its drug resistance if they are tenable. They should differentiate the subgroups of malignant tumors from molecular level in addition to taking other clinical indexes such as tissue differentiation, TNM staging system, and tissue type into consideration, in order to avoid unsuitable chemotherapy and use of MDR-drugs especially lipophilic. Combined treatment with reverser of *mdr-1* gene and supressor of P-gp should be used to improve curative effect if it has been proved to be effective. Some researchers held that MDR of tumors could not be completely explained by *mdr-1* gene and its P-gp system<sup>[10]</sup>, and further research should be made. In our phase II study, a control study will be made on the difference of *mdr-1* gene expression in cancer and normal tissues as well as in those before and after chemotherapy. We believe that the theory of MDR will be an important reference index for chemotherapy of tumors as a result of our better understanding of it.

Surgical treatment is the commonly used treatment for esophageal carcinoma. Its curative effect is chiefly decided by TNM stages, histological differentiation and types. Generally speaking, it is better for the early and well differentiated squamous cell carcinoma than the late and poorly differentiated adenocarcinoma or the undifferentiated one. However, exceptions in clinic suggest that further research at the molecular level of gene is needed in esophageal carcinoma which has its unique biological characteristics independent of its morphological parameters as other malignant tumors.

Since the finding of *mdr-1* gene and its product P-gp (P-glycoprotein, p170), they have been ap-

plied to researches on their relations to cytotoxic chemotherapeutic drugs, especially to the lipophilic drugs. Many of these researches were in the field of hematic malignancies, and new ways were explored to reverse MDR. However, attention was seldom paid to the congenital expression of *mdr-1* gene in tissues of esophageal carcinoma and its relation with morphological parameters. It was found in this study that the congenital expression of *mdr-1* gene was 37% in tissues of the 46 cases of esophageal carcinoma without chemotherapy before operation. It was much higher than that reported in leukemia<sup>[4,9-13]</sup>, melanoma<sup>[6]</sup>, and breast cancer<sup>[1,3,5,7]</sup>. This is one of the possible reasons why no progress has been achieved in the curative effect of chemotherapy for esophageal carcinoma in the past years. It indicates that only by attaching importance to the selection of chemotherapeutic drugs and suitable chemotherapy for esophageal carcinoma, can its curative effect be achieved. It also suggests that surgical treatment for it at present should be stressed. Many researches have demonstrated that cancer is a genetic disease. Besides traditional morphological indexes, the following factors were found to be related with the prognosis of esophageal carcinoma such as antioncogene, oncogene and their abnormal products as well as others at the level of gene molecules, and have been taken into account in clinic. Overexpression of *mdr-1* gene was believed to be an index of drug resistance and further malignization of the histological behavior of cancer cells<sup>[10]</sup>. The theory of drug resistance of tumors was advanced by Goldie and Codman<sup>[8]</sup> in 1979 in the light of gene change. It held that drug resistance was resulted from gene mutation of tumor cells produced in frequency of the tumor, and that the larger the tumor, the more the frequency of proliferation and the stronger the drug resistance. This theory also indicates that drug resistance of tumors has a positive correlation with the stage of tumors. No significant difference was found in the expression of *mdr-1* gene in tissues of esophageal carcinoma on the basis of its morphology, differentiation and TNM. It was suggested that expression of *mdr-1* gene is a

molecular parameter independent of surgical pathomorphological indexes. This results show that surgical treatment is the first choice for esophageal carcinoma at present due to its drug resistance.

It was held that expression of *mdr-1* gene was a protective mechanism of cells, which was found in some normal tissue cells in addition to cancer cells<sup>[10]</sup>. The results in our study seemed to support it. Long follow-up study is needed to decide whether overexpression of *mdr-1* gene in esophageal carcinoma is an index of its further malignization, because no comparison was made for its difference in cancer and normal tissues as well as before and after its chemotherapy.

Although surgical treatment of esophageal carcinoma is destructive and will exert some influence on the quality of life of the patients, it remains the first choice before a breakthrough is made in chemotherapy. In order to improve the curative effect of chemotherapy, the reverse mechanism of MDR should be further studied while the drug-resistant mechanism is comprehensively researched.

## REFERENCES

- 1 Charpin C, Vietho P, Duffaud F. Quantitative immunocytochemical assays of P-glycoprotein in breast carcinoma: correlation to messenger RNA expression and to immunohistochemical prognostic indicators. *J Natl Cancer Inst*, 1994;86:1539
- 2 Chen KN, Xing HP, Cheng BC. Expression of *mdr-1* gene in cancer tissue and its association with morphological indexes of esophageal carcinoma in Anyang. *Natl Med J China*, 1998;78:462
- 3 Goldstein LJ. MDR-1 gene expression in solid tumors. *Eur J Cancer*, 1996;32A:1039
- 4 Bertolini F, de Monte L, Corsini C. Retrovirus mediated transfer of the multidrug resistance gene into human haemopoietic progenitor cell. *Br J Haematol*, 1994;8:318
- 5 Benchekroun MN, Schneider E, Safa AR. Mechanisms of resistance to ansamycin antibiotics in human breast cancer cell line. *Mol Pharmacol*, 1994;46:677
- 6 Berger W, Elbling L, Minai-Pour M. Intrinsic MDR-1 gene and P-glycoprotein expression in human melanoma cell lines. *Int J Cancer*, 1994;59:717
- 7 Veneroni S, Zaffaroni Z, Daidone MG. Expression of P-glycoprotein and *in vitro* or *in vivo* resistance to doxorubicin and cisplatin in breast and ovarian cancers. *Eur J Cancer*, 1994;30A:1002
- 8 Gottesman MM. How cancer cells evade chemotherapy. *Cancer Res*, 1993;53:747
- 9 Rowinsky EK, Adjei A, Donehower RC. Phase I and pharmacodynamic study of the topoisomerase I inhibitor topotecan in patients with refractory acute leukemia. *J Clin Oncol*, 1994;12:2193
- 10 Beck J, Niethammer D, Cekeler V. High *mdr-1* and *mrp*, but low topoisomerase II alpha-gene expression in B cell chronic lymphocytic leukemias. *Cancer Lett*, 1994;86:135
- 11 Yamashita T, Watannabe M, Onodera M. Multidrug resistance gene and P-glycoprotein expression in anaplastic carcinoma of the thyroid. *Cancer Detect Prev*, 1994;18:407
- 12 Hart SM, Ganeshaguru K, Hoffbrand AV. Expression of the multidrug resistance associated protein (MRP) in acute leukemia. *Leukemia*, 1994;8:2163
- 13 Schneider E, Cowan KH, Bader H. Increased expression of the multidrug resistance-associated protein in relapsed acute leukemia. *Blood*, 1995;85:186

# Preparation and distribution of 5-fluorouracil <sup>125</sup>I sodium alginate-bovine serum albumin nanoparticles

YI Yi-Mu<sup>1</sup>, YANG Tang-Yu<sup>2</sup> and PAN Wei-Min<sup>3</sup>

**Subject headings** 5-fluorouracil (5-FU); sodium alginate-albumin; preparation of nanoparticle (NP); distribution

## Abstract

**AIM** To prepare 5-FU sodium alginate <sup>125</sup>I bovine serum albumin nanoparticles (BSA NP), to determine the radioactive count in different organs of rats at different time points after oral administration of 5-FU <sup>125</sup>I sodium alginate-BSA NP and to calculate the kinetic parameters of its metabolism.

**METHODS** Emulsion solidification method was used to prepare 5-FU <sup>125</sup>I sodium alginate-BSA NP, and to determine its diameter under transmission electronic microscope (TEM). Then the rate of NP and external drug releasing velocity were measured. Radioactive counting in different organs of rats was made after oral administration of the NP by GAMA Counter, and the kinetic parameters of drug metabolism were calculated by handling the data with the two-department model.

**RESULTS** The average arithmetic diameter of the NP was 166nm±34nm, the rate of 5-FU was 32.8% and the cumulative external releasing ratio amounted to 84.0% within 72 hours. The NP was mainly distributed in the liver, spleen, lungs and kidneys after NP oral administration to rats. The micro-radioautographic experiment showed that NP was distributed in the Kupfers cells of liver, liver parenchymal cells and the

phagocytes of spleen and lungs. The kinetic parameters of metabolism were:  $T_{1/2} = 9.42\text{h}$ ,  $C_{\max} = 2.45 \times 10^7 \text{Bq}$ ,  $T_{\max} = 2.18\text{h}$ ,  $\text{AUC} = 148 \times 10^9 \text{Bq}$ . **CONCLUSION** NP is difficult to pass through the blood-cerebral barrier, and <sup>125</sup>I sodium alginate-BSA NP enters the body circulation by gastrointestinal passage.

## INTRODUCTION

Nanoparticle (NP) is a colloidal dispersion system, with diameters ranging from 10nm to 1000nm. The particles exist mainly in the organs rich in phagocytes after absorption, such as liver, spleen and lymph system. Since its introduction in the 1980s, scientists have done a lot of researches on its preparation, stability and targeting<sup>[1,2]</sup>. Now most materials used to prepare NP are synthetic substances, e.g. cyanoacrylate, methylacrylate and polylactic acid. However, we selected natural substances-sodium alginate and bovine serum albumin as carriers, and 5-fluorouracil (5-FU) as model drug to prepare NP by emulsion solidification, and studied its distribution after oral administration.

## MATERIALS AND METHODS

### Animal

The Kunming rats weighing 20 g±2 g, were provided by the Experimental Animal Centre of Tongji Medical University.

### Reagent

Sodium alginate (chemical reagent), bovine serum albumin (Sigma), pentane dialdehyde (biochemical reagent, Merck), Na <sup>125</sup> I (specific activity 7.78 TBq/L, Chinese Atomic Energy Institution), IV liquid nuclear emulsion (Physics Institute of Chinese Atomic Energy Research Institution).

### Preparation of <sup>125</sup>I bovine serum albumin (BSA)

The BAS (10mg) was dissolved in 10mL distilled water and marked with I<sup>125</sup> according to the chloramine-T method. After the reaction was completed, the mixture was separated by column chromatography (10 mm×340 mm), using Sephadex G-50 as column material and Na<sub>2</sub>S<sub>2</sub>O<sub>3</sub> as eluant. Then the

<sup>1</sup>Pharmaceutics Department of School of Pharmacy, Tongji Medical University, Wuhan 430030, China

<sup>2</sup>Materia Medica Department of School of Pharmacy, Tongji Medical University, Wuhan 430030, China

<sup>3</sup>Nuclear Medicine Department of Medical Experimental Research Center, Tongji Medical University, Wuhan 430030, China

YI Yi-Mu, born on January 15, 1954 in Huanggang County, Hubei Province, graduated from School of Pharmacy of Tongji Medical University in 1975, now working in the Pharmaceutics Department of the same university, mainly engaged in researches in new dosage forms of drugs and new drug-products, having 3 papers published and ten papers presented at international and national academic conferences.

\*The project supported by the National Natural Science Foundation of China, No.39270809

Correspondence to: YI Yi-Mu, Pharmaceutics Department of School of Pharmacy, Tongji Medical University, Wuhan 430030, China

Received 1998-11-091

radio-chemical purity of eluate was determined by dichloroacetic acid method.

#### **Preparation of <sup>125</sup>I sodium alginate-BAS NP**

According to the literature, 1 mL-above I<sup>125</sup>-BAS (1g/L, SpA 107 Bq) was added into sodium alginate solution to prepare sodium alginate- BSA NP.

#### **Determination of the diameter of nanoparticles**

The NP size in the suspension was detected on TEM.

#### **Determination of the encapsulation efficiency**

The standard curve of 5-FU was drawn first. One hundred and five mg of 5-FU was weighed precisely, dissolved in thin HCL solution (9-1000) and adjusted to given volume. This solution was diluted to its half concentration. After 3.0, 6.0, 9.0, 12.0 and 15.0 mL-diluted solution were taken into 100mL-volumetric flasks and adjusted to given volume respectively, their absorbance (A) values were detected on ultraviolet-visible spectrophotometer at 265 nm. The following regression equation was obtained:  $C = 16.72A \pm 0.0416$  ( $r = 0.9998$ ).

A total of 1.0 mL 5-FU NP suspension was added accurately to a test tube with 9 mL 6mol/HCl. The mixture was hydrolyzed for 20h at 100°C water bath. The hydrolyzate was adjusted to given volume with distilled water to detect its A value as standard curve item, the hydrolyzate of bland NP suspension served as control. The result showed that the control group had no obvious absorption at 265nm (A=0.01). By putting the A value into the regression equation we worked out the concentration of 5-FU in the hydrolyzate and got the encapsulation efficiency consequently.

#### **Determination of recovery rate**

The same quantities of albumin, sodium alginate and pentane dialdehyde as "Preparation of NP" items were mixed with 5-FU weighed precisely, the mixture was dissolved in distilled water. Its A value was detected according to the standard curve and the content of 5-FU was calculated.

#### **Determination of drug release**

Appropriate quantity of 5-FU NP suspension was taken precisely, washed for three times with distilled water, and suspended in 200mL-thin HCL solution (9-1000). The drug release state of the suspension was measured at 37°C by paddle method (100r/min). The samples were taken at the beginning, the 2nd, 4th, 8th, 12th, 24th, 48th and 72nd hour, and filtered through 0.2µm microporous membrane. The filter liquor was detected at 265nm

to get its A value and cumulative rate of drug release.

#### **The distribution of <sup>125</sup>I sodium alginate-BSA in rats**

Fourty-five Kunming rats were divided into 15 groups (3 rats per group). After starvation for 16h, the rats were given the 5-FU NP orally 148× 10<sup>8</sup>Bq per rat. Right after its blood was taken from the eye at different time points (heparin was added to prevent coagulation), the rats were sacrificed by breaking its spine. The relevant tissues and organs were taken. When the water had been absorbed with filter paper after washing, they were weighed. The amounts of the NP in unit weight in different tissues were measured by GAMA Counter. In accordance with the counting result, we calculated the tissue blood ratio at different time points and used two-department model to process the data in order to get pertinent kinetic parameters.

#### **Radioautography**

While carrying out the histological experiment, we chose the tissues of liver, spleen, lungs, and kidneys at some time points (the 4th, 8th and 12th hour), and frozen sections and paraffin wax sections about 6µm-thick were made. IV liquid emulsion was used for microradioautography.

## **RESULTS**

#### **Diameter of NP**

On the 5-time enlarged photograph (diagram 1) of TEM, the average arithmetic mean diameter of 300 detected NPs was 166 nm±33 nm, 8% < 130 nm, 36% 130 nm - 150 nm, 42% 150 nm - 170 nm and 14% >180nm.

#### **Encapsulation efficiency**

After two batches of 5-FU NPs were hydrolyzed in acid medium, their encapsulation efficiency was calculated (Table 1).

**Table 1 Encapsulation efficiency of 5-FU in NP**

Weight of drug added (g)	A value	Weight of drug encapsulated (g)	Encapsulation efficiency (%)
0.6162	0.679	0.208	33.8
0.6113	0.625	0.193	31.6
0.5917	0.676	0.195	32.9

#### **Rate of recovery**

The rate of recovery of three batches of samples is shown in Table 2.

**Table 2 Rate of recovery of 5-FU**

Weight of 5-FU added (g)	Weight of 5-FU determined (g)	Rate of recovery (%)
0.1348	0.1326	98.4
0.1463	0.1449	99.1
0.1429	0.1395	97.6

**Varitation of drug releasing ratio of 5-FU NP before and after storage**

The cumulative ratio of drug release within 72 h decreased from 84.8% before storage to 80.6% after storage under 40°C±1°C for three months.

**The pharmacokinetics of <sup>125</sup>I sodium alginate-BAS NP in rats**

Thirty min after the rats administrated <sup>125</sup>I sodium alginate-BSA NP orally, obvious radioactivity was shown in its blood. Eight hours after the adminis-

tration, the radioactivity of their liver, spleen and lungs was 2.08 times, 2.32 times and 1.60 times, as much as that of blood, while 24 hours after the administration, they decreased to 1.18, 1.22 and 0.87 times respectively (Table 3).

The data in the parentheses show the ratio of radioactivity of the relative organ to that of blood. The data in Table 3 were put into computer, and processed according to the two-department model to calculate the relevant pharmacokinetical parameters. The results are shown in Table 4.

**Radioautography**

The microradioautographical experiment indicated that the <sup>125</sup>I sodium alginate-BSA NP were mainly distributed in the Kupffer cells of liver and liver parenchymal cells (Figure 2) after oral administration to rats. And there were Ag particles in the phagocytes of spleen (Figure 3) and also in the pulmonary cells (Figure 4).

**Table 3 Distribution of <sup>125</sup>I sodium alginate-BSA NP in rats (n = 3, dosage 148×10<sup>8</sup>Bq per rat, po.)**

Organ	Value of radioactive counting of 100mg tissue in 30s at different time points					
	1h	4h	8h	16h	24h	36h
Blood	502±100	601±135	373±22	298±19	191±17	129±23
Heart	436±110(0.86)	801±66(0.33)	265±23(0.71)	230±23(0.77)	190±10(0.99)	87±35(0.67)
Liver	436±110(0.86)	908±100(1.51)	777±69(2.08)	405±97(1.36)	226±16(1.18)	153±21(1.19)
Spleen	663±140(1.32)	1029±168(1.71)	834±272(2.32)	436±195(1.46)	233±25(1.22)	169±27(0.95)
Lungs	717±314(1.42)	818±172(1.36)	597±121(1.60)	443±31(1.49)	166±4(0.87)	119±27(0.92)
Kidneys	526±139(1.05)	185±39(0.14)	401±71(1.08)	387±105(1.30)	133±13(0.69)	123±14(0.95)
Brain	105±31(0.21)	112±49(0.19)	111±47(0.30)	96±27(0.32)	50±5(0.26)	39±11(0.30)
Stomach	89654±7143	28674±3647	8362±1902	4641±1400	698±34	527±114
Intestine	765±137	5573±891	30±599	403±118	115±64	204±46
Bowel	1256±664	639±1023	30±599	3221±863	125±60	256±102

**Table 4 Pharmacolinetical parameters of <sup>125</sup>I sodium alginate-BSA NP in rats**

Parameter	Unit	Value
A	Bq	3022×10 <sup>2</sup>
α	1/h	0.07
B	Bq	3.03×10 <sup>3</sup>
β	1/h	-0.11
Ka	1/h	1.46
V/F	Bq	1428×10 <sup>3</sup>
T <sub>1/2α</sub>	h	9.42
T <sub>1/2β</sub>	h	-6.07
T <sub>1/2Ka</sub>	h	0.47
K <sub>21</sub>	1/h	-0.11
K <sub>10</sub>	1/h	0.07
K <sub>12</sub>	1/h	-0.00035
AUC	Bq×h	3.9×10 <sup>9</sup>
CL(s)	Bq×h/Bq	105×10 <sup>3</sup>
T(peak)	h	2.18
Cmax	Bq	2.45×10 <sup>7</sup>

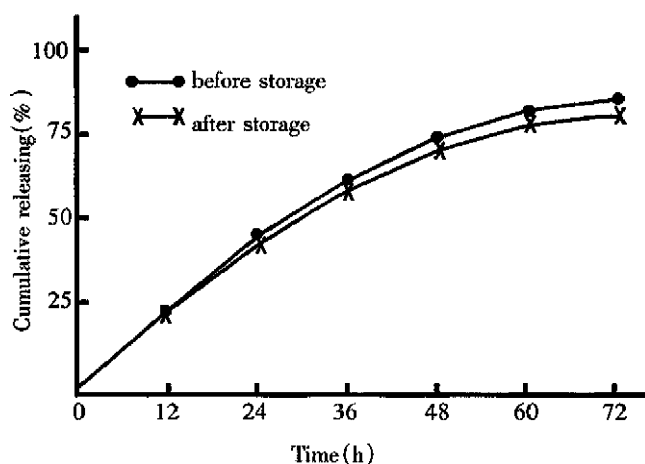


**Figure 1** Releasing of 5-FU from NP.

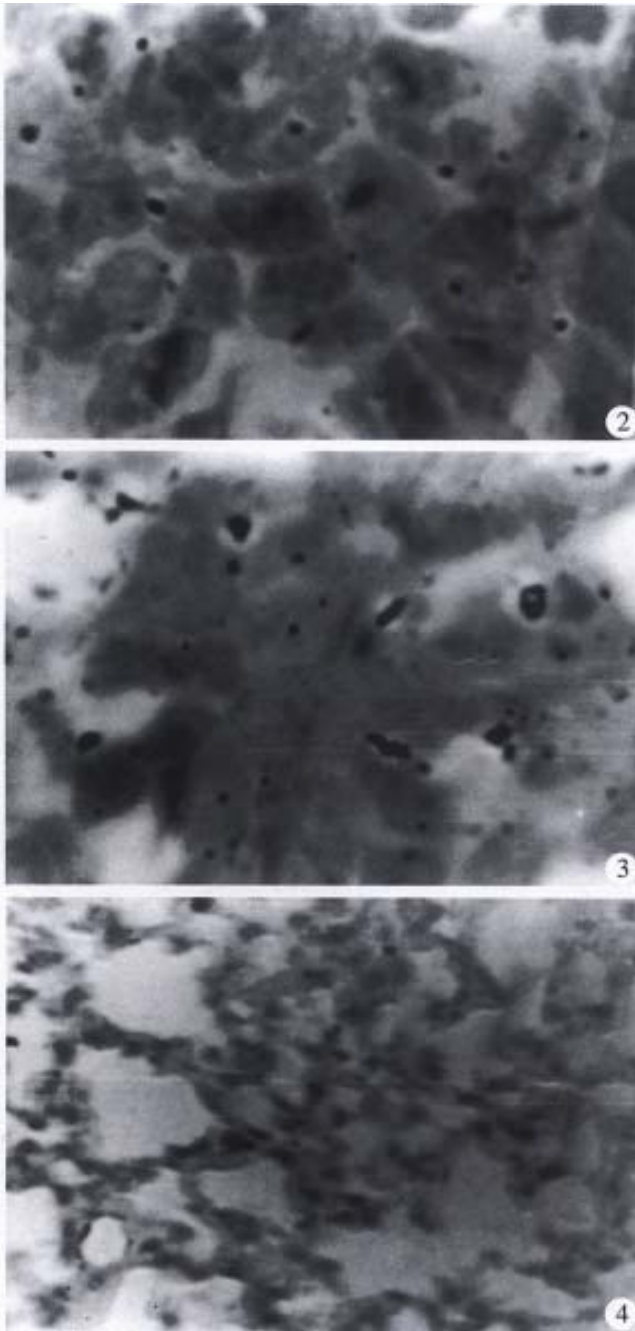


**Figure 2** NP in liver.  $\times 1000$

**Figure 3** NP in spleen.  $\times 1000$

**Figure 4** NP in lungs.  $\times 1000$

## DISCUSSION

Since the introduction of NP in the early 80s, scientists have done a lot of researches in its preparation, stability, distribution and targeting. It is suggested that the stability of NP is better than that of liposome and it can carry more drug than liposome.

At present, the materials, which are reported to prepare NP in literature abroad, are all man-made synthetic materials. While NP is mostly administered in travenously, we chose natural polysaccharide and protein to compose the carrier, and observed its distribution and metabolism after oral administration to rats.

Thirty minutes after the rats administrated  $^{125}\text{I}$  sodium alginate-BSA NP orally, the radioactive substances in their blood were detected.

The results indicate that NP is mainly distributed in the liver, spleen and lungs, quantitatively in heart and slightly in brain. This shows NP is difficult in passing through the blood-cerebral barrier. The experiments also display that the  $^{125}\text{I}$  sodium alginate-BSA NP enters the body-circulation by gastrointestinal passage and is chiefly distributed in the tissues rich in phagocytes, such as in the liver and spleen.

In the study of its distribution, we discovered that there is still a large amount of radioactivity in the gastrointestinal passage 12 hours after the administration. This illustrates that the absorption of NP is not complete because NP exists in the suspension as cloudy polymer but not mono-dispersion, and the large diameter of the polymer makes it difficult for the NP to be absorbed by the gastrointestinal passage.

## REFERENCES

- 1 Keyser JLDE, Poupaert JH, Dumont P. Poly (diethyl methylenemalonate) Nanoparticles as a potential drug carrier: preparation, distribution and elimination after intravenous and peroral administration to mice. *J Pharm Sci*, 1991;80: 67-70
- 2 Alain R, Brigitte C, Roger LV, Louis T. Blood clearance and organ distribution of intravenously administered polymethacrylic nanoparticles in mice. *J Pharm Sci*, 1989;78:481-484
- 3 Dieter Scherer, J.R. Robinso N, Jorg Kreuter. Influence of enzymes on the stability of polybutylcyanoacrylate nanoparticles. *In J Pharm*, 1994;101: 165-168
- 4 Nazin Ammoury, Hatem Fessi, Devissaguet JP, Puisieux F, Benita S. In vitro release kinetic pattern of indomethacin from poly (D, L-Lactide) Nanocapsules. *J Pharm Sci*, 1990;79:763-767

Edited by MA Jing-Yun

# Plasma L-ENK, AVP, ANP and serum gastrin in patients with syndrome of Liver-Qi-stagnation \*

CHEN Ze-Qi, CHEN Guo-Lin, LI Xue-Wen, ZHAO Yu-Qiu and SHI Lin-Jie

**Subject headings** Syndrome of Liver-Qi stagnation; leucine enkephalin/ blood; arginine vasopressin/ blood; atrial natural polypeptide/ blood; gastrin/blood

## Abstract

**AIM** To investigate the pathophysiologic basis of syndrome of Liver-Qi stagnation and parameters for clinical differentiation.

**METHODS** Plasma L-ENK, AVP, ANP and serum gastrin were determined by RIA in 84 patients with neurasthenia, mastodynia, chronic gastritis, and chronic cholecystitis presenting the same syndrome of Liver-Qi stagnation in traditional Chinese medicine (TCM). Healthy subjects served as controls in comparison with patients having the same syndrome but with different diseases.

**RESULTS** Among the patients with Liver-Qi stagnation, the plasma L-ENK, ANP and gastrin levels were  $38.83 \text{ ng/L} \pm 6.32 \text{ ng/L}$ ,  $104.11 \text{ ng/L} \pm 29.01 \text{ ng/L}$  and  $32.20 \text{ ng/L} \pm 6.68 \text{ ng/L}$ , being significantly lower than those in the healthy controls ( $P < 0.01$ ,  $t = 3.34, 6.17, 4.48$ ). The plasma AVP of the patient group ( $52.82 \text{ ng/L} \pm 19.09 \text{ ng/L}$ ) was significantly higher than that of the healthy controls ( $P < 0.01$ ,  $t = 5.79$ ). The above changes in patients having the same symptom complex but different diseases entities showed no significant differences,  $P > 0.05$ .

**CONCLUSION** The syndrome of Liver-Qi stagnation is closely related to the emotional modulatory abnormality of the brain, with decrease of plasma L-ENK, ANP and gastrin, and increase of plasma AVP as the important pathophysiologic basis.

Department of TCM, Affiliated Xiangya Hospital, Hunan Medical University, Changsha 410008, Hunan Province, China

Dr. CHEN Ze-Qi, male, born on 1951-10-04, in Ningxiang County, Hunan Province, graduated from Hunan Medical University in 1973, now associate professor, Deputy Chief Physician of Department of Integrated Chinese and Western Medicine, majoring in liver disease study in TCM (Traditional Chinese Medicine), having 30 papers published.

\*Project Supported by the National Natural Science Foundation of China, No.39330240

**Correspondence to:** Dr. CHEN Ze-Qi, Department of TCM, Affiliated Xiangya Hospital, Hunan Medical University, 141 Xiangya Road, Changsha 410008, Hunan Province, China

Received 1998-07-06

## INTRODUCTION

Liver-Qi stagnation syndrome is common in liver disease. The predominant clinical manifestations were characterized by emotional alterations and digestive disturbances. In order to explore the pathophysiological basis and indexes of differentiation, we investigated the alterations of neurohumoral parameters in association with modulating emotional and digestive function.

## MATERIALS AND METHODS

### Subjects

Fifty-four patients with Liver-Qi stagnation syndrome selected from Xiangya Hospital and several general hospitals of Hunan Province from May 1995 to October 1996 were examined for plasma L-ENK, AVP and ANP. Seven were males and 47 females. Age ranged from 14-60 years, averaging  $39 \pm 11.2$  years. The diagnoses were mastodynia (19), neurasthenia (17), chronic gastritis (10), and chronic cholecystitis (8). Another 30 patients selected from Xiangya Hospital through March 1997 to October 1997 were added, they were all females, aged 20-53 years, averaging  $34.7 \pm 12.7$  years. Mastodynia was diagnosed in eleven cases, neurasthenia in nine cases, chronic gastritis in seven, and chronic cholecystitis in three.

The healthy controls were selected from the blood donors and employees in our hospital, all of them were negative in physical examination, blood routine, liver function test and chest fluoroscopy to rule out organic disease of heart, liver, lung, kidney, and nervous system diseases. L-ENK, ANP and AVP were detected in 30 cases, whereas serum gastrin was examined in 33 cases.

### Differentiation and diagnosis by TCM

Based on previous criteria derived by our department<sup>[1]</sup>, they were modified according to the clinical epidemiological survey as: hypochondrial, breast and lower abdominal pain; depression; restless and easily irritated; obstruction sensation at the pharynx; dysmenorrhea, amenorrhea, or irregular menstrual cycle; and the tense pulse. The patients presented with 3 or more of the above six items were considered to have Liver-Qi stagnation syndrome. (The disease entities selected including mastodynia, neurasthenia, chronic gastritis, chronic cholecystitis

were diagnosed according to the textbook listed criteria and diagnosed by the departments of breast disease, neurology, general surgery, and digestive medicine).

### Laboratory methods

All the 4 parameters were determined by radioimmunoassay. The apparatus used was FJ-2008 P-type gamma immunocounter. Venous blood samples were collected during fasting in the morning and determined subsequently. Radioimmunoassay kits for L-ENK and AVP were provided by the Department of Neurobiology of the 2nd Military Medical University, and the ANP and gastrin immunoassay kits were provided by Northern Institute of Immunoreagents, Beijing. The standard curve for L-ENK was  $r = 0.998$ ,  $CV = 3.07\%$ ,  $RER = 0.039$ ; for ANP,  $r =$

$0.998$ ,  $CV = 7.15\%$ ,  $RER = 0.035$ ; for AVP,  $r = 0.998$ ,  $CV = 3.15\%$ ,  $RER = 0.039$ ; and for gastrin,  $r = 1.000$ ,  $CV = 3.18\%$ ,  $RER = 0.038$ ; all fitted the quality control criteria.

### Statistical analysis

All data were expressed as  $\bar{x} \pm s$ . Student's  $t$  test and  $F$  test were used for comparison between groups 2 and 3.

### RESULTS

Table 1 lists the results of measurement of plasma L-ENK, AVP, ANP and serum gastrin of the Liver-Qi stagnant patients group (LQSP) and of the normal controls and Table 2 shows the results of measurements in patients with different disease entities.

**Table 1 The plasma L-ENK, AVP, ANP and serum gastrin levels in Liver Qi stagnation patients**

Group	L-ENK	AVP	ANP	Gastrin
LQSP	38.83±6.32(40) <sup>b</sup>	52.82±19.09(30) <sup>b</sup>	104.11±29.01(32) <sup>b</sup>	32.20±6.68(30) <sup>b</sup>
Control	45.19±9.58(30)	29.88±10.35(30)	149.50±28.89(30)	47.02±15.64(30)

In brackets are the number of cases; <sup>b</sup> $P < 0.01$ , vs control.

**Table 2 The plasma and serum neurohumeral parameters of patients with Liver Qi stagnation syndrome of different disease entities**

Group	L-ENK	AVP	ANP	Gastrin
Neurathenia	40.72±17.18(14)	42.95±1078(8)	110.24±39.40(10)	31.03±7.79(9)
Mastodynia	36.40±21.12(10)	61.31±23.57(13)	104.73±34.43(13)	33.49±7.08(11)
Gas-Chole*	40.87±26.02(16)	49.32±12.85(9)	99.83±20.15(9)	31.24±4.52(10)
$F$ value	0.15	2.28	0.24	0.40
$P$	>0.05	>0.05	>0.05	>0.05

Note: in the brackets are the number of cases; \*Gas-Chole stands for chronic gastritis and chronic cholecystitis.

### DISCUSSION

In TCM, the function of liver is mainly dredging and storing of blood. The dredging function of the liver is extremely important in regulating the flow of Qi and blood in the body, the psychoemotion, digestion and absorption, water and fluid metabolism, menstruation and reproductive function. Psychoemotional disturbance is the main cause of Liver-Qi stagnation, and in turn, psychoemotional change is the clinical feature of Liver-Qi stagnation, such as easily irritated and arousal of angry, depression and sighing, insomnia with nightmares, even suspicious and indifferent and grieving. RIA of the psychoemotional and digestive function related neurohumoral parameters in this series showed that among the Liver-Qi stagnation patients, plasma L-ENK, ANP and serum gastrin were significantly decreased and the plasma AVP increased as compared with

those of the normal controls. However, between the different disease entities of various organ systems in modern Western medicine observed no significant difference. It strongly indicates that these alterations are the pathophysiological basis of Liver-Qi stagnation in common. These parameters are the indexes of syndrome, rather than the indexes of the disease entity. This study preliminarily explored the relationship between Liver-Qi stagnation syndrome and the modulatory neurohumeral factors associated with psychoemotional changes.

L-ENK is an active neuropeptide, its secretory neurons are distributed in the thalamic body thalamus, periaqueductal gray matter, and dorsal glial region of spinal cord, and are the modulators of emotional activity within the central nervous system<sup>[2]</sup>. Gastrin is a gastrointestinal hormone secreted by G cells distributed in pylorus and upper duodenum.

Recent study reveals that some of the gastrointestinal peptide is also situated in CNS, the dual distribution of these peptides were called as brain enteric peptide<sup>[3]</sup>. Immunohistochemical studies demonstrated that gastrin and leucine enkephalin are also presented in the brain, stomach, intestine and pancreas<sup>[4]</sup>. Enkephalin is extensively distributed in the central nervous system and the digestive tract, and its secretory cells coincided with gastrin secretory cells<sup>[5]</sup>. In this study, both plasma L-ENK and serum gastrin were significantly decreased in the patients with Liver-Qi stagnant syndrome, which might play an important role in the pathogenesis of psychoemotional modulation disorder and result in unstable emotional activity. Since the brain-enteric peptide secretion and release are closely related with the functional status of CNS and the vegetative nervous system, decreased brain-enteric peptide during Liver-Qi stagnation would certainly affect the gastric acid secretion, the intestinal, pancreatic juice, bile secretion and motility of the digestive tract, ultimately leading to digestive disturbance.

Vasopressin, the antidiuretic hormone (ADH), is synthesized by the neurons of supraoptic nucleus of hypothalamus. Release of ADH is normally modulated by plasma osmotic pressure, blood volume and blood pressure; but pain, vomiting and emotional tension may promote ADH release, and antagonize the diuresis<sup>[4]</sup>.

Atrial natriuretic polypeptide is mainly distributed in the brain, which is high in the hypothalamus and the diaphragmatic sellae region. Its secre-

tion is influenced by physical, humoral and neural factors. Its functions include natriuresis, vasodilation, and decrease of blood pressure<sup>[6]</sup>. It was reported that ANP significantly inhibited the release of AVP via hypothalamus-neurohypophyseal axis, the antagonistic effect of ANP and renin-angiotensin not only existed peripherally, but also in the CNS, particularly in regulating the blood volume, electrolyte balance and maintenance of blood pressure<sup>[7]</sup>. Decrease of plasma ANP and elevation of AVP might be one of the pathophysiologic basis of the CNS regulatory dysfunction resulting in increased vascular tension, sodium and water retention, and hypertension in Liver-Qi stagnation syndrome. But the cause-effect relationship, the precise mechanism of the elevated AVP and decreased ANP, as well as the validity of the four neurohumeral parameters in this study as reference indexes in differentiation of the Liver-Qi stagnant syndrome await further clarification.

#### REFERENCES

- 1 Chen GL, Pan QM, Zhao YQ, Chen ZQ, Li XQ, Fu MR. Studies on the clinical diagnostic criteria of liver disease syndromes in TCM. *Zhonguo Yiyao Xuebao*, 1990;6:66-73
- 2 Yan DY, Li TD. Neurophysiology. Hefei: China University Publisher of Science and Technology, 1992:79-104
- 3 Zhang JR. Physiology. Beijing: People's Health Publisher, 1997:198-194
- 4 Luo ZQ, Xu ML, Yang SR (translators). Neuroendocrinology. Beijing: People's Health Publisher, 1986:267
- 5 Cheng ZP. Endocrine physiology. Beijing: People's Health Publisher, 1981:267
- 6 Tang J, Tang VQ. Endocrine function of circulatory system. Beijing: Jointed Press of Beijing Medical University and Peking Union Medical College, 1989: 2-29
- 7 Zhang DM, Xu LS (eds). Neuroendocrinology. Beijing: China Medical Technology Publisher, 1991:295-308

Edited by MA Jing-Yun

Review

# Current medical therapy for ulcerative colitis

XU Chang-Tai and PAN Bo-Rong

**Subjects heading** colitis, ulcerative/drug therapy; inflammatory bowel diseases/drug therapy; cyclosporin; glucocorticosteroids; sulphasalazine 5-aminosalicylic acids

## INTRODUCTION

In recent years, the advances in therapy of ulcerative colitis (UC) have been characterized mainly by the more extensive use of immunosuppression. Cyclosporin (CSA) may become a drug of choice to treat severe UC, but its long-term effect is insufficient. Topically, glucocorticosteroids (GCS) are hopeful in right ileocolonic UC, but no action for maintenance therapy<sup>[1-3]</sup>. The most significant development in recent years is the introduction of immunomodulatory treatments using cytokines and anticytokines. Immunomodulation therapy creates great expectations since early reset of the immunostat might be able to control inflammation in a long term. Current treatment strategies are anti-inflammatory and to modulate the immune response. Standard therapies with sulphasalazine (SAS) or 5-aminosalicylic acids (5-ASA, mesalazine or mesalamine), GCS and antibiotics yield a fair immediate success, but long-term response to these therapies is poor. The greatest advance has been the introduction of immunosuppressive strategies. The indexes like the clinical activity index (CAI) proposed by Rachmilewitz<sup>[1]</sup>, although useful, have not received general acknowledgement.

Patients with an inflammatory bowel disease (IBD), such as UC or Crohn's disease, have recurrent symptoms with high morbidity. Mild disease requires only symptomatic relief and dietary manipulation. Mild to moderate disease can be managed with 5-ASA, including olsalazine and mesalamine. Mesalamine enemas and suppositories are useful in treating proctosigmoiditis. Corticosteroids are beneficial in patients with more severe symptoms, but side effects limit their use, particularly for chronic

therapy. Immunosuppressant therapy may be considered in patients with refractory disease that is not amenable to surgery. IBD in pregnant women can be managed with 5-ASA and corticosteroids<sup>[2]</sup>. Since longstanding IBD is associated with an increased risk of colon cancer, periodic colonoscopy is warranted.

Since lesions in UC are quite diffuse and uniform endoscopic indexes used are quite straightforward, clinical activity, endoscopic activity and histology show a reasonable correlation and it is useful to monitor disease activity also with flexible proctosigmoidoscopy. The persistence of active inflammatory lesions at histology in the presence of endoscopic remission predicts relapse. Bresci G *et al*<sup>[3]</sup> reported that the activity of the disease was evaluated by a Clinical Activity Index and an Endoscopic Index. Of 112 cases of UC observed, 95 showed no change in extent and were studied as examples of non-progressive UC, and in this group the extension of the disease was: pancolitis in 19%, left sided colitis in 39%, proctosigmoiditis in 17% and proctitis in 25%. A colectomy had to be performed in 5%. None of the enrolled cases developed a cancer during the follow up. The patients with ulcerative pancolitis or left-sided colitis were treated with 5-ASA-1.6g/d in a delayed-release formulation, while the patients with proctosigmoiditis or proctitis were treated with 5-ASA enem as 4g/d. The patients with more than one relapse/year accounted for 39%. The proportion of patients with only one relapse/year was 53%. The patients with steady remission for all the seven years of the trial were only 8%, but with a statistically significant difference between the groups with initial diagnosis of proctosigmoiditis or proctitis and the group with initial diagnosis of pancolitis or left-sided colitis (12% vs 5%). Among the patients with continuous remission, 37% showed colonic alterations, with an endoscopic score higher than 4 but a clinical score less than 6. Side effects were observed in 6% of patients but without treatment withdrawal. Non-progressive UC throughout the colon has a relatively good prognosis, which seems to be independent of the location of the disease, even if Bresci G *et al*<sup>[3]</sup> have found a statistically significant higher percentage of patients with steady remission among the patients with more distal diseases.

Department of J 4th Milit Med Univ, Fourth Military Medical University, 17 Changle Xilu, 710033 Xi'an, Shaanxi Province, China

**Correspondence to:** Dr. XU Chang-Tai, Department of J 4th Milit Med Univ, Fourth Military Medical University, 17 Changle Xilu, 710033 Xi'an, Shaanxi Province, China

Tel. +86-29-3374765

Email: changtai@mail.igd.edu.cn

**Received** 1998-11-10 **Revised** 1998-12-30

## CURRENT TREATMENT OF ULCERATIVE COLITIS

Ulcerative colitis is a mucosal disease and therefore well suited for treatment in most instances with topically acting drugs at the level of the colonic mucosa. UC is controlled mainly using GCS and 5-ASA.

Ardizzone *et al*<sup>[4]</sup> had reviewed the role of corticosteroids, ASA and mesalazine (5-ASA, mesalamine), immunosuppressive agents and alternative novel drugs for the treatment of distal UC. Short cycles of traditional, rectally administered corticosteroids (methylprednisolone, betamethasone, and hydrocortisone) are effective for the treatment of mild to moderately active distal UC. In this context, their systemic administration is limited to patients who are refractory to either oral 5-ASA, topical mesalazine or topical corticosteroids. Of no value in maintaining remission, the long-term use of either systemic or topical corticosteroids may be hazardous. A new class of topically acting corticosteroids [budesonide, fluticasone, beclomethasone dipropionate, prednisolone 21-methasulphobenzoate, tixocortol (tixocortol pivalate)] represents a valid alternative for the treatment of active UC, and may be useful for refractory distal UC. Although there is controversy concerning dosage or duration of therapy, oral and topical mesalazine is effective in the treatment of mild to moderately active distal UC. Sulfasalazine and mesalazine remain the first-choice drugs for the maintenance therapy of distal UC. Evidence shows a trend to a higher remission rate with higher doses of oral mesalazine. Topical mesalazine (suppositories or enemas) is also effective in maintenance treatment. For patients with chronically active or corticosteroid-dependent disease, azathioprine and mercaptopurine are effective in reducing either the need for corticosteroids or clinical relapses. Moreover, they are effective for long-term maintenance remission. CSA may be useful in inducing remission in patients with acutely severe disease that does not achieve remission with an intensive intravenous regimen. Existing data suggest that azathioprine and mercaptopurine may be effective in prolonging remission in these patients. The role of alternative drugs in the treatment of distal UC and its different forms are reviewed. In particular data are reported concerning the effectiveness of 5-lipoxygenase inhibitors, topical use of short chain fatty acids, nicotine, local anesthetics, bismuth subsalicylate enema, sucralfate, clonidine, free radical scavengers, heparin and hydroxychloroquine. The management of patients with acute severe UC requires careful in-hospital assessment of the patient and the coordinated treatment of a team of experienced gastroenterologists and

surgeons. Complete understanding of the potential complications and their management, especially toxic megacolon, is essential.

The current medical arsenal advocates a standardized approach to management that includes continuous, high dose iv hydrocortisone, more aggressive use of topical steroids as well as feeding the patients and continuing (but not initiating) oral 5-ASA agents was reviewed<sup>[5]</sup>. For those patients whose disease proves refractory to iv steroids, iv. CSA (with an acute response rate of 82%) is an essential component in the medical management of these patients. Antibiotics should be used only when specifically indicated. Total parental nutrition has not been shown to be helpful in the acute setting. Air contrast barium enema and colonoscopy have been used to predict response but may be dangerous diagnostic modalities in these acutely ill patients and are not better than good clinical judgement. Marion *et al*<sup>[5]</sup> review and advocate long-term management of acute response using 6-mercaptopurine or azathioprine. The surgical experience and the postoperative complications of the ileal pouch anal anastomosis, which include acute pouchitis in 50% - 60%, chronic pouchitis in 5%-10% and recent reports of dysphasia among patients with chronic pouchitis, must be considered before colectomy is advised. Over 80% of patients with acute severe colitis can be spared colectomy using the current arsenal of medical therapies.

The inhibited release of 5-lipoxygenase products may account for some of the anti-inflammatory effects of ropivacaine seen in the treatment of UC<sup>[6]</sup>. Prompt diagnosis and exclusion of infection require a minimum of rigid sigmoidoscopy, rectal mucosal biopsy and stool culture. Admission to hospital is mandatory for patients with features of severe disease, or who are in their first attack of UC and have bloody diarrhea, even if the criteria for severe disease are not met. Once admitted, plain abdominal X-ray, full blood count, and serum albumin and C reactive protein should be used to monitor the patients on alternate days; temperature and pulse rate should be recorded four times per day. Treatment should be instituted as soon as the diagnosis is made with an intravenous corticosteroid (hydrocortisone 100mg iv. four times daily or equivalent). Antibiotics may be included if infection cannot be confidently excluded. Free diet is allowed but attention should be given to nutritional, fluid and electrolyte status with intravenous replacement if necessary. Any evidence of colonic dilatation occurring despite maximal therapy should be regarded as an absolute indication for colectomy. The patient should be kept fully informed from an early stage about the

likely natural history of the condition and about the possible therapeutic options including surgery. CSA therapy should be reserved for patients who have a poor response to the first 3d-4d of corticosteroid therapy, particularly those with serum C reactive protein >45mg/L and who do not yet have absolute indications for colectomy. Most patients who have not convincingly responded within 10 days of starting medical therapy should undergo colectomy, although some responders who are febrile may reasonably continue for up to 14 days before a final decision. Approximately 30%-40% of patients with severe colitis will need colectomy within the first 6 months. With optimal management, mortality can be zero, but better medical therapies are urgently needed to reduce the colectomy rate<sup>[7]</sup>.

Finnie *et al*<sup>[8]</sup> speculated that corticosteroids might cause beneficial stimulation of mucus synthesis, since this is a known action of carbenoxolone, a corticosteroid itself, and has also been proposed as a possible mechanism for the protective effect of smoking on UC. We have therefore compared the effects of corticosteroids including carbenoxolone, and nicotine on mucin synthesis, assessed by incorporation of N-[3H] acetylglucosamine into mucin by colonic epithelial biopsies in culture. In histologically normal biopsies from the left colon, hydrocortisone and prednisolone caused a very marked concentration-dependent increase in mucin synthesis, with maximal effect at 6 nmol/L ( $P < 0.001$ ) and 1.5 nmol/L ( $P < 0.001$ ) respectively. The maximal effect of hydrocortisone was significantly greater than that of prednisolone ( $P < 0.05$ ). Carbenoxolone, 0.17 mmol/L, also increased mucin synthesis in the left colon [ $P < 0.05$ ,  $n = 15$  (three patients)]. In contrast, these corticosteroids caused only a small, non-significant increase in mucin synthesis in the histologically normal right colon; fludrocortisone, 2 nmol/L and 20 nmol/L, and aldosterone, 0.1 nmol/L - 10 nmol/L had no effect. Nicotine significantly increased mucin synthesis between 62.5 nmol/L and 6.25 nmol/L ( $P < 0.05$  at all concentrations) in both the right and left colon. In biopsies from the relatively uninvolved right colon of patients with UC, corticosteroids and nicotine caused relatively smaller increases in mucin synthesis. The marked stimulation of mucin synthesis by corticosteroids suggests that this may account, at least in part, for their therapeutic effect in UC.

GCS act by binding to the GCS-R (glucocorticosteroid receptor). The activated receptor assembles to a dimer that is transported in the nucleus of the cell where it binds to DNA and acts *via* enhanced or reduced transcription, reduced translation and breakdown of DNA. GCS have a very extensive

anti-inflammatory and immunosuppressive action. Since the receptor is the same for all body cells, GCS in the circulation have many systemic effects. Many actions have been described for the aminosalicylates<sup>[9]</sup>. SAS and 5-ASA inhibit the production of cyclooxygenase, thromboxane synthetase, platelet-activating-factor synthetase, and IL-1 by macrophages and can decrease immunoglobulin production by plasma cells. Both SAS and 5-ASA inhibit the production of reactive oxygen species and scavenge reactive oxygen metabolites. 5-ASA lacks the antibacterial effect of SAS.

#### TREATMENT OF ACTIVE ULCERATIVE COLITIS

The two variables determining the therapeutic approach in UC are disease extent and disease severity (Table 1).

Effective medical treatment of UC is available. However, 20% - 40% of patients remains refractory and become steroid dependent or chronic active. Azathioprine and its metabolite 6-mercaptopurine have been found effective in this setting, although duration of treatment and doses are not entirely clear. Methotrexate has no definitive part in the treatment of refractory colitis. Iv. CSA induces remission in a considerable number of patients; follow-up treatment is, however, not defined. This approach may be useful for elective surgery. A number of other treatments have been proposed including chloroquine, interferons and anti-cytokines. None of these can currently be recommended for clinical practice. Anti-inflammatory cytokines such as IL-10 may be good candidates<sup>[5,10]</sup>.

In the presence of proctitis or distal colitis, a topical approach should always be the first choice. To control active distal disease rectal 5-ASA is at least as effective as rectal GCS<sup>[11]</sup>. In patients with left-sided colitis, enemas are the best choice because of the retrograde spread up to the splenicflexure. GCS enemas have been used for a long time in the treatment of distal UC. Prednisolone (20 mg - 30 mg), hydrocortisone (100 mg-125 mg), and betamethasone (5 mg) have all been shown to be effective. To minimize side effects, poorly absorbable GCS have been used for enema therapy including hydrocortisone foam and prednisolone metasulphobenzoate or molecules with increased first-pass metabolism in the liver, e.g., betamethasone dipropionate and tixocortol pivalate. Budesonide enemas carry almost no systemic effects because of a very high first-pass effect. Doses of 2 mg are as effective as 20 mg - 30 mg of prednisone. Repeated therapy courses with budesonide enemas have been found safe without suppression of the HPA axis<sup>[5,12]</sup>.

CSA has been proposed in the management of patients with acute UC in whom standard therapy failed and who were candidates for colectomy<sup>[13]</sup>. Seven academic hospitals contributed to this retrospective study which included 29 patients (median age: 33 years, 12 females and 17 males). The median duration of the disease was 4 years. For the responders, maintenance therapy included tapering dose of steroids ( $n = 12$ ), azathioprine ( $n = 12$ ), 5-ASA or salazopyrine ( $n = 10$ ), methotrexate ( $n = 1$ ) or oral CSA ( $n = 11$ ). The median duration of follow-up was 12 months (4 to 48 months). Among the 20 responders, 7 were subsequently referred for colectomy either selectively ( $n = 3$ ) or because of recurrence of the disease ( $n = 4$ ). Among the 12 patients treated by azathioprine as a maintenance therapy, only 3 (25%) had to be referred for surgery. Among the 8 patients who did not receive azathioprine, 4 (50%) were subsequently subject to a colectomy (NS). In patients with acute refractory UC who received CSA, the short-term efficacy (avoidance of immediate colectomy) was obtained in 20 (69%) out of 29 patients. However, after a median follow-up of 12 months, only 13 (45%) patients were colectomy free.

Refractory distal colitis is a difficult medical problem and is defined as active distal inflammation unresponsive within 4 wk - 6 wk to a topical treatment with 5-ASA or corticosteroids associated with oral salicylates or sulphasalazine<sup>[6,7]</sup>. Although there is little controlled evidence, it is logical to increase the dose of the topically administered drug or to continue the drug for a longer time. A further step is to switch drugs. All clinicians have experience with patients in whom proctitis not responsive to 5-ASA responded to GCS enemas and *vice versa*. Another valuable approach seems to combine 5-ASA and GCS in one enema. Frequently, patients with refractory distal disease do not respond even to oral therapy with GCS and a rectal drip of GCS over several hours together with administration of antidiarrheals in hospital may be necessary or iv administration of high doses of GCS. Active disease extending beyond the rectum necessitates oral therapy. In mild-to-moderate disease oral SAS or 5-ASA formulations in high doses can be used or a combined approach of oral 5-ASA and topical 5-ASA. Many physicians prefer this approach because of the low incidence of side effects and the reluctance of the patients to take GCS<sup>[4-6]</sup>.

Oral salicylates at doses of over 2g have been shown to be more effective than placebo to control mild-to-moderate attacks of UC<sup>[14]</sup>. There probably is a dose-response effect with doses up to 3.8g being

increasingly more effective, but this was not demonstrated in all studies. 5-ASA was not more effective than SAS and was beneficial especially to the SAS-sensitive patient. Recent data<sup>[15]</sup> have shown that balsalazide is more effective and better tolerated than mesalamine in the treatment of active UC. Patients taking balsalazide not only experienced more asymptomatic days and achieved the first asymptomatic day more rapidly but with side effects. Differences were highly significant.

Improvement of symptoms of UC with 5-ASA may be slow and overall 5-ASA or sulphasalazine are certainly less effective to control active UC than GCS. There is a dose effect for oral GCS, 40 mg prednisolone daily being more effective than 20 mg; while 60 mg offers little extra benefit but is associated with a considerable increase in side effects<sup>[3,4]</sup>.

Severe UC is defined using the criteria of Tnielove and Witts<sup>[16]</sup> as six or more bloody stools in a patient with fever, tachycardia, hypoalbuminemia and raised ESR. These patients will mostly be admitted to hospital to receive a continuous iv infusion of GCS. In severe left-sided or extensive disease GCS are mandatory and combined therapy with 5-ASA is probably not more efficacious than GCS alone. As soon as symptoms are controlled, tapering of the GCS can be started but proctoscopic monitoring of disease activity is valuable.

Recently parameters predictive of outcome of severe colitis under 3 days of intravenous glucocorticosteroids have been revised<sup>[17]</sup>. The need for colectomy was predicted in 85% of the patients on the basis of the presence of eight or more stools per 24 h or 4-5 stools per 24 h together with C-reactive protein >45mg/L. Based on these criteria one could make the decision to introduce intravenous CSA or to decide for colectomy. In patients who deteriorate or are admitted with toxic colonic dilatation, immediate colectomy has to be performed. If a pouch-anal anastomosis is constructed, a temporary diversion ileostomy is indicated. Many surgeons' three-step procedures, i.e. first colectomy with closure of a short rectal stump, subsequent construction of an ileoanal pouch with temporary ileostomy and finally closure of the stoma. The side effects of CSA are multiple (Table 2) and opportunistic infections by pneumocystis and cytomegalovirus may be life-threatening. These complications were encountered especially in elderly patients treated with long-term CSA and GCS. Another serious side effect is epileptiform fits due to the CSA hydrophobic vehicle. Patients with lowered serum cholesterol or magnesium should not receive CSA.

**Table 1 Treatment of active ulcerative colitis**

Severity	Extent		
	Distal	Left-sided	Extensive
Mild	Topical GCS or 5-ASA	Topical GCS or 5-ASA +oral 5-ASA	Oral 5-ASA (+topical therapy)
Moderate/severe	Topical GCS or 5-ASA (+oral 5-ASA?)	Oral GCS	Oral or GCS iv
Refractory	Increase dose and duration	GCS iv+CSA	GCS iv+CSA
	Switch enemas	Surgery	Surgery
	Combine topical GCS and 5-ASA		
	Oral GCS		
	Others		

**Table 2 Adverse events reported with use of cyclosporin (iv+oral) in IBD<sup>[18]</sup>**

Type of side effect	%	Type of side effect	%
Paresthesias	26	Headache	5
Miscellaneous	13	Infection	3
Hypertrichosis	13	Hepatotoxicity	3
Hypertension	11	Gingival hyperplasia	2
Tremor	7	Seizure	1
Nausea/vomiting	6	Anaphylaxis	0.3
Renal insufficiency	6	Side effects/patient	0.94

**Table 3 Major side effects of glucocorticosteroids**

	Short-term and long-term therapy	Long-term therapy
CNS	Pseudotumor cerebri Psychosis	
Musculoskeletal	Myopathy Aseptic necrosis	Osteoporosis
Ocular	Graucoma	Cataracts
Gastrointestinal	Ulcer-pancreatitis	
Cardiovascular	Hypertension Fluid retention	
Endocrinological		Permanent suppression of HPA-axis Growth failure
Metabolic	Hyperglycemia Hyperosmolar state Hyperlipidemia	Fatty liver Hypokalemia
Skin	Acne, ecchymosis	Striae, atrophy, wound Infection Cushingoid fat Distribution

**Table 4 Immunosuppressives used in inflammatory bowel diseases**

Drug	Mode of action	Mechanism of action
AZT/6-MP	Inhibition of ribonucleotide synthesis	Inhibition of proliferation of T-cell clones
Methotrexate	Folic acid inhibitor	Inhibition of T and B-cell Function decrease of IL-1 and IL-6
Cyclosporin (CsA)	Inhibition of T-cell-receptor-stimulated	Inhibition of IL-2 production and
Tacolimua (FK 506)	Transcription of lymphokine genes	IL-2 receptors; inhibition of cytokines(TNF $\alpha$ ,IFN $\gamma$ )
Mycophenolate	Inhibition of guanosin nucleotide synthesis	

**Table 5 Immunomodulation therapy in inflammatory bowel disease**

	Cytokines	Anticytokines	Antisense nucleotides
Current studies	rhu IL-10, rhu IL-11	TNF antibodies, inhibitors	ICAM-1
Future studies		IL-1 antibodies IL-1 ra IFN- $\gamma$ antibodies IL-12 antibodies	NF $\kappa$ B

Side effects of drug therapy in patients with refractory colitis result from cumulative toxicity of high-dose iv CSA and GCS. The exact role of CSA in the treatment of severe colitis needs to be defined and will greatly depend on the long-term outcome of patients treated with this drug. The side effects associated with GCS therapy are important (Table 3). Short-term treatment carries mild side effects in the majority of patients but long-term therapy are sinecures associated with irreversible complications. In the past years, therefore, attempts have been made to develop GCS with high topical activity lacking the systemic activity of the drug and hence carrying fewer side effects.

Other approaches to therapy of UC are currently under investigation. Transdermal nicotine in doses of 15 mg - 25 mg daily added to conventional therapy was effective against placebo to control active disease<sup>[19]</sup>. The rationale to use this therapy is clear. Most UC patients are nonsmokers, and patients with a history of smoking usually acquire their disease within a few years after they have stopped smoking<sup>[20]</sup>. Among patients who continue to smoke, symptoms may improve, suggesting that smoking may have a beneficial effect. Another recent trial confirmed the moderate efficacy of nicotine in the treatment of UC. The use of nicotine as a treatment, however, remains highly controversial. The use of oral ridogrel, a thromboxane synthase inhibitor in UC is currently investigated. A study suggests that there is no benefit of adding azathioprine in patients with chronic stable colitis, whereas the drug is efficacious to maintain UC in remission. The evidence for the use of methotrexate in the treatment of chronic active UC is largely negative. It should be emphasized that UC is a curable disease. Colectomy with ileo-anal pouch anastomosis is a valuable treatment alternative in chronically active or intractable disease.

Rectal treatment with mesalazine enemas is the first-line therapy for distal UC. In order to improve the benefits of rectal therapy, a new 60 mL- 5-ASA rectal gel enema preparation has been developed using a device that excludes direct contact of the inert propellant gas with the active drug<sup>[21]</sup>. Twelve patients with active UC administered 4 g of the mesalazine rectal enema labelled with 100MBq technetium sulfur colloid (99mTc-SC). Anterior scans of the abdomen were acquired at intervals of 4 hours. Scans were analyzed to evaluate the extent of retrograde flow and homogeneity of distribution of the radiolabelled enema in the rectum, sigmoid, descending and transverse colon. In addition, plasma levels of 5-ASA and Ac-5-ASA were measured for 6 hours. All patients retained the entire rectal gel

throughout the course of the study without adverse events. In 11 (92%) out of 12 patients, the gel had spread homogeneously beyond the sigmoid colon and had reached the upper limit of disease in all cases. The maximum spread (splenic flexure) was observed in 6 (50%) out of 12 patients within the first 2 hours. The systemic absorption of mesalazine and its metabolite Ac-5-ASA were low. The new mesalazine enema represents an adequate alternative and a further technological improvement in the topical treatment of distal UC<sup>[20,21]</sup>.

The choice between sulfasalazine and 5-aminosalicylate (5-ASA) drugs in the management of UC patients often depends on idiosyncrasies of drug tolerance and control of the disease in individual patients. Walker *et al*<sup>[22]</sup> sought to evaluate whether there were population differences in the effect of 5-ASA and SAS on the occurrence of clinically recognized adverse events. We also attempted to determine whether there were differences in the use of concomitant steroids and in the rates of hospitalization. A large computerized database drawn from general practices in the United Kingdom was reviewed. The 2894 patients who were diagnosed having UC were receiving ongoing medical therapy specific to UC. The period of data availability ran from early 1990 to late 1993. The average duration of observation was 2.1 years per patient. Patient histories were categorized into distinct periods according to the dose of 5-ASA and SAS, steroids, and immunosuppressants, and were further divided based on the UC activity. Within these categories, they examined the initiation and discontinuation of steroids, rate of new hospitalizations for UC, and clinical complaint of adverse events. The results show new clinical mentions of hepatic, pancreatic, renal, and hematological events other than anemia were similar among the 5-ASAs and were very infrequent generally. Hospitalizations for UC occurred with similar frequency (about 15 hospitalizations per 100 patients per year) among users of those drugs. Patients receiving SAS had lower rates of initiation of prednisolone than patients receiving 5-ASA, but SAS was used proportionately less often in patients who had been recently hospitalized, and it may be that SAS patients were somewhat less sick than patients using 5-ASA. The choice of drug did not affect discontinuation rates for prednisolone among established users. In the United Kingdom, during the period of this study, serious adverse reactions to drugs were not an important aspect of the management of patients with UC. Renal and pancreatic complications of SAS and 5-ASA therapy were extremely rare. SAS and 5-ASA drugs have similar steroid-sparing properties. Disease-specific

hospitalizations are approximately 100 times more common in UC patients than serious adverse drug effects. Considerations of drug efficacy should therefore dominate the choice between the therapeutic agents.

The efficacy and safety of 5-ASA suspension enema were compared with oral SAS in patients with active mild to moderate distal UC<sup>[23]</sup>. Thirty-seven patients were randomly assigned to treatment with either rectal mesalamine, 4 g at night ( $n = 19$ ) or oral SAS, 1 g four times a day ( $n = 18$ ) in a 6 week, double blind, double-dummy, parallel-group, multicenter study. A physician-rated Disease Activity Index (DAI), which included symptom evaluations and sigmoidoscopic findings, assessed efficacy, by physician-rated Clinical Global Improvement (CGI) scores, and by Patient Global Improvement (PGI) scores. Adverse event reports, clinical laboratory tests, and physical examination assessed safety. Mean DAI scores indicated significant improvement from baseline in both treatment groups. CGI scores indicated that 94% of the 5-ASA patients were either "very much improved" or "much improved" at wk 6 vs 77% of the SAS patients. PGI ratings showed more improvement in the 5-ASA treatment group than in the SAS group at week 2 ( $P = 0.02$ ) and at 4 week ( $P = 0.04$ ). Adverse events, primarily headache and nausea, occurred significantly more frequently ( $P = 0.02$ ) in the SAS than in the 5-ASA group (83% vs 42%). Three patients were withdrawn from SAS treatment because of adverse events. Rectally administered 5-ASA is as effective as oral SAS in treatment of active distal UC but is associated with fewer and milder adverse events. Patients treated with 5-ASA reported improvement earlier than those treated with SAS.

Since transdermal nicotine is of value in the treatment of active UC but is often associated with side effects, an alternative in the form of topical therapy with nicotine enemas has been developed. In an open study<sup>[24]</sup>, 22 patients with active colitis, all non-smokers, were asked to take a 100mL enema containing 6mg of nicotine every night for 4 weeks. Pre-trial treatment using mesalazine ( $n = 16$ ), oral prednisolone (8), cyclosporin (1) and azathioprine (1) was kept constant for the month prior to assessment and during the study period. Symptoms, with stool frequency, were recorded on a diary card and an endoscopy was performed with rectal biopsy at the beginning of the study and after 4 weeks. Seventeen of the 22 patients completed 1 month of treatment. Mean duration of relapse was 29 weeks. Sixteen of 17 improved their St Mark's score. Urgency and stool frequency improved in 12 patients, sigmoidoscopic and histological scores in

10. Three patients had a full remission of symptoms with normal sigmoidoscopy. Six of 10 patients with a partial response continued with the enemas for the second month, and five showed further improvement with full remission in two. The enema appeared effective when added to conventional treatment and produced few side effects. Topical nicotine therapy for UC may have a place in future management, but case control studies are needed<sup>[25]</sup>. Immunosuppressives used in IBD (Table 4), and immunomodulation therapy in IBD are directed toward suppressing the action of proinflammatory cytokines for enhancing the effects of antiinflammatory mediators (Table 5).

#### MAINTENANCE THERAPY IN ULCERATIVE COLITIS

Aminosalicylates are used as standard treatment for maintaining remission in UC<sup>[26]</sup>. As yet, there is no other existing alternative with proven efficacy. In the light of the hypothesis that the intestinal environment may contribute to the pathophysiology of UC, a trial was conducted to test the effects of probiotic treatment with an oral preparation of non-pathogenic *E. coli*. A total of 120 patients with inactive UC were included in a double blind, double-dummy study comparing mesalazine 500mg three times daily. An oral preparation of viable *E. coli* strain Nissle (Serotype 06:K5:H1) for 12 weeks was studied with regard to their efficacy in preventing a relapse of the disease. Study objectives were to assess the equivalence of the clinical activity index (CAI) under the two treatment modalities and to compare relapse rates, relapse free times and global assessment. The start and end scores of the CAI demonstrated no significant difference between the two treatment groups. Relapse rates were 11.3% under mesalazine and 16.0% under *E. coli* Nissle 1917 (NS). Life table analysis showed a relapse-free time of  $103 \pm 4$  d for mesalazine and  $106 \pm 5$  d for *E. coli* Nissle 1917 (N.S.). Global assessment was similar for both groups. Tolerability to the treatment was excellent. No serious adverse events were reported. From the results of this preliminary study, probiotic treatment appears to offer another option for maintenance therapy of UC. Additional support is provided for the hypothesis of a pathophysiological role for the intestinal environment in UC.

Distal UC can be maintained with a topical approach. Regimens such as alternate-day enema administration has been shown to be effective, while for maintenance, the use of suppositories may be feasible as far as compliance is concerned, and the long-term use of enemas is difficult. The benefit of

maintenance treatment with oral 5-ASA of extensive UC is well established. SAS reduces the relapse rate by fourfold and all 5-ASA formulations have comparable efficacy with fewer side effects. The rate of GI side effects is especially decreased with 5-ASA. The optimal 5-ASA dose may be 2 g. A dose effect was not demonstrated for most 5-ASA formulations and SAS, except for olsalazine<sup>[27]</sup>.

## PROSPECTS

There is overwhelming evidence that genetic factors play a role in the predisposition to develop the chronic IBD<sup>[28-30]</sup>. The genetic analysis of complex diseases, such as UC, is difficult. The presence of disease heterogeneity, the relative low frequency in the population, the degree to which first-degree relatives are affected (approximately 10%), the presence of genes with minor genetic effects, and ethnic differences are some of the difficulties encountered in identifying disease susceptibility loci. Two major approaches to identify these genes are being followed at present. The first, family-based, consists of studying linkage analysis in sibling pairs and parental transmission in genome-wide screening using microsatellite markers. These studies are appropriate and helpful for finding genes of major or moderate effects but may be difficult in identifying genes with minor effects; and can be considered in the future in genome-wide screens with technologic advances. The second approach is based on conventional epidemiological designs, population-based studies, using candidate genes in the framework of a biologic hypothesis. Recent data using both approaches in both Crohn's disease and UC are reviewed. The results of genome-wide linkage studies have not reached consensus, but suggest that these diseases are different and polygenic in nature. We have started our studies with the hypothesis that an abnormal immune disbalance contributes to the biologic basis of the disease. Therefore, polymorphisms in genes encoding proinflammatory and regulatory cytokines were studied. Preliminary data of these association studies suggest the importance of several genes with small effects in determining the severity and prognosis of these diseases. If the promised breakthrough of immunomodulation therapy is achieved in IBD, one may anticipate quite dramatic changes in the treatment of IBD. GCS still are the mainstay of therapy of UC within 5-10 years.

This review<sup>[29]</sup> focuses on current developments in the major categories of the therapy used in the management of IBD. Conventional corticosteroids, although a mainstay of the acute treatment of IBD for many years, have many drawbacks, including a

variety of side effects, particularly with chronic use. Budesonide appears to be relatively safe and at least moderately effective in inducing remission in active distal UC. Aminosalicylates, both oral and topical, have been proved useful in managing mild to moderate active UC, as well as in maintaining remission. Data from recent trials suggest that higher doses of mesalamine are generally more efficacious than lower doses. In addition, a combination of oral and rectal formulations is successful, but is not so when single route is used. The immunomodulatory agents azathioprine, 6-mercaptopurine, and methotrexate have been shown to be effective in the treatment of IBD and are now widely accepted as valuable parts of the therapeutic armamentarium. CSA, although effective, is associated with much toxicity, and patients must be monitored closely in centers experienced with this agent. Clinical trials of IL-10, IL-11, and anti-TNF- $\alpha$  have also shown promise. Antibiotics have been used empirically for many years in the treatment of IBD. Larger clinical trials are warranted to explore the potential efficacy of antibiotic therapy. The acemannan, heparin, and transdermal nicotine have also shown variable degrees of promise as possible therapies for IBD. Despite the variety of agents available for the treatment of IBD, none is ideal or universally accepted. Ongoing research into the well-established therapeutic agents, as well as novel drugs with more precise targets, may contribute to the design of a more optimal regimen for IBD in the not too distant future.

Both UC and Crohn's disease are considered to be the result of an unrestrained inflammatory reaction, but an explanation for the aetiopathogenesis has still not emerged<sup>[30]</sup>. Until the predisposing and trigger factors are clearly defined, therapeutic and preventive strategies for these disorders must, therefore, rely on interrupting or inhibiting the immunopathogenic mechanisms involved. Current therapies, such as glucocorticoids and 5-ASA, inhibit raised concentrations of interdependent, soluble mediators of inflammation, which may amplify one another or have parallel effects. Future medical options for treatment of UC aim at removing perpetuating antigens, blocking entry of inflammatory cells by manipulating adhesion molecules, targeting soluble mediators of inflammation by blocking proinflammatory molecules or by preserving endogenous suppressive molecules, or correcting genetic defects. It remains, however, to be determined whether targeting multi-inflammatory actions or a single key pivotal process is the better therapeutic strategy and whether subgroups of UC with different clinical courses will require different treatment approaches<sup>[24,31]</sup>.

## REFERENCES

- 1 Rachmilewitz D. Coated mesalazine (5-aminosalicylic acid) versus sulphasalazine in the treatment of active ulcerative colitis: a randomised trial. *BMJ*, 1989;298:82-86
- 2 Botoman VA, Bonner GF, Botoman DA. Management of inflammatory bowel disease. *Am Fam Physician*, 1998;57:57-68, 71-72
- 3 Bresci G, Parisi G, Gambardella L, Banti S, Bertoni M, Rindi G, Capria A. Evaluation of clinical patterns in ulcerative colitis: a long-term follow-up. *Int J Clin Pharmacol Res*, 1997;17:17-22
- 4 Ardizzone S, Porro GB. A practical guide to the management of distal ulcerative colitis. *Drugs*, 1998;55:519-542
- 5 Marion JF, Present DH. The modern medical management of acute, severe ulcerative colitis. *Eur J Gastroenterol Hepatol*, 1997;9:831-835
- 6 Martinsson T, Haegerstrand A, Dalsgaard CJ. Effects of ropivacaine on eicosanoid release from human granulocytes and endothelial cells *in vitro*. *Inflamm Res*, 1997;46:398-403
- 7 Leiper K, London IJ, Rhodes JM. Management of the first presentation of severe acute colitis. *Baillieres Clin Gastroenterol*, 1997;11:129-151
- 8 Finnie IA, Campbell BJ, Taylor BA, Milton JD, Sadek SK, Yu LG, Rhodes JM. Stimulation of colonic mucin synthesis by corticosteroids and nicotine. *Clin Sci Colch*, 1996;91:359-364
- 9 Hanauer SB. Inflammatory bowel disease. *N Engl J Med*, 1996;334:841-848
- 10 Scholmerich J. Immunosuppressive treatment for refractory ulcerative colitis—where do we stand and where are we going. *Eur J Gastroenterol Hepatol*, 1997;9:842-849
- 11 Marshall JK, Irvine EJ. Rectal corticosteroids versus alternative treatments in ulcerative colitis: a meta analysis. *Gut*, 1997;40:775-781
- 12 Pruitt R, Katz S, Bayless T, Levine J. Repeated use of budesonide enema is safe and effective for the treatment of acute flares of distal ulcerative colitis. *Gastroenterology*, 1996;110:A995
- 13 Van-Gossum A, Schmit A, Adler M, Chioccioli C, Fiasse R, Louwagie P, D'Haens G, Rutgeerts P, De-Vos M, Reynaert H, Devis G, Belaiche J, Van-Out-ryve M. Short and long-term efficacy of cyclosporin administration in patients with acute severe ulcerative colitis. Belgian IBD Group. *Acta Gastroenterol Belg*, 1997;60:197-200
- 14 Sutherland LR, May GR, Shaffer EA. Sulfasalazine revisited: a meta-analysis of 5-aminosalicylic acid in the treatment of ulcerative colitis. *Ann Intern Med*, 1993;118:540-549
- 15 Green JR, Lobo AJ, Holdsworth CD, Leicester RJ, Gibson JA, Kerr GD, Hodgson HJ, Parkins KJ, Taylor MD. Balsalazide is more effective and better tolerated than mesalamine in the treatment of acute ulcerative colitis. The Abacus Investigator Group. *Gastroenterology*, 1998;114:15-22
- 16 Truelove SC, Witts LJ. Cortisone in ulcerative colitis: final report on a therapeutic trial. *BMJ*, 1955;2:1041-1048
- 17 Travis SP, Farrant JM, Ricketts C, Nolan DJ, Mortensen NM, Kettlewell MGW, Donlop SP. Predicting outcome in severe ulcerative colitis. *Gut*, 1996;38:905-910
- 18 Wadworth AN, Fitton A. Olsalazine. A review of its pharmacodynamic and pharmacokinetic properties, and therapeutic potential in inflammatory bowel disease. *Drugs*, 1991;41:647-664
- 19 Pullan RD, Rhodes J, Ganesh S, Mani V, Morris JS, Williams GT, Newcombe RG, Russell MA, Feyerabend C, Thomas GA. Transdermal nicotine for active ulcerative colitis. *N Engl J Med*, 1994;330:811-815
- 20 Motley RJ, Rhodes J, Kay S, Morris TJ. Late presentation of ulcerative colitis in ex-smokers. *Int J Colorectal Dis*, 1988;3:171-175
- 21 Gionchetti P, Venturi A, Rizzello F, Corbelli C, Fanti S, Ferretti M, Boschi S, Miglioli M, Campieri M. Retrograde colonic spread of a new mesalazine rectal enema in patients with distal ulcerative colitis. *Aliment Pharmacol Ther*, 1997;11:679-684
- 22 Walker AM, Sznede P, Bianchi LA, Field LG, Sutherland LR, Dreyer NA. 5-Aminosalicylates, sulfasalazine, steroid use, and complications in patients with ulcerative colitis. *Am J Gastroenterol*, 1997;92:816-820
- 23 Kam L, Cohen H, Dooley C, Rubin P, Orchard J. A comparison of mesalamine suspension enema and oral sulfasalazine for treatment of active distal ulcerative colitis in adults. *Am J Gastroenterol*, 1996;91:1338-1342
- 24 Green JT, Thomas GA, Rhodes J, Williams GT, Evans BK, Russell MA, Feyerabend C, Rhodes P, Sandborn WJ. Nicotine enemas for active ulcerative colitis: a pilot study. *Aliment Pharmacol Ther*, 1997;11:895-863
- 25 Garey KW, Streetman DS, Rainish MC. Azathioprine hypersensitivity reaction in a patient with ulcerative colitis. *Ann Pharmacother*, 1998;32:425-428
- 26 Kruis W, Schutz E, Fric P, Fixa B, Judmaier G, Stolte M. Double-blind comparison of an oral *Escherichia coli* preparation and mesalazine in maintaining remission of ulcerative colitis. *Aliment Pharmacol Ther*, 1997;11:853-858
- 27 Travis SP, Tysk C, de-Silva HJ, Sandberg-Gertzen H, Jewell DP, Jarnerot G. Optimum dose of olsalazine for maintaining remission in ulcerative colitis. *Gut*, 1994;35:1282-1286
- 28 Pena AS, Crusius JB. Genetics of inflammatory bowel disease: implications for the future. *World J Surg*, 1998;22:390-393
- 29 Robinson M. Optimizing therapy for inflammatory bowel disease. *Am J Gastroenterol*, 1997;92(12 Suppl):12S-17S
- 30 Rask-Madsen J. From basic science to future medical options for treatment of ulcerative colitis. *Eur J Gastroenterol Hepatol*, 1997;9:864-871
- 31 Rhodes J, Thomas G, Evans BK. Inflammatory bowel disease management. Some thoughts on future drug developments. *Drugs*, 1997;53:189-194

Edited by MA Jing-Yun

# Species differentiation and identification in the genus of *Helicobacter*

HUA Jie-Song, ZHENG Peng-Yuan and HO Bow

**Subject Headings** *Helicobacter*; genus; species; biological features; biochemical tests; identification; differentiation

As early as nineteenth century, incidental presence of spiral organisms was noted in the stomachs of dogs<sup>[1]</sup>, rats and cats<sup>[2]</sup>. In the early years of this century, spiral organisms were also found in the gastric contents of patients with ulcerative carcinoma<sup>[3]</sup>. During the ensuing 30 years, there were scattered reports of these organisms being found in the stomach of patients with benign peptic ulcers. Dogenes<sup>[4]</sup> showed a prevalence of 43% of spiral organisms in a comprehensive autopsy study in 242 human stomach specimens. However, he did not associate the presence of the spiral organism with various gastric diseases.

Controversy existed over the possible role of these spiral organisms in human gastric disease. It was suggested that the bacteria observed in gastric biopsies might represent bacterial contaminants introduced from mouth. This hypothesis gained support with the publication of an extensive histologic study of gastric biopsies from 1000 subjects by Palmer<sup>[5]</sup>. After the publication of the report the interest in gastric bacteria waned.

Interest in the role of gastric bacteria in the pathogenesis of peptic ulcer disease was rekindled when Steer and Colin Jones<sup>[6]</sup> reported the presence of bacteria deep in the mucus layer of gastric mucosa in patients with gastric ulceration. It was suggested that the bacteria might cause a reduction in gastric mucosal resistance via predisposal to ulceration. Attempts to culture this bacterium yielded growth of *Pseudomonas aeruginosa*. Retrospectively, careful examination of the figures in this publication<sup>[6]</sup> suggests that the organism seen on the mucosa is a spiral bacterium, a morphological form not associated with *P. aeruginosa*. It is now assumed that the culture of *P. aeruginosa* by these authors represents a

contaminant cultured from the endoscope. With the discovery of *Helicobacter pylori* by Warren and Marshall<sup>[7]</sup>, it has been shown that *H. pylori* is associated with gastroduodenal disease<sup>[8,9]</sup>.

The spiral organism was first named *Campylobacter pyloridis* in 1984<sup>[10]</sup>. However, the rules of Latin grammar changed the name to *Campylobacter pylori*<sup>[11]</sup>. Ribosomal ribonucleic acid sequences showed that the bacterium did not belong to the *Campylobacter* genus<sup>[12-14]</sup>. In 1989, Goodwin *et al*<sup>[15]</sup> proposed a new genus called *Helicobacter* on the bases of 5 major taxonomic features: ultrastructure and morphology, cellular fatty acid profiles, menaquinones, growth characteristics and enzyme capabilities. *C. pylori* was, therefore, transferred to the new genus and renamed as *Helicobacter pylori*. The major features<sup>[15,29]</sup> of *Helicobacter* genus consist of ① Helical, curved or straight unbranched morphology. ② Gram negative. ③ Endospores are not produced. ④ Rapid, darting motility by means of multiple sheathed flagella that are unipolar or bipolar and lateral, with terminal bulbs. ⑤ Optimal growth at 37°C; growth at 30°C but not at 25°C; variable growth at 42°C. ⑥ Microaerophilic, variable growth in air enriched with 100mL/L -CO<sub>2</sub> and anaerobically. ⑦ External glycocalyx produced in broth cultures. ⑧ Susceptible to penicillin, ampicillin, amoxicillin, erythromycin, gentamicin, kanamycin, rifampin and tetracycline. Resistance to nalidixic acid, cephalothin, metronidazole and polymyxin. ⑨ G+C content of chromosomal DNA of 200mol/L-440 mol/L.

It has been a decade since the genus of *Helicobacter* was created. This genus expands rapidly from at first only two species, viz. *H. pylori* and *Helicobacter mustelae*, to 20 species<sup>[15-35]</sup> and one associated species<sup>[36]</sup> with a wide variety of sources isolated from either human beings and/or different animals. The characteristic details of the *Helicobacter* genus, which might be useful in the differentiation and identification of different *Helicobacter* species in microbiological laboratory, are listed in Table 1, 2, 3 and 4. The genus of *Helicobacter* will surely continue to enlarge as more data of *Helicobacter* features are available and more animal hosts are investigated. Molecular methods, such as PCR, will provide the most accurate tests in differentiation and identification in future with the publication of the genomic library of *H. pylori*<sup>[37]</sup>.

Department of Microbiology, Faculty of Medicine, National University of Singapore, Lower Kent Ridge Road, Singapore 119260, Republic of Singapore

**Correspondence to:** Dr. HUA Jie-Song, Department of Microbiology, National University of Singapore, Lower Kent Ridge Road, Singapore 119260, Republic of Singapore  
Tel. +65-8743285, Fax. +65-7766872  
Email. michuajs@nus.edu.sg

Received 1999-01-16

**Table 1 Locations, key morphological features and growth characteristics of *Helicobacter* species colonizing either humans and/or animals**

Characteristic	<i>H. pylori</i>	<i>H. canis</i>	<i>H. cinaedi</i>	<i>H. felis</i>	<i>H. fennelliae</i>	<i>H. pullorum</i>	<i>H. westmeadii</i>
Host	Human	Dog, human	Human	Cat, dog, human	Human	Poultry, human	Human
Location	Stomach	Intestine	Blood, rectum	Stomach	Intestine	Intestine	Blood
Cell size (µm)	0.5×3.0-5.0	4.0	0.3-0.5×1.5-5.0	0.4×5-7.5	0.3-0.5×1.5-5.0	3×4	0.5×1.5-2.0
Flagella							
Number	4-8	2	1-2	14-20	1-2	1	1
Distribution	Polar	Biopolar	Polar	Biopolar	Polar	Monopolar	Monopolar
Sheath	+	+	+	+	+	-	+
Periplasmic fibers	-	-	-	+	-	-	-
Growth at:							
25°C	-	-	-	-	-	-	-
37°C	+	+	+	+	+	+	+
42°C	-	+	-	+	-	+	-
Growth on:							
10g/L glycine	-	-	+	-	+	-	-
15g/L NaCl	-	-	-	-	-	-	-
Tolerance to:							
10g/L bile	-	+	Vary	-	-	+	-
Safrain 'O'	-	-	-	-	+	-	-
Methyl orange	-	-	+	-	Vary	+	-
Growth under:							
Aerobic conditions	-	-	-	-	-	-	-
Microaerobic conditions	+	+	+	+	+	+	Weak+
Anaerobic	Weak+	-	-	+	-	-	+
Susceptibility to:							
Nalidixic acid	R	S	S	R	S	S	S
Cephalothin	S	S	I	S	S	R	R
Cefoperazone	S	S	S	S	S	R	-
Metronidazole	S	S	S	S	S	-	-

**Table 2 Locations, key morphological features and growth characteristics of *Helicobacter* species colonizing animals**

Characteristic	<i>H. acinonyx</i>	<i>H. bilis</i>	<i>H. bizzozeronii</i>	<i>H. cholecystus</i>	<i>H. hepaticus</i>	<i>H. nuridarum</i>	<i>H. mustelae</i>	<i>H. nemestrinae</i>	<i>H. pametensis</i>	<i>H. rodentium</i>	<i>H. salomonis</i>	<i>H. trogontum</i>
Host	Cheetah	Mice	Dog	Hamster	Mice	Rat, mice	Ferret	Macaque	Bird, swine	Mice	Dog	Rat
Location	Stomach	Bile, live, intestine	Stomach	Gallbladder	live, intestine	Intestine	Stomach	Stomach	Intestine	Intestine	Stomach	Intestine
Cell size (µm)	0.3×1.5-2.0	0.5×4.0-5.0	0.3×5-10	0.5-0.6×3.0-5.0	0.2-0.3×1.5-5.0	0.5×3.5-5.0	0.5-2.5×5.0	0.2×2.0-5.0	0.4-1.5	0.3×1.5-5.0	0.8-1.2×5.0-7.0	0.6-0.7×4.0-6.0
Flagella												
Number	2-5	3-14	10-20	1	2	10-14	4-8	4-8	2	2	10-23	3-7
Distribution	Monopolar	Biopolar	Biopolar	Polar	Biopolar	Biopolar	Peritrichous	Polar	Biopolar	Biopolar	Biopolar	Biopolar
Sheath	+	+	+	+	+	+	+	+	+	-	+	+
Periplasmic fibers	-	+	-	-	-	+	-	-	-	-	-	+
Growth at:												
25°C	-	-	-	-	-	-	-	-	-	-	-	-
37°C	+	+	+	+	+	+	+	+	+	+	+	+
42°C	-	+	+	+	-	-	+	+	+	+	-	+
Growth on:												
10g/L glycine	-	+	-	+	+	-	-	-	+	+	-	-
15g/L NaCl	-	-	-	-	+	-	-	-	-	+	-	-
Tolerance to:												
10g/L bile	-	+	-	+	-	-	-	-	-	-	-	-
Safrain 'O'	-	-	-	-	-	-	-	-	-	-	-	-
Methyl orange	-	-	-	-	-	-	-	-	-	-	-	-
Growth under:												
Aerobic conditions	-	-	-	-	-	-	-	-	-	-	-	-
Microaerobic conditions	+	+	+	+	+	+	+	+	+	+	+	+
Anaerobic	-	-	-	+	+	-	+	Weak+	Weak+	+	-	-
Susceptibility to:												
Nalidixic acid	R	R	R	I	R	R	S	R	S	R	R	R
Cephalothin	S	R	S	R	R	R	R	S	S	R	S	R
Cefoperazone	S	S	S	S	S	S	R	S	S	S	S	S
Metronidazole	S	S	S	S	S	S	S	S	S	S	S	S

**Table 3 Key and differential biochemical characteristics of *Helicobacter* species colonizing either humans and/or animals**

Characteristic	<i>H. pylori</i>	<i>H. canis</i>	<i>H. cinaedi</i>	<i>H. felis</i>	<i>H. fennelliae</i>	<i>H. pullorum</i>	<i>H. westmeadii</i>
Catalase activity	+	-	+	+	+	+	+
Urease activity	+	-	-	+	-	-	-
Oxidase activity	+	+	+	+	+	+	+
Alkaline phosphatase activity	+	+	-	+	+	-	+
γ-Glutamyl transpeptidase activity	+	-	-	+	-	-	-
H <sub>2</sub> S production	-	-	-	-	-	-	-
Indoxyl acetate hydrolysis	-	+	-	-	+	-	-
Hippurate hydrolysis	-	-	-	-	-	-	+
Nitrate reduction	-	-	+	+	-	+	+
C <sub>4</sub> esterase	+	-	+	+	+	-	+
C <sub>8</sub> esterase lipase	+	-	+	-	+	-	+
Leucine arylamidase	+	-	-	+	-	-	+
Acid phosphatase	+	-	+	+	+	-	+
Naphthol-AS-B1-phosphohydrolase	+	-	+	-	+	-	+
DNase activity	+	-	-	+	-	-	-
G+C content (mol%)	35-37	48	37-38	43	37-38	34-35	-

**Table 4 Key and differential biochemical characteristics of *Helicobacter* species colonizing animals**

	<i>H. acinonyx</i>	<i>H. bilis</i>	<i>H. bizzozeronii</i>	<i>H. cholecystus</i>	<i>H. hepaticus</i>	<i>H. muridarum</i>	<i>H. mustelae</i>	<i>H. nemestrinae</i>	<i>H. pametensis</i>	<i>H. rodentium</i>	<i>H. salomonis</i>	<i>H. trogontum</i>
Catalase activity	+	+	+	+	+	+	+	+	+	+	+	+
Urease activity	+	+	+	-	+	+	+	+	-	-	+	+
Oxidase activity	+	+	+	+	+	+	+	+	+	Weak+	+	+
Alkaline phosphatase activity	+	+	+	+	+	+	+	+	+	-	+	-
$\gamma$ -Glutamyl transpeptidase activity	+	+	+	-	+	+	+	+	-	-	+	+
H <sub>2</sub> S production	-	+	-	-	+	-	-	-	-	-	-	-
Indoxyl acetate hydrolysis	-	-	+	-	+	+	+	-	-	-	+	-
Hippurate hydrolysis	-	-	-	-	-	-	-	-	-	-	-	-
Nitrate reduction	-	+	+	+	+	-	+	-	+	+	+	+
DNase activity			+								+	
G+C content (mol%)	30					35		36	24		38	

## REFERENCES

- Bizzozero B. Ueber die schlauchfoermigen Drusen des magendarmkanaals und die beziehung ihrer epithels zu dem oberflaechene epithel der schleimhaut. *Arch F Mikr Anat*, 1893;23:82-152
- Salomon H. Ueber das spirillum des saugtiermagens und sein verhalten zu den belegzellen. *Zentralbl Bakteriell Microbiol Hyg*, 1896;19:433-442
- Krienitz W. Ueber das auftreten von spirochaeten verschiedener form im magenin-halt bei carcinoma ventriculi. *Dtsch Med Wochenschr*, 1906;32:872-876
- Doenges JL. Spirochetes in the gastric glands of macacus rhesus and humans without definite history of related disease. *Proc Soc ExpMed Biol*, 1938;38:536-538
- Palmer ED. Investigation of gastric mucosa spirochetes of the human. *Gastroenterology*, 1954;27:218-220
- Steer HW, Colin-Jones DG. Mucosal changes in gastric ulceration and their response to carbenoxolone sodium. *Gut*, 1975;16:590-597
- Warren JR, Marshall BJ. Unidentified curved bacilli on gastric epithelium in active chronic gastritis. *Lancet*, 1983;1:1273-1275
- Goodwin CS, Armstrong JA, Marshall BJ. Campylobacter pyloridis, gastritis, and peptic ulceration. *J Clin Pathol*, 1986;39:353-365
- Wee A, Kang JY, Toh M. Helicobacter pylori and gastric cancer: correlation with gastritis, intestinal metaplasia and tumor histology. *Gut*, 1992;33:1029-1032
- Marshall BJ, Royce H, Annear DL, Goodwin CS, Pearman JW, Warren JR. Original isolaton of Campylobacter pyloridis from human gastric mucosa. *Biomed Letts*, 1984;25:83-88
- Marshall BJ, Goodwin CS. Revised nomenclature of Campylobacter pyloridis. *Int J Syst Bacteriol*, 1987;37:68
- Lau PP, de Brunner Vossbrinck B, Dunn B, Miotto K, Macdonell MT, Rollins DM. Phylogenetic diversity and position of the genus Campylobacter. *Syst Appl Microbiol*, 1987;9:231-241
- Romaniuk PJ, Zoltowska B, Trust TJ, Lane DJ, Olsen GJ, Pace NR. Campylobacter pylori, the spiral bacterium associated with human gastritis, is not a true Campylobacter sp. *J Bacteriol*, 1987;169:2137-2144
- Thompson LM, Smibert RM, Johnson JL, Krieg NR. Phylogenetic study of the genus Campylobacter. *Int J Syst Bacteriol*, 1988;38:190-199
- Goodwin CS, Armstrong JA, Chilvers T, Peters M, Collins MD, Sly L. Transfer of Campylobacter pylori and Campylobacter mustelae to Helicobacter gen. nov. as Helicobacter pylori comb. nov. and Helicobacter mustelae comb. nov. respectively. *Int J Syst Bacteriol*, 1989;39:397-409
- Hua JS, Ho B. General Microbiology. In: Fan XG, Xia HX eds. *Helicobacter pylori* infection: basic principals and clinical practice. Hunan Science and Technology Press, 1997:7-11
- Eaton KA, Dewhirst FE, Radin MJ, Fox JG, Paster BJ, Krakowka S. Helicobacter acinonyx sp. nov. isolated from cheetahs with gastritis. *Int J Syst Bacteriol*, 1993;43:99-106
- Fox JG, Yan LL, Dewhirst FE, Paster BJ, Shames B, Murphy JC. Helicobacter bilis sp. nov. a novel Helicobacter species isolated from bile, livers, and intestines of aged, inbred mice. *J Clin Microbiol*, 1995;33:445-454
- Hanninen ML, Happonen I, Saari S, Jalava K. Culture and characteristics of Helicobacter bizzozeronii, a new canine gastric Helicobacter sp. *Int J Syst Bacteriol*, 1996;46:839:160-166
- Stanley J, Linton D, Burnens AP, Dewhirst FE, Owen RJ, Porter A. Helicobacter canis. sp. nov. a new species from dogs: an integrated study of phenotype and genotype. *J Gen Microbiol*, 1993;139:2495-2504
- Franklin CL, Beckwith CS, Livingston RS, Riley LK, Gibson SV, Besch-Williford CL. Isolation of a novel Helicobacter species, helicobacter cholecystus- sp. nov. from the gallbladders of Syrian hamsters with cholangiofibrosis and centrilobular pancreatitis. *J Clin Microbiol*, 1996;34:2952-2958
- Paster BJ, Lee A, Fox JG, Dewhirst FE, Tordoff LA, Fraser GJ. Phylogeny of Helicobacter felis sp. nov. Helicobacter mustelae, and related bacteria. *Int J Syst Bacteriol*, 1991;41:31-38
- Fennell CL, Totten PA, Quinn TC, Patton DL, Holmes KK, Stamm WE. Characterization of Campylobacter-like organisms isolated from homosexual men. *J Infect Dis*, 1984;149:58-66
- McNulty CA, Dent JC, Curry A, Uff JS, Ford GA, Gear MW. New spiral bacterium in gastric mucosa. *J Clin Pathol*, 1989;42:585-591
- Hazell SL. Isolation of "Helicobacter heilmannii" from human tissue. *Eur J Clin Microbiol Infect Dis*, 1996;15:4-9
- Fox JG, Dewhirst FE, Tully JG, Paster BJ, Yan L, Taylor NS. Helicobacter hepaticus sp. nov. a microaerophilic bacterium isolated from livers and intestinal mucosal scrapings from mice. *J Clin Microbiol*, 1994;32:1238-1245
- Lee A, Phillips MW, O'Rourke JL, Paster BJ, Dewhirst FE, Fraser GJ. Helicobacter muridarum sp. nov. a microaerophilic helical bacterium with a novel ultrastructure isolated from the intestinal mucosa of rodents. *Int J Syst Bacteriol*, 1992;42:27-36
- Fox JG, Taylor NS, Edmonds P, Brenner DJ. Campylobacter pylori subsp. Mustelae subsp. Nov. isolated from the gastric muscosa of ferrets (Mustela putorius furo), and an emended description of Campylobacter pylori. *Int J Syst Bacteriol*, 1988;38:367-370
- Bronsdon MA, Goodwin CS, Sly LI, Chilvers T, Schoenknecht FD. Helicobacter nemestrinae sp. nov. a spiral bacterium found in the stomach of a pigtailed macaque. *Int J Syst Bacteriol*, 1991;41:148-153
- Dewhirst FE, Seymour C, Fraser GJ, Paster BJ, Fox JG. Phylogeny of Helicobacter isolates from bird and swine feces and description of Helicobacter pametensis sp. nov. *Int J Syst Bacteriol*, 1994;44:553-560
- Stanley J, Linton D, Burnens AP, Dewhirst FE, On SL, Porter A. Helicobacter pullorum sp. nov. genotype and phenotype of a new species isolated from poultry and from human patients with gastroenteritis. *Microbiology*, 1994;140 (Pt12):3441-3449
- Shen Z, Fox JG, Dewhirst FE, Paster BJ, Foltz CJ, Yan L. Helicobacter rodentium sp. nov. a urease negative Helicobacter species isolated from laboratory mice. *Int J Syst Bacteriol*, 1997;47:627-634
- Jalava K, Kaartinen M, Utriainen M, Happonen I, Hanninen M. Helicobacter salomonis sp. nov., a canine gastric Helicobacter sp. related to Helicobacter felis and Helicobacter bizzozeronii. *Int J Syst Bacteriol*, 1997;47:975-982
- Mendes EN, Queiroz DM, Dewhirst FE, Paster BJ, Moura SB, Fox JG. Helicobacter trogontum sp. nov., isolated from the rat intestine. *Int J Syst Bacteriol*, 1996;46:916-921
- Trivett Moore NL, Rawlinson WD, Yuen M, Gilbert GL. Helicobacter westmeadii sp. nov., a new species isolated from blood cultures of two AIDS patients. *J Clin Microbiol*, 1997;35:1144-1150
- Schauer DB, Ghori N, Falkow S. Isolation and characterization of "Flexispira rappini" from laboratory mice. *J Clin Microbiol*, 1993;31:2709-2714
- Tomb JF, White O, Kerlavage AR, Clayton RA, Sutton GG, Fleischmann RD. The complete genome sequence of the gastric pathogen: Helicobacter pylori. *Nature*, 1997;388:539-547

# Transient expression and antigenic characterization of HBsAg of HBV nt551 A to G mutant<sup>\*</sup>

FANG De-Xing<sup>1</sup>, LI Fa-Qing<sup>1</sup>, TAN Wei-Guo<sup>1</sup>, CHEN Hua-Biao<sup>1</sup>, JIN Hui-Ying<sup>1</sup>, LI Su-Qin<sup>1</sup>, LIN Hou-Ji<sup>2</sup> and ZHOU Zhen-Xian<sup>2</sup>

**Subject headings** hepatitis B virus;HbsAg;point mutation;antibodies.monoclonal

## INTRODUCTION

From the late 80s, there have been increasing number of reports on hepatitis B (HB) patients with atypical HBV serological markers, some of them even lack any HBV immunological markers. Analysis of the HBV in those patients demonstrated mutants. Mutations could be found within the C, S, P and X genes<sup>[1]</sup>. The most important S gene mutants are those which affect the antigenicity of HBsAg  $\alpha$  determinant (HBsAg amino acid residue 124 to 147). There are several reports on HBV S gene mutants affecting amino acid position 126, 144 and 145 of HBsAg<sup>[1-3]</sup>. We have described another HBV mutant with a point mutation at nt551 (A to G) of HBV genome, leading to a substitution of Met to Val at amino acid residue 133 of HBsAg<sup>[4]</sup>. In this study, we investigated the antigenicity of the mutant HBsAg by different mAb.

## MATERIALS AND METHODS

The recombinant bacteriophage pM13T was constructed and the mutant HBsAg coding region was sequenced (GenBank accession number AF052576)<sup>[4]</sup>. Construction of the mutant HBsAg expression plasmid pSHBsT and transfection of COS7 cell followed the reference<sup>[1]</sup>. The reactivity of the expressed HBsAg protein to mAb was detected by using a solid RIA kit (Beijing Atomic Energy Institute, China).

## RESULTS

The wild HBsAg<sup>[1]</sup> and mutant HBsAg were expressed under the regulation of SV40 early promoter in COS7 cell in a transient fashion. A mAb against

HBsAg  $d$  determinant (anti- $d$ ), S4 (Shanghai Institute of Biological Products, China), was used for the quantitation of the expressed HBsAg proteins. After a series of dilution and detection, both HBsAg preparations were adjusted to a concentration of 2.1  $\mu\text{g/L}$ .

Three different mAb against HBsAg- $\alpha$  determinant (anti- $\alpha$ ), A6, A11 and S17, from different manufacturers were selected to characterize the binding activity of the expressed HBsAg. Under the condition of the same concentration of HBsAg proteins determined by anti- $d$ , the reactivity of the mutant HBsAg to three anti- $\alpha$  mAb was weaker than that of the wild HBsAg, as shown in Table 1. The result implied that the Met to Val substitution at amino acid position 133 of HBsAg resulted in the alteration of the antigenicity.

**Table 1** Detection of the reactivity of the expressed HBsAg to anti- $\alpha$  mAb by radioimmunoassay<sup>\*</sup>

Anti- $\alpha$ mAb	pSHBs(133Met)	pSHBsT(133Val)
A6	1118(5.82)	774(3.93)
A11	932(4.80)	744(3.76)
S17	945(4.87)	630(3.14)

<sup>\*</sup>Counter per minute (cpm), the number in the parentheses is P/N-value. According to the solid RIA kit producer's instructions,  $P/N = (\text{sample cpm} - \text{background}) / (\text{negative control cpm} - \text{background})$ . Untransfected cells were used as negative control, average cpm was 240. Blank polystyrene beads were used as background, average cpm 58.  $P/N \geq 2.10$  is considered to be positive reactivity. The more the P/N value, the stronger the reactivity.

## DISCUSSION

Since Carman *et al*<sup>[3]</sup> described the HBV immune escape mutant in 1990, many researchers have reported that HBV DNA mutations are related to immune escape, but most of which are limited to the detection by PCR amplification and direct nucleotide sequencing. So far, only the mutant HBsAg with substitution of Ile to Ser at aa126<sup>[1]</sup>, HBsAg with substitution of Asp to Ala at aa144<sup>[2]</sup>, and HBsAg with substitution of Gly to Arg at aa145<sup>[3]</sup> were

<sup>1</sup>Huadong Research Institute for Medical Biotechnics, Nanjing 210002, China

<sup>2</sup>Nanjing Second Hospital, Nanjing 210003, China

<sup>\*</sup>Project supported by Natural Science Foundation of Jiangsu Province, No.BK97188

**Correspondence to:** Dr. FANG De-Xing, Huadong Research Institute for Medical Biotechnics, Nanjing 210002, China  
Tel. +86-25-4542419, Fax. +86-25-4541183

Email: dfang@public1.ptt.js.cn

Received 1998-11-10

characterized in detail. Because the mutation of A to G at nt551 affect the HBsAg  $\alpha$  determinant, it was likely that the mutation could cause immune escape<sup>[4]</sup>. This study showed that the mutation resulted in decreased reactivity of the HBsAg to anti- $\alpha$  monoclonal antibodies, confirming the hypothesis that the HBV is a new immune escape mutant.

The finding of HBV immune escape mutant has caused attention from scientists all over the world. Some experts recommended that it is worth considering to add mutant immunogen (HBsAg) into the future hepatitis B vaccine. But it is very important to know what mutants are immune escape ones and prevalent ones. A mutation specific PCR (msPCR)

method for detecting the mutation at nt551 of HBV genome was established and the investigation and survey of the mutant among child and adult patients is in progress.

#### REFERENCES

- 1 Fang DX, Gan RB, Zhang Q, Li ZQ, Duan SC, Yin Z. Transient expression and antigenic characterization of HBsAg 126Ser of hepatitis B virus aa126 Ile to Ser mutant. *Chin J Virol*, 1998;14:1-9
- 2 Ni F, Fang D, Gan R, Li Z, Duan S, Xu Z. A new immune escape mutant of hepatitis B virus with an Asp to Ala substitution in aa144 of the envelope major protein. *Res Virol*, 1995;146:397-407
- 3 Carman WF, Zanetti AR, Karayiannis P, Waters J, Manzillo G, Tanzi E. Vaccine-induced escape mutant of hepatitis B virus. *Lancet*, 1990;336:325-329
- 4 Fang DX, Lin HJ, Li FQ, Zhou ZX, Tan WG, Wang YL. Nucleotide sequencing of the S gene of a new hepatitis B virus immune escape mutant. *Chin J Microbiol Immunol*, in press.

Edited by MA Jing-Yun

# Experimental study of cholagogic cream for refractory jaundice

GUO Guang-Hua<sup>1</sup>, XU Jian-Heng<sup>2</sup>, SUN Shu-Ming<sup>2</sup>, MA Tao<sup>2</sup>, WU Li-Biao<sup>2</sup>, YANG Yi-Hua<sup>1</sup>, ZHUANG Qing-Wu<sup>1</sup> and JING Xu-Bin<sup>1</sup>

**Subject headings** jaundice; cholagogic cream bile duct stenosis; cholestatic hepatitis

## INTRODUCTION

“The refractory jaundice” in this paper implies the benign icteric disease which was repeatedly treated with either western or traditional Chinese medicine but gave no evidence of improvement, mainly including primary sclerosing cholangitis, intrahepatic sand-like calculi, bile duct stenosis and cholestatic hepatitis etc<sup>[1,2]</sup>. Such diseases are difficult to treat by both traditional Chinese and western medicine. In this study, the cholagogic and anti-inflammatory effects of cholagogic cream, and the combined effects with trepibutone on refractory jaundice were observed and evaluated by experimental pathologic and biochemical examination.

## MATERIALS AND METHODS

### *Ingredients of cholagogic cream*

Dandelion herb 20 g, curcuma root 15 g, Fructus Aurantii 10 g, Sichuan chinaberry 10 g, oriental wormwood 20g, lysimachia 20g, gentian root 10g, Chicken's gizzard-skin-15 g, root bark of the tree peony 15 g, red peony root 15 g, red sage root 20 g, burreed tuber 15 g, zedoary 15 g, rhubarb 10 g, mirabilite 10 g, Herba Lycopi 15 g, earthworm 15 g.

### *Animal experiment*

Thirty-two healthy adult hybrid dogs of either sex (mean weight, 18.1 kg) were selected. The animals were anesthetized intravenously with 2% pentobarbital sodium (30 mg/kg). Epigastric median incision was performed to reveal the common bile duct and hepatic porta. One percent formaldehyde solution was evenly and carefully infiltrated into the ex-

trahepatic bile duct wall with a small needle. The volume depended on appearance of white on the bile duct wall. A mushroom like catheter (a catheter with a mushroom tip) was placed into the gallbladder, fixed on the abdominal wall, and the abdomen was closed after gastrostomy. The appearance of jaundice after one month indicated the success in model preparation.<sup>[2]</sup> The 32 dogs were randomly divided into control group, cholagogic cream group, trepibutone group, and cholagogic cream plus trepibutone group, 8 for each.

### *Route of drug administration*

The medicine was administered through the gastrostomy tube, followed by 1/2 hour observation to make sure that no vomiting occurred.

The administration regimens (1 week) were:

Cholagogic cream plus trepibutone group: cholagogic cream 0.3 g/kg, twice a day; and trepibutone 0.75g/kg, three times a day.

Cholagogic cream group: cholagogic cream 0.3 g/kg, twice a day.

Trepibutone group: trepibutone 0.75 mg/kg, Three times a day.

Control group: normal saline 100 mL, twice a day.

### *Observation methods*

The bile flow from the cholecystostomy tube in 24 hours was recorded at 08:00 every day, and 5 mL bile was taken for viscosity measurement. The remaining bile was transfused back to duodenum via the gastrostomy tube. The bile in the gallbladder was also collected regularly before and after operation for viscosity measurement.

Changes of the serum total bilirubin, direct bilirubin and glutamic-pyruvic transaminase were routinely detected.

The preparation and observation of the scanning electron microscopic sections were carried out in the Center for Computation and Test, Nankai University, Tianjin. Hitachi-650 scanning electron microscope was used, the maximal resolving power was 60A. The paraffin-embedded sections by routine HE staining were observed under optical microscope.

<sup>1</sup>Department of Gastroenterology, <sup>2</sup>Department of General Surgery, First Affiliated Hospital, Medical College of Shantou University, Shantou 515041, Guangdong Province, China

Guo Guang-Hua, male, born on 1950-07-21 in Chaoyang City, Guangdong Province, graduated from Medical College of Shantou University, now an associate professor, having 15 papers published.

**Correspondence to** Dr. Guang-Hua Guo, Department of Gastroenterology, First Affiliated Hospital, Medical College of Shantou University, Shantou 515041, Guangdong Province, China

Tel. +86-754-8258290 Ext. 3387, 3412

Received 1998-11-09

## RESULTS

After therapy, the bile flow showed no significant change in the control group, but dramatically increased in trepibutone group and cholagogic cream group, especially in cholagogic cream plus trepibutone group.

The bile viscosity displayed no significant change in the control group, but dropped significantly in trepibutone group and cholagogic cream group, especially in cholagogic cream plus trepibutone group.

Serum total bilirubin and direct bilirubin were apparently decreased in all the groups except the control group.

Glutamic-pyruvic transaminase (GPT) was significantly decreased in all the groups, especially in cholagogic cream plus trepibutone group, except the control group.

Seven days later, the sections were observed under optical microscope. In the control group, inflammatory cell infiltration occurred in the bile duct wall, especially in the mucous submucous layers. In trepibutone group, inflammatory cell infiltration reduced, but the mucosal exfoliation was obvious. In cholagogic cream group, the inflammatory cells were decreased, and the endoscopic appearance of the gallbladder mucosa returned to normal. In cholagogic cream plus trepibutone group, the inflammatory cells were markedly decreased, and many new mucous membranes were observed.

The mucous membrane of the bile duct was observed under scanning electron microscope for 7 days. It was found that the mucosal membrane was swollen, and the microvilli were exfoliated from the surface of the mucosa in the control group. The edema was markedly alleviated, and the microvilli were quite rare in trepibutone group. A part of the microvilli appeared, and the edema was markedly reduced in cholagogic cream group. The edema was completely resolved and many neoformative microvilli were seen in cholagogic cream plus trepibutone group.

## DISCUSSION

Sclerosing cholangitis, representative of the typical refractory jaundice clinically, served as the icterus model. This experiment found that cholagogic cream possesses a strong cholagogic effect (soothing

the liver and normalizing the function of the gallbladder, eliminating blood stasis and removing obstruction in the meridians, and relieving jaundice), which results mainly from its ingredients such as dandelion herb, lysimachia, oriental wormwood, curcuma root, gentian root and rhubarb. The mechanism might be explained in two aspects. Cholagogic cream, on one hand, can promote the bile secretion from liver cells and bile capillaries, resulting in marked increase of bile flow, and sharp decrease of bile viscosity and serum total bilirubin; and on the other hand, it can also resolve mucosal edema in the bile duct and relax the sphincter, which can be explained by the observation under the scanning electron microscope and change of the serum direct bilirubin. Therefore, it is extremely beneficial to patients with refractory jaundice.

This experiment also proves that cholagogic cream has a strong anti-inflammatory effect (clearing away heat and toxic materials or expelling toxin by cooling, and promoting Qi flow and blood circulation). It could increase the phagocytosis of inflammatory cells by regulating the immunologic function, leading to the elimination of the inflammations in the liver cells and the bile duct wall, which can be proved by the sharp decrease of serum GPT level and the rapid resolution of the inflammation in bile duct wall observed under the optical microscope. The clinical experiences indicated that many refractory jaundices were mutually affected with other hepatic diseases, such as liver dysfunction, hepatic interstitial cells, the bile duct stenosis, edema and inflammation. So, we believe that the cholagogic cream possesses a unique advantage of overall regulation, which is absent in western medicine.

Besides, the combination of cholagogic cream and trepibutone can enhance the effects, the mechanism, beyond profound discussion here, might be complex, but it is certain that the combination of the traditional Chinese and western medicine for refractory jaundice is undoubtedly practicable.

## REFERENCES

- 1 Huang ZQ. Primary sclerosing cholangitis. In: Wu JP, Qiu FZ, eds. *Surgery of Huang Jiashi*. 4th ed. Beijing: People's Health Publishing House, 1979:1269-1271
- 2 Houry S. Sclerosing cholangitis induced by formaldehyde solution injected into the biliary tree of rats. *Arch Surg*, 1990;125:1059-1061

# Application of BRV-R mAbs to detection of corresponding receptors

ZI Zi-Qiang, XU Yan, SUN Wen-Min and REN Zhong-Yuan

**Subject headings** rotavirus; antibodies, monoclonal; IgG

## INTRODUCTION

Rotavirus is a major pathogen of acute gastroenteritis in human infants and young animals. It has been the second cause of infant death especially in developing countries. The infections sometimes occur in adults too. We have used the BRV-R mAb to study the BRV and the BRV-R on MA104 cell surface in three aspects: ① the conjugation test of the BRV-R mAb and rabbit anti-BRV IgG; ② the anti-infectious action of the BRV-R mAb; and ③ the immuno-spot test of the BRV-R mAb.

## MATERIALS AND METHODS

### *Conjugation test of BRV-R mAb and anti-BRV IgG*

**Preparation of rabbit anti-BRV IgG** Virosomes were extracted from the BRV (NCDV strain) suspension concentrated by PEG using ultracentrifugation and observed under electron microscope. Using the virus ( $10^7$ /mL), we prepared the rabbit anti-BRV immune serum. Antibody titre was determined by the complement fixation test. The rabbit anti-BRV IgG was extracted by salting-out method and DE52 chromatographic analysis. Antibody protein was 7.2 g/L measured by Lowry method and was preserved at  $-20^{\circ}\text{C}$ .

**Preparation of ascities BRV-R mAb** The conventional procedure adopted in our lab was used.

### *Conjugation test of BRV-R mAb and rabbit anti-HBV IgG*

ELISA was employed for the detection. The main procedures were: The 96-pore polyethylene plate (America Costor) coated with rabbit anti-BRV IGG (130 mg/L) was incubated for 24 h at  $4^{\circ}\text{C}$ , washed and enclosed. Its horizontal rows were added with doubling diluted ascitic type BRV-R mAb. The first spot of each row was added with diluted fluid as blank control, and the SP<sub>2/0</sub> ascities

was used as a negative control. After that, the plate was incubated, washed and added with goat anti-mouse IgG-HRP. It was then put in substrate fluid for color reaction Bio-RAD (America) 2550 type enzyme linked immune measurer was used to detect A (the OD value,  $\lambda = 492$ ). The titre of BRV-R mAb was determined and the IgG of BRV-R mAb was extracted by DE52.

### *Anti-infectious action of BRV-R mAb*

MA104 strain culture and BRV (NCDV strain) suspension preparation were completed using our own procedure. We set up five control groups: ① the normal MA104 strain; ② BRV; ③ rabbit anti-BRV IgG; ④ BRV-R mAb; ⑤ fluid combined with the rabbit anti-BRV IgG and BRV. Test groups: ① MA104 strain tube was first incubated with BRV-R mAb for 30min at  $37^{\circ}\text{C}$  and then added with BRV (NCDV strain) suspension. It was supplemented with maintenance media after 30min at  $37^{\circ}\text{C}$ ; ② The rabbit anti-BRV IgG and BRV-R mAb were quantitatively mixed, incubated for 30min at  $37^{\circ}\text{C}$ , and then put in the MA104 strain tube. After another 30min at  $37^{\circ}\text{C}$ , it was added to BRV (NCDV strain) suspension. Maintenance media was added in the tube after the third 30min at  $37^{\circ}\text{C}$ . The cells of the control and test groups were cultured at  $37^{\circ}\text{C}$  and CPE was observed.

### *Immuno-spot test of BRV-R*

**Preparation for BRV-R** After routinely cultured, amplified, digested, collected and washed with PBS, the MA104 strain cells were suspended in the 0.01 mol/L PB (pH 7.0), swollen thoroughly at  $4^{\circ}\text{C}$  and mechanically splitted. Supernatant was collected after centrifugation  $1000\times g$  for 5 min and discarded after immersing cell membrane-via-centrifugation  $20\ 000\times g$  for 1 h. Add 3g/L sodium deoxycholate-Tris chlorhydric acid and incubate for 40min at  $4^{\circ}\text{C}$ . After centrifugation  $100\ 000\times g$  for 45min, supernatant was taken, which is BRV-R, and preserved at  $-20^{\circ}\text{C}$ .

**Immuno-spot test** After drying at room temperature, BRV-R was dropped on the pyroxylin membrane (British product) with a total dose of  $30\mu\text{m}$ , and then put in the 10% ovi albumin-0.1 mol/L glucine-Tris chlorhydric acid buffer solution for 1h at  $37^{\circ}\text{C}$  for enclosing. After washing, it was placed into the BRV-R mAb preparation for 1h at  $37^{\circ}\text{C}$ ,

Department of Microbiology, Tianjin Medical University, Tianjin 300070, China

ZI Zi-Qiang, female, professor, engaged in research and teaching of medical microbiology for 28 years and medical virology for 20 years, having about 30 papers published.

**Correspondence to:** Dr. ZI Zi-Qiang, Department of Microbiology, Tianjin Medical University, Tianjin 300070, China

**Received** 1998-10-04

rewashed and added with the goat anti-mouse IgG-HRP conjugate for 1h at 37°C. Substrate solution was added for color reaction and observed with naked eye.

## RESULTS

### *The conjugation test of BRV-R mAb and rabbit anti-BRV IgG*

The positive result was judged if the OD value of the sample was 0.1 higher than that of the negative control determined by ELISA. The conjugation titre of the ascitic type BRV-R mAb and rabbit anti-BRV IgG was 1:5120 and when the BRV-R mAb was extracted by DE52 chromatographic analysis it was 1:2560.

### *Anti-infectious action of BRV-R mAb*

The BRV was inoculated into the MA104 strain cells. The CPE of each group was observed at different time points every day. The result is shown in Table 1.

### *Immuno-spot test*

The result indicated that the BRV-RmAb can combine with the BRV-R, and colored brown, while the control groups showed no color.

**Table 1 The anti-infectious action of the BRV-R mAb**

Groups	CPE at different time point (h)			
	24	48	72	96
Control group 1	-	-	-	-
Control group 2	+	++	+++	++++
Control group 3	-	-	-	-
Control group 4	-	-	-	-
Control group 5	-	-	-	-
Test group 1	-	-	-	+/-
Test group 2	+	++	+++	++++

## DISCUSSION

The conjugation reaction was produced by the rabbit anti-BRV IgG and BRV-R mAb when detecting the plate coated with rabbit anti-BRV IgG using ELISA. The cytoprotection test indicated that the BRV-R mAb was able to prevent the corresponding sensitive cell strain MA104 from being infected by the BRV. We inferred that the BRV-R mAb and BRV shared the correlative antigen determinants, which were related to the BRV-R on the cell surface. The immuno-spot test demonstrated that the antigenicity of the BRV-R on the bovine enteric mucosal cell surface was correlated with that of the BRV-R on the MA104 strain cell surface. To a certain extent, it has laid a basis for purifying the BRV-R on the MA104 strain cells by affinity chromatography, studying its property, and searching the correlative receptors on different tissues and cell surface *in vivo* utilizing labelled BRV-R mAb.

Edited by MA Jing-Yun

# A successful case of combined liver and kidney transplantation for autosomal dominant polycystic liver and kidney disease \*

HE Xiao-Shun, HUANG Jie-Fu, CHEN Gui-Hua, ZHENG Ke-Li and YE Xiao-Ming

**Subject headings** liver; transplantation; kidney transplantation; kidney disease; liver disease

With advances in transplantation, multiorgan transplantation has become a treatment of choice for end-stage organ failure which can not be reversed with other modalities. In 1984, the first case of combined liver and kidney transplantation was introduced by Witts at Innsbruck University Hospital in a 30-year-old man with HBsAg positive cirrhosis. He survived more than 9 years<sup>[1]</sup>. Since then, an increasing number of such combined transplantation has been performed. But in Asia, this technique has not been put into clinical practice yet. We report such a case below.

## CASE REPORT

### Physical examination

A 52-year-old woman was admitted to our hospital with fatigue, jaundice and severe abdominal pain. She suffered from congenital polycystic liver and kidney disease at 40 years of age. Two weeks before her admission, she underwent laparotomy in a local hospital for unbearable abdominal pain. She was found to have anemia and jaundice in physical examination. She had an enormous liver extending to pelvic cavity with an enlarged spleen. Biochemical tests showed hemoglobin 103 g/L, WBC  $3.2 \times 10^9$ /L, platelet  $7.4 \times 10^9$ /L, serum total bilirubin 42.7  $\mu\text{mol/L}$ , albumin 30 g/L, creatine 62  $\mu\text{mol/L}$ , BUN-8.5  $\mu\text{mol/L}$  and prothrombin time 18 seconds (control 12 seconds). The renogram indicated that her renal function had been slightly damaged. Two weeks after her admission, she re-

ceived combined liver and kidney transplantation.

### Procurement of donor organs

The donated liver and kidney were harvested using the rapid multiple organs harvesting technique<sup>[2]</sup>. Both organs were flushed *in situ* and then cold preserved in the Winsconson University solution. Lymphocyte cross-matching was negative and the panel reactive antibody (PRA) was 8%.

### Operative and postoperative course

The liver was transplanted orthotopically using venovenous bypass during anhepatic phase. Following implantation of the liver, the kidney was placed intraperitoneally into the right iliac fossa after 12.5h of cold ischemia. Bile was produced promptly, indicating immediate graft function. The kidney assumed normal color and consistency after revascularization and produced copious amounts of urine. The total operative blood loss was 3500mL, and 2800mL blood products were infused. Immunosuppressive regimen including cyclosporine A, 2mg/kg per day intravenously, and methylpredisone (starting with 1 g per day and tapering to 10 mg daily) was given.

### Results

The early postoperative course was uneventful. The patient was discharged two months after combined liver and kidney transplantation. Six months after transplantation, however, she developed jaundice though her general condition was good. Following the jaundice period, liver function began to show signs of deterioration. The biliary sludge was diagnosed. She was reoperated due to biliary obstruction. The biliary sludge which was 2.0 cm  $\times$  0.5 cm in size located in the middle portion of common bile duct. The patient was soon recovered from the second operation and discharged on the 20th day with nearly normal liverfunction. She is doing well and is in good health.

## DISCUSSION

The high success rate achieved with single organ transplantation has stimulated the assumption of double organ transplantation for patients with complex multiorgan failure. The development of new immunosuppressive agents and improved surgical ap-

Organ Transplantation Centre, First Affiliated Hospital of Sun Yet-Sen University of Medical Sciences, Guangzhou 510080, China

HE Xiao-Shun, MD, PhD, male, born on 1964-09-15 in Anqing, Anhui Province, graduated from Sun Yat-Sen University of Medical Sciences, working as a visiting scholar in University of Sydney and Australian National Liver Transplantation Unit between 1997-1998, now associate professor of surgery, tutor of post graduates, majoring in transplantation surgery, having 20 papers published.

\*Project supported by the National Natural Science Foundation of China, No.39470714

**Correspondence to:** Dr. HE Xiao-Shun, Organ Transplantation Centre, First Affiliated Hospital of Sun Yet-Sen University of Medical Sciences, 58 Zhongshan Erlu, Guangzhou 510080, China  
Tel. +86-20-87755766 Ext. 8753, Fax. +86-20-87750632  
Email sean@gzsums.edu.cn.

Received 1998-11-10

proaches as well as sophisticated postoperative management make assumption become clinical practice.

The main concern in combined liver and kidney transplantation is the selection of candidates. According to Margreiter<sup>[3]</sup>, the indications for combined liver-kidney transplantation are divided into three categories: ① Disease affecting both organs, such as autosomal dominant polycystic disease. ② Renal disorders with liver involvement or liver disorders with renal involvement, including primary type I hyperoxaluria, type I glycogen storage disease, cholesterol acyltransferase deficiency, etc. ③ Separate diseases of both organs. This category consisting of patients on hemodialysis with liver disease and patients with end-stage liver disease and renal function impairment other than hepatorenal syndrome is the main indication for combined liver and kidney transplantation.

Autosomal dominant polycystic kidney disease is often present in newborns, but does not become clinically evident until adulthood. It is often associated with liver cysts which may reach enormous size (in our case, it weighs 5.0kg) and can therefore be extremely disabling considering both the rigors of renal ischemia during transplantation and nephrotoxic effects of cyclosporine A, and some necessitating antibiotics may worsen the previously impaired renal function and lead to postoperative renal failure. We treated the patient with combined liver-kidney transplantation.

The surgical technique of combined liver-kidney transplantation was exactly the same as for transplantation of the liver or the kidney alone. For the reason that liver is more subject to cold ischemia damage than kidney, the liver is generally implanted prior to the kidney. In case a venovenous bypass

should be needed, the axilla and thigh, preferentially on the left side, must be prepared. Because of the poor coagulation status of the recipient, heparin may not be required for prevention of clotting.

A protective role of the liver allografts in the survival of other solid organ transplants has been noted, but the exact mechanism of this phenomenon has not been elucidated. The liver has the potential to protect the other organs immunologically. The efficacy of simultaneous liver-kidney transplantation in the prevention of hyperacute renal rejection in patients with reformed anti-HLA lymphocytotoxic antibodies is also demonstrated in clinical practice. However, these observations have been challenged by reports documenting hyperacute rejection of kidney or/and liver allografts when the roles of ABO matching and donor/recipient crossmatching have been violated<sup>[4-5]</sup>. Although our patient did not experience any rejection and showed some protection of the transplanted kidney by the liver graft, we believe that careful selection of suitable donor with HLA typing crossmatching and PRA test are essential to success in combined liver-kidney transplantation.

#### REFERENCES

- 1 Watts RWE, Calne RY, Williams R. Primary hyperoxaluria (type I): attempted treatment by combined hepatic and renal transplant. *Q J Med*, 1985;57:697-699
- 2 He XS, Huang JF, Chen GH. Clinical orthotopic liver transplantation for the treatment of end stage liver diseases. *Chin J Organ Transplant*, 1996;17:60-62
- 3 Margreiter R. Combined technique. In: Kremer B, Broelsch CE, Henne-Bruns D, eds. Atlas of liver, pancreas, and kidney transplantation. New York: Georg Thieme Verlag Stuttgart, 1994
- 4 Shaked A, Thompson M, Wilkinson AH. The role of combined liver/kidney transplantation in end-stage hepato-renal disease. *Am Surgeon*, 1993;9:606-609
- 5 Eid A, Moore SB, Wiesner RH. Evidence that the liver does not always protect the kidney from hyperacute rejection in combined liver-kidney transplantation cross positive lymphocyte crossmatch. *Transplantation*, 1990;50:331-334

Edited by MA Jing-Yun

# Resection of gastric carcinoma with preservation of pancreas and clearance of lymph nodes along splenic artery: theory, technique and results

LIN Chao-Hong

**Subject headings** stomach neoplasms / surgery; lymph nodes; pancreas / blood supply; splenic artery

## INTRODUCTION

Cancers of whole gastric stomach, cardia, and gastric corpus often metastasize to splenic hylus and lymph nodes along the splenic artery<sup>[1]</sup>. There is ample statistical evidence to support the routine clearance of the lymph nodes along the splenic artery in cases of cancers in whole stomach, gastric corpus, cardia, and in certain invasive cancers in gastric antrum. Beginning from the mid 1940s, many surgeons adopted the procedure of resection of the spleen together with pancreatic body and tail in order to clear the lymph nodes of splenic hylus and along the splenic artery (pancreatic resection procedure). However, combined resection procedure carries the disadvantage of increased operative complication and mortality, and reduction of pancreatic function, especially in insulin output, hence increasing the incidence or aggravating diabetes mellitus. Based on the data and rationale of all those mentioned above, we began in 1968 our research on the operative procedure for gastric cancer, with preservation of pancreatic parenchyma with clearance of lymph nodes along the splenic artery (pancreatic preservation procedure)<sup>[2]</sup>.

## MATERIALS AND METHODS

### *Theoretical grounds of pancreatic preservation*

The lymph flow from the stomach does not enter into the pancreas. By injecting 2ml of methylene blue into the gastric cardia or corpus subserous space during operation, we observed the direction of gastric lymph flow in 54 cases. The direction of cardia lymph flow could be judged from the flow direction during operation and from anatomic examination of lymph nodes specimens. ① The direction of the lymph flow from the gastric cardia is ascending toward mediastinal lymph nodes along the esophageal

wall. ② Lymph from the lesser curvature flows toward the left gastric artery and then into lymph nodes along the celiac artery. ③ Lymph flowing along the short gastric arteries is running away from the greater curvature, and drains into lymph nodes of splenic hylus, then out along the splenic artery and finally to lymph nodes along the celiac artery. ④ Lymph from the posterior gastric wall along the post-gastric artery flows to retroperitoneal space and then into the lymph nodes along the splenic artery at the upper border of pancreas. ⑤ Lymph flowing along esophagocardiac branch of left subdiaphragmatic artery comes from the left side of gastric cardia, and drains to the para-aortic lymph nodes. The direction of lymph flow from the upper gastric corpus, besides being the same as that from cardia, may enter into lymph nodes of the splenic hylus and along the splenic artery via the left gastropiploic artery and its lymph nodes, and finally accumulate into lymph nodes along the celiac artery. Not a single case was found with lymphatic flow entering into pancreatic parenchyma.

It is infrequent for cancers from gastric cardia, gastric corpus, and whole stomach to invade pancreas itself. During the period from 1968 to 1986, in our hospital 439 cases of cancers in gastric cardia, gastric corpus, and whole stomach could be resected, of which 25 (5.7%) cases were found invading into the pancreas. From examination of the resected specimens of pancreatic body and tail in 22 cases, we found that direct invasion of gastric cancer to pancreatic parenchyma and capsule occurred in only 6 cases, with no metastasis to lymph nodes. This result is in agreement with the conclusion of the research on gastric lymphatic flow.

No necrosis of pancreatic body and tail occurred after resection of splenic artery and vein. The pancreatic body and tail is vascularized by pancreatic transverse artery, splenic artery, great pancreatic artery and pancreatic tail artery. The pancreatic transverse artery is the left branch of pancreatic dorsal artery. The splenic artery arises from the celiac artery and gives off 2-10 arterioles supplying the pancreas, one of which is called greater pancreatic artery, located between the middle and distal thirds of the pancreas. The right branch anastomoses with branches from pancreatic transverse artery and the splenic artery and a left branch anastomoses

Department of Surgery, Shanghai Sixth People's Hospital, Shanghai Second Medical University, Shanghai, China

Dr. LIN Chao-Hong, author of 74 papers, professor and postgraduate instructor of Shanghai Second Medical University. Director of the Department of Surgery, Shanghai Sixth People's Hospital, Shanghai 200233, China

**Correspondence to:** Dr. LIN Chao-Hong, Department of Surgery, Shanghai Sixth People's Hospital, Shanghai 200233, China.

Tel. +86-21-64369181

**Received** 1998-09-23

with artery of the pancreatic tail. The artery of the pancreatic tail arises from the distant 1/3 of splenic artery or from the left gastroepiploic artery. The pancreas has an abundant venous anastomosis, with the veins mainly accompanying synonymous arteries. There are 3-13 veins from the pancreatic body and tails (average 7). They drain into the splenic vein, more often into the upper mesenteric vein and upper part of the inferior mesenteric vein or left gastroepiploic vein. There is usually a vein which accompanies the inferior pancreatic artery and drains into the upper mesenteric vein, sometimes into the inferior mesenteric vein or the splenic vein<sup>[3]</sup>. Since about 40% of the pancreatic dorsal artery arises from the first part of the splenic artery, it is enough to resect the splenic artery at the distal end of the pancreatic dorsal artery. The pancreatic body and tail may be supplied by the left branch of the dorsal pancreatic artery, i.e., the transverse pancreatic artery. After resection of splenic vein, the pancreatic body and tail can be drained by transverse pancreatic vein and collateral vein with surrounding tissues several days after operation, therefore necrosis of pancreatic body and tail will not occur.

***Procedure for preservation of pancreatic parenchyma with resection of the splenic artery and vein and pancreatic capsule with surrounding lymphatic and neural connective tissues***

We first resected the omentum with concomitant freeing of the transverse mesocolon to the lower border of pancreas. After clearance of the capsule in front of the pancreas from the lower pancreatic border, the spleno-renal ligament was then resected up to gastric fundus and the left side of the cardia. After lifting up the spleen, we freed the pancreatic body and tail along the retroperitoneal space, and cleared the lymph nodes along the common hepatic artery, celiac artery and the root of left gastric artery together with the attached fatty and connective tissues. After the roots of the left gastric artery and the splenic artery were exposed, these arteries were separated and ligated. If the pancreatic dorsal artery arised from the first part of the splenic artery, one should ligate the splenic artery to the left of the dorsal artery, or when it arised from other arteries at the root of the splenic artery. After the operator changed his position to the left side of the patient, the assistant lifted the spleen and pancreatic body and tail out of the incision and turned them to the right side. After incising the splenic vein sheath, the splenic vein was exposed and resected at the left of the entrance of the inferior mesenteric vein. With slight traction of the severed ends of the splenic artery and vein, the vascular

branches which arose from the splenic artery and entered into the pancreatic parenchyma, the most important of which were the great pancreatic artery and artery of the pancreatic tail, should be freed and ligated. Concomitantly, we resected several venous tributaries arising from the pancreatic parenchyma and draining into the splenic vein. In the end, we freed completely the pancreatic body and tail, the splenic artery and vein, the pancreatic capsule and surrounding lymphatic, fatty, nerve and connective tissues.

By adopting the procedure described above, we found the operation expedient and with less possibility of injuring the pancreatic dorsal artery and inferior mesenteric vein. The lymph nodes and connective tissue were cleared in front of distal splenic vessels and at the periphery from the branch of the distal splenic artery and vein to the root of splenic vessels and finally the pancreatic capsule and splenic artery and vein surrounding lymphatic, fatty, neural and connective tissues were freed from the pancreatic body and tail. The other operative procedure was the same as the radical operation for gastric cancer.

## RESULTS

***Comparison of lymph node metastasis between two different operation groups***

From 1968 to 1992, we performed radical resection of gastric carcinoma by two different techniques, on 216 cases with preservation of pancreas and clearance of lymph nodes along the trunk of splenic artery and 30 cases with resection of pancreas. The metastasis rates of lymph nodes in splenic hylus and those along the trunk of splenic artery were 20.8% (45/216) and 25% (54/216) in the first group, and 20% (6/30) and 23.3% (7/30) in the second group. There was no significant difference statistically ( $P>0.05$ ).

***Comparison of postoperative complication, mortality and survival rates***

In the first operation group (preservation of pancreas), the postoperative complications occurred in 9 (4.2%), diabetes mellitus in 2 (0.9%) and death in 2 (0.9%); and in the second operation group in 12 (40%) diabetes mellitus in 3 (10%) and death in 1 (3.3%). The 5-year survival rates were 57% and 36% and 10-year survival rates were 47% and 30%, respectively. There was significant statistical difference ( $P<0.05$ ) between the two in the incidence of complication, but no marked difference in the mortality rate.

## DISCUSSION

The severe organic deficiency caused by expanded resection of gastric cancer has been of great concern

in recent years. It is a subject of dispute among surgeons that after clearance of lymph nodes along the splenic artery, whether one should adopt the procedure of pancreatic body and tail preservation or resection. After 20 years' research on this subject, we think that pancreatic preservation conforms better to the rationale of radical gastric cancer resection. The reasons are: ① The results of our research on lymphatic flow of gastric cardia and corpus indicated that the direction of the lymphatic flow from those area is along the upper border of the pancreas and the splenic artery, draining to relevant lymph nodes, but not into pancreatic parenchyma. Maruyama<sup>[4]</sup> found no case with gastric lymphatic flow entering into pancreatic parenchyma with preoperative gastroscopic photography after injection of opaque medium into inferior posterior wall of gastric cardia and upper part of gastric corpus and photography of specimens 1 to 5 days later and by injecting dye into gastric subserous space during operation. ② By serial sections of autopsy material of gastric cancer and pancreatic body and tail resected together with gastric cancer, Maruyama<sup>[5]</sup> found that only a small part of gastric cancer lesion invaded pancreas directly from the serous surface without any intrapancreatic lymphatic metastasis. We got the same conclusion from pathologic examination of resected pancreatic body and tail. ③ Maruyama<sup>[5]</sup> adopted the procedure of pancreatic preservation with clearance of lymph nodes along the splenic artery in 76 cases after 1976, with an operative mortality of 1.1%. Various common complications occurred in 25% cases, and pancreatic complication in 6.5%, but not a single case of diabetes mellitus occurred postoperatively. During the same period, Maruyama adopted pancreatic resection procedure in 58 cases and common complications occurred in 59.2% and pancreatic complications in 25%, and postoperative diabetes mellitus in 9.2%, and the operative mortality was 2.6%. In our group of 216 cases, postoperative complication occurred in 4.2%, the mortality rate being 0.9%, and the postoperative diabetes mellitus was found in 0.9%. In 30 cases with resection of pancreas, the postoperative complication occurred in 40%, and the postoperative mortality being 3.3%, postoperative diabetes mellitus in 10%. The incidence of postopera-

tive complications and diabetes mellitus of pancreatic preservation adopted by our group and Maruyama were lower than those applying procedures with pancreatic resection ( $P < 0.05-0.001$ ). The postoperative survival rates after pancreatic preservation operation by our group and Kinoshita, Maruyama<sup>[6]</sup> were higher than those applying pancreatic resection procedure ④. The lymph nodes of splenic hilus and along the splenic artery can be completely removed by pancreatic preservation procedure with resection of spleen, splenic artery and vein, pancreatic capsule, and surrounding lymphatic tissues together with the fatty, nerve and connective tissues. Maruyama<sup>[5]</sup> first cleared the lymph nodes along the splenic artery with preservation of pancreatic parenchyma, then resected the pancreas and the specimens were examined histologically. The result showed that on lymph nodes were left. In summary, the procedure with pancreatic preservation has advantages of easy performance, complete clearance of lymph nodes along the splenic artery, and low incidence of common postoperative complications and diabetes mellitus, and the 5-year survival rates being higher than that with pancreatic resection.

The indications for pancreatic preservation procedure are cancers from gastric cardia, corpus, whole stomach and certain cases with cancer from gastric antrum requiring clearance of lymph nodes along the splenic artery. Patients with preoperative diabetes mellitus or diabetic tendency are indicated absolutely for this procedure. If, however, the cancerous lesion or metastatic lymph nodes have invaded the pancreas parenchyma and Borrmann 4 type carcinoma, the combined resection procedure should be adopted.

## REFERENCES

- 1 Lin CH. Gastric carcinoma study of lymphatic metastasis. *J Abdom Surg*, 1992; 5:43-44
- 2 Lin CH, Wang RS. A new operation procedure method for gastric cancer with preservation of pancreas and clearance of lymph nodes along the splenic artery. *Shanghai Med J*, 1990;13:125-128
- 3 Chen GX. The morphologic basis of abdominal surgery. Fuzhou: Fujian Science and Technology Publishing House. 1981:175-177
- 4 Maruyama K. Lymphatic flow of gastric cardia and metastasis of cancer: a study of endoscopic lymphography. *Stomach & Intestine*, 1978;13:1535-1542
- 5 Maruyama K. A new dissection technique of superior pancreatic lymph nodes: pancreas preserving operation with removal of splenic artery and vein. *Jpn J Gas-trentrol Surg*, 1979;12:961-966
- 6 Kinoshita T, Maruyama K, Sasako M. Lymph node dissection around the splenic artery for gastric cancer: a comparative study of pancreatectomy and pancreas preserving operation. *Nippon Geka Gakkai Zasshi*, 1992;93:128-132

Edited by MA Jing-Yun

# Comparison of serum Zn, Cu and Se contents between healthy people and patients in high, middle and low incidence areas of gastric cancer of Fujian Province \*

LU Hua-Dong<sup>1</sup>, WANG Zhi-Qiang<sup>2</sup>, PAN Yu-Rong<sup>1</sup>, ZHOU Tian-Shu<sup>1</sup>, XU Xi-Zhu<sup>1</sup> and KE Tian-Wang<sup>1</sup>

**Subject headings** stomach neoplasms/etiology; stomach neoplasms/mortality; trace elements/blood; copper/blood; selenium/blood; zinc/blood

## INTRODUCTION

To find out the difference of Zn, Cu and Se contents in the sera between healthy group in high gastric cancer incidence area and in low incidence area, and the difference among healthy, gastric cancer or other tumor groups, we collected 453 serum samples from healthy, gastric cancer or other tumor groups in high gastric cancer incidence areas of Changle and Putian, middle incidence area of Shaxian, and low incidence area of Fuan between 1992 and 1995, and measured and compared the serum contents of Zn, Cu and Se. The results are presented as follows.

## MATERIALS AND METHODS

### Sampling objects

According to the gastric cancer mortality from the data of resident retrospective survey on death causes in 1986-1988, we selected high gastric cancer incidence area Changle with a gastric cancer mortality of  $92.26/10^5$  and Putian with a mortality of  $58.61/10^5$ , middle incidence area Shaxian with a mortality of  $18.86/10^5$  and low incidence area Fuan with a mortality of  $7.76/10^5$ . Samples were collected in terms of sex and age proportion from healthy check-up people in the three areas, and from patients with gastric cancer and other tumors diagnosed by hospitals. Table 1 shows the number of samples collected.

<sup>1</sup>Hygiene and Anti-Epidemic Station of Fujian Province, Fuzhou 350001, Fujian Province, China

<sup>2</sup>Department of Environmental Health, Fujian Medical University, Fuzhou 350004, Fujian Province, China

Dr. LU Hua-Dong, male, born on 1949-11-23 in Quanzhou, Fujian Province, China, graduated from Xiamen University as a postgraduate in 1975, now associate chief technician of environmental and health, having 22 papers published.

\*Supported by "8.5" national major project, No.95-914-01-10.

Correspondence to: Dr. LU Hua-Dong, Hygiene and Anti-Epidemic Station of Fujian Province, Fuzhou 350001, Fujian Province, China  
Tel. +86-591-3707042

Received 1998-10-08

**Table 1** Sample number of different groups among the three areas

Area of incidence	County	Healthy (group I)	Gastric cancer (group II)	Other tumor (group III)
High	Changle	100	41	3
	Putian	52	39	14
Middle	Shaxian	95	14	15
Low	Fuan	49	15	16
Total		296	109	48

### Sampling method

All appliances and recipients were washed carefully and disinfected to avoid contamination during sampling. Blood was collected from veins. Sera were separated by centrifugation of samples and transferred into plastic tubes, sealed up, frozen, then stored at low temperature.

### Sample analysis and measurement

**Cu and Zn** The samples were diluted and contents of Cu and Zn were measured by flame spectroscopy in Pekin-Elmer 5000 atomic absorption spectrophotometer.

**Se** The samples were digested and content of Se was determined by hydride generating method in Pekin-Elmer 5000 atomic absorption spectrophotometer.

### Quality control

To assure the accuracy of analysis, we adopted the strict quality-control measures, i. e. analyzed each batch of samples while analyzing national standard referential material GBW-09 cattle serum.

### Data analysis and statistics

SYSTAM software was used to manage and analyze the data of this survey.

## RESULTS AND DISCUSSION

### Difference of serum microelement contents of healthy group in high, middle and low gastric cancer incidence areas

Results of serum Zn, Cu and Se in healthy people of different areas were analyzed (Table 2).

**Table 2 Serum contents of trace elements in healthy group in high, middle and low gastric cancer incidence areas ( $\bar{x}\pm s$ )**

	<i>n</i>	Zn(mg/L)	Cu(mg/L)	Se( $\mu$ g/L)	Cu/Zn
High (I)	152	0.886 $\pm$ 0.015	0.911 $\pm$ 0.015	84.82 $\pm$ 2.18	1.065 $\pm$ 0.025
Middle (II)	95	0.885 $\pm$ 0.015	0.942 $\pm$ 0.019	84.57 $\pm$ 1.23	1.099 $\pm$ 0.035
Low (III)	152	1.002 $\pm$ 0.019	0.867 $\pm$ 0.032	76.87 $\pm$ 3.22	0.867 $\pm$ 0.033
Analysis of variance		<i>F</i> = 9.326 <i>P</i> = 0.00012	<i>F</i> = 2.479 <i>P</i> = 0.086	<i>F</i> = 2.297 <i>P</i> = 0.102	<i>F</i> = 9.939 <i>P</i> = 0.000066
Newmen-Keul test in comparison of different areas	I:III I:II II:III	<i>q</i> = 5.782 <sup>a</sup> <i>q</i> = 0.0303 <i>q</i> = 5.456 <sup>a</sup>			<i>q</i> = 6.827 <sup>a</sup> <i>q</i> = 0.955 <i>q</i> = 6.105 <sup>a</sup>

<sup>a</sup>*P*<0.01.**Table 3 Contents of Zn, Cu and Se in sera of healthy, gastric cancer and other tumor groups ( $\bar{x}\pm s$ )**

	<i>n</i>	Zn(mg/L)	Cu(mg/L)	Se( $\mu$ g/L)	Cu/Zn
Healthy (I)	294	0.905 $\pm$ 0.010	0.914 $\pm$ 0.011	83.22 $\pm$ 1.32	1.044 $\pm$ 0.018
Gastric cancer (II)	109	0.843 $\pm$ 0.019	1.045 $\pm$ 0.023	73.58 $\pm$ 1.68	1.308 $\pm$ 0.035
Other tumor (III)	48	0.858 $\pm$ 0.028	1.127 $\pm$ 0.040	75.29 $\pm$ 2.33	1.404 $\pm$ 0.078
Analysis of variance		<i>F</i> = 5.137 <i>P</i> = 0.006	<i>F</i> = 29.168 <i>P</i> < 0.00001	<i>F</i> = 9.278 <i>P</i> = 0.000073	<i>F</i> = 35.220 <i>P</i> < 0.000001
Newmen-Keul test in comparison of different groups	I:III I:II II:III	<i>q</i> = 4.305 <sup>a</sup> <i>q</i> = 2.362 <sup>b</sup> <i>q</i> = 0.673	<i>q</i> = 7.660 <sup>b</sup> <i>q</i> = 8.949 <sup>b</sup> <i>q</i> = 3.094	<i>q</i> = 5.852 <sup>b</sup> <i>q</i> = 3.426 <sup>a</sup> <i>q</i> = 0.664	<i>q</i> = 9.423 <sup>b</sup> <i>q</i> = 9.113 <sup>b</sup> <i>q</i> = 2.673

The serum Zn content of healthy group had no difference as compared with that in high incidence area and that in middle incidence area, but was obviously lower than in low incidence area. The ratio of Cu/Zn in high incidence was inconsiderably different from that in middle incidence area, but significantly higher than in low incidence area, the difference being statistically significant. However, no obvious difference was found in serum Cu and Se contents among these areas.

The correlation between contents of Cu and Se in healthy human serums and gastric cancer mortality among different areas was insignificant, but in high incidence area the content of Zn was much lower than in low incidence area and the ratio of Cu/Zn was higher. The result indicated that contents of microelement had a certain relationship with gastric cancer incidence although we could not conclude the contents affected gastric cancer incidence. Because of limited investigation scope, the conclusion was uncertain in a way, nevertheless it provides a clue to further study the causes of gastric cancer.

#### **Comparison of microelement contents in human serum between healthy and gastric cancer groups**

Zn, Cu and Se in the samples collected from healthy, gastric cancer and other tumor groups in

the three areas were measured and the ratio of Cu/Zn was calculated. The results of statistics and analysis are presented in Table 3.

According to Table 3, the serum levels of Zn, Cu and Se and the ratio of Cu/Zn are significantly different statistically between the healthy group and gastric cancer group, however the difference between the gastric cancer group and other tumor group was not significant. Newmen-Keuls test was used in comparison of all groups.

#### **Zn content**

The Zn content in the serum of gastric cancer and other tumor patients was lower than in healthy group, and the difference being statistically significant. However this difference did not exist between gastric cancer group and other tumor groups. Zn was considered one of the necessary compositions of many enzymes in human body, involved in the synthesis of DNA and RNA polymeric enzymes, took part in the nucleic acid metabolism and immunosurveillance protection, affecting the process of cancerization directly or indirectly. Epidemiological studies also indicated that content of Zn in serum of tumor patients was lower than in healthy persons. The results of this study showed that the serum content of Zn was closely related to gastric cancer. Though it was uncertain that there existed a cause and effect relationship. Zn was proved to play an

important role in physiological and biochemical process, disease production and cancerization.

#### ***Cu content***

The Cu content in serums in gastric cancer and other tumor patients was obviously higher than in healthy group, the difference being statistically significant. Though the relationship between Cu and cancer are controversial and the mechanism remained ambiguous, most clinical and experimental studies showed that a large variety of cancers are connected with considerably higher Cu content in serum and enhanced activity of cuprein in plasma. Our results were similar to theirs.

#### ***Ratio of Cu/Zn***

It was reported that contents of Cu and Zn in human serum existed proportionally and affected each other. The determination of ratio of Cu/Zn was helpful for diagnosing many diseases, observing their transformations, preventing recrudescence, and reflected the nutritive status of Zn in human body more effectively than Zn content in serum. It was said that if the ratio was above 2, it would lead to cancerization. The ratio of Cu/Zn in healthy group was markedly lower than in gastric cancer and other tumor groups, with statistically significant difference. In many gastric cancer cases, the ratio exceeded 2, indicating its implication in observing, diagnosing and distinguishing gastric cancer cases. It also provided references on etiology.

#### ***Se content***

Researches on relationship between Se and cancer were popular. Though they did not come to an

agreement in etiology, many epidemiological reports supported that Se content in serum decreased in cancer cases, especially those who suffered from tumors of alimentary canal. Measurement of Se content in serum is of some value in diagnosing and distinguishing the kinds of cancers. Se was one of the necessary composites of glutathione peroxidase (GSH-Px), thus can prevent lipid peroxidation from producing free radicals. Most clinical and experimental studies showed that the activity of GSH-Px in consumptive chronic and cancer patients decreased obviously. Our results indicated the content of Se in serum of gastric cancer and other tumor patients was much lower than in healthy population, with statistically significant difference. Most researches supported such a hypothesis.

#### **CONCLUSION**

A great deal of investigations have demonstrated that contents of Zn, Cu and Se are connected with tumor. Our study indicated that in healthy population, Zn contents in serum and ratio of Cu/Zn had significant differences between high incidence area and low incidence area while contents of serum Se and Cu were similar, and Zn and Cu in sera of gastric cancer patients were found much higher than in healthy population by determining contents of Zn, Cu and Se in 453 serum samples collected from healthy, gastric cancer and other tumor population in high, middle and low incidence areas. Such results were identical to those presented in most epidemiological surveys. The result is of reference value for diagnosing and differentiating tumors, and has provided fundamental data for further investigation on etiology of tumors.

Edited by MA Jing-Yun

# nm23 expression in gastric carcinoma and its relationship with lymphoproliferation

WANG Yang-Kun<sup>1</sup>, JI Xiao-Long<sup>2</sup> and MA Nai-Xu<sup>1</sup>

**Subject headings** stomach neoplasms; nm23 protein; gene expression; lymphoproliferation; lymphocytes

## INTRODUCTION

Tumor spread is a complex biological process closely related to tumor growth, which is regulated by many genes within the cell. Recent studies have revealed that nm23 is intimately related to tumor metastasis in its biochemical nature, structure and function and its regulating role of the gene itself<sup>[1]</sup>. In this study, gene product nm23 expression was performed in 97 cases of gastric cancer and observations were made on its relationship to hyperplasia of lymphatic tissue.

## MATERIALS AND METHOD

Specimens were collected from 97 cases of gastric cancer treated by radical surgery together with 482 enlarged regional lymph nodes (including 214 with reactive hyperplasia and 268 showing cancer metastases). Specimens were fixed in 100mL/L-formalin solution and embedded in paraffin wax. Sections of 4µm in thickness were made and routinely stained with HE stain. In accordance with the literature<sup>[2]</sup>, gastric carcinoma was divided into: stage T1, where cancer tissue invades the mucosa or submucosa; stage T2, with invasion of muscular layer; stage T3, with invasion of serosa; stage T4, with invasion of tissue outside the serosa or of adjacent organs.

### *Observation of lymphocytes surrounding the cancer*

Lymphocytes in the advancing aspect of cancerous invasion were observed but excluding lymphocytes in between cancer nests and the submucosal lymphocytic reaction.

Observations were made separately for each type and each stage of gastric carcinoma.

### *Observation of lymph node metastasis*

Changes were observed in lymph node metastasis, which were into 4 stages<sup>[3]</sup>: Stage 1, structure of lymph nodes is undamaged. Peripheral sinuses or elsewhere show invasion by solitary or multiple cancer cells which may be scattered or form cancerous foci comprised of 3 - 5 cells each; Stage 2, metastatic cancer cells comprise < 1/3 of surface area of section of lymph gland and usually with intact lymph follicles, dilated lymph sinuses filled with cancer cells and an intact lymph node capsule; stage 3, metastatic cancer cells comprise > 2/3 of cross sectional area with intact lymph node capsule; and stage 4, the lymph node and its capsule are both invaded by metastatic cancer cells, or there is invasion of surrounding fibrofatty tissue, muscle fibres, glands etc. with little residual lymphatic tissue.

### *Antibody and staining methods*

One section was randomly selected from the sections made from the 4 pieces of tissue obtained from around the cancer and tested for expression of nm23 gene product using the streptomyces antibiotin peroxidase linkage method (S-P). DAB was used coloration, and haematoxylin for background staining.

## RESULT

Expression of nm23 of gastric carcinoma and results of examination for lymphocytes around the cancer are shown in Table 1.

### *Relationship between expression of nm23 and reactive hyperplasia in lymph nodes*

In each type of gastric cancer showing enhanced expression of nm23, reactive hyperplasia of regional lymph nodes was active, whereas this was diminished in those cases showing negative or weak expression of nm23. High expressivity of nm23 shows positive correlation with the amount of reactive hyperplasia of lymph nodes in the drainage area of the cancer, and the latter was related somewhat with the histological type of tumor. In papillary adenocarcinoma and tubular adenocarcinoma there was a greater amount of reactive hyperplasia, while the hyperplasia was low in adenocarcinoma, with low grade differentiation, mucinous adenocarcinoma and signet ring cell carcinoma.

<sup>1</sup>Department of Pathology, Chinese PLA 91 Hospital, Yanzhou 272000, Shandong Province, China

<sup>2</sup>Department of Pathology, Chinese PLA General Hospital, Beijing 100853, China

**Correspondence to:** Dr. WANG Yang-Kun, Department of Pathology, Chinese PLA 91 Hospital, Yanzhou 272000, Shandong Province, China

Tel. +86-537-3413106 Ext. 63739

Received 1998-07-07

**Table 1 Results of positive expression of nm23, hyperplasia of lymphatic tissue and metastasis in various types of gastric carcinoma**

Type of cancer	Number of cases	Positive expression of nm23 cases (%)	Enlarged lymph nodes (nodes)	Reactive hyperplasia of lymph nodes (nodes)	Cancer metastasis of lymph nodes (nodes)				Lymphocytes around cancer (cases)			
					I	II	III	IV	-	+	++	+++
Papillary adenocarcinoma	8	7(87.5)	34	26	2	4	2	0	1(12.5)	3(37.5)	3(37.5)	1(12.5)
Tubular adenocarcinoma	17	14(82.4)	105	38	4	28	29	6	0(0.0)	3(17.6)	8(47.1)	6(35.3)
Poorly differentiated adenocarcinoma	37	30(81.1)	163	97	2	16	29	19	4(10.8)	7(45.9)	11(29.7)	5(13.5)
Mucinous adenocarcinoma	23	16(69.6)	89	35	1	14	26	13	3(13.0)	12(52.2)	6(26.1)	2(8.7)
Signet ring cell carcinoma	12	9(75.0)	91	18	2	24	32	15	1(12.5)	6(50.0)	5(41.7)	0(0.0)
Total	97	76(78.4)	482	214	1	86	118	53	9(9.3)	41(42.3)	33(34.0)	14(14.4)

**Table 2 Relationship between stage of gastric cancer and expression of nm23 and hyperplasia of lymphatic tissue**

Group	No. of cases	Positive nm23 expression No. (%)	Lymphocytes around cancer cases (%)	Reactive hyperplasia of lymph nodes (nodes)	Metastatic lymph nodes (nodes)
T 1	6	6(100.0)	6(100.0)	48	0
T 2	15	14(93.3)	14(93.3)	52	4
T 3	27	24(85.2)	25(92.6)	63	19
T 4	49	33(67.3)	43(97.8)	51	245
Total	97	76(78.4)	88(90.7)	214	268

### **Relationship between expression of nm23 and lymph node metastasis**

In all types of gastric cancer when positive expression of nm23 protein was enhanced there was generally no spread to the lymph nodes in the drainage area of the cancer. When expression was negative, there was usually metastasis to regional nodes. There was a negative correlation between high expressivity of nm23 and the number and degree of regional lymph node involvement (Table 2).

### **Relationship between expression of nm23 and histological type and depth of infiltration in gastric carcinoma**

There was some relationship between expression of nm23 protein and the histological type of gastric cancer and the depth of invasion. A high positive rate was seen in papillary adenocarcinoma, tubular adenocarcinoma and poorly differentiated adenocarcinoma as compared with mucinous adenocarcinoma and signet ring cell carcinoma, but the difference was not marked ( $P>0.05$ ). Positive rate of nm23 expression decreased as depth of invasion increased. Stages T1 and T2 show marked difference as compared with Stage T4 ( $P<0.01$ ).

## **DISCUSSION**

The appearance of large numbers of lymphocytes around a cancer is the morphological expression of the body's immunological reaction to the tumor.

Tumors can indirectly inhibit the antineoplastic cellular immunity of the host by means of lymphocytes. The degree of inhibition shows a parallel relationship with the degree of malignancy of the tumor<sup>[4]</sup>. A considerable portion of these lymphocytes are immunoresponsive and having lethal activity on tumor cells. They directly prevent tumor growth by releasing lymphokines or through the lethal action of cytotoxins<sup>[5,6]</sup>. Our results are basically the same with those reported in literature. The degree of lymphocytic infiltration around a cancer is related to the stage of the tumor. The covatation degree in the early stage of adenocarcinoma is more serious, and the lymph nodes with reactive hyperplasia are higher in number than those in the late stage. The degree of lymphatic tissue hyperplasia was not significantly related to the age and sex of the patient.

Gene *nm23* is a type identified through the CD-NA archives for low grade metastasing melanoma cell line K-1735 of mice using different hybridization technics. In this gene, the levels of mRNA and the encoded protein are markedly lowered in many experimental tumors of high metastatic phenotype, hence it is considered as a metastasis-inhibiting gene. Human *nm23* gene has two subtypes: *nm23-H1* and *nm23-H2*<sup>[7,8]</sup>, located in human chromosome number 17 in its long arm in the vicinity of the centromere, its encoded product being a 17kD protein composed of 152 aminoacids<sup>[9]</sup>. The relationship between human *nm23* genetic protein and nu-

cleoside diphosphate kinase (N DP K) expression universally present inside cells and tumor spread and prognosis, is still controversial in the literature<sup>[10,11]</sup>. In this group of 97 cases, positive expression is seen in 78.4% which is intimately related to the degree of lymphatic tissue hyperplasia. Lymphocytic infiltration was found around the cancer in 88 cases accounting for 90.7% of the total. Marked surrounding infiltration was seen with positive expression of nm23 in 79% of 14 such cases, while in 9 cases with absence of lymphocytic infiltration, nm23 expression was found in 32.5%, difference being significant between the two groups ( $P < 0.01$ ).

Lymph nodes in the area of drainage of the cancer were presented with a stage of reactive hyperplasia and a stage of metastasis, each showing corresponding characteristic changes in histological structure, and difference in quantity and in degree<sup>[12]</sup>. In this study, the degree of reactive hyperplasia of the regional lymph nodes and lymph node metastasis is related closely to nm23 gene expression. In this group, of the 482 enlarged lymph nodes, 21 had reactive hyperplasia and 268 had metastasis. When reactive hyperplasia is large in number and severe in degree, the positive expression rate of nm23 is increased, if opposite, the rate decreased. When the number of metastatic lymph nodes is large and the degree of involvement is severe, the positive expression of nm23 is reduced, and increased if opposite. This shows that level of expression of nm23 is intimately related to enlargement of lymph nodes in the drainage area. This means specifically, that expressivity of nm23 is in direct ratio to the amount and degree of reactive hy-

perplasia in lymph nodes, but inverse ratio to the number and degree of lymph node involvement in metastasis. It is likely that nm23 gene inhibits the metastatic action of the tumor after cell malignancy transformation. Such close relationship of nm23 with inhibition of tumor spread and the reduction of lymphatic tissue hyperplasia in gastric carcinoma awaits further investigations. Expression of nm23 gene which helps understand hyperplasia and metastasis of lymphatic tissue, and evaluate the depth of invasion of gastric carcinoma provides a useful method in radiotherapy and chemotherapy.

## REFERENCES

- 1 Hennessy C, Henry JA, May FE, Westley BR, Angus B, Lennard TW. Expression of the antimetastatic gene nm23 in human breast cancer: an association with good prognosis. *J Natl Cancer Inst*, 1991;83:281-285
- 2 Liu TH, Li WH. Diagnostic pathology. 1st ed. Beijing: People's Health Press, 1994:68-74
- 3 Wang YK, Ma NX, Wang XL, Sun MG. Histopathological study on the phase of metastatic carcinoma of lymph node and its significance. *Cancer Res Clin*, 1996; 8:76-78
- 4 Ioannides CG, Whiteside TL. T cell recognition of human tumors: implications for molecular immunotherapy of cancer. *Clin Immunol Immunopathol*, 1993; 66: 91-106
- 5 Alexander D, Shiroo M, Robinson A, Biffen M, Shivan E. The role of CD45 in T-cell activation-resolving the paradoxes. *Immunol Today*, 1992;13:477-481
- 6 Fujii Y, Okumura M, Inada K, Nakahara K. Reversal of CD45R isoform switching in CD8+T cells. *Cell Immunol*, 1992;139:176-184
- 7 Steeg PS, Bevilacqua G, Kopper L, Thorgeirsson UP, Talmadge JE, Liotta LA. Evidence for a novel gene associated with low tumor metastatic potential. *J Natl Cancer Inst*, 1988;80:200-204
- 8 Stahl JA, Leone A, Rosengard AM, Porter L, King CR, Steeg PS. Identification of a second human nm23 gene, nm23 H2. *Cancer Res*, 1991;51:445-449
- 9 Backer JM, Mendola CE, Kovacs I, Fairhurst JL, O'Hara B, Eddy RL. Chromosomal localization and nucleoside diphosphate kinase activity of human metastasis-suppressor genes nm23-H1 and nm23-H2. *Oncogene*, 1993;8:497-502
- 10 Cohn KH, Wang FS, Desoto-Lapaix F, Solomon WB, Patterson LG, Arnold MR. Association of nm23-H1 allelic deletions with distant metastasis in colorectal carcinoma. *Lancet*, 1991;338:722-724
- 11 Royds JA, Cross SS, Silcocks PB, Scholefield JH, Rees RC, Stephenson TJ. nm23 'anti-metastatic' gene product expression in colorectal carcinoma. *J Pathol*, 1994;172:261-266
- 12 Wang YK, Fu JB, Liu L, Dong RC. Histopathological study of the reaction hyperplasia of lymph node in the cancer drainage area. *Chin J Clin Oncol*, 1993; 20:723-724

# Clinical significance of Fas antigen expression in gastric carcinoma \*

LIU Hai-Feng<sup>1</sup>, LIU Wei-Wen<sup>1</sup>, FANG Dian-Chun<sup>1</sup>, LIU Feng-Xian<sup>2</sup> and HE Guang-You<sup>2</sup>

**Subject headings** stomach neoplasms/pathology; Fas antigen; lymphatic metastasis; prognosis; immunohistochemistry

## INTRODUCTION

In order to determine whether Fas antigen plays a role in the gastric carcinogenic sequence, an immunohistochemical study of Fas antigen expression in gastric carcinoma and its relation to clinical status, pathomorphological parameters and prognosis was carried out and reported below.

## MATERIALS AND METHODS

### *Histological specimens*

Fifty-nine cases of surgically resected gastric carcinomas (male 37, female 22; mean age 55.6 years) were selected from the files of the Department of Pathology of our hospital. All blocks were fixed in 10% formalin and embedded in paraffin. Serial sections were cut from each block in 4 $\mu$ m, HE stained and confirmed pathologically. All patients underwent curative resection, and followed up for 2.7 to 52 months.

### *Immunohistochemical methods*

Immunohistochemical staining for Fas antigen was performed using SP technique. Slides were deparaffinized and then were hydrated and detected with immunohistochemical kit according to the manual of the manufacturer. The sections were then counterstained with hematoxylin. With each batch of test samples, a positive control consisting of a tissue section from liver was evaluated. A negative control was prepared for each sample using an irrelevant antibody of the same isotype as the primary antibody. The immunostaining of Fas antigen was visually classified into negative and positive groups.

### *Statistics*

Correlations between Fas antigen expression and

<sup>1</sup>Department of Gastroenterology, <sup>2</sup>Department of Pathology, Southwest Hospital, Third Military Medical University, Chongqing 400038, China

Dr. LIU Hai-Feng, Physician in charge, having 18 papers published.

\*Key project of the 9th 5-Year Plan for Medicine and Health of Army, No.96Z047.

**Correspondence to:** Dr. LIU Hai-Feng, Department of Gastroenterology, Southwest Hospital, Third Military Medical University, Chongqing 400038, China

Tel. +86-23-65317511 Ext. 73049

Received 1998-08-27

clinicopathologic parameters were examined using Chi-square test. Survival data was analyzed by a log-rank test.  $P < 0.05$  was considered to be statistically significant.

## RESULTS

### *Expression of Fas antigen in gastric carcinoma*

Twenty-seven (45.8%) of the 50 gastric carcinomas showed immunoreactivity for Fas antigen in gastric carcinoma cells. The Fas antigen immunoreactivity appeared brown or dark brown, which was mainly located in the cytoplasm (Figure 1), a few specimens simultaneously expressed Fas antigen on the cell membrane of tumor cells. Some of the mature lymphocytes infiltrating in the stroma of gastric carcinoma had Fas antigen expression with a strong staining intensity.

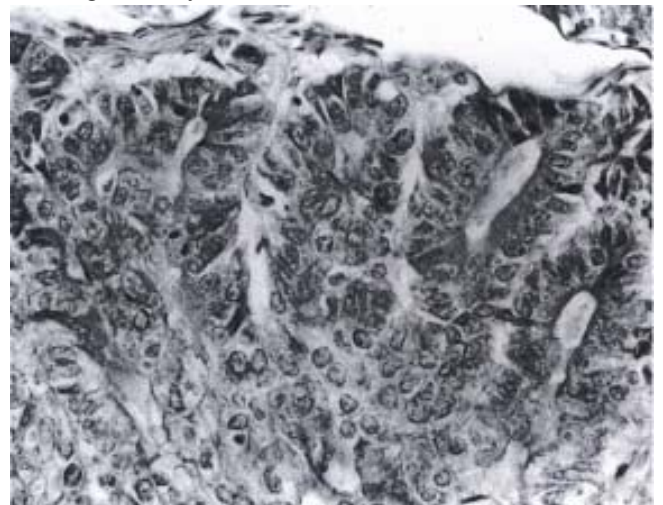


**Figure 1** Immunoreactivity of Fas antigen detected in the cytoplasm of gastric carcinoma cells. SP $\times$ 200

### *Correlation between Fas antigen expression and clinico-pathological parameters of gastric carcinomas*

Fas antigen expression was related to clinical pathological staging of gastric carcinoma. The rate of Fas antigen expression was not correlated with patient age, sex, tumor size, grades of differentiation and depth of invasion ( $P > 0.05$ ). The immunoreactivity of Fas antigen was significantly associated with lymph node status and clinical stages of gastric carcinoma. Sixteen (61.5%) of 26 gastric carcinomas without lymph node metastasis were immunoreactive

versus 11 (33.3%) of 33 cases with lymph node metastasis ( $P<0.05$ ). Twenty-one (58.3%) of 36 gastric carcinomas in clinical stages I and II were immunoreactive versus 6 (26.1%) of 23 gastric carcinomas in clinical stages III and IV ( $P<0.05$ ).

#### **Relationship between Fas antigen expression and prognosis**

The survival rate of patients with Fas antigen expression was compared with that of those without Fas antigen expression. Patients with Fas antigen expression in gastric carcinomas showed a significantly longer survival period as compared with those without Fas antigen expression ( $P<0.05$ ).

#### **DISCUSSION**

Fas antigen is a type I transmembrane protein, its molecular weight is 45 000, and it belongs to the tumor necrosis factor/nerve growth factor receptor family<sup>[1]</sup>. Fas antigen as a receptor exists in the body and can induce a poptosis in target cells. In recent studies, Fas antigen expression has been identified in various human organs, e. g., heart, liver, lung, kidney, and ovary<sup>[2,3]</sup>. But, little is known about Fas antigen expression and its relationship with the biological behavior and prognosis of human gastric carcinoma.

In this study, we found that Fas antigen also expressed in gastric carcinoma tissues. Since Fas antigen is a transmembrane protein, it should appear both on the surface and in the cytoplasm of gastric carcinoma cells. But, in our study, most of the specimens expressed Fas antigen only in the cytoplasm of tumor cells, a few specimens expressed Fas antigen both on the surface and in the cytoplasm of tumor cells. There are several possible explanations for this. First, under pathological conditions, normal Fas antigen expression may be down-regulat-

ed, but expressi on of soluble Fas antigen is up regulated<sup>[4]</sup>. Second, Fas antigen may be affected by mutation on its DNA, or certain abnormalities may occur in the maturation process of this protein. Third, the structure of Fas antigen, which originally expressed on the surface, may be destroyed through a certain mechanism, e. g., its binding site on the membrane undergoes proteolysis, and only cytoplasmic Fas antigen expression remains. However, the mechanism remains to be elucidated in future in vitro studies.

Our findings concerning the relationship between Fas antigen expression and the pathological characteristics of gastric carcinoma showed that Fas antigen expression could relate to lymph node status and clinical stages. The rate of Fas antigen expression was significantly higher in gastric carcinomas without lymph node metastasis than in those with lymph node metastasis, and in clinical stages I and II than in clinical stages III and IV gastric carcinomas. This indicated that aberrant Fas antigen expression may be involved in lymph node metastasis of gastric carcinoma. In addition, the survival period of patients with Fas antigen expression was longer than those without Fas antigen expression. The results demonstrated that Fas antigen expression may be of some value in predicting prognosis in patients with gastric carcinoma.

#### **REFERENCES**

- 1 Nagata S, Goldstein P. The Fas death factor. *Science*, 1995;267:1449-1456
- 2 Higaki K, Yano H, Kojiro M. Fas antigen expression and its relationship with apoptosis in human hepatocellular carcinoma and noncancerous tissues. *Am J Pathol*, 1996;149:429-437
- 3 Leithauser F, Dhein J, Mechttersheimer G, Koretz K, Bruderlein S, Henne C. Constitutive and induced expression of APO-1, a new member of the nerve growth factor/tumor necrosis factor receptor superfamily, in normal and neoplastic cells. *Lab Invest*, 1993;69:415-429
- 4 Cheng J, Zhou T, Liu C, Shapiro JP, Brauer MJ, Kiefer MC. Protection from Fas-mediated apoptosis by a soluble form of the Fas molecule. *Science*, 1994;263:1759-1762

# Distribution of nitric oxide synthase in stomach wall in rats

PENG Xi, FENG Jing-Bin and WANG Shi-Liang

**Subject headings** stomach/ physiology; nitric oxide synthase/analysis

## INTRODUCTION

It has been shown that neuronal nicotinamide adenine dinucleotide phosphate-diaphorase (NADPH-d) may correspond to the neuronal nitric oxide synthase (NOS), and may be used as a marker for NOS in the central and peripheral nervous system. Thus, NADPH-d histochemistry provides us with a mean to specifically identify neurons producing nitric oxide (NO)<sup>[1,2]</sup>.

Recent pharmacological and physiological studies demonstrated that NO is a neurotransmitter in the non-adrenergic non-cholinergic (NANC) inhibitory nerves in the mammalian gastrointestinal tract. It may play a very important role in the neuronal regulation of gut. NOS activity is present in neurons and fibers of the major enteric nerve layer in intestine<sup>[3]</sup>. However, there have been far fewer studies of NOS activity in stomach wall. If NO is a transmitter of NANC in inhibitory nerves, it should be present in neurons innervating the muscularis. What proportion of nerves produce NO? What is the pattern of innervation of these neurons? To answer these questions, we examined the distribution and morphological feature of NOS positive neurons in the stomach wall with improved whole mount preparation technique.

## MATERIALS AND METHODS

Adult male Wistar rats weighing 210g-250g were provided by the Center of Laboratory Animals of our university. The experimental rats were fasted overnight prior to the experiment, and anaesthetized with sodium pentobarbitone (50 mg·kg<sup>-1</sup>, ip). Stomach was excised and rinsed with PBS and dipped in 40 mL/L paraformaldehyde for 4 h, then stored in 200 g/L sucrose in PBS for 48 h at 4°C. Thereafter, whole mount preparations were made, and histochemistry staining of NADPH-d and control test were performed as previously reported<sup>[4]</sup>.

Institute of Burn Research, Southwest Hospital, Third Military Medical University, Chongqing 400038, China

Dr. PENG Xi, male, born on 1968-10-21 in Beijing, graduated from Third Military Medical University, with a master degree of surgery, having 10 papers published.

**Correspondence to:** Dr. PENG Xi, Institute of Burn Research, Southwestern Hospital, Third Military Medical University, Chongqing 400038, China

Tel. +86-23-68753479

Received 1998-11-09

## Statistical analysis

All results were expressed as the  $\bar{x} \pm s$ , and data were analyzed by Student's *t* test. *P* values <0.05 were considered statistically significant.

## RESULTS

Our study showed that NOS was widely distributed in the gastric wall, and most of them were located in the myenteric plexus, and distributed in submucosal plexus, gastric mucosal epithelium and gastric gland. In the myenteric plexus, the cytoplasm of the NOS positive neurons completely labelled except for the nucleus. The cell body shape was basically similar, most of them shaped round, oval or fusiform while their density, size and staining intensity varied greatly in the different parts of stomach. The density was (62 ± 38) cells/mm<sup>2</sup>, (43 ± 32) cells/mm<sup>2</sup> and (32 ± 28) cells/mm<sup>2</sup> respectively in the antrum, body and fundus (*P*<0.01). Two subtypes of NOS positive neurons could be distinguished on the basis of size, staining intensity and number of processes. In fundus, about 75% neurons were large, and dark-stained. Neurons of the second subtype were slightly smaller, with only one or two processes and were mainly located in the antrum (approximately 65%). In the body of stomach, the character of NOS positive neurons was an intermediate state from fundus to antrum.

## DISCUSSION

The results of our experiment provide the first morphological evidence for the presence of NOS positive neurons in the stomach myenteric plexus. Nerve bundles also contained a large number of reactive fibers. Many bead-like structures strung together by NOS positive varicosities in nerve fibers, some were closely adherent to the outer walls of blood vessels and smooth muscle fibers. This finding has provided morphological evidence of NO involved in the modulation of motility and blood circulation of gastrointestinal tract. The significant difference of the distribution of NOS positive neurons among the myenteric plexus in different parts of the stomach may be related to the physiological function of the stomach.

## REFERENCES

- 1 Richard B, Lynn M, Suzanne L, Crook WJ. Colocalization of NADPH-d staining and VIP immunoreactivity in neurons in opossum internal anal sphincter. *Dig Dis Sci*, 1995;40:781-788
- 2 Barbier M, Timmermans JP. NADPH-diaphorase and nitric oxide synthase colocalization in enteric neurons of pig distal colon. *Microsc Res Tech*, 1994;29:78-85
- 3 Konturek SK, Konturek PC. Role of nitric oxide in the digestive system. *Digestion*, 1995;56:1-13
- 4 Peng X, Feng JB, Wang SL. The methods of display myenteric plexus of stomach in rats. *Chin J Anat*; 1999;22:72-73

Edited by MA Jing-Yun

# Appearance of an inhibitory cell nuclear antigen in rat and human serum during variable degrees of hepatic regenerative activity

N Assy<sup>1,2</sup>, YW Gong<sup>3</sup>, M Zhang<sup>3</sup> and GY Minuk<sup>3,4</sup>

**Subject headings** liver regeneration; hepatectomy; inhibitory cell nuclear antigen; cross-reacting protein; antibodies, monoclonal; proliferating cell nuclear antigen

## Abstract

**AIM** To determine whether proliferating cell nuclear antigen (PCNA) is present in the peripheral circulation and whether PCNA levels correlate with enhanced regenerative activity.

**METHODS** In animal studies, adult male Sprague-Dawley rats ( $n = 3-4/\text{group}$ ) were sacrificed at 0, 12, 24, 36, 48, 72 and 96 hours following 70% partial hepatectomy. At each interval, sera were analyzed by Western blot for PCNA by two monoclonal antibodies (PC-10 and 19F-4). In human studies, sera from 4 patients with liver cirrhosis and 4 healthy controls were tested in a similar manner.

**RESULTS** The PC-10 monoclonal antibody identified a protein with a molecular mass of 120 KD which remained stable in rat sera for 24 hours following partial hepatectomy, then increased 1.5-fold at 48 hours prior to returning to baseline at 96 hours after partial hepatectomy. However, it was not detected in the sera of patients with or without liver disease. In the 19F-4 monoclonal antibody, a protein with a molecular mass of approximately 46 KD was found, which was present in rat sera prior to partial hepatectomy and for 12 hours after surgery. Thereafter, levels fell by approximately 50% at 24 hours, 65% at 36 hours and 75% at 48 hours where they remained until 96 hours after partial hepatectomy. The de-

crease in levels correlated with the extent of partial hepatectomy. In human sera, the appearance of this inhibitory cell nuclear antigen (ICNA) was higher in the sera of patients with cirrhosis than in healthy controls.

**CONCLUSION** The PC-10 monoclonal antibody can detect a protein in the circulation when active hepatic regenerative activity is taking place. The 19F-4 monoclonal antibody, however, identifies a protein in both rat and human sera that inversely correlates with hepatic regenerative activity. This protein which is tentatively referred to as inhibitory cell nuclear antigen (ICNA) may be used in documenting the extent of suppression of hepatic regeneration.

## INTRODUCTION

Serologic markers of hepatic regenerative activity are lacking. Those that are available (ornithine decarboxylase, thymidine kinase and alpha-fetoprotein levels) correlate with enhanced regenerative activity and only appear when the stimulus to regeneration is significant (large partial hepatectomies)<sup>[1]</sup>. To date, serologic markers of attenuated hepatic regenerative activity has yet been identified. In this study, we set out to determine whether proliferating cell nuclear antigen (PCNA) might serve as a more sensitive marker of enhanced hepatic regenerative activity than presently available enzymatic assays.

PCNA is a 261 amino acid nuclear protein that has been identified as an auxiliary protein of DNA polymerase delta and is involved in the progression of cell cycle and DNA synthesis<sup>[2,3]</sup>. Monoclonal antibodies to PCNA are increasingly used for evaluation of cell proliferation in situ<sup>[4,5]</sup>. Of the 17 known monoclonal antibodies to PCNA, PC-10 and 19F-4 are two of the most commonly used ones<sup>[6,7]</sup>. Recently, using the PC-10 and the 19F-4 monoclonal antibodies, we demonstrated that tissue levels of PCNA correlate well with hepatic regenerative activity when compared with PCNA immunostain-

<sup>1</sup>Liver Unit, Rambam Medical Center, Haifa, <sup>2</sup>The Bruce Rappaport Faculty of Medicine, Technion-Israel Institute of Technology, Haifa, Israel and <sup>3</sup>Liver Diseases Research Laboratory, <sup>4</sup>Liver Diseases Unit, Departments of Medicine & Pharmacology, University of Manitoba, Winnipeg, Manitoba, Canada

**Correspondence to:** Nimer Assy, MD, Fassouta, Upper Galilee 251 70, P.O.Box 428, Israel

Tel. +972 • 4 • 9870 • 080 Fax. +972 • 4 • 9870 • 080

E-mail. drnimer@netvision.net.il

Received 1999-03-02

ing, [<sup>3</sup>H] thymidine incorporation into DNA and other markers of hepatic regenerative activity<sup>[8]</sup>.

In the present study, we employed both the PC-10 and 19F-4 monoclonal antibodies in an attempt to determine whether circulating PCNA levels correlate with regenerative activity in rats following partial hepatectomy and in humans with various forms of liver diseases.

## MATERIAL AND METHODS

### *Animals and surgery*

Adult male Sprague-Dawley rats (250 g/body-300 g/body weight) were maintained on Purina rat chow and water ad libitum until the day prior to surgery. All animals were kept in similar housing units on a 12 h light and 12 h dark cycle. Thirty and 70% partial hepatectomies were performed under light ether anesthesia between 9:00 a.m. and noon each day according to the methods of Higgins and Anderson<sup>[9]</sup>. Sham operations in which appropriate portions of the liver were exteriorized for the same length of time as rats undergoing partial hepatectomy were also carried out. Blood samples (1 mL-2 mL) were taken from groups of rats ( $n = 3-4$ /group) at the time of death by exsanguination at 0, 12, 24, 48, 72 and 96 hours after surgery. Sera from the samples were stored at -20°C until batch tested. Sera were also collected from 4 patients with histologic evidence of liver cirrhosis (2 HBV, and 2 HCV related) and from 4 healthy laboratory volunteers.

### *Immunoblotting*

Equal amounts of serum protein (100 µg/lane) as quantified by the Lowry method<sup>[10]</sup>, were passed through a 10% SDS-PAGE at 100V for two hours at room temperature. Resolved proteins were transferred electrophoretically to nitrocellulose (Bio-Rad, Hercules, CA) at room temperature for one hour at 100V in a buffer containing 25mM-glycine, 192mM Tris, and 20% methanol. Nonspecific binding of the antibodies to the membranes was diminished by preincubating the blots in TBS (50mM-Tris-HCl and 150mM-NaCl, pH 7.4) in the presence of 3% dry milk for one hour at room temperature. Blots were incubated with PC10 monoclonal antibody (1:500, DAKO Corporation, Carpinteria, CA) and 19F4 monoclonal antibody (1:500, Boehringer Mannheim, Germany) in TBS containing 0.5% dry milk and 0.1% Tween-20 (Bio-Rad, Hercules, CA) at 4°C for 16 hours followed by peroxidase-labeled anti-mouse antibody (1:500 dilution, Amersham, Quebec) in the same buffer at room temperature for one hour. After each incubation,

blots were washed twice with TBS containing 0.1% Tween-20 for 10 minutes. Immunoreactive bands were visualized using an enhanced chemiluminescence kit (ECL, Amersham, Quebec). Films were scanned by a PC scanner and the optical densities (OD) determined by an NIH.IMAGE program (NIH, Bethesda, Maryland).

### *Statistics*

Data were presented as means ± SD. Differences between groups and differences over time were analyzed using the Man-Whitney test, repeated measure analysis of variance and Kruskal-Wallis analysis where appropriate. *P* values less than 0.05 were considered significant.

## RESULTS

Figure 1 provides the results of 19F-4 protein determinations in rat sera following partial hepatectomy. As reported elsewhere, the molecular mass of the 19F-4 protein was 46KD. In sham operated rats, 19F-4 levels remained unchanged throughout the study. However, in partial hepatectomized rats, 19F-4 levels fell significantly to a nadir of approximately 50% baseline values at 24 hours after partial hepatectomy ( $P < 0.001$ ). Thereafter, levels remained low until 96 hours when they returned to baseline. Figure 2a shows the results of serum 19F-4 levels following various degrees of partial hepatectomy at 48 hours after surgery. Levels were lowest in rats having undergone 70% partial hepatectomy, highest in sham operated controls and intermediate in the 30% partial hepatectomy group ( $P < 0.05$ ). Finally, in the human sera, 19F-4 was again identified at 46KB, but levels were significantly higher in cirrhotic patients than in healthy controls (Figure 2b,  $P < 0.05$ ).

The results of sera PC-10 protein determinations are shown in Figure 3. The molecular mass of PC-10 was 120KD. Serum levels remained relatively constant for 24 hours prior to a gradual increase of approximately 1.5 times baseline at 48 hours following partial hepatectomy ( $P < 0.05$ ). Serum levels of PC-10 were not detected in either cirrhotic patients or healthy controls.

## DISCUSSION

Two proteins were described in rat sera that crossreact with monoclonal antibodies to proliferating cell nuclear antigens. The results also indicate that the levels of these crossreacting proteins changes significantly following partial hepatectomy and in the case of 19F4.4, they change inversely in proportion to the extent of partial hepatectomy. They are also

higher in sera of cirrhotic patients as compared with healthy controls.

The cross reactivity reported here does not represent an isolated phenomenon with such antibodies. Waseem et al reported that PC-10 reacted with a faint band at 120KD besides reacting with 36KD protein HeLa cell<sup>[6]</sup>. However, no investigation of the functional role of this crossreacting protein was given in a model of liver regeneration, neither was this protein documented in the blood previously. The fact that PC-10 protein increased significantly at 48 hours after partial hepatectomy stresses its possible role as a marker of liver regeneration in the blood. Whether the crossreactivity is due to direct binding to the immunogenic peptide of new proteins or involve secondary changes of the PCNA molecule (degradation product) with difference in the amino acid sequences of the immunogenic protein is unknown.

A similar crossreactivity has been shown with other monoclonal antibodies especially when used with different concentrations<sup>[11-13]</sup>. However, the concentration of the monoclonal antibodies used here were the same as used previously in the liver tissues and in which no crossreacting proteins were seen<sup>[8]</sup>. Thus, differences in concentration are unlikely responsible for the crossreactivity observed here. Another possibility is that the crossreactivity is due to the binding of the secondary antibody (anti-mouse IgG) with the protein, however incubation of the membrane with secondary antibody alone did not reveal the above crossreacting protein suggesting that the crossreactivity is due to the presence of monoclonal antibodies.

It must be appreciated that identical or closely related similar epitopes may occur on otherwise unrelated protein<sup>[11]</sup>. The 19F-4 protein expression shown here may reflect a profile of an inhibitory protein during liver regeneration.

Three explanations are in favor of the above hypothesis. First, it decreased sharply to reach a nadir level at 24-36 hours after partial hepatectomy, a period that corresponded to the peak of DNA synthesis<sup>[14]</sup>. Second, the 19F-4 protein was expressed more in the sera of patients with cirrhosis than in the sera of normal persons. Finally, and most importantly, the fact that 19F-4 protein expression decreased significantly with the extent of hepatic resection may reflect its possible role as an inhibitory protein which is synthesized by the liver.

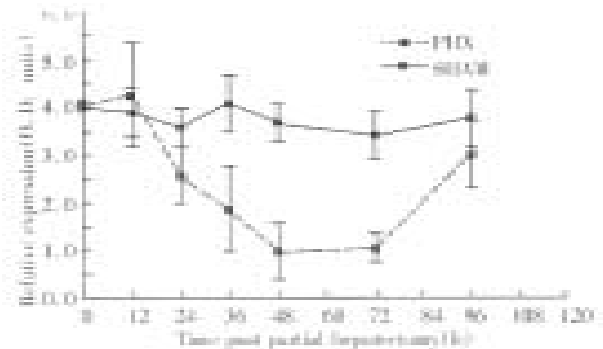


**Figure 1** Expression of 19F-4 protein (ICNA) in rat sera at different time intervals following 70% partial hepatectomy and in sham operated rats. The molecular mass of the 19F-4 protein was 46KD.  $P < 0.001$  between both groups at 24, 36, 48 and 72 hours post PHX.

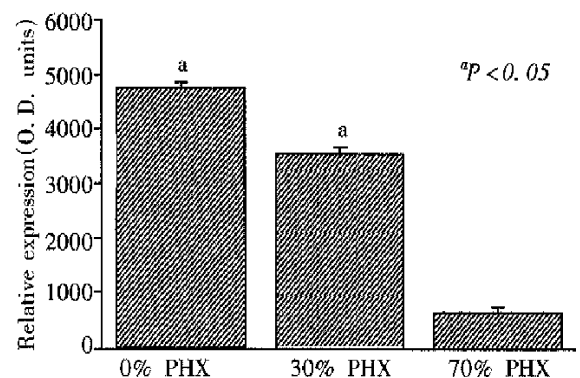


**Figure 2a** Serum 19F-4 protein levels following various degrees of partial hepatectomy at 48 hours post surgery.  $^aP < 0.05$ .

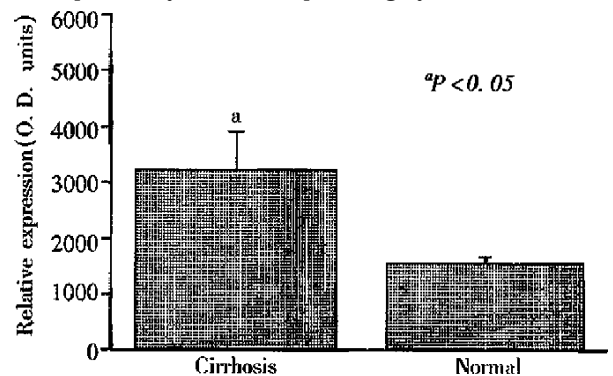


**Figure 2b** 19F-4 levels in the human sera of 4 cirrhotic patients as compared to 4 healthy controls.  $^aP < 0.05$ .

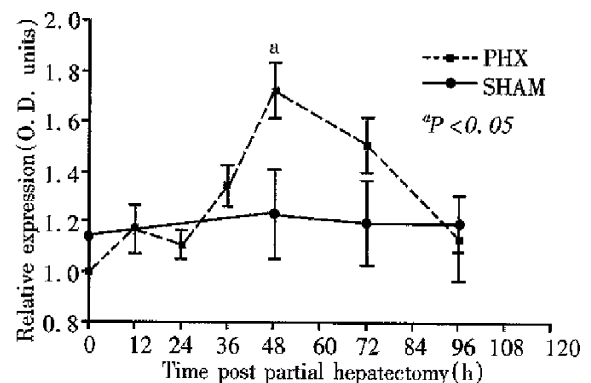


**Figure 3** Expression of PC-10 protein in rat sera following 70% partial hepatectomy and in sham operated rats. The molecular mass of PC-10 was 120KD.  $^aP < 0.05$  at 48 hours post PHX.

It has been established that the 19F-4 and PC-10 reacts with a protein region of 14 at length<sup>[15]</sup>. The reasons why both monoclonal antibodies detect the same PCNA protein at a molecular mass of 36KD in the liver tissue while each detect or immunoreact with different molecular mass protein in the blood, is unknown (PC-10-120KD and 19F-4-46KD). Theoretically, the unsophisticated epitopes recognized by these monoclonal antibodies might be present in another protein in the blood. One explanation for the inability of PC-10 to recognize the peptide recognized by 19F-4 in the blood is the length of the protein. In a recent mini-review, Laver *et al* stressed that conformational epitopes on native proteins are comprised of 15-22aa residues<sup>[16]</sup>.

One could suggest that the early appearance of 19F-4 protein followed by a decrease at 24 hours after partial hepatectomy reflect a parameter of injury or represent an acute phase reactant protein rather than being related to the process of growth after partial hepatectomy. However, the appearance of the protein in the serum of sham rats argues against this possibility, moreover, the presence of such a protein in the serum of normal persons, also argue against this hypothesis.

## CONCLUSION

PC-10 crossreacting protein (120KD) correlates positively with the regenerative rate after 70% partial hepatectomy whereas 19F-4 protein correlates negatively. The 19F-4 (46KD) protein is clearly of interest in that it is a cell cycle dependent protein, being undetectable in the serum during rapidly dividing cells, prominent in the serum of intact normal liver and more prominent in the serum of patients with liver cirrhosis. Crossreacting proteins detected by monoclonal antibodies are not always non-specific and fortuitous but may have an important role in clinical biology. Ongoing studies to isolate and se-

quence the corresponding protein are under investigation.

## REFERENCES

- 1 Fausto N. Hepatic regeneration. In: D Zakim, TD Boyer, eds. *Hepatology: a textbook of liver disease*. Philadelphia: W.B. Saunders, 1990:49-62
- 2 Prelich G, Tan CK, Kostura M, Mathews, MB, So AJ, Downey KM, Stillman B. Functional identity of proliferating cell nuclear antigen and a DNA polymerase-delta auxillary protein. *Nature (Lond)*, 1987;326:517-520
- 3 Jaskulski D, DeRiel JK, Mercer WE, Calabretta B, Baserga R. Inhibition of cellular proliferation by antisense oligodeoxynucleotides to PCNA cyclin. *Science*, 1988;240:1544-1546
- 4 Yang CL, Zhang SJ, Toomy NL, Palmer TN, Lee M. Induction of DNA polymerase activity in the regenerating rat liver. *Biochemistry*, 1991;30:7534-7541
- 5 Theocharis SE, Skopelitou AS, Margeli AP, Pavlaki KJ, Kittas C. Proliferating cell nuclear antigen (PCNA) expression in regenerating rat liver after partial hepatectomy. *Dig Dis Sci*, 1994;39:245-252
- 6 Waseem NH, Lane DP. Monoclonal antibody analysis of the proliferating cell nuclear antigen (PCNA): Structural conservation and the detection of a nucleolar form. *J Cell Sci*, 1990;96:121-129
- 7 Ogata K, Ogata Y, Nakamura Y, Tan EM. Monoclonal antibodies to a nuclear protein (PCNA/CYCLIN) associated with DNA replication. *Expl Cell Res*, 1987;168:475-486
- 8 Assy N, Gong YW, Zhang M, Minuk GY. The use of proliferating cell nuclear antigen as a marker of liver regeneration following partial hepatectomy in rats. *J Lab Clin Med*, 1998;131:251-256
- 9 Higgins GM, Anderson RM. Experimental pathology of the liver: Restoration of the liver of the white rat following partial surgical removal. *Arch Path*, 1931;12:186-201
- 10 Lowry OH, Rosebrough NJ, Farr AL, Randall RJ. Protein measurement with the folin phenol reagent. *J Biol Chem*, 1951;193:265-275
- 11 Nigg EA, Walter G, Singer SJ. On the nature of crossreaction observed with antibodies directed to defined epitopes. *Proc Nat Acad Sci USA*, 1982;79:5939-5943
- 12 Dulbecco R, Unger M, Bologna M, Battifor A, Syka P, Okada S. Crossreactivity between THY-1 and a component of intermediate filaments demonstrated using a monoclonal antibody. *Nature*, 1981;292:772-774
- 13 Lane DP, Hoeffler WK. SV 40 large T shares an antigenic determinant with a cellular protein of molecular weight 68000. *Nature*, 1981;288:167-170
- 14 Grisham JW. A morphologic study of DNA synthesis and cell proliferation in regenerating rat liver, autoradiography with thymidine-H3. *Cancer Res*, 1961;22:842-849
- 15 Roos G, Landberg G, Huff JP, Houghten R, Takasaki Y, Tan EM. Analysis of the epitopes of proliferating cell nuclear antigen recognized by monoclonal antibodies. *Lab Invest*, 1993;68:204-210
- 16 Laver WG, Air GM, Webster RG, Smith-Gill SJ. Epitopes on protein antigens: misconceptions and realities. *Cell*, 1990;61:553-556

Edited by MA Jing-Yun

# A comparison between previous and present histologic assessments of chronic hepatitis C viral infections in humans

N Assy<sup>1</sup> and GY Minuk<sup>2</sup>

**Subject headings** hepatitis C/pathology; hepatitis/pathology; liver/pathology; hepatitis/chronic active

## Abstract

**AIM** To compare the previously employed classification of liver histology (minimal, chronic persistent hepatitis, chronic active hepatitis and cirrhosis) with a new classification recently described by Sheuer *et al* (activity grade and fibrosis stage) in percutaneous liver biopsies from patients with chronic hepatitis C viral infections.

**METHODS** Liver biopsies from 79 untreated patients were reviewed. Anti-HCV testing had been performed by ELISA and confirmed by a recombinant immunoblot assay. With respect to the new classification, all the specimens were evaluated using the Knodell score for activity.

**RESULTS** A good correlation was revealed between the previous and more recent histologic classifications in patients with abnormal liver enzyme tests. However, in 13/15 (87%) of patients with normal aminotransferase values, changes were consistent with chronic persistent hepatitis whereas normal activity and no fibrosis were demonstrated by the Sheuer classification.

**CONCLUSION** The old classification is more often misleading but correlates well with the new classification and thereby permits comparisons between historically clinical studies.

## INTRODUCTION

Despite recent advances in biochemical, serologic and radiologic techniques, liver biopsies remain an essential component of diagnostic and management decisions in patients with chronic viral hepatitis. The importance of liver biopsies in this patient population has been emphasized by the International Hepatology Informatics Group, the METAVIR group in France, and a working group of the International Congress of Gastroenterology who address the terminology, grading, staging and related histologic aspects of chronic viral hepatitis<sup>[1-3]</sup>. Liver biopsy provides information about the extent and distribution of inflammation and allows grading and staging of the disease (the amount of fibrosis). Furthermore, the liver biopsy enables some assessment of the rate of disease progression whenever the date of onset of infection is known. The presence of diffuse fibrosis or cirrhosis correlates with a lower likelihood of response to antiviral therapy, and the finding of severe necroinflammatory and fibrotic changes is helpful in determining the relative importance of early treatment rather than deferring therapy<sup>[4]</sup>.

Recently, Desmetts and colleagues proposed a new classification for chronic hepatitis which incorporates the first three components of the Knodell score for grading activity and a description of staging the extent of fibrosis as none, mild, moderate, severe, or cirrhosis<sup>[3,5]</sup>. This new classification is intended to replace the longstanding descriptions of chronic hepatitis as nonspecific hepatitis, chronic persistent hepatitis, chronic active hepatitis, and cirrhosis. Such a change in nomenclature is advantageous, in that the previous classification is largely confined to a system of grading rather than staging and is thus less complete. Nonetheless, as the previous classification has been widely employed for many decades, it is important for comparative purposes to determine whether there is a reasonable correlation between the two forms of classification. Thus, in the present study, we classified percutaneous liver biopsies from 79 patients with chronic hepatitis C viral infections by both classifications and compared the results using a Spearman rank test and cross-tabulation method for correlation.

<sup>1</sup>Liver Unit, Rambam Medical Center, Haifa, and The Bruce Rappaport Faculty of Medicine, Technion-Israel Institute of Technology, Haifa, Israel and <sup>2</sup>Liver Diseases Unit, Departments of Medicine & Pharmacology, University of Manitoba, Winnipeg, Manitoba, Canada  
**Correspondence to:** Dr. Assy Nimer, Fassouta, Upper Galilee, 2517 0 Box 428

Tel. (04)9870-080 Fax. (04)9870-080  
E-mail. drnimer@netvision.net.il

Received 1999-03-02

## PATIENTS AND METHODS

Liver biopsies from 79 untreated patients (47 males, 32 females) were reviewed for the purpose of this study. The mean age of the study population was  $44 \pm 11$  years. A total of 49 patients were believed to have acquired their infections from needle sharing, 25 from previous blood transfusions, and 10 were considered sporadic infections. Anti-HCV testing had been performed by a second or third generation ELISA test and confirmed by a recombinant immunoblot assay (Ortho Diagnostic System, Raritan, NJ).

Paraffin-embedded sections of specimens were stained with hematoxyline and eosine, masson trichrome, reticulin, and periodic acid-shiff after diastase digestion. Descriptions of normal, nonspecific, chronic persistent hepatitis, chronic active hepatitis and cirrhosis were as described originally<sup>[6]</sup>. With respect to the new classification, all specimens were evaluated using the first three components of the Knodell score for activity<sup>[5]</sup>: periportal  $\pm$  bridging necrosis (range of score 0-10), intralobular degeneration and focal necrosis (score 0-4), portal inflammation (score 0-4). Thus, the total score for activity could range from 0-18. Total scores of 1-3 indicate minimal chronic hepatitis, 4-8 mild chronic hepatitis, 9-12 moderate chronic hepatitis, and 13-18 severe chronic hepatitis. The scoring system for staging fibrosis included: no fibrosis, 0; periportal fibrous expansion (mild) without septa formation, 1; portal septa ( $>1$  septum) with intact architecture (moderate), 2; portal-central septa ( $>1$  septum) with architectural distortion (severe), 3; and cirrhosis, 4. To eliminate inter-observer variability, biopsies were interpreted by one observer (NA.) unaware of the clinical or laboratory status of the patients.

## Statistics

A Spearman rank test and crosstabulation method for correlation were used. Discriminative analyses were made to relate serum AST and ALT values (independent variables) to histologic features (dependent nominal variables with more than two values). Differences were considered significant when *P* values were  $<0.05$ . All statistical analyses were performed with Statistica and Winstat computer programs (Statsoft Inc, Tulsa, OK and Kalmia Co, Cambridge, MA respectively).

## RESULTS

Table 1 shows the frequency of different histologic features in both the traditional and the new classification system. Thirty-four patients (34/41, 83%) with normal activity according to the new classifica-

tion, had chronic persistent hepatitis by the old classification and twenty-seven patients (27/29, 93%) with mild activity according to the new classification had chronic active hepatitis by the old classification system, suggesting that the old classification was more often misleading than the new classification system.

**Table 1 The frequency of histologic features of chronic HCV viral infection in 79 adults classified by the new and the old classification \***

Old classification	New classification			
	Normal	Mild	Moderate	Total
Normal(minimal)	7	0	0	7
CPH	34	4	0	38
CAH	0	27	2	29
Cirrhosis	0	4	1	5
Total	41	35	3	79

\* Number of patients, Chi-square = 66.9,  $P < 0.001$ .

Table 2 provides the results of comparisons between the old and new histologic classifications. In general, the grading of activity and staging of fibrosis in the new classification tended to correlate with the histologic classifications employed with the old classification system. Not surprisingly, correlation coefficients were stronger when activity was graded rather than fibrosis staged ( $r = 0.6$  and  $r = 0.48$  respectively).

**Table 2 Correlation of traditional histologic diagnosis with aminotransferases, activity grade, and fibrosis stage in 79 patients with chronic HCV viral infection \***

Old classification	ALT	AST	Activity score	Fibrosis score
Normal	$57.6 \pm 31.4$	$39.0 \pm 0.0$	$1.0 \pm 0.0$	$0.0 \pm 0.0$
CPH	$94.0 \pm 67.5$	$59.7 \pm 31.8$	$2.0 \pm 1.1$	$0.2 \pm 0.5$
CAH	$153.8 \pm 67.8$	$112.9 \pm 42.0$	$5.4 \pm 1.4$	$1.8 \pm 1.2$
Cirrhosis	$144.3 \pm 49.2$	$142.0 \pm 52.7$	$5.5 \pm 1.7$	$4.0 \pm 0.0$

Values are presented as mean  $\pm$  SD. Activity grade; 1-3 normal, 4 - 8 mild, 9 - 12 moderate, 12 - 18 severe. Fibrosis stage; 0 non, 1 mild, 2 moderate, 3 severe, and 4 cirrhosis.

As shown in Table 3, in patients with persistently normal aminotransferase values, the old classification was more often misleading than the new classification. Specifically, 13/15 patients with normal AST values were found to have chronic persistent hepatitis on liver biopsy whereas according to the new classification, the overall activity in these patients ( $1.8 \pm 0.8$ ) was still within the normal range (0-3).

By discriminative regression analysis, serum AST values correctly classified the grade of activity

in 59/79 (75%) patients and the stage of fibrosis in 50/79 (63%) patients when employing the Desmet *et al* classification. However, when the 'traditional' classification was employed, serum AST values predicted the histology in only 34/79 (43%) of cases. Serum ALT values correctly classified the grade of activity in 53/79 (67%) patients and the stage of fibrosis in 43/79 (54%) patients by the Desmet *et al* classification as compared with 41/79 (52%) patients by the traditional classification. Serum ALT values did not add to the predictive value of AST determinations using either histological classifications.

**Table 3 Histologic distribution of chronic HCV viral infection according to aminotransferases levels**

	Normal AST n = 15	Abnormal AST n = 64
Old classification*		
Normal	2	0
CPH	13	30
CAH	0	29
Cirrhosis	0	5
New classification		
Overall activity	1.8±0.8	3.7±2.2
Fibrosis	0.06±0.2	1.2±1.4

\* Number of patients.

## DISCUSSION

The new recommendations for nomenclature, grading, and staging of chronic hepatitis and related biliary and other disorders are attempts to standardize the criteria and simplify the terminology used in making these diagnoses. The inclusion of a system of grading and staging, whether it is numerical or descriptive, simple or complex, matters less than the need for it to communicate important information about the degree of necroinflammatory activity (grade) and the extent of the disease (stage of fibrosis) that are likely factors of prognostic and therapeutic significance<sup>[7]</sup>.

To our knowledge, this study represents the first attempt to determine whether the previously employed classification of histologic disease in patients with chronic viral hepatitis correlates with the proposed classification by Desmet and colleagues. The fact that a good correlation does exist between these two methods indicates that comparison between natural history and treatment studies performed hereafter with studies reported using the old classification system are likely to be valid. The results also indicate that in general, nonspecific histologic disease correlates with Desmet activity scores of 1, chronic persistent hepatitis with 2, chronic active hepatitis with 5, and cirrhosis with 5.5. Simi-

larly, by the old classification, normal or nonspecific findings are associated with a Desmet fibrosis score of 0, chronic persistent hepatitis with 0.2, chronic active hepatitis with 2 and cirrhosis with 4.

The reason(s) why AST but not ALT values correlated better with certain histologic findings is unclear. One possible explanation is that co-existing non-viral related fatty infiltration of the liver disproportionately contributes to the ALT elevations in some of these patients. Another possible explanation concerns the intracellular tropism of HCV. Because AST is a mitochondrial enzyme whereas ALT is predominantly cytosolic, a stronger correlation would be expected with AST values if HCV-induced liver injury was more extensive in the mitochondrial fraction of hepatocytes. The recent detection of HCV antigens in the microsomal but not mitochondrial fraction of hepatocytes argues against that possibility<sup>[8]</sup>. Nonetheless, isoenzyme analyses of the AST elevations would be of interest. Finally, ALT activity may be less stable than AST activity and therefore the findings may be artifactual in origin<sup>[9]</sup>.

Numerous previous studies have documented that serum ALT levels are increased in the majority of patients with chronic hepatitis C viral infections and decline to the normal range with spontaneous or treatment-induced remissions<sup>[10,11]</sup>. However, these and other studies failed to demonstrate that ALT values reliably reflect the histologic severity of the disease as graded by more traditional histologic classifications<sup>[12,13]</sup>, and the degree of viremia based on HCV-RNA quantitation<sup>[14,15]</sup>. Only changes in ALT values over time appear to reflect changes in the severity of disease<sup>[16]</sup>. Our findings that ALT values do not predict efficiently the histologic activity according to the new classification is in accordance with these previous studies.

In conclusion, these results show a good correlation between the old and new histologic classifications of liver disease in patients with chronic hepatitis C viral infections. Aminotransferases correlates better with the necroinflammatory activity according to new classification than the traditional classification.

## REFERENCES

- 1 International Group. Acute and chronic hepatitis revisited. *Lancet*, 1977;2:914-919
- 2 METAVIR Cooperative Study Group. Intra and interobserver variation in liver biopsy interpretation in patients with chronic hepatitis C. *Hepatology*, 1994;20:15-20
- 3 Desmet VJ, Gerber M, Hoofnagle JH, Manns M, Scheuer PJ. Classification of chronic hepatitis: diagnosis, grading, and staging. *Hepatology*, 1994;19:1513-1520
- 4 Perrillo RP. The role of liver biopsy in hepatitis C. *Hepatology*, 1997;26:57S-61S
- 5 Knodell RG, Ishak KG, Black WC. Formulation and application of a

- numerical scoring system for assessing histological activity in asymptomatic chronic active hepatitis. *Hepatology*, 1981;1:431-435
- 6 Ludwig J. The nomenclature of chronic active hepatitis: an obituary. *Gastroenterology*, 1993;105:274-278
- 7 Ludwig J. Histopathological diagnosis and terminology of chronic hepatitis. *J Hepatol*, 1995;23(Suppl 1):49-53
- 8 Tsutsumi M, Urashima S, Takada A, Date T, Tanaka Y. Detection of antigens related to hepatitis C virus RNA encoding the NSS region in the livers of patients with chronic type C hepatitis. *Hepatology*, 1994;19:265-272
- 9 Cuccherini B, Naussbaum SJ, Seeff LB, Lukacs L, Zimmerman HJ. Stability of aspartate aminotransferase and alanine aminotransferase activities. *J Lab ClinMed*, 1983;102:370-376
- 10 Mutimer D, Shaw J, Harrison R, Ala F, Neuberger J, Elias E. Hepatitis C virus antibody positive blood donors. *GUT*, 1993;34:S54
- 11 Alberti A, Chemello L, Cavallo D. Antibody to hepatitis C virus and liver disease in volunteer blood donors. *Ann Int Med*, 1991;114:1010-1012
- 12 Wong DKH, Bhusnurmath SR, Chang NK. Chronic hepatitis C: Clinicopathologic correlation in 80 patients. *Hepatology*, 1992;16:225
- 13 Haber MM, West AB, Haber AD, Reuben A. Relationship of aminotransferases to histological status in chronic hepatitis C. *Am J Gastroenterol*, 1995;90:1250-1257
- 14 Brianti S, Folli M, Gaiani S, Masci C, Miglioli M, Barbara L. Persistent hepatitis C viremia without liver disease. *Lancet*, 1993;20:404-405
- 15 Navas S, Castillo I, Carreno V. Detection of plus and minus HCV RNA in normal liver of anti HCV positive patients. *Lancet*, 1993;3:904-905
- 16 Di Bisceglie AM, Goodman ZD, Ishak KJ, Hoofnagle JH, Melpolder JJ, Alter HJ. Long term clinical and histopathological follow-up of chronic post-transfusion hepatitis. *Hepatology*, 1991;14:969-974

Edited by MA Jing-Yun

# Relationship between expression of $\alpha$ -fetoprotein messenger RNA and some clinical parameters of human hepatocellular carcinoma \*

HE Ping, TANG Zhao-You, YE Sheng-Long and LIU Bin-Bin

**Subject headings** liver neoplasms; carcinoma, hepatocellular; AFP mRNA; polymerase chain reaction

## Abstract

**AIM** To certify the relationship between AFP-mRNA and some pathological parameters of hepatocellular carcinoma (HCC).

**METHOD** We detected the expression of AFP in mRNA level in tissue samples from 52 patients suffering from HCC by RT-PCR method.

**RESULTS** The positive rate of AFP mRNA was 76.9% in the HCC tumor tissues, and 69.4% in the paratumor tissues from the HCC patients with severe cirrhosis. However, in HCC patients without cirrhosis, the positive rate reached 50% in tumor tissues, but no AFP mRNA expression was found in the related paratumor tissues.

**CONCLUSION** The AFP protein was specially expressed by HCC cells and mutated hepatocytes. The AFP mRNA was positively related with cirrhosis, but no significant relationship was found between AFP mRNA and tumor size, capsule status and tumor metastasis.

## INTRODUCTION

The value of  $\alpha$ -fetoprotein (AFP) as a useful marker for hepatocellular carcinoma (HCC) has been widely accepted since its discovery in 1956 and detection in serum of patients with HCC (reviewed by Abelev 1971)<sup>[1]</sup>. Further evaluation of AFP, particularly for much earlier detection of HCC and early detection of subclinical recurrence or metastasis, remains an important approach to improving the overall 5-year survival rate of HCC before breakthroughs are made in basic researches. Recent progress in the development of PCR amplification of AFP from HCC tissues, will assist the clinical evaluation of AFP.

Serum AFP concentrations are increased in the majority of patients with HCC. In China, the serum AFP level of 60%-70% of the HCC patients was higher than normal values. Histochemical studies have shown the presence of AFP in malignant hepatocytes<sup>[2]</sup>, and serum AFP concentrations rapidly return to normal after radical resection of HCC, indicating that malignant hepatocytes are responsible for production of AFP. Possible explanations for the reinitiating of AFP synthesis by neoplastic hepatocytes include either increased transcription of the AFP gene or post-translational modifications affecting AFP production.

In the present study, we have developed the competitive reverse transcription followed by polymerase chain reaction (RT-PCR) assays to evaluate messenger RNA (mRNA) level of AFP in tissue specimens obtained by biopsy. In addition, AFP mRNA levels in human HCC were quantitated in comparison with those of non-neoplastic portion to elucidate the relationship of AFP gene expression in human HCC and some pathological parameters.

## MATERIALS AND METHODS

### *Human HCC and paratumor tissues*

Surgical specimens of 52 patients with HCC were obtained in Liver Cancer Institute of Shanghai Medical University from February 1996 to March 1998. Thirty-two cases (61.5%) had abnormal serum AFP (>20  $\mu$ g/L). The controls were operative specimens of patients with liver cyst (3 cases) and hepatic hemangioma (2 cases). Surgical specimens were immediately frozen in liquid nitrogen and stored at

Liver Cancer Institute & Zhong Shan Hospital, Shanghai Medical University, Shanghai 200032, China

Dr. HE Ping, female, born on 1964-10-29 in Jiaxing City, Zhejiang Province, Han nationality, graduated from Shanghai Medical University as a Ph.D. in 1998, assistant researcher of molecular biology, majoring molecular biology of liver cancer, having 7 papers published. Presented at the Third National Meeting of Advances of Diagnosis and Treatment in Hepatocellular Carcinoma, Dalian, 23-25 July, 1997.

\*Project supported by the National Natural Science Foundation of China, No.3900050.

**Correspondence to:** Dr. HE Ping, Liver Cancer Institute, Zhong Shan Hospital, Shanghai Medical University, Shanghai 200032, China. Tel. +86 • 21 • 64041990 • 2136, Fax. +86 • 21 • 64037181

Received 1998-11-14

-80°C until use.

### Primers for PCR

The primers for amplifying AFP and  $\beta$ -actin gene were synthesized by Shanghai Biochemistry Institute, Chinese Academy of Sciences. The sequences of primers for AFP were 5'-ATT CAG ACT GCT GCA GCC AA-3' (sense, 272 bp-291 bp) and 5'-GTG CTC ATG TAC ATG GGC CA-3' (antisense, 728 bp-747 bp). The sequences of the sense and antisense primers for the  $\beta$ -actin gene were 5'-CTA TTG GCA ACG AGC GGT TC-3' and 5'-CTT AGG AGT GGG GGT GGC TT-3', respectively.

### Isolation of mRNA

Total cellular RNA was isolated by the guanidinium isothiocyanate extraction method of Chomezynski and Sacchi<sup>[3]</sup>. Approximately 0.5 g-1.0 g of each tumor and corresponding non-tumorous liver tissues were minced and homogenized with 1 mL denaturing solution (4 mol/L guanidinium isothiocyanate, 25 mmol/L-sodium citrate at pH 7.0, 0.5% sarkosyl, 0.1 mol/L mercaptoethanol). Sodium acetate 0.1 mL-2 mol/L (pH 4.0), 1 mL- phenol (water saturated) and 0.2 mL- chloroform/isoamyl alcohol mixture (49:1) were sequentially added to the homogenate. The final suspension was shaken vigorously for 10s and cooled in ice-water for 15 min. After centrifugation at 10 000×g for 20 min at 4°C, the aqueous phase, in which RNA was present, was taken and mixed with 1 mL isopropanol, and then placed at -20°C for 1 h to precipitate RNA. Sedimentation at 10 000×g for 20 min was performed again and the resulting RNA pellet was dissolved in 0.3 mL denaturing solution, transferred into a 1.5 mL Eppendorf tube, and precipitated with 0.3 mL- isopropanol at -20°C for 1 h. After centrifugation for 10 min at 4°C, the RNA pellet was dissolved in diethyl-pyrocabonate (DEPC)-treated water.

### RT-PCR

A 5  $\mu$ L sample of total RNA, 20IU RNasin, 5  $\mu$ L -oligo (dT) (100 mg/L), 5  $\mu$ L- dNTP (20 mM), 30IU avian myeloblastosis virus reverse transcriptase (Promega), 10  $\mu$ L- 5×reaction buffer and 13  $\mu$ L- DEPC-treated water were added to a 0.5 mL-tube and incubated at 42°C for 1h. The PCR system for amplifying AFP and  $\beta$ -actin gene each contained equal amounts of RT products (10  $\mu$ L), sense and antisense primers (50 pmol each), Taq DNA polymerase (3IU), PCR reaction buffer and double-distilled H<sub>2</sub>O. Samples were amplified through 35 consecutive cycles, each amplification cycle consisting of a denaturation at 94°C for 1 min, primer anneal-

ing at 55°C for 1 min, and extension at 72°C for 2 min. Cycles were preceded by incubation at 95°C for 5 min to ensure full denaturation of the target DNA, and were followed by an extra 7 min of incubation at 72°C after the final cycle to ensure full extension of the product. The PCR reactions were performed on a DNA thermal cycler (Perkin Elmer/Cetus Instruments, Norwalk, Conn.). The amplified fragments of AFP and  $\beta$ -actin gene were analyzed by 2% agarose gel.

### Analysis of AFP gene expression

The PCR products from HCC and paratumor tissues were separated by 2% agarose, the electrophoresis results were printed. The absorbance (A) and the areas of fragment were read by ImageMaster VDS (Pharmacia Biotech). The expression level of the AFP gene was calculated as follows: AFP gene expression (%) = [AFP fragment area × (A<sub>fragment</sub> - A<sub>background</sub>)] / [  $\beta$ -actin fragment area × (A<sub>fragment</sub> - A<sub>background</sub>)].

### Relationship of AFP mRNA and some clinical parameters

The clinical parameters of patients with HCC were cirrhosis, HBsAg, differentiation, tumor size, metastasis and tumor capsule. The differences among the groups were analyzed by Chi-square test.

## RESULTS

### Transcriptional level of AFP mRNA in HCC and paratumor tissues

The total RNAs from samples were analyzed by electrophoresis (Figure 1). The RNAs containing 28s, 18s and 5s were not contaminated by DNA and degraded.

### Analysis of RT-PCR products

The expected sizes of the amplified AFP fragment and  $\beta$ -actin fragment were 475 bp and 759 bp respectively (Figure 2). In 52 patients, the AFP positive rates in HCC tissues were 76.9% (40/52). Among these patients, 25 (69.4%) of 36 cases accompanied with serious cirrhosis had positive AFP mRNA in paratumor tissues, but no AFP mRNA expression was found in normal liver tissues of patients with liver cyst or hepatic hemangioma.

The expression level of AFP in HCC samples (58.4%±6.4%) was higher than that in paratumor tissues (30.2%±6.1%,  $P<0.01$ ). The expression level of AFP in different HCC groups is shown in Table 1. AFP expression in HCC with cirrhosis (65.6%±5.4%) was higher than that in HCC without cirrhosis (48.2%±4.3%,  $P<0.01$ ). Nosigni-

ficant differences in AFP expression were found between HCCs with and without metastasis ( $57.1\% \pm 6.4\%$  vs  $55.2\% \pm 7.8\%$ ,  $P > 0.05$ ), as well as between HCCs with different capsule status or between large HCCs ( $>5$  cm) and small HCCs ( $\leq 5$  cm).

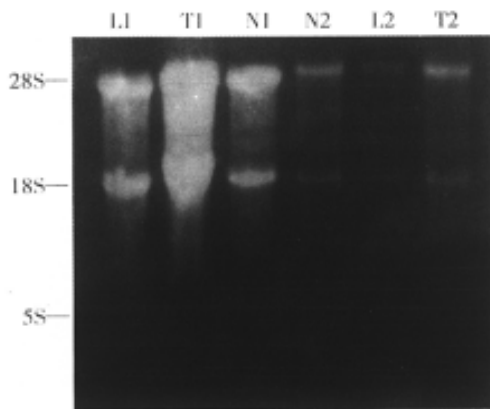


**Figure 1** The denaturing gel electrophoresis of RNA in HCC, paratumor and normal tissues. L: paratumor tissues, T: hepatoma tissues, N: normal liver tissues.

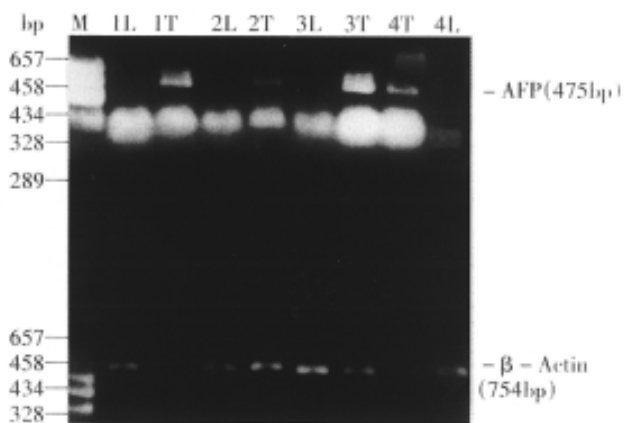


**Figure 2** The expression of AFP mRNA in hepatoma, paratumor tissues by RT-PCR. L: paratumor tissues, T: hepatoma tissues, M: markers (bp): 657, 458, 434, 328, 289.

### Relationship between AFP mRNA and some clinical parameters

The HCC patients with severe cirrhosis had highest AFP positive rates in HCC tissues (88.8%) and in paratumor tissues (69.4%) among these patients. But the HCC patients without cirrhosis had lower AFP positive rates in HCC tissues (50%) and were negative in all of paratumor tissues. A significant difference in AFP mRNA expression was found between the HCC patients with serum HBsAg (HCC tissues was 82.6%, paratumor was 52.2%) and without serum HBsAg. But, no significant difference was found between the HCC with different differentiation, metastasis, or different capsule status (Table 2).

**Table 1** The correlation of AFP mRNA in hepatoma tissues and some clinical parameters

Histological parameter	Cases	Positive tumor AFP mRNA	Positive paratumor AFP mRNA
<b>Cirrhosis<sup>a</sup></b>			
Yes	36	88.8 (32/36)	69.4 (25/36)
No	16	50.0 (8/16)	0.0 (0/16)
<b>HBsAg<sup>b</sup></b>			
(+)	46	82.6 (38/46)	52.2 (24/46)
(-)	6	33.3 (2/6)	16.7 (1/6)
<b>Differentiation</b>			
Well	18	77.8 (14/18)	33.3 (6/18)
Poor	34	76.5 (26/34)	55.9 (19/34)
<b>Tumor size</b>			
$\leq 5$ cm	20	75.0 (15/20)	25.0 (5/20)
$> 5$ cm	32	78.1 (25/32)	62.5 (20/32)
<b>Metastasis</b>			
Yes	11	81.8 (9/11)	45.5 (5/11)
No	41	75.6 (31/41)	48.5 (20/41)
<b>Capsule</b>			
Yes	20	85.0 (17/20)	40.0 (8/20)
No	32	71.9 (23/32)	53.1 (17/32)

<sup>a</sup> $P < 0.01$ , <sup>b</sup> $P < 0.05$ .

**Table 2** The expression levels of AFP gene in HCC

Group	No. of cases	AFP gene expression $\bar{x} \pm s_x$ (%)	P
Total			
HCC	52	58.4 $\pm$ 6.4	
Paratumor	52	30.2 $\pm$ 6.1	<0.01
<b>Cirrhosis</b>			
Yes	36	65.5 $\pm$ 5.4	
No	16	48.2 $\pm$ 4.3	<0.01
<b>Metastasis</b>			
Yes	11	57.1 $\pm$ 6.4	
No	41	55.2 $\pm$ 7.8	>0.05
<b>Capsule</b>			
Complete	20	53.1 $\pm$ 8.2	
Incomplete	32	51.8 $\pm$ 6.5	>0.05
<b>Tumor</b>			
$\leq 5$ cm	20	48.5 $\pm$ 5.3	
$> 5$ cm	32	53.6 $\pm$ 8.3	S>0.05

### Relationship between AFP mRNA levels in HCC tissues and serum AFP levels

AFP cDNA fragments were amplified from all HCC tissues of 32 patients with serum AFP  $> 20$   $\mu\text{g/L}$ , while from paratumor tissues of 14 HCC patients. Among 20 HCC patients with serum AFP  $\leq 20$   $\mu\text{g/L}$ , there were 8 patients with AFP mRNA in HCC tissues. In other words, the positive rates of AFP mRNA had a significant difference between HCC patients with serum AFP  $> 20$   $\mu\text{g/L}$  (100%) and those with serum AFP  $\leq 20$   $\mu\text{g/L}$  (40%,  $P < 0.01$ ).

### DISCUSSION

Human AFP gene is present on chromosome 4q11-21 and consists of 15 exons<sup>[4]</sup>. AFP is an oncofetal protein, and its gene expression is shown mainly by hepatocytes and endoderm cells of the visceral yolk sac in the early stages of fetal liver development, but repressed soon after birth. Reactivation of AFP

gene expression is shown during massive liver necrosis and in hepatocarcinogenesis. Many experiments demonstrated that the major control of AFP production is probably at the level of gene transcription<sup>[5]</sup>.

In the current study, RNA was extracted from the tissues by acid guanidinium thiocyanate-phenol-chloroform extraction method according to Chomczynski and Sacchi<sup>[3]</sup>. Because the amount of RNA was small when extracted from biopsy samples, we adopted this procedure for better yield of RNA in comparison with the CsCl gradient extraction of Chirgwin<sup>[6]</sup>. The portions of extracted RNA from surgically resected samples were electrophoresed through formaldehyde agarose gel, stained with ethidium bromide, and clear bands of 18S and 28S ribosomal RNA were observed. In this method, an amount of contaminating DNA in the prepared RNA was less than detectable level (Figure 1).

The results showed that the total positive rate of AFP mRNA in hepatoma tissues was 76.9%. It demonstrated that AFP gene was activated in HCC cells of most HCC patients. Among them, the positive rate of HCC patients with severe cirrhosis was highest (88.8%), while 69.4% in their paratumor tissues. But the HCC patients without cirrhosis had lower AFP mRNA levels: 50% in HCC tissues and negative in paratumor tissues. These results showed that the transcription levels of AFP mRNA were correlated to cirrhosis<sup>[7]</sup>. Koa and his colleagues found that the tumorigenesis rate of HCC patients with cirrhosis and serum AFP < 20 µg/L was 26%, but the patients with cirrhosis and AFP ≥ 20 µg/L was 46% in a five-year observation<sup>[8]</sup>. This suggested that the cells of paratumor tissues secreting AFP protein may be precarcinomatous cells. They were of some characteristics of embryonic hepatocytes or HCC cells, and expressed this embryonic antigen before genesis of HCC. Therefore, it aids earlier detection of HCC by assaying AFP mRNA in biopsy of HCC patients with cirrhosis<sup>[8]</sup>. We conclude that the expression levels of AFP mRNA in HCC tissues were higher than that in paratumor tissues. The activation of AFP gene in paratumor tissues may be related to precarcinomatous changes.

Muguti, *et al* reported that the serum AFP level of HCC patients with serum HBsAg was higher than that of patients without HBsAg. They suggested that serum AFP levels had significant differences among different HBsAg titers<sup>[9]</sup>. Lee also found that most of patients with serum HBsAg had high serum AFP levels and demonstrated that the motivate observation of AFP had great value for early diagnosis of HCC<sup>[10]</sup>. Our study suggested that the transcriptional activation of AFP in HCC tissues may be related to HBV infection<sup>[11-13]</sup>.

In our experiment, the positive rate of AFP mRNA of patients with serum AFP ≤ 20 mg/L was 40% in HCC tissues, and 15% in paratumor tissues. But, the positive rate of AFP mRNA of patients with serum AFP > 20 mg/L was 100% in HCC tissues, and 68.8% in paratumor tissues. These results were supported by the reported paper<sup>[14]</sup>. Total positive rate of HCC tissues was 76.9%, but that of serum AFP was 61.5%. These suggested that the activated AFP gene in transcription level was higher than that in translation level. Therefore, the activation of AFP gene included both gene transcription and translation levels.

On the other hand, our experiments certified that AFP gene re-expression had no relationship with tumor capsule status, differentiation and tumor mass size. Thus, although the motion of serum AFP level can predict the recurrence and metastasis of HCC patients after resection or treatment, there is no relationship between AFP mRNA expression in HCC tissues and recurrence and metastasis of HCC. In other words, AFP expression is not one of the reasons that result in the recurrence and metastasis of HCC.

Finally, gene therapy for HCC using retrovirus or adenovirus vectors carrying human AFP promoter for tissue specific expression of suicide genes or cytokines are now under investigation in some laboratories<sup>[15,16]</sup>, including ours<sup>[17]</sup>. Quantitation of AFP transcripts in HCC shown in this study could provide a clue for selection of patients for such a targeted gene therapy, since expression of transduced genes could be expected in AFP-producing HCCs only.

## REFERENCES

- 1 Abelev GI. Alpha-fetoprotein in ontogenesis and its association with malignant tumors. *Adv Cancer Res*, 1971;14:295-358
- 2 Hirohashi S, Shimamoto Y, Ino Y, Kishi K, Ohkura H, Mukojima T. Distribution of alpha fetoprotein and immunoreactive carcinoembryonic antigen in human hepatocellular carcinoma and hepatoblastoma. *Jpn J Clin Oncol*, 1983; 13:37-43
- 3 Chomczynski P, Sacchi N. Single-step method of RNA isolation by acid guanidinium thiocyanate-phenol-chloroform extraction. *Anal Biochem*, 1987;162:156-159
- 4 Dugaiczak A, Harper ME, Minghetti PP. Chromosomal localization, structure, and expression of the human alpha-fetoprotein gene. *Kroc Found Ser*, 1985;19:181
- 5 Tilghman SM, Belayew A. Transcription control of the murine albumin/fetoprotein locus during development. *Proc Natl Acad Sci USA*, 1982;79:5254-5257
- 6 Chirgwin JM, Przybyla AE, MacDonald RJ, Rutter WJ. Isolation of biologically active ribonucleic acid from sources enriched in ribonuclease. *Biochem J*, 1979;18:5294-5299
- 7 Di Bisceglie AM, Dusheiko GM, Paterson AC, Alexander J, Shouval D, Lee CS. Detection of alpha fetoprotein messenger RNA in human hepatocellular carcinoma and hepatoblastoma tissue. *Br J Cancer*, 1986;54:779-785
- 8 Oka H, Tamori A, Kruoki T, Kobayashi K, Yamamoto S. Prospective study of α-fetoprotein in cirrhotic patients monitored for development of hepatocellular carcinoma. *Hepatology*, 1994;19: 61-66
- 9 Muguti G, Tait N, Richardson A, Little JM. Alpha-fetoprotein expression in hepatocellular carcinoma: A clinical study. *J Gastroenterol Hepatol*, 1992;7:374-378

- 10 Lee HS, Chung YH, Kin CY. Specificities of serum  $\alpha$ -fetoprotein in HBsAg(+) and HBsAg(-) patients in the diagnosis of hepatocellular carcinoma. *Hepatology*, 1991;14:68-72
- 11 Songsivilai S, Dharakul T, Senawong S. Hepatitis B and hepatitis C-associated hepatocellular carcinoma: evaluation of alpha fetoprotein as a diagnostic marker. *Asian Pac J Allergy Immunol*, 1995;13:167-171
- 12 Wong CB, Attar BM, Shimoda SS. Marked episodic elevations of alpha-fetoprotein without hepatocellular carcinoma in a patient with hepatitis B. *Am J Gastroenterol*, 1995;90:1015-1016
- 13 Parkinson AJ, McMahan BJ, Zanis L, Lanier AP, Wainurigh RB. Detection of alpha fetoprotein and hepatitis-B surface antigen in blood spotted on filter paper: use as a screen for hepatocellular carcinoma in Alaska natives. *Arctic Med Res*, 1996;55:123-128
- 14 Peng SY, Lai PL, Chu JS, Lee PH, Tsung PT, Chen DS, Hsu HC. Expression and hypomethylation of  $\alpha$ -fetoprotein gene in unicentric and multicentric human hepatocellular carcinomas. *Hepatology*, 1993;17:35-41
- 15 Kanai F, Lan KH, Shiratori Y, Tanaka T, Ohashi M, Okudaira T. In vivo-gene therapy for  $\alpha$ -fetoprotein-producing hepatocellular carcinoma by adenovirus-mediated transfer of cytosine deaminase gene. *Cancer Res*, 1997;57:461-465
- 16 Mawatari F, Tsuruta S, Ido A, Ueki T, Nakao K, Kato Y. Retrovirus-mediated gene therapy for hepatocellular carcinoma: selective and enhanced suicide gene expression regulated by human alpha-fetoprotein enhancer directly linked to its promoter. *Cancer Gene Ther*, 1998;5:301-306
- 17 He P, Liu BB, Ye SL, Tang ZY. The cloning of the combined transcriptional regulatory sequence of human  $\alpha$ -fetoprotein enhancer/albumin promoter. *Chin J Hepatol*, 1998;6:136-138

Edited by MA Jing-Yun

# Study of angiogenesis induced by metastatic and non-metastatic liver cancer by corneal micropocket model in nude mice \*

SUN Hui-Chuan, LI Xiao-Ming, XUE Qiong, CHEN Jun, GAO Dong-Mei and TANG Zhao-You

**Subject headings** liver neoplasms; angiogenesis; corneal micropocket model; neoplasms metastasis

## Abstract

**AIM** To study the angiogenesis induced by liver cancer with different metastatic potentials using corneal micropocket model in nude mice.

**METHODS** Corneal micropockets were created in nude mice. Tumor tissues and liver tissues were implanted into the corneal micropockets. Angiogenesis was observed using a digital camera under slit-lamp biomicroscope, and compared among different grafts and incision alone. Vascular responses were recorded in regard to the range, number and length of new blood vessels toward the grafts or incisions.

**RESULTS** Vascular responses induced by tumor tissues were greater than those by incision alone and liver tissue grafts. LCI-D20 induced more intensive angiogenesis than LCI-D35.

**CONCLUSION** Highly metastatic liver cancer LCI D20 was more angiogenic than low metastatic cancer LCI D35 and liver tissue. Micropocket was a useful model to study dynamic process of angiogenesis *in vivo*.

## INTRODUCTION

Angiogenesis is a tumor growth and metastasis dependent process. It has been proved that subtype of tumor with metastatic potential is more angiogenic than non-metastatic one<sup>[1]</sup>. Corneal micropocket is an ideal model to observe the dynamic change in angiogenesis *in vivo*<sup>[2]</sup>. Therefore, this model was created in nude mice to study the angiogenesis induced by different grafts.

## MATERIALS AND METHODS

### Materials

**Animals:** Six-week-old male BALB/c nu/nu mice were provided by Shanghai Pharmaceutical Institute. The eyes of each mouse were treated with aureomycin ointment everyday for one week before operation to prevent any potential infection. A slit-light biomicroscope (Wuxi Optical Instrument Factory, Jiangsu Province, China) was used to observe the eyes of mice. Highly metastatic LCI D20 and lowly metastatic LCI D35 human hepatoma models were established by orthotopic implantation of surgical specimens of liver cancer patients in nude mice<sup>[3]</sup>. In LCI D20 model, metastasis to the lung, peripheral liver and celiac lymph nodes was found 20 days after transplantation to the liver. Rapid deterioration and death occurred in nude mice. On the contrary, in LCI D35 model, 35 days after orthotopic transplantation, no metastatic lesion appeared, the nude mice survived for more than two months without distant metastasis<sup>[4]</sup>.

### Methods

Operations were performed in aseptic condition under anesthesia with 0.06 mL 3% pentobarbital and 0.9% natural solution was used to wash the eyes. Under an anatomic microscope, the eyes were fixed and moved forward by two sutures through the conjunctiva near cornea. With a modified blade (Gillette Limited, Shanghai, China), a superficial incision about 1.5 mm long not through the cornea was made on the corneal dome near the pupil. A modified spatula made from a sterilized 27gauge needle was used to make a 1.5 mm × 0.8mm-micropocket in the corneal stroma from incision toward the cornea-scleral junction. A graft, about 0.1 mm × 0.1 mm × 0.5mm, was put into the bottom of the micropocket using the modified spatula. The inci-

Liver Cancer Institute and Zhongshan Hospital, Shanghai Medical University, Shanghai 200032, China

Dr. SUN Hui-Chuan, male, born on 1968-12-12 in Deyang City, Sichuan Province, Han Nationality, graduated from Shanghai Medical University in 1992. Now he is a Ph.D. graduate student in the Graduate School of Shanghai Medical University, studying the mechanisms of metastasis of liver cancer, especially in the field of angiogenesis. He has published 6 papers.

\*Supported by the Fund for Leading Specialty of Shanghai Metropolitan Bureau of Public Health.

**Correspondence to:** Dr. SUN Hui-Chuan, Liver Cancer Institute, Zhongshan Hospital, Shanghai Medical University, #136 Yi Xue Yuan Road, Shanghai 200032, China  
Tel/Fax. +86 • 21 • 64037181  
E-mail. zytang@srcap.stc.sh.cn

Received 1999-01-03

sion could be self-closed (Figure 1). Aureomycin ointment was applied to the operated eyes to prevent postoperative infection for 3 days. On the 3rd, 5th, 7th, 10th, 15th and 20th days after operation, the operated eyes were observed under slit-lamp biomicroscope with their images recorded in computer via a digital camera (Figures 2, 3). Angiogenesis induced by the implanted tissues was defined as those blood vessels originating at the adjacent limbal plexus toward the implants. The methods of quantitative study followed those reported in the literature<sup>[5]</sup>. Briefly, the circle of the cornea was evenly divided into 24 parts to present the range of angiogenesis. For example, if the range of angiogenesis was one-fourth of circle, it was 6. The distance from the cornea-scleral junction to the pupil was divided evenly into 5 parts. The length of blood vessels could be calculated from one to five. The number of blood vessels was counted from the pictures.

## RESULTS

The angiogenesis on the cornea of nude mice could be separated into two phases. In the first phase, the blood vessels originating from the limbal plexus at the cornea-scleral junction and pointing to the incision in the operated areas were caused by the surgical manipulations. If there was no graft, the blood vessels disappeared 3 days after operation. However, the angiogenesis on the fourth day after operation was different in case of different grafts (Table 1). Vascular response was described in detail as follows.

**Table 1 Comparison of angiogenesis among different grafts and incision alone (t test)**

Angiogenesis	LCID20 (n=4)	LCID35 (n=4)	Liver tissues (n=4)	Incision alone (n=4)	P value
Range ( $\bar{x}\pm s$ )	24.00±0.00	11.50±1.29	7.25±0.96	4.50±0.58	<0.01
Number ( $\bar{x}\pm s$ )	24.75±2.63	16.50±2.98	12.50±1.29		<0.01
Length ( $\bar{x}$ )	5.1	4.4	4.3		>0.05

### Incision alone

On the 1st day after operation, the new blood vessels developed from the limbal plexus and pointed to the operating site. But on the 2nd day, the number of blood vessels decreased, and no blood vessel was found on the cornea on the 3rd day.

### Liver tissues

On the 7th day after operation, the blood vessels reached the implants, which were the peak of angiogenesis induced by liver tissues. Its range was 7.25. Its average length and number were 4.4 and 12.5 respectively. On the following days, the size of grafts was decreased, with the length and number of new blood vessels reduced as well.

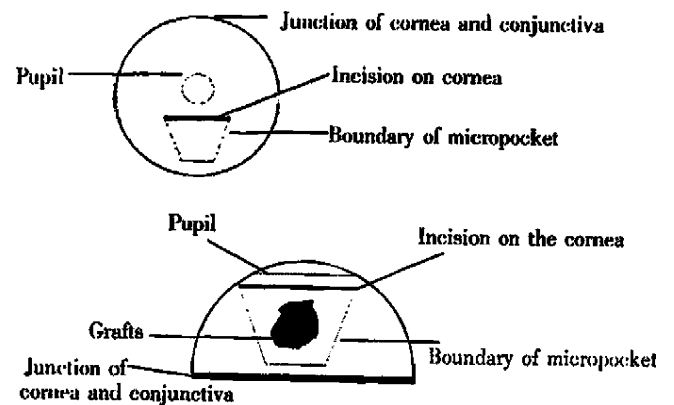


**Figure 1** Schematic description of the establishment of corneal micropocket.

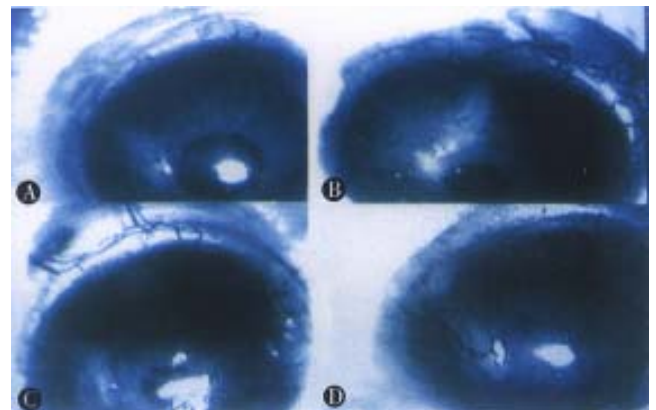


**Figure 2** Angiogenesis induced by LCID35 in corneal micropocket in nude mice.

A: 4th day; B: 7th day; C: 10th day; D: 13th day.

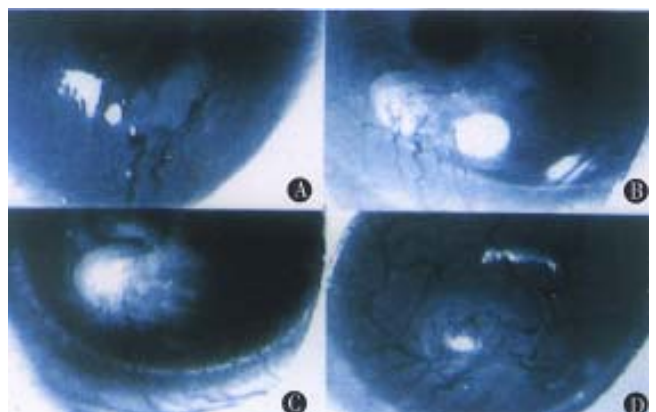


**Figure 3** Angiogenesis induced by LCID20 in corneal micropocket in nude mice.

A: 4th day; B: 7th day; C: 10th day; D: 13th day.

### LCID35 tumor tissues

On the 7th day after operation, the blood vessels reached the tumor implants. The tumor was larger than that when it was implanted. The range of angiogenesis was 11.5, and the average length and

number of new blood vessels were 4.4 and 16.5 respectively.

#### LCI D20 tumor tissues

On the third day after operation, the blood vessels reached the tumor implants. On the 7th day, the blood vessels were penetrating to the tumor tissues with the tumor implants enlarged. On the 15th day, the blood vessels originating from the counterpart of the operative limbal plexus could be found. The range was 24, the average length and number of blood vessels were 5.1 and 24.75 respectively. The tumor graft was 2-3 times larger than its original size. Hemorrhagic necrosis is often presented at the central part of the tumor. The sizes of blood vessels were obviously bigger than those of others.

#### DISCUSSION

The human hepatoma metastatic model LCI D20 and LCI D35 were good tools for the study of metastasis. We have observed that the LCI D20 tumor was ruddier than LCI D35 tumor, and there were more blood vessels in LCI D20, suggesting LCI D20 is more angiogenic than LCI D35.

To study angiogenesis *in vivo*, we established a corneal micropocket model in nude mice to show the angiogenic reaction induced by human hepatoma tissues *in vivo*. Because *in vivo* study can dynamically demonstrate angiogenesis, it is more reliable than *in vitro* study.

It was demonstrated that the blood vessels on cornea induced by incision alone disappeared 3 days after operation, which was considered as a normal blood vessel reaction caused by trauma. Liver graft induced mild reaction on the cornea of nude mice, which was greater than incision alone. It may result from the slight difference in their histological compatibility between the donor mice and recipient mice in our corneal micropocket model. Folkman *et al*

also reported the rejection caused by xenogenic implantation in the corneal micropocket model<sup>[2]</sup>. However, the angiogenesis induced by xenogenic tissue implantation and tumor tissues were very different. Tumor angiogenesis was more potent and durable than others, and the grafts grew rapidly instead of disappearing in case of liver grafts.

Our experiment also indicated that tumor tissues with different metastatic potentials had different angiogenicities. LCI D20 induced a relatively stronger angiogenesis than LCI D35 did. In addition, the growth rate of LCI D20 tumor was greater than that of LCI D35. A peak of angiogenesis was observed in LCI D35 implants. Our hypothesis is that proliferation of tumor was balanced by apoptosis due to lack of enough blood supply. However, no peak of angiogenesis was found in LCI D20 grafts, indicating angiogenesis induced by LCI D20 became more intensive at the end of the observation period.

In preparation of the corneal micropocket model in nude mice, the depth of incision into the cornea, the size of micropockets and grafts are vitally important for success.

Observation of dynamic changes in angiogenesis shown by our model is very helpful for screening anti-angiogenic drugs or other anti-tumor drugs.

#### REFERENCES

- 1 Folkman J. Tumor angiogenesis. In: Holland JF, Bast RC, Morton DL, Frei E, Kufe DW, Weichselbaum RR, eds. Cancer medicine, 4th Edition. Baltimore, Maryland: Williams & Wilkins, 1996: 181-204
- 2 Gimbrone MA, Cotran RS, Leapman SB, Folkman J. Tumor growth and neovascularization: an experimental model using the rabbit cornea. *J Natl Cancer Inst*, 1974;52:413-419
- 3 He B, Liu KD, Tang ZY, Xue Q. Different mutation and expression patterns in LCI D20 and LCI D35 models. *Chinese Hepatology*, 1997;5:245-246
- 4 Sun FX, Tang ZY, Liu KD, Ye SL, Xue Q, Gao DM, Ma ZC. Establishment of a metastatic model of human hepatocellular carcinoma in nude mice via orthotopic implantation of histologically intact tissues. *Int J Cancer*, 1996;66:1-5
- 5 Voest EE, Kenyon BM, O'Reilly MS, Truitt G, D'Amato RJ, Folkman J. Inhibition of angiogenesis *in vivo* by interleukin 12. *J Natl Cancer Inst*, 1995;87:581-586

Edited by WANG Xian-Lin

# Gene expression of hepatocyte growth factor and its receptor in HCC and nontumorous liver tissues

LUO Yun-Quan, WU Meng-Chao and CONG Wen-Ming

**Subject headings** liver neoplasm; hepatocyte growth factor receptor, hepatocyte growth factor; gene expression

## Abstract

**AIM** To study the changes of gene expression of hepatocyte growth factor (HGF) and hepatocyte growth factor receptor (HGFr) in hepatocellular carcinoma (HCC) tissue and nontumorous liver tissue and the relationship between these changes and the biological behavior of the tumor.

**METHODS** Gene expression of HGF and HGFr in 26 cases of HCC tissue and their adjacent nontumorous liver tissues was determined with digoxigenin-labeled DNA probes.

**RESULTS** Positive expression of HGF in HCC tissue was similar to that in the adjacent nontumorous liver tissue, but positive rate of HGF expression was lower than HGFr gene expression. However, HGFr expression was higher in the metastatic cases than in those without metastasis. It was found that HGFr was overexpressed in HCC tissue as well as in the adjacent nontumorous liver tissue.

**CONCLUSION** There seems to be a close relationship between overexpression of HGFr gene and tumor metastasis, and the HGF and HGFr system plays an important role in regulating tumor growth and metastasis.

## INTRODUCTION

Gene mutation is the pathogenetic basis and essence of canceration induced by various carcinogenic factors. Mutation of oncogene and anti-oncogene, alteration of growth factor and growth factor receptor as well as instability of chromosome are the essential causes of tumor genesis. Using the hepatocyte growth factor (HGF) and hepatocyte growth factor receptor (HGFr) gene (c-met) DNA probe, we conducted an auto-control study on primary liver cancer tissues and their adjacent nontumorous tissues in 26 patients suffering from hepatocellular carcinoma (HCC) in an attempt to observe expression of gene products at a transcription level and thus to explore the role and significance of these products in the development and growth of liver cancer.

## MATERIALS AND METHODS

### Specimens

Tissue specimens used in the present study were sampled from 26 patients with pathologically confirmed hepatocellular carcinoma and the nontumorous liver tissue (2 cm away from the carcinoma), including 22 males and 4 females ranging in age from 34 to 63 years with a mean of 48.5 years. The fresh tissue was surgically excised under aseptic conditions and stored in liquid nitrogen.

### RNA extraction<sup>[1]</sup>

A tissue mass of 0.5 g with addition of 4 mol/L-guanidinium thiocyanate, 25 mmol/L-sodium citrate, 5 g/L-Sarcosyl and 5 mL of 0.1 mol/L- $\beta$ -mercaptoethanol solution was ultracentrifuged in an ice bathed centrifuge tube for 1 min-2 min, followed by addition of 0.5 mL of 2 mol/L-NaAc (pH 4.0), 5 mL-saturated phenol and 1 mL chloroform-amylen alcohol (49:1), which were mixed up thoroughly by oscillation for 5 min and ice bathed for 15 min. The stock solution was centrifuged at 4°C at 9 200rpm for 20 min. The supernatant was mixed with isopropanol thoroughly, centrifuged at 9 200rpm for 20 min, precipitated at -20°C for 2 h, and then centrifuged at 2 200rpm at 4°C to discard the supernatant. The precipitate was washed with 75% alcohol and vacuum dried. The RNA was dissolved in 0.5 mL-water pretreated with diethylpyrocarbonate (DEPC) and then stored at -70°C for use.

Eastern Hospital of Hepatobiliary Surgery, Second Military Medical University, Shanghai 200438, China

Dr. LUO Yun-Quan, male, born on 1963-10-10 in Huoqiu County, Anhui Province, Han nationality, graduated from Second Military Medical University as a doctor postgraduate in 1995, associate professor of hepatobiliary surgery, majoring hepatobiliary surgery, having 25 papers published.

\*Presented at the 6th Meeting of National General Surgery Association for the Study of Hepatobiliary Surgery Diseases, Qindao, 16-20 September, 1998.

**Correspondence to:** Dr. LUO Yun-Quan, Eastern Hospital of Hepatobiliary Surgery, Second Military Medical University, Shanghai 200438, China.

Tel. +86 • 21 • 25070844

E-mail. yqluo@guomai.sh.cn

Received 1998-11-20

### Preparation and labeling of the probe

**Source of the probe** The HGF probe plasmid was kindly donated by the American Gene Engineering Co., and the HGFr plasmid (c-met plasmid) given by the Gene Bank of the Japanese Cancer Research Resources.

**Preparation and labeling of the probe** The probe was prepared and labeled as described<sup>[2]</sup>. The HGF plasmid was enzyme-cut with -EcoR I-EcoR-V to obtain a 1.4 kb segment as the probe. The c-met plasmid was enzyme-cut with -EcoR-I-Sal-I to obtain a 1.6 kb segment as the probe. Labeling was performed by the digoxin random primer method.

### RNA dot blot hybridization

**Preparation of the hybridization membrane**  $\mu$ LRNA was mixed with the following solutions: 20  $\mu$ L 1L/L- formamide, 7  $\mu$ L 370 mL/L-formaldehyde, 2  $\mu$ L 20 $\times$ SSC at 68 $^{\circ}$ C, which was cooled in ice bath promptly at 15 min. The denatured RNA was spotted on to the nitrocellulose membrane, with 10  $\mu$ L-at each spot (the membrane was wet with water and then soaked in 20 $\times$ SSC for 1h), dried in a vacuum drying oven at 80 $^{\circ}$ C for 2 h, and then sealed in a plastic bag for use.

**Hybridization** Hybridization was conducted according to the instructions of the digoxin DNA labeling test kit.

### In situ molecular hybridization

**Treatment of the slide** The slide was soaked in sulfuric acid overnight, washed, dried at 180 $^{\circ}$ C for 3 h, and then coated with gelatin to which 0.1% DEPC was added to inhibit RNase activity.

**Preparation of frozen sections** Frozen sections of 6  $\mu$ m in thickness dried with cool air flow were fixed with 4% paraformaldehyde buffer solution for 10 min, gradient dehydrated with ethanol, and stored at -70 $^{\circ}$ C for use.

**Procedures of hybridization in situ** This was done according to the instructions of the digoxin DNA labeling test kit.

### Statistical treatment

Percentage of the specimens was compared by  $\chi^2$  test.

## RESULTS

### Results of RNA dot blot hybridization

The results showed that HGF was expressed both in the liver cancers (5/26) and in the nontumorous liver tissues (6/26); the positive rates of expression were low, but they showed no significant difference

between the two groups; c-met expression was relatively high in the liver cancers and the nontumorous liver tissues, the former being higher than the latter (17/26 vs 8/26), showing significant difference ( $P < 0.05$ ).

### Results of hybridization in situ (ISH)

The results of hybridization in situ were classified into four grades (Table 1): negative, weak, moderate and strong. HGF gene expression was not high either in the liver cancers or in the nontumorous liver tissues, while c-met gene expression was high, similar to the result of dot blot hybridization. So far as distribution was concerned, weak and moderate grades dominated HGF gene expression while moderate and strong grades dominated c-met gene expression.

Table 1 The results of RNA ISH of HCC tissue and nontumorous liver tissue

Group	n	HGF expression				c-met expression			
		N	W	M	S	N	W	M	S
HCC	26	20	2	3	1	9	1	6	10
Nontumorous	26	18	3	3	2	13	4	6	3

N: Negative; W: Weak(10%-20%); M: Moderate(40%-60%); S: Strong (70%-80%).

### Relationship between c-met gene expression in cancer tissues and tumor metastasis

Comparative study showed that c-met gene expression was much higher in the group with associated metastasis than that in the group without associated metastasis (15/18 vs 2/8), showing significant difference between the two groups ( $P < 0.01$ ).

## DISCUSSION

### Traits and significance of HGF and HGFr expression in liver cancer and nontumorous liver tissue

HGF has a wide spectrum of biological activity. Recent studies also showed that HGF could inhibit growth of HCC cells as well as AFP gene expression of HCC<sup>[3]</sup>. HGFr is the product of c-met cancer gene, and c-met mRNA has been found to be over-expressed in various tumor tissues<sup>[4]</sup>. No report has been seen about the law of change in HGF and HGFr gene expression in liver cancer. The results of our study showed that although HGF expression was observed both in the liver cancer and the nontumorous liver tissues, its positive rate was much lower than c-met gene expression; c-met gene expression was high both in the liver cancer and in the nontumorous liver tissue, and expression in the former was higher than that in the latter. The mode of c-met expression here was similar to that in other tumor tissues. There was no difference in HGF ex-

pression in the liver cancer and nontumorous liver tissues. In the presence of high expression of c-met gene, sensitivity of malignant tumor cells to HGF was increased; only small amounts of HGF would trigger pronounced response, resulting in extension and metastasis of the tumor. Therefore, determination of c-met gene expression may help assess malignancy and prognosis of a tumor.

### ***C-met gene overexpression and tumor metastasis***

Studies have shown that c-met mRNA concentration is very low or undetectable in normal tissue, whereas it has high expression in the corresponding cancerous tissues. Once a cell with negative HGF is infected, its receptors may be irritated by HGF and activate the cells, which then invade the basement membrane. Malignant cells with high concentration of HGFr have more sensitive and stronger response to HGF<sup>[5]</sup>. Studies reveal that cancerous cells have a defect of c-met protein retrotranscription and processing. The production of this protein involves synthesis of 190kb primary gene, cleavage of  $\alpha$  and  $\beta$  sub-units of c-met and formation of mature HGFr which all need the integration of HGF<sup>[6]</sup>. Some cancerous cells have defective cleavage. As the primary gene itself is active, the cancerous cells would be out of HGF control even if the cells do not split. Cell activity would be increased even in the absence of exogenous HGF. The expression of HGFr on the malignant cell is different from that on the normal cell. Although HGFr expression of normal cells may be increased temporarily after resection of the liver or the kidney, it restores to normal soon after inju-

ry. This is because normal cells and organs are capable of lowering receptor expression and regulating their response to HGF, whereas persistent overexpression of HGFr in malignant tumor cells leads to its excessive reaction with HGF, providing malignant tumor cells with kinetic and aggressive traits<sup>[7]</sup>. The present study revealed that there was a tendency of overexpression of c-met gene in patients with metastatic malignancy, over expression of c-met gene was closely correlated with tumor metastasis and infiltration, and that HGF and its receptor system play an important role in regulating growth and metastasis of liver tumors.

### **REFERENCES**

- 1 Chomczynski P, Sacchi N. Single step method of RNA isolation by acid guanidinium thiocyanate phenol chloroform extraction. *Anal Biochem*, 1987;162:156
- 2 Sambrook J, Fritsch EF, Maniatis T. Molecular cloning. A laboratory manual (second edition) Cold Spring Harbor Laboratory Press, 1989:1345-1356
- 3 Noguchi O, Enomoto N, Ikeda T, Kobayashi F, Marumo F, Sato C. Gene expressions of c met and hepatocyte growth factor in chronic liver disease and hepatocellular carcinoma. *J Hepatol*, 1996 Mar;24:286-292
- 4 Kaji M, Yonemura Y, Harada S, Liu X, Terada I, Yamamoto H. Participation of c-met in the progression of human gastric cancers: anti c-met oligonucleotides inhibit proliferation or invasiveness of gastric cancer cells. *Cancer Gene Ther*, 1996;3:393-404
- 5 Jeffers M, Rong S, Woude GF. Hepatocyte growth factor/scatter factor-met signaling in tumorigenicity and invasion/metastasis. *J Mol Med*, 1996;74:505-513
- 6 Schirmacher P, Odenthal M, Steinberg P, Dienes HP. Growth factors in liver regeneration and hepatocarcinogenesis. *Verh Dtsch Ges Pathol*, 1995;79:55-60
- 7 Lamszus K, Jin L, Fuchs A, Shi E, Chowdhury S, Yao Y, Polverini PJ, Latterra J, Goldberg ID, Rosen EM. Scatter factor stimulates tumor growth and tumor angiogenesis in human breast cancers in the mammary fat pads of nude mice. *Lab Invest*, 1997;76:339-359

Edited by LU Han-Ming

# Long-term effectiveness of infancy low-dose hepatitis B vaccine immunization in Zhuang minority area in China \*

LI Hui<sup>1</sup>, LI Rong-Cheng<sup>2</sup>, LIAO Su-Su<sup>1</sup>, GONG Jian<sup>2</sup>, ZENG Xian-Jia<sup>1</sup> and LI Yan-Ping<sup>2</sup>

**Subject headings** hepatitis B vaccine; immunization; HBsAg; risk factor

## Abstract

**AIM** To observe the long-term effectiveness of low-dose immunization strategy and risk factors of HBsAg carriers in immunized children of Zhuang minorities of Longan County in the 9th year after infancy immunization.

**METHODS** Two epidemiologic methods, a cross sectional follow up study and a case-control study, were used for the evaluation of the serological effect and the determination of the risk factors. Hepatitis B virus markers were detected with radioimmunoassay.

**RESULTS** The protective anti-HBs-positive rate was 43.8% in 1183 children aged 1-9 years, who were immunized with three doses of 10 µg hepatitis B vaccine in infancy according to 0, 1 and 6 months schedule. It declined from 87.9% in the first year to 37.1% in the 9th year after vaccination. The HBsAg-positive rate was 1.6%, not increasing with age during 9 years after the infant immunization program. Compared with 14.0% of HBsAg-positive rate of the baseline survey in 1985, the effectiveness of hepatitis B vaccine immunization was 88.6%. Of 36 immunized children with positive HBsAg, 89.1% were likely attributable to HBsAg positivity of their mothers.

**CONCLUSION** The long-term effectiveness of infancy low-dose hepatitis B vaccine immunization

**is high, and the booster is not needed 9 years after the vaccination in the Zhuang minority area where hepatitis B is highly endemic. A high-dose immunization strategy should be recommended in order to further decrease the current HBsAg-positive rate.**

## INTRODUCTION

Hepatitis B (HB) infection is a major public health problem in developing countries, and hepatitis B vaccine immunization has become a principal strategy to control this disease<sup>[1-3]</sup>. Longan County, inhabited mostly with Zhuang minorities, is a high endemic area of hepatitis B and hepatocellular carcinoma in China. The infant low-dose immunization program integrated with EPI has been implemented in this county for 9 years. In order to provide the evidences for developing the strategy to further improve the effectiveness of immune protection, a study on long-term effectiveness of the low-dose strategy and the risk factors of immunized children with positive HBsAg was conducted in Longan.

## MATERIALS AND METHODS

### *Sample size and subjects*

A total of 1183 children aged 1-9 years were sampled as a vaccination group for the observation of long-term effectiveness in terms of cluster sampling. Those children were born in the period between 1987 and 1996 in Longan County, who had the vaccination record of three doses of 10 µg-plasma-derived hepatitis B vaccine, according to 0, 1 and 6 months schedule of the regimen in which the infancy vaccination was integrated with EPI and without predelivery HBsAg and HBeAg screening for their mothers, and without the booster. In this county, the infant HB vaccination covered 90%, ranging from 75% to 97% between 1987 and 1996.

A total of 3645 children aged 1-9 years were selected as a control group from the subjects of a cross-sectional survey on hepatitis B virus infection of children aged 1-10 years of Longan in 1985. None of the controls had received HB vaccines. The prevalences of their hepatitis B infection markers were representative of the infection level of the -

<sup>1</sup>Institute of Basic Medical Sciences, Chinese Academy of Medical Sciences, Beijing 100005, China

<sup>2</sup>Guangxi Anti-Epidemic & Hygiene Center, Nanning 530021, Guangxi Zhuang Autonomous Region, China

Professor LI Hui, M.D., M.P.H., male, born on 1943-06-20 in Jiangjin County, Sichuan Province, China, Han nationality, graduated from Beijing Medical University as a graduate in 1970 and from Peking Union Medical College as a postgraduate in 1982, now professor of epidemiology, majoring hepatitis B control and etiology of cardiologic vascular diseases, having 28 papers and 7 books published.

\*Supported by the China Medical Board of New York, Inc., USA, Grant No.93-582.

**Correspondence to:** Prof. LI Hui, Department of Epidemiology, Institute of Basic Medical Sciences, CAMS & PUMC, 5# Dong Dan San Tiao, Beijing 100005, China

Tel.+86 • 10 • 65296971(O) +86 • 10 • 65141591(H)

Received 1999-02-05

young population before HB immunization.

Mothers of vaccinated children were selected from both groups of the families of the immunized children, who were HBsAg-positive confirmed serologically after 1987 and who were HBsAg negative in 1996, respectively.

**Study methods**

A cross-sectional follow-up study and a case-control study were adopted for the evaluation of the serological effect and the determination of risk factors of HBsAg carriers after infancy vaccination.

**Hepatitis B vaccine**

Plasma-derived hepatitis B vaccines used from 1987 to 1996 were produced by the National Institute of Biological Products, Beijing (10 µg/per ampoule).

**Lab test**

Radioimmunoassay (RIA) was used for the detection of anti-HBs, anti-HBc and HBsAg. The protective anti-HBs-positive was defined as S/N-ratio ≥ 10.0, and anti-HBc inhibition ratio ≥ 75% and HBsAg S/N-ratio ≥ 2.1 (need confirmation in lab testing) were defined as the sera positive. When comparing with the result of the baseline survey, the anti-HBs-positive was defined as S/N-ratio ≥ 5.0 (retesting for specimens with anti-HBs level of 2.1 to 5 S/N-ratio). RIA reagent kits were provided by the National Institute of Biological Products, Beijing.

**Data analysis**

Both softwares, dBase-III and EPI-info 6.01, were used for the data base and the statistics analysis.

**RESULTS**

**Comparison of positive rates of anti-HBs before and after immunization**

The protective anti-HBs-positive rate was 48.8% on average in 1183 immunized children aged 1-9 years after infancy vaccination, which decreased from 87.9% in the first year to 37.1% in the 9th year. Comparison with the results of the baseline survey in 1985 and the anti-HBs-positive rates for both groups of children before and after the immunization program are shown in Table 1.

**Table 1 Comparison of anti-HBs-positive rates between the immunized children and the unimmunized children**

Age group (year)	Immunized children			Unimmunized children		
	n	Positive <sup>a</sup>	%	n	Positive <sup>a</sup>	%
1	219	165	75.3	759	117	15.4
3	317	198	62.5	539	121	22.4
5	310	148	44.7	590	204	34.6
7	248	131	52.8	655	238	36.3
9	89	49	55.1	364	125	34.1
Total	1 183	691	58.4	2 907	805	27.7

<sup>a</sup>Anti-HBs-positive was defined as S/N ratio ≥ 5.

Table 1 shows that the anti-HBs-positive rate for each age group of vaccinees after the immunization was significantly higher than that of controls ( $P < 0.01$ ), suggesting that the infant low-dose immunization in Longan was effective; however, the anti-HBs-positive rate significantly decreased with age 9 years after the infancy immunization.

**Comparison of positive rates of anti-HBc before and after immunization**

The anti-HBc-positive rates for both groups of children are shown in Table 2.

**Table 2 Anti-HBc-positive rates between the immunized and the unimmunized children**

Age group (year)	Immunized children			Unimmunized children		
	n	Positive <sup>a</sup>	%	n	Positive <sup>a</sup>	%
1	219	7	3.2	759	85	11.2
3	317	8	2.5	539	92	17.1
5	310	16	5.2	590	142	24.1
7	248	9	3.6	655	181	27.6
9	89	8	9.0	364	111	30.5
Total	1 183	48	4.1	2 907	611	21.0

<sup>a</sup>Anti-HBc-positive was defined as inhibitory ratio ≥ 75%.

Table 2 shows that the anti-HBc-positive rate of the vaccinees after the immunization was significantly lower than that of the controls ( $P < 0.01$ ), indicating that the HBV infection frequency in the immunized children 9 years after the vaccination was lower than before; and among the immunized children the anti-HBc-positive rate had a trend of increasing with age, but there was no significant difference between the age groups ( $P > 0.05$ ).

**Comparison of positive rates of HBsAg before and after immunization**

Of 1183 immunized children, 19 (1.6%) HBsAg-positive children was found. The results of pre and post-vaccination are shown in Table 3.

**Table 3 HBsAg-positive rates between the immunized and the unimmunized children**

Age group (year)	Immunized children			Unimmunized children		
	n	Positive <sup>a</sup>	%	n	Positive <sup>a</sup>	%
1	219	2	1.6	1 115	56	5.0
3	317	3	1.0	638	98	15.4
5	310	7	2.3	691	131	18.9
7	248	4	1.6	772	147	19.0
9	89	2	2.3	429	77	18.0
Total	1 183	19	1.6	3 645	509	14.0

<sup>a</sup>HBsAg-positive was defined as S/N ratio ≥ 5.

Table 3 shows that the HBsAg-positive rate was 1.6% in the immunized children, being significantly lower than 14.0% in the unimmunized children ( $P < 0.01$ ), and the effectiveness of the hepatitis B vaccine immunization was 88.6% 9 years after in-

fancy vaccination; in addition, the HBsAg-positive rate was not increasing with age ( $P>0.05$ ).

#### Study on the risk factors of HBsAg-positivity of immunized children

A case-control study on the risk factor of HBsAg-positivity of immunized children was conducted. A number of 36 individuals were sampled from the HBsAg-positive children (sampling proportion of 85.7%) as a case group, and 516 individuals from the HBsAg-negative children as control group (sampling proportion of 44.6%), in the vaccination population. The results of sera HBsAg detection for their mothers are shown in Table 4.

**Table 4 Comparison of HBsAg-positive mothers between case and control groups**

Positive HBsAg of mother	Case group	Control group	Total	OR	P
Yes	23	84	107	9.16	<0.01
No	13	435	448		
Total	36	519	555		

Table 4 shows that among the immunized children, the HBsAg-positive rate of the mothers of 36 HBsAg-positive children after infancy vaccination was 9.16 times that of the mothers of the control (OR = 9.16,  $P<0.01$ ), and the attributable risk (AR) was estimated as 89.1%. It is indicated that after the immunization, the possibility of HBsAg seroconversion of offsprings for the HBsAg-positive mothers was significantly higher than that for the negative mothers, and the HBsAg positivity of immunized children was mainly due to the HBsAg carrying mothers.

#### DISCUSSION

Longan County is a remote minority area, and an area of high HBV endemicity in China. To evaluate the effectiveness of the immunization strategy with low-dose of HB vaccine for infants and without predelivery HBV markers screening for their mothers is of important significance for the control of HBV infection of this kind of areas. The HBsAg-positive rate decreased from 14.0% of the unimmunized children aged 1-9 years in 1985 to 1.6% of the immunized children 9 years after the infancy vaccination, and the effectiveness of the vaccine protection was 88.6% for the immunized population. Based on this data, the HBsAg-positive rate of children aged 1-9 years in the whole county was estimated as 2.84% ( $0.9 \times 0.016 + 0.1 \times 0.14$ ), and the effectiveness of the HB vaccination was 79.7% for the

whole population with same age. The HBV infection will be effectively controlled in the Zhuang minorities of Longan as the HBsAg carriers decreased obviously in children below age of 9 years. The results indicate that the low-dose immunization strategy used in Longan is successful for the hepatitis B control, and beneficial in health economics for the remote minority areas in China.

To further improve the protective effectiveness of HB vaccine immunization in population is still a problem which calls for studies. In recent years, the average coverage of HB immunization of infants was around 90%, ranging from 75% to 97%, in this area. If the coverage can be expanded, a higher effectiveness will be obtained. In addition, it is also important to determine the risk factors of HBsAg-positive children after vaccination. Our results from a case-control study revealed that the yielded HBV infection among the immunized infants was mainly due to the HBsAg positivity of their mothers (AR = 89.1%), therefore, perinatal HBV infection, i.e., failure of HB vaccine immunization, was probably the most important reason for this. It is imperative and of great benefit to recommend a high-dose immunization strategy for neonates of mothers carrying HBeAg based on the predelivery screening with the improvement of economic condition of this area.

The results of our study showed that the vaccine-induced antibody level was decreasing year by year, but the HBsAg-positive rate always fluctuated around 2% among the immunized population. Our findings are similar to the results of Edward<sup>[4]</sup>, Whittle<sup>[5]</sup> and Xu<sup>[6]</sup>. This phenomenon can be explained with the vaccine-induced immunologic memory for hepatitis B surface antigen. This study indicates that the time table for booster of HB vaccine has not been determined due to lack of relative evidences 9 years after this immunization strategy, and the follow-up studies should be continued in Longan.

#### REFERENCES

- 1 Coursaget P, Chotard J, Vincelot P, Diopmar I, Yvonnet B, Sarr M. Seven-year study of hepatitis B vaccine efficacy in infants from an endemic area (Senegal). *Lancet*, 1986;ii:1143-1145
- 2 Sung JL and Asian Regional Study Group. Hepatitis B virus eradication strategy for Asia. *Vaccine*, 1990;8(Suppl):95-99
- 3 Chao HL. Study on immune persistence and protective effect of hepatitis B vaccine. *Chin J Experiment Clin Virol*, 1995;9:1-4
- 4 Edward T, James C, Robert JG, Anne CB. Nine-year follow-up study of a plasma-derived hepatitis B vaccine in a rural African setting. *J Med Virol*, 1993;40:204-209
- 5 Whittle HC, Maine N, Pikington J, Menely M, Fortuin M, Bunn L. Long-term efficacy of continuing hepatitis B vaccination in infancy in two Gambian villages. *Lancet*, 1995;345:1089-1092
- 6 Xu ZY, Chao HL, Liu CB, Yang JY, Yan TQ, Shun YD. A cross-sectional study of long-term effectiveness of universal infant hepatitis B vaccination program. *Chin J Experiment Clin Virol*, 1995;9:13-16

# Cloning of the non-structural gene 3 of hepatitis C virus and its inducible expression in cultured cells \*

ZHANG Shu-Zhong<sup>1</sup>, LIANG Jia-Jing<sup>1</sup>, QI Zhong-Tian<sup>2</sup> and HU Yi-Ping<sup>1</sup>

**Subject headings** hepatitis C virus; gene, viral; gene expression; cells, cultured

## Abstract

**AIM** To study the inducible expression of hepatitis C virus *ns3* gene (HCV-*ns3*) in eukaryotic cells.

**METHODS** The *ns3* gene was obtained from plasmid pBns3 by polymerase chain reaction and inserted into the cloning vector pGEM-T. Then, the *ns3* was subcloned into the vector pMSG to generate dexamethasone (DM)inducible expression plasmid pMSG-*ns3*. CHO cells were transfected by pMSG-*ns3* using calcium phosphate precipitation method and cultivated for 12 h-24 h. The transfected cells were induced with DM and the transient expression of NS3 protein was analyzed by ELISA and Western-blot methods.

**RESULTS** After treated with  $3 \times 10^{-8}$  mol/L DM, the expression of NS3 was observed in the transfected CHO cells. A slightly higher level of NS3 was shown along with the time of DM treatment.

**CONCLUSION** The inducible expressing vector pMSG-*ns3* might be helpful for further studies of the characteristics of the *ns3* gene *in vivo*.

## INTRODUCTION

Hepatitis C virus (HCV) is a recently identified enveloped positive-strand RNA virus, with a genome size of approximate 9.5 kb, that exhibits a considerable degree of sequence variation. HCV genotypes vary in different geographical areas<sup>[1,2]</sup>. Data show that the viral protease plays a key role in the HCV polyproteins processing<sup>[3-5]</sup>. Whether the NS3 protein, a viral protease, has a putative influence during the HCV pathogenesis is unknown. By using PCR method, we obtained the *ns3* fragment from the recombinant cloning vect or pBns3 which contained the Chinese HCV *ns3* gene and then subcloned it to construct the inducible expressing vector pMSG-*ns3*. The successful expression of *ns3* gene *in vitro* is helpful for the study of the NS3 protein biological activities *in vivo*.

## MATERIALS AND METHODS

### Materials

Plasmids Recombinant vector pBns3 was provided by the Microbiological Department; cloning vector pGEM-T vector system kit was purchased from Promega; and expressing vector pMSG was provided by Dr. ZHENG Wen-Chao.

Cells *E. Coli* DH5 $\alpha$  and CHO cells were preserved in our department.

**PCR primers design and synthesis** Primers were provided by Dr. WANG Su-Ming (Human Gene Therapy Research Institute). Postive primer: 5'-GTCGCTAGCCATGGAATTCCTACG-3' with the *Nhe*-I (GCTAGC) restriction site, the initiation codon ATG and the Kozak sequence. Negative primer: 5'-CGGCGCT CGAGTGGAAATTCATAC-AA 3' with the *Xho* I restriction site (CTCGAG). The recombinant plasmids pBns3 were used as template to amplify the *ns3*-690 bp fragments.

**Main reagents** Restriction enzymes, T4 ligase, calf intestinal alkaline phosphatase (CIP), protoblot Western-blot AP system kit and fmol DNA sequencing system kit were all purchased from Promega, QIA quick gene gel kit from QIA gene. Human anti-HCV serum and anti-HCV EIA kit (TMB) were provided by the Microbiology Department.

<sup>1</sup>Department of Cell Biology, Department of Basic Medicine, Second Military Medical University, Shanghai 200433, China

<sup>2</sup>Department of Microbiology, Department of Basic Medicine, Second Military Medical University, Shanghai 200433, China

M.D. ZHANG Shu-Zhong, male, born on December 18, 1968 in Jinan, Shandong, China, graduated from Second Military Medical University in July 1997, lecturer, engaged in the researches of transgenic animals under the instruction of Professor HU Yi-Ping, having three papers published.

\*Project supported by the National Natural Science Foundation of China, No.39470290.

Correspondence to: HU Yi-Ping, Department of Cell Biology, Department of Basic Medicine, Second Military Medical University, Shanghai 200433, China

Tel. +86 • 21 • 25070240

Received 1998-11-09 Revised 1999-01-16

## Methods

**Plasmid construction** The 690 bp fragments of *ns3* gene were amplified from the recombinant plasmid pBns3 by PCR and subcloned into the cloning vector pGEM-T. The positive clones selected from the transfected DH5 $\alpha$  were performed as described by the pGEM-T vector systems (Promega). The constructed plasmids (designated as pGEM-*ns3*) were identified by the restriction enzyme analysis and verified by sequencing. The corresponding *ns3* gene was excised from the pGEM-*ns3* digested with *Nhe*I and *Xho*I and then religated with the pMSG to generate the dexamethasone (DM) inducible expressing plasmids pMSG-*ns3* (Figure 1).

## Transient expression of NS3 protein

Transient expression of NS3 protein was analyzed in CHO cells transfected with the pMSG-*ns3* by the calcium phosphate coprecipitation method. Four hours after the addition of DNA, the cells were glycerol shocked with 10% glycerol in PBS for 2 min and replenished with fresh medium to grow for 24 h. After 8 h, 24 h and 32 h in the presence of DM, respectively, the transfected cells were collected to detect the NS3 proteins. The similar cell preparations untransfected by the pMSG-*ns3* served as negative control. The collected cells were treated with lysis buffer (50mM-Tris.cl, pH 8.0, 10 mg/L- phenyl methylsulfonyl fluoride, 1% Nonidet P-40) for 20 min in ice bath and then centrifuged for 15 min in a microfuge. The supernatants were isolated and prepared to be analyzed by ELISA and Western-blot methods.

## Statistical analysis

Results were shown as  $\bar{x} \pm s$  (mean  $\pm$  SD) and a paired Student's *t* test was used for quantitative information, and  $P < 0.05$  was considered statistically significant. Statistical analysis of the results was carried out using Duncan's multiple range test with computer.

## RESULTS

**Amplification of HCV-*ns3* by PCR** Using the plasmid pBns3 as template, PCR was performed to amplify a 690bp fragment and then cloned into *Xho*-I and *Nhe*-I sites of the cloning vector pGEM-T (Figure 2).

**Plasmid construction** All plasmids described in this study were constructed in DH5- $\alpha$ . The extracted DNA sequencing showed that the inserted fragments contained: the Kozak sequence, the initiation codon ATG and the *Nhe*I, *Xho*I restriction sites; the 690bp corresponding sequence of the *ns3* gene; the correct reading frame of the NS3 proteins (Figures 3 and 4).

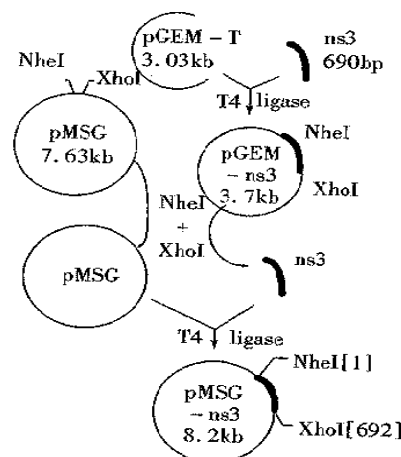


Figure 1 The construction of pGEM-*ns3* and pMSG-*ns3*.

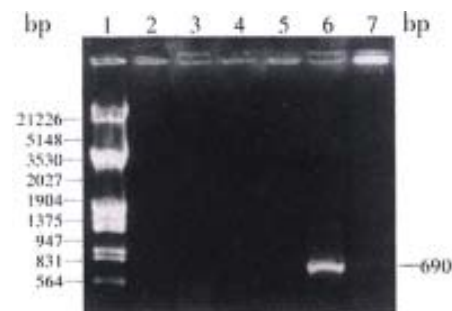


Figure 2 The PCR results of pBns3.

Lane 1:  $\lambda$ /EcoR-I + Hind-III marker; Lane 2, 3: negative controls; Lane 4, 5: PCR results from other primers; Lane 6: PCR products of *ns3* gene annealing at 58°C; Lane 7: PCR result from another annealing temperature.

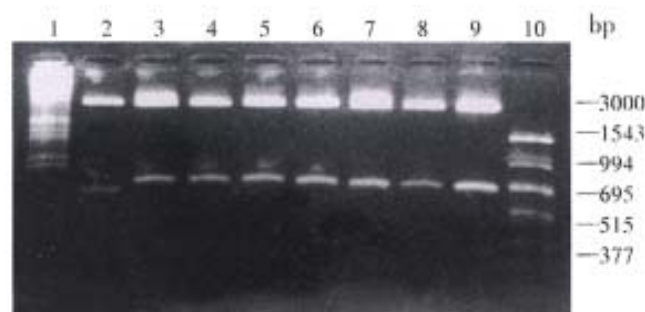


Figure 3 pGEM-*ns3* digested with *Nhe*-I and *Xho*-I.

Lane 1:  $\lambda$ /EcoR-I + Hind-III marker; Lane 2-9: clone 8-1; Lane 10: PCR marker



Figure 4 pMSG-*ns3* (clone 1) digested with *Sac*-I and *Hind*-III. Lane 1:  $\lambda$ /Hind-I marker; Lane 2: Clone 1 digested with *Hind*-III; Lane 3: Clone 1 digested with *Sac*-I; Lane 4:  $\lambda$ /EcoR-I + Hind III marker.

**Expression of the NS3 proteins in mammalian cells** In the groups transfected by DM induced pMSG-*ns3*, the ELISA results were different as compared with the negative control ( $P < 0.05$ ) (Table 1). A-M-r 30 000 protein was detected by Western blot analysis (Figure 5).

**Table 1** The ELISA results CHO cells transfected by pMSG-*ns3* and induced by DM ( $\bar{x} \pm s$ )

Serial dilution	Negative control	Treatment periods (t/h)			
		0	8	24	32
1:16	0.08±0.02	0.18±0.01 <sup>a</sup>	0.20±0.01 <sup>a</sup>	0.20±0.02 <sup>a</sup>	0.22±0.01 <sup>a</sup>
1:32	0.04±0.02	0.19±0.02 <sup>a</sup>	0.17±0.01 <sup>a</sup>	0.18±0.01 <sup>a</sup>	0.22±0.01 <sup>a</sup>
1:64	0.02±0.00	0.14±0.02 <sup>a</sup>	0.15±0.01 <sup>a</sup>	0.14±0.01 <sup>a</sup>	0.20±0.02 <sup>a</sup>
1:128	0.03±0.02	0.12±0.01 <sup>a</sup>	0.15±0.00 <sup>a</sup>	0.12±0.01 <sup>a</sup>	0.16±0.01 <sup>a</sup>
1:256	0.01±0.01	0.06±0.01 <sup>a</sup>	0.09±0.03 <sup>a</sup>	0.11±0.01 <sup>a</sup>	0.07±0.01 <sup>a</sup>

<sup>a</sup> $P < 0.05$  vs negative control.



**Figure 5** The Western-blot of the NS3 protein transfected cells induced by DM.

Lane 1: negative control (untransfected); Lane 2, 3: groups induced after by DM 24 h and 32 h ( $3 \times 10^{-7}$  mol/L); Lane 4-6: groups induced by DM after 8 h, 24 h and 32 h ( $3 \times 10^{-8}$  mol/L); Lane 7: uninduced group.

## DISCUSSION

Epidemiological data show that more than 1% of the world population are infected with HCV and HCV patients often develop chronic hepatitis, with long-term complications of cirrhosis and hepatocellular carcinoma (HCC)<sup>[6]</sup>. Some reports suggest that several viral proteases do harm their hosts, such as human immunodeficiency virus type 1 protease (HIV-1 PR) which can destroy the cytoskeletons (the latter involves the cell shapes, the initiation of mitoses may play an essential part in cell signal transportations) and cause the cell abnormal proliferation leading to carcinogenesis<sup>[7,8]</sup>. Whether the NS3 proteins, also being a viral protease, would injure the host cytoskeletons and attribute to the high incidence of HCC in HCV patients is worth investigation.

To facilitate the expression of NS3 protein *in vitro* in our study, an inducible expressing vector

pMSG-*ns3* containing both the initiation codon ATG and the Kozak sequence (GCCATGG) was created. Surprisingly, however, no significant differences of ELISA results were found in other cells (such as HeLa, SMMC-7721, etc.). Under the low level of the protein expression, the non-specific agents existing in the cell extracts from the human beings might have across-reaction with the detection antibody to cause a high background. The same initiation codon might be affected by several regulation elements existing in different cells and lead to different efficiencies in the expression. To avoid the interferences resulting from certain non-specific agents, CHO cells were used as transfected hosts. Subsequently, the NS3 proteins with Mr-30 000 were detected in all the transfected groups after the treatment of DM and their contents increased slightly along with the time of treatment. Although the ELISA results of the transfected group apparently increased in the absence of DM ( $P < 0.05$ ), no NS3 proteins were detected by the Western-blot analysis. Thus, in order to eliminate the fault results, the Western-blot method are more reliable and convincing for analyzing the proteins expression than the other means such as ELISA, etc.. Our study of the transient expression of NS3 proteins *in vitro* is not only available for further selecting cell lines with a stable integrants of *ns3* gene, but also helpful for the development of the *ns3* transgenic mice and the study of the NS3 biological functions *in vivo*.

## REFERENCES

- 1 Choo QL, Kuo G, Weiner AJ, Overby LR, Bradley D, Houghton M. Isolation of a cDNA clone hepatitis genome. *Science*, 1989; 244:359-362
- 2 Qi ZT, Pan W, Kong XT. Immunoscreening and identification of Chinese HCV genomic cDNA  $\lambda$ gt11 Library. *Acad J Sec Mil Med Univ*, 1992;13:401-410
- 3 Tomei L, Failla C, Santolini E, Francesco RD, Monica NL. NS3 is a serine protease required for processing of hepatitis C virus polyprotein. *J Virol*, 1993;67:4017-4026
- 4 Takamizawa A, Mori C, Fuke I, Manabe S, Murakami S, Fujita J, Onishi E, Andoh T, Yoshida I, Okayama H. Structure and organization of the hepatitis C virus genome isolated from human carriers. *J Virol*, 1991;65:1105-1113
- 5 Bartenschlager R, Ludwina AL, Mous J, Jacobsen H. Nonstructural protein 3 of the hepatitis C virus encodes a serine type proteinase required for cleavage at the NS3/4 and NS4/5 junctions. *J Virol*, 1993;67:3835-3844
- 6 Plageman PGW. Hepatitis C virus brief review. *Arch Virol*, 1991; 120:165-180
- 7 Shoeman RL, Honer B, Mothes E, Traub P. Potential role of the viral protease in human immunodeficiency virus type 1 associated pathogenesis. *Med Hypotheses*, 1992;37:137-150
- 8 Wang Ning. Modulation of cytoskeletal stiffness and cancer inhibition In: LI Chun-Hai, GUO Ya-Jun, eds. Current Advance in Tumor Molecular Biology. Beijing: Military Medical Science Press, 1996:53-56

Edited by WANG Xian-Lin

# Surgical resection for hepatoportal bile duct cancer

HE Xiao-Shun, HUANG Jie-Fu, LIANG Li-Jian, LU Ming-De and CAO Xiu-Hu

**Subject headings** biliary tract neoplasms/surgery;  
prognosis hepatic portal

## Abstract

**AIM** To discuss the effect of surgical procedures on the prognosis of patients of bile duct cancer and their indications.

**METHODS** A retrospective analysis was made for 52 cases of hepatoportal bile duct cancer treated from January 1991 to December 1996. All the cases were classified according to the modified Bismuth-Corlette system and received appropriate operation. Therapeutic effects were evaluated on the basis of their survival rates, jaundice elimination, comfort index, operative mortality and complications.

**RESULTS** Seventeen cases received surgical resection (32.7%). The survival rate was 71.4%, 35.7% and 10.4% for one, two and three years respectively, and was 30%, 16.8% and 0% for those with drainage ( $P < 0.05$ ). The mortality rate was 6.0% for the drainage group and 5.9% for the resection group ( $P > 0.05$ ). Of the 17 resected patients, 8 (47.1%) had curative resection and 9 (52.9%) noncurative resection. Their mean survival time was 21.1 months and 7.5 months respectively ( $P < 0.05$ ).

**CONCLUSION** Proper surgical procedure should be used on the basis of the local and general conditions of the patients, and aggressive resection with or without liver resection is a valid procedure for the treatment of hepatoportal bile duct cancer and can significantly improve the prognosis of patients.

## INTRODUCTION

Surgical resection is the only effective way for hepatoportal bile duct cancer. However, the treatment is very troublesome due to its low resectability and poor prognosis. The purpose of this paper is to discuss the effect of surgical procedures on its prognosis and indications.

## PATIENTS AND METHODS

From January 1991 to December 1996, 52 patients with hepatoportal bile duct cancer (53.6% of extrahepatic bile duct cancer) were treated in our hospital. Of them, 39 were male and 13 female aged from 37 to 70 years, averaging 56.8. The patients aged from 50 to 70 years made up 65.4%. The diagnosis was confirmed by histological examination in 46 and by operation in 6. All the tumors were classified according to the modified Bismuth-Corlette system. Therapeutic effect was evaluated by their survival rate, jaundice elimination, comfort index, operative mortality and complications. The data collected during the follow-up were analysed with the help of American SAS software. The parameters were compared by Chi-square test and Student's t test. Differences between the survival rates were analysed by Likelihood Ratio Test or Wilcoxon test, and significant difference ( $P < 0.005$ ) was found.

## RESULTS

### *Pathological findings*

Out of the 52 patients (88.5%), the diagnosis of bile duct cancer was confirmed by histological examination in 46 and by operation in 6. Adenocarcinoma was found in 97.8% and sclerotic cholangiocarcinoma in 52.9% of the 17 resected patients. Local or distant metastatic tumors were found in 7 patients, which were confirmed in the 6th, 55th, 45th, 15th, 14th, 25th and 15th month after operation respectively by fine needle aspiration biopsy (FNAB), CT, or B-US.

Based on macroscopic appearance, complete excision of the tumor was not achieved in six cases. Involvement of the stem of the portal vein was discovered in one case during dissection. Of the 17 resected patients, a macroscopic curative resection was achieved in 11 (11/52, 21.2%). Residual cancer cells were found at the surgical resection margins in 3 cases. Thus, curative resection was performed only in 8 patients (8/52, 15.4%).

Department of Surgery, First Affiliated Hospital of Sun Yat-Sen University of Medical Sciences, Guangzhou 510080, Guangdong Province, China

**Correspondence to:** Dr. HE Xiao-Shun, Department of Surgery, First Affiliated Hospital of Sun Yat-Sen University of Medical Sciences, 58 Zhongshan Er Road, Guangzhou 510080, Guangdong Province, China

Received 1998-12-22

### Surgical findings

The types of operation for hepatoportal bile duct cancer are shown in Table 1.

**Table 1 Operative procedures for 52 hepatoportal bile duct cancer and their mortality**

Operative procedure	No. of patients	No. of death
Resection	17	1
Local resection (LR)	(3)	(0)
LR+Caudate segment resection	(1) <sup>a</sup>	(0)
LR+Median segment resection	(4) <sup>a</sup>	(1)
LR+Right/left hemihepatectomy	(9) <sup>b</sup>	(0)
Bypass	33	2
Segment III cholangiojejunostomy	(20)	(2)
Segment V cholangiojejunostomy	(9)	(0)
Choledochojejunostomy	(3)	(0)
Intubation	1	0
Exploration	2	0
Total	53	3

<sup>a</sup>Partial excision of portal vein and repair of its lateral wall;

<sup>b</sup>Reconstruction of right hepatic artery in one case.

### Operative survival rate and complications

The total operative mortality rate was 5.8% (3/52) and 5.9% (1/17) and 6.0% (2/33) respectively in resection group and drainage group with no statistical significance ( $P = 0.5422$ ). No death was found in 30 days after extensive excision. One patient died 27 days after palliative excision due to massive hemorrhage in the upper digestive tract caused by stress ulcer.

The total operative complication rate was 44.2% (23/52), 52.9% in the resection group and 42.4% in the drainage one with no statistical significance ( $P = 0.4797$ ). The operative complication rate was 50.0% (4/8) in those who received curative resection, and was 55.6% in those who had palliative excision.

### Survival rate

The average survival of the 52 patients was 9.1 months. The survival rate for 1, 2, 3, 4 and 5 years was 43.2%, 25.9%, 25.9%, 12.9% and 4.0%.

**Types of operation and quality of life** The average survival time was 6.4 months in the drainage group and was 15.6 months ( $P < 0.05$ ) in the resection group. The quality of life after operation was evaluated according to the elimination of jaundice, and the comfort index. Complete elimination of jaundice means that serum bilirubin is returned to normal while partial elimination implies that serum bilirubin is dropped by 50% at least as compared with that before operation, and no reduction refers to its

decrease of less than 50%. The duration of well-being is known as the period of time in which the patient is free of jaundice, pruritus, cholangitis and malaise after surgery. The comfort index is taken as the duration of well-being expressed in percentage of total survival time, which is close to 100% when the disease is completely relieved (Table 2).

$$\text{Comfort Index} = \frac{\text{Duration of well-being (mon.)}}{\text{Duration of survival (mon.)}} \times 100\%$$

**Comparison of the survival rates between resection and drainage** The survival rate was 71.4%, 35.7% and 10.4% for the patients who underwent resection, and 30.0%, 16.8% and 0% for the patients underwent drainage. There was a significant difference between them ( $P < 0.05$ ).

**Table 2 Average survival time and comfort indices of the patients after resection and drainage**

Operative procedure	No. of patients	Mean survival time (mo)	Comfort index (%)
Resection	17	15.62 <sup>a</sup>	91 <sup>b</sup>
Drainage	33	6.37 <sup>a</sup>	74 <sup>b</sup>

<sup>a</sup> $P < 0.005$ , <sup>b</sup> $P < 0.05$ .

### DISCUSSION

The treatment of hepatoportal bile duct cancer is very troublesome. Untreated patients usually die of recurrent cholangitis and hepatic failure within 3 months when their diagnosis is confirmed<sup>[1]</sup>. Before 1970, many authors held that bile duct cancer should be treated vigorously. Therapeutic effect of excision for it has been gradually improved as a result of accurate diagnosis and better operative techniques.

It was reported that 15%-95% patients with hepatoportal bile duct cancer upon the spectrum of cases referred to any particular surgical unit and the cancer received excision, which has exceeded 30%<sup>[2,3]</sup>. In our study 32.7% patients received excision. The excision rate and survival rate were much higher than those from 1986 to 1990 ( $P < 0.05$ )<sup>[4]</sup>.

The data in our study provides strong support for other surgeons<sup>[2,3,5]</sup>. The survival rate for 1, 3 and 5 years after radical operation of hepatoportal bile duct cancer was 71.4%, 35.7% and 5.9% while the operative mortality and complications had no remarkable increase. The operative death rate due to hepatic failure and bile leakage at the anastomosis was 5.9% in our study, while it was from 0% to 27% in the literature.

It is controversial whether radical operation

should be performed for hepatoportal bile duct cancer. Some authors held that it is not necessary to have partial hepatectomy because it can not improve the survival and will increase postoperative mortality and complications on the contrary<sup>[6,7]</sup>. The residual rate of cancer cell at its incisional margin was 28%-92% in the literature. Furthermore, the recurrent rate of tumor was high even after radical operation. Others advocate radical operation for cholangiocarcinoma with right or left hemihepatectomy, trisegmentectomy, vascular resection and its reconstruction and caudate lobe resection, even total hepatectomy and orthotopic liver transplantation<sup>[2,3,8]</sup> in order to remove more tumor tissues, prolong the survival and reduce its recurrence. In our study, out of the 17 resected patients, 14 (82.4%) had hepatectomy which was characterized by: ① Hepatoportal parenchyma was excised if it was involved or in an effort to eliminate residual cancer cells at its incisional margins; ② Hepatolobectomy was a curative procedure for the patient when unilateral bile duct was involved; ③ Unilateral bile duct was involved beyond second order; ④ Unilateral portal vein or hepatic artery was involved. The average survival was 16.1 months. Of the 17 patients who underwent resection, curative excision was performed in 8, and non-curative excision in 9. Their average survival was 21.1 and 7.5 months respectively ( $P < 0.05$ ). The 1 and 2-year survival of those with no residual cancer cells at their incisional margins was 87.5% and 44.5%, while it was 57.1% and 30.1% ( $P < 0.05$ ) for those with residual cancer cells at their incisional margins. No significant difference was found in operative complication and death rate between the two groups. Therefore, hepatolectomy should be taken into consideration when the patient's local conditions and general conditions are good.

However, a considerable number of patients could not endure major operations due to their severe jaundice and poor liver function when they came to see a doctor. Major hepatectomy would undoubtedly lead to further damage of liver function and postoperative hepatic failure. Median hepatolectomy should be performed for such patients because it has the advantages of less hepatic injury and a higher cure rate<sup>[9]</sup>. In our study, 4 of the 17 resected patients received median hepatolectomy, 2 curative excision, and 2 palliative excision. One died of massive gastrointestinal bleeding due to stress ulcer on the 27th day after operation. The other 3 had significant improvement in their life Quality with an average survival of 14.7 months, and one is still alive 25 months after operation with no recurrence.

Cholangiocarcinoma is inclined to invade its peripheral tissues, such as portal vein, hepatic artery and parenchyma as well as the caudate lobe because there is no muscular layer of mucosa in the wall of bile duct. It was reported that better prognosis could be achieved by caudatolectomy<sup>[3,10]</sup>. One patient received this operation in our study. We advocate resection of the caudate lobe when considerable involvement of the caudate ducts or parenchyma is confirmed by preoperative or intraoperative assessment. Angiotomy and reconstruction are advisable for selected patients when their blood vessels are involved<sup>[11]</sup>. In this study, wedge resection and reconstruction of portal vein were performed in one patient due to involvement of portal veins; and right hepatic artery reconstruction and left hemihepatectomy in another due to involvement of portal vein, left and right arteries. They recovered after operation. It is believed that residual cancer cells in the connective tissue around the hepatoduodenal ligament may play a major role in the tumor recurrence. Major hepatic resection, including excision of the whole hepatoduodenal ligament, is experimentally feasible, and its clinical results are promising<sup>[12,13]</sup>. However, tumor cells were found in some patients even after such extensive excisions. So its indication should be taken into careful consideration in clinical practice.

Although, excision is the only way to cure hepatoportal bile duct cancer, a considerable number of patients are not suitable to receive it in spite of great advances having made in diagnostic techniques and surgical treatment. Palliative operation has advantages of less complications and better life quality over conservative treatment<sup>[14]</sup>. The curative effect of palliative operation is characterized by the level of jaundice elimination. In our study, complete elimination of jaundice was made in 85% of the 20 patients treated by segment III hepatocholecholejojunostomy with a comfort index of 74%, and with a 10% operative mortality. The curative effect of SV hepatocholecholejojunostomy in the other 9 patients was similar to that of segment III hepatocholecholejojunostomy. Drainage tube may be placed for those who can not receive excision and intrahepatic drainage. Since long-standing external drainage of bile may lead to water and electrolyte imbalance, recurrence of jaundice, and cholangitis. Intrahepatic anastomosis to segment III or V hepatic duct, or both should be the first choice in palliative treatment.

From the above analysis, we believe that the following preoperative examinations must be made for cholangiocarcinoma, such as serological and biological tests, liver and renal function test, blood co-

agulation tests, B-US, PTC/ERCP, angio graphy, etc. Only when there are no contraindications and the patient's general condition is good, should a tumor excision with or without liver resection be performed. Resection and reconstruction of hepatoportal vessels should be carried out for selected patients. If resection is not feasible, palliative biliary drainage is worthwhile. More extensive resection (like block resection) should be selected very carefully. It is not wise to lay undue stress on a more radical operation. What we advocate is the surgical procedure selected according to the extent, gross appearance and degree of infiltration of tumor to its adjacent tissues or organs in order to achieve the most effective result and to relieve the patient's sufferings.

#### REFERENCES

- 1 Denbesten L, Liechty RD. Cancer of the biliary tree. *Am J Surg*, 1965;109:587
- 2 Baer HU, Stain SC, Dennison AR, Eggars B, Blumgart LH. Improvements in survival by aggressive resections of hilar cholangiocarcinoma. *Ann Surg*, 1993;217:20
- 3 Sugiura Y, Nakamura S, Iida S, Hosoda Y, Ikeuchi S, Mori S, Sugio-ka A, Tsuzuki T. Extensive resection of bile ducts combined with liver resection for cancer of the main hepatic duct junction. *Surgery*, 1994;115:445
- 4 Cao XH. A clinical analysis of 106 cases of extrahepatic bile duct cancer. *Shi Yong Wai Ke Za Zhi*, 1992;12:578
- 5 Huang JF, Li SP, Cao XH. A discussion on surgical option for proximal bile duct cancer. *FU Bu Wai KE*, 1992;3:179
- 6 Hadjis NS, Blenkham JI, Alexander N, Benjamin IS, Blumgart LH. Outcome of radical surgery in hilar cholangiocarcinoma. *Surgery*, 1990;107:597
- 7 Bengmark S, Ekberg H, Evander A, Stahl BK, Tranberg KG. Major liver resection for hilar cholangiocarcinoma. *Ann Surg*, 1988; 207:120
- 8 Pichlmayr R, Weimann A, Ringe B. Indication for liver transplantation in hepatobiliary malignancy. *Hepatology*, 1994;20:33s
- 9 White TT. Skeletonization resection and central hepatic resection in the treatment of bile duct cancer. *World J Surg*, 1988;12:48
- 10 Nimura Y, Hayakawa N, Kamiya J, Kondo S, Shionoya S. Hepatic segmentectomy with caudate lobe resection for bile duct carcinoma of the hepatic hilus. *World J Surg*, 1990;14:535
- 11 Nimura Y, Hayakawa N, Kamiya J, Maeda S, Kondo S, Yasui A, Shionoya S. Combined portal vein and liver resection for carcinoma of the biliary tract. *Br J Surg*, 1991;78:727
- 12 Mimura H, Takakura N, Kim H. Block resection of the hepatoduodenal ligament for carcinoma of bile duct and gallbladder: Surgical technique and a report of 11 cases. *Hepatogastroenterology*, 1991;36:561
- 13 Kumada K, Ozawa K, Shimahara Y, Morikawa S, Okamoto R, Moriyasu F. Truncumbilical bypass of the portal vein in radical resection of biliary tract tumors involving the hepatic duct confluence. *Br J Surg*, 1990;77:749
- 14 Langer JC, Langer B, Taylor BR, Zeldin R, Cummings B. Moreover, the cytotoxicity of abdominal cavity infiltrating lymphocytes induce hepatic bile ducts: results of an aggressive surgical approach. *Surgery*, 1985;98:752

Edited by WANG Xian-Lin

# Evaluation of dot immunogold filtration assay for anti-HAV IgM antibody \*

WU Wei, XU De-Zhong, YAN Yong-Ping, ZHANG Jing-Xia, LIU Ying and LI Ru-Lin

**Subject headings** hepatitis A virus; immunoglobulin/analysis; immunogold filtration assay

## Abstract

**AIM** To detect hepatitis A virus-specific immunoglobulin M (IgM) antibody rapidly.

**METHODS** Colloidal gold with an average diameter of 15 nm was prepared by controlled reduction of a boiling solution of 0.2 g/L-chloroauric acid with 10 g/L-sodium citrate and labeled with anti-HAVIgG as gold probe. Dot immunogold filtration assay (DIGFA) has been developed by coating anti-human  $\mu$  chain on nitrocellulose membrane (NCM) for capturing the anti-HAV IgM in serum, then using cultured hepatitis A antigen as a "bridge", connecting anti-HAV IgM in sample and anti-HAV IgG labeled colloidal gold. If there was anti-HAV IgM in sample, gold probes would concentrate on NCM, which will appear a pink dot.

**RESULTS** A total of 264 serum samples were comparatively detected with both DIGFA and ELISA by "blind" method. Among them, 88 were positive and 146 were negative with the two methods. The sensitivity and the specificity of DIGFA were 86.27% and 90.12%, respectively. Fifteen negative serum samples and 15 positive serum samples were detected 3 times repeatedly, the results were the same.

**CONCLUSION** DIGFA is a simple, rapid, sensitive, specific and reliable method without expensive equipment and is not interfered with rheumatoid factor (RF) in serum. It is suitable for basic medical laboratories. The test could be applied for diagnosis and epidemiological survey of hepatitis A. It has a broad prospect in application.

Department of Epidemiology, Fourth Military Medical University, Xi'an 710033, Shaanxi Province, China

Dr. WU Wei, female, born on 1973-05-20 in Hohhot City, Inner Mongolia, Manchu nationality, graduated from Fourth Military Medical University as a post graduate in 1998, assistant of epidemiology, majoring viral hepatitis, having 2 papers published.

\*Supported by the mandatory key project for the Ninth-Five year plan of PLA, No.96L049.

**Correspondence to:** Dr. WU Wei, Epidemiology Department, Fourth Military Medical University, 17 Changle Xilu, Xi'an 710033, Shaanxi Province, China.

Tel. +86 • 29 • 3374871

Email. ww520@263.net

Received 1999-01-04

## INTRODUCTION

Hepatitis A virus-specific immunoglobulin M antibody (anti-HAV IgM) is the specific serological marker for the early diagnosis of acute hepatitis A. It can be detected by radioimmunoassay (RIA), enzyme-linked immunosorbent assay (ELISA), solid phase hemagglutination inhibition test (SPHIA) and other methods. At present, double sandwich ELISA is in widespread use<sup>[1]</sup>. However, it takes more time to finish the test and the procedure is complicated. The need of a simple, rapid, and noninstrumented test is evident in many basic units, where laboratory facilities and trained personnel are limited. In 1989, Chun developed a rapid test, DIGFA<sup>[2]</sup>. It has been used to detect HCG, C-reactive protein, immunoglobulin G antibody and others<sup>[3,4]</sup>. We developed DIGFA for detection of anti-HAV IgM. The evaluation of this test is presented below.

## MATERIALS AND METHODS

### Materials

**Agents** Gold chloride (HAuCl<sub>4</sub>) was produced by Shanghai No.1 Chemical Reagent Factory, and nitrocellulose membrane by Amersham International Co. (England). Anti-human  $\mu$  chain was obtained from DAKO Co. (Denmark). Anti-HAV IgG and cell cultured hepatitis A virus were prepared by Nanjing Military Medical Institute. ELISA kits for detection of anti-HAV IgM and anti-HBcIgM were produced by Shanghai Kehua Biotech. Co., Ltd, and ELISA kits for detection of anti-HCV by Sino-American Biotechnology Co.

**Samples** From 1994 to 1997, 137 serum samples of acute viral hepatitis were collected from 5 hospitals in Xi'an city. During the outbreak of hepatitis A in a college in 1997, sera of 14 patients, 40 contacts and 33 classmates with no contact history were collected. Ten RF positive sera were obtained from Xijing Hospital. Sera of 30 normal blood donors were taken from blood bank of Xijing Hospital. All samples were stored at -20°C.

### Methods

**Preparation of gold probe** Colloidal gold with an average diameter of 15nm was prepared by controlled reduction of a boiling solution of 0.2 g/L-chloroauric acid with 10 g/L-sodium citrate according to the method of Frens<sup>[5]</sup>. The quality of colloidal gold was controlled by transmission electron microscope

(TEM) and spectrophotometers. Freshly prepared 10 g/L-K<sub>2</sub>CO<sub>3</sub> solution was added into colloidal gold to adjust its pH. The minimal protecting amount was determined by constructing a concentration variable isotherm (CVAI)<sup>[6]</sup>. Anti-HAVIgG was added while stirring. It was incubated for 5-10 minutes at room temperature and followed by addition of bovine serum albumin (BSA) to final concentration of 10 g/L. After this was centrifuged, supernatant was discarded and the pellet was suspended. Gold probe obtained by the method described above was stored at 4°C.

**DIGFA** An immunofiltration system containing a NCM was coated with anti-human  $\mu$  chain, filter paper and an adsorbent pad. The NCM was positioned over an adsorbent pad covered by a plastic layer with a hole exposing the NCM (Figure 1). A drop of liquid positioned over the hole was rapidly sucked through the NCM. Thus, anti-HAVIgM in serum was captured by anti-human  $\mu$  chain on the NCM. Sequentially, hepatitis A antigen and gold probe were added. Cultured hepatitis A antigen as a “bridge” connected anti-HAV IgM in sample and anti-HAV IgG labeled colloidal gold. If there was anti-HAV IgM in sample, gold probes would concentrate on NCM, which would present a pink dot. The assay was routinely performed as follows. The membrane was activated by adding one drop of washing solution. Then 15  $\mu$ L-serum was added. After it was soaked in, one drop of washing liquid was added and followed by 15  $\mu$ L-cultured hepatitis A antigen. After it was soaked in, one drop of washing liquid were added, and gold probe and after this was soaked in, one drop of water was added. The process was completed within 10 minutes at room temperature.

**ELISA** All commercial kits were used according to their manufacturers' instruction.

**Statistical analysis** The following definitions and formulae were used in the analysis of the data generated in this study. A true-positive (a) sample was reactive by DIGFA and ELISA. A true-negative (d) sample was nonreactive by DIGFA and ELISA. A

false-positive (b) sample was reactive by DIGFA but negative by ELISA and a false-negative (c) sample was negative by DIGFA but positive by ELISA (Table 1). The sensitivity of DIGFA was defined as the probability that a sample containing anti-HAV IgM would be positive in DIGFA. The specificity of DIGFA was defined as the probability that a sample without anti-HAV IgM would be negative in DIGFA. The formulae are shown in Table 2.

**Table 1 Comparison of DIGFA results with ELISA**

		ELISA		Total
		+	-	
DIGFA	+	a	b	a+b
	-	c	d	c+d
	Total	a+c	b+d	N

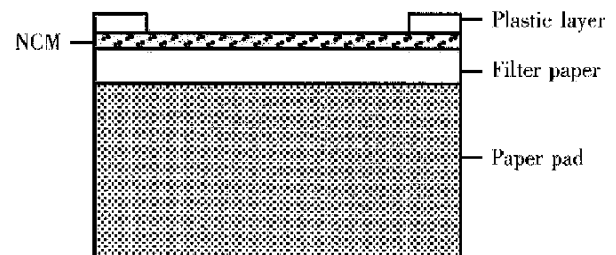


**Figure 1** Immunofiltration system.

## RESULTS

### Validity

A total of 264 serum samples were comparatively detected with both DIGFA and ELISA by “blind” method, 88 were positive and 146 were negative (Table 3). The sensitivity, the specificity, the accuracy, the positive and the negative predictive value, the positive likelihood ratio, the negative likelihood ratio and Youden index of DIGFA were 86.27%, 90.12%, 88.64%, 84.62% 91.25%, 8.735, 0.1523, 0.7639, respectively. Sensitivity, specificity and accuracy (95% CI) were 75.59%, 92.95%, 85.53%, 94.71% and 84.81%, 92.45%, respectively. Serum samples of 34 hepatitis B, 15 hepatitis C and 10 RF positive patients were determined with DIGFA, none of them was positive.

**Table 2 Formulae for evaluation of DIGFA**

Index	Formulae	Index	Formulae
Sensitivity	$a / (a+c)$	Specificity	$d / (b+d)$
Positive predictive value	$a / (a+b)$	Negative predictive value	$d / (c+d)$
Accuracy	$(a+d) / N$	Youden index	$\frac{a}{a+c} + \frac{d}{b+d} - 1$
Positive likelihood ratio	$[a / (a+c)] / [b / (b+d)]$	Negative Likelihood ratio	$[c / (a+c)] / [d / (b+d)]$

**Table 3 Comparison of DIGFA results with ELISA**

		ELISA		Total
		+	-	
DIGFA	+	88	16	104
	-	14	146	160
Total		102	162	264

**Repeatability**

NCM coating anti-human  $\mu$  chain and gold probe were kept at 4°C. In order to establish the stability of the reagents, 15 negative and 15 positive serum samples were selected at random and detected 3 times once a month. All results were the same. It indicates that the reagents are stable at least for 3 months at 4°C and repeatable.

**DISCUSSION**

Incidence of hepatitis A is very high in developing countries, especially in poor hygiene area. In order to control epidemic of hepatitis A, it is very important to detect anti-HAV IgM as early as possible. DIGFA is a rapid method, requiring 10 minutes to perform. Additionally, it is simple enough to be used by paramedical personnel without special training. It allows reliable measurement of anti-HAV IgM from a small volume of serum (15 $\mu$ L) without using special equipment. DIGFA showed very good performance. Its sensitivity and specificity are similar to that of ELISA. Rheumatoid factor, anti-HB-cIgM and anti-HCV do not markedly interfere with

the assay. It attributes to double sandwich method used in DIGFA and cell cultured hepatitis A antigen which is purer. The sample is drawn quickly through the porous membrane, thereby reducing low-affinity nonspecific binding and minimizing chemical interference. However, if there is fibrin clot or much blood lipid in serum, they will interfere with reaction between antigen and antibody, and the drawing rate of NCM, which will result in false positive or false negative. So, before detection, such sera must be centrifuged with fibrin clot and blood lipid removed.

In brief, rapid and simple procedure, with the visual interpretation of results and reagent stability make DIGFA particularly suitable for field testing and epidemiological surveys.

**REFERENCES**

- 1 Guo KS. Detection of virus-specific immunoglobulin antibody. *Chin J Exp Clin Virol*, 1988;2:79-81
- 2 Urdal P, Borch SM, Landaas S, Krutnes MB, Gogstad GO, Hjortdahl P. Rapid immunometric measurement of C-Reactive protein in whole blood. *Clin Chem*, 1992;38:580-584
- 3 Beristain CN, Rojkin LF, Lorenze LE. Evaluation of dipstick method for detection of human immunodeficiency virus infection. *J Clin Lab Anal*, 1995;9:347-350
- 4 Spielberg F, Kabeya CM, Ryder RW, Kifuani NK, Harris J, Bender TR. Field testing and comparative evaluation of rapid visually read screening assays for antibody to human immunodeficiency virus. *Lancet*, 1989;1:580-584
- 5 Frens G. Controlled nucleation for the regulation of the particle size in monodisperse gold suspensions. *Nature Phys Sci*, 1977; 241:20-22
- 6 Horisberger M. Colloidal gold, a useful marker for transmission and scanning electron microscopy. *J Histochem Cytol*, 1977;25:295-299

Edited by WANG Xian-Lin

# Experimental study of bioartificial liver with cultured human liver cells \*

WANG Ying-Jie, LI Meng-Dong, WANG Yu-Ming, NIE Qing-He and CHEN Guo-Zheng

**Subject headings** artificial liver; cell, cultured; hepatocytes; fulminant hepatic failure; animal model; liver support

## Abstract

**AIM** To establish an extracorporeal bioartificial liver support system (EBLSS) using cultured human liver cells and to study its support effect for fulminant hepatic failure (FHF).

**METHODS** The liver support experiment of EBLSS consisting of aggregates cultured human liver cells, hollow fiber bioreactor, and circulation unit was carried out in dizhepatic dogs.

**RESULTS** The viability of isolated hepatocytes and nonparenchymal liver cells reached 96%. These cells were successfully cultured as multicellular spheroids with synthetic technique. The typical morphological appearance was retained up to the end of the artificial liver experiment. Compared with the control dogs treated with EBLSS without liver cells, the survival time of artificial liver support dogs was significantly prolonged. The changes of blood pressure, heart rate and ECG were slow. Both serum ammonia and lactate levels were significantly lowered at the 3rdh and 5thh. In addition, a good viability of human liver cells was noted after 5h experiment.

**CONCLUSION** EBLSS playing a metabolic role of cultured human hepatocytes, is capable of compensating the function of the liver, and could provide effective artificial liver support and therapy for patients with FHF.

Clinical Center of Infectious Diseases, Southwest Hospital, Third Military Medical University, Chongqing 400038, China

Dr. WANG Ying-Jie, associate professor of the Center of Infectious Diseases, Southwest Hospital, Third Military Medical University, born on October 3, 1960, graduated and obtained a bachelor degree from Yanan University in 1985, and M.D. from Third Military Medical University in 1997. Specialized in the study of hepatic failure and severe hepatitis, having 65 papers published.

\*Supported by the national key project fund of the "9th Five Year Plan", No.96-920-12-02.

**Correspondence to:** Dr. WANG Ying-Jie, Center of Infectious Diseases, Southwest Hospital, Third Military Medical University, Chongqing 400038, China

Tel. +86 • 23 • 68754217

Received 1998-12-24

## INTRODUCTION

Despite the progress of intensive therapy for patients with fulminant hepatic failure (FHF), their death rate is still up to 90%. Liver transplantation is the only curative treatment for FHF at present. Unfortunately, it is limited by a severe shortage of donor organs and the short time available to find a suitable liver. Since some patients with FHF are potentially reversible, it is believed that if liver support system could be provided, their natural liver tissue could regenerate with the liver function maintained stable until an appropriate organ was obtained. Over the past 30 years, various liver support systems have been investigated, such as cross-circulation, whole liver perfusion, hemadsorption, charcoal hemoperfusion, hemodialysis, plasma exchange, total body washout, etc. However, a lot of clinical trials showed that these detoxification systems could promote the recovery of consciousness in some patients, but the survival rate has not been improved<sup>[1]</sup>, and none of these therapeutic procedures succeeded in gaining wide clinical acceptance. Recent development of bioartificial liver support system containing living hepatocytes is an important advance in this field. Because this system has potential metabolic and synthetic functions of liver, it may provide certain essential nutrients and factors necessary for regeneration of the liver tissue<sup>[2,3]</sup>. Further development of the bioartificial liver is expected to provide very interesting and valuable results in the treatment of FHF<sup>[4]</sup>.

The purpose of our experimental study was to establish an optimal extracorporeal bioartificial liver support system (EBLSS) with cultured human hepatocytes and to furnish a new therapeutic method for these patients.

## MATERIAL AND METHODS

### *Isolation of hepatocytes*

Human liver obtained from normal donors was transported in ice-cold physiological saline. Liver cells were isolated by the two-step perfusion method. The perfusion solution was Ca<sup>2+</sup>/Mg<sup>2+</sup> free Hanks balanced salt solution and 0.05% collagenase (all chemical and cell culture reagents were purchased from Sigma Chemical CO). The hepatocytes and nonparenchymal liver cells were harvested by centrifugation at 50×g for 3 min and at 500×g for 3 min. The viability of the isolated liver cells was determined by the trypan blue exclusion test.

### Aggregate culture of hepatocytes

Freshly isolated liver cells were suspended in hepatocytes and nonparenchymal liver cells of about  $4 \times 10^5$  and  $2 \times 10^5$  viable cells/mL. After 1 h of incubation at  $37^\circ\text{C}$ , they were seeded in culture flasks precoated with poly (2-hydroxyethyl methacrylate) and cultured with hormonally defined medium (HDM) in a humidified atmosphere of 5%  $\text{CO}_2$  and 95% air at  $37^\circ\text{C}$ . In order to suppress attachment on their wells and promote their aggregation, the flasks were rotated at regular intervals. Cell morphology in the aggregate culture was observed by an Olympus phase contrast microscope.

### The bioartificial liver design

The bioartificial liver consisted of aggregate liver cells (about  $1 \times 10^8$ ), circulating and hollow-fiber bioreactor containing 200 cellulose nitrate/cellulose acetate porous fibers (pore size of  $0.2 \mu\text{m}$ , fiber length of 21 cm, fiber inside diameter of  $660 \mu\text{m}$ ). The extrafiber volume was about 40 mL while the intrafiber volume was about 45 mL. The external fiber surface area was  $0.34 \text{ m}^2$ .

### Animal model

Mongrel dogs (provided by Experimental Animal Center of Third Military Medical University), weighing between 11 kg and 14 kg, were used in the study. Under pentobarbital (30 mg/kg, intravenously) anesthesia, all dogs received side to side portocaval shunts with their portal vein and hepatic artery tied off to form dizhepatic model.

### In vivo EBLSS studies

Animals were divided into two groups: group 1 ( $n = 5$ ) was treated by EBLSS without liver cells and group 2 ( $n = 5$ ) was supported by EBLSS with spheroids liver cells. After cannulation of their femoral arteries and veins, they received 5 h successive hemoperfusion with EBLSS at a rate of 30 mL/min to 50 mL/min. Heparin was administered at 50 U/kg. Perfusion was carried out for 5 h. Blood samples were obtained at 0, 1, 3 and 5 h. Ammonia and lactate were determined in our laboratory using standard techniques. The cell viability and aggregate adherence rate of EBLSS were observed under phase contrast microscope.

## RESULTS

### Cell yield and viability

The total isolated hepatocytes and nonparenchymal liver cells by the simplified two step perfusing method were  $13.6\text{--}14.7 \times 10^7$  cell/100 g of liver. Their estimated viability judged by the trypan blue test was 92%–96%.

### Aggregate culture

Under the defined culture environment and by gen-

tly shaking repeatedly, the freshly isolated hepatocytes were attached to each other within 4 h–8 h, multiple aggregates in different sizes were loosely formed, and the multiplicity of aggregates increased with the lapse of time. Up to 48 h a lot of regular spheroid aggregates were found in flasks. The aggregate hepatocyte spheroids appeared tight and dense in the center and on the surface of the spheroids attached to a lot of single cells. By the action of single cell, some spheroids were also attached to each other. The characteristics of multicellular spheroid aggregates can be maintained up to the end of the bioartificial liver support experiment (Figure 1).

### In vivo EBLSS animal support

Dogs supported with EBLSS showed significant improvement in their survival time as compared with the control group ( $10.7 \text{ h} \times 1.1 \text{ h}$  and  $5.8 \text{ h} \times 0.5 \text{ h}$ , respectively) ( $P < 0.01$ , Figure 2). The changes in blood pressure, heart rate and ECG of the support dogs were slow. After 3 h and 5 h of treatment, the blood ammonia and serum lactate levels were significantly lower in the support group as compared with the control animals ( $P < 0.01$ , Figures 3 and 4). Liver cell viability at the end of the 5 h experimental period was 52.3% to 70.8%, and the aggregate adherence rate was about 50%.

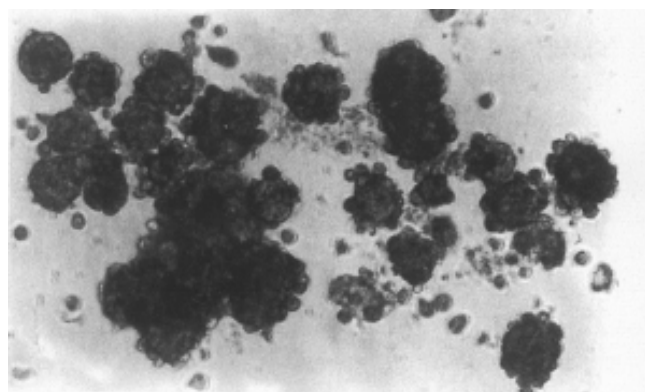


Figure 1 Multicellular spheroids of human hepatocytes and nonparenchymal liver cells. Phase-contrast microscope.  $\times 400$

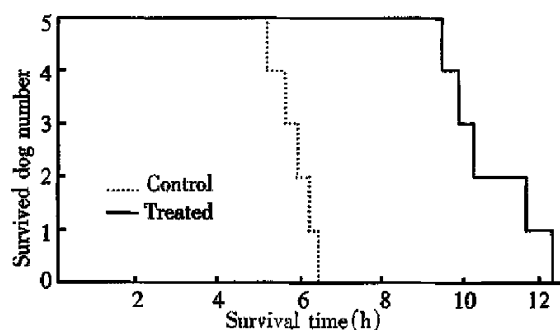


Figure 2 Survival curve in the support and control groups.

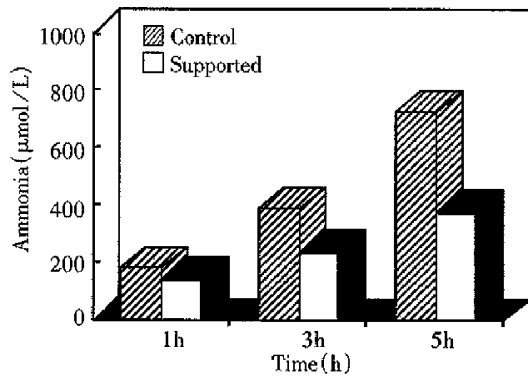


Figure 3 Changes of serum ammonia in dizhepatic dogs.

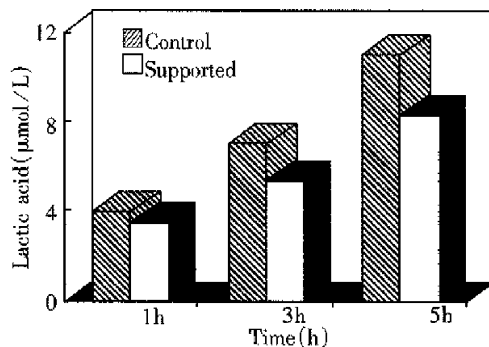


Figure 4 Changes of serum lactate in dizhepatic dogs.

## DISCUSSION

Up to now, considerable progress has been made in the bioartificial liver system. There are two extracorporeal systems, which have reached the stage of preliminary clinical assessment. One based on a human hepatoblastoma cell line was developed by Sussman and Kelly (extracorporeal liver assist devices)<sup>[5]</sup> and the other on isolated pig hepatocytes (bioartificial liver) was developed by Demetriou's group<sup>[6]</sup>. Although primarily isolated porcine hepatocytes proliferate poorly *in vitro*, they possess normal liver function and the source is almost unlimited. Unfortunately, animal hepatocytes can not replace the synthesis of human plasma proteins. On the other hand, it should be considered that besides the immunological rejection of xenogenic biological tissue, xenogenic proteins and enzymes in the blood will produce side effects. Human cell line is readily available in large quantities, but its differential function is rather poor. Sufficient replacement of liver function by the lines cannot be expected. Besides, they are all genetically transformed, potentially tumorigenic, and characterized by tremendous alterations in genetic, metabolic and synthetic parameters. The side effects and risks of these cells cannot be ruled out completely.

Recently, a workshop sponsored by the National Digestive Diseases Advisory Board on "Current Issues in the Management of Fulminant Hepatic

Failure" discussed the development of EBLSS<sup>[7]</sup>. The ideal hepatocyte for such devices was described as being human in origin, of normal (nonmalignant) phenotype, readily available, rapidly and easily grown in cell culture to a high density, stable and remaining in a well-differentiated state for days or weeks, and capable of the full range of synthetic and detoxifying features of mature hepatocytes.

In this study, we found that the human hepatocytes and nonparenchymal cells could be easily isolated by an alternative extracorporeal two-step perfusion method. The viability of cells was 92% to 96% and the yield of cells reached 10.8/100 g of liver. Using a synthetic technique, we successfully performed the aggregate culture of hepatocytes and nonparenchymal cells. Hepatocytes grown in suspension as self-induced multicellular spheroids with three-dimensional structures resembled *in vivo*. It has become clear that three dimensional rather than monolayer growth is particularly important for maintaining differentiated hepatocyte function in culture<sup>[8]</sup> and the co-culture with nonparenchymal cells also significantly enhances hepatocyte viability and function. Perhaps for this reason, our EBLSS consisting of hepatocyte aggregate spheroids and hollowfiber reactor not only possesses metabolic function (metabolism of ammonia and lactate) but also prolongs the survival in dizhepatic dogs.

These results have important implications concerning use of human hepatocytes in bioartificial liver design. Such EBLSS has provided effective liver support for dizhepatic animal, at least in a short time. It can be expected to maintain the patients in the best condition until an adequate liver graft becomes available or provide liver support for a longer period of time to await liver regeneration in some patients.

## REFERENCES

- Nyberg SL, Peshwa MV, Payne WD, Hu WS, Cerra FB. Evolution of the bioartificial liver: the need for randomized clinical trials. *Am J Surg*, 1993;166:512-521
- Hughes RD, Williams R. Use of bioartificial and artificial liver support devices. *Semin Liver Dis*, 1996;16:435-444
- Rozga J, Holzman MD, Ro MS, Gniffin DW, Neuzil DF, Giorgio T, Moscioni AD, Demetriou AA. Development of a hybrid bioartificial liver. *Ann Surg*, 1993;217:502-511
- Bismuth H, Figueiro J, Samuel D. What should we expect from a bioartificial liver in fulminant hepatic failure. *Artif Organs*, 1998; 22:26-31
- Sussman NL, Kelly JH. Extracorporeal liver support: cell based therapy for the failing liver. *Am J Kidney Dis*, 1997;30(Suppl 4): S66-71
- Demetriou AA, Rozga J, Podesta L, LePage E, Morsiani E, Moscioni AD, Hoffman A, McGrath M, Kong L, Rosen H, Villamil F, Woolf G, Vierling J, Makowka L. Early clinical experience with a hybrid bioartificial liver. *Scand J Gastroenterol*, 1995;30(Suppl 208):111-117
- Hoffnagle JH, Carithers RL, Shapiro C, Ascher N. Fulminant hepatic failure: summary of a workshop. *Hepatology*, 1995;21: 240-245
- Roide N, Sakaguchi K, Koide Y, Asano K, Kawaguchi M, Matsushima H, Takenami T, Shinji T, Mori M, Tsuji T. Formation of multicellular spheroids composed of adult rat hepatocytes in dishes with positively charged surfaces and under other non adherent environments. *Exp Cell Res*, 1990;186:227-235

# Chemoprevention of 2-amino-1-methyl-6-phenylimidazo [4, 5-*b*] pyridine-induced carcinogen-DNA adducts by Chinese cabbage in rats \*

TAN Wen<sup>1</sup>, LIN Dong-Xin<sup>1</sup>, XIAO Ying<sup>2</sup>, FF Kadlubar<sup>3</sup> and CHEN Jun-Shi<sup>4</sup>

**Subject headings** heterocyclic amine; DNA-adduct; Brassica vegetable; colonic neoplasms; cytochrome P450

## Abstract

**AIM** The food-borne carcinogen 2-amino-1-methyl-6-phenylimidazo [4,5-*b*] pyridine (PhIP) induces colon and mammary gland tumors in rats and has been implicated in the etiology of human colorectal cancer. This study was conducted to examine the potentially preventive effect of Chinese cabbage (*Brassica chinensis*), a brassica vegetable most commonly consumed in China, against this carcinogen induced DNA adduct formation in rats and its possible mechanisms.

**METHODS** Sprague-Dawley rats were maintained for 10 days on basal diet or diet containing 20% (w/w) freeze-dried cabbage powder prior to administration of a single dose of PhIP (10 mg/kg) by oral gavage. Rats were sacrificed at 20 h after PhIP treatment and PhIP-DNA adducts in the colon, heart, lung and liver were analyzed using <sup>32</sup>P-postlabeling technique. Levels of hepatic cytochrome P450 (CYP) 1A1 and 1A2, as indicated by 7-ethoxyresorufin O-deethylase and 7-methylxresorufin O-demethylase activity, and cytosolic glutathione-S-transferases (GSTs) towards 1-chloro-2, 4-dinitrobenzene (CDNB) in the liver, lung and colon were measured.

**RESULTS** Rats pre-treated with Chinese cabb-

age and given a single dose of PhIP had reduced levels of PhIP-DNA adducts in the colon, heart, lung and liver, with inhibition rates of 82.3%, 60.6%, 48.4% and 48.9%, respectively ( $P < 0.01$ ). The enzyme assays revealed that Chinese cabbage induced both CYP1A1 and 1A2 activity, but the induction was preferential for CYP1A1 over 1A2 (81% vs 51%). GST activity towards CDNB in the liver and lung, but not colon, was also significantly increased by cabbage treatment.

**CONCLUSION** The results indicate that Chinese cabbage has a preventive effect on PhIP-initiated carcinogenesis in rats and the mechanism is likely to involve the induction of detoxification enzymes.

## INTRODUCTION

The incidence of colorectal cancer is generally lower in China as compared to Western countries, but has been increasing consistently and rapidly in urban population in the last two decades, presumably due to the change of lifestyle, particularly in dietary habits, e.g., increased consumption of animal foods<sup>[1]</sup>. It has been shown that a large number of heterocyclic amine carcinogens are formed in meat and fish during cooking. Among them, one of the most abundant heterocyclic amines, 2-amino-1-methyl-6-phenylimidazo [4,5-*b*] pyridine (PhIP), has been proved to be carcinogenic for the colon and mammary gland of rats<sup>[2]</sup>. As several heterocyclic amines including PhIP have been detected in human urine after intake of normally cooked food<sup>[3]</sup>, it would appear that humans are continuously exposed to these carcinogens from their diet. After metabolic activation via oxidation and esterification, PhIP binds to DNA to form PhIP-DNA adducts<sup>[4]</sup>, which is widely believed to represent an important genotoxic step in the initiation of carcinogenesis. It has recently been found that PhIP-DNA adducts were

<sup>1</sup>Department of Chemical Etiology and Carcinogenesis, Cancer Institute, Chinese Academy of Medical Sciences and Beijing Union Medical College, Beijing 100021, China

<sup>2</sup>Department of Nutrition & Food Hygiene, School of Public Health, Beijing Medical University, Beijing 100083, China

<sup>3</sup>Division of Molecular Epidemiology, National Center for Toxicological Research, Jefferson, Arkansas 72079, USA

<sup>4</sup>Institute of Nutrition and Food Hygiene, Chinese Academy of Preventive Medicine, Beijing 100050, China

\*Supported by the National Natural Science Foundation of China, No.39570627.

**Correspondence to:** Dr. LIN Dong-Xin, Department of Chemical Etiology and Carcinogenesis, Cancer Institute, Chinese Academy of Medical Sciences, P.O. Box 2258, Beijing 100021, China  
Tel. +86 • 10 • 67722460, Fax. +86 • 10 • 67713359  
Email: dlin@public.net.cn

Received 1998-12-29

present in surgical samples of human colon<sup>[5]</sup>. These findings strongly suggest the importance of PhIP in the etiology of human colorectal cancer. Epidemiological data also support this hypothesis, showing that consumption of meat, especially well-done meat, is associated with an increased risk for human colorectal cancer<sup>[6]</sup>. In view of the fact that absolute avoidance of exposure of human to food-borne heterocyclic amines is impossible, seeking chemopreventive agents against these carcinogens is thus warranted.

The hypothesis that plant foods are protective against cancers at various sites has drawn interest in recent years and has been supported by many studies. A large number of potentially anticarcinogenic agents found in vegetables, may act as inhibitors in initiation, promotion and progression of the carcinogenesis. Brassica vegetables and their components are considered to be able to modulate expression of enzymes involving in metabolism of carcinogenic compounds, thereby preventing the carcinogenicity of the carcinogens<sup>[7]</sup>. Numerous epidemiological studies have consistently indicated that regular consumption of brassica vegetables reduces the incidence of human cancer including colorectal cancer<sup>[8]</sup>. Chinese cabbage (*Brassica chinensis*) is one of the most commonly consumed vegetables in China. In the present study, we examined the preventive effects of Chinese cabbage on PhIP-DNA adduct formation in rats and its possible mechanisms.

## MATERIALS AND METHODS

### Materials

PhIP was purchased from Toronto Research Chemicals (Ontario, Canada). Resorufin, 7-methoxyresorufin and 7-ethoxyresorufin were obtained from Sigma Chemical Company (St Louis, MO, USA). Reagents and materials for <sup>32</sup>P-postlabeling analyses were from sources described previously<sup>[4]</sup>. Chinese cabbage was locally purchased and its fine powder was made by freeze-drying.

### Animals and treatments

Weanling male Sprague-Dawley rats (146 g ± 15 g body wt) were obtained from Laboratory Animal Services, Chinese Academy of Medical Sciences (Beijing, China) and housed in a climate controlled room with a 12 h light/day cycle. Animals maintained on basal diet and tap water ad libitum for one week before experiment were randomly divided into three groups (5 rats/group). Group A and B were given basal diet, while group C was given basal diet containing 20% (w/w) Chinese cabbage powder. After 10 days on the diets, the animals in group B and C received a single dose of PhIP

(10 mg/kg- body wt) by oral gavage administration. Control rats (group A) were given the same volume of 55% ethano l in saline (pH 4.5) used as vehicle for PhIP. Animals were killed under ether anesthesia at 20 h after PhIP treatment and the liver, lung, heart and colo n from each rat were removed. The tissues were immediately placed in cold saline, and then frozen quickly in liquid nitrogen and stored at -80°C.

### Preparation of microsomes and cytosols

The liver and lung were thawed and washed at 4°C with phosphate-buffered saline. The minced tissues were homogenized in an ice-cold Teflon-glass homogenizer in 10 mmol/L-potassium phosphate buffer (pH 7.4) containing 1.4 mm ol/L-β-mercaptoethanol and 0.25 mol/L-sucrose. The col on mucosal cells were removed from the tissues using a spatula and were homogenized as described for the liver and lung. Homogenates were centrifuged at 9 000 g for 20 min, microsomes and cytosols were obtained by centrifuging the resulting supernatant at 105 000 × g for 45 min. After collecting cytosol fractions, the microsomes were washed once by resuspension in 100 mmol/L-potassium phosphate buffer (pH 7.0) and followed by recentrifugation at 105 000 × g for 45 min. The washed microsomes were resuspended in 3-weight volume of 100 mmol/L-potassium phosphate buffer (pH 7.0) containing 20% (v/v) glycerol. Cytosols and microsomal suspensions were stored in aliquots at -80°C until assayed.

### Analysis of PhIP-DNA adducts

DNA was isolated from each liver, lung, heart and colon, and PhIP-DNA adducts were analyzed using <sup>32</sup>P-postlabeling technique as described<sup>[4]</sup> previously with minor modifications. Briefly, DNA samples were digested with micrococcal nuclease and spleen phosphodiesterase. The digests were then extract ed with n-butanol and <sup>32</sup>P-labeled with [ $\gamma$ -<sup>32</sup>P] ATP. After treatment with nuclease P1, the <sup>32</sup>P-labeled adducts were separated by thin-layer chromatography (PEI-cellulose). Adducts were then detected using electronic autoradiography system (Packard Instrument Company, USA) with PhIP-modified calf thymus DNA as a standard.

### Enzyme assays

Cytosolic glutathione S-transferase (GST) activity was determined with 1-chloro-2-dinitrobenzene (CDNB) as substrate as described by Habig *et al*<sup>[9]</sup>. The reaction mixture consisted of 1 mmol/L-GSH and 1 mmol/L-CDNB in 1mL of 100 mmol/L potassium phosphate buffer, pH 6.5. The reaction was started by adding cytosol, and the increase in ab-

sorbance at 340 nm due to the formation of CDNB-GSH conjugates was recorded for 5 min. Ethoxyresorufin O-dealkylase (EROD) and methoxyresorufin O-dealkylase (MRO D) activities were determined by a fluorometric measurement of resorufin formation as described<sup>[10]</sup>. The reaction mixtures consisted of 3 mL-50 mmol/L-Tris buffer (pH 7.5), 25 mmol/L-MgCl<sub>2</sub>, 1.7 μmol/L-ethoxyresorufin or 5 μmol/L methoxyresorufin and 1 mg microsomal protein in a quartz cuvette at 20°C. The reactions were initiated by adding 125 μmol/L NADPH to the cuvette. The increase of fluorescence (excitation wavelength 522 nm and emission wavelength 586 nm) due to resorufin was recorded for 5 min. Enzyme activities were calculated by comparison with a resorufin standard curve. The background activity observed in the absence of microsomal protein was subtracted from each value.

### Statistical analysis

The results were analyzed using a one-way ANOVA procedure, and pair-wise comparisons were made using the Student's t test procedure in SigmaStat statistical computer software (Jandel Scientific, San Rafael, CA, USA).

## RESULTS

The body weight gain of rats over a 10-day period was similar in groups A, B and C, with the values (g) being 42 g ± 2.8 g, 46 g ± 6.2 g and 45 g ± 5.0 g, respectively ( $P > 0.05$ ). This suggests that feeding rats with the diet containing 20% Chinese cabbage did not alter their nutritional status.

PhIP-DNA adducts were detected by <sup>32</sup>P-postlabeling in the heart, lung, liver and colon of rats given PhIP. Adduct pattern was similar in these four tissues and chromatographically identical to that observed in DNA modified *in vitro* with N-hydroxy-PhIP (Figures 1A, 1C and 1D). The major adduct (spot 1) was previously characterized as N-(2'-deoxyguanosin-8-yl)-PhIP<sup>[4]</sup>. No adducts were detectable in any of the tissues in the control rats without PhIP treatment (Figure 1B). As previously reported<sup>[11]</sup>, DNA adduct levels (adducts/108 nucleotides) were highest in the colon (53.1 ± 8.7), followed in the heart (41.4 ± 14.9) and lung (22.1 ± 5.0), while adduct levels in the liver were relatively low (4.7 ± 3.7) (Figure 2). Following a single dose of PhIP, rats pre-treated with Chinese cabbage had significantly reduced adduct levels in the colon (9.4 ± 5.1), heart (16.3 ± 5.8) and lung (11.4 ± 3.2) as compared with those consuming basal diet without cabbage ( $P < 0.01$ ). The adduct level in the liver of rats fed cabbage also decreased (2.4 ± 1.7), although the difference from that of control rats was not significant (Figure 2).

Figure 3 presents results from the EROD and MROD assays. Cytochrome P450 (CYP) 1A1 catalyzes primarily the dealkylation of ethoxyresorufin in the EROD assay, whereas CYP1A2 is mainly responsible for dealkylation of methoxyresorufin in the MROD assay<sup>[10]</sup>. In rats treated with Chinese cabbage and given a single dose of PhIP, hepatic microsomes displayed a marked induction of EROD activity (82.7 pmol/mg ± 14.1 pmol/mg protein/min). This value was 2.7- and 1.8-fold higher than that in the two control groups (31.1 pmol/mg ± 3.8 pmol/mg and 45.8 pmol/mg ± 3.9 pmol/mg protein/min), respectively ( $P < 0.05$ ). Similar results were found in the hepatic MROD assay (Figure 3). In our experiment, rats given basal diet and a single dose of PhIP had EROD activity that was 1.5-fold higher than that of rats given no PhIP, while the MROD activity was not significantly induced as compared with the controls (Figure 3). These results are generally in accordance with previous studies showing induction of CYP1A by heterocyclic amines<sup>[11]</sup>.

A comparison of GST activity towards CDNB in the liver, lung and colon mucosa of rats given different treatments indicated that rats pretreated with cabbage had elevated GST activity in the liver and lung. The mean values of the activity in the liver and lung increased by 18.2% and 35.6%, respectively, as compared with that in controls ( $P < 0.05$ ). However, no significant differences in GST activity towards CDNB was observed in colon mucosa of rats given different treatments (Table 1).

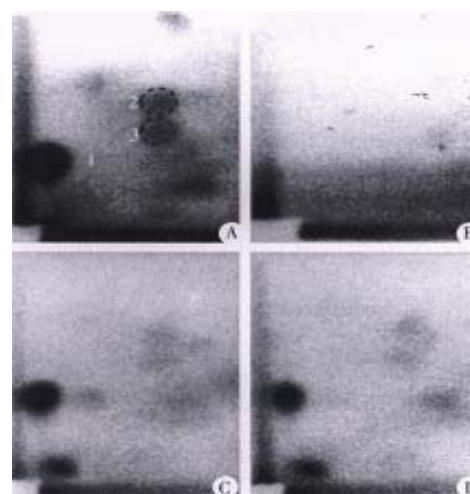


**Figure 1** Autoradiograms of PhIP-DNA adducts analyzed by <sup>32</sup>P-postlabeling.

(A) N-Hydroxy-PhIP modified calf thymus DNA; (B) colon DNA from control rats without PhIP treatment; (C) colon DNA from rats given 10 mg/kg PhIP and control diet; (D) colon DNA from rats given 10 mg/kg PhIP after 10 days on the diet containing 20% (w/w) Chinese cabbage.

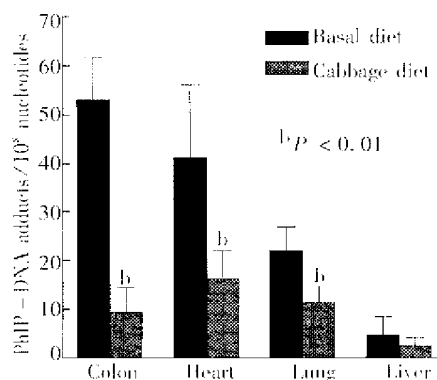


**Figure 2** PhIP-DNA adduct levels in tissues of rats given PhIP (10 mg/kg) with or without pretreatment with Chinese cabbage for 10 days. Values shown are  $\bar{x} \pm s$  from 5 rats/group. Asterisk-designates a response significantly different from control at  $P < 0.01$  with ANOVA.

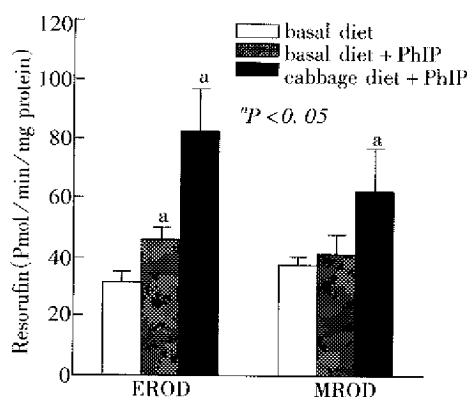


**Figure 3** Activity of 7-ethoxyresorufin O-deethylase (EROD) and methoxyresorufin O-demethylase (MROD) in hepatic microsomes from rats received different treatments. Activity values shown are the  $\bar{x} \pm s$  from three experiments, each from 5 individual microsome samples. Asterisk-designates a response significantly different from control at  $P < 0.05$  with ANOVA.

**Table 1** Effect of Chinese cabbage on glutathion S-transferase activity

Treatment group <sup>a</sup>	GST activity (nmol • mg protein <sup>-1</sup> • min <sup>-1</sup> ) <sup>b</sup>		
	Colon	Lung	Liver
Control diet+solvent	135±19	60±10	1 842±298
Control diet+PhIP	134±26	73±8	1 871±351
Cabbage diet+PhIP	142±29	99±9 <sup>c</sup>	2 212±423 <sup>c</sup>

<sup>a</sup>Animals were given a single dose of PhIP (10 mg/kg body wt) or its vehicle solvent after ten days on the diets. The cabbage diet was a basal diet containing 20% (w/w) freeze-dried Chinese cabbage powder.

<sup>b</sup>Glutathion S-transferase activity towards CDNB (nmol • mg prot ein<sup>-1</sup> • min<sup>-1</sup>) was determined in triplicate. Values given are  $\bar{x} \pm s$ .

<sup>c</sup> $P < 0.05$  as compared to control diet+PhIP group (Student's t test).

## DISCUSSION

The present study has shown for the first time that Chinese cabbage inhibits the formation of DNA adducts induced by PhIP. Since carcinogen-DNA adduct formation is generally believed to represent an important genotoxic step in the initiation of carcinogenesis,

these results support that Chinese cabbage has a chemopreventive role against PhIP-induced colon carcinogenesis. The findings are in accordance with epidemiological evidence, which has consistently indicated that regular consumption of brassica vegetables reduces the incidence of human colorectal cancer<sup>[8]</sup>. Furthermore, our findings provide an insight into the mechanisms of the anticarcinogenic action of vegetables.

PhIP, like most chemical carcinogens, undergoes enzymatic biotransformation *in vivo*. These metabolic pathways are binary in terms of toxicological consequences, leading to both activation and/or detoxification of the carcinogen. Hydroxylation of exocyclic amino groups of PhIP by CYP1A2 is believed to be an initial activation step, whereas ring-hydroxylation catalyzed principally by CYP1A1 seems to serve as a detoxification pathway<sup>[12]</sup>. The balance between metabolic activation and detoxification is one of the important determinants in chemical toxicity and carcinogenicity. We thus examined the induction of CYP1A1 versus 1A2 by Chinese cabbage. It was found that both CYP1A1 and 1A2 were induced by the cabbage, but the induction was preferential for CYP1A1 over CYP1A2 (80.6% vs 50.2%). These results are consistent with a protective effect against PhIP-DNA adduct formation, suggesting that the action mechanism of the cabbage is likely to be via induction of CYP1A1.

Another detoxification pathway of PhIP is GST catalyzed redox reaction of N-acetoxy-PhIP, an ultimate DNA-damaging metabolite of PhIP *in vivo*, with GSH<sup>[13]</sup>. The results presented herein clearly demonstrated that Chinese cabbage could induce GST activity in rats. This mechanism may also play an important role in suppression of PhIP-DNA formation in rats pretreated with the cabbage. The oxidation of PhIP by CYP1A2 results in the formation of N-hydroxy-PhIP, which can undergo further activation via O-acetylation by acetyltransferase to form N-acetoxy-PhIP. This metabolic process occurs mostly in the liver and is believed to be an essential step in forming highly reactive electrophiles that cause DNA damage and consequently initiate carcinogenesis. It has been shown that both N-hydroxy-PhIP and N-acetoxy-PhIP can be transported from the liver through the circulation to extrahepatic tissues where it forms PhIP-DNA adducts<sup>[14]</sup>. Therefore, to protect against PhIP, induction of GST activity in the liver is extremely important because it can eliminate N-acetoxy-PhIP formed *in situ* and prevent this ultimate carcinogen from being transported to the target tissues. This detoxification pathway may partially explain why the levels of PhIP-DNA adducts in the colon of rats treated with

Chinese cabbage were greatly decreased although the activity of GST in the tissue was not induced.

Brassica vegetables are rich in glucosinolates, which can be hydrolyzed to isothiocyanates or indoles. Isothiocyanates and indole derivatives such as indole-3-carbinol are potent inducers of biotransformation enzymes including CYP1A and GSTs<sup>[7]</sup>. It was shown that the levels of glucosinolates in Chinese cabbage ranged from 170 mg/kg to 1 360 mg/kg<sup>[7]</sup>. The induction of CYP1A and GSTs in rats by Chinese cabbage observed in the present study is likely associated with these compounds. Although CYP1A1 mainly catalyzes detoxification of PhIP, it may also catalyze activation of certain carcinogens such as polycyclic aromatic hydrocarbons (PAHs). In view of this fact, one may raise a question that consumption of Chinese cabbage could enhance the carcinogenicity of PAHs, which also widely occurs in the environment. However, many experimental studies have indicated that brassica vegetables and certain hydrolysis products of their glucosinolates also have anticarcinogenic properties against PAHs<sup>[7]</sup>, suggesting that brassica vegetables may preferentially induce enzymes involving detoxification of PAHs. In addition, brassica vegetables also contain many other compounds, which may act via different protective mechanisms against chemical carcinogenesis.

In conclusion, this study indicates a preventive effect of Chinese cabbage against a colon carcinogen, PhIP, initiated carcinogenesis in rats, and the mechanism is likely to involve induction of detoxification enzymes. In view of this observation and epidemiological evidence, regular consumption of Chinese cabbage and other brassicas in diet is highly recommended for reducing potential cancer risk of PhIP and other heterocyclic amine carcinogens.

## REFERENCES

- Ji BT, Devesa SS, Chow WH, Jin F, Gao YT. Colorectal cancer incidence trends by subsite in urban Shanghai, 1972-1994. *Cancer Epidemiol, Biomarkers & Prev*, 1998;7:661-666
- Ito N, Hasegawa R, Sano M, Tamano S, Esumi H, Takayama S, Sugimura T. A new colon and mammary carcinogen in cooked food, 2-amino-1-methyl-6-phenylimidazo [4,5-b] pyridine (PhIP). *Carcinogenesis*, 1991;12:1503-1506
- Boobis AR, Lynch AM, Murray S, De la Torre R, Solans A, Farre M, Segura J, Gooderhan NJ, Davies DS. CYP 1A2-catalyzed conversion of dietary heterocyclic amines to their proximate carcinogens is their major route of metabolism in humans. *Cancer Res*, 1994;54:89-94
- Lin DX, Kaderlik KR, Turesky RJ, Miller DW, Lay JO, Jr, Kadlubar FF. Identification of N-(deoxy-gunosin-8-yl)-2-amino-1-methyl-6-phenylimidazo-[4,5-b] pyridine as the major adduct formed by the food-borne carcinogen, 2-amino-1-methyl-6-phenylimidazo [4,5-b] pyridine, with DNA. *Chem Res Toxicol*, 1992;5:691-697
- Friesen MD, Kaderlik K, Lin DX, Garren L, Bartsch H, Lang NP, Kadlubar FF. Analysis of DNA adducts of 2-amino-1-methyl-6-phenylimidazo [4,5-b] pyridine in rat and human tissues by alkaline hydrolysis and gas chromatography/electron capture mass spectrometry: validation by comparison with 32P-postlabeling. *Chem Res Toxicol*, 1994;7:733-739
- World Cancer Research Fund and American Institute for Cancer Research. Food, Nutrition and Prevention of Cancer: a global perspective. Washington, DC, USA: American Institute for Cancer Research, 1997:216-251
- Verhoeven DTH, Verhagen H, Goldbohm RA, van den Brandt PA, van Poppel G. A review of mechanisms underlying anticarcinogenicity by brassica vegetables. *Chem Biol Interact*, 1997;103:79-129
- Verhoeven DTH, Goldbohm RA, van Poppel G, Verhagen H, van den Brandt PA. Epidemiological studies on brassica vegetables and cancer risk. *Cancer Epidemiol, Biomarkers & Prev*, 1996;5:733-748
- Habig WH, Pabst MJ, Jokoby WB. Glutathione S-transferases. The first enzymatic step in mercapturic acid formation. *J Biol Chem*, 1974;249:7130-7139
- Sohn OS, Surace A, Fiala ES, Richie JP, Jr, Colosimo S, Zang E, Weisburger JH. Effects of green and black tea on hepatic xenobiotic metabolizing systems in the male F344 rat. *Xenobiotica*, 1994; 24:119-127
- Degawa M, Kobayashi K, Miura S, Arai H, Esumi H, Sugimura T, Hashimoto Y. Species difference among experimental rodents in induction of P4501A family enzymes by 2-amino-1-methyl-6-phenylimidazo [4,5-b] pyridine. *Jpn J Cancer Res*, 1992;83:1047-1051
- Lin DX, Lang NP, Kadlubar FF. Species differences in the biotransformation of the food-borne carcinogen 2-amino-1-methyl-6-phenylimidazo [4,5-b] pyridine by hepatic microsomes and cytosols from human, rats, and mice. *Drug Metab Disp*, 1995;23:518-524
- Lin DX, Meyer DJ, Ketterer B, Lang NP, Kadlubar FF. Effects of human and rat glutathione S-transferases on the covalent DNA binding of the N-acetoxy derivatives of heterocyclic amine carcinogens in vitro: a possible mechanism of organ specificity in their carcinogenesis. *Cancer Res*, 1994;54:4920-4926
- Kaderlik KR, Minchin RF, Mulder GJ, Ilett KF, Daugaard-Jenson M, Teitel CH, Kadlubar FF. Metabolic activation pathway for the formation of DNA adducts of the carcinogen 2-amino-1-methyl-6-phenylimidazo [4,5-b] pyridine (PhIP) in rat extrahepatic tissues. *Carcinogenesis*, 1994;15:1703-1709

Edited by WANG Xian-Lin

# Glutamine: a precursor of glutathione and its effect on liver \*

YU Jian-Chun, JIANG Zhu-Ming and LI De-Min

**Subject headings** glutamine; glutathione/biosynthesis; liver/drug effects

## Abstract

**AIM** To investigate the relationship between alanyl-glutamine (ALA-GLN) and glutathione (GSH) biosynthesis in hepatic protection.

**METHODS** Twenty male Wistar rats were randomly divided into two groups: one receiving standard parenteral nutrition (STD) and the other supplemented with or without ALA-GLN for 7 days. The blood and liver tissue samples were examined after 5-fluorouracil (5-FU) was injected peritoneally.

**RESULTS** The concentration measurements were significantly higher in ALA-GLN group than in STD group in serum GLN ( $687 \mu\text{mol/L} \pm 50 \mu\text{mol/L}$  vs  $505 \mu\text{mol/L} \pm 39 \mu\text{mol/L}$ ,  $P < 0.05$ ), serum GSH ( $14 \mu\text{mol/L} \pm 5 \mu\text{mol/L}$  vs  $7 \mu\text{mol/L} \pm 3 \mu\text{mol/L}$ ,  $P < 0.01$ ) and in liver GSH content ( $6.9 \mu\text{mol/g} \pm 2.5 \mu\text{mol/g}$  vs  $4.4 \mu\text{mol/g} \pm 1.6 \mu\text{mol/g}$  liver tissue,  $P < 0.05$ ). Rats in ALA-GLN group had lesser elevations in hepatic enzymes after 5-FU administration.

**CONCLUSION** The supplemented nutrition ALA-GLN can protect the liver function through increasing the glutathione biosynthesis and preserving the glutathione stores in hepatic tissue.

## INTRODUCTION

Glutamine (GLN) was considered as a nonessential amino acid previously which is most abundant in the circulation system and in the amino acid pool of the body. The traditional standard amino acid solution does not contain glutamine since glutamine is unstable during sterilization at high temperature. In recent studies, GLN has also been demonstrated as a conditional essential amino acid, which plays a central role in the response to injury; and GLN also supports acid-base homeostasis<sup>[1]</sup>, maintains the function and morphology of the gastrointestinal epithelium<sup>[2,3]</sup>, preserves the stores of antioxidants in tissues<sup>[4,5]</sup>, enhances the immune response<sup>[6]</sup> and augments host defenses. The standard parenteral nutrition supplemented with GLN could significantly increase GSH stores and the survival rate of injured animal models. Therefore, GLN plays a major role in various anti-injury processes.

In this study, we used alanyl-glutamine dipeptide (ALA-GLN) solutions which are stable with the same biological effects as GLN and selected a model of 5-FU induced free radical-mediated hepatic injury, so as to establish a causal relationship between preservation of hepatic glutathione stores by glutamine administration and diminished hepatic injury caused by the toxicity of chemotherapy.

## MATERIAL AND METHODS

### Animals

Male Wistar rats ( $211 \text{ g} \pm 16 \text{ g}$ ) obtained from Animal Laboratories of Chinese Academy of Medical Sciences were allowed to acclimatize for 5-7 days at constant temperature with a 12 h light/dark cycle. Only those animals demonstrating normal food intake and weight gain were entered into the study. The rats were randomized to receive either the standard as control (STD,  $n = 10$ ) or alanyl-glutamine (ALA-GLN,  $n = 10$ ) parenteral nutrition. At the fifth day after catheterization 5-FU, a chemotherapeutic drug, was administered intraperitoneally ( $100 \text{ mg/kg}$ ) for GSH depletion as a model of stress injury and intestinal inflammation. Animals were killed on the seventh day after catheterization for harvest of tissue and blood. Mortality rate was assessed.

Department of Surgery, Peking Union Medical College Hospital, Chinese Academy of Medical Sciences, Beijing 100730, China

YU Jian-Chun, M.D., female, born on 1962-03-25 in Changchun City, Jilin Province, graduated from Postgraduate School of Peking Union Medical College, as a postgraduate in 1988, associate professor of general surgery, majoring gastrointestinal surgery, parenteral and enteral nutrition, having 15 papers published.

\*Supported by the Youth Scientific Foundation of Chinese Academy of Medical Sciences, No.31016.

**Correspondence to:** YU Jian-Chun, M.D., Department of Surgery, Peking Union Medical College Hospital, Chinese Academy of Medical Sciences, 1 Shuaifuyuan, East District, Beijing 100730, China  
Tel. +86 • 10 • 65296038, Fax. +86 • 10 • 65124875

E-mail: yujch@csc.pumch.ac.cn

Received 1998-11-20

### **Catheterization for parenteral nutrition**

The animals were anesthetized with intraperitoneal sodium pentobarbital (45 mg/kg). The hair was clipped from the cervical and interscapular regions, and the skin prepared with alcohol and povidone-iodine. Under sterile conditions, a Silastic catheter with an internal diameter of 0.76 mm and external diameter of 1.52 mm (Dow Corning Corp, USA) was inserted into the right jugular vein, advanced into the superior vena cava, and secured in place. The catheter was tunneled subcutaneously to the interscapular region and anchored to the deep fascia using a stainless steel button and prolene (Ethicon, USA). After threading the catheter through a flexible wire sheath, the combined unit was attached to a swivel apparatus (Instech Laboratories, Inc. USA) that allowed free movement of the animal during sustained intravenous feeding. After recovery from anesthesia, the animals were housed in individual metabolic cages.

### **Diet preparation**

Parenteral feeding solutions were prepared in a laminar flow hood and were sterilized using membrane filtration (0.22  $\mu\text{m}$  filter). Stock solutions were prepared on the day of catheterization and stored at 4°C. Both the standard glutamine-free parenteral solution (STD) and the 3% alanine-glutamine dipeptide supplemented solution (ALA-GLN) provided the necessary calories, nitrogen, vitamins, and minerals required for the growing rats<sup>[7]</sup>. The diets were isocaloric (260 Kcal  $\cdot$  kg<sup>-1</sup>  $\cdot$  d<sup>-1</sup>, in which 20% Intralipid provides 20% calories) and isonitrogenous (1.66 g  $\cdot$  kg<sup>-1</sup>  $\cdot$  d<sup>-1</sup>), and differed only in the composition of alanine-glutamine dipeptide (alanine-glutamine 6 g + standard amino acid solution 100 mL + non-protein caloric solution 100 mL, i.e. 3% ALA-GLN, equals to 2% GLN). After catheterization and recovery from anesthesia, animals were randomized to receive either the STD ( $n = 10$ ) or ALA-GLN ( $n = 10$ ) parenteral nutrition at an initial rate of 24 mL/day. On the second day after the operation, the infusion rate was increased to 48 mL/day and maintained at this level throughout the experiment. At 08:00 am of the fifth day after catheterization, 5-FU was administered intraperitoneally (100 mg/kg). Animals were killed on the seventh day after catheterization for harvest of tissue and blood. Mortality rate was assessed only in those animals killed at 24 hours.

### **Harvest procedures**

At the time of harvest, animals were weighed and

anesthetized with intraperitoneal sodium pentobarbital (45 mg/kg) and the skin prepared with povidone-iodine. Under sterile conditions, a midline incision was made from the pubis to the suprasternal notch, and whole blood was drawn from the right ventricle into a heparinized syringe. The whole blood was centrifuged immediately and plasma obtained for determination of glutathione, glutamine, alanine aminotransferase (ALT), alkaline phosphatase (ALP), total and direct bilirubin concentration. The plasma (200  $\mu\text{L}$ ) added with 86.2 g/L-SSA (5-sulfosalicylic acid solution 200 mL) was centrifuged for 1 minute immediately. The supernatant was removed and stored at -80°C for determination of the reduced glutathione. A 400 mg liver without capsule was resected from the middle lobe and immediately placed in a 4.31% SSA solution with a weight to volume ratio of 1:10. These samples were then homogenized in a glass manual tissue grinder. The acid suspension was centrifuged and the supernatant sample was removed. For determination of disulfidated glutathione (GSSG), an aliquot of previous supernatant was mixed with TRIS buffer and 2-vinylpyridine (Sigma Company) to protect the SH group directly during harvesting. Those samples were stored at -80°C until analysis of the GSH and the oxidized form of glutathione (GSSG).

### **Analytical procedures**

Biochemical assay of plasma and hepatocyte cellular glutathione was based on the "Glutathione, Glutathione Reductase-DTNB Recycling Method" originally described by Tietze<sup>[8]</sup>:  $2\text{GSH} + \text{DTNB} \rightarrow \text{GSSG} + \text{TNB} + 2\text{H}^+$ ;  $\text{GSSG} + \text{NADPH} + \text{H}^+ \rightarrow 2\text{GSH} + \text{NADP}^+$ .

The principle of the assay is illustrated as follows. GSH is oxidized by 5,5'-dithiobis-2-nitrobenzoic acid (DTNB) (Sigma Company), yielding 2-nitro-5-thiobenzoic acid (TNB) monitored at 412 nm spectrophotometrically (UVIKON 930, KONTRON INSTRUMENTS); and GSSG is reduced by nicotinamide-adenine dinucleotide phosphate (NADPH, reduced form, Sigma) in the presence of glutathione disulfide reductase. In the process, GSH is oxidized to GSSG, and the reaction is maintained by adding the enzyme glutathione reductase (Sigma Company) and the electron donor NADPH, so that the concentration of GSH is rate limiting. The GSSG was measured with the samples treated with 2-vinylpyridine masking GSH specifically. A standard curve with known concentration of glutathione was generated for each sample analy-

sis. Plasma glutamine was determined with amino acid autoanalyzer (Model 119 CL, Beckman, USA). ALT, ALP and total and direct bilirubin concentrations were assayed using an automated laboratory analyzer (RA 2000).

#### Statistical analysis

All calculations were performed on an Apple Macintosh SE computer using STATVIEW standard statistical software. Data were expressed as mean  $\pm$  standard error. Chi square analysis was used for mortality data. Other data were analyzed with ANOVA.

## RESULTS

### Body weight

Although the body weight loss occurred during parenteral nutrition (PN) and 5-FU treatment, there were no significant differences in body weight between STD and ALA-GLN groups before starting PN (215.2 g  $\pm$  22.5 g vs 207.2 g  $\pm$  14.6 g,  $P > 0.05$ ) or after finishing PN (188.1 g  $\pm$  19.9 g vs 190.6 g  $\pm$  19.8 g,  $P > 0.05$ ).

### Plasma glutamine and glutathione

Forty-eight hours after 5-FU administration, animals in the experimental group had significantly higher plasma concentrations of GLN (687.3  $\mu\text{mol/L} \pm 49.8 \mu\text{mol/L}$  vs 504.9  $\mu\text{mol/L} \pm 39.6 \mu\text{mol/L}$ ,  $P < 0.05$ ) and GSH (14.37  $\mu\text{mol/L} \pm 5.16 \mu\text{mol/L}$  vs 7.08  $\mu\text{mol/L} \pm 3.16 \mu\text{mol/L}$ ,  $P < 0.01$ ) than in the control group (Figure 1).

### Hepatic glutathione

Forty-eight hours after drug administration, hepatic glutathione concentrations were significantly lowered in the STD group. But the GSSG level was similar between the two groups. The GSH concentration was in the normal range in the ALA-GLN group, but significantly higher than that in the STD group (6.9  $\mu\text{mol/g} \pm 2.5 \mu\text{mol/g}$  vs 4.4  $\mu\text{mol/g} \pm 1.6 \mu\text{mol/g}$  liver tissue,  $P < 0.05$ ). The redox ratio of GSSG/GSH in ALA-GLN group was significantly lower than that in the STD group (0.12  $\pm 0.03$  vs 0.47  $\pm 0.33$ ,  $P < 0.05$ , Figure 1).

### Hepatic injury and mortality

Forty-eight hours after drug administration, STD animals had greater elevations in plasma ALT, ALP and total and direct bilirubin levels as compared with the ALA-GLN animals ( $P < 0.05$ ) (Figure 2). One rat in ALA-GLN group and two rats in STD group died at 24 hours after drug administration,

and one rat in STD group died at 34 hours after drug administration. Although mortality rate was higher in STD (30%) than in ALA-GLN animals (10%), there was no significant difference in mortality rate between the two groups ( $P > 0.05$ ).

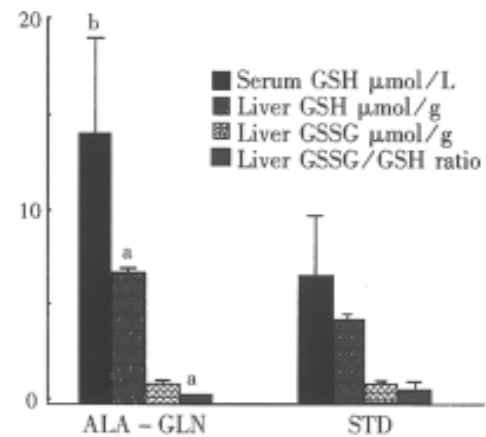


**Figure 1** Glutathione concentrations in serum and in liver tissue after 5-FU administration.

<sup>a</sup> $P < 0.05$ , <sup>b</sup> $P < 0.01$  as compared with STD.

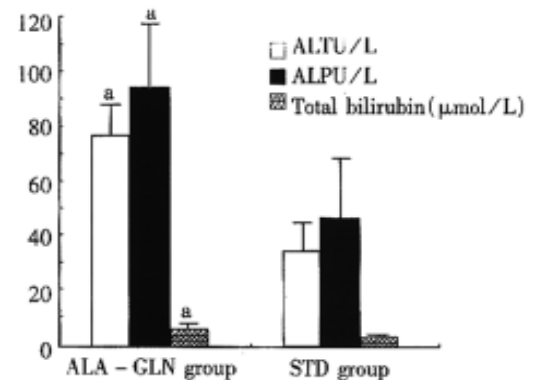


**Figure 2** Liver function changes after 5-FU administration. <sup>a</sup> $P < 0.05$  compared with STD group.  $\times 10$

## DISCUSSION

Glutathione (GSH) is a major antioxidant and a vital component of host defenses. It protects tissues from free radical injury via detoxification of active species and/or repair of injury, and plays an important role in the metabolism of drugs and endogenous substances<sup>[9]</sup>. The depletion of tissue GSH concentration and protein alkylation results in the drug toxicity of target tissues. The drug toxicity to normal tissues limits the chemotherapy doses.

GSH is a tripeptide consisting of glutamate, cysteine and glycine. Although experiments showed that GSH biosynthesis is rate-limited by cysteine during glutathione depleted states<sup>[10]</sup>, the availability of glutamine appears to be important for the regeneration of glutathione stores during our experi-

ment of hepatic injury. The reason is that glutamate is poorly transported into cells. Under various experimental conditions, the glutamate portion of the molecule is derived from glutamine. Glutamine is efficiently transported across the cell membrane and deaminated in the mitochondria to produce glutamate and NH<sub>3</sub>. Glutamate is then transported back to the cytosol, where it is readily available for glutathione synthesis. GLN is a vital precursor of glutamate for GSH synthesis.

After 5-FU was administered in our study, STD animals exhibited a significantly lower glutathione stores as compared with that in the ALA-GLN group animals. The concentration of GSH which was in the normal range in GLN group was significantly higher than that in the STD group. Ninety-six hours after chemotherapeutic drug administration, hepatic glutathione concentrations, GSH concentration and the GSH/GSSG-ratio in STD animals did not recover to the normal range. The possible reason may be the deficiency of GLN as a precursor for GSH biosynthesis, limiting glutathione synthesis. This level of GSH depletion was associated with increased hepatic injury, as suggested by higher concentrations of hepatic enzymes. The normal concentration of GSH was associated with better hepatic function in the ALA-GLN animals.

These results suggest that 3% ALA-GLN has equivalent biological and metabolic effects with 2% GLN<sup>[11]</sup>. The study confirms the important function of glutamine in the causal relationship between preservation of hepatic glutathione stores by glutamine administration and decrease of hepatic injury and

mortality. This may be due to the mechanism of increased cellular reduced glutathione through the cell membrane<sup>[12]</sup>. GSH may also protect cells via detoxification by binding with the toxicant and repairing the injury of hepatocytes.

## CONCLUSION

We demonstrated that alanyl-glutamine could protect the liver function after chemotherapy through increasing the glutathione biosynthesis and preserving the glutathione stores of hepatic tissue.

## REFERENCES

- 1 Welbourne TC, Joshi S. Interorgan glutamine metabolism during acidosis. *JPEN*, 1990;14(Suppl):77s
- 2 Hwang TL, O'Dwyer ST, Smith RJ, Wilmore DW. Preservation of small bowel mucosa using GLN-enriched parenteral nutrition. *Surg Forum*, 1986;37:56
- 3 Rene RWJ, Bernard K, Maarten F. Glutamine and the preservation of gut integrity. *Lancet*, 1993;334:1364
- 4 Wilmore DW, Smith RJ, O'Dwyer ST. The gut: A central organ after surgical stress. *Surgery*, 1988;104:917
- 5 Roy W Hong, Jan D Rounds, William S Helton. Glutamine preserves liver glutathione after lethal hepatic injury. *Ann Surg*, 1992;215:114-119
- 6 Burke D, Alverdy JC, Aoye E, Moss GS. Glutamine supplemented total parenteral nutrition improves gut immune function. *Arch Surg*, 1989;124:1396
- 7 Popp MB, Brennan MF. Growth and body composition during long-term total parenteral nutrition in the rat. *Am J Clin Nutr*, 1982;36:1119-1128
- 8 Meister A, Anderson ME. Glutathione. *An Rev Biochem*, 1983;52:711-760
- 9 Deneke SM, Fanburg BL. Regulation of cellular glutathione. *Am J Physiol*, 1989;257:L163-L173
- 10 Black M. Acetaminophen hepatotoxicity. *Gastroenterology*, 1980;78:382-392
- 11 Jiang ZM, Wang LJ, Qi Y. Comparison of parenteral nutrition supplemented with L glutamine or glutamine dipeptides. *JPEN*, 1993;17:134
- 12 Le CT, Hollaar L, Van der Valk EJ. Protection of myocytes against free radical induced damage by accelerated turnover of the glutathione redox cycle. *Eur Heart J*, 1995 Apr;16:553-562

Edited by MA Jing-Yun

# Expression of B7 costimulation molecules by colorectal cancer cells reduces tumorigenicity and induces anti-tumor immunity \*

HU Jin-Yue, WANG Sa, ZHU Jian-Gao, ZHOU Guo-Hua and SUN Qu-Bing

**Subject headings** colorectal neoplasms; B7 gene; gene expression; immunohistochemistry

## Abstract

**AIM** To study the tumorigenicity of colorectal cancer cells transfected with B7 gene and the anti-tumor immunity induced by B7 gene modified colorectal cancer cells.

**METHODS** B7 gene was transfected into mouse colon cancer cell line CMT93. The transfectants were selected in DMEM containing 800mg/L-G418, and B7 molecules were detected by immunohistochemistry. Experiments *in vivo* include: ①  $5 \times 10^6$  B7+ CMT93 cells were inoculated into the back of C57BL/6 mice subcutaneously to determine their tumorigenicity ( $n = 4$ ). As control, wild type CMT93 cells were inoculated the same as the experimental group ( $n = 3$ ). ② The mice primed by B7+ CMT93 cells whose tumors vanished were rechallenged with wild type CMT93 to observe the immune protection of these mice against the wild type CMT93 ( $n = 4$ ). Non-primed 4 native mice inoculated with wild type CMT93 were used as control. With *in vitro* cytotoxicity assay, the mice were immunized with B7+ CMT93 or the wild type CMT93 by intraperitoneal injection ( $n = 4 \times 2$ ). The spleen cells and the abdominal cavity infiltrating lymphocytes were obtained and cultured for two days. Cytotoxicity of these cells against the B7 gene modified or wild type CMT93 was detected by MTT assay.

**RESULTS** B7 high expression clones were obtained after the transfection of the B7 gene into CMT93 cells by electroporation. Immunohisto-

chemistry results showed mainly membrane staining and partly cytoplasm staining in B7 gene transfected CMT93 cells. **In vivo-experiments:** ① After the inoculation of the B7+ CMT93 cells into the back of C57BL/6 mice, they lost their tumorigenicity greatly ( $P < 0.01$ ). All the small tumors growing in the early period in the experimental group vanished in one month, and the tumors in control group grew progressively. ② No tumors were found in all 4 mice primed by B7+ CMT93 cells after they were rechallenged with wild type CMT93. In the control group all mice had grown tumors ( $P < 0.05$ ). **In vitro-cytotoxicity assay,** the CTLs induced by B7+ CMT93 had a higher cytotoxicity against the wild type CMT93 than that induced by wild type CMT93 ( $P < 0.05$ ), and the cytotoxicity of CTLs induced by B7+ CMT93 against B7+ CMT93 cells was higher than that against wild type CMT93 cells ( $P < 0.05$ ).

**CONCLUSION** The results suggest that the expression of costimulation B7 molecules by colorectal cancer cells can decrease their tumorigenicity greatly, and the B7 molecule can augment the activation of the CTLs against colorectal cancer, and it plays an important role in CTL effector function as well.

## INTRODUCTION

For efficient activation of T cells, two signals are required. The first antigen-specific signal is mediated by the T cell receptors after their interaction with peptide-MHC complexes. The second signal is antigen-nonspecific costimulatory signals, such as that delivered by the CD28 molecule on the T cells interacting with B7 molecule on the APCs<sup>[1]</sup>. When tumor antigen is presented to T cells, there are three distinct pathways to deliver costimulatory signals: trans-costimulation, cis-costimulation and transfer cis-costimulation. Among them, the cis-costimulation in which two signals are delivered by one tumor cell simultaneously is the most efficient mode<sup>[2]</sup>. Usually, B7 molecule is not expressed on

Institute of Cancer Research, Hunan Medical University, Changsha, 410078, Hunan Province, China.

MD. HU Jin-Yue, male, born on 1966-07-30 in Hunan Province, graduated from Hunan Medical University as a postgraduate in 1995, now lecturer and doctorate candidate, majoring tumor immunology.

\*Supported by the National Natural Science Foundation of China, No.3950076.

Presented at the 6th Meeting of Colorectal Cancer of China and the First China-Japan-Korea International Congress of Colorectal Cancer, Haerbin, 17-20, September 1998

Correspondence to: Professor SUN Qu-Bing, Cancer Research Institute, Hunan Medical University, Changsha 410078, Hunan Province, China.

Tel. +86 • 731 • 4474411 Ext. 2316, Fax. +86 • 731 • 4471339

Received 1998-12-22

the surface of most tumor cells, so tumor antigen can not activate T cells by cis-costimulation. After the tumor cells were transfected with B7 gene however, efficient anti-tumor immunity can be induced by cis-costimulatory mode. The mice primed with B7 gene modified tumor cells can reject not only B7 gene modified tumor cells, but also the wild type tumor cells<sup>[3,4]</sup>. Our experimental results showed that after the transfection of colorectal cancer cells CMT93 with B7 gene, the tumorigenicity of the B7 gene modified tumor cells decreased, and B7 molecules augmented the immunity against tumor cells.

## MATERIALS AND METHODS

### Materials

Male or female C57BL/6 mice, 6.8 weeks old, were purchased from Shanghai Experimental Animal Center of Chinese Academy of Sciences. Colorectal cancer cell line CMT93 was bought from ATCC. Plasmid pLNSX containing mouse B7.1 gene (pLNSXB7) was provided kindly by Dr. CHEN Lie-Ping *et al*<sup>[5]</sup>. Rat IgG anti-mouse B7 molecule was purchased from Pharmingen. Alkaline phosphatase-conjugated goat IgG anti-rat Ig was bought from Organon Teknik. G418 was obtained from Gibco.

### Transfection of tumor cells

Plasmid pLNSX-mB7 was constructed by cloning murine B7 PCR product into the PCR<sup>TM</sup> II vectors and then subcloning it into retroviral vector pLNSX<sup>[5]</sup>. Plasmid was transfected into colorectal cancer cells CMT93 by electroporation. After transfection, the CMT93 cells were selected in DMEM containing 800 mg/L-G418. Two weeks later, the G418-resistant cells were cultured in DMEM containing 400 mg/L-G418.

### Immunohistochemistry analysis

Colorectal cancer CMT93 cells were digested and cultured in 8-room Slide Chamber (Costar). The immunohistochemistry analysis was performed when the cells were confluent to 50%-60%. Briefly, CMT93 cells were fixed with 0.15% glutaraldehyde solution for 15min at room temperature, and rinsed 3 times with PBS (0.01 M, pH 7.2). Then the cells were incubated for 2 h at 37°C with rat IgG anti mouse B7 molecule antibody (1:200 dilution). After rinsed with PBS for 3 times, the cells were incubated for 1 h at 37°C with alkaline phosphatase-conjugated goat IgG anti-rat Ig (1:50 dilution). The cells were rinsed with PBS 3 times again, and the staining substrate NBT/BCIP (10:1) was added. The cells were stained for 30 min at room temperature. Then the cells were rinsed by PBS to terminate the reaction.

### Tumorigenicity of B7 gene transfected cells

The B7+ CMT93 (CMT93-B7) or wild type CMT93 cells were digested when they grew confluent to 95%. Four mice were inoculated with  $5 \times 10^6$  CMT93-B7 cells in their backs. Three mice were inoculated with  $5 \times 10^6$  wild type CMT93 cells as control. Ten days later, the grown tumors were observed, and the long and short diameters of the tumors were measured by caliper (0.02 cm) every two days.

### Immune protection

Four mice rejecting the initial inoculation of CMT93-B7 tumor cells were rechallenged with  $2.5 \times 10^6$  wild type CMT93 cells in their backs by subcutaneous injection. Four non-primed mice were inoculated with  $2.5 \times 10^6$  wild type CMT93 cells in their backs as control. After five days, when the tumors in control group became palpable, all mice were examined to see whether the tumors existed or not, and the long and short diameters of the tumors were measured by caliper every three days. One month later, when the tumor size was approximately 1.5 cm  $\times$  1.5 cm, all mice were killed.

### In vitro cytotoxicity

Four mice were primed with  $5 \times 10^6$  CMT93-B7 cells by intraperitoneal injection. Another four mice were primed with  $5 \times 10^6$  wild type CMT93 cells as control. Seven days after injection, all mice were killed with their abdominal cavities rinsed with 5 mL-Hank's solution. All cells taken from the abdominal cavities were cultured in RPMI 1640 medium supplemented with 10% FCS. After two days of culture, the macrophages and the non-rejected tumor cells were removed by adherence, and the cytotoxicity of CTL from abdominal cavities against CMT93-B7 cells and wild type CMT93 cells were detected by MTT assay<sup>[6]</sup>. In addition, the spleen cells were prepared from all CMT93-B7 or wild type CMT93 primed mice, and their cytotoxicity against CMT93-B7 cells and wild type CMT93 cells were detected as well.

## RESULTS

### Identification of plasmid pLNSX-B7

Plasmid pLNSX is a retroviral vector<sup>[3]</sup>. There is a *Hind* III site in front of and behind the inserted B7 DNA fragment respectively. Figure 1 shows that pLNSX-B7 was cleaved into two fragments after the digestion with *Hind* III. They represented plasmid DNA and B7 DNA respectively.

### Immunohistochemistry staining

Positive staining was found in G418-resistant CMT93-B7 cells. The positive staining was mainly

located in the cell membrane, and some plasma staining was found as well (Figure 2). The percentage of staining of CMT93-B7 cells was 62%. The percentage of staining of wild type CMT93 cells was less than 5% (Figure 2), so we considered this wild type cells did not express B7 costimulation molecules.

#### **Tumorigenicity of CMT93-B7**

After inoculation with  $5 \times 10^6$  tumor cells, all mice grew palpable tumors on the seventh day. Then the tumors of the mice in the control group grew progressively. Yet the tumors of the mice in the experimental group shrank gradually from the second week. The tumors of the four mice in the experimental group disappeared on day 12, day 14, day 14 and day 32 respectively. The size of the biggest tumor was  $0.996 \text{ cm} \times 0.302 \text{ cm}$  (No 4, on day 12). By unpaired Student's *t* test, significant difference was found between the data from the experimental group and the control group in each measurement ( $P < 0.01$ , Figures 3 and 4).

#### **Protective immunity**

Four mice primed with CMT93-B7 were rechallenged with  $2.5 \times 10^6$  wild type CMT93. From day 1 to day 32 after rechallenge, no tumor was found in them. In the control group, however, tumors were found in all the four mice injected with  $2.5 \times 10^6$  wild type CMT93 cells on day 7. In the second week, the tumors in the control group shrank partly. Among them, one tumor was rejected completely on day 16, but the others grew progressively from the third week. By unpaired Student's *t* test, significant difference was found between the data from experimental group and control group in each measurement ( $P < 0.05$ , Figure 5).

#### **In vitro cytotoxicity**

Inoculation of CMT93 or CMT93-B7 cells in the mice by intraperitoneal injection induced infiltration of lymphocyte in abdominal cavities, but the infiltrating lymphocytes induced by inoculation of CMT93 were less than that induced by inoculation of CMT93-B7 (data not shown). The cytotoxicity assay showed that the abdominal cavity infiltrating lymphocytes induced by CMT93-B7 were more cytotoxic against CMT93 than that induced by wild type CMT93. The results of the spleen cells were the same as the abdominal cavity infiltrating lymphocytes (Figure 6). Moreover, the cytotoxicity of abdominal cavity infiltrating lymphocytes induced by CMT93-B7 against CMT93-B7 was higher than that against wild type CMT93. These results suggested that B7 molecule might play an important role in CTL cytotoxicity.

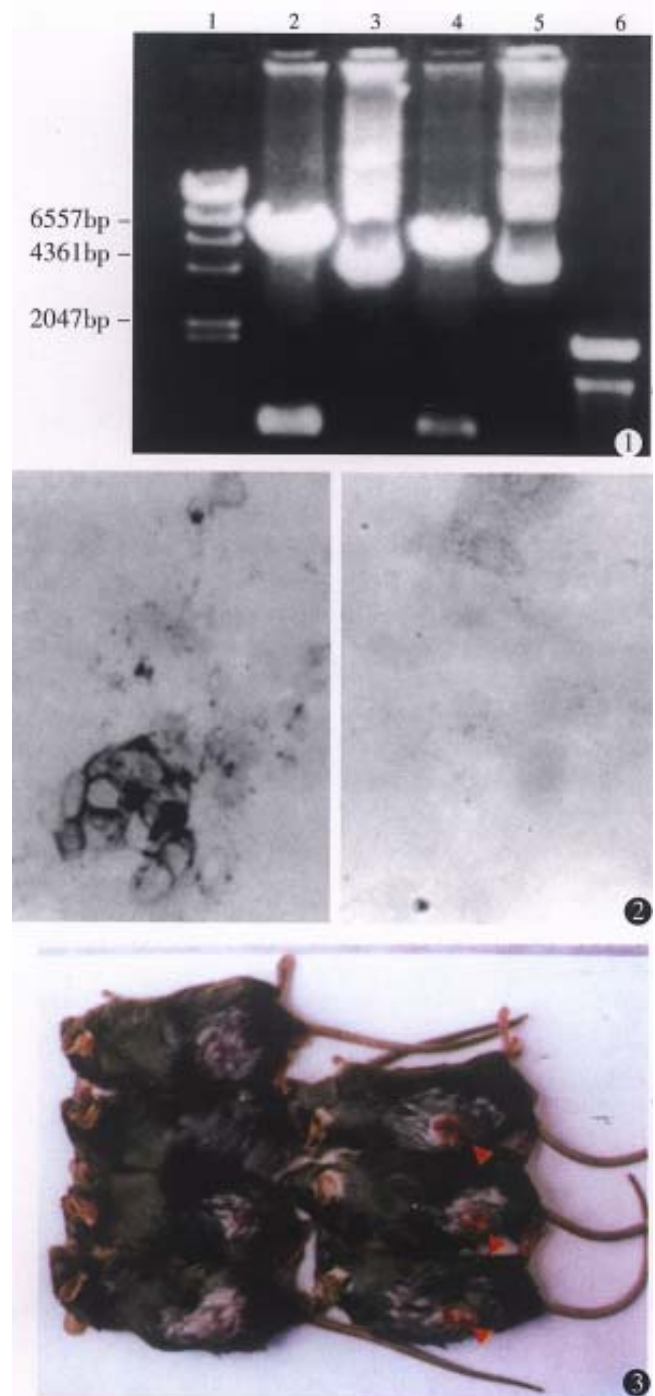


**Figure 1** Electrophoretic result of plasmid pLNSXmB7. After digestion by Hind III, pLNSX-mB7 was cleaved into two fragments. They represented plasmid DNA and B7 DNA respectively.

Lane 1:  $\lambda$ /Hind-III marker; Lane 2, 4: pLNSX-mB7 digested by Hind III; Lane 3, 5: pLNSX-mB7 non-digested; Lane 6: 100bp ladder marker

**Figure 2** Results of immunohistochemistry.  $\times 100$

The left is the staining of CMT93-B7 cells. Positive staining is mainly located in the cell membrane. The right is the negative staining of wild type CMT93 cells.

**Figure 3** Tumorigenicity of CMT93-B7 (I).

In the left experimental group, all the four mice rejected the tumors completely. In the right control group, one big tumor was found in each mouse. The arrows showed the location of the tumors.

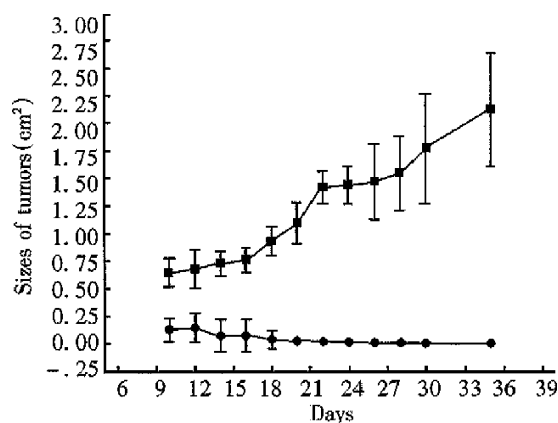


**Figure 4** Tumorigenicity of CMT93-B7(II).  
 ■ The tumors in control mice injected wild type CMT93 grew progressively ( $n = 3$ ).  
 ● The tumors in experimental mice inoculated CMT93-B7 vanished gradually ( $n = 4$ ,  $P < 0.01$  compared with control group).

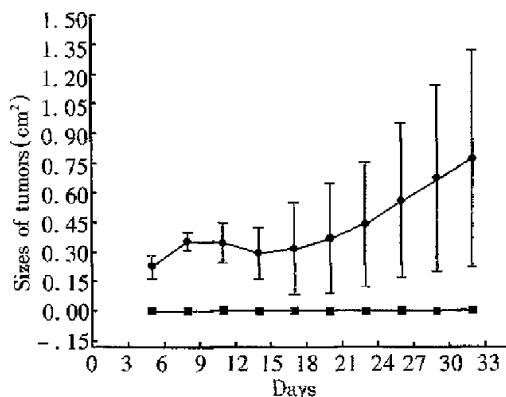


**Figure 5** Protective immunity.  
 ● In control group, four native mice injected  $2.5 \times 10^6$  wild type CMT93 cells, one mouse's tumor vanished. Three mice's tumor grew progressively.  
 ■ In experimental group, four mice primed with CMT93-B7 were rechallenged with  $2.5 \times 10^6$  wild type CMT93 cell, and no tumors were found. ( $P < 0.05$  compared with control group).

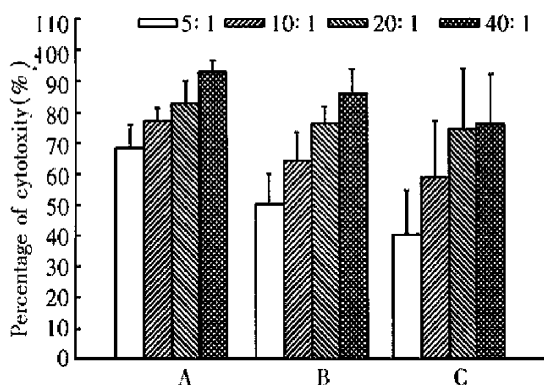


**Figure 6** Cytotoxicity of abdominal cavity infiltrating lymphocytes (ACIL) against tumor cells.  
 A: Cytotoxicity of CMT93-B7 induced ACIL against CMT93-B7 tumor cells,  $n = 4$ .  
 B: Cytotoxicity of CMT93-B7 induced ACIL against CMT93 wild type tumor cells,  $n = 4$ .  
 C: Cytotoxicity of CMT93 induced ACIL against CMT93 wild type tumor cells,  $n = 4$ .  
 By paired Student's  $t$  test: A is different from B significantly,  $P < 0.05$ ; B is different from C significantly,  $P < 0.05$ .

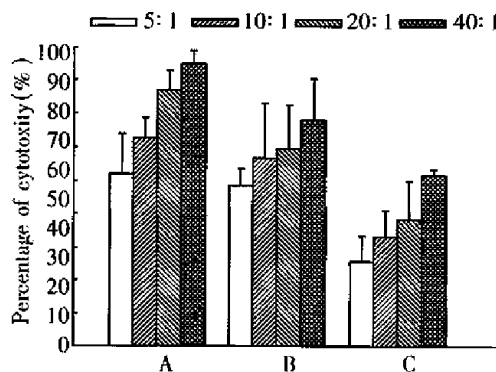


**Figure 7** Cytotoxicity of spleen cells against tumor cells.  
 A: Cytotoxicity of CMT93-B7 induced spleen cells against CMT93-B7 tumor cells,  $n = 4$ .  
 B: Cytotoxicity of CMT93-B7 induced spleen cells against CMT93 wild type tumor cells,  $n = 4$ .  
 C: Cytotoxicity of CMT93 induced spleen cells against CMT93 wild type tumor cells,  $n = 4$ .  
 By paired Student's  $t$  test: A is different from B significantly,  $P < 0.05$ ; B is different from C significantly,  $P < 0.01$ .

**DISCUSSION**

Tumor-bearing host can not reject tumor cells efficiently. The unresponsiveness of T cells to tumor antigens should be considered as ignorance rather than tolerance<sup>[7]</sup>. Three critical parameters contribute to the ignorance of the immune system. They are low levels of antigen presentation, lack of availability of costimulation signals, and a relatively low frequency of relevant CTL precursors<sup>[7]</sup>. These factors may play a role singly or simultaneously. B7 molecules deliver costimulation signal in three different ways. Among them, the cis-costimulation is the most efficient mode<sup>[2]</sup>.

Tumor cells expressing B7 molecules activate T cells by cis-costimulation. In this process, tumor's antigenicity is required. The tumor cells without antigenicity or with poor antigenicity can not induce efficient anti-tumor immunity though they express B7 costimulation molecules<sup>[5]</sup>. CMT93 is a weak immunogenicity cell line. We found that its tumorigenicity decreased greatly after the transfection with B7 gene. The inoculated CMT93-B7 tumor cells proliferated and formed some palpable tumors in the early stage after inoculation. But a short time later the tumors disappeared completely. Yet in the control group, all tumors grew progressively (Figure 4). The reason why CMT93-B7 cells formed some small tumors in the early stage after inoculation is that the immune system of the host needs a short time to recognize the tumor antigen and to produce immune response to the tumor cells.

B7 gene transfected tumor cells can induce a strong anti-tumor immunity. The mechanism is that in the presence of B7 costimulation, the CTL clones against the domain epitopes of tumor cells are am-

plified more greatly than ever, and more importantly the CTL repertoire against subdomain epitopes of tumor antigen is expanded. Chen<sup>[2]</sup> considered that besides providing a unique signal for T cell activation, B7 costimulation may also reduce the threshold of interaction between peptide-MHC complex and TCR which is required for CTL activation. So the subdomain epitopes which usually can not activate T cells induce T cell activation. In this study, we found that the tumors growing initially after the inoculation of CMT93-B7 vanished in a short time, and the mice primed with CMT93-B7 rejected the rechallenge of wild type CMT93 completely. It suggested that when wild type tumor cells rechallenged the mice primed with B7 expressing tumor cells, T cells had already been activated, so the rechallenged wild type tumor cells could be rejected quickly and completely<sup>[8]</sup>.

B7 costimulation signal is needed for T cell activation. During T cells displaying their effector function, this signal is considered no longer required, but few exceptions have been reported<sup>[9]</sup>. In the rechallenge experiment, the mice primed with CMT93-B7 rejected the rechallenged wild type CMT93 cells completely. The activated CTL from primed mice can kill the wild type tumor cells. In cytotoxicity experiment *in vitro*, the CTL induced by CMT93-B7 had a higher cytotoxicity against CMT93-B7 than against wild type CMT93 (Figures 6, 7). This phenomenon showed that B7 molecules play an important role in effector function. The mechanism may be that the interaction of B7 with

CD28 promoted the lymphocyte adherence to target cells, and that the interaction of B7 with CD28 promoted the combination of peptide-MHC with TCR, i.e., B7 costimulation reduced the threshold of interaction between peptide-MHC complex and TCR. According to the above results, we consider that the CTL induced by B7 positive tumor cells can kill wild type tumor cells, and the B7 molecules can augment the cytotoxicity of CTL against tumor cells.

## REFERENCES

- 1 Chen L, Linsley PS, Hellstrom KE. Costimulation of T cells for tumor immunity. *Immunol Today*, 1993;14:483-496
- 2 Chen L. T cell costimulation and tumor immunity. *Chin J Cancer Biother*, 1996;3:86-95
- 3 Baskar S, Ostrand-Rosenberg S, Nabavi N, Nadler LM, Freeman GJ, Grimcher LH. Constitutive expression of B7 restores immunogenicity of tumor cells expressing truncated MHC class II molecules. *Proc Natl Acad Sci USA*, 1993;90:5676-5690
- 4 Li Y, Hellstrom I, Li Y, McGowan P, Hellstrom I, Hellstrom KE, Chen L. Costimulation of tumor reactive CD4+ and CD8+ T lymphocytes by B7, a natural ligand for CD28, can be used to treat established mouse melanoma. *J Immunol*, 1994;153:421-428
- 5 Chen LP, McGowan P, Ashe S, Johnston J, Li Y, Hellstrom I. Tumor immunogenicity determines the effect of B7 costimulation on T cell-mediated tumor immunity. *J Exp Med*, 1994;179:523-532
- 6 Heo DS, Park JG, Hata K, Day R, Herberman RB, Whiteside TL. Evaluation of Tetrazolium-based Semiautomatic Colorimetric Assay for measurement of human antitumor cytotoxicity. *Cancer Research*, 1990;50:3681-3690
- 7 Melero I, Bach N, Chen L. Costimulation, tolerance and ignorance of cytolytic T lymphocytes in immune responses to tumor antigens. *Life Sciences*, 1997;60:2035-2041
- 8 Yang G, Hellstrom KE, Hellstrom I, Chen L. Antitumor immunity elicited by tumor cells transfected with B7-2, a second ligand for CD28/CTLA-4 costimulatory molecules. *J Immunol*, 1995;154:2794-2800
- 9 Ramarathnam L, Castle M, Wu Y, Liu Y. T cell costimulation by B7/BB1 induces CD8 T cell-dependent tumor rejection: an important role of B7/BB1 in the induction, recruitment, and effector function of antitumor T cells. *J Exp Med*, 1994;179:1205-1214

Edited by WANG Xian-Lin

# Study of differential polymerase chain reaction of C-erbB-2 oncogene amplification in gastric cancer \*

JI Feng, PENG Qing-Bi, ZHAN Jing-Biao and LI You-Ming

**Subject headings** stomach neoplasms; C-erbB-2 gene; polymerase chain reaction; oncogene amplification

## Abstract

**AIM** To study the significance of C-erbB-2 oncogene amplification in gastric cancer.

**METHODS** C-erbB-2 oncogene amplification was examined by using differential polymerase chain reaction (dPCR) in surgical and endoscopic specimens of 83 cases of gastric cancer and 101 metastatic lymph nodes.

**RESULTS** C-erbB-2 amplification was found in 28.9% (24/83) surgical specimens and 20.5% (17/83) endoscopic ones of gastric cancer patients. The amplification was significant in both types of specimens of advanced cancer cases ( $P<0.05$ ) and surgical specimens with lymph node metastasis ( $P<0.01$ ). The incidence of C-erbB-2 amplification in lymph nodes with metastasis was higher than in primary sites (surgical specimens,  $P<0.05$ ). The patients with amplification tumors had poorer 5-year survival rates than those with unamplification ones in the early cancers and well to moderately differentiated adenocarcinomas ( $P<0.05$ ). The same surgical samples were tested again by Southern blot hybridization to ascertain C-erbB-2 amplification, and the positive rate of C-erbB-2 amplification (15.7%) was lower than that of dPCR (28.9%,  $P<0.05$ ).

**CONCLUSION** Examining C-erbB-2 amplification by dPCR is a quick, simple, reliable and independent method, and is helpful in predicting prognosis and metastatic potential of gastric cancer.

Department of Gastroenterology, 1st Affiliated Hospital, Medical College of Zhejiang University, Hangzhou 310003, Zhejiang Province, China  
Dr. JI Feng, male, born on 1962-11-26 in Lingbo City, Zhejiang, graduated from Zhejiang Medical University as a M.D. in 1989, associate professor of internal medicine and Director of master student, having 25 papers published.

\*Project supported by the Zhejiang Natural Science Foundation, No.925006.

**Correspondence to:** Dr. JI Feng, Department of Gastroenterology, 1st Affiliated Hospital, Medical College of Zhejiang University, No. 261, Qing Chun Road, Hangzhou 310003, Zhejiang Province, China  
Tel. +86 • 571 • 7072524 Ext. 4402, Fax. +86 • 571 • 7072577

Received 1998-11-21

## INTRODUCTION

Human proto-oncogene, C-erbB-2, has been showed to share homology with the closely related V-erbB oncogene and with the epidermal growth factor receptor (EGFR) by DNA sequence analysis. The amplification of C-erbB-2 gene is frequently found in many cancers and has relation to the gene protein overexpression in cancer cells. In breast cancer, the C-erbB-2 amplification or protein overexpression of C-erbB-2 is a signal of poor prognosis and in gastric cancer, the overexpression of C-erbB-2 protein examined by immunohistochemistry has relation to differentiation, progress and metastasis of tumor<sup>[1]</sup>. The current study was designed to examine the possible association between the amplification of C-erbB-2 gene which was examined by differential polymerase chain reaction (dPCR) and clinicopathologic features of gastric cancer. We compared the dPCR with Southern blot analysis, in order to demonstrate its superiority, reliability and practical value.

## MATERIALS AND METHODS

### *Clinical samples*

The surgical and endoscopic biopsy specimens and 101 metastatic lymph nodes in 83 patients with resected gastric cancers diagnosed pathologically were collected. All specimens and normal gastric mucosa for control were immediately washed to remove blood and fat, and stored in liquid nitrogen.

### *Reagents and primer synthesis*

Taq DNA polymerase and a C-erbB-2 probe were obtained from Promega (U.S.A.) and Wako Pure Chemical Industries (Japan) respectively. The human C-erbB-2 primers were: A:5'-ACGTCTA AGATTTCTTTGTT 3', B:5'-ACCTTGGCAATCTGCATAC A 3'. The  $\beta$ -actin primers were: A:5'-CAAAGACCTCATACGCTTACA 3' B:5'-ATAAGCCATGCCAAAGTG ATC-3'. The amplifying DNA fragments of above two pairs of primers were 104bp and 296bp respectively and all primers were synthesized in the Cell Biology Research Institute of Shanghai.

### *DNA extraction and dPCR examination*

Total DNA from cancer, normal mucosa and

metastatic lymph node cells were extracted by using the phenol-chloroform method. The purity and content of DNA extracted were examined by spectrophotometer analysis. The dPCR was manipulated according to the article<sup>[2]</sup> in detail. A total amount of 25  $\mu$ L- reaction solution contained 0.1  $\mu$ g DNA sample and 0.05 nmol/L- of each pair primers. The amplification of C-erbB-2 and  $\beta$ -actin was carried out in one reaction system and PCR procedure was as follows: predenaturation at 95°C for 5 min, addition of Taq DNA polymerase, denaturation at 94°C for 60 s, annealing at 52°C for 60 s and extension at 72°C for 50 s, and the thermal cycles from denaturation at 94°C to extension were repeated 30 times. Then 10  $\mu$ L DNA amplifying product was subjected to electrophoresis in 4% agarose gel, stained with ethidium bromide and observed under ultraviolet light. The level of amplification was determined by densitometry (Beckman CD2000). The number of gene copy was calculated according to the ratio of the OD value of C-erbB-2 and that of  $\beta$ -actin and the ratio  $\times 296/104$  was thought to be corrected number of gene copy.

#### Southern blot analysis

DNA from surgical specimens was digested with EcoR-I, and 10  $\mu$ g of completely digested DNA was subjected to electrophoresis in 0.8% agarose gel and then denatured, neutralized, and transferred to nylon filters. According to classical Southern blot hybridization<sup>[3]</sup>, the filters were hybridized with <sup>32</sup>P-labeled C-erbB-2 cDNA probes. DNA from normal gastric mucosa was used as a control. After hybridization, the filters were washed and exposed to XAR-5 film. The level of amplification was determined by densitometry, and the densitometric signals of all the bands were summed up.

#### Statistical analysis

The significance of differences among groups was determined by the  $\chi^2$  test. Five-year survival rate was calculated by Kaplan- Meier method and tested with Log-rank method.

## RESULTS

### C-erbB-2 amplification of dPCR in surgical and endoscopic specimens of gastric cancer (Table 1)

Within the extent of 0.17-0.49 (99% convincing range) was the numbers of gene copy of C-erbB-2 in 30 control cases (normal gastric mucosa). After multiplying 296/104, the extent of the number was corrected to be 0.48-1.39. Every case with the number of gene copy of C-erbB-2 over 1.39 was thought to be of gene amplification. Twenty-four

surgical and seventeen endoscopic specimens of 83 cases with gastric cancer showed a positive gene amplification and the multiples of amplification were within the extent of 2-33 and 2-29 in the two types of specimens respectively. No difference in the incidence of positive rate of amplification was found between surgical and endoscopic specimens.

The cases of gastric cancer with positive C-erbB-2 amplification in endoscopic specimens were all associated with positive amplification in their surgical ones. The amplification of C-erbB-2 was correlated with the depth of invasion (in the both types of specimens,  $P < 0.05$ ) and lymph node metastasis (only in surgical specimens,  $P < 0.01$ ), but not correlated with the age, sex, gross appearance of tumor and liver metastasis in cases with gastric cancer. C-erbB-2 amplification was detected more often, but not to a significant extent, in well-moderately differentiated adenocarcinoma ( $\chi^2 = 3.75$ ,  $P > 0.05$ ).

**Table 1 Relationship between clinicopathologic features and incidence of C-erbB-2 amplification**

Variable	Case number	C-erbB-2 amplification (%)	
		Surgical specimen	Endoscopic specimen
Age (yr)			
<60	16	(31.3)	4(25.0)
$\geq 60$	67	19(28.4)	13(19.4)
Sex			
Male	51	15(29.4)	10(19.6)
Female	32	9(28.1)	7(21.9)
Gross appearance			
Borrmann1	8	3(37.5)	2(25.0)
Borrmann 2	37	9(24.3)	7(18.9)
Borrmann 3	32	10(31.2)	7(21.9)
Borrmann 4	6	2(33.3)	1(16.7)
Depth of invasion			
Early cancer	28	4(14.3) <sup>a</sup>	2(7.1)a
Advanced cancer	55	20(36.4)	15(27.3)
Differentiation			
Well-mod	45	17(37.8)	12(26.7)
Poor	38	7(18.4)	5(13.2)
Lymph node metastasis			
Positive	21	11(52.4) <sup>b</sup>	7(33.3)
Negative	62	13(21.0)	10(16.1)
Liver metastasis			
Positive	13	6(46.2)	4(30.8)
Negative	70	18(25.7)	13(18.6)

Compared with the other results of same variable group, <sup>a</sup> $P < 0.05$ ; <sup>b</sup> $P < 0.01$ . Well-mod: Well to moderately differentiated carcinoma; Poor: Poorly differentiated carcinoma.

### C-erbB-2 amplification at primary sites and in metastatic nodes of gastric cancer

Regardless of the presence or absence of C-erbB-2 amplification at the primary site, the rate of C-erbB-2 amplification in lymph nodes with metastasis (44.6%) was significantly higher than that at primary sites (28.9%,  $P < 0.05$ ).

### Gene amplification examined by Southern blot

The rate of C-erbB-2 amplification (15.7%, 13/83) examined by Southern blot was significantly lower than that (28.9%) examined by dPCR in surgical specimens of gastric cancer ( $P < 0.05$ ). C-erbB-2 amplification was detected by using dPCR in 12 of 13 amplification cases examined by Southern blot.

### Association between C-erbB-2 amplification in surgical specimens of gastric cancer and prognosis of the patient

No difference between the 5-year survival rates of gastric cancer patients with C-erbB-2 amplification and those without was found. The 5-year survival rates of patients with the gene amplification tumors and those without were 50.0% and 95.8% respectively for early cancers, 47.1% and 78.6% respectively for well to moderately differentiated adenocarcinomas. Thus, the prognosis was significantly worse among patients with C-erbB-2 amplification tumors than among those without amplification in the early cases ( $P < 0.05$ , Figure 1) and in the well to moderately differentiated cancers ( $P < 0.05$ , Figure 2).

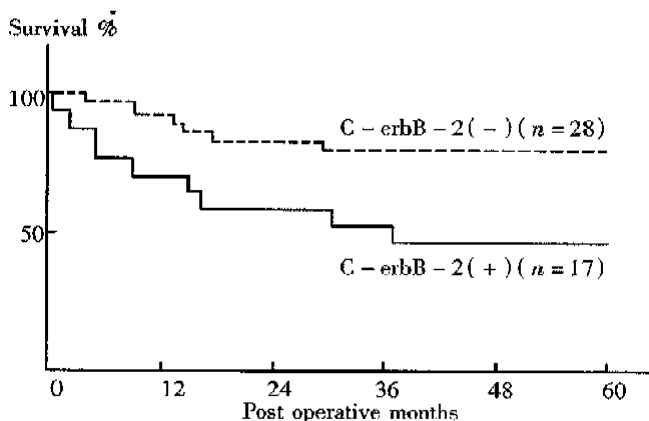
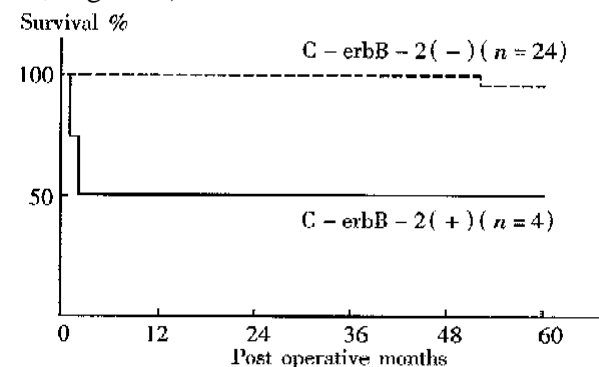


**Figure 1** Survival curves for patients with early cancer with C-erbB-2 amplification ( $n = 4$ ) and for those with no C-erbB-2 amplification ( $n = 24$ ,  $P < 0.05$ ).

**Figure 2** Survival curves for patients with well-moderately differentiated carcinoma with C-erbB-2 amplification ( $n = 17$ ) and for those with no C-erbB-2 amplification ( $n = 28$ ,  $P < 0.05$ ).

### DISCUSSION

In recent years, some studies have revealed a correlation of C-erbB-2 amplification with poor prognosis in breast or gastric cancers. However, there are few systematic studies about C-erbB-2 changes in gastric cancer in China. In the current study, the C-erbB-2 amplification were observed in 24 surgical specimens of 83 cases by dPCR. High rates of the gene amplification in advanced cancers showed a tendency to deep invasion in such cancers. C-erbB-2 amplification seemed to exist more often in cancers with nodal involvement than in those without. Therefore, cancers with the amplification might have a tendency to show a greater degree of lymph node metastasis. Recent studies have showed that p185, the protein products of C-erbB-2, which is located in microvillus and pseudopodia of cancer cells is able to accelerate cell movement. Amplification of C-erbB-2 might therefore be related to the regulation of cancer cell invasion and metastasis<sup>[4]</sup>. In the present study C-erbB-2 amplification was found more often in well to moderately differentiated cancers, suggesting its correlation with cell differentiation; such a result was similar to the report of Yokota<sup>[5]</sup>. Our result also showed that the incidence of C-erbB-2 amplification in metastatic lymph nodes was higher than that at the primary sites. Therefore, the gene amplification might be related to nodal involvement of gastric cancer, and the oncogene possibly allowed the cancer cells to spread from the primary site to lymph nodes. The activated C-erbB-2 gene has been indicated to enhance the metastatic potential of colon cancer cells, suggesting participation of the gene in the metastasis process<sup>[6]</sup>. In a 5-year follow-up of all cases, we found that there was no difference in prognosis between cases with C-erbB-2 amplification and those without. But in cases of early and well to moderately differentiated gastric cancer, patients with C-erbB-2 amplification tumors were found to have a worse prognosis than those without amplification, perhaps because of the greater degree of deep invasion and lymph metastasis in C-erbB-2 amplification tumors.

The dPCR in the current study is a semi-quantitative analysis which can be used to detect gene changes rapidly and sensitively without using isotopic technique<sup>[7]</sup>. The basic property of dPCR is that both the target gene samples to be tested and the monocopy reference gene in PCR are run in one reactive system. The amplification copy number of the sample gene DNA is calculated on the basis of the ratio of OD values of amplifying products of the sample and reference genes. As compared with Southern blot hybridization, dPCR is simpler, needs

less sample or DNA and no isotope, and causes less error. Although less amount of DNA from endoscopic specimens was used in dPCR, the rate of C-erbB-2 amplification reached 20.5% and was not significantly lower than that done with surgical specimens. Our results indicated that the prognosis of gastric cancer might be predicted preoperatively by using dPCR to examine C-erbB-2 amplification. The rate of C-erbB-2 amplification was significantly higher by using dPCR than using Southern blot hybridization in surgical specimens. These results prove that dPCR is a highly sensitive method. Therefore examining C-erbB-2 amplification by dPCR might be helpful in predicting prognosis and metastatic potential of gastric cancer, especially early and well to moderately differentiated cancers.

## REFERENCES

- 1 Uchino S, Tsuda H, Maruyama K, Kinoshita T, Sasako M, Saito T, Kobayashi M, Hirohashi S. Overexpression of C-erbB-2 protein in gastric cancer. *Cancer*, 1993;72:3179-3184
- 2 Neubauer A, Neubauer B, He M. Analysis of C-erbB-2 gene amplification in archival tissue by differential PCR. *Oncogene*, 1992;7:1019-1025
- 3 Southern EM. Detection of specific sequences among DNA fragments separated by gel electrophoresis. *J Mol Biol*, 1975;98:503-517
- 4 De Potter Cr, Quatacker J. The p185 protein is localized on cell organelles involved in cell motility. *Clin Exp Metastasis*, 1993;11:463-471
- 5 Yokota J, Yamamoto T, Miyajima N, Toyoshima K, Nomura N, Sakamoto H, Yoshida T, Terada M, Sugimura T. Genetic alteration of the C-erbB-2 oncogene occur frequently in tubular adenocarcinoma of the stomach and are often accompanied by amplification of the v-erbA homologue. *Oncogene*, 1988;2:283-287
- 6 Yusa K, Sugimoto Y, Yamori T, Toyoshima K, Tsuruo T. Low metastatic potential of clone from murine colon adenocarcinoma 26 increased by transfection of activated C-erbB-2 gene. *J Natl Cancer Inst*, 1990;82:1633-1636
- 7 Frye RA, Benz CC, Liu E. Detection of amplified oncogenes by differential polymerase chain reaction. *Oncogene*, 1989;4:1153-1157

Edited by LU Han-Ming

# Gastroduodenal ulcer treated by pylorus and pyloric vagus-preserving gastrectomy

LU Yun-Fu<sup>1</sup>, ZHANG Xin-Xin<sup>2</sup>, ZHAO Ge<sup>1</sup> and ZHU Qing-Hua<sup>1</sup>

**Subject headings** peptic ulcer/surgery; stomach ulcer/surgery; duodenal ulcer/surgery; pylorus/surgery; gastrectomy

## Abstract

**AIM** To evaluate the curative effect of pylorus and pyloric vagus-preserving gastrectomy (PPVPG) on peptic ulcer.

**METHODS** Treating 132 cases of GU and DU with PPVPG, and comparative studies made with 24 cases treated with Billroth I (B I) and 20 cases with Billroth II (B II); advantages and shortcomings evaluated.

**RESULTS** Not a single death after PPVPG. No recurrence of the disorder in the subsequent follow-up for an average of 6.5 years. Curative effect (visik I-&II) 97.7%. Acidity reduction similar to that found in B I and B II, but 97.7% of the B I and all B II cases having more than second degree intestinal fluid reflux, in contrast to 7.1% in PPVPG cases. Dumping syndrome occurred in the B I and B II cases, none in PPVPG cases. With regard to gastric emptying, food digestion, absorption, body weight and life quality, PPVPG proved to be superior to Billroth procedure.

**CONCLUSION** PPVPG has the advantages of conventional Billroth gastrectomy in reducing acid, removing ulcer focus, and at the same time preserves the pylorus and pyloric vagus for maintaining the normal gastric physiological function. Dumping syndrome, intestinal fluid reflux and other complications of conventional gastrectomy may be avoided.

## INTRODUCTION

Subtotal resection of stomach (Billroth, 1881), usually referred to as the conventional procedure, has been used for over 100 years in the surgical treatment of peptic ulcer. However, such operation, owing to the loss of pyloric function, often causes postoperative problems, such as rapid gastric emptying, dumping syndrome, intestinal content reflux, indigestion, poor absorption, etc. In order to avoid such complications to the fullest extent, we designed the PPVPG and did repeated animal experiments before its clinical application in January 1988. Since that time we treated 132 cases of gastric and duodenal ulcers with gratifying results, with 44 cases treated with Billroth operation for comparison.

## MATERIALS AND METHODS

### Patients

The patients under treatment were 121 males and 11 females, 17-67 years old, medium age 46. They had ulcer histories from 1 year to 31 years, averaging 8.3 years. Most (97%) of them had symptoms, such as pains in the upper abdomens, nausea and vomiting, poor appetite, acidic cructation and heartburn. They took medicines regularly as part of the treatment. Film takings of the digestive tracts with barium meal and gastroscopy indicated the presence of ulcers, in diameters area of 10 mm-30 mm (51 gastric and 81 duodenal including four cases of compound ulcers). Pylorus stenosis occurred in 4 cases, and duodenal stenosis in 3 cases.

### PPVPG technique

The operation started with dissecting the greater curvature from a point 2 cm above the pylorus to the last two branches of the left gastroepiploic artery. The lesser close to the gastric wall, was set free by dissection. The anterior and posterior vagal trunks, hepatic branches and the last 2-3 branches of Lataget vagus innervating the pyloric region, together with attached blood vessels, were carefully preserved; only the vagus branches innervating the body of the stomach and blood vessels were selectively excised. With the upper part of the gastric body cut off, we sutured the out-edge-of the lesser curve side conventionally in one layer, reserving 3.5 cm of the greater curve side for anastomosis. The antral cut-edge was trimmed to a

<sup>1</sup>Surgery Department of the Second Clinical College, Shanxi Medical University, No.382, Wuyi Road, Taiyuan 030001, Shanxi Province, China

<sup>2</sup>The Third Shanxi Provincial People's Hospital

LU Yun-Fu, M.D. male, born on Dec 15, 1949 in Wuyuan County, Jangxi Province, China, Han nationality, graduated from Shanxi Medical University in 1976, now head of surgery department, engaged in gastroduodenal and liver diseases, having 69 papers published.

**Correspondence to:** LU Yun-Fu, Surgery Department of the Second Clinical College, Shanxi Medical University, No.382, Wuyi Road, Taiyuan 030001, Shanxi Province, China

Received 1998-08-20

concave shape. The antral seromuscular layer from the lesser curvature to the greater curvature where Latarget nerve senter were preserved. The antral mucosa 7 mm-10 mm-proximal to the pyloric ring was excised, and then the mucosal edge 6 cm proximal to the pyloric ring was sutured round all layers of cut edge near the greater curvature (stoma for anastomosis). The antral seromuscular flap with attaching vagus branches was sutured to the region of anastomosis (Figure 1).

Treatment of the ulcer focus. The ulcer was resected together with large part of the stomach in 47 cases; longitudinal section and transverse suture were done in 42 cases of duodenal ulcer and the ulcer of pyloric canal; in 4 cases of bulbar posterior duodenal penetrating ulcer, we freed the back wall of duodenum and the ulcer was transversely sutured, the 4 cases of gastric and duodenal compound ulcers were treated respectively according to the afore-mentioned principle; in those cases with concurrent duodenal or pylorus stenosis, 3 cases were treated with duodenoplasty and 4 cases with pylorus dilatation; and no particular treatment was given in 28 cases, and the ulcers were allowed to heal by themselves.

**RESULTS**

PPVPG has been done in 132 patients with peptic ulcers. Comparative studies were made between PPVPG and Billroth procedures (B I 24 cases and B II 20 cases).

**Reduction of gastric acid**

Postoperative examinations (10-15 days) of gastric juice and serum gastrin were carried out in 64 patients. By comparing with the preoperative basic level, the mean basic acid output (BAO) reduction rate was 70.5%, and the mean maximal acid output (MAO) reduction rate 76.3%. The above two indices and postprandial serum gastrin reduction rate were more or less similar to those in cases undergoing B I and B II operations in the same period (Tables 1, 2 and 3).

**Table 1 Basic acid output before and after operation ( $\bar{x}\pm s$ , mmol/L)**

Operation mode	n	Preoperation	Postoperation
PPVPG	64	7.75±2.43	2.29±1.25 <sup>b</sup>
B I	24	7.51±2.76	2.16±1.28 <sup>b</sup>
B II	20	7.21±2.58	2.06±1.23 <sup>b</sup>

<sup>b</sup>P<0.01, vs preoperation.

**Table 2 Maximal acid output before and after operation ( $\bar{x}\pm s$ , mmol/L)**

Operation mode	n	Preoperation	Postoperation
PPVPG	64	66.23±13.76	15.68±5.53 <sup>b</sup>
B I	24	67.21±20.23	15.96±10.32 <sup>b</sup>
B II	20	66.18±7.19	16.15±11.04 <sup>b</sup>

<sup>b</sup>P<0.01, vs preoperation.

**Table 3 Serum gastrin concentration before and after operation ( $\bar{x}\pm s$ , ng/g)**

Operation mode	n	Preoperation	Postoperation
PPVPG	64	284.9±52.5	129.5±11.3 <sup>b</sup>
B I	24	299.2±45.0	124.8±18.0 <sup>b</sup>
B II	20	260.0±64.3	136.8±46.8 <sup>b</sup>

<sup>b</sup>P<0.01, vs preoperation.

**Gastric emptying time**

A test meal consisting of noodles soup 150 g + 100 g barium sulfate was given to patients of different groups 4 weeks after operation. A normal gastric complete emptying time was seen in 81.8% of the PPVPG group, 50% of the B I group and all cases of the B II group in which complete emptying occurred in 30 minutes. The results demonstrate that the conventional subtotal gastrectomy with Billroth anastomosis has the disadvantage of greatly quickened gastric emptying time. Furthermore, 9.1% gastric retention occurred in Billroth operation, whereas only 2.3% (3/132) of the PPVPG patients had such complication.

**Dumping syndrome**

Three months postoperatively, patients with one of the following three complaints were suggestive of having dumping syndrome: a. postprandial dizziness, b. cold sweating and c. palpitation<sup>[2]</sup>. Thus, the dumping syndrome was noted in 16.7% of the B I group and 15.0% of the B II group, but in none of the PPVPG group.

**Duodenogastric reflux**

Four weeks after the operation, duodeno-gastric reflux was measured by dynamic scanning by means of intravenous injection of 99 mTc-EHIDA 185MBq (5mci). The degree of reflux was divided into six grades, and only those higher than grade II had an apparent clinical value<sup>[3]</sup>. In 96 patients after PPVPG, only 7 (7.3%) had reflux to a small extent, with no clinical symptoms; whereas those undergoing B I and B II, reflux occurred in 97.9% of the patients (Figure 2, Table 4), either with or without subjective symptoms. Bacterial cultures of the gastric juice were positive in all cases with reflux.

**Table 4 Duodenogastric reflux (n)**

Operation mode	n	Reflux indexes grades (%)						Total	%
		I <5%	II -10%	III -20%	IV -30%	V -40%	VI >40%		
PPVPG	84	6	0	0	0	0	6	7.1	
B I	24	0	6	7	5	5	23	95.8	
B II	20	0	0	5	6	4	20	100.0	

Significantly different from groups PPVPG and B I and B II (P<0.005,  $\chi^2 = 99.6608$ ). No marked difference between groups B I and B II (P>0.05,  $\chi^2 = 0.8536$ ).

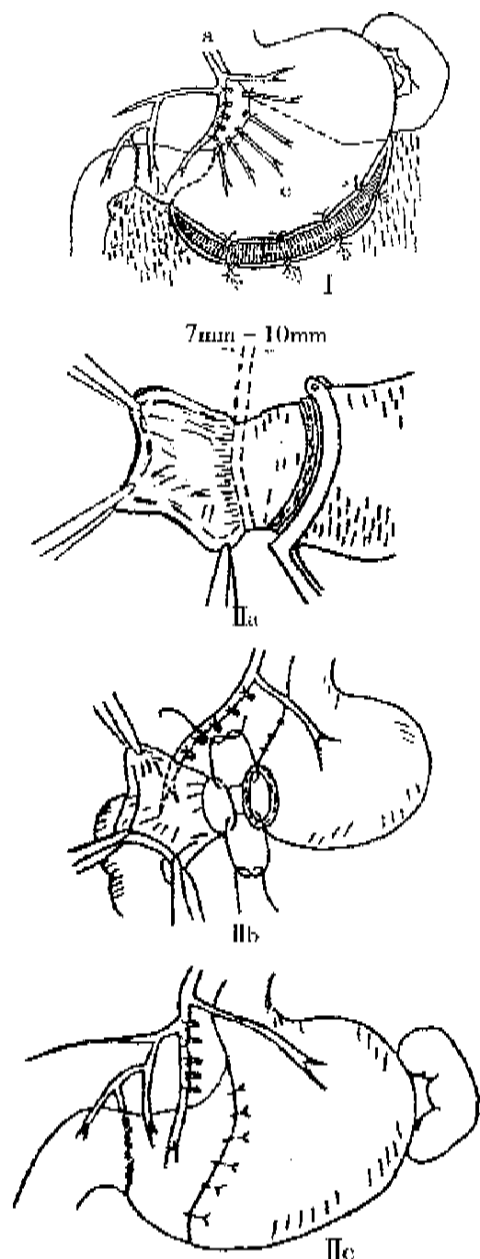


**Figure 1** Schema of PPVPG. I a: Vagus preserved; I b: antral mucosa stripped region; I c: stomach resection region. II a: the antral mucosa 7mm-10mm proximal to the pyloric ring is excised; II b: the distal mucosal edge is sutured round all layers of the cut edge near the greater curvature (stoma for anastomosis); II c: antral seromuscular layer is sutured to the region of anastomosis.

#### **Digestion and absorption of food**

Beginning on the 7th postoperative day, the patients were given a specially prepared diet for 4 consecutive days. It was discovered that ① diarrhea occurred in 11.4% of the cases with the Billroth operations, but in none of the cases with PPVPG; ② the amount of fat globules in the stool of PPVPG cases was much less than that in B I and B II cases; ③ the postoperative urinary nitrogen excretion was

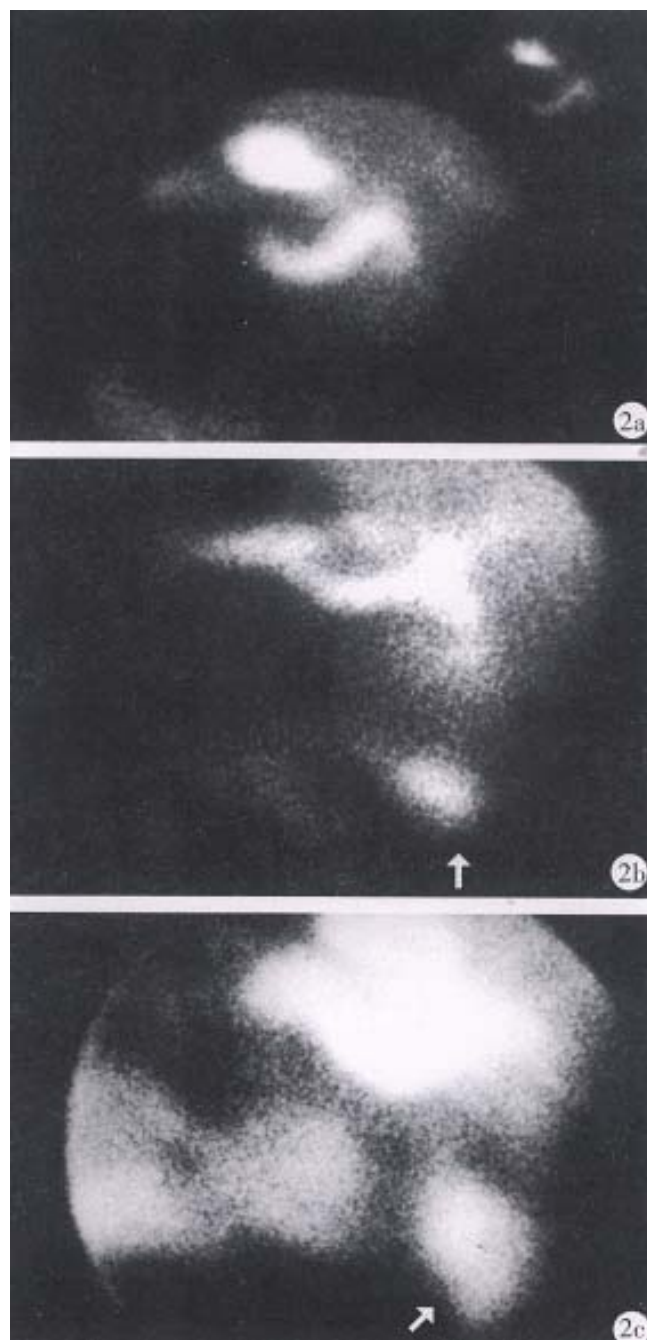


**Figure 2** Intestinal content reflux after an intravenous injection of  $^{99m}\text{Tc}$ -EHIDA resulted from different operation modes. A. No reflux resulted from PPVPG; B. Reflux resulted from B I; C. Serious reflux resulted from B II.

13.1gm per day in the PPVPG cases, 17 gm in B I cases and 20.1 gm in B II cases. These results suggested that patients undergoing Billroth operations had relatively poorer function of digestion and absorption, and their catabolism increased; and ④ body weight was measured three months before and after operations, 92.8% of the patients with **PPVPG** showed no body weight loss, a result much better than 79% with BI and 65% with BII.

### Follow-ups

Through phone calls or by mails and re-examinations at the outpatient department, our follow-ups have lasted over a period of 1-10 years, averaging 6.5 years as a whole. To our satisfaction, no ulcer relapses or complications have been found in the surveys of 132 patients, Visik grades I, II 97.7%. Gastroscopic examinations done in 72 (54.5%) of 132 patients showed a complete disappearance of the original ulcer foci together with normal remanent gastric mucosa and pylorus.

### DISCUSSION

Despite different explanations for the causation and evolution of peptic ulcer, acknowledged explanation for gastric acid is involved. Therefore, a reduction of gastric acid secretion is regarded as the principle of surgical treatment of ulcer. In the conventional Billroth operation, this point has been fully asserted, but also considered as an important standard for judging ulcer recurrence rate. In this regard, PPVPG and Billroth are equally effective. PPVPG effectively reduces gastric acid by stripping off the antral mucosa containing many G cells, resulting in decreased hormonal stimulation, and by subtotal resection of stomach corpus which leads to greatly reduced parietal cells. As the vagus branch innervating the remanent stomach body is separated by excision and its direct effect on the parietal cells thus stopped, so the operation effectively reduces gastric acid. The mean BAO decreased by 70.5% and the mean MAO by 76.3%, they bore no marked difference with those of homochronous Billroth operations ( $P>0.05$ ). The small part of antral mucosa was preserved for the purpose of anastomosing it with the cut edge near the greater curve so as to avoid the stenosis of anastomotic more likely to occur in stoma directly anastomosing the cut edge with the mucosa of the pyloric tube and also to avoid the possibility that excessive excision would affect the function and integrity of pyloric sphincter. The small part of antrum mucosa retained, in fact, would be just good enough for being scarred. The scar width of the anastomotic stoma in experimental dogs was 6 mm-8 mm 6 months after operation and would lose its function of promoting secretion. Care must be taken,

however, to make the antral mucosa 7 mm-10 mm wide. The width less than 7 mm may lead to the stenosis of anastomotic stoma, but more than 10 mm will affect the reduction of gastric acid. AN NN *et al*<sup>[4]</sup> considered the optimal free HCl concentration after the resection of stomach as 20 clinical units, and the mean free HCl of PPVPG was 15.68 clinical units (equal to 15.68 mmol/L). What is more important is that in the postoperative follow-ups, not a single case of relapse was found and the curative effect was proved to be highly gratifying. All these demonstrate that PPVPG designed is scientific enough to meet all clinical requirements. With the vagus resected, the action potential of gastric smooth muscle is 8-20 times less than normal<sup>[1]</sup>, leading to a delay of gastric emptying and retention. The preservation of vagus in the operation is to avoid this condition and also to retain the physiological function of pyloric sphincter. The small part of seromuscular flap retained in PPVPG protects the branches of latarjer vagus passing through it to the pylorus along with the attaching blood vessels and also reinforce the anastomotic stoma to prevent from leaking. PPVPG has the advantages of conventional Billroth gastrectomy in reducing acid, removed ulcer focus, at the same time preserves pylorus and pyloric vagus, which enables the pylorus and the remanent stomach to function normally. PPVPG has greatly avoided postoperative complications of the subtotal gastric resection, such as dumping syndrome, intestinal fluid reflux and so on. Safe and adaptable to wide variety of indications, PPVPG carves not only a new course for the surgical treatment of peptic ulcer, including perforated ulcer, profuse bleeding due to gastroduodenal ulcer, and slight duodenal or pylorus stenosis, but also can be applied to other benign gastric lesion such as polyposis, leiomyoma and ectopic pancreas.

### REFERENCES

- 1 Lu YF, Hou YD, Jia SR, Guo CY. Experimental study of pyloric vagus preserving gastrectomy. *World J Surg*, 1993;17:525-529
- 2 Sekine T, Stato T, Maki T, Shiratori T. Pylorus-preserving gastrectomy for gastric ulcer one to nine year follow up study. *Surgery*, 1975;77:92-99
- 3 Gu SQ. Determination of duodenal gastric reflex. *Beijing Yixue*, 1988;4(Suppl):78-81
- 4 An NN, Ky R, Wang MS. Clinical experience of 18 cases of gastrectomy preserving pylorus. *Shiyong Waike Zazhi*, 1986;6:245-247

Edited by LU Han-Ming

Review

# Expression of proliferating cell nuclear antigen in polyps from large intestine

LUO Yu-Qin<sup>1</sup>, MA Lian-Sheng<sup>2</sup>, ZHAO Yi-Ling<sup>3</sup>, WU Kai-Chun<sup>4</sup>, PAN Bo-Rong<sup>5</sup> and ZHANG ssXue-Yong

**Subject heading** colonic polyps; adenomas; proliferating cell nuclear antigen; colonic neoplasms

Colon cancer has a high incidence in the world, especially in Western countries, and the incidence is also increasing in China in recent years. To reduce the incidence, it is essential to identify individuals at high risk and to eradicate risk factors. Although colorectal neoplasia is a multi-stage process, hyperproliferation is the main factor leading to the initiation of carcinogenesis<sup>[1]</sup>. In animal models of colonic cancer, an increased colonic proliferative rate resulted from inherited differences, pharmacological or surgical intervention, which increase the susceptibility of the colonic mucosa to carcinogens<sup>[2]</sup>. On the other hand, interventions that decrease colonic proliferation are associated with decreased susceptibility to carcinogens<sup>[3]</sup>. PCNA (proliferating cell nuclear antigen) is an accessory protein of DNA polymerase and is thought to play an important role in the elongation or replication of the DNA chain. Its accumulation in the nucleus during the G-1 and S stages of the cell cycle has been reported<sup>[4]</sup>, and the labeling index, which is the percentage of PCNA-positive cells, has been reported to be correlated with the proliferative activity and the prognosis of various malignant tumors<sup>[5]</sup>. Thus it is valuable to assess what role PCNA plays during the transformation of the colonic polyps to colonic cancer.

## PCNA AREA RATE AND PCNA LABELING INDEX

Fujishima<sup>[6]</sup> has measured the PCNA labeling index

<sup>1</sup>Department of Gastroenterology, Chinese PLA 222 Hospital, Jilin 132011, Jilin Province, China

<sup>2</sup>P.O. Box 2345, Beijing 100023, China

<sup>3</sup>Department of Pathology, Fourth Military Medical University, Xi'an 710033, Shaanxi Province, China

<sup>4</sup>Department of Gastroenterology, Xijing Hospital, Fourth Military Medical University, Xi'an 710033, Shaanxi Province, China

<sup>5</sup>Rm 12 Bildg 621, Fourth Military Medical University, Xi'an 710033, Shaanxi Province, China

Dr. LUO Yu-Qin, female, born on 1961-05-12 in Jilin City, Jilin Province, graduated from Department of Medicine, Jilin Medical College, specialized in the study of digestive disease, having 15 papers published.

**Correspondence to: Dr. LUO Yu-Qin, Department of Gastroenterology, Chinese PLA 222 Hospital, Jilin 132011, Jilin Province, China**

Tel. +86 • 432 • 2050789

Received 1999-01-07

(PCNA-LI) by visual inspection and the PCNA area rate (PCNA-AR), determined with the newly developed image processor for analytical pathology (IPAP), in tissue samples obtained by biopsy and polypectomy under endoscopic observation. Samples from 20 patients with serrated adenoma, 10 subjects with normal mucosa of the large intestine, 9 patients with hyperplastic polyp, 11 with tubular adenoma low-grade atypia, 15 with tubular adenoma in high-grade atypia, and 15 with well differentiated adenocarcinoma were studied. In serrated adenoma, the crypts were divided into upper, middle, and lower zones with each zone examined microscopically. In the lower zone of crypt of the serrated adenoma, the PCNA-LI and PCNA-AR were found to be approximate to the values of tubular adenoma, indicating the presence of high proliferative activity in the bottoms of crypts. Determination of the pattern of distribution of PCNA-positive cells indicated the presence of a proliferative zone in the lower region or bottom of the serrated adenoma. However, 5 of the 20 serrated adenomas exhibited an irregular or widely extended proliferative zone, and 2 were complicated by cancer. These findings indicated that serrated adenoma is also a highly proliferative tumor and that it may be complicated by cancer if atypia is increased and disturbance of the proliferative zone is present. The PCNA-AR and PCNA-LI increased in the following order: normal mucosa of the large intestine, hyperplastic polyp, tubular adenoma with low grade atypia, and tubular adenoma with high-grade atypia and adenocarcinoma, in proportion to the degree of atypia (Table 1).

**Table 1 Colonic mucosa pathology and PCNA ( $\bar{x}\pm s$ , %)**

Pathological diagnosis	PCNA-area rate	PCNA-labeling index
Normal colonic mucosa	12.8±2.5	32.8±5.8
Hyperplastic polyp	18.2±5.7	27.6±10.3
Tubular adenoma with low-grade atypia	31.0±8.1	40.9±11.8
Tubular adenoma with high-grade atypia	44.6±10.1	59.2±9.8
Adenocarcinoma	69.2±11.8	74.3±13.6
Serrated adenoma (upper zone)	16.4±7.5	25.6±6.1
Serrated adenoma (middle zone)	31.9±9.9	40.4±8.9
Serrated adenoma (lower zone)	49.6±11.6	60.2±10.1

The difference of both PCNA-AR and PCNA-LI between tubular adenoma with low-grade atypia

and hyperplastic polyp was significant ( $P < 0.01$ ), as were the differences between tubular adenoma with high-grade atypia and tubular adenoma with low-grade atypia ( $P < 0.01$ ), and between adenocarcinoma and tubular adenoma with high-grade atypia ( $P < 0.01$ ). Proliferative activity of epithelial tumor cells was evaluated by Bielicki *et al.*<sup>[7]</sup> with immunohistochemistry and anti-PCNA monoclonal antibodies in alcohol fixed, paraffin embedded sections of 44 colonic adenomas, including 33 tubular, 5 villous and 6 tubulovillous adenomas. The mean PCNA-LI was  $24.7\% \pm 10.9\%$ ,  $24.8\% \pm 6.2\%$  and  $24.8\% \pm 14.0\%$  in tubular, villous and tubulovillous adenomas respectively. In 12 tubular adenomas with dysplasia the mean PCNA index in areas with dysplasia was significantly higher ( $38.2\% \pm 11.5\%$ ) as compared to areas without dysplasia ( $17.0\% \pm 8.9\%$ ;  $P < 0.05$ ). The results indicate that PCNA-LI of epithelial tumor cells is significantly increased in adenomas with high grade of dysplasia irrespective of histological type or size of the tumour.

#### DISTRIBUTION PATTERN OF PCNA-POSITIVE CELLS

Carr *et al.*<sup>[8]</sup> compared PCNA immunoreactivity in hyperplastic polyps, adenomas, and inflammatory cloacogenic polyps of the human colon and rectum using paraffin embedded tissue. The monoclonal antibody PC10 was used to demonstrate PCNA immunoreactivity in 88 polypoid lesions from 68 patients. Cases in which immunoreactivity was completely absent were excluded, leaving 32 hyperplastic polyps, 31 adenomas, and seven inflammatory cloacogenic polyps for analysis. Labelling indices for the upper and lower third of each lesion and for adjacent normal mucosa were calculated. It was found that the upper third labelling indices for adenomas were substantially higher than those for hyperplastic polyps or normal mucosa, whereas those for the upper thirds of hyperplastic polyps and normal mucosa did not differ greatly. The differences between the lower third samples were not significant. In 16 (50%) hyperplastic polyps positive cells persisted onto the luminal surface. Some adenomas showed the most intense staining and the highest labelling indices in the upper third, with strong staining of surface cells; this pattern was not seen in the other lesions. The inflammatory cloacogenic polyps did not show a consistent pattern of immunoreactivity. They concluded that differences in cell kinetics between adenomas, hyperplastic polyps, and normal mucosa may be shown in formalin fixed, paraffin embedded tissue using PC10 as a marker of proliferative activity. PCNA expression also persists into the

upper portion of hyperplastic polyps. Assuming that hyperplastic polyps are hypermature lesions with a slower rate of cell migration, this finding suggests that there may be an alteration in PCNA protein metabolism. Fujishima *et al.*<sup>[6]</sup> has compared the upper, middle and lower zones of serrated adenomas, both the PCNA area rate and PCNA labeling index increased from the upper zone to the lower zone. The difference in both the PCNA-AR and PCNA-LI was very significant ( $P < 0.01$ ). Meanwhile, the values in the upper zone of serrated adenomas were higher than those in the normal mucosa of large intestine, and those in the middle zone and lower zone were similar to those in tubular adenomas with low-grade atypia and tubular adenomas with high-grade atypia respectively. In the distribution pattern of PCNA-positive cells, the lower crypt type was predominant in the normal mucosa of the large intestine and in the hyperplastic polyps. Whereas 75% cases of tubular adenoma with low-grade atypia were upper crypt type, 71% of the cases of tubular adenoma with high-grade atypia had labelled cells distributed in all the layers, and 100% of adenocarcinomas had labeled cells distributed in all layers. Of the serrated adenomas, 75% were the lower crypt type, with PCNA-positive cells being distributed in the lower to the bottom regions of the crypt. The remaining 25% were the total crypt type. Thus, labeled cells were predominantly located in the lower regions of serrated adenomas, although some were distributed throughout the crypts. Two cases of total crypt type of serrated adenoma were complicated by cancer.

#### PCNA, A MARKER OF CELL KINETICS

Tranchina *et al.*<sup>[9]</sup> has evaluated proliferating cell index in colonic adenomas, using anti PCNA-PC10 antibody. The results have been compared by grading. A high proliferating grade has been shown in patients with multiple adenomas. This finding suggests a prognostic value of proliferating cell index. In Adam's study<sup>[10]</sup>, colon cancer was induced in 40 Sprague Dawley rats using a 10-week course of 1, 2 dimethylhydrazine (DMH). Twenty animals received cimetidine in their drinking water, commencing from the 5th week after concluding the course of DMH. After five weeks treatment the animals were sacrificed with the colon and rectum excised. Tumors were assessed histologically for depth of invasion, inflammatory cell response and stained for proliferating cell nuclear antigen (PCNA), as a measure of tumor proliferative index. PCNA staining was measured by a computerized image analysis system. There were 25 tumors in the cimetidine treated group and 20 in

controls. In the control group, 10% of the tumors were benign, 35% malignant polyps, 40% invading through submucosa and 15% invading through the bowel wall, as opposed to 40%, 44%, 8% and 8%, respectively in the cimetidine group (Chi-square test,  $P = 0.002$ ). The mean proliferative index was 27.9% for control tumors and 23.1% for the cimetidine treated tumors (t test,  $P = 0.002$ ). It is concluded that cimetidine inhibits colon cancer cellular proliferation and slows down early tumor invasion in this animal model. Winde *et al*<sup>[11]</sup> studied PCNA and KI-67 proliferation indices (PI) by point counting. Prostaglandin PG E2 and PGF2 alpha were quantified by time-resolved competitive fluorescence immunoassay. All patients responded to sulindac therapy within 6 to 24 weeks. Complete adenoma reversion was achieved in 60 and 87 percent of patients after 48 weeks at 53 mg and 67 mg of sulindac per day per patient on average, respectively. Reversion was evident compared with the control group. Dose reduction by one-sixth to one-eighth of the usual oral dose was significant (Mann's trend test,  $P < 0.05$ ). PCNA and KI-67 PIs of adenomatous and flat mucosa were significantly reduced (Wilcoxon's test,  $P < 0.05$ ). Correlation of PCNA and KI-67 PIs indicates similar reaction of different tissue structures (Spearman's rank correlation test,  $P < 0.01$ ). Nonsteroidal anti-inflammatory drug-induced redifferentiation from high-grade to low-grade dysplasia occurred in all but two patients. Tissue-PGE2 levels were greatly reduced. Unwanted, curable side effects were rare (gastritis,  $n = 2$ ), and laboratory controls were within detection limits. These indicated that low-dose rectal sulindac maintenance therapy was highly effective in achieving complete adenoma reversion without relapse in 87 percent of patients after 33 months. Rectal FAP phenotype should be crucial for the surgical decision. Colectomy with ileorectal anastomosis and regular chemoprevention might be a promising alternative to pouch procedures. Chemoprevention of FAP-related tumors with lower incidence via dysplasia reversion may be possible in the future. Shpitz *et al*<sup>[12]</sup> also believed that proliferating cell nuclear antigen is a marker of cell kinetics in aberrant crypt foci, hyperplastic polyps, adenomas, and adenocarcinomas of the human colon. They made serial sections with paraffin-embedded ACF (aberrant crypt foci) stained with a monoclonal antiproliferating cell nuclear antigen (PCNA) antibody and macroscopic lesion. The PCNA-labelling index (PCNA-LI), expressed as a ratio of positively stained nuclei to total nuclei counted, was calculated separately for basal, middle, and upper colonic crypt compartments. A

comparison of the PCNA-LI was made for each compartment in normal mucosa, and hyperplastic lesions. A stepwise increase in the PCNA-LI was observed during neoplastic progression of colonic lesions. The two most important variables of increased cell proliferation, expressed as PCNA-LI per crypt compartment, were the presence of dysplasia and the size of dysplastic lesions. Their conclusions are as follows. In colorectal carcinogenesis, all stages of malignant progression are characterized by hyperproliferation with upward expansion of proliferative compartment. In vitro uptake of bromodeoxyuridine and expression of proliferating cell nuclear antigen (PCNA) were evaluated histochemically by Risio *et al*<sup>[13]</sup> in rectal mucosa of control subjects with colorectal neoplasia in large intestine adenomas and adenocarcinomas. Both labeling indices increased progressively along the path of tumor progression, as did the difference between them (PCNA labeling indices were always greater than those of bromodeoxyuridine). The correlation between them was fairly close in the controls and in adenomas with low-grade dysplasia, whereas no significant linear correlation was noted in adenomas with high-grade dysplasia or in adenocarcinomas. The progressive increase in PCNA would thus seem to be related to both hyperproliferation and neoplastic deregulation of PCNA synthesis. In the mucosa of subjects with colorectal neoplasia, PCNA labeling revealed hyperproliferation but not the surface-wards shift of the proliferative compartment detected by bromodeoxyuridine. PCNA expression, therefore, is not a sufficiently sensitive marker of the risk of tumor transformation in the intestinal mucosa.

#### PCNA AND ONCOGENE EXPRESSION AND DNA PLOIDY

p53 is a nuclear phosphoprotein which controls normal cell growth. Normal p53 protein can not be detected by standard immunohistochemical staining and the over-expression found in neoplastic cells correlates with the presence of point mutations of evolutionary conserved regions of the p53 gene. Pignatelli *et al*<sup>[14]</sup> examined the expression of p53 protein in a series of 36 colorectal adenomas (13 tubular, 17 tubulovillous, 6 villous) showing different degrees of dysplasia (11 mild, 19 moderate, 6 severe), using the polyclonal antibody CM1 which recognises p53 protein in conventionally fixed and processed histological material. They found that 15 out of 36 colorectal adenomas showed p53 immunoreactivity although the staining was very focal in 4 positive cases (26%) (less than 0.1% positive cells). More than 80% of severely

dysplastic adenomas showed strong p53 immunoreactivity, and this over-expression was correlated with increased cell proliferative rate as detected by the proliferating cell nuclear antigen (PCNA) staining, p53 nuclear staining was also seen in 8 out of 11 (65%) colorectal adenocarcinomas as previously shown. Their data suggest that the p53 gene mutation with the subsequent over-expression of the protein, occurs in colorectal adenomas and may therefore be a fundamental genetic event underlying the dysplasia and loss of proliferative control that are characteristic of adenomas with malignant potential. Tomita<sup>[15]</sup> investigated the colonic adenoma-adenocarcinoma progression sequence and analyzed DNA ploidy on hyperplastic polyps to adenocarcinomas. DNA ploidy data were then compared with immunocytochemical staining for proliferating cell nuclear antigen (PCNA). In hyperplastic polyps to villous adenomas, all cases were diploid except one aneuploid villous adenoma. In three adenomas, diploid in situ adenocarcinomas were present. As diploid percentage decreased from hyperplastic polyps to villous adenomas, aneuploid percentage increased. In adenocarcinomas, the Dukes classification corresponded well to DNA ploidy status. All four stage A carcinomas were diploid, whereas three cases each of stage C1 and C2 carcinomas were aneuploid or multiploid. A surprising finding was that S-phase percentage in adenocarcinomas was not parallel with PCNA-positive tumor cell numbers. It is concluded that multistep adenoma-adenocarcinoma progression is partially reflected in DNA ploidy pattern from hyperplastic polyps to villous adenomas. In adenocarcinomas, the Dukes classification parallels well with the DNA ploidy status from stage A diploid to stage D aneuploid, but is not accompanied by increasing PCNA-positive cell numbers.

#### PCNA AND TYROSINE KINASE

Tyrosine kinase and a number of growth factors, especially EGF- $\alpha$  are known to stimulate proliferation of cells in the gastrointestinal tract, including colon. In humans increased colonic mucosal proliferative activity has been observed in numerous premalignant lesions including adenomatous polyps and ulcerative colitis. In the present study Malecka-Panas *et al*<sup>[16]</sup> determined the differences of proliferative patterns in patients with adenomatous polyps, ulcerative colitis and colonic adenocarcinoma as reflected by rectal mucosa tyrosine kinase, EGF receptor tyrosine kinase and PCNA to evaluate the role of tyr-k in colonic mucosal cell proliferation during carcinogenic

process. The study population comprised 40 patients, aged 17-74 years (mean 57). Of them, 10 patients had adenomatous polyps, 10 ulcerative colitis in remission phase, 10 colon adenocarcinoma and 10 healthy controls. After informed consent 6-8 rectal mucosal biopsy specimens were obtained at 10 cm from the anal verge at the beginning of colonoscopy examination and at least 10 cm away from any macroscopic mucosal changes. They found that mean PCNA labeling indices in patients with colon adenocarcinoma, adenomatous polyps, ulcerative colitis and healthy controls were  $27.6\% \pm 5.75\%$ ;  $12.8\% \pm 6.76\%$ ;  $10.9\% \pm 5.34\%$  and  $1.5\% \pm 0.97\%$  respectively. PCNA labeling index in rectal mucosa of patients with adenomatous polyps, ulcerative colitis and colon cancer was significantly higher ( $P < 0.01$ ) than that in the control group. An upward expansion of the proliferative compartment was also observed in patients with premalignant and malignant colon conditions. Total tyrosine kinase activity was elevated by 219%, 224% and 600% in the rectal mucosa of patients with polyps, ulcerative colitis and colorectal carcinoma respectively as compared with the control group. EGF receptor tyrosine kinase was increased in colonic mucosa by 35.2% in patients with adenomatous polyps, by 40.6% in patients with ulcerative colitis and 123% in patients with colon cancer. They concluded that increased values of this enzyme in the above mentioned groups of patients may suggest that tyrosine phosphorylation represents an early sign of colonic mucosa susceptibility for cancer development. Overall, EGF receptor-associated tyrosine kinase plays an important role in the development of hyperproliferative state of the colon mucosa and colon carcinogenesis.

The first step in multistage colonic carcinogenesis are increased cell proliferation and an upward shift of the proliferation zone of colonic crypts. In the present study, progression in cell kinetics was followed up at sequential stages of colonic carcinogenesis, starting with aberrant crypt foci (ACF), the earliest putative preneoplastic lesions, hyperplastic and dysplastic polyps, and invasive carcinomas<sup>[12]</sup>. In humans, increased colonic mucosal proliferative activity and expansion of proliferative compartment have been observed in numerous premalignant lesions including adenomatous polyps, familial polyposis coli and ulcerative colitis<sup>[17]</sup>.

Furthermore, the colonic mucosa of individuals with colon carcinoma has been demonstrated to be diffusely hyperproliferative as compared to that from normal individuals<sup>[18]</sup>. It also suggested that

colonic hyperproliferation, including an increased proliferative rate and expansion of proliferative zone could be used as an intermediate marker of colon cancer risk, therefore PCNA detection helps with early diagnosis of large intestinal cancer and assessment of the prognosis of patients.

## REFERENCES

- 1 Barnard A, Beauchamp RD, Russell W, Dubois R, Coffery R. Epidermal growth factor related peptides and their relevance to gastrointestinal pathophysiology. *Gastroenterology*, 1995; 108:564-580
- 2 Malecka-Panas E, Mea N, Dinda J, Dutta S, Majumdar APN. Azoxymethane enhances ligand induced activation of EGF receptor tyrosine kinase in the colonic mucosa of rats. *Carcinogenesis*, 1996;17:233-237
- 3 Zhang SZ, Luk GD, Hamilton SR. Alpha-difluoromethyl-lornithine-induced inhibition of Growth of autochthonous experimental colonic tumours produced by azoxymethane in male F344 rats. *Cancer Res*, 1988;48:6498-6503
- 4 Morris GF, Mathews MB. Regulation of proliferation cell nuclear antigen during the cell cycle. *J Biol Chem*, 1989;264:13856-13864
- 5 Al-Sheneber IF, Shibata HR, Sampalis J. Prognostic significance of proliferating cell nuclear antigen expression in colorectal cancer. *Cancer*, 1993;71:1954-1959
- 6 Fujishima N. Proliferative activity of mixed hyperplastic adenomatous polyp/serrated adenoma in the large intestine, measured by PCNA (proliferating cell nuclear antigen). *J Gastroenterol*, 1996;31:207-213
- 7 Bielicki D, Markiewski M, Wielondek M, Chosia M, Domagala W. PCNA defined proliferative activity of epithelial tumor cells in adenomas of the colon. *Pol J Pathol*, 1995;46:151-154
- 8 Carr NJ, Monihan JM, Nzeako UC, Murakata LA, Sobin Lit. Expression of proliferating cell nuclear antigen in hyperplastic polyps, adenomas and inflammatory cloacogenic polyps of the large intestine. *J Clin Pathol*, 1995;48:46-52
- 9 Tranchina MG, Puzzo L. Possible prognostic role of PCNA in colonic adenomas. *Pathologica*, 1993;85:679-685
- 10 Adams WJ, Lawson JA, Nicholson SE, Cook TA, Morris DL. The growth of carcinogen-induced colon cancer in rats is inhibited by cimetidine. *Eur J Surg Oncol*, 1993;19:332-335
- 11 Winde Q, Schmid KW, Schlegel W, Fischer R, Osswald H, Bunte It. Complete reversion and prevention of rectal adenomas in colectomized patients with familial adenomatous polyposis by rectal low-dose sulindac treatment. Advantages of a low-dose non-steroidal anti-inflammatory drug regimen in reversing adenomas exceeding 33 months. *Dis Colon Rectum*, 1995;38:813-830
- 12 Shpitz B, Bomstein Y, Mekori Y, Cohen R, Kaufman Z, Gronkin M, Bronheim J. Proliferating cell nuclear antigen as a marker of cell kinetics in aberrant crypt foci, hyperplastic polyps, adenomas, and adenocarcinomas of the human colon. *Am J Surg*, 1997;174:425-430
- 13 Risio M, Candelaresi G, Rossini FP. Bromodeoxyuridine uptake and proliferating cell nuclear antigen expression throughout the colorectal tumor sequence. *Cancer Epidemiol Biomarkers Prev*, 1993;2:363-367
- 14 Pignatelli M, Stamp GW, Kafiri G, Lane D, Bodmer WF. Overexpression of p<sup>53</sup> nuclear oncoprotein in colorectal adenomas. *Int Cancer*, 1992;50:683-688
- 15 Tomita T. DNA ploidy and proliferating cell nuclear antigen in colonic adenomas and adenocarcinomas. *Dig Dis Sci*, 1995;40:996-1004
- 16 Malecka-Panas E, Kordek R, Bierant W, Tureaud J, Liberski PP, Majumdar AP. Differential activation of total and EGF receptor (EGF-R) tyrosine kinase (tyr-k) in the rectal mucosa in patients with adenomatous polyps ulcerative colitis and colon cancer. *Hepatogastroenterology*, 1997;44:435-440
- 17 Lightdale C, Lipkin M, Deschner E. In vivo measurement in familial polyposis: kinetics and location of proliferating cells in colonic adenomas. *Cancer Res*, 1982;42:4280-4283
- 18 Biasco G, Paganelli GM, Miglioli M. Rectal cell proliferation and colon. Cancer risk in ulcerative colitis. *Cancer Res*, 1990;50:1156-1159

Edited by WANG Xian-Lin

# Long-term efficacy of plasma-derived hepatitis B vaccine among Chinese children: a 12-year follow-up study \*

LIAO Su-Su<sup>1</sup>, LI Rong-Cheng<sup>2</sup>, LI Hui<sup>1</sup>, YANG Jin-Ye<sup>2</sup>, ZENG Xian-Jia<sup>1</sup>, GONG Jian<sup>2</sup>, WANG Shu-Sheng<sup>2</sup>, LI Yan-Ping<sup>2</sup> and ZHANG Kong-Lai<sup>1</sup>

**Subject headings** Hepatitis B vaccines; hepatitis B virus; HBsAg; follow-up study

## INTRODUCTION

To evaluate long-term efficacy of a plasma-derived hepatitis B vaccine and provide evidence for decision-making on the vaccine booster doses, we conducted a prevalent follow-up study to examine serologic changes in hepatitis markers and vaccine efficacy in 350 children from the original cohort of 513 children who participated in a randomized, double-blind and placebo-controlled trial on a plasma-derived hepatitis B vaccine in Longan County, Guangxi Autonomous Region, China, in 1982. In this paper, we report the serologic changes in hepatitis markers and vaccine efficacy during 12 years after the initial vaccination in 350 children from the original cohort vaccinated in 1982.

## METHODS

### Immunization procedures

Between October 1981 and April 1982, 789 children, ranging in age from 3 to 36 months (mean age, 21 months), were recruited from seven vaccination clinics in Longan County, Guangxi Autonomous Region, China, an endemic area for HBV infections. Participants at each clinic were randomly allocated into vaccine ( $n = 408$ ) or control ( $n = 381$ ) groups. The two groups were comparable in age, sex and prevalence of hepatitis B virus (HBV) markers. The group allocation was unknown to the parents of the children and the

<sup>1</sup>Institute of Basic Medical Sciences, Peking Union Medical College and Chinese Academy of Medical Sciences

<sup>2</sup>Provincial Anti-epidemic Station of Guangxi Autonomous Region  
Dr. LIAO Su-Su, female, born in 1955 in Beijing, graduated and received medical bachelor from School of Public Health, Beijing Medical University in 1986, and studied as a doctoral candidate in Peking Union Medical College (PUMC) and obtained Ph.D in epidemiology in 1991. As a full-time professor in the Department of Epidemiology, PUMC, she is teaching epidemiology as well as doing research primarily on hepatitis B, HIV/AIDS and STDs-related public health issues. She has published more than 10 papers and translated 4 books (as one of the co-translators) since 1991.

\*This study was supported by grant from China Medical Board, New York, Grant No. 93-582.

**Correspondence to:** LIAO Su-Su, MD, Ph.D, Department of Epidemiology, Peking Union Medical College, 5 Dong Dan San Tiao, Beijing 100005, China

Tel+ 86 • 10 • 65296971 Fax. +86 • 10 • 65133604

E-mail.susuliao@mx.cei.gov.cn

Received 1998-11-10

staff. Children in the vaccine group received three 17.5  $\mu\text{g}$  doses of a plasma-derived hepatitis B vaccine (produced by Beijing Institute of Biological Products, China) by intramuscular injection, according to the conventional 0.16 month schedule. Children in the control group were administered a placebo (vaccine diluent) at the same time. The blood specimens were collected before the administration of vaccine or placebo from each child for testing anti-HBs, antibody to hepatitis B core antigen (anti-HBc) and hepatitis B surface antigen (HBsAg).

Of 789 children, 513 (255 in vaccine group and 258 in control group) had no serologic markers of HBV infection (HBsAg, anti-HBc and anti-HBs) before the first vaccine/placebo dose. In this paper, we refer to the 513 children without HBV serologic markers before vaccination as the original study cohort.

### The 12-year follow-up study

In 1994, we obtained blood specimens from 350 (68%) of the original cohort of 513. Of the 350 participants, 167 were from the vaccinated group and 183 from the control group. Blood samples were tested for anti-HBs, anti-HBc and HBsAg. The loss to follow-up was attributed to temporary migration.

During the 12 years after vaccination, eight prevalent follow-up studies were conducted in the original cohort at 6 months, 1, 2, 3, 5, 8, 10 and 12 years after the first dose of vaccine/placebo. Each of the 350 children studied at the 12-year follow-up was observed for one to eight times, averaging 4.8 times in the vaccinated group and 4.9 in the control group during the 12 years.

### Laboratory tests (Table 1)

**Table 1 Testing methods and diagnosis of HBV infections and immunologic response**

Time of testing	Methods and criteria of diagnosis			Manufacturer
	HBsAg	Anti-HBc	Anti-HBs	
Before and 6-month, 1-year after vaccination	RPHA $\geq 18$	PHA $\geq 18$	RIA,S/N ratios $\geq 2.1$	Beijing Institute of Biological Products
2 to 10 years after vaccination	RIA,S/N ratios $\geq 2.1$	RIA, inhibitory ratios $\geq 75\%$	RIA,S/N ratios $\geq 2.1$	Beijing Institute of Biological Products
12 years after vaccination	RIA,S/N ratios $\geq 2.1$	RIA, inhibitory ratios $\geq 75\%$	RIA,S/N ratios $\geq 2.1$	Abbot, USA

S/N ratio: sample to negative control ratio, RIA: radioimmunoassays, RPHA: reverse passive hemagglutination, PHA: passive hemagglutination

## RESULTS

## Levels of anti-HBs during the 12 years (Figure 1)

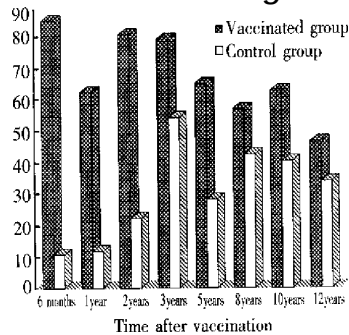


**Figure 1** Percentage of children with anti-HBs levels of 10 S/N ratios or more.

In 1994, 46.1% of vaccinated children had a protective level of anti-HBs, compared with 33.9% of controls ( $P < 0.05$ ).

Among the vaccinated children with detectable anti-HBs (S/N ratios  $\geq 2.1$ ), the titers of anti-HBs declined gradually during the 12-year period. At 6 months after the first dose, the median S/N ratio of anti-HBs in the vaccinated group was 143, and 33 at one year after, but at the 12-year follow-up, the median S/N-ratio of anti-HBs in the vaccinated group was lower than that of controls (15 vs 36,  $P < 0.0001$ ). HBV infections during 12-year follow-up (Table 2).

**Table 2** Hepatitis B infections at each follow-up observation

Time since first dose	% of HBsAg			% of anti-HBc		
	Vaccinated group	Control group	Efficacy (%)	Vaccinated group	Control group	Efficacy (%)
6 months	2.9	7.4	60.8	5.9	10.8	45.4
1 year	3.4	3.9		2.5	13.4 <sup>c</sup>	81.3
2 years	1.2	8.6 <sup>a</sup>	86.0	2.5	24.7 <sup>d</sup>	89.9
3 years	1.0	10.4 <sup>c</sup>	90.4	12.2	29.6 <sup>b</sup>	58.8
5 years	0.0	14.6 <sup>c</sup>	100.0	1.3	24.0 <sup>d</sup>	94.6
8 years	5.9	13.6	56.6	7.8	23.7 <sup>b</sup>	67.1
10 years	1.3	14.6 <sup>c</sup>	91.1	1.3	14.6 <sup>c</sup>	91.2
12 years	1.8	10.9 <sup>c</sup>	83.5	9.6	37.7 <sup>d</sup>	74.5

<sup>a</sup> $P < 0.1$  and  $> 0.05$ ; <sup>b</sup> $P < 0.005$ ; <sup>c</sup> $P < 0.01$ ; <sup>d</sup> $P < 0.0001$ .

Table 2 shows the HBV infections and protective efficacy of the vaccine against HBsAg during the 12 years.

At 12 years, 14 chronic HBsAg carriers were detected in the control group, whereas only one carrier was noted in the vaccinated group (7.6% vs 0.6%,  $P < 0.0001$ ), which corresponded to a protective efficacy of 92%. The only HBsAg carrier

in the vaccinated group had been HBsAg positive since 6 months after the first dose of vaccine. This finding suggests that infection was present before protection could be elicited. In the control group, however, 4 of the 14 chronic carriers were identified as HBsAg positive from six months after the first dose of placebo, and 8 carriers had been infected since or after one year. In the other 2 control children who were chronic carriers, the time of infection could not be established.

## DISCUSSION

We found in this study that protective efficacy against HBsAg at the 12 years after vaccination was 83% and the efficacy against chronic HBsAg carriage was 92%. The immunogenicity of the vaccine, which was a vaccine on field trial, was slightly lower and the level of anti-HBs decreased more rapidly in our study than those used by Wainwright and Coursaget<sup>[1,2]</sup>. However, the medium and long-term protection against HBV infection in our study did not differ greatly from that in these studies. Coursaget *et al*<sup>[12]</sup> studied the efficacy of the hepatitis B vaccine in three groups of children: nonvaccinated, vaccinated with a booster dose at school-age, and vaccinated without a booster dose. At 9 to 12 years after vaccination, they reported a protective efficacy against HBsAg of 88%, with no difference in efficacy between groups with and without a booster dose. Xu *et al*<sup>[3]</sup> reported a protective efficacy against HBsAg of 77% in preschool and school-age children at six years after vaccination. But none of these studies reported the protective efficacy against chronic HBsAg carriage status. Vaccine protection did not parallel the decrease in titres of anti-HBs. This finding indicates the persistence of immunologic memory and supports the recommendation that administration of booster doses should not be based only on the level of anti-HBs but also on the measure of protection against HBV infections<sup>[4]</sup>. Because of the protection of the vaccine against HBV infections shown in this study, we do not recommend administration of booster doses of the hepatitis B vaccine for at least 12 years after the initial vaccination.

## REFERENCES

- 1 Wainwright RB, McMahon BJ, Bulkow LR, Parkinson AJ, Harpster AP. Protection provided by hepatitis B vaccine in a Yupik Eskimo population: seven-year results. *Arch Intern Med*, 1991;151:1634-1636
- 2 Coursaget P, Leboulleux D, Soumare M, Cann PL, Yvonne B, Chiron JP, Coll-Seck AM. Twelve-year follow-up study of hepatitis B immunization of Senegalese infants. *J Hepatol*, 1994;21:250-254
- 3 Xu HW, Sui XF, Men BY. Evaluation of efficacy of plasma derived hepatitis B vaccine at six years after vaccination. *J Xi'an Med Univ*, 1995;16:368-371
- 4 Hadler SC. Are booster doses of hepatitis B vaccine necessary. *Ann Intern Med*, 1988;108:457-458

# HBeAg gene expression with baculovirus vector in silk worm cells

DENG Xiao-Zhao, DIAO Zhen-Yu, HE Liang, QIAO Ren-Liang and ZHANG Lin-Yuan

**Subject headings** hepatitis B virus; HBeAg BmNPV vector; gene expression; DNA, viral

## INTRODUCTION

Miyanohara *et al*<sup>[1]</sup> first obtained products with the expression of HBeAg activity by constructing a yeast expression system; later researches discovered HBeAg expression in xeropus oocytes<sup>[2]</sup>, COS cells<sup>[3]</sup>, *E. coli* cells<sup>[4]</sup>, *Bacillus subtilis*<sup>[5]</sup>, which allow us to know more certainly about HBeAg gene. HBeAg has the same 149 amino acid sequence as the amino-terminal of HBcAg which is encoded by c-gene and consists of 183 amino acids. The c-gene has a 89bp pre-c-sequence in the upstream of it. The co-expressed product of the two genes (pre-c protein) is cleaved off the amino-terminal signal peptide sequence and the c-terminal alkaline region by hydrolases in the membrane of endoplasmic reticulum, forming the secretable HBeAg<sup>[6]</sup>. The most important thing is that the signal peptide encoded by pre-c region directs the formation and secretion of HBeAg, suggesting that only by eukaryotic expression systems can we produce HBeAg with high purity and activity. The domestic HBeAg/anti-HBe diagnostic kit is produced in *E. coli* cells, containing a high proportion of HBeAg which affects the quality of the kit. Recently, the technique with baculovirus vector to express foreign gene efficiently in worm cells and body has been applied and popularized<sup>[7]</sup>. We have replaced the polyhedron protein gene encoding sequence with human INF- $\alpha$  in Bombyx mori nuclear polyhedrosis virus (*Bm NPV*), suggesting that silk worm cells can recognize the signal peptide of human INF- $\alpha$  gene and cut correctly<sup>[8]</sup>. Ninety-nine percent protein becomes mature only after the secreting stage, the *Bm NPV*-

*Bm N* will be a good expression system. For this purpose, we amplified the pre-c signal peptide sequence and the same 149 amino acids sequence homologous with HBcAg at the N-end by PCR, and added appropriate restriction endonuclease sites on both 5' and 3' ends, cloned it into-Bm-NPV transfer vector pBmo30, the Bm-N cells were co-transfected by p-Bm-HBe and wild-type Bm-NPV DNA, and at length the recombinant virus with high expression HBeAg were efficiently obtainable after plaque purification.

## MATERIALS AND METHODS

### Viruses and vectors

Bm NPV transfer vector pBmo30 and silk worm cells were supplied by Virus Research Institute of Wuhan University. The cells were cultured in Tc-100 (containing 100 mL/L-fetal calf serum) and then stored frozen. HBeAg gene was generated by PCR from the template DNA obtained from the HBV Library of the Virus Research Institute of Wuhan University<sup>[9]</sup>.

### DNA extraction and fragment recollection

The transfer vector pBmo30 and recombinant vector pBm HBe DNA were extracted from *E. coli* cells by ordinary method. The silk worm cells were infected by *Bm NPV* DNA, then cultured for 5-7 days at 27 °C, centrifuged at low speed when nuclear polyhedrons emerged. The supernatants containing virus particles were harvested to infect *Bm N* cells again, and the cells were cultured, observed as before, and centrifuged to maintain the cells and supernatants. The *Bm N* DNA was extracted from polyhedrons and viruses according to Summers program. The amplified fragments and enzyme-excised fragments were subjected to 7 g/L-10 g/L agarose gel electrophoresis respectively, and recovered by DE81 membrane method<sup>[10]</sup>.

### PCR amplification

At the 3' and 5' ends of the HBV e gene, we took artificially synthesized 30bp sequence as the primers. *Bgl*-II locus was added to the (+) 5' end of the primer, and *xba*-I-TAA-*Sma*-I locus to (-) 5' end of the primer.

Primer 1(+): 5'AGATCTCATGGAACTTT-TTACCTCTGCCT 3'

Huadong Research Institute for Medical Biotechnics, Nanjing 210002, Jiangsu Province, China

Dr. DENG Xiao-Zhao, female, born on 1956-10-02 in Nanjing, Jiangsu Province, Han nationality, graduated from Nanjing Normal University as a Ph.D. in 1995, Associate Professor of Biology, major in molecular biology, having 15 papers published.

\*Supported by the Natural Science Foundation of Jiangsu Province, No.BK95140306

**Correspondence to:** Dr. DENG Xiao-Zhao, Huadong Research Institute for Medical Biotechnics, 293 Zhongshan East Road, Nanjing 210002, Jiangsu Province, China.

Tel. +86 • 25 • 4540749

Received 1998-10-18 Revised 1998-11-16

Primer 2(-): 5'CCCGGGTTATCTAGAAA-CAACAGTAGTTTCCGGAA3'

PCR reaction was performed from the template PHB24 plasmid containing entire genic HBV and the above primers. PCR product was subjected to 7 g/L-agarose gel electrophoresis.

#### DNA sequence analysis

DNA sequence was analyzed to identify the amplified fragment through ddNTP/PCR/silver-stained sequence analysis system. PCR amplification was performed under the template DNA of purified 537bp fragment, with the same primers, and under the presence of one type ddNTP according to silver-stained sequence analysis protocol. The samples were subjected to the 80 g/L PAG gel electrophoresis, then fixed, stained and colorized and the DNA sequence was read up.

#### Clone ligation and transformation

The plasmid pBm DNA and PCR fragment were digested respectively by *Bgl* II and *Sma* I, ligated, then transfected into competent *E. coli* cells. The resistance colonies were selected from ApILB plates. *Bgl* II and *Sma* I digested the extracted recombinant DNA, the DNA samples were subjected to 100 g/L-agarose gel electrophoresis to identify the positive recombinant.

#### BmN cells co-transfected by transfer vector DNA and wild-type BmNPV DNA

The extracted recombinant transfer vector DNA and wt Bm NPV DNA were mixed by 5:1 molar ratio, and then co-transfected the fresh growing well wall-adhering-Bm-N cells, through the mediation of lipofectin as previously described. Two hours later the medium was removed, and TC-100 (containing 100 mL/L- fetal calf serum) was added and the cells were cultured for 7-10 days at 27°C. Cells containing recombinant viruses were chosen with plaque purification on agars plates. Those plaques of 0<sup>-</sup> (occlusion) phenotype without polyhedrons, which were the positive recombinant viruses, were selected.

#### HBeAg expression and determination

Bm N cells were infected by recombinant viruses, cultured for 4 days at 27°C, centrifuged to get cells and supernatants, a 50 g/L SDS-PAG electrophoresis was performed as general method, stained with Cormassie blue, and the prote in expression was observed.

Cells were lysed with guanidine hydrochloride to rupture cell membrane and centrifuged to get supernatants. Anti-HBe/HBcAg kit from Medicine

Research Institute of Nanjin was used to perform ELISA, separately by using the HBeAg-positive serum of HBV patients and HBcAg generated from engineered bacteria as positive controls, and by using reaptured -Bm-N cell medium containing normal receptor and cultured supernatant as negative controls. P, N values were calculated on the basis of OD value (A), P/N ≥ 2 was considered as positive.

#### Purification of HBeAg expressed in Bm N cells

Cell culture supernatants were collected, precipitated by 27% ammonium sulfate, and then dissolved by PBS (0.02 mol/L-PB, pH 7.0, 0.03 mol/L- NaCl). After separation from pre-balanced sephacryls-200 (1 cm×100 cm) column, electrophoresis and ELISA detection were performed. The peak HBeAg-activity was captured. After gradient elution through DEAE-Sepharose FF ion exchange column, detection of HBeAg activity and SDS-PAG electrophoresis were performed. The general pressured liquid chromatographic system used was from Pharmacia Co.

#### HBeAg expressed in silk worm cells used in conjunction with anti-Hbe antibody in ELISA kit

The purified HBeAg expressed in silk worm cells was used to coat the enzyme labeled reaction plate (100 ng/well), incubated throughout the night at 4°C, then serum to be detected was added to it, and after 30 min at 40°C, the sametype of HBeAg was added to it. At last, TMB H<sub>2</sub>O<sub>2</sub> was used to colorize it. Those P/N ≥ 2.1 were positive.

## RESULTS

#### PCR amplification and sequence analysis of HBeAg gene

A series of PCRs were performed with the synthesized primers and plasmid PHB24 as template DNA; each PCR generated a fragment about 0.5 kb that was homologous with the HBeAg gene, within the 361 bp sequence from 5'end analyzed except one site (the 375, T→A), by using ddNTP/PCR/silver staining. The 88 bp sequence from 273-361 of the amplified fragment was identified as HBeAg gene (Figure 1). The amplified HBeAg gene was 537 bp from the 5'signal peptide sequence. We designed *Bgl*-II site at 5'end and *Xba*-I, *Sma*-I sites at 3'end for cloning.

```
TGG GGG GAA TTG ATG ACT
CTA GCT ACC TGG GTG GGT
AAT AAT TTG GAA GAT CCA
GCA TCT AGG GAT CTT GTA
GTA AAT TAT GTT AAT ACT
```

Figure 1 Partial sequence of HBeAg amplified by PCR.

### Construction and identification of the inserted vectors carrying HBeAg gene

The *Bm* NPV transfer vector *pBm* 030 was 6.3 kb, containing polycloning site. *pBm* 030 DNA and the amplified fragment by PCR was digested by *Bgl*-II/*Sam*-I respectively, ligated by T4 DNA ligase, and allowed the *e* gene to be inserted into the polycloning site under the control of *plh* promoter. The constructive processes was shown in Figure 2. The ligated DNA was transferred into *E. coli* cells, and positive colonies were selected. *Bgl*-II/*Sma*-I were used to digest the recombinant vector, and a fragment of 0.5 kb was obtained on agarose gel electrophoresis, indicating that HBeAg gene cloning was successful. Constructed recombinant viruses carried HBeAg gene.

### *Bm*N cells were co-transfected by the transfer vector *pBm* HBe DNA and *wt-BmNPV* DNA

Polyhedrosis observed in most cells was the signal of successful co-transfection. Other cells turned to have pathologic characteristics of infection, such as enlargement of cells and their nuclei, condensation of intracellular contents, and irregular granules. Polyhedrosis was not the typical characters of infection in recombinant viruses. So, after co-transfection gene recombination has completed between both *plh* gene on the 3', 5' ends of *pBm* HBe DNA and the homologous gene of the *wt Bm* NPV *plh* gene. The *plh* gene was exchanged for the *Pplh*/HBe gene expression box, as controlled by *plh* promoter. The recombinant virus by plaque-purification was named *r-Bm*-HBe (Figure 3).

### Expression and detection of HBeAg in silk worm cells

The silk worm cells were infected by recombinant virus *rBm*HBe, cultured for 72 hours. And the cells and supernatants were harvested for SDS-PAGE electrophoresis (Figure 4). The *wt Bm* NPV could produce polyhedron protein ( $M_r$  32 000), while the recombinant virus *rBm* HBe produced HBeAg about  $M_r$  18 000 instead of polyhedrosis because of the exchange of *plh* gene. The expression of HBeAg was also observed in the cultured medium, but with smaller molecular weight. So most of the expressed HBeAg was secreted out of cells induced by the signal peptide at N-end. ELISA was performed on culture cell lysate and cell culture supernatant to detect the activity of the expressed HBeAg (Table 1). A positive reaction can be found when the culture cell lysate was diluted 1 : 2 000. The antigenic activity of the culture supernatant was much higher, reaching a dilution of 1 : 32 000. Also no HBcAg was

detected in the cell culture supernatant, and HBcAg in culture cell lysate was detectable only at a dilution lower than 1 : 160. The above results definitely proved that HBeAg antigenicity was expressed in silk worm cells.

**Table 1** HBeAg antigenicity detection with ELISA

Sample	Dilution						
	1:1000	1:2000	1:4000	1:8000	1:16000	1:32000	1:64000
Cell culture medium	+	+	+	+	+	+	-
Culture cell lysate	+	+	-	-	-	-	-

### Detection of anti-HBe antibody by double antibody sandwich method

The HBeAg expressed in silk worm cells was used to coat the enzyme-labelled plate, then anti-HBe antibodies in samples were detected. The results were showed in Table 2.

**Table 2** Comparison of two methods in anti-HBe antibody detection

Conventional method	n	Positive (n)	
		Double sandwich method <sup>a</sup>	Indirect <sup>b</sup>
Anti-HBe(+) and anti-HBc(-)	35	35	35
Anti-HBe(-) and anti-HBc(+)	52	4	52
Anti-HBe(+) and anti-HBc(+)	37	37	37
Anti-HBe(-) and anti-HBc(-)	42	2	0

<sup>a</sup>The purified HBeAg expressed in karyotic cells was used to coat enzyme-labeled reaction plate (100 ng/well), incubated throughout the night at 4 °C, and then serum to be detected was added to it. After 30 min at 40 °C, HRP-Labeled HBeAg expressed in karyotic cells was added to it, and at last this was colorized by application of TMB-H<sub>2</sub>O<sub>2</sub>. Those P/N ≥ 2.1 were positive.

<sup>b</sup>The anti-HBe antibody detection kit for sale in market employed the competition inhibition method.

### Purification of HBeAg

Sephacryls-200 chromatography was performed firstly, and showed five protein peaks. ELISA detection indicated that most HBeAg existed in the fourth peak fraction. After concentration, DEAE-Sepharose FF chromatography was performed to get purified HBeAg. The recovery rate was about 52% (Table 3).

**Table 3** Purification of HBeAg Produced by *Bm* N cells

Method	Total activity (by ELISA)	Specific activity (per mg protein)	Purification factor		Total recovery (%)
			A	B	
Cell culture medium	1:1.60×10 <sup>6</sup>	1:2.9×10 <sup>5</sup>	1.0	/	/
(NH <sub>4</sub> ) <sub>2</sub> SO <sub>4</sub>	1:1.32×10 <sup>6</sup>	1:8.5×10 <sup>5</sup>	2.9	2.9	80
Sephacryl S-200	1:1.12×10 <sup>6</sup>	1:5.3×10 <sup>4</sup>	6.3	18.3	70
DEAE Sepharose FF	1:8.40×10 <sup>5</sup>	1:5.0×10 <sup>5</sup>	9.4	172.0	52

A: Individual steps; B: Accumulated results.

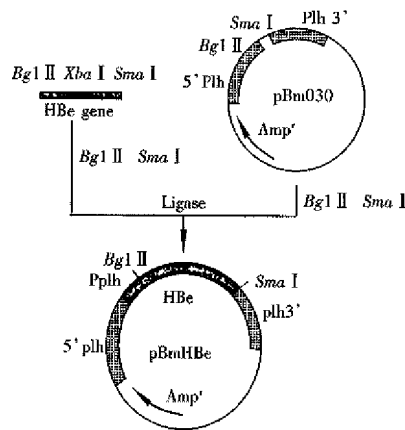


Figure 2 Construction of recombinant vector pBm HBe.

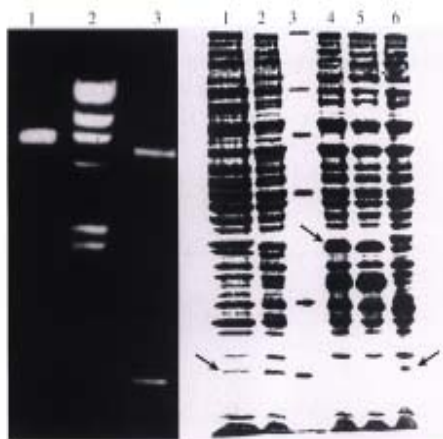


Figure 3 Restriction endonuclease analysis plasmid pBm HBe (Left).

1. p Bm HBe/Bgl II, linearization; 2. λ DNA/Hind III marker; 3. p Bm Hbe/Bg-II + Sma I, released 0.54 kb HBeAg gene.

Figure 4 PAG Electrophoresis analysis of HBeAg prote in expressed in Bm N cells(Right). 1 and 2: Bm N cells infected withr Bm-HBe, the arrow shows HBeAg protein, M,18 000; 3: Standard protein molecular weight marker, M,94 000,17 000,43 000,20 000, 17 500; 4 and 5: Bm- N cells infected with wt Bm NPV, the arrow shows M,32 000 polyhe dea protein; 6: Culture supernatant, the arrow shows HBeAg protein.

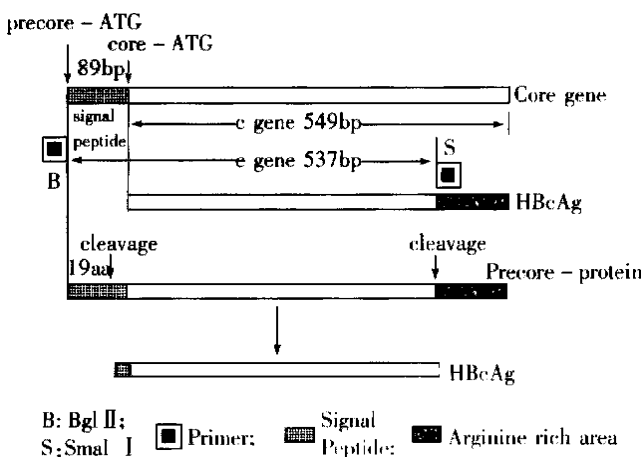


Figure 5 Structure of HBeAg gene and PCR design.

### Characteristics of HBeAg expressed in silk worm cells as compared with those in E. coli cells

The purified HBeAg expressed in silk worm cells and E. coli-cells was adjusted to a protein concentration of 2 g/L-each, then detected by HBeAg detection kit and detection anti-HBe antibody kit sallied in market (Table 4). Those values indicated in Table 4 were dilution magnitude; the P/N ≥ 2.1 was used to determine the end point.

Table 4 Characteristics of HBeAg expressed in E. coli cells as compared with those in karyotic cells with the double-antibody Sandwich

Antigen	Cell	HBeAg kit	Anti-HBc kit
HBeAg 1	karyotic	10-7	10-1
HBeAg 2	E. coli	10-5	10-3

### DISCUSSION

We constructed a transfer vector pBm HBe with HBeAg gene fragment from PCR. This vector was used together with wt Bm NPV to co-transfect the silk worm cells, and the recombinant viruses carrying HBeAg gene was obtained. The amplified HBeAg gene was 537 bp long, including an 89 bp sequence of signal peptide from 5'-end to 3'-end of e gene. The relation between c gene and it was shown in Figure 5. While HBeAg was expressed in silk worm cells, the signal peptide was clipped off in granular endoplasmic reticulum, and 19 amino acids were lost with the HBeAg secreting into cell cultured medium. And some antigens in non-secretary form also existed in cells. On the basis of gene sequence analysis, an ATG was found to locate at both 5'-and 3'-ends of the signal peptide, and the second ATG obeyed the Kozak rule completely. When 40s subgroup of ribosome was scanned to the first AUG codon, some of the 40s submits and 60s submits would fit into ribosomes, begin to transcribe and produce protein carrying signalpeptide, which was processed and secreted out of the cells as soluble HBeAg. The HBeAg reaction rate was 100-fold higher, and the anti-HBc cross reaction rate was 100-fold lower, compared with the reaction using expression by prokaryotic cell in the same concentration of protein, because prokaryotic cell system did not differentiate and cut message peptide sequence. The products expressed were cellular c antigen (Table 4).

The other 40s subgroup continued to scan until the second AUG, combined with the 60s subgroup and began to transcribe, and produce protein without signal peptid e, which remained inside of

the cells. Such a result was consistent with the the orctic basis of the initial regulation of mRNA transcription<sup>[2]</sup>. The exp ressed product inside cells should be HBcAg according to the c gene sequence ana lysis, but ELISA results proved it was HBeAg (1:2 000) mostly, with little HBcAg (<1:160). So the phenomenon suggested that the arginine abundant region at the carboxyl end should be very important for HBcAg expression; it took part in the self-fitting into core particle of HBcAg protein. The amplified e gene fragment did not contain the arginine abundant region, so its expressed product contained little HBcAg.

## REFERENCES

- 1 Miyano-hara A. Expression of hepatitis B virus cores antigen in *Saccharomyces cerevisiae*: synthesis of two polypeptides translated from different initiation codes. *J Virol*, 1986;59:176-180
- 2 Standing DJ. A signal peptide encoded within the precore region of hepatitis B virus directs the secretion of a heterogeneous population of e antigens in *Xenopus* oocytes. *Proc Natl Acad Sci USA*, 1988;85:8405-8409
- 3 Ou JH, Yen CT, TS Benedict Yen. Transport of hepatitis B virus precore protein into the nucleus after cleavage of its signal peptide. *J Virol*, 1989;63:5238-5243
- 4 Deng XZ, Zhang LY, He L, Zhang Z. High expression of Hepatitis B e gene in *E. Coli*. *J China Pharmaceutical Univ*, 1992;23:290-293
- 5 Qi YP, Ma XW, Hung YX, Tan YP. Cloning and expression of hepatitis B virus e gene in bacillus cells. *J Wuhan Univ*, 1993;39:99-106
- 6 Gerlich WH, Heermann KH. Function of hepatitis B virus protein and virus assembly. In: Girlish WH6 *et al* Eds. *Viral hepatitis and liver disease*, New York: 1991:121-134
- 7 Lu M, Iatrou K. Characterization of a domain of the genome of Bm-NPV containing a functional gene for a small capsid protein and harboring deletions eliminating three open reading frames that are present in Ac-NPV. *Gene*, 1997;185:69-75
- 8 Deng XZ, Zhang LY, Yu MG, Li GF, Diao ZY, Zhong J. The replication of recombinant bombyx mori nuclear polyhedrosis virus (r-Bm-NPV) and expression of Hu IFN- $\alpha$  gene. *J Wuhan Univ*, 1995;41:324-328
- 9 Qi YP, Hung YX, Wei ZY. Construction of gene band for Hepatitis B virus ayw subtype. *J Wuhan Univ*, 1989;(2):112-116
- 10 Simbraok J, Fritsch EF, Maniatis T. Molecular cloning, A laboratory manual, 2nd ed. *Cold Spring Harbor Laboratory Press*, 1989:776-786

Edited by LU Han-Ming

# Establishment of a pig model of combined pancreas-kidney transplantation

XU Ze-Kuan, LIU Xun-Liang, ZHANG Wei, MIAO Yi and DU Jing-Hui

**Subject headings** pancreas transplantation; kidney transplantation; pig; animal model

## INTRODUCTION

We studied the recipient and graft pathophysiologic changes after transplantation, the inducement of immunotolerance, the regularity of chronic rejection and its prophylactico-therapeutic measures by establishing a model of pancreas-kidney transplantation in large animals.

## MATERIALS AND METHODS

### *Animals*

Twenty-six local healthy hybrid pigs, male or female, weighing  $18.4 \text{ kg} \pm 2.8 \text{ kg}$  used as donors and recipients, were provided by Experimental Animals Centre of Jiangsu Province and fasted for 24 hours.

### *Operative procedure*

Ketamine (15 mg/kg) was intramuscularly injected 15 minutes before anesthesia. A trocar was placed in the auricular vein for fluid infusion. The anesthesia was maintained with 30 g/L pentobarbital sodium. Ventilation was provided by tracheal intubation. ① donor operation: the whole stomach was excised. After dissection of the hepatoduodenal ligament, the portal vein was isolated. The proper hepatic artery and common bile duct were then ligated and divided. The jejunum was transected 5 cm distal to the ligament of Treitz. The superior mesenteric artery and vein were identified. The uncinate lobe, body and tail of the pancreas were mobilized. At this point, the pancreas was only attached to its arterial blood supply (consisting of the celiac axis and superior mesenteric artery and the portal vein). The aortic cannula was placed, through which 200 mL blood was drawn and kept for use. In situ flushing with 4°C hyperosmotic citrate adenine (HCA) containing 12 mL/L of 20 g/L ligustrazin hydrochloride was performed. The perfusate pressure was about 80 cm high of water column. The aorta was clamped, and the portal vein and inferior

vena cava were divided. Perfusion was stopped when the effluent from the portal vein was clear, and pancreas, duodenum, two kidneys became blanched. About-300 mL of cold perfusate solution was used. The entire pancreas and attached duodenum, spleen, two kidneys and ureters were removed in continuity with abdominal aorta, inferior vena cava and portal vein. They were placed in 0°C-4°C HCA soon after they had been removed. Then the preparation of the graft was made. The abdominal aorta was ligated and divided 1 cm distal to the left renal artery. The right kidney was removed. The distal of the portal vein and the left renal vein were immobilized. The issue whether the left renal vein should be transected or hold an inferior vena cava button was decided in accordance with the diameter of the distal end of the portal vein. The two veins were anastomosed in an end to end fashion. Reperfusion was done through the aortic cannula with cold perfusate solution to check the anastomotic stoma. The duodenum was rinsed with metronidazole and then its ends were closed. ② Recipient operation: After anesthesia worked, a cannula was placed in the external jugular vein and was immobilized behind the ear through the tunnel under the skin. The recipient pig received 1.0 g cephadrine, 100 mL of 5 g/L metronidazole and fluid infusion. A cannula was placed in the left femoral artery to detect the average arterial pressure. After entering into the abdomen, the entire pancreas was removed. The abdominal aorta between the common iliac artery and renal artery was freed, and the lumbar arteries were ligated and divided. The inferior vena cava was also freed by ligating and dividing all the branches. The proximal aorta was clamped, 30 mL of normal saline containing 1 mg/kg of heparin was injected from the distal aorta. Then, the distal end of the abdominal aorta was clamped. An oval opening was made on the anterior wall of the recipient abdominal aorta, its caliber was similar to the diameter of the proximal end of the donor abdominal aorta. The lacuna was rinsed with normal saline containing heparin. The donor aorta anastomosis was performed in an end to side fashion to the recipient aorta, and the portal vein was anastomosed to the inferior vena cava (Figure 1). The graft was covered with ice bag during the procedure of vascular anastomosis. Soon after circulation to the graft was restored, the graft

Department of Surgery, The First Affiliated Hospital of Nanjing Medical University, Nanjing 210029, Jiangsu Province, China

**Correspondence to:** XU Ze-Kuan, Department of Surgery, The First Affiliated Hospital of Nanjing Medical University, Nanjing 210029, Jiangsu Province, China

**Received** 1999-01-04

became pink with its arteriopalms and peristalsis recovered. Urine overflowing from the ureter graft was perceived. The duodenum allograft was then anastomosed to the host's bladder in a side to side fashion. The ureterostomosis of the graft was performed. The graft was fixed to the posterior side of the abdominal wall. The donor's spleen was removed. Just before closing the incision, a drainage-tube was placed in the left iliac fossa. The amount and kinds of fluid infusion depended on the monitoring results during the operation. However, 200 mL of blood was regularly transfused intravenously.

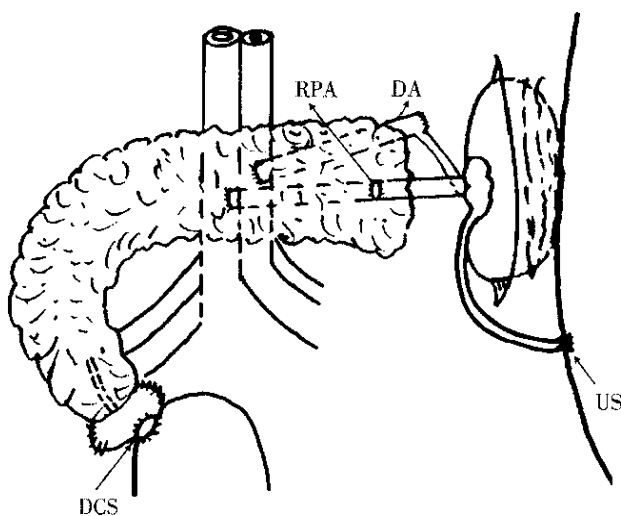


**Figure 1** The postoperative sketch map. DA: donor aorta; RPA: reno-portal anastomosis; DCS: duodeno-cystostomy; US: ureterostomosis.

### Postoperative management

The graft function was intensively monitored by urine amylase, plasma glucose, urine volume of kidney allograft. All recipients received 1 500 mL-2 000 mL fluid infusion intravenously per day in the first few postoperative days containing 500 mL of low molecular dextran, 1.0 g of cephadrine and 100 mL of 5 g/L metronidazole. The drainage-tube was extracted on the third postoperative day. The recipients were allowed to eat on the fourth or fifth postoperative day. The fluid infusion was then decreased or stopped. No immunosuppression was administered to the pigs.

## RESULTS

### Operative time

There was no warm ischemia, the cold ischemia of the transplant was  $151.4 \text{ min} \pm 15.7 \text{ min}$ . The vascular anastomosis was  $55.6 \text{ min} \pm 4.9 \text{ min}$ .

### Survival of the recipients and monitoring of the graft functions

The survivors usually began to defecate 3 d-4 d after surgery, and then were allowed to eat. Listlessness, hypodynamia and anorexia were found 7 d-9 d after surgery with rapid weight loss. The survivors died 1 d-2 d after a lump could be palpated in the abdomen, due to disturbance of internal environment and anastomosis bleeding. The other 11 pigs survived a mean period of  $9.1 \text{ d} \pm 2.4 \text{ d}$ . Among them, number 9 603 and 9 610 were killed on the seventh day and ninth day respectively because of obvious decrease in urine amylase and in urine volume of the kidney graft and increase in fasting blood glucose. The graft turned dark, and necrotic areas were noted. The histopathology showed acute rejection. The destruction of the graft induced by acute rejection was evaluated by urine amylase, blood glucose and urine volume of the kidney graft. The urine amylase concentrations usually began to decline 5 d-6 d and became obvious 2 d-3 d before the pig died. The urine volume of the kidney allograft decreased rapidly 4 d-5 d before the death of the pig. The fasting blood glucose elevated significantly 1 d-2 d before the pig died.

## DISCUSSION

### The technical improvement of this model

The transplantation technique was improved on the basis of the old one as follows<sup>[1,2]</sup>: ① the donor aortic segment and the recipient abdominal aorta were anastomosed in an end-to-end fashion; ② a renoportal end-to-end anastomosis was performed between the left renal vein and the distal end of portal vein before the end-to-side anastomosis of the proximal end of portal vein to the recipient inferior vena cava; ③ the donor duodenum was anastomosed to the host bladder in a side-to-side fashion; and ④ the ureterostomosis of the graft was performed. The present technique has the following advantages: ① Iliac blood vessels are too slender to be operated, whereas it is simple to anastomose the donor abdominal aorta to the host abdominal aorta in an end-to-side fashion and the donor portal vein to the host inferior vena cava in an end-to-side fashion. This technique enjoys a high success rate. ② The kidney allograft function can be monitored in ureterostomosis. ③ Only two vascular end-to-side anastomoses were performed, which shortened the interruption time of blood flow. It is important to modify the disturbance of the recipient's physiological process and maintain the graft function. ④ The pancreas allograft function is easy to monitor by urine amylase when the pancreas

exocrine secretion drainage is established with duodenocystostomy.

### Summary

① The spleen instead of pancreas allograft was harvested, prepared and implanted in order not to damage the pancreas allograft and the circulation of the pancreas allograft was monitored. ② Since pig's systema lymphaticum is very abundant, when the recipient abdominal aorta and the inferior vena cava are isolated, the lymph-vessels should be ligated carefully in order to avoid lymph extravasation after operation. ③ The recipient's internal environment should be kept stable. Number 9601 pig's tracheal intubation could not be pulled out, and the pig died 8 hours after operation. The amount and variety of fluid infusion depended on the monitoring results of

average arterial pressure, blood gas, electrolytes, blood glucose and urine volume. Two hundred mL donor blood was regularly transfused to the recipient. The interruption time of blood flow was shortened. The left renal vein and the distal end of portal vein were anastomosed first. Then, only one donor vein should be anastomosed to recipient vein. After the above-mentioned measures were adopted, satisfactory transplantation results were achieved.

### REFERENCES

- 1 Ganger KH, Mettler D, Boss HP, Ruchti C, Stoffel M, Schilt W. Experimental duodeno-pancreatic-renal composite transplantation: a new alternative to avoid vascular thrombosis. *Transplantation Proceedings*, 1987;19:3960-3964
- 2 Gruessner RW, Nakhleh R, Tzardis P, Schechner R, Platt JL, Gruessner A, Tomadze G, Najaran JS, Sutherland DER. Differences in rejection grading after simultaneous pancreas and kidney transplantation in pigs. *Transplantation*, 1994;57:1021-1028

Edited by WANG Xian-Lin

# Detection of human liver-specific F antigen in serum and its preliminary application \*

FENG Tao<sup>1</sup>, ZENG Zhao-Chun<sup>1</sup>, ZHOU Lan<sup>2</sup>, CHEN Wen-Yuan<sup>1</sup> and ZUO Yu-Ping<sup>1</sup>

**Subject headings** liver-specific F antigen/blood; liver neoplasms/diagnosis; carcinoma, hepatocellular/diagnosis; liver diseases/diagnosis

## INTRODUCTION

Aspartate aminotransferase (AST) and alanine aminotransferase (ALT) activity are usually used as biochemical criteria for the evaluation of liver lesion. These enzymes will release into the blood when the integrity of hepatocyte is compromised. Although the aminotransferase has been used as a criterion of liver function for decades, it can not show the accurate hepatohistological characteristics when it is abnormal in patients with chronic liver disease<sup>[1]</sup>.

Human liver-specific F antigen (F-Ag), a  $M_r$  44 000 cytosolic protein of unknown function, is found predominantly in the liver. Previous studies using relatively insensitive assays have shown that the concentration of F-Ag in the serum rises when the liver is severely damaged<sup>[2]</sup>. The sensitive radioimmunoassay has enabled measurements in serum from healthy humans and patients with mild hepatic damage. The results suggest that F-Ag may be a sensitive and specific marker of hepatocellular damage<sup>[1]</sup>. To avoid the effects of radioactive isotope, Biotin-Avidin ELISA (BAELISA) was established to detect F-Ag, and its clinical value as guidelines of liver function was discussed and compared with that of AST and  $\alpha$ -AFP.

## MATERIALS AND METHODS

### Materials

**Subjects and serum samples** The vein blood samples of 25 healthy subjects, 54 patients with various liver diseases and 10 patients with non-liver diseases were

provided by Department of Gastroenterology of the First and Second Colleges of Clinical Medicine affiliated to Chongqing Medical University, and were centrifuged at 2 000r/min and stored at  $-20^{\circ}\text{C}$ .

**Reagents** Standard F-Ag antibody (guinea pig against human F-Ag antiserum) purchased from DAKO (Denmark) and purified human F-Ag was used as the standard. F-Ag antibody (guinea pig against human F-Ag antiserum) was prepared by our department (1:32). D-biotin-N-hydroxysuccinimide esters (BNHS) and avidin-HRP (A-HRP) were provided by Shanghai Biochemistry Institute and Chemistry Department of Shanghai Medical University respectively.

### Methods

**Preparation of biotin-IgG (B-IgG)** One g/L BNHS (resolved in N, N-dimethyl formamide) and purified anti-F-Ag IgG (v/v = 5:1) were mixed up quickly and placed for 4 h at room temperature. The mixture was dialysed to remove free biotin mixed with distilled glycerol (v/v = 1:01) and then stored at  $-20^{\circ}\text{C}$ .

**BA-ELISA** Coating 96-well plate was coated with anti-F-Ag IgG (5 mg/L, 200  $\mu\text{L}$ /well) diluted with 60 mmol/L  $\text{NaHCO}_3$  (pH 9.6) and placed overnight at  $4^{\circ}\text{C}$  or for 2 h at  $37^{\circ}\text{C}$ , blocked with buffer A (10 mmol/L PB, 150 mmol/L NaCl, 1.5% BSA, pH 7.6) for 30 min (200  $\mu\text{L}$ /well). Standard F-Ag solution and serum samples were put into 96-well plate (100  $\mu\text{L}$ /well) for 60 min. B-IgG and A-HRP diluted (1:200) with buffer B (10 mmol/L PB, 150 mmol/L NaCl, 1% BSA, 0.05% Tween-20) were put into the plate again (100  $\mu\text{L}$ /well). The substrate of HRP was 0-phenylenediamine (OPD) and  $\text{H}_2\text{O}_2$  (100  $\mu\text{L}$ /well). The reaction was stopped by 2 mol/L  $\text{H}_2\text{SO}_4$  (50  $\mu\text{L}$ /well). The OD value of each well in the plate was detected under 492 nm wavelength. Concentration of F-Ag in serum was measured in triplicate.

**Detection of  $\alpha$ -AFP and AST ELISA** (normal value  $<20 \mu\text{g/L}$ ) and routine assay of AST (normal value 5U/L - 35U/L) were used.

**Statistical method** *t* test and correlative analysis

<sup>1</sup>Department of Biochemistry, Chongqing University of Medical Sciences, Chongqing, 400016, China

<sup>2</sup>Department of Molecular Biology, Chongqing University of Medical Sciences, Chongqing 400016, China

FENG Tao, male, born on 1963-07-26 in Maerkang City, Sichuan Province, Han nationality, graduated from Beijing Normal University in 1984 and earned master's degree in Chongqing Medical University in 1991, lecturer of Biochemistry, majoring purification and production of antiserum of protein, having 5 papers published.

\*Supported by the Educational Committee of Sichuan Province.  
**Correspondence to:** FENG Tao, Department of Biochemistry, Chongqing Medical University, Chongqing 400016, China

Tel. +86 • 23 • 68808038, Fax. +86 • 23 • 68817090

Received 1998-12-21

were made by computer.

## RESULTS

### BA-ELISA

The minimum detection limit of BA-ELISA was 0.01U/mL (1U = 1.0 µg F-Ag). The linear range of the standard curve was 0.01U/mL-50U/mL. The intra-and inter-assay coefficient of variation (CV) was 6.2% and 7.7% respectively. Recovery rate was 95.9%-105.2% when the known amount of F-Ag was put into the serum of normal subjects. All serum samples were detected with BA-ELISA, and the results were shown in the following Table 1. The serum F-Ag concentration of 25 healthy subjects was 0.08 U/mL ± 0.03 U/mL. The values under 0.08 U/mL ± 0.03 U/mL were regarded as negative. Compared with control group (healthy subjects), increase was found in the serum F-Ag of all liver diseases with no change in non-liver diseases ( $P>0.05$ ). AST activity was 124.5 U/L ± 62.5 U/L in non-carcinomatous liver diseases (31 cases). No obvious correlation was found between their AST activity and serum F-Ag concentration ( $n = 31, r = 0.13, P>0.05$ ). AST activity was 91.5 U/L ± 47.8 U/L in acute hepatitis (8 cases). A close correlation was found between their AST activity and serum F-Ag concentration ( $n = 8, r = 0.89, P<0.05$ ). The concentration of α-AFP in hepatocellular carcinoma (23 cases) was 113.7 µg/L ± 50.2 µg/L. An obvious correlation was found between their α-AFP and serum F-Ag ( $n = 23, r = 0.84, P<0.05$ ).

**Table 1 The serum F-Ag concentration of liver diseases and non liver diseases**

Groups	Total cases	Positive cases	Positive rate (%)	F-Ag ( $\bar{x} \pm s, U/mL$ )
Control	25	0	0.00	0.08±0.03
Acute hepatitis	8	7	87.5	9.43±4.02
Chronic hepatitis	10	8	80.0	6.72±3.17
Hepatocellular cancer	23	21	91.3	15.15±5.48
Liver cirrhosis	8	6	75.0	8.31±3.59
Alcoholic liver diseases	5	4	80.0	5.28±2.64
Non-liver diseases	10	1	10.0	0.11±0.04

<sup>a</sup> $P<0.05$ ; <sup>b</sup> $P<0.01$ .

## DISCUSSION

Making use of high affinity between biotin and

avidin ( $K_d = 10^{-15}$  mol/L), we coupled biotin with anti-F-Ag IgG and developed BA-ELISA for detecting F-Ag of human serum which is highly sensitive, stable (recovery rate 95.9%-105.2%), easy and safe with a wide range (0.01 U/mL-50 U/mL). It is advisable for clinical use.

Positive serum F-Ag was found in 46 out of 54 cases of liver disease (its average level was 13.5 U/mL and its positive rate was 85.2%), while positive serum F-Ag was found in only 1 out of 10 cases of non-liver diseases. It indicates that F-Ag is rather specific and has a high detectable rate for liver disease. Compared with present criteria for the evaluation of liver function, serum F-Ag level is correlated with AST activity in acute hepatitis patients, and is not correlated with AST activity in patients with chronic hepatitis, liver cirrhosis and cancer. It is suggested that F-Ag is of great practical value to the diagnosis, treatment and prognosis of liver diseases, and is a more sensitive and specific marker of liver damage and pathological features as compared with the routine criteria of liver function.

The detectable rate of serum F-Ag was 91.3% in 23 cases of liver cancer. The level of serum F-Ag was higher (the mean level was 14.3 U/mL) than that of other liver diseases. Serum F-Ag was negative in 4 cases of non-liver tumors out of 10 cases of non-liver disease, which was consistent with that of stomach cancer reported by Grewal<sup>[3]</sup>. It is suggested that serum F-Ag is a specific marker of liver tumor and has a high detectable rate. The level of F-Ag and α-AFP has a positive correlation. Therefore, detection of serum F-Ag is helpful for the correct diagnosis of liver diseases.

Further research is to be made in the function of F-Ag in order to find out the direct evidences and theoretical bases of F-Ag as a marker of liver damage.

## REFERENCES

- 1 Foster GR, Goldin RD, Oliveira DBG. Serum F protein: a new sensitive and specific test of hepatocellular damage. *Clinica Chimica Acta*, 1989;184:85-92
- 2 Mori Y, Mori Y, Iesato K, Ueda S, Wakashin Y, Wakashin M, Okuda K. Purification and immunological characterization of human liver-specific F antigen. *Clinica Chimica Acta*, 1981;112:125-134
- 3 Grewal GK, Oliveira DBG. Why serum F protein is a sensitive and specific marker of liver damage in man. *Clinica Chimica Acta*, 1990; 191:93-96

Edited by WANG Xian-Lin

# Vagus effect on pylorus-preserving gastrectomy

LU Yun-Fu, ZHAO Ge, GUO Cui-Ying, JIA Shou-Ren and HOU Yi-Ding

**Subject headings** vagus; pylorus; gastrectomy; gastric emptying

## INTRODUCTION

Maki and others reported in 1967 the study of a pylorus-preserving gastrectomy (PPG)<sup>[1]</sup>. It successfully prevented dumping syndrome and duodenogastric reflux, but failed in gaining proper speed of gastric emptying, thus leading to new complications such as gastric retention, etc. To inquire into this subject, we have made the following experimental studies.

## MATERIALS AND METHODS

Twelve mongrel dogs of either sex weighing 15 kg to 25 kg were divided randomly into two groups 6 in each. Group A: preserving the pyloric vagus (Figure 1). Figure 1, I Make an incision on the antral wall, strip off antral mucosa and suture seromuscular layer with its attaching vagus branches to form a small pouch in which a water bag pressure sensor had been installed. In addition, a bipolar electrode was put into the antral smooth muscle layer. Through separate transducers the pressure sensor and electrode were connected to a bichanneled physiologic kymograph for recording the intra-antral pressure curve and the electromyographic curve. Figure 1 II are the curves after pylorus and pyloric vagus preserving gastrectomy (PPVPG)<sup>[2]</sup>. Figure 1 III shows the curves of the control group. Group B: not preserving the pyloric vagus (Figure 2). According to Maki's surgical mode, transect the antrum from the gastric body 2 cm above the pylorus and cut all the vagus branches innervating the antrum and pylorus. The rest of the procedures followed those described in Group A.

## RESULTS

Group A. It can be seen from the figure that an action potential is immediately followed by a rhythmic stomach contraction. Figure 1 shows the curves after PPVPG, resembling those of the

control group (Figure 1), demonstrating that rhythmic sphincter action is preserved by retaining the pyloric vagus. Group B. It can be seen in Figure 2, action potential of smooth muscle decreasing significantly, 8-12 times lower than that of the normal; asynchronous action between potential and contraction; and frequent spastic contraction of pylorus. The spastic contraction was apparently caused by the action of intramural nerve plexus or automatic rhythm of the smooth muscle, not by the action potential of the vagus.



**Figure 1** Electromyogram and intraluminal pressure. A. Intraluminal pressure; B. Electromyogram; I. Sutured antrum seromuscular flap; II. Postoperation of PPVPG; III. Control group.

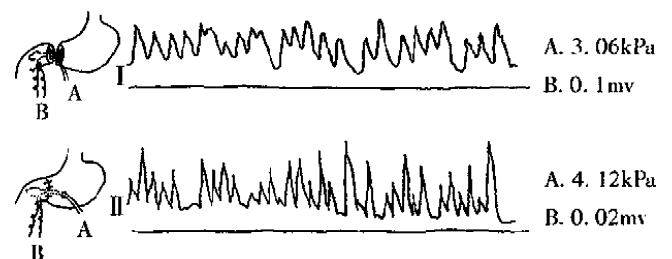


**Figure 2** Electromyogram and intraluminal pressure of gastrectomy without preserving pyloric vagus. A. Intraluminal pressure; B. Electromyogram; I. Transecting antrum and pyloric vagus; II. Transecting antrum and pyloric vagus, with the antrum anastomosed.

Table 1 shows the effect of pyloric vagus on electromyogram and intraluminal pressure with the vagus preserved or resected.

Department of Surgery, the Second Clinical College, Shanxi Medical University, Taiyuan 030001, Shanxi Province, China

**Correspondence to:** LU Yun-Fu, Department of Surgery, the Second Clinical College, Shanxi Medical University, Taiyuan 030001, Shanxi Province, China

**Received** 1998-08-20

**Table 1 Effect of pyloric vagus on electromyography and intraluminal pressure ( $\bar{x}\pm s$ )**

Parameters	Vagus preserved (n = 6)	Vagus resected (n = 6)
Action potential (mV)	0.855±0.26 <sup>b</sup>	0.057±0.043
Intraluminal pressure (kPa)	3.273±0.426	3.645±0.608

<sup>b</sup>P<0.01, vs vagus resected.

## DISCUSSION

In an attempt to prevent dumping syndrome and alkaline reflux gastritis as much as possible, Flynn<sup>[3]</sup>, Killen *et al*<sup>[4]</sup> once performed resection of 50%-70% canine stomach, retaining 2 cm of the distal antrum, removing the remained antrum mucosa and anastomosing mucosa of the corpus and duodenal, then suturing the seromuscular coat. However, the operation has not been applied clinically because of its high mortality and the difficulty in stripping the mucosa. Later, Maki continued the study and formally advanced a PPG<sup>[1]</sup>, which resected most of the antrum and the corpus 2 cm from the pyloric ring and retained the remaining antrum mucosa. PPG successfully prevented dumping syndrome and duodenogastric reflux in 50 cases of gastric ulcer since its clinical application in October 1964, but failed in keeping normal gastric emptying. According to some reports, gastric retention reached 40%, lasting as long as 6 months<sup>[5]</sup>. The chief reason of gastric retention, judged by our experimental study, could be attributed to incision of vagus innervating pylorus, which consists of excitatory and inhibitory postganglionic fibers. The former speeds the spread of the basic electric rhythm (slow wave), facilitates the formation of an action potential which causes rhythmic contraction of stomach, and the latter, relaxes the stomach. By the coordination of the

two, the stomach contracts and relaxes rhythmically. With the vagus resected, the action potential of gastric smooth muscle decreases notably, autonomous contraction of gastric smooth muscle induced by the homogenetic rhythm of smooth muscle and the intramural nerve plexus occurs. The uncontrolled spastic contraction will lead to the delay of gastric emptying as well as gastric retention. In our view, the physiological function of pyloric sphincter can not be really preserved without preserving vagus innervating pylorus. To preserve the vagus, we designed a PPVPG through a large number of experimental studies on animals<sup>[4]</sup>. This operation mainly consists of stripping off antrum mucosa, excising the bulk of the corpus, preserving pylorus, vagus trunks, Latarjer vagus and the last two to three branches of avian claw vagus innervating the pyloric region; it has been applied clinically since January, 1988. As many as 132 cases of peptic ulcer were so treated with good results. The fact that there was not a single case of gastric retention and ulcer relapse in the follow-up survey. All these demonstrate that PPVPG was scientific enough to meet all clinical requirements. At the same time, it has proved that preserving vagus is rather important in preventing gastric retention after PPG.

## REFERENCES

- 1 Maki T, Shiratori T, Hatafuku T, Sugawara K. Pylorus-preserving gastrectomy as an improved operation for gastric ulcer. *Surgery*, 1967;61:838-845
- 2 Lu YF, Hou YD, Jia SR, Guo CY. Experimental study of pylorus and pyloric vagus preserving gastrectomy. *World J Surg*, 1993;17:525-529
- 3 Flynn PJ, Longmire WP. Subtotal gastrectomy with pyloric sphincter preservation. *S Forum*, 1960;10:185-191
- 4 Killen DA, Symbas PN, Tennessee N. Effect of preservation of the pyloric sphincter during antrectomy on postoperative gastric emptying. *Am J Surg*, 1962;104:836-843
- 5 Nanna AN. Clinical experience of 18 cases of gastrectomy preserving pylorus. *Shiyong Waiké Zazhi*, 1986;6:245-246

Edited by LU Han-Ming

# Activation of killer cells with soluble gastric cancer antigen combined with anti-CD<sub>3</sub> McAb \*

CHEN Qiang, YE Yun-Bin and CHEN Zeng

**Subject headings** stomach neoplasms; antigens, neoplasm; killer cells; interleukin-2; CD3 McAb

## INTRODUCTION

There have been many reports on cancer therapy with lymphokine-activated killer (LAK) cells and interleukin-2 (IL-2), but the proliferative response and anti-cancer effect of LAK cells are dependent on IL-2 dose. Other methods to improve the anti-tumor activity of cytotoxic T cells by activation with anti-CD3 McAb in conjunction with IL-2 are being investigated in recent years. In this study, we attempted to explore the physiologic and biologic effects of T-killer cells (TAK) co-stimulated with soluble gastric cancer antigen, anti-CD3 McAb and IL-2.

## MATERIALS AND METHODS

### Materials

Interlukin-2 was produced by Shanghai Bio-Chemical Institute and anti-CD3 monoclonal antibody was prepared from Tumor Institute, Chinese Academy of Medical Sciences. Medium 1640 was produced by Gibco Company of America.

Target cell: K562 and SGC-7901 were prepared by Radio biology Research Laboratory of our hospital, hepatocarcinoma cell line (SMC) was prepared by Tumor Research Laboratory of Fujian Medical University. All tumor cells were maintained in medium 1640 with 100 ml/L calf serum.

### Methods

Tumor soluble antigen was extracted from SGC cells by salting-out method previously described by Chen YX *et al*<sup>[1]</sup> and stored at -20°C. The mononuclear cells (MNC) were isolated from 50 mL venous blood of normal donor by centrifugation over a Ficoll-Hypaque gradient and a final concentration of  $1 \times 10^9/L$  was obtained in each culture bottle. Three kinds of cytotoxic T cells by activation was maintained in medium 1640 with 750 kU/L IL-2 for LAK cells, 750 kU/L IL-2 and 100 mg/L CD3

McAb for CD3AK cells. TAK cells were stimulated with IL-2, CD3 McAb and the extracted tumor antigen at a dose of 100 mg/L of culture. All the cells were refed with new media every 2-3 days of incubation at 37°C in air atmosphere containing 50 mL/L CO<sub>2</sub> and were diluted to  $1 \times 10^9/L$ .

Expansion of the three kinds of killer cells was tested with typan blue staining. The cytotoxicity of the three different killer cells were tested with MTT methods<sup>[2]</sup>, and the ratio of killer cells and the target cells was 10:1.

Having cultured for 10 days, TAK cells were tested for CD3, CD4, CD8, NK and CD19 by Flow Cytometry.

## RESULTS

### The killer cells cultured with various stimulators

There was a similar growth tendency among the three kinds of killer cells. In LAK cells group, the maximum cell number of expansion was found about 10 days of culture, the cell number decreased rapidly on the 15th day and was fewer than the initial number on the 20th day. However, in TAK group and CD3AK group, the peaks of the cell expansion were found on the 13th day and the cell number was more than that in LAK group. The activity of cell expansion was TAK > CD3AK > LAK (Figure 1).

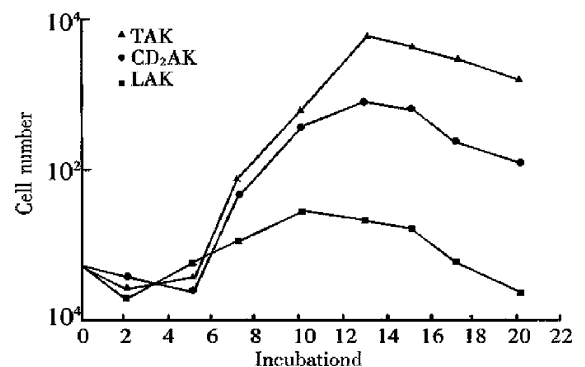


**Figure 1** The proliferation tendency among the three kinds of killer cells.

### Comparison of the anti-tumor activity among the three kinds of killer cells during culture

Table 1 shows that the killing activity of all the killer cells to K562 was low in the early stage of culture, but it increased as the rapid expansion occurred. On the 20th day, TAK and CD3AK cells maintained killing activity from the 15th day. On the

Department of Internal Medicine, Fujian Provincial Tumor Hospital, Fuzhou 350014, Fujian Province, China

Dr. CHEN Qiang, male, born on 1956-12-13 in Fuzhou City, Fujian Province, Han nationality, graduated from Fujian Medical University in 1982, associate chief of Internal Medicine Department, having 16 papers published.

\*Supported by the Scientific Foundation of Fujian Provincial Scientific & Technical Commission, No.95-J-14.

**Correspondence to:** Dr. CHEN Qiang, Fujian Tumor Hospital, Fuma road, Fuzhou 350014, China.

Tel. +86 • 591 • 3660063, Fax. +86 • 591 • 3660011

Received 1998-12-22

other hand, the killing activity of TAK, CD3AK and LAK to SGC-7901 was 98.5%, 82.1%, and 62.1%, and was 74.9%, 51.3% and 52.4% to SMC respectively.

#### Analysis of surface markers in the killer cells

By flow cytometry, it showed that TAK cells were dominated by CD8+ T cells (Table 2).

#### Effect of anti CD3 monoclonal antibody on TAK

Anti-CD3 monoclonal antibody and IL-2 could co-stimulate the expansion of lymphocytes, and make the cells become higher in anti-tumor activity (Table 3).

**Table 1 Comparison of anti-tumor activity among the three kinds of killer cells during culture**

Group	Incubation day						
	3	7	10	12	15	17	20
TAK	30.3	42.8	58.7	54.0	49.9	47.0	36.9
CD3AK	25.4	39.7	47.5	50.2	38.9	38.4	27.0
LAK	23.5	34.7	38.5	30.8	14.5	10.4	8.9

**Table 2 Analysis of surface markers on the killer cells (n = 6)**

Incubation	CD <sub>3</sub>	CD <sub>4</sub>	CD <sub>8</sub>	CD <sub>4</sub> /CD <sub>8</sub>	NK	CD <sub>19</sub>
0d	52.80	49.40	26.40	1.87	23.30	7.20
10d	49.88	44.36	62.80	0.76	4.53	0.20

**Table 3 Influence on the killer cells with various stimulation**

Group	Stimulated by	Duplication of proliferation	Killing activity
1	IL-2 alone	2.1	38.5%
2	IL-2 alone after costimulation with anti-CD3 mAb for 48 h	3.8	40.1%
3	Coexistence of anti-CD3 mAb and IL-2 during incubation	5.3	58.7%

#### Morphological observation of the killer cells

Under the inverted microscope, the killer cells were found to be round and bright large lymphocytes. They were aggregated into lumps with TAK lumps bigger than LAK lumps, and CD3AK lumps smaller. As the cell culture was continued, the shape of the killer cells changed and became irregular.

*In vitro*, we found that under the microscope the effect cells were aggregated onto the target cells after mixed cultivation for 1h, and that the target cells became enlarged after mixed culture for 6 h; and that cell debris could be seen after mixed culture for 15 h only in TAK group and CD3AK group.

#### DISCUSSION

Since Rosenberg *et al*<sup>[3]</sup> reported the anti-tumor therapy by LAK cell and IL-2 in 1985, it has been widely used. Its effective rate was 20%-35%. However, its adverse reaction was severe due to high doses of IL-2. For this reason, scientists are

now trying to look for a certain kind of effect cells which has higher anti-tumor activity and requires lower doses of IL-2 to maintain its activity.

In the study, CD8+ dominated cytotoxic T cells (TAK), generated from PBMC co-stimulated with soluble gastric cancer antigen (TSA) and anti-CD3 McAb, showed much higher cytotoxic activity against gastric cancer cell line from which TSA was extracted than that against hepatoma cell line (SMC). Moreover, we found that the expansion of TAK *in vitro* required lower IL-2 concentration than CD3AK did. It was encouraging that we have laid a foundation to solve the LAK activity which is dependent on IL-2.

As immune cells for treatment, the ratio between subtypes and its relative stability was of great importance. The results in flow cytometry showed that in the course of TAK culture, CD<sub>8</sub><sup>+</sup> cell number increased obviously, CD<sub>3</sub><sup>+</sup> decreased slightly and CD<sub>4</sub><sup>+</sup> had no change. It is suggested that TAK cells were dominated with CD<sub>8</sub><sup>+</sup> cells. We knew CD<sub>8</sub><sup>+</sup> T cells could be subdivided into Tc cells and Ts cells. If the number of Tc cells increased in the culture, the anti-tumor activity would be greatly enhanced. This may explain why CD<sub>8</sub><sup>+</sup> dominant TAK had strong anti-tumor activity. Further identification of Tc and Ts cells in the culture will be our next focus of research. Our results also showed that on the 10<sup>th</sup> day of culture, CD<sub>19</sub><sup>+</sup>, CD<sub>16</sub><sup>+</sup> and CD<sub>56</sub><sup>+</sup> cells were rare, suggesting that anti-tumor effect of TAK cells was chiefly dependent on CD<sub>8</sub><sup>+</sup> T cells.

Tao *et al*<sup>[4]</sup> reported that stimulation of PBMC with anti-CD3 McAb and IL-2 for 48 hours and then with IL-2 alone achieved a better anti-tumor activity. Our results showed that coexistence of anti-CD3 McAb and IL-2 during cell culture is of benefit to cell proliferation and cytotoxicity.

Our conclusion is that the immune effect cells generated from the PBMC stimulated with anti-CD3 McAb, IL-2 and TSA may be characterized by rapid proliferation *in vitro*, high cytotoxicity and low IL-2 dependence. Clinically, it is worth being considered.

#### REFERENCES

- Chen YX, Shi W, Wan YX, Chen JD, Li YF, Zhai H. Soluble tumor antigens and anti-CD3 McAb costimulated tumor killer cells-TAK cells. *Chin J Microbiol Immunol*, 1995;15:293-296
- Ferrari M, Chiara M, Isetta O. MTT colorimetric assay for testing macrophage cytotoxic activity *in vitro*. *J Immunol Methods*, 1990;131:165-168
- Rosenberg SA, Lotze MT, Munn LM. A progress report on the treatment of 157 patients with advanced cancer using lymphokine-activated Killer cells and interleukin-2 or high dose interleukin-2 alone. *N Engl J Med*, 1987;316:889-893
- Tao JX, Zhang YK. Adoptive immunotherapy on cancer. *Chin J Cell Biol*, 1994;16:1-7

# Clinical significance of changes of perioperative T cell and expression of its activated antigen in colorectal cancer patients

WANG Yi-Xing<sup>1</sup>, RUAN Can-Ping<sup>2</sup>, LI Li<sup>3</sup>, SHI Jing-Hua<sup>2</sup> and KONG Xian-Tao<sup>3</sup>

**Subject headings** colorectal neoplasms; perioperative period; T lymphocytes; surface antigen

## INTRODUCTION

Immune function status is corresponded to genesis and progress of tumor, and cell immune plays a major role in anti-tumor immunity. In recent years, there has been more and more interest in the effect of tumor on functional imbalance of T lymphocyte subgroups. In order to study changes of immune status in colorectal cancer patients before and after operation, we determined six kinds of T lymphocyte surface antigens including CD<sub>3</sub>, CD<sub>4</sub>, CD<sub>8</sub>, CD<sub>16</sub>, CD<sub>69</sub> and CD<sub>3</sub><sup>+</sup>/HLA-DR<sup>+</sup> in 35 patients with colorectal cancer from April 1996 to March 1997, and the results were compared with those in patients with benign diseases.

## MATERIAL AND METHODS

### Patients

Among the twenty-five patients with benign disease in the control group, sixteen were patients with inguinal hernia, nine with varicose, their average age was  $46.61 \pm 11.63$ . They did not take any medicine recently and had no complications. Among the thirty-five patients in the colorectal group, eighteen were male and seventeen female. Their average age was  $60.13 \pm 8.15$ . All of them were operated upon, twenty-seven patients received radical resection and eight patients palliative resection. The diagnosis was confirmed by pathological examination.

### Material

A murine monoclonal antibody to human CD<sub>3</sub>, CD<sub>4</sub>, CD<sub>8</sub>, CD<sub>16</sub>, CD<sub>69</sub> and a double-color fluorescent labeled CD<sub>3</sub>-FITC/HLA-DR-PE were purchased from Coulter-Immunotech Company.

<sup>1</sup>Department of General Surgery, Anda Hospital, Pudong New Area, Shanghai 201204, China

<sup>2</sup>Department of General Surgery, Changzheng Hospital, Fengyang Road 415, Shanghai 200003, China

<sup>3</sup>Department of Laboratory Diagnosis, Changzheng Hospital, Fengyang Road 415, Shanghai 200003, China

**Correspondence to:** WANG Yi-Xing, Department of General Surgery, Anda Hospital, Pudong New Area, Shanghai 201204, China

Tel. +86 · 21 · 58918622 Ext. 8888

**Received** 1998-12-21

## Methods

Peripheral vein blood was collected in heparin tubes 3 days before operation in control, 3 days before operation and 10 days after operation in cancer patients respectively. Ten  $\mu$ L- fluorescent labeled antibodies (Coulter) was mixed into 100  $\mu$ L heparinized blood (or  $10^6$  cells with nucleus) in a tube. The mixture was incubated at room temperature for 15 min, and was processed in a Q-prep machine and determined in a Coulter Epics XL flow cytometer (Coulter Company, USA) with relative softwares. The Dot Plot was made according to the detected value of the forward scatter light and the side scatter light (at a 90° angle from the laser axis) of flowing cells excited by an air-cooled 488 nm argon-ion laser. Green and red emissions of the lymphocyte group were detected with a 530 nm  $\pm$  10 nm bandpass filter and a 515 nm  $\pm$  10 nm bandpass filter respectively. The same type of non-fluorescent-labeled murine monoclonal antibodies was used as control in each group of samples. A combination of volt of the photomultiplier tubes (PMT1 and PMT2) was adjusted according to the non-fluorescent-labeled murine monoclonal antibodies to keep background fluorescent below 2% and CD<sub>3</sub>/CD<sub>4</sub>, color complement was adjusted in permitting width.

## Statistical analysis

Data was analyzed by Student's t test and Chi-square test.

## RESULTS

### Changes of T cell and its subgroups in colorectal cancer patients before and after operation

The results in Table 1 show that: ① CD<sub>3</sub>, CD<sub>4</sub> and CD<sub>4</sub>/CD<sub>8</sub> were significantly lower in cancer patients before operation than those in control while CD<sub>8</sub> was much higher in cancer patients ( $P < 0.05$ ). ② T cell and its subgroups changed obviously after operation. CD<sub>3</sub>, CD<sub>4</sub> and CD<sub>4</sub>/CD<sub>8</sub> were significantly higher in cancer patients after operation than those before operation ( $P < 0.05$ ), but CD<sub>8</sub> decreased obviously ( $P < 0.05$ ). No significant difference was found in CD<sub>3</sub>, CD<sub>4</sub> and CD<sub>4</sub>/CD<sub>8</sub> of the postoperative cancer patients and the controls.

**Table 1 Change of T cell and its subgroups in colorectal cancer patients before and after operation (% ,  $\bar{x} \pm s$ )**

Groups	Cases	CD <sub>3</sub>	CD <sub>4</sub>	CD <sub>8</sub>	CD <sub>4</sub> /CD <sub>8</sub>
Control	25	68.41 ± 7.30	39.88 ± 9.11	25.15 ± 7.34	1.79 ± 0.90
Colorectal cancer before operation	35	62.57 ± 7.46 <sup>a</sup>	38.81 ± 8.23 <sup>a</sup>	30.71 ± 4.03 <sup>a</sup>	1.13 ± 0.28a
Colorectal cancer after operation	35	65.38 ± 8.19	37.31 ± 11.47	25.26 ± 5.98	1.69 ± 1.07a

*P*<0.05 vs control and colorectal cancer after operation.

**Table 2 Expression of T cell activated antigen and CD16 in patients with colorectal cancer (% ,  $\bar{x} \pm s$ )**

Groups	Cases	CD <sub>16</sub>	CD <sub>69</sub>	CD <sub>3</sub> <sup>+</sup> /HLA-DR <sup>+</sup>
Control	25	11.11 ± 6.25	10.98 ± 6.41	4.44 ± 3.22
Colorectal cancer before operation	35	7.37 ± 2.61 <sup>ac</sup>	5.99 ± 2.07 <sup>ac</sup>	3.81 ± 1.72 <sup>c</sup>
Colorectal cancer after operation	35	11.62 ± 4.23	10.87 ± 2.81	7.62 ± 3.01 <sup>b</sup>

<sup>a</sup>*P*<0.05; <sup>b</sup>*P*<0.01 vs control; <sup>c</sup>*P*<0.05 vs colorectal cancer after operation.

### Expression of T cell activated antigen and CD16 in patients with colorectal cancer

The results in Table 2 show that: ① CD<sub>16</sub> and CD<sub>69</sub> were significantly lower in cancer patients before operation than those in control, and no significant difference was found in CD<sub>3</sub><sup>+</sup>/HLA-DR<sup>+</sup> between the postoperative cancer patients and the control. ② T cell activated antigen CD<sub>69</sub>, CD<sub>3</sub><sup>+</sup>/HLA-DR<sup>+</sup> and CD<sub>16</sub> increased obviously postoperatively (*P*<0.05). No significant difference was found in CD<sub>16</sub> and CD<sub>69</sub> between the postoperative cancer patients and the controls, while CD<sub>3</sub><sup>+</sup>/HLA-DR<sup>+</sup> was much higher than that in control (*P*<0.01).

### DISCUSSION

It was found in the study that CD<sub>3</sub>, CD<sub>4</sub>, CD<sub>4</sub>/CD<sub>8</sub>, CD<sub>69</sub> and CD<sub>16</sub> on NK cell surface in cancer patients before operation were lower than those in control, but CD<sub>8</sub> was much higher than that in control. The cell immune function decreased significantly in colorectal cancer patients before operation. Elevation of CD<sub>8</sub> was caused by increase of T suppressive cells (Ts), while reduced CD<sub>16</sub> was due to decrease of NK cells and increase of serum immune suppressive factor along with the tumor growing<sup>[1,2]</sup>. No statistical difference was found in activated T cell CD<sub>3</sub><sup>+</sup>/HLA-DR<sup>+</sup> between the cancer patients before operation and the controls. It might be caused by the on-going of TH cell mediated ADCC effect when TH cell (CD<sub>4</sub>) having recognized APC antigen in body with tumor was activated. Though the body immune function was suppressed at different extent, activation of T cell which was important in cell immune was still going on<sup>[3]</sup>.

Both T cell subgroups and T cell activated antigen changed obviously in colorectal cancer patients after operation with CD<sub>3</sub>, CD<sub>4</sub>/CD<sub>8</sub>, CD<sub>16</sub> and CD<sub>69</sub> increased significantly, and CD<sub>8</sub> decreased

obviously. Except the activated T cell CD<sub>3</sub><sup>+</sup>/HLA-DR<sup>+</sup> which was much higher than that in control, no significant difference was found in other parameters between the colorectal cancer patients after operation and the controls. The mechanism is that immune suppression in colorectal cancer patient is caused by the soluble immune suppression factor originated from tumors related to differentiation. Since the level of the immune suppression factor decreased, the body immune function and host anti-tumor immune function recovered gradually after the tumor was resected, strong T cell immune response induced by MHC II antigen HLA-DR activated CD<sub>4</sub> positive T cell to produce cellular factors, and augmented effect of CD<sub>8</sub> or CD<sub>4</sub> positive T cell mediated ADCC<sup>[4,5]</sup>. Increased CD<sub>3</sub> positive T cell, T help cell and CD<sub>16</sub> expression, and decreased suppressive T lymphocyte after operation showed that resection of tumor is helpful in improving patient cell immune functions. Increased T cell activated antigen CD<sub>69</sub> and CD<sub>3</sub><sup>+</sup>/HLA-DR<sup>+</sup> showed that host cell immune function was enhanced. So we hold that radical or palliative excision of colorectal tumor may be helpful in enhancing patient immune functions and postoperative treatment. Monitoring patient immune status after operation may have definite clinical significance in predicting the prognosis of patients.

### REFERENCES

- 1 Phillips JH, Sanier LL. Dissection of the lymphokine-activated killer phenomenon: relative contribution of peripheral blood natural killer cells and T lymphocytes to cytotoxicity. *J EXP Med*, 1986;164:814
- 2 Ortado JR, Manson A, Overton R. Lymphokine-activated killer cells: analysis of progenitors and effectors. *J EXP Med*, 1986;164:1193
- 3 Bi AH. Medical immunology. The People's Surgeon Press, Beijing, 1996:106
- 4 Jackson PA, Green MA, Marks CG, King RJB, Hubbard R, Cook MG. Lymphocyte subset infiltration patterns and HLA antigen status in colorectal carcinomas and adenomas. *Gut*, 1996;38:85
- 5 Peters PJ, Geuze HJ, Van Der HA. A new model for lethal hit delivery by cytotoxic T lymphocytes. *Immunol Today*, 1990;11:28

# Role of intracellular calcium in contraction of internal anal sphincter

NIU Wei-Xin<sup>1</sup>, QIN Xin-Yu<sup>1</sup>, LU Ying-Qing<sup>2</sup>, SHI Nian-Ci<sup>2</sup> and WANG Cheng-Pei<sup>1</sup>

**Subject headings** intracellular calcium; internal anal sphincter; ryanodine; muscle contraction

## INTRODUCTION

Internal anal sphincter (IAS) is a continuation of the smooth circular muscle layer thickened at the rectum, innervated by vegetative nerve. IAS is a special smooth muscle, which is different from colonic smooth muscle in physiology and pharmacology<sup>[1]</sup>. It was found that contraction of gastric smooth muscle depends on the influx of extracellular calcium and release of intracellular calcium<sup>[2]</sup>. In present study, we observed and compared the effects of extra and intracellular calcium on the contraction of IAS and colonic smooth muscle.

## MATERIALS AND METHODS

IAS and colonic smooth muscle (circular muscle) were taken from 10 patients undergoing abdomino-perineal resection of the rectal carcinoma. The strips containing muscle were approximately 1.2 cm long and 0.2 cm wide. The samples were immediately immersed in Krebs-Henseleit solution. The muscle segments were held by the extremities in the direction of the fibres and suspended in a 35mL organ bath containing Krebs-Henseleit solution at  $36.5^{\circ}\text{C} \pm 0.1^{\circ}\text{C}$  and gassed with 95% oxygen-5% carbon dioxide. Segments were attached to an isometric transducer coupled to a polygraph recorder.

Responses of the strips to acetylcholine (Ach) and noradrenaline (NA) were examined using cumulative concentration responses. After this, repeated steps were made in calcium-free and

calcium solution respectively to test effects of extracellular calcium on the contraction of the muscle. Finally, ryanodine of different doses was given to the strips in solution containing calcium to study the role of intracellular calcium in contraction of the muscle.

Anal manometry was made in 32 healthy volunteers to obtain the contracting figures of anal sphincter. The average age was 47 years (ranging from 33-61). The manometry consisted of a perfused open-ended polyethylene catheter (inside diameter 1mm) attached to an external transducer (CYS, China), and a micro computer (Laser-310).

Statistical results were compared using Student's test.  $P < 0.05$  was considered to be significant.

## RESULTS

### *Contracting frequency of colonic smooth muscle and IAS*

In vitro spontaneous contraction of 7-12 and 11-17 cycles per min (cpm) could be seen in colonic smooth muscle and IAS respectively. The contracting frequency of anal sphincter from the manometric figures was 12 cpm-18 cpm under the resting condition in these volunteers.

### *Effects of Ach and NA on colonic smooth muscle and IAS*

Ach had a dose-dependent relation with contraction of colonic smooth muscles and had no effect on internal anal sphincter. NA had a dose-dependent relation with contraction of internal anal sphincter and had no effect on colonic smooth muscles (Table 1).

### *Contracting effects of extracellular calcium on colonic smooth muscle and IAS*

Significant difference was found in contractions of colonic smooth muscles in calcium and calcium-free solutions, but no difference was found in contraction of IAS in calcium and calcium-free solutions (Table 2).

### *Effects of ryanodine on contraction of colonic smooth muscle and IAS*

Ryanodine had a remarkably inhibiting effect on contractions of IAS, but had no effect on contractions of colonic smooth muscles (Table 3).

<sup>1</sup>Department of General Surgery, Zhongshan Hospital, Shanghai Medical University, Shanghai 200032, China

<sup>2</sup>Laboratory of Basic Pharmacology, Shanghai Medical University, Shanghai 200032, China

Dr. NIU Wei-Xin, male, born on 1958-01-26 in Hefei City, Anhui Province, Han nationality, graduated from Shanghai Medical University as a postgraduate in 1991, associate professor of surgical department, having 8 papers published.

Presented at the 95th Annual Congress of Japan Surgical Society, Nagoya, 10-12 April, 1995.

Correspondence to: Dr. NIU Wei-Xin, Surgical Department, Zhongshan Hospital, Shanghai Medical University, 136 Yi-xue-yuan road, Shanghai 200032, China.

Tel. +86 • 21 • 64041990 Ext. 2810 or 2640

Received 1998-12-22

**Table 1 Dose-response correlation of Ach and NA in colonic smooth muscle and IAS ( $\bar{x} \pm s$ ,  $n = 10$ )**

Ach (mol/L)	Colonic smooth muscle		Internal anal sphincter (IAS)	
	Contraction strength (g)		NA (mol/L)	Contraction strength (g)
$10^{-6}$	$1.2 \pm 0.39$		$10^{-6}$	$0.70 \pm 0.23$
$10^{-5}$	$2.4 \pm 0.41$		$5 \times 10^{-6}$	$1.34 \pm 0.41$
$10^{-4}$	$4.1 \pm 1.20$		$10^{-5}$	$1.74 \pm 0.41$
$10^{-3}$	$6.4 \pm 1.60$		$5 \times 10^{-5}$	$2.20 \pm 0.44$
$10^{-2}$	$9.3 \pm 1.75$		$10^{-4}$	$2.68 \pm 0.45$

**Table 2 Contraction of colonic smooth muscle and IAS in different solutions ( $\bar{x} \pm s$ ,  $n = 10$ )**

Solution	Contraction strength (g)	
	Colonic smooth muscle	Internal anal sphincter
Ca <sup>2+</sup> solution	$8.30 \pm 2.01$	$2.44 \pm 1.20$
Ca <sup>2+</sup> -free solution	$4.27 \pm 0.91^a$	$1.84 \pm 0.77$

<sup>a</sup> $P < 0.01$ ,  $t = 3.72$ , compared with Ca<sup>2+</sup> containing solution.

**Table 3 Inhibiting effect of ryanodine on colonic smooth muscle and IAS ( $\bar{x} \pm s$ ,  $n = 10$ )**

Ryanodine ( $\mu\text{mol/L}$ )	Percentage of contractile strength without ryanodine (%)	
	Colonic smooth muscle	Internal anal sphincter (IAS)
0.1 <sup>a</sup>	$85 \pm 17.9$	$91 \pm 11$
1.0	$87 \pm 13$	$71 \pm 24^b$
10.0	$85 \pm 14$	$57 \pm 20^c$

<sup>b</sup> $P < 0.05$ ,  $t = 2.48$ ; <sup>c</sup> $P < 0.01$ ,  $t = 3.61$ ; compared with a.

## DISCUSSION

Smooth muscle of gut is innervated by cholinergic and adrenergic nerves. Acetylcholine is effective in contracting colonic smooth muscles, whereas epinephrine inhibits it. It is these nerves that regulate and control the movement of the smooth muscles of digestive tract.

The contracting frequency of IAS is basically in accordance with anal sphincter in the volunteers. The contracting frequency of IAS is higher than that of colonic circular muscle. It is possibly related to the maintenance of continence because anal resting pressure is mainly produced by contraction of IAS<sup>[3]</sup>.

It is well known that contraction of muscular cell is associated with Ca<sup>2+</sup>, and contraction of

colonic smooth muscle is chiefly produced by influx of Ca<sup>2+</sup>. From present study we found that contraction of colonic smooth muscle was weakened by about 50% when no extracellular calcium exists, whereas contraction of IAS was not affected. It is suggested that releases of Ca<sup>2+</sup> from intracellular storage may occur at the time when IAS contracts.

Ryanodine is an alkaloid extracted from rhizome of *Ryania speciosa* Vahl. It has been found in animal experiments that when Ryanodine is combined with Ryanodin receptor of sarcoplasmic reticulum in smooth muscular cells, contraction of the muscular cells will be prevented because Ca<sup>2+</sup> storage is exhausted after release of Ca<sup>2+</sup> from it<sup>[4-7]</sup>. In the present study we found that contraction of IAS induced by agonist was significantly inhibited in contrast with colonic smooth muscle when Ryanodin was given. It is indicated that release of intracellular calcium may play an important role in contraction of IAS. IAS is a special smooth muscle, being principally responsible for the generation and maintenance of resting anal canal pressure<sup>[3]</sup>. It is still unknown whether the contracting property of IAS is associated with the release of intracellular calcium. Further studies should be made.

## REFERENCES

- O'Kelly TJ, Brading A, Mortensent NJM. In vitro response of the human anal canal longitudinal muscle layer to cholinergic and adrenergic stimulation: evidence of sphincter specialization. *Br J Surg*, 1993;80:1337-1341
- Bitar KN, Bridford P, Putney JW, Makhlof GM. Cytosolic calcium during contraction of isolated mammalian gastric muscle cell. *Science*, 1986;232:1143-1145
- Frenker B, Euler CV. Influence of pudendal block on the function of the anal sphincter. *Gut*, 1975;16:482-489
- Jender DJ, Fairhurst AS. The pharmacology of ryanodine. *Pharmacol Rev*, 1969;21:1-25
- Iino M, Kobayashi T, Endo M. Use of ryanodine for functional removal of the calcium store in smooth muscle cells of the guinea-pig. *Biochem Biophys Res Comm*, 1988;152:417-422
- Burgoyne RD, Check TR. Locating intracellular calcium stores. *Science*, 1991;16:319-320
- Kwan CY, Zhang ZD, Bourreau JP. Intracellular calcium release channel in smooth muscle as studied with ryanodine. *Acta Pharmacol Sin*, 1992;13:76-77

Edited by WANG Xian-Lin

# Gastric emptying measured by ultrasonography

Odd Helge Gilja, Trygve Hausken, Svein Ødegaard and Arnold Berstad

**Subject headings** gastric emptying; stomach/ultrasonography; stomach/pathophysiology

A number of different methods have been used to estimate gastric emptying in humans, and all have their advantages and disadvantages. The method of choice will depend on whether solid or liquid meals are studied, the level of precision required, the degree of invasiveness that the subject or patient will tolerate, ethical considerations, and not at least the facilities available. Scintigraphy, with appropriate labelling of the test meal components and appropriate corrections applied, is considered so far the gold standard for measurement of gastric emptying. However, its application is limited by the need to restrict exposure to ionising radiation. Other methods are gastric aspiration techniques, radiography, ultrasonography, magnetic resonance imaging, epigastric impedance measurements, applied potential tomography, tracer methods (e.g. paracetamol), and breath tests. Regardless of the method used, the investigator must be aware of the limitations of the method in use, the large inter-individual variability and of the factors known to influence gastric emptying.

Ultrasonography is non-invasive, cheap, widely available, and can be repeatedly performed because of its safety. Two-dimensional ultrasound has, for many years, been widely used to assess gastric emptying rates<sup>[1-5]</sup>, and good correlation to radionuclide estimates of emptying rates have been detected<sup>[3,6]</sup>. In one study, ultrasound measurements of gastric emptying gave comparable sensitivity to scintigraphy in quantifying emptying of both low and high nutrient liquids<sup>[7]</sup>.

Ultrasound imaging of the proximal stomach is usually considered inappropriate due to the presence of gas-pockets and its relative inaccessibility close to the intra-thoracic cavity. However, an ultrasonographic method has been developed to overcome these problems and it demonstrated a moderate day-

to-day variation and low intra and interobserver error<sup>[8]</sup>. This method has been applied to study accommodation of the proximal stomach in patients with functional dyspepsia and the effect of different drugs on the stomach<sup>[9-12]</sup>.

In addition to ordinary B-mode imaging, the movements of gastroduodenal contents and velocity curves of transpyloric flow can be synchronously visualised by duplex ultrasound, that is combination of Doppler measurement and B-mode imaging<sup>[13-16]</sup>. By use of duplex scanning, it was revealed that, in the fed state, a short gush of duodenogastric reflux normally precedes the peristaltic closure of the pylorus<sup>[14]</sup>.

One of the latest advances in ultrasound technology is three-dimensional (3-D) imaging. An early system for acquisition and processing of 3-D ultrasound data was developed in an attempt to enhance the accuracy of volume computation of the distal stomach<sup>[17]</sup>. Using a motor device, the transducer was tilted through an angle of 90°, capturing sequential two-dimensional frames before the data set was transferred to a graphic workstation for final 3-D processing. This 3-D ultrasound system was validated both in vitro and in vivo, and yielded high accuracy and precision in volume estimation of abdominal organs<sup>[18,19]</sup>. This 3-D scanning system was also used to evaluate patients with functional dyspepsia<sup>[20-22]</sup>. Despite the significant achievements with respect to accuracy in volume estimation and 3-D reconstruction of tissue and organs, this 3-D system could only acquire a 90° fan-like data set from a predetermined, single position of the transducer.

Random or free-hand acquisition of 3-D ultrasound data has been achieved by utilizing mechanical<sup>[23,24]</sup>, acoustic<sup>[25-28]</sup>, or electromagnetic<sup>[29,30]</sup> devices to locate the exact position and orientation of the transducer in space. To enable scanning of a large organ like the fluid-filled stomach, a commercially available magnetometer-based position and orientation measurement (POM) device was chosen, which is relatively immune to metallic influence and electronic noise from the scanner. This system for magnetic scanhead tracking has been validated with respect to both its precision in locating specific points in space<sup>[30]</sup> and its accuracy in volume estimation<sup>[31,32]</sup>. In these studies, the sensor system worked well in scanning human organs, and high precision and accuracy were revealed in point location and volume estimation.

Department of Medicine, Haukeland University Hospital, University of Bergen, Norway

**Correspondence to:** Odd Helge Gilja, Department of Medicine, Haukeland University Hospital, University of Bergen, N-5021 Bergen, Norway

Tel. +4755 • 298060/972134 Fax. +4755 • 972950

E-mail. Odd.Gilja@meda.uib.no

URL. <http://www.uib.no/med/avd/med/a/oddgilja.html>

Received 1999-02-09

In one study, 14 male volunteers were examined with 3-D ultrasound after ingestion of a 500 mL soup meal up to 35 min postcibally<sup>[33]</sup>. The average half-emptying time of this meal was 22.1min±3.8min. Intra-gastric distribution of the meal, expressed as proximal/distal volume, varied on average from 3.6±2.1 (5 min postprandially) to 2.7±1.9 (30 min postprandially). This 3-D ultrasound system using magnetic scanhead tracking demonstrated excellent in vitro accuracy, calculated gastric emptying rates more precisely than by two-dimensional ultrasound, and enabled estimation of intra-gastric distribution of a soup meal in healthy subjects. The same 3-D imaging system was also used to evaluate gastric emptying and duodenogastric reflux stroke volumes using a digital colour Doppler imaging model<sup>[34]</sup>.

In conclusion, ultrasonography is a reliable and safe method to assess gastric emptying in humans. Ordinary two-dimensional ultrasound imaging can be supplied with Doppler analysis and 3-D scanning to obtain a higher level of information on pathophysiology of the stomach.

## REFERENCES

- Bateman DN, Whittingham TA. Measurement of gastric emptying by real-time ultrasound. *Gut*, 1982;23:524-527
- Bolondi L, Bortolotti M, Santi V, Calletti T, Gaiani S, Labo G. Measurement of gastric emptying time by real time ultrasonography. *Gastroenterology*, 1985;89:752-759
- Holt S, Cervantes J, Wilkinson AA, Wallace JH. Measurement of gastric emptying rate in humans by real-time ultrasound. *Gastroenterology*, 1986;90:918-923
- Duan LP, Zheng ZT, Li YN. A study of gastric emptying in non-ulcer dyspepsia using a new ultrasonographic method. *Scand J Gastroenterol*, 1993;28:355-360
- Ricci R, Bontempo I, Corazziari E, La Bella A, Torsoli A. Real time ultrasonography of the gastric antrum. *Gut*, 1993;34:173-176
- Marzio L, Giacobbe A, Conoscitore P, Facciorusso D, Frusciante V, Modoni S. Evaluation of the use of ultrasonography in the study of liquid gastric emptying. *Am J Gastroenterol*, 1989;84:496-500
- Hveem K, Jones KL, Chatterton BE, Horowitz M. Scintigraphic measurement of gastric emptying and ultrasonographic assessment of antral area: relation to appetite. *Gut*, 1996;38:816-821
- Gilja OH, Hausken T, Odegaard S, Berstad A. Monitoring postprandial size of the proximal stomach by ultrasonography. *J Ultrasound Med*, 1995;14:81-89
- Gilja OH, Hausken T, Wilhelmsen I, Berstad A. Impaired accommodation of proximal stomach to a meal in functional dyspepsia. *Dig Dis Sci*, 1996;41:689-696
- Gilja OH, Hausken T, Bang CJ, Berstad A. Effect of glyceryl trinitrate on gastric accommodation and symptoms in functional dyspepsia. *Dig Dis Sci*, 1997;42:2124-2131
- Gilja OH, Hausken T, Odegaard S, Berstad A. Accommodation of the proximal stomach is fat dependent in functional dyspepsia. *Eur J Ultrasound*, 1996;4:S21
- Vingerhagen S, Hausken T, Gilja OH, Berstad A. Influence of a 5HT<sub>1</sub> receptor agonist (Sumatriptan) on gastric accommodation and initial transpyloric flow of a liquid meal examined by duplex sonography. *Gut*, 1997;41:A41
- King PM, Adam RD, Pryde A, McDicken WN, Heading RC. Relationships of human antroduodenal motility and transpyloric fluid movement: non invasive observations with real-time ultrasound. *Gut*, 1984;25:1384-1391
- Hausken T, Odegaard S, Matre K, Berstad A. Antroduodenal motility and movements of luminal contents studied by duplex sonography. *Gastroenterology*, 1992;102:1583-1590
- Hausken T, Gilja OH, Odegaard S, Berstad A. Flow across the human pylorus soon after ingestion of food, studied with duplex sonography. Effect of glyceryl trinitrate. *Scand J Gastroenterol*, 1998;33:484-490
- Hausken T, Gilja OH, Undeland KA, Berstad A. Timing of post-prandial dyspeptic symptoms and transpyloric passage of gastric contents. *Scand J Gastroenterol*, 1998;33:822-827
- Thune N, Hausken T, Gilja OH, Matre K. A practical method for estimating enclosed volumes using 3D ultrasound. *Eur J Ultrasound*, 1996;3:83-92
- Gilja OH, Thune N, Matre K, Hausken T, Odegaard S, Berstad A. In vitro evaluation of three-dimensional ultrasonography in volume estimation of abdominal organs. *Ultrasound Med Biol*, 1994;20:157-165
- Gilja OH, Smievoll AI, Thune N, Matre K, Hausken T, Odegaard S, Berstad A. In vivo comparison of 3D ultrasonography and magnetic resonance imaging in volume estimation of human kidneys. *Ultrasound Med Biol*, 1995;21:25-32
- Hausken T, Thune N, Matre K, Gilja OH, Odegaard S, Berstad A. Volume estimation of the gastric antrum and the gallbladder in patients with non-ulcer dyspepsia and erosive prepyloric changes, using three dimensional ultrasonography. *Neurogastroenterol Mot*, 1994;6:263-270
- Gilja OH, Hausken T, Odegaard S, Berstad A. Three-dimensional ultrasonography of the gastric antrum in patients with functional dyspepsia. *Scand J Gastroenterol*, 1996;31:847-855
- Berstad A, Hausken T, Gilja OH, Thune N, Matre K, Odegaard S. Volume measurement of gastric antrum by 3 D ultrasonography and flow measurements through the pylorus by duplex technique. *Dig Dis Sci*, 1994;39:97-100
- Dekker DL, Piziali RL, Dong EJr. A system for ultrasonically imaging the human heart in three dimensions. *Comput Biomed Res*, 1974;7:544-553
- Nikraves PE, Skorton DJ, Chandran KB, Attarwala YM, Pandian N, Kerber RE. Computerized three dimensional finite element reconstruction of the left ventricle from cross-sectional echocardiograms. *Ultrasound Imaging*, 1984;6:48-59
- Moritz WE, Shreve PL, Mace LE. Analysis of an ultrasonic spatial locating system. *IEEE Trans Instrum Meas*, 1976;25:43-50
- Brinkley JF, Muramatsu SK, McCallum WD, Popp RL. In vitro evaluation of an ultrasonic three-dimensional imaging and volume system. *Ultrasound Imaging*, 1982;4:126-139
- Handschumacher MD, Lethor JP, Siu SC, Mele D, Rivera JM, Picard MH, Weyman AE, Levine RA. A new integrated system for three-dimensional echocardiographic reconstruction: Development and validation for ventricular volume with application in human subjects. *J Am Coll Cardiol*, 1993;21:743-753
- Levine RA, Handschumacher MD, Sanfilippo AJ, Hagege AA, Harrigan P, Marshall JE, Weyman AE. Three-dimensional echocardiographic reconstruction of the mitral valve, with implications for the diagnosis of mitral valve prolapse. *Circulation*, 1989;80:589-598
- Kelly IM, Gardener JE, Brett AD, Richards R, Lees WR. Three-dimensional US of the fetus. Work in progress. *Radiology*, 1994;192:253-259
- Detmer PR, Bashein G, Hodges TC, Beach KW, Filer EP, Burns DH, Strandness JrDE. 3D ultrasonic image feature localization based on magnetic scanhead tracking: In vitro calibration and validation. *Ultrasound Med Biol*, 1994;20:923-936
- Hodges TC, Detmer PR, Burns DH, Beach KW, Strandness JrDE. Ultrasonic three-dimensional reconstruction: In vitro and in vivo volume and area measurement. *Ultrasound Med Biol*, 1994;20:719-729
- Gilja OH, Hausken T, Olafsson S. In vitro evaluation of three-dimensional ultrasonography based on magnetic scanhead tracking. *Ultrasound Med Biol*, 1998;24:1161-1167
- Gilja OH, Detmer PR, Jong JM, Leotta DF, Li XN, Beach KW, Martin R, Strandness DEJ. Intra-gastric distribution and gastric emptying assessed by three-dimensional ultrasonography. *Gastroenterology*, 1997;113:38-49
- Hausken T, Li XN, Goldman B. Quantification of gastric emptying and duodenogastric reflux stroke volumes using three-dimensional guided digital color Doppler Imaging. *Eur J Ultrasound*, 1998;7:(S1)3421

# Fine-needle aspiration cytology of liver diseases

Ji Xiao-Long

See article on page 98

**Subject headings** biopsy, needle/cytology; liver neoplasms/pathology

Ultrasonography, CT and magnetic resonance have been widely used in the diagnosis of liver diseases in the past 20 years, but the final definite diagnosis of liver space occupying (LSO) lesions can not be made only by imaging methods. Ultrasonography has been used in combination with fine-needle aspiration biopsy in the diagnosis of liver diseases since the 1970s. The accuracy of differential diagnosis of both benign and malignant lesions could reach 88.8%. Since then, this technique has become popular in the diagnosis of LOS lesions in large hospitals in China. Dr. Edoute reported 279 cases of LSO lesions in 1976-1988 diagnosed by non-ultrasonically-guided aspiration biopsy, which is of great importance in the diagnosis of LSO lesions by ultrasonically-guided fine-needle aspiration biopsy.

## ADVANTAGES AND DISADVANTAGES OF FINE-NEEDLE ASPIRATION CYTOLOGY(FNAC)

FNAC leads to little tissue damage and few complications. Pneumothorax occurred in only one case of the 279 cases reported by Dr. Edoute. It has been proved in our practice that one focus can be aspirated 3-5 times.

The disadvantage of FNAC is that smear cytological examination can only determine whether the cells are malignant, but can not type the tissues. Big needle aspiration biopsy should be performed in order to make the final definite classification of tumors, e.g., to differentiate the subtypes of primary hepatic cancer, but it has more complications than fine-needle aspiration biopsy. Furthermore, fine-needle aspiration biopsy can reduce the risk of punc-

ture by incorporating the advantages of both fine-needle and big-needle aspiration biopsies, but the tissue core is relatively small which sometimes can not meet the needs of multiple biopsies of tissue slices.

## INDICATIONS AND CONTRAINDICATIONS OF FNAC

FNAC is mainly used at present in the diagnosis of LSO lesions by ultrasonography and CT. Fine-needle liver aspiration biopsy is performed when the final definite diagnosis can not be made. Big-needle aspiration biopsy is usually used in the diagnosis of diffuse hepatic lesions while fine-needle aspiration biopsy is mainly used in the diagnosis of focal hepatic lesions.

### *Indications of FNAC*

Indications of FNAC are: primary liver cancer, secondary liver cancer, deep hepatic hemangioma, hepatic abscess, circumscribed fatty liver, and cystic tumor or cancer of liver.

### *Contraindications of FNAC*

The contraindications of FNAC are: patients with hemorrhagic tendency such as those with noticeably prolonged prothrombine time, patients with suspected extrahepatic obstructive jaundice, patients with suspected hepatic echinococcosis, patients with hepatic surface hemangioma, and those who fail to cooperate.

## PREOPERATIVE PREPARATION, PROCEDURES AND POSTOPERATIVE MANAGEMENT

### *Preoperative preparation*

Preoperative examination of prothrombine time, bleeding and clotting time.

Ultrasonography is used to determine the site of LSO lesions, and the site of needle insertion and its depth.

### *Aspiration needle*

The external diameter of the fine-needle is less than 1mm, while that of the big-needle is greater than 1mm. Berlin Charife Hospital succeeded in fine-needle (its external diameter was 1mm) aspiration cytology biopsy in 1931. Swedish physicians began to use it in the 1950s and named it fine-needle aspiration biopsy.

Department of Pathology, Chinese PLA General Hospital, Beijing 100853, China

Ji Xiao-Long, M.D., male, born on August 22, 1952 in Ju Rong City, Jiangsu Province, graduated from the Third Military Medical University in 1978, specializing in surgical pathology of digestive system, and having more than 200 papers published.

**Correspondence to:** Dr. Ji Xiao-Long, Fu Xing Road 28, Beijing 100853, China

Tel. +86 • 10 • 68228362 Fax. +86 • 10 • 68228362

E-mail. xlji@plagh.com.cn

**Received** 1999-03-20

**Fine-needle.** PTC needle is used for aspiration biopsy in China, which consists of the needle scabbard and the needle core. The needle is 15 cm-20 cm-long and its external diameter is 0.6 mm-0.8 mm. Its tip is sharp with a 30° -45° oblique angle. Fine-needle aspiration can be performed in both cytological examination and the diagnostic aspiration biopsy of various cysts and fluid lesions.

**Big-needle.** The external diameter of big-needle for transcutaneous aspiration is greater than 1 mm. Its appearance, structure and length are identical to fine-needle, but the needle with 1.2 mm external diameter are commonly used.

**Fine-needle aspiration histology.** Number 21-23 Sute-cut needles, which are identical in external diameter with fine-needle, are usually used in hepatic tumor biopsy. When the needle is being inserted into the light target, the operator lifts the piston in the needle handle, making the needle core move up, so that the tissue strips can be inlaid in the space of the needle sheath in which the pressure is negative. The aspirated tissue for biopsy is 0.4 mm in diameter and 3 mm long.

**Guiding needle.** The fine-needle (its external diameter is 0.7 mm) is rather soft and easy to bend in the process of transcutaneous aspiration, which often results in failure. When the guiding needle (it is 5 cm-long and its external diameter is 1.6 mm) is supplemented, success can be achieved. After the guiding needle is inserted into subcutaneous tissues, the fine-needle is used to aspirate in order to avoid its bending.

#### OPERATIONAL PROCEDURES OF ULTRASONICALLY-GUIDED FNAC

Preoperative measurement of blood pressure and pulse for postoperative control. For determination of the site of LSO lesions by ultrasonography, horizontal position is taken for patients with lesions in the left hepatic lobes, while left lateral position is taken for patients with lesions in the right hepatic lobes. After routine sterilization, the aspiration site is determined by aspiration probe. The guiding needle is inserted into subcutaneous tissues after local anesthesia reaches Glisson's capsule. The fine-needle is inserted into the guiding needle hole. The patient is asked to hold his breath while the fine-needle is inserted into the target of the liver along the aspiration line displayed on the screen of ultrasonic detector. A solid sense can be felt when the needle has been inserted into the focal tissues. Then, the patient is asked to resume his normal respiration while the needle core is pulled out and connected to a 10-mL injector. Soon after the negative pressure is removed by lifting and inserting the needle point

3 or 4 times, the needle is pulled out. The aspirated tissues are placed on a glass slide and prepared into a round-shaped smear to observe whether there are yellowish particles. The liver tissues are aspirated when yellowish particles are found. After the dried smear is fixed in 95% alcohol for 10 min, it is taken out and stained for cytological examination. The second aspirated tissues are placed on a piece of filter paper and fixed in 100 mL/L formalin for histological examination. The third ones are placed on a piece of filter paper and fixed in 30 mL/L-glutaraldehyde for electron microscopy.

**Postaspiration treatment.** The patient is asked to rest in bed for 4 h-6 h. Two hours after aspiration, blood pressure and pulse are measured every 30 minutes, then once an hour for 4 successive times if no change is found.

#### COMPLICATIONS AND DEATH RATE

Fine-needle aspiration results in little liver damage and has a high safety. It was reported by Livraghi *et al*<sup>[1]</sup> in 1983 that the occurrence rate of complications was 0.05% in the 11 700 cases receiving fine-needle abdominal aspiration biopsy. Smith *et al*<sup>[2]</sup> in 1985 reported a total rate of complication of 0.16% and a death rate of 0.006% in the 63 108 cases receiving fine-needle abdominal aspiration biopsy. Among them, noticeable bleeding was found in 17, bile leakage in 51, infection in 16, and death in 4. In the study by Cheng MH *et al*<sup>[3]</sup>, bleeding was found in 2 cases, liver cancer in 1 case, and cavernous hemangioma in 1 case among the 160 cases of LSO lesions receiving ultrasonically-guided fine-needle aspiration biopsy.

In theory, pulling out the fine-needle when it has been inserted into tumor may result in contamination of a small number of malignant cells on the surface of fine needles. However, TAO *et al*<sup>[4]</sup> reported that no tumor implantation was found in the 2 500 cases receiving transcutaneous aspiration biopsy, while it was found in 2 cases among the 11 700 cases reported by Livraghi *et al*.<sup>[1]</sup> No tumor implantation has been reported so far in China, although tens of thousands cases received fine-needle aspiration biopsies.

#### FUTURE DEVELOPMENT

It is not difficult to find out LSO lesions with wide application of imaging methods, but it is still troublesome to make an accurate and definite diagnosis of tumors. Combined methods should be advocated for the diagnosis of LSO lesions by ultrasonically-guided fine-needle aspiration biopsy in order to improve the accuracy of its diagnosis.

**Ultrasonically-guided FNAC biopsy**

The positive rate of the diagnosis of liver parenchyma occupying malignant lesions is 77%-90%. FNAC biopsy is helpful for the rapid diagnosis of liver cancer and can provide the basis for cytological diagnosis and avoid unnecessary exploratory laparotomies.

However, it is difficult for FNAC to classify tumors and to make differential diagnosis of atypical proliferation of liver cells and well-differentiated hepatocellular carcinoma. FNAC can not serve as an exclusive diagnostic method for malignant tumors due to its 10%-23% false positive rate.

**Ultrasonically-guided fine-needle aspiration histology (FNAH) biopsy**

In our studies, the aspirated tissues are placed on a small piece of filter paper and fixed in 100 mL/L-formalin for histological examination since FNAC could not classify the tissues. Among the 4 cases of liver cancer, 2 were diagnosed by FNAC as having interdegenerative cells and the other 2 as having hepatocytes due to cirrhosis, while all of them were diagnosed by FNAH as well-differentiated hepatocellular carcinoma. Positive cancer cells were found in 8 cases of secondary liver cancer by FNAC. Of them, 1 case was diagnosed as leiomyoma, 2 as squamous epithelial carcinoma, and 5 as adenocarcinoma by FNAH.

**Ultrasonically-guided fine-needle aspiration ultrastructural (FNAU) biopsy**

Histological classification could not be made since the tissues taken by FNAH were small. Ghadially reported that 1%-8% tumors could not be diagnosed only by histological examination (optical microscope). We have achieved satisfactory results in the diagnosis of tumors by electron microscopy, which can further confirm the histological diagnosis of tumor and show their histogenesis, and is helpful for the localization of the primary focus of hepatic

metastatic carcinoma. Combination of FNAC and FNAU can increase the positive rate of tumor diagnosis, but FNAU is limited in its use due to the difficulties in specimen preparation and tissue localization.

**Ultrasonically-guided fine-needle immunohistochemistry**

It is advocated to label the different cell antigens by immunohistochemistry for the differentiation of their types when it is difficult to diagnose the fine-needle aspirated cells by routine staining. For instance, neuroendocrine labelling is helpful for the diagnosis of carcinoid and positive AFP labelling supports the diagnosis of hepatocellular carcinoma. The current tendency is to prepare more specific antibodies so as to make the differential diagnosis of tumors more accurate and easier.

**Ultrasonically-guided fine-needle molecular biology**

The wide application of molecular biology techniques has made it possible to detect the level of nucleic acid and various kinds of oncogenes. A large number of biopsies can not be performed due to the limited specimens of fine-needle aspirated tissues or cells while oncogene biopsy is not limited by the amount of specimens because the diagnosis of tumors at gene level can be made on the basis of a few cells. Therefore, molecular biology biopsies such as in situ hybridization and PCR are the future hot points of fine-needle aspiration cytology.

**REFERENCES**

- 1 Livraghi T, Damascelli B, Lombardi C, Spagnoli I. Risk in fine-needle abdominal biopsy. *J Clinical Ultrasound*, 1983;11:77-81
- 2 Smith EH. Fine-needle aspiration: are there any risks. In: Holm HH, ed. *Interconventional ultrasound*. Copenhagen: Munksgaard, 1985:1-10
- 3 Cheng MH, Li JG, Wang B, Yuan Z, Xue D. Ultrasonically-guided fine-needle aspiration biopsy of LSO lesions. *Zhonghua Wuli Zazhi*, 1985;7:85-88
- 4 Tao LC, Pearson FG, Delarue NC, Langer B, Sanders DE. Percutaneous fine-needle aspiration biopsy. *Cancer*, 1980;45:1480-1485

Edited by MA Jing-Yun

Original Articles

# Non-imaging-guided fine-needle aspiration of liver lesions: a retrospective study of 279 patients

Yeouda Edoute<sup>1,4</sup>, Ehud Malberger<sup>2,4</sup>, Orly Tibon-Fishe<sup>2</sup> and Nimer Assy<sup>3,4</sup>

See invited commentary on page 95

**Subject headings** liver neoplasms/diagnosis; liver neoplasms/secondary; fine-needle aspiration; liver/pathology

## Abstract

**AIM** To determine the value of nonimaging-guided (direct) fine-needle aspiration cytology in diagnosing liver lesions.

**METHODS** Detection by technetium-99m, ultrasound or computed tomographic scanning of the liver was made in 279 patients with 332 aspirations.

**RESULTS** Based on histologic, cytologic and clinical findings, final liver diagnoses were reached in 265 patients, of whom 171 had malignant and 94 benign liver disease. Among the 171 patients with malignant liver disease, the cytologic findings indicated suspected malignancy in 8 patients, suggested definite malignancy in 130, but failed to disclose malignancy in 33 patients. In 93 of the 94 patients with benign liver disease, the cytologic findings were reported as benign, while in one patient the report of malignancy was false. The overall sensitivity, specificity, and positive and negative predictive values for cytologic results were 80.7%, 98.9%, 99.3% and 73.8%, respectively. The diagnostic accuracy of fine-needle aspiration cytology was 87.2%. The only major complication attributable to the procedure consisted of one case of pneumothorax.

**CONCLUSION** Direct fine-needle aspiration of palpable liver mass and blind fine-needle aspiration of non-palpable liver lesions for cytodiagnosis are simple, safe, and cost-effective diagnostic method for evaluating the nature of liver lesions. The aspiration procedure including potential complications could be cut short by early finding of abnormal cells.

Department of <sup>1</sup>Internal Medicine C, <sup>2</sup>Diagnostic Cytology, <sup>3</sup>Liver Unit, Rambam Medical Center, Haifa, and <sup>4</sup>The Bruce Rappaport Faculty of Medicine, Technion-Israel Institute of Technology, Haifa, Israel.

**Correspondence to:** Nimer Assy, MD., Fassouta, Upper Galilee 25170, P.O.B. 428, Israel

Tel. +972 • 4 • 9870-080, Fax. +972 • 4 • 9870-080

E-mail. drnimer@netvision.net.il

Received 1999-03-02

## INTRODUCTION

Imaging-guided fine-needle aspiration (FNA) for cytodiagnosis is well established as a reliable and cost-effective method for diagnosing malignant lesions in all systems and organs of the human body. FNA of liver lesions guided by ultrasound (US) or computed tomography (CT) has proven to be a safe, very sensitive and specific method for diagnosing hepatocellular carcinoma<sup>[1-8]</sup> and liver metastases<sup>[3,9-11]</sup>. A sensitivity between 66.9% and 100% has been reported in major centers<sup>[12-28]</sup>. However, its value in small peripheral centers remains to be determined. From 1976, and before the US and CT imaging methods were introduced in our hospital, we performed direct FNA of palpable abdominal<sup>[29]</sup> and liver mass and blind FNA of nonpalpable lesions detected by technetium-99m, US and CT liver scan. Our findings encouraged us to use this method as the initial diagnostic tool in patients suspected of having malignant liver disease (MLD). To date, a large retrospective evaluation describing the accuracy of direct FNA or the safety of the technique has not been reported.

The aspiration procedure using guided needle aspiration seems excessive for routine use with potential for complications. Whether the procedure could be cut short by early finding of abnormal cells remains to be determined. The aim of this study was to report our experience gained with nonguided FNA of palpable and non palpable liver and to compare our results with the method of imaging guided FNA as reported in the literature.

## MATERIAL AND METHODS

During the years 1976-1988 we performed 332 direct FNAs of liver in 279 patients at Rambam Medical Center. Of the 332 aspirations, 50 (45 patients) were direct aspirations of palpable liver lesions, and 282 (234 patients) were blind aspirations of non-palpable liver lesions. The aspirations were made in order to either confirm or rule out suspicions of primary or metastatic malignancy in the liver, based on clinical findings and supported by the presence of unifocal or multifocal liver lesions on a radioisotope, US or CT scan. Informed consent was obtained from each patient, and the study protocol conformed to the ethical guidelines of the Declaration of Helsinki as reflected in a priori approval by the hospital's Human Research Committee.

### Technique

The specimens for cytologic examination were obtained by direct insertion of a long (0.8 mm×80 mm) 22-gauge needle. All aspirations were performed by one operator, and the penetrating sites of the liver were subcostal. An attendant cytopathologist was present in all cases to verify that adequate numbers of cells of the expected type were present in the sample. In cases of palpable liver mass, or of hepatomegaly arousing a strong suspicion of liver malignancy but without any palpable mass, the aspiration was usually performed prior to any imaging exploration of the liver. In cases of unifocal or multifocal lesion (s) demonstrated by imaging methods (with or without an enlarged liver), the puncture sites and directions of the needles were blindly directed towards the estimated site of the lesion. Three to five aspirations from different insertion points were made in each FNA procedure, with six to eight needle passes for each aspiration. The aspirate was expelled onto glass slides, smeared and fixed with 95% ethyl alcohol, and later stained by Papanicolaou's method. One slide was air-dried for May-Grünwald/Giemsa staining.

### Exclusion

The only contraindications for FNA were a history of marked hemorrhagic tendency, a high increase in D-dimers, reduced platelet count, or prolonged prothrombin or partial thromboplastin time.

### Cytopathologic interpretation

Cytologic findings were reported as follows: acellular, unsatisfactory, no malignancy, atypical-reactive, malignancy cannot be ruled out (inconclusive), suspected malignancy and definite malignancy. The tumor cell type was specified whenever possible. The clinical, laboratory, radiologic, imaging, operative, histologic and cytologic data were compiled in each patient. Follow up information for each patient was obtained in order to reach a final diagnosis and to evaluate the diagnostic role played by FNA. Data were obtained by reviewing Rambam Medical Center charts, the discharge summaries of other hospitals and telephone communication.

### Statistical analysis

To determine the sensitivity and specificity of cytologic diagnoses, it is necessary to classify cytologic findings for each patient as either malignant or benign. For this purpose, patients with cytologic findings of 'no malignancy' and 'atypical-reactive' were classified as having benign cytologic diagnoses, while patients with cytologic findings in liver aspirations from the right or left side of 'suspected' and

'definite malignancy' were diagnosed as having malignancy. The cytologic findings of FNA were categorized as true-positive, true-negative, false-positive and false-negative. The accuracy of true and false cytologic diagnoses was verified against histologic, cytologic and clinical categories. A cytologic diagnosis was defined as true-positive if a patient with malignant cytologic diagnosis had one or more of the followings:

**Histologic findings** Histologic findings of malignancy based either on liver tissue obtained by liver needle biopsy, surgery or autopsy or on histologic findings of malignancy from another site revealing malignant cells similar to those obtained by FNA of the liver.

**Cytologic findings** Malignant cells from other organs or from body fluids, exhibiting malignant cells similar to those obtained by FNA of the liver.

**Clinical findings** A combination of the followings: ① palpable liver mass, hepatomegaly or elevated serum alkaline phosphatase; ② imaging scan of the liver suggesting malignancy and ③ steady deterioration, with survival time not exceeding 12 months, with or without indication of MLD on death certificate.

A cytologic diagnosis was defined as true-negative if a patient with negative cytologic diagnosis also had benign histologic diagnosis of a liver biopsy or no evidence for MLD during surgery and/or his subsequent clinical course was considered characteristic of a benign disease (improvement either spontaneously or following therapy). Specificity was determined by dividing true-negatives by the number of lesions ultimately found to be benign. Basing on histologic, cytologic and clinical findings, we reached final diagnoses in 308 aspirations from 265 patients.

### RESULTS

Twenty-four out of 332 aspirations were excluded from the study: ten because the aspirates were unsatisfactory, five because the cytological findings were inconclusive, and nine because the conclusive cytology findings could not be verified by histology, adequate clinical follow-up, or autopsy. The study included 265 patients (308 aspirations) with final diagnosis, of whom 171 (203 aspirations) had a malignant liver disease and 94 (105 aspirations) had a benign liver disease. Sixty-one (21.9%) patients had histories of prior malignancy, 56 with one prior tumor and 5 with two prior tumors.

Table 1 lists the patients' clinical characteris-

tics. All the patients underwent at least one of the following liver imaging explorations: technetium-99m scanning, US or CT. Among 94 patients with BLD, the imaging scans suggested malignancy in less than 20%. One hundred and fifty-five of the 171 patients with malignant liver disease underwent at least liver imaging scanning, malignancy was suggested in 134 (86.5%) patients. In patients with malignant liver disease, malignant multifocal lesions were found in 79% and unifocal lesions in only 21%.

Table 2 shows the conclusive cytological findings from FNA according to the final diagnosis of liver disease. Among 130 patients with definite cytological findings of malignancy, primary liver carcinoma was diagnosed in 26 (20%), 24 of whom had hepatocellular carcinoma. Adenocarcinoma was specified in 59 (64.1%) of 92 patients (70.8%) with cytologically diagnosed liver metastases. Other cytologic diagnoses included anaplastic carcinoma, lymphoma, sarcoma, etc. Histologic findings verified the cytologic diagnosis of malignancy in 62 (36.3%) patients. In 35 (20.5%) patients the cytologic diagnosis of malignancy was verified by matching with cytologic tumor cells obtained from other organs or from body fluids, and in 74 (43.2%) patients by clinical findings alone. Clinical findings suggesting malignancy were observed in only two (2.1%) of 94 patients with benign liver disease and corresponding cytologic findings. In these two patients, the survival time was shorter than 12 months due to cardiovascular events.

Table 3 shows the relationship between nonguided FNA cytodiagnosis in patients with MLD and type of suspected malignant liver lesion detected by various kinds of liver imaging scanning. Among 230 liver scans suggesting malignancy, 166 (72%) were suggestive of multifocal lesions, and 64 (28%) of unifocal lesions. The proportion of true-positive cytologic diagnosis was 73.5% (122/153) among patients with liver scans suggesting multifocal lesions, while 68.8% (44/66) indicated unifocal lesions. The final clinical diagnoses in the benign liver lesions were liver cirrhosis, various types of chronic hepatitis, liver abscess, and hemangioma. Using the defined histologic, cytologic, and clinical criteria for malignant and benign liver diseases, the sensitivity of FNA cytology for the diagnosis of malignancy was 80.7%, while the specificity and positive and negative predictive values were 98.9%, 99.3% and 73.8% respectively. The overall diagnostic accuracy rate of FNA cytology was 87.2%.

Sensitivity = proportion of correctly diagnosed malignant lesions.

Specificity = proportion of correctly diagnosed benign lesions.

Table 4 shows the effect of repeated FNA on

the accuracy of liver disease diagnosis. In 37 patients clinically suspected of having malignant liver disease, nondiagnostic or benign cytologic diagnosis was made in 18 patients, thus increasing the sensitivity and decreasing the false-negative rate. The one case originally classified as malignant (false-positive cytologic finding) was, on review of the cytologic slides, subsequently classified as benign lesion with marked cellular atypia.

One case of non-fatal pneumothorax was the only major complication following the procedure, while pain and tenderness at the puncture site was not an infrequent complaint.

The median survival of patients with malignant liver disease was 2 months (range, 1-19 months), whereas the median survival of patients who died of benign liver disease was 12 months (range, 1-95 months).

**Table 1 Characteristics of patients with final diagnosis of liver disease**

	Malignant	Benign
Number of patients	171	94
Male	99	46
Female	72	48
Age (years)		
Median	69	67
Range	22-99	7-86
Symptoms (% of patients)		
Weight loss	71.3	48.9
Abdominal pain	64.7	51.0
Jaundice	18.8	19.4
Signs (% of patients)		
Hepatomegaly	74.3	45.7
Palpable liver mass	19.9	5.3
Ascites	16.5	15.3
Abdominal mass	7.6	5.1
Abnormal liver tests (% of patients)		
Alkaline phosphatase	88.9	60.6
Aspartate aminotransferase	48.2	22.4
Bilirubin	44.1	36.7

**Table 2 Direct fine-needle aspiration (FNA) diagnosis for liver lesions compared with the final diagnosis**

Direct FNA cytology	Final diagnosis	
	Malignant	Benign
Non-malignant	49	99
Atypical-reactive	03	05
Suspicious	16	0
Malignancy	135	1
Total	203	105

**Table 3 Relationship between nonguided fine-needle aspiration cytodiagnosis and type of suspected malignant liver lesions demonstrated by different kinds of imaging liver scanning among patients with malignant liver disease**

Type of imaging and lesions *	No. of imagings	True-positives	False-negatives	True-negatives	False-positives
Radioisotope					
Unifocal	35	23	5	7	0
Multifocal	96	71	17	7	1
US					
Unifocal	21	15	2	4	0
Multifocal	61	46	11	3	1
CT					
Unifocal	18	6	1	1	0
Multifocal	9	5	3	1	0

\* Patient may have more than one imaging scanning.

**Table 4 Accuracy of non-guided FNA cytodiagnosis according to first FNA (number of FNAs) or most meaningful FNA when it was repeated (number of patients)**

	FNAs No. (%)	Patients No. (%)
True positive	151(74.4)	138(80.7)
True negative	104(99.0)	93(98.9)
False positive	1(1.0)	1(1.1)
False negative	52(25.6)	33(19.3)
Non-diagnostic	24(7.2)	14(5.0)
Total	332	279

## DISCUSSION

FNA is a procedure available for more than two decades. FNA of the liver guided by US or CT has proven to be a safe and accurate method for diagnosing hepatocellular carcinoma<sup>[1-8]</sup> and liver metastases<sup>[3,9-11]</sup>. The most important requirement for such cytodiagnosis is a representative sample from the lesion. Except for some cases of well-differentiated hepatocellular carcinoma, the identification of malignancy in liver aspirate can be made by any experienced cytopathologist (our cytopathologist has a high expertise in obtaining an accurate diagnosis by FNA). The reported sensitivity of US- and CT-guided FNA ranges between 66.9% and 100%<sup>[12-28]</sup>. In the present study, the sensitivity, specificity, and positive and negative predictive values of nonguided FNA for cytodiagnosis of liver lesions were 80.7%, 98.9%, 99.3% and 73.8%, respectively. The overall accuracy rate was 87.2%. These data indicate that the diagnostic accuracy of nonguided FNA of liver lesions is similar to imaging-guided FNA.

What, in the present study, produced representative tissue sampling by nonguided FNA ① Sampling representing a larger liver volume: this was achieved by a number of aspirations in various directions (multiple insertion points) and by multiple (6-8) long passes in each aspiration; ② direct sampling by aspiration of palpable liver masses including cleaning of the needle with saline solution after each pass to remove residual cellular material and/or debris: this explanation applies to 19.9% of patients (34 out of 171) with malignant liver diseases; and ③ large parts of the liver being affected: imaging scannings suggesting malignant multifocal lesions were more prevalent than those indicative of unifocal lesions. Thus, among 230 liver scans suggesting malignancy, 166 (79%) pointed to multifocal lesions and only 64 (21%) to unifocal ones.

Furthermore, nondetection of pathologic findings by imaging liver scans does not preclude the presence of malignancy. Heiken *et al.*<sup>[30]</sup> prospectively evaluated the ability of CT to detect malignant lesions in eight patients who subsequently underwent hepatic lobectomy or transplantation. Among the 37 malignant lesions demonstrated by

pathologic evaluation, only 14 (38%) were detected by contrast-enhanced CT, but none of the 18 lesions smaller than 1cm in diameter were detected by the CT. We therefore suggest that actual malignancy is more frequent than its on-screen appearance.

Histopathologic examinations of patients with rectal carcinoma showed that the depth and distance involvement of the tumor exceeds the macroscopically defined tumor border<sup>[31,32]</sup>. Consequently, although the aspirating needle does not necessarily aspirate the actual imaged lesion, it certainly aspirates some surrounding malignant cells since the enlarged liver is accessible to needles and do not require radiological visualization. This argument may be supported by the facts that 74.3% of patients with MLD had hepatomegaly which could only be attributed to malignancy and that the rate of malignant cytologic findings in patients with unifocal malignant liver lesion was only slightly less than that of patients with multifocal lesions (69% vs 73%).

The present study was conducted in order to establish the cytologic examination as a reliable diagnostic method. Evaluation of the diagnostic accuracy of our cytologic findings was carried out on three levels. In 62 (36.3%) of the 171 patients with MLD, the cytologic diagnosis was verified by histologic findings obtained by liver needle biopsy, at surgery, at autopsy or on histologic findings of malignancy from another site revealing malignant cells similar to those obtained by FNA of the liver. This constituted the highest level of verification. The cytologic diagnosis of malignancy was confirmed in 35 (20.5%) patients by matching with cytologic tumor cells obtained from other organs or from body fluids, and in 74 (43.2%) by clinical findings alone. The defined clinical findings suggesting malignancy were observed in only two (2.1%) of 94 patients with BLD and corresponding cytologic findings. In these two patients the survival time was shorter than 12 months due to cardiovascular events. The validity of the cytologic findings is also supported by the survival time. The median survival for patients in whom the cytologically diagnosed MLD was verified against histologic, cytologic and clinical findings was 2, 3 and 2 months, respectively.

There were 33 (19.3%) patients with false negative cytologic findings, which was due to failure to obtain a representative malignant sample rather than to misinterpretation of the smears. It has been shown that superficial nonrepresentative FNA of a malignant tumor may reveal only necrotic material, degenerative changes or inflammatory reactions, which are frequently observed but do not reveal the presence of an underlying tumor<sup>[19]</sup>. In order to lower the rate of false-negative cytologic findings, we suggest that FNA should be repeated in patients clinically suspected of having malignancy despite negative cytologic findings. In doing so, we were able to increase the sensitivity of the cytologic

findings from 74.4% to 80.7%. Negative cytologic findings must be viewed with caution because of their false-negative rate (19.2%). However, because a malignant cytologic diagnosis is considered to be equivalent to a malignant histologic diagnosis, high specificity is a necessary requirement. In our series one false-positive cytologic diagnosis due to marked cellular atypia was reported. False-positive cytologic diagnoses have been reported in the literature<sup>[9,13,19,20]</sup>, ranging from 4% (20) to 20% (9). One case of pneumothorax is the only major complication reported following the procedure<sup>[33]</sup>, while pain, tenderness and local skin hemorrhage at the puncture site were not infrequent. In general, use of a thin (23 gauge) needle is usually safe and is less likely associated with major complications such as bleeding.

The results of this retrospective study may lead to the impression that FNA is easy and accurate for use by physicians who perform FNA. However, it does not mean to replace the current general practice of ultrasound guided needle biopsy in major centers, and does not provide rejection of available and more useful methods, particularly in the diagnosis of localized lesions of the liver. The aspiration procedure seems excessive for routine use with potential for complications and this study indicates that the procedure could be cut short by early findings of abnormal cells. Moreover, as funding for health care becomes increasingly a global issue of paramount importance, a less-time consuming and less expensive procedure with high clinical benefit for both diagnosis and therapy will be the goal of clinicians, health care policymakers, and patients. Our data suggest that nonguided (direct and blind) FNA of palpable and nonpalpable liver lesions is a simple, accurate and cost-effective method that allows rapid microscopic diagnosis. When repeated nonguided FNA fails to demonstrate malignancy, guided FNA should be considered.

## REFERENCES

- 1 Geboes K, Bossaert H, Nijs L. Carcinoma of the liver: cytopathologic diagnosis. *J Am Geriatr Soc*, 1978;26:411-413
- 2 Tao LC, Donat EE, Ho CS, McLoughlin MJ. Percutaneous fine needle aspiration biopsy of the liver. Cytodiagnosis of hepatic cancer. *Acta Cytol*, 1979;23:287-291
- 3 Rosenblatt R, Kutcher R, Moussouris HF, Schrieber K, Koss LG. Sonographically guided fine-needle aspiration of liver lesions. *JAMA*, 1982;248:1639-1641
- 4 Jacobsen GK, Gammelgaard J, Fugløj M. Coarse needle biopsy versus fine needle aspiration biopsy in the diagnosis of focal lesions of the liver. Ultrasonically guided needle biopsy in suspected hepatic malignancy. *Acta Cytol*, 1983;27:152-156
- 5 Gondos B, Forouhar F. Fine needle aspiration cytology of liver tumors. *Ann Clin Lab Sci*, 1984;14:155-158
- 6 Tao LC, Ho CS, McLoughlin MJ, Evans WK, Donat EE. Cytologic diagnosis of hepatocellular carcinoma by fine needle aspiration biopsy. *Cancer*, 1984;53:547-552
- 7 Tatsuta M, Yamamoto R, Kasugai H. Cytohistologic diagnosis of neoplasms of the liver by ultrasonically guided fine-needle aspiration biopsy. *Cancer*, 1984;54:1682-1686
- 8 Kasugai H, Yamamoto R, Tatsuta M *et al*. Value of heparinized fine-needle aspiration biopsy in liver malignancy. *AJR Am J Roentgenol*, 1985;144:243-244
- 9 Ho CS, McLoughlin MJ, Tao LC, Blendis L, Evans WK. Guided percutaneous fine-needle aspiration biopsy of the liver. *Cancer*, 1981;47:1781-1785
- 10 Plafker J, Noshier JL. Fine needle aspiration of liver with metastatic adenoid cystic carcinoma. *Acta Cytol*, 1983;27:323-325
- 11 Holm HH, Torp-Pedersen S, Larsen T, Juul N. Percutaneous fine needle biopsy. *Clin Gastroenterol*, 1985;14:423-449
- 12 McLoughlin MJ, Ho CS, Langer B, McHattie J, Tao LC. Fine needle aspiration biopsy of malignant lesions in and around the pancreas. *Cancer*, 1978;41:2413-2419
- 13 Schwerek WB, Schmitz Moormann P. Ultrasonically guided fine-needle biopsies? in neoplastic liver disease: cytohistologic diagnoses and echo pattern of lesions. *Cancer*, 1981;48:1469-1477
- 14 Cornud F, Vissuzaine C, Sibert A, Lenoir S, Blangy S. Sensibilite de la ponction-biopsie a l'aiguille fine dans la diagnostic histologique des tumeurs malignes hepatiques et pancreatiques. *Gastroenterol Clin Biol*, 1985;9:47-50
- 15 Whitlatch S, Nunez C, Pitlik DA. Fine needle aspiration biopsy of the liver. A study of 102 consecutive cases. *Acta Cytol*, 1984;28:719-725
- 16 Bell DA, Carr CP, Szyfelbein WM. Fine needle aspiration cytology of focal liver lesions. Results obtained with examination of both cytologic and histologic preparations. *Acta Cytol*, 1985;30:397-402
- 17 Cochand-Priollet B, Chagnon S, Ferrand J, Blery M, Hoang C, Galian A. Comparison of cytologic examination of smears and histologic examination of tissue cores obtained by fine needle aspiration biopsy of the liver. *Acta Cytol*, 1987;31:476-480
- 18 Pinto MM, Avila NA, Heller CI, Criscuolo EM. Fine needle aspiration of the liver. *Acta Cytol*, 1988;32:15-21
- 19 Bogner C, Rougier P, Leclere J, Duvillard P, Charpentier P, Prade M. Fine needle aspiration of the liver and pancreas with ultrasound guidance. *Acta Cytol*, 1988;32:22-26
- 20 Pilotti S, Rilke F, Claren R, Milella M, Lombardi L. Conclusive diagnosis of hepatic and pancreatic malignancies by fine-needle aspiration. *Acta Cytol*, 1988;32:27-38
- 21 Nguyen GK. Fine-needle aspiration biopsy cytology of hepatic tumors in adults. *Pathol Annu*, 1986;21:321-349
- 22 Verma K, Bhargava DK. Cytologic examination as an adjunct to laparoscopy and guided biopsy in the diagnosis of hepatic and gallbladder neoplasia. *Acta Cytol*, 1982;26:311-316
- 23 Schultenover SJ, Ramzy I, Page CP, LeFebvre SM, Cruz AB Jr. Needle aspiration biopsy: role and limitations in surgical decision making. *Am J Clin Pathol*, 1984;82:405-410
- 24 Prior C, Kathrein H, Mikuz G, Judmaier G. Differential diagnosis of malignant intrahepatic tumors by ultrasonically guided fine needle aspiration biopsy and by laparoscopic/intraoperative biopsy. A comparative study. *Acta Cytol*, 1988;32:892-895
- 25 Farnum JB, Patel PH, Thomas E. The value of Chiba fine-needle aspiration biopsy in the diagnosis of hepatic malignancy: a comparison with Menghini needle biopsy. *J Clin Gastroenterol*, 1989;11:101-109
- 26 Civardi G, Fornari F, Cavanna L, Di Stasi M, Sbolli G, Buscarini L. Value of rapid staining and assessment of ultrasound guided fine needle aspiration biopsies. *Acta Cytol*, 1988;32:552-554
- 27 Silverman JF, Finley JL, O'Brien KF. Diagnostic accuracy and role of immediate interpretation of fine needle aspiration biopsy specimens from various sites. *Acta Cytol*, 1989;33:791-796
- 28 Buscarini L, Sbolli G, Cavanna L. Clinical and diagnostic features of 67 cases of hepatocellular carcinoma. *Oncology*, 1987;44:93-97
- 29 Edoute Y, Ben-Haim SA, Malberger E. Value of direct fine needle aspirative cytology in diagnosing palpable abdominal masses. *Am J Med*, 1991;91:377-382
- 30 Heiken JP, Weyman PJ, Lee JKT. Detection of focal hepatic masses: prospective evaluation with CT, delayed CT, CT during arterial portography, and MR imaging. *Radiology*, 1989;171:47-51
- 31 Chan KW, Boey J, Wong SKC. A method of reporting radial invasion and surgical clearance of rectal carcinoma. *Histopathology*, 1985;9:1319-1327
- 32 Madsen PM, Christiansen J. Distal intramural spread of rectal carcinomas. *Dis Colon Rectum*, 1986;29:279-282
- 33 Malberger E, Edoute Y, Nagler A. Rare complications after transabdominal fine needle aspiration. *Am J Gastroenterol*, 1984;79:458-460

# Prospect of gastroenterology and hepatology in the next century \*

Rudi Schmid

**Subject headings** gastroenterology; hepatology; next century

The task of predicting what Gastroenterology and Hepatology may look like in the coming century is a great personal challenge and at the same time an awe-inspiring assignment. Not only have these two medical specialties become very large and diversified but there are so many new discoveries and ideas that it is a capricious undertaking to attempt fore-telling which of them may become part of the next century's medical practice. I therefore will take the personal privilege of being highly selective, choosing only topics for discussion which I believe have a distinct potential of generating novel scientific concepts, fresh approaches or new therapeutic modalities.

Over the past few decades, the biological sciences which form the basis of contemporary medicine have evolved enormously, producing an ever-increasing volume of new information and technology that is keeping Gastroenterology and Hepatology changing and advancing at an accelerating pace. Looking back half a century to the end of WWII and China's liberation, it may seem astounding how elementary gastroenterology had been at that time. Modern science hardly had touched it and most of the diagnostic and therapeutic dogmas were still those of the 19th century. But over the past 50 years, Gastroenterology and Hepatology have profoundly been remade. We have witnessed a dramatic increase of insight into the causes and mechanisms of disease and our diagnostic and therapeutic capabilities have vastly expanded and improved, for example, the discovery of the viruses causing infectious hepatitis, of transplantation of the liver, pancreas and small bowel, or of the introduction of fiberoptic endoscopy. And to top it all, recall the recent revolution in peptic ulcer disease which

unceremoniously has toppled old dogmas about gastric acid and made it instead a readily curable infectious disease.

I believe with confidence that this dynamic evolution will continue and probably accelerate in the coming century. And there is no question that it will bring much novel and unanticipated clarification about currently obscure diseases. It will also greatly refine diagnostic procedures and expand therapeutic choices. What seems more difficult to predict though, is what directions this evolution will take, and how we are going to make use of the new opportunities and how we will pay for them.

## *Human Genome Project*

The Human Genome Project is a joint enterprise that undoubtedly will have an enormous and irreversible impact on the future of Gastroenterology and Hepatology. It probably is the largest international scientific project ever undertaken. Once its ultimate goals are reached, presumably early in the next century, the entire human genome will have been sequenced and mapped and it will be possible and perhaps become routine to screen an individual's genome from a simple blood sample. Genetic mutations which result in hereditary diseases of the gastrointestinal tract or the liver will readily be identifiable. Individuals or families at risk for a hereditary disease may be screened for the genetic defect. And eventually, such screening may become available even for prenatal use. It is likely, of course, that the function of many of the new genes identified by the sequencing initially will not be known and will have to be determined stepwise, one by one. This will be a huge task which may well take several decades of painstaking investigations. But once this has been accomplished, gastroenterologists of the future will look at intestinal and liver diseases from a vastly different perspective, and they will use treatments which are far beyond today's imagination.

The sequencing of the full human genome will have far-reaching consequences in many other ways. Many genetic diseases are polygenic, i.e., there is more than one allele in the same location or the phenotypic expression of a primary gene defect is modified by one or several additional as yet unidentified genes. This probably accounts for the

Rudi Schmid, M.D., Ph.D., F.R.C.P., M.A.C.P.  
Member of the National Academy of Sciences, U.S.A.  
Emeritus Professor of Medicine and former Dean University of California  
513 Parnassus Avenue, Room S-357  
San Francisco, California 94143-0410, USA  
Tel. +01 • 415 • 4762342, Fax. +01 • 415 • 4760689

\*Expanded and updated text of a previously published article in *World Journal of Gastroenterology*, vol. 4, Suppl. 2, Pages 1-3, October 1998.

Received 1999-05-01

wide spectrum of clinical expression that is seen in many inherited diseases. For example, homozygous Wilson disease, copper storage disease, may clinically present as progressive cirrhosis, as a severe chronic disease of the central nervous system, or as acute hemolytic anemia. This phenotypic variability probably reflects the polygenic nature of this disease, a hypothesis which is likely to be resolved by the successful sequencing of the human genome. Another example of highly variable expression of a genetic defect is observed in  $\alpha$ -1 antitrypsin deficiency type ZZ. Here, only 20% of the patients homozygous for the defect actually develop progressive liver disease and cirrhosis. In the majority of patients, the liver merely exhibits scattered hepatocytes bearing variable amounts of defective and hence misfolded and precipitated antitrypsin which accumulates in the cells, eventually killing them by apoptosis. The variation in phenotypic expression of this hereditary defect may reflect genetic differences in the activity of cellular metalloproteases fitted to degrade the precipitated antitrypsin. Again, the genome project is likely to resolve this puzzle.

Another benefit of the genome project will be identification of the genetic factors which determine individual susceptibility to environmental assaults, such as viral, bacterial or fungal infections or exposure to toxins or poisons. Clearly, different people respond to such noxious assaults differently. For example, some experts believe that inflammatory bowel disease, such as ulcerative colitis or Crohn's disease, may be the result of a genetically determined aberration of the immune response to the trillions of microorganisms inhabiting the intestinal lumen. To date, no such genetic immune defect has been identified but the sequencing of the genome may change this. A similar differentiated response is also observed in chronic alcoholism. Surprisingly, only 25% of chronic alcoholics develop cirrhosis of the liver. Why is it that the majority escapes hepatic injury? It clearly is not due to dietary factors or to a preferred alcoholic beverage. Rather, I suspect that this striking difference is caused by genetic factors which determine how the liver is reacting to the metabolic products or reactive oxygen radicals which are produced when alcohol is metabolized. Here, too, the sequencing of the genome in the next century may provide plausible answers.

The Human Genome Project is of importance also for the future of gene therapy for inherited diseases. This is because it will facilitate identification of the nature of the genetic error in a mutated gene e.g., transposition of a base pair, missense mutations, deletion of several nucleotide sequences etc. This information is crucial for construction of the new gene to be transposed. As you are aware, somatic gene therapy *in vivo* has

been used successfully in many animal models and in a few highly selected genetic defects in humans. There are still problems which need to be addressed, but I am confident that they will be resolved in the not too distant future. One of these problems concerns the vehicle or vectors which are used to transport the replacing gene to the targeted cells or organ. At present, this is usually accomplished by packaging it into liposomes, adeno or retroviruses, or more recently, adeno-associated viroids. But these RNA viruses often cause immune or toxic reactions which limit their usefulness as vectors. Moreover, it is difficult to target live viruses to specific cells or tissues in which the mutation is being expressed.

As an attractive alternative a highly imaginative new approach has been proposed (Kren *et al.* Nature Medicine, March 1998) which employs a chimeric RNA/DNA oligonucleotide embedded in a short stretch of DNA. This is coated with a polycation containing a ligand that permits targeting of specific cells. And it is the cells' own DNA mismatch repair mechanism which is used for integration of the new oligonucleotide into the cells' DNA. This new technology has been tested successfully for site-specific introduction of a single base-pair mutation in rat hepatocytes *in vitro* and *in vivo*. It is very promising particularly for gene therapy of hereditary diseases expressed in the liver and it undoubtedly will play a commanding role in the next century.

A second problem with current gene therapy is that the somatic cells selected for gene repair have a limited natural life span and then undergo apoptosis. A repaired gene therefore can be expressed no longer than the life span of its cell, which may range from a few days for intestinal mucosa cells to several hundred days for hepatocytes. To overcome this major limitation, one would need to repair the genetic defect in embryonic germ cells, an approach which at present is neither possible nor ethically justifiable. A more promising design might be to target gene therapy to an organ's stem cell compartment. Stem cells are undifferentiated pluripotential progenitor cells, which can either replicate themselves or undergo differentiation to more mature cells. (Science, March 5, 1999). Such pluripotential stem cells have been identified in, or isolated from, a variety of animal and human tissues, including bone marrow, intestinal mucosal crypts and brain. In the liver, unequivocal identification of stem cells has not yet been reported, but so-called oval cells have been identified and isolated (Petersen *et al.* Hepatology, February 1998). Ovalocytes are believed to represent stem cell-derived intermediary precursor cells which are able to differentiate into hepatocytes or bile ductular cells (Matsusake *et al.* Hepatology, March 1999). They typically are found in regenerating liver under experimental conditions in

which replication of mature hepatocytes has been blocked. Since ovalocytes' differentiation potential is limited, identification of the authentic hepatic stem cell compartment currently is a top research priority. Once this has been accomplished, it should be feasible to transpose new genetic information into the stem cells' genome thereby making it available indefinitely to daughter cells. I am confident that in the coming century, such technology will become available which would represent a true breakthrough in gene therapy of a large number of hereditary diseases. At present, of course, permanent cure of hereditary diseases of the liver, such as Crigler-Najjar disease, OTC deficiency and hereditary analbuminemia, can be accomplished only by orthotopic liver transplantation.

Other new and promising applications of gene therapy recently have been described for the treatment of malignant tumors or cancer metastases in the liver. The trick here obviously is to package the genetic information to be transposed in a vehicle that is able to recognize specific molecular features of cancer cells, particularly cell membrane receptors or membrane-bound antigens. The majority of malignant tumor cells exhibits mutations in genes expressing so-called cancer repressor proteins, such as p53, p16 and others, which act primarily by controlling the cells' mitotic cycle. When these genes are mutated or lost, the result is unregulated cell replication and tumor growth. In animal models, gene therapy targeted specifically to surface receptors of malignant cells was able to successfully reconstitute functioning p53 or p16 genes, resulting in sustained tumor shrinkage and prolonged survival. In an alternative approach, the DNA sequence to be transposed into tumor cells was coupled to a monoclonal antibody which recognized a glycoprotein abundantly expressed in hepatocellular carcinomas (Mohr *et al. Hepatology*, January 1999). Although to date, these and other novel techniques of gene therapy have been tested only in experimental animals or in cell cultures, they obviously have great promise for cancer therapy of the future and eventually may substitute for surgery, radiation or chemotherapy.

I have discussed the Human Genome Project and particularly gene therapy in some detail because within their frame of reference both will have an epochal impact on the future practice of Gastroenterology and Hepatology. But the enormous advances in the basic biomedical sciences, particularly in molecular and cell biology and in molecular virology and genetics, will literally revolutionize the way physicians of the future will think about mechanisms of disease. And the next generation of gastroenterologists and hepatologists will be handed a staggering array of new therapeutic modalities, most of which have not yet been invented. To illustrate what I mean, I arbitrarily

have chosen for discussion three recent major scientific contributions which I believe have the potential to make an immense impact on clinical medicine of the future.

The first scientific break-through is the so-called nucleic acid or naked DNA vaccine. As you know, most of the currently available antiviral vaccines consist of attenuated live DNA or RNA viruses which have lost most of their virulence but retained their antigenic potential. Examples are vaccines against viral hepatitis, poliomyelitis, measles, varicella, yellow fever, etc. All of these, of course, are modeled, as it were, after Edward Jenner's classic experiment with cowpox as protection against the deadly smallpox. Although most of these live vaccines are highly protective, reservations often are expressed whether avirulent viruses could spontaneously undergo back mutation to a more virulent form; or whether attenuated live viruses could cause unsuspected morbidity decades after they had been used in a vaccine. The advent of recombinant DNA technology now has made it possible to design novel vaccines which provide strong and sustained antigen expression but exclude these lingering doubts about live-vaccines' safety.

The principle of this new approach is relatively simple. A gene from a pathogenic microbe encoding a microbial antigen, is spliced into a bacterial plasmid. The vaccine consisting of the plasmid bearing the spliced gene, is injected into muscle tissue where it directs the muscle cells to manufacture microbial antigen. The latter evokes a sustained immune response, involving both, antibody formation and a T-cell response. Although, to date, this new naked DNA vaccine has been tested only in experimental animals, persistent high titers of circulating antibodies have been obtained and the animals were protected against infection. It is thus evident that this new approach to vaccination has great promise and is likely to be a relatively inexpensive procedure. Indeed, naked DNA vaccine looks like the vaccine of the 21st century.

#### TRANSPLANTATION OF ISOLATED SYNGENEIC HEPATOCYTES

The second subject I have selected for discussion is still in its experimental phase but its great potential for future medical applications already is unmistakable. It concerns the transplantation of isolated syngeneic hepatocytes into a recipient's liver *in vivo*. Development of such a technique for clinical use obviously would open new avenues not only for correction of genetic defects, but also for the management of acute hepatic failure. It eventually may contend with, if not substitute for, orthotopic liver transplantation which in view of the scarcity of available organs might be a solace.

The first satisfactory technique for isolation of intact and functioning hepatocytes from

experimental animals was developed by Berry and Friend in 1969 (J Cell Biol, vol. 43). It stimulated a profusion of attempts to culture such isolated cells in vitro or to introduce them into various organs of congenic recipients *in vivo*, but with few exceptions, the cells failed to survive, let alone to proliferate. In 1982, Mito *et al* in Japan (Gastroenterology, Vol. 82) reported the exciting finding that in rats, syngeneic hepatocytes transferred into a recipient's spleen not only survived and retained their characteristic physiologic functions, but also proliferated. In fact, partial hepatectomy of the recipient a few days after transfer of hepatocytes into its spleen greatly magnified the number of mitotic figures in the transplanted cell population. And then, in 1991, Gupta *et al* (Proc Natl Acad Sci USA, Vol. 88) announced the surprising observation that a major fraction of the hepatocytes extant in the spleen eventually migrated to the host's liver where they were fully integrated into existing liver cell plates, properly functioning and apparently surviving indefinitely (*Hepatology*, February 1999).

Since the spleen is a relatively small organ, only a limited number of donor hepatocytes can be transferred to the liver with this procedure. Nonetheless, in rats and mice, it was able to at least partially correct genetic defects such as analbuminemia and unconjugated hyperbilirubinemia. Fortunately, a complementary experimental stratagem has been developed (Laconi *et al*. Am J Pathol, Vol. 153, 1998) which allows for a significant increase of the number of donor hepatocytes which can be delivered to the liver via the spleen. This consists of preparatory treatment of the designated recipient animal with the pyrrolizidine alkaloid retrorsine which is taken up selectively by the liver. It blocks the resident hepatocytes' cell cycle and therefore suppresses their proliferative potential. When combined with a subsequent two-third hepatectomy, the proliferative thrust generated by this resection is lost on the blocked resident hepatocytes thereby greatly favoring the transplanted cells. In preliminary studies with this approach, one to two months after the procedure, up to 80 percent of the recipient liver's cells consisted of transplanted hepatocytes and their progeny.

Although these are unusually exciting experimental findings, in its present form, this technology clearly is far from being applicable to clinical medicine. Nonetheless, I believe that on the basis of the new scientific information and technical expertise gained from these experiments, it will only be a question of time until a clinically acceptable and promising version of this approach will be developed. Given the rapid progress in research on inducible immune tolerance, it even may become possible to use allogeneic hepatocytes for transplantation instead of being limited to

syngeneic donor cells. To start with, I can think of two important groups of liver diseases in which hepatocyte transplantation via the spleen may be the therapeutic approach of choice. One is fulminant hepatic failure of variable etiology, including potentially fatal tylenol poisoning, in which the number and/or condition of surviving liver cells during the acute phase may be insufficient to sustain life and eventual recovery. The other consists of genetic defects expressed in the liver for which conventional gene therapy may be unavailable or lacking promise. These include  $\alpha$ -1 antitrypsin deficiency type ZZ, Wilson disease, analbuminemia, Crigler-Najjar disease and several others. Two different technical approaches are possible. One is to transplant hepatocytes obtained from a syngeneic donor; the other is to use the patients' own hepatocytes after the genetic defect had been corrected *ex vivo* with DNA supplied by an unrelated donor. Either approach would seem attractive and technically feasible. I am confident that in the next century, this cellular approach to liver transplantation will become a very important and frequently used procedure.

#### ACTIVE BIDIRECTIONAL EXCHANGE OF NUCLEATED BLOOD CELLS BETWEEN FETUS AND MOTHER

The third scientific issue that I wish to discuss is really a working hypothesis, but one that is supported by powerful, though indirect, evidence. It concerns the recent demonstration that in pregnancy there often an active bidirectional exchange of nucleated blood cells between fetus and mother, producing what has been called microchimerism. In the maternal circulation, immune-competent fetal cells are detectable not only during pregnancy but often for several decades thereafter (Bianchi *et al*. Proc Natl Acad Sci USA, Vol. 93, 1996). It is unknown, of course, how these immunologically foreign cells are able to survive and proliferate in the mother and what consequences, if any, this may have for her own immune system.

The original discovery in maternal blood of cyncytial trophoblasts derived from fetal placenta was recorded in 1959 (Lewis Thomas *et al*. Trans Assoc Am Phys, Vol. 72). At that time, identification of these giant multinucleated cells was possible only by morphological means. But in the last decade, much more refined technology has become available for cell identification and isolation, such as polymerase chain reaction and fluorescence-activated cell sorters. With these new methods, forty middle-aged women were studied, all of whom had given birth to at least one son over the past three decades. The DNA of the Y chromosome was used for identification of male fetal cells in the mother's blood. Quantitative results were expressed in terms of the number of male fetal-cell DNA equivalents identified in a

specified sample of maternal blood (Nelson *et al.* The Lancet, Vol. 351, 1998). In the blood of healthy women aged 35.61, the range of male cell DNA equivalents was found to be very low (range 0.2, mean 0.38). But surprisingly, in women with established systemic sclerosis, a presumably autoimmune disease, the values were 30 times higher (range 0.61, mean 11.1, *P value* = 0.0007). In a comparable albeit less carefully controlled study of a larger group of women suffering from systemic sclerosis, male DNA sequences were identified in maternal blood in 46 percent, but only in 4 percent of healthy controls (Artlett *et al.* N Engl J Med, Vol. 338, 1998). These striking findings demonstrate not only a much higher incidence of fetal microchimerism in women with systemic sclerosis, but also a much more elevated level of fetal-cell DNA equivalents in the patients as compared to healthy controls.

To interpret these startling novel observations, Nelson in 1996 proposed the bold but attractive hypothesis that many chronic diseases of supposedly autoimmune nature in fact may be the result of allogeneic fetal cells which during pregnancy had gained access to the maternal blood and subsequently had engrafted and are surviving in the mother for decades (Arthritis Rheum, Vol. 39, 1996). This almost heretic hypothesis is bolstered by a number of supporting observations, such as the following:

① Many diseases of supposedly autoimmune etiology have a strong female predilection, particularly those affecting the liver, such as autoimmune hepatitis, primary sclerosing cholangitis, systemic sclerosis and primary biliary cirrhosis; the last has a female-to-male ratio of almost 10:1.

② All of these presumably autoimmune diseases exhibit morphological, immunological and chemical features characteristic of graft-versus-host disease which is a chimeric condition observed in recipients of allogeneic stem cell or bone marrow transplantations.

③ Moreover, in most of these supposedly autoimmune diseases and in graft versus host disease, intrahepatic bile ducts are a principal target of the pathological process. Furthermore, all of the above diseases tend to be associated with accessory "autoimmune" phenomena, such as Sj-gren's syndrome, systemic sclerosis, the CREST syndrome, thyroid dysfunction and others.

Although these diverse clinical observations persuasively imply a common pathogenic mechanism for this group of diseases, by themselves they of course do not prove this novel hypothesis. But I believe that in the coming century, this issue will receive great attention and will emerge as one of immunology's leading scientific problems. And when all the scientific information is in, I would not be surprised if Nelson's hypothesis would turn out to be

correct.

The three novel scientific contributions which I have discussed above are examples of work that has passed through most of its experimental phase and whose exciting potential for clinical application is quite obvious. It seems just a matter of time until it will be ready for testing in humans. But we should realize that there still are countless obscure diseases for whose full exploration we currently lack the required intellectual basis and experimental tools. It is in these areas that I expect molecular and cell biology, virology and genetics of the future to provide the necessary conceptual framework and methodology to make progress and achieve scientific breakthroughs.

One of these areas is the vast field of viral hepatitis, particularly of the types B and C which world-wide are causing immense morbidity and mortality. Despite recent remarkable advances, we still do not understand how these viruses are surviving indefinitely and how they are causing chronic liver injury nor do we have effective, reliable and safe therapies to arrest their progression, let alone to achieve permanent cure. Some of us are old enough to recall the complete failure of steroid treatment of chronic active hepatitis B which only a few decades ago had been flaunted as the ultimate therapy for this chronic liver disease. Against this background, the current hyperbole about interferon treatment of chronic viral hepatitis appears somewhat uncritical, if not misleading. I hope and actually anticipate that early in the next century, new scientific information and technology will become available which will allow development of a definitive therapy for chronic viral hepatitis which causes no more than minor side effects to the patient and whose costs are affordable.

#### MOLECULAR DIAGNOSTICS

And finally, the rapid evolution of molecular biology has created a new discipline, molecular diagnostics, which is offering an ever-increasing number of tests of previously unthinkable variety, sophistication and sensitivity. For example, molecular techniques already are used to quantitate viral loads in viral hepatitis. But one of molecular diagnostics' most promising applications will be in the search for new infectious agents which to date have escaped detection by available staining or immunological methods. As you are aware, several gastrointestinal diseases, previously of unknown etiology, have recently been found to be caused by newly discovered microorganisms. These include, of course, peptic ulcer, but also Whipple's disease, bacillary angiomatosis and most recently, nanobacteria which cause connective tissue calcification in systemic sclerosis, sclerosing cholangitis and the CREST syndrome associated with primary biliary cirrhosis (Kajander, *et al.*

Proc Natl Acad Sci USA, July 1998). But there are several other gastrointestinal diseases of unknown etiology whose clinical and pathological features seem consistent with, if not suggestive of, an infective origin. These certainly include Crohn's disease, ulcerative colitis, granulomatous hepatitis and sarcoidosis and perhaps primary biliary cirrhosis and sclerosing cholangitis. Many experts of course have postulated an immunologic origin of these diseases and a recent report, that an antibody to tumor necrosis factor  $\alpha$  is profoundly down-regulating inflammation in Crohn's ileocolitis is supporting, but of course not proving, this hypothesis. (Baert *et al.* Gastroenterology, January 1999). Now, that highly sensitive molecular RNA and DNA probes and PCR have become available, I am confident that the hunt for elusive microorganisms will be intensified. And I would not be surprised if one or more of these diseases eventually would be discovered to have an infectious etiology.

#### DIAGNOSTIC AND THERAPEUTIC INSTRUMENTS AND MECHINERY

Predicting the future of Gastroenterology and Hepatology would be incomplete without briefly considering what new diagnostic and therapeutic instruments and machinery may become available in the next century. Here, progress, driven by intense market competition, is so rapid that precise predictions are quite impossible. Nonetheless, some trends seem to become detectable. Radiology is likely to progress by leaps and bounds, particularly spiral computerized tomography and three-dimensional imaging. They increasingly will replace invasive diagnostic procedures, including fiberoptic endoscopy. The only exception may be fiberoptic, laser-induced fluorescence spectroscopy which uses either tissue-intrinsic or extrinsically-elicited fluorescence; this is a novel procedure which appears to greatly enhance diagnostic accuracy. On the other hand, Magnetic Resonance Imaging, with its very expensive equipment, appears to be taking a back seat. And in gastrointestinal surgery, an ever-increasing proportion of invasive procedures will be performed by laparoscopy, which often makes hospitalization unnecessary and thereby reduces costs.

#### ECONOMICS OF HEALTH CARE

And this brings me to a true megafactor which in a major way will shape and restrain the practice of Gastroenterology in the next century. This is the economics of health care. All over the world, per capita costs of medical care are rising steeply, far outpacing the rate of inflation. To a considerable extent, this is due to the accelerated appearance on the market of new or advanced but always more

expensive machines, procedures and drugs which seem necessary to keep up with contemporary medicine. In the US, this continuing price increase has driven health care costs to a level, equaling 15% of gross domestic product (GDP), and other developed countries are not far behind. Although in the developing world, health care costs generally are lower, the cost increase in proportion is at least similar. It seems evident that if this trend should continue, health care eventually will consume a major part of the GDP. But I am afraid that as long as medical care continues to be unregulated or is remaining a competitive market commodity, it will be very difficult, if not impossible to bring quality of medical care and its costs into some sort of reasonable balance. Consider, for example, who would be qualified and publicly acceptable as decision makers. Would it fall to third party payers, that is insurance companies or health maintenance organizations. Or to employers who are funding the costs of health care Or to the medical care establishment, that is to physicians and hospitals Or perhaps to the government. However this paramount issue will be resolved, it will have an enormous impact on the future practice of Gastroenterology and Hepatology, both in the developed and in the developing world. As developing countries are striving to catch up with modern Western medicine, they rapidly are coming on mainstream, offering an almost unlimited market for aggressive pharmaceutical and medical equipment industries. This of course is further destabilizing the rapidly rising costs of adequate medical care.

#### CONCLUSION

In concluding, I believe that this brief glimpse into the science and practice of Gastroenterology and Hepatology in the next century is offering us a mixed perspective, one of an ever-widening disparity between rising opportunities on the one hand, and strained resources on the other. I am afraid that unless this serious imbalance will be dealt with early in the next century, the practice of Gastroenterology and the quality of health care world-wide will suffer. We need to learn how to reduce expenses by voluntarily lowering our dependence on technical procedures and complex equipment, and by avoiding use of expensive but only marginally effective medications and surgical interventions. And last but not least, in hopelessly ill patients, we should have the courage to abstain from using every possible means at our disposal to prolong dying and suffering, as unreasonable terminal care is one of modern health system's most expensive components. These, I am afraid, will be painful adjustments for the medical establishment but they must be faced better sooner than later.

# Escherichia Coli O157: H7 and Shiga-like-toxin-producing Escherichia Coli in China \*

XU Jian-Guo, CHENG Bo-Kun and JING Huai-Qi

**Subject headings** Escherichia coli O157:H7; Shiga-like-toxin; enteritis

*Escherichia coli* (*E. coli*) is one of the facultative anaerobes of the human intestinal tract, usually harmless. Infections due to pathogenic *E. coli* may result in urinary tract infections, sepsis, meningitis and enteric disease. Diarrheagenic *E. coli* has been classified into several categories, such as enterotoxigenic *E. coli* (ETEC), entero-invasive *E. coli* (EIEC), entero-pathogenic *E. coli* (EPEC), entero-aggregative *E. coli* (EaggEC) and entero-hemorrhagic *E. coli* (EHEC). A variety of virulence or potential virulence factors for diarrheagenic *E. coli* have been identified. The nomenclature of diarrheagenic *E. coli* is based on virulence factors<sup>[1,2]</sup>.

In 1977 Konowalchuk *et al*<sup>[3]</sup> reported that some strains of pathogenic *E. coli* O26 : H11 produced a toxin with a profound cytopathic effect on Vero cells, and named it verotoxin (VT). O'Brien *et al* noted<sup>[4]</sup> that the VT reported by Konowalchuk *et al*<sup>[3]</sup> was strikingly similar to Shiga toxin (Stx) produced by *Shigella dysenteriae* type 1, and it could be neutralized by anti-Stx, thus a new nomenclature, Shiga-like toxin (SLT), appeared. An alternative nomenclature is "Shiga toxin" (ST), which indicated that the specific cytotoxin described by Konowalchuk *et al*<sup>[3]</sup> is essentially identical at the genetic and protein levels with the Stx produced by *S. dysenteriae* I discovered some 100 years ago. Consequently, SLT, ST and VT have been used interchangeably, resulting in the name of verotoxin-

producing *E. coli* (VTEC), shiga-like-toxin-producing *E. coli* (SLTEC) and shiga-toxin-producing *E. coli* (STEC) coexisted in literature<sup>[5]</sup>. However, it must be noted that *E. coli* O157 : H7 is the main serotype of EHEC recognized at present<sup>[1,2,6]</sup>. Hemorrhagic colitis (HC) and hemolytic uremic syndrome (HUS) are life threatening, which are often caused by STEC or EHEC. So far as the diseases are concerned, *E. coli* O157 : H7 should belong to EHEC. All of the EHEC strains are believed to be pathogenic. As for its toxin, *E. coli* O157 : H7 should belong to VTEC, SLTEC or STEC. However, not all of the STEC strains could cause HC or HUS<sup>[7]</sup>. The confusion from the nomenclature may be clarified in future when the pathogenic mechanisms of bacteria are fully understood.

Food-borne outbreaks of SLTEC disease appear to be increasing in the world. Mass-produced and mass-distributed food can involve large numbers of people in short time. SLTEC strains belong to a very diverse range of serotypes, among which O157 : H7 is most commonly associated with large outbreaks<sup>[8]</sup>. In the summer of 1996 in Japan, a largest outbreak in the world caused by *E. coli* O157 : H7 was reported, in which about 10 000 cases were identified<sup>[9]</sup>. Chinese government and society became aware of the importance of *E. coli* O157 : H7 from the Japanese outbreak. An informal national network for detection of *E. coli* O157 : H7 was organized in April 1997, involving about 30 public health laboratories from different provinces and municipalities.

## *E. coli* O157 : H7 IN CHINA

The studies of *E. coli* O157 : H7 in China can be divided into two phases. In phase 1, starting from 1986 up to August 1996, the bacteriologists who studied the pathogen were mainly motivated by their scientific interests, few organized projects were carried out<sup>[2]</sup>. In phase 2, starting from August 1996 up to now, the public health authorities and most of the scientists have paid more attention to *E. coli* O157 : H7, and a new trend of isolation of *E. coli* O157 : H7 has been attempted in various parts of China.

The first group of patients with HC caused by *E. coli* O157 : H7 were identified in Beijing in 1988,

Key Laboratory of Molecular Medical Bacteriology, Ministry of Health, Institute of Epidemiology and Microbiology, Chinese Academy of Preventive Medicine, Beijing 102206, China

Dr. XU Jian-Guo, male, born on 1952-04-19 in Pinglu County, Shanxi Province, graduated from Shanxi Medical University as a medical student in 1976, from Chinese Academy of Medical Sciences as graduate student with Master degree in 1982, from Chinese Academy of Preventive Medicine with doctoral degree in 1993, now professor of microbiology, majoring medical bacteriology, having 70 papers published.

\*Supported by Outstanding Young Scientist Award from National Natural Science Foundation of China, Grant No. 39625001.

**Correspondence to:** Professor XU Jian-Guo, Key Laboratory of Molecular Medical Bacteriology, Ministry of Health, Institute of Epidemiology and Microbiology, Chinese Academy for Preventive Medicine, Beijing 102206, China

Tel. +86 • 10 • 61739579, Fax. +86 • 10 • 61730233

Email. xujg@public.bta.net.cn

Received 1999-02-05

as the etiologic agents isolated in Xuzhou city, Jiangsu Province of China<sup>[10]</sup>. In the three years from 1986 to 1988, 24 of 486 sporadic diarrhea patients were diagnosed as having HC, 5 strains of *E.coli* O157 : H7 were isolated, all of which were hybridized with SLT1, SLT2 and EHEC specific probe<sup>[10]</sup>. In 1993, two strains of *E.coli* O157 : H7 were isolated from a patient with HC and a patient with HUS, in Shandong Province. In the same period, several groups of scientists failed to isolate *E.coli* O157 : H7 in other cities of China, possibly due to lack of proper diagnostic techniques and reagents. Kain *et al*<sup>[11]</sup> reported that, in a study carried out in Beijing, about 7% of fecal samples were collected from diarrhea children hybridized with EHEC probe pCVD419<sup>[6]</sup>. However, similar amount of positive samples were also observed in the control group, but without strain isolation. The 168 strains of EPEC isolated before 1982 were detected with SLT1, SLT2 and EHEC specific probes, no EHEC or STEC was found<sup>[2]</sup>.

In 1997, a Chinese national network for detection of *E.coli* O157 : H7 was organized, *E.coli* O157 : H7 strains were isolated from diarrhea patients in Zhejiang, Anhui Provinces and Ningxia Autonomous Region. Nine strains were isolated from pigs in Fujian Province. It was interesting to note that all of the 9 strains from pig source were negative for SLT1, SLT2, and Hly genes. In 1998, several public health laboratories in China have attempted to isolate *E.coli* O157 : H7 from various sources, such as diarrhea patients, pigs, cattle, food and cow's milk. A total of 48 strains were isolated from cattle, pigs and milk. Some strains were found to be hybridized with Hly, Sl1 or Sl2 gene probes, most of the strains, however, were not. And, this result was demonstrated and confirmed by PCR method in the reference laboratory. The *E.coli* O157 : H7 isolation data in China are summarized in Table 1.

**Table 1** *E.coli* O157 : H7 strains isolated in China

No. Strains	Year	Source	Hly <sup>a</sup>	SLT1	SLT2	Province
5	1986-1988	HC	+	+	+	Jiangsu
3	1993	HC, HUS	+	+	+	Shandong
1	1997	Diarrhea	+	+	+	Anhui
1	1997	Diarrhea	+	-	-	Zhejiang
1	1997	Diarrhea	+	ND	ND	Ningxia
1	1997	Diarrhea	-	-	-	Passenger
9	1997	Cattle	-	-	-	Fujian
2	1997	Food	+	+	+	Fujian
1	1998	Milk	+	+	+	Guangdong
2	1998	Food	ND	ND	ND	Guangdong
4	1998	Pig				Liaoning
1	1998	Cattle	+	+	+	Liaoning
2	1998	Cattle	+	ND	ND	Hebei
14	1998	Cattle	ND	ND	ND	Ningxia

<sup>a</sup>Hly: hemolysin gene.

It is shown in literature, that *E.coli* O157 : H7

strains have been isolated from samples of beef, lamb, deer, wild boar, ostrich, partridge, antelope, and reindeer<sup>[11,12]</sup>. Cattles have long been regarded as the principal reservoir of *E.coli* O157 : H7. STEC strains were found prevalent in the gastrointestinal tracts of other domestic animals, including sheep, pig, goat, dog, and cat<sup>[2,5]</sup>. Many domestic animals carrying pathogens are asymptomatic. Strains of *E.coli* O157 : H7 have also been detected in cats and dogs with diarrhea<sup>[2,5]</sup>. *E.coli* O157 : H7 can potentially enter the human food chain from a number of animal sources, most commonly by contamination of meat with feces or intestinal contents after slaughter. One of the most common sources of human *E.coli* O157 : H7 infections is hamburger patty, made from ground beef. Hence, most of the outbreaks of *E.coli* O157 : H7 infection all over the world have been linked to hamburgers. In the outbreak of United States in 1993, more than 700 people were infected, and over 50 cases of HUS were diagnosed. So far, this is the largest outbreak of *E.coli* O157 : H7 associated with hamburger.

In China, only few sporadic cases of *E.coli* O157 : H7 infections have been identified. No outbreak as yet has been reported. The strains of *E.coli* O157 : H7 were isolated from cattle, pigs and milk. These results suggest that risk of infection with these microbes existed in China. It occurred to us that the prevalence of *E.coli* O157 : H7 seems to be higher in pigs than one expected. It should be emphasized that the consumption of pork in China is very popular and the risk seems to be much higher than that from beef. Further investigation of *E. coli* O157 : H7 in pigs should be conducted in China. Fortunately, no known virulence gene was found in the strains isolated from pigs in China such as SLT1, SLT2 and hemolysin gene as well. However, it was reported recently that the SLT2 containing phage from sewage, as the phage containing virulence gene, could infect non-pathogenic *E.coli* rather easily. The risk of such microbe infection seems fairly high.

#### SLTEC OTHER THAN O157 : H7 IN CHINA

*E.coli* O157 : H7 has not been recognized as a big public health problem in China up to now. However, STEC seems to be serious<sup>[13]</sup>. In clinical or public health bacteriological laboratories, only EPEC, ETEC and EIEC used to be diagnosed by serotyping techniques. Nevertheless, it has been noted not infrequently that almost pure cultures of *E.coli* were seen and new varieties of *E.coli* were isolated from certain fecal samples of diarrheal patients, which could not be serotyped with the

typesera available. Whether they should be recognized as pathogenic *E.coli* or not still remains a question. We assumed that some of these strains isolated as *E.coli* might be pathogenic in nature, which had been overlooked because of lacking proper techniques for identification. In order to verify this hypothesis, we collected 174 named nonpathogenic *E.coli* strains in Beijing from 1988 to 1990 and detected them with DNA probes<sup>[14]</sup>. The DNA probes covered almost all the virulence genes reported, such as heat-stable toxin (ST) heat-labile toxin (LT), EPEC adherence factor (EAF), diffuse adherence gene (DA), EHEC specific probe pCVD419, EAggEC specific probe, 2.5 Kb specific probe for invasive plasmid (INV) of EIEC and Shigella-species, shiga-like toxin 1 or 2 (SLT1 or SLT2), EPEC attaching and effacing genes (*eae*). It was observed that 59.3% strains tested were hybridized with at least one of the used probes, with a higher percentage of (29.7%) *E.coli* strains hybridized with SLT2 and INV probes<sup>[13,14]</sup>.

In general, strains of EHEC and some of EPEC hybridize with SLT1 or/and SLT2 probe. INV probe is a 2.5-Kb fragment derived from the invasive plasmid of *S.flexneri* 2a, and used as a diagnostic tool specific for Shigella species and EIEC strains<sup>[14,15]</sup>. The fragment was subsequently sequenced and named invasive associated locus (*ial*). However, none of the known EIEC or Shigella flexneria species was found to hybridize SLTs probes<sup>[16]</sup>. To clarify the relationship between EIEC and some of our strains isolated, the invasive plasmid antigen BCD (*ipaBCD*), the key genes for invasive ability of EIEC and Shigella, were synthesized by PCR labeled by Digoxin and used as probe. The absence of DNA hybridization signals indicated a lack of *ipaBCD* genes in *E.coli* F171. We also found that *E.coli* F171 could not provoke keratoconjunctivitis in guinea pigs. Sereny test was used as a critical marker for virulence of EIEC and Shigella species. However, with HEP-2 cell assay, the *E.coli* F171 is able to invade the epithelial cells. The data suggested that the genes encoding invasive ability of *E.coli*-F171 differed from EIEC, and *E.coli* F171 was therefore not a member of EIEC<sup>[13,14]</sup>.

Adherence of bacteria to epithelial cells has been recognized as a virulence characteristic of enteric pathogen<sup>[1]</sup>. Three adherence patterns were defined i.e., localized adherence, diffuse adherence and aggregative adherence<sup>[17]</sup>. Many of our *E.coli* strains hybridized with SLT2 and INV DNA probes demonstrated HEP-2 cell aggregative adherence pattern<sup>[13,14]</sup>. However, none of them were hybridized with EAggEC specific probe, which

was derived from the genes encoding EAggEC adherence factor I (EAF/I), and used as an identification marker for EAggEC. The aggregative adherence pattern to HEP-2 cells is the characteristic feature as EAggEC strains<sup>[18]</sup>. Under electron microscope, a unique kind of fimbria was observed on the surface of cells of *E.coli* F171. The subunit size of the fimbriae protein was 19KDa, and the genes encoding the fimbriae were located on a 60 MDa plasmid. *E.coli* HB101 cells containing the cloned genes were able to adhere onto the HEP-2 cells. The analysis of N terminal amino acid sequence indicated that *E.coli* F171 has its unique features<sup>[14]</sup>.

The shiga-like toxins have been demonstrated as the virulence factors for *E.coli* strain, which could cause HC and HUS<sup>[19]</sup>. Many of EPEC and EHEC strains contain genes for SLT1 or SLT2. The toxin producing ability of *E.coli* F171 was studied with Vero cell assay, which was originally used for study SLTs since *E.coli* F171 was hybridized with SLT2 probe. Both cell culture filtrate and a crude toxin preparation of *E.coli* F171 were found toxic to Vero cells. The Vero cell toxicity of *E.coli* F171 could not be neutralized by SLT2 antibody. The fact that hybridization of *E.coli* F171 with SLT2 probe suggested that it has DNA fragment homologous to SLT2 gene or it has an entire SLT2 gene<sup>[14]</sup>.

The invasiveness, toxin production activity and epithelial cell adherence ability have been described as key features for EIEC, ETEC and EAggEC respectively<sup>[20]</sup>. *E.coli* F171 could adhere onto and invade into HEP-2 cells and produce toxins. It combines many key features of EIEC, EHEC, EPEC, and EAggEC. Based on the data obtained, it seems that *E.coli* F171 represents a new variety of STEC. Hence the name of enteric SLTs-producing and invasive *E.coli* (ESIEC) was proposed. Since 31.4% of collected *E.coli* strains were tested in our studies shared similar features as *E.coli* F171, infections presumably caused by this kind of pathogenic *E.coli* seems to be an important public health problem in China.

In order to confirm the virulence and pathogenesis to human beings, a study in adult volunteers was carried out. By oral in take of  $10^9$ - $10^{10}$  colony forming units (CFU) of *E.coli* F171, all of 8 volunteers developed diarrhea, 3 of 8 developed high fever ( $39.8^{\circ}\text{C}$ ). The incubation period ranged from 7 to 49 hours. Unformed stools were 3-6 times a day. The volumes of stools of 4 volunteers were above 1 000 mL a day. Antibiotic therapy was given to 5 of the 8 volunteers. No diarrhea was observed for the control group consisting of 4 volunteers, who ingested  $10^9$  CFU of

non-pathogenic strain *E.coli*-HB101. Typical clinical symptoms for ESIEC in volunteers were bowel movement, diarrhea, general abdominal pain, moderate fever and unformed stool. It was revealed that ingested *E.coli* F171 could colonize and replicate for up to 7 days. By examining the stool samples of the volunteers, it was observed that the bacteria could reach an amount of  $2.74 \times 10^{12}$  CFU. The strains isolated from the patient stool samples of volunteers were confirmed as *E.coli* F171 by specific antiserum in animal against it.

Although the human pathogenic nature of *E.coli* F171 was recognized, the key virulence factors of ESIEC have not been studied in detail. The pathogenic mechanism of ESIEC, for instance, has not been understood. The "pathogenicity island", which refers to the large chromosomal segment carrying genes involved in pathogenicity, has recently revolutionized our understanding of bacterial pathogenesis<sup>[21]</sup>. The GC content of pathogenesis islands is different from that of the other host chromosome, suggesting that they may originate from horizontal transfer between different bacterial general. The number of gram-negative bacterial species known to harbor pathogenicity islands has grown steadily, including uropathogenic *E.coli* (UPEC), EHEC, EPEC, *Helicobacter pylori*, salmonella typhimurium and *Vibrio cholerae*<sup>[21]</sup>. It is believed that there is no pathogenicity island in the non-pathogenic *E.coli*. We must investigate the pathogenicity island so as to confirm the medical significance of ESIEC. Recently, we have observed an *irp2* gene in many strains of ESIEC. The *irp2* gene is involved in iron uptake and has been considered as one of the virulence genes located on the high pathogenicity island (HPI) of *Yersinia*-species<sup>[22]</sup>. This gene was observed in many strains of adherent *E.coli* and in *E.coli* isolated from blood, but rarely observed in EPEC, EIEC or ETEC. No *-irp2-* was found in EHEC, *Shigella* and *Salmonella enterica* strains. It seems that pathogenicity island existed in ESIEC. The HPI of the *Y. pestis* is disseminated among species of the Enterobacteriaceae family which are pathogenic to humans.

## REFERENCES

- Levine MM. *Escherichia coli* that cause diarrhea: enterotoxigenic, enteropathogenic, enteroinvasive, enterohemorrhagic, and enteroadherent. *J Infect Dis*, 1987;155:377-389
- Xu JG, Qi GM. The clinical and epidemiological features of enterohemorrhagic *E.coli* and its diagnostic methods. *Chin J Epidemiol*, 1996;12:367-369
- Konowalchuk J, Speirs JI, Stavric S. Vero response to a cytotoxin of *Escherichia coli*. *Infect Immun*, 1977;18:775-779
- O'Brien AD, Holmes RK. Shiga and Shiga-like toxins. *Microbiol Rev*, 1987;51:206-220
- James CP, Paton AW. Pathogenesis and diagnosis of Shiga toxin-producing *Escherichia coli* infections. *Clin Microbiol Rev*, 1998; 11:450-479
- Levine MM, Xu J, Kaper JB, Lior H, Prado V, Ball T. A DNA probe to identify enterohemorrhagic *Escherichia coli* of O157 : H7 and other serotypes that cause hemorrhagic colitis and hemolytic uremic syndrome. *J Infect Dis*, 1987;156:175-182
- Xu JG, Chen BK, Wu YP, Huang LB, Deng QD, Lai XH. A new bacterial pathogen: entero adherent-invasive-toxigenic *E.coli*. *Chin Med J*, 1996;109:16-17
- Griffin PM, Tauxe RV. The epidemiology of infections caused by *Escherichia coli* O157 : H7, other enterohemorrhagic *E.coli*, and the associated hemolytic uremic syndrome. *Epidemiol Rev*, 1991; 13(suppl):60-98
- Fukushima H, Hashizume T, Kitani T. The massive outbreak of enterohemorrhagic *E.coli* O157 infections by food poisoning among the elementary school children in Sakai, Japan. 3rd International Symposium and Workshop on Shiga Toxin (Verotoxin) Producing *Escherichia coli* Infections. Melville, NY: Lois Joy Galler Foundation for Hemolytic Uremic Syndrome Inc. 1997: 111
- Xu JG, Quan TS, Xiao DL, Fan RR, Li LM, Wang CA. Isolation and characterization of *Escherichia coli* O157 : H7 strains in China. *Curr Microbiol*, 1990;20:299-303
- Kain KC, Barteluk RL, Kelly MT, He X, Hua G, Ge YA. Etiology of childhood diarrhea in Beijing, China. *J Clin Microbiol*, 1991;29: 90-95
- Clarke RC, Wilson JB, Read SC, Renwick S, Rahn K, Johnson RP. Verocytotoxin producing *Escherichia coli* (VTEC) in the food chain: preharvest and processing perspectives. In: Karmali, MA, Goglio AG eds. Recent advances in verocytotoxin producing *Escherichia coli* infections. Amsterdam, The Netherlands: Elsevier Science BV, 1994:17-24
- Xu JG, Cheng BQ, Wu YP, Huang LB, Lai XH, Liu BY. Cell adherence patterns and DNA probe types of *E.coli* strains isolated from diarrheal patients in china. *Microbiol Immunol*, 1996;40: 88-99
- Xu JG, Wu YP, Deng QD, Xiao HF, Hall R, Lai XH. Characterization of a Shiga -like toxin producing and invasive *Escherichia coli* strain: a possible new variety of diarrheagenic pathogen. In: Kusch GT, Kawakami M, eds. Cytokines, cholera and the gut. OMN Ohmsha, Japan: IOS Press, 1996:321-328
- Small PL, Falkow S. Development of a DNA probe for the virulence plasmid of *Shigella* spp. and enteroinvasive *Escherichia coli*. In: Leive L, Bonventre PF, Morello JA, Silver SD, Wu WC, eds. Microbiology. Washington D.C: American Society for Microbiology, 1986:121-124
- Smith HR, Scotland SM, Chart H, Rowe B. Vero cytotoxin production and presence of VT genes in strains of *Escherichia coli* and *Shigella*. *FEMS Microbiol Lett*, 1987;42:173-177
- Nataro JP, Kaper JB, Robins-Browne B, Prado V, Vial P, Levine MM. Patterns of adherence of diarrheagenic-*Escherichia coli* to HEp-2 cells. *Pediatr Infect Dis J*, 1987;6:829-831
- Vial PA, Robins-Browne B, Lior H, Prado V, Kaper JB, Nataro JP. Characterization of enteroadherent aggregative *Escherichia coli*, a putative agent of diarrheal disease. *J Infect Dis*, 1988;158:70-78
- Karmali MA. Infection by verotoxin-producing *Escherichia coli*. *Clin Microbiol Rev*, 1989;2:15-38
- Nataro, JP, Kaper JB. Diarrheagenic *Escherichia coli*. *Clin Microbiol Rev*, 1998;11:142-201
- Hacker J, Blum-Oehler G, Mühldorfer I, Tsch-pe H. Pathogenicity islands of virulent bacteria: structure, function and impact on microbial evolution. *Mol Microbiol*, 1997;23:1089-1097
- Schubert S, Rakin A, Karch H, Carniel E, Heesemann J. Prevalence of the "high pathogenicity island" of *Yersinia* species among *Escherichia coli* strains that are pathogenic to humans. *Infect Immun*, 1998;66: 480-485

# The Hsp90 chaperone complex-A potential target for cancer therapy ?

Beatrice D. Darimont

See article on page 199

## ORIGINAL ARTICLE

Down-regulation of Hsp90 could change cell cycle distribution and increase drug sensitivity of tumor cells.

## MAJOR POINTS OF THE COMMENTED ARTICLE

Using an antisense RNA approach, Liu *et al* studied the consequence of lowering Hsp90  $\beta$  expression in two human gastric (SGC7901, SGC7901/VCR), one hepatic (HCC7402) and one esophageal (Ec109) cancer cell line. For two of the investigated cell lines (SGC7901/VCR and Ec109) cell growth slowed down upon decrease of the Hsp90  $\beta$  level due to an increase in G1 cell phase. The growth rate of the SGC7901 cell line was unaffected by lowering the concentration of Hsp90  $\beta$ , however the duration of G1 was decreased while G2 increased. No Hsp90  $\beta$  dependent change in the growth was detectable for the hepatic cancer cell line HCC7402, which expressed Hsp90  $\beta$  in lower levels than the other cell lines. Upon lowering the Hsp90  $\beta$  concentration, all cell lines became more sensitive to chemotherapeutic drugs. Increases in the efficacy of mitomycin C (MMC) and cyclophosphamide (CTX) were generally modest (0-5 fold), although the SGC7901 cell line exhibited a 24.8 fold increased sensitivity to MMC. With the exception of the cell line SGC7901/VCR, dramatic effects were observed on the sensitivity of the cell lines to adriamycin (ADR) and vincristine (MMC) with a  $10^4$  fold and  $3 \times 10^4$  fold increase in sensitivity of SGC7901 to VCR, or Ec109 to ADR, respectively.

## COMMENTARY

Molecular chaperones are one of the life-guards of a living cell. They coordinate and execute basic and essential cell functions, such as facilitation of protein folding and oligomeric assembly of proteins, as well as the regulation of ligand binding and

release, subcellular localization and turnover of proteins<sup>[1,2]</sup>. They are important for cell viability, and have been proposed to act as evolutionary tools, that produce a pool of mutant proteins under stress conditions<sup>[3,4]</sup>. Not surprisingly, aberrant chaperone action has been linked to numerous diseases<sup>[5-8]</sup>, and the clinical interest in chaperones as targets for drug based treatments is increasing.

### *Hsp90 assembles into multiprotein complexes*

Hsp90, a highly conserved and ubiquitously expressed chaperone of animal and plant cells, is one of the most abundantly expressed proteins (1%-2% of the cytosolic protein in unstressed mammalian cells)<sup>[2,9-11]</sup>. Most eukaryotic cells contain at least two Hsp90 isoforms-the heat shock induced Hsp90  $\beta$  and the usually less regulated Hsp90  $\beta$ <sup>[12]</sup>. Another close relative, Grp94, is expressed in the endoplasmic reticulum<sup>[11,13]</sup>. Hsp90 assembles into large multiprotein complexes, that have partially overlapping compositions and include other chaperones such as Hsp70, Hip ("Hsp70-interacting protein"), Hop ("Hsp90-Hsp70 organizing protein", also called p60, Sti1), p23, and one of three large immunophilins FKBP51, FKBP52 (Hsp56), or Cyp40, which are peptidyl prolyl isomerases<sup>[2,10]</sup>.

### *Hsp90 folds and controls the activity of regulatory proteins involved in signaling*

The predominant role of these complexes may be to facilitate the maturation, functional regulation, cellular localization and stress-dependent protection and repair of proteins rather than to assist the folding of de novo synthesized proteins<sup>[14-16]</sup>. Interestingly, many of the substrates of these Hsp90 chaperone complexes are regulatory proteins, or proteins involved in structural organization such as actin and tubulin<sup>[2]</sup>. One of the best studied substrates of Hsp90 chaperone complexes are intracellular receptors, especially but not exclusively steroid receptors<sup>[10,17-22]</sup>. *In vivo* association of unliganded steroid receptors with Hsp90 chaperone complexes is required for optimal steroid binding<sup>[23-25]</sup>, and may also affect receptor subcellular trafficking<sup>[26]</sup>. Hsp90 chaperone complexes also assist in the folding, maturation, membrane localization and degradation of many

Department of Cellular and Molecular Pharmacology, University of California, San Francisco, USA

**Correspondence to:** Beatrice D. Darimont, Department of Cellular and Molecular Pharmacology, University of California, San Francisco, CA 941430450, USA

Fax. 415-502-8644

E-mail: darimon@itsa.ucsf.edu

Received 1999-05-17

protein kinases<sup>[2,10,20]</sup>, such as v-Src<sup>[27]</sup>, Raf<sup>[28]</sup>, eIF-2- $\alpha$ -kinase<sup>[29]</sup>, casein kinase II (CK II)<sup>[30]</sup>, mitogen-activated protein kinase (MEK)<sup>[31]</sup>, cyclin-dependent kinase 4 (CDK4)<sup>[32,33]</sup>, and the cyclin-dependent kinase regulator Wee1<sup>[34]</sup>. Association of these kinases with Hsp90 chaperone complexes is mediated by p50 cdc37, an homolog of the yeast cell cycle control protein, cdc37<sup>[33,35]</sup>. The ability to interact functionally with a wide variety of regulatory proteins suggests that Hsp90 chaperone complexes may also coordinate and establish crosstalk between different signal transduction pathways. A recent study by Le Bihan *et al*<sup>[36]</sup> gave evidence for modulation of progesterin- and glucocorticosteroid receptor-mediated transcription by calcium/calmodulin kinases (CaMK types II and IV), presumably through Hsp90 chaperone complexes.

#### ***The role of Hsp90 in cell cycling and cancer***

Hsp90 action has been connected to cell cycle and cell differentiation<sup>[2,37,38]</sup>, most likely as a consequence of their role in folding and functional regulation of intracellular receptors, protein kinases and other potential substrates such as p53<sup>[9,39]</sup>. Moreover, the expression pattern of Hsp90 itself can be cell cycle dependent<sup>[40]</sup>. Increased levels of Hsp90 (mostly Hsp90  $\alpha$ ) have been found in various malignant cell lines and cancers and usually correlate with vigorous proliferation of the malignant cells<sup>[2,41-44]</sup>.

In a complementary study Liu *et al*<sup>[45]</sup> (this issue) investigate the consequence of lowering Hsp90  $\beta$  expression in several human cancer cell lines using an antisense RNA approach. In agreement with the trend seen in other studies<sup>[41-44]</sup>, they find that in some but not all cancer cell lines growth slows upon decrease of the Hsp90  $\beta$  level, with various changes in cell cycle phasing. For one cell line, the hepatic cancer cell line HCC7402, growth and cell cycle phasing is not affected by reduced expression of Hsp90  $\beta$ . Thus, overexpression of Hsp90 is not essential for cancerous growth. In fact, in an invasive and tumorigenic subline of 8701-BC breast cells down-regulation of Hsp90  $\beta$  has been observed<sup>[46]</sup>. In view of the differences in the regulation of Hsp90  $\alpha$  and Hsp90  $\beta$ , it would be interesting to extend the studies of Liu *et al* to Hsp90  $\alpha$ , whose expression is usually more directly linked to the cell cycle than that of Hsp90  $\beta$ .

#### ***Hsp90 as target for anti-tumor drugs***

Pharmacologically, the influence of Hsp90 activity on tumor growth is well established. Hsp90 chaperone complexes are targets for several pharmacological drugs<sup>[2,9,47]</sup>. The antibiotic geldanamycin is an anti-tumor drug that binds to the

ATP/ADP binding site in the N-terminal domain of Hsp90<sup>[48]</sup>. Geldanamycin interferes with the folding, maturation, cellular localization and degradation of various intracellular receptors and kinases<sup>[2,9,47]</sup>, and initially was described as an inhibitor for cell cycle kinases<sup>[49]</sup>. Another, unrelated antibiotic, Radicicol, also binds to the ATP-ADP-binding site of Hsp90 and suppresses transformation by diverse oncogenes such as Src, Ras and Mos<sup>[50,51]</sup>. Geldanamycin prevents binding of p23 to Hsp90<sup>[19]</sup>, however whether its anti-tumor activity is due directly to this interference remains to be investigated. Although the role of ATP/ADP in the function of Hsp90 is not fully understood, the functional consequence of the binding of these structurally unrelated antibiotics to the Hsp90 ATP/ADP-binding site marks this site as an interesting target for drug design. Other potential and probably more selective drug targets in the Hsp90 chaperone complex are the immunophilins FKBP51, FKBP52 or Cyp40 that bind the immunosuppressants FK506, rapamycin or cyclosporin A<sup>[10,19]</sup>.

#### ***Hsp90 mediated multidrug resistance***

In addition of being target for several pharmacological drugs, Hsp90 chaperone complexes influence the sensitivity of cells to many drugs, and high Hsp90 expression is often associated with multidrug resistance<sup>[52]</sup>, a major impediment of successful cancer chemotherapy. In their present study, Liu *et al*<sup>[45]</sup> demonstrate that upon lowering the Hsp90  $\beta$  concentration the sensitivity of cancer cell lines to chemotherapeutic drugs increases, however the extent of these changes was strongly dependent on the drug. With exception of some cancer cell lines, their Hsp90  $\beta$  dependent increases in the efficacy are generally modest (0-5-fold) for the drugs mitomycin C and cyclophosphamide, and more dramatic (up to  $3 \times 10^4$ -fold) for the drugs adriamycin and vincristine.

The mechanisms underlying multidrug resistance appear to be complex and are not well understood. In many tumor cells multidrug resistance is associated with overexpression of either the 170 kDa P-glycoprotein (Pgp) or members of the ATP-binding cassette transporter superfamily, such as the multidrug resistance protein (MRP) or the breast cancer resistance protein (BCRP), that act as drug export pumps<sup>[53-55]</sup>. A third form of multidrug resistance (atypical MDR) correlates with quantitative or qualitative alterations in topoisomerase ii  $\alpha$ , that actively participates in the lethal action of cytotoxic drugs<sup>[56,57]</sup>. The mechanism of Hsp90 mediated multidrug resistance remains largely to be characterized. The contribution of Hsp90 might be a general strengthening of the stress response and the cellular

resistance to cytotoxic drugs. However, in some drug resistant cell lines Hsp90  $\beta$  was found to stabilize and enhance the function of Pgp<sup>[52]</sup> suggesting a more direct role of Hsp90 in regulating multidrug resistance.

## CONCLUSIONS AND PERSPECTIVES

Hsp90 chaperone complexes are vital and versatile coordinators and regulators of multiple signal transduction pathways. In higher organisms their action goes beyond that of a single cell and also affects complex regulatory systems such as the immune response. Hsp90, Grp94 and Hsp70 bind peptides and deliver them to MHC class I molecules, which increases the efficiency of the immune response<sup>[58]</sup> and often enhance tumor immunogenicity<sup>[59]</sup>. These pleiotropic functions make Hsp90 chaperone complexes ideal targets for the treatment of cancers.

Antisense Hsp90 mRNA expression, as used by Liu *et al*<sup>[45]</sup> is a powerful tool for regulating Hsp90 expression and reducing proliferation in some cancer cell lines. However, the inherent difficulty of selectively targeting antisense constructs to tumor cells impedes the usage of this strategy for clinical therapy. In contrast, the role of Hsp90, Grp94 and Hsp70 in tumor immunogenicity may offer new strategies for anti-tumor vaccination. Presently, the most promising strategy for an Hsp90 targeted therapy is the functional regulation of Hsp90 by drugs such as geldanamycin or radicicol. The solution of the molecular structures of Hsp90 : ATP/ADP and Hsp90 : geldanamycin complexes<sup>[48,60]</sup> allows the identification of structural features required for Hsp90 binding, and to develop new drugs with different pharmacological properties by structure based design. Other attractive targets for drug based regulation of Hsp90 chaperone complexes are the sites for the interaction with the kinase specific p50<sup>cdc37</sup> or immunophilins that appear to mediate specificity by directing Hsp90 chaperone complexes to particular substrates. Future elucidation of the composition, structure and function of those complexes will certainly open new possibilities for the treatment of cancer.

## REFERENCES

- Hartl FU. Molecular chaperones in cellular protein folding. *Nature*, 1996;381:571-579
- Csermely P, Schnaider T, Söiti C, Prohászka Z, Nardai G. The 90-kDa molecular chaperone family: structure, function, and clinical applications. A comprehensive review. *Pharmacol Ther*, 1998; 79:129-168
- Csermely P. Proteins, RNAs, chaperones and enzyme evolution: a folding perspective. *Trends Biochem Sci*, 1997;22:147-149
- Rutherford SL, Lindquist S. Hsp90 as a capacitor for morphological evolution. *Nature*, 1998;396:336-342
- Welch WJ. Mammalian stress response: cell physiology, structure/function of stress proteins, and implication for medicine and disease. *Physiol Rev*, 1992;72:1063-1081
- Burdon RH. Heat shock proteins in relation to medicine. *Mol Aspects Med*, 1993;14:83-165
- Jindal S. Heat shock proteins: applications in health and disease. *Trends Biotechnol*, 1996;14:17-20
- Brooks DA. Protein processing: a role in the pathophysiology of genetic disease. *FEBS Lett*, 1997;409:115-120
- Scheibel T, Buchner J. The Hsp90 complex-a super-chaperone machine as a novel drug target. *Biochem Pharmacol*, 1998;56: 675-682
- Pratt WB. The Hsp90 based chaperone system: involvement in signal transduction from a variety of hormone and growth factor receptors. *Proc Soc Exper Biol Med*, 1998;217:420-434
- Scheibel T, Buchner J. The Hsp90 family: an overview. In: Gething MJ, ed. Guidebook to molecular chaperones and protein catalyses. Oxford: Oxford University Press, 1997:147-151
- Krone PH, Sass JB. Hsp90  $\alpha$  and Hsp90  $\beta$  genes are present in the zebrafish and are differentially regulated in developing embryos. *Biochem Biophys Res Comm*, 1994;204:746-752
- Gupta RS. Phylogenetic analysis of the 90kD heat shock family of protein sequences and an examination of the relationship among animals, plants, and fungi species. *Mol Biol Evol*, 1995; 12:1063-1073
- Nair SC, Toran EJ, Rimerman RA, Hjermsstad S, Smithgall TE, Smith DF. A pathway of multi-chaperone interactions common to diverse regulatory proteins-estrogen receptor, fcs tyrosine kinase, heat shock transcription factor, HSF1, and the aryl hydrocarbon receptor. *Cell Stress Chaperones*, 1996;1: 237-250
- Johnson JL, Craig EA. Protein folding in vivo: unraveling complex pathways. *Cell*, 1997;90:201-204
- Nathan DF, Vos MH, Lindquist S. *In vivo* function of the Saccharomyces cerevisiae Hsp90 chaperone. *Proc Natl Acad Sci USA*, 1997;94:12949-12956
- Smith DF, Toft DO. Steroid receptors and their associated proteins. *Mol Endo*, 1993;7:4-11
- Bohen SP, Yamamoto KR. Modulation of steroid receptor signal transduction by heat shock proteins. In: The biology of heat shock proteins and molecular chaperones. Cold Spring Harbor: Cold Spring Harbor Laboratory Press, 1994:313-334
- Pratt WB, Toft DO. Steroid receptor interactions with heat-shock protein and immunophilin chaperones. *Endo Rev*, 1997;18:306-360
- Pratt WB. The role of the Hsp90 based chaperone system in signal transduction by nuclear receptors and receptors signaling via MAP kinase. *Annu Rev Pharmacol Toxicol*, 1997;37: 297-326
- Holley SJ, Yamamoto KR. A role for Hsp90 in retinoid receptor signal transduction. *Mol Biol Cell*, 1995;6:1833-1842
- Pongratz I, Mason GG, Poellinger L. Dual roles of the 90-kDa heat shock protein Hsp90 in modulating functional activities of the dioxin receptor. Evidence that the dioxin receptor functionally belongs to a subclass of nuclear receptors which require Hsp90 both for ligand binding activity and repression of intrinsic DNA binding activity. *J Biol Chem*, 1992;267: 13728-13734
- Picard D, Khurshed B, Garabedian MJ, Fortin MG, Lindquist S, Yamamoto KR. Reduced levels of Hsp90 compromise steroid receptor action *in vivo*. *Nature*, 1990;348:166-168
- Bohen SP, Yamamoto KR. Isolation of Hsp90 mutants by screening for decreased steroid function. *Proc Natl Acad Sci USA*, 1993; 11424-11428
- Nathan DF, Lindquist S. Mutational analysis of Hsp90 function: interactions with a steroid receptor and a protein kinase. *Mol Cell Biol*, 1995;15:3917-3925
- DeFranco DB, Ramakrishnan C, Tang Y. Molecular chaperones and subcellular trafficking of steroid receptors. *J Steroid Biochem Molec Biol*, 1998;65:51-58
- Xu Y, Lindquist S. Heat-shock protein Hsp90 governs the activity of pp60v-src kinase. *Proc Natl Acad Sci USA*, 1993;90: 7074-7078
- van der Straten A, Rommel C, Dickson B, Hafen E. The heat shock protein 83 (Hsp83) is required for Raf-mediated signalling in Drosophila. *EMBO J*, 1997;16:1961-1969
- Uma S, Hartson SD, Chen JJ, Matts RL. Hsp90 is obligatory for the hemeregulated eIF-2 $\alpha$  kinase to acquire and maintain an activable conformation. *J Biol Chem*, 1997; 272:11648-11656
- Miyata Y, Yahara I. The 90-kDa heat shock protein, Hsp90, binds and protects casein kinase II from selfaggregation and enhances its kinase activity. *J Biol Chem*, 1992;267: 7042-7047
- Stancato LF, Silverstein AM, Owens-Grillo JK, Chow YH, Jove R, Pratt WB. The Hsp90 binding antibiotic geldanamycin decreases Raf levels and epidermal growth factor signaling without disrupting

- formation of signaling complexes or reducing the specific enzymatic activity of Raf kinase. *J Biol Chem*, 1997;272:4013-4020
- 32 Dai K, Kobayashi R, Beach D. Physical interaction of mammalian CDC37 with CDK4. *J Biol Chem*, 1996;271:22030-22034
- 33 Stephanova L, Leng X, Parker SB, Harper JW. Mammalian p50Cdc37 is a protein kinase-targeting subunit of Hsp90 that binds and stabilizes Cdk4. *Genes Dev*, 1996;10:1491-1502
- 34 Aligue R, Akhavan-Niak H, Russell P. A role for Hsp90 in cell cycle control: wee 1 tyrosine kinase requires interaction with Hsp90. *EMBO J*, 1994;13:6099-6106
- 35 Kimura Y, Rutherford SL, Miyata Y, Yahara I, Freeman BC, Yue L, Morimoto RI, Lindquist S. Cdc37 is a molecular chaperone with specific functions in signal transduction. *Genes Dev*, 1997;11:1775-1785
- 36 Le Bihan S, Marsaud V, Mercier Bodard C, Baulieu EE, Mader S, White JH, Renoir JM. Calcium/calmodulin kinase inhibitors and immunosuppressant macrolides rapamycin and FK506 inhibit progesterin and glucocorticosteroid receptor-mediated transcription in human breast cancer T47D cells. *Mol Endo*, 1998;12:986-1001
- 37 Sato N, Torigoe T. The molecular chaperones in cell cycle control. *Annals New York Acad Sci*, 1998;851:61-66
- 38 Galea-Lauri J, Latchman DS, Katz DR. The role of the 90-kDa heat shock protein in cell cycle control and differentiation of the monoblastoid cell line U937. *Exp Cell Res*, 1996;226:243-254
- 39 Sepehrnia B, Paz IB, Dasgupta G, Momand J. Heat shock protein 84 forms a complex with mutant p53 protein predominantly within a cytoplasmic compartment of the cell. *J Biol Chem*, 1996;271:15084-15090
- 40 Jerome V, Vourc'h C, Baulieu EE, Catelli MG. Cell cycle regulation of the chicken Hsp90 $\alpha$  expression. *Exp Cell Res*, 1993;205:44-51
- 41 Ferrarini M, Heltai S, Zocchi MR, Rugarli C. Unusual expression and localization of heat shock proteins in human tumor cells. *Int J Cancer*, 1992;51:613-619
- 42 Yufu Y, Nishimura J, Nawata H. High constitutive expression of heat shock protein 90 $\alpha$  in human acute leukemia cells. *Leuk Res*, 1992;16:597-605
- 43 Franzen B, Linder S, Alaiya AA, Eriksson E, Fujioka K, Bergman AC, Jornvall H, Auer G. Analysis of polypeptide expression in benign and malignant human breast lesions. *Electrophoresis*, 1997;18:582-587
- 44 Nanbu K, Konishi I, Komatsu T, Mandai M, Yamamoto S, Kuroda H, Koshiyama M, Mori T. Expression of heat shock proteins HSP70 and Hsp90 in endometrial carcinomas. Correlation with clinicopathology, sex steroid receptor status, and p53 protein expression. *Cancer*, 1996;77:330-338
- 45 Liu XL, Xiao B, Yu ZC, Guo JC, Zhao QC, Xu L, Shi YQ, Fan DM. Down-regulation of Hsp90 could change cell cycle distribution and increase drug sensitivity of tumor cells. *W J G*, 1999;199-208
- 46 Luparello C, Noel A, Pucci-Minafra I. Intratumoral heterogeneity for Hsp90 beta mRNA levels in a breast cancer cell line. *DNA Cell Biol*, 1997;16:1231-1236
- 47 Cardenas ME, Sanfridson A, Cutler NS, Heitman J. Signal-transduction cascades as targets for therapeutic intervention by natural products. *Trends Biotechnol*, 1998;16:427-433
- 48 Stebbins CE, Russo AA, Schneider C, Rosen N, Hartl FU, Pavletich NP. Crystal structure of an Hsp90 geldanamycin complex: targeting of a protein chaperone by an antitumor agent. *Cell*, 1997;89:239-250
- 49 Uehara Y, Murakami Y, Suzukake-Tsuchiya K, Moriya Y, Sano H, Shibata K, Omura S. Effects of herbimycin derivatives on src oncogene function in relation to antitumor activity. *J Antibiot (Tokyo)*, 1988;41:831-834
- 50 Sharma SV, Agatsuma T, Nakano H. Targeting of the protein chaperone, Hsp90, by the transformation suppressing agent, radicicol. *Oncogene*, 1998;16:2639-2645
- 51 Roe SM, Prodromou C, O'Brien R, Ladbury JE, Piper PW, Pearl LH. Structural basis for the inhibition of the Hsp90 molecular chaperone by the antitumor antibiotics radicicol and geldanamycin. *J Med Chem*, 1999;42:260-262
- 52 Bertram J, Palfner K, Hiddemann W, Kneba M. Increase of P-glycoprotein-mediated drug resistance by Hsp90 beta. *Anti-Cancer Drugs*, 1996;7:838-845
- 53 Persidis A. Cancer multidrug resistance. *Nature Biotech*, 1999;17:94-95
- 54 Bradshaw DM, Arceci RJ. Clinical relevance of transmembrane drug efflux as a mechanism of multidrug resistance. *J Clin Oncol*, 1998;16:3674-3690
- 55 Doyle LA, Yang W, Abruzzo LV, Krogmann T, Gao Y, Rishi AK, Ross DD. A multidrug resistance transporter from human MCF-7 breast cancer cells. *Proc Natl Acad Sci USA*, 1998;95:15665-15670
- 56 Volm M. Multidrug resistance and its reversal. *Anticancer Res*, 1998;18:2905-2917
- 57 Nooter K, Stoter G. Molecular mechanisms of multidrug resistance in cancer chemotherapy. *Pathol Res Pract*, 1996;192:768-780
- 58 Multhoff G, Botzler C, Issels R. The role of heat shock proteins in the stimulation of an immune response. *Biol Chem*, 1998;379:295-300
- 59 Campbell FA, Redmond HP, Bouchier-Hayes D. The role of tumor rejection antigens in host antitumor defense mechanisms. *Cancer*, 1995;75:2649-2655
- 60 Prodromou C, Roe SM, O'Brien R, Ladbury JE, Piper PW, Pearl LH. Identification and structural characterization of the ATP/ADP binding site in the Hsp90 molecular chaperone. *Cell*, 1997;90:65-75

# Down-regulation of Hsp90 could change cell cycle distribution and increase drug sensitivity of tumor cells

LIU Xian-Ling<sup>1</sup>, XIAO Bing, YU Zhao-Cai, GUO Jian-Cheng, ZHAO Qing-Chuan, XU Li, SHI Yong-Quan and FAN Dai-Ming

See invited commentary on page 195

**Subject headings** Hsp90; antisense RNA; cell cycle; gene transfection; drug resistance, multiple

## Abstracts

**AIM** To construct Hsp90 antisense RNA eukaryotic expression vector, transfect it into SGC7901 and SGC7901/VCR of MDR-type human gastric cancer cell lines, HCC7402 of human hepatic cancer and Ec109 of human esophageal cancer cell lines, and to study the cell cycle distribution of the gene transected cells and their response to chemotherapeutic drugs.

**METHODS** A 1.03kb cDNA sequence of Hsp90 $\beta$  was obtained from the primary plasmid pHSP90 by EcoR I and BamH I nuclease digestion and was cloned to the EcoR I and BamH I site of the pcDNA by T4DNA ligase and an antisense orientation of Hsp90 $\beta$  expression vector was constructed. The constructs were transfected with lipofectamine and positive clones were selected with G418. The expression of RNA was determined with dot blotting and RNase protection assay, and the expression of Hsp90 protein determined with western blot. Cell cycle distribution of the transfectants was analyzed with flow cytometry, and the drug sensitivity of the transfectants to Adriamycin (ADR), vincristine (VCR), mitomycin (MMC) and cyclophosphamide (CTX) with MTT and intracellular drug concentration of the transfectants was determined with flow

## cytometry.

**RESULTS** In EcoR I and BamH I restriction analysis, the size and the direction of the cloned sequence of Hsp90 $\beta$  remained what had been designed and the gene constructs were named pcDNA-Hsp90. AH-SGC790, AH-SGC7901/VCR, AH-HCC7402 and AH-Ec109 cell clones all expressed Hsp90 anti-sense RNA. The expression of Hsp90 was down-regulated in AH-SGC7901, AH SGC7901/VCR, AH-HCC7402 and AH-Ec109 cell clones. Cell cycle distribution was changed differently. In AH-SGC7901/VCR and AH-Ec109 cells, G1 phase cells were increased; S phase and G2 phase cells were decreased as compared with their parental cell lines. In AH-SGC7901 cell, G1 phase cells were decreased, G2 phase cells increased and S phase cells were not changed, and in AH-HCC7402 cells G1, S and G2 phase cells remained unchanged as compared with their parental cell lines. The sensitivity of AH SGC7901, AH-SGC7901/VCR, AH-HCC7402 and AH-Ec109 to chemotherapeutic drugs, the sensitivity of AH-SGC7901/VCR to ADR, VCR, MMC and CTX the sensitivity of AH-HCC7402 to ADR and VCR, and the sensitivity of Ec109 to ADR, VCR and CTX all increased as compared with their parental cell lines. The mean fluorescence intensity of ADR in AH-SGC7901, AH-SGC7901/VCR, AH-HCC7402 and AH-Ec109 was also significantly elevated ( $P < 0.05$ ).

**CONCLUSION** Down-regulation of Hsp90 could change cell cycle distribution and increase the drug sensitivity of tumor cells.

## INTRODUCTION

Heat shock proteins (HSPs) are a highly conserved group of intracellular proteins whose synthesis is increased in response to a variety of stressful stimuli<sup>[1]</sup>. HSPs are classified by molecular weight into groups of HSP110, HSP90, HSP70, HSP60, small molecular HSP and ubiquitin. HSP90 is a main chaperone protein in the cell plasma<sup>[2]</sup>. Recent studies have suggested that HSP90

<sup>1</sup>Institute of Digestive Diseases, Xijing Hospital, Fourth Military Medical University, Xi'an 710032, Shaanxi Province, China  
Dr. LIU Xian-Ling, female, born on 1962-04-12 in Shaanxi Province, received Ph.D. degree in 1998 from Fourth Military Medical University, now attending physician in the department of gastroenterology, having 10 papers published.

\*Project supported by the National Natural Science Foundation of China, No. 39570806 and National Excellent Youth Scientific Foundation, No. 3952020.

**Correspondence to:** LIU Xian-Ling, Institute of Digestive Diseases, Xijing Hospital, Fourth Military Medical University, 15 Western Chang Le Road, Xi'an 710032, Shaanxi Province, China  
Tel. +29 • 3375226

Received 1999-01-03 Revised 1999-03-19

expression is increased in tumor tissues<sup>[3,4]</sup> and is closely related to multi-drug resistance protein P-gp<sup>[5,6]</sup>. To further investigate the biological roles of HSP90 in the processes of carcinogenesis and the possibility of down regulation of HSP90 to reverse the drug resistance of tumor cells, we have constructed the Hsp90 antisense RNA eukaryotic expression vector, transfected it into SGC7901 of human gastric cancer SGC7901/VCR of multi-drug resistant human gastric cancer, HCC7402 of human hepatic cancer and Ec109 of human esophageal cancer cell lines. We also studied the cell cycle distribution of the gene transected cells and their response to chemotherapeutic drugs.

## MATERIAL AND METHODS

### Materials

**Reagents** EcoR I and BamH I nuclease was purchased from Sino-American Biotech Inc T4 DNA ligase from Promega Company. Other reagents included guanidinium isothiocyanate lysis solution (guanidinium isothiocyanate, citric acid sodium, sarkosyl, ( $\gamma$ -<sup>32</sup>P) ATP, T4 phage polynucleotide kinase, 20 × SSC (NaCl, citric acid sodium), 50 × Denhardt (Ficoll, N-Polyvinylpyrrolidone and BSA), pre-hybridization solution (6 × SSC, 0.5% SDS, 5 × Denhardt, 100 mg/L salmon sperm DNA) TBE (89 mmol/L Tris-boric acid, 2 mmol/L EDTA), 5 × hybridization buffer (200mM-PIPES pH 6.4, 2mM-NaCl, 5mM EDTA), formamide hybridization buffer (formamide: 5 × hybridization buffer = 4:1), RNase S<sub>1</sub>, RNase S<sub>1</sub> buffer (10mM Tris-Cl pH 7.5, 300mM NaCl, 5mM EDTA), 50mg/L proteinase K, 0.5% SDS (w/v), phenol, chloroform, RNA loading buffer (80% formamide, 1mM EDTA pH 8.0, 0.1% bromophenol blue, 0.1% Xylene Cyanol), acrylamide, bisacrylamide, 10% saturated ammonium sulfate, urea, lipofactamine, G418, RPMI1640, goat anti-human HSP90  $\beta$  monoclonal antibody, HRP-labeled donkey anti-goat IgG, Lysis buffer (50 mmol/L Tris • Cl, pH 8.0, 150 mmol/L NaCl, 0.02% NaN<sub>3</sub>, 0.1% SDS, 100  $\mu$ L/mL PMSF, 1 mg/L aprotinin, 1% NP-40, 0.5% deoxycholic acid), TEMED, Tris-glycine working solution (25 mmol/L Tris • Cl, 250 mmol/L glycine, 0.1% SDS), 2 × SDS gel-loading buffer (100 mmol/L Tris • Cl, pH 6.8, 200 mmol/L DTT, 4% SDS, 0.2% bromophenol blue, 20% glycerol), electroblotting buffer (39 mmol/L glycine, 48 mmol/L Tris • Cl, 0.037% SDS, 20% methanol), tetrachloride naphenol, propidium iodide, adriamycin (ADR), vincristine (VCR), Mitomycin (MMC) and cyclophosphamide (CTX).

**Cell lines** SGC7901 of human gastric cancer cell line was provided by the Military Medical Scientific Chinese Academy, of Military Medical Sciences, SGC7901/VCR of MDR-type

human gastric cancer cell line was from our institute, HCC7402 of human hepatic cancer cell line from Pathological Department of Fourth Military Medical University (FMMU). Ec109 of human esophageal cancer cell line was from Biochemical Department of FMMU.

### Methods

**Construction of HSP90 antisense RNA eukaryotic expression vector** pHSP90 of HSP90 cDNA plasmid was supplied by YAMAMOTO. Eukaryotic expression vector pcDNA 3.1(+) was supplied by Yang Jing-Hua. *E. coli* JM109 was introduced by original source our institute. ① Plasmid map analyses: Analysis of the nuclease site of pHSP90 plasmid map of HSP90 prokaryotic expression vector found that there were two EcoR I nuclease sites and one BamH I nuclease sites in the gene sequence of HSP90 cDNA, of which EcoR I nuclease site is located at 0.99kb and 1.07kb respectively and BamH I nuclease site is located at 2.1kb. There was another EcoR I nuclease site at prime 3 of the pHSP90 plasmid following the stop codon of HSP90 cDNA (Figure 1). There was one EcoR I and one BamH I nuclease site on the multi-clonal nuclease sites of prokaryotic expression vector pcDNA 3.1(+), of which EcoR I is located at prime 3 and BamH I is located at prime 5 (Figure 2). With EcoR I and BamH I nuclease, a 1.03kb fragment of 1.07kb-2.1kb could be digested from HSP90 cDNA (EcoR I was at prime 3, BamH I at prime 5). By inserting the digested fragment (1.03kb) into EcoR I and BamH I nuclease site of pcDNA 3.1(+), the HSP90 antisense RNA eukaryotic expression vector could be constructed.

② The primary plasmid pHSP90 was extracted by alkali lysis. First, pHSP90 was digested by EcoR I and electrophoresed on agarose-gel. Two fragments of 1.43kb and 3.99kb could be seen under ultraviolet from the gel. Of them, the 1.43kb-DNA was excised from the gel and purified by the frozen-melting method. The purified DNA was further digested by BamH I nuclease and electrophoresed, and a 1.3kb fragment (EcoR-I was at prime 3, BamH I was at prime 5) was obtained. The specific fragment (0.5  $\mu$ g) and 0.1  $\mu$ g-pcDNA 3.1(+) linearized by EcoR I and BamH I nuclease was ligated by T4 DNA ligase under 16°C for 18 h (Figure 3). The ligated products were transformed into the sensitized *E. coli* JM109, grew on ampicilline resistant agarose gel. Positive clones were selected and amplified and a small amount of plasmid was extracted. The reconstructed plasmid was digested by either EcoR I or BamH I or by both EcoR I and BamH I nuclease to determine the size and the direction of the fragment.

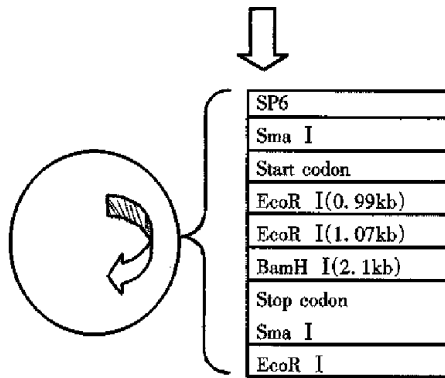


**Figure 1** Plasmid map of phHSP90.

Vector: pSP64(3kb); Inserts: human HSP90 $\beta$  cDNA (2.5kb); Insert site: Sma I of multiclone enzyme restriction site of pSP64; Promoter: SP6; Drug resistance: Amp

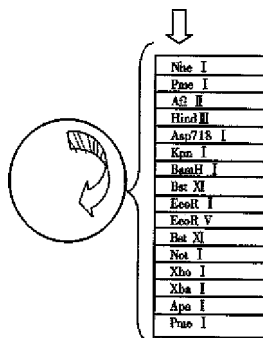


**Figure 2** Plasmid map of eukaryotic expression vector pcDNA 3.1 (+). (5.4kb)

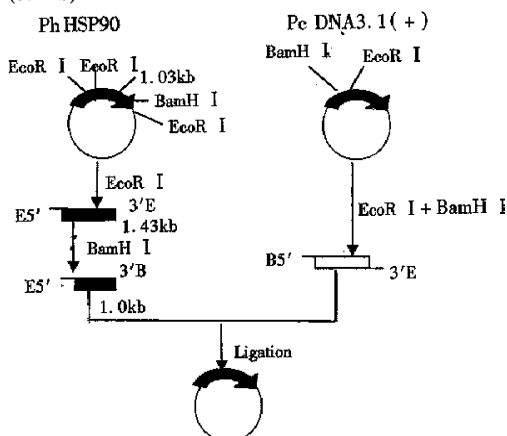


**Figure 3** Construction of pcDNA-HSP90 of HSP90 antisense RNA eukaryotic expression vector.

**Gene transfection and clone selection.** The pcDNA-HSP90 of HSP90 anti-sense RNA constructs was extracted by the alkali lysis method, purified by PEG, transfected into SGC7901, SGC7901/VCR, HCC7402 and Ec109 by Lipofectamine and selected by G418. In a six-well culture plate, seed  $1 \times 10^5$  cells per well in 2 mL appropriate complete growth

medium. Incubate the cells at 37°C in a CO<sub>2</sub> incubator until the cells are 80% confluent. After rinsing the cells with serum free and antibiotics-free medium, add pcDNA-HSP90-Lipofectamine mixture (or pcDNA 3.1(+)-Lipofectamine mixture as control). Incubate the cells at 37°C in a CO<sub>2</sub> incubator for 6 hours. Then change the medium with RPMI1640 culture medium containing 10% fetal bovine serum. G418 (400 mg/L) was added to select the resistant clone after 48-72 hours. The medium was changed every 3-4 days and colonies were collected approximately 3 weeks later.

**RNA analyses.** ① Probe designing and synthesizing. Reading 30bp from 1641<sup>st</sup> bp of HSP90 cDNA, the gene sequence is 5' ATT GAC GAG TAC TGT GTG CAG CAG CTC AAG-3'. This gene fragment was matched with the gene bank from the Internet. We found that this sequence could only match with the HSP90 gene, and no homology with any other available genes. So this selected sequence was used as a probe and was synthesized by the Shanghai Biotech Company.  $\beta$ -actin was donated by Dr. Zhao Qing-Chuan and the sequence is  $\beta$ -actin-2095: 5'-ACT ATG TTT GAG ACC TTC AA-3'. ② Oligonucleotide probes labeled by T4 phage polynucleotide kinase. Add pure water to a total volume of 19.5  $\mu$ L in 10pmol/ $\mu$ L Oligonucleotide (1.0  $\mu$ L), 10  $\times$  T4 buffer (2.0  $\mu$ L) and 10pmol [ $\gamma$ -<sup>32</sup>P]ATP (5.0  $\mu$ L). After being mixed, suck 0.5  $\mu$ L-10  $\mu$ L 10 mmol/L Tris-Cl (pH 8.0) to assay the radioactivity ratio. Then 1  $\mu$ L T4 phage polynucleotide kinase was added and mixed and bathed in 37°C for 45 min, then bathed in 68°C for 10min to inactive T4 phage polynucleotide kinase. Afterwards, suck 0.5  $\mu$ L above solution and added to 10  $\mu$ L 10 mmol/L Tris-Cl (pH 8.0) to assay the radioactivity ratio. Precipitate the probes with ethanol and resolubilized to 20  $\mu$ L 1mmol/L EDTA deionized water and stored at -20°C. Radioactivity ratio of the oligonucleotide was assayed by the TCA method<sup>[7]</sup>. ③ RNA isolation. Total RNA was obtained from the cells by the guanidium isothiocyanate-phenol-chloroform extraction method. Cells of  $1 \times 10^6$  were collected and washed with PBS, guanidinium isothiocyanate lysis solution 500  $\mu$ L, 3 mol/L- NaAc 100  $\mu$ L, water saturated phenol and chloroform each 500  $\mu$ L-were added, ice bathed for 20 min and centrifuged at 4°C (12 000r/min) for 15 min. The upper water layer was sucked up to another eppendoff tube, extracted with anequal volume of phenol/chloroform (1/1), precipitated by isopropanol, centrifuged at 4°C (12 000r/min) for 15 min, washed with 70% ethanol once, resuspended to three-evaporated water, treated by

50  $\mu$ L DEPC quantitated and stored at  $-20^{\circ}\text{C}$ . ④ RNA dot blotting. The quantitated RNA was denatured by formaldehyde and was dropped to the nitrocellulose membrane and was dried in  $80^{\circ}\text{C}$  dry oven for 2 h. After pre-hybridization at  $68^{\circ}\text{C}$  water bathing for 2 h, probes were added to the hybridization bag and water bathed for 16 h-24 h at  $68^{\circ}\text{C}$ . The hybridization membrane was picked out and washed with  $2 \times \text{SSC}$  and 0.1% SDS for 20 min at room temperature and with  $0.2 \times \text{SSC}$  and 0.1% SDS at  $68^{\circ}\text{C}$  3 times for 10 min. Then the nitrocellulose membrane was dried by filter paper and was covered by fresh-keeping film. The membrane was exposed to X-ray film in the presence of intensifying screens at  $-20^{\circ}\text{C}$  for 48 h-72 h. The film was then developed to observe the results. ⑤ RNase protection assay<sup>[8]</sup>. RNA (10  $\mu$ L) from the cells were precipitated and resuspended in 30  $\mu$ L formamide hybridization buffer. Radiolabeled Oligonucleotide probes (1  $\mu$ L) and  $\beta$ -actin probes (1  $\mu$ L) diluted to  $1 \times 10^5$  cpm with hybridization buffer were added to the total RNA. The mixture was heated at  $85^{\circ}\text{C}$  for 5 min and the RNAs hybridized at  $45^{\circ}\text{C}$  or  $50^{\circ}\text{C}$  overnight. After hybridization, 2  $\mu$ L RNase S1 buffer, 16  $\mu$ L water and 2  $\mu$ L RNase S1 (2 mg/L) were added and the mixture was incubated at  $37^{\circ}\text{C}$  for 60 min. The solution, which now contained RNase protected fragments, was deproteinized with 50 mg/L proteinase K and 0.5% SDS (w/v) at  $37^{\circ}\text{C}$  for 15 min, extracted with an equal volume of phenol/chloroform (1/1), coprecipitated with 10  $\mu$ g yeast RNA, and resuspended in 8  $\mu$ L loading buffer. The samples were electrophoresed on a 18% acrylamide/6M urea polyacrylamide sequencing gel (200 v, 120 min). Gels were radioautographed at  $-20^{\circ}\text{C}$  for 48 h. Its size was determined according to the standard molecular weight marker.

**Protein analyses** Cells were lysed by lysis buffer and the protein was quantitated. Then SDS-PAGE and immunoblot was performed as usual. Goat anti-HSP90- $\beta$  (1:100) was reacted with the electroblotting for 2 h and HRP-labeled donkey anti-goat IgG (1:500) reacted with the electroblotting for 1 h at room temperature. After washing with PBS (0.01 mol/L pH 7.4), tetrachloride naphenol was used to develop the protein strip and photographed.

**Growth analyses** The pcDNA-HSP90 gene transfected cells and their parental cells were seeded into 24-well plates as pairs at a concentration of  $1 \times 10^4$ /well, 2 mL each well, and cultured in the incubator with a condition of 5%  $\text{CO}_2$ ,  $37^{\circ}\text{C}$ . The cell morphology and growth feature were observed

under microscope. Three wells of each kind of cells were digested by 0.25% trypsin and counted, and its mean value was used to draw the growth curve. Cell doubling time of the exponential phase was calculated by Patterson's formula,  $T_d = T \cdot \lg 2 / \lg (N_1/N_0)$ . Here  $T_d$  is cell doubling time (hour),  $T$  is the time needed for cell growth from  $N_0$  to  $N_1$

**Cell cycle analyses.** Cells growing well were digested by 0.25% trypsin, washed by PBS, fixed by cold ethanol at  $4^{\circ}\text{C}$  and dyed with PI, and then were analyzed by flow cytometry.

**The drug sensitivity analyses.** MTT methods were used. The pcDNA-HSP90 gene transfected cells and their parental cells were seeded into 96well plates as pairs at a concentration of  $5 \times 10^3$ /well, 200  $\mu$ L each well, cultured in the incubator with a condition of 5%  $\text{CO}_2$ ,  $37^{\circ}\text{C}$  overnight. Add adriamycin, vincristine, mitomycin or cyclophosphamide at a concentration of 2  $\mu$ g/ $\mu$ L, 2  $\mu$ g/ $\mu$ L, 2  $\mu$ g/ $\mu$ L and 400  $\mu$ g/ $\mu$ L according to the peak plasma concentration of different antineoplastic drugs, and diluted at a ratio of 1:10 respectively and seed 3 weeks for each concentration. Forty-eight hours later, add tetrazolium blue 20  $\mu$ L to each well at a concentration of 5 mg/L PBS. Culturing was continued for 4 hours and the supernatant was removed. Add 150  $\mu$ L DMSO to react for 15 minutes. ELISA reader was used to measure the OD value of each well at A490 nm and the ratio of living cells. The living cell ratio = A490 of the experimental well/that of control well. Dose-effector curve was drawn and  $\text{IC}_{50}$  and resistant index (RI) were determined.  $\text{RI} = \text{IC}_{50}$  of parental cells/that of the gene transfected cells.

**Intracellular drug concentration analyses** In a 35 mm tissue culture plate, seed  $3 \times 10^5$  cells in to 2 mL complete growth medium. Incubate the cells at  $37^{\circ}\text{C}$  in a  $\text{CO}_2$  incubator until the cells are 70% confluent. Add adriamycin to make its final concentration to 10 mg/L. After culture for 1 hour, cells were digested by 0.25% trypsin, washed by PBS and were analyzed by flow cytometry at 575 nm.

#### Statistical analysis

The growth of pcDNA-HSP90 transfectants and their associated controls were compared using two sample *t* tests. Cell cycle fractions, sensitivity of tumor cells to chemotherapeutic drugs and intracellular drug concentrations of pcDNA-HSP90 transfectants and their associated controls were compared using ANOVA.

#### RESULTS

### The constructed HSP90 antisense RNA expression vector

Two gene fragments of 1.43kb and 3.99kb were isolated by agarose-gel electrophoresis after the primary plasmid pHSP90 was digested by EcoR. After the 1.43kb gene fragment was further digested by BamH I, a 1.03kb fragment was obtained, of which BamH I was at its prime 3, EcoR I was at its prime 5. The eukaryotic expression vector pcDNA 3.1(+) was digested by EcoR I and BamH I nuclease and formed linearized plasmid, of which EcoR I was at its prime 3 and BamH I was at its prime 5. With the ligated positive reconstructs digested by EcoR I and BamH I nuclease, we could obtain a 5.4kb vector DNA and 1.03kb inserted fragment. If the ligated positive reconstructs were digested by either EcoR I or BamH I nuclease, we could see a linearized reconstructs (Figure 4). These results indicated that the size and the direction of the inserted HSP90 cDNA fragment was what had been expected. The reconstructed expression vector was named pcDNA-HSP90.



**Figure 4** Nuclease restriction analysis of pcDNA-HSP90 of HSP90 anti-sense RNA eukaryotic expression vector.

1. pHSP90; 2. pHSP90/EcoR I; 3. HSP90/EcoR I-BamH I; 4.  $\lambda$  DNA/EcoR I+Hind III marker (21227, 5148, 4268, 2027, 1375, 125bp); 5. pcDNA 3.1(+); 6. pcDNA 3.1 (+)/EcoR I+BamH I; 7. pcDNA-HSP90; 8. pcDNA-HSP90/EcoR I+BamH; 9. pcDNA-HSP90/EcoR I; 10. pcDNA-HSP90/BamH I

### Gene transfection and clone selection

The positive colonies were selected approximately 3 weeks later. pcDNA-HSP90 of HSP90 anti-sense RNA constructs transfected cell lines were named AH-SGC7901, AH-SGC7901/VCR, AH-HCC7402 and AH-Ec109 respectively (Figure 5). pcDNA3.1 (+) transfected cell lines were named SGC7901-pcDNA, SGC7901/VCR-pcDNA, HCC7402 pcDNA and Ec109-pcDNA.

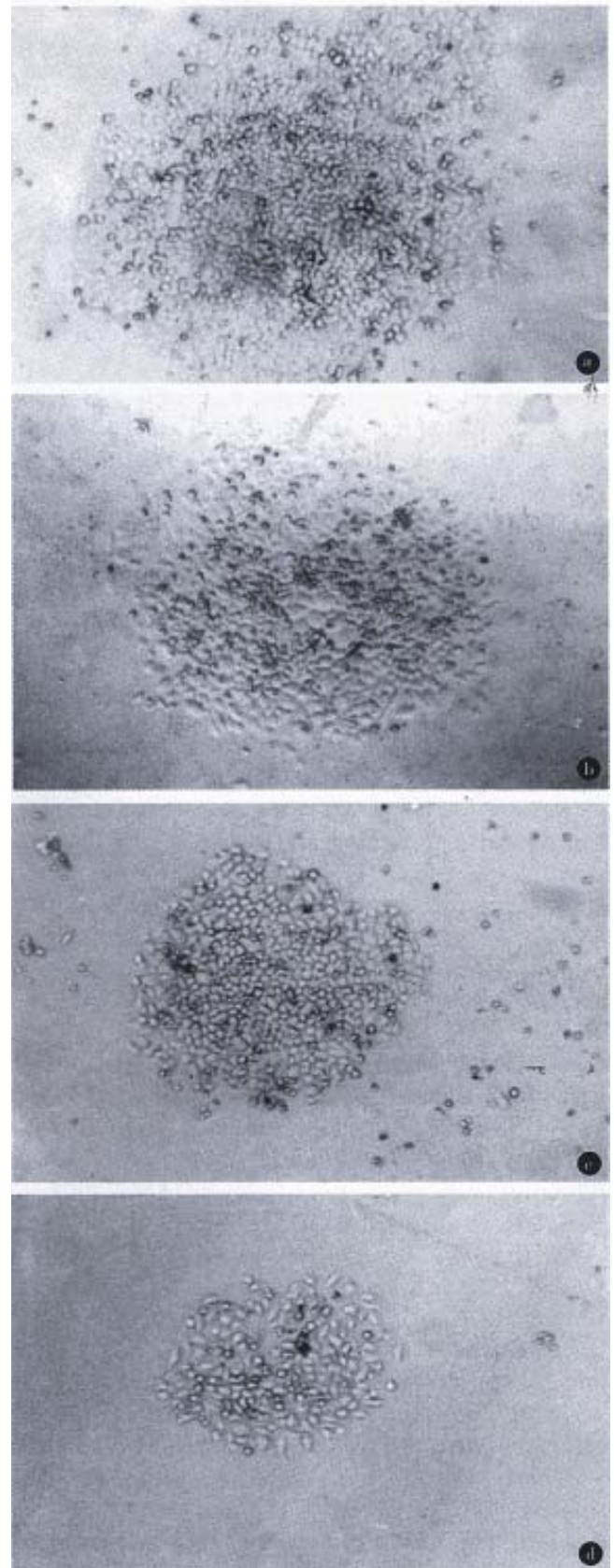


**Figure 5** SGC7901, SGC7901/VCR, HCC7402 and Ec109 cells transfected with pcDNA-HSP90 of HSP90 antisense RNA constructs, selected by G418, positive clones were obtained and were named a. AH-SGC7901; b. AH-SGC7901/VCR; c. AH-HCC7402; d. AH-Ec109.

### Dot blotting and RNase protection assay

**Dot blotting.** All three groups of pcDNA-HSP90 transfectants, pcDNA3.1(+) transfectants and their parental cells had positive signals of  $\beta$ -actin (Figure 6). Only pcDNA-HSP90 transfected cell group had positive signals of HSP90 anti-sense RNA (Figure 7), indicating that pcDNA-HSP90 transfected cell group had the expression of HSP90 anti-sense RNA.

**RNase protection assay (Figure 8).** HSP90 anti-sense RNA transfectants AH-SGC7901/VCR (1), AH-SGC7901 (4), AH-HCC7402 (7) and AH-Ec109 (10) cells had two positive stripes (Hsp90 anti-sense RNA,  $\beta$ -actin) while pcDNA3.1(+) transfected group and the blank control cell group (parental cell line) had only one positive stripe ( $\beta$ -actin), also indicating that pcDNA-HSP90 transfected cell group had the expression of HSP90 anti-sense RNA and further confirmed that pcDNA-HSP90 had been transfected into the aim cells and had the expression of HSP90 anti-sense RNA.

**The expression of Hsp90 protein in the gene transfected cells.** Western blot results showed that the expression of Hsp90 $\beta$  in pcDNA 3.1(+) transfected cells and in their parental cells were almost the same. In Hsp90 antisense RNA transfected cells (AH-SGC7901, AH-SGC7901/VCR, AH-HCC7402 and AH-Ec109), Hsp90 $\beta$  expression was lower than that of their parental cells and pcDNA3.1(+) transfected cells (Figure 9).

**Growth of the gene transfected cell lines.** Compared with their parental cells, the growth of pcDNA-HSP90 gene transfected cells was inhibited in different degrees (Figure 10). The growth inhibiting rate of the 10th day AH-SGC7901 to SGC7901 was 24.28%, of AH-SGC7901/VCR to SGC7901/VCR 27.58%, AH-HCC7402 to HCC7402 10.51% and AH-Ec109 to Ec109 66.91%.

In SGC7901 and AH-SGC7901, the Td calculated from the cell growth curve was 26.6 h and 27.72 h, respectively. The Td of AH-SGC7901 was prolonged 1.12 has compared with its parental cell SGC7901. Td of SGC7901/VCR and AH-SGC7901/VCR was 55.53 h and 72.22 h, respectively. Td of HCC7402 and AH-HCC7402, and Ec109 and AH-Ec109 was 40.66 h and 43.40 h, and 25.03 h and 41.00 h, respectively. These results indicated that the Td of AH-SGC7901/VCR and AH-Ec109 was significantly longer than that of their parental cells ( $P < 0.05$ ), while that of AH-SGC7901 and AH-HCC7402 had no obvious changes as against that of their parental cells ( $P > 0.005$ ).

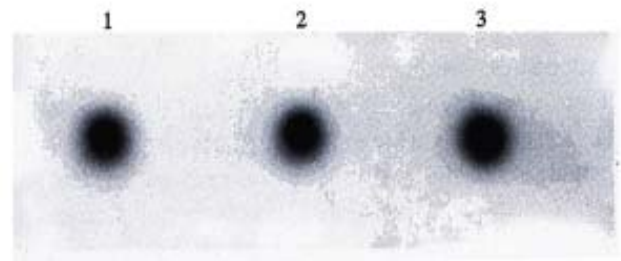


**Figure 6** The expression of  $\beta$ -actin mRNA in AH-SGC7901 of pcDNA-HSP90 transfected cell line, SGC7901-pcDNA of pcDNA 3.1(+) transfected cell line and its parental cell line SGC7901 by Dot blot. 1: SGC7901; 2: SGC7901-pcDNA; 3: AH-SGC7901

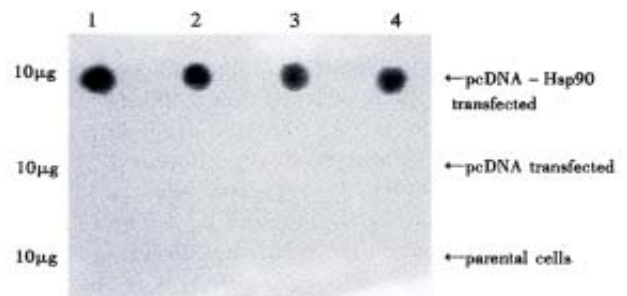


**Figure 7** The expression of HSP90 anti-sense RNA in pcDNA-HSP90 transfected, pcDNA 3.1(+) transfected and the parental cell lines of SGC7901, SGC7901/VCR, HCC7402 and Ec109 by Dot blot. 1: SGC7901; 2: SGC7901/VCR; 3: HCC7402; 4: Ec109

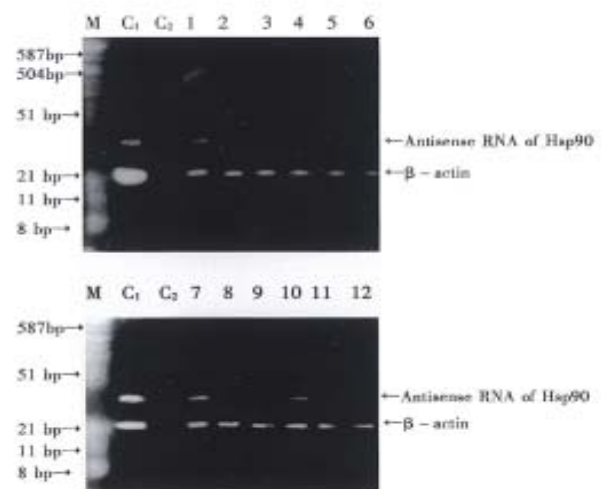


**Figure 8** Expression of hsp90 anti-sense RNA by RNase protection assay. M: PBR322 DNA/Hae III Marker; C1: Positive control,  $\beta$ -actin (20bp) and HSP90 probe (30bp); C2: negative control, probe plus RNase S1, no RNA. 1. AH-SGC7901/VCR; 2. SGC7901-pcDNA/VCR; 3. SGC7901/VCR; 4. AH-SGC7901; 5. SGC7901-pcDNA; 6. SGC7901; 7. AH-HCC7402; 8. HCC7402-pcDNA; 9. HCC7402; 10. AH-Ec109; 11. Ec109-pcDNA; 12. Ec109

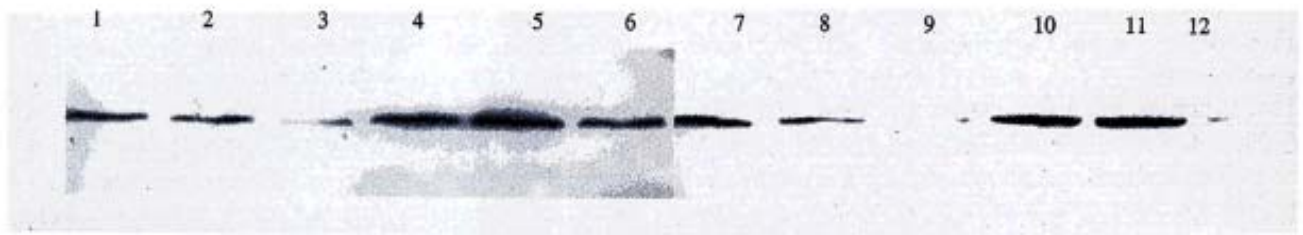


**Figure 9** The expression of HSP90 protein in pcDNA-HSP90 transfected cells. 1. SGC7901; 2. SGC7901-pcDNA; 3. AH-SGC7901; 4. SGC7901/VCR; 5. SGC7901/VCR-pcDNA; 6. AH-SGC7901/VCR; 7. HCC7402; 8. HCC7402pcDNA; 9. AH-HCC7402; 10. Ec109; 11. Ec109pcDNA; 12. AHEc109

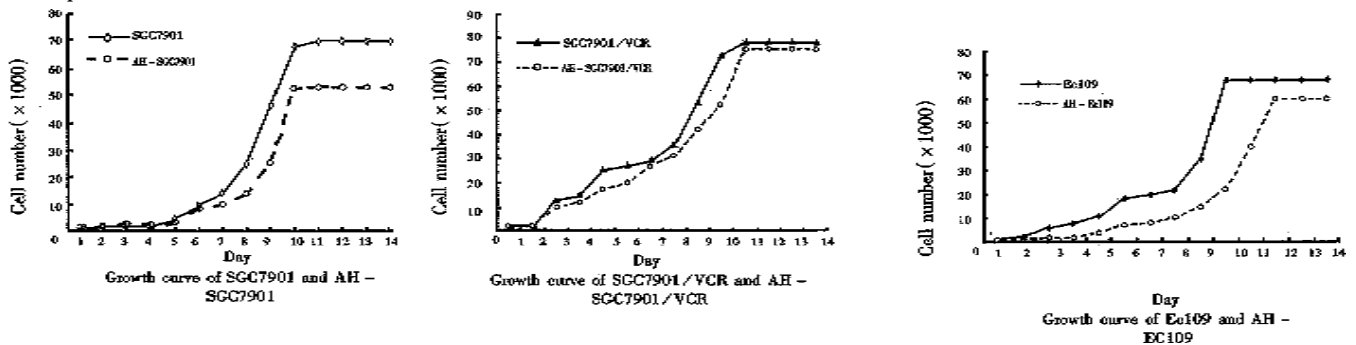


**Figure 10** Growth of gene transfected cell lines.

**Cell cycle distribution of the transfected cells (Table 1).** We can see from Table 1 that G<sub>1</sub> phase cells of AH-SGC7901 were decreased, G<sub>2</sub> phase cells were increased and S phase had no obvious change as compared with their parental cells, while G<sub>1</sub> phase cells of AH-SGC7901/VCR were increased and S phase and G<sub>2</sub> phase cells were decreased. G<sub>1</sub> phase, S phase and G<sub>2</sub> phase cell of AH-HCC7402 had no obvious changes and G<sub>1</sub> phase cells of AH-Ec109 were increased, S and G<sub>2</sub> phase cells were significantly decreased as compared with their parental cells.

**Table 1** Kinetics of pcDNA-HSP90 transfected cells and their parental cells analyzed with flow cytometry

Cell lines	Cell cycle fraction (%)		
	G <sub>0</sub> -G <sub>1</sub>	S	G <sub>2</sub> -M
SGC7901	61.6	28.0	10.4
AH-SGC7901	55.7	28.1	16.2
SGC7901/VCR	62.2	23.5	14.3
AH-SGC7901/VCR	74.7	13.6	11.7
HCC7402	70.7	21.1	8.2
AH-HCC7402	69.5	20.0	10.4
Ec109	56.2	29.5	14.8
AH-Ec109	72.5	19.5	8.0

**Drug sensitivity of the gene transfectants.** IC<sub>50</sub> of SGC7901 to ADR, VCR, MMC and CTX was 1.58 × 10<sup>-6</sup>, 1.99 × 10<sup>-3</sup>, 3.10 × 10<sup>-2</sup> and 630 mg/L and IC<sub>50</sub> of AH-SGC7901 to ADR, VCR, MMC and

CTX was 1.58 × 10<sup>-7</sup>, 1.99 × 10<sup>-7</sup>, 1.25 × 10<sup>-3</sup> and 630 mg/L respectively. RI of SGC7901 to ADR, VCR, MMC and CTX was 10, 10 000, 24.8 and 1 compared with AH-SGC7901, i.e., the sensitivity of AH-SGC7901 to ADR, VCR and MMC increased 10, 10 000 and 24.8 times respectively as compared with their parental cell lines, and the sensitivity to CTX had no obvious changes.

IC<sub>50</sub> of SGC7901/VCR to ADR, VCR, MMC and CTX was 0.398, 1.25, 0.199 and 3981.07 mg/L, IC<sub>50</sub> of AH-SGC7901/VCR to ADR, VCR, MMC and CTX was 0.1, 0.199, 0.063 and 794.32 mg/L. RI of SGC7901/VCR to ADR, VCR, MMC and CTX was 3.98, 6.28, 3.15 and 5.01 as compared with AH-SGC7901.

IC<sub>50</sub> of HCC7402 to ADR, VCR, MMC and CTX was 1.20 × 10<sup>-3</sup>, 6.33 × 10<sup>-4</sup>, 3.0 × 10<sup>-2</sup> and 1258.92 mg/L and IC<sub>50</sub> of AH-HCC7402 to ADR, VCR, MMC and CTX was 2.51 × 10<sup>-6</sup>, 6.33 × 10<sup>-5</sup>, 3.00 × 10<sup>-2</sup> and 1258.92 mg/L. RI of HCC7402 to ADR, VCR, MMC and CTX was 477.7, 10, 1 and 1 or the sensitivity of AH-HCC7402 to ADR and VCR increased 477.7 and 10 times respectively compared with their parental cell lines, and its sensitivity to MMC and CTX had no obvious changes.

IC<sub>50</sub> of Ec109 to ADR, VCR, MMC and CTX was 1.0 × 10<sup>-1</sup>, 44.66, 1.99 and 1258.92 mg/L and IC<sub>50</sub> of Ec109 to ADR, VCR, MMC and CTX was 3.16 × 10<sup>-6</sup>, 1.99, 1.99 and 398.10 mg/L respectively. RI of Ec109 to ADR, VCR, MMC and CTX was 31 622.77, 22.44, 1.00 and 3.16.

**Intracellular drug concentration of the gene transfectants.** The mean fluorescence intensity of ADR was  $0.286 \pm 0.02$  in SGC7901,  $0.290 \pm 0.026$  in AH-SGC7901 and  $0.279 \pm 0.009$  in SGC 7901 control, which was significantly increased in AH-SGC7901 ( $P < 0.05$ ).

The mean fluorescence intensity of ADR in SGC7901/VCR was  $0.320 \pm 0.050$ ,  $0.323 \pm 0.054$  in AH-SGC7901/VCR which was significantly increased ( $P < 0.05$ ).

The mean fluorescence intensity of ADR was  $0.480 \pm 0.122$  in HCC7402, and significantly increased in AH-HCC7402 ( $0.503 \pm 0.188$ ) ( $P < 0.05$ ).

The mean fluorescence intensity of ADR was  $1.300 \pm 0.361$  in Ec109, and significantly increased in AH-Ec109 ( $1.680 \pm 0.590$ ) ( $P < 0.05$ ).

## DISCUSSION

Antisense RNA is the RNA that is complementary with the mRNA. The antisense RNA could combine with mRNA specifically and inhibit the translation of the RNA. It is one of the gene expression and modulating modes in prokaryotic cells. Antisense RNA also exists in eukaryotic cells but its function is still unknown. Antisense RNA technique is to transfect artificially-composed antisense RNA into the eukaryotic cells, transcript antisense RNA, block the translation of the gene, inhibit the expression of the specific gene and block the function of the gene, and to evaluate the influence of the gene to the cell growth and cell differentiation. In comparison of the ribozyme technique<sup>[8]</sup>, antisense RNA technique has the advantages of simple designing, strong specificity, easy operating, and being economic and time saving. According to the two common nucleases EcoR I and BamH I and their different directions of pHSP90 and pcDNA 3.1(+), the nuclease digested fragment was inserted to pcDNA 3.1(+), and the nuclease restriction analysis showed that the gene clone was successful. This study has laid ground for further understanding the biological roles of HSP90 in tumor cells.

In order to determine whether the HSP90 antisense RNA gene transfected and G418 selected cell clones had the expression of HSP90 antisense RNA, a 30-bp oligonucleotide was synthesized and was labeled with ( $\gamma$ -<sup>32</sup>P) ATP by T4 phage polynucleotide kinase. RNA isolated from the selected clones was first analyzed by dot blotting with the labeled probes. The results showed that the pcDNA-HSP90 transfected cell group had positive signals while the pcDNA 3.1(+) transfected cell group and the blank control cell group had no positive signals, indicating that the pcDNA-HSP90 transfected cell group had the expression of HSP90 antisense RNA.

RNase protection assay<sup>[9,10]</sup> or RNase mapping

is a highly sensitive method for gene expression analysis. This method was primarily used to analyze and quantitate specific RNAs. In the research of gene's characters, it is used to determine the size of the exons. The principle of RNase protection assay is: the labeled oligonucleotide probes were hybridized with cell total RNA or mRNA. The unhybridized single chain RNA was digested by RNase S1. The hybridized double chain was protected and could not be digested by RNase S1. Electrophoresis on acrylamide/urea polyacrylamide sequencing gel, the protected chain could be isolated. Radioautograph could develop the protected chain. Its size could be determined according to the standard-molecular-weight-marker. By this method, 0.1pg globin RNA could be assayed. Its specificity and sensitivity is far greater than Northern blot. In this research, RNase protection assay was also used to determine the expression of HSP90 antisense RNA in the gene transfected and the control cells. The results showed that pcDNA-HSP90 transfected cells had the expression of HSP90 antisense RNA. Analysis of RNA by RNase protection assay is simpler than Northern blot and more specific than Dot blot.

Western blot showed that the expression of HSP90  $\beta$  in AH-SGC7901, AH-SGC7901/VCR, HCC7402 and Ec109 was decreased as compared with their parental cells and their pcDNA transfected groups. This indicated that the antisense RNA of HSP90 has partly blocked the mRNA of HSP90 and inhibited the translation of HSP90 protein.

Both Dot blot and RNase protection assay showed that pcDNA-HSP90 transfected AH-SGC7901, AH-SGC7901/VCR, AH-HCC7402 and AH-Ec109 all had the expression of HSP90 antisense RNA, and with western blot, the expression of HSP90 $\beta$  protein in these cells was decreased when compared with their parental cells and their pcDNA transfected groups. This has established a cell model for further studying the role of HSP90 in these cell lines.

It is known that cell growth is closely related to cell cycle distribution, and cell cycle is regulated by many factors. Oesterreich S<sup>[11]</sup> and Mairesse N<sup>[12]</sup> showed in their studies that hsp27 may be involved in the regulation of cell growth. Fuse *et al*<sup>[13]</sup> had investigated the alternations of cytokinetics and HSP70 expression by hyperthermia in the *in vitro* experimental systems, using two rat glioma cell lines, two human glioblastoma cell lines and rat glioblast cells. They found that HSP70 was increased in all the heat-treated cells. S phase and/or G2/M phase cells were increased in these heat-treated cells. Faassen<sup>[14]</sup> suggested that *in vivo* aging of human T cells resulted in a general defect in the

induction of gene products required for transition from quiescence into the S phase of the cell cycle. This conclusion is supported by observations of diminished inducibility of the lymphokine IL-2 and its receptor during aging. Faassen's study demonstrated that decreased proliferative response to phytohemagglutinin (PHA) was also paralleled by decreased induction during the prereplicative interval of two of the most strongly enhanced proteins in mitogen-activated T cells: HSP90 and P73, which are also members of the heat shock protein family. Diminished induction of HSP90 and p73 was observed in lymphocytes from older subjects (mean age 75 years), regardless of differences in health status of the subject populations.

The above two researches indicated that HSP plays a regulation role in cell growth. Hyperthermic treatment could induce the expression of HSP70, promote the synthesis of DNA and increase the S phase and G<sub>2</sub>/M-phase cell and is beneficial to cell proliferation. In the aged subjects, T cell proliferative response was decreased because of the defects in the induction of HSP90 and P73.

In order to further understand whether decreased expression of HSP90 could influence the tumor growth, we used the cell model we had established and studied their growth. From the cell growth curve it can be seen that the cell growth of the HSP90 antisense RNA transfectants was inhibited in different degrees. Among them, the growth of AH-SGC7901/VCR and AH-Ec109 was significantly decreased as compared with their parental cells, and the cell doubling time prolonged 16.69 h and 15.97 h respectively. The growth of AH-SGC7901 was also inhibited to some degree as compared with its parental cells.

Cell cycle analyses showed that, G<sub>1</sub> phase cells of AH-SGC7901/VCR and AH-Ec109 were increased and S phase cells were decreased as compared with their parental cells, indicating that there was G<sub>1</sub> arrest, causing the growth inhibition of the above two cell groups. G<sub>1</sub> phase cells of AH-SGC7901 were diminished, G<sub>2</sub> phase cells were increased and S phase had no obvious change, indicating that there was G<sub>2</sub>/M arrest, causing slower mitosis, and the decrease of cell mitosis and proliferation. G<sub>1</sub> phase S phase and G<sub>2</sub> phase of AH-HCC7402 all had no obvious changes compared with their parental cells. These results indicate that the expression of HSP90 $\beta$  is related to cell growth. Low expression of HSP90 could cause G<sub>1</sub> arrest and inhibit the synthesis of DNA or cause G<sub>2</sub>/M-arrest and inhibit cell mitosis, therefore inhibiting the cell growth and proliferation. The different inhibition rate in different cell lines may be because of the different heritage background and different blocking rate of HSP90 antisense RNA to HSP90

gene in these gene transfected cells. We concluded that down-regulate the expression of HSP90 $\beta$  could change the cell cycle distribution and inhibit the tumor cell growth.

The development of resistance of tumor cells to anti-cancer drugs is one of the critical issues for successful chemotherapy. Multi-drug resistance is an adaptable reaction of tumor cells to chemotherapeutic drugs. Various kinds of protein expression and/or the changes of enzyme activity could be seen in MDR-type tumor cells. Through the changes of these proteins, tumor cells could avoid being killed by chemical agents. Much evidence suggests that the heat shock proteins (hsp) may be involved in drug resistance<sup>[5,6,11,15-17]</sup>. In our study, the sensitivity of the pcDNA-HSP90 transfected cells to chemotherapeutic drugs increased more significantly than their parental cells. This means that lowered expression of HSP90 could increase sensitivity of the tumor cells to chemotherapeutic drugs. We also found that drug accumulation was increased in the pcDNA-HSP90 transfected cells. HSP90 might be related to the efflux of chemical agents. When HSP90 is decreased, the retention of chemical agents is increased and the intracellular drug concentration is increased, so is the sensitivity of the cells to the anti-cancer drugs. HSP90 is a major cytoplasmic chaperone protein and is related to many protein substrates, e.g. actin, tubulin, protein kinase and steroid receptor<sup>[18,19]</sup>. HSP90 may form hetero-oligomeric complex with some plasmic proteins such as HSP70, p60, Hip/p48, p23, FKBP52, FKBP51 and Cyp-40, involve protein folding, transportation and degradation, and regulate the activity of the protein<sup>[20-25]</sup>.

We thought that HSP90 may regulate the sensitivity of tumor cells to chemotherapeutic drugs through regulating the activity and function of P-gp. Bertram J and co-workers have reported that heat-shock protein hsp90 beta is associated with the P-glycoprotein (P-gp or P170), one of the most prominent components of the drug resistance machinery. They demonstrated that hsp90 beta can be co-precipitated along with P-gp and vice versa. In native agarose gels, both proteins migrated together as one single band as shown by Western blot analysis. This intracellular protein-protein interaction may present a mechanism for the modulation of P-gp function possibly by a stabilization of the protein which seems to be attributed to hsp90 beta. This study supports our research.

Oesterreich S and co-workers<sup>[1]</sup> found that when hsp was induced by elevated temperatures, resistance to doxorubicin (Dox), but not to other commonly used chemotherapeutic agents, was

induced in breast cancer cells. To evaluate the role of hsp27 in this phenomenon, they have transfected MDA-MB-231 breast cancer cells, which normally express low levels of hsp27, with a full-length hsp27 construct. These hsp27-overexpressing cells now display a 3-fold elevated resistance to Dox. They have also derived a MCF-7 breast cancer cell line with amplified endogenous hsp27 which is highly resistant to Dox. When these cells were transfected with an antisense hsp27 construct, they were rendered sensitive to Dox (3-fold). These results suggest that hsp27 specifically confers Dox resistance in human breast cancer cells. Our studies showed that HSP90 was related to MDR, and lowered expression of HSP90 could increase the drug sensitivity of tumor cells by 3-30 000 times indicating that regulation of HSP90 is more effective than hsp27 in this aspect. In different cells with different chemicals, the effect is different, possibly because of the different biological characteristics of the tumor cells and the different mechanism of the anti-cancer drugs.

The mechanisms of HSP90 in sensitizing tumor cells to anti-cancer drugs need to be further studied. This study gives some clues in using HSP inhibitors as a sensitizer to increase the sensitivity of tumor cells to anti-cancer drugs. In conclusion, down-regulation of HSP90 could change the cell cycle distribution and slow the tumor cell growth and increase the sensitivity of tumor cells to anti-cancer drugs.

## REFERENCES

- Schlesinger MG. Heat shock proteins. *J Biol Chem*, 1990;265:12111-12114
- Jill L, Elizabeth AC. Protein folding *in vivo*: unraveling complex pathways. *Cell*, 1997;90:201-204
- Yano M, Naito Z, Tanaka S and Asano G. Expression and roles of heat shock protein in human breast cancer. *Jpn J Cancer Res*, 1996;87:908-915
- Jameel A, Skilton RA, Campbell TA. Clinical and biological significance of Hsp90 $\beta$  in human breast cancer. *Int J Cancer*, 1992;50:409-415
- Bertram J, Palfner K, Hiddemann W, Kneba M. Increase of P-glycoprotein-mediated drug resistance by hsp 90 beta. *Anticancer Drug*, 1996;7:838-845
- Kim SH, Hur WY, Kang CD, Lim YS, Kim DW, Chung BS. Involvement of heat shockfactor in regulating transcriptional activation of MDR1 gene in multidrug-resistance cell. *Cancer Letters*, 1997;115:9-14
- Zhou DY. Experimental methods of molecular biology. *Beijing: People's Military Medical Publishing House*, 1995:42
- Lau ET, Kong RY, Cheah KSE. A critical assessment of the RNase protection assay as a means of determining exon sizes. *Analytical Biochem*, 1993;209:360-366
- Altman S. RNA enzyme-directed gene therapy. *Pro Natl Acad Sci USA*, 1993;90:10898-10900
- Sambrook J, Fritsch EF, Maniatis T. Molecular cloning: a laboratory manual. 2nd ed. Cold Spring Harbor: *Cold Spring Harbor Laboratory Press*, 1989:374
- Oesterreich S, Weng CN, Qiu M, Hilsenbeck SG, Osborne CK, Fuqua SAW. The small heat shock protein Hsp27 is correlated with growth and drug resistance in human breast cancer cell lines. *Cancer Res*, 1993;53:4443-4448
- Mairesse N, Horman S, Mosselmans R, Galand P. Antisense inhibition of the 27kDa heat shock protein production affects growth rate and cytoskeletal organization in MCF-7 cells. *Cell Biol Int*, 1996;20:205-212
- Faassen AE, O'Leary JJ, Rodysill KJ, Bergh N, Hallgren HM. Diminished heat-shock protein synthesis following mitogen stimulation of lymphocytes from aged donors. *Exp Cell Res*, 1989;183:326-334
- Ciocca DR, Fuqua SA, Lock Lim S, Toft DO, Welch WJ, McGuire WL. Response of human breast cancer cells to heat shock and chemotherapeutic drugs. *Cancer Res*, 1992;52:3648-3654
- Ciocca DR, Oesterreich S, Chamness GC, McGuire WL, Fuqua SA. Biological and clinical implications of heat shock protein 27000 (Hsp27): a review. *J Natl Cancer Inst*, 1993;83:1558-1570
- Sliutz G, Karlseder J, Tempfer C, Orel L, Holzer G, Simon MM. Drug resistance against gemcitabine and topotecan mediated by constitutive hsp70 overexpression *in vitro*: implication of quercetin as sensitizer in chemotherapy. *Brit J Cancer*, 1996;74:172-177
- Smith DF. Dynamics of heat shock protein 90-progesterone receptor binding and the disactivation loop model for steroid receptor complexes. *Mol Endocrinol*, 1993;7:1418-1429
- Xu Y, Lindquist S. Heat-shock protein Hsp90 governs the activity of pp60v-src kinase. *Proc Natl Acad Sci USA*, 1993;90:7074-7078
- Yhonehara M, Minami Y, Kawata Y. Heat-induced chaperone activity of Hsp90. *J Biol Chem*, 1996;271:2641-2645
- Wiech H, Buchner J, Zimmermann R, Jakob U. Hsp90 chaperones protein folding *in vitro*. *Nature*, 1992;358:169-170
- Jakob U, Buchner J. Assisting spontaneity: the role of Hsp90 and small HSPs as molecular chaperones. *TIBS*, 1994;19:205-211
- Pennisi E. Expanding the eukaryote's cast of chaperones. *Science*, 1996;274:1613-1614
- Freeman BC, Toft DO, Morimoto RI. Molecular chaperone machine: chaperone activities of cyclophilin Cyp-40 and the steroid aporeceptor-associated protein p23. *Science*, 1996;274:1718-1720
- Johnson J, Corbisier R, Stensgard B. The involvement of p23, hsp90, and immunophilins in the assembly of progesterone receptor complexes. *J Steroid Biochem Mol Biol*, 1996;56:21-37
- Jakob U, Lilie H, Meyer I. Transient interaction of Hsp90 with early unfolding intermediates of citrate synthase. Implications for heat shock *in vivo*. *J Biol Chem*, 1995;270:7288-7294

# Cyclosporin A protects Balb/c mice from liver damage induced by superan tigen SEB and D-GalN

YIN Tong<sup>1</sup>, TONG Shan-Qing<sup>2</sup>, XIE Yu-Cai<sup>3</sup> and LU De-Yuan<sup>2</sup>

**Subject headings** cyclosporin A; liver necrosis; apoptosis; staphylococcal enterotoxin B; D-galactosamine

## Abstract

**AIM** To investigate the pathogenic effect of SEB and D-GalN on liver and the protection of cyclosporin A, the relationship between hepatic apoptosis and necrosis and the possible mechanism of acute hepatic necrosis.

**METHODS** After staphylococcal enterotoxin B (SEB) mixed with D-galactosamine (D-GalN) were injected intraperitoneally into Balb/c mice and those previously treated with cyclosporin A, blood samples were collected and livers were isolated at 2, 6, 12, 24h. Patterns of hepatocellular death were studied morphologically and biochemically, circulating cytokines (TNF- $\alpha$ , IFN- $\gamma$ ) and mice mortality within 24h was assessed.

**RESULTS** The SEB could induce the typical apoptotic changes of hepatocytes, the D-GalN could induce hepatocytes apoptosis and degeneration at the same time, and the mice having received the SEB+D-GalN injections developed apoptosis at 2 and 6h, but after 12h hepatocytes were characterized by severe injury, whereas all the examinations in the cyclosporin A treated mice were normal.

**CONCLUSION** Hepatic cell apoptosis might be related to necrosis, and massive hepatocyte apoptosis is likely the initiating step of acute hepatic necrosis in mice. The effects induced by SEB and D-GalN on hepatocytes might be mediated by T cells, and could be prevented by cyclosporin A.

<sup>1</sup>Faculty of Medical Laboratory Sciences, Ruijin Hospital, Shanghai Second Medical University, Shanghai 200025, China

<sup>2</sup>Department of Microbiology, Shanghai Second Medical University, Shanghai 200025, China

<sup>3</sup>Department of Internal Medicine, Ruijin Hospital, Shanghai Second Medical University, Shanghai 200025, China

YIN Tong, female, born on 1967-07-28 in Zhenjiang City, Jiangsu Province, graduated from Shanghai Second Medical University as a postgraduate in 1996, lecturer, majoring infection and immunology, having 4 papers published.

\*Supported by Shanghai Institute of Immunology Foundation, No.9508.

**Correspondence to:** YIN Tong, Faculty of Medical Laboratory Sciences, Ruijin Hospital, Shanghai Second Medical University, Shanghai 200025, China

Tel. +86 • 21 • 63846590 Ext. 470

Received 1999-01-04

## INTRODUCTION

Patterns of cell death are defined as apoptosis and necrosis<sup>[1]</sup>. After staphylococcal enterotoxin B (SEB) together with D-Galactosamine (D-GalN) were injected ip. into BALB/c mice as well as those previously treated with cyclosporin A, we studied the patterns of hepatocellular death to investigate the pathogenic effect of SEB and D-GalN on liver and the protection of cyclosporin A, the relationship between hepatic apoptosis and necrosis, and the possible mechanism of acute hepatic necrosis.

## MATERIALS AND METHODS

### Main reagents

Cyclosporin A was given by Prof. Fan Li-An, Shanghai Institute of Immunology. D-GalN was purchased from Sigma Chemical Co. SEB was purchased from Institute of Microbiology and Epidemiology, Academy of Military Medical Sciences.

### Mice

Six-week-old male Balb/c mice weighing 20 g were purchased from the Department of Experimental Animal, Shanghai Institute of Biological Products, Ministry of Health of China.

### Groups

Mice were randomly divided into 6 groups: NS, CSA, SEB, D-GalN, SEB+D-GalN and CSA+SEB+D-GalN. Each group was divided into 4 subgroups each containing 6 mice according to 2, 6, 12 and 24 h. After pretest, SEB amount was set at 50  $\mu$ g/mice; D-GalN, 16 mg/mice; and CSA, 0.5 mg/mice. CSA was injected 0.5 h earlier. After mixed *in vitro*, SEB and D-GalN were injected. Control group was treated with normal saline in the same way. All drugs were injected intraperitoneally.

### Light microscopic examination

Livers were isolated at 2, 6, 12 and 24 h, and immediately fixed in 100 mL/L formalin, 5  $\mu$ m thick sections were stained with HE for light microscopic examination. Incidence of apoptosis bodies (ABs) was counted<sup>[2]</sup>.

### Transmission electron microscopic examination

Immediately after sacrifice, 1 mm<sup>3</sup> section from the

liver were fixed in 20 g/L glutaraldehyde. After stained, ultrathin sections were examined under a 200CX electron microscope.

#### **Agarose gel electrophoresis of hepatocellular DNA**

DNA was purified from hepatocytes and subsequently analyzed on 10 g/L agarose gels<sup>[3]</sup>.

#### **Serum alanine aminotransferase (ALT) assay**

Serum ALT activities were measured by a CX4 automatic biochemical analyzer (Beckman).

#### **Serum tumor necrosis factor (TNF- $\alpha$ ) assay**

It was performed according to L929 cell-killing method<sup>[4]</sup>.

#### **Serum interferon $\gamma$ (IFN- $\gamma$ ) assay**

IFN- $\gamma$  assay was made by cytopathic effect reduction method<sup>[5]</sup>.

#### **Statistical analysis**

Statistical significance was evaluated according to paired student's *t* test.

## **RESULTS**

### **Tissue histology**

Hepatocytes of SEB 2 h and 6 h groups showed nuclear pycnosis (Figure 1A) and no necrosis was found in 12 h and 24 h, suggesting that SEB only induce hepatocyte apoptosis in Balb/c-mice. Hepatocytes of D-GalN 2 h group developed chromatin condensation and organella edema (Figure 1B), 6 h group showed hepatocyte coexistence of degeneration and apoptosis bodies, no necrosis occurred after 12 h. Hepatocytes of SEB+D-GalN 2 h group showed nuclear pycnosis, nucleus was fragmented in 6 h group, after 12 h, besides some hepatocytes apoptosis, necrosis characters such as widespread destruction of the liver structure, massive erythrocyte agglutination, etc (Figure 1C) were found. Hepatocytes of the CSA+SEB+D-GalN group were normal (Figure 1D).

In SEB and D-GalN group, the incidence of ABs was strikingly raised at 6 h, rapidly decreased after 6 h, and decreased to normal in 24 h. But in SEB+D-GalN group it continuously increased till 24 h, and in CSA+SEB+D-GalN group it had no obvious changes.

### **Agarose gel electrophoresis of hepatocellular DNA**

The groups of SEB 6 h, D-GalN 6 h, SEB+D-GalN 6h and, 12 h showed typical "ladder" pattern, but SEB+D-GalN 24 h present "smear" pattern, and no abnormalities were found in CSA+SEB+D-GalN group (Figure 2).

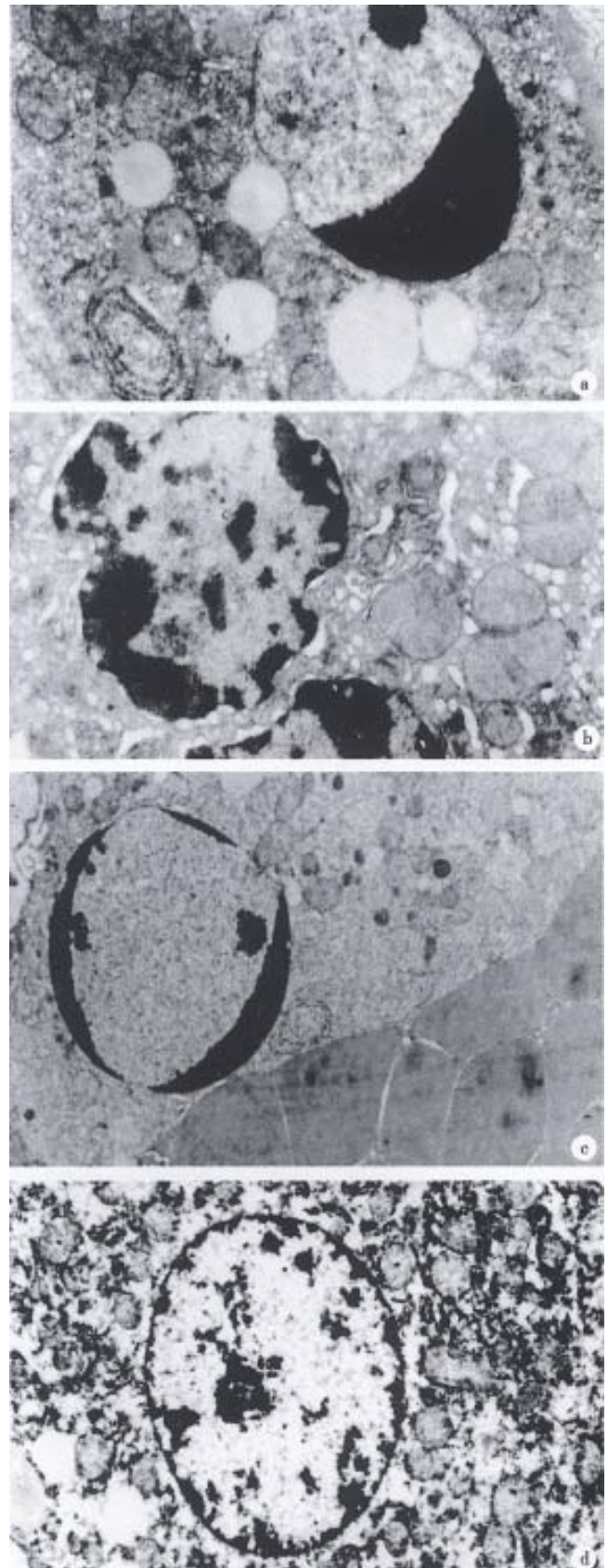


**Figure 1** Hepatocytes of Balb/c mice under TEM.

A. SEB 6 h, chromatin condensation,  $\times 10\ 000$ ; B. D-GalN 2 h, nuclear pycnosis and organelle edema,  $\times 10\ 000$ ; C. SEB+D-GalN 12 h, nuclear pycnosis and erythrocyte agglutination,  $\times 4\ 000$ ; D. CSA+SEB+D-GalN 6 h, nuclear of hepatocyte,  $\times 6\ 000$

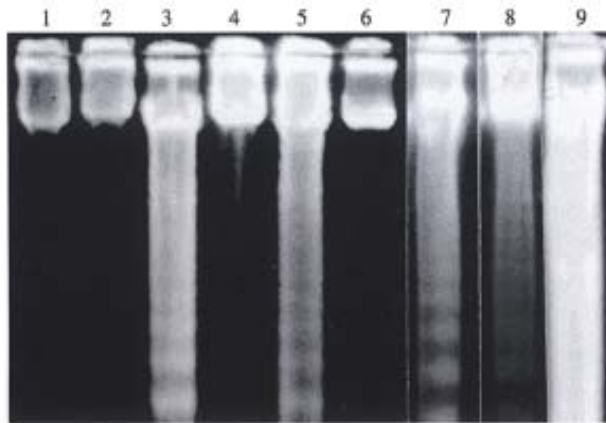


**Figure 2** DNA agarose gel electrophoresis in livers of Balb/c mice. 1. CSA 6 h; 2. CSA+SEB+D-GalN 6 h; 3. SEB+D-GalN 6 h; 4. CSA+SEB+D-GalN 12 h; 5. SEB+D-GalN 12 h; 6. NS; 7. SEB 6 h; 8. D-GalN 6 h; 9. SEB+D-GalN 24 h.

### Serum ALT assay

Compared with control group, there was very obvious difference in the activities of serum ALT of SEB+D-GalN 6 h and 12 h groups ( $P < 0.01$ ), and there was obvious difference in D-GalN 2, 6 h and SEB+D-GalN 2 h groups ( $P < 0.05$ ), but there was no difference in each of SEB groups, CSA, CSA+SEB+D-GalN, D-GalN 12 h and 24 h groups ( $P < 0.05$ ). Among these groups, activities of serum ALT of SEB+D-GalN 12 h even up to several thousand units (Table 1).

**Table 1** Serum ALT activities of Balb/c mice in different time (IU/L, 1IU/L = 16.67 nmol · s<sup>-1</sup>/L)

t/h	NS	CSA	SEB	D-GalN	SEB+D-GalN	CSA+SEB+D-GalN
2	51.8 ± 16.4	51.5 ± 17.8	59.5 ± 18.8	71.3 ± 25.7 <sup>a</sup>	69.0 ± 24.6 <sup>a</sup>	54.2 ± 24.5
6	56.0 ± 21.3	63.0 ± 18.1	60.5 ± 20.3	81.3 ± 24.7 <sup>a</sup>	95.7 ± 38.7 <sup>b</sup>	60.7 ± 29.4
12	54.8 ± 14.9	55.5 ± 27.5	56.5 ± 16.9	63.8 ± 22.8	4 109.2 ± 1910.1 <sup>b</sup>	60.5 ± 26.7
24	59.7 ± 24.5	59.0 ± 24.7	59.5 ± 24.7	60.7 ± 26.3		65.7 ± 24.2

<sup>a</sup> $P < 0.05$ , <sup>b</sup> $P < 0.01$  vs normal saline.

**Table 2** Lethality within 24 hours

D-GalN (mg/mice)	SEB (µg/mice)	CSA (mg/mice)	24 h lethality (death/total)
	10		0/3
	50		0/6
	100		0/3
	150		0/3
16			0/6
16	10		0/3
16	50		3/6
16	100		2/3
16	150		3/3
16	50	0.5	0/6
		0.5	0/6
			0/6 <sup>a</sup>

<sup>a</sup>Mice treated with normal saline.

### Circulating cytokine levels

Serum TNF- $\alpha$  levels of SEB 2 h (210 ng/L ± 80 ng/L) and SEB+D-GalN 2 h (300 ng/L ± 110 ng/L) reached a peak, thereafter sharply decreased in SEB 6 h (50 ng/L ± 30 ng/L) and SEB+D-GalN 6 h (50 ng/L ± 20 ng/L). Serum IFN- $\gamma$  levels of SEB and SEB+D-GalN groups began to increase after 2 h of administration (SEB 2 h 400 ng/L ± 120 ng/L, SEB+D-GalN 2 h 400 ng/L ± 150 ng/L), and peaked at 6 h-12 h (SEB 6 h 1480 ng/L ± 480 ng/L, 12 h 1620 ng/L ± 590 ng/L, 24 h 780 ng/L ± 350 ng/L, SEB+D-GalN 6 h 1360 ng/L ± 520 ng/L, 12 h 1 860 ng/L ± 680 ng/L 24h 790 ng/L ± 320 ng/L). Our data showed that there was no difference in the kinetics of appearance of serum cytokines between mice of SEB and SEB+D-GalN groups ( $P < 0.05$ ). In CSA+SEB+D-GalN groups both serum of TNF- $\alpha$  or IFN- $\gamma$  levels were negative.

### Twenty-four lethality

None of the Balb/c mice died at a dose of SEB up to 150 µg/mouse alone, and D-GalN of 16 mg/mouse within 24 h, whereas the lethality was elevated within 24 h with increased dose of D-GalN when the two were used in combination, for example, 50 µg SEB caused death in about half of the mice, 150 µg SEB up to 100%. But pretreated with CSA 0.5 h earlier, the mice were all survived (Table 2).

## DISCUSSION

Hepatocytes of SEB groups only showed apoptosis morphologically, and the course seems to finish within 12 hours, DNA agarose gel electrophoresis of hepatocytes exhibited the "ladder" pattern at 6 h-12 h, but activities of serum ALT were always normal. This result indicates that SEB caused hepatocytes nuclear pycnosis while membrane was intact. Mice lethality within 24 hours is 0. Because SEB did not exhibit any direct toxic effect on hepatocytes<sup>[6]</sup>, we analysed the mechanism of SEB-induced hepatocyte apoptosis may be related to biological features of superantigen nonspecific stimulating massive T cell proliferation and

releasing cytokines (TNF- $\alpha$ , IFN- $\gamma$ , etc.). D-GalN could induce both hepatocyte apoptosis and degeneration morphologically. The result of DNA agarose gel electrophoresis was similar to that of SEB groups, but activities of ALT rose between 2 and 6 hours, probably due to ( $P < 0.05$ ), hepatocyte degeneration which elevated membrane permeability. Mice lethality within 24 hours is 0. D-GalN is a kind of indirect toxin to liver, which can cause a selective depletion of urine nucleotides in mouse liver, thus leading to secondary hepatic injury. High doses can cause hepatocyte injury in mice resembling human viral hepatitis<sup>[1]</sup>.

Balb/c mice treated with SEB+D-GalN showed typical features of hepatocyte apoptosis within 6 hours, but after 12 hours, extensive cell necrosis was prominent besides apoptosis in a few hepatocyte. After 12 hours, the incidence of ABs became too high to count because a majority of hepatocytes were destructed. In biochemistry, DNA agarose gel electrophoresis demonstrated typical "ladder" between 6 and 12 hours, but a "smear" pattern at 24 hours. Serum ALT increased from the 2nd hour ( $0.01 < P < 0.05$  at 2 hours, as compared  $P < 0.01$ , at 6 hours  $68 \mu\text{mol} \cdot \text{s}^{-1} \cdot \text{L}^{-1}$  to at 12 hours. This indicated a great amount of hepatocytes were destructed, with a 24 h lethality of 50% whereas the mice pretreated with CSA were all normal. Superantigen had no direct toxic effect on hepatocytes, only nonspecifically stimulated massive T cell proliferation and released cytokines while CSA can inhibit T lymphocyte releasing cytokines. Therefore, we think that the acute injury to hepatocytes is mediated by T cells thus it can be inhibited by CSA.

Leist<sup>[7]</sup> reported that D-GalN+LPS/TNF induced hepatocyte apoptosis in Balb/c mice in the early stage and necrosis in the late stage. Our results are in agreement with Leist's. Based on the studies of transgenic mice in literature<sup>[8]</sup> and our experiment, we assume that the process of hepatic

injury induced by SEB+D-GalN is: massive hepatocyte apoptosis occurred, then the neutrophils and macrophages were attracted by endogenous mediators and activated by apoptotic hepatocytes releasing massive cytokines, and finally, the secondary acute hepatic necrosis, occurred leading to the death of mice. D-GalN in addition to its sensitization of hepatocyte, D-GalN may prevent the rapid uptake of apoptotic cells by neighboring hepatocytes and Kupffer's cells<sup>[7]</sup>. Gantner<sup>[9]</sup> reported apoptotic hepatocytes can induce procoagulant activities in endothelial cells and platelets that eventually result in thrombin deposition and sinusoidal congestion. Therefore, there might be some relationship between apoptosis and necrosis. If the number of apoptotic hepatocytes is small and can be rapidly phagocytized by the nearby hepatocytes and Kupffer's cells, secondary necrosis will not occur while if it is massive and can not be phagocytized rapidly, secondary necrosis will develop.

## REFERENCES

- 1 Alison MR, Sarraf CE. Liver cell death: pattern and mechanisms. *Gut*, 1994;35:577
- 2 Faa G, Ledda-Columbano GM, Ambu R, Congiu T, Coni P, Riva A. An electron microscopic study of apoptosis induced by cycloheximide in rat liver. *Liver*, 1994;14:270
- 3 Sambrook J, Fritsch EF, Maniatis T. Molecular cloning, 2nd ed. Beijing: Science and Technology Press, 1993:309
- 4 Hu BY, Zhang BZ, Zhu YM. Assay of TNF induced by whole blood. *Shanghai J Immunol*, 1991;11:160
- 5 Yong TP, Yi XN. Practical immunology, 1st ed. Changchun: Changchun Publishing House, 1994:596
- 6 Uchiyama T, Yan XJ, Imanishi K, Imanishi KI, Yagi J. Bacterial superantigen-mechanism of T cell activation by the superantigen and the role in the pathogenesis of infectious diseases. *Microbiol Immunol*, 1994;38:245
- 7 Leist M, Gantner F, Bohlinger I, Tiegs G, Germann PG, Wendel A. Tumor necrosis factor-induced hepatocyte apoptosis precedes liver failure in experimental murine shock models. *Am J Pathol*, 1995; 146:120
- 8 Chisari FV. Hepatitis B virus transgenic mice: insights into the virus and the disease. *Hepatology*, 1995;22:1316
- 9 Gantner F, Leist M, Jilgs S, Germann PG, Freudenbeg MA, Tiegs G. Tumor necrosis factor-induced hepatic DNA fragmentation as an early marker of T cell-dependent liver injury in mice. *Gastroenterology*, 1995;109:166

Edited by MA Jing-Yun

# Nitric oxide synthase distribution in esophageal mucosa and hemodynamic changes in rats with cirrhosis

HUANG Ying-Qiu<sup>1</sup>, XIAO Shu-Dong<sup>2</sup>, ZHANG De-Zhong<sup>2</sup> and MO Jian-Zhong<sup>2</sup>

**Subject headings** esophagus; nitric oxide synthase; liver cirrhosis; hemodynamics

## Abstract

**AIM** To observe the nitric oxide synthase (NOS) distribution in the esophageal mucosa and hemodynamic changes in cirrhotic rats.

**METHODS** NOS distribution in the lower esophagus of rats with carbon tetrachloride-induced cirrhosis was assessed by using NADPH-diaphorase (NADPH-d) histochemical method. Concentration of NO in serum were measured by fluorometric assay. Mean arterial pressure (MAP), cardiac output (CO), cardiac index (CI), splanchnic vascular resistance (SVR), and splanchnic blood flow (SBF) were also determined using <sup>57</sup>Co-labeled microsphere technique.

**RESULTS** Intensity of NOS staining in the esophageal epithelium of cirrhotic rats was significantly stronger than that in controls. There was a NOS-positive staining area in the endothelia of esophageal submucosal vessels of cirrhotic rats, but the NOS staining was negative in normal rats. NO concentration of serum in cirrhotic rats were significantly higher in comparison with that of controls. Cirrhotic rats had significantly lower MAP, SVR and higher SBF than those of the controls.

**CONCLUSION** Splanchnic hyperdynamic circulatory state was observed in rats with cirrhosis. The endogenous NO may play an important role in development of esophageal varices and in changes of hemodynamics in cirrhosis.

## INTRODUCTION

Cirrhosis with portal hypertension is associated with hyperdynamic circulation characterized by generalized vasodilation and increased cardiac output and splanchnic regional blood flows. Endogenous NO, a very potent vasodilator factor, may play a very important role in the pathogenesis of hemodynamic changes in cirrhosis. It is unclear whether NO is involved in the pathogenesis of esophageal varices as one of severe complications of hepatic cirrhosis. The present study was aimed at investigating the effects of endogenous NO on esophageal varices and hemodynamic changes in cirrhotic rats.

## MATERIALS AND METHODS

### *Experimental animal*

Male Sprague-Dawley (SD) rats (supplied by the Shanghai Laboratory Animal Center of Chinese Academy of Sciences) weighing between 250 g and 300 g were used. Cirrhotic rat model was induced by injection of 60% CCl<sub>4</sub> oily solution twice weekly subcutaneously (0.3 mL/100 g, first time 0.6 mL/100 g) for two months<sup>[1]</sup>. After the model was established, there were 8 cirrhotic rats in experimental group and 8 normal SD rats served as controls.

### *Hemodynamic studies*<sup>[2]</sup>

Under Ketamine anesthesia (100 mg/kg intramuscularly), the right femoral artery and the femoral vein were cannulated with a polyethylene 50 catheters, which went forward respectively to the abdominal aorta and inferior vena cava. The left ventricle was catheterized under pressure monitoring through the right carotid artery with a polyethylene 50 catheter for injection of <sup>57</sup>Co-labeled microspheres. All catheters were connected to highly sensitive pressure transducers that were calibrated before each study, and blood pressures were registered on a multichannel recorder (Lifescope 6). An abdominal incision (1.5 cm-2.0 cm) was performed, and the portal pressure (PP) was indirectly measured through puncture of spleen with a No.4 needle<sup>[3]</sup>. Cardiac output and splanchnic blood flows were measured by using <sup>57</sup>Co-labeled microspheres technique. A reference blood sample was obtained from the femoral artery

<sup>1</sup>Department of Gastroenterology, General Hospital of Benxi Iron & Steel Co., Benxi 117000, China

<sup>2</sup>Shanghai Institute of Digestive Diseases, Renji Hospital, Shanghai Second Medical University, Shanghai 200001, China

HUANG Ying-Qiu, male, born on 1962-03-30 in Benxi City, Liaoning Province, graduated from Shanghai Second Medical University, with a master degree in 1997, now chief of Department of Gastroenterology, General Hospital of Benxi Iron & Steel Co., physician and associate professor of China Medical University, member of Liaoning Digestive Branch of Chinese Medical Association (CMA), and member of Liaoning Internal Medicine Branch of CMA, majoring digestive medicine, having 30 papers published.

**Correspondence to:** Dr. HUANG Ying-Qiu, Department of Gastroenterology, General Hospital of Benxi Iron & Steel Co., Benxi 117000, China

Received 1999-02-05 Revised 1999-04-14

catheter for 70 seconds at a constant rate of 1 mL/min with a continuous-withdrawal pump (model WZ-50, Zhejiang Medical University, China). Meanwhile, approximately 50 000 microspheres labeled with  $^{57}\text{Co}$ -labeled microspheres (diameter,  $15\ \mu\text{m} \pm 0.6\ \mu\text{m}$ , Du Pont Co., USA) were injected into the left ventricle 10 seconds after the start of blood withdrawal. Then 2 mL blood sample was withdrawn from the right femoral vein and stored at  $-70\ ^\circ\text{C}$  for determination. The rats were then killed, the lower esophagus was quickly excised and quick-frozen in nitrogen solution for NADPH-d histochemical staining, and then liver specimens were fixed in 10% formalin for histologic examination. Other abdominal organs and mesentery were also taken out, weighed, and cut into small pieces, and placed in  $\gamma$  counter (model GP1, Shanghai Electronic Apparatus Co., China) for determining the radio-activity (cpm).

### Calculations

Cardiac output (CO) (mL/min) = injected  $^{57}\text{Co}$  (cpm)  $\times$  reference blood sample (mL/min)/reference blood  $^{57}\text{Co}$  (cpm).

Cardiac index (CI) (mL  $\cdot$  min $^{-1}$   $\cdot$  100 g-1BW) = CO (mL/min)/100 g BW.

Splanchnic blood flow (SBF) (mL/min) = organ  $^{57}\text{Co}$  (cpm)  $\times$  reference blood sample (mL/min)/reference blood  $^{57}\text{Co}$  (cpm).

Portal vein blood flow (PVF) (mL/min) = the sum of gastric, splenic, intestinal, mesenteric and pancreatic venous flows.

Splanchnic vascular resistance (SVR) (kPa  $\cdot$  mL $^{-1}$   $\cdot$  min $^{-1}$ ) = [MAP-PP (kPa)]/PVF (mL/min).

### NADPH-d histochemical staining<sup>[4]</sup>

Esophageal samples were fixed in 4% paraformaldehyde and 0.4% picric acid in 0.16 mol/L sodium phosphate buffer, pH 6.9, for 4 hours. Then they were transferred to 10% sucrose in 0.1 mol/L sodium phosphate buffer, pH 7.2, at  $4\ ^\circ\text{C}$  for 24 hours. Cryostat sections (10  $\mu\text{m}$  thick,  $-20\ ^\circ\text{C}$  Minotome cryostat, USA) were immersed for 10 minutes in 0.01 mol/L phosphate buffer, pH 8.0, and were incubated for 40 minutes at  $37\ ^\circ\text{C}$  in prewarmed solution consisting of 0.01 mol/L phosphate buffer, pH 8.0; 0.3% Triton X100; 0.5 mmol/L nitroblue tetrazolium (NBT, Sigma, USA); and were 1.0 mmol/L NADPH (Sigma, USA). After washing in 0.01 mol/L phosphate buffer, pH 7.4, the sections were dehydrated with graded alcohol and mounted on microscopic glass slides.

### Serum NO determination

This assay is a modification of the method of

Damiani and Burini<sup>[5]</sup> for the fluorometric determination of nitrite. Briefly, the serum sample is added with 20% sodium sulfosalicylic acid to remove protein. After centrifugation, the filtrate is added with 0.01 mol/L EDTA and 2,3-Diaminonaphthalene (DAN, Fluka, Switzerland) hydrochloric acid solution. The reaction is terminated after 10 min at  $20\ ^\circ\text{C}$  by addition of 2.8 mol/L-NaOH solution. The intensity of fluorescent signal of 1(H) naphthotriazole in the serum sample were obtained in a luminescence spectrofluorometer (Model F-4 000, Hitachi, Japan) with excitation at 365 nm, emission at 420 nm and slits at 3 nm. Nitrite levels in samples were then calculated as a standard curve for nitrite.

### Liver histologic examination

The liver samples were fixed in 10% formalin, processed routinely, and embedded in paraffin. The sections were stained with HE and were then observed using a microscope.

### Statistical analysis

The results were expressed as  $\bar{x} \pm s$ , and were analyzed with Student's *t* test.  $P < 0.05$  was regarded as of statistical significance.

## RESULTS

The liver histology of all the animals treated with CCl<sub>4</sub> in the study had a granulated surface, and histological examination showed the characteristic features of cirrhosis.

Areas with a positive reaction for NADPH diaphorase were stained dark blue. The reaction was negative in specimens stained without NADPH. NADPH-diaphorase histochemical staining showed that intensity of NOS staining in lower esophageal epithelium of cirrhotic rats was significantly stronger than that in normal SD rats. There was a NOS positive staining area in the endothelium of esophageal submucosal vessels, but the NOS staining was negative in normal controls (Figures 1, 2).

Hyperdynamic circulatory status associated with portal hypertension was observed in all rats with cirrhosis (Tables 1, 2). Serum NO level in cirrhotic rats were significantly higher than that in normal controls ( $4.204\ \mu\text{mol/L} \pm 1.253\ \mu\text{mol/L}$  vs  $0.532\ \mu\text{mol/L} \pm 0.257\ \mu\text{mol/L}$ ,  $P < 0.01$ ).

**Table 1 Hemodynamics parameters ( $\bar{x} \pm s$ )**

	Controls (n = 8)	Cirrhotic rats (n = 8)
MAP (kPa)	$17.05 \pm 0.34$	$14.42 \pm 0.47^a$
PP (kPa)	$1.123 \pm 0.096$	$1.665 \pm 0.067^a$
CO (mL/min)	$135.5 \pm 3.55$	$189.99 \pm 9.26^a$
CI (mL $\cdot$ min $^{-1}$ $\cdot$ 100 g-1 BW)	$39.68 \pm 1.64$	$55.89 \pm 1.82^a$
PVF (mL $\cdot$ min $^{-1}$ $\cdot$ 100 g-1 BW)	$3.762 \pm 0.094$	$4.295 \pm 0.155^a$
SVR (kPa $\cdot$ mL $^{-1}$ $\cdot$ min $^{-1}$ )	$4.234 \pm 0.118$	$2.974 \pm 0.186^a$

<sup>a</sup> $P < 0.01$ , compared to control group.

**Table 2** Blood flow of splanchnic organs ( $\text{mL} \cdot \text{min}^{-1} \cdot \text{g}^{-1}$ ,  $\bar{x} \pm s$ )

Organ	Controls ( $n = 8$ )	Cirrhotic rats ( $n = 8$ )
Stomach	$0.544 \pm 0.045$	$0.881 \pm 0.065^a$
Spleen	$0.946 \pm 0.060$	$0.725 \pm 0.057^a$
Pancreas	$0.819 \pm 0.031$	$0.998 \pm 0.055^a$
Intestine & mesentery	$1.451 \pm 0.037$	$1.686 \pm 0.057^a$
Kidney	$0.465 \pm 0.038$	$0.686 \pm 0.046^a$

<sup>a</sup> $P < 0.01$ , compared to control group.

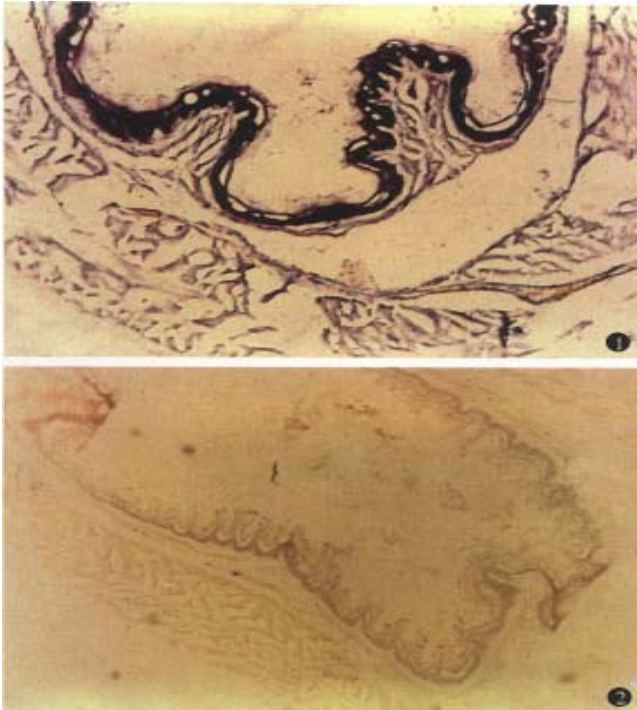


**Figure 1** Esophageal NADPH-d histochemical staining in cirrhotic rats.  $\times 200$

**Figure 2** Esophageal NADPH-d histochemical staining in normal rats.  $\times 200$

## DISCUSSION

Lower esophageal varices are the main clinical manifestation and the cause of upper gastrointestinal hemorrhage in cirrhosis associated with portal hypertension. Cirrhosis with portal hypertension is often associated with hyperdynamic circulation characterized by generalized vasodilation and increased cardiac output and splanchnic regional blood flows. However, the mechanisms responsible for the development of lower esophageal varices and the hyperdynamic circulatory status are still unclear.

Our study showed that intensity of NOS staining in esophageal epithelium of cirrhotic rats associated with portal hypertension was significantly stronger than that in normal SD rats. There was a NOS positive staining area in the endothelium of esophageal submucosal vessels, but the NOS staining

was negative in normal rats. In addition, we also found that the levels of serum NO were all significantly elevated in cirrhotic rats as compared to normal rats. The hyperdynamic circulatory state of cirrhosis with portal hypertension could provide continuous stimuli (such as a progressive increase in blood flow, high oxygenation in portal blood, or endotoxemia) for nitric oxide synthase (NOS) induction in the portal collateral bed<sup>[6]</sup>. Our findings suggest that NO may play an important role in the collateralization of the portal system because inhibition of NO synthesis reduces portal systemic shunting without affecting portal pressure in cirrhotic rats<sup>[7]</sup>. Therefore, overexpressed NOS in the mucosa of the lower esophagus of cirrhotic rats significantly shows a mechanism for the predisposition of collaterals to develop at this site by enhancing NO production. Therefore, greater NOS content in the lower esophageal mucosa of cirrhotic rats would produce increased amounts of NO, adding to the hyperdynamic circulation in the region.

In order to determine NOS, we used a kind of histochemical staining method depended on the presence of diaphorase. The technique of "diaphorase" staining is based on the ability of the C-terminal portion of nitric oxide synthase to transfer electrons from NADPH to nitroblue tetrazolium (NBT) reducing the substrate NBT to an insoluble purple formazan product giving the characteristic "diaphorase" reaction<sup>[8]</sup>. Other studies showed that the overexpression of NOS visualized by immunohistochemical staining and of NADPH-d staining in brain and peripheral tissues were identical<sup>[9,10]</sup>. It seems that the NADPH-d staining technique is a useful and simple method to determine the expression of NOS<sup>[11]</sup>. In the present study, we found a strong expression of NADPH-d activity in the lower esophagus, reflecting NOS. The findings are identical to Tanoue's report<sup>[4]</sup>. Tanoue *et al* found that expression of NOS proteins in endothelium of submucosal veins was markedly higher in portal-hypertensive rats than in controls. We postulate that because NO is a very potent vasodilator factor, overexpression of NOS may be an important cause of esophageal variceal rupture to give rise to hemorrhage.

In the present study, increment of splanchnic blood flow associated with portal hypertension was observed in all 8 rats with cirrhosis except that splenic vein flow was lower than controls. Moreover, there were 6 cirrhotic rats with ascites in the 8 rats with cirrhosis. Although the cause of this hyperdynamic circulation is still a matter of

controversy, it seems that vasodilatation, induced by increased activity of endothelia-independent and endothelia-dependent vasodilators, initiates the hyperdynamic state. Recently, a role of endogenous nitric oxide in the regulation of blood flow and vascular tone of the systemic and splanchnic circulations in portal hypertension has been suggested by several *in vivo* and *in vitro* studies, implying that excessive synthesis of NO could be responsible for the these circulatory abnormalities. Our previous studies had suggested that an excessive release of NO may be involved in the splanchnic hyperemia<sup>[12]</sup>.

In conclusion, the results of the present study show that endogenous NO may play an important role in development of esophageal varices and in changes of hemodynamics pattern in cirrhosis.

## REFERENCES

- 1 Huang YQ, Zhang DZ, Mo JZ, Xiao SD, Li RR. Effects of nitric oxide on hemodynamics in cirrhotic rats. *Chin J Hepatol*, 1997;5: 153-155
- 2 Nagasawa M, Kawasaki T, Yoshimi T. Effects of calcium antagonists on hepatic and systemic hemodynamics in awake portal hypertensive rats. *J Gastroenterol*, 1996;31:366-372
- 3 Benoit JN, Womack WA, Hernandez L. "Forward" and "backward" flow mechanisms of portal hypertension. Relative contributions in the rat model of portal vein stenosis. *Gastroenterology*, 1985;89:1092-1096
- 4 Tanoue K, Ohta M, Tarnawski AS, Wahlstrom KJ, Sugimachi K, Sarfeh IJ. Portal hypertension activates the nitric oxide synthase gene in the esophageal mucosa of rats. *Gastroenterology*, 1996; 110:549-557
- 5 Damiani P, Burini G. Fluorometric determination of nitrite. *Talanta*, 1986;33:649-652
- 6 Miller VM, Aarhus LL, Vanhoutte PM. Modulation of endothelium-dependent responses by chronic alteration of blood flow. *Am J Physiol*, 1986;251:H520-H527
- 7 Lee FY, Albilos A, Colombato LA, Groszmann RJ. The role of nitric oxide in the vascular hyporesponsiveness to methoxamine in portal hypertensive rats. *Hepatology*, 1992;16:1043-1048
- 8 Norris PJ, Charles IJ, Scorer CA, Emson PC. Studies on the localization and expression of nitric oxide synthase using histochemical techniques. *Histochemical J*, 1995;27:745-756
- 9 Dawson TM, Brecht DS, Fotuhi M, Hwang PM, Snyder SH. Nitric oxide synthase and neuronal NADPH diaphorase are identical in brain and peripheral tissues. *Proc Natl Acad Sci USA*, 1991;88: 7797-7801
- 10 Hope BT, Maichel JG, Knigge KM, Vincent SR. Neuronal NADPH diaphorase is a nitric oxide synthase. *Proc Natl Acad Sci USA*, 1991;88:2811-2814
- 11 Ward SM, Xue C, Shuttleworth W, Brecht DS, Snyder SH, Sanders KM. NADPH diaphorase and nitric oxide synthase colocalization in enteric neurons of canine proximal colon. *Am J Physiol*, 1992; 263:G277-G284
- 12 Huang YQ, Xiao SD, Zhang DZ, Mo JZ. Effects of erythropoietin or nitric oxide synthesis inhibitor on hyperdynamic circulatory state in cirrhotic rats. *Natl Med J China*, 1998;78:139-142 (in Chinese with English abstract)

Edited by MA Jing-Yun

# Expression of perforin and granzyme B mRNA in judgement of immunosuppressive effect in rat liver transplantation \*

ZHANG Shao-Geng<sup>1</sup>, WU Meng-Chao<sup>2</sup>, TAN Jing-Wang<sup>1</sup>, CHEN Han<sup>2</sup>, YANG Jia-Mei<sup>2</sup> and QIAN Qi-Jun<sup>2</sup>

**Subject headings** liver transplantation; immunosuppression; perforin granzyme B genes; graft rejection

## Abstract

**AIM** To explore the expression of perforin and granzyme B genes mRNA to judge the effect of immunosuppression in acute rejection of liver transplantation.

**METHODS** The expression of perforin and granzyme B genes mRNA was examined by reverse transcription-polymerase chain reaction (RT-PCR) in hamster to rat liver grafts under the immunosuppression of cyclosporine or/and splenectomy. Histological findings were studied comparatively.

**RESULTS** Cyclosporine could obviously decrease the cellular infiltration, and completely repress the expression of mRNA for perforin and granzyme B, but could not change severe hepatocyte necrosis and hemorrhage. Splenectomy could significantly lighten hepatocyte necrosis, and completely eliminate hemorrhage, but not affect the cellular infiltration and the expression of perforin and granzyme B genes mRNA. Cyclosporine or splenectomy alone could not prolong the survival time, however, their combination could completely repress the rejection of liver grafts. The survival time of animals were significantly prolonged (37.1 days). The architecture of hepatic lobules was preserved. There was slight

**cellular infiltration in the portal tracts and no expression of perforin and granzyme B genes mRNA could be seen in three weeks after transplantation.**

**CONCLUSION** Perforin and granzyme B genes are valuable in judging the effect of immunosuppression in liver transplantation.

## INTRODUCTION

Rejection is one of major factors influencing the outcome of the patients after liver transplantation, and acute rejection is more harmful to the grafts and recipients. The cellular immunity has been proved to be a chief mechanism in rejecting liver transplantation, and cytotoxic T lymphocyte (CTL) is the major effector cell, the perforin lytic pathway to granzyme B, plays a critical role in the T-cell immune response<sup>[1]</sup>. It is a hot issue of the moment to search for special early markers to judge the effect of immunosuppression in acute rejection of liver transplantation. In this study, the expression of perforin and granzyme B mRNA was examined by reverse transcriptase-polymerase chain reaction (RT-PCR) under the immunosuppression of Cyclosporine (CsA) and splenectomy based on the establishment of a stable and reliable model of hamster to rat concordant xenogeneic orthotopic liver transplantation.

## MATERIALS AND METHODS

### Animals

Female golden hamsters weighing 150 g-180 g were the donors of liver xenografts, and male Wistar rats weighing 230 g-260 g were the recipients. The animals were purchased from Xi Bi Experimental Animal Centre and Shanghai Experimental Animal Centre of Chinese Academy of Sciences.

### Liver transplantation

Orthotopic liver transplantation was performed according to simplified three-cuff technique<sup>[2]</sup> with some modifications. Donor cholecystectomy was performed at the time of cuff preparation, without reconstruction of hepatic artery, and splenectomy at the time of transplantation with simple ligation of the splenic hilum and excision. No microscope was

<sup>1</sup>The Department of Hepatobiliary Surgery, Fuzhou Military General Hospital, Fuzhou 350025, Fujian Province, China

<sup>2</sup>Shanghai East Hepatobiliary Hospital of Second Military Medical University, Shanghai 200433, Shanghai, China

Dr. ZHANG Shao-Geng, male, born on 1964-02-16 in Nanchang city, Jiangxi Province, graduated from Shanghai Second Military Medical University in 1997, under the instruction of professor Wu Meng-Chao, he was engaged in the studies of liver transplantation and obtained M.D. and Ph.D. Now he is working in the Department of Hepatobiliary Surgery, Fuzhou Military General Hospital.

\*Project supported by the National Natural Science Foundation of China, No. 39500152.

**Correspondence to:** Dr. ZHANG Shao-Geng, Department of Hepatobiliary Surgery, Fuzhou Military General Hospital, 156 Xi Huan Bei Road, Fuzhou 350025, Fujian Province, China

Tel. +86 • 591 • 3709089

Received 1999-02-05

used for all the operations.

### Experimental groups

Liver xenografts were studied in four groups: A, untreated controls ( $n = 8$ ); B, treated with cyclosporine 30mg/kg/daily ( $n = 6$ ); C, treated with splenectomy ( $n = 6$ ); D, treated with splenectomy and cyclosporine 30 mg · kg · day ( $n = 7$ ).

### Immunosuppressants

CsA was administered to recipients intramuscularly beginning on the first day of operation, at an interval of 12 hours. Splenectomy was done at the time of transplantation.

### Histology

Postoperative specimens at rejection and specimens taken at sacrifice were fixed in 10% formalin and stained with hematoxylin and eosin.

### RNA extraction

Total RNA was extracted according to the Qiagen kit directory. In brief, after homogenization and lysis with lytic buffer RLT in QIA shredder, same volume of 70% ethanol were added. Samples were then moved into RNeasy spin column and centrifuged for 15sec at  $8\,000 \times g$ , buffer RW1 and buffer PRE were added and centrifuged for 15 sec at  $8\,000 \times g$  step by step. Finally, RNA was eluted with diethylpyrocarbonate (DEPC)treated water and centrifuged for 1min at  $8\,000 \times g$ . The approximate quantity of RNA was determined with an OD 260 nm and the purity was confirmed with an OD ratio of 260 : 280 to be greater than 1.8 in all specimens. RNA was extracted from rat splenocytes stimulated in culture for 18 hours with PHA (10 mg/L), Con A (10 mg/L) and IL-2 (20 units/mL) for the positive control. The RNA of normal rat liver served as negative control.

### Reverse transcription and polymerase chain reaction

The cDNA synthesis was performed with GIBCOL BRL kit. RNA mixtures were prepared as follows: 2  $\mu$ g of total RNA and 0.5  $\mu$ g of oligo (dT) 12-18, were added with DEPC-treated water and diluted to 12  $\mu$ L, water bathed at 70°C for 10 min and incubated on ice for at least 1min, then added with 2  $\mu$ L of  $10 \times$  PCR buffer, 2  $\mu$ L of 25mM MgCl<sub>2</sub>, 1  $\mu$ L of 10mM dNTP, and 2  $\mu$ L of 0.1M DTT and incubated at 42°C for 5 min. 200U Super Script II RT was added and incubated at 42°C for 50 min and the reaction was terminated at 70°C for 15 min and chilled on ice, and finally 1  $\mu$ L of Rnase H was added to each tube and incubated for 20 min at 37°C. The cDNA was stored at -20°C.

The DNA was amplified using RT-PCR on a

Perkin-Elmer 2 400 thermocycler, and RT-PCR primer was designed according to the exon of rat gene sequences. The primer set for perforin was ① 5' GCCATCCTGCGTCTGGACCTG3', ② 5' CATTTCGCGGTGCACG ATGGAG3'; primer set for the granzyme was ① GACTTTGTGCTGACTGCTGC TCAC3', ② 5' TTGTCCATAGGAGACGATGCC GC3'; and for the  $\beta$ -actin: ① 5' TGCTAC ACTGCCA CT CGGTCA3', ② 5' GCATGCTCTGTGGAGCTGT TA3'<sup>[3]</sup>. The reaction mixture contained 2  $\mu$ L cDNA, 1  $\mu$ L of 10 mmol/L dNTP, 3  $\mu$ L of 25 mmol/L MgCl<sub>2</sub>, 5  $\mu$ L of  $10 \times$  buffer, 1  $\mu$ L Taq polymerase, 2  $\mu$ L each of the forward and reverse primer, and 34  $\mu$ L of dual-distilled water for each 50  $\mu$ l amplification reaction. Reactions were performed for 30 cycles. The conditions were 94°C for 3 min prior to cycling, denaturing at 95°C for 15 sec, annealing at 60°C for 20 sec and extension at 70°C for 30 sec. Following amplification, ten  $\mu$ L PCR products were run on a 1.5% agarose gel stained with ethidium bromide, gene specific bands were visualized by photography under UV fluorescence.

## RESULTS

### Survival time

Graft survival is shown in Table 1. Groups A, B and C showed rejection in 6-9 days. Groups B and C had rejection with a time course similar to group A ( $P > 0.05$ ). Survival in group D was significantly prolonged to  $37.1 \pm 9.9$  days ( $P > 0.01$ ).

**Table 1 Survival of hamster to rat liver transplantation**

Groups	Therapy	Survival (days)	$\bar{x} \pm s$
A	None	6,7,7,7,7,7,7	$6.9 \pm 0.4$
B	CsA 30 mg · kg · day	6,7,7,7,8,9	$7.3 \pm 1.0$
C	Splenectomy	6,7,7,7,7,8	$7.0 \pm 0.6$
D	CsA 30mg · kg · day+splenectomy	27,29,30,35,39,46,54	$37.1 \pm 9.9^a$

<sup>a</sup> $P < 0.01$  as compared with groups A, B and C.

### Histological examination

The liver xenografts in group A showed diffuse mononuclear cell infiltration, massive necrosis and interstitial hemorrhage (Figure 1A). In group B, CsA at dose of 30 mg · kg · day obviously decreased cellular infiltration, but severe hepatocyte necrosis and hemorrhage remained unchanged (Figure 1B). Splenectomy (group C) significantly alleviated hepatocyte necrosis and hemorrhage, but did not change diffuse mononuclear cell infiltration (Figure 1C). In group D, CsA and splenectomy abated cellular infiltration and hepatocyte necrosis and hemorrhage, the architecture of the hepatic lobule was preserved, but there was slight cellular infiltration in the portal tracts (Figure 1D).

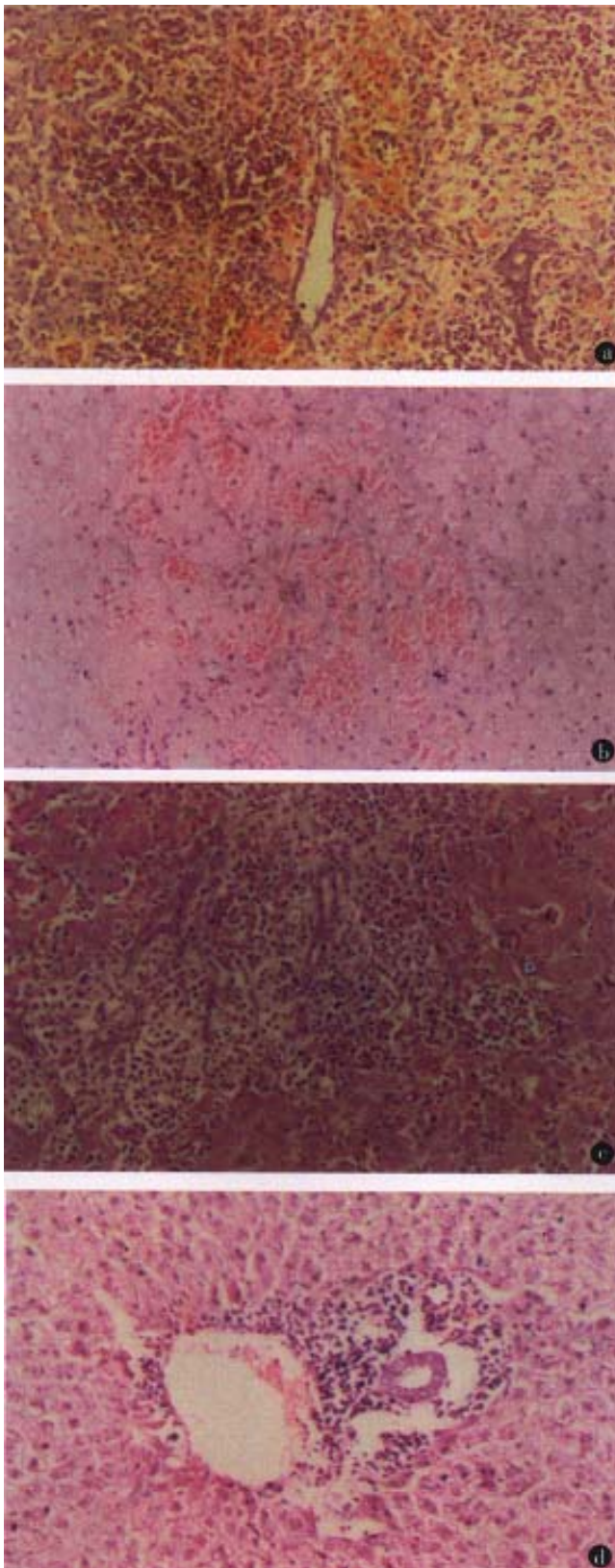


**Figure 1** Histology of liver grafts. (A) Diffuse mono nuclear cell infiltration, massive necrosis and interstitial hemorrhage; (B) Cellular infiltration obviously decreased, but severe hepatocyte necrosis and hemorrhage unchanged; (C) Splenectomy significantly alleviated hepatocyte necrosis and hemorrhage, but did not change diffuse mononuclear cell infiltration; (D) The architecture of the hepatic lobule was preserved, but there was slight cellular infiltration in the portal tracts.

**Expression of perforin and granzyme B genes mRNA**

All recipients had the expression of perforin and granzyme B genes mRNA in group A on post-transplantation day (POD) 5; only one (1/6) in group B expressed mRNA of these genes on POD 5; and five recipients (5/6) in group C expressed mRNA of both genes on POD 5. There was no expression of both genes in group D on POD 5 and 14, but only one recipient (1/7) expressed mRNA of perforin and granzyme B genes on POD 21 (Figure 2).

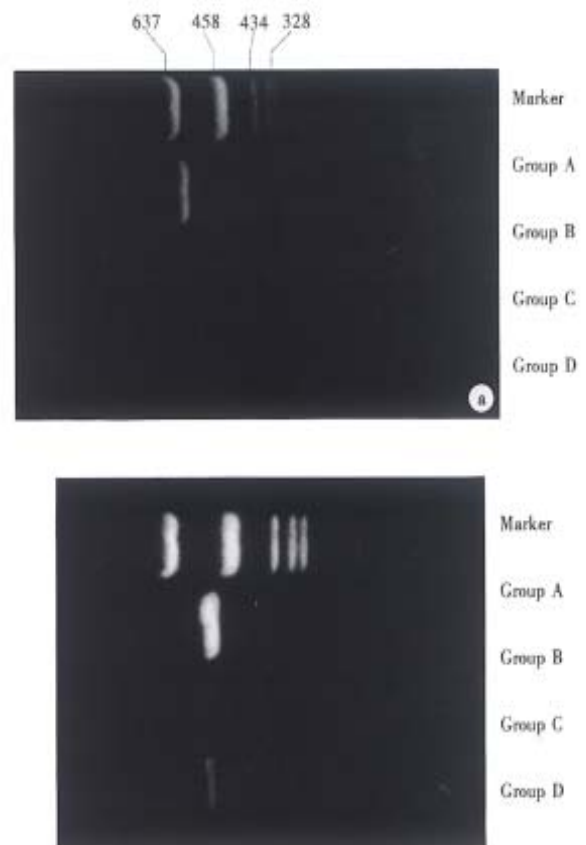


**Figure 2** Expression of perforin and granzyme B genes in liver xenografts on POD 7. A. Perforin; B. Granzyme B.

**DISCUSSION**

Gold hamster to rat orthotopic liver transplantation is concordant and heterotransplantation and presents with acute rejection. The recipient's survival can not prolong until both cellular and humoral rejection are depressed due to its dual immune mechanism. Splenectomy can effectively inhibit antibody formation, obviously abated hepatocyte necrosis and hemorrhage, but is unable to improve the diffuse mononuclear cellular infiltration in the grafted liver. CsA can significantly decrease cellular infiltration, but can not improve hepatocyte necrosis and hemorrhage,

neither of them can prolong the recipient's survival when used alone, but they can inhibit both cellular and humoral rejection, normalize the architecture of the grafted liver, and significantly prolong the recipient's survival to 37.1 days when used in combination. The result is better than that reported abroad<sup>[4]</sup>.

CTL is believed to play an important role in the mechanism of rejection, and effect mechanism of perforin and granzyme B, in spite of the regulatory and effect mechanism underlying the rejection process, remains incompletely understood. Effect of immunosuppression on the expression of perforin and granzyme B mRNA has become a hot topic in recent years. Mueller *et al*<sup>[5]</sup> analyzed the expression of perforin and granzyme A genes in situ hybridization in cellular infiltrates of MHC mismatched mouse heart transplants both in immunosuppressed recipients treated with CsA and untreated recipients. In untreated grafts, there were many perforin and granzyme A-expressing cells and heart transplants were completely rejected on POD 10. In contrast, CsA treatment significantly decreased the positive cells and prolonged survival of the transplants to 30 days. CsA did not obviously decrease infiltration of CD8<sup>+</sup> cells but significantly reduced the number of perforin and granzyme A-positive cells. It shows that CsA treatment mainly depressed the activation of CTL rather than decreased the number of infiltrating cells. Rapamycin can completely block

the expression of granzyme B gene in infiltrating cells of grafts, obviously prolong the survival of grafts<sup>[6]</sup>.

Our experimental results show that combined CsA and splenectomy could effectively depress rejection in hamster to rat orthotopic liver transplantation. The architecture of the hepatic lobule was undamaged, and the survival was significantly prolonged, and there were no expression of perforin and granzyme B genes mRNA.

In conclusion, expression of the CTL-associated gene perforin and granzyme B provides two valuable markers to judge the effect of immunosuppression in acute rejection of liver transplantation. But this should be further confirmed clinically.

## REFERENCES

- 1 Griffiths GM, Mueller C. Expression of perforin and granzymes *in vivo*: potential diagnostic markers for activated cytotoxic cells. *Immunol Today*, 1991;12:415-419
- 2 Zhang SG, Tan JW, Yang JM. Three cuff in hamster to rat orthotopic liver transplantation. *J Sec Milit Med Univ*, 1998;19:89-90
- 3 McDiarmid SV, Farmer DG, Kuniyoshi JS. Perforin and granzyme B. *Transplant*, 1995;59:762-766
- 4 Valdivia L, Monden M, Gotoh M. Prolonged survival of hamster-to-rat liver xenografts using splenectomy and cyclosporine administration. *Transplant*, 1987;44:759-763
- 5 Mueller C, Shao Y, Altermatt HJ. The effect of cyclosporine treatment on the expression of genes encoding granzyme A and perforin in the infiltrate of mouse heart transplants. *Transplant*, 1993;55:139-145
- 6 Wieder KJ, Hancock WW, Schmidbauer G. Rapamycin treatment depresses intragraft expression of RC/MMP 2, granzyme B and IFN gamma in rat recipients of cardiac allografts. *J Immunol*, 1993;151:1158-166

Edited by MA Jing-Yun

# Cultivation of human liver cell lines with microcarriers acting as biological materials of bioartificial liver \*

GAO Yi, XU Xiao-Ping, HU Huan-Zhang and YANG Ji-Zhen

**Subject headings** bioartificial liver; liver cell lines; microcarrier

## Abstract

**AIM** To improve the cultivation efficiency and yield of human liver cell line CL-1.

**METHODS** High-density cultivation of CL-1 on microcarriers was carried out with periodic observation of their growth and proliferation. The specific functions of human liver cell were also determined.

**RESULTS** Cells of CL-1 cell line grew well on microcarrier Cytodex-3 and on the 7th day the peak was reached. The amount of CL-1 cells was  $2.13 \times 10^8$  and the total amount of albumin synthesis reached 71.23  $\mu\text{g}$ , urea synthesis 23.32 mg and diazepam transformation 619.7  $\mu\text{g}$  respectively. The yield of CL-1 on microcarriers was 49.3 times that of conventional cultivation. The amounts of albumin synthesis, urea synthesis and diazepam transformation were 39.8 times, 41.6 times and 33.3 times those of conventional cultivation, respectively.

**CONCLUSION** The human liver cell line CL-1 can be cultivated to a high density with Cytodex-3 and has better biological functions. High-density cultivation of CL-1 on microcarriers can act as the biological material of bioartificial liver.

## INTRODUCTION

The animal experiments of extracorporeal bioartificial liver suggested that the device could provide special assistance to hepatic functions, and the effects of its primary clinical application was encouraging<sup>[1-3]</sup>. Although few successful studies were reported on human cell line acting as the biological material of bioartificial liver, it is rather conspicuous<sup>[4,5]</sup>, and has opened up a new path for the study of bioartificial liver.

To meet the principal needs of bioartificial liver functions, microcarrier technique was used to cultivate high density human liver cell line to improve the cultivation efficiency and yield in this study. The growth of liver cells on microcarriers was observed and the specific functions of liver cells were determined periodically. The feasibility and value of human liver cell line cultivated on microcarriers as the biological material of bioartificial liver were inquired.

## MATERIALS AND METHODS

### Materials

The tissue of human liver cell line CL-1 was taken from normal adult liver. Microcarrier Cytodex-3 was produced by Pharmacia in Sweden. Magnetic stirrer (0r/min-200r/min) and stirring culture vessel was made by Bellco Biotechnology in USA. The culture matrix consisted of DMEM was soluted in 10% NCS and L-Glutamine at a concentration of 3 g/L, products of Gibco.

### Methods

Common culture of CL-1 CL-1 cells 100mL, at a concentration of  $2 \times 10^5$  mL, were inoculated into a cubic culture flask. On the 1st, 3rd, 5th and 7th day the growth of cells was observed on an upside-down microscope and the cells were counted respectively. The amount of the cells in the culture system was also calculated. superficial clear liquid was obtained periodically to determine the functions of the liver cells.

**Microcarrier culture of CL-1** Cell suspension 100 mL, at a concentration of  $2 \times 10^5$  mL, was inoculated into a stirring culture vessel containing 500 mg Cytodex-3 and stirred intermittently for 8 hours. Then the culture system was placed into a fixed temperature culture case at a temperature of

Department of General Surgery, Zhujiang Hospital, First Military Medical University, Guangzhou 510282, Guangdong Province, China

Dr. GAO Yi, male, born on 1961-04-06 in Beijing, Han nationality, graduated from Second Military Medical University as M.D. in 1992, associate professor of general surgery, director of postgraduate.

\*Supported by the National Natural Science Foundation of China, No.39570212.

**Correspondence to:** Dr. GAO Yi, Department of General Surgery, Zhujiang Hospital, First Military Medical University, Guangzhou 510282, Guangdong Province, China

Tel. +86 • 20 • 84339888 Ext.43549

Received 1998-12-21

37°C and stirred continuously at a speed of 300 r/min. From the 2nd day on, whether to change the culture substrate or not and how much volume to change were determined by the color of the matrix and the value of its pH and the interval of changing liquid was about 24 hours-36 hours.

**Morphological observation and counting of the cells cultivated on microcarriers** On the 1st, 3rd, 5th, 7th and 9th day 0.1 mL samples were taken at a well-distributed state of stirring, and growth of the cells was observed on the upside-down microscope. One mL samples were collected every other day to calculate the amount of cells in the culture system by means of crystal ester-calculating.

**Observation of cells cultivated on microcarriers under electron scanning microscope** On the 7th day cell sample was taken at a well-distributed state and culture matrix was discarded. After it was rinsed with phosphate buffer solution and fixed for 0.5 hour with 2 mL 2% pentanal, it was rinsed with phosphate buffer solution again, fixed for 0.5 hour with 1% osmic acid, dehydrated gradiently for 10 minutes each stage, exchanged with acetic isopental ester for 4 hours, and dried by CO<sub>2</sub> drier (HITACHI HCP-2, JAPAN). Finally it was splashed with ion platinum vacantly. Growth of the cells was observed under S-450 electron scanning microscope (JAPAN).

**Determination of albumin synthesis** When the culture substrate was changed, superficial clear liquid was obtained to determine the concentration of human albumin by radio-immunity competition.

**Determination of diazepam transformation** Standard diazepam was added to the culture vessel at a concentration of 20 µg/mL. The superficial clear liquid was taken periodically and the concentration of diazepam was determined according to XUE Guo-Zhu *et al*<sup>[6]</sup>. The amounts of diazepam transformation were calculated.

**Determination of urea in superficial clear liquid** Superficial clear liquid (0.2 mL) was taken and determined by BECKMAN biochemical auto-detector. The amount of urea was calculated on the basis of the culture volume.

## RESULTS

### *Comparison of cell amounts after expanded by cultivation*

After 1-3 days of cultivation, the CL-1 cells in common culture adhered and grew slowly, and part of them in suspension was devitalized. From then on the adhering CL-1 cells grew rapidly, and cell amount reached  $4.32 \times 10^6/100$  mL on the 5th day.

On the 7th day the amount decreased to  $3.83 \times 10^6/100$  mL while in the microcarrier culture the growth of CL-1 accelerated on the 3rd day and reached the peak of  $2.13 \times 10^8$  on the 7th day, and decreased to  $1.83 \times 10^8$  on the 9th day (Figure 1). The ratio of the peak amounts of CL-1 between microcarrier culture and common culture was 49.3:1.

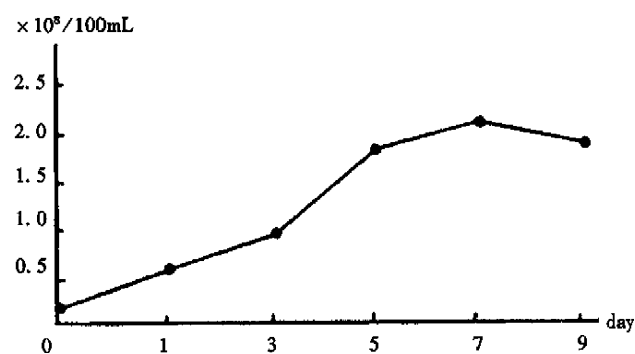


**Figure 1** Change of the amount of CL-1 cultivated on microcarriers.

### *Morphological observation of CL-1 cultivated on microcarriers*

**Observation under upside-down microscope** On the 1st day over 50% microcarriers were attached with cells and the cells were beginning to expand. On the 5th day more than 80% microcarriers were covered with cells (Figure 2). The multi-morphological growth of liver cells could be observed under high-amplification microscope. On the 7th day the phenomenon of bridge-link could be observed between microcarriers, i.e., the microcarriers were linked to each other through cells (Figure 3).

**Observation under electron microscope** On the 7th day of cultivation, electron microscopy showed that the cells adhered fast to the microcarriers semi-spherically (Figure 4). The microvilli on the surfaces of the cells could be observed clearly.

**Changes of specific functions of cells** When CL-1 cells were cultivated on microcarriers, the specific functional indexes such as albumin synthesis, urea synthesis and diazepam transformation rose gradually along with the prolonging of the cultivation. On the 7th day these indexes peaked, and then decreased gradually, while CL-1 cells were commonly cultivated, the functional indexes as described above reached their peaks on the 5th day and decreased noticeably on the 7th day. All the functional indexes determined at various time points in microcarrier culture were obviously higher than those in common culture

(Tables 1, 2). When functional indexes of CL-1 cells reached their peaks on the 7th day, the albumin synthesis, urea synthesis and diazepam transformation of CL-1 in microcarrier culture were 39.8, 41.6 and 33.3 times over those in common culture on the 5th day.

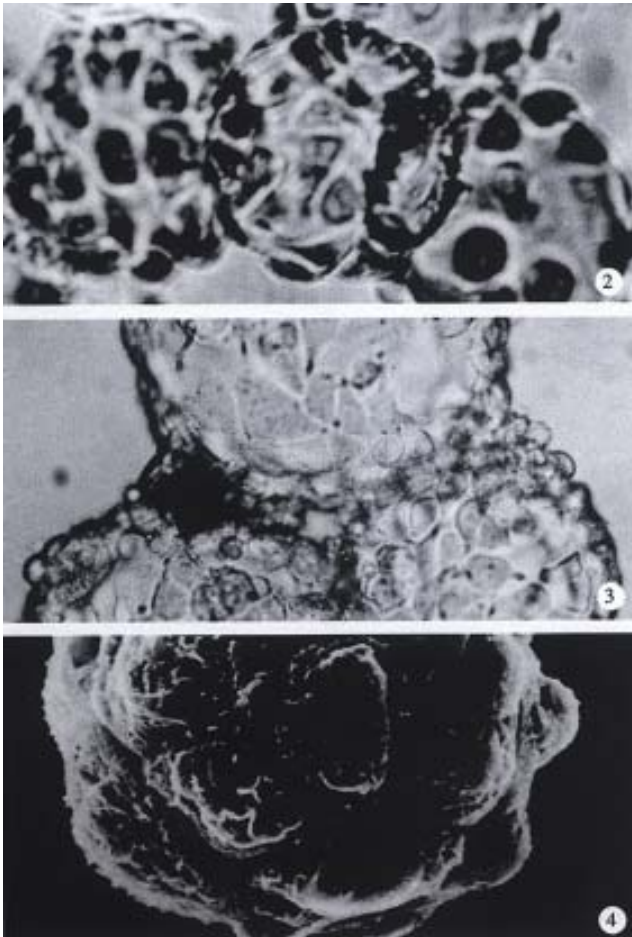


**Figure 2** On the 5th day more than 80% microcarriers were covered with CL-1 cells under upside-down microscope.  $\times 120$

**Figure 3** On the 7th day the phenomenon of bridge-link could be observed between microcarriers under upside-down microscope.  $\times 200$

**Figure 4** On the 7th day of cultivation, the electron microscope showed that the cells adhered fast to the microcarriers semi-spherically under scanning electronic microscope.  $\times 950$

**Table 1** Changes of specific functions of CL-1 under two culture conditions

Indexes of functions	1st day	3rd day	5th day	7th day	9th day
Albumin synthesis ( $\mu\text{g}$ )					
Microcarrier culture	21.34	35.87	58.35	71.32	67.98
Common culture	0.43	1.21	1.79	1.65	
Urea synthesis (mg)					
Microcarrier culture	7.45	11.49	19.62	23.32	20.18
Common culture	0.08	0.34	0.56	0.42	
Diazepam transformation ( $\mu\text{g}$ )					
Microcarrier culture	112.2	271.3	544.1	619.7	573.3
Common culture	3.4	8.9	18.6	13.5	

**Table 2** Comparison of peak function values of CL-1 under two culture conditions

Indexes of functions	Albumin synthesis ( $\mu\text{g}$ )	urea synthesis (mg)	Diazepam transformation ( $\mu\text{g}$ )
Microcarrier culture	71.23	23.32	619.7
Common culture	1.79	0.56	18.6
Ratio	39.8:1	41.6:1	33.3:1

## DISCUSSION

Microcarrier culture can improve the culture efficiency and yield. As the biological material of bioartificial liver, the liver cells must meet two needs: ① possessing the specific functions of liver; and ② providing biological function enough to satisfy the patients. The former demands high differentiation of the cells, and the latter sufficient amount of liver cells. Our primary study on the human liver cell line at early stage showed the characteristics of high differentiation and good specific liver functions of CL-1. It is extremely valuable as the biological material of bioartificial liver<sup>[6]</sup>. In common culture, however, the yield of human cell line can only reach the level of  $10^6$ - $10^7$ , not enough to meet the need of necessary amount to survive an individual. So the urgent question on the biological material of bioartificial liver is how to increase the amount of the cells. The technique of microcarrier culture in cell engineering makes cultivating the human liver cell line possible in high-density in that it possesses a high ratio of surface area to volume, which provides a comparatively large area for cells to adhere in small culture volume. Few successful cultivations of animal primary liver cells on microcarriers have been reported both at home and abroad<sup>[7,8]</sup>, while there was no report on cultivation of human liver cells on microcarriers yet. Microcarrier culture of CL-1 was studied by using Cytodex-3 and slow stirring in our work. After 100 mL suspension of CL-1 was inoculated at a concentration of  $2 \times 10^5/\text{mL}$ , the cells grew and adhered to the microcarriers in great amount and reached the peak on the 7th day. The maximal yield of cells cultivated on microcarrier was 49.3 times over that in 100 mL common cubic flask. The reasons for the increase of cell yield in a big margin when CL-1 was cultivated on microcarrier were as follows: ① The surface area in the culture system for cells to grow was greatly improved by using microcarriers. 0.5 g Cytodex-3 was added into 100 mL culture matrix each and the cultivating surface area could reach 2 300  $\text{cm}^2$ ; while the efficient surface area of the common culture flask was only 28  $\text{cm}^2$ . The quantity of the cells increased correspondingly with the improvement of the cultivating surface; ② Cytodex-

3 is primarily characterized by a thin layer of collagen chemically coupled to a matrix of cross-linked dextran, so that it can attach the liver cells strongly, stimulate the expanding and growth of them and promote their growth<sup>[5,9]</sup>; and ③ Low speed stirring employed to cultivate CL-1 cells made them easy to adhere to the surfaces of the suspending microcarriers and expand to mono-layers gradually.

The overall functions of CL-1 cultivated in microcarrier system were improved. Due to the marked increase of the amount of cells, the function indexes of CL-1 cultivated on microcarrier were greatly improved and predominated over those in common culture. Such improvement was the prerequisite for CL-1 cultivated on microcarrier to act as the biological material of bioartificial liver. Furthermore, the time for the highest cell amount and function indexes in microcarrier culture was later than that in common culture. It may be due to the improvement of efficient surface area for cultivating which delayed the peak of growth and reproduction of CL-1 afterwards.

Further improvement is needed in microcarrier culture of liver cells. Matsumura held that about 25 g-75 g liver cell ( $2.5 \times 10^9$ - $7.5 \times 10^9$  liver cells) was enough to provide the necessary liver functions to survive an individual when his liver weight was 1 200 g<sup>[10]</sup>. Although the amount of CL-1 had been

greatly improved to the level of  $2 \times 10^8$  in a culture volume of 100 mL in this study, it can not meet the need of the bioartificial liver yet. Expansion of the volume of microcarrier culture to several or even several tens of liters is to be further studied. Perfusion culture with microcarrier is promising.

## REFERENCES

- 1 Sussman NL, Finegold MJ, Kelly JH. Recovery from syncytial giant-cell hepatitis (SGCH) following treatment with an extracorporeal liver assist device (ELAD). *Hepatology*, 1992;15:51A
- 2 Rozga J, Holzamn MD, Ro MS. Development of a hybrid bioartificial liver. *Ann Surg*, 1993;217:502-511
- 3 Demetriou AA, Rozga J, Podesta L, Lepage E, Morsiani E, Moscioni AD, Hoffman A, McGrath M, Kong L, Rosen H. Early clinical experience with a hybrid bioartificial liver. *Scand J Gastroenterol Suppl*, 1995;208:111-117
- 4 Sussman L, Kelly JH. Artificial liver: a forthcoming attraction. *Hepatology*, 1994;17:1163-1164
- 5 Nyberg SL, Rimmel RP, Mamn HJ. Primary hepatocytes outperform HepG2 cells as the source of biotransformation function in a bioartificial liver. *Ann Surg*, 1994;220:59-67
- 6 Xue GZ, Gao Y, Yang JZ. Primary study on human cell line acting as the biological material of artificial liver. *J Chin Infiltr Artif Organ*, 1996;7:1-4
- 7 Rozga J, Williams F, Ro MS, Neuzil DF, Giorgio TD, Backfisch G, Moscioni AD, Hakim R, Demetriou AA. Development of a bioartificial liver: properties and function of a hollow module inoculated with liver cells. *Hepatology*, 1993;17:258-265
- 8 Wang YJ, Li MD, Wang YM. Cultivation of rat liver cells adhered on microcarriers. *J Chin Exp Surg*, 1997;14:61
- 9 Kasai S, Sawa M, Mito M. Is the biological artificial liver clinically applicable. A historic review of biological artificial liver support system. *Artif Organ*, 1994;18:348-354
- 10 Matsumura KN, Guevara GR, Huston H, Hamilton WL, Rikimaru M, Yamasaki G, Matsumura MS. Hybrid bioartificial liver in hepatic failure: preliminary clinical report. *Surgery*, 1987;101:99-103

Edited by WANG Xian-Lin

# CT arterial portography and CT hepatic arteriography in detection of micro liver cancer

LI Li, WU Pei-Hong, MO Yun-Xian, LIN Hao-Gao, ZHENG Lie, LI Jin-Qing, LU Li-Xia, RUAN Chao-Mei and CHEN Lin

**Subject headings** liver neoplasms/diagnosis; CT arterial portography; CT hepatic arteriography

## Abstract

**AIM** To recognize the characteristic findings of micro-liver cancer (MLC) and to evaluate the effect of CT arterial portography (CTAP) and CT hepatic arteriography (CTHA) in diagnosis of MLC.

**METHODS** Between April 1996 to December 1998, CTAP and CTHA were performed in 12 patients with MLC, which were not detected by conventional CT examinations. After CTHA, 3 mL-5 mL mixture of lipiodol, doxorubicin and mitoycin C were injected into hepatic artery through the catheter, and the followed up by CT three or four weeks later (Lipiodol CT Lp-CT).

**RESULTS** A total of 22 micro-tumors (0.2 cm-0.6 cm in diameter) were detected in 12 patients, which manifested as small perfusion defects in CTAP and small round enhancement in CTHA. The rate of detectability of CTAP and CTHA was 68.2% (15/22) and 77.3% (17/22) respectively, and the rate of the simultaneous use of both procedures reached 86.4% (19/22). All micro-tumors were demonstrated as punctate lipiodol deposit foci in Lp-CT. After Lp-CT, the elevated serum level of  $\alpha$ -fetoprotein (AFP) dropped to the normal level in all patients.

**CONCLUSION** The CTAP and CTHA are the most sensitive imaging methods for detecting micro-liver cancer. Confirmed by the change of the elevated serum AFP level and lipiodol deposit foci in Lp-CT, small perfusion defects in CTAP and punctate enhancement in CTHA may suggest micro-liver cancer.

Cancer Center, Sun Yat-Sen University of Medical Sciences, Guangzhou 510060, Guangdong Province, China

Dr. LI Li, male, born on 1968-10-08 in Changsha City, Hunan Province, graduated from Sun Yat-Sen University of Medical Sciences as a postgraduate in 1996, now attending doctor of medical imaging, majoring oncological imaging diagnosis and interventional radiology, having 8 papers published.

\*Supported by "9 • 5" National Major Project of National Committee of Sciences and Technology, No. 96-907-03-02.

**Correspondence to:** Dr. LI Li, Department of Imaging & Interventional Radiology, Cancer Center, Sun Yat-Sen University of Medical Sciences, 651 Dongfeng Road E, Guangzhou 510060, Guangdong Province, China

Tel. +86 • 20 • 87765368 Ext 3216, Fax. +86 • 20 • 87754506

Email. Liliixj@public.guangzhou.gd.cn

Received 1998-10-08

## INTRODUCTION

With combined the findings of diagnostic imaging and elevated serum AFP level, more and more small liver cancer were detected earlier, and the therapeutic effect was significantly improved<sup>[1,2]</sup>. Except for other causes, such as hepatitis and teratoma, the elevated serum AFP level (higher than 400  $\mu$ g/L) strongly suggests the occurrence of primary hepatocellular carcinoma. However, sometimes no tumors could be found on conventional CT scanning (contrast material administered by intra-venous injection). These patients were further examined with were CTAP and CTHA. From April 1996 to December 1998, 12 patients with micro-cancer were examined with CTAP and CTHA in our hospital.

## MATERIALS AND METHODS

### Materials

From April 1996 to December 1998, 12 patients (10 men, 2 women) suspected to have liver cancer were examined with CTAP and CTHA. They ranged in age from 23 to 54 years (mean age, 36.4 years). The serum level of AFP was elevated in all the patients with a range of 201  $\mu$ g/L to 1 405  $\mu$ g/L (including 8 cases > 400  $\mu$ g/L, 4 cases < 400  $\mu$ g/L). Cirrhosis occurred in 7 cases. The tumors were 0.2 cm-0.6 cm in size with a mean of 0.46 cm. Multiple nodules were found in 7 cases.

### Methods

CTAP examinations were performed with incremental scanning of the liver in cranial-to-caudal direction with 2.7 mm to 8 mm collimation on bi-spiral-*Elscint* Twin Flash scanner (*Elscint*-Corp.). CT images were obtained 25sec-35sec after the initiation of transcatheter (5-F) superior mesenteric artery injection of 30 mL-40 mL of non-ionic contrast medium at a rate of 2.5 mL/sec-3.0 mL/sec with an automatic power injector (Medrad, Pittsburgh). During the catheterization, contrast medium administered before CT scanning was limited to 5 mL-10 mL injected by hand to visualize any aberrant vessels and to facilitate proper catheter placement.

CTHA examinations were done by injecting contrast medium into proper hepatic artery or

common hepatic artery. Twenty mL to 30 mL of contrast medium was injected at a rate of 3.0 mL/sec-3.5 mL/sec. Consecutive scanning of the liver was started 6sec-8sec after the initiation of injection of the contrast medium. After CTHA examinations, 3 mL-5 mL mixture of lipiodol, doxorubicin (10 mg-15 mg), and mitoycin C (2 mg-4 mg) were injected into hepatic artery, and the follow-up CT was performed three or four weeks later (Lp-CT). The serum AFP level was detected in all the patients two or three weeks later, and all returned to normal within 1-6 months.

## RESULTS

### *Detectable rate of micro-tumors*

A total of 22 micro-tumors were found in our group. The tumors measured 0.2 cm-0.6 cm with a mean of 0.46 cm. CTAP and CTHA images were carefully interpreted by two experienced radiologists. Fifteen tumors were demonstrated as fleckly perfusion defects on CTAP images with a detectable rate of 68.2%, and 17 manifested as punctate enhancement foci on CTHA with a detectable rate of 77.3%. Nineteen were found by simultaneous use of both procedures with a detectable rate of 84.4%. But 3 tumors were not detected by CTAP and CTHA in 2 patients. All 22 micro-tumors manifested as punctate lipiodol deposit foci in Lp-CT, which was performed two or three weeks later. Because the tumors in our series were extremely small, no pathologic diagnosis was acquired in all patients.

### *Follow-up of patients*

The serum AFP level was examined two or three weeks after Lp-CT. The AFP level dropped to the normal level in all the patients. Within 1-6 months. All survived without any signs of recurrence in our group, and the survival period ranged from 3 to 33 months (mean, 15.2 months).



**Figure 1** CTAP image obtained in a 40-year-old man with liver micro-cancer shows a punctuate perfusion defect in right lobe.

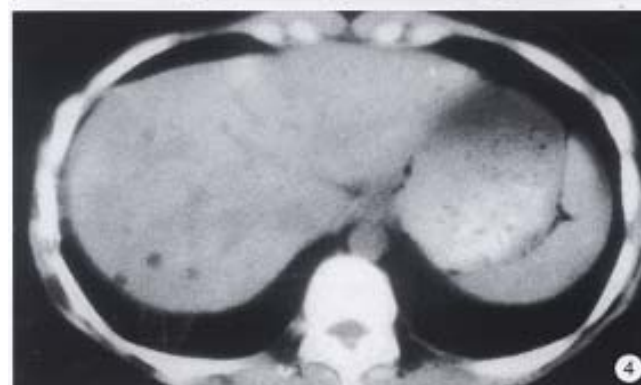
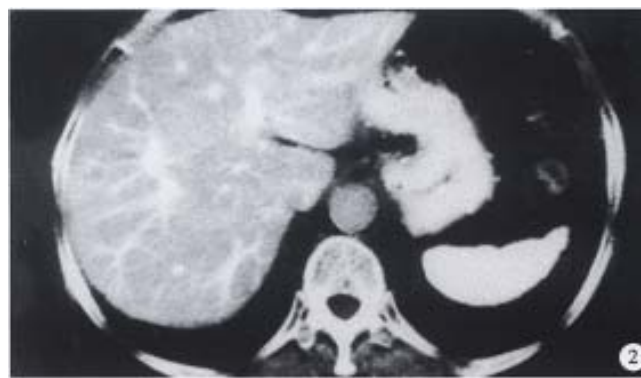


**Figure 2** CTHA image obtained on the same slice to Figure 1, the micro-tumor manifested as an small round enhancement nodule.

**Figure 3** CTHA in a 45-year-old man shows a micro-cancer with a diameter of 0.3 cm.

**Figure 4** A punctuate lipiodol deposit focus with 0.2 cm in diameter is shown on Lp-CT in a 28-year-old woman with elevated serum AFP level of 860  $\mu\text{g/L}$  detects which was not detected by CTAP and CTHA.

**Figure 5** CTHA in a 35-year-old man shows two punctuate non-pathologic enhancement foci on the edge of right lobe.

## DISCUSSION

In some of our patients found with elevated serum level by AFP, no tumors were detected by conventional CT scanning. For those patients, CTAP and CTHA examinations were recommended. Fleckly perfusion defects were found on CTAP (Figure 1) and punctate enhancement foci on CTHA (Figure 2). After CTHA examination, 3 mL-5 mL mixture of lipiodol and anticancer drug was tentatively injected in to hepatic artery for Lp-CT diagnosis, which was repeated three or four weeks later. Micro-foci of lipiodol deposit was found with elevated serum AFP level, which dropped continuous to normal. The prognosis of these patients was very good. Since April 1996, 12 patients with such findings have been examined in our hospital. All patients were surviving without any signs of recurrence, and the longest survival being 33 months. Due to its special clinical significance, we suggested the definition of micro-cancer in liver (0.2cm-06cm in diameter) which includes: ① elevated serum AFP level (AFP $\geq$ 400  $\mu$ g/L, or rising continuously); ② no micro-tumors were detected by conventional imaging methods, but by CTAP and CTHA; ③ Punctate lipiodol deposit foci were demonstrated on Lp-CT; and ④ after Lp-CT, serum AFP level lowered continuous or turned to normal level. CTAP and CTHA are considered as the most sensitive imaging methods for detecting small hepatocellular carcinoma<sup>[3]</sup>. The development of spiral CT technique greatly facilitated procedures and improved the quality of CT images<sup>[4]</sup>. Detectability of CTAP and CTHA for very small tumors (as small as 0.2 cm in diameter, Figure 3) was high, being 68.2% and 77.3% respectively, and that of simultaneous use of both procedures was 84.4%. But there were still some cases of micro-tumors which could not be detected by CTAP and CTHA. In a 28-year-old female patient with elevated AFP level of 860  $\mu$ g/L, no tumors were found either on conventional CT scanning or on CTAP and CTHA images. Three weeks later, Lp-CT detected a punctate lipiodol deposit focus of 0.2 cm in diameter in her left lobe with AFP continuous dropping to normal level (Figure 4). This patient had survived for 33 months without any signs of recurrence. With the widespread use of CTAP and CTHA, there have been more reports on non-pathologic perfusion defects detected with CTAP and non-pathologic enhancement detected with CTHA. Due to aberration of blood supply for some parts of the liver, such as arterio-portal shunt<sup>[5]</sup>, cirrhotic nodule, focal nodular hyperplasia, and focal fatty infiltration, the normal tissue could manifest as perfusion defects in CTAP, especially in the

medial segment of the left lobe<sup>[6]</sup>. Peterson *et al* reported that perfusion defects on CTAP were sometimes nonspecific, and peripheral flat or wedge-shaped perfusion defects indicated benignity<sup>[7]</sup>. In our study, the occurrence rate of non-pathologic perfusion defects detected with CTAP was 15.1%, and peripheral wedge-shaped perfusion defects were most common<sup>[8]</sup>. Similar to findings of CTAP, pseudo-lesion enhancement of normal liver tissue also occurred in CTHA. Kanematsu *et al* supposed that local non-pathologic enhancement detected with CTHA might result from the cystic venous drainage or peripheral arterio-portal shunts<sup>[9]</sup>. In our study, the occurrence rate of non-pathologic enhancement detected with CTHA was 22.0%, and small round peripheral enhancement was seen most commonly<sup>[8]</sup> (Figure 5). Thus, we do not recommend to use CTAP or CTHA alone to interpret small hepatocellular carcinomas. The combined use of both procedures can help distinguish micro-cancer from the false-positive findings on CTAP and CTHA, and increase the accuracy of diagnosis for small hepatocellular carcinoma<sup>[10]</sup>. Besides the findings on CTAP and CTHA images, combination of lipiodol deposit foci on Lp-CT and dropping of elevated serum AFP level are also helpful for the establishment of diagnosis for liver micro-cancer.

## REFERENCES

- 1 Wu MC. Clinical research advantage in primary liver cancer. *WJG*, 1998;4:471-474
- 2 Tang ZY. Advances in clinical research of hepatocellular carcinoma in China. *WCJD*, 1998;6:1013-1016
- 3 Hori M, Murakami T, Oi H, Kin T, Takahashi S, Matsushita M. Sensitivity in detection of hypervascular hepatocellular carcinoma by helical CT with intra-arterial injection of contrast medium, and by helical CT and MR imaging with intravenous injection of contrast mediums. *Acta Radiol*, 1998;39:144-151
- 4 Murakami T, Oi H, Hori K, Kim T, Takahashi S, Tomoda K. Helical CT during arterial portography and hepatic arteriography for detecting hypervascular hepatocellular carcinoma. *AJR*, 1997; 169:131-135
- 5 Tamura S, Kihara Y, Yuki Y, Sugimura H, Shimice T, Adjei O. Pseudolesion on CTAP secondary to arterio portal shunts. *Clin Imaging*, 1997;21:359-365
- 6 Matusi O, Kadoya M, Yashikawa J, Gadate T, Kawanori Y. Posterior aspect of hepatic segment IV: Patterns of portal venule branching at helical CT during arterial portography. *Radiology*, 1997; 205:159-162
- 7 Peterson MS, Baron RL, Dodd III GD, Zajko AJ, Oliver JH, Miller WJ. Hepatic parenchymal perfusion defects detected with CTAP: imaging-pathologic correlation. *Radiology*, 1992;185:149-155
- 8 Li L, Wu PH, Lin HG, Li JQ, Mo YX, Zheng L. Findings of non-pathologic perfusion defects by CT arterial portography and non-pathologic enhancement of CT hepatic arteriography. *WJG*, 1998; 4:513-515
- 9 Kanematsu M, Hoshi H, Imado T, Yamawaki Y, Mizuno S. Non-athological focal enhanced on spiral CT hepatic angiography. *Abdom Imaging*, 1997;22:55-59
- 10 Irie T, Takeshita K, Wada Y, Kisano S, Terahata S, Tamai S. Evaluation of hepatic tumors: comparison of CT with arterial portography, CT with infusion hepatic arteriography, and simultaneous use of both techniques. *AJR*, 1995;164:1407-1412

# Effect of apolipoprotein E gene Hha I restricting fragment length polymorphism on serum lipids in cholecystolithiasis

LIN Qi-Yuan, DU Jing-Ping, ZHANG Ming-Yi, YAO Yu-Gwei, Li Lin, CHENG Nan-Sheng, YAN Lu-Nan and XI-AO Lu-Jia

**Subject headings** apolipoprotein E; polymorphism; lipids; cholecystolithiasis; polymerase chain reaction

## Abstract

**AIM** To investigate the role of apolipoprotein E (apoE) polymorphism in the lithogenesis of gallstone and the hereditary pathogenesis of the disease.

**METHODS** Polymerase chain reaction (PCR) was used to study apoE phenotypes and allele frequencies in patients with gallstones and control, and the fasting serum lipids of subjects were also measured by enzymatic methods.

**RESULTS** The levels of triglyceride (TG) and very low density lipoprotein cholesterol (VLDL-C) were much higher in E<sub>2</sub>/E<sub>3</sub> patients than that in E<sub>2</sub>/E<sub>3</sub> control. E<sub>3</sub>/E<sub>3</sub> patients were accompanied with remarkably low levels of high density lipoprotein cholesterol (HDL-C) and its subforms. But in E<sub>3</sub>/E<sub>4</sub> patients there were only slight changes in levels of VLDL-C and low density lipoprotein cholesterol (LDL-C).

**CONCLUSION** Different apoE phenotype patients with gallstones have different characteristics of dyslipidemia and the average level of serum lipids in patients with gallstones are higher than subjects without gallstones in the same apoE gene phenotype. ε<sub>2</sub> allele is possibly one of the dangerous factors in the lithogenesis of cholecystolithiasis.

Department of General Surgery, First Hospital, West China University of Medical Sciences

Dr. LIN Qi-Yuan, Male, born on 1964-01-01 in Nanchong City, Sichuan Province, graduated from West China University of Medical Sciences and earned a Doctor degree in 1996, now an associate professor, majoring hepatic-biliary-pancreatic surgery having 16 articles published.

\*Project supported by National Natural Science Foundation of China, No. 39670709.

**Correspondence to:** LIN Qi-Yuan, Department of General Surgery, First University Hospital, West China University of Medical Sciences, Chengdu 610041, Sichuan Province, China

Tel. +86 · 28 · 5551078, Fax. +86 · 28 · 5530724

Received 1999-01-20

## INTRODUCTION

The apolipoprotein E (apoE) gene locus possesses three alleles, ε<sub>2</sub>, ε<sub>3</sub> and ε<sub>4</sub>, which are inherited in co-domain fashion and code for three isoprotein E<sub>2</sub>, E<sub>3</sub> and E<sub>4</sub> making up six phenotypes, three heterozygous E<sub>2</sub>/E<sub>3</sub>, E<sub>3</sub>/E<sub>4</sub> and E<sub>2</sub>/E<sub>4</sub>, three homozygous E<sub>2</sub>/E<sub>2</sub>, E<sub>3</sub>/E<sub>3</sub> and E<sub>4</sub>/E<sub>4</sub><sup>[1-7]</sup>. The differences of these main isoprotein alter the receptor-binding affinity of the apolipoprotein-containing lipoproteins and affect the metabolism of cholesterol and lipids<sup>[2,4]</sup>. It is putative that apoE polymorphisms are closely related to hyperlipidemia<sup>[5]</sup>, coronary heart disease<sup>[6]</sup> and diabetes mellitus<sup>[7]</sup>. The formation of gallstones is frequently associated with the changes in biliary lipid compositions, the lithogenic bile being usually supersaturated with cholesterol and decreased with bile acids and lecithin<sup>[8,9]</sup>. A prerequisite for the formation of gallstones is the lithogenic bile, which is often the result of disorders in lipid metabolism or dyslipidemia. The important role of apoE in the regulation of lipid metabolism raises the possibility that apoE polymorphisms may be involved in the formation of gallstones. This case-control cohort study is designed to investigate the significance of apoE polymorphisms as a predisposing factor in the pathogenesis of cholecystolithiasis.

## SUBJECTS AND METHODS

### Subjects

Eighty-seven consecutive patients with gallstones were investigated. The treatment group consisted of 39 men and 48 women (mean age 52 years, ranging from 16 to 83 years). All of them suffered from non-symptomatic cholecystolithiasis and underwent operation in the First Hospital from January 1994 to December 1995. The control group included 50 subjects with 27 men and 23 women (mean age 49 years, ranging from 15 to 78 years), and they were also matched in sex and age distribution with the patients with gallstones.

### DNA amplification

Leukocyte DNA of venous blood collected in EDTA tubes were extracted by Hixson slotting-out method<sup>[10]</sup>. Model DNA was amplified by polymerase chain reaction (PCR) thermal cycles using oligonucleotides primers F4 (5'-ACAGAATTCGCC CCGGCTGGTACAC-3') and F6 (5'-TAAGCTTGG CACGGCTG TCCAAGGA-3'). Each amplification reaction system contained 1 μg DNA, 1 pmol/L

of each primer and 25 kilo units/L of Taq-polymerase up to a final volume of 30 μL. Each reaction mixture was heated at 95°C for 5 minutes for predenaturation, and followed by 30 cycles of amplification for annealing at 60°C for 1 minute, elongation at 70°C for 2 minutes, denaturation at 95°C for 1 minute, and then a prolonged elongation time up to 7 minutes at 56°C.

**Analysis of restricting fragment length polymorphism for apoE**

Twenty-five μL of PCR amplified products in each reaction system were mixed with 5 units of Hha I enzyme for digestion apoE sequences at 37°C for 1 hour. Each reaction mixture was loaded onto 85 g/L polyacrylamide gel, after electrophoresis for 3 hours under constant current (45 mA) and visualized by ultraviolet light. The size of apoE Hha I restricting fragment length polymorphisms were estimated by comparison with marker DNA PBR32. On the basis of the size and the number of various fragments, apoE phenotypes were determined as E2 with 91bp, and 83bp E3 with 91bp, 48bp and 35bp, as well as E4 with 72bp, 48bp and 35bp.

**Lipids analysis**

Serum total cholesterol (TC) and total triglyceride (TG) were determined by enzymatic methods with the OUL 3 000 automatic analyzer. High density lipoprotein cholesterol (HDL-C) was measured enzymatically and formed in the serum supernatant after precipitation of low density lipoprotein cholesterol (LDL-C) and very low density lipoprotein cholesterol (VLDL-C) with dextrin sulfate and MgCl2. The LDL-C and VLDL-C levels were calculated according to Friedwald's formula<sup>[11]</sup>.

**Statistical analysis**

All results were expression as  $x \pm s$ . The *F* test and  $\chi^2$  test were used for statistical analysis, *P* values less than 0.05 were regarded as significant.

**RESULTS**

**Distribution of apoE phenotypes and allele frequencies**

In the six common apoE phenotypes, E<sub>2/3</sub>, E<sub>3/3</sub> and E<sub>3/4</sub> phenotypes existed in either patients with gallstones or control subjects. There were only 2 E<sub>2/4</sub> phenotype cases in the control, and no E<sub>2/2</sub> and E<sub>4/4</sub> were detected in both groups. The overall distribution of apoE phenotypes and apoE allele frequencies in the patients with gallstones were analogous to that of the control (Table 1).

**Table 1 Apolipoprotein E phenotype distributions and allele frequencies in patients with gallstones and controls**

Groups	n	Phenotype				Allele		
		E <sub>2/3</sub> (%)	E <sub>2/4</sub> (%)	E <sub>3/3</sub> (%)	E <sub>3/4</sub> (%)	ε2(%)	ε3(%)	ε4(%)
Patients	87	10(11.4)	0	69(79.4)	8(9.2)	5.8	89.6	4.6
Male	39	4(10.2)	0	31(79.4)	4(10.2)	5.1	89.8	5.1
Female	48	6(12.5)	0	38(79.1)	4(8.9)	6.3	89.6	4.2
Controls	50	5(10.0)	2(4.0)	37(74.1)	6(12.0)	7.0	85.0	8.0
Male	27	3(10.0)	1(3.7)	20(74.0)	3(11.0)	7.4	85.2	7.4
Female	23	2(8.6)	1(4.3)	17(74.6)	3(13.0)	6.5	84.8	8.7

**Serum lipids**

The levels of TG (1.43 mmol/L) and VLDL-C (0.68 mmol/L) in E<sub>2/3</sub> patients with gallstones were markedly higher than that in E<sub>2/3</sub> control (1.06 mmol/L, *P*<0.05 and 0.48 mmol/L, *P*<0.05). LDL-C (1.41 mmol/L) was significantly lower in E<sub>2/3</sub> patients than that in the control (2.04 mmol/L, *P*<0.05). No statistical differences were noted in TC, HDL-C, HDL2-C and HDL3-C between E<sub>2/3</sub> patients and control subjects (Table 2).

In E<sub>3/3</sub> patients with gallstones, the HDL-C (0.89 mmol/L), HDL2-C (0.49 mmol/L) and HDL3-C (0.39 mmol/L) were significantly decreased as compared with that in E<sub>3/3</sub> control (1.28 mmol/L, *P*<0.05; 0.73 mmol/L *P*<0.001; and 0.55 mmol/L, *P*<0.001). LDL-C and VLDL-C showed no difference in both groups (Table 2). E<sub>3/3</sub> female patients had lower levels of HDL-C (0.82 mmol/L), HDL2-C (0.46 mmol/L) and HDL3-C (0.36 mmol/L) than E<sub>3/3</sub> female controls (1.33 mmol/L, *P*<0.001; 0.77 mmol/L, *P*<0.01; and 0.57 mmol/L, *P*<0.01). Serum lipid levels were not changed in E<sub>3/3</sub> male patients and controls (Table 3).

LDL-C increased (1.92 mmol/L) and VLDL-C decreased (0.42 mmol/L) in E<sub>3/4</sub> patients with gallstones as compared with E<sub>2/3</sub> patients (LDL-C-1.41 mmol/L, VLDL-C-0.68 mmol/L) and E<sub>3/3</sub> patients (LDL-C 1.87 mmol/L, VLDL-C 0.46 mmol/L), but the differences were not significant. No obvious changes occurred in TC or HDL-C and its subforms among E<sub>2/3</sub>, E<sub>3/3</sub> and E<sub>3/4</sub> patients with gallstones (Table 2).

**Table 2 Comparisons of lipid levels in E<sub>2/3</sub>, E<sub>3/3</sub>, E<sub>3/4</sub> both gallstone patients and controls**

Lipids (mmol/L)	E <sub>2/3</sub>		E <sub>3/3</sub>		E <sub>3/4</sub>	
	Patients (n=10)	Controls (n=5)	Patients (n=69)	Controls (n=37)	Patients (n=8)	Controls (n=6)
TG	1.43 ± 0.35 <sup>a</sup>	1.06 ± 0.10	0.97 ± 0.21	0.64 ± 0.44	1.11 ± 0.33	0.92 ± 0.16
TC	2.99 ± 0.65	2.52 ± 0.53	3.14 ± 0.59	3.67 ± 0.76	3.94 ± 0.45	3.62 ± 0.63
LDL-C	1.41 ± 0.56 <sup>a</sup>	2.04 ± 0.16	1.87 ± 0.49	2.43 ± 0.67	1.92 ± 0.64	2.46 ± 0.32
VLDL-C	0.68 ± 0.26 <sup>a</sup>	0.48 ± 0.20	0.46 ± 0.20	0.30 ± 0.11	0.42 ± 0.13	0.44 ± 0.10
HDL-C	0.95 ± 0.23	1.02 ± 0.15	0.89 ± 0.30 <sup>a</sup>	1.28 ± 0.23	0.86 ± 0.21	0.90 ± 0.36
HDL2-C	0.53 ± 0.13	0.62 ± 0.22	0.49 ± 0.18 <sup>b</sup>	0.73 ± 0.13	0.44 ± 0.19	0.55 ± 0.18
HDL3-C	0.42 ± 0.12	0.56 ± 0.28	0.39 ± 0.12 <sup>b</sup>	0.55 ± 0.11	0.40 ± 0.13	0.46 ± 0.12

<sup>a</sup>*P*<0.05, <sup>b</sup>*P*<0.01, vs controls; *F* test.

**Table 3 The comparisons of lipid levels in E<sub>3/3</sub> same gender either gallstone patients or controls**

Lipids (mmol/L)	Male		Female	
	Patients (n = 31)	Controls (n = 20)	Patients (n = 38)	Controls (n = 17)
TG	0.85 ± 0.50	0.53 ± 0.22	1.10 ± 0.30	0.72 ± 0.57
TC	3.05 ± 0.44	0.41 ± 0.57	3.23 ± 0.85	3.87 ± 0.63
LDL-C	1.86 ± 0.68	2.71 ± 0.49	1.89 ± 0.86	2.20 ± 0.56
VLDL-C	0.40 ± 0.24	0.25 ± 0.10	0.52 ± 0.14	0.35 ± 0.17
HDL-C	0.94 ± 0.33	1.21 ± 0.28	0.82 ± 0.27 <sup>b</sup>	1.33 ± 0.19
HDL2-C	0.52 ± 0.22	0.69 ± 0.16	0.46 ± 0.15 <sup>b</sup>	0.77 ± 0.10
HDL3-C	0.42 ± 0.12	0.52 ± 0.13	0.36 ± 0.12 <sup>b</sup>	0.57 ± 0.10

<sup>b</sup>P<0.01, vs controls, F test.

## DISCUSSION

E<sub>2/3</sub>, E<sub>3/3</sub>, and E<sub>3/4</sub> are three common apolipoprotein E gene phenotypes, accounting for more than 50%, E<sub>2/4</sub> and E<sub>4/4</sub> for less than 6.2%<sup>[12]</sup>. In the present study, only 2 E<sub>2/4</sub> phenotype cases were detected in control, and no E<sub>2/2</sub> and E<sub>4/4</sub> homozygotes were found in both groups. The results show that ε2 and ε4 alleles resulting from the inheridary variations of apoE gene existed mainly in heterozygous way in population.

There were racial differences in the distribution of apoE alleles and phenotypes. In this study and Wang's literature<sup>[13]</sup>, the frequencies of E<sub>3/3</sub> phenotype were 85%-86% in healthy Chinese people, but 75% in Finnish people. Frequencies of ε4 were lower in Chinese people (8%-9%) than 20% in the Finnish (20%). The frequencies of E<sub>3/3</sub> phenotype in Chinese patients with gallstones were 79.3% as compared with 62.2% in Finnish, and E<sub>3/4</sub> phenotype in Chinese patients with gallstones were 9.2% but 28.9% in Finnish<sup>[14]</sup>. Kamboth<sup>[15]</sup> also reported that there may be some variations of apoE allele and phenotype in different regional population from western to oriental countries.

Patients of different apoE phenotype with gallstones had different characteristics of dyslipidemia. Higher mean serum TG, VLDL-C levels and lower mean LDL-C levels were found in E<sub>2/3</sub> patients. The E<sub>3/3</sub> patients, especially in women, had markedly lower concentrations of HDL-C, HDL2-C and HDL-3-C, while E<sub>3/4</sub> patients had only slight lower levels of VLDL-C and higher levels of LDL-C as compared with the E<sub>2/3</sub> and E<sub>3/3</sub> patients with gallstones.

The difference in the changes of serum lipid levels in different apoE phenotype patients with gallstone may be associated with apoE locus gene polymorphisms. E2, E3 and E4 isoproteins resulted from the single amino acid interchange between 112 site cysteine and 118 site arginine, E3 with cysteine at 112 site and arginin at 18 site, E2 with cysteine and E4 with arginine at either 112 site or 118 sites. Because of arginine bearing positive charge, E4 possessed more than one charge, the activity of receptor-binding to apoE-contained lipoprotein was stronger than E3. On the contrary, E2 possessed less than one charge, the activity of receptor-binding was lower<sup>[1-3]</sup>. Accordingly, ε2 allele

predisposes to serum triglyceride elevation<sup>[7]</sup>, the correlative change to serum lipid levels can be found in E<sub>2/3</sub> patients with gallstones in this study. ε4 allele was responsible for the increase of serum cholesterol<sup>[16]</sup>, but in E<sub>3/4</sub> phenotype patients, the increments of VLDL-C had no statistical difference, this may be associated with the low frequency of ε4 allele in population.

E<sub>3/3</sub> phenotype is putative normal type, but the E<sub>3/3</sub> patients with gallstones possessed the low level of HDL-C and its subforms as well. The changes may be related to other pathogenesis except apoE polymorphisms<sup>[17]</sup>. The results suggest that cholecystolithiasis may be a multigenic disease but not a monogenic one.

This study demonstrates that patients of different apoE phenotype with gallstones possess different dyslipidemia. The average level of serum lipids are much higher in patients with gallstones than that in non-gallstone subjects in the same apoE phenotype population. ε2 allele is likely one of the high-risk factors in the lithogenesis of cholecystolithiasis.

## REFERENCES

- Weisgraber KH. Apolipoprotein E distribution among human plasma lipoproteins: role of the cysteine-arginine interchange at residue 112. *J Lipid Res*, 1990;31:1503-1511
- Gajra B, Candlish JK, Saha N, Heng CK, Soemantri AG, Tay JS. Influence of polymorphisms for apolipoprotein B (ins/del, Xba I, EcoR I) and apolipoprotein E on serum lipids and apolipoproteins in a Javanese population. *Genet Epidemiol*, 1994;11:19-27
- Miettinen TA. Impact of apoE phenotype on the regulation of cholesterol metabolism. *Ann Med*, 1992;23:181-186
- Rall SC Jr, Mahley RW. The role of apolipoprotein E genetic variants in lipoprotein disorders. *J Intern Med*, 1992;231:653-659
- Walden CC, Hegele RA. Apolipoprotein E in hyperlipidemia (comments). *Ann Intern Med*, 1994;120:1026-1036
- Lenzen HJ, Assmann G, Buchwalsky R, Schulte H. Association of apolipoprotein E polymorphism, low-density lipoprotein cholesterol, and coronary artery disease. *Clin Chem*, 1986;32:778-781
- Ukkola O, Kervinen K, Salmela PI, Von Dickschiff K, Laakso M, Kesaniemi YA. Apolipoprotein E phenotype is related to macro and microangiopathy in patients with non-insulin-dependent diabetes mellitus. *Atherosclerosis*, 1993;101:9-15
- Johnston DE, Kaplan MM. Pathogenesis and treatment of gallstones. *New Eng J Med*, 1993;116:412-421
- Carey MC. Pathogenesis of gallstones. *Am J Surg*, 1993;165:410-419
- Hixson JE, Vernier DT. Restriction isotyping of human apolipoprotein E by gene amplification and cleavage with Hha I. *J Lipid Res*, 1990;31:548
- Friedewald WT, Levy RI, Friedrickson DS. Low-density lipoprotein cholesterol estimation of the concentration of in plasma without use of the preparative ultracentrifuge. *Clin Chem*, 1972;18:499-502
- Wilson PW, Myers RH, Larson MG, Ordovas JM, Wolf PA, Schaefer EJ. Apolipoprotein E alleles, dyslipidemia, and coronary heart disease. The Framingham offspring study. *JAMA*, 1994;272:1666-1671
- Wang KQ, He JL, Xie YH. Studies on human apolipoprotein E genetic isoform and their phenotypes among the Chinese population. *Proc CAMS and PUMC*, 1987;2:133-139
- Juvonen T, Kervinen K, Kairaluoma MI, Lajunen LH, Kesaniemi YA. Gallstone cholesterol content is related to apolipoprotein E polymorphism. *Gastroenterology*, 1993;104:1806-1813
- Kamboh MI, Aston CE, Ferrell RE, Hamman R. Impact of apolipoprotein E polymorphism in determining interindividual variation in total cholesterol and low density lipoprotein cholesterol in Hispanics and non-Hispanic whites. *Atherosclerosis*, 1993;98:201-211
- Jikkanen MJ, Huttunen JK, Ehnholm C, Pietidnen. Apolipoprotein E4 homozygosity predisposes to serum cholesterol elevation during high fat diet. *Arteriosclerosis*, 1990;10:285-288
- Juvonen T, Savolainen MJ. ApoA1 and cholesteryl ester protein gene loci in patients with gallbladder disease. *J Lipid Res*, 1995;36:80

# Studies on the flow and distribution of leukocytes in mesentery microcirculation of rats \*

JIANG Yong, LIU Ai-Hua and ZHAO Ke-Seng

**Subject headings** microcirculation; leukocyte; leukocyte-endothelium interaction; mesentery

## Abstract

**AIM** To study the effect of leukocyte-endothelium interaction (LEI) on the flow and distribution of leukocytes in microcirculation under physiological condition.

**METHODS** A microcirculation image multiple parameter computer analysis system (MIMPCAS) was used to study the flow and distribution of leukocytes in mesentery microcirculation of rats *in vivo*.

**RESULTS** The difference of visible leukocyte flux (VLF) was as high as 131 times in the arterioles and venules with similar diameter and blood velocity. The visible leukocytes rolled along the blood vessel wall as a "jerky" movement. The frequency distribution of the visible leukocyte velocity (VLV) showed a "two-peak" curve. The low peak value was on 10  $\mu\text{m/s}$ -15  $\mu\text{m/s}$  while the high peak fell between 25  $\mu\text{m/s}$ -30  $\mu\text{m/s}$ . With the increase of diameter of venules, VLF increased while the VLV remained at the same level. With the increase of RBC velocity, VLV trends to elevate and VLF to fall down.

**CONCLUSION** The results herein might provide a basic theory for the study on the mechanism of LEI under physiological condition and novel methods for the prevention and treatment of high LEI in many pathological processes.

## INTRODUCTION

Leukocyte-endothelium interaction (LEI) exists in many pathophysiological processes, such as inflammation, burns, tumor and shock<sup>[1,2]</sup>. In the recent two decades, quantitative studies on the interaction of leukocyte-endothelium have been carried out and the change of the flow and distribution of leukocytes is the basis for the abnormal increase of LEI<sup>[3-5]</sup>. High level LEI would bring about the blockage of blood vessels and decrease of blood perfusion<sup>[6,7]</sup>. Therefore, it is important to study the flow and distribution of leukocytes in microcirculation. We used a microcirculation image multiple parameter computer analysis system (MIMPCAS)<sup>[4]</sup> to study the characteristic of the flow and distribution of leukocytes in mesentery microcirculation of rats, and analyzed its influencing factors.

## MATERIALS AND METHODS

Five Sprague-Dawley rats were anesthetized with a mixture of 133 g/L urethane and 10 g/L chloralose (6 mL/kg, im)<sup>[4]</sup>. The abdomen of rats was open by the incision on the midline under the xiphoid. Small intestinal loops were pulled out and the mesentery was mounted on a hollowed transparent pedestal for observation. The specimen was suffused with a balanced 37°C Krebs's solution to maintain relatively normal condition in temperature and environment.

An Olympus microscope with a halogen lamp and Leitz long distance lens (20 × ) was used to observe the third order arterioles and venules. Being transmitted through a low-light level camera of model 1319, the signal was displayed on a Hitachi color monitor. A JVC recorder was used for off line measurement. Each specimen was recorded no more than 30 minutes so as not to affect the mesentery microcirculation<sup>[3]</sup>. The MIMPCAS was used to measure the diameter (D) of blood vessels, the velocity of red blood cells (V<sub>rbc</sub>), the visible leukocyte velocity (VLV), the visible leukocyte flux (VLF) and the adhesive leukocyte count (ALC) following the procedure described previously<sup>[4]</sup>.

The following formula was used to calculate the parameters of microcirculation<sup>[4,6,9]</sup>: 1. mean blood velocity,  $V_{\text{mean}} = V_{\text{rbc}}/1.6$ ; 2. flow volume of blood,

Chinese PLA Key Laboratory for Shock and Microcirculation, The First Military Medical University Guangzhou 510515, China

Dr. JIANG Yong, male born on 1964-10-25 in Henan Province, graduated and got a Ph.D. degree from the Academy of Military Medical Sciences in 1997, now professor of pathophysiology, majoring shock and cellular signal transduction, having more than 50 papers published in international or national major journals .

\*Project supported by National Natural Science Foundation of China, No. 39270852.

**Correspondence to:** Dr JIANG Yong, Chinese PLA Key Laboratory for Shock and Microcirculation, The First Military Medical University, Guangzhou 510515, China.

Tel. +86 · 20 · 85148376, Fax. +86 · 20 · 87705671

Received 1999-01-20

$F = V_{\text{mean}} \times \pi \times D^2/4$ ; 3. shearrate,  $\dot{\gamma}_w = 8 \times (V_{\text{mean}}/D)$ ; 4. total leukocyte flux,  $\text{TLF} = (60 \times F) \times K \times 10^{-6}$ ,  $K$  is the amount of leukocytes in the blood<sup>[7]</sup>; 5. invisible leukocyte flux,  $\text{ILF} = \text{TLF} - \text{VLF}$ .

The results were represented by mean  $\pm$  standard deviation ( $\bar{x} \pm s$ ) and the significance of difference was judged by Student's  $t$  test.

## RESULTS

### *Leukocytes flow and distribution in microcirculation of rat mesentery under physiological condition*

Twenty arterioles with a diameter between 11  $\mu\text{m}$ -45  $\mu\text{m}$  were selected for observation. Only one leukocyte rolled along the wall and there was no leukocyte sticking on it in the third order arterioles. In the 20 capillaries with an average diameter of  $6.3 \mu\text{m} \pm 1.7 \mu\text{m}$ , the visible leukocyte flux was  $0.2 \text{ cells/min} \pm 0.4 \text{ cells/min}$  and there were no plugging leukocytes. In the 20 venules with a diameter of 10  $\mu\text{m}$ -50  $\mu\text{m}$ , the visible leukocyte flux was  $13.3 \text{ cells/min} \pm 7.2 \text{ cells/min}$  and there were about  $0.3 \pm 0.3$  leukocytes sticking on the wall within a length of 94  $\mu\text{m}$  of blood vessels (Table 1). Under the physiological condition, the flow and distribution of leukocytes in different blood vessels varies to a large extent. The visible leukocyte flux (VLF) differed significantly between the venules and arteries with comparable diameter and blood velocity and the value of VLF in venules was as high as 131 times that of arterioles. Due to the interaction of leukocyte and endothelium which mainly occurred in venules, further studies were carried out on the flow and distribution of leukocytes in mesentery venules.

**Table 1** The flow and distribution of leukocytes in the mesentery microvasculature of rats under physiological condition

	Arteriole	Capillary	Venule
Number	20	20	20
D( $\mu\text{m}$ )	$22.6 \pm 9.1$	$6.3 \pm 1.7$	$25.1 \pm 10.6$
Vmean(mm/s)	$1.07 \pm 0.3$	$0.45 \pm 0.12$	$0.86 \pm 0.27$
Flow(pL/s)	$440.1 \pm 439.2$	$14.1 \pm 6.7$	$430.7 \pm 412.4$
$\dot{\gamma}_w(\text{s}^{-1})$	$371.1 \pm 212.8$	$570.4 \pm 189.7$	$272.1 \pm 189.2$
TLF(cells/min)	$91.1 \pm 90.9$	$2.9 \pm 1.4$	$89.2 \pm 85.4$
VLF(cells/min)	$0.1 \pm 0.2^b$	$0.2 \pm 0.4$	$13.1 \pm 7.2^b$
ILF(cells/min)	$91.0 \pm 90.9$	$2.7 \pm 1.3$	$76.1 \pm 77.8$
ALC(cells/94 $\mu\text{m}$ )	0	0	$0.3 \pm 0.3$

<sup>b</sup> $P < 0.01$ ,  $t = 8.07$ .

### *The characteristic of the flow and distribution of visible leukocytes*

**The space characteristic of the flow and distribution of visible leukocytes** Ten sampling lines on vessel with equal distance were set perpendicular to the longitudinal

vessel and the velocity of leukocyte passing through each line was measured. The variation of the velocity of leukocyte reflected the characteristic of its temporal distribution. Each leukocyte passing through the sampling lines with a large variation on velocity suggested that leukocyte rolling along the wall of blood vessels took a "jerky" movement (Figure 1). However, the average velocity for a leukocyte passing through a vessel with a definite length was similar, about 20  $\mu\text{m/s}$ .

**The time characteristic of the flow and distribution of visible leukocytes** For the measurement, one line was set on a third order venule (D: 37  $\mu\text{m}$ ) of mesentery of rat. The velocity and flux of all the visible leukocytes passing the measuring line were determined in 10s as one unit, and measurements were continuously performed 6 times in 1 minute. It was found that visible leukocyte velocity and visible leukocyte flux changed temporarily (Figure 2).

**Frequency distribution of VLV** The velocities of 400 visible leukocytes in 30 third branch venules were measured, of which the frequency distribution is shown in Figure 3. The frequency distribution of VLV presented with the characteristic of double peaks. Low peak value was about 10  $\mu\text{m/s}$ -15  $\mu\text{m/s}$  while the high peak was around 25  $\mu\text{m/s}$ -30  $\mu\text{m/s}$ . Leukocytes with velocity below 5  $\mu\text{m/s}$  or above 50  $\mu\text{m/s}$  were rarely found.

### *The influence of vessel diameter and blood velocity on the flow and distribution of leukocytes*

Visible leukocyte flux and visible leukocyte velocity were measured in 20 capillaries of mesentery of rats. Eight venules with similar blood velocity (Vrbc:  $1.2 \text{ mm/s} \pm 0.1 \text{ mm/s}$ ) and vessel diameter (D: 10  $\mu\text{m}$ -50  $\mu\text{m}$ ) were selected for the observation of influence of vessel diameter on the flow and distribution of leukocytes. It was found that with the increase of blood vessel diameter, visible leukocyte flux increased while visible leukocyte velocity remained relatively stable. Twelve venules with similar diameter ( $31.5 \mu\text{m} \pm 1.1 \mu\text{m}$ ) were selected for the observation of the influence of blood velocity on the flow and distribution. The blood velocity in these vessels ranged from 0.27 mm/s to 1.38 mm/s. Following the increase of Vrbc, visible leukocyte velocity increased while visible leukocyte flux decreased as shown in Figure 4.

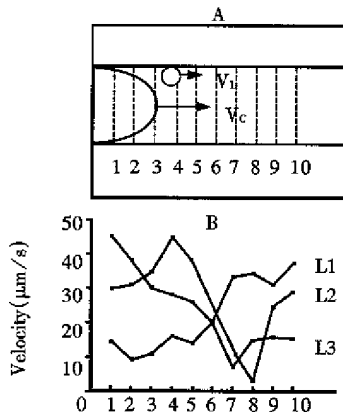


**Figure 1** Leukocytes rolling along the blood vessel wall showed a “jerky” movement. (A. Multiple sampling scheme for the velocity determination used by MIMPCAS; B. Three leukocytes passed through 10 sampling lines with a large variation of velocity.)

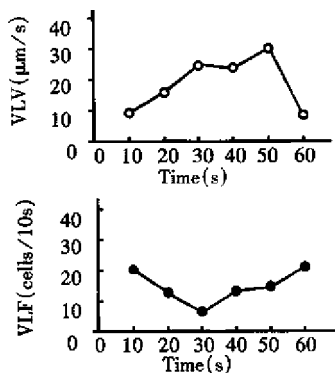


**Figure 2** The time-dependent changes of VLV and VLF in the third order venules of rat mesentery.

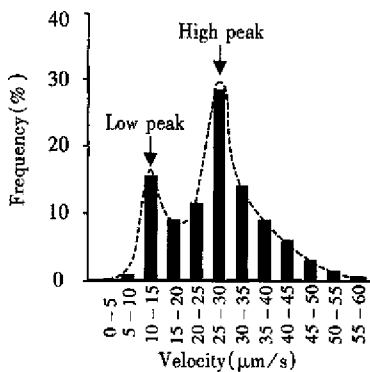


**Figure 3** The frequency histogram of VLV.

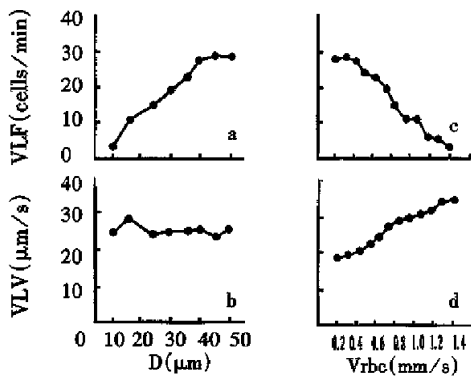


**Figure 4** Effect of vessel diameter and red blood cell velocity on the flow and distribution of visible leukocytes in the venules of rats.

**DISCUSSION**

Recently, wide interest has been shown in the research of leukocyte-endothelium interaction. Studies on the rheological behavior of leukocytes in the microcirculation have promoted the understanding on the mechanism of cellular adhesion. These studies mainly involved two aspects, i.e., one is the interaction between leukocytes and red blood cells and the other is that between leukocytes and endothelial cells<sup>[6,7]</sup>.

It was found in this study that leukocytes scarcely rolled on the wall or firmly stuck in arterioles. Under normal condition, sticking leukocytes in venules were rarely observed while some leukocytes rolled along the vessel wall in the marginal stream, suggesting that the flow and distribution of leukocyte in venules and arterioles was significantly different. There exist some interactions between leukocytes and endothelium in venules, for which the major phenomenon is the leukocytes rolling on the endothelium of venule wall. The development of leukocyte rolling and sticking on endothelium depends on two forces: leukocyte-endothelium adhesive forces and hemodynamic dispersal forces, i.e., shear stress<sup>[1,8]</sup>. Mayrovitz had suggested that the adhesion of leukocytes on the vessel wall might be mainly related to shear stress, for the adhesion of leukocytes existed on the wall of post-capillary venules<sup>[7]</sup>. However, the results herein showed that VLV varied to a large extent even in the arterioles and venules with a similar shear stress, suggesting that under physiological condition the difference of leukocyte flow and distribution in different vessels mainly came from the characteristic of endothelial cells and the micro-environment around leukocytes<sup>[9]</sup>.

The rolling of leukocytes along the walls presented with an uneven “jerky” movement. The balance between adhesive forces and dispersal forces was broken by the non-homogeneity of endothelium and that of hemodynamic forces, which brought about the rolling of leukocytes with the characteristic of non-stable speed<sup>[3,8,10]</sup>. The factors that influence homogeneity of endothelium include non-even surface of endothelium, local characteristic of endothelium, surface distribution of charge, the concentration of reactive substances, etc., while that for hemodynamic force, were temporal variation of blood velocity and local concentration of red blood cells. The results from the analysis on the frequency of VLV showed that the rolling leukocytes with a velocity lower than 10 µm/s had a potential to stick on the endothelium of blood vessels, while the rolling leukocytes with

a speed higher than 30  $\mu\text{m/s}$  tended to merge into the central stream of blood. The two peaks of the distribution of VLV suggested that there were at least two kinds of adhesive molecules with different property, by which two different velocities of leukocyte rolling along the walls were mediated. However, the adhesive molecules involved in the leukocyte-endothelium interaction are waiting to be identified and it is also necessary to pay more attention to the study on the mechanism of cellular adhesion.

In this study, the impact of diameter of blood vessels and blood flow of venules on the flow and distribution of leukocytes was analyzed. The diameter of blood vessels were found to have a significant effect on the flow and distribution of leukocytes. In the blood vessels with a larger diameter, visible leukocyte flux (VLF) increased significantly, but the visible leukocyte velocity (VLV) kept stable. Atherton had suggested that the temporal contact between leukocyte and endothelium should be taken as an inelastic collision<sup>[3]</sup>. The increase of adhesion force would bring about more chances of random collision and higher degree of inelastic collision between leukocytes and endothelium. Visible leukocyte flux mainly reflects the random collision between leukocyte and endothelium, while visible leukocyte velocity indicates the degree of inelastic collision. In the larger vessels, the leukocyte flux and the area of endothelium are also larger, so the random contact chances increase to bring about high flux of visible leukocyte. The change of diameter would not impact the adhesion force, so visible leukocyte velocity was the same.

Given a certain extent of blood viscosity, shear stress is determined by blood velocity under the condition of definite vessel diameter<sup>[2,6,8,10]</sup>. The

shear stress is high in the blood vessels with fast flow of blood, which will reduce the chance of collision between leukocyte and endothelium. Therefore in the vessels with fast blood flow, visible leukocyte flux is low while visible leukocyte velocity is high.

In summary, the flow and distribution of leukocytes in the mesentery microcirculation of rats was studied *in vivo*, and the influential factors on which were explored under normal conditions. The result of this study is helpful for the understanding of the mechanism for leukocyte endothelium interaction in physiological state and provides theoretic basis for the study and treatment of increased LEI in pathological processes.

## REFERENCES

- 1 Harlan JM. Leukocyte-endothelial interactions. *Blood*, 1985;65: 513-525
- 2 Zhao K, Wu KY, Zhu ZJ, Huang XL. The role of leukocyte in the disorder of microcirculation during shock. *Natl Med J Chin*, 1986; 66:722-725 (Chin)
- 3 Atherton A, Born GVR. Quantitative investigations of the adhesiveness of circulating polymorphnuclear leukocytes to blood vessel walls. *J Physiol (Lond)*, 1972;222:447-474
- 4 Jiang Y, Zhao KS, Li SX. Computer assisted analysis of leukocyte rheological behavior in microvasculature. *Chin Med J*, 1993;106: 883-888
- 5 Zentl H, Sack FU, Intaglietta M, Messmer K. Computer assisted leukocyte adhesion measurement in intravital microscopy. *Int J Microcirc: Clin Exp*, 1989;8:293-302
- 6 House SD and Lipowsky HH. Leukocyte-endothelium adhesion: microhemodynamics in mesentery of the cat. *Microvasc Res*, 1987; 34:363-379
- 7 Mayrovitz HN, Kang SJ, Herscovici B, Sampsel RN. Leukocyte adherence initiation in skeletal muscle capillaries and venules. *Microvasc Res*, 1987;33:22-34
- 8 Zhao KS. Cytorheology-A new project for shock research. *Med J Chin PLA*, 1986;11:137-139 (Chin)
- 9 Schmid-Schibein GW, Usami S, Skalak R, Chen S. The interaction of leukocytes and erythrocytes in capillary and postcapillary vessels. *Microvasc Res*, 1980;19:45-70
- 10 Jones DA, Smith CW, and McIntire LV. Effect of fluid shear stress on leukocyte adhesion to endothelium cells. In: Granger DN and Schmid-Schonbein GW, eds. Physiology and pathophysiology of leukocyte adhesion. 1st ed. New York: Oxford University Press, 1995:148-168

Edited by MA Jing-Yun

# Study on the quality of recombinant proteins using matrix-assisted laser desorption ionization time of flight mass spectrometry \*

ZHOU Guo-Hua<sup>1</sup>, LUO Guo-An<sup>1</sup>, SUN Guo-Qing<sup>2</sup>, CAO Ya-Cheng<sup>2</sup> and ZHU Ming-Sheng<sup>3</sup>

**Subject headings** recombinant proteins; molecular weight; flight mass spectrometry; erythropoietin tryptic digests

## Abstract

**AIM** To study the possibility of matrix-assisted laser desorption/ionization time of flight mass spectrometry (MALDI-TOF MS) for controlling the quality of recombinant proteins.

**METHODS** By using MALDI-TOF MS, the molecular weights and purity of recombinant bioactive proteins were analyzed.

**RESULTS** The molecular weights and purity were obtained in nine recombinant bioactive proteins, including interleukin 2, tumor necrosis factor  $\alpha$ , granulocyte-macrophage colony stimulating factor, interferon  $\alpha 2b$ , interferon  $\alpha 1$ , erythropoietin, calmodulin and its fragment, and neuronal nitric oxide synthase were obtained. MALDI-TOF MS was also used to assay specific proteins in the mixtures and to characterize the erythropoietin tryptic digests.

**CONCLUSION** The results showed that MALDI-TOF MS can be employed for the effective quality control of recombinant proteins.

## INTRODUCTION

Since Hillenkamp *et al*<sup>[1]</sup> first introduced matrix-assisted laser desorption/ionization time of flight mass spectrometry (MALDI-TOF MS) to analyze proteins with molecular masses greater than Mr 10 000, MALDI-TOF MS has been widely used to study different classes of biomolecules such as proteins, oligonucleotides, polysaccharides and polymers<sup>[2-5]</sup>. Compared to the traditional techniques, such as sodium dodecyl sulfate polyacrylamide gel electrophoresis (SDS-PAGE), MALDI-TOF MS has several advantages in the determination of protein molecular weight (Mr), peptide mapping, and purity.

In the present report, MALDI-TOF MS was used to accurately determine the Mr and purity of nine biological samples including recombinant bioactive proteins, such as: interleukin-2 (IL-2), interferon-alpha 2b (IFN $\alpha 2b$ ), interferon-alpha 1 (IFN $\alpha 1$ ), erythropoietin (EPO), granulocyte-macrophage-colony stimulating factor (GM-CSF), tumor necrosis factor alpha (TNF $\alpha$ ), calmodulin (CaM) and its fragment, and neuronal nitric oxide synthase (nNOS). In addition, the protein mixtures and EPO peptide mapping were characterized by the technique.

## MATERIALS AND METHODS

### Materials

**Chemicals** 3,5-dimethoxy-4-hydroxycinnamic acid (Sinapinic acid), 2,5-dihydroxybenzoic acid (DHB) and acetonitrile were produced by Sigma (St. Louis, USA). Trifluoroacetic acid (TFA) was from Merk-Schuchardt. Ammonium hydrogencarbonate, acetic acid and ethanol were produced by Nanjing Chemical Reagent Plant (Nanjing, China). All water used in the experiment was ultra high quality produced by a Milli-Q Plus Ultra Pure Water System.

**Proteins** Horse heart myoglobin, carbonic anhydrase B,  $\beta$ -lactoglobulin, bovine serum albumin and trypsin were obtained from Sigma (St. Louis, USA). IL-2 (*E.coli*), IFN $\alpha 1$  (Silkworm cell), GM-CSF (*E.coli*), IFN $\alpha 2b$  (*E.coli*), EPO (CHO), nNOS, and CaM and its fragments were supplied by the East China Institute for Medicine and Biotechnology (Nanjing, China).

<sup>1</sup>Department of Chemistry, Tsinghua University, Beijing 100084 Beijing, China

<sup>2</sup>Institute of Soil Science, Chinese Academy of Sciences, Nanjing 210018, Jiangsu Province, China

<sup>3</sup>Huadong Research Institute for Medicine and Biotechnics, No. 293 Zhongshan East Road, Nanjing 210002, Jiangsu Province, China.

Dr. ZHOU Guo-Hua, male, born on 1964-12-03 in Nantong County, Jiangsu Province, Han nationality, graduated from Tsinghua University as a Ph.D graduate in 1998, associate professor of Pharmacy, majoring in drug analysis, having 30 papers published.

\*Supported by the National Natural Science Foundation of China, No. 692350220.

**Correspondence to:** Prof. LUO Guo-An, Department of Chemistry, Tsinghua University, Beijing 100084 Beijing, China

Tel. +86 • 10 • 62784764 or +86 • 25 • 4540665, Fax. +86 • 10 • 62784764 or +86 • 25 • 4541183

Email.galuo@sam.chem.tsinghua.edu.cn or GHZHOU@publicl.ptt.js.cn

Received 1999-01-04

## Methods

**Tryptic digestion of EPO** Approximately 200 µg EPO protein was lyophilized and dissolved in 200 µL 1% ammonium bicarbonate (pH 8.5). Trypsin protease was added to the solution which was incubated at 37°C for 16h in a substrate: enzyme ratio of 50:1 (w:w). The digestion was quenched by storing the sample at -70°C. The sample was lyophilized and reconstituted in 50 µL 10% acetic acid before use.

**MALDI-TOF MS** Analyses were performed on a Finnigan Laser MAT 2 000 time-of-flight mass spectrometer (Finnigan MAT, Hemel Hempstead, Herts, UK). The system used a nitrogen laser (337 nm, 2 ns pulse) to desorb ions from the sample specimen. The desorbed ions were accelerated to 20kV into a free long tube. The time recorded for a molecule to travel the length of the tube to a detector was proportional to the mass of the ion, which was its molecular weight. All spectra were obtained using the positive-ion mode. Standard stainless-steel targets (with a sample application area of about 3.14 mm<sup>2</sup>) obtained from the manufacturer were employed for all analyses. The lasermat software allowed the user to irradiate one of the four possible target regions or quadrants of about 0.02 mm<sup>2</sup>. The spectra in this study were calibrated using instrumental calibration, based on the parameters determined from analysis of a number of standard proteins and peptides.

**Sample preparation for MALDI-TOF MS determination** The samples of each protein were prepared to 0.8 g/L-1.0 g/L in dilute TFA (0.05%, 0.09 mol/L sinapinic acid in acetonitrile-ethanol-water(60:4:36, v/v/v) was used as protein matrix and 0.1 mol/L 2,5-dihydroxybenzoic (DHB) in formic acid-water (9:1, v/v) was used as peptide matrix. The matrix solution was kept in the dark and prepared fresh every few days.

The samples for mass spectrometric analysis were mixed with the matrix in an Eppendorf tube. Typically, 5 µL of sample solution was added to a tube containing 10 µL of matrix solution. The solution was stirred in a vortex mixer, and then approximately 0.5 µL of sample solution was applied to the target and followed by drying at room temperature and atmospheric pressure. For some protein samples in which the buffer contained salts at high concentrations, the dried sample/matrix preparation on the target was washed by depositing a droplet of cold distilled water for a few seconds on the sample spot surface to dissolve excess salt crystals, and followed by removing the droplet.

## RESULTS AND DISCUSSION

### *Mr* measurement for purified proteins

**Nonglycosylated proteins** The *M<sub>r</sub>* of recombinant proteins, IL-2, TNFα, GM-CSF, TNFα-2b, CaM fragments and nNOS expressed in *E.coli* were determined using MALDI-TOF MS. Table 1 shows the number of amino acids, theoretical *M<sub>r</sub>*, measured *M<sub>r</sub>* and relative determination error for these nonglycoproteins.

**Table 1** *M<sub>r</sub>* of non-glycoproteins measured by MALDI-TOF MS

Protein	Number of amino acids	Theoretical <i>M<sub>r</sub></i>	Measured <i>M<sub>r</sub></i>	Relative error (%)
IL-2	134 <sup>a</sup>	15478	15610	2.8
GM-CSF	127	14477	15451	5.56
TNF-α	158 <sup>a</sup>	17484	17517	0.18
nNOS	199 <sup>a</sup>	22248	22306	0.26
IFN-α2b	166 <sup>a</sup>	19378	19533	0.79
CaM fragment	95	10846	10851	0.05

<sup>a</sup>An additional methionine at the NH<sub>2</sub>-terminal.

As table 1 shows, the *M<sub>r</sub>* relative error of the protein GM-CSF was 5.56%, which was much higher than the systematic error of the instrument. In addition, the peak in the GM-CSF mass spectrum was very sharp, indicating that the product was very pure. However, the results of Edman sequencing showed that there were 8 additional amino acids, MMKSDNSH, at the NH<sub>2</sub>-terminus. The relative error was 0.12% when the 8 amino acids were added to the regular GM-CSF amino acid sequence. The relative errors of interleukin-2 and interferon α2b were approximately 0.8%. The increased mass was approximately equal to the *M<sub>r</sub>* of an amino acid, which may have been added during the modifications, such as phosphorylation and cystinylation. The details were not achieved in the present report. An asymmetric single charged peak was observed in the interferon α2b mass spectrum (Figure 1), with an unresolved impurity peak on the left side that could be seen when the mass spectrum was amplified partially. This may be caused by partially removing N terminal methionine residue in the interferon α2b.

**Glycosylated proteins** Proteins expressed in mammal cells are generally glycosylated. Because of the microheterogeneity of the carbohydrates, the final product is a complicated heterogeneous mixture. In some cases, the functions of the biomolecules depend on the carbohydrate components<sup>[11,12]</sup>. For example, recombinant human erythropoietin will lose its *in vivo* bioactivity without sialic acid residues<sup>[13,14]</sup>. Thus, it is very important to characterize the carbohydrate parts in glycoproteins<sup>[15,16]</sup>. In this article, MALDI-TOF MS

was used to determine  $M_r$  and carbohydrate percentages of erythropoietin (EPO) and interferon  $\alpha 1$  (Table 2).

**Table 2**  $M_r$ s of glycoproteins measured by MALDI-TOF MS

Protein	Number of amino acids	Measured $M_r$	Carbohydrate content (%)
EPO	166	28 707	35.6
IFN $\alpha 1$	166	20 465	5.2

As can be seen in Figure 2, the half-intensity-width of EPO was much larger, indicating that EPO was a heterogeneous protein. The carbohydrate percentage was so high that electrospray mass spectrometry could not be employed to determine the heterogeneity. The  $M_r$  obtained using MALDI-TOF MS was 28 707, while the  $M_r$  obtained using the traditional SDS-PAGE technique was about 34 000. The mass difference of 5 293 suggested that SDS-PAGE could measure the apparent  $M_r$  of the glycoprotein with high carbohydrate content. Since the results of SDS-PAGE for the molecular weight were related to the gel concentration, the determination procedure was difficult to control. The degree of glycosylation for biomolecules expressed in silkworm cells was generally lower, with only 5.2% carbohydrates found in recombinant protein interferon  $\alpha 1$  by MALDI-TOF MS, which was consistent with theoretical calculations. The TOF mass spectra for EPO and IFN $\alpha 1$  showed that the half-intensity-widths were 8 000 and 3 000, respectively, much wider than that of nonglycoproteins in Table 1, Figures 4 and 5. Ordinarily the half-intensity-widths are produced by isotopes, and are no more than 500<sup>[17]</sup>. Therefore, half-intensity-widths of 500 in singly charged MS peaks may be employed as a simple criterion to evaluate the heterogeneity of glycoproteins. The MS peak width will increase as glycoprotein becomes more heterogeneous.

#### Determination of protein mixture

##### Mixture composed of known standard proteins

Methods used to analyze each component in multi-protein mixtures without tedious separation are of great value. The advantage of MALDI-TOF MS in multicomponent characterization is the ability to simultaneously determine the  $M_r$  of each ingredient during one scan. However, singly charged oligomers with multiply charged monomers and multiply charged oligomers would complicate the mass spectra. Peaks could be specified only according to their  $M_r$  and the number of charges.

Figure 3 shows the MALDI-TOF mass spectrum for mixed proteins composed of myoglobin from horse heart, carbonic anhydrase B,  $\beta$ -lactoglobulin

and bovine serum albumin. Both molecular ion and the multiply charged monomers or oligomers were observed. The  $M_r$  measurement accuracy for the four proteins was 0.0%, 0.04%, 0.12%, and 0.18%, respectively.

#### Determination of a specific protein in mixtures

The mass spectrum of *E. coli* expressed products containing calmodulin in Figure 4, showed a protein mixture containing a protein with an observed  $M_r$  of 16 934, together with a doubly charged monomer and a singly charged dimer, indicating that the mixture contained calmodulin with a theoretical  $M_r$  of approximately 17 000. In addition, the spectrum showed that there was very little singly charged dimer, because calmodulin seldom formed dimers.

#### Measurement of the purity of expressed products and the relative content of impurities

Since MALDI-TOF MS can give the  $M_r$  of all components in a mixture, the relative purity of the expressed product, along with the  $M_r$  of the impurity and its abundance, can be obtained from the mass spectrum. Figure 5 shows the mass spectrum of calmodulin fragment expressed in *E. coli* had small amounts of impurities with  $M_r$  of 9643.8 and 9074.0. In addition, few impurities were observed in the recombinant proteins, IL-2, TNF $\alpha$ , GM-CSF, IFN $\alpha 2b$ , nNOS, IFN $\alpha 1$  and EPO.

#### Characterization of tryptic peptide mapping for erythropoietin

The MALDI-TOF peptide mapping strategy has been used successfully to analyze proteins in enzymatic digests and has thus been applied to verify the primary structure of some proteins<sup>[18]</sup>. As a technique, it offers a number of advantages over conventional peptide mapping with HPLC since it reduces the actual analysis time and also provides a means of assigning peptide fragments from their respective  $M_r$ . Peptide mapping is the "fingerprint" of the protein, so it can be employed to rapidly identify the correctness of the primary structure of protein during expression or purification<sup>[19]</sup>. This report introduces the peptide map of recombinant human erythropoietin by MALDI-TOF MS. Protease trypsin can theoretically digest the erythropoietin into 21 peptide fragments, including three glycopeptide fragments and two disulfide bonds (one between fragments T<sub>1</sub> and T<sub>20</sub>, and another inside T<sub>5</sub>). The proteolytic digests were subjected directly to MALDI-TOF MS analysis without any prior purification. Figure 6 shows the mass spectrum of the tryptic digest with 13 peaks corresponding to peptide fragments. The observed mass values of the digests were consistent with the theoretical mass values as calculated from the amino acid sequence of rhEPO (Table 3). The mass value

of 1612.7 indicated the formation of a disulfide bond between T<sub>1</sub> nor T<sub>20</sub>, which was verified by the fact that neither T<sub>1</sub> nor T<sub>20</sub> was observed. Peptide mixtures generated by enzymatic digestion do not always allow for complete evaluation of peptide fragments by MALDI-TOF MS. As can be seen in Table 3, about 76.5% of the entire amino acid sequence was confirmed. In the lower mass range (below m/z 400), analyte molecules could not be identified since the matrix peaks overlap with the signals from the analytes. In addition, the three glycosylated peptides were also not observed, because EPO was heterogeneous and the MS sensitivity to carbohydrates was much lower than that of peptides. Several matrices, including 2,5-dihydroxy benzoic acid (DHB), 2-aminobenzoic acid and  $\alpha$ -cyano-4-hydroxycinnamic acid, were tested to obtain the best resolution and sensitivity in the mass spectrum measurement. The results in Figures 6, 7 and 8, show that the best matrix was DHB, which produced large analytical signals with good resolution. The 2-aminobenzoic acid matrix gave signals with lower sensitivity and poorer resolution, but it was better than the  $\alpha$ -cyano-4-hydroxycinnamic acid matrix that is more suitable for "big" proteins rather than "small" peptides. The matrix concentration also affects the mass resolution and analyte signals. For example, with saturated DHB solution employed as the matrix, only two main peaks with mass values of about 480 and 2550 were obtained, possibly due to poor crystallization over the entire sample area in the target.

In general, the choice of MALDI-TOF matrix is very critical to the homogeneous crystallization and the homogeneous embedding of the analyte molecules in the matrix. In addition, the matrix is responsible for the high mass resolution and high analyte signals.

**Table 3 MALDI-TOF-MS analysis of the tryptic digests of EPO**

rhEPO peptide	Position	Calculated mass value	Observed mass value	Relative mass value error (%)
T <sub>1</sub>	1-4	439.5	440.5	0.23
T <sub>3</sub>	11-14	515.6	517.8	0.39
T <sub>4</sub>	15-20	735.9	735.5	-0.05
T <sub>5</sub>	21-45	glycopeptide		
T <sub>6</sub>	46-52	927.1	928.4	0.14
T <sub>7</sub>	53	174.2		
T <sub>8</sub>	54-76	2525.3	2525.5	0.01
T <sub>9</sub>	77-97	glycopeptide		
T <sub>10</sub>	98-103	601.7	600.8	-0.15
T <sub>11</sub>	104-110	802.5	803.4	0.11
T <sub>12</sub>	111-116	586.3	585.5	-0.14
T <sub>13</sub>	117-131	glycopeptide		
T <sub>14</sub>	132-139	923.0	923.5	0.05
T <sub>15</sub>	140	146.2		
T <sub>16</sub>	141-143	434.5	*	
T <sub>17</sub>	144-150	898.0	899.1	0.12
T <sub>18</sub>	151-152	203.2		
T <sub>19</sub>	153-154	259.3		
T <sub>21</sub>	163-166	447.4	*	
T <sub>2-S-S-T<sub>20</sub></sub>	1615.8	1612.7		-0.19

\*A wide unresolved peak caused by T<sub>1</sub>, T<sub>16</sub> and T<sub>21</sub>.

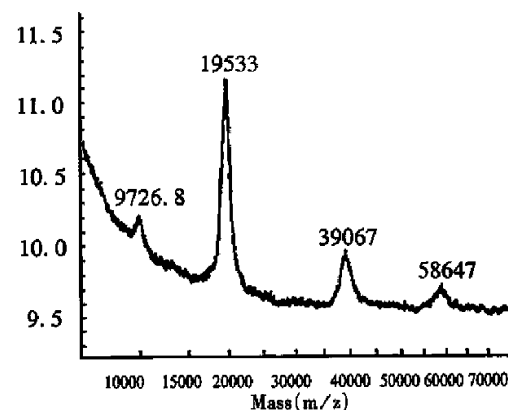


**Figure 1** MALDI-TOF mass spectrum of interferon  $\alpha$ 2b using sinapinic acid as matrix.

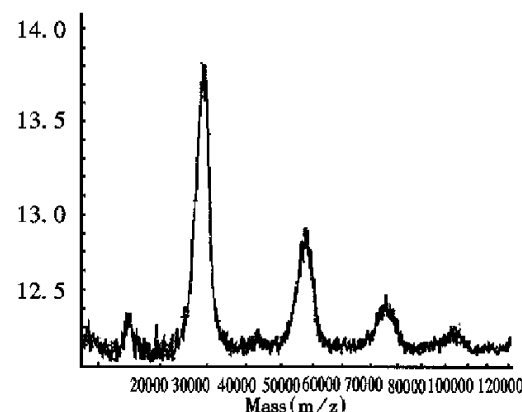


**Figure 2** MALDI-TOF mass spectrum of recombinant human erythropoietin using sinapinic acid as matrix.

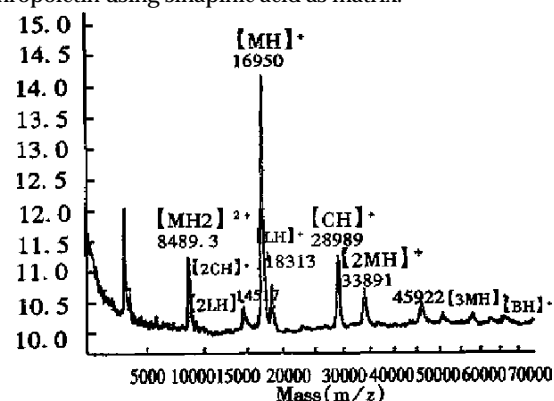


**Figure 3** MALDI-TOF mass spectrum of standard protein mixtures using sinapinic acid as matrix. M: Myoglobin; C: Carbonic anhydrase B; L:  $\beta$ -lactoglobulin; B: Bovine serum albumin.

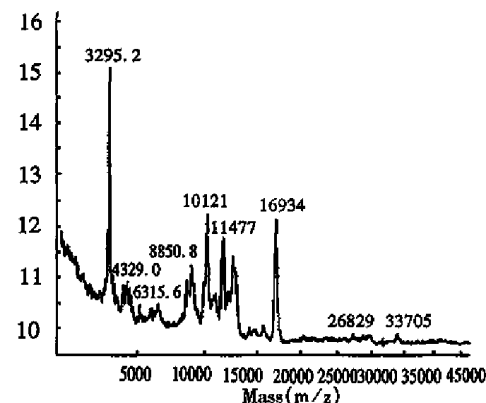


**Figure 4** MALDI-TOF mass spectrum of mixtures containing calmodulin using sinapinic acid as matrix.

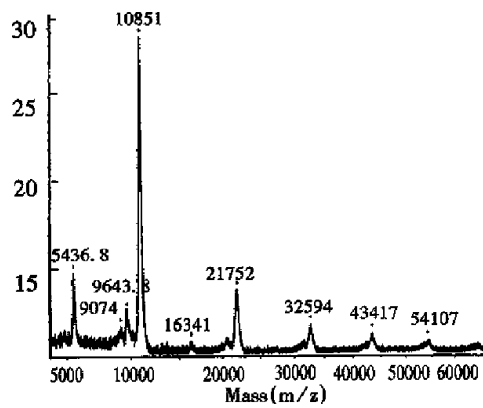


**Figure 5** MALDI-TOF mass spectrum of calmodulin fragment using sinapinic acid as matrix.

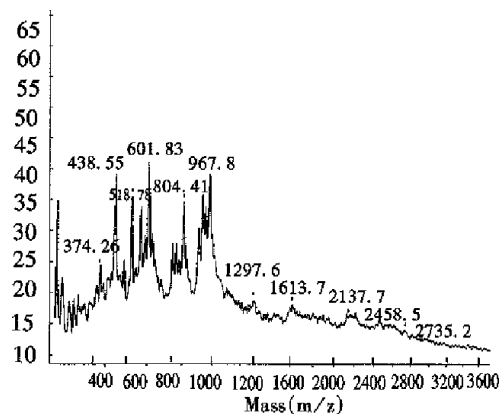


**Figure 6** MALDI-TOF mass spectrum of tryptic digests of recombinant human erythropoietin using 100mM DHB as matrix.

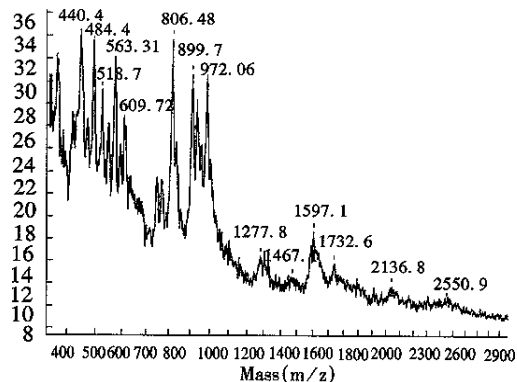


**Figure 7** MALDI-TOF mass spectrum of tryptic digests of recombinant human erythropoietin using 2-Aminobenzoic acid as matrix.

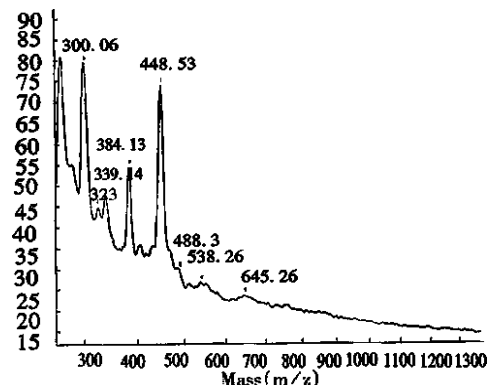


**Figure 8** MALDI-TOF mass spectrum of tryptic digests of recombinant human erythropoietin using  $\alpha$ -cyano-4-hydroxycinnamic acid as matrix.

## CONCLUSION

The present investigations clearly show that MALDI-TOF MS is a powerful tool for measuring protein molecular weight, identifying unknown components in mixtures, determining purity and the relative content of impurities, and characterizing peptide mapping. The MALDI-TOF analysis validated that SDS-PAGE is unreliable in determining the  $M_r$  of glycoproteins. Since the broad MS peaks reflect the carbohydrate heterogeneity, half-intensity widths, MALDI-TOF MS peaks are recommended as a criterion to evaluate the heterogeneity of glycoproteins. The advantages of MALDI-TOF MS were described in this paper, such as its accuracy, small volume sample consumption and rapid response. It is suggested that this technique should be the first choice when studying the quality of scarce or precious samples during the early stages in the development of engineered proteins.

## REFERENCES

- 1 Karas M, Hillenkamp F. Laser desorption/ionization of proteins with molecular masses exceeding 10000 daltons. *Anal Chem*, 1988; 60:2299-2301
- 2 Papac DI, Wong A, Jones AJS. Analysis of acidic oligosaccharides and glycopeptides by matrix-assisted laser desorption/ionization time-of-flight mass spectrometry. *Anal Chem*, 1996; 68:3215-3223
- 3 Karas M, Bahr U, Strupat K, Hillenkamp F. Matrix dependence of metastable fragmentation of glycoproteins in MALDI TOF mass spectrometry. *Anal Chem*, 1995;67:675-679
- 4 Feistner GJ, Faull KF, Barofsky DF, Roepstorff P. Mass spectrometric peptide and protein charting. *J Mass Spectr*, 1995;30: 519-530
- 5 Harmon BJ, Gu X, Wang DIC. Rapid monitoring of site-specific glycosylation microheterogeneity of recombinant human interferon- $\gamma$ . *Anal Chem*, 1996;68:1465-1473
- 6 Russell DH, Edmondson RD. High-resolution mass spectrometry and accurate mass measurements with emphasis on the characterization of peptides and proteins by matrix-assisted laser desorption/ionization time-of-flight mass spectrometry. *J Mass Spectrom*, 1997;32:263-276
- 7 Powell, AK, Harvey DJ. Stabilization of sialic acids in N-linked oligosaccharides and gangliosides for analysis by positive ion matrix-assisted laser desorption/ionization mass spectrometry. *Rapid Commun Mass Spectrom*, 1996;10:1027-1032
- 8 Rosinke B, Strupat K, Hillenkamp F, Rosenbusch J, Dencher N, Krüger U, Galla HJ. Matrix-assisted laser desorption/ionization mass spectrometry (MALDI-MS) of membrane proteins and non-covalent complexes. *J Mass Spectrom*, 1995; 30:1462-1468
- 9 Tang X, Sadeghi M, Olumee Z, Vertes A, Braatz JA, McIlwain LK, Drefuss PA. Detection and quantitation of  $\beta$ -2-microglobulin glycosylated end products in human serum by matrix-assisted laser desorption/ionization mass spectrometry. *Anal Chem*, 1996;68: 3740-3745
- 10 Edmondson RD, Russell DH. Evaluation of matrix-assisted laser desorption ionization-time-of-flight mass measurement accuracy by using delayed extraction. *J Am Soc Mass Spectrom*, 1996;7: 995-1001
- 11 Wasley BC, Timony G, Murtha P, Stoudemire J, Dorner AJ, Caro J, Kriege M, Kaufman RJ. The importance of N- and O-linked oligosaccharides for the biosynthesis and *in vitro* and *in vivo* biologic activities of erythropoietin. *Blood*, 1991;77:2624-2632
- 12 Yamaguchi K, Akai K, Kawanishi G, Ueda M, Masuda S, Sasaki R. Effects of site directed removal of N-glycosylation sites in human erythropoietin on its production and biological properties. *J Biol Chem*, 1991;266:20434-20439

- 13 Higuchi M, Oh-eda M, Kuboniwa H, Tomonoh K, Shimonaka Y, Ochi N. Role of sugar chains in the expression of the biological activity of human erythropoietin. *J Biol Chem*, 1992;267:7703-7708
- 14 Takeuchi M, Takasaki S, Shimada M, Kobata A. Role of sugar chains in the in vitro biological activity of human erythropoietin produced in recombinant Chinese hamster ovary cells. *J Biol Chem*, 1990;265:12127-12130
- 15 Narhi LO, Arakawa T, Aoki KH, Elmore R, Rohde MF, Boone T, Strickland TW. The effect of carbohydrate on the structure and stability of erythropoietin. *J Biol Chem*, 1991;266:23022-23026
- 16 Lai PH, Everett R, Wang FF, Arakawa T, Goldwasser E. Structural characterization of human erythropoietin. *J Biol Chem*, 1986;261:3116-3121
- 17 Depaous AM, Advani JV, Sharma BG. Characterization of erythropoietin dimerization. *J Pharmac Sci*, 1995;84:1281-1284
- 18 Apffel A, Chakel J, Udiavar S, Hancock WS, Soubers C, Jr EP. Application of capillary electrophoresis, high performance liquid chromatography, on line electrospray mass spectrometry and matrix assisted laser desorption ionization time of flight mass spectrometry to the characterization of single chain plasminogen activator. *J Chromatogr A*, 1995;717:41-60
- 19 Rush RS, Derby PL, Strickland TW, Rohde MF. Peptide mapping and evaluation of glycopeptide microheterogeneity derived from endoproteinase digestion of erythropoietin by affinity high-performance capillary electrophoresis. *Anal Chem*, 1993;65:1834-1842

Edited by WANG Xian-Lin

# Cloning and identification of an angiostatic molecule IP-10/crg-2 \*

LIU Zhi-Guo<sup>1</sup>, YANG Jing-Hua<sup>2</sup>, AN Hua-Zhang<sup>1</sup>, WANG Hai-Yan<sup>1</sup>, HE Feng-Tian<sup>1</sup>, HAN Zhe-Yi<sup>1</sup>, HAN Ying<sup>1</sup>, WU Han-Ping<sup>1</sup>, XIAO Bing<sup>1</sup> and FAN Dai-Ming<sup>1</sup>

**Subject headings** IFN- $\alpha$ ; IFN- $\gamma$ ; inducible protein; cytokine responsive gene-2; DNA

## Abstract

**AIM** To obtain human and murine cDNAs encoding IFN- $\gamma$  inducible protein 10 (IP-10) and cytokine responsive gene-2 (Crg-2).

**METHODS** The encoding genes of IP-10 and Crg-2 were amplified by RT-PCR from cultured human fibroblast cells and Balb/c mouse liver treated by IFN- $\gamma$  and TNF- $\alpha$ , respectively, and cloned into plasmids of pUC19 and pGEM3Zf(+).

**RESULTS** The nucleotide sequences of the amplified DNA were confirmed by endonucleases digestion and sequencing.

**CONCLUSION** Recombinant IP-10/crg-2 gene clones with 306 bp and 314 bp inserts were established for further research on biological activities and ligands of hIP-10/mCrg-2.

## INTRODUCTION

Angiogenesis plays an important role in tumorigenesis and metastasis, and gene therapy targeting vasculature of neoplasms has become a hot topic<sup>[1]</sup>. Many new molecules, including endostatin and angiostatin, were discovered with significant inhibitory effect on neovascularization of tumor. Besides these molecules, some 'old' cytokines were also found to possess the bioactivity of inhibiting angiogenesis, including IP-10/Crg-2<sup>[2]</sup>. Human IP-10 belongs to a superfamily called chemokines and Crg-2 is its murine analogue. As a member of chemokines, IP-10/Crg-2 was primarily characterized as a proinflammatory molecule. However, recent findings showed that IP-10/Crg-2 had a powerful inhibitory effect in neovascularization of tumor, and tumor regression induced by IL-12 was closely related with high level of IP-10 expression and subsequent vasculature destruction<sup>[3]</sup>. However, little has been known about its properties, especially the mechanisms of its inhibitory effect on endothelium, since the receptor of IP-10/Crg-2, CXCR3, was predominantly distributed in activated T cells, but not in endothelial cells<sup>[4]</sup>. To further clarify the bioactivity of IP-10/Crg-2 and explore its potential application in gene therapy against angiogenesis, we amplified the gene sequence encoding IP-10 and Crg-2 by RT-PCR from primary human fibroblast cells and mouse liver, and cloned them into pUC19 and pGEM3Zf(+) vector, respectively.

## MATERIAL AND METHODS

### Material

Recombinant human IFN- $\gamma$  was purchased from Bonding Co., Beijing. Recombinant TNF- $\alpha$  was kindly provided by Genetic Diagnosis Institute of our University. Endonucleases, T4 ligase and reverse transcriptase were purchased from Gibco BRL. Taq DNA polymerase was obtained from Perkin Elmer. 100bp PCR marker was purchased from New England Biolabs. The kit for purification of plasmids and PCR products were obtained from Promega. Primers were synthesized by the Shanghai Bioengineering Center of Chinese Academy of Sciences. Host bacterial cell line DH5 $\alpha$ , cloning vector pUC19 and pGEM3Zf(+) were stored in our lab.

<sup>1</sup>Department of Gastroenterology, Xijing Hospital, the Fourth Military Medical University, Xi'an 710032, China

<sup>2</sup>Department of Cellular and Molecular Biology, Harvard University, USA

Dr. LIU Zhi-Guo, male, born on 1974-03-24 in Harbin of China, graduated from Department of Medicine, the Fourth Military Medical University (FMMU) with bachelor degree of medicine in 1997, and now as a postgraduate in Department of Gastroenterology of Xijing Hospital, FMMU.

\*Supported by the Outstanding Youth Fund from National Natural Science Foundation of China, No. 39625023.

**Correspondence to:** Dr. FAN Dai-Ming, Department of Gastroenterology, Xijing Hospital, The Fourth Military Medical University, Xi'an 710032, Shaanxi Province, China

Tel. +86 • 29 • 2539041, Fax. +86 • 29 • 2539041

Email. zhiguoliu@163.net

Received 1998-12-03 Revised 1999-03-01

## Methods

### Template preparation of human and mouse cDNA

Human primary fibroblast cell was obtained by cultured surgically resected specimens of normal adult. Four hours before RNA extraction, human IFN- $\gamma$  was added to reach a final concentration of  $1 \times 10^6$  U/L for cell culture and Balb/c mice was individually injected with TNF- $\alpha$   $5 \times 10^6$  U. The total RNAs were then purified from fibroblast cells and mouse liver respectively by the method of guanidium/phenol, and reverse-transcribed to cDNA according to literature<sup>[5]</sup>.

### PCR amplification of IP-10 and Crg-2 encoding sequence

Primers were designed according to the sequence of IP-10/crg-2. For human IP10, endonuclease sites were introduced: 5' primer GGGCGCTAGC (*Nhe* I)CATATG(*Nde* I) AATCAAAGTGGCGATTCTGATT, 3' primer AAGCTT(*Hind* III) GGTACC(*Kpn* I) TTAA GGAGATCTTTAGACATTTC. For murine crg-2, no endonucleases were introduced: 5' primer ACCATGAACCCAAGTGCTGC; 3' primer GCTTCACTCCAGTTAAGGAG. PCR cycle parameters: 94°C 45s, 60°C 45s, 72°C 45s, 30 cycles in all. PCR reaction mixture consists of cDNA template (human or murine origin) 2  $\mu$ L, 25 mmol/L MgCl<sub>2</sub> 8  $\mu$ L, 10XPCR buffer 10  $\mu$ L, 10 mmol/L dNTPs 4  $\mu$ L, Taq DNA polymerase 2  $\mu$ L, 50  $\mu$ mol/L upstream and downstream primers 2  $\mu$ L each, and distilled water was supplemented to 100  $\mu$ L.

### Construction of human IP-10 recombinant plasmid

PCR amplification product was digested by endonucleases *Nhe* I and *Kpn* I, meanwhile pUC19 was cut by *Xba* I and *Kpn* I. After purification by agarose electrophoresis, these two fragments were ligated by cohesive ends and then the recombinant plasmid was introduced into *E. coli* line DH5 $\alpha$ . Clones were picked randomly by blue/white screening, and identified by endonucleases digestion of *Xba* I/*Eco*R I and *Hind* III/*Bgl* II.

### Construction of murine crg-2 recombinant plasmid

Murine crg-2 recombinant plasmid was constructed by T/A cloning according to literature<sup>[6]</sup>. Five  $\mu$ g pGEM3Zf(+) was digested by *Sma* I. After purification by electrophoresis, 10  $\mu$ l 10 $\times$  PCR buffer, 1  $\mu$ L 100 mmol/L dTTP, 1  $\mu$ L Taq DNA polymerase and distilled water were added to make a final volume of 100  $\mu$ L and incubated at 75°C for 2 h. The PCR product was ligated with vector and the recombinant was transformed into DH5 $\alpha$ , clones

were selected by blue/white screening, minipreps were extracted and the right insert was confirmed by endonuclease digestion with *Bam*H I or *Hin* d III.

**Sequence analysis** DNA sequence analyses were conducted in the Central Lab of our university with automatic DNA analyzer (PE373-A, USA) according to the methods of Sanger.

## RESULTS

### PCR amplification of IP-10/Crg-2 encoding sequence

PCR reactions were carried out using the obtained cDNAs of human fibroblast and murine liver treated by IFN- $\gamma$  or TNF- $\alpha$  as the templates. Electrophoresis of PCR products indicated that fragments of about 300bp were amplified in each of the reaction mixture, which were consistent with our expectation of 322bp and 314bp(Figure 1).



**Figure 1** Amplification of human IP-10 and murine crg-2 gene by PCR.

1. crg-2 gene fragment (306 bp); 2. IP-10 gene fragment (314 bp); 3. 100 bp PCR marker (1500, 1200, 1000, 900, 800, 700, 600, 500, 400, 300, 200 and 100 bp fragment, from top to bottom. The 500 and 1000 bp fragments serve as reference bands).

### Construction and identification of recombinant plasmids

For recombinant construction of human IP-10, purified PCR product was ligated with endonucleases-digested pUC19, and the recombinant was transformed into *E. coli* line DH5 $\alpha$ . White clones were picked and confirmed by dual endonucleases digestion with *Xba* I/*Eco*R I and *Hin* d III/*Bgl* II. Electrophoresis of 20  $\mu$ g/L showed that fragments of about 237 bp and 318 bp were released respectively. This clone was identified as positive and named pUC19/h-IP-10 (Figure 2, lane 1-3). For vector construction of crg-2, the amplified fragment was ligated directly with pGEM3Zf(+) T vector, and recombinants were analyzed by single endonuclease digestion with

*Bam* H I or *Hin* d III. Electrophoresis of 20 g/L showed that a fragment of 251 bp or 204 bp was released the positive clones were named pGEM3Zf(+)/*crg-2* (Figure 2, lane 5-7).

### Sequence analysis

Minipreps of pUC19/IP-10 and pGEM3Zf(+)/*crg-2* were prepared according to the manual of Promega Wizard Minipreps kit. Samples were analyzed with automatic sequence analyzer. Sequencing results showed that the 306 bp and 314 bp inserts were completely identical with reported sequences of IP-10<sup>[7]</sup> and *crg-2*<sup>[8]</sup>, flanked by introduced endonuclease sites or added single T (Figure 3).

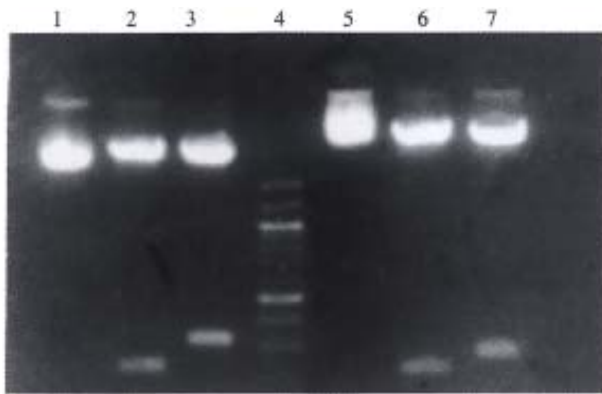


**Figure 2** Identification of pUC 19/IP-10 and pGE M3Zf(+)/*crg-2* recombinant clones by restriction endonucleases digestion. 1. pUC19/IP-10 control; 2. pUC19/IP-10 by *Xba*-I+*Eco* R I; 3. pUC 19/IP-10 by *Hin* d III+*Bgl* II; 4. 100bp PCR marker; 5. pGEM3Zf (+)/*crg-2* control; 6. pGEM3Zf(+)/*crg-2* by *Hin* d III; 7. pGEM3Zf (+)/*crg-2* by *Bam* H I.

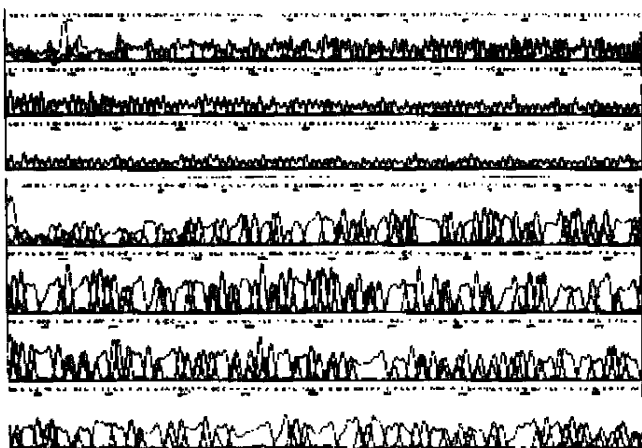


**Figure 3** The nucleotide sequence of IP-10/*crg-2* gene encoding region. Human IP-10 sequence (*above*); murine-*crg-2* sequencing (*below*).

### DISCUSSION

The growth of tumor is dependent on the vasculature for nutrition and oxygen. Destruction of established vasculature will lead tumor cells to necrosis or apoptosis, that is the main idea of angiostatic therapy. Tumor cells are highly heterogenic and multiple drug resistance (MDR) is very likely to be induced. But its endothelium, is more stable and susceptible to treatment and causes little<sup>[9]</sup> MDR. In normal adult, endothelium remains in dormant status except for wound-healing and menstruation. So inhibiting the process of active angiogenesis of tumor will eventually selectively cure the neoplasms and its metastasis without induction of MDR.

IP-10 was initially identified in 1985 as a member of CXC subfamily in chemokine superfamily<sup>[7]</sup>. The family of chemokines is characterized by 4 highly conservative cysteines at the N terminus of protein. Most chemokines are basic heparin binding protein possessing the activity of chemotaxis, which play important roles in inflammation and wound healing. According the different structures, gene location and bioactivities, this family can be divided into 2 subfamilies, CC and CXC subfamily. The first 2 cysteines of CC subfamily are adjacent with each other, while in CXC subfamily the cysteines were separated by a single random residue. IP-10/Crg-2 is a secreted protein consisting of 98 amino acids, of which the first 21 amino acids represent a signal peptide, with a  $M_r$  of 6000-7000 for mature form. Its receptor CXCR3 was successfully cloned in 1996<sup>[4]</sup>. The receptor belonging to seven transmembrane G-protein coupled receptors expressed primarily on activated T cell. The best-described bioactivities of IP-10/Crg-2 include angiogenesis inhibition, bone marrow hemopoietic stem cell inhibition, chemotaxis for activated T cell and monocyte-macrophage<sup>[10]</sup>. Among them, the most attracting property is the effect on vasculature, especially after it is found to be the downstream molecule for IFN- $\gamma$  or IL-12 to induce the regression of tumor<sup>[3, 11]</sup>. But most researches are focused on its induction or its effects on various kinds of tissues and cells, and are far from the insight of its biological activity and signal transduction process.

We amplified the complete cDNA sequences of IP-10/Crg-2. The target gene clones were established and confirmed by endonuclease digestion and sequence analysis. This will help us further clarify the bioactivity of IP-10/Crg-2 and the downstream mechanism after receptor binding.

## REFERENCES

- 1 Folkman J. Antiangiogenic gene therapy. *Proc Nat Acad Sci USA*, 1998;95:9064-9066
- 2 Keane MP, Arenberg DA, Lynch JP, Whyte RI, Iannettoni MD, Wilke CA, Morris SB, Glass MC, DiGiovine B, Kunkel SL, Strieter RM. The CXC chemokines, IL-8 and IP-10, regulate angiogenic activity in idiopathic pulmonary fibrosis. *J Immunol*, 1997;159:1437-1443
- 3 Sgadari C, Angiolillo AL, Tosato G. Inhibition of angiogenesis by interleukin 12 is mediated by the interferon-inducible protein 10. *Blood*, 1996;87:3877-3882
- 4 Marcel L, Basil G, Pius L, Simon AJ, Luca P, Ian C, Marco B, Bernhard M. Chemokine receptor specific for IP-10 and Mig: structure, function and expression in activated T lymphocytes. *J Exp Med*, 1996;184:963-969
- 5 Sambrook J, Fritsch EF, Maniatis T. Molecular cloning: a laboratory manual. 2nd ed. New York: Cold Spring Harbor Laboratory Press, 1989:60-87
- 6 Borovkov AY, Rivkin MI. Xcm I-containing vector for direct cloning of PCR products. *Bio Techniques*, 1997;22:812-814
- 7 Andrew DL, Jay CU, Jeffrey VR.  $\gamma$ -interferon transcriptionally regulates an early response gene containing homology to platelet proteins. *Nature*, 1985;315:672-676
- 8 Vanguri P, Farber JM. Identification of CRG-2: An interferon inducible mRNA predicted to encode a murine monokine. *J Biol Chem*, 1990;265:15049-15057
- 9 Thomas B, Judah F, Timothy B, Michael SO. Antiangiogenic therapy of experimental cancer does not induce acquired drug resistance. *Nature*, 1997;390:404-407
- 10 Baggiolini M, Dewald B, Moser B. Human chemokines: an update. *Annu Rev Immunol*, 1997;15:675-705
- 11 Yu WG, Ogawa M, Mu J, Umehara K, Tsujimura T, Fujiwara H, Hamaoka T. IL-12 induced tumor regression correlates with in situ activity of IFN-gamma produced by tumor-infiltrating cells and its secondary induction of anti-tumor pathways. *J Leukoc Biol*, 1997;62:450-457

Edited by MA Jing-Yun

# Pathogenic effects of O-polysaccharide from *Shigella flexneri* strain \*

ZHONG Qi-Ping

**Subject headings** *Shigella flexneri* strain;bacterial antigen;O-polysaccharide,virulence

## Abstract

**AIM** To investigate the specific pathogenesis of O-polysaccharide (O-PS) which is on the outer membrane of lipopolysaccharides (LPS) from *Shigella flexneri*.

**METHODS** The O-PS was isolated and purified from *Shigella flexneri*- 5 M90T by enzymatic hydrolysis and gel chromatography. Effects of O-PS were observed by *in vitro* experiment, (HeLa cell culture), and *in vivo* experiment (rabbit ileal loop assay).

**RESULTS** *In vitro* and *in vivo* experiments with the purified O-PS from *Shigella flexneri*-revealed that the O-PS alone was toxic to Hela cells and caused mucosal inflammation and hemorrhagic exudation in ileal loop of rabbit.

**DISCUSSION** O-PS might be one of the factors causing diarrhea and its mechanism was different from endotoxin reaction of LPS. The molecular mechanism of O-PS need further studies.

## INTRODUCTION

*Shigella flexneri* is one of the pathogens which causes diarrhea and its pathogenic mechanism is still unclear, even though extensive investigations were carried out worldwide. It has been known that the invasive outer membrane protein encoded by its plasmid DNA plays a primary role in bacterial infection. The roles of other factors, especially lipopolysaccharides (LPS), were also better understood. The specific pathogenesis of O-polysaccharide (O-PS) which is on the outer membrane of lipopolysaccharides remains unclear. To understand the pathogenesis of the O-PS of *Shigella flexneri*, we isolated and purified the O-PS from *Shigella flexneri*- 5 M90T and observed the pathogenesis of O-PS *in vitro* and *in vivo*.

## MATERIALS AND METHODS

### Materials

**Strain** Wild-type *Shigella flexneri* 5 M90T was provided by Pasteur Institute (French).

**Medium** Lauria-Bertani (LB) medium.

**Reagents** Proteinase K was purchased from Merck, Sephadex G50 from Sigma, fetal bovine serum (FBS) from Institute of Hematology, Chinese Academy of Medical Sciences, 1640 medium from GIBCO, and nuclease from Huamei.

### Methods

**Preparation of O-PS** ① Cultivation of bacteria and harvest. A single colony of *Shigella flexneri*-5 M90T was inoculated onto LB plates, incubated at 37°C overnight and harvested into a clean centrifuge tube. The bacteria were washed with 20 mmol/L Tris-HCl (pH 7.4) buffer, lyophilised and ground to powder in a mortar. ② Isolation of LPS by enzymatic hydrolysis and gel chromatography<sup>[1,2]</sup>. Bacterium powder (25 mg) was suspended in 1.0 mL ddH<sub>2</sub>O, boiled for 15 min and centrifuged to remove cell debris. The supernatant was added with DNase (50 mg/L) and RNase (100 mg/L) and incubated at 37°C for 1 hour, then added with proteinase K (1mg), incubated at 60°C for 1 hour, boiled for 5 min and centrifuged for supernatant. The supernatant was then dialyzed against ddH<sub>2</sub>O overnight and centrifuged again. The supernatant, the crude LPS, was separated by a Sephadex G50 chromatography

Department of Microbiology, Tianjin Medical University, Tianjin 300070, China

ZHONG Qi-Ping, female, born on 1955-10-02 in Tianjin, graduated from Nankai University in 1982, graduated from Tianjin Medical University with a master degree in 1997, engaged in bacteriological research, now associate professor of microbiology, having 9 papers published.

\*Project supported by the National Natural Science Foundation of China, No. 39370040.

**Correspondence to:** ZHONG Qi-Ping, Department of Microbiology, Tianjin Medical University, Tianjin 300070, China

Tel. +86 • 22 • 23525615

Received 1998-12-13 Revised 1999-04-02

column with elution of ddH<sub>2</sub>O. The first peak was collected, lyophilized and stored at 4°C. ③ Preparation of O-PS by acid hydrolysis<sup>[2,3]</sup>. LPS was hydrolyzed in 1% acetic acid at 100°C for 2 hours. The solution was then centrifuged and the supernatant was separated by gel chromatography and O-PS was collected as described above.

**Quantification of carbohydrates by the sulfuric acid-phenol method<sup>[4]</sup>** A proper amount of O-PS was dissolved in 2 mL ddH<sub>2</sub>O, mixed well with 1 mL 5% phenol and then added with 5 mL sulfuric acid. The mixture was incubated at room temperature for 10 min and transferred to 25°C-30°C water bath for 10 min-20 min. The carbohydrate content was quantified by measuring absorbance at 480 nm with 10 mg/L-100 mg/L rhamnose as standard.

**Antigenicity measurement of O-PS by ELISA** Rabbit antisera against *Shigella flexneri*-5 M90T and enzyme-conjugated goat antirabbit IgG were added to the plate coated with 50 mg/L O-PS. The antigenicity of O-PS was determined by color reaction density after adding TMB.

**Effects of O-PS on HeLa cell** With 1640 medium containing 10% bovine sera, penicillin and streptomycin, HeLa cells were cultured into monolayer and transferred into a 12 hole tissue culture plate. When cells grew onto the plate walls and formed small clumps, the medium was replaced by fresh one. O-PS was added to each hole to reach a final concentration of 100, 200, 500 and 1000 µg/L respectively and incubated under 5% CO<sub>2</sub> at 37°C. Growth and morphology of the HeLa cells were observed every 24 hours.

**Rabbit ileal loop assay** Rabbits were fasted for 24 hours. The rabbit ligated ileal loops (5 cm) were prepared in rabbits (weight 2 kg) anesthetized with procaine hydrochloride by local infiltration. Twenty µg O-polysaccharides in 0.5 mL saline was injected into the loop. Rabbits were sacrificed 24 hours later. Portions of tested loops were taken and fixed in 10% buffered formalin immediately. The pathologic slices of the specimen were prepared with standard procedures.

## RESULTS

**Purification of O-PS from *Shigella flexneri* 5 M90T** Separation of the crude O-PS by Sephadex G50 showed three major peaks of carbohydrates measured with the sulfuric acid-phenol method (Figure 1). According to references<sup>[3]</sup> and the

molecular weight, the peak I was thought to be the long-chain O-PS. This was confirmed by ELISA analysis which gave rise to positive results with peak I by using antisera against *Shigella flexneri*-5 M90T. On the contrast, peak II yielded negative results with ELISA analysis. Peak III was not analyzed due to its small amount and low molecular weight. Therefore, it is plausible that peak II and III were the fragments generated in acid-hydrolysis. Peak I is the O-PS based on its molecular weight and antigenicity.

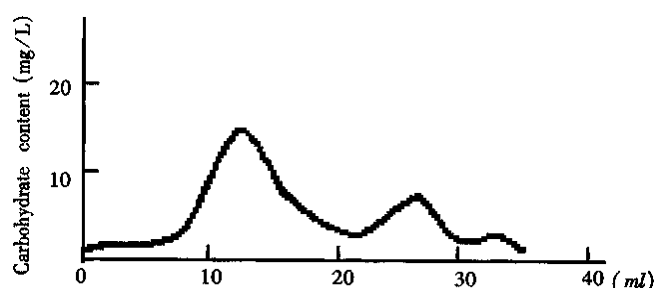


**Figure 1** The curve of carbohydrate content quantified. The crude O-PS was separated by Sephadex G50 with elution of ddH<sub>2</sub>O.

### **Toxicity of O-PS to HeLa cells**

The toxicity of O-PS to HeLa cells demonstrated as cell shrinking and falling off from plate walls within 48 hours. The cytopathic effect of HeLa cells was positively related to the concentration of O-PS in medium (Figure 2).

### **Effects of O-PS on ileal loop of rabbits**

After 24 hours of injection of 20 µg O-PS into ileal loop of rabbit, mucosal inflammation and hemorrhagic exudation in ileal loop of rabbit could be observed. When observing the pathologic slice of the specimen under light microscope, we could see inflammatory reaction, the mucosa and submucosa had moderate to severe hyperemia and infiltration of neutrophils and lymphocytes, the muscularis and serosa had mild hyperemia and infiltration of white blood cells. There were necrotic substances and hemorrhage in the lumen.

## DISCUSSION

*Shigella flexneri* is an intracellular pathogen which causes acute inflammation by infection of the

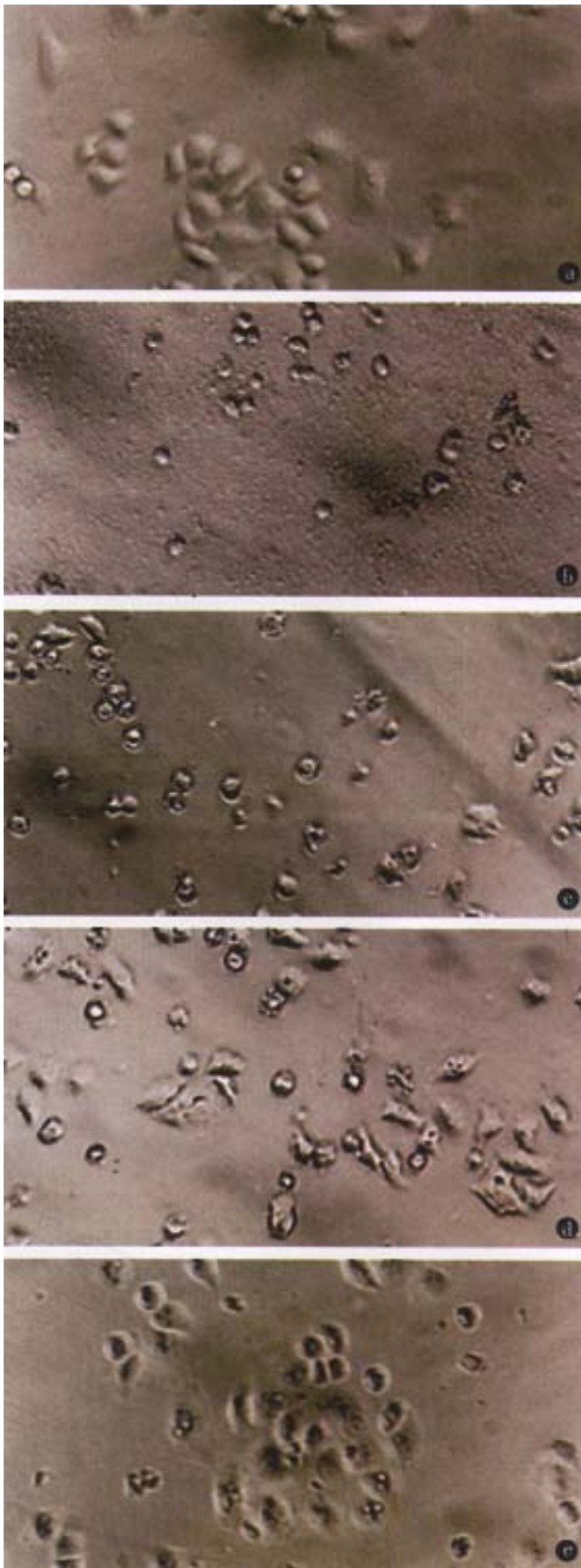


**Figure 2** Effect of various doses of O-PS on HeLa cell. Normal HeLa cells (A), and HeLa cells in the medium containing 1000 (B), 500 (C), 200 (D), 100 (E)  $\mu\text{g}/\text{mL}$  O-PS respectively.  $\times 200$

mucosal membrane of the large intestine and damages the mucosal epithelial cells, leading to ulcer. It has been shown that the infection of *Shigella flexneri* is accomplished by releasing the across membrane signals which induce aggregation of actin and polymerization of myosin to trigger the endocytosis. This will bring about the breakdown of membrane and allow bacteria to get into cells, proliferate and move in cells, diffuse into surrounding cells and eventually kill the cells infected by inhibiting respiration<sup>[5]</sup>. These functions were dependent on the presence of O antigen and involved in form a “tail-like” actin structure on the bacterium surface as a motile apparatus. As for the infection of *Shigella flexneri*, LPS plays an important role in inducing inflammation. For example, antibodies against LPS showed protective effects for inflammatory reaction and the mutants defective in O-antigen can not cause keratitis in guinea pigs, although it is able to invade HeLa cells. However, little is known about the roles and mechanisms of LPS played in the infection of cells.

LPS of gram negative bacteria is composed of lipid A, core polysaccharide and O-PS. Among them, lipid A, the principal component of LPS, causes pathological or physiological damages by inducing some cellular factors<sup>[6]</sup>. But O-PS is generally thought to determine the antigenicity of the bacterium and its resistance to the defence of the host cells<sup>[7]</sup>. In recent years, the specific pathogenesis of O-PS has received increasing attention worldwide<sup>[8,9]</sup>. There are reports using whole bacterium in the research, but the role played by each component of LPS has not been distinguished. For example, enteroinvasive *Escherichia coli* (EIEC) can be strongly recognized by the antisera against O-PS, suggesting that the structure of O-PS may be related to its toxicity. The *Shigella* vaccine of the same serotype was efficient; the mAb against O-PS of *Shigella flexneri* could inhibit contact hemolytic activity<sup>[10]</sup>. All these indicate the importance of O-PS in pathogenesis of *Shigella flexneri*. Therefore, it is important to investigate the pathogenesis by using purified O-PS.

In this paper, we studied *Shigella flexneri* pathogenesis by using purified O-PS both *in vitro* and *in vivo*. We have modified Eidhin’s method to improve the preparation of crude LPS by conducting additional steps of nuclease digestion and Sephadex G50 gel chromatography. The experiment showed that M90 O-PS alone was toxic to HeLa cells and caused mucosal inflammation and hemorrhagic exudation of ileal loop in rabbits. It appears that the toxicity to HeLa cells and ileal loop pathogenesis resulted from a common factor. Our experiments

showed that *Shigella flexneri* O-PS may also be one of the factors which cause diarrhea. However, its molecular mechanism is still unclear and needs further investigations. The methods and results presented in this report provide a basis to study diarrhea pathogenesis and a new thought to develop diarrhea vaccines.

**Acknowledgments** We are grateful to Professor Chen En-Lin for his overall guide to this paper, to Mr. He Jian-Min for his technical assistance in preparing LPS, to Dr. Li Fang-Tao, Li Bao-Yan and Kang Ning for participating in the animal experiment, and Department of Pathology for pathological diagnosis.

#### REFERENCES

- 1 Eidhin DN, Mouton C. A rapid method for preparation of rough and smooth lipopolysaccharide from *Bacteroides*, *Porphyromonas* and *Prevotella*. *FEMS Microbiol Lett*, 1993;110:133-138
- 2 Xu XP, Chen ZH, Su X. Study on immunogenicity of *S. sonnei* polysaccharide-protein conjugate. *Chin J Microbiol Immunol*, 1992;12:141-144
- 3 Muller-Seitz E. Degradation studies on and investigation of O specific and core polysaccharides. *FEBS Lett*, 1968;1:311-314
- 4 L Blay K, Caroff M, Richards JC, Perry MB, Chaby R. Specific and cross-reacting monoclonal antibodies to *Bordetella parapertussis* and *Bordetella bronchiseptica* lipopolysaccharides. *Microbiology*, 1994;140(pt 9):2459-2465
- 5 Sansonetti PJ. Genetic and molecular basis of epithelial cell invasion by *Shigella* species. *Rev Infect Dis*, 1991;13(Suppl 4):S285-292
- 6 Jiao BH. Molecular endotoxicology. *Shanghai: Shanghai Scientific and Technological Publishing House*, 1995:151-156, 232-253
- 7 Lindberg AA, Karnell A, Weintraub A. The lipopolysaccharide of *Shigella* bacteria as a virulence factor. *Infect Dis*, 1991;13(Suppl 4):S279-284
- 8 Rajakumar K, Jost BH, Sasakawa C, Okada N, Yoshikawa M, Adler B. Nucleotide sequence of the rhamnose biosynthetic operon of *Shigella flexneri* 2a and role of lipopolysaccharide in virulence. *J Bacteriol*, 1994;176:2362-2373
- 9 Sandlin RC, Lampel KA, Keasler SP, Goldberg MB, Stolzer AL, Maurelli AT. Avirulence of rough mutants of *Shigella flexneri*: requirement of O antigen for correct unipolar localization of IcsA in the bacterial outer membrane. *Infect Immun*, 1995;63:229-237
- 10 Mei Y, Su X, Li H, Xu XP. Analysis of biological characteristics of monoclonal antibodies to *Shigella flexneri* 2a O-side chain of LPS. *Chin J Microbiol Immunol*, 1992;12:322-323

Edited by MA Jing-Yun

# The mechanism of actions of Octreotide, Bupleurum-Peony Cheng Qi decoction and Dan Shan in severe acute pancreatitis

WU Xie-Ning

**Subject headings** Pancreatitis/therapy; Octreotide; bupleurum peony Cheng Qi decoction

The pathogenesis of severe acute pancreatitis (necrotizing pancreatitis) is complicated and has not been elucidated up to date. In my opinion, it is multifactorial, and aggressive treatment should be directed to the multifaceted pathophysiology<sup>[1]</sup>. A cumulative series of twenty cases were treated with the regimen i.e., combined traditional Chinese and modern medicine. No death, almost no morbidity and no serious complications, such as ARDS and DIC occurred, only mental confusion as sequela occurred in a patient with previous cerebral infarction. The present article is to discuss the mechanism of actions of the medicines used in this treatment regimen.

## THE PATHOGENESIS OF SEVERE ACUTE PANCREATITIS

It involves ① the release of pancreatic and lysosomal enzymes by the pancreatic acini which induce pancreatic autodigestion; ② the increase of vascular permeability, resulting in microcirculatory impairment; and ③ overstimulation of macrophages and neutrophils with release of many cytokines, inflammatory mediators (leukotrienes, prostaglandins, platelet activating factor) and free radicals. These factors interact with one another producing pancreatic acinar damage and intestinal epithelial barrier dysfunction. If not corrected instantly, it might lead to gut barrier damage and translocation of intestinal bacteria and endotoxin, resulting in a "second attack" caused by infection and endotoxemia, producing multiorgan dysfunction syndrome and eventually multiorgan failure.

Severe acute pancreatitis is most frequently precipitated by gallstone, biliary sludge,

microlithiasis with or without bile reflux, obstruction of biliary-pancreatic common pathway, high fat and high protein diet, alcohol consumption and ischemia here in Shanghai, hence, I think it is multifactorial and multifaceted a disease. The detailed mechanism will be delineated in another paper.

## OCTREOTIDE AND SOMATOSTATIN

On reviewing the medical literature, octreotide and somatostatin are found to act on many facets. Either of them inhibits cholecystokinin which stimulates the synthesis, secretion and release of pancreatic enzymes<sup>[2]</sup>, concomitantly it also stimulates and activates the monocytic-macrophagic system, lower the endotoxin level in acute necrotizing pancreatitis<sup>[3]</sup>. An experimental study showed that somatostatin could cause the blockage of endotoxin, IL-1, IL-6, IL-2, TNF- $\alpha$  and restore them to a near normal level<sup>[4]</sup>. Microcirculatory impairment is the initiating as well as aggravating factor in necrotizing pancreatitis, octreotide could decrease the small intestinal and colonic blood flow, and cause redistribution intrapancreatically, as well as decrease of the blood flow to the islets and to the cells secreting hormones with vasodilating property<sup>[5]</sup>. This is a very important point in contrast to the viewpoint that octreotide decreased pancreatic blood flow in the past. Another experimental study also showed the pancreatic microcirculatory impairment mimicked the ischemia-reperfusion damage in humans, with impaired arteriolar perfusion, increased vascular permeability and aggregation and stasis of neutrophils in the postcapillary venules. Via the mediation of the adhesive molecules on the vascular endothelium, the neutrophils interacted with the endothelial cells, the oxygen free radicals produced by the neutrophils damaged the vascular endothelium, resulted in endothelial swelling, making the capillary lumen narrowed and obstructed, and the functional capillary density decreased. By given octreotide, the changes in the postcapillary venules were much lessened as compared with those not given octreotide, the statistical difference was significant<sup>[6]</sup>. No adhesion of neutrophils in the

Department of Gastroenterology, Shanghai First People's Hospital, Shanghai 200080, China

Dr. WU Xie-Ning, Professor of Medicine, B.S., M.D. Editor of Ten books on Hepatology and Gastroenterology, having 185 papers published.

**Correspondence to:** Dr. WU Xie-Ning, Department of Gastroenterology and Central Research Laboratory, Shanghai First People's Hospital, No. 85, Wujing Road, Shanghai 200080, China

**Received** 1999-04-08

postcapillary venules were seen, indicating that octreotide attenuated the interaction between neutrophils and endothelial cells, thus providing a protective effect. Octreotide also increased PGI<sub>2</sub> level<sup>[7]</sup>, inhibited the synthesis of vasoconstricting leukotrienes and decreased the eicosanoid products<sup>[6]</sup>. Basing on the above facts, octreotide or somatostatin is a requisite in the treatment of severe acute pancreatitis.

#### BUPLEURIUM-PEONY CHENG QI DECOCTION

The herbal mixture Bupleurium-Peony Cheng Qi decoction has seven constituents: *Bupleurum*, *White peony*, *Scutellaria*, *Rhubarb (Rhei Rhizome)*, *Unripe bitter orange*, *Magnolia bark*, *Refined mirabilite*. This herbal mixture also acts on multifacets of the disease, among which, rhubarb is the major constituent<sup>[8]</sup>. It inhibits the secretion and activity of the pancreatic enzymes, such as trypsin, lipase, phospholipase A<sub>2</sub>, chymotrypsin, elastase, amylase, kallikren-kinin and is synergistic with octrotide (or somatostatin) in this aspect. It stabilizes the lysosomal membrane of acinar cells<sup>[9]</sup>, which is important in attenuating the acinar damage. It inhibits the inflammatory cytokines, its ant hracene derivative inhibits the phagocytic function of phagocytes, thereby inhibiting their overstimulation. As it is known, cytokines, such as IL-6, IL-1, IL-8 and TNF- $\alpha$ , are released by overstimulation of macrophages. A recent experimental study showed that acute phase proteins were induced by IL-6 and inhibited by rhubarb. Furthermore, the neutrophilic infiltration was only minimal in the necrotizing pancreatitis rats. The chemotactic effect of neutrophils on the inflamed area was by IL-8. Rhubarb can neutralize and expel the endotoxin, resulting in low blood endotoxin level with subsequent low release of TNF- $\alpha$ , these are the indirect evidences of rhubarb's inhibitory effect on cytokine release<sup>[4]</sup>. Rhubarb also inhibits vascular permeability, after oral administration, rhubarb is more concentrated in the pancreas, liver and kidney, whereas the brain and the lung are the next, and inhibition of the vascular permeability can cause cessation of exudation in the above organs and tissues. This is crucial in the prevention of local complications of the pancreas itself as well as prevention of leakage of fluid into the peritoneal cavity which causes peritonitis, hypovolemia and hypoalbuminemia, adult respiratory distress syndrome (ARDS) and pancreatic encephalopathy<sup>[5]</sup>. It also inhibits Na<sup>+</sup>, K<sup>+</sup>ATPase, impedes the transport of Na<sup>+</sup> from intestinal lumen into the cells and increases the volume of luminal contents, as the osmotic pressure increases within the colonic lumen, intestinal wall is

then stimulated and peristalsis increased. Concomitantly, the plasma oncotic pressure increases, water switches to the blood circulation from the tissue. In this recipe, bupleurum and unripe bitter orange can increase the gastric emptying and small intestinal propulsion, refined mirabilite can also promote small intestinal peristalsis. As a whole, the herbal mixture restores the gut motility and absorptive function of the GI tract, relieving intestinal paresis and even paralysis. Magnolia bark and white peony relax the gut smooth musculature to restrain the overaction of the rest constituents. When the tongue becomes moistened, it indicates the gut function is restored<sup>[6]</sup>. Rhubarb has also broad-spectrum antibiotic action, *in vitro* it inhibits bacteroid fragilis, streptococci, B.Coli etc., neutralizes and expels the endotoxin in the intestinal lumen. It is of particular importance in the prevention of dislocation of intestinal bacteria and endotoxin<sup>[7]</sup>. It decreases blood lipids, inhibits protein catabolism, reduces urea synthesis and promotes urinary excretion of urea and creatinine<sup>[8]</sup>. Rhubarb has another important effect, i.e., a powerful relaxant of Oddi's sphincter, it can antagonize and abolish the contracting effect of octrotide, in favor of pancreatic fluid and bile drainage. This is of particular importance in the management of severe acute pancreatitis especially in cases with stone in the common bile duct. One of the precautions is that rhubarb cannot be decocted too long, i.e., two minutes is enough, otherwise many of its beneficial effects will be lost.

Bupleurum has tranquilizing and analgesic effects, it also inhibits the growth of hemolytic streptococcus, staphylococcus aureus *in vitro*, also protects liver cells and decreases serum cholesterol and triglyceride, moreover, it enhances the intestinal contractility by acetylcholine. Another important effect is that it can stimulate the secretion of endogenous glucocorticoids<sup>[11]</sup> which can inhibit excessive secretion of cytokines and inflammatory mediators and protect acinar cells.

Unripe bitter orange has biphasic action on gut smooth muscle, low concentration stimulates, high concentration inhibits, which is dependent upon the functional status of the GI tract and the concentration of the herbal medicine. It has a synergistic effect on the GI musculature with bupleurum, refined mirabilite and rhubarb.

White peony inhibits amylase and has a weak relaxing effect on the Oddi's sphincter.

Scutellaria has antibiotic effect on staphylococcus aureus, streptococcus, B.Coli, pseudomonas bacillus, etc. It decreases free fatty acid, triglyceride, serum and hepatic cholesterol and transaminase levels. High fat diet is often one of the precipitating factors of severe acute

pancreatitis, free fatty acid can cause lipoperoxidation and damage the vascular endothelium and acinar cells, and scutellaria inhibits lipoperoxidation both via vitamin C-Fe and NADPH-ADP routes. It can also inhibit release of histamine by mast cells, and the cyclo-oxygenase and lipo-oxygenase pathways which produce inflammatory mediators. Besides, it inhibits thromboxane A<sub>2</sub> synthase, reduces platelet aggregation and its adhesive function, promotes PGE<sub>1</sub> and PGE<sub>2</sub> levels, and transformation of fibrinogen to fibrin and prevents endotoxin induced disseminated intravascular coagulation (DIC). Finally, scutellaria also has the effect of lowering the elevated temperature.

### SALVIA MILTIORRHIZA

*Salvia Miltiorrhiza* (Dan Shen) inhibits platelet aggregation, decreases blood viscosity, improves blood rheology and microcirculation, and inhibits the release of lysosomal enzymes and chemotacting neutrophils as well. Besides, it is an antioxidant as well as a calcium ion antagonist, the latter is also of great importance in improving the microcirculation. Experimental studies revealed that Ca<sup>2+</sup> influx occurred via the acinar cell membrane before the exocrine pancreatic secretion started<sup>[13]</sup>, and then some proteases were secreted. Ca<sup>2+</sup> influx also occurred before the macrophages produced and released the cytokines such as TNF- $\alpha$ , IL-6 and IL-1. TNF- $\alpha$  is the crucial mediator of systemic complications, it upregulates adhesive molecules and induces excessive nitric oxide formation and superoxide free radicals, damaging the pancreas substance and other organs. Furthermore, it causes increased vascular permeability inducing microcirculatory ischemia. Calcium ion antagonist inhibits the release of TNF- $\alpha$ , improves the ischemia and increases the vascular perfusion, and it also inhibits the acinar cells to produce protease, ameliorating the inflammation and tissue damage. In our experience, Dan Shen is also an important therapeutic agent in the management of severe acute pancreatitis.

By and large, the above seven constituents of the herbal mixture have an overall effect on interruption of the cascade in severe acute pancreatitis. The herbal mixture restores the gut

motility; inhibits release of cytokines and inflammatory mediators with subsequent attenuation of neutrophilic infiltration; improves pancreatic ischemia; prevents the dislocation of intestinal bacteria and endotoxin; and lowers blood lipoids, decreases lipoperoxidation and reduces damages of vascular endothelium and acinar cell membrane. Together with octreotide (or somatostatin) and Dan Shen, these would provide a synergistic as well as a complementary effect. During the treatment, the patients usually run a smooth course without fluctuation and recover uneventfully, hence, their combined use is of practical value and worth recommendation of wide use in clinical practice.

### REFERENCES

- 1 Wu XN. Management of severe acute pancreatitis. *WJG*, 1998;4: 90-91
- 2 Shiratori K, Watanabe SI, Takeuchi T. Somatostatin analogues SMS 201-995 in hibits pancreatic exocrine secretion and release of secretin and cholecystokinin in rats. *Pancreas*, 1991;6:23-30
- 3 Büchler MW, Binder M, Friess H. Role of somatostatin and its analogues in the treatment of acute and chronic pancreatitis. *Gut*, 1994;3(Suppl):S15-S19
- 4 Zhang QH, Cai D, Wu SC. Changes of inflammatory mediators in acute necrotizing pancreatitis rats and the effect of somatostatin. *Natl Med J China*, 1997;77:355-358
- 5 Carlsson PO, Jansson L. The long-acting somatostatin analogue octreotide decreases pancreatic islet blood flow in rats. *Pancreas*, 1994;9:361-364
- 6 Hoffmann TF, Uhl E, Messmer K. Protective effect of the somatostatin analogue octreotide in ischemic/reperfusion induced acute pancreatitis rats. *Pancreas*, 1996;12:286-293
- 7 Van Ooljen R, Tinga CT, Kat WJ. Effect of long-acting somatostatin analog (SMS 201-995) on eicosanoid synthesis and survival in rats with necrotizing pancreatitis. *Dig Dis Sci*, 1992;37: 1434-1440
- 8 Li YK, Jiang MY (eds). Pharmacology of Chinese herbal medicine. Traditional Chinese Medicine Publisher, 1992
- 9 Xu JY, Yu DJ, Jiang SH. Experimental study on the treatment of acute hemorrhagic necrotizing pancreatitis with target liposome of emodin. Shanghai International Conference of Gastroenterology, Nov. 28-30, 1996, Shanghai
- 10 Zhao Q, Quai NC, Li QK, Wu SZ. Clinical and experimental studies on the effect of Dachengqi decoction on acute phase protein levels in multiple organ:dysfunction syndrome. *Chin J Integrated Tradit Western Med*, 1998;18:453-456
- 11 Kimura K, Shimosagawa T, Sasano H. Endogenous glucocorticoids decrease the acinar cell sensitivity to apoptosis during cerulein pancreatitis in rats. *Gastroenterology*, 1998;114:372-381
- 12 Zhen SS, Wei QJ, Wu HG. Study on the effects of Dan Shan and Anisodamine hydrochloride injection on early pulmonary damage in dogs with acute hemorrhagic necrotizing pancreatitis. *Chin J Integrated Western Med*, 1989;9:158-360
- 13 Hughes CB, El-Din MAB, Koto M. Calcium channel blockade inhibits release of TNF- $\alpha$  and improves survival in a rat model of acute pancreatitis. *Pancreas*, 1996;13:22-28

**Review**

# Diagnostic approach to patients with cholestatic jaundice

N Assy, G Jacob, G Spira and Y Edoute

**Subject headings** bile ducts, intrahepatic; biopsy; cholangiography; cholestasis; diagnosis, differential; jaundice; tomography, X-ray computed; ultrasonography

Conjugated hyperbilirubinemia due to any form of hepatobiliary disease is essentially the result of impairment in bile formation and/or bile flow, a condition known as cholestasis<sup>[1,2]</sup>. Cholestatic jaundice is often accompanied by a broad spectrum of laboratory, clinical, and histological abnormalities. Laboratory abnormalities include increased serum levels of alkaline phosphatase and gamma-glutamyltransferase (GGT), and variable elevation of bilirubin, serum copper, ceruloplasmin, cholesterol, lipoprotein X, and serum bile acids, as well as of prothrombin time, which is corrected by vitamin K supplementation. There is minimal or no elevation of aminotransferases. Clinically, pruritus, fatigue, xanthomas, back pain from osteoporosis, pale stools, or even steatorrhea may be present, with evidence of fat-soluble vitamin deficiency. Histologically, conjugated hyperbilirubinemia is characterized by bile plugs (bilirubinostasis), feathery degeneration of hepatocytes (cholestasis), small-bile-duct destruction, pericholangitis, portal edema, bile lakes and infarcts (typically with extrahepatic obstruction), and finally, biliary cirrhosis<sup>[1-3]</sup>.

## MECHANISM OF CHOLESTASIS

Bile formation originates in hepatocytes with the uptake and production of organic anions, bilirubin, and bile salts through diverse cellular transporters that may be either sodium-dependent or independent<sup>[4]</sup>. Bile salts taken up at the sinusoidal surface of the hepatocytes are generally conjugated to increase their water solubility and subsequently

are excreted into the biliary tree at the apical (canalicular) surface. Secretion is achieved via the combined process of Na<sup>+</sup> coupled, carrier-mediated, or vesicular-transport systems<sup>[4]</sup>. Multiple factors contribute to the impairment of bile flow: Endotoxins are potent stimuli for activating cytokine production from macrophages<sup>[5,6]</sup> and have acute cholestatic effects on hepatic bile production<sup>[7]</sup>. Endotoxins and several proinflammatory cytokines [tumor necrosis factor (TNF)alpha, interleukin (IL)-1, and IL-6] down-regulate hepatic transport mechanisms that determine bile acid-dependent bile flow, affecting both bile acid uptake and canalicular secretion<sup>[8,9]</sup>. These proinflammatory cytokines also promote the expression of MHC class II molecules on target cells, thereby enhancing target antigen presentation<sup>[10]</sup>. Proinflammatory cytokines activate neutrophils and T and B cells, increase the expression of intercellular adhesion molecules (ICAMs), and may promote tissue damage by direct action. It is proposed that these portal tract inflammatory events can contribute to the down-regulation of hepatocellular bile salt transport, and hence aggravate cholestasis. Unfortunately, there are few cases of cholestatic jaundice in which the specific cellular defect has been identified. For most cholestatic process, multiple defects may act in concert to produce disease.

## EVALUATION OF THE PATIENT WITH CHOLESTATIC JAUNDICE

The first question to be resolved is whether the cholestasis results from intrahepatic or extrahepatic disease process, bearing in mind that several intrahepatic causes of cholestatic jaundice can mimic extrahepatic obstruction to varying degree<sup>[2,11]</sup>. Comprehensive clinical evaluation comprising the history, physical examination, and basic laboratory tests and the additional information provided by ultrasonography (US) or computed tomography (CT) are highly successful in making this important distinction (Figure 1). Clinically important clues to extrahepatic obstructions include abdominal pain, a palpable gallbladder or upper abdominal mass, evidence of cholangitis, and a history of previous biliary surgery. Clinical clues to intrahepatic

Liver Disease Unit and Department of Internal Medicine C, Rambam Medical Center, Haifa, and Department of Anatomy, the Bruce Rappaport Faculty of Medicine, Technion-Israel Institute of Technology, Haifa, Israel

**Correspondence to:** Dr. Nimer Assy, P.O.Box 428, 25170 Fassouta, Upper Galilee, Israel

Tel. +972 • 4 • 987 • 0080, Fax. +972 • 4 • 987 • 0080

Email.drnimer@netvision.net.il

**Received** 1999-04-08

cholestasis include pruritus, as in primary biliary cirrhosis (PBC) and primary sclerosing cholangitis (PSC) patients<sup>[12]</sup>. Pruritus may be prominent in alcoholic hepatitis and has been reported in about 10% of patients with acute viral hepatitis<sup>[13]</sup>.

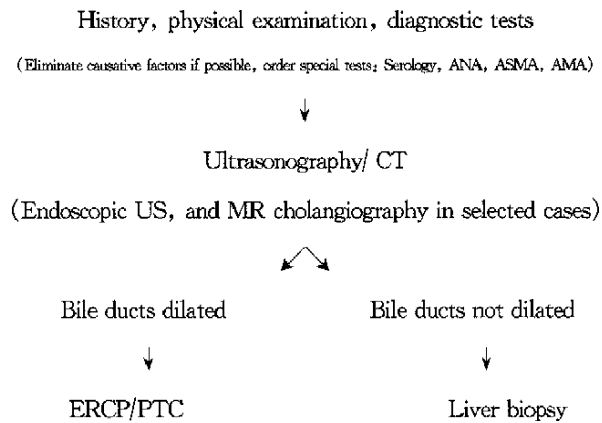


**Figure 1** Schematic of work-up of cholestatic jaundice. AFP, alpha-fetoprotein; AMA, antimitochondrial antibodies; ANA, antinuclear antibody; ASMA, anti-smooth muscle antibody; CT, computed tomography; ERCP, endoscopic retrograde cholangiography; MR, magnetic resonance; PTC, percutaneous transhepatic cholangiography; US, ultrasonography.

The patient should be asked about risk factors, including alcohol intake, medications, sexual contact, drug abuse, needle punctures, and travel history. The family history is of value in benign recurrent intrahepatic cholestasis (BRIC). Details regarding the onset of jaundice and its duration, whether intermittent or progressive, as well as its associated symptoms like darkening of the urine, acholic stools, arthralgia, rash, weight loss, fever, chills, and pain in the right upper quadrant should be obtained<sup>[3]</sup>. Physical examination should involve careful observation of stigmata of chronic liver disease, xanthelasma, clubbing, and lymphadenopathy. Hepatomegaly is usual in alcoholic liver disease, primary or secondary hepatic neoplasm, infiltrative disease, and primary biliary cirrhosis (PBC)<sup>[14,15]</sup>. Marked splenomegaly suggests cirrhosis with portal hypertension or lymphoproliferative disease<sup>[16,17]</sup>.

Laboratory work-up for cholestatic jaundice should include complete blood count with differential, urea, creatinine, electrolytes, and a liver panel including alkaline phosphatase, GGT, aminotransferases, albumin, bilirubin, and prothrombin time. Immunological markers such as AMA, ANA, ASMA, ANCA, and immunoglobulins and serological markers for viral hepatitis are

helpful. Serum alpha-fetoprotein, carcinoembryonic antigen, and CA19.9 may be increased in patients with malignancies<sup>[18]</sup>.

Clinical evaluation is quite sensitive, but has a positive predictive value of only about 75%; that is, about 25% of patients with suspected obstruction actually have hepatocellular disease<sup>[2]</sup>. The rare case of obstruction that is missed in the initial clinical evaluation will probably become apparent on follow-up evaluation, and the delay in establishing the correct diagnosis is unlikely to harm the patient. If, on the other hand, obstruction is suspected, then a more aggressive work-up is appropriate.

US and CT have comparable sensitivity (85%-96%) in detecting dilatation of the intrahepatic and extrahepatic biliary tree in patients with proven obstruction<sup>[3]</sup>. US is widely recommended as the first-line imaging procedure in the evaluation of cholestatic jaundice. Although gallbladder stones are readily detected by US, common bile duct stones may be missed in 60% of patients because of the interference caused by intestinal gas. Obesity may also lead to an unsatisfactory study. Moreover, with the exception of mass lesion in the head of the pancreas, US usually does not identify the type of obstruction.

CT is more likely to yield information regarding the level of the obstruction, localizing this in 90% of patients<sup>[3,19]</sup>. CT is also a reasonable first choice in patients with lymphoma, in whom it may provide information regarding retroperitoneal lymph node involvement<sup>[20]</sup>. Although a negative US or CT may represent a logical stopping point in the diagnostic work-up of a patient in whom obstruction is not strongly suspected on clinical grounds, a negative study should not dissuade the clinician from further evaluation of a patient in whom obstruction is considered highly likely. In patients in whom the clinical suspicion of biliary obstruction is supported by CT or US, direct visualization of the biliary tree with percutaneous transhepatic cholangiography (PTC) or endoscopic retrograde cholangiography (ERCP) is appropriate and necessary. PTC and ERCP have in common 99% sensitivity and specificity for the diagnosis of biliary obstruction, and both are capable of demonstrating the site and the nature of the obstruction in more than 90% of patients<sup>[21]</sup>. Both also provide therapeutic interventions including removal of stones, dilatation of strictures, and the placement of stents across obstructing lesions, as well as the placement of biliary drainage catheters<sup>[22]</sup>.

ERCP is the procedure of choice in suspected ampullary or duodenal lesions in pancreatic

carcinoma and when gallstone obstruction is suspected, in which case sphincterectomy and stone extraction can be implemented. Palliative stenting of neoplastic obstruction and temporary stenting of certain types of traumatic lesions of the common bile duct are frequently accomplished with ERCP<sup>[22]</sup>. ERCP is also a logical first procedure in patients with suspected PSC and in patients who have undergone cholecystectomy in whom jaundice is suspected on the basis of choledocholithiasis, since US is often unhelpful in this setting, as the stone is likely to be missed and ductal dilatation may be absent<sup>[23]</sup>.

PTC is often preferred when an obstructing lesion high in the biliary tree is anticipated, as it will permit visualization of the proximal extent of the lesion and enable immediate biliary drainage of obstructed intrahepatic ducts. PTC is also preferred in patients with previous gastrointestinal surgery like Billroth II gastrectomy<sup>[24]</sup>. PTC is usually contraindicated in patients with marked ascites and coagulopathy. In some instances, both PTC and ERCP may be used together in a combined therapeutic approach from above and below to maneuver guidewires and stents across a difficult obstruction. Sometimes hepatobiliary scintigraphy, which is of established value in the diagnosis of acute cholecystitis, may help in evaluating biliary leaks and congenital malformations<sup>[25]</sup>.

Recently, endoscopic CT and magnetic resonance cholangiography have been found to be very helpful in the diagnosis of biliary obstruction, especially in the setting of liver transplantation<sup>[26,27]</sup>. A negative study obtained by ERCP or PTC represents a reasonable endpoint to the work-up of obstruction in the jaundiced patient. Liver biopsy may be appropriate at this time point. Minor complications of a cutting needle biopsy, such as prolonged right upper quadrant pain, occur in up to 6% of cases<sup>[28]</sup>. Major complications such as clinically significant intra-abdominal bleeding are uncommon, and mortality (almost always from hemorrhage) is approximately 0.01%<sup>[29,30]</sup>. Cholestasis per se does not appear to increase the risk of a major complication. Percutaneous liver biopsy is contraindicated in patients with a significant coagulopathy or substantial ascites; in these instances, performance of a transjugular liver biopsy<sup>[31]</sup> or not performing a biopsy at all are alternatives. Weighing against these negative considerations are the potential benefits of obtaining histological information.

Liver biopsy may be of great value in differentiating hepatocellular cholestasis from obstructive cholestasis<sup>[32]</sup>. Unfortunately,

differentiating drug-induced cholestatic hepatitis from other causes cannot be performed histologically. A chief question in a patient with cholestatic jaundice is whether there is significant underlying chronic liver disease<sup>[33]</sup> or an infiltrative process, particularly granulomatous disease, lymphoma, or metastatic carcinoma<sup>[34]</sup>. Portal tract neutrophilic infiltrates seen in liver biopsy are a common accompaniment of biliary obstruction, ascending cholangitis, outright sepsis, cholangiolytic drug reactions, and hyperalimentation<sup>[35]</sup>. Finally, biopsy of the liver is particularly helpful in differentiating the cholestatic picture of alcoholic hepatitis from that of cholangitis<sup>[36]</sup>.

### DIFFERENTIAL DIAGNOSIS

Cholestatic liver disease can be broadly categorized as extra- or intrahepatic. The extrahepatic component is best approached anatomically. The intrahepatic component comprises intrinsic disease, infiltrative disease, systemic disease, and space-occupying lesions. Prevalent clinical abnormalities (Tables 1, 2) will be detailed in subsequent sections.

### EXTRAHEPATIC CAUSES OF CHOLESTATIC JAUNDICE

Among the extrahepatic causes of chronic cholestasis, secondary sclerosing cholangitis due to choledocholithiasis or biliary surgery is probably the most common. This is usually related to a single stricture of the common hepatic duct or common bile duct. Other causes of extrahepatic cholestasis are listed in Table 1.

**Table 1 Differential diagnosis of cholestasis and hyperbilirubinemia (cholestatic jaundice)**

CBD dilated: Best approach is anatomically
Ampulla of Vater
Stones, carcinoma of pancreas, chronic pancreatitis, ampullary neoplasm, diverticulum, pancreatic cyst, abscess of pancreas, sphincter of Oddi dysfunction
Common bile duct
Benign traumatic stricture, stones, choledochal cyst, cholangiocarcinoma, parasites, hemobilia, extrahepatic atresia
Gallbladder
Carcinoma of gallbladder
Portal nodes
Cholangiocarcinoma, lymphoma, metastatic carcinoma, cavernous portal vein

### CHOLEDOCHOLITHIASIS

Although gallstones produce jaundice by impaction in the common bile duct, acute cholecystitis is associated with mild jaundice in up to 20% of

patients. This is attributed to edema of the common duct (Mirizzi syndrome) or to direct involvement of the porta hepatis by inflammation<sup>[37]</sup>. Common duct stones retained after cholecystectomy may produce jaundice in the immediate postoperative period or even several years after cholecystectomy. Acute gallstone obstruction is often associated with pain from biliary colic or from acute pancreatitis resulting from ampullary obstruction. Sudden impaction of a stone in the common duct may be associated with a rapid rise in aminotransferases 20-50 above normal, followed by an equally rapid decline within 72 hours<sup>[38]</sup>. Cholangitis is relatively common in patients with choledocholithiasis and manifests as fever with chills, abdominal pain, and jaundice, a syndrome known as Charcot's triad, although jaundice may be absent in one third of patients with cholangitis<sup>[39]</sup>.

#### **BENIGN STRICTURES OF THE BILE DUCTS**

Benign biliary stricture in adults following previous surgery and biliary atresia in the pediatric population are the two most common type of strictures<sup>[18]</sup>. PSC may produce multiple or diffuse strictures that are not associated with proximal ductal dilatation<sup>[40]</sup>. In patients with chronic alcoholic pancreatitis, a long stricture may develop in the intrapancreatic portion of the common duct, leading initially to cholestasis and eventually to secondary biliary cirrhosis<sup>[41]</sup>. Ampullary stenosis may result in patients with acquired immunodeficiency syndrome (AIDS)<sup>[42]</sup> or from the trauma of passing a stone. Cholangitis is frequent in patients with benign biliary obstruction, in contrast to its relative infrequency in the framework of malignant obstruction<sup>[18]</sup>.

#### **NEOPLASTIC OBSTRUCTION**

Pancreatic carcinoma is the commonest neoplasm producing obstructive jaundice. Other tumors include cholangiocarcinoma, ampullary tumors, and carcinoma of the gallbladder<sup>[18,43]</sup>. Abdominal pain radiating into the back, along with loss of appetite and weight loss, may be present, but jaundice may also develop without pain (usually progressive and deep jaundice). Cholangiocarcinoma may obstruct the biliary system at any level, and the clinical presentation is similar to pancreatic cancer<sup>[44]</sup>. Cholangiocarcinoma of the extrahepatic bile ducts may be growing into the lumen. The sclerosing variant of cholangiocarcinoma, which frequently arises at the confluence of the right and left hepatic ducts (Klatskin's tumor), may be difficult to distinguish from PSC both radiologically and on biopsy. This tumor infiltrates early into the wall of

the bile duct, where it elicits a markedly sclerotic response<sup>[45]</sup>.

Tumors producing complete obstruction of the common bile duct may be accompanied by marked, palpable dilatation of the gallbladder (Courvoisier's law). Ampullary tumors may produce intermittent jaundice because of sloughing of the tumor and partial relief of the block. Metastatic cancer may obstruct the bile duct, as may lymphoma<sup>[46]</sup>. Hepatocellular carcinoma may uncommonly rupture into the biliary system and give rise to tumor emboli that lodge in and obstruct the common duct<sup>[47]</sup>. The extrahepatic ducts may be compressed by adjacent tumor, by peribiliary lymph node infiltrated by lymphoma, or by metastatic carcinoma of breast<sup>[46]</sup>. Direct infiltration of the ducts by lymphoma may also lead to obstruction<sup>[48]</sup>.

#### **UNCOMMON CAUSES OF OBSTRUCTIVE JAUNDICE**

Choledochal cyst may first manifest as obstructive jaundice after 17 years of age<sup>[49]</sup>. A duodenal diverticulum is a rare cause of biliary obstruction. Hemobilia, mostly a result of hepatic trauma, including invasive procedures or neoplasm, presents with the triad of biliary colic, jaundice and gastrointestinal bleeding<sup>[50]</sup>. Invasion of the common bile duct with *Ascaris* or with liver flukes of the *Fasciola*, *Clonorchis*, or *Opisthorchis* genera may produce cholangitis<sup>[51]</sup>. Secondary sclerosing cholangitis due to opportunistic infection of immunodeficient patients has become increasingly common since the advent of AIDS. *Cryptosporidium parvum*, cytomegalovirus (CMV), and *Microsporidia* are the organisms most frequently found<sup>[52]</sup>.

#### **INTRAHEPATIC CAUSES OF CHOLESTATIC JAUNDICE**

Intrahepatic cholestasis may arise from many sources and presents, therefore, a particular challenge when it develops in the seriously ill patient (Table 2). Many insults may cause local and systemic activation of the inflammatory cytokine system, and thus these proinflammatory events are potent inducers of intrahepatic cholestasis.

#### **INTRINSIC DISEASES**

Drug-induced cholestasis. Drugs may be responsible for 2%-5% of cases of jaundice in in-patients, and this percentage is probably substantially higher in the elderly<sup>[53]</sup>. The clinical presentation may mimic viral hepatitis or biliary tract disease. Serum sickness like features, including rash, arthralgia, and eosinophilia, are clues to a drug-induced etiology<sup>[53]</sup>. Chronic cholestasis tends to occur as a rare idiosyncratic reaction to certain commonly used drugs, including ampicillin-clavulanic acid,

chlorpromazine, cotrimoxazole, erythromycin, flucloxacillin, phenytoin, and tetracycline (Table 3)<sup>[54]</sup>. The histological features vary from case to case and over time. Generally, in the acute phase there is parenchymal bilirubinostasis, in the chronic phase bilirubinostasis commonly resolves, and features of cholestatic stasis persist and ductopenia develops<sup>[55]</sup>. A different pattern of drug-induced liver injury leading to chronic cholestasis is drug-induced sclerosing cholangitis, as seen following floxuridine treatment<sup>[56]</sup>. Sclerotic agents, injected into intrahepatic hydatid cysts, may escape into the biliary system and cause stricture formation that may ultimately lead to biliary cirrhosis<sup>[57]</sup>. In patients taking numerous medicines, the only practical approach is to eliminate the drug with the highest likelihood of cholestatic injury and monitor for improvement.

**Table 2 (continued): Differential diagnosis of cholestatic jaundice**

Normal CBD	
Extrahepatic	Stone too early, stone too late, cholangiocarcinoma, and primary sclerosing cholangitis
Intrahepatic	
	Intrinsic diseases
	Drugs, alcoholic hepatitis, viral hepatitis, AIDS, primary biliary cirrhosis, autoimmune cholangitis, primary sclerosing cholangitis, idiopathic adulthood ductopenia, Autoimmune hepatitis, decompensated liver cirrhosis
	Infiltrative diseases
	Granulomatous hepatitis (Tuberculosis, amyloidosis), sarcoidosis, Lymphoma, leukemia, fatty liver
	Systemic diseases
	Sepsis, total parenteral nutrition (TPN), benign recurrent intrahepatic cholestasis (BRIC), cholestasis of pregnancy, cystic fibrosis, disappearing intrahepatic ducts syndrome, allograft rejection, graft versus host disease (GVHD), sickle cell syndrome, mastocytosis, hypereosinophilic syndrome, Hyperthyroidism
	Space occupying lesions
	Blood-hematoma, peliosis; pus-bacterial, amebic; cyst-hydatid, polycystic Cancer-primary, secondary

**Table 3 Common drugs known to cause cholestatic jaundice**

Antimicrobial agents	Augmentin (amoxicillin-clavulanic acid), cloxacillin, erythromycin, ethambutol, dapsone, fluconazole, nitrofurantoin, griseofulvin, ketoconazole, terbinafine
Cardiovascular agents	Disopyramide beta-blockers, ACE inhibitors, propafenone, ticlopidine, warfarin, methyl dopa
Endocrine agents	Sulfonyleureas, clofibrate, estrogens, tamoxifen, androgens, niacin, oral contraceptives
Gastrointestinal agents	H2 blockers (e.g., ranitidine), penicillamine
Immunosuppressive agents	Azathioprine, cyclosporine, gold salts, NSAIDs (e.g. diclofenac, nimesulide, piroxicam)
Psychopharmacologic agents	Tricyclic antidepressants, benzodiazepines, phenothiazines, phenytoin, halothane

ACE: angiotensin-converting enzyme; NSAIDs: non-steroidal anti-inflammatory drugs.

**Alcoholic hepatitis.** Alcoholic hepatitis with severe cholestasis must always be considered. Marked hepatomegaly with hepatic tenderness and evidence of hepatocellular failure (aminotransferases <500U/L), along with a compatible history of alcohol intake and fever, suggests the diagnosis. Alkaline phosphatase can vary from normal to values in the thousands U/L. Bilirubin levels range from normal to 340 µmol/L • 510 µmol/L<sup>[58]</sup>.

**Viral hepatitis.** Infrequently, a severe cholestatic syndrome may follow the acute phase of viral hepatitis; this is most commonly seen with hepatitis A<sup>[59]</sup>, Hepatitis C<sup>[60]</sup>, and hepatitis E<sup>[61]</sup>. Despite the fact that jaundice may be profound for up to 6 months, complete recovery is the rule. Recently, we described a case of severe cholestatic jaundice in the elderly due to Epstein-Barr virus infection, which led to a diagnostic delay since the clinical presentation mimicked biliary obstruction<sup>[62]</sup>.

**AIDS.** In AIDS-related cholangiopathy, *Cryptosporidium* is the most frequent cause, but *Microsporidia*, CMV, *Mycobacterium avium-complex*, and *Cyclospora* have also been reported. Papillary stenosis may be present in patients with CD4 lymphocyte counts of <100/mm<sup>[3]</sup> and alkaline phosphatase >500IU/L. Jaundice is an unusual manifestation of AIDS-related cholangiopathy. If present, it suggests other disorders, including drug or alcohol abuse or neoplasm<sup>[63]</sup>.

**Primary biliary cirrhosis.** PBC could account for cholestatic jaundice. Classic PBC is described as a chronic non-suppurative cholangitis associated with AMA positivity in 95% of cases (anti-M2). Thirty percent will have positive ANA<sup>[64]</sup>. Histologically, bile duct injury along with portal inflammation are the usual findings, which are most often associated with elevation in alkaline phosphatase, IgM, and cholesterol. A female predominance is characteristic. Patients may, most commonly, be asymptomatic at presentation or may describe fatigue, pruritus, or right upper quadrant pain. Less than 20% of patients will have jaundice at time of presentation, and less than 5% will exhibit complications of portal hypertension<sup>[64]</sup>. The majority of patients will have associated autoimmune disorders (Sjögren's syndrome, scleroderma, and arthritis). Ursodeoxycholic acid (UDCA) is the only drug shown to prolong survival and to improve biochemical abnormalities. However, there is no evidence that it improves liver histology<sup>[65]</sup>. Presentation of HLA-II antigens as well as the expression of ICAM-1 and LFA3 induced by proinflammatory cytokines like TNF-alpha and interferon-gamma appear to

contribute to the biliary cell lysis observed in PBC<sup>[66]</sup>.

*Autoimmune cholangitis.* AIC is a recent entity in which liver biopsy findings are indistinguishable from classic PBC, but AMA positivity is lacking. Clinical and biochemical parameters are similar to PBC, except that in AIC other autoantibodies such as ANA and ASMA are often found in varying titers. The IgM titers are typically lower as well. These patients are treated as if they have PBC<sup>[67]</sup>.

*Primary sclerosing cholangitis.* PSC patients are more likely to be young men. PSC is associated with inflammatory bowel disease in 40% of cases<sup>[68]</sup>. Current information suggests immune-mediated damage of the biliary epithelium, although a precise mechanism has not been defined. Patients typically present with cholestasis, although occasionally jaundice and less commonly portal hypertension are present. Serum ANCA is positive in up to 80% of patients<sup>[69]</sup>. Both intra and extrahepatic bile ducts are involved, although a small percentage of patients have their disease confined to the hilar extrahepatic duct. Liver histology is not particularly useful in making the diagnosis, but does aid in the diagnosis of small-duct PSC (pericholangitis). Recurrent bacterial cholangitis as well as the development of cholangiocarcinoma and (in 15%-30% of cases) carcinoma of the colon constitute the morbid complications<sup>[70]</sup>. UDCA has no benefit in these patients regarding survival and quality of life. Whether other therapies such as FK-506 and colchicine offer significant benefit has not been established<sup>[71]</sup>.

*Idiopathic adulthood ductopenia.* This entity is rare and is defined by the presence of ductopenia (decrease of bile ducts in >50% of the portal triads) and cholestasis in the absence of known cholestatic liver disease. It is a diagnosis of exclusion<sup>[72]</sup>. In addition to ductopenia, the biopsy may show lymphocytic cholangitis and features of chronic cholestasis. In some patients the process progresses to biliary cirrhosis. A recent report suggests that UDCA may result in biochemical improvement<sup>[72]</sup>.

*Autoimmune hepatitis.* AIH can present as a primary cholestatic disorder<sup>[73]</sup>. By the criteria proposed by the International Autoimmune Hepatitis Group, a score can be calculated that defines the probability of a diagnosis of AIH. Patients are usually females (70% of cases) ANA and ASMA are present in the serum of the majority of patients. Furthermore hypergammaglobulinemia is present in 80% of cases. Associated autoimmune disorders include arthritis, rash, thyroiditis, Sjögren's syndrome, and ulcerative colitis<sup>[74]</sup>.

*Decompensated chronic liver disease.* Jaundice

may occur during the course of chronic hepatitis or cirrhosis. In cirrhosis, jaundice often is accompanied by other evidence of severe hepatocellular dysfunction and is a prognostically grave sign. Cirrhosis induced by extrahepatic obstruction is associated with increased levels of circulating endotoxins<sup>[75]</sup>, and elevated levels of proinflammatory cytokines can be documented in patients with cirrhosis of biliary or viral origin<sup>[76]</sup>.

## INFILTRATIVE DISEASES

*Granulomatous hepatitis.* GH is a common cause of cholestatic liver disease. Most often the liver manifestations are secondary to a more disseminated process, but isolated GH has been described<sup>[77]</sup>. GH is a well-described entity associated with a long list of causes, including sarcoidosis, infection (tubercular and fungal, especially histoplasmosis), hypersensitivity reaction, foreign-body reaction, malignant conditions, inflammatory bowel disease, drug reaction, and as a manifestation of other chronic liver disease<sup>[77]</sup>. In one series, approximately 20% of cases of patients with granulomas were attributed to associated liver conditions. On the other hand, idiopathic GH accounts for 5%-36% of cases in which hepatic granulomas are found<sup>[78]</sup>. Pathologically, hepatic granulomas are usually multiple nodular infiltrates consisting of aggregates of epithelioid cells or macrophages surrounded by a rim of mononuclear cells. Multinucleated giant cells are sometimes present. The normal architecture of the liver is usually not disturbed. In some cases, granuloma may be confined to the liver with no evidence of extrahepatic granulomatosis. Clinically, patients are often asymptomatic, and granulomas are found as part of a work-up for abnormal liver function tests or in the evaluation of fever of unknown origin (FUO). In studies of FUO, GH accounts for up to 13% of cases<sup>[79]</sup>. In GH, nonspecific symptoms are the rule, usually including malaise, anorexia, and fever. Manifestations of profound cholestasis or hepatic failure are rare<sup>[77]</sup>. In such cases, routine bacterial and fungal blood culture as well as special culture and stains of involved tissue would be required. GH tends to follow a benign course, with spontaneous recovery in most cases.

*Sarcoidosis.* Sarcoidosis is a systemic disease characterized by non-caseating granuloma of multiple organs. Seventy percent of patients have hepatic granuloma. Localization of portal granuloma may result in cholestasis with destruction of interlobular bile ducts<sup>[80]</sup>. A non-caseating granuloma indicates a combined role of activated CD4 T cells and macrophages. Elevated alkaline

phosphatase is the most characteristic abnormality found on liver testing and may be reduced by treatment with corticosteroids used to treat other manifestations of the disease. Concomitant intrathoracic disease, pulmonary symptoms, and significant anemia/leukopenia make this diagnosis very likely<sup>[81]</sup>.

**Lymphoma.** Between 3% and 10% of patients with lymphoma develop jaundice during the course of their disease and its treatment<sup>[82]</sup>. The causes of jaundice include hepatic infiltration, portal tract destruction, obstruction of the extrahepatic biliary tree, and jaundice associated with chemotherapy<sup>[82]</sup>. Histiocytic lymphoma may produce a rapidly progressive syndrome characterized by fever, hepatosplenomegaly, deep jaundice, lymphadenopathy, and pancytopenia. A rare syndrome of lymphoma<sup>a2</sup> associated idiopathic cholestasis has been reported most commonly with Hodgkin's disease, but may also occur with non-Hodgkin's lymphoma<sup>[84]</sup>.

**Fatty liver.** Fatty liver, or non-alcoholic steatohepatitis, most commonly occurs in middle-aged women with obesity, diabetes, and hyperlipidemia and a variety of other medical problems. Cholestasis can be seen in about 5% of patients with fatty liver<sup>[85]</sup>.

## SYSTEMIC DISEASES

**Bacterial infection (sepsis).** Mild hyperbilirubinemia develops in 1%-6% of patients with bacterial infections. The bilirubin is usually <170  $\mu\text{mol/L}$ . Serum alkaline phosphatase levels range from 1.5 to 3-fold above normal, whereas serum aminotransferases usually show less than a 2-fold increase<sup>[86]</sup>. The organisms most commonly associated with infections producing cholestatic jaundice are the gram-negative bacteria. Gram-positive infection from *Staphylococcus aureus*, in particular toxic shock syndrome and streptococcal pneumonia, may also be associated with jaundice<sup>[86]</sup>. The pathogenesis of cholestasis in sepsis is unclear, but direct hepatotoxicity from gram-negative bacterial endotoxins, gram-positive bacterial lipoteichoic acid, hepatic hypoxia, destruction of transfused red cells, and hematomas may all play a role. Endotoxins and inflammation-induced cytokines such as TNF are potent cholestatic agents<sup>[87-90]</sup>. Bile may also precipitate within larger intrahepatic bile ducts in conditions in which sepsis is playing a role, producing massive ductular dilatation with retained bile at the interface of the hepatic parenchyma and portal tracts, so-called "cholangitis lenta"<sup>[91]</sup>. Other uncommon infections may produce cholestatic jaundice include

leptospira, clostridium, and borrelia.

**Total parental nutrition.** TPN-associated cholestatic jaundice in adults usually follows infusions containing in excess of 60% of calories as lipids for a period longer than 3-4 weeks. Gallbladder stasis is almost universal in patients on TPN, with a marked increase in the incidence of gallstones<sup>[92]</sup>. If the TPN cannot be discontinued, it should be cycled around 10 hours per day. Excess caloric infusion can be avoided by keeping glucose <6 g/kg per day and lipid <2 g/kg per day. Recent reports have demonstrated improvement in cholestatic parameters by administration of UDCA<sup>[93]</sup>. Patients receiving hyperalimentation are susceptible to developing cholestasis because of the diminished stimulus to bile flow associated with the absence of oral feeding and release of hormones that stimulate bile flow<sup>[94]</sup>, as well as the direct oxidant stress to the liver. Whether there are toxic effects of the hyperalimentation solutions has never been clearly established<sup>[95]</sup>. However, hyperalimentation fluids are hypertonic and may aggravate a cholestatic state by further desiccating bile through osmotic effects<sup>[95]</sup>.

**Benign recurrent intrahepatic cholestasis.** BRIC is characterized by recurrent episodes of jaundice with pruritus, biochemical signs of cholestasis, and histological hepatocanicular bilirubinostasis, with normal intra- and extrahepatic bile ducts and absence of inflammation and fibrosis, absence of factors known to produce intrahepatic cholestasis such as drugs or pregnancy, and symptom-free intervals<sup>[96]</sup>. Cholestatic episodes may last for many months. BRIC may occur in sporadic or familial form; the latter has recently been attributed to genetic abnormalities on chromosome 18<sup>[97]</sup>. As in Byler disease, GGT is normal in the presence of high alkaline phosphatase. The episodes eventually resolve without morphological sequelae.

**Cholestasis of pregnancy.** This entity occurs recurrently in the third trimester of pregnancy in susceptible individuals and resolves after parturition. It is characterized by biochemical cholestasis with pruritus, usually accompanied by jaundice. Contraceptive drugs are a risk factor. Histology of the liver is similar to BRIC. It is associated with increased risk of premature delivery or stillborn births<sup>[98]</sup>. UDCA has been used with success<sup>[99]</sup>.

**Cystic fibrosis.** In the liver, mutation and deletion in cystic fibrosis transmembrane conductance regulator impair biliary secretion and result in cholestasis in 15% of cystic fibrosis patients<sup>[100]</sup>. UDCA also may be useful in these cases<sup>[101]</sup>. Biliary cirrhosis occurs in approximately

5% of patients and affects more males than females<sup>[100]</sup>.

*Disappearing intrahepatic bile ducts.* Disappearance of intrahepatic bile ducts occurs in a variety of congenital and disease conditions (Table 4). The pathogenic mechanism responsible for bile duct destruction remains poorly defined. Moreover, it is likely that multiple mechanisms are operative in individual diseases. The primary mechanism includes direct or indirect cytotoxicity of biliary epithelial cells, ischemic injury and necrosis, and progressive obliterative peribiliary fibrosis<sup>[102]</sup>.

**Table 4 Causes and syndromes of ductopenia in the adult patient**

Syndromatic ductopenia (Alagille syndrome)
Non-syndromatic adult ductopenia
Ductal plate malformation (congenital hepatic fibrosis, biliary atresia)
Primary biliary cirrhosis, autoimmune cholangitis
Primary sclerosing cholangitis
Chronic rejection
Graft-versus-host disease
Sarcoidosis
Cystic fibrosis
Byler disease (progressive familial intrahepatic cholestasis)
Histiocytosis X and
Different drugs (amoxicillin-clavulanic acid, carbamazepine)
Duct destruction after regional chemotherapy (e.g. floxuridine)
Idiopathic adulthood ductopenia

*Allograft rejection.* Causes of cholestasis after liver transplantation are multifactorial, including postoperative dysfunction of the biliary tree (ductular or vascular), infection, recurrence of the primary disease, drugs, and rejection. In both acute and chronic rejection, small bile ducts are destroyed, resulting in cholestatic changes. Alkaline phosphatase, bilirubin, and GGT, along with aminotransferases, are elevated. Because of their lack of specificity, histological evaluation is needed to make the diagnosis<sup>[103]</sup>.

*Graft-versus-host disease.* GVHD is the major complication of allogeneic bone marrow transplantation. Donor T cells recognize foreign host antigens in an immunocompromised host, resulting in injury to skin, intestine, and liver. In liver, the small bile duct cells are the primary targets of injury. The diagnosis is based on the development of rash, diarrhea, and elevated alkaline phosphatase. Acute GVHD usually begins in the third week, whereas chronic GVHD develops at around the sixth month after transplant. The extreme hyperbilirubinemia seems out of proportion to the degree of bile duct or hepatocellular damage<sup>[104]</sup>. Although liver biopsy can be

performed, skin or rectal biopsy is preferred.

*Sickle cell anemia.* In patients with sickle cell anemia, jaundice may occur from a variety of factors, including viral hepatitis, choledocholithiasis, hepatic sickle cell crisis, and a syndrome of severe intrahepatic cholestasis. Hepatic sickle cell crisis is characterized by severe right upper quadrant pain, fever, leukocytosis, jaundice, tender hepatomegaly, and moderate elevation of alkaline phosphatase. Resolution of acute symptoms with hydration and analgesia may be followed by persistent cholestatic jaundice for several weeks<sup>[105]</sup>.

*Postoperative jaundice.* The prevalence of jaundice following major surgery has been estimated at 17% for bilirubin levels of 2 mg/dl-4 mg/dl, with 4% of patients developing more pronounced elevations. The etiology of cholestatic jaundice in the postoperative period may be discrete or multifactorial. Responsible factors include sepsis, drug- or anesthetic-induced hepatitis, and obstruction of the biliary tree resulting from pancreatitis, choledocholithiasis, or direct injury to the biliary tree<sup>[106]</sup>. The entity termed "benign postoperative cholestatic jaundice" occurs between 1 and 10 days following major surgery. The jaundice may be profound, with a 2 to 4-fold elevation of alkaline phosphatase levels and only mild increases in serum aminotransferases. Liver biopsy reveals cholestasis without inflammation. The condition is self-limited and requires differentiation from obstructive jaundice<sup>[106]</sup>.

*Sweet's syndrome.* This is an idiopathic condition, but approximately 20% of patients have an associated malignancy<sup>[107]</sup>. The disease is thought to be a hypersensitivity reaction, either as a parainflammatory (e.g., infections, autoimmune disorders, vaccination) or paraneoplastic event. The most frequently observed neoplasm is acute myelogenous leukemia; lymphomas, chronic leukemia, myelomas, myelodysplastic syndromes, and a variety of solid tumors also are represented. The onset of Sweet's syndrome is widely distributed around the time of development of malignancy, appearing most often within 2 months before or after the clinical diagnosis of overt malignancy. A definitive derangement in neutrophil function in Sweet's syndrome has not been identified. Rather, elevated levels of circulating granulocyte colony-stimulating factor and IL-6 or of local cytokines have been implicated<sup>[108-110]</sup>.

## OTHER INTRAHEPATIC CAUSES OF CHRONIC CHOLESTASIS

Nodular regenerative hyperplasia (NRH), bone marrow transplant (BMT), connective tissue diseases (CTD), Felty's syndrome, mastocytosis,

hypereosinophilic syndrome, hyperthyroidism, and space occupying lesions that can lead to chronic intrahepatic cholestasis are listed in Table 1. The pathology of these entities is not discussed further here.

## CONCLUSIONS

The causes of cholestatic jaundice can usually be identified if one keeps in mind the important steps of transport of bilirubin and secretion of bile flow through the intra and extrahepatic biliary tree.

Most causes of cholestatic jaundice are a result of diseases of the liver or biliary tract, including intrahepatic forms caused by drugs, alcohol, infection, and destruction of the interlobular ducts. In postoperative jaundice, multiple mechanisms, such as a combination of pigment load with hypoxic injury to the liver, can result in jaundice. It is easy to visualize how mechanical obstruction of the biliary tree will give rise to jaundice, as in a patient with carcinoma of the bile duct or PSC. There is no substitute for a good history, physical examination, and review of the standard chemistries. With the initial information, the correct diagnosis can be made 85% of the time. In the remaining cases, non-invasive scanning procedures will help in confirming suspicions, but the final diagnosis will usually be made only with direct forms of cholangiography and/or liver biopsy. Occasionally we encounter a case of cholestatic jaundice where we cannot readily establish the diagnosis. Tincture of time generally will lead to the appearance of further signs and symptoms that eventually will clarify the disease.

In every case, the responsibility rests on the physician to adopt a thoughtful approach to minimize risk, expense, and time involved in obtaining sufficient information for a definitive diagnosis and treatment.

## REFERENCES

- Stazi F, Fareello P, Stazi C. Intrahepatic cholestasis. *Clin Ter*, 1996; 147:575-583
- Scharschmidt BF, Goldberg HI, Schmid R. Current concepts in diagnosis. Approach to the patient with cholestatic jaundice. *N Engl J Med*, 1983;308:1515-1519
- Frank BB. Clinical evaluation of jaundice. A guideline of the Patient Care Committee of the American Gastroenterological Association. *JAMA*, 89;262:3031-3034
- Moseley RH. A molecular basis for jaundice in intrahepatic and extrahepatic cholestasis. *Hepatology*, 1997;6:1682-1684
- Crawford JM. Cellular and molecular biology of the inflamed liver. *Curr Opin Gastroenterol*, 1997;13:175-185
- Uhl B, Speth V, Wolf B, Jung G, Bessler WG, Hauschildt S. Rapid alterations in the plasma membrane structure of macrophages stimulated with bacterial lipopeptides. *Eur J Cell Biol*, 1992;58: 90-98
- Spitzer JA, Zhang P. Hepatic cellular interactions in endotoxaemia and sepsis. *Biochem Soc Trans*, 1995;23:993-998
- Roelofsen H, Schoemaker B, Bakker C, Ottenhoff R, Jansen PLM, Elferink RPJO. Impaired hepatocanalicular organic anion transport in endotoxemic rats. *Am J Physiol*, 1995;269:G427-G434
- Moseley RH, Wang W, Takeda H, Lown K, Shick L, Ananthanarayanan M, Suchy FJ. Effect of endotoxin on bile acid transport in rat liver: a potential model for sepsis-associated cholestasis. *Am J Physiol*, 1996;271: G137-G146
- Ayres RCS, Neuberger JM, Shaw J, Joplin R, Adams DH. Intercellular adhesion molecule-1 and MHC antigens on human intrahepatic bile duct cells: effect of pro-inflammatory cytokines. *Gut*, 1993;34:1245-1249
- Edoute Y, Lachter J, Furman E, Assy N. Severe cholestatic jaundice induced by EBV infection in the elderly. *J Gastroenterol Hepatol*, 1998;13:821-824
- McKnight JT, Jones JE. Jaundice. *Am Fam Physician*, 1992;45: 1139-1148
- Fisher DA, Wright TL. Pruritus as a symptom of hepatitis C. *J Am Acad Dermatol*, 1994;30:629-632
- Mainenti PP, Petrelli G, Lamanda R, Amalfi G, Castiglione F. Primary systemic amyloidosis with giant hepatomegaly and a swiftly progressive course. *J Clin Gastroenterol*, 1997; 24:173-175
- Chang HC, Nguyen B, Regan F. Hepatomegaly and multiple liver lesions. *Post grad Med J*, 1998;74:439-440
- Shah SH, Hayes PC, Allan PL, Nicoll J, Finlayson ND. Measurement of spleen size and its relation to hypersplenism and portal hemodynamics in portal hypertension due to hepatic cirrhosis. *Am J Gastroenterol*, 1996;91:2580-2583
- O'Reilly RA. Splenomegaly in 2505 patients at a large university medical center from 1913 to 1995. 1963 to 1995: 449 patients. *West J Med*, 1998;169:88-97
- Bass NM. An integrated approach to the diagnosis of jaundice. In: Neil Kaplowitz, eds. Liver and biliary disease. Baltimore: Williams & Wilkins, 1996:651-672
- Pasanen PA, Pikkarainen P, Alhava E, Partanen K, Janatuinen E. Evaluation of a computer-based diagnostic score system in the diagnosis of jaundice and cholestasis. *Scand J Gastroenterol*, 1993; 28:732-736
- Brice P. Staging of Hodgkin's disease. *Rev Prat*, 1998;48:1070-1074 (in French with English Abstract)
- Khan MA, Khan AA, Shafiqat F. Comparison of ultrasonography and cholangiography (ERCP/PTC) in the differential diagnosis of obstructive jaundice. *JPMA J Pak Med Assoc*, 1996; 46:188-190
- Liu CL, Lo CM, Lai EC, Fan ST. Endoscopic retrograde cholangiopancreatography and endoscopic endoprosthesis insertion in patients with Klatskin tumors. *Arch Surg*, 1998;133: 293-296
- de Ledinghen V, Lecesne R, Raymond JM, Gense V, Amouretti M, Drouillard J, Couzigou P, Silvain C. Diagnosis of choledocholithiasis. EUS or magnetic resonance cholangiography. A prospective controlled study. *Gastrointest Endosc*, 1999;49:26-31
- Dixit VK, Jain AK, Agrawal AK, Gupta JP. Obstructive jaundice—a diagnostic appraisal. *J Assoc Physicians India*, 1993;41:200-202
- Roca I, Ciofetta G. Hepatobiliary scintigraphy in current pediatric practice. *Q J Nucl Med*, 1998;42:113-118
- Mendler MH, Bouillet P, Sautereau D, Chaumerliac P, Cessot F, Le Sidaner A, Pillegand B. Value of MR cholangiography in the diagnosis of obstructive diseases of the biliary tree: a study of 58 cases. *Am J Gastroenterol*, 1998;93:2482-2490
- Meduri B, Aubert A, Chiche R, Fritsch J. Laparoscopic cholecystectomy and lithiasis of the common bile duct: prospective study on the importance of preoperative endoscopic ultrasonography and endoscopic retrograde cholangiography. *Gastroenterol Clin Biol*, 1998;22: 759-765
- Froehlich F, Lamy O, Fried M, Gonvers JJ. Practice and complications of liver biopsy: results of a nationwide survey in Switzerland. *Dig Dis Sci*, 1993;38:1480-1484
- Garcia-Tsao G, Boyer JL. Outpatient liver biopsy: how safe is it. *Ann Intern Med*, 1993;118:150-153
- Tobkes AI, Nord HJ. Liver biopsy: review of methodology and complications. *Dig Dis*, 1995;13:267-274
- Sawyer AM, McCormick PA, Tennyson GS, Chin J, Dick R, Scheuer PJ, Burroughs AK, McIntyre N. A comparison of transjugular and plugged-percutaneous liver biopsy in patients with impaired coagulation. *J Hepatol*, 1993;17:81-85
- Desmet VJ. Cholestasis: extrahepatic obstruction and secondary biliary cirrhosis. In: MacSween RNM, Anthony PP, Scheuer PJ, Burt AD, Portmann BC, eds. Pathology of the liver. *Edinburgh: Churchill Livingstone*, 1994;425-476
- Van Ness MM, Diehl AM. Is liver biopsy useful in the evaluation of patients with chronically elevated liver enzymes. *Ann Intern Med*, 1989;111:473-478

- 34 Jenkins D, Gilmore IT, Doel C, Gallivan S. Liver biopsy in the diagnosis of malignancy. *Q J Med*, 1995;88:819-825
- 35 Snover DC. Biopsy diagnosis of liver disease. *Baltimore: Williams & Wilkins*, 1992:28
- 36 Jensen K, Gluud C. The Mallory body: morphological, clinical and experimental studies (Part I of a literature survey). *Hepatology*, 1994;20:1061-1077
- 37 Mergener K, Enns R, Eubanks WS, Baillie J, Branch MS. Pseudo-Mirizzi syndrome in acute cholecystitis. *Am J Gastroenterol*, 1998;93:2605-2606
- 38 Seitz U, Bapaye A, Bohnacker S, Navarrete C, Maydeo A, Soehendra N. Advances in therapeutic endoscopic treatment of common bile duct stones. *World J Surg*, 1998;22:1133-1144
- 39 Csendes A, Diaz JC, Burdiles P, Maluenda F, Morales E. Risk factors and clas40 Teefey SA, Baron RL, Rohrmann CA, Shuman WP, Freeny PC. Sclerosing cholangitis: CT findings. *Radiology*, 1988;169:635-639
- 41 Smits ME, Rauws EA, van Gulik TM, Gouma DJ, Tytgat GN, Huibregtse K. Long-term results of endoscopic stenting and surgical drainage for biliary stricture due to chronic pancreatitis. *Br J Surg*, 1996;83:764-768
- 42 Cello JP. Acquired immunodeficiency syndrome cholangiopathy: spectrum of disease. *Am J Med*, 1989;86:539-546
- 43 Pasanen PA, Partanen KP, Pikkarainen PH, Alhava EM, Janatuinen EK, Pirinen A E. A comparison of ultrasound, computed tomography and endoscopic retrograde cholangiopancreatography in the differential diagnosis of benign and malignant jaundice and cholestasis. *Eur J Surg*, 1993;159:23-29
- 44 Iwatsuki S, Todo S, Marsh JW, Madariaga JR, Lee RG, Dvorchik I, Fung JJ, Starzl TE. Treatment of hilar cholangiocarcinoma (Klatskin tumors) with hepatic resection or transplantation. *J Am Coll Surg*, 1998;187:358-364
- 45 Wetter LA, Ring EJ, Pellegrini CA, Way LW. Differential diagnosis of sclerosing cholangiocarcinomas of the common hepatic duct (Klatskin tumors). *Am J Surg*, 1991;161:57-62
- 46 Fidiyas P, Carey RW, Grossbard ML. Non-Hodgkin's lymphoma presenting with biliary tract obstruction. A discussion of seven patients and a review of the literature. *Cancer*, 1995;75:1669-1677
- 47 Buckmaster MJ, Schwartz RW, Carnahan GE, Strodel WE. Hepatocellular carcinoma embolus to the common hepatic duct with no detectable primary hepatic tumor. *Am Surg*, 1994;60:699-702
- 48 Maes M, Depardieu C, Dargent JL, Hermans M, Verhaeghe JL, Delabie J, Pittaluga S, Troufleau P, Verhest A, De Wolf-Peeters C. Primary low-grade B-cell lymphoma of MALT-type occurring in the liver: a study of two cases. *J Hepatol*, 1997;27:922-927
- 49 Jesudason SR, Govil S, Mathai V, Kuruvilla R, Muthusami JC. Choledochal cysts in adults. *Ann R Coll Surg Engl*, 1997;79:410-413
- 50 Mosenkis BN, Brandt LJ. Bleeding causing biliary obstruction after endoscopic sphincterotomy. *Am J Gastroenterol*, 1997;92:708-709
- 51 Liu LX, Harinasuta KT. Liver and intestinal flukes. *Gastroenterol Clin North Am*, 1996;25:627-636
- 52 Forbes A, Blanshard C, Gazzard B. Natural history of AIDS related sclerosing cholangitis: a study of 20 cases. *Gut*, 1993;34:116-121
- 53 Farrell GC. Drug-induced hepatic injury. *J Gastroenterol Hepatol*, 1997;12:S242-S250
- 54 Erlinger S. Drug-induced cholestasis. *J Hepatol*, 1997;26(suppl 1):1-4
- 55 Feuer G, Di Fonzo CJ. Intrahepatic cholestasis: a review of biochemical-pathological mechanisms. *Drug Metabol Drug Interact*, 1992;10:1-161
- 56 Ludwig J, Kim CH, Wiesner RH, Krom RA. Floxuridine-induced sclerosing cholangitis: an ischemic cholangiopathy. *Hepatology*, 1989;9:215-218
- 57 Sherlock S. The syndrome of disappearing intrahepatic bile ducts. *Lancet*, 1987;2:493-496
- 58 Nissenbaum M, Chedid A, Mendenhall C, Gartside P. Prognostic significance of cholestatic alcoholic hepatitis. *Dig Dis Sci*, 1990;35:891-896
- 59 Schiff ER. Atypical clinical manifestations of hepatitis A. *Vaccine*, 1992;10(Suppl 1):S18-S20
- 60 Chia SC, Bergasa NV, Kleiner DE, Goodman Z, Hoofnagle JH, Di Bisceglie AM. Pruritus as a presenting symptom of chronic hepatitis C. *Dig Dis Sci*, 1998;43:2177-2183
- 61 Khuroo MS, Rustgi VK, Dawson GJ, Mushahwar IK, Yattoo GN, Kamili S, Khan BA. Spectrum of hepatitis E virus infection in India. *J Med Virol*, 1994;43:281-286
- 62 Edoute Y, Baruch Y, Lachter J, Furman E, Bassan L, Assy N. Severe cholestatic jaundice induced by Epstein Barr virus infection in the elderly. *J Gastroenterol Hepatol*, 1998;13:821-824
- 63 Lefkowitz JH. The liver in AIDS. *Semin Liver Dis*, 1997;17:335-344
- 64 Leung PS, Coppel RL, Ansari A, Munoz S, Gershwin ME. Antimitochondrial antibodies in primary biliary cirrhosis. *Semin Liver Dis*, 1997;17:61-69
- 65 Heathcote J. Treatment of primary biliary cirrhosis. *J Gastroenterol Hepatol*, 1996;11:605-609
- 66 Bloom S, Fleming K, Chapman R. Adhesion molecule expression in primary sclerosing cholangitis and primary biliary cirrhosis. *Gut*, 1995;36:604-609
- 67 Sherlock S. Ludwig Symposium on biliary disorders. Autoimmune cholangitis: a unique entity. *Mayo Clin Proc*, 1998;73:184-190
- 68 Ponsoen CI, Tytgat GN. Primary sclerosing cholangitis: a clinical review. *Am J Gastroenterol*, 1998;93:515-523
- 69 Bansi DS, Fleming KA, Chapman RW. Importance of antineutrophil cytoplasmic antibodies in primary sclerosing cholangitis and ulcerative colitis: prevalence, titre, and IgG subclass. *Gut*, 1996;38:384-389
- 70 Chapman RW. The colon and PSC: new liver, new danger? *Gut*, 1998;43:595-596
- 71 Stiehl A. Ursodeoxycholic acid therapy in treatment of primary sclerosing cholangitis. *Scand J Gastroenterol Suppl*, 1994;204:59-61
- 72 Ludwig J. Idiopathic adulthood ductopenia: an update. *Mayo Clin Proc*, 1998;73:285-291
- 73 Motoo Y, Sawabu N, Watanabe H, Okai T, Nakanuma Y. Prolonged intrahepatic cholestasis in acute-onset, severe autoimmune hepatitis. *J Gastroenterol*, 1997;32:410-413
- 74 Czaja A, Carpenter HA. Validation of scoring system for diagnosis of autoimmune hepatitis. *Dig Dis Sci*, 1996;41:305-314
- 75 Grinko I, Geerts A, Wisse E. Experimental biliary fibrosis correlates with increased numbers of fat-storing and Kupffer cells, and portal endotoxemia. *J Hepatol*, 1995;23:449-458
- 76 Shindo M, Mullin GE, Braun-Elwert L, Bergasa NV, Jones EA, James SP. Cytokine mRNA expression in the liver of patients with primary biliary cirrhosis (PBC) and chronic hepatitis B (CHB). *Clin Exp Immunol*, 1996;105:254-259
- 77 Sartin JS, Walker RC. Granulomatous hepatitis: a retrospective review of 88 cases at the Mayo Clinic. *Mayo Clin Proc*, 1991;66:914-918
- 78 McCluggage WG, Sloan JM. Hepatic granulomas in Northern Ireland: a thirteen year review. *Histopathology*, 1994;25:219-228
- 79 Zoutman DE, Ralph ED, Frei JV. Granulomatous hepatitis and fever of unknown origin. An 11-year experience of 23 cases with three years' follow-up. *J Clin Gastroenterol*, 1991;13:69-75
- 80 Moreno-Merlo F, Wanless IR, Shimamatsu K, Sherman M, Greig P, Chiasson D. The role of granulomatous phlebitis and thrombosis in the pathogenesis of cirrhosis and portal hypertension in sarcoidosis. *Hepatology*, 1997;26:554-560
- 81 Albu E, Saraiya RJ, Carvajal SJ, Sehonanda A, Balar N, Gerst PH. Sarcoidosis presenting as obstructive jaundice. *Am Surg*, 1995;61:516-517
- 82 Abe H, Kubota K, Makuuchi M. Obstructive jaundice secondary to Hodgkin's disease. *Am J Gastroenterol*, 1997;92:526-527
- 83 Young IF, Roberts Thomson IC, Sullivan JR. Histiocytic lymphoma presenting with extrahepatic biliary obstruction: a report of three cases. *Aust N Z J Surg*, 1981;51:181-183
- 84 Hubscher SG, Lumley MA, Elias E. Vanishing bile duct syndrome: a possible mechanism for intrahepatic cholestasis in Hodgkin's lymphoma. *Hepatology*, 1993;17:70-77
- 85 French SW, Nash J, Shitabata P, Kachi K, Hara C, Chedid A, Mendenhall CL. Pathology of alcoholic liver disease. VA Cooperative Study Group 119. *Semin Liver Dis*, 1993;13:154-169
- 86 Navasa M, Rimola A, Rodes J. Bacterial infections in liver disease. *Semin Liver Dis*, 1997;17:323-333
- 87 Green RM, Whiting JF, Rosenbluth AB, Beier D, Gollan JL. Interleukin-6 inhibits hepatocyte taurocholate uptake and sodium potassium adenosinetriphosphatase activity. *Am J Physiol*, 1994;267:G1094-G1100
- 88 Green RM, Crawford JM. Hepatocellular cholestasis: pathobiology and histological outcome. *Semin Liver Dis*, 1995;15:372-389
- 89 Moseley RH. Sepsis-associated cholestasis. *Gastroenterology*, 1997;112:302-306
- 90 Shiomi M, Wakabayashi Y, Sano T, Shinoda Y, Nimura Y,

- Ishimura Y, Suematsu M. Nitric oxide suppression reversibly attenuates mitochondrial dysfunction and cholestasis in endotoxemic rat liver. *Hepatology*, 1998;27:108-115
- 91 Lefkowitz JH. Bile ductular cholestasis. an ominous histopathologic sign related to sepsis and "cholangitis lenta". *Hum Pathol*, 1982;13:19-24
- 92 Klein S, Nealon WH. Hepatobiliary abnormalities associated with total parenteral nutrition. *Semin Liver Dis*, 1988;8:237-246
- 93 Spagnuolo MI, Iorio R, Vegnente A, Guarino A. Ursodeoxycholic acid for treatment of cholestasis in children on long-term total parenteral nutrition: a pilot study. *Gastroenterology*, 1996;111:716-719
- 94 Wiechmann DA, Heubi JH. Pediatric hepatobiliary disease. *Curr Opin Gastroenterol*, 1997;13:427-431
- 95 Bhatia J, Moslen MT, Haque AK, McCleery R, Rassin DK. Total parenteral nutrition associated alterations in hepatobiliary function and histology in rats: is light exposure a clue. *Pediatr Res*, 1993;33:487-492
- 96 Nakamuta M, Sakamoto S, Miyata Y, Sato M, Nawata H. Benign recurrent intrahepatic cholestasis: a long-term follow-up. *Hepatogastroenterology*, 1994;41:287-289
- 97 Bull LN, van Eijk MJ, Pawlikowska L, De Young JA, Juijn JA, Liao M, Klomp LW, Lomri N, Berger R, Scharschmidt BF, Knisely AS, Houwen RH, Freimer NB. A gene encoding a P-type ATP ase mutated in two forms of hereditary cholestasis. *Nat Genet*, 1998;18:219-224
- 98 Assy N, Minuk GY. Liver disease in pregnancy. *J Am Coll Surg*, 1996;183:643-653
- 99 Diaferia A, Nicastrì PL, Tartagni M, Loizzi P, Iacovizzi C, Di Leo A. Ursodeoxycholic acid therapy in pregnant women with cholestasis. *Int J Gynaecol Obstet*, 1996;52:133-140
- 100 Strazzabosco M. Transport systems in cholangiocytes: their role in bile formation and cholestasis. *Yale J Biol Med*, 1997;70:427-434
- 101 Lindblad A, Glaumann H, Strandvik B. A two-year prospective study of the effect of ursodeoxycholic acid on urinary bile acid excretion and liver morphology in cystic fibrosis associated liver disease. *Hepatology*, 1998;27:166-174
- 102 Woolf GM, Vierling JM. Disappearing intrahepatic bile ducts: the syndromes and their mechanisms. *Semin Liver Dis*, 1993;13:261-275
- 103 Mor E, Solomon H, Gibbs JF, Holman MJ, Goldstein RM, Husberg BS, Gonwa TA, Klintmalm GB. Acute cellular rejection following liver transplantation: clinical pathologic features and effect on outcome. *Semin Liver Dis*, 1992;12:28-40
- 104 Crawford JM. Graft-versus-host disease of the liver. In: Ferrara JLM, Deeg J, Burakoff S, eds. Graft-versus-host disease. *New York: Marcel Dekker*, 1996:315-336
- 105 Krauss JS, Freant LJ, Lee JR. Gastrointestinal pathology in sickle cell disease. *Ann Clin Lab Sci*, 1998;28:19-23
- 106 Becker SD, Lamont JT. Postoperative jaundice. *Semin Liver Dis*, 1988;8:183-190
- 107 Cohen PR, Talpaz M, Kurzrock R. Malignancy associated Sweet's syndrome: review of the world literature. *J Clin Oncol*, 1988;6:1887-1897
- 108 Reuss-Borst MA, Pawelec G, Saal JG, Horny HP, Muller CA, Waller HD. Sweet's syndrome associated with myelodysplasia: possible role of cytokines in the pathogenesis of the disease. *Br J Haematol*, 1993;84:356-358
- 109 Park JW, Mehrotra B, Barnett BO, Baron AD, Venook AP. The Sweet syndrome during therapy with granulocyte colon-stimulating factor. *Ann Intern Med*, 1992;116:996-998
- 110 Paydas S, Sahin B, Seyrek E, Soyul M, Gonlusen G, Acar A, Tuncer I. Sweet's syndrome associated with G-CSF. *Br J Haematol*, 1993;85:191-192

Edited by MA Jing-Yun

# Clarithromycin resistance in *Helicobacter pylori* and its clinical relevance

Xia<sup>1</sup> Harry Hua-Xiang, FAN Xue-Gong and Talley<sup>1</sup> Nicholas J.

**Subject headings** *Helicobacter pylori*; *Helicobacter* infections; clarithromycin resistance

## INTRODUCTION

The macrolide clarithromycin has emerged as the most important antibiotic in combined therapy for eradication of *H. pylori* infection<sup>[1,2]</sup>. However, concerns about increasing clarithromycin resistance in *H. pylori* and its impact on the efficacy of eradication therapy have been raised since its widespread acceptance in *H. pylori* therapy<sup>[3,4]</sup>. Here, we sought to review the geographic prevalence of clarithromycin resistance in *H. pylori* and its molecular mechanisms, and assess the clinical relevance of clarithromycin resistance.

## Geographic prevalence of clarithromycin resistant *H. pylori*

The worldwide prevalence of primary (pre-treatment) clarithromycin resistance to *H. pylori* ranges from 0.8% to 18% (Figure 1)<sup>[5-29]</sup>. The reported prevalence in China is between 4.8% and 7.5%, while the rate in Australia ranges from 6.1% to 7.8%<sup>[5,6,11,12]</sup>.

## Molecular mechanisms of clarithromycin resistance

Versalovic *et al* were the first to identify an A→G transition mutation within a conserved loop of 23S rRNA of *H. pylori*, and its association with clarithromycin-resistance<sup>[30]</sup>. The mutation occurs commonly at two gene positions cognate with positions 2058 and 2059 of *Escherichia coli*-23S rRNA, which were re-named 2143 and 2144, and now revised as 2142 and 2143, respectively<sup>[4,31]</sup>. Point mutations may occasionally occur at other positions, and can be a transition (A→G) or a transversion (A→C), but the transition is far more frequent<sup>[4,32-35]</sup>. Moreover, Versalovic *et al*<sup>[32]</sup> also observed that the A2142G mutation was associated with a high level of resistance (MIC>64 mg/L)

than the A2143G mutation<sup>[32]</sup>. These observations are supported by others studies<sup>[33,36]</sup>.

It has been reported that macrolide-resistance was not stable in some strains of *H. pylori in vitro*<sup>[17]</sup>. This phenomenon was also observed *in vivo*; i.e., strains developed resistance post-treatment and then reverted to being susceptible after a period of follow-up<sup>[17,30]</sup>. Versalovic *et al* cultured five genotypically identical isolates subsequently from one patient before and after treatment with clarithromycin alone<sup>[30]</sup>. They observed that the first two post-treatment isolates with a low-level clarithromycin resistance had an A2143G mutation, which was not present in the susceptible pretreatment isolate or in the last two post-treatment isolates with reverted susceptibility<sup>[30]</sup>. This suggests that the mutation may be unstable<sup>[35]</sup>. However, Hulten *et al* reported that clarithromycin resistance was stable after 50 subcultures *in vitro*<sup>[35]</sup>, which is consistent with other studies<sup>[37]</sup>.

Cross-resistance between macrolides in *H. pylori* has been observed<sup>[12,17,30]</sup>. Generally, *H. pylori* strains resistant to clarithromycin are also resistant to erythromycin, azithromycin and roxithromycin or vice versa. These observations have been confirmed at the molecular level<sup>[36]</sup>.

## Detection of clarithromycin resistance in *H. pylori*

The methods currently used for susceptibility testing of *H. pylori* to clarithromycin include agar dilution method, broth dilution method, disc diffusion test and the Epsilon meter test (E-test)<sup>[17,38]</sup>. The agar dilution method determines the minimal inhibitory concentrations (MICs) of antibiotics against bacteria. This method is time consuming and not feasible for routine use. However, it is a reliable technique which is usually carried out as a reference method for other techniques<sup>[17,38,39]</sup>. Broth dilution method is rarely used because of the difficulty in growing *H. pylori* in broth. The disc diffusion test is the easiest and cheapest way of testing susceptibility. However, this test requires strict standardization before it can be used<sup>[39]</sup>. The E-test, developed in 1988, provides the MIC of a strain directly by using a diffusion-like method<sup>[40]</sup>. A plastic-coated strip contains a preformed antimicrobial gradient on one side and a scale on the other. The reading is taken at the point where the

<sup>1</sup>Department of Medicine, University of Sydney, Nepean Hospital, Sydney, Australia

<sup>2</sup>Department of Infectious Diseases, Xiang-Ya Hospital, Hunan Medical University, The People's Republic of China

**Correspondence to:** Harry Hua-Xiang Xia, Clinical Sciences Building, Department of Medicine, The University of Sydney, Nepean Hospital, P.O. Box 63, Penrith NSW 2751, Australia  
Tel. +61 • 2 • 47 • 242682, Fax. +61 • 2 • 47 • 242614  
Email. xia@med.usyd.edu.au

Received 1999-04-08

ellipse of growth inhibition intersects the strip. Standardization and correlation with the agar dilution method are also required prior to application. This method is now widely used by many investigators<sup>[12,13,15,16,18,22-28]</sup>. At present, no "gold standard" method has been proposed for testing *H. pylori* susceptibility to antibiotics including clarithromycin and metronidazole, as there is still a need for standardization regarding the appropriate medium, the supplementation, the size of the inoculum, the incubation atmosphere, the appropriate time to read the plates and the breakpoint differentiating resistance and susceptibility<sup>[38]</sup>. Since cross-resistance exists between macrolides, erythromycin susceptibility testing may be useful in predicting (determining) clarithromycin resistant *H. pylori* strains<sup>[12,17]</sup>. Erythromycin susceptibility testing is well established in many microbiological laboratories, and it is much cheaper than clarithromycin susceptibility testing at present.

The association between point mutations on the 23S rRNA gene and macrolide resistance in *H. pylori* potentially provides a new approach for diagnosing macrolide resistant *H. pylori* strains. Although cycle DNA sequencing of the 23S rRNA gene amplicons is regarded as the reference method, simpler techniques have been developed<sup>[38]</sup>. These include polymerase chain reaction based restriction fragment length polymorphism (PCR-RFLP), an oligonucleotide ligation assay (PCR-OLA), a DNA enzyme immunoassay (PCR-DEIA), a reverse hybridisation line probe assay (PCR-LiPA), and a preferential homoduplex formation assay (PCR-PHFA)<sup>[30,31,33,41-43]</sup>. The PCR-based molecular techniques are quicker than microbiological susceptibility testing, and more importantly, they can be performed directly on gastric biopsies and gastric juice<sup>[10,44,45]</sup>.

#### **Clinical relevance of clarithromycin resistance in *H. pylori***

Studies have shown that clarithromycin resistance in *H. pylori* substantially affects the success rate of eradication regimens containing clarithromycin (Table 1). Generally, dual therapy with an antisecretory agent (e.g., H<sub>2</sub> antagonist or proton pump inhibitor) and clarithromycin achieves eradication rates of 60% to 80% for susceptible strains, but less than 40% for resistance strains (Table 1). Triple therapy with an antisecretory agent, clarithromycin and another antibiotic (i.e., amoxicillin or metronidazole) increases the eradication rates to 80%-95% for susceptible strains, but the rates remain under 40% for resistant ones (Table 1). A preliminary study reported that a combination of ranitidine bismuth citrate and

clarithromycin eradicated *H. pylori* at a rate of 98% and 92%, respectively, for both susceptible and resistant strains, but remains to be confirmed<sup>[13]</sup>.

Current anti *H. pylori* treatment regimens consisting of clarithromycin do not achieve an eradication rate of 100%. Emergence of clarithromycin-resistant strains during ineffective treatment has also been observed; the prevalence of clarithromycin-resistant strains cultured after treatment ranges between 40% and 100% (Table 1). This implies a likelihood of potential spread of clarithromycin-resistant strains in the population. Thus, the prevalence of clarithromycin resistance in *H. pylori* may exhibit a similar trend to the prevalence of metronidazole resistance in *H. pylori*. In Ireland, the prevalence of metronidazole resistant strains was 7% in 1989, 34% in 1992 and 38% in 1996<sup>[17]</sup>. In Australia, the prevalence of metronidazole resistance was 17% in 1988, but increased to 40% in 1995 and over 60% in 1998<sup>[11,47]</sup>. It is most likely that this increase is due to the use of metronidazole as a key agent in classic triple therapy (consisting of bismuth, metronidazole and tetracycline or amoxicillin), or increased use of this drug for other infections. Similarly, the current prevalence of clarithromycin-resistant strains of 6%-8% in Australia is much higher than the rate of 1.9% reported four years ago in this country<sup>[11,12,48]</sup>. This increase in the prevalence of clarithromycin resistance has been also reported in Europe and the United States<sup>[14,20,27,49]</sup>. It is assumed that prescriptions of macrolides, especially the new members such as spiramycin, roxithromycin, azithromycin and clarithromycin have been increased over the past years for the treatment of respiratory infection, sexually transmitted diseases and other infectious diseases. Thus, patients treated with any member of macrolides alone may select macrolide resistant *H. pylori* organisms (if infected), as cross-resistance exists between macrolides.

Overall, *H. pylori* resistance to clarithromycin is of less clinical relevance as compared with resistance to metronidazole, mainly because of the low prevalence and the possible reversibility of resistance in some strains. Susceptibility testing is not routinely required before treatment because of the low prevalence of clarithromycin resistance (Figure 1). However, *H. pylori* should be cultured and tested for clarithromycin susceptibility in patients who have failed the therapy containing clarithromycin (Table 1). Moreover, any previous use of macrolides not aimed at anti-*H. pylori* infection should be also taken into account when clarithromycin is chosen for eradication of *H. pylori*.

**Table 1** Effect of primary clarithromycin resistance on the efficacy of eradication therapy for *Helicobacter pylori* infection

Authors	Treatment regimens	Eradication rate (%)		Prevalence of resistant strains post-treatment (%)*
		Susceptible strains	Resistant strains	
Liu <i>et al.</i> , 1996 <sup>[5]</sup>	LFC or BFC	98(45/46)	0(0/4)	100(5/5)
Suzuki <i>et al.</i> , 1998 <sup>[8]</sup>	LAC	94(66/70)	0(0/1)	40(2/5)
Miyaji <i>et al.</i> , 1997 <sup>[9]</sup>	OC or LC	64(9/14)	0(0/5)	80(20/25)
	OAC or LAC	85(57/67)	28(2/7)	(Overall)
	OCM or LCM	86(68/79)	38(3/8)	
Maeda <i>et al.</i> , 1998 <sup>[10]</sup>	LAC	85(29/34)	40(2/5)	63(5/8)
Megraud <i>et al.</i> , 1997 <sup>[13]</sup>	OC	70(33/47)	38(3/8)	81(17/21)
	RbCC	98(42/43)	92(11/12)	(Overall)
Debets-Ossenkopp <i>et al.</i> , 1996 <sup>[16]</sup>	RC	81(58/72)	0(0/1)	73(11/15)
Tompkins <i>et al.</i> , 1997 <sup>[18]</sup>	OC	80(101/127)	0(0/4)	74(14/19)
Moayyedi <i>et al.</i> , 1998 <sup>[19]</sup>	OCT	91(104/114)	40(2/5)	Nor reported
Schutze <i>et al.</i> , 1996 <sup>[24]</sup>	RC	75(21/28)	20(1/5)	91(10/11)
Laine <i>et al.</i> , 1998 <sup>[25]</sup>	AC	35(73/208)	7.7(2/2.6)	53(70/131)
	OAC	81(153/190)	27(4/15)	(Overall)
Yousfi <i>et al.</i> , 1996 <sup>[26]</sup>	RanMC	87(20/23)	25(1/4)	67(4/6)
Buckley <i>et al.</i> , 1997 <sup>[46]</sup>	OMC	85(71/84)	0(0/3)	58(7/12)

O, omeprazole; C, clarithromycin; A, amoxicillin; Ran, ranitidine; M, metronidazole; Rbc, ranitidine bismuth citrate; L, lansoprazole; Rox, Roxithromycin; B, colloidal bismuth subcitrate (CBS).

\*The number of resistant strains post treatment was greater than the number of resistant strains before treatment in all the studies, suggesting acquisition of clarithromycin resistance during the unsuccessful treatment.

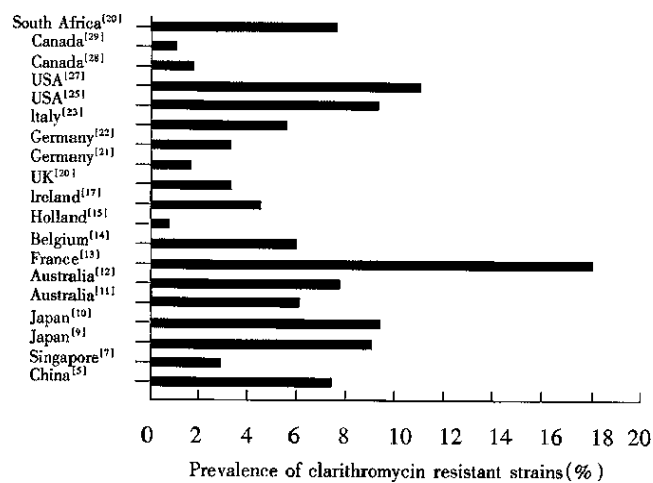


**Figure 1** Worldwide prevalence of clarithromycin resistant *H. pylori* strains. Each of these studies included at least 50 strains. The number after each country is the reference number.

### Conclusions

The prevalence of clarithromycin resistant *H. pylori* is low, but appears to be increasing. Point mutations in the 23S rRNA gene, mainly at the positions 2142 and 2143 with a transition of A→G, are responsible for the resistance. Although current triple therapies containing clarithromycin are able to eradicate up to 90% of susceptible strains, the eradication rates may be significantly reduced for resistant strains. Moreover, unsuccessful treatment with regimens containing clarithromycin can be associated with acquisition of resistance to the drug, which may explain the increasing rate of clarithromycin resistance.

### REFERENCES

- Graham DY. Clarithromycin for treatment of *Helicobacter pylori* infections. *Eur J Gastroenterol Hepatol*, 1995;7 (Suppl 1): S55-S58
- Xia H H-X, Talley NJ. Prospects for improved therapy for *Helicobacter pylori* infection. *Exp Opin Invest Drugs*, 1996;5: 959-976
- Xia HX, Buckley M, Hyde D, Keane CT, O' Morain CA. Effects of antibiotic-resistance on clarithromycin-combined triple therapy for *Helicobacter pylori*. *Gut*, 1995;37(Suppl.1):A55
- Megraud F. Epidemiology and mechanism of antibiotic resistance in *Helicobacter pylori*. *Gastroenterology*, 1998;115:1278-1282
- Liu W, Lu B, Xiao S, Xu W, Shi L, Zhang D. Clarithromycin combined short-term triple therapies for eradication of *Helicobacter pylori* infection. *Chin J Intern Med*, 1996;35: 803-806
- Hu P, Li Y, Chen M, Wu H, Cui J, Li Q. Clinical study of one week clarithromycin combination therapy for the treatment of *H. pylori* infection. *Chin J Dig*, 1997;17:204-206
- Hua J, Ng HC, Yeoh KG, Ho KY, Ho B. Characterization of clinical isolates of *Helicobacter pylori* in Singapore. *Microbios*, 1998;94:71-81
- Suzuki J, Mine T, Kobayashi I, Fujita T. Assessment of a new triple agent regimen for the eradication of *Helicobacter pylori* and the nature of *H. pylori* resistance to this therapy in Japan. *Helicobacter*, 1998;3:59-63
- Miyaji H, Azuma T, Ito S, Suto H, Ito Y, Yamazaki Y. Susceptibility of *Helicobacter pylori* isolates to metronidazole, clarithromycin and amoxicillin in vitro and in clinical treatment in Japan. *Aliment Pharmacol Ther*, 1997;11:1131-1136
- Maeda S, Yoshida H, Ogura K, Kanra F, Shiratori Y, Omata M. *Helicobacter pylori* specific nested PCR assay for the detection of 23S rRNA mutation associated with clarithromycin resistance. *Gut*, 1998;43:317-321
- Xia H H-X, Kalantar J, Talley NJ. Metronidazole- and clarithromycin-resistant *Helicobacter pylori* in dyspeptic patients in Western Sydney as determined by testing multiple isolates from different gastric sites. *J Gastroenterol Hepatol*, 1998;13:1027-1032
- Midolo PD, Bell JM, Lambert R, Turnidge JD. Antimicrobial resistance testing of *Helicobacter pylori*: a comparison of E test and disk diffusion methods. *Pathology*, 1997;29:411-414
- Megraud F, Pichavant R, Palegry D, French PC, Roberts PM, Williamson R. Ranitidine bismuth citrate (RBC) co-prescribed with clarithromycin is more effective in the eradication of *Helicobacter pylori*

- than omeprazole with clarithromycin. *Gut*, 1997;41(Suppl 1): A92
- 14 De Koster E, Cozzoli A, Jonas C, Ntounda R, Butzler JP, Deltenre M. Six years resistance of *Helicobacter pylori* to macrolides and imidazoles. *Gut*, 1996;39(Suppl 2):A5
  - 15 Van Zwet AA, de Boer WA, Schneeberger PM, Weel J, Jansz AR, Thijs JC. Prevalence of primary *Helicobacter pylori* resistance to metronidazole and clarithromycin in the Netherlands. *Eur J Clin Microbiol Infect Dis*, 1996;15:861-864
  - 16 Debets Ossenkopp YJ, Sparrius M, Kusters JG, Kolkman JJ, Vandenbroucke-Grauls CMJE. Mechanism of clarithromycin resistance in clinical isolates of *Helicobacter pylori*. *FEMS Microbiol Lett*, 1996;142:37-42
  - 17 Xia H X, Buckley M, Keane CT, O' Morain CA. Clarithromycin resistance in *Helicobacter pylori*: prevalence in untreated dyspeptic patients and stability *in vitro*. *J Antimicrobial Chemother*, 1996;37:473-481
  - 18 Tompkins DS, Perkin J, Smith C. Failed treatment of *Helicobacter pylori* infection associated with resistance to clarithromycin. *Helicobacter*, 1997;2:185-187
  - 19 Moayyedi P, Raganathan PL, Mapstone N, Axon ATR, Tompkins DS. Relevance of antibiotic sensitivities in predicting failure of omeprazole, clarithromycin, and tinidazole to eradicate *Helicobacter pylori*. *J Gastroenterol*, 1998;33(Suppl X):62-65
  - 20 Morton D, Bardhan D. A six-year assessment of tinidazole, metronidazole, clarithromycin, tetracycline and amoxicillin resistance in *Helicobacter pylori*-clinical isolates: a rising tide of antibiotic resistance. *Gastroenterology*, 1998;114:A907
  - 21 Adamek RJ, Suerbaum S, Pfaffenbach B, Opferkuch W. Primary and acquired *Helicobacter pylori* resistance to clarithromycin, metronidazole, and amoxicillin influence on treatment outcome. *Am J Gastroenterol*, 1998;93:386-389
  - 22 Wolle K, Nilius M, Leodolter A, Muller WA, Malfertthneiner P, Konig W. Prevalence of *Helicobacter pylori* resistance to several antimicrobial agents in a region of Germany. *Eur J Clin Microbiol Infect Dis*, 1998;17:519-521
  - 23 Piccolomini R, Di Bonaventura G, Catamo G, Carbone F, Neri M. Comparative evaluation of the E test, agar dilution, and broth microdilution for testing susceptibilities of *Helicobacter pylori* strains to 20 antimicrobial agents. *J Clin Microbiol*, 1997;35:1842-1846
  - 24 Schutze K, Hentschel E, Hirschl AM. Clarithromycin or amoxicillin plus high dose ranitidine in the treatment of *Helicobacter pylori*-positive functional dyspepsia. *Eur J Gastroenterol Hepatol*, 1996;8:41-46
  - 25 Laine L, Suchower L, Frantz J, Connors A, Neil G. Low rate of emergence of clarithromycin resistant *Helicobacter pylori* with amoxicillin co therapy. *Aliment Pharmacol Ther*, 1998;12:887-892
  - 26 Yousfi MM, El Zimaity HMT, Cole RA, Genta RM, Graham DY. Metronidazole, ranitidine and clarithromycin combination for treatment of *Helicobacter pylori* infection (modified Bazzoli's triple therapy). *Aliment Pharmacol Ther*, 1996;10:119-122
  - 27 Vakil N, Hahn B, McSorley D. Clarithromycin-resistant *Helicobacter pylori* in patients with duodenal ulcer in the United States. *Am J Gastroenterol*, 1998;93:1432-1435
  - 28 Best LM, Haldane DJM, Bezanson GS, Veldhuyzen van Zanten SJO. *Helicobacter pylori*: primary susceptibility to clarithromycin *in vitro* in Nova Scotia. *Can J Gastroenterol*, 1997;11:298-300
  - 29 Loo VG, Fallone CA, De Souza E, Lavallee J, Barkun AN. *In vitro* susceptibility of *Helicobacter pylori* to ampicillin, clarithromycin, metronidazole and omeprazole. *J Antimicrob Chemother*, 1997;40:881-883
  - 30 Versalovic J, Shortridge D, Kibler K, Griffy MV, Beyer J, Flamm RK. Mutation in 23S rRNA are associated with clarithromycin resistance in *Helicobacter pylori*. *Antimicrobial Agents Chemother*, 1996;40:477-480
  - 31 Taylor DE, Ge Z, Purych D, Lo T, Hiratsuka K. Cloning and sequence analysis of two copies of a 23S rRNA gene from *Helicobacter pylori* and association of clarithromycin resistance with 23S rRNA mutations. *Antimicrob Agents Chemother*, 1997;41:2621-2628
  - 32 Versalovic J, Osato MS, Spakovsky K, Dore MP, Reddy R, Stone GG. Point mutation in the 23S rRNA gene of *Helicobacter pylori* associated with different levels of clarithromycin resistance. *J Antimicrob Chemother*, 1997;40:283-286
  - 33 Stone GG, Shortridge D, Versalovic J, Beyer J, Flamm RK, Graham DY. A PCR-oligonucleotide ligation assay to determine the prevalence of 23S rRNA gene mutations in clarithromycin-resistant *Helicobacter pylori*. *Antimicrob Agents Chemother*, 1997;41:712-714
  - 34 Occhialini A, Urdaci M, Doucet Populaire F, Bebear CM, Lamouliatte H, Megraud F. Macrolide resistance in *Helicobacter pylori*: rapid detection of point mutations and assays of macrolide binding to ribosomes. *Antimicrob Agents Chemother*, 1997;41:2724-2728
  - 35 Hulten K, Gibreel A, Skold O, Engstrand L. Macrolide resistance in *Helicobacter pylori*: mechanism and stability in strains from clarithromycin treated patients. *Antimicrob Agents Chemother*, 1997;41:2550-2553
  - 36 Wang G, Taylor DE. Site specific mutations in the 23S rRNA gene of *Helicobacter pylori* confer two types of resistance to macrolide-lincosamide streptogramin B antibiotics. *Antimicrob Agents Chemother*, 1998;42:1952-1958
  - 37 Debets Ossenkopp YJ, Brikman AB, Kuipers EJ, Vandenbroucke Grauls CMJE, Kusters JG. Explaining the bias in the 23S rRNA gene mutations associated with clarithromycin resistance in clinical isolates of *Helicobacter pylori*. *Antimicrob Agents Chemother*, 1998;42:2749-2751
  - 38 Megraud F. Resistance of *Helicobacter pylori* to antibiotics. *Aliment Pharmacol Ther*, 1997;11(Suppl 1):43-53
  - 39 Xia HX, Keane CT, Beattie S, O' Morain CA. Standardization of disc diffusion test and its clinical significance for susceptibility testing of metronidazole against *Helicobacter pylori*. *Antimicrob Agents Chemother*, 1994;38:2357-2361
  - 40 Xia HX, Daw MA, Keane CT, O' Morain CA. Prevalence of metronidazole resistant *Helicobacter pylori* in dyspeptic patients. *Irish J Med Sci*, 1993;162:91-94
  - 41 Pina M, Occhialini A, Monteiro L, Doermann HP, Megraud F. Detection of point mutation associated with resistance of *Helicobacter pylori* to clarithromycin by hybridization in liquid phase. *J Clin Microbiol*, 1998;36:3285-3290
  - 42 Van Doorn L J, Debets Ossenkopp YJ, Marais A, van Hoek K, Sanna R, Megraud F. Detection of 23S rRNA mutation associated to macrolide-resistance of *Helicobacter pylori* by PCR and a reverse hybridization line probe assay. *Gut*, 1998;43(Suppl 2):A7-8
  - 43 Maeda S, Yoshida H, Ogura K, Maysunaga H, Kawamata O, Shiratori Y. Detection of *Helicobacter pylori* 23S rRNA gene mutation associated with clarithromycin resistance using preferential homoduplex formation assay (PCR-PHFA). *Gut*, 1998;43(Suppl 2):A7
  - 44 Bjorkholm B, Befrils R, Jaup B, Engstrand L. Rapid PCR detection of *Helicobacter pylori* associated virulence and resistance genes directly from gastric biopsy material. *J Clin Microbiol*, 1998;36:3689-3690
  - 45 Sevin E, Lamarque D, Delchier JC, Soussy CJ, Tankovic J. Co-detection of *Helicobacter pylori* and its resistance to clarithromycin by PCR. *FEMS Microbiol Lett*, 1998;165:369-372
  - 46 Buckley MJM, Xia HX, Hyde DK, Keane CT, O' Morain CA. Metronidazole resistance reduces efficacy of triple therapy and leads to clarithromycin resistance. *Dig Dis Sci*, 1997;42:2111-2115
  - 47 Katelaris PH, Nguyen TV, Robertson GJ, Bradbury R, Ngu MC. Prevalence and determinants of metronidazole resistance by *Helicobacter pylori* in a large cosmopolitan cohort of Australian dyspeptic patients. *Aust NZ J Med*, 1998;28:633-638
  - 48 Lian JX, Carrick J, Lee A, Daskalopoulos G. Metronidazole resistance significantly affects eradication of *H. pylori* infection. *Gastroenterology*, 1993;104:A133
  - 49 Xia HX, Keane CT, O' Morain CA. A 5-year survey of metronidazole and clarithromycin resistance in clinical isolates of *Helicobacter pylori*. *Gut*, 1996;39(Suppl 2):A6-7

# Clinical study on the treatment of liver fibrosis due to hepatitis B by IFN- $\alpha_1$ and traditional medicine preparation \*

CHENG Ming-Liang<sup>1</sup>, WU Ya-Yun<sup>1</sup>, HUANG Ke-Fu<sup>2</sup>, LUO Tian-Yong<sup>1</sup>, DING Yi-Shen<sup>1</sup>, LU Yin-Yin<sup>1</sup>, LIU Ren-Cai<sup>3</sup> and WU Jun<sup>1</sup>

**Subject headings** hepatitis B; liver cirrhosis/therapy; interferon- $\alpha$ ; drugs, Chinese herbal

## INTRODUCTION

In China, liver fibrosis in most patients resulted from the viruses of hepatitis B. Both anti-virus and anti-fibrosis should be considered in designing a program for the treatment of liver fibrosis. Therefore, 40 cases of liver fibrosis due to hepatitis B were treated by using IFN- $\alpha_1$  and traditional medicinal preparations from February 1994 to April 1996. Good curative effect was achieved.

## MATERIALS AND METHODS

### *Clinical materials*

A group of 40 patients (33 men and 7 women) was investigated. Their age ranged from 28 years to 45 years with a mean of 36. Their course of disease was from 4 years to 12 years, averaging 7 years. All patients had the typical history of hepatitis B. The diagnosis of liver fibrosis was confirmed by experimental serology and liver biopsy (the criteria of diagnosis referred to the criteria amended during the 5th National Academic Conference on Infectious Diseases and Parasitic Diseases). Patients whose clinical manifestations were not consistent with the findings in serological and pathohistological tests were not included in the study.

<sup>1</sup>Department of Infectious Diseases, Affiliated Hospital, Guiyang Medical College, Guiyang 550004, Guizhou Province, China

<sup>2</sup>Central Hospital of the Fifth Engineering Bureau of Railway Ministry

<sup>3</sup>Hospital of Bijie County, Guizhou Province, China

Dr. CHENG Ming-Liang, male, born on January 17, 1959 in Guiyang, Guizhou Province, graduated from Guiyang Medical College as B.S. in 1982. Professor of Infectious Diseases, specialized in hepatitis and hepatofibrosis, having 38 papers and books published.

\*Supported by the key project of the "8th Five Year Plan" of Scientific Committee of Guizhou Province (1993 No. 2037) and the key project of the "9th Five Year Plan" of Scientific Committee of Guizhou Province. (1996 No.1028)

**Correspondence to:** Professor CHENG Ming-Liang, Department of Infectious Diseases, Affiliated Hospital, Guiyang Medical College, Guiyang 550004, China.

Tel. +86 • 851 • 6829499 (H), 6855119 Ext. 3263 (O)

Received 1997-12-02 Revised 1999-01-18

### *Therapeutic*

All the patients received intramuscular injection of 3 000 000U IFN- $\alpha_1$  (Produced by Shengzhen Kexing Company, batch number 94010), once a day for the first month, and once two days after a month. Traditional medicinal preparation (composed mainly of Tetrandrae, Salvia miltiorrhiza Bge, Semen Ginkgo, Radix paeoniae rubrae, each gram has 0.8 g herb, produced by Duyun Pharmaceutical Factory, Guizhou Province, batch number 940102) was taken, three times a day for 3 months (45 g/d). Besides vitamin E and C, none of other medicines had been used in this group.

### *Observation index and methods*

Detection of serum liver fibrosis indexes and hepatitis B virus marker: 6 mL serum was taken from the patients before treatment, by the end of treatment and 6 months after treatment respectively. Laminin (LN), hyaluronic acid (HA) and precollagen type III (PC III) were measured by radioimmunoassay (the reagents were purchased from Shanghai Naval Medical Research Institute and Chongqing Tumor Research Institute). Radioimmunoassay was also used to detect the markers of hepatitis B virus such as HBsAg, anti-HBs, HBcAg, anti-HBc, HBeAg and anti-HBe. HBV-DNA was measured by PCR (the reagent was bought from 3V Company, Shandong Province).

### *Ultrasonography and fibergastroscopy*

Each patient was detected once by HPSONOS-1000 Colour Doppler (HP Company of USA) before and after the treatment and by direct vision fibergastroscopy (Olympus-XQ20, Japan).

### *Liver biopsy*

The liver tissue was quickly taken by fine needle under local anesthesia. The liver tissue was about 3 cm long. It was fixed by 10% formalin, then imbedded in paraffin, sliced and routinely stained. These slices taken from 12 biopsied patients before and after the treatment were read by single blind method. After a pathologist read these slices according to the criteria, another pathologist reported the results after reread them.

**Table 1 Comparison of the 5 serum indexes of the 40 patients before and after treatment and after 6 months of follow-up ( $\bar{x} \pm s$ )**

Time	n	LN	PCIII	HA	Albumin	Globulin
		(ng/L)		(ng/L)	(g/L)	
Before treatment	40	420.0 ± 68.0	146.2 ± 44.8	182.40 ± 42.20	30.51 ± 2.42	26.25 ± 6.84
After treatment	40	290.3 ± 36.4 <sup>b</sup>	112.4 ± 30.6 <sup>b</sup>	136.32 ± 39.20 <sup>b</sup>	35.25 ± 4.46 <sup>b</sup>	31.32 ± 6.74 <sup>b</sup>
Effective type after 6 months follow-up	22	142.6 ± 32.8 <sup>c</sup>	80.0 ± 31.8 <sup>c</sup>	84.54 ± 36.33 <sup>c</sup>	39.13 ± 3.24 <sup>c</sup>	25.98 ± 3.22 <sup>c</sup>
Non-effective type after 6 months follow-up	18	403.5 ± 41.5 <sup>a</sup>	156.3 ± 43.9 <sup>a</sup>	178.20 ± 38.60 <sup>a</sup>	29.35 ± 2.71 <sup>a</sup>	37.00 ± 4.54 <sup>a</sup>

<sup>a</sup> $P < 0.05$ ; <sup>b</sup> $P < 0.001$ , compared with those before treatment; <sup>c</sup> $P < 0.001$  the effective type compared with the non-effective type.

## RESULTS

The serum LN, HA, PC III and globulin of the 40 cases after treatment were noticeably lower than those before treatment ( $P < 0.001$ ). The albumin was obviously increased compared with that before treatment ( $P < 0.001$ ). After 6 months of follow-up, LN, HA and globulin in the effective type (HBsAg, HBeAg and HBV-DNA turned negative after using IFN $\alpha_1$ , suggesting that the viruses of hepatitis B were temporarily suppressed. Otherwise, it was considered to be non-effective type) were obviously lower than those in the non-effective type ( $P < 0.001$ ), while the albumin was obviously higher than that in the non-effective type ( $P < 0.001$ , Table 1).

Before treatment, 32 patients were found with HBsAg, anti-HBc and HBeAg; 8 patients with HBsAg and anti-HBc; and 21 patients with HBV-DNA. After 3 months of treatment, HBsAg, HBeAg and HBV-DNA became negative in 6 (15%), 16 (50%), and 16 (76.2%) patients, respectively. Among the 12 patients who received liver puncture biopsy, dekris-type necrosis disappeared in 3 patients, no obvious proliferation of fiber with more new-born liver cells in one patient, improvement of bridge-joint necrosis with elimination of the ramus septi-fibrosis in 3 patients, improvement of bridge-joint with new-born liver cells and unclear ramus septi-fibrosis in 2 patients, complete foliole with a great number of liver cells in 3 patients. Before treatment, the portal vein of 34 patients was  $\geq 14$  mm in width among the 40 patients, while after treatment, the portal vein of 28 patients was  $\leq 12$  mm. After 6 months of follow-up, among the 28 patients, the portal vein of 23 patients was  $\leq 11$  mm, the others remained 12 mm. Before treatment, the blood flow rate of portal vein in 36 patients was  $\geq 16$  mm/s, while after treatment, it was  $\leq 12$  mm/s in 32 patients. No change was found in the rest. By using fibergastroscopy the line or snake-shaped grey-white or grey-blue changes could be seen at the lower segment of esophageal mycoderma in 32 patients before treatment, while the changes disappeared in 28 patients after treatment. No obvious changes were found in 4 patients.

## DISCUSSION

Up to now, there has been no good way to cure liver fibrosis resulting from chronic hepatitis B. A number of researches have been made by domestic scientists who had made great progress by using traditional medicines such as *Salvia miltiorrhiza* Bge, *Tetrandrae*, *Radix paeoniae rubrae* and *Prunus persicac* (L), batsch et al<sup>[1-3]</sup>. However these methods have not been considered to suppress the virus of hepatitis B. For this reason, some tests were made by using IFN $\alpha_1$  and traditional medicinal preparations to treat 16 patients with early-stage hepatic cirrhosis, and have achieved rather good curative effect which was confirmed by liver biopsy before and after treatment<sup>[4]</sup>. On the other hand, short-term curative effect was significant in 20 patients treated simply by the traditional medicinal preparations<sup>[5]</sup>, but there was recurrence in some patients. Therefore, IFN $\alpha_1$  and traditional medicinal preparation were used to treat hepatitis and liver fibrosis at the same time. At present IFN $\alpha_1$  is regarded as one of the most effective agents to treat hepatitis B because it is a biologically regulatory and active material with antiviral and immunoregulatory function<sup>[6,7]</sup>. *Tetrandrine* is an effective ingredient of *Tetrandrae*. In modern medicine the research has proved that it can block the channel of calcium on the cytomembrane of liver, obstruct the depletion of ATP in the cytomembrane, protect the liver cells, and inhibit the proliferation of internal lipocyte of liver and synthesis of collagen. The effective ingredients of dansheng are *Tanshinone* and *tanshine* which may suppress the reaction of inflammation and promote the regeneration of liver cells by reducing the degeneration and necrosis of liver cells. The effective ingredient of chichao is *paeoniflorin* which may improve the microcirculation of liver, decrease the portal pressure and promote the histologic change of liver fiber. Flavonoid substance in ginkgo leaves can strengthen the immunologic function of body, decrease the free radical of oxygen, increase the activity of NK cells and intensify the anti virus capacity of body<sup>[8,9]</sup>. After 3 months of treatment with the herbal medicinal preparations, the changes of LN, HA, PC III, albumin and globulin were

obviously different from those before treatment, which were confirmed by liver biopsy, ultrasonography and fibergast roscopy. It is suggested that this preparation can improve the function of liver and suppress the fibrosis of liver in a short time. Follow-up was made for 6 months after withdrawing the medicine. The result proved that the difference between IFN $\alpha_1$  effective type and ineffective type was very obvious. It indicated that the virus of hepatitis B was suppressed in the patients cured by IFN $\alpha_1$ , and the liver fibrosis due to clinical hepatitis B was continuously improved or reversed by using the traditional herbal preparations which can cure liver fibrosis. The patients in this group are being followed up continuously.

#### REFERENCES

- 1 Ma XH, Zhao YC, Yi L. The action of dansheng to reabsorption of hepatofibrosis. *Chin J Integrated Traditional West Medi*, 1988;8: 161-163
- 2 Liu P, Liu C, Hu Ying. The clinical observation of supporting the healthy energy and eliminate the evil to cure hepatic cirrhosis after hepatitis. *Chin J Integrated Traditional West Medi*, 1996;16: 459-462
- 3 Yang DG, Wang LJ, Song WY. The comparison of histology in liver puncture by re-using chichao to treat chronic hepatitis before and after treatment. *Chin J Integrated Traditional West Medi*, 1994;14:207-208
- 4 Cheng ML, LT, Wu YY. The histological study on IFN $\alpha_1$  and traditional medicine preparation to treat early stage hepatic cirrhosis. *Chin J Integrated Traditional West Medi*, 1995;15: 300-301
- 5 Cheng ML, Ding YS, Luo YF. The clinical study on handanbituo to treat chronic hepatitis hepatofibrosis. *Chin J Integrated Traditional West Medi*, 1996;1:431-432
- 6 Billiau A. The model of action of interferons in viral infections and their possible role in the control of hepatitis B. *J Hepatol*, 1986; 3(suppl):S171
- 7 Yao GB, Fei GH, Wu XH. The study on IFN to treat chronic hepatitis B. *Chin J Digest*, 1991;11:133-136
- 8 Cheng ML, Liu SD. The basic study and clinics of hepatofibrosis. First edition. Beijing: People's Health Publishing House, 1996: 228-248
- 9 Li W, Dai QT, Liu ZE. The first-step observation of early-stage fibrosis after the dissolvable of the complex prescription sinkgo to treat chronic hepatitis B. *Chin J Integrated Traditional West Medi*, 1995; 15:593-595

Edited by WANG Xian-Lin

# Antibody detection and sequence analysis of sporadic HEV in Xiamen region \*

HUANG Ru-Tong, LI Xiao-Yu, XIA Xiao-Bing, YUAN Xin-Tong, LIU Min-Xia and LI De-Rong

**Subject headings** hepatitis E virus; antibodies; viral/analysis; nucleotide sequences; sequence analysis

## INTRODUCTION

Hepatitis E virus (HEV) is transmitted through a fecal-oral route<sup>[1]</sup>. HEV induces acute hepatitis and is responsible for a significant portion of the fulminant hepatitis in epidemic and sporadic cases, especially in the mixed infection patients and women in their third trimester of pregnancy<sup>[1]</sup>. It has been reported that HEV infection is more prevalent in underdeveloped and developing countries in Asia, Africa, and Central America, but is rare in developed countries<sup>[1]</sup>. In China, a large outbreak occurred between 1986 and 1988 in Xinjiang, and sporadic spread was often found in other regions.

HEV is a non-enveloped virus, approximately 27 nm-34 nm in diameter and has a positive-sense, single-stranded RNA genome of approximately 7.2 kb. The viral genome consists of three discontinuous open reading frames (ORFs). Since the molecular cloning and sequencing of HEV were described<sup>[2]</sup>, several genomic analyses of HEV strains obtained from different geographic areas have been reported<sup>[3]</sup>. The existing variations on the gene structure of HEV strains from some regions of China was reported by us<sup>[4]</sup>. In this study, after the collection of the serum samples of patients with acute hepatitis in Xiamen, anti-HEV antibody and HEV RNA in serum were detected, further HEV RNA was cloned and sequenced. The results are described and discussed.

## PATIENTS AND METHODS

### Patients

From September 1996 to March 1997, 81 samples of serum of patients (71 male and 10 female, aged 13

Institute of Microbiology and Epidemiology, Academy of Military Medical Sciences, Beijing 100850, China

Dr. HUANG Ru-Tong, male, born on 1942-11-11 in Zhejiang Province, graduated from Shanghai Fudan University as a postgraduate in 1966, now associate professor of microbiology, majoring aetiology of medical virology, having 60 papers published.

\*Supported by the Foundation of General Logistics Department of Chinese PLA, No.9608037.

**Correspondence to:** Dr. HUANG Ru-Tong, Institute of Microbiology and Epidemiology, Academy of Military Medical Sciences, Beijing 100850, China

Tel. +86 • 10 • 66931535, Fax. +86 • 10 • 68213044

Received 1999-01-20

-69 years) with acute hepatitis at clinic and admitted to the Infections Disease Hospital in Xiamen were collected. These serum samples were provided by professor LIAO Mian-Chu and were stored at -25 °C before test. The sera showed elevated ALT levels. The serum of patients with acute hepatitis was tested for detection of serum IgM anti-HAV, HBsAg, IgM anti-HBc, anti-HCV and anti-HEV antibodies. According to above detections, all samples suspected of hepatitis E were taken to our laboratory and were further studied. One case (sample No.3, Zhou, male aged 52 years) used in the determination of sequence was diagnosed as fulminant hepatitis. He had complained of tiredness, anorexia, urine-yellow, jaundice in skin and sclera and spider nevus, with ALT 20420 nmol • s<sup>-1</sup>/L and SB-205.2 μmol/L, and virus markers of anti-HAV IgM and anti-HEV IgM positive.

### Detection of anti-HEV antibody

Anti-HEV IgG and IgM antibodies were further detected by ELISA with recombinant antigens (Institute of Virology, Chinese Academy of Preventive Medicine) according to the manufacturer's instructions.

### Cloning and sequencing of HEV RNA

Two sets of pair primers were synthesized at Institute of Microbiology of Chinese Science Academy according to the Burmese HEV sequence<sup>[3]</sup>. The sequence of each oligonucleotide primer was: outer primers (F1) 5'-GCT ATT ATG GAG GAG TGT GG 3' and (R1) 5'-CAG GGC CCC AAT TCT TCT 3', inner primers (F2) 5'-GCG TGG ATC TTG CAG GCC 3' and (R2) 5'-TTC AAC TTC AAG CCA CAG CC 3'. HEV RNA was extracted from 200 μL serum by proteinase K (10 g/L) guanidine thiocyanate buffer (4.2M guanidine thiocyanate and 5 g/L N-lauroyl sarcosine and 0.025 mol/L Tris-HCl, pH 8.0) phenol/choroform<sup>[5]</sup>. All viral RNA were used to be transcribed and nested-PCR<sup>[4]</sup>. The amplified PCR products were ligated into pGEM-T vector (Promega products) according to the manufacturer's instructions. The ligation mixture was transformed to *E. coli* strain JM 109. The positive clones were picked up and cultured in LB medium. The positive

recombinant clones were identified and sequenced. The nucleotide sequence (location 4522-4761) of X-S1 isolate of HEV was compared with those of other known HEV strains. Percentage of similarity and divergence were calculated as described previously<sup>[4]</sup>.

**RESULTS**

**Detection of anti-HEV and HEV RNA in serum samples of patients with acute hepatitis**

Twelve of 81 serum samples of acute hepatitis in Xiamen were positive for anti-HEV IgG, of them, 11 were also positive for anti-HEV IgM. Eight of 12 serum samples of positive anti-HEV IgG were used to detect HEV RNA, 2 samples were found positive for HEV RNA. The results are shown in Table 1.

**Cloning and sequencing of HEV**

The amplified PCR positive products obtained from X-S1 and X-S6 samples were purified and ligated into pGEM-T vector, then transformed to *E.coli* JM 109. One of two white specks obtained from X-S1 had a band of about 239 bp in gel electrophoresis. Two white specks of the X-S6 were positive and a band of 239 bp was found after digested by *EcoR* I and *Hind* III. One positive clone of X-S1 was sequenced. HEV sequence of the X-S1 isolate could be recognized, this HEV X-S1 strain was neither lost nor inserted in length 239 bp compared with Burma strain of HEV. Aberrance occurred in 48 bases, 5 of them took place at the first codon position, 4 at the second position and 39 at the third codon position. The nucleotide sequence of X-S1 isolate is shown in Figure 1.

**Table 1 Results of anti-HEV antibody and HEV RNA detection in serum of patients from Xiamen**

Patients	Name	Sex	Age	Collection time	Anti-HEV <sup>a</sup>		Results of HEV RNA detection
					IgG	IgM	
1	Ling JD	M	31	97-03-05	+	+	ND <sup>b</sup>
2	Du YM	M	24	97-02-05	+	+	-
3	Zhou SL	M	52	97-02-15	+	+	+
4	Huang JC	M	50	97-02-19	+	-	ND
5	Qiu SS	M	53	97-02-19	+	+	-
6	Huang JZ	M	45	97-01-28	+	+	-
7	Mei SP	F	31	96-02-17	+	+	ND
8	Zhen MC	M	68	96-12-09	+	+	-
9	Zhang MS	M	60	97-12-09	+	+	-
10	Zhong M	M	29	96-11-13	+	+	+
11	Kang CR	M	24	96-10-10	+	+	N
12	Jiang XW	M	29	97-02-19	+	+	-

<sup>a</sup>A>0.30 +  $\bar{x}$  of negative samples; positive.<sup>b</sup>Not done.

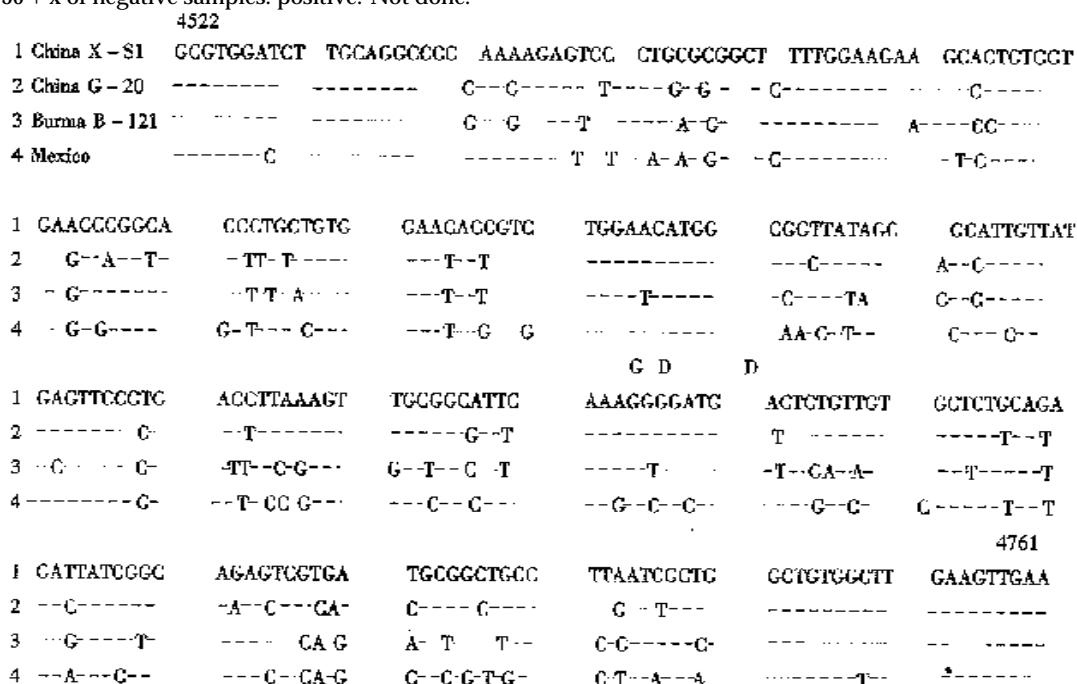


**Figure 1** Comparison of the nucleotide sequences among four strains of HEV.

### Comparison of the nucleotide sequence of HEV

The sequence of HEV X-S1 strain was compared with the Chinese (G-20), Burmese (B-121) and Mexican strains of HEV. The similarity of nucleotide sequences was 85.4%, 79.2% and 76.4% respectively. The divergence of nucleotide sequences was 14.2%, 19.9% and 22.3% respectively.

### DISCUSSION

This paper reports the results of serological survey on hepatitis E virus infection in Xiamen population. The serum samples from 81 patients with acute hepatitis were tested for anti-HEV IgG and IgM antibodies with HEV recombination antigen by ELISA. Twelve (14.8%) of 81 patients with acute hepatitis had antibody to HEV, 11 were positive for IgM anti-HEV and 2 positive for HEV RNA. The results show that there is hepatitis E virus infection in Xiamen again, but there has been no documented report of detection of HEV RNA in anti-HEV positive patients from this area.

The mixed infection of HEV and HBV were described previously<sup>[4]</sup>. This paper reports the co-infection of HEV and HAV. This case is positive for both antibodies of HAV and HEV. The patient presented as severe hepatitis in the clinical characteristics, with very high ALT ( $20420 \text{ nmol} \cdot \text{s}^{-1}/\text{L}$ ). This shows that both the HEV and HAV are transmitted primarily through a fecal-oral route. In this study, the partial nucleotide sequence of Xiamen X-S1 isolate of sporadic HEV was described and compared. It is shown that Xiamen (X-S1) strain and Guangzhou (G-20) strain<sup>[4]</sup> are most

identical to each other (85.4%), with a lower range of identities to the Burmese strain<sup>[2]</sup> and Mexican strain<sup>[3]</sup> (80.1%-77.3%). The nucleotide sequences of the X-S1 strain and the G-20 strain may belong to a novel and unique branch. Similar results have been reported by other investigators<sup>[6,7]</sup>. Recently the HEV-US-1 strain was discovered by George G. Schlauder<sup>[8]</sup>, it is significantly divergent from other human HEV isolates, which may be the fourth genotype. The discovery of these HEV variants may be important in understanding the worldwide distribution of HEV infection.

### REFERENCES

- 1 Gust ID, Purcell RH. Report of a workshop: waterborne non-A, non-B hepatitis. *J Infect Dis*, 1987;156:630-635
- 2 Tam AW, Smith MM, Guerra ME, Huang CC, Bradley DW, Fry KE, Reyes GR. Hepatitis E virus (HEV): molecular cloning and sequencing of the full-length viral genome. *Virology*, 1991;185:120-131
- 3 Huang CC, Nguyen D, Fernandez J, Yun KY, Fry KE, Bradley DW, Tam AW, Reyes GR. Molecular cloning and sequencing of the Mexico isolate of hepatitis E virus. *Virology*, 1992;191:550-558
- 4 Huang RT, Nakazono N, Ishii K, Kawamata O, Kawaguchi R, Tsukada Y. Existing variations on the gene structure of hepatitis E virus strains from some regions of China. *J Med Virol*, 1995;47:303-308
- 5 Tsarev SA, Emerson SU, Reyes GR, Tsareva TS, Legters LJ, Malik IA, Iqbal M, Purcell RH. Characterization of a prototype strain of hepatitis E virus. *Proc Natl Acad Sci USA*, 1992;89:559-563
- 6 Wei SJ, Walsh P, Tong YB, Dong HQ, Cai XL. Nucleic acid sequence analysis of the sporadic hepatitis E virus strains in Guangzhou. *Chin J Microbiol Immunol*, 1998;18:92-95
- 7 Wu JC, Sheen IJ, Chiang TY, Sheng WY, Wang YJ, Chan CY, Lee SD. The impact of traveling to endemic areas on the spread of hepatitis E virus infection: epidemiological and molecular analyses. *Hepatology*, 1998;27:1415-1420
- 8 Schlauder GG, Dawson GJ, Erker JC, Kwo PY, Kningge F, Smalley L, Rosenblatt JE, Desai SM, Mushahwar IK. The sequence and phylogenetic analysis of a novel hepatitis E virus isolated from a patient with acute hepatitis reported in the United States. *J Gen Virol*, 1998;79:447-456

Edited by MA Jing-Yun

# Primary malignant tumor of the small intestine

ZHOU Zhi-Wei, WAN De-Sen, CHEN Gong, CHEN Ying-Bo and PAN Zhi-Zhong

**Subject headings** intestinal neoplasms/diagnosis; intestinal neoplasms/therapy; small intestine; survival analysis

## INTRODUCTION

Primary malignant tumors of the small intestine are easy to be misdiagnosed because of its low morbidity, nonspecific clinical manifestations and the limited examination methods. Most cases are already in advanced stage at the time of diagnosis, so therapeutic result is very poor. In order to have a better understanding of the clinical characteristics of malignant tumor of the small intestine, an analysis was made for the diagnosis, treatment and prognosis-influencing factors of 75 cases with their diagnoses confirmed by pathological examination from 1964 to August, 1995 in our hospital, so as to improve their early diagnosis, timely treatment and therapeutic effect.

## MATERIALS AND METHODS

### General data

This group consisted of 75 cases, 42 males and 33 females. The onset age ranged from 4 to 75 years with an average of 47 years. The course of disease was 1 to 99 months, averaging 47 months.

### Pathological type and tumor site

The diagnoses of the 75 cases were confirmed by pathological examination, 26 were cases of leiomyosarcoma, 25 adenocarcinomas, 20 malignant lymphomas, and 4 other malignant neoplasms. The tumors were located at duodenum, jejunum and ileum in 18, 28 and 29 cases respectively (Table 1).

### Clinical manifestations

Clinical manifestations of these malignant tumors are shown in Table 2.

Cancer Centre, Sun Yat-Sen University of Medical Sciences, Guangzhou 510060, Guangdong Province, China

ZHOU Zhi-Wei, male, born on 1964-01-28 in Pengze County, Jiangxi Province, Han nationality, graduated from Sun Yat-Sen University of Medical Sciences in 1984, associate professor, majoring in gastroenteric oncology, having 10 papers published.

**Correspondence to:** Dr. ZHOU Zhi-Wei, Department of Abdominal Surgery, Cancer Centre, Sun Yat-Sen University of Medical Sciences, Guangzhou 510060, Guangdong Province, China

Tel. +86 • 20 • 87765368 Ext.5214

Received 1998-11-09

**Table 1 Pathological types and distributions**

Type of neoplasms	Number by region			
	Duodenum	Jejunum	Ileum	Total
Leiomyosarcoma	5	14	7	26
Adenocarcinoma	10	9	6	25
Malignant lymphoma	2	4	14	20
Malignant fibrous histiocytoma		1	1	2
Malignancy of neurofibroma			1	1
Malignancy of fibroma	1			1
Total	18	28	29	75

### Preoperative diagnosis

Before the exploratory laparotomy, 33 cases were diagnosed as intestinal carcinoma, 25 cases as abdominal mass, and 17 cases were misdiagnosed as other diseases, such as intestinal perforation, acute peritonitis, ovary tumor, colon carcinoma, and intussusception of ileum to cecum, and so on.

### Accessory examinations

No abnormal CEA (carcinoembryonic antigen) was detected in 10 cases. Twenty-three out of 26 cases were found to have abdominal mass by B-type ultrasonography. CT (computed tomography) scans showed a clear demonstration of tumor on the diseased region and the structures around it in 20 cases. Of the 13 cases accepted barium meal roentgenography, 11 were diagnosed as intestinal tumor, with an accuracy of 84.6%. Of the 7 cases of duodenal tumors, 6 were diagnosed as duodenal tumor by fibroscopy which were confirmed by pathological examination. Barium enema was performed in 18 cases and 8 of them were found to have tumor in their ileum.

### Methods of treatment

Surgical treatment was the main therapeutic method for this group of cases. Thirty-seven cases received radical resection, 21 palliative resection, and 10 bypass operation, 3 exploratory laparotomy and 3 direct biopsy. The operation mortality was 1.4%. Four cases did not receive surgical operation. 27 cases received adjuvant chemotherapy. 5-fluorouracil (5-FU), mitomycin (MMC), cyclophosphamide (CTX) and adriamycin (ADM) were commonly used.

## RESULTS

Survival rates were calculated with Life Table, and computer's COX multivariate analysis model was used for survival analysis.

**Table 2 Clinical manifestations**

Symptom	Abdominal pain	Abdominal mass	Emaciation	Intestinal obstruction	Melena	Acute peritonitis	Jaundice	Fever	Anemia
Number	45	43	18	11	6	5	5	4	3
%	60	57.3	24	14.7	8	6.7	6.7	5.3	5

**Follow-up data**

Duration of follow-up ranged from 1 to 30 years, the follow-up rate was 94.2%. One-, 3- and 5-year survival rates of the 71 operated cases were 70.7%, 49.9% and 35.1% respectively (Tables 3-5).

**Table 3 Survival rate by operation type**

Operation type	n	Survival rate (%)		
		1 year	3 years	5 years
Radical resection	37	87.5	68.7	48.1
Palliative resection	21	57.9	33.8	24.1
Symptom- relieving and exploratory operation	13	42.9	21.4	0.0

**Table 4 Survival rate by pathological type**

Pathological type	n	Survival rate (%)		
		1 year	3 years	5 years
Adenocarcinoma	25	53.9	27.9	14.0
Leiomyosarcoma	26	95.8	82.1	57.5
Malignant lymphoma	20	48.6	39.7	23.8

**Table 5 Survival rate by location of tumor**

Location of tumor	n	Survival rate (%)		
		1 year	3 years	5 years
Duodenum	17	69.2	38.5	0.0
Jejunum	27	81.8	59.6	50.4
Ileum	27	51.1	29.2	17.5

**Prognostic factors analysis by computer's COX multivariate analysis model**

An analysis was made by COX multivariate analysis model, for the following factors which may influence prognosis such as patient sex, age, clinical course, histological type, tumor site, tumor size, gross type, lymph node metastasis, liver metastasis, invasion to adjacent organs, operation type, and chemotherapy. The critical value of alpha was 0.05. Statistical results showed that patient age, histological type, tumor site and operation type had significant influence on survival rate. But chemotherapy had no significant effect on prognosis.

**DISCUSSION****General consideration**

The incidence of primary malignant tumor of the small intestine is very low, accounting for 1%-3.6% of all gastrointestinal malignant neoplasms and 0.2%-0.3% of that of the whole body<sup>[1,2]</sup>.

From 1964 to 1995, 75 cases of primary malignant tumor of the small intestine were admitted to our hospital, constituting about 1.4% of 4427 cases of malignancy of all GI tract in the same period. In China, the leiomyosarcoma, adenocarcinoma, and malignant lymphoma account for the most of the small intestine malignancies, but carcinoid is rare. However, in other countries the most frequently encountered malignancies of small intestine are in order of adenocarcinoma and carcinoid, malignant lymphoma and leiomyocarcinoma<sup>[3]</sup>.

Relationship between pathology and tumor site. The predilection site of leiomyosarcoma is jejunum, ileum and duodenum. The predilection site of adenocarcinoma is in order of duodenum, jejunum and ileum, while the predilection site of malignant lymphoma is ileum and jejunum, and is lower in duodenum<sup>[3]</sup>. The tumor distribution rates in this group cases are consistent with those reported in the literature (Table 1).

Tumor distribution in small intestine. Adenocarcinoma accounts for about 50%-66% of tumors in the duodenum (55.6% in this group), and followed by malignant lymphoma and leiomyosarcoma. In the jejunum, leiomyosarcoma is the most encountered (accounting for 50% in this group), the next is adenocarcinoma and malignant lymphoma. But in the ileum, malignant lymphoma constitutes about half of all malignancies (48.3% in this group), and followed by adenocarcinoma and leiomyosarcoma.

Many scholars hold that the low incidence of malignant tumors in small intestine is associated with the following factors: ① Alkalinity in the small intestinal lumen is unfit for the growth of tumor. ② Rapid peristalsis of small intestine is suggested to minimize the time of mucosal exposure to potential carcinogens from food, and liquid content in lumen may dilute carcinogens, which will lead to the reduction of carcinogenicity. ③ The lack of intraluminal bacterial flora obviously reduces carcinogenic agents, and these bacteria are necessary in the process of metabolism. ④ A large concentration of IgA produced mainly in the lymphoid tissue of small intestine, is protective against tumorigenesis by neutralizing virus and potential carcinogenic agents. ⑤ The T-lymphocyte with strong immunity, accounting for the majority

of lymphocytes in collecting lymphadens of small intestines, has a strong ability and specific characteristics to protect against tumor growing. ⑥ Benzopyrene hydroxylase is present in large amounts in the mucosa of small intestine and may detoxify carcinogens<sup>[1]</sup>.

### Diagnosis

Primary malignant tumor of small intestine is easy to be misdiagnosed because of its low incidence, its vague and nonspecific clinical presentations, and the limited diagnostic methods. Misdiagnosis rate in literature reports is 40%-80%<sup>[4]</sup>, and 56% in our group. We hold that following are the key points to increase its diagnostic accuracy and to decrease its misdiagnostic rate.

A better understanding should be acquired in primary malignant tumor of small intestine. In clinics the following should be highly suspicious of the disease: unknown abdominal pain, abdominal mass, melena, and obstruction, especially when an abdominal mass is palpable.

Barium meal roentgenography is the routine method for detecting primary malignant tumor of small intestine, its diagnostic accuracy can be as high as 50%<sup>[2,5]</sup>. We think that for the patients who are suspicious of tumor in small intestine, barium meal roentgenography should be performed if possible. In our studied group, diagnoses were established by barium meal X-rays in 11 out of 13 cases with an accuracy of 84.6%. Air-barium contrast roentgenography, in which a large amount of barium and air are injected into the duodenum lumen through a gastric tube, is suggested to be performed to visualize small intestine segment by segment, so as to increase its diagnostic accuracy rate. The distal ileum usually is poorly visualized in upper GI series studies, but it may be demonstrated through barium enema in which contrast material from colon is refluxed into the distal small intestine through the ileocecal valve. Combination of barium meal roentgenography and barium enema can achieve a positive rate of 50%-80%.

Flexible endoscopic examination and direct biopsy are the most reliable methods to establish the diagnosis, especially in early stage of the disease. It is also helpful and reliable for diagnosis of tumors in the duodenum. In our studied group, the diagnosis was established in 6 of 7 cases by flexible endoscopic examination and were confirmed by pathological examination. In foreign countries, the flexible endoscopy for small intestine was used in clinic in 1969. But it developed very slowly because of its technical difficulties in inserting and the great suffering of patients<sup>[5]</sup>.

Computed Tomography (CT) scans can show a good demonstration of the tumor-involved region and the structures around it. Furthermore, CT scan can define whether there is local or distant metastasis. Especially for those whose diagnosis can not be confirmed by GI barium roentgenography, CT scan is an effective method<sup>[6]</sup>.

### Treatment

Surgical resection is so far the most effective therapeutic method for malignant tumor of small intestine. If diagnosis is established, radical resection should be performed as early as possible, which requires at least segmental resection of 10cm of the involved region, including removal of the corresponding mesentery and its lymph nodes<sup>[7]</sup>. It was reported the 5-year survival rate of radical resection is 25%-54%<sup>[1,8]</sup>, which is consistent with that (48.1%) in our study. For carcinoma in the duodenum, Whipples operation should be performed if possible. Tumor in the distal ileum should be treated by right hemicolectomy. Palliative resection of tumor is somewhat valuable and should not be given up easily. Its 5-year survival rate is 0%-25% reported in literature<sup>[1]</sup>, and is 24.1% in our study. Bypass operation can temporarily relieve symptoms but could not prolong the patient's life. Reexploratory resection should be performed for recurrence if possible<sup>[9,10]</sup>.

Adjuvant postoperative chemotherapy for malignant lymphoma is necessary. The unresectable malignant lymphoma of small intestine should be treated mainly by chemotherapy in order to relieve symptoms and prolong life. The usual chemotherapy regimen is CHOP (CTX+VCR+ADM+Prednisone). Leiomyosarcoma of small intestine is partly sensitive to chemotherapeutic agents. For huge leiomyosarcoma, preoperative combination chemotherapy of ADM and CTX can minimize the size of tumor and improve resection rate. Chemotherapy has no effect on adenocarcinoma of small intestine due to its nonsensitivity to chemotherapeutic agents. In our study, 27 cases had accepted chemotherapy, but neither postoperative adjuvant nor palliative chemotherapy is effective in prolonging the survival, which is possibly associated with the late stage of the disease.

### Prognostic factors

It was reported that prognostic factors of primary malignant tumor of the small intestine are chiefly the operation type, histological type, tumor site and tumor size<sup>[1,7]</sup>, and each of them was analyzed by monovariate analysis. Up to now there have been no reports in the world about the prognostic factors

studied by multivariate analysis model. In our study, 12 factors were analyzed by computer's COX multivariate analysis model, including patient sex, age, clinical course, histological type, tumor site, tumor size, gross type, lymph node metastasis, liver metastasis, invasion to adjacent organs, operation type, and chemotherapy. The results showed that significant prognostic factors were histological type, operation type, patient age and tumor site in order, neither tumor size nor chemotherapy had significant effect on prognosis.

## REFERENCES

- 1 Han YF, Zhang QZ. An analysis of 36 cases of primary tumor of the small bowel. *Tumor*, 1995;15:406-407
- 2 Wang WD, Chen XY. A report of 77 cases of Primary malignant tumors of the small bowel. *Tumor*, 1990;10:44-45
- 3 Wang D, Xu JX, Wang ZX. CT diagnosis of Primary malignant tumors of the small bowel. *J Clin Radiol*, 1995;15:220-222
- 4 Wei JZ, Zhu YF, Wang JH. A diagnostic analysis of 27 cases of Primary malignant tumors of the small bowel. *Prac J Cancer*, 1993;8:175-176
- 5 Ciccarella O, Welch JP, Kent GG. Primary malignant tumors of the small bowel. *Am J Surg*, 1987;153:350-354
- 6 He SW. A clinical analysis of 41 cases of Primary malignant tumors of the small bowel. *J Prac Oncol*, 1992;6:54-55
- 7 Chen YR, Wang L. Tumor of the small bowel in China. *J Prac Surg*, 1991;11:437-439
- 8 Zheng YL, Zhao QY. A synthetic analysis of malignant tumor of the small bowel in China. *Prac J Cancer*, 1989;4:138-139
- 9 Sellner F. Investigation on the significance of the adenocarcinoma sequence in the small bowel. *Cancer*, 1990;66:702-711
- 10 Zhou HG, Chen ZP, Kuang YL. Diagnosis and treatment of Primary malignant tumors of the small bowel. *Shanghai Dier Yike Daxue Xuebao*, 1995;15:138-141

Edited by WANG Xian-Lin

# The evaluation of gastrointestinal function in diabetic patients

Eamonn M.M. Quigley

**Subject headings** diabetic gastroenteropathy; diabetic gastroparesis; gastric dysmotility; gastric emptying

Nowadays, a number of options are available for the assessment of gastric motor function. Thus, a global evaluation of gastric motor function may be obtained by tests of gastric emptying while regional function of the antrum and fundus may be evaluated by such techniques as antral manometry and the barostat, respectively. Traditionally, given widespread access to a variety of tests of gastric emptying, gastric dysmotility has been classified according to the patient's gastric emptying status. Accordingly, a given patient will be defined as having either delayed (gastroparesis) or accelerated (the dumping syndrome) gastric emptying. The limitations of this approach must be appreciated. Thus, it is evident from a variety of recent studies that gastric emptying rate and symptoms may not correlate. Secondly, and this is particularly relevant to diabetes mellitus, the same disease process may at different times lead to accelerated, delayed or normal emptying, in the same patient. These caveats notwithstanding, the clinical approach to gastric dysmotility usually begins with a gastric emptying test. Recently, electrogastrography has been proposed as an alternative test of global gastric motor function.

## TESTING GASTRIC EMPTYING

For most clinicians, the scintigraphic assessment of the emptying rate of a liquid, solid or liquid/solid meal represents the primary investigational tool for the detection of gastric motor dysfunction in the diabetic, or in other clinical situations<sup>[1]</sup>. Scintigraphy is widely available and should be within the capabilities of any nuclear medicine department. By using different isotopes to label liquid and solid, one can either separately or simultaneously measure the rate of emptying of the

liquid and solid components of the meal. Apart from the radiation exposure involved, this is a relatively noninvasive test. Importantly, in an area of medicine where most data is qualitative, scintigraphy provides truly quantitative data. Of the various meals available, the emptying rate of indigestible solids is the most sensitive in detecting gastric motor dysfunction but, in practice, a semi-solid meal such as chicken liver or scrambled eggs is more practical and appears to yield clinically relevant results in the diabetic population. It is important to be aware, however, that several technical factors may significantly influence the results of gastric emptying studies. For this reason, it is recommended that each laboratory defines its own normal values, obtained using its particular meal and imaging technique. As mentioned already, one also needs to be aware of the limitations of gastric emptying tests in the evaluation of symptoms, given the often imperfect correlation between symptoms and gastric emptying rate.

In normal individuals, the emptying curve for a liquid meal follows a simple exponential pattern. Liquid emptying is thought to reflect the effects of a pressure gradient generated by an increase in fundic tone. Autonomic neuropathy, such as occurs in diabetes, leads to a loss of fundic accommodation and can lead to an acceleration of liquid emptying. The normal emptying curve for solid meals is quite different. Initially, following solid ingestion, no emptying takes place (the lag phase). This lag phase corresponds to the time it takes for high amplitude antral contractions to grind down, or triturate, the solid particles of the meal until they are small enough to empty, suspended in the liquid phase, through the pylorus. Once trituration has been accomplished, solid emptying now follows an exponential pattern similar to that of the liquid phase. In diabetes, impaired antral contractility will lead to a prolonged lag phase and a significant prolongation of the total time for gastric emptying of solids. From gastric emptying curves, a number of parameters can be obtained and used to describe the rate of gastric emptying. These include the time it takes for half of the meal to be emptied ( $t_{1/2}$ ) and the percentage of the meal that has been emptied at a given time, such as at 30 minutes, 1 hour or 2 hours.

Internal Medicine-Gastroenterology and Hepatology, University of Nebraska Medical Center, Nebraska, USA

**Correspondence to:** Eamonn M.M. Quigley, M.D., Internal Medicine Gastroenterology and Hepatology, University of Nebraska Medical Center, 600S. 42nd St, Omaha, Nebraska 69198-2000, USA  
Tel. +402-559 Ext.4356, Fax.+402-559 Ext.9004

Received 1999-05-19

Indigestible solids are emptied only on return of the fasting motor pattern, long after meal ingestion. Phase 3, a band of high amplitude contractions which periodically sweeps through the gastrointestinal tract while fasting, empties indigestible particles. Typically, antral Phase 3 activity is lost in those with advanced autonomic neuropathy; thus, their predilection for bezoar formation.

Several alternatives have recently become available for the assessment of gastric emptying. Of greatest potential for clinical relevance is the description of a breath test based on  $^{13}\text{C}$  octanoic acid<sup>[2]</sup>. As this is a stable isotope, radiation exposure is not involved and this test has the potential to become an office-based assessment of gastric motor function. Preliminary studies demonstrate good intra-individual reproducibility, though correlations with scintigraphy have not been perfect. Ultrasonography can evaluate antral contractile activity and can provide an indirect assessment of gastric emptying rate. It is, however, highly dependent on the presence of a skilled ultrasonographer, and provides a relatively brief assessment of antral motor function. Magnetic resonance imaging can provide, not only a global assessment of gastric emptying, but also detailed information on regional gastric function. Given the costs of this methodology, it is unlikely, however, that it will achieve widespread use as a test of gastric function. Others have evaluated impedance-based techniques in the assessment of gastric emptying. Again, it seems unlikely that these will achieve widespread use in clinical practice, despite promise in clinical research.

### ELECTROGASTROGRAPHY

Electrogastrography has been available since the turn of the century for the assessment of gastric electrical activity. Recent advances in electronics have considerably simplified this approach to the assessment of gastric motor function. ECG-type electrodes, placed on the abdominal wall over the surface markings of the stomach, are used to record gastric electrical activity. Direct comparisons with serosal electrodes have demonstrated that surface electrogastrography accurately records a representation of gastric slow wave activity. Typically, electrogastrographic recordings are performed, first in the fasting state and then following administration of a meal. Two parameters are of primary importance, namely, the prevalence of abnormal gastric rhythms (such as bradygastria and tachygastria) and secondly, the change in the amplitude (or "power") of the EGG following meal ingestion. In normal circumstances, the EGG power should increase significantly following a meal.

Electrogastrography is a relatively simple and noninvasive technique<sup>[3]</sup>. Several studies have clearly demonstrated that it can reproducibly record a representation of the gastric slow wave and that it can detect dysrhythmias in the fasting and post-prandial states. This technique is, however, highly susceptible to motion artifact and is therefore only appropriate for recordings in relatively still individuals. Signal amplification and processing are required to produce a meaningful trace but this is now readily provided by commercially available equipment. The greatest limitation to electrogastrography now lies in its clinical application. Despite the suggestion that it could serve as a screening test of gastric function, few studies have compared the relative value of electrogastrography to other modalities such as scintigraphy, in the assessment of gastric motor function. Available data has indeed provided somewhat conflicting results. Until truly prospective studies examine the role of electrogastrography in detecting gastric motor dysfunction among patients with a variety of gastrointestinal symptoms and provide direct comparisons, not only in terms of efficacy, but also in terms of cost and patient acceptability, with other commonly available modalities, the place of electrogastrography will remain uncertain.

### MANOMETRY

Antral motility serves to grind down or triturate the meal. In assessing antral motor function, an important goal, therefore, is to record the frequency, amplitude and propagation of antral contractions. As gastric emptying also depends, in large part, on coordination between the antrum, pylorus and duodenum, an assessment of coordinated antral, pyloric and duodenal activity has become a further goal of tests applied to this area. Ultrasonography, by detecting dynamic changes in antral diameter over time, can also assess antral contractile activity. Recordings, are, however, usually short-lived and are most successful with a liquid meal. They are also highly-dependent on a high level of skill of the interpreter. For this reason, manometry remains the primary technique for the direct assessment of antral contractile activity<sup>[4]</sup>. Most commonly, this is performed using a multi-lumen perfused catheter assembly passed via the nares and positioned under fluoroscopy, so that sensors simultaneously record intraluminal pressure activity from the antrum, duodenum and jejunum. To accurately record antro-pyloric activity, multiple closely-spaced sensors must be employed. Otherwise, oral displacement of the assembly, on meal ingestion, will lead to loss of contact between sensors and the antrum and the pylorus in the post-

prandial period and lead to uninterpretable artifact. Some have recommended the inclusion of a "sleeve" device to accurately monitor pyloric activity.

In order to record normal variations in both fasting and postprandial motor activity, some have advocated the use of a solid-state assembly. Because they do not rely on perfusion, these assemblies permit prolonged ambulatory recordings in the patient's usual environment. During fasting, several cycles of the migrating motor complex can be evaluated and the response to a number of meals can also be assessed. Most importantly, recordings can be performed during sleep and diurnal variations in motor patterns thereby assessed.

Regardless of which technique is employed, the primary goals of antroduodenal manometry are to assess antral and duodenal intraluminal pressure changes during fasting and in response to the meal and also to provide an assessment of antro-duodenal coordination. During fasting, motor activity in the antrum and duodenum is organized into the migrating motor complex. Each cycle of this complex comprises three phases which occur in sequence and continue to recur as long as the individual remains fasted. Each cycle lasts between 90 and 120 minutes and begins with Phase 1, or motor quiescence. This is followed by sporadic or irregular activity, Phase 2, which increases in intensity over time and culminates in the most distinctive phase of the migrating motor complex, Phase 3 (or the activity function), a band of uninterrupted rhythmic contractions which migrates slowly in an aboral direction along the length of the intestine. The migrating motor complex is initiated in the proximal small intestine and is typically associated with the onset of related activity in the stomach. Thus, for example, Phase 3 in the duodenum is associated with intense rhythmic contractile activity in the antrum. Following meal ingestion, the migrating motor complex is abolished and is replaced in the duodenum, by irregular but intense contractile activity (the postprandial motor response) and in the antrum by intense and relatively rhythmic high amplitude contractions. The duration of this postprandial response depends on the volume and caloric content of the meal and can vary anywhere from 2 to 6 hours. If no further food is ingested, the migrating motor complex returns. At night, migrating motor complex activity is usually most prominent but differs in that Phase 2 activity is markedly suppressed or even may be absent. The migrating motor complex at night, therefore, features Phase 3 complexes in relative isolation.

Antroduodenal manometry provides a direct and simultaneous measure of intraluminal pressure changes in the antrum and duodenum. Normal

patterns of motor activity in the antrum and duodenum have now been defined and the manometric features of several disease states, including intestinal neuropathy, autonomic neuropathy and intestinal myopathy, have been defined. This is, however, an invasive test and requires prolonged (at least 4 hours) recordings during fasting and following meal ingestion. Several recent studies have emphasized the importance of intrinsic variations in normal patterns of antral and duodenal motor activity. Furthermore, the clinical significance of some reported "abnormal" patterns has been disputed. What then is the role of antroduodenal manometry in the assessment of gastric motor function. My own belief is that its primary role lies in the definition of normal motility among those in whom there is some suggestion of dysmotility, yet, less invasive studies have proven either inconsistent, uninterpretable or unexpectedly normal<sup>[5]</sup>. More problematic is the definitive diagnosis of the underlying cause of dysmotility in an individual patient. The sensitivity and specificity for manometry in the detection of neuropathy and myopathy have been questioned and the range of normal variation continues to be extended. I am most happy therefore, when manometry is entirely normal, in this situation, I feel confident in reassuring the patients and their physicians that there is no evidence of a primary motor disorder of the upper gastrointestinal tract. In the diabetic patient, manometry should rarely prove necessary. If symptoms are appropriate and screening tests such as scintigraphy, ultrasonography, other tests of gastric emptying or electrogastrography prove abnormal, then there should be no need to proceed to manometry. It should be reserved for those patients with symptoms suggestive of dysmotility and in whom the less invasive tests have proven inconclusive.

#### TESTS OF FUNDIC TONE

In contrast to the antrum, where high amplitude contractile activity is the most important feature of normal motor function, the proximal stomach mediates its motor function primarily through the generation of, and fluctuations in tone. Following meal ingestion, the fundus and proximal corpus undergoes vagally-mediated relaxation (receptive relaxation) to accommodate the meal. Subsequent fluctuations in proximal gastric tone mediate emptying of liquids and solid particles suspended in the liquid phase. Manometry is not valuable in the assessment of proximal gastric function and, until recently, this was a relatively unexplored area of the gastrointestinal tract. The development of the barostat, a technique which can record fluctuations in pressure or volume within an organ while the

other parameter is varied, has provided tremendous insights into the function of the proximal stomach in health and in a variety of disease states, including diabetic gastropathy. A clinical role for the barostat, or other techniques to assess compliance and accommodation, has not, as yet, been established.

#### GASTROINTESTINAL FUNCTION IN DIABETES

Diabetes may be associated with several effects on gastrointestinal motor function. These include gastroparesis, accelerated emptying of liquids, esophageal dysmotility, small intestinal dysmotility (including the pseudo-obstruction syndrome), delayed colonic transit, megacolon and fecal incontinence. For this reason, the term diabetic gastroenteropathy is to be preferred over the more commonly used term diabetic gastroparesis<sup>[6]</sup>. The latter has become outmoded and is indeed misleading as it suggests, firstly, the limitation of diabetic dysmotility to the stomach and, secondly, a preponderance of delayed gastric emptying. As already mentioned, liquid emptying may, in fact, be accelerated in diabetes. Reflecting this spectrum of dysfunction, there is a similarly wide-range of symptomatology in diabetic gastroenteropathy. Thus, esophageal dysfunction may lead to dysphagia, gastroparesis to nausea, vomiting, postprandial fullness and abdominal pain, and accelerated emptying to the features of the "dumping syndrome". Delayed intestinal and colonic transit may contribute to constipation and abdominal pain, and rapid intestinal transit to diarrhea. Gall bladder dysfunction may contribute to the prevalence of gallstones among these patients and neuropathy of the anal sphincter to incontinence.

Diabetic gastropathy is common and has been reported in up to 50% of patients with long-standing Type I diabetes mellitus. While most prevalent among those with Type I diabetes, it is clear from recent studies that gastropathy may be equally prevalent among those with Type II disease. In the general population, therefore, Type II related gastropathy will be most common. Gastropathy is usually, but not invariably, associated with an autonomic neuropathy. Consequences of gastropathy may include delayed emptying of solids and indigestible particles, rapid emptying of liquids, bezoar formation, malnutrition and weight loss.

Gastric emptying rate may also influence blood sugar control. Delayed gastric emptying may lead to hypoglycemia. If a meal is not emptied and insulin continues to be administered timed to a meal, hypoglycemia will result indeed, unexplained hypoglycemia should always lead to a suspicion of gastric emptying delay. It has been suggested that accelerated emptying could contribute to hyperglycemia, but recent studies suggest a

relatively minor role for gastric emptying rate in the pathogenesis of postprandial hyperglycemia, among those with Type II diabetes and accelerated gastric emptying. Recent studies have also emphasized the variability of gastric emptying rate within a given diabetic patient. Thus, longitudinal studies have demonstrated that even in the same individual, gastric emptying may be, at different times, normal, accelerated or delayed<sup>[7]</sup>. This observation is extremely important in the assessment of therapeutic interventions. Furthermore, symptoms and gastric emptying rate correlate poorly in diabetics as in other patients with gastric dysmotility. While severely delayed emptying is consistently associated with delayed postprandial vomiting of undigested material, more modest degrees of delay bear an inconsistent relationship to such symptoms as early satiety, postprandial fullness, bloating, nausea and vomiting.

While tests of gastric emptying will remain, for the foreseeable future, the cornerstone of the evaluation of the diabetic with suspected gastric dysmotility, the clinician needs to be aware of their limitations. Normal gastric emptying does not exclude the stomach as the origin of the patient's symptoms, neither does delayed emptying, implicating the stomach as the cause of their symptoms. It is to be hoped that future studies will serve to further define relationships between symptoms, motor function and therapeutic response in this population. Diabetic gastropathy has traditionally been ascribed to the effects of extrinsic autonomic denervation. Recently, a role for hyperglycemia has been emphasized<sup>[6]</sup>. Studies involving normal individuals, as well as patients with diabetes mellitus, have illustrated the potential of hyperglycemia to delay gastric emptying, suppress the gastric component of the migrating motor complex, induce antral hypomotility and provoke gastric dysrhythmias, such as tachygastria. Furthermore, some recent work in an animal model has suggested the direct involvement of the enteric nervous system and gastrointestinal smooth muscle in diabetes. Finally, the acid-base and electrolyte abnormalities associated with this complication may lead to the development of ileus and gastroparesis during the course of ketoacidosis.

#### MANAGEMENT OF DIABETIC GASTROENTEROPATHY

In the approach to a patient with gastrointestinal dysmotility, several factors need to be addressed. These include the patient's nutritional status, pain management, prokinetic therapy, symptom suppression and the consideration of endoscopic or surgical approaches. Attention to nutritional status is of paramount importance in the management of these patients. Specific deficiencies should be identified and appropriate replacement instituted. In patients with gastroparesis, a low fat, low

residue diet should be instituted, given the known effects of these dietary factors on gastric emptying rate and, in the diabetic patient, on bezoar formation. Several options are now available, in terms of the form and mode of delivery of nutrition, for the patient with gastroparesis and gastroenteropathy. In the first instance, every attempt should be made to institute an adequate nutritional intake via the oral route, by the use of diets of variable composition and consistency, and the addition of appropriate oral supplements. For the patient who cannot tolerate or achieve an adequate caloric intake by the oral route, either in the short or in the long-term, a number of alternatives are available. In the short-term, enteral nutrition can be delivered via a nasogastric or nasoenteric tube. If oral intake cannot be reinstated in the long-term, access to the gastrointestinal tract may be achieved through a gastrostomy or jejunostomy. One approach is to commence enteral feeding via the nasogastric or nasoenteric route on a trial basis. If this is tolerated, a jejunostomy is placed and continued in the long-term. In patients with severe gastroparesis, gastrostomy feeding may, by definition, prove unsuccessful. A gastrostomy may, however, help by allowing the patient to periodically "vent" the stomach and relieve distressing distention and bloating. Indeed, one approach to the management of patients with severe intractable gastroparesis is the simultaneous placement of a gastrostomy for venting and a jejunostomy for enteral feeding.

Several pharmacological agents are available for the management of patients with diabetic gastropathy. These include prokinetic and antiemetic agents, analgesics for pain management, agents that modulate sensation and other symptomatic remedies. The first prokinetic agents were non-specific cholinergic agonists such as bethanechol. While these agents were capable of stimulating gastric emptying, there is little evidence for efficacy in gastrointestinal motor disorders and their use was complicated by a high prevalence of side effects outside of the gastrointestinal tract. Metoclopramide, a dopamine antagonist, represented, therefore, a significant advance in prokinetic therapy<sup>[8]</sup>. Through its central actions, metoclopramide is an effective antiemetic, its peripheral actions lead to an acceleration of gastric emptying and promote esophageal motor activity. While metoclopramide has been shown to be effective, in the short-term, in the symptomatic therapy of diabetic gastroparesis, its long-term use has been complicated by tolerance and a relatively high prevalence of central nervous and hyperprolactinemia-related side effects. One advantage of metoclopramide, however, is its availability in several formulations, not only in tablet form but also as a suspension and for

subcutaneous injection. Domperidone, another dopamine antagonist, does not cross the blood-brain barrier and is therefore not associated with the central nervous system, extrapyramidal side effects which have complicated metoclopramide use. It is, however, both an antiemetic and prokinetic and has been shown to be valuable in the symptomatic management of patients with diabetic gastroparesis<sup>[9]</sup>. It may cause hyperprolactinemia, however, and is not, as yet, approved for use in the United States.

Cisapride facilitates acetylcholine release in the enteric nervous system through a 5HT-4-mediated affect and has been shown to promote motor activity along the length of the gastrointestinal tract. It has been shown to accelerate liquid and solid emptying both in the short-term (6weeks) and to sustain this effect beyond one year<sup>[10,11]</sup>. It has, therefore, become an important component of the management of patients with gastroparesis and other gastrointestinal motor disorders. It is available in tablet and suspension form. Concerns have recently been raised regarding its potential to induce cardiac conduction and rhythm disturbances, especially when employed in conjunction with agents which modify its metabolism. This agent should not, therefore, be used in conjunction with agents which are known to inhibit cytochrome P-450 3A4 metabolism in the liver or in individuals predisposed to cardiac conduction or rhythm abnormalities.

Erythromycin acts as a motilin agonist to stimulate motor activity, primarily in the upper gastrointestinal tract. When given intravenously, erythromycin in low doses (50mg - 100mg) is a potent gastro-prokinetic and will effectively correct gastroparesis even in patients with refractory symptoms. Intravenous erythromycin has become, therefore, an important component of the management of patients with intractable diabetic gastroparesis, particularly in those who require hospitalization<sup>[12]</sup>. Oral erythromycin, even when used in suspension form, has proven disappointing. Whether this reflects the relatively poor bioavailability of this agent, or the development of tolerance, remains unclear. The latter seems less likely given the recent demonstration of the long-term efficacy of intravenous administration for up to 18 months in patients with refractory gastroparesis<sup>[13]</sup>. Several related compounds are currently under investigation. The goal is to produce an agent with minimal antibiotic activity but similar prokinetic properties to erythromycin and which is effective when administered orally.

Among patients with diabetic gastropathy, nausea is a prominent symptom. Many of these patients describe awaking each morning with nausea and, in fact, find nausea a much more distressing

symptom than vomiting. For this reason, antiemetic agents assume an important role in the symptomatic treatment of these patients. Some of the prokinetic agents, such as metoclopramide and domperidone, have antiemetic actions whereas others, such as cisapride and erythromycin do not. In these latter circumstances, an antiemetic such as a phenothiazine derivative or a 5HT-3 antagonist should therefore be used in conjunction, and can often be used successfully on a p.r.n. basis. In choosing a particular antiemetic, attention should be paid to whether they are available in the appropriate formulation, as well as to their duration of action and, of course, cost.

### SURGERY IN THE MANAGEMENT OF DIABETIC GASTROPARESIS

In general, there is no role for gastrectomy, either partial or complete in the patient with diabetic gastroparesis. Limited experience suggests a poor response to this approach, which is no surprise, given the relatively diffuse involvement of the gastrointestinal tract in this disorder. The surgical approach which has achieved significant importance is the simultaneous placement of a gastrostomy and jejunostomy in patients with intractable gastroparesis who are unable to tolerate p.o. intake and who have significant distention. Nowadays this can be most efficiently and effectively achieved by the laparoscopic approach. An endoscopic approach which involves the simultaneous placement of a gastrostomy and jejunostomy has also been advocated but experience has been inconsistent. Most recently, electrical pacing of the stomach, through electrodes surgically implanted on the surface of the stomach, using a cardiac-type pacemaker, has been shown, in pilot studies, to produce a dramatic reduction in symptoms and a variable improvement in gastric emptying rate in intractable gastroparesis<sup>[14-16]</sup>. Randomized, prospective controlled studies are currently in progress and results are eagerly awaited.

### THE APPROACH TO GASTRIC DYSMOTILITY IN DIABETIC PATIENTS

In this review, the status of currently available tests for the evaluation of gastric motor function has been discussed. Limitations have been highlighted and, in particular, the often-times poor correlation between symptoms and objective evidence of motor dysfunction emphasized. How should the clinician approach the evaluation and management of the patient with diabetes who has symptoms suggestive of dysmotility? Firstly, mindful of the non-specificity of symptoms, the clinician should ensure that mucosal or mechanical causes have been ruled

out. In particular, consideration should be given to peptic ulcer disease, gastro-esophageal reflux disease and low-grade intestinal obstruction. Medications should be carefully reviewed for iatrogenic causes of nausea and vomiting and the possible contribution of psychological factors, and depression, in particular, borne in mind. If, at this stage, symptoms remain unexplained, two options are available. One begins with a screening test of gastric function such as gastric emptying scintigraphy (or electrogastrography) and then decides on further therapy based on its results. The second approach is to initiate empiric therapy with a prokinetic or prokinetic/anti-emetic combination. Testing, in this approach, is limited to those who fail to respond to therapy. More detailed and invasive tests of motor function such as manometry should be reserved for those with persisting and disabling symptoms who do not respond satisfactorily to empiric therapy.

### REFERENCES

- 1 Minami H, McCallum RW. The physiology and pathophysiology of gastric emptying in humans. *Gastroenterology*, 1984;86:1592-1610
- 2 Choi MG, Camilleri M, Burton DD, Zinsmeister AR, Forstrom LA, Nair KS. Reproducibility and simplification of <sup>13</sup>C octanoic acid breath test for gastric emptying of solids. *Am J Gastro*, 1998;93:92-98
- 3 Camilleri M, Hasler WL, Parkman HP, Quigley EMM, Soffer E. Measurement of gastroduodenal motility in the gastrointestinal laboratory. *Gastroenterology* (In press)
- 4 Quigley EMM. Gastric and small intestinal motility in health and disease. *Gastro Clin N Amer*, 1996;25:113-145
- 5 Byrne KG, Quigley EMM. Antroduodenal manometry: an evaluation of an emerging methodology. *Dig Dis*, 1997;15:53-63
- 6 Quigley EMM. The pathophysiology of diabetic gastropathy—more vague than vagal. *Gastroenterology*, 1997;115:1790-1794
- 7 Nowak TV, Johnson CP, Kalbfleisch JH, Roza AM, Wood CM, Weisbruch JP, Soergel KH. Highly variable gastric emptying in patients with insulin-dependent diabetes mellitus. *Gut*, 1995;37:23-29
- 8 Malagelada JR, Rees WDW, Mazzotta LJ, Go VLW. Gastric motor abnormalities in diabetic and post-vagotomy gastroparesis; effect of metoclopramide and bethanechol. *Gastroenterology*, 1980;78:286-293
- 9 Silvers D, Kipnes M, Broadstone V, Patterson D, Quigley EMM, McCallum R, Joslyn A. Domperidone significantly improves gastrointestinal symptoms associated with diabetic gastroparesis. *Gastroenterology*, 1997;112:A826
- 10 Camilleri M, Malagelada JR, Abell TL, Brown ML, Hench V, Zinsmeister AR. Effect of six weeks of treatment with cisapride in gastroparesis and intestinal pseudo-obstruction. *Gastroenterology*, 1989;96:704-712
- 11 Abell TL, Camilleri M, DiMaggio EP, Hench VS, Zinsmeister AR, Malagelada JR. Long term efficacy of oral cisapride in symptomatic upper gut dysmotility. *Dig Dis Sci*, 1991;36:616-620
- 12 Janssens J, Peeters TL, Vantrappen G, Tack J, Urbain JL, De Roo M, Muls E, Bouillon R. Improvement of gastric emptying in diabetic gastroparesis by erythromycin. *N Engl J Med*, 1990;322:1028-1031
- 13 DiBaise JK, Quigley EMM. Efficacy of long term intravenous erythromycin in the treatment of severe gastroparesis: one center's experience. *Am J Gastro*, 1997;92:1613
- 14 Familoni BO, Abell TL, Voeller G, Galem A, Gaber O. Electrical stimulation at a frequency higher than basal rate in human stomach. *Dig Dis Sci*, 1997;42:885-891
- 15 McCallum RW, Chen JDZ, Lin Z, Schirmer BD, Williams RD, Ross RA. Gastric pacing improves emptying and symptoms in patients with gastroparesis. *Gastroenterology*, 1998;114:456-461
- 16 Tougas G, Huizinga JD. Gastric pacing as a treatment for intractable gastroparesis: shocking news? *Gastroenterology*, 1998;114:598-601

# Assessment of severity of acute pancreatitis: a comparison between old and most recent modalities used to evaluate this perennial problem

Raffaele Pezzilli and Francesco Mancini

**Subject headings** pancreatitis/diagnosis; pancreatitis/radiography; severity assessment; evaluating studies

Acute pancreatitis is an acute inflammatory process of the pancreatic gland. According to the Atlanta classification system, there are two forms of acute pancreatitis: mild acute pancreatitis, characterized by interstitial edema, which is self-limiting and severe acute pancreatitis characterized by local complications such as necrosis, abscesses, pseudocysts and the presence of organ dysfunction<sup>[1]</sup>. The mortality due to severe pancreatitis is about 25%-50% and is due mainly to infection of the necrosis<sup>[2]</sup>. Early identification of patients with severe acute pancreatitis is essential for the correct care of the disease and the avoidance of complications.

Over the past 20 years, many schemes have been proposed for identifying severe pancreatitis. The aim of this paper is to review the current criteria for the early assessment of severity of acute pancreatitis.

## CLINICAL CRITERIA

Bank *et al*<sup>[3]</sup> analyzed the incidence of cardiac, pulmonary, kidney, hematological, metabolic and neurological complications in 75 patients with acute pancreatitis and they reported a mortality rate of 56% if one or more complications were present. Subsequently, Agarwall and Pitchumoni<sup>[4]</sup> conducted a retrospective study involving 76 patients and proposed a scheme comprised of simplified clinical criteria. In both studies, a 48-hour observation period was necessary for the clinical criteria. Furthermore, these clinical assessments depend on the experience of the clinical team and are difficult to standardize.

## CLINICAL AND LABORATORY CRITERIA

Ranson *et al*<sup>[5]</sup> identified a series of 11 criteria

Emergency Department, Sant'Orsola Hospital, Bologna, Italy  
**Correspondence to:** Raffaele Pezzilli, Medicina d'Urgenza e Pronto Soccorso, Ospedale Sant'Orsola, Via Massarenti 9, 40138 Bologna, Italy  
Tel. +39-51-6364701, Fax. +39-51-6364794  
Email.pezzilli@orsola-malpighi.med.unibo.it  
**Received** 1999-06-21

evaluated in 100 patients with acute pancreatitis in 1974. The Ranson score is still widely used at present in judging severity. Five of the 11 criteria are considered upon hospital admission and 6 in the following 48 hours. They reported that most patients with less than two positive items survived; in those with 3 or 5 positive items, the mortality rate was about 20%, and in those with 6 or more positive items, the mortality reached about 50%. There is a correlation between 3 or more Ranson positive criteria and the high incidence of pancreatic necrosis and systemic complications. Later studies confirmed a sensitivity from 40% to 90%<sup>[4,6]</sup>. The Ranson score has been recently criticized for the following reasons: a good assessment of severity requires the determination of all items and requires 48 hours of observation for the judgement of severity, thus delaying the proper treatment after the onset of pain. Talamini *et al*<sup>[7]</sup> have simplified the original Ranson score by evaluating only the items considered on admission and concluded that this simplified system is of little use for predicting severity. Finally, this criteria correlate to the severity of acute pancreatitis only at the opposite ends of the scheme (<2 and >6 items) but not between 3 and 5 positive items. Twelve to 24 hours after the onset of pain, the score is completely useless. It can be applied only to biliary pancreatitis and the same authors have therefore proposed a new modified score<sup>[8]</sup>.

Imrie *et al*<sup>[9]</sup> have proposed a score called the Glasgow score which seems to be more precise than that of Ranson, with a sensibility for the assessment of severe acute pancreatitis of 56%-85%<sup>[10,11]</sup>.

Another simplified score has been set up by Fan *et al*<sup>[12]</sup>, utilizing only two biochemical parameters (azotemia and glycemia). This score system has a sensitivity of about 75% in the assessment of the severity of acute pancreatitis.

More recently the APACHE II score<sup>[13]</sup> which takes into consideration age, presence of chronic associated diseases and some biochemical parameters has been proposed for the assessment of the severity of acute pancreatitis. Wilson *et al*<sup>[14]</sup> have reported a score of 6.3 in patients with mild acute pancreatitis, of 9.4 in those with severe pancreatitis and of 14.1 in those with fulminant pancreatitis.

## BIOCHEMICAL CRITERIA

The search for a marker able to evaluate the severity of acute pancreatitis at the early stage is the aim of the present research in the field of pancreatology. The evaluation of the severity of acute pancreatitis by means of serum pancreatic enzyme determination has been a boon<sup>[15-17]</sup>. We recently evaluated serum amylase and lipase in 66 patients with acute pancreatitis<sup>[15]</sup>. Most of these patients were studied within 24 hours from the onset of pain. Twenty patients had no alterations of the pancreatic gland at imaging, 36 had pancreatic edema and 10, pancreatic necrosis. The elevation of the serum pancreatic enzymes overlapped in the three groups.

The determination of serum C-reactive protein<sup>[18]</sup> is at present widely used for the assessment of the severity of acute pancreatitis. Serum levels of this protein greater than 100mg/L indicate a severe acute pancreatitis in about 60%-80% of the cases. The determination of the C-reactive protein is easy to perform and inexpensive. However, its sensitivity is good only after the first 48 hours from the onset of pain<sup>[6,19]</sup>.

Granulocyte elastase has been evaluated in the search for biochemical markers able to evaluate the severity of acute pancreatitis even earlier than the C-reactive protein determination. This protein is released by activated neutrophils and it is able to damage cellular membranes and the extracellular matrix. Gross *et al*<sup>[20]</sup> and Dominguez-Munoz *et al*<sup>[21]</sup> have reported that 70%-80% of the patients with severe acute pancreatitis studied within 48 hours from the onset of the pain were correctly identified using this protein. More recently interleukin 6, released by activated macrophages and the interleukin 8 released by neutrophils have been proposed as markers of the severity of acute pancreatitis. These two cytokines are released rapidly in severe forms of acute pancreatitis (within 24 hours from the onset of pain) and have a specificity greater than that of C-reactive protein (80%-100%)<sup>[22-24]</sup>.

The soluble receptor of interleukin 2, which is released by the activated lymphocytes is able to identify 70% of the patients with severe acute pancreatitis studied within 24 hours from the onset of pain<sup>[25]</sup>. We have demonstrated<sup>[26]</sup> that the human pancreatic secretory trypsin inhibitor, produced by the pancreatic acinar cells and the hepatocytes is able to correctly identify 70% of the cases studied within 24 hours from the onset of pain. All these studies demonstrate that the immune system is early activated at an early phase during the course of acute pancreatitis. However, the determination of these proteins, except for C-reactive protein and granulocyte elastase, is not feasible for routine use. We hope that in the near

future simple techniques for the determination of these proteins will be developed.

## RADIOLOGICAL CRITERIA

Balthazar *et al*<sup>[27]</sup> have demonstrated that contrast enhanced computed tomography is able to assess the severity of acute pancreatitis. They divided the severity of acute pancreatitis into 5 categories. In 83 patients with acute pancreatitis, they found that the mortality was nil in stages A, B and C, and reached 17% in those of grade E. The findings of left-sided or bilateral effusions on chest radiograph within 24 hours of admission were associated with a severe outcome<sup>[28]</sup>.

## RADIOLOGICAL AND BIOCHEMICAL CRITERIA

Serum creatinine greater than 152.6  $\mu\text{mol/L}$  and/or the presence of pathological chest radiographs (pulmonary densification and/or pleural effusions) are capable of identifying, within 24 hours of admission to the hospital, subgroups of both patients at higher risk of adverse clinical outcome and of patients with necrotizing pancreatitis<sup>[29]</sup>.

## CONCLUSION

In conclusion, the Ranson, Glasgow and Fan criteria are at present useful in clinical practice for their simplicity and low costs. The APACHE II score gives useful information in patients with a more severe form of acute pancreatitis. Serum determination of interleukins may play a role in the assessment of the severity of acute pancreatitis only when rapid techniques for their determination are developed. At present, C-reactive protein is the marker which is the easiest to perform and which has the lowest cost. The evaluation of both chest radiographs and serum creatinine is also simple to carry out in the Emergency Room.

## REFERENCES

- 1 Bradley EL. A clinically based classification system for acute pancreatitis. Summary of the International Symposium on Acute Pancreatitis, Atlanta, GA, September 11 through 13, 1992. *Arch Surg*, 1993;128:586-590
- 2 Banks PA. Predictors of severity in acute pancreatitis. *Pancreas*, 1991;6(Suppl 1):S7-S12
- 3 Bank S, Wise L, Gersten M. Risk factors in acute pancreatitis. *Am J Gastroenterol*, 1983;78:637-640
- 4 Agarwall N, Pitchumoni CS. Simplified prognostic criteria in acute pancreatitis. *Pancreas*, 1986;1:69-73
- 5 Ranson JHC, Rifkind KM, Roses DF, Fink SD, Eng K, Spencer FC. Prognostic signs and the role of operative management in acute pancreatitis. *Surg Gynecol Obstet*, 1974;139:69-81
- 6 Wilson C, Heads A, Shenkin A, Imrie CW. C reactive protein, antiproteases and complement factors as objective markers of severity in acute pancreatitis. *Br J Surg*, 1989;76:177-181
- 7 Talamini G, Bassi C, Falconi M, Sartori N, Frulloni L, Di Francesco V, Vesentini S, Pederzoli P, Cavallini G. Risk of death from acute pancreatitis. Role of early, simple "routine" data. *Int J Pancreatol*, 1996;19:15-24
- 8 Ranson JHC. The timing of biliary surgery in acute pancreatitis. *Ann Surg*, 1979;189:654-663

- 9 Imrie CW, Benjamin IS, Ferguson JC, McKay AJ, Mackenzie I, O'Neill JO, Blumgart LH. A single center double blind trial of Trasylol therapy in primary acute pancreatitis. *Br J Surg*, 1978;65:337-341
- 10 Blamey SL, Imrie CW, O'Neill J, Gilmour WH, Carter DC. Prognostic factors in acute pancreatitis. *Gut*, 1984;25:1340-1346
- 11 London NJM, Neoptolemos JP, Lavelle J, Bailey I, James D. Contrast-enhanced abdominal computed tomography scanning and prediction of severity of acute pancreatitis: a prospective study. *Br J Surg*, 1989;76:268-272
- 12 Fan ST, Choi TK, Lai ECS, Wong J. Prediction of severity of acute pancreatitis: an alternative approach. *Gut*, 1989;30:1591-1595
- 13 Knaus WA, Draper EA, Wagner DP, Zimmerman JE. APACHE II: a severity of disease classification. *Crit Care Med*, 1985;13:818-829
- 14 Wilson C, Heath DI, Imrie CW. Prediction of outcome in acute pancreatitis: a comparative study of APACHE-II, clinical assessment and multiple factor scoring systems. *Br J Surg*, 1990;77:1260-1264
- 15 Pezzilli R, Billi P, Miglioli M, Gullo L. Serum amylase and lipase concentrations, and lipase/amylase ratio, in the assessment of etiology and severity of acute pancreatitis. *Dig Dis Sci*, 1993;38:1265-1269
- 16 Pezzilli R, Billi P, Platè L, Bongiovanni F, Morselli Labate AM, Miglioli M. Human pancreas specific protein/procarboxypeptidase B: a useful serum marker of acute pancreatitis. *Digestion*, 1994;55:73-77
- 17 Gullo L, Ventrucci M, Pezzilli R, Platè L, Naldoni P. Diagnostic significance of serum elastase I in pancreatic disease. *Br J Surg*, 1987;74:44-47
- 18 Mayer AD, McMahon MJ, Bowen M, Cooper EH. C-reactive protein: an aid to assessment and monitoring of acute pancreatitis. *J Clin Pathol*, 1984;37:207-211
- 19 Pezzilli R, Billi P, Cappelletti O, Barakat B. Serum C-reactive protein in the acute biliary pancreatitis. Is it a reliable marker for the early assessment of severity of the disease. *Italian J Gastroenterol Hepatol*, 1997;29:554-557
- 20 Gross V, Scholmerich J, Leser HG, Salm R, Lausen M, Ruckauer K, Schoffel U, Lay L, Heinisch A, Farthmann EH, Gerok W. Granulocyte elastase in assessment of severity of acute pancreatitis. Comparison with acute phase proteins C-reactive protein,  $\alpha_1$  antitrypsin, and protease inhibitor  $\alpha_2$  macroglobulin. *Dig Dis Sci*, 1990;35:97-105
- 21 Dominguez Munoz JE, Carballo F, Garcia MJ, De Diego JM, Rabago L, Simon MA, de la Morena J. Clinical usefulness of polymorphonuclear elastase in predicting the severity of acute pancreatitis: results of a multicenter study. *Br J Surg*, 1991;78:1230-1234
- 22 Heath DI, Cruickshank A, Gudgeon M, Jehanli A, Shenkin A, Imrie CW. Role of interleukin 6 in mediating the acute phase protein response and potential as an early means of severity assessment in acute pancreatitis. *Gut*, 1993;34:41-45
- 23 Gross V, Andreesen R, Leser HG, Ceska M, Liehl E, Lausen M. Interleukin 8 and neutrophil activation in acute pancreatitis. *Eur J Clin Invest*, 1992;22:200-203
- 24 Pezzilli R, Billi P, Miniero R, Fiocchi M, Cappelletti O, Morselli Labate AM, Barakat B, Sprovieri G, Miglioli M. Serum interleukin 6, interleukin 8 and  $\alpha_2$  microglobulin in the early assessment of the severity of acute pancreatitis. A comparison with serum C-reactive protein. *Dig Dis Sci*, 1995;40:2341-2348
- 25 Pezzilli R, Billi P, Gullo L, Beltrandi E, Maldini M, Mancini R, Incorvaia L, Miglioli M. Behavior of serum soluble interleukin-2 receptor, soluble CD8 and soluble CD4 in the early phases of acute pancreatitis. *Digestion*, 1994;55:268-273
- 26 Pezzilli R, Billi P, Plate L, Barakat B, Bongiovanni F, Miglioli M. Human pancreatic secretory trypsin inhibitor in the assessment of the severity of acute pancreatitis. A comparison with C reactive protein. *J Clin Gastroenterol*, 1994;19:112-117
- 27 Balthazar EJ, Ranson JHC, Naidich DP, Megibow AJ, Caccavale R, Cooper MM. Acute pancreatitis: prognostic value of CT. *Radiology*, 1985;156:767-772
- 28 Pezzilli R, Billi P, Barakat B, Broccoli P, Morselli Labate AM. The use of the peripheral leukocyte count and chest X-ray in early assessment of the severity of acute pancreatitis in comparison with the Ranson score system. *Panminerva Med*, 1999;41:39-42
- 29 Talamini G, Uomo G, Pezzilli R, Rabitti PG, Billi P, Bassi C, Cavallini G, Pederzoli P. Serum creatinine and chest radiographs in the early assessment of acute pancreatitis. *Am J Surg*, 1999;177:7-14

*Invited Commentary*

# Bioartificial liver support for fulminant hepatic failure

Robert S. Brown, Jr.<sup>1</sup> and Howard J. Worman<sup>2</sup>

See article on page 308

## ORIGINAL ARTICLE

Effects of a bioartificial liver support system on acetaminophen-induced acute liver failure canines.

## MAJOR POINTS OF THE COMMENTED ARTICLE

Investigations of bioartificial liver support systems are rather novel in mainland China. In this issue of the *World Journal of Gastroenterology*, Xue *et al*<sup>[1]</sup> report on the safety and efficacy of a bioartificial liver support system developed in Hong Kong (TECA-I, TECA Ltd.) in dogs with fulminant hepatic failure. In the TECA-I bioartificial liver system, whole blood is perfused through hollow fiber tubes containing porcine hepatocytes. These investigators induced acute hepatocyte necrosis, as evidenced by elevations in the serum aminotransferase activities and subsequent histological examinations, by administering overdoses of acetaminophen (multiple injections of 115mg/kg). Fulminant hepatic failure with concomitant elevations in the serum ammonia concentrations resulted. Six of 9 dogs treated with TECA-I bioartificial liver system survived for more than 30 days, suggesting full recovery of hepatic function. In contrast, 10 dogs treated with either intravenous glucose or with arginine, glutamic acid and branch chain amino acids all died within 36 hours after treatment. These results represent an initial step towards clinical trials of a bioartificial liver support system in China.

## COMMENTARY

### *Fulminant hepatic failure*

The liver can fail acutely with rapid loss of hepatocyte function. In the otherwise healthy

individual, the presentation is dramatic and can cause mental status alterations, coma and a rapidly deteriorating course that leads to death. The term fulminant hepatic failure is used to describe the presence of hepatic encephalopathy in liver disease of short duration<sup>[2]</sup>.

There are several causes of fulminant hepatic failure including viral infections, drugs (overdose of acetaminophen is one example<sup>[3]</sup>), toxins, hemorrhagic shock, congestive heart failure, severe fluid depletion, sepsis and various metabolic derangements. In some hospitalized patients, the cause of fulminant hepatic failure may never be established. This may be because the patient deteriorates too rapidly for diagnostic testing to be completed or because the precipitating event, such as ingestion of a toxin or overdose of a drug, is not witnessed or reported.

Individuals with fulminant hepatic failure will have various signs and symptoms of liver dysfunction. As already mentioned, hepatic encephalopathy, with elevated serum ammonia concentrations, is part of the diagnosis. Increased intracranial pressure and cerebral edema can lead to irreversible brain damage and is a common cause of death. All patients are jaundiced with significantly elevated serum bilirubin concentrations. The serum prothrombin time is elevated and abnormal bleeding may result. Renal failure from acute tubular necrosis or hepatorenal syndrome often complicates the picture. Disseminated intravascular coagulation, infections, sepsis and respiratory failure may also occur. In contrast to individuals with cirrhosis, complications of portal hypertension such as ascites and bleeding esophageal varices are generally not significant problems in patients with fulminant hepatic failure.

In fulminant hepatic failure, aminotransferase activities may be markedly elevated as a result of the massive hepatocyte necrosis that occurs after a sudden insult to the liver. This is especially with sudden, massive hepatocyte necrosis seen in acetaminophen overdose<sup>[3]</sup> and shock liver<sup>[4]</sup>. Serum aminotransferase activities may only be elevated for a few days and then return to normal or near normal, despite the presence of severe hepatic dysfunction<sup>[3,4]</sup>. Therefore, their normalization does not necessarily indicate an improvement in

<sup>1</sup>Departments of Medicine and of Pediatrics, College of Physicians and Surgeons, Columbia University, New York, NY, USA

<sup>2</sup>Departments of Medicine and of Anatomy and Cell Biology, College of Physicians and Surgeons, Columbia University, New York, NY 10032 USA

**Correspondence to:** Dr. Robert S. Brown or Dr. Howard J. Worman, Department of Medicine College of Physicians and Surgeons, Columbia University, 630 West 168th Street, 10th Floor, Room 508, New York, NY 10032, USA  
Tel. (212)305-8156, Fax. (212)305-6443  
Email: hjw14@columbia.edu(Dr. Worman); rb464@columbia.edu (Dr. Brown)

Received 1999-07-14

condition because they cannot remain elevated if no more hepatocytes are left to die.

### **Treatment**

Hepatic stem cells (oval cells), which may originate in the bone marrow<sup>[5]</sup>, and/or hepatocytes can divide and are capable of repopulating a liver in which up to 90% of the hepatocyte mass is destroyed. In fulminant hepatic, complete recovery is therefore possible if the cause of hepatocyte death is reversed, adequate supportive care is provided, and cerebral edema does not occur. Unfortunately, many or most patients succumb before hepatocytes can regenerate to restore adequate liver function.

The treatment goal in fulminant hepatic failure is to keep the patient alive and free of serious complications either until: ① liver function spontaneously recovers or ② emergency liver transplantation, which is effective in cases of fulminant hepatic failure<sup>[6]</sup>, can be performed. A significant advance in treatment of it would be the ability to “buy time” either until adequate hepatocyte regeneration occurs and the patient recovers or until a donor organ becomes available for transplantation. If temporary liver support could be provided, the need for emergency transplantation may even be obviated as adequate function may eventually return in the damaged liver.

### **Bioartificial liver support**

One way to “buy time” in fulminant hepatic failure bioartificial liver support<sup>[7]</sup>. This is achieved with biomechanical devices in which plasma or blood is subjected to living hepatocytes extracorporeally. Several studies, including one of the first from China<sup>[1]</sup> reported in this issue of the *World Journal of Gastroenterology*, have reported experimental trials of bioartificial liver support systems in animals with fulminant hepatic failure.

In the United States and Europe, a few trials of bioartificial liver support devices have been conducted in human subjects. Several others are currently in progress. Clinical experience with bioartificial liver systems has focused on two different types of devices. The first, developed by Demetriou and colleagues<sup>[8]</sup> at Cedar Sinai Medical Center in Los Angeles, is now manufactured by Circe Biomedical (Lexington, MA). This device uses plasma perfusion and requires plasma separation with the Cobe Spectra (Lakewood, CO). The plasma is passed through a charcoal column, warmed and oxygenated and then passed through a hollow fiber cartridge containing approximately 40 grams of porcine hepatocytes. The hepatocytes are cryopreserved and thawed with a viability greater than 70% prior to use. Treatments are for 7 hours

per day. The second device, initially developed by Sussman and colleagues<sup>[9]</sup> at Baylor in Houston with the trade name Hepatix, is now being manufactured by VitaGen (La Jolla, CA). This device uses whole blood perfusion and a transformed human cell line, C3A cells, in its hollow fiber cartridge. This device can be used continuously. Both devices use venovenous access via a standard dual lumen dialysis catheter usually placed in the femoral vein.

The advantages of whole blood perfusion are simplicity, less personnel costs (no pheresis nurse required), the ability to use devices in parallel (e.g. continuous venovenous hemofiltration), ability to use the device continuously and lower volume loads. Plasma separation requires the use of large volumes of citrate resulting in both a volume load as well as a risk of hypocalcemia, which often requires continuous calcium infusion. It is also more labor intensive and requires an extra device. However, plasma separation does result in less hemolysis and thrombocytopenia and avoids the need for systemic heparin administration. Finally there is a potential advantage to the lack of cellular components in the cartridge, which could lead to immune activation. Overall the major advantages of whole blood perfusion, continuous use, devices in parallel, and lower volume loads makes this method preferable.

The ideal cells to populate a liver support system would be human liver cells. However, until human liver stem cells can be isolated reliably, this remains limited by shortage. Transformed human liver cells will make human proteins, are able to multiply, and will pack more densely in hollow fiber devices allowing for increased hepatocyte mass (approximately 100 grams). However, liver function is often variable and reduced compared with primary hepatocytes, particularly with regard to cytochrome p450 activity and glucuronidation<sup>[10]</sup>. Finally there are concerns regarding tumorigenic risk, particularly in patients who receive a liver transplant and subsequent immunosuppression. Non-human hepatocytes will have normal liver function but will make non-human proteins. There are also concerns regarding antibody responses to xenogenic tissues and potential zoonoses. Most research to date has used porcine hepatocytes due to availability of adequate mass of cells. The concerns regarding porcine endogenous retroviruses appear theoretical; no porcine retroviral sequences have been detected by reverse transcription-polymerase chain reaction in patients treated with the Circe device (Chris Stevens, MD, personal communication). Finally early clinical data has supported efficacy of porcine hepatocyte-based devices, including lowering intracranial hypertension in acute liver failure.

Phase I data on the circe liver assist system have been very encouraging. In a group of patients

with acute liver failure ( $n = 18$ ) or primary non-function of a transplanted liver ( $n = 3$ ), survival was 90% with one patient having spontaneous recovery<sup>[8]</sup>. Importantly, patients treated with the device had lower intracranial pressure readings during treatment. Among patients with acute or chronic liver dysfunction ( $n = 10$ ), results were worse with high mortality<sup>[8]</sup>. Thus the device is currently being tested only for patients with acute liver failure or primary non-function of a transplanted liver in a multi-center phase II/III randomized controlled clinical trial at liver transplant centers in the United States and Europe. This trial will likely complete enrollment in the next year. The device from VitaGen was previously tested under the trade name Hepatix in a non-controlled Phase I trial and a pilot controlled trial. In the Phase I trial 11 patients with acute liver failure were treated with 6 deaths, 1 spontaneous recovery and 4 transplants<sup>[9]</sup>. Neurologic or biochemical improvement was seen in 10 of 11 patients treated, but 5 of the 6 deaths were due to intracranial hypertension. In the controlled trial ( $n = 24$ ), there was no survival benefit seen either in transplant patients (78% survival among controls, 75% with the device,  $n = 17$ ) and 25% and 33% respectively among non-transplant patients<sup>[11]</sup>. This device is currently undergoing further phase I testing in the United States.

In summary, early clinical evidence supports some efficacy for bioartificial liver support systems in fulminant hepatic failure. Future discoveries in basic cell biology will undoubtedly lead to superior systems. Of those currently available, the porcine hepatocyte system is further developed. Additional

research and human clinical trials are needed to define the best cell lines, method of perfusion (whole blood vs plasma) and methods to expand the clinical indications for bioartificial liver support systems.

## REFERENCES

- 1 Xue YL, Zhao SF, Zhang ZY, Wang YF, Fi XJ, Huang XQ, Luo Y, Huang YC, Liu DG. Effects of a bioartificial liver support system on acetaminophen-induced acute liver failure canines. *World J Gastroenterol*, 1999;5:308-311
- 2 Bernau J, Rueff B, Benhamou JP. Fulminant and subfulminant hepatic failure: definitions and causes. *Sem Liver Dis*, 1986;6: 97-106
- 3 Prescott LF, Wright N, Roscoe P, Brown SS. Plasma-paracetamol half-life and hepatic necrosis in patients with paracetamol overdose. *Lancet*, 1971;i:519-521
- 4 Gitlin N, Serio KM. Ischemic hepatitis: widening horizons. *Am J Gastroenterol*, 1992;87:831-836
- 5 Petersen BE, Bowen WC, Patrene KD, Mars WM, Sullivan AK, Murase N, Boggs SS, Greenberger JS, Goff JP. Bone marrow as a potential source of hepatic oval cells. *Science*, 1999;284:1168-1170
- 6 Ascher NL, Lake JR, Emond JC, Roberts JP. Liver transplantation for fulminant hepatic failure. *Arch Surg*, 1993;128:677-682
- 7 Sussman NL, Gislason GT, Kelly JH. Extracorporeal liver support. Application to fulminant hepatic failure. *J Clin Gastroenterol*, 1994;18:320-324
- 8 Watanabe FD, Mullon CJ, Hewitt WR, Arkadopoulos N, Kahaku E, Eguchi S, Khalili T, Arnaout W, Shackleton CR, Rozga J, Solomon B, Demetriou AA. Clinical experience with a bioartificial liver in the treatment of severe liver failure: a phase I clinical trial. *Ann Surg*, 1997;225:484-491
- 9 Sussman NL, Gislason GT, Conlin CA, Kelly JH. The hepatix extracorporeal liver assist device: initial clinical experience. *Artif Organs*, 1994;18:390-396
- 10 Nyberg SL, Rimmel RP, Mann HJ, Peshwa MV, Hu WS, Cerra FB. Primary hepatocytes outperform Hep G2 cells as the source of biotransformation functions in a bioartificial liver. *Ann Surg*, 1994; 220:59-67
- 11 Ellis AJ, Hughes RD, Wendon JA, Dunne J, Langley PG, Kelly JH, Gislason GT, Sussman NL, Williams R. Pilot controlled trial of the extracorporeal liver assist device in acute liver failure. *Hepatology*, 1996;24:1446-1451

# Establishment and characterization of four human hepatocellular carcinoma cell lines containing hepatitis B virus DNA

Jae-Ho Lee<sup>1</sup>, Ja-Lok Ku<sup>1</sup>, Young-Jin Park<sup>1,2</sup>, Kuhn-Uk Lee<sup>2</sup>, Woo-Ho Kim<sup>3</sup> and Jae-Gahb Park<sup>1,2</sup>

**Subject headings** carcinoma, hepatocellular; liver neoplasms; hepatitis B virus; hepatitis x-antigen; cell line

## Abstract

**AIM** To investigate the characteristics of newly established four hepatocellular carcinoma cell lines (SNU-739, SNU-761, SNU-878 and SNU-886) from Korean hepatocellular cancer patients. **METHODS** Morphologic and genetic studies were done.

**RESULTS** All four lines grew as a monolayer with an adherent pattern, and their doubling times ranged from 20 to 29 hours. The viability rate was relatively high (88%-94%). Neither mycoplasmal nor bacterial contamination was present. The lines showed different patterns in fingerprinting analysis. The hepatitis B virus (HBV) DNA was integrated in the genomes of all four lines, and in all of them HBx, HBc and HBs transcripts were detected by reverse transcriptase-PCR methods. Among the three cell lines used as control (Hep 3B, SK Hep1 and Hep G2), only Hep 3B showed HBx expression, and this line was used as a HBV integrated control. The RNA of albumin was detected in three lines (SNU-761, SNU-878 and SNU-886), that of transferrin in two lines (SNU-878, SNU-886), and that of IGF-II was detected in none of the cell lines.

**CONCLUSION** These well characterized cell lines may be very useful for studying the biology of hepatocellular carcinoma in association with the hepatitis B virus.

## INTRODUCTION

Hepatocellular carcinoma (HCC) is one of the most prevalent malignant diseases encountered in the world, killing up to 1 million people annually. Geographically, its prevalence varies greatly, with a very high incidence in sub-Saharan Africa and south and northeast Asia, including Korea<sup>[1-3]</sup>. Although many risk factors for HCC such as aflatoxin, persistent hepatitis C viral infection and alcoholic cirrhosis have been reported, hepatitis B viral infection has been known to be the most important etiologic factor. Epidemiological and laboratory studies have confirmed a strong association between the hepatitis B virus (HBV) and HCC. Prospective studies have shown that in those infected with HBV, the risk of HCC was several hundred times higher than in uninfected individuals<sup>[4,5]</sup>.

Despite this well-known close epidemiological relationship between HBV and HCC, the direct evidence of a causal relationship is inconclusive; HBV does not contain real oncogenes, and the mechanism by which HBV induces hepatocellular carcinoma has not been clearly demonstrated. It has been noticed that HBx, a protein encoded by HBV, is a molecule critically involved in HBV-induced hepatocellular carcinogenesis, and the HBx protein has been shown to transactivate various viral and cellular genes, including growth related genes such as c-fos<sup>[6]</sup>, c-myc<sup>[7]</sup> and IGF<sup>[8]</sup>. Thus, the HBx protein has been suspected to be a critical molecule in the HBV induced carcinogenesis of HCC, which was supported further by report that the HBV x gene product induces HCC in transgenic mice<sup>[9]</sup>. HBV, however, has a very narrow host range and restricted tissue tropism to hepatocytes, and it is therefore difficult to study HBV-related HCC. The role of HBV in hepatic carcinogenesis has mainly been studied either by transfecting cloned viral DNA into permanent cell lines or by using HBV transgenic mice<sup>[10]</sup>. Another useful approach may be to use established HCC cell lines that are integrated with HBV DNA. Although HBV integrated HCC cell lines are very useful in hepatocellular carcinogenesis research, such cell lines are not yet sufficient. Furthermore, the

<sup>1</sup>Laboratory of Cell Biology, Korean Cell Line Bank, Cancer Research Center and Cancer Research Institute, Seoul National University College of Medicine, Seoul 110-744, Korea; Departments of <sup>2</sup>Surgery and <sup>3</sup>Pathology, Seoul National University College of Medicine, Seoul, Korea

This work was supported in part by a grant from the Korea Science and Engineering Foundation (KOSEF) through the Korean Cell-Line Bank and Cancer Research Center at Seoul National University, KOSEF-CRC-97-8

**Correspondence to:** Jae-Gahb Park, M.D., Ph.D., Laboratory of Cell Biology, Cancer Research Institute, Seoul National University College of Medicine, 28 Yongon-dong, Chongno-gu, Seoul 110-744, Korea

Tel.(82-2)760-3380, Fax.(82-2)742-4727

Email.jgpark@plaza.snu.ac.kr

Received 1999-06-25

establishment of HCC cell lines has been more difficult since the usage of transcatheter embolization with lipiodol and chemotherapeutic agents in the treatment of HCC. The preoperative application of this therapeutic modality induces extensive necrosis of tumor tissue and leaves only a small amount of viable tumor cells available for culture at the time of operation<sup>[11]</sup>.

After reporting eight HCC cell lines<sup>[12]</sup>, we established four more lines from Korean HCC patients infected with HBV (SNU-739, SNU-761, SNU-878, SNU-886). We analyzed phenotypes such as *in vivo* and *in vitro* (cell line) cell morphology and *in vitro* growth pattern, DNA finger printing, expression of HBV viral transcripts, albumin transferrin and insulin like growth factor II. The relationship between HBx and *p53* gene mutation in eight previously reported cell lines and these four newly reporting cell lines was already described<sup>[13]</sup>.

## MATERIALS AND METHODS

### Cell culture

Cell lines were established from pathologically proven hepatocellular carcinomas. Solid tumors were finely minced and disassociated into small aggregates by pipetting. Appropriate amounts of fine neoplastic tissue fragments were seeded into 25cm<sup>2</sup> flasks. Initial culture was performed in ACL-4 medium supplemented with 5% heat inactivated fetal bovine serum (AR5 medium). ACL-4 is a fully defined medium formulated for the selective growth of the human lung adenocarcinoma<sup>[14]</sup> and has proved to be useful in the establishment of colorectal cancer cell lines and HCC cell lines<sup>[12,15]</sup>. The composition of ACL-4 includes RPMI 1640 as the basal medium, insulin (20 mg/L), transferrin (10mg/L), sodium selenite (25 nM), hydrocortisone (50nM), epidermal growth factor (1µg/L), ethanolamine (10 µM), phosphorylethanolamine (10 µM), triiodothyronine (100 pM), bovine serum albumin (2g/L), HEPES buffer (10mM), glutamine (2mM) and sodium pyruvate (0.5mM). RPMI 1640, glutamine and sodium pyruvate were obtained from GIBCO/BRL (Grand Island, NY); epidermal growth factor was obtained from Collaborative Research (Waltham, MA); all other reagents were obtained from Sigma (St. Louis, MO). For the maintenance of the cultures, the medium was replaced with RPMI 1640 supplemented with 10% heat inactivated fetal bovine serum (R10 medium). Initial cell passages were performed when heavy tumor cell growth was observed, and subsequent passages were performed every 1 or 2 weeks. Adherent cultures were passaged at sub-confluence after trypsinization. If stromal cell growth was noted during initial growth, differential trypsinization was used to obtain a pure

tumor cell population, as previously described by Park *et al*<sup>[15]</sup>. Cultures were maintained in humidified incubators at 37°C in an atmosphere of 5% CO<sub>2</sub> and 95% air. Well characterized and widely used HCC cell lines (Hep 3B and SK-Hep1) and one hepatoblastoma cell line (Hep G2) were obtained from American Type Culture Collection (ATCC, Rockville, MD) and used as controls in DNA profile and transcript analysis.

### Morphologic characteristics

Surgically removed tissue samples were fixed in 10% neutral formalin for 24 hours. After routine processing, they were embedded in paraffin for light microscopic examination. Four mm thick sections were stained with hematoxylin and eosin (HE), and tumor cells were classified using the WHO classifications<sup>[16]</sup>. For the morphological studies of the cell lines, cells grown in a 75cm<sup>2</sup> culture flask were observed daily under a phase-contrast microscope (Olympus, CK2). For light microscopic examination, cells grown on Flaskette Chamber Slides (Nunc Inc., Naperville, IL) were washed with phosphate buffered saline (PBS), fixed in 4% paraformaldehyde in 0.1M sodium cacodylate for 30min, and then stained with HE.

### Growth properties and microorganism contamination

To determine the population doubling time, about 3 × 10<sup>5</sup> viable cells were seeded into 15 - 20 identical 25cm<sup>2</sup> flasks. The number of cells was counted daily for at least 14 days. Cultures were fed every 3 or 4 days and 24 hours prior to counting. To determine cell viability, a dye-exclusion procedure using 0.4% trypan blue staining methods performed and the number of viable cells was counted under a microscope using a hemocytometer.

Mycoplasma contamination was tested by direct agar isolation and the Hoechst 33342 stain method (Microbiological Associates, Bethesda, MD) and rRNA based PCR method<sup>[17]</sup>. All lines were tested for bacterial contamination.

### DNA and RNA extraction

Total cellular RNA and DNA were obtained from washed cell pellets by homogenization in guanidine thiocyanate followed by centrifugation over a cesium chloride cushion. Subsequently, total genomic DNA was prepared by the proteinase K digestion and phenol chloroform extraction method<sup>[15]</sup>.

### DNA fingerprinting

For DNA profile analysis, three polymorphic DNA probes, pYNH24 on chromosome No.2 (ATCC, Rockville, MD), ChdTC 15 on chromosome No.12

and ChdTC 114 on chromosome No.20 (from Dr. H. Mizusawa, JCRB, Tokyo, Japan) were used to detect variable number of tandem repeats (VNTRs). The probes were labeled with [ $\alpha$ - $^{32}$ P] dCTP (3000Ci/mmol) using a random primed DNA labeling kit (Boehringer Mannheim, Indianapolis, IN). Prior to separation by 0.7% agarose gel electrophoresis, 10 $\mu$ g of each DNA sample was digested with 70 units of Hinf I restriction endonuclease, and Southern blots were then performed<sup>[18]</sup>.

### **HBV DNA integration**

For the identification of HBV DNA integration, 10 $\mu$ g of each DNA sample was digested with 10 units of Hind III, separated by electrophoresis, and transferred to a nylon membrane as described above. A  $^{32}$ P labeled 3.2kb full length HBV DNA clone (pAM6) was used as a probe. Hybridization and autoradiography were done by the same methods described in Southern blot.

### **RT-PCR of HBV *x*, *s* and *c* gene**

Total RNA was prepared from the cell lines and treated with DNase to exclude cellular DNA contamination. cDNA was made using MMLV reverse transcriptase (Boehringer Mannheim, Indianapolis, IN) and random hexamer. A reverse transcriptase reaction was performed at 42°C for 1 hour with 2 $\mu$ g of template RNA. The PCR primer sequences were as follows: *x* gene (forward 5-acggggcgcacctctctta-3' reverse 5-tgcctacagcctcctagtag-3'), *c* gene (forward 5'-gtctctgtggagtactctc-3', reverse 5'-gtcgaatccacactccaaa-3), and *s* gene (forward 5'-tctcaatttctagggggag-3', reverse 5'-gcactagtaaactgagccag-3'). PCR reaction was performed with annealing temperature of 55°C for 30 seconds. PCR product was resolved in 1% agarose gel and detected by EtBr staining. To confirm this result, we also performed Southern blot with HBx, HBs, and HBc probes labeled with [ $\alpha$ - $^{32}$ P] dCTP (3000Ci/mmol).

## **RESULTS**

### **Establishment of the cell lines**

The four HCC cell lines designated SNU-739, SNU-761, SNU-878 and SNU-886 were established from Korean HCC patients, all of whom had previously been treated by transcatheter arterial embolization. Preoperative serologic testing had revealed the presence of hepatitis surface antigen in all patients from whom the specimens were obtained (Table 1).

All cell lines showed the monolayer growth pattern, and population doubling times ranged from 20 to 29 hours. All lines were free from contamination with bacteria and mycoplasma.

### **Morphologic studies**

The gross and histologic features of the original tumors were categorized using the WHO classification. Grossly, the original tumors from which the cell lines were derived were either single nodular type or the single nodular with perinodal extension type (Table 2).

Histologically, the original tumor of the SNU-739 cell line was the mixed microtrabecular and compact type; individual tumor cells were similar to normal hepatocytes (cirrhotomimetic type), but scattered multinuclear syncytial cells with clear cytoplasm were seen within the area of compact histology. Eosinophilic hyaline globules were occasionally seen, and scattered or aggregated neutrophils were encountered throughout the tumor (Figure 1a). Cultured cells grew as an adherent pattern; they were monotonous spindle shaped cells, containing single round nuclei and flattened cytoplasm. The nucleoli were inconspicuous (Figure 2a).

The original tumor of cell line SNU-761 was the homogenous macrotrabecular type. The tumor cells were uniform cirrhotomimetic cells of grade III differentiation. Sinusoids were well developed and multinuclear giant cells were occasionally encountered (Figure 1b). The individual cultured cell was polygonal, with a single ovoid nucleus and abundant cytoplasm. The cells occasionally produced short cytoplasmic processes at the free lateral border. In large part, they formed an adherent monolayer, and tended to overlap (Figure 2b).

The original tumor of cell line SNU-878 was the macrotrabecular type with a minor area of compact histology. Its cells belong to the cirrhotomimetic group, and most were moderately differentiated (grade II or III). Clusters of cells containing clear cytoplasm were seen in the central part of tumor cell nests. The tumor cells occasionally contained Mallory body-like amorphous materials in their cytoplasm (Figure 1c). The cultured cells of SNU-878 grew as a monolayer of tightly packed colonies, consisting of polygonal cells of variable shapes in a mosaic pattern. Most tumor cells contained multiple nuclei, simulating syncytium, while a few were detached from the compact colony. Single or double conspicuous nucleoli were noted (Figure 2c).

The original tumor of cell line SNU-886 consisted of cirrhotomimetic cells in a macrotrabecular pattern. The nuclear shape of individual cells varied and large anaplastic cells were scattered throughout the tumors; the degree of cellular differentiation was categorized as grade II-IV (Figure 1d). The growing cells of cell line SNU-886 formed an adherent monolayer of mixed spindle shaped and polygonal cells. Most of the tumor cells contained one or two nuclei, with small multiple nucleoli (Figure 2d).

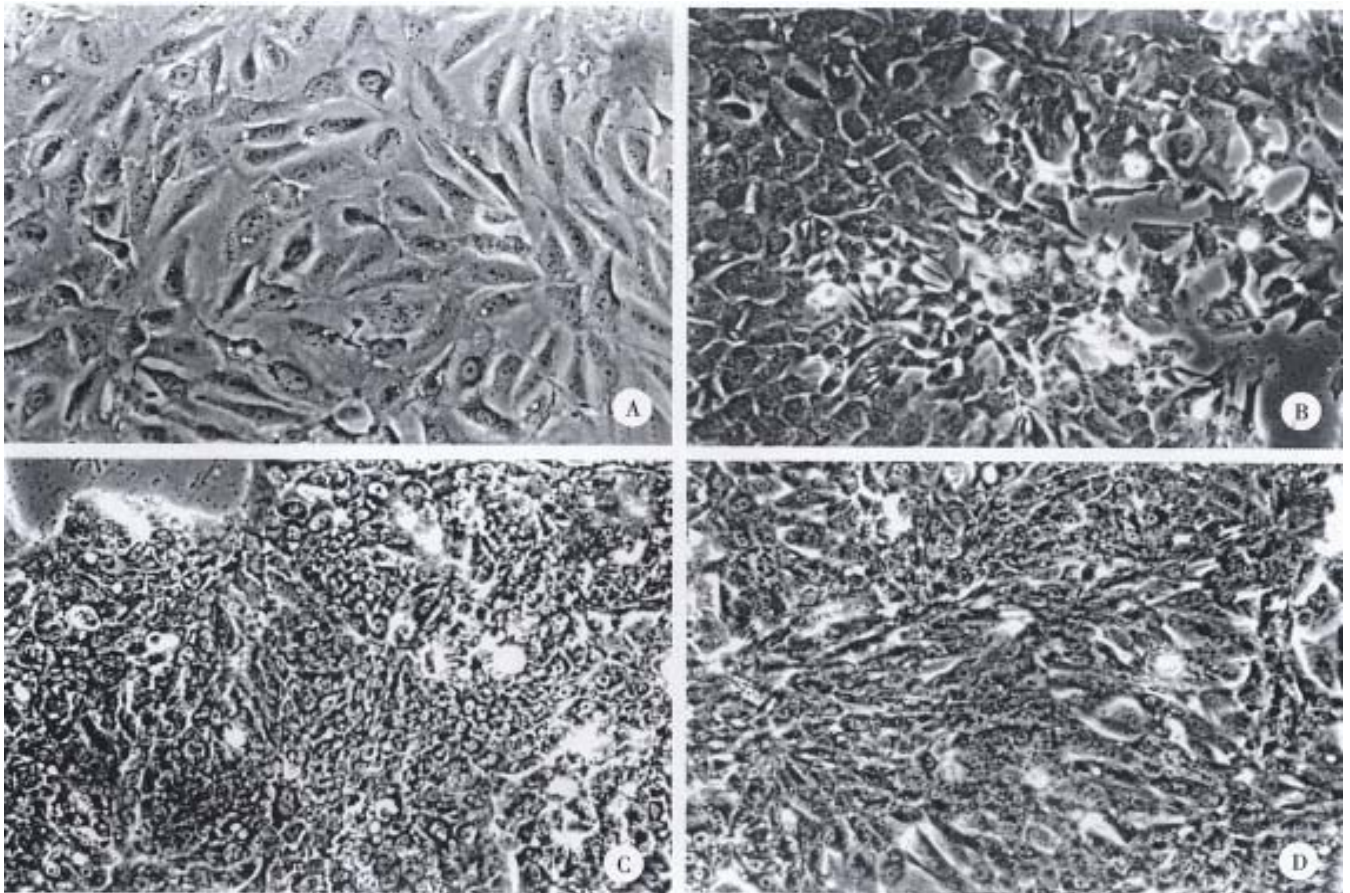


**Figure 1** Microscopic features of cell lines and their original tumors where the cell lines were derived. A, B, C, D, show cell line morphology of SNU-739, SNU-761, SNU-878 and SNU-886 respectively.

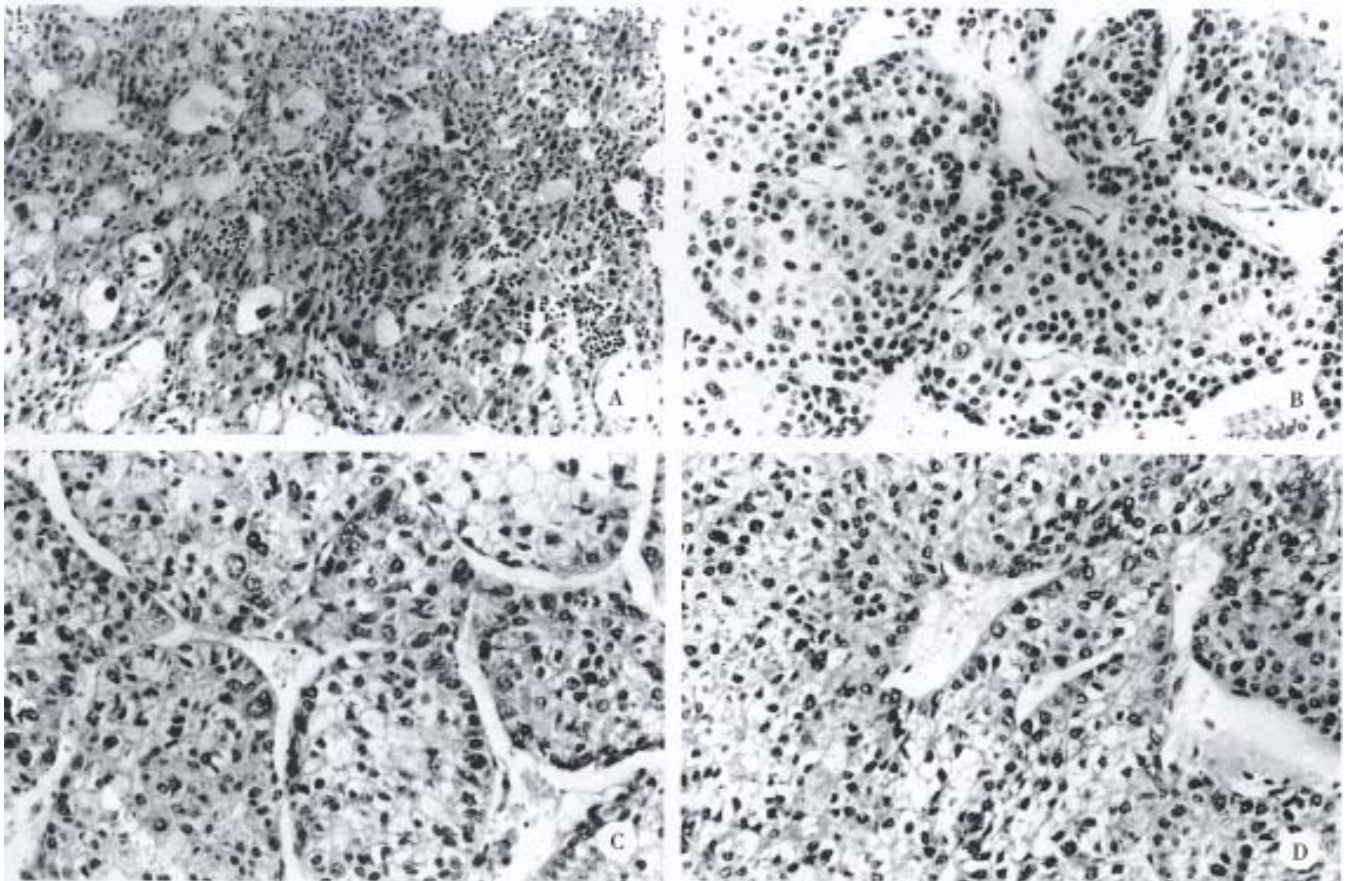


**Figure 2** A, B, C, and D, show original tumor morphology of each cell line. Scale bars, 50 $\mu$ m.

### DNA Profiles and HBV DNA integration

DNA profiles using restriction endonuclease Hinf I and polymorphic DNA probes pYNH24, ChdTC 15, and ChdTC 114 showed more than 12 allelic bands with the size range of 4.4 to 10kb (Figure 3).

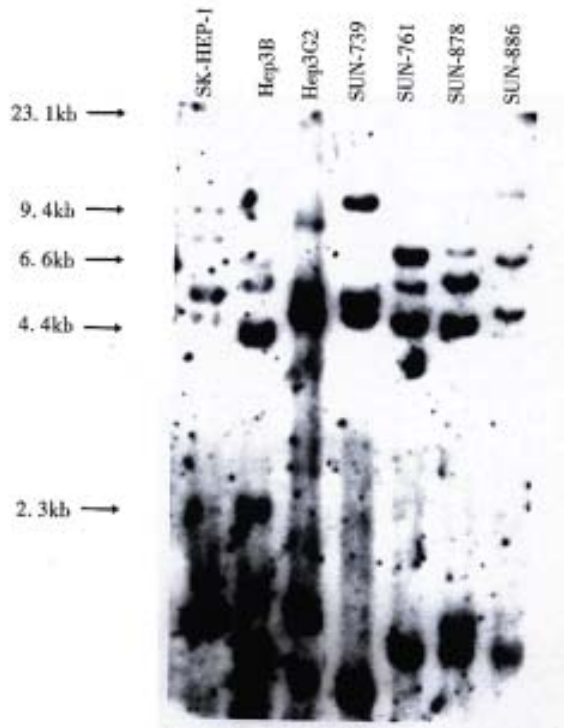


**Figure 3** DNA profile of 4 HCC cell lines. The DNA profiles of Southern blotting. Genomic DNAs from 4 HCC cell lines were digested with Hinf-I and hybridized with ChdTC-15, ChdTC-114 and pYNH24. It is evident that the 4 HCC cell lines are unique and unrelated.

All four cell lines showed different band pattern, and this indicates that these cell lines were unique and unrelated. In addition, their DNA profiles were different from those of three previously reported ATCC cell lines, SK-Hep1, Hep3B, and Hep G2. These results exclude possible cross contamination between the cell lines.

Hepatitis B virus DNA was detected in all cell lines by Southern-blot hybridization with cellular DNA after digestion using Hind III. Relatively high molecular weight bands with enzyme digestion suggest integrated form of HBV DNA. Each cell line showed a different pattern of HBV integration (Figure 4).

### HBV viral RNA

Using the RT-PCR method, HBx RNA was detected in all four cell lines and the Hep3B line. HBs and HBc RNA were detected in all four newly established cell lines (Figure 5). Among the three control cell lines, only Hep3B showed HBx RNA expression, and this line was known to be integrated with HBV DNA and express HBx RNA. SK-Hep1 and HepG2, reported to have no association with HBV, and did not show HBx RNA expression.

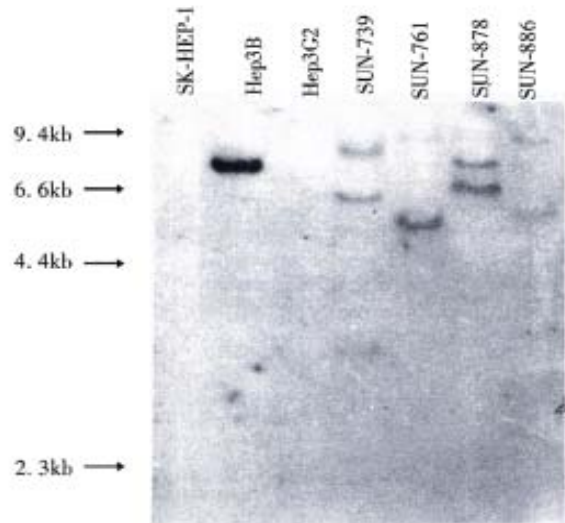


**Figure 4** Integration of HBV DNA in genomic DNA of 4 HCC cell lines. Different size and pattern of bands indicate random integration of HBV DNA in genome of the cell lines. A band is also seen in Hep3B, which is a HBV integrated cell line.

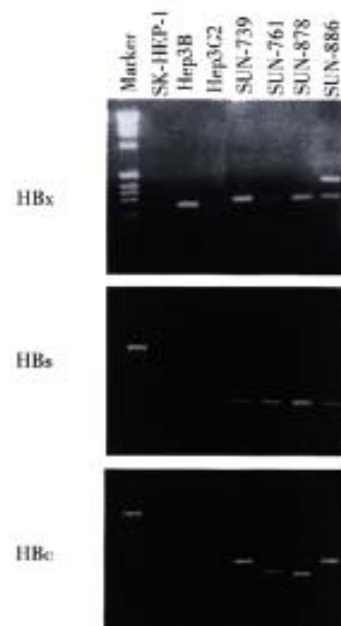


**Figure 5** HBx, HBs and HBc RNA transcripts in 4 HCC cell lines. In RT-PCR analysis, HBx, HBs, and HBc gene transcripts were detected in all presenting cell lines. Among the cell lines used as control (SK-HEP-1, Hep3B and HepG2), HBx gene transcript was detected in Hep3B line. HBs and HBc gene transcripts were not detected in any of the three control lines.

### RNA expression of albumin, transferrin and IGF-II

In Northern blot, the expression of RNA coding for albumin was detected in the SNU-761, SNU-878, and SNU-886 cell lines (Figure 6). RNA for transferrin was expressed in the SNU-878 and SNU-886 cell lines. RNA for IGF-II was expressed in none of these cell lines (Table 3).

**Table 1 Tumor of hepatocellular carcinoma cell lines**

Cell line	Age/Sex	Blood type	Prior therapy	HBsAg	Serum $\alpha$ -FP ( $\mu$ g/L)	Histology and differentiation <sup>a</sup>	Background pathology
SNU739	52/M	O+	TAE <sup>b</sup>	+	207	HCC, grade II IV/IV	Cirrhosis
SNU761	49/M	AB+	TAE	+	21400	HCC, grade III/IV	Cirrhosis
SNU878	54/F	O+	TAE	+	7	HCC, grade II III/IV	Cirrhosis
SNU886	57/M	A+	TAE	+	33	HCC, grade II IV/IV	CAHc

<sup>a</sup>Differentiation based on Edmondson Steiner's classification; <sup>b</sup>TAE: transcatheter arterial embolization; <sup>c</sup>CAH: chronic active hep atitis

**Table 2 Morphological characteristics of cell lines *in vitro* and *in vivo* (tumor specimen)**

Cell line	<i>In vitro</i>			<i>In vivo</i>			
	Growth character	Cell morphology	Nuclear morphology	Histology	Cell type	Gross type	Grade
SNU739	Ad <sup>a</sup>	Spindle	Single	Micro-trabecular compact	C <sup>b</sup> /clean	SN <sup>c</sup>	II-IV
SNU761	Ad	Polygonal	Single	Macro-trabecular	C	SN	III
SNU878	Ad	Polygonal	Single multinuclear	Macro-trabecular	C	SE <sup>d</sup>	II-III
SNU886	Ad	Polygonal-spindle	Single-double	Macro-trabecular	C	SN	II-IV

<sup>a</sup>Ad: adherent; <sup>b</sup>C: cirrhotomimetic; <sup>c</sup>SN: single nodular; <sup>d</sup>SE: single nodular with perinodal extension

**Table 3 Characteristics of hepatocellular carcinoma cell lines**

Cell lines	Viability (%)	Doubling time (hr)	HBV DNA integration	HBV RNA expression			Albumin	Transferrin	IGF-II
				X	preS/S	C			
SNU-739	94	20	+	+	+	+	-	-	-
SNU-761	91	24	+	+	+	+	+	-	-
SNU-878	88	25	+	+	+	+	+	+	-
SNU-886	90	29	+	+	+	+	+	+	-

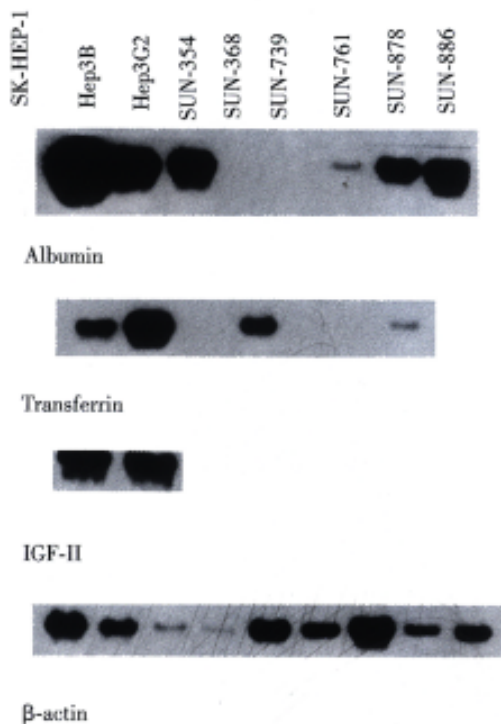


**Figure 6** RNA expression of albumin, transferrin and IGF-II in 4 HCC cell lines. RNA for albumin was detected in the SNU-761, SNU-878, SNU-886, Hep 3B, HepG2 and SNU-354 (previously reported HBV integrated cell line). RNA for transferrin was detected in the SNU-878 and SNU-886 cells lines, however the band in SNU-886 line was very faint to be hardly visible. The same sized band was also detected in Hep3B, HepG2 and SNU-368 (another previously reported HBV integrated cell).

RNA for IGF-II was expressed in none of the presenting four cell lines, but it was expressed in Hep3B and HepG2 lines.

## DISCUSSION

Cell lines established from human cancers provide very useful tools for studying the biology of cancer and the development and testing of new therapeutic approaches. In HCC, well-characterized HCC cell lines make possible various studies that cannot be performed with biopsy or postmortem tissues. The frequent integration of the HBV gene in hepatocellular carcinoma suggests that it play an essential role in carcinogenesis of hepatocellular carcinoma. Permanent cell lines derived from HCCs with the HBV gene integration offer good models not only for the investigation of HCC carcinogenesis but also for the elucidation of the regulatory mechanisms of HCC cell specific gene expression. In spite of their definite value as a resource for research in HCC, reports of established HCC cell lines have been decreasing since 1985, and only a few cases have been reported<sup>[11]</sup>. Furthermore, permanent HCC cell lines integrated with the HBV gene are rarer, and other than our previous report of eight lines, only a few cases have been reported in the literature. Recent attempts to culture HCC cells as permanent lines have been rather disappointing. The use of transcatheter arterial embolization (TAE) with lipiodol or chemotherapeutic drugs before surgical resection is now common, and it is thus difficult to obtain HCC tissues suitable for isolation and cultivation of intact

viable cells. In our establishment of these herein reported cell lines, the success rate was only 9% (4 lines out of 44 trials), which is much lower than our previously reported 8 cell lines (success rate 29%, 8 lines out of 28 trials) due to extensive necrosis caused by the preoperative TAE. All four of these cell lines were in fact derived from HCC tissues of patients who underwent preoperative TAE. In these cases that the cell lines were successfully established, the necrotic portion was diverse, ranging from 30% to 70%. However, in cases that establishment of cell lines were failed, the necrotic portion was usually more extensive.

HBV is a 3.2Kb sized DNA virus with only four genes known to encode for the inner "c" and "e" antigen, "s" (surface) proteins, a DNA polymerase and the "x" protein. According to recent reports on the carcinogenic mechanism of the HBS virus, the x gene of HBV (HBx), capable of gene transactivation, is considered to play an important role<sup>[19,20]</sup>. In order to investigate the transcriptional activity of HBV genes in our cell lines, HBx, preS/S and HBc RNA expression was examined using the RT-PCR methods. The HBV gene RNA transcript which encodes the x, preS/S and c was detected in these four lines and in Hep 3B; this is known to have one or two copies of HBV DNA integrated into the host genome and to express HBV viral transcripts of various size<sup>[21]</sup>. This RNA expression indicates that HBV genes integrated into the cell lines are transcriptionally active, though an exact quantitative assay was not possible.

Among our previously reported eight cell lines, x gene RNA was detected in only two cell lines (SNU-354, SNU-368) by Northern blot analysis<sup>[12]</sup>. We re-examined the RNA transcript of x gene in those eight cell lines using the RT-PCR methods, and detected RNA expression in six of them (SNU-182, SNU-354, SNU-368, SNU-387, SNU-449, SNU-475). This may indicate that for detecting a very tiny amount of viral transcript, RT-PCR is more sensitive than Northern blot; thus, the viral DNA actually transcribed should be determined by RT-PCR analysis.

These high expression rates of x gene transcription (10 of 12 lines) in HCC cell lines established from Korean HCC patients who were serologically proved to be HBS antigen positive suggest that, in Korea, HBV plays an important role in the etiology of HCC. This is further supported by the prevalence of HBV infection in Korea, which affects as much as 8% of general population<sup>[22]</sup>.

In this report, we have described the characteristics of four newly established HCC cell lines in which HBV DNA was integrated into the genomes. Considering that fresh specimens for the

establishment of new cell lines are difficult to obtain, these four cell lines would be invaluable future resources.

## REFERENCES

- 1 World Health Organization. Causes of deaths by sex and age. In: World Health Statistics Annals. WHO, Geneva: WHO, 1993
- 2 Omata M. Current perspectives on hepatocellular carcinoma in Oriental and African countries compared to developed Western countries. *Dig Dis*, 1987;5:97-115
- 3 Simonetti RG, Camma C, Fiorello F, Politi F, D'Amico G, Pagliaro L. Hepatocellular carcinoma. A worldwide problem and the major risk factors. *Dig Dis Sci*, 1991;36:962-972
- 4 Szmunn W. Hepatocellular carcinoma and the hepatitis B virus: evidence for causal association. *Prog Med Virol*, 1978;24:40-69
- 5 Beasley RP. Hepatitis B virus as the etiologic agent in hepatocellular carcinoma epidemiologic considerations. *Hepatology*, 1982; 2:21S-27S
- 6 Twu JS, Lai MY, Chen DS, Robinson WS. Activation of protooncogene c-jun by the X protein of hepatitis B virus. *Virology*, 1993;192:346-350
- 7 Balsano C, Avantaggiati ML, Natoli G. Transactivation of c-fos and c-myc protooncogenes by both full length and truncated versions of the HBV-X protein. In: Hollinger FB, Lemon SM, Margolis H, eds. Viral hepatitis and liver disease. Baltimore: Williams & Wilkins Co., 1991:572-578
- 8 Menzo S, Clementi M, Alfani E, Bagnarelli P, Iacovacci S, Manzin A, Dandri M, Natoli G, Levrero M, Carloni G. Transactivation of epidermal growth factor receptor gene by the hepatitis B virus X-gene product. *Virology*, 1993;196:878-882
- 9 Kim CM, Koike K, Saito I, Miyamura T, Jay G. HBx gene of hepatitis B virus induces liver cancer in transgenic mice. *Nature*, 1991;351:317-320
- 10 Chisari FV, Klopchin K, Moriyama T, Pasquinelli C, Dunsford HA, Sell S, Pinkert CA, Brinster RL, Palmiter RD. Molecular pathogenesis of hepatocellular carcinoma in hepatitis B virus transgenic mice. *Cell*, 1989;59:1145-1156
- 11 Miyazaki M, Namba M. Hepatocellular carcinomas. In: Hay RJ, Park JG, Gazdar A, eds. Atlas of human tumor cell lines. San Diego: Academic Press, 1994:185-212
- 12 Park JG, Lee JH, Kang MS, Park KJ, Jeon YM, Lee HJ, Kwon HS, Park HS, Yeo KS, Lee KU. Characterization of cell lines established from human hepatocellular carcinoma. *Int J Cancer*, 1995;62:276-282
- 13 Kang MS, Lee HJ, Lee JH, Ku JL, Lee KP, Kelley MJ, Won YJ, Kim ST, Park JG. Mutation of p53 gene in hepatocellular carcinoma cell lines with HBx DNA. *Int J Cancer*, 1996;67:898-902
- 14 Brower M, Carney DN, Oie HK, Gazdar AF, Minna JD. Growth of cell lines and clinical specimens of human non small cell lung cancer in serum free defined medium. *Cancer Res*, 1986;46:798-806
- 15 Park JG, Oie HK, Sugarbaker PH, Henslee JG, Chen TR, Johnson BE, Gazdar A. Characteristics of cell lines established from human colorectal carcinoma. *Cancer Res*, 1987;47:6710-6718
- 16 Gibson JB, Sobin LH. Histologic typing of tumors of the liver, biliary tract and pancreas. In: International Histological Classification of Tumors. Geneva: WHO, 1978:20
- 17 Deng S, Hiruki C, Robertson JA, Stemke GW. Detection by PCR and differentiation by RFLP of *Acholeplasma*, *Spiroplasma*, *Mycoplasma*, and *Ureaplasma*, based upon 16S rRNA Genes. *PCR Method Applications*, 1992;1:202-204
- 18 Sambrook J, Fritsch EF, Maniatis T. Molecular cloning: a laboratory manual, 2nd Ed. Cold Spring Harbor: Cold Spring Harbor Laboratory Press, 1989
- 19 Shirakata Y, Kawada M, Fujiki Y, Sano H, Oda M, Yaginuma K, Kobayashi M, Koike K. The X gene of hepatitis B virus induced growth stimulation and tumorigenic transformation of mouse NIH3T3 cells. *Jpn J Cancer Res*, 1989;80:617-621
- 20 Balsano C, Billet O, Bennoun M, Cavard C, Zider A, Grimber G, Natoli G, Briand P, Levrero M. Hepatitis B virus X gene product acts as a transactivator *in vivo*. *J Hepatol*, 1994;21:103-109
- 21 Knowles B, Howe CC, Aden DP. Human hepatocellular carcinoma cell lines secrete the major plasma proteins and hepatitis surface antigen. *Science*, 1980;209:497-499
- 22 Shin HR. HBV or HCV infection and risk of HCC in Korea. Proceedings of the Federation Meeting of Korean Basic Medical Scientists, 1993:86

# Clinical implication of VEGF serum levels in cirrhotic patients with or without portal hypertension

Nimer Assy<sup>1,4</sup>, M Paizi<sup>3,4</sup>, D Gaitini<sup>2</sup>, Y Baruch<sup>1,4</sup> and G Spira<sup>3,4,5</sup>

**Subject headings** VEGF; growth factors; liver cirrhosis; liver regeneration; hypertension portal; duplex sonography; angiogenesis

## Abstract

**AIM** To determine whether serum vascular endothelial growth factor (VEGF) levels correlates with the severity of liver cirrhosis and whether portal hypertension impacts on the expression of serum VEGF protein.

**METHODS** Fifty-three patients (mean age  $56 \pm 2$  years) with HCV ( $n = 26$ ), HBV ( $n = 13$ ), and cryptogenic liver cirrhosis ( $n = 14$ ) (Child-Pugh's class A: 24, B: 19 and C: 12) and normal renal function constitute the patient population, who were all diagnosed by clinical, histological and radiologic findings. Six healthy people and six patients with acute hepatitis served as controls. Severity of liver disease was evaluated by the CP score. Serum levels of IGF-1 and VEGF were measured by radioimmunoassay and ELISA, respectively. Portal hypertension was assessed using pulsed Doppler ultrasound.

**RESULTS** The mean serum VEGF levels in all cirrhotic patients ( $73 \pm 58$ ) were significantly lower than those of healthy controls ( $360 \pm 217$ ,  $P < 0.01$ ) and acute hepatitis ( $1123 \pm 1261$ ,  $P < 0.01$ ) respectively. No significant difference in median serum VEGF levels were noted among the different Child-Pugh-s classes (class A: median, 49.4 ng/L, range, 21 ng/L-260 ng/L, Class B: median 59.9 ng/L; range 21-92, and Class C: median 69; range 20 ng/L - 247 ng/L). A significant correlation was noted between serum VEGF and two accurate parameters of portal hypertension: portal blood flow velocity ( $r = 0.6$ ) and spleen size ( $r = 0.55$ ). No correlation

was found between VEGF serum levels and serum albumin, IGF-1, platelets count and aminotransferases ( $r = 0.2$ ,  $r = 0.1$ ,  $r = 0.2$  and  $r = 0.2$ , respectively).

**CONCLUSION** Circulating VEGF level in patients with liver cirrhosis could not serve as an indicator of the progression of chronic liver disease but rather, they may reflect increased portal hypertension or decreased hepatic regenerative activity or the combination of both.

## INTRODUCTION

Angiogenesis or formation of new blood vessels, is a tightly regulated process in which blood vessels supply growing tissue with nutrients, growth factors, hormones, and oxygen to meet the needs of development or repair of injured tissues<sup>[1]</sup>. Liver growth also depends on angiogenesis. When angiogenesis is reduced, growth and repair decrease significantly<sup>[2]</sup>. In human subjects with liver cirrhosis, liver regeneration is impaired<sup>[3]</sup>. This raises questions about angiogenesis as a mediator for the growth of hepatic parenchymal cells and consequently whether angiogenesis reflects the severity of liver disease or not. Vascular endothelial growth factor (VEGF) was closely related to angiogenesis in various human cancers. However, little is known of its circulating levels in liver cirrhosis with or without portal hypertension. The presence or absence of collateral circulation significantly impacts the natural history of portal hypertension in cirrhotic patients. Collateral growth involves two different mechanisms: capillary collateral develops by sprouting (angiogenesis) and muscular collateral develops in situ from preexisting arterioles (arteriogenesis)<sup>[4]</sup>. The process is mediated also by various angiogenic growth factors such as VEGF, FGFs, IGF-1 and PDGF<sup>[5]</sup>. The clinical relevance of serum VEGF levels in portal hypertension patients has not been previously described and remains to be clarified.

VEGF is a secreted, 46kDa dimeric protein active as a direct and specific mitogen for vascular endothelial cells and the only angiogenic factor

Departments of <sup>1</sup>Medicine B, Liver Unit, <sup>2</sup>Ultrasound, Rambam Medical Center, Haifa, <sup>3</sup>Department of Anatomy and Cell Biology, <sup>4</sup>Bruce Rappaport Faculty of Medicine, Technion, Haifa, <sup>5</sup>Rappaport Institute for Research of the Medical Sciences, Technion, Haifa, Israel  
**Correspondence to:** Dr Assy Nimer, Fassouta 25170, Box 428, Upper Galilee, Israel  
Tel. 972-4-9870-080, Fax. 972-4-9870-080  
Email.drnimer@netvision.net.il  
Received 1999-05-19

exhibiting vascular permeability inducing activity. Five distinct human VEGF molecules having 121, 145, 165, 189 and 206 amino acids, respectively, were identified in man, all the result of alternative splicing of the same VEGF gene<sup>[1]</sup>. VEGF production is known to be upregulated by several substances, including oxygen, steroid hormones, reactive oxygen metabolites and protein kinase C agonists<sup>[6]</sup>. The level of VEGF gene expression was high in several human cancer cell lines and in tumors of the human gastrointestinal tract, brain, kidney and liver<sup>[7-11]</sup> as well as in normal tissues. Monacci *et al* reported by *in situ* hybridization studies that VEGF gene in the rat liver was located in hepatocytes and a small number of Kupffer cells<sup>[12]</sup>. However, the function of hepatocytes derived VEGF is not clear. VEGF has been shown to induce the proliferation of hepatic sinusoidal cells by virtue of increased expression of its receptors flt-1 and flk-1 following partial hepatectomy. Furthermore, VEGF gene expression increased in hepatocytes isolated from 70% resected rat liver<sup>[13]</sup>. We have noted recently that exogenous VEGF 165 administration to partially hepatectomised rats stimulates liver cell proliferation<sup>[2]</sup>. The aim of the present study was to determine whether serum VEGF levels in patients with liver cirrhosis reflects the degree of liver dysfunction and to determine whether portal hypertension impacts on VEGF serum levels.

## PATIENTS AND METHODS

### Study population

The protocol of this study was approved by the Helsinki committees of the Rambam Medical Center and the Israel Ministry of Health. Subjects were briefed on the experimental nature of the study and signed informed consent form. Fifty-three patients (mean age  $56 \pm 2$  years) with HCV ( $n = 26$ ), HBV ( $n = 13$ ), and cryptogenic ( $n = 14$ ) liver cirrhosis and normal renal function constitutes the patient population of this study. All patients were diagnosed by clinical, histological and radiological findings. Twenty-two patients belonged to Child-Pugh's class A, 19 to Child class B, and 12 to Child class C. Patients with renal failure (creatinine  $> 106.8 \mu\text{mol/L}$  and creatinine clearance  $< 50\text{mL/min}$ ), dysthyroidism, and patients with known hepatocellular carcinoma were excluded. Severity of liver disease was evaluated by the CP score (Child-Pugh's score)<sup>[14]</sup> and by the generation of IGF-1<sup>[15]</sup>. Portal hypertension was defined as the presence of varices or/and portal vein diameter (PVD)  $> 13\text{cm}$ , portal blood flow velocity (PFV)  $< 15\text{cm/sec}$  and spleen size  $> 13\text{cm}$ <sup>[16]</sup>. Sera were obtained from 53 patients with liver cirrhosis, six healthy controls and six patients with acute

hepatitis. None of the patients with liver cirrhosis had acute illness during the study period.

### Serum levels of IGF-1

Serum levels of IGF-1 were measured by radioimmunoassay kit (Incstar Corp, Stillwater, MN, USA) including extraction of octadecasilylsilica (Sep-Packs). Sensitivity of the assay was  $2.0\text{nmol/L}$  (normal values male:  $11\text{nmol/L} - 48\text{nmol/L}$ ; female,  $9\text{nmol/L} - 46\text{nmol/L}$ , with intra and inter assay variation of less than 8.4% and 10.3%, respectively.

### Serum levels of VEGF

ELISA was employed to determine the level of VEGF. As the concentration of serum VEGF is  $15\text{ng/L} - 550\text{ng/L}$ , a sandwich ELISA based on chemiluminescence rather than spectrophotometry is required. Black ELISA plates (Corning) were coated with rabbit anti-VEGF IgG purified on protein G Sepharose chromatography column and blocked with 0.1% gelatin. Samples to be tested are added, followed by anti-EGF monoclonal antibody. Biotinylated rabbit anti-mouse IgG-1 and streptavidin horseradish peroxidase were then used and the presence of horseradish peroxidase was visualized by luminol substrate (Super Signal, Pierce). Photons released were read in a microplate luminometer, and translated to ng/L according to a titration curve of VEGF included in the plate.

### Duplex Doppler ultrasonography

Thirty-three patients were examined with duplex Doppler ultrasonography equipped with an ultrasonic system consisting of a mechanical sector scanner (IGE rt 3600) and a pulsed Doppler device with an insonating frequency of 3.5MHz and a pulse repetition frequency of 2KHz. A wall filter of 100Hz was used to avoid a false positive diagnosis of portal vein thrombosis, due to an inadequate high pass filter. The study was carried out by the same examiner (DG) to avoid interobserver variability. The examiner was unaware of the grade of cirrhosis so as to prevent from bias in the results. All the patients were kept fasting overnight prior to the sonography. Portal flow measurements were taken in the supine position during expiration. The portal trunk was scanned longitudinally with the sector scanner. We preferred the intercostal approach to keep the angle of insonation below  $60^\circ$ . The portal flow velocity (PFV) in cm/sec was measured directly. Over a given period, by the dedicated software supplied with the Doppler equipment. Each measurement was repeated until good and reproducible spectral patterns and blood flow sounds

were obtained. Portal flow velocity and diameter were measured in triplicate and accepted if the coefficient of variation was less than 10%. The arithmetic mean of the three values was analyzed.

### Statistics

Results were expressed as mean  $\pm$  SD ( $\bar{x} \pm s$ ). Differences among groups were analyzed using Scheffes multiple comparison test. Difference between two groups was assessed by Mann-Whitney test for non-parametric data. The correlation between serum VEGF levels and, IGF-1, albumin, and portal blood flow were evaluated using simple regression analysis and Spearman correlation coefficient analysis.  $P < 0.05$  was considered to be significant.

### RESULTS

The clinical, radiological and laboratory data of our patients with liver cirrhosis are shown in Table 1. The mean serum VEGF levels in all cirrhotic patients were significantly lower than those of healthy controls (73 ng/L  $\pm$  58 ng/L versus 360 ng/L  $\pm$  217 ng/L,  $P < 0.01$ ) and lower than patients with acute hepatitis (1123 ng/L  $\pm$  1261 ng/L,  $P < 0.01$ ) respectively (Figure 1). No significant difference in the median serum VEGF levels were noted among different Child-Pugh classes. The median serum VEGF levels of class A were 49.4 ng/L, ranging from 21 ng/L to 260 ng/L; Class B 59.9 ng/L, ranging from 21 ng/L to 92 ng/L; and Class C 69 ng/L ranging from 20 ng/L to 247 ng/L (Figure 2).

The mean serum VEGF levels were significantly different between patients with mild or non-portal hypertension and patients with moderate to severe portal hypertension (mean 39.8 ng/L  $\pm$  16.5 ng/L, median 37.7 ng/L range 20 ng/L - 69.8 ng/L vs mean 80.8 ng/L  $\pm$  5.7 ng/L, median 67.4 ng/L, range 20 ng/L - 260 ng/L,  $P < 0.005$ , respectively, Figure 3). A significant correlation was found between VEGF and two accurate parameters of portal hypertension, portal blood flow velocity ( $r = 0.6$ ) (Figure 4) and spleen size ( $r = 0.55$ ). However, weak correlation was found between VEGF and portal vein diameter ( $r = 0.3$ ) and no significant correlation was noted between VEGF serum levels and serum albumin, IGF-1, and aminotransferases ( $r = 0.2, 0.1,$  and  $0.2$ , respectively), suggesting that VEGF reflect neither the hepatic synthetic function in patients with liver cirrhosis nor inflammatory activity. Decreased VEGF levels were not associated with both portal vein thrombosis seen in two of our patients and platelet count ( $r = 0.2$ ).

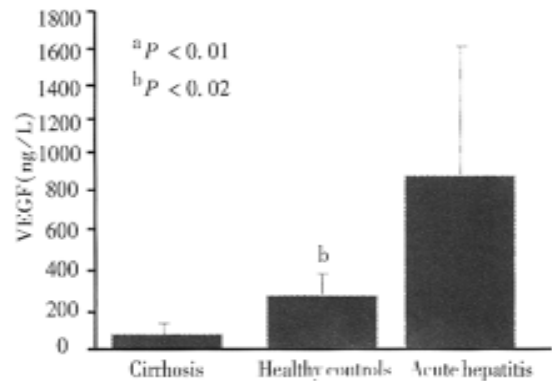


**Figure 1** Serum VEGF levels of patients with liver cirrhosis, healthy controls and acute hepatitis. The mean serum level of the cirrhotic patients was significantly lower than that of healthy controls and acute hepatitis patients ( $P < 0.01$ ,  $P < 0.02$ ), respectively.

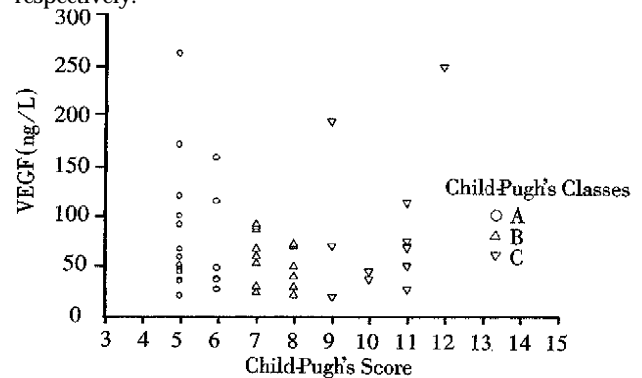


**Figure 2** Serum VEGF levels in patients with different grades of liver cirrhosis (Child-Pugh's class). The mean serum VEGF level was not significantly different among the three classes.

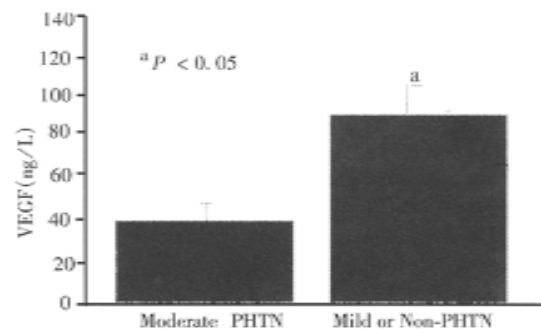


**Figure 3** Serum VEGF levels of patients with liver cirrhosis with or without portal hypertension. The mean serum level of the cirrhotic patients with portal hypertension was significantly lower than of those without portal hypertension ( $P < 0.005$ ).

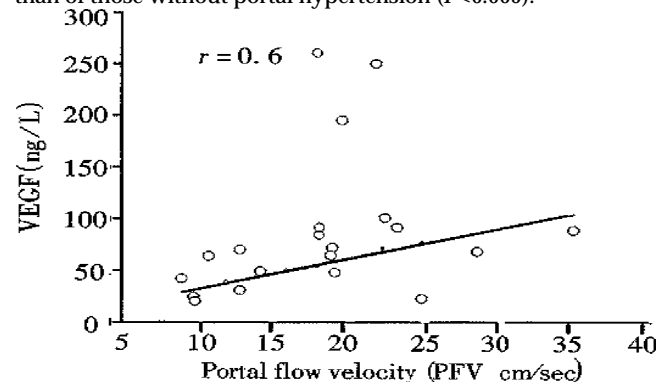


**Figure 4** Correlation between serum VEGF levels and portal blood flow velocity in all patients with liver cirrhosis ( $r = 0.6$ ).

**Table 1** The clinical, biochemical and radiological characteristics of the patients with different stages of liver cirrhosis

	Child-Pugh's A n=22	Child-Pugh's B n=19	Child Pugh's C n=12
Age (yrs)	56.3±12	49.0±12.9	53.3±14
Gender (m/f)	9/13	13/6	10/2
Albumin (g/dl)	4.1±0.3	3.3±0.4	2.7±0.3
Bilirubin (mg%)	1.1±0.3	1.8±1.0	3.8±1.1
PT (%)	81±13.5	66.3±14.4	51.7±9.4
AST (U)	66±38	62±45	94±76
ALT (U)	67±50	44±42	58±59
VEGF (ng/L)	78±13.5	63±9.4	87±20
IGF-1 (nmol/L)	16.7±1.4	13.3±1.06	10.9±1.1
PFV (cm/sec)	19.2±2.7	17.2±8.3	17.2±5.3
Pv diameter (mm)	14.5±2.3	11.7±3.5	13±2.5
Spleen size (cm)	15.1±2.4	16.2±1.9	15.4±2.7

## DISCUSSION

Vascular endothelial growth factor (VEGF) is closely related to angiogenesis in various human cancers<sup>[8-11]</sup>. However, little is known of its circulating levels in liver cirrhosis. We examined the circulating VEGF levels in chronic liver disease to assess their clinical significance. The results of this study clearly indicate that serum VEGF levels decreased which did not correlate with the disease severity in patients with liver cirrhosis. Moreover, the serum levels were down-regulated in the presence of portal hypertension and may be associated with the grade of hepatocyte regeneration.

Decreased serum VEGF levels in our patients with cirrhosis are in accordance with the study of Kraft A *et al*, which showed that ascitic fluid from patients with cirrhosis contained only a median of 303 ng/L (range 116 ng/L-676 ng/L) of VEGF, corresponding to the low serum levels in our series<sup>[17]</sup>. Our study is in agreement with the study by Chow *et al* that VEGF expression did not correlate with the biochemical liver profile, and clinical stage of cirrhosis<sup>[18]</sup>. That VEGF did not correlate with IGF-1, an accurate marker of synthetic function<sup>[15]</sup>, suggests that expression of serum VEGF may characterize a progression toward lower proliferation rate in cirrhosis *in vivo*<sup>[3]</sup>. In a recent report, as well as in our study, patients with acute hepatitis demonstrated a significantly higher level of VEGF than the control group. This high level was not accompanied by serum aminotransferase, suggesting that the serum VEGF is not the result of damaged hepatocytes but rather a high regenerative capacity<sup>[19]</sup>.

VEGF production is known to be down-regulated by several substances including angiostatin, and endostatin<sup>[20]</sup>. Thus, the low serum VEGF in these patients may be related to the

increased activity of these inhibitors. Unfortunately, these inhibitors were not measured in our study subjects. On the other hand, acute phase proteins are upregulated in liver cirrhosis<sup>[21]</sup>. VEGF induces capillary hypermeability, which may contribute to acute inflammatory changes<sup>[1]</sup>. However, in spite of the necroinflammatory changes observed in some patients with increased aminotransferases, the serum VEGF levels remained low. Moreover, no correlation between VEGF and aminotransferases levels was noted in the study population.

Lower VEGF serum levels in the patients with cirrhosis may reflect the lower platelet count. However, no correlation between serum VEGF and platelets count was found in our patients. According to that postulation, the VEGF levels were expected to be elevated since activation of platelets during serum preparation increased the VEGF content by 8-10 times<sup>[22]</sup>. Finally, the serum VEGF in the liver was not associated with sonographic portal vein thrombosis, which also activates platelets. Low circulating VEGF levels in our patients with cirrhosis also indicate that VEGF was derived from neither the large burden of tumor cells superimposed on cirrhosis, nor platelets activated by the vascular invasion of HCC cells since HCC was excluded from our patients.

The clinical relevance of serum VEGF levels in portal hypertension patients has not been previously described and remains to be clarified. Previous experimental studies have suggested that the paracrine system of endothelin and other growth factors may participate in the regulation of hepatic hemodynamics in cirrhosis<sup>[23]</sup>. The present study assessed the relationship between increased portal pressure (portal blood flow velocity < 15) and serum VEGF levels in human cirrhosis. The results indicate that expression of VEGF in the serum is down-regulated in the presence of moderate to severe portal hypertension. The reasons for this remain unclear. The expression and localization of PDGF, bFGF, EGF, and TGF- $\alpha$  in gastric coronary vein of cirrhotic and non-cirrhotic patients was investigated using immunohistochemical technique by Yang *et al*<sup>[24]</sup>. The strongly positive immunostaining rates were 93%, 89%, 70% and 68%, respectively in cirrhotic patients with portal hypertension whereas the immunostaining was negative in non-cirrhotic patients. These results suggested that gastric coronary vein could produce angiogenic growth factor during cirrhosis, the growth factor might act on the vascular function and/or structure via autocrine-paracrine mechanism and not via endocrine mechanism.

The potential usefulness of duplex sonography in the diagnosis of portal hypertension has been assessed previously by Iwao *et al*<sup>[16]</sup>. A portal vein diameter greater than 13cm or a portal vein flow velocity less than 15cm/sec indicated portal hypertension with a sensitivity and specificity of over 80%. That VEGF correlates well with the portal blood flow velocity indicates that VEGF is down-regulated in patients with portal hypertension. However, patients with portal blood flow velocity above 15cm/sec (no or mild portal hypertension) still had lower VEGF serum levels as compared to controls. This finding supports the notion that decreased VEGF serum levels are related to not only increased portal hypertension but also reduced regenerative capacity. This has an important clinical implication since the clinical outcome of these patients may be related to liver regenerative capacity.

In contrast to VEGF, Hsu *et al* found that serum bFGF, another angiogenic factor, was significantly increased in patients with liver cirrhosis and HCC when compared with those with chronic hepatitis or normal subjects. However, as for VEGF, none of the liver function test findings were correlated with the levels of basic FGF<sup>[25]</sup>. These results suggest that angiogenic factors play different roles in liver cirrhosis. The reason for the difference in circulating levels between VEGF and bFGF remains unclear.

## CONCLUSION

Circulating VEGF levels in patients with liver cirrhosis can not serve as an indicator of the progression of chronic liver disease but rather, they may reflect increased portal hypertension or decreased regenerative capacity of the cirrhotic liver or combination of both. Further studies are warranted to determine the clinical value of soluble VEGF as a prognostic factor, and a surrogate indicator of angiogenesis.

## REFERENCES

- 1 Neufeld G, Cohen T, Gengrinovitch S, Poltorak Z. Vascular endothelial growth factor (VEGF) and its receptors. *FASEB J*, 1999; 13:9-22
- 2 Assy N, Spira G, Paizi M, Shankar L, Kraizer Y, Cohen T, Neufeld G, Dabbah B and Baruch Y. Effect of vascular endothelial growth factor on hepatic regenerative activity following partial hepatectomy in rats. *J Hepatol*, 1999;30:911-915
- 3 Nakano K, Chijiwa K, Kameoka N. Impaired hepatic ketogenesis and regeneration after partial hepatectomy in cirrhotic rats. *Eur Surg Res*, 1994;26:257-265
- 4 Sumanovski LT, Battagay E, Stumm M, van der Kooij M, Sieber CC. Increased angiogenesis in portal hypertensive rats: role of nitric oxide. *Hepatology*, 1999;29:1044-1049
- 5 Tanoue K, Tarnawski AS, Santos AM, Hanke S, Sugimachi K,

- Sarfeh II. Reduced expression of basic fibroblast growth factor and its receptor mRNAs and proteins in portal hypertensive esophageal mucosa: a mechanism responsible for muscularis mucosae thinning and variceal rupture. *Surgery*, 1996;119:442-430
- 6 Shweiki D, Itin A, Soffer D, Keshet E. Vascular endothelial growth factor induced by hypoxia may mediate hypoxia-initiated angiogenesis. *Nature*, 1992;359:843-845
- 7 Kondo S, Asano M, Suzuki H. Significance of vascular endothelial growth factor/vascular permeability factor for solid tumor growth, and its inhibition by the antibody. *Biochem Biophys Res Commun*, 1993;194:1234-1241
- 8 Brown LF, Berse B, Jackman RW, Tognazzi K, Manseau EJ, Senger DR, Dvorak HF. Expression of vascular permeability factor (vascular endothelial growth factor) and its receptors in adenocarcinomas of the gastrointestinal tract. *Cancer Res*, 1993;53:4727-4735
- 9 Plate KH, Breier G, Weich HA, Risau W. Vascular endothelial growth factor is a potential tumour angiogenesis factor in human gliomas *in vivo*. *Nature*, 1992;359:845-848
- 10 Brown LF, Berse B, Jackman RW, Tognazzi K, Manseau EJ, Dvorak HF, Senger DR. Increased expression of vascular permeability factor (vascular endothelial growth factor) and its receptors in kidney and bladder carcinomas. *Am J Pathol*, 1993;143:1255-1262
- 11 Suzuki K, Hayashi N, Miyamoto Y, Yamamoto M, Ohkawa K, Ito Y, Sasaki Y, Yamaguchi Y, Nakase H, Noda K, Enomoto N, Arai K, Yamada Y, Yoshihara H, Tujimura T, Kawano K, Yoshikawa K, Kamada T. Expression of vascular permeability factor/vascular endothelial growth factor in human hepatocellular carcinoma. *Cancer Res*, 1996;56:3004-3009
- 12 Monacci WT, Merrill MJ, Oldfield EH. Expression of vascular permeability factor/vascular endothelial growth factor in normal rat tissues. *Am J Physiol*, 1993;264:C995-1002
- 13 Yamane A, Seetharam L, Yamaguchi S, Gotoh N, Takahashi T, Neufeld G, Shibuya M. A new communication system between hepatocytes and sinusoidal endothelial cells in liver through vascular endothelial growth factor and Flt tyrosine kinase receptor family (Flt-1 and KDR/Flk-1). *Oncogene*, 1994;9:2683-2690
- 14 Pugh RN, Murray layon IM, Dawson JL, Pietroni MC, Williams R. Transection of the esophagus for bleeding esophageal varices. *Br J Surg*, 1973;60:646-649
- 15 Assy N, Hochberg Z, Amit T, Shenn-Orr Z, Enat R, Baruch Y. Growth hormone stimulated insulin-like growth factor (IGF-1) and IGF-binding protein-3 in liver cirrhosis. *J Hepatol*, 1997;27:796-802
- 16 Iwao T, Toyonaga A, Oho K, Tayama C, Masumoto H, Sakai T, Sato M, Tanikawa K. Value of Doppler ultrasound parameters of portal vein and hepatic artery in the diagnosis of cirrhosis and portal hypertension. *Am J Gastroenterol*, 1997;92:1012-1017
- 17 Kraft A, Weindel K, Ochs A, Marth C, Zmija J, Schumacher P, Unger C, Marme D, Gastl G. Vascular endothelial growth factor in the sera and effusions of patients with malignant and non-malignant disease. *Cancer*, 1999;85:178-187
- 18 Chow NH, Hsu PI, Lin XZ, Yang HB, Chan SH, Cheng KS, Huang SM, Su IJ. Expression of vascular endothelial growth factor in normal liver and hepatocellular carcinoma: an immunohistochemical study. *Hum Pathol*, 1997;28:698-703
- 19 Akiyoshi F, Sata M, Suzuki H, Uchimura Y, Mitsuyama K, Matsuo K, Tanikawa K. Serum vascular endothelial growth factor levels in various liver diseases. *Dig Dis Sci*, 1998;43:41-45
- 20 Raymond E. Tumor angiogenesis inhibitors: media and scientific aspects. *Presse Med*, 1998;27:1221-1224
- 21 Moshage H. Cytokines and the hepatic acute phase response. *J Pathol*, 1997;181:257-266
- 22 Verheul HM, Hoekman K, Luyckx de Bakker S, Eekman CA, Folman CC, Broxterman HJ, Pinedo HM. Platelet: transporter of vascular endothelial growth factor. *Clin Cancer Res*, 1997;3: 2187-2190
- 23 Poo JL, Jimenez W, Maria Munoz R, Bosch-Marce M, Bordas N, Morales-Ruiz M, Perez M, Deulofeu R, Sole M, Arroyo V, Rodes J. Chronic blockade of endothelin receptors in cirrhotic rats: hepatic and hemodynamic effects. *Gastroenterology*, 1999;116:161-167
- 24 Yang Z, Tian L, Peng L, Qiu F. Immunohistochemical analysis of growth factor expression and localization in gastric coronary vein of cirrhotic patients. *J Tongji Med Univ*, 1996;16:229-233
- 25 Hsu PI, Chow NH, Lai KH, Yang HB, Chan SH, Lin XZ, Cheng JS, Huang JS, Ger LP, Huang SM, Yen MY, Yang YF. Implications of serum basic fibroblast growth factor levels in chronic liver diseases and hepatocellular carcinoma. *Anticancer Res*, 1997;17: 2803-2809

# Liver biopsy: complications and risk factors

Pornpen Thampanitchawong and Teerha Piratvisuth

**Subject headings** liver/pathology; biopsy; risk factor

## Abstract

**AIM** To study the complications and the risk factors of percutaneous liver biopsy, and to compare the complication rate between the periods of 1987-1993 and 1994-1996.

**METHODS** Medical records of all patients undergoing percutaneous liver biopsy between January 1, 1987 to September 31, 1996 in Songklanagarind Hospital were reviewed retrospectively.

**RESULTS** There were 484 percutaneous liver biopsies performed. The total complication rate was 6.4%, of which 4.5% were due to major bleeding; the death rate was 1.6%. The important risk factors correlated with bleeding complications and deaths were a platelet count of  $70 \times 10^9/L$  or less, a prolonged prothrombin time of  $>3$  seconds over control, or a prolonged activated partial thromboplastin time of  $>10$  seconds over control. Although physician inexperience was not statistically significantly associated with bleeding complications and deaths, there was a reduction of death rate from 2.2% in 1987-1993 to 0% in 1993-1996. This reduction is thought to result from both increased experience of senior staff and increased supervision of residents.

**CONCLUSIONS** Screening of platelet count, prothrombin time, and activated partial thromboplastin time should be done and need to be corrected in case of abnormality before liver biopsy. Percutaneous liver biopsy should be performed or supervised by an expert in gastrointestinal diseases, especially in high risk cases.

## INTRODUCTION

Percutaneous liver biopsy is a helpful diagnostic procedure which has been used for 100 years<sup>[1-3]</sup>. Although ultrasonography, computed tomography, and magnetic resonant imaging are useful in investigation of liver disease, liver biopsy is still essential for diagnosis<sup>[4]</sup> in the majority of patients. To avoid fatal complications, biopsy must be performed in patients with indications for and no contraindications against biopsy<sup>[5]</sup>. In our hospital, this procedure has been practised for several years. In 1992 there was an unofficial report of an unusual high complication rate, but this is the first investigative study. After 1994, all liver biopsies were performed by well-trained gastroenterologists or under their supervision; this seemed to lead to a decrease in the complication rate. Thus this study reviewed the incidence of complications in unsupervised biopsy performed between 1987-1993, and compare it with the incidence of complications in supervised biopsy performed between 1994-1996. Risk factors and additional procedures required for complications were evaluated.

## MATERIALS AND METHODS

We retrospectively collected all percutaneous liver biopsies performed in inpatients between January 1, 1987 and September 31, 1996. Eligible patients were aged 15 years or older and underwent biopsy performed by medical staff or residents using Menghini needle. Recorded data included: demographic data (age and gender); indication for biopsy; post-biopsy notes, both immediate and follow-up; hematocrit (Hct) result within 48 hours pre-biopsy and 5-48 hours post-biopsy (if several Hct were reported, the median was calculated); prothrombin time (PT), partial thromboplastin time (PTT), platelet count and liver function test within 10 days pre-biopsy; history of FFP and/or platelet transfusion prior to biopsy; ultrasonography report and pathological diagnosis.

Complications were defined as follows: Major bleeding: a decrease in Hct of 4% or more requiring packed red cell (PRC) transfusion and/or surgical intervention. Minor bleeding: a decrease in Hct of 4% or more not requiring intervention (PRC-transfusion or surgery). Transient hypotension: blood pressure of lower than 90/60mmHg, a decrease in systolic pressure of 20mmHg or more or a decrease in diastolic pressure of 15mmHg or more.

Department of Medicine, Songklanagarind Hospital, Hat Yai, Songkhla, Thailand

**Correspondence to:** Pornpen Thampanitchawong, MD, Department of Medicine, Songklanagarind Hospital, Hat Yai 90110, Thailand  
Fax. 66-74-212 912

Email: tpornpen@ratree.psu.ac.th

Received 1999-06-23

Data analysis. A Chi-square and two-tailed Fisher exact test was used to compare proportions; a two-tailed Student's *t* test was used to compare means; and a logistic regression analysis was used to determine the best predictors among several independent variables. Probability (*P*) value of less than 0.05 was considered to be statistically significant.

## RESULTS

Of 484 percutaneous liver biopsies, 50 biopsies were performed in 25 patients (2 biopsies/1 patient). The distribution of biopsies in each time period is summarized in Table 1.

**Demographic data.** The mean age of patients was 50 years (range 15-85 years), 76.9% (372 of 484) of patients were men and 23.1% (112 of 484) were women. There was no difference of age and gender between the periods of 1987-1993 and 1994-1996 (Table 1).

**Indications for biopsy and pre-biopsy data.** Indications for liver biopsy are shown in Figure 1. The most frequent indication was presence of a space occupying lesion, 57.2% (277 of 484), other indications were unexplained hepatomegaly or liver function test abnormality, 21.9% (106 of 484), acute or chronic hepatitis, 7.2% (35 of 484), acute or chronic jaundice, 5.2% (25 of 484), infection, 4.5% (22 of 484), cirrhosis 1.9% (9 of 484), alcoholic liver disease, 1.7% (9 of 484), drug related liver disease, 0.2% (1 of 484), and glycogen storage disease, 0.2% (1 of 484). All pre-biopsy data comparing between 1987-1993 and 1994-1996 showed no statistically significant difference (Table 1).

**Blood transfusion.** FFP was transfused in 11.2% (54 of 484) of all liver biopsies, of which 69.8% had PT prolonged >3 seconds over control, 41.2% had PTT prolonged >10 seconds and 25.9% had abnormal PT and PTT. The average amount of FFP given was  $1.8 \pm 0.3$  units (range 2-32 units). Platelet concentrates were transfused in 1.9% (9 of 484) of all liver biopsies, of which 55.6% had a platelet count  $70 \times 10^9/L$  or less and the average amount of platelet concentrate was  $1.9 \pm 0.1$  units (range 4-21 units).

**Physicians involved in liver biopsy.** Between 1987-1993, most percutaneous liver biopsies were performed by non-gastroenterologist without supervision; after 1994 all liver biopsies were performed by well-trained gastroenterologists or by residents under their supervision.

**Pathological results.** There was a significant decrease of hepatic malignancy from 49.3% (181 of 367) in 1987-1993 to 36.8% (43 of 117) in 1994-1996 ( $P=0.019$ , Table 1).

**Complications.** The overall complication rate was 6.4% (31 of 484); 4.5% (17 of 484) were due to major bleeding, 2.7% (13 of 484) due to transient hypotension, and 1.0% (5 of 484) due to minor bleeding. The death rate was 1.6% (8 of 484) but when patients who died from other causes were excluded, it was 1.2%. There was no association between age or gender and complication ( $P > 0.05$ ). There was no significant difference between major bleeding between 1987-1993 and 1994-1996 (4.72%, 17 of 360) vs 3.4% (5 of 124,  $P=0.617$ ). The death rate was reduced from 2.2% (8 of 360) during first period to 0% (0 of 124) in the later period; but this was not statistically significant ( $P=0.0208$ ). Bleeding complication of hepatic malignancy (3.5%, 9 of 260) and non-hepatic malignancy (5.8%, 13 of 224) were not different. 38.7% of pathological findings of complicated cases were hepatic malignancy. Coagulopathy was related to both bleeding complications and death. In patients with a normal PT the bleeding complication rate was 3.6% (15 of 416) and the death rate was 1.0% (4 of 416). The rates increased to 10.5% (6 of 57) and 7% (4 of 57), respectively, when PT was prolonged by >3 seconds over control, ( $P=0.017$  and  $P=0.009$ ). Patients with a PTT prolonged by >10 seconds over control also had increased rates of bleeding complications (10.3% vs 3.8%) among patients with normal PTT ( $P=0.079$ ). The death rate in patients with prolonged PTT, on the other hand, was significantly higher than that in patients with a normal PTT (7.7% vs 1.2%,  $P=0.023$ ). There was also a significant difference in both bleeding and death rates between patients with platelet counts  $70 \times 10^9/L$  and those with platelet counts greater than  $70 \times 10^9/L$  (bleeding rate: 25.0% vs 4.0%,  $P=0.014$ ; death rate: 33.3% vs 0.8%,  $P=0.001$ ).

Logistic regression analysis of the independent variables demonstrated that the most important predictors for bleeding ( $P=0.000$ ) and death ( $P=0.003$ ) was only platelet count  $70 \times 10^9/L$  or less.

Eight patients (1.6%) died after liver biopsy between 1987-1993. Only five of these deaths could be definitely attributed to liver biopsy and one additional death was probably related to biopsy procedures. Therefore, the actual death rate should be 1.2% (6 of 484). In three of the attributable deaths, bleeding and puncture wounds were observed during laparotomy; in two other cases, Hct was markedly decreased both 3 and 24 hours post-biopsy. One patient developed sudden dyspnea

and in which pneumothorax could not be excluded; thus, this death is probably related to biopsy. Two of the deaths may not have been associated with liver biopsy; the first patient died of pulmonary hemorrhage and the second of pneumonia with sepsis.

**Table 1** The number of liver biopsies, demographic data, pre-biopsy laboratory data and pathological results comparing between 1987-1993 and 1994-1996

	1987-1993	1994-1996	P- value
Liver biopsies (%)	367 (75.8)	117 (24.2)	NS
Mean age (years)	51	48	NS
Gender (%)			NS
Male (n=372)	74.5	80.4	
Female (n=112)	25.5	19.6	
Hct (%)	34.40±8.33	33.35±8.39	NS
PT (sec)	14.15±2.34	13.61±1.63	NS
PTT (sec)	32.61±6.67	33.19±5.88	NS
Platelet ( $\times 10^9/L$ )	298±172	332±162	NS
TB+ (g/dl)	1.33±1.22	1.30±1.30	NS
AST+ (U/L)	125±117.64	148.44±134.36	NS
ALT+ (U/L)	82.03±80.37	90.86±78.72	NS
ALP+ (U/L)	355.69±278.32	347.10±303.76	NS
Alb+ (g/dl)	3.54±0.75	3.58±0.81	NS
Hepatic malignancy	49.3	36.8	0.019

NS: No statistical significant, TB: Total bilirubin, AST: Aspartate aminotransferase, ALT: Alanine aminotransferase, ALP: Alkaline phosphatase, Alb: Albumin

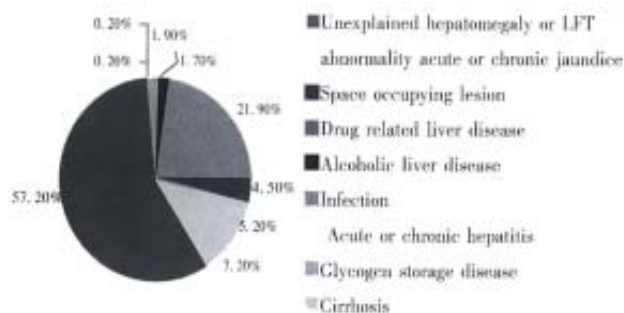


**Figure 1** Indications for liver biopsy. The most common indication was presence of a space occupying lesion (57.2%, 277 of 484), other indications were found less frequent respectively.

## DISCUSSION

In this patient population, the overall complication rate was 6.4% and the overall death rate was 1.6%. Our complication and death rates were unusually high as compared with other studies which have shown a complication rate of 0.13% - 3.2%, and a mortality rate 0% - 0.33%<sup>[1,6,7]</sup>. However, MaVay and associates also reported a high rate of major bleeding (4.5%)<sup>[6]</sup>.

We found the most important independent risk factors for bleeding complications and death were platelet count of  $70 \times 10^9/L$  or less. However, prolonged PT > 3 seconds over control and prolonged PTT > 10 seconds over control also

contributed to the increasing bleeding complications. Our study supports those of commonly considered contraindications for liver biopsy that is a platelet count of  $50-80 \times 10^9/L$  or less or a PT > 3 seconds<sup>[1,8]</sup>. Shama *et al* also found no bleeding in 16 patients with platelet counts of  $61-90 \times 10^9/L$ , but 3 of 13 patients with platelet counts of  $30-60 \times 10^9/L$  bled<sup>[9]</sup>. Ewe, while investigating laparoscopic liver bleeding time, found bleeding from the biopsy site occurred in cases with a platelet count of  $50 \times 10^9/L$  or less, but this bleeding could be stopped with compression<sup>[10]</sup>. Although these studies demonstrated no increased risk of bleeding with a platelet count greater than  $60 \times 10^9/L$ , one patient in our study with platelet count of  $63 \times 10^9/L$  had post liver biopsy bleeding. Therefore, we chose a platelet count of greater than  $70 \times 10^9/L$  as the safety margin for doing liver biopsy. Sherlock also recommended that liver biopsy should not be performed when platelet count was less than  $80 \times 10^9/L$ <sup>[11]</sup>. In this study, PT being greater than 3 seconds is a risk for bleeding complication, but McVay *et al* have reported that mild prolongation of PT and PTT 1.1-1.5 times that of normal is not associated with increased bleeding complications<sup>[6]</sup>. Other studies have also shown no increased risk for bleeding in open surgical procedures if PT and PTT were prolonged by 1.5 times or less<sup>[3,11]</sup>. Therefore, it has been suggested that bleeding after liver biopsy is a random event that cannot be predicted by currently available methods<sup>[9,11]</sup>, local intrahepatic clotting and elastic factors may prevent bleeding<sup>[10]</sup>.

In this study, the death rate decreased from 2.2% in 1987-1993 to 0% in 1994-1996. This decrease was not statistically significant probably due to the small sample size of patients biopsied between 1994-1996. Gilmore *et al* reported a frequency of bleeding complications of 3.25% when biopsies were performed by inexperienced physicians (less than 20 previous biopsies performed), which was higher than the complication rate of 1.1% when biopsies were performed by physicians who had done more than 100 biopsies before<sup>[3]</sup>. A survey in Switzerland also showed the complication rate was markedly higher in physicians with less experience (0.88% in physicians who performed biopsies less than 12 times per year vs 0.06% in physicians who performed biopsies 50 or more times per year)<sup>[12]</sup>. This may suggest that liver biopsy complication rate is determined by both the experience and training of those performing the procedure.

As in other studies, the most frequent indication for liver biopsy was the presence of a space occupying lesion and the most frequent

pathological diagnosis was hepatic malignancy<sup>[6,9]</sup>. Our study showed no association between pathological findings and bleeding complications. Hepatic malignancy and cirrhosis have previously been identified as risk factors by Gonzalez-Vallina, Mc Gill, and Fisher *et al*<sup>[6,8,13]</sup>. In these reports, Vim-Silverman and Tru-cut needles were frequently used and may have caused increased bleeding. Malignancy may also predispose to bleeding because of hypervascularity and capillary fragility, cirrhosis is thought to increase the risk of bleeding due to large subcapsular venous pooling<sup>[9]</sup>. However, Paisal showed no significant increase in bleeding due to cirrhosis<sup>[14]</sup>.

### CONCLUSIONS

Bleeding complications of percutaneous liver biopsy may occur in the setting of a platelet counts of  $70 \times 10^9/L$  or less, a prolonged PT > 3 seconds over control, or a PTT > 10 seconds over control. In order to minimize complications, all pre biopsy patients should be screened with platelet counts, PT, and PTT. If any of these value is abnormal, it should be corrected with FFP or platelet concentrate before liver biopsy. This study showed that physician experience is not a statistically significant risk factor for complications of liver biopsy. However other reports have suggested that performance of liver biopsy by untrained or inexperienced physician increase complications. Therefore, percutaneous liver biopsy should be performed or supervised by an expert in gastroenterology; this is especially important in high risk cases.

**Acknowledgements** The authors are grateful to Ms. Nualta Arpakopkul of the Department of Epidemiology for her help in statistical analysis, and to Ms. Anne Kasmar, and Mr. Ben Worley for their help in English language advice.

### REFERENCES

- 1 Sherlock S. Diseases of the liver and biliary system: needle biopsy of the liver. 8th ed. Boston, Melbourne: Blackwell Scientific Publications, 1989:36-48
- 2 Valori R, Elias E. How to perform a percutaneous liver biopsy. *Bri J Hos Med*, 1989;42:408-409
- 3 Gilmore IT, Burroughs A, Murray-Lyon IM, Williams R, Jenkins D, Hopkins A. Indication, methods, and outcomes of percutaneous liver biopsy in England and Wales: an audit by the British Society of Gastroenterology and the Royal College of Physicians of London. *Gut*, 1995;36:437-441
- 4 Stotland BR, Lichtenstein GR. Liver biopsy complications and routine ultrasound. *Am J Gastroenterol*, 1996;91:1295-1296
- 5 McGill DB. Predicting hemorrhage after liver biopsy. *DigDis Sci*, 1981;26:235-237
- 6 McVay PA, Toy PTCY. Lack of increased bleeding after liver biopsy in patients with mild hemostatic abnormalities. *Am J Clin Pathol*, 1990;94:747-753
- 7 Hegarty JE, Williams R. Liver biopsy: techniques, clinical applications, and complications. *Br Med J (Clin Res Ed)*, 1988; 288:1254-1256
- 8 Schiff ER, Schiff L. Disease of the liver: needle biopsy of the liver. 7th ed. Philadelphia: Lippincott, 1993:216-225
- 9 Sharma P, McDonald GB, Banaji M. The risk of bleeding after percutaneous liver biopsy: relation to platelet count. *J Clin Gastroenterol*, 1982;4:451-453
- 10 Ewe K. Bleeding after liver biopsy does not correlate with indices of peripheral coagulation. *Dig Dis Sci*, 1981;26:388-393
- 11 Pasha T, Gabriel S, Thrneau T, Dickson ER, Lindor KD. Cost-effectiveness of ultrasound guided liver biopsy. *Hepatology*, 1998; 27:1220-1226
- 12 Froehlich F, Lamy O, Fried M, Gonvers JJ. Practice and complications of liver biopsy: results of a nationwide survey in Switzerland. *Dig Dis Sci*, 1993;38:1480-1484
- 13 Gonzalez-Vallina R, Alonso EM, Rand E, Black DD, Whittington PF. Outpatient percutaneous liver biopsy in children. *J Pediatr Gastroenterol Nutr*, 1993;17:370-375
- 14 Pongchairerks P. Ultrasound-guided liver biopsy: accuracy, safety and sonographic findings. *J Med Assoc Thai*, 1993;76:597-600

Edited by MA Jing-Yun

# Effects of heparin on hepatic regeneration and function after partial hepatectomy in rats

Li Y, Wang HY and Chi Hin Cho

**Subject headings** heparin; hepatectomy; liver regeneration; alanine aminotransferase; rats

## Abstract

**AIM** To investigate the effects of heparin on the regenerative rate and serum alanine aminotransferase level in partial-hepatectomized (two-thirds) rats.

**METHOD** Three different doses of heparin (100, 500 or 1000 U/kg) were given after partial hepatectomy through the tail vein at a 12h interval for 2 or 3 days. After drug treatment, rats were killed and the remnant livers were weighed for the assessment of regenerative rate. Blood samples were also collected to measure serum alanine aminotransferase levels.

**RESULTS** Heparin given in the present dosages for 2 or 3 days neither stimulated the regeneration of the liver nor improved the hepatic function as indicated by an insignificant change both on remnant liver weight and serum alanine aminotransferase activity as compared with the control.

**CONCLUSION** Heparin alone has no beneficial effects on the regeneration of livers and improvement of hepatic function in hepatectomized rats.

## INTRODUCTION

It is known that liver regenerates quickly in response to tissue damage. Hepatocyte growth factor (HGF) has been implicated in the regulation of liver growth after partial hepatectomy<sup>[1,2]</sup>. It has been reported that heparin is a potent inducer of HGF production in various types of cells, including human embryonic lung and skin dermal fibroblasts, and promyelocytic leukemic and umbilical vein endothelial cells as well<sup>[3]</sup>. Furthermore, it was also demonstrated that heparin, when given to partially hepatectomized rats, could increase the plasma HGF level and stimulate DNA synthesis in hepatocytes of the remnant livers during the early stage of liver regeneration. However, this indirect indicator of tissue growth in the early phase of liver regeneration can not extrapolate and ascertain whether heparin is a true hepatotrophic factor for liver regeneration at the later stage of the regenerative process. Also, there was no clear indication that heparin can indeed restore the liver function along with its regenerative capacity.

The purpose of this study is to investigate the effects of heparin on liver regeneration and function by measuring the regenerative rate and serum alanine aminotransferase level, respectively in partially hepatectomized rats. The results of this study could be useful for assessing the therapeutic implication of heparin as a hepatotrophic agent in man.

## MATERIALS AND METHODS

### Animals

Male Sprague-Dawley rats (180 g - 200 g) purchased from the Laboratory Animal Unit, the University of Hong Kong, were reared on a standard laboratory diet (Ralston Purina Co., USA), and given tap water. They were kept in a room where the temperature ( $22^{\circ}\text{C} \pm 1^{\circ}\text{C}$ ), humidity (65%-70%), and day:night cycle (12:12 light:dark) were controlled.

### Drug

Heparin (Sigma, St. Louis, MO, USA; sodium salt, 174 USP units/mg) was prepared in 0.9% w/v NaCl (British Drug House, UK) solution (normal saline) in a concentration series of 50, 250, and 500U/mL for intravenous injection. Different doses of heparin 100, 500 and 1000U/kg, i.e. 0.2 mL/100 g body weight were given, respectively. Similar volume of normal saline was

Department of Pharmacology, Faculty of Medicine, The University of Hong Kong, 5 Sassoon Road, Hong Kong, China

**Correspondence to:** Professor Chi Hin Cho, Department of Pharmacology, Faculty of Medicine, The University of Hong Kong, 5 Sassoon Road, Hong Kong, China

Tel.(852)2819 9252, Fax.(852)2817 0859

Email.chcho@hkusua.hku.hk

Received 1999-05-19

injected through the same route as the control.

### Partial hepatectomy, drug treatment and hepatic regeneration assessment

Partial (two-thirds) hepatectomy was performed by excision of the median and left hepatic lobes according to the method of Higgins and Anderson<sup>[4]</sup> under pentobarbitone anaesthesia. The heparin at doses of 100, 500, and 1000U/kg or its vehicle (normal saline) were administered intravenously through tail vein every 12h starting 6h after operation for 2 (4 injections) or 3 (7 injections) days. The rats were killed 3h after the last dose. Blood samples were collected for the measurement of serum alanine aminotransferase level. At the time of killing, the remnant livers were removed and weighed to assess the hepatic regeneration. The hepatic regenerative rate in each postoperative rat was calculated from the wet weight of the remaining liver divided by the estimated preoperative weight of the whole liver times 100<sup>[5]</sup>.

### Measurement of serum alanine aminotransferase level

The serum alanine aminotransferase activity was measured by the method used in our laboratory with modifications<sup>[6]</sup>. Lactate dehydrogenase (LDH), L-alanine, reduced nicotinamide adenine dinucleotide (NADH) and  $\alpha$ -ketoglutarate were prepared at concentrations of 20U/mL, 0.8M, 2mM and 0.1 mM, respectively. Serum (0.1 mL) was added to 0.1 mL NADH, 0.1 mL alanine, 0.1mL  $\alpha$ -ketoglutarate and 0.5mL of 0.2M phosphate buffer mixture. The final solution was incubated at 37°C for 1min. LDH in 0.1mL was then added and the absorbance of the mixture was measured at 340nm for 3min with a spectrophotometer (Beckman, DU 650, USA), using mixture without LDH as the blank. The rate of decrease in absorbance was determined and the amount of alanine aminotransferase present was calculated with a formula. Serum alanine aminotransferase levels were expressed as U/mL.

### Statistical analysis

The results were expressed as mean  $\pm$  S.E. ( $\bar{x} \pm s_{\bar{x}}$ ) and statistical analysis was performed with an analysis of variance (ANOVA) followed by a Dunnett *t* test. A value of  $P < 0.05$  was considered to be statistically significant.

## RESULTS

### Liver regeneration

The remaining liver tissue regenerated along with the time after partial hepatectomy. Two or three days after hepatectomy the regenerative rates were 51% or 84%, respectively in the vehicle treatment groups. Heparin had no significant effect on hepatic regeneration. The regenerative rates in all three doses of heparin treated for 2 or 3 days, except for

the highest dose in the 3 days group, remained similar to those of the control. The highest dose of heparin treated for 3 days, however, significantly attenuated the liver regeneration when compared with control group (Figure 1).

### Serum alanine aminotransferase level

Serum alanine aminotransferase activity was significantly increased after partial hepatectomy at day 2 when compared with the enzyme level of normal rats. These levels seemed to be recovered back to normal level at the 3rd day after operation. Heparin at all three doses treated for 2 or 3 days did not significantly affect the serum alanine aminotransferase activity in partially hepatectomized animals (Figure 2).

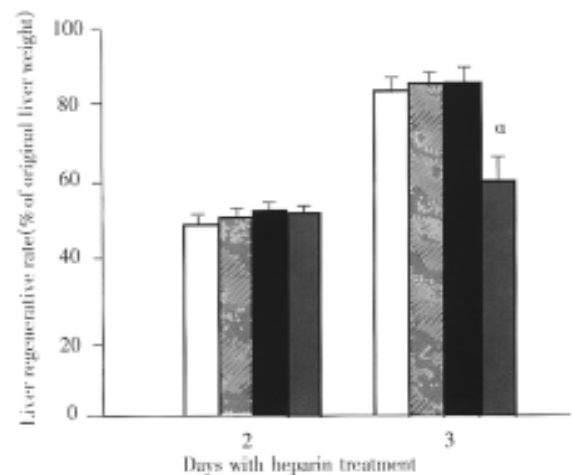


**Figure 1** Effect of different doses of heparin treated for 2 or 3 days on liver regeneration in partially hepatectomized rats. Open columns represent groups with normal saline treatment. Hatched, solid, or cross-hatched columns stand for groups treated with heparin at doses of 100, 500, or 1000U/kg, respectively. Each column represents the mean  $\pm$  S.E.M. of 5 animals. <sup>a</sup> $P < 0.05$  vs corresponding group with normal saline treatment.

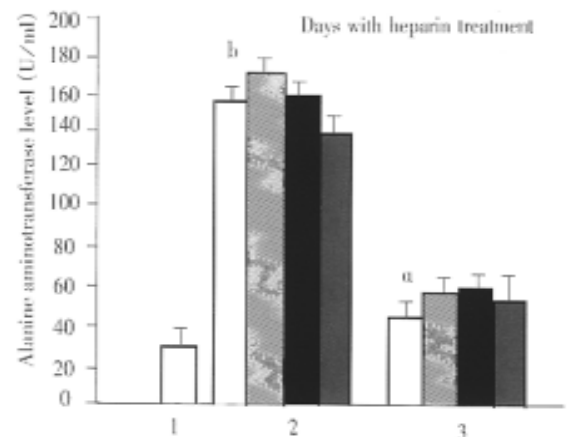


**Figure 2** Effect of different doses of heparin treated for 2 or 3 days on serum alanine aminotransferase level in partially hepatectomized rats. Open columns represent groups with normal saline treatment. Hatched, solid, or cross-hatched columns stand for groups treated with heparin at doses of 100, 500, or 1000U/kg, respectively. Each column represents the mean  $\pm$  S.E.M. of 5 animals. <sup>a</sup> $P < 0.05$ , <sup>b</sup> $P < 0.001$  vs 0 day with normal saline treatment.

## DISCUSSION

The present study showed that partial hepatectomy stimulated the remnant liver to regenerate in a time-dependent manner which was comparable with the previous study<sup>[5]</sup>. Liver regeneration is a compensative mechanism to restore the organ function after injury or related diseases. After partial hepatectomy, liver mass doubled within 48h and completely recovered in 7-10 days. This process was relatively well synchronized with the peaks of DNA synthesis and mitosis occurring at approximately 24 and 30h, respectively<sup>[4,7]</sup>. It has been reported that heparin could stimulate endogenous HGF production and consequently enhance DNA synthesis in hepatocytes *in vivo* after hepatic injury. The latter effect was significant within 36h after hepatectomy, but the same effect was not examined thereafter. More importantly, the actual liver regeneration and function had not been assessed<sup>[8]</sup>.

Although the early phase of liver regeneration is important for liver growth, the later stage of liver development and maturation of hepatocytes is the final determinant for a normal functional liver. The present study determined the effects of heparin on liver regeneration and its function 48 and 72h after hepatectomy. Our results demonstrated that heparin at all doses accelerated no hepatic regeneration. The highest dose instead significantly retarded liver regeneration on the 3rd day. This finding suggested that higher dose and longer period of heparin treatment might be harmful rather than beneficial to liver regeneration.

Increased liver regeneration is reflected by improvement of hepatic functions. Serum alanine aminotransferase level is one of the indicators for hepatic functions in clinical practice. In the present study, partial hepatectomy induced a significant

increase in serum enzyme activity and tended to recover along with the natural liver regeneration at the 3rd day after hepatectomy. These findings were in accord with the previous study<sup>[5]</sup>. Our present data also indicated that heparin could not accelerate the recovery of alanine aminotransferase level as liver regenerated on the 2nd and 3rd after hepatectomy. Although heparin could stimulate DNA synthesis of hepatocytes at the first day after partial hepatectomy<sup>[8]</sup>, it could not improve the deteriorated action on the liver due to hepatectomy beyond that period of time. Taken together, heparin is not an ideal hepatotrophic drug when it is used alone in liver injury or related diseases.

---

**Acknowledgments** The project is supported in part by the CRCG and RGC grants from the University of Hong Kong and the Hong Kong Research Grant Council, respectively.

## REFERENCES

- 1 Michalopoulos GK. Liver regeneration: molecular mechanisms of growth control. *FASEB J*, 1990;4:176-187
- 2 Zarnegar R, Defrances MC, Kost DP, Lindroos P, Michalopoulos GK. Expression of hepatocyte growth factor mRNA in regenerating rat liver after partial hepatectomy. *Biochem Biophys Res Commun*, 1991;177:559-565
- 3 Matsumoto K, Tajima H, Okazaki H, Nakamura T. Heparin as an inducer of hepatocyte growth factor. *J Biochem*, 1993;114:820-826
- 4 Higgins GM, Anderson RM. Experimental pathology of the liver: restoration of the liver of the white rat following partial surgical removal. *Arch Pathol*, 1931;12:186-202
- 5 Lee SD, Wang JY, Cho CH, Wu JC, Lu RH, Lai KH, Tsai YT, Lo KJ. Effects of H2-receptor antagonists on the rat liver after partial hepatectomy or carbon tetrachloride-induced hepatic injury. *Scand J Gastroenterol*, 1986;21:984-990
- 6 Woo PCY, Kaan SK, Cho CH. Evidence for potential application of zinc as an antidote to acetaminophen-induced hepatotoxicity. *Eur J Pharmacol*, 1995;293:217-224
- 7 Grisham JW. A morphologic study of deoxyribonucleic acid synthesis and cell proliferation in regenerating rat liver: autoradiography with thymidine-H<sup>3</sup>. *Cancer Res*, 1962;22:842-849
- 8 Matsumoto K, Nakamura T. Heparin functions as a hepatotrophic factor by inducing production of hepatocyte growth factor. *Biochem Biophys Res Commun*, 1996;227:455-461

Edited by MA Jing-Yun

# Effects of a bioartificial liver support system on acetaminophen induced acute liver failure canines

XUE Yi-Long<sup>1</sup>, ZHAO Shi-Feng<sup>2</sup>, ZHANG Zuo-Yun<sup>1</sup>, WAND Yue-Feng<sup>1</sup>, LI Xin-Jian<sup>1</sup>, HUANG Xiao-Qiang<sup>3</sup>, LUO Yun<sup>1</sup>, HUANG Ying-Cai<sup>4</sup> and LIU Cheng-Ggui<sup>1</sup>

See invited commentary on page 286

**Subject headings** liver support system; acute liver failure; canines; porcine hepatocytes; bioartificial liver; acetaminophen

## Abstract

**AIM** To evaluate the safety and efficacy of the bioartificial liver support system in canines with acute liver failure (ALF).

**METHODS** Nine canines with acute liver failure by acetaminophen-induced received TECA-I bioartificial liver support system (BALSS) from Hong Kong TECA LTD Co. Blood was perfused through a hollow fiber tube containing (1-2) × 10<sup>10</sup> the porcine hepatocytes. In contrast, another 10 canines with a cute liver failure by Acetaminophen received drugs. Each treatment lasted 6 hours.

**RESULTS** BALSS treatment resulted in beneficial effects for acetaminophen-induced ALF canines with survival and with the recovery of the liver functions and tissues, and plasma ammonia decreased from 135.9 μmol/L ± 17.5 μmol/L to 65.7 μmol/L ± 22.0 μmol/L, 32.5 μmol/L ± 8.8 μmol/L, GPT from 97.8U/L ± 8.7U/L to 64.8U/L ± 11.9U/L, 19.0U/L ± 6.3U/L, GOT from 103.0U/L ± 16.7U/L to 75.7U/L ± 19.6U/L, 26.5U/L ± 5.0U/L, and AKP from 158.3U/L ± 12.1U/L to 114.5U/L ± 19.8U/L, 43.8U/L ± 5.6U/L during and after the treatment. In contrast, 10 ALF canines in both the drug and control groups died 1 or 2 days after treatment.

**CONCLUSION** TECA-1 artificial liver support system is safe and efficacious for canines with acute liver failure.

<sup>1</sup>Institute of Basic Medical Sciences; <sup>2</sup>Department of Emergency; <sup>3</sup>Department of Hepatobiliary Surgery; <sup>4</sup>Department of Digestion, PLA General Hospital, Beijing 100853, China

Dr. XUE Yi-Long, female, born on 1953-10-29 in Nanjing City, Jiangsu Province, graduated from Fourth Military Medical University in 1978, Associate Professor, majoring in artificial organs, having 22 papers published.

\*Project supported by the Scientific Research Fund of Ministry of Education for Overseas Chinese Fellows who Returned Home, No.94-001 and Hong Kong TECA LTD Co.

Correspondence to: Dr. XUE Yi-Long, Institute of Basic Medical Science, PLA General Hospital, Beijing 100853, China

Tel. +86-10-66937914

Email: xueyl@plagh.com.cn

Received 1999-04-28

## INTRODUCTION

Acute liver failure (ALF) is a well-known complication in clinical diseases and the current comprehensive treatment is not satisfactory. The recent developed artificial liver support systems, especially the bioartificial liver support systems (BALSS), which perfuse the ALF blood with the exotic hepatocytes to temporarily replace the complex functions of illed liver such as synthesis, detoxication and biotransformation, provide a brand-new approach to treat the ALF<sup>[1-8]</sup>. But the difficulties in acquiring high-density culturing of hepatocytes, lack of a stable and well-reproducible big animal model of ALF impeded the development of BALSS researches. In the present study, we have introduced the basic techniques of a hollow fiber bioartificial liver system, used the Chinese experimental miniature swines as the donor of hepatocytes, improved the culturing conditions of porcine hepatocytes in the bioartificial liver system and developed an acetaminophen-induced ALF canine model so as to assess the efficacy, safety and feasibility of the BALSS in treating the ALF canines.

## MATERIALS AND METHODS

### Animal

The healthy adult hybrid canines weighing 15kg and adult Chinese experimental miniature swines weighing 10kg, the male or female, were provided by the Experimental Animal Center of PLA General Hospital.

### Reagent

All chemicals were obtained from Hong Kong TECA LTD Co. or Sigma Chemical Co.

### The development of a canine model of ALF

The canines received multi-subcutaneous injections (sc) with acetaminophen (115mg/kg) to induce the ALF models.

### The isolation and culturing of porcine hepatocytes

Hepatocytes were isolated from Chinese experimental miniature swines by collagenase digestion. Viability of the cells was assayed by trypan blue exclusion and AO/PI fluorescence staining.

### The procedure of BALS treatment

Freshly isolated hepatocytes were cultured in the TECA-IBALSS from Hong Kong TECA LTD Co. and used to treat the ALF canines. The porcine hepatocytes were circulating through the exterior space of capillary hollow fibers in the BALSS. A circuit was developed between the femoral artery and vein on one side of the ALF canine and connected to the hollow fibers of BALSS. The canine's blood circulated through the inner space of capillary hollow fibers and the substances exchanged through the membrane of hollow fibers with the porcine hepatocytes to achieve the perfusing function.

### Experimental groups

Nineteen ALF canines were randomly divided into three groups: ① BALSS perfusion group ( $n = 9$ ): perfused with the hollow fiber tube BALSS; ② drug group ( $n = 5$ ): intravenous injection with arginine, sodium glutamate and acidi amino chaini branchi; ③ control group ( $n = 5$ ): intravenous injection of 5% dextrose solution. Each treatment lasted six hours.

### Biochemical assays

The plasma levels of ammonia, GPT, GOT, AKP and BUN were measured before and 2, 4, 6 hours, 1, 3, 5, 7, 14, 30 days after treatment.

### Morphological observation

The liver, kidneys, heart, lungs were taken out when the canines died or survived for 30 days for paraffin section and HE stained and examined under light microscope.

### Statistical analyses

The values of blood biochemical parameters were expressed as means $\pm$ SD. Data between the three groups and pre-and post-treatment were compared using *t* test. Statistical significance was considered when  $P < 0.05$ .

## RESULTS

### The development of a canine model for acetaminophen-induced ALF

After injected with acetaminophen, the thirty-eight healthy canines (21 male, 17 female) demonstrated a significantly increased level of  $\text{NH}_3$ , GPT, GOT and AKP at 48 hours ( $P < 0.01$ , Figure 1) while plasma concentration of BUN had no change. In the mean time, symptoms appeared such as vomiting, food refusal and listlessness. Histologic examination showed massive necrosis of the hepatic tissues. Sixty-three per cent had ALF, in which the plasma levels of  $\text{NH}_3$  and GPT were higher than 100  $\mu\text{mol/L}$  and 60U/L respectively.

### The porcine hepatocytes

Using the modified enzymatic digestive method, each liver yielded approximately  $0.8 - 5 \times 10^{10}$  hepatocytes. Viability of the final suspensions averaged 60% - 80% by trypan blue exclusion and AO/PI fluorescence staining.

### The liver function recovery of ALF canines after treatment with BALSS

All ALF canines in the control group, with increasing levels of plasma ammonia, GPT, GOP and AKP died 2 - 30 hours after treatment. All the five ALF canines in drug group died 6 - 36 hours after treatment. The plasma levels of ammonia, GPT, GOT and AKP declined slightly during the treatment, but it had no significant difference compared with that in the control group ( $P > 0.05$ ). In BALSS perfusion group, all nine ALF canines showed remarkable liver function recovery. During BALSS treatment, the levels of plasma ammonia, GPT, GOT and AKP began to decline at the 2nd hour and the declination was even more obvious compared with pre-treatment at the 4th hour and 6th hour ( $P < 0.01$ ) (Figures 2, 3, 4, 5). The levels of these biochemical parameters had significant differences at the 6th hour of treatment between BALSS perfusion group and the drug group ( $P < 0.01$ ). Except three canines in BALSS perfusion group who died 6 and 12 hours and 5 days after treatment because of narcotization and wound bleeding, the other 6 canines survived more than 30 days.

### The morphological changes of liver in ALF canines after treatment with BALSS

The liver, heart, kidneys and lungs were taken out for pathological examination when the canines died and survived for 30 days after treatment. The liver tissues of the dead ALF canines showed massive necrosis in the drug and control groups. Thirty days after treatment, the liver tissue of ALF canines in BALSS perfusion group had no obvious hepatocyte necrosis but a slight cholestasis and fibrosis.

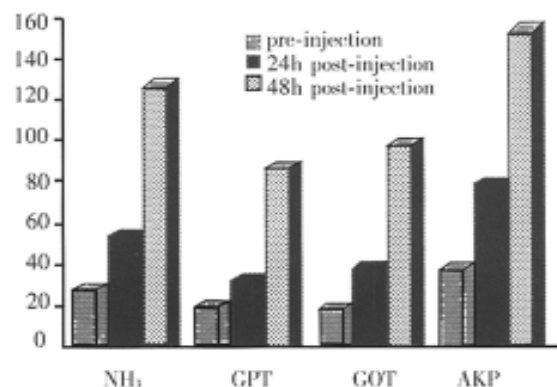


**Figure 1** The changes of canines' biochemistry parameters before and after injections of acetaminophen.

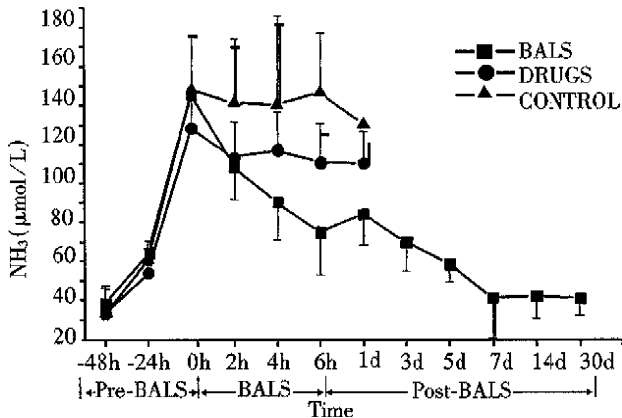


**Figure 2** Effects of the BALS on ammonia of acetaminophen-induced ALF canines.

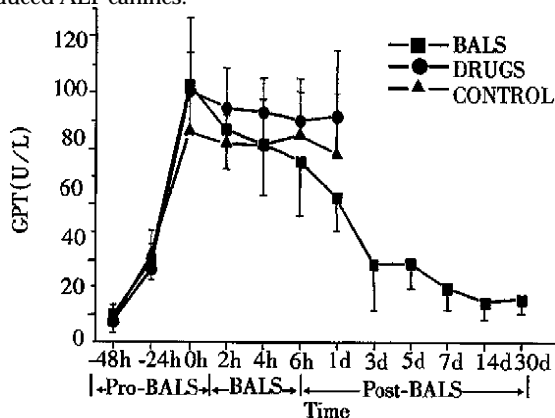


**Figure 3** Effects of the BALS on GPT of acetaminophen-induced ALF canines.

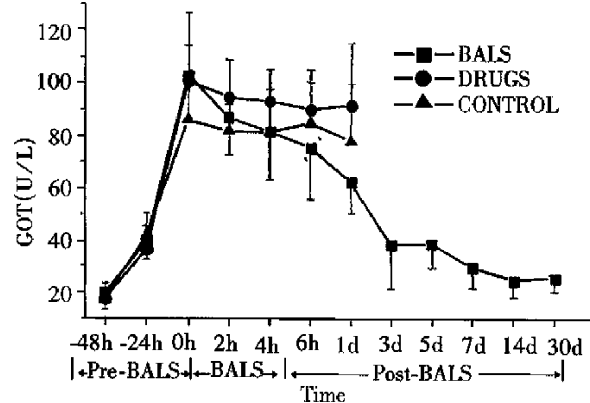


**Figure 4** Effects of the BALS on GOT of acetaminophen-induced ALF canines.

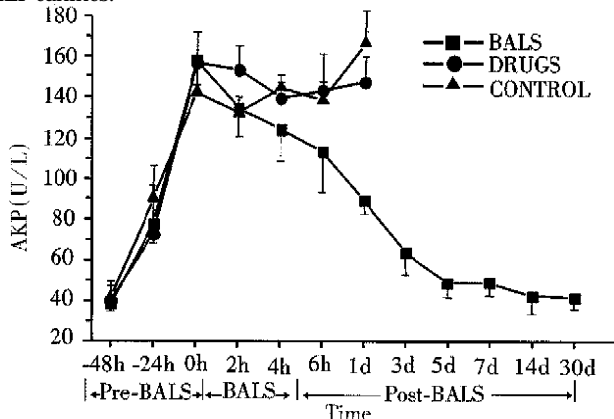


**Figure 5** Effects of the BALS on AKP of acetaminophen-induced ALF canines.

## DISCUSSION

ALF is usually an integrative response caused by viruses, drugs and toxins which leads to severe hepatocyte injury and the rapid loss of synthetic, metabolic and regulative functions, followed by the release of non-inflammatory cellular factors and other indefinite toxins into the circulation. Its mortality was as high as 50% - 80% and no effective clinical therapy is available currently. Because the ill liver has a tendency of reversibility, a reproduction can occur if we replace the hepatic functions by artificial methods. Since the liver has more than 500 complex physiological functions, the current non-biological ALS such as activated charcoal absorption can not replace the liver functions completely although it can clear some middle and small molecular weight substances in the circulation. In BALSS the exotic hepatocytes were used to exchange the substances with the ALF blood, so that it can temporarily replace the complex liver functions of ALF patients directly from the exotic hepatocytes. Now there are several types of BALSS and a few small animal experiments and clinical study reports with various therapeutic effects<sup>[1-7,9-11]</sup>. The studies of BALSS in China are still in the initial stage and the BALSS techniques are not mature. This experiment studied the main problems such as the source and culturing of hepatocytes, the development of ALF canines model and a assessment of the efficacy and safety of BALSS treatment based on the advanced techniques of hollow fiber tube BALSS introduced from abroad.

A large quantity of hepatocytes with a well-functioned condition and high-density in culture in the BALSS is a key factor in success. Some authors used the human liver tumor cell lines, human embryo hepa tocytes and porcine hepatocytes as the sources of hepatocytes<sup>[9-11]</sup>. But the possible dangers of the tumor cells to the receptors and the scarce of the embryonic cell hampered the studies of BALSS. Our experiment selected the quarantined pure strain Chinese experimental miniature swine as the source of hepatocytes. Using the modified enzymatic digesting and culturing method, we acquired a large quantity of porcine hepatocytes that can meet the needs of BALSS. The development of a large animal ALF model, especially with high-reproductivity, stability and a similar pathological changes to ALF patients, is still a major difficulty. Some people established the ALF canine models by surgical operation to occlude the blood supply for liver temporarily<sup>[12]</sup>. But this kind of models can not suit the studies of ALF or drugs because of the multiple organs failure induced by ischemic-reperfusion injury and the variability of death time. We used the multiple injections of acetaminophen to

induce the ALF canines. Forty-eight hours after injection, the blood hepatic biochemistry parameters had obvious changes. The canines' liver tissues manifested massive necrosis. The ALF canines would die within 56 - 84 hours without treatment. This disease model had a good reproductivity and the changes of blood biochemical parameters were similar to ALF patients except the plasma BUN. The death time of ALF canines is relatively stable and suits the studies of BALSS and drugs.

In our experiment, we developed an ALF canine model induced by acetaminophen and then treated with the clinical routine drugs, BALSS and infusion of dextrose solution for evaluating the efficacy, safety and feasibility of BALSS to treat the ALF canines. The biochemical parameters related to hepatic functions of the ALF canines in the control group were elevated except for the plasma BUN. The canines died within 2 days. The drug therapy could partly correct the changes of biochemical parameters of the ALF canines, but with a very limited efficacy, and the canines died 2 days after treatment. The perfusion treatment with the BALSS of cultured Chinese experimental miniature porcine hepatocytes lasted 6 hours. The blood biochemical parameters of hepatic functions of the ALF canines were corrected obviously at the 4th hour of perfusion. The effect was significantly superior to which used in the other two groups. ALF canines can survive more than 30 days after perfusion therapy. The pathological changes of liver were also recovered obviously. The results showed that the porcine hepatocytes in this kind of BALSS could temporarily replace the hepatic functions of ALF canines by perfusion through the membrane of

the hollow fiber tube, and then offered a chance for regeneration and repairment of the canine liver. It is suggested that the BALSS could temporarily replace the hepatic function of ALF patients safely and effectively, and may become a brand-new method for the treatment of ALF.

## REFERENCES

- Demetriou AA, Rozga J, Podesta L, Lepage E, Morsiani E, Moscioni AD, Hoffman A, McGrath M, Kong L, Rosen H, Villamil F, Woolf G, Vierling J, Makowka L. Early clinical experience with a hybrid bioartificial liver. *Scand J Gastroenterol*, 1995;208:111-117
- Sussman NL, Podestál L, Lepage E. The hepatic extracorporeal liver assist device: initial clinical experience. *Artif Organs*, 1994; 18:390-395
- Rozga J, Podesta L, LePage E, Morsiani E, Moscioni AD, Hoffman A, Sher L, Villamil F, Woolf G, McGrath M, Kong L, Rosen H, Lanman T, Vierling J, Makowka L, Demetriou AA. A bioartificial liver to treat severe acute liver failure. *Ann Surg*, 1994;219:538-546
- Harland RC, Bollinger R. Extracorporeal hepatic perfusion in the treatment of patients with acute hepatic failure. *Transplant Rev*, 1994;8:73-79
- Dixit V. Transplantation of isolated hepatocytes and their role in extrahepatic life support systems. *Scand J Gastroenterol*, 1995; 30(Suppl):101-110
- Tompkins RG, Yarmush ML. Prospects for an artificial liver. *Transplant Rev*, 1993;7:191-199
- Rozga J, Holzman MD, Ro MS, Griffin DW, Neuzil DF, Giorgio T, Moscioni AD, Demetriou AA. Development of a hybrid bioartificial liver. *Annals Surg*, 1993;217:502-511
- Xue YL, Zhang ZY, Huang YC, Liu CG. The present and development of the artificial liver researches. *Junyi Jinxu Xueyuan Xuebao*, 1996;17:293-297
- Nyberg SL, Rimmel RP, Mann HJ, Peshwa MV, Hu WS, Cerra FB. Primary hepatocytes outperform Hep G<sub>2</sub> cells as the source of biotransformation functions in a bioartificial liver. *Annals Surg*, 1994;220:59-67
- Sussman NL, Chong MG, Koussayer T, He DE, Shang TA, Whisnand HH, Kelly JH. Reversal of fulminant hepatic failure using an extracorporeal liver assist device. *Hepatology*, 1992;16:60-65
- Sielaff TD, Hu MY, Amiot B, Rollins MD, Rao S, McGuire B, Bloomer JR, Hu WS, Cerra FB. Gel entrapment bioartificial liver therapy in galactosamine hepatitis. *J Surg Res*, 1995;59: 179-184
- Misra MK, Peng FK, Sayhoun A, Kashii A, Derry CD, Caridis T, Slapak M, Chir M. Acute hepatic coma: A canine model. *Surgery*, 1972;72:634-642

Edited by MA Jing-Yun

# A study of the ameliorating effects of carnitine on hepatic steatosis induced by total parenteral nutrition in rats

LIANG Li-Jian, YIN Xiao-Yu, LUO Shi-Min, ZHENG Jin-Fang, LU Ming-De and HUANG Jie-Fu

**Subject headings** carnitine; hepatic steatosis; total parenteral nutrition; rats

## Abstract

**AIM** To investigate the effects of carnitine on ameliorating hepatic steatosis induced by total parenteral nutrition (TPN) in animal model.

**METHODS** Eighteen normal Wistar rats and 19 cirrhotic Wistar rats induced by carbon tetrachloride were randomly divided into three groups, i. e., free access to food and drink (group A), TPN (group B) and TPN+carnitine (group C) for one week, respectively. Hepatic function, histology and its fat content were determined on the 7th day.

**RESULTS** Hepatic triglyceride (TG) and cholesterol (CHO) contents were significantly higher in groups B and C than in group A, and significantly lower in group C than in group B in both normal and cirrhotic rats (all  $P < 0.05$ ). Histopathological examinations revealed that hepatic steatosis was more severe in group B than in group C in both normal and cirrhotic rats.

**CONCLUSION** Carnitine can ameliorate hepatic steatosis associated with TPN in both non-cirrhotic and cirrhotic rats.

## INTRODUCTION

Long-term total parenteral nutrition (TPN) can frequently lead to the development of hepatic steatosis. Although its incidence has decreased with modifications of the TPN regimen, such as increasing content of lipid and decreasing content of glucose, hepatic steatosis still remains the most common complication of TPN. The exact pathogenesis of TPN-associated hepatic steatosis is still unclear. A number of factors may contribute to the development of hepatic steatosis following TPN. Of them, the absolute or relative deficiency of carnitine is commonly postulated to be an important mechanism. Previous studies showed that patients with long-term TPN had carnitine deficiency<sup>[1-4]</sup>, however, the prophylactic effects of carnitine supplementation on hepatic steatosis have not been well documented. In this study, we investigated the effects of carnitine on minimizing TPN-associated hepatic steatosis in both normal and cirrhotic rats.

## MATERIALS AND METHODS

### *Animals and grouping*

**Normal groups** Eighteen male Wistar rats weighing 250g-300g, obtained from the Laboratory Animal Center of our university, served as normal groups. They were randomly divided into three groups: A1, B1 and C1, with six in each group.

**Cirrhotic groups** Twenty-five male Wistar rats, weighing 218g-245g, were used for inducing liver cirrhosis. They were treated with subcutaneous injection of 60% carbon tetrachloride (CCl<sub>4</sub>) at a dose of 0.3mL/100g body weight twice each week for 10 weeks, and 5% ethanol water solution was ingested as drink water through the period of time<sup>[5]</sup>. A total of six rats died during CCl<sub>4</sub> treatment. The remaining 19 rats were taken as cirrhotic groups, and randomly divided into three groups: A2, B2 and C2, with six, seven and six rats, respectively.

### *Feeding*

Groups A (A1 and A2), B (B1 and B2) and C (C1 and C2) had free access to food and water, carnitine-free TPN, and TPN with carnitine

Department of Hepatobiliary Surgery, The First Affiliated Hospital, Sun Yat-Sun University of Medical Sciences, Guangzhou 510080, Guangdong Province, China

Dr. LIANG Li-Jian, Male, Professor of hepatobiliary surgery, having 96 papers published.

**Correspondence to:** Dr. HUANG Jie-Fu, MD, Department of Hepatobiliary Surgery, The First Affiliated Hospital, Sun Yat-Sun University of Medical Sciences, 56 Zhongshan Er Lu, Guangzhou 510080, China

Tel. +86-20-87755766 Ext.8096, Fax.+86-20-87755766 Ext.8663

Received 1999-04-08

supplementation, respectively, for one week. Both group B and C were fasted when TPN was applied.

TPN solution was prepared according to physiological needs of growing rats<sup>[6]</sup>. It offered a total non-protein energy of 166kcal/kg body weight daily, with 40% provided by MCT/LCT lipid emulsion, and a nitrogen quantity of 1140mg/kg body weight daily. In normal rats, 10% compound amino acids solution was used as source of nitrogen, while 8% essential amino acids and branch-chained amino acids solution was used in cirrhotic rats. In group C, carnitine ("Hepadif", HANSEO Pharmaceutical Company, Seoul, Korea) was added to TPN solution at a dose of 100mg/kg body weight per day.

### Implementation of TPN

A 0.9mm silicon cannula was placed into the internal jugular vein of rat under ether anesthesia. The cannula was coursed subcutaneously, and was brought outside and fixed at the back neck. Rats were kept in cages without limiting activity after cannulation, and TPN solution was infused continuously via the cannula over 24 hours a day.

### Investigation

By the end of one week feeding, rats were weighed and then sacrificed under ether anesthesia. Blood sample was collected for determining total bilirubin (TBIL), aspartate transaminase (AST), alanine transaminase (ALT) and albumin (ALB). The liver was excised. One part of the liver was taken for quantitative assessment of triglyceride (TG) and cholesterol (CHO) content by using solvent extraction method. The remaining liver was fixed in 10% formalin and embedded in paraffin, and the sections were stained with hematoxylin and eosin (HE) and Sudan IV for histopathological examination. The severity of hepatic steatosis was evaluated semi-quantitatively according to the following grading system suggested by Ruwart *et al*<sup>[7]</sup>:

-: absence of steatosis.

+: mild steatosis with presence of lipid, mainly macrovesicular, in no more than 1/3 hepatocytes.

++: Moderate steatosis with presence of both micro- and macro-vesicular lipid in 1/3 to 2/3 of hepatocytes.

+++: severe steatosis with mixed micro and macro-vesicular lipid in more than 2/3 of hepatocytes.

++++: severe steatosis with presence of macrovesicular lipid in all or almost all hepatocytes.

### Statistical analysis

Results were expressed as mean  $\pm$  SD ( $\bar{x} \pm s$ ). Statistical analysis was performed using commercially available SPSS package, and one-way ANOVA and Student's *t* test were employed to compare the means between groups. Statistical significance was considered at  $P < 0.05$ .

### RESULTS

One rat in group B2 died of pulmonary edema during TPN due to an overly rapid infusion rate, and was excluded from the study. All other rats remained alive up to the end of study. There was no statistically significant difference in the initial body weight among normal groups (A1, B1 and C1) and cirrhotic groups (A2, B2 and C2) (Table 1).

With respect to liver function, Table 2 shows no significant difference in TBIL, AST, ALT and ALB among normal groups, and no significant difference in TBIL, AST and ALT among cirrhotic groups. ALB was significantly lower in group B2 and C2 than in group A2 (both  $P < 0.05$ ). Group C2 tended to have a lower ALT and higher ALB than group B2 (Table 2), but the difference was not statistically significant.

In normal groups, hepatic TG and CHO content was remarkably elevated in groups B1 and C1 in comparison with A1 (all  $P < 0.05$ ), but were significantly lower in C1 when compared with B1 (both  $P < 0.05$ , Table 3). Similarly, in cirrhotic groups, B2 and C2 had a significantly higher hepatic TG and CHO level than A2 (all  $P < 0.05$ ), and C2 had a markedly lower hepatic TG and CHO content as compared with B2 (both  $P < 0.05$ , Table 3).

Semi-quantitative assessment of hepatic steatosis revealed that group A1 was negative, A2 +, both B1 and B2 +++, and both C1 and C2 ++ (Figure 1).

**Table 1** The initial body weight (BW) of rats in different groups ( $\bar{x} \pm s$ )

	Normal group			Cirrhotic group		
	A1	B1	C1	A2	B2	C2
<i>n</i>	6	6	6	6	6	6
BW(g)	263.8 $\pm$ 13.5	268.1 $\pm$ 11.8	270.8 $\pm$ 10.1	318.2 $\pm$ 7.1	318.7 $\pm$ 5.3	321.8 $\pm$ 6.9

**Table 2** Liver function in various groups ( $\bar{x}\pm s$ )

	Normal group			Cirrhotic group		
	A1	B1	C1	A2	B2	C2
TBIL( $\mu\text{mol/L}$ )	12.4 $\pm$ 3.2	13.8 $\pm$ 4.8	2.0 $\pm$ 5.1	13.0 $\pm$ 2.7	13.2 $\pm$ 2.1	12.0 $\pm$ 2.5
AST(IU/L)	156.9 $\pm$ 28.6	187.2 $\pm$ 29.6	179.7 $\pm$ 22.3	264.0 $\pm$ 23.6	269.5 $\pm$ 26.7	269.5 $\pm$ 102.0
ALT(IU/L)	54.0 $\pm$ 11.0	43.8 $\pm$ 11.7	44.8 $\pm$ 15.1	106.0 $\pm$ 24.0	117.7 $\pm$ 25.0	89.2 $\pm$ 22.7
ALB(g/L)	38.8 $\pm$ 1.7	37.8 $\pm$ 1.0	39.5 $\pm$ 3.1	32.2 $\pm$ 2.8	5.8 $\pm$ 1.9 <sup>a</sup>	27.2 $\pm$ 2.4 <sup>a</sup>

<sup>a</sup> $P < 0.05$ , vs group A2.

**Table 3** Hepatic fat content in various groups ( $\bar{x}\pm s$ )

Group	Normal group			Cirrhotic group		
	A1	B1	C1	C1	A2	B2
TG( $\mu\text{mol/g}$ )	5.15 $\pm$ 0.76	39.33 $\pm$ 2.42 <sup>a</sup>	17.00 $\pm$ 3.95 <sup>a,e</sup>	9.05 $\pm$ 0.78	26.58 $\pm$ 2.76 <sup>c</sup>	13.11 $\pm$ 8.42 <sup>c,g</sup>
CHO( $\mu\text{mol/g}$ )	5.59 $\pm$ 0.66	13.13 $\pm$ 1.06 <sup>a</sup>	8.98 $\pm$ 1.50 <sup>a,e</sup>	6.30 $\pm$ 0.65	10.2 $\pm$ 0.83 <sup>c</sup>	7.98 $\pm$ 0.99 <sup>c,g</sup>

<sup>a</sup> $P < 0.05$ , vs group A1; <sup>c</sup> $P < 0.05$ , vs group A2; <sup>e</sup> $P < 0.05$ , vs group B1; <sup>g</sup> $P < 0.05$ , vs group B2.

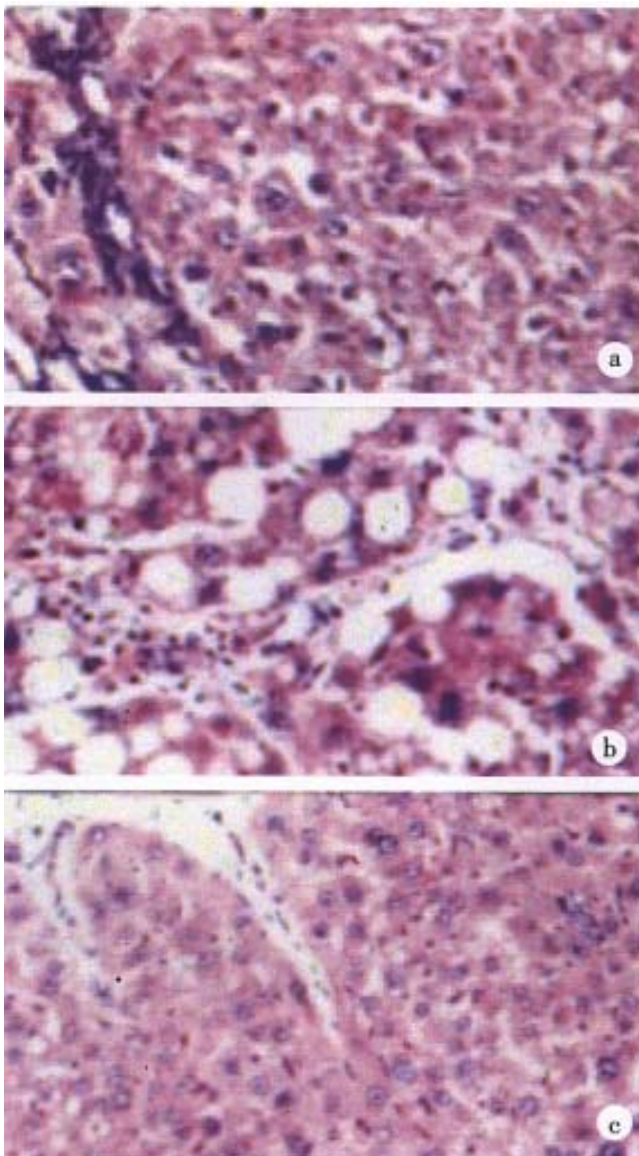


**Figure 1** Histopathological features of hepatic steatosis (HE staining,  $5 \times 10$ ), showing grade + (a), ++++ (b) and ++ (c). (a) Group A2, (b) Group B2, (c) Group C2.

## DISCUSSION

TPN has been widely applied to patients who are temporarily or permanently unable to intake sufficient nutrition enterally. It, however, can cause some metabolic disorders, especially in long-term users. Of them, hepatic steatosis is the most serious and frequently encountered disorder. The TPN-associated hepatic steatosis may be related to the high concentration of dextrose or glucose in its regimen, and impaired TG secretion by the liver. TPN with the use of glucose or lipid emulsion as the sole energy source usually leads to a more severe hepatic steatosis than that using both glucose and lipid in combination, which was also observed in our preliminary study (data not shown). In cirrhotics, the liver tends to utilize less glucose and more lipid to produce energy. Hence, the glucose-lipid ratio of TPN should be adjusted in cirrhotic patients with, ideally, 55% - 60% of energy provided by glucose and 40%-45% provided by lipid.

To date, the effect of lipid emulsion itself on liver function is controversial. It is commonly thought that LCT predisposes to liver function damage. But, Fan *et al*<sup>[8]</sup> reported that the MCT/LCT clearance rate was not impaired in cirrhotic livers, and hence believed that MCT/LCT was suitable for TPN in patients with liver cirrhosis. Our study showed that TPN using MCT/LCT could lead to hepatic steatosis in both normal rats (group B1) and cirrhotic rats (group B2). In addition, ALB in group B2 was significantly lowered. It was postulated that hepatic steatosis caused by TPN further damaged the compromised liver function, and consequently influenced the synthesis of ALB. Regardless of the causes of hepatic steatosis, it is certainly deleterious to liver function, especially in patients with liver cirrhosis and impaired liver function. Therefore, it is necessary to treat the hepatic steatosis in long-term TPN users, and to supplement ALB simultaneously in those with liver

cirrhosis and impaired liver function.

Many factors contribute to the development of TPN-associated hepatic steatosis. Absolute or relative deficiency of carnitine is an important factor. Long-term TPN can lead to a reduced level of carnitine, and chronic liver disease itself can also cause deficiency of carnitine. Rudman *et al*<sup>[9]</sup> determined serum carnitine level in 273 hospitalized patients and 12 normal subjects, and found that serum carnitine level in cirrhotic patients was only 25% of that in non-cirrhotic patients as well as in normal subjects; and autopsy study revealed that the content of carnitine in liver, kidney, muscle and brain of cirrhotics was only 1/3 to 1/4 that of noncirrhotic patients.

Carnitine plays an important role in  $\beta$ -oxidation of free fatty acid and tricarboxylic acid cycle in mitochondria. In a carnitine deficiency,  $\beta$ -oxidation of free fatty acids would be inhibited, which leads to the lipid infiltration of hepatocytes as well as the insufficient production of ATP and consequent liver failure. Supplementation of carnitine probably can help prevent the TPN-associated hepatic steatosis, and promote oxidation of fat and recovery of liver function. The present study demonstrated that carnitine supplementation could minimize TPN-associated hepatic steatosis in both normal and cirrhotic rats. In addition, group C2 tended to have a lower ALT and higher ALB in comparison with

group B2. It suggested that carnitine supplementation during TPN was helpful in reducing the severity of hepatic steatosis and subsequently protecting liver function. It is reasonable to speculate that carnitine supplementation in long-term TPN is of therapeutic value, particularly for patients with impaired liver function. Further studies are still, however, needed to fully evaluate its clinical usefulness.

## REFERENCES

- 1 Bowyer BA, Fleming CR, Ilstrup D, Nelson J, Reek S, Burnes J. Plasma carnitine levels in patients receiving home parenteral nutrition. *Am J Clin Nutr*, 1986;43:85-91
- 2 Hahn P, Allardyce DB, Frohlich J. Plasma carnitine levels during total parenteral nutrition of adult surgical patients. *Am J Clin Nutr*, 1982;36:569-572
- 3 Moukartzel AA, Dahlstrom KA, Buchman AL, Ament ME. Carnitine status of children receiving long term total parenteral nutrition: a longitudinal prospective study. *J Pediatr*, 1992;120:759-762
- 4 Bonner CM, DeBrie KL, Hug G, Landrigan E, Taylor BJ. Effects of parenteral L-carnitine supplementation on fat metabolism and nutrition in premature neonates. *J Pediatr*, 1995;126:287-292
- 5 Wu MC, Yang GS. The establishment of liver cirrhosis animal model in rats. *Zhonghua Shiyan Waike Zazhi*, 1984;1:145-147
- 6 Tao RC, Yoshimura NN, Chinn IB, Wolfe AM. Determination of intravenous non-protein energy and nitrogen requirements in growing rats. *J Nutr*, 1979;109:904-915
- 7 Ruwart YJ, Rush BD, Snyder KF, Peters KM, Appelman HD, Henley KS. 16, 16-Dimethyl prostaglandin E2 delays collagen formation in nutritional injury in rat liver. *Hepatology*, 1988;8:61-64
- 8 Fan ST, Wong J. Metabolic clearance of a fat emulsion containing medium-chain triglycerides in cirrhotic patients. *J Parenter Enteral Nutr*, 1992;16:279-283
- 9 Rudman D, Sewell CW, Ansley JD. Deficiency of carnitine in cachectic cirrhotic patients. *J Clin Invest*, 1977;60:716-723

Edited by MA Jing-Yun

# Telomerase activity in gastric cancer and its clinical implications \*

ZHAN Wen-Hua, MA Jin-Ping, PENG Jun-Sheng, GAO Jing-Song, CAI Shi-Rong, WANG Jian-Ping, ZHENG Zhang-Qing and WANG Lei

**Subject headings** stomach neoplasms; telomerase; tumor markers

## Abstract

**AIM** To study the telomerase expression in gastric carcinoma and its clinical implications.

**METHODS** Telomerase activity was examined in gastric cancer and corresponding normal tissues using a modified TRAP (telomeric repeat amplification protocol) assay (TRAP-eze) in tissue samples from 94 gastric carcinomas and 58 normal tissues, 12 gastric adenomas and 9 gastric ulcer lesions.

**RESULTS** Telomerase activity was present in 81 of the 94 (86.2%) gastric cancer tissues, whereas no telomerase activity was detected in any normal tissues. The incidence of telomerase activity in gastric cancer tissues was unrelated to the tumor diameter, histological grade, tumor invasion in depth, lymph node metastasis and TNM stage.

**CONCLUSION** Telomerase plays an important role in carcinogenesis and progression of gastric cancer, and it is suggested to be a useful tumor marker.

## INTRODUCTION

The development of carcinoma results from multiple independent genetic changes that activate proto-oncogenes or inactivate the action tumor suppressor genes. Although several authors have reported findings in gastric cancer that support this concept<sup>[1]</sup>, the molecular mechanism of gastric carcinogenesis has not been fully explored. Recent studies showed that telomerase activity expression was closely correlated with the occurrence and development of human malignant tumors. Telomerase activity expression was detected in most of human tumors<sup>[2,3]</sup>.

Telomerase is a ribonucleoprotein complex that adds telomeric repeats onto chromosomal ends using an intrinsic RNA as a template, thus extending telomeric DNA<sup>[4,5]</sup>. Telomeres are special structures containing unique repeats and associated proteins at the ends of eukaryotic chromosomes, which consist of short tandem DNA repeat sequences and telomere-binding proteins. Human telomeres repetitive sequence is TTAGGG/AATCCC. Telomeres are thought to be important for protecting the ends of the chromosomes from fusion, degradation and random breakage, and for maintaining the stability of the chromosomes. Telomeres apply for the important structure fundament for solving the so-called "end replication problem". According to the so-called "end replication problem", the cellular chromosomes lose 50 bp - 200 bp of telomeric sequences during each cell division, leading to a limited replicative capacity and eventually resulting in cellular senescence. Therefore, telomere is considered to play a role of "mitotic clock"<sup>[6,7]</sup>. In germline cells, telomere length maintained stable because of telomerase enzyme, which resynthesizes telomeric DNA sequences at chromosome ends, in contrast, telomere length is kept balanced because of telomerase reactivity in the malignant cells.

During the past 20 years, the mortality rates of gastric cancer have been rising constantly in our country, and the mortality rate of gastric cancer ranks first in the analyses of variation trends and short-term detection of Chinese malignant tumor mortality<sup>[8]</sup>. Therefore, it is urgent to put emphasis on the study of the experimental and clinical studies. The study of telomerase expression in

Department of Surgery, Sun Yat-Sen University of Medical Sciences, the First Affiliated Hospital, Guangzhou, China

\*The study was supported by the research grant from Natural Science Foundation of Guangdong Province and Public Health Commission of Guangdong Province.

**Correspondence to:** Professor ZHAN Wen-Hua, Department of Surgery, The First Affiliated Hospital, Sun Yat-Sen University of Medical Sciences, Guangzhou, China

Tel.+86-10-20-87755766-8804, Fax.+86-10-20-87750632, 87331061

Email. whzhan@gzsums.edu.cn

Received 1999-01-20

primary gastric cancer could help us better understand the carcinogenesis of gastric cancer at molecular level, and search for a new gastric tumor marker, which are of benefit for development of drugs or methods to inhibit telomerase activity<sup>[9]</sup>.

The non-isotopic TRAP assay was used in this study to detect telomerase activity expression and clinical pathological data in gastric carcinomas.

## MATERIALS AND METHODS

### Tissue samples

Surgically resected tissue samples from 94 gastric carcinomas, 58 normal gastric mucosa tissues, 12 gastric adenomas and 9 gastric ulcer lesions were taken from operations performed during the period of February 1997 to September 1998. The gastric cancer samples were collected from 50 males and 44 females aged from 30 to 82 years (mean age 63). The mean diameter of tumors is 4.6cm (ranging from 2cm to 12cm), and according to the depth of invasion, there were 2 of T<sub>1</sub>, 14 of T<sub>2</sub>, 38 of T<sub>3</sub> and 40 of T<sub>4</sub>. Two were of stage I, 23 of stage II, 42 of stage III, and 27 of stage IV. Tumor sizes were measured immediately after gastrectomy. All samples were obtained within 1h after surgical removal. Specimens were snap frozen and stored in liquid nitrogen until use. The histopathological factors were evaluated by our pathologists and operators according to the international established criteria.

### Extract preparation

Frozen samples of 50 mg-100 mg, including gastric cancer, normal gastric mucosa, gastric adenoma and metaplastic lesions, were washed twice with ice wash buffer, all of which was then carefully removed. The samples were kept in liquid nitrogen and ground with a pestle until a smooth consistency was achieved, and then homogenized until a uniform consistency was reached and mixed with 200μL × CHAP Lysis Buffer. After 30 minutes incubation on ice, the lysates were centrifuged at 16000rpm for 30 minutes at 4°C. The 160μL supernatant was placed into two fresh tubes, and the protein concentration was determined. The remaining extract was aliquoted and quickly frozen and stored at -80°C.

### TRAP assay

All operational procedures were finished on the super-clean desk in ice water, and all reagents were thawed on ice. The amount of reagent required in each TRAP assay is 50.0μL containing: 10×TRAP buffer 5.0 μL, 50 × dNTPs mixture 1.0 μL, TS primer 1.0μL, CX primer [5'(CCCTTA)<sub>3</sub>-CCCTAA 3'] 1.0μL, Taq polymerase (5U) 0.4μL (2U), ddH<sub>2</sub>O 9.6μL and tissue extract 2.0μL,

which was incubated for 30 minutes at 30°C. The reaction mixture was then subjected to 31 PCR cycles at 94°C for 45 sec, 50°C for 45 sec and 72°C for 90 sec.

The PCR products were analyzed by electrophoresis in a 12.5% polyacrylamide nondenaturing gel for 1 hour at 100 volts for a 10cm-12cm vertical gel, or until the bromophenol blue just run off the gel. After electrophoresis, the gel was stained with silver nitrate solution. The positive enzyme activity was confirmed when the telomerase specific, 6bp DNA ladder, was observed.

### Statistics

Statistical analysis was made with SAS. Telomerase positive ratio between groups was tested for significance with  $\chi^2$  test and Fisher exact test.

## RESULTS

The expression of telomerase in gastric carcinoma (Table 1).

**Table 1 Telomerase expression in gastric cancer**

Groups	Telomerase activity		Positive rate(%)
	Positive	Negative	
Gastric cancer (n=94)	81	13	86.2
Normal tissue (n=58)	0	58	0
Gastric ulcer (n=9)	1	8	11.1
Gastric adenoma (n=12)	1	11	8.38

Telomerase activity was detected in 81 (86.2%) of 94 gastric carcinomas examined, 1 of 12 gastric adenoma and 1 of 9 gastric ulcer lesions. However, no telomerase activity ( $P<0.001$ ) was detected in all the 58 normal tissues from the same patients (Figure 1).

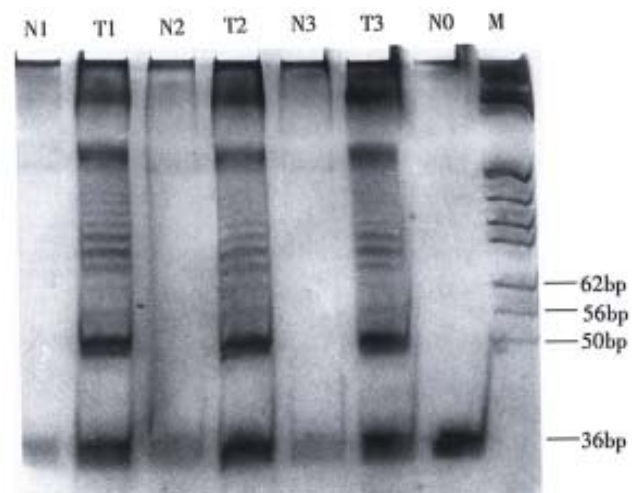


**Figure 1** Representative results of telomerase activity in gastric cancer and normal tissues. Most of the gastric cancer tissues (T) showed telomerase activity whereas it was not detected in the corresponding normal tissues (N).

The relationship between telomerase activity and clinical pathological parameters in gastric carcinoma.

The incidence of telomerase activity in gastric carcinoma tissues was not correlated to tumor diameter, histological grade, tumor invasion in depth, lymph node metastasis and TNM stage ( $P>0.05$ , Table 2).

**Table 2 Clinical data in gastric cancer cases**

Groups	Telomerase activity		$\chi^2$	P
	Positive(n=81)	Negative(n=13)		
<b>Tumor size (cm)</b>				
<5 (n=42)	35	7	0.839	0.657
5.8 (n=32)	29	3		
>8 (n=20)	17	3		
<b>Histological grade</b>				
Well differentiated (n=28)	23	5	0.564	0.754
Moderately and well differentiated(n=18)	16	2		
Poorly differentiated (n=48)	42	6		
<b>Invasion depth</b>				
T1 (n=2)	1	1	0.392	0.531
T2 (n=14)	12	2		
T3 (n=38)	33	5		
T4 (n=40)	35	5		
<b>Lymph node metastasis</b>				
<3cm (n=38)	30	8	2.792	0.095
>3cm (n=56)	51	5		
<b>TNM stage</b>				
I(n=2)	1	1	0.135	0.714
II (n=23)	20	3		
III (n=42)	37	5		
IV (n=27)	23	4		

## DISCUSSION

Telomeres, the distal ends of human chromosomes composed of tandem repeats of the sequence TTAGGG, are believed to play an essential role in maintaining the stability and protection of chromosomes. Normal human somatic cells lose 50bp-100bp of terminal telomeric DNA with each round of replication. Telomerase is a ribonucleoprotein containing an RNA template that synthesizes telomeric DNA. Cells with the activated enzyme appear to escape from progressive telomeric shortening and acquire an indefinite growth potential<sup>[10]</sup>. Telomerase activity has been demonstrated in multiple tumor lines and is absent in corresponding normal tissues. In our study, telomerase activity was positive in 81 (86.2%) of 94 gastric carcinoma tissues, whereas it was negative in normal tissues. According to a recent review, 758 (85%) of 895 malignant tumors, but none of 70 normal somatic tissues, expressed telomerase activity<sup>[11]</sup>. These strong associations of telomerase activity with malignant tumors is good evidence that

telomerase can be an important marker for diagnosing cancer.

In our study, telomerase activity was also detected in 1 of 2 early gastric cancers, and 1 of 12 gastric adenomas and 9 gastric ulcer lesions, respectively. The results from Maruyama *et al* are similar to those of the present study in which telomerase activity was detected in 10 (45%) of 22 adenomas and 2 (15%) of 12 metaplastic lesions<sup>[12]</sup>. Tahara *et al* demonstrated telomerase activity in 10 tubular adenoma samples. These results support the hypothesis that telomerase activation is an early event in the malignant process. According to the previous report<sup>[14,15]</sup>, telomerase activity expression could take place in the early stage of gastric cancer even in the precancerous lesions, which implicated the importance of the early diagnosis of gastric cancer.

It is interesting that about 15% of malignant tumors expressed no telomerase activity, and in our study, no telomerase activity has been detected in about 14% gastric cancer samples. It is unclear what mechanism is responsible for this phenomenon. Long-term chromosome stability in humans depends on the addition of telomeric repeats, and telomerase is essential for telomere length maintenance. However, in a survey of immortal cell lines, Kim *et al* found that approximately 10% of tumors maintained long stretches of terminal repeats without detectable telomerase activity<sup>[16]</sup>. Bryan *et al* also found that 40% of the immortal lines showed no telomerase activity, yet these cell lines had very long and heterogeneous telomeres of up to 50kb<sup>[17]</sup>. Recombination has been proposed as a possible elongation mechanism in these cases, however, direct evidence is still lacking<sup>[18]</sup>. In a recent research, Smith *et al* found a second enzyme, *tankyrase*, which may enable telomerase to do its work. These evidence suggests that *tankyrase* can control the action of telomerase by removing TRF 1, a telomere-specific DNA binding protein that otherwise blocks telomerase's access to the chromosome ends<sup>[19]</sup>.

We found no significant correlation between levels of telomerase activity and other clinicopathological variables, including tumor diameter, histological grade, tumor invasion in depth, lymph node metastasis and TNM stage. This is in contrast to the results of Hiyama *et al*, who reported that telomerase activity was present mostly in large tumors or those of advanced stage, including metastatic tumors. Furthermore, the survival rate of tumor patients with detectable telomerase activity was significantly lower than that of patients without telomerase activity. However,

our results are in agreement with the studies by Ahn *et al.* These contradictory results need further investigations.

## REFERENCES

- 1 Wright PA, Williams GT. Molecular biology and gastric carcinoma. *Gut*, 1993;34:145-147
- 2 Rhyu MS. Telomeres, telomerase, and immortality. *J Natl Cancer Inst*, 1995;87:884-894
- 3 Shay JW, Gazdar AF. Telomerase in the early detection of cancer. *J Clin Pathol*, 1997;50:106-109
- 4 Greider CW. Telomerase activity, cell proliferation, and cancer. *Proc Natl Acad Sci USA*, 1998;95:90-92
- 5 Kim NW, Piatyszek MA, Prowse KR, Harley CB, West MD, Ho PLC, Coviello GM, Wright WE, Weinrich SL, Shay JW. Specific association of human telomerase activity with immortal cells and cancer. *Science*, 1994;266:2011-2015
- 6 Blackburn EH. Structure and function of telomeres. *Nature*, 1991;350:569-573
- 7 Zakian VA. Telomeres:beginning to understand the end. *Science*, 1995;270:1601-1607
- 8 Li LD, Lu FZ, Zhang SW. Trend of change in mortality from malignant neoplasms over the past 20 years and predictive analysis. *Chin J Oncol*, 1997;19:3-9
- 9 Morin GB. Is telomerase a universal cancer target? *J Natl Cancer Inst*, 1995;87:859-861
- 10 Blasco MA, Rizen M, Greider CW, Hanahan D. Differential regulation of telomerase activity and telomerase RNA during multi-stage tumorigenesis. *Nat Genet*, 1996;12:200-204
- 11 Shay JW, Bacchetti S. A survey of telomerase activity in human cancer. *Eur J Cancer*, 1997;33:787-791
- 12 Maruyama Y, Hanai H, Fujita M, Kaneko E. Telomere length and telomerase activity in carcinogenesis of the stomach. *Jpn J Clin Oncol*, 1997;27:216-220
- 13 Tahara H, Kuniyasu H, Yokozaki H. Telomerase activity in premalignant and neoplastic gastric and colorectal lesions. *Clin Cancer Res*, 1995;1:1245-1251
- 14 Hiyama E, Yokoyama T, Tatsumoto N, Hiyama K, Imamura Y, Murakami Y, Kodama T, Piatyszek MA, Shay JW, Matsuura Y. Telomerase activity in gastric cancer. *Cancer Res*, 1995;55:3258-3262
- 15 Ahn MJ, Noh YH, Lee YS, Lee JH, Chung TJ, Kim IS, Choi IY, Kim SH, Lee JS, Lee KH. Telomerase activity and its clinicopathological significance in gastric cancer. *Eur J Cancer*, 1997;33:1309-1313
- 16 Kim NW. Clinical implications of telomerase in cancer. *Eur J Cancer*, 1997;33:781-786
- 17 Bryan TM, Englezou A, Gupta J, Bacchetti S, Reddel RR. Telomere elongation in immortal human cells without detectable telomerase activity. *EMBO J*, 1995;14:4240-4248
- 18 Biessmann H, Mason JM. Telomere maintenance without telomerase. *Chromosoma*, 1997;106:63-69
- 19 Smith S, Giriat I, Schmitt A, de-Lange T. Tankyrase, a poly (ADP-ribose) polymerase at human telomeres. *Science*, 1998;282:1484-1487

Edited by MA Jing-Yun

# Survey of coverage, strategy and cost of hepatitis B vaccination in rural and urban areas of China\*

ZENG Xian-Jia<sup>1</sup>, YANG Gong-Huan<sup>2</sup>, LIAO Su-Su<sup>1</sup>, CHEN Ai-Ping<sup>2</sup>, TAN Jian<sup>2</sup>, HUANG Zheng-Jing<sup>2</sup> and LI Hui<sup>1</sup>

**Subject headings** Hepatitis B vaccine; coverage rate; immunization strategy; hepatitis B/prevention and control

## Abstract

**AIM** In order to understand the coverage, immunization strategy and cost of hepatitis B (HB) vaccination of China in recent years.

**METHODS** A two-stage household random sampling method was used in the survey.

**RESULTS** The survey carried out at 112 Disease Surveillance Points (DSPs) of 25 provinces, autonomous regions and municipalities of China in 1996, showed that the coverage rates of HB vaccination among neonates were 96.9% in the urban DSPs and 50.8% in the rural DSPs in 1993-1994, while in students aged 7-9 years, they were 85.8% and 31.5% in 1994, respectively. Up to 1994, 97.5% of the urban DSPs and 73.9% of the rural DSPs on a neonate vaccination against HB program were included in EPI. About 93% of the urban DSPs and 44% of the rural DSPs did HBsAg and HBeAg screening for all or part of pregnant women. The neonates received the regimen of high-dose HB vaccine in combination with hepatitis B immune globin (HBIG) if their mothers were HBsAg and/or HBeAg positive in pregnancy, otherwise they received the low-dose vaccine (10 $\mu$ g $\times$ 3). Part of DSPs had a lower neonate coverage due to unreasonable allocation of the vaccines (used for adults not at risk) or higher cost or insufficient supply of the vaccines. It is necessary to evaluate the quality of serological lab test to HBVMs in the maternal prescreening.

**CONCLUSION** Remarkable achievements have been made according to the national planning and policy of HB immunization in China.

## INTRODUCTION

Some studies demonstrated that HBsAg and anti-HBc-positive rates of the immunized populations after hepatitis B (HB) vaccination were significantly lower than those of a parallel or a historical control population, and the efficacy or effectiveness of protection against HBsAg was over 85% 1-12 years after infancy vaccination<sup>[1,2]</sup>. Since the 1990s hepatitis B vaccination has become a principal strategy for the control of HB in China<sup>[3]</sup>, however, special attention should be paid to the rational use of HB vaccine and the improvement of coverage rate of vaccination in the implementation of national HB immunization program. At present, there has been few data on national coverage of infancy vaccination, immunization strategy and regimen, allocation and cost of HB vaccine because of lack of the corresponding survey in the whole country. To improve the benefit of the national vaccination program and to provide the evidences relative to immunization compliance used for the evaluation of effectiveness of this HB control program, we conducted an epidemiological survey in the national disease surveillance points (DSPs) between December 1995 and January 1996 in China.

## MATERIALS AND METHODS

### Definition of terms

Coverage rate of hepatitis B vaccination: this rate means the percentage of immunized individuals with hepatitis B vaccine among infants and children aged 7-9 years, and is estimated through the sampling survey.

Reported coverage rate of infant hepatitis B vaccination: this rate means the percentage of immunized individuals with hepatitis B vaccine among all infants of the rural counties or the urban districts in 1994, and is reported by the local anti-epidemic stations according to the routine communicable disease reporting system.

Immunization strategy and regimen: the strategy is referred to the selection of target population for immunization, hepatitis B vaccine integrated with or without EPI, screening hepatitis B surface antigen and eantigen or not to mothers before delivery, and in conjunction with or without hepatitis B immune globin (HBIG); and regimen is referred to dosage of vaccine and schedule of

<sup>1</sup>Institute of Basic Medical Sciences, CAMS & PUMC, Beijing 100005, China

<sup>2</sup>Institute of Epidemiology and Microbiology, Chinese Academy of Preventive Medicine, China

\*Supported by China Medical Board of New York, Inc. USA, Grant No. 93-582

Correspondence to: ZENG Xian-Jia, Department of Epidemiology, Institute of Basic Medical Sciences, CAMS & PUMC, Beijing 100005, China

Tel. +86-10-65296971

Received 1999-04-08

vaccination.

Allocation of vaccine: allocation of vaccine means the proportion of vaccine amount allocated to different populations of immunization.

Cost of vaccination: the cost is the fee used for injection of HB vaccine or/and HBIG in each infant as well as the fee for predelivery screening of mothers.

### Subjects

All infants born in the period from January 1, 1993 to December 31, 1994 and children aged 7-9 years: all children born between January 1, 1986 and December 31, 1988 among the identified eligible households were selected as eligible subjects for interview.

### Sampling methods

Two-stage random sampling method with a same sample size was used to determine eligible villages or neighbourhood committees and households for the survey in each DSP. The procedure is as follows: ① making first-stage sampling frame that all villages or neighbourhood committees in each DSP are defined as first-stage sampling unit for coding, then 20 sampling units are randomly drawn in terms of a table of random number (if the sampling unit less than 20, then only 10 sampling units drawn); ② making second-stage sampling frame that all households in each village or neighbourhood committee drawn in the first-stage sampling are referred to as second-stage sampling unit, 50 or 100 households (if only 10 units drawn in the first-stage, then sampling 100 units) are randomly sampled, and 20% of households as candidates for the replacement of non responders or families lost to follow-up.

### Method of data collection

Household survey and schooling interview were carried out for the collection of the data of individuals from the families, schools and clinics according to a standardized questionnaire. The data relative to status of infancy HB vaccination of the eligible children were collected through interviewing their parents or caretakers and checking the Immunization Record Card; the information of the children aged 7-9 years were provided by their parents, and the validity was determined after checking with their teachers and health workers if necessary. The data on reported coverage of HB vaccination and the status of allocation of the vaccines were provided by three departments, EPI, epidemiology and disease surveillance in an anti epidemic station in terms of the standardized questionnaire.

## RESULTS

### Status of hepatitis B vaccination

**Coverage rates of infant hepatitis B vaccination and children aged 7-9 years** Among the 112 DSPs of 25 provinces, autonomous regions and municipalities (PARMs), except for 2 DSPs of the Tibet Autonomous Region and 1 DSP of the Gansu Province which did not carry out the hepatitis B vaccination, the remaining 109 DSPs had the hepatitis B vaccination program up to 1994. We interviewed a total of 10900 families of the 109 DSPs in the survey, including 8248 children and 17883 junior students. The coverage rate of HB vaccine immunization is shown in Table 1.

**Table 1 Coverage rates of hepatitis B vaccine immunization among infants and primary school students in 109 DSPs of China**

Target population	Areas	No. of DSPs	Sample size	Coverage		Coverage with 3 doses	
				No. of vaccinees	%	No. of vaccinees	%
Infants	Total	109	8248	5376	65.2	5190	96.5
	Urban	40	2572	2492	96.9	2434	97.7
	Rural	69	5676	2884	50.8	2756	95.6
Students	Total	108	17883	8143	45.5	7815	96.0
	Urban	40	4621	3965	85.8	3933	99.2
	Rural	68 <sup>a</sup>	13262	4178	31.5	3882	92.9

<sup>a</sup>In one DSP, no hepatitis B vaccination for primary school students was conducted in 1994.

It can be seen from Table 1, that the coverage rate of infant HB vaccine immunization in the urban areas was 96.9%, significantly higher than that in the rural areas (50.8%) during the period of 1993-1994 ( $\chi^2 = 1655.9$ ,  $P < 0.01$ ). The coverage of students aged 7-9 years was 85.5% in the urban, significantly higher than 31.5% in the rural ( $\chi^2 = 4074.3$ ,  $P < 0.01$ ). The coverage with 3 doses of HB vaccine was over 92% in both.

### The reported coverage rates of hepatitis B vaccination by the local anti-epidemic stations

According to the reported coverage of the anti-epidemic stations of the 112 DSPs (41 in the urban and 71 in the rural) in 1994, 92.7% of the urban DSPs and 45.1% of the rural DSPs, had a coverage rate of over 60% for neonatal HB vaccination, the difference between the two areas was statistically significant ( $\chi^2 = 25.1$ ,  $P < 0.01$ ).

### Status of the implemented strategies of hepatitis B vaccine immunization

#### Selection of target population for HB immunization

Up to 1994, 97.3% (109/112) of the anti-epidemic stations located in the surveyed DSPs had implemented the infant HB vaccine immunization program. The number of DSPs without HB vaccination for preschool children, primary school students and middle school students was 18 (6 in the urban and 12 in the rural), 41 (15 in the urban and 26 in the rural) and 68 (22 in the urban and 46 in the rural), respectively, and the number of DSPs conducting HB vaccination for adults at risk, even for the general population, was 43 (18 in the urban and 25 in the rural) and 34 (13 in the urban and 21 in the rural), respectively.

**Status of hepatitis B vaccination integrated with EPI** Totally 82.6% of 109 DSPs integrated infant HB vaccine immunization into EPI program in 1994. This percentage was 97.5% in the urban, significantly higher than 73.9% in the rural ( $\chi^2=9.8, P<0.01$ ).

**Pattern and quality of maternal predelivery HBeAg and HBsAg screening** Of 40 urban DSPs the proportion of DSPs with the predelivery screening for all pregnant women or a part of pregnant women and the proportion without the predelivery screening was 60.0%, 32.5% and 7.5% in 1994, respectively. However, the corresponding proportion was 5.8%, 37.7% and 55.1% in 69 rural DSPs. The former two proportions of the urban DSPs were significantly higher than that of the rural DSPs ( $\chi^2=25.7, P<0.01$ ). The results of the predelivery screening obtained from the household survey in the urban and rural DSPs are shown in Table 2.

**Table 2 Results of predelivery screening HBeAg and HBsAg among mothers of 2 252 infants in 1994**

	Urban	Rural
Number of screening	1775	477
Isolated HBsAg-positive	13	14
Isolated HBeAg-positive	5	0
HBeAg- and HBsAg-positive	7	0
HBsAg-positive rate	1.1%(20/1775)	2.9%(14/477)
HBeAg-positive rate	0.7%(12/1775)	0.0%

The results of Table 2 showed that HBsAg-positive and HBeAg-positive rates were 1.1% and 0.7% in the urban, and 2.9% and 0% in the rural.

**Dosage and regimen of infant HB vaccination and in combination with HBIG** The regimen of immunization, 0, 1, 6 months schedule, was used for infancy vaccination in all 109 DSPs. The status

of regimen for infant HB vaccination and in combination with HBIG in the DSPs with the predelivery screening in all pregnant women (14 DSPs), a part of pregnant women (18 DSPs) and without screening (39 DSPs) is shown in Table 3.

**Table 3 Regimen of infant HB vaccination or/and in combination with HBIG in 71 DSPs**

Screening	Maternal HBVMs	Regimen	No. of DSPs			
			Total	Urban	Rural	
Yes	HBeAg- and HBsAg-positive	30 $\mu$ g+10 $\mu$ g $\times$ 2	6	5	1	
		HBIG $\times$ 1+30 $\mu$ g+10 $\mu$ g $\times$ 2	10	2	8	
		30 $\mu$ g $\times$ 3	7	3	4	
	Isolated HBsAg-positive	30 $\mu$ g $\times$ 3	Others	9	7	2
			30 $\mu$ g+10 $\mu$ g $\times$ 2	11	9	2
			HBIG $\times$ 1+30 $\mu$ g+10 $\mu$ g $\times$ 2	9	2	7
		10 $\mu$ g $\times$ 3	30 $\mu$ g $\times$ 3	6	3	3
			10 $\mu$ g $\times$ 3	2	0	2
			Others	4	2	2
HBeAg- and HBsAg-negative	10 $\mu$ g $\times$ 3	10 $\mu$ g $\times$ 3	25	12	13	
		HBIG $\times$ 1+10 $\mu$ g $\times$ 3	1	1	0	
		30 $\mu$ g+10 $\mu$ g $\times$ 2	6	3	3	
No		10 $\mu$ g $\times$ 3	36	3	33	
		HBIG $\times$ 1+30 $\mu$ g $\times$ 3	1	0	1	
		30 $\mu$ g+10 $\mu$ g $\times$ 2	2	0	2	

Table 3 showed that among the DSPs with the maternal predelivery screening, the regimen of first dose of 30 $\mu$ g, second and third doses of 10 $\mu$ g-HB vaccine was adopted for the infants whose mothers were HBeAg or/and HBsAg-positive in the majority of DSPs, next was the regimen of three doses of 30 $\mu$ g; combination with HBIG only in 18 DSPs, and the regimen of three doses of 10 $\mu$ g was used for the infants of mothers with negative screening results and in the DSPs without the maternal screening. Almost all the DSPs used China-made plasma-derived HB vaccines.

#### Allocation of vaccines

Based on the reported infancy coverage rates from anti-epidemic stations where DSPs were located in 1994, a total amount of HB vaccines and the proportion of the vaccines allocated to various populations and the pattern of the vaccine allocation were analyzed. The results showed that of 109 DSPs, 22 DSPs where the coverage rate of infant HB vaccination was not up to 60% in 1994 allocated less than 80% of the vaccines to infants for HB vaccination integrated with EPI, indicating that a considerable amount of the vaccines was unreasonably allocated to other populations, leading to the lower coverage of infant vaccination against HB in these DSPs. This phenomenon often occurred in the rural DSPs. In addition, although over 80% of HB vaccines was allocated to infants, the infant

coverage was still less than 60% in 7 DSPs, suggesting that the amount of the vaccines ordered for that year was not enough for infant vaccination.

### Cost of vaccination

It was found that there was a big difference in the vaccination fee for each child and maternal predelivery screening, even in a same DSP, the rate was different. In a few DSPs, families had to pay very high fee for their baby immunization. Among 63 DSPs with the regimen of three doses of 10 $\mu$ g vaccine, 8 DSPs (12.7%) charged over 50 yuan RMB, 2 DSPs of which over 100 yuan per infant, approximately 2 - 5 times higher than the common standard of 21 yuan. Of 18 DSPs using combined HBIG, 4 DSPs charged a fee over 60 yuan, the highest being up to 140 yuan.

### DISCUSSION

The results of this survey showed that the coverage rate of infant HB vaccine immunization in the urban areas was 96.9%, significantly higher than in the rural areas (50.8%) during the period of 1993 - 1994; the coverage of students aged 7 - 9 years was 85.5% in the urban, also significantly higher than in the rural (31.5%), indicating that these coverage rates in 1994 met with the expected standard in "the National Hepatitis B Vaccine Immunization Protocol"<sup>[4]</sup>. On the other hand, the data from this survey are similar to the results reported by the local anti epidemic stations, which basically reflected the real status of HB vaccination in China, and may be recommended as evidence related to the compliance in the evaluation of effectiveness of hepatitis B immunization prevention in the future. Because HBsAg-positive rate declined to 1% - 2% 1-9 years after HB vaccination<sup>[2]</sup>, further raising the coverage of infant immunization, especially in the rural areas, is a crucial factor to control the prevalence of hepatitis B. It was found in this study that the unreasonable allocation of the vaccines was one of the causes leading to less than 60% of the coverage in infant HB vaccination in some DSPs. The short of vaccine supply was another important problem in some DSPs.

The high HB vaccination fee (including maternal prescreening) is probably one of the reasons for lower coverage of infant immunization. We, therefore, suggest that ① vaccines must be allocated rationally so as to insure a coverage of

85% and over for neonates in the rural areas first, and then for adults at high risk; ② a national standard payment for HB vaccination should be implemented; ③ infant hepatitis B vaccine immunization should be integrated into EPI for a better administration in the rural areas. In addition, we recommend that the HB vaccination for adult should be discontinued at present so as to avoid the waste of health resources.

The maternal predelivery HBsAg and HBeAg screening is of great significance to select a valuable regimen of HB vaccination for infants and to interrupt the transmission of HBV between mother and infant. The fact that only 5.8% and 37.7% of DSPs conducted the maternal prescreening for all and a part of pregnancy women is mainly attributable to a poor lab condition, technician training and lack of fund. On the other hand, there might be some problems with the quality of the screening in some areas, especially in the rural areas, which was also demonstrated by Liu PB *et al*<sup>[5]</sup> in their studies. Thus, it is necessary to investigate the quality of the maternal HBsAg and HBeAg prescreening by the local health institutions of our country. In addition, it is also found in our survey that there were the multiple strategies and regimens of infant HB immunization, therefore, their cost-effectiveness and cost-benefit should be evaluated as soon as possible, so as to recommend an optimum strategy and regimen for areas with different HBV infection and economic status.

**Acknowledgments** We would like to thank the staff from the 112 anti-epidemic stations and disease surveillance points of 25 provinces, municipalities and autonomous regions of China for their help with this survey.

### REFERENCES

- 1 Coursaget P, Leboulleux D, Soumare M, Cann PL, Yvonnet B, Chiron JP. Twelve-year follow-up study of hepatitis B immunization of Senegalese infants. *J Hepatol*, 1994;21:250-254
- 2 Xu ZhY, Cao HL, Liu ChB, Yang JY, Yan TQ, Su YD. A cross-sections study of long-term effectiveness of universal infant hepatitis B vaccination program. *Zhonghua Shiyuan yu Linchuang Bingduxue Zazhi*, 1995;9:13-16
- 3 Qin XH, Jiang HB (eds): Module on use of hepatitis B vaccine and reagents of immunological diagnosis. *Beijing: Editorial Office of Chin J Microbiol Immunol*, 1991:6
- 4 Qin XH, Jiang HB (eds): Module on use of hepatitis B vaccine and reagents of immunological diagnosis. *Beijing: Editorial Office of Chin J Microbiol Immunol*, 1991:78-83
- 5 Liu PB, Li BF, Zeng XJ, Fang YCH, Wang BL, Liu XJ. Feasibility study on neonates hepatitis B vaccination strategy: mother predelivery screening. *Zhonghua Yufang Yixue Zazhi*, 1996;30(Suppl):37-40

# Codon 249 mutations of *p53* gene in non-neoplastic liver tissues

PENG Xiao-Mou, YAO Chun-Lan, CHEN Xue-Juan, PENG Wen-Wei and GAO Zhi-Liang

**Subject headings** liver; *p53* gene; codon 249 mutation; liver neoplasms; hepatitis, viral; liver cirrhosis; polymerase chain reaction

## Abstract

**AIM** To study the significance of *p53* gene in hepatocarcinogenesis through analyzing codon 249 mutations of *p53* gene in non-neoplastic liver tissues.

**METHODS** Codon 249 mutation was detected using single-stranded conformational polymorphism analysis and allele-specific PCR in liver tissues from 10 cases of chronic hepatitis, 5 cases of cirrhosis and 20 cases of HCCs.

**RESULTS** The detection rate of codon 249 mutation in chronic hepatitis, cirrhosis and pericancerous tissues was 70% (7/10), 100% (5/5) and 70% (14/20), respectively by AS-PCR. These mutations could not be detected by SSCP analysis. The detection rates were 65% (13/20) and 45% (9/20) in cancerous tissues by AS-PCR and SSCP analysis.

**CONCLUSION** Codon 249 mutations of *p53* gene were very popular in non-neoplastic liver tissues though the number of those mutant cells was only in subsection. Those mutations in cancerous tissues might take place in the stage before the formation of tumor.

## INTRODUCTION

Since AGG to AGT mutations in codon 249 of the *p53* gene resulting in an arginine to serine substitution were observed in up to 50% - 60% of HCC from Southern Africa and some provinces of China<sup>[1,2]</sup>, the significance of *p53* gene and the specific mutations of codon 249 in hepatocarcinogenesis has been widely accepted<sup>[3,4]</sup>. It is controversial, however, whether the specific mutations of codon 249 are involved in the initiation of HCC. Some authors believed that codon 249 AGT transversions were only involved in the differentiation stage of HCC because they had found that these mutations were only observed in HCC of later stage or bad differentiation<sup>[5,6]</sup>. Obviously, the crucial point to solve this problem is to clarify whether codon 249 AGT transversions take place in non-neoplastic tissues, such as hepatitis or cirrhotic tissues. Direct DNA sequencing, single-stranded conformational polymorphism (SSCP) and restriction fragment length polymorphism (RFLP) of PCR products were the main methods to detect gene mutations in the past. With lower sensitivity, these methods can not be used to demonstrate mutations in tissues other than massive, uniform tumor tissues. Recently, AS-PCR, a 100-fold more sensitive assay, has been used in the detection of codon 249 AGT transversions<sup>[7]</sup>. For these reasons, the occurring time of codon 249 mutation was investigated using AS-PCR to detect codon 249 mutations of *p53* gene in non-neoplastic liver tissues from Chinese patients in this study.

## MATERIALS AND METHODS

### Materials

**Specimens** Ten pieces of liver biopsy specimens of chronic hepatitis B, and 5 pieces of autopsy liver specimens were collected from our third affiliated hospital, and 20 pieces of surgically dissected specimens of HCCs were from our cancer hospital. All patients were Chinese living in Southern China. Cancerous and pericancerous tissues of surgically dissected specimens of HCCs were separated by pathologists genomic DNA was extracted by digesting with proteinase K and followed by phenol-chloroform extraction. All extract products were stored at -70°C.

**Reagents** All primers used in this research were designed according to the sequence of HSP53G from GenBank, and are shown in Table 1.

Department of Infectious Diseases, Third Affiliated Hospital, Sun Yat-Sen University of Medical Sciences, Guangzhou 510630, Guangdong Province, China

Dr. PENG Xiao-Mou, male, born on October 28, 1963 in Chaling County, Hunan Province, graduated from Department of Medicine, Hunan University of Medical Sciences, now instructor, engaged in the study on viral hepatitis, having 16 papers published.

\*Supported by the China Medical Board (CMB) of New York, Inc, Grant No. 93-582.

**Correspondence to:** Dr. PENG Xiao-Mou, Department of Infectious Diseases, Third Affiliated Hospital, Sun Yat-Sen University of Medical Sciences, Guangzhou 510630, Guangdong Province, China  
Tel. +86-20-85516867 Ext.2019

Received 1999-03-10

**Table 1 Primers for PCR and AS-PCR**

Code	Oligonucleotide sequence	Position
S1	5' -GGCGA CAGAG CGAGA TTCCA	13890-13909
A1	5' -GATTC TCTTC CTCTG TGC GC	14534-14515
S2	5' -TGGGC GGCAT GAACC GGAGT	14055-14074
S3	5' -TGGGC GGCAT GAACC GGAGG	14055-14074
A2	5' -GGGTC AGCGG CAAGC AGAGG	14175-14156

**Methods**

**PCR** Using primers S1 and A2 from intron sequences upper and lower flank of exon 7, 286bp fragment was amplified. Procedures were described in brief as follows: 0.5µg genomic DNA was added to 30µL of PCR mixture. The mixture was denatured at 98°C for 5 minutes, and then added to 1.5U Taq polymerase at 80°C. The amplification was carried out for 30 cycles composed of 40 seconds at 94°C, 50 seconds at 64°C, 1 minute at 72°C, and another 10 minutes at 72°C after the last cycle. Amplified products were visualized by running them on 2% agarose gel and staining with ethidium bromide.

**SSCP** Twenty µL of PCR products was precipitated at -20°C for 1 hour by adding 2.5 vol of alcohol and 0.1 vol of 4M sodium acetate. Pellets were re-suspended in 10µL of formamide dye mixture (95% formamide; 20mmol/L EDTA; 0.05% bromphenol blue). Samples were heated at 95°C for 5 minutes, chilled on ice and immediately loaded (5 µL) on 6% polyacrylamide gel. Gels were run at 40W for 4 hours at room temperature. Silver staining was used to visualize the bands, HepG2215 cell line without codon 249 mutation served as negative control.

**DNA sequencing** SSCP positive products were purified using low-melting agarose. DNA sequencing was carried out using automatic sequencing system.

**AS-PCR** Kirby' s semi-nested PCR protocol was modified by nested PCR for AS-PCR analysis in order to promote the specificity of the amplified products. About 0.25µg genomic DNA was added to 50µL of PCR I mixture containing primers S1 and A1. The amplification was carried out for 30 cycles composed of 40 seconds at 94°C, 40 seconds at 55°C, and 1 minute at 72°C. Five µL PCR I product (1:100) was added to a flesh tube, and 45µL of PCR II mixture containing primers S2 (allele-specific primer with T replacement in the third base pair of codon 249) or S3 and A2 was added. The amplification was performed just as above. Amplified products were analyzed by running on 2% agarose gel and visualized by staining with ethidium bromide. 121bp band was observed.

**RESULTS**

**PCR/SSCP/DNA sequencing analysis**

Exon 7 was successfully amplified in all tissue samples with nucleotide number as expected. PCR/SSCP analysis of tissue samples showed that SSCP positive results were only observed in cancerous tissues of some HCCs (Table 2), and that the pattern of band shift was identical (Figure 1). All SSCP positive amplified products were identified to be codon 249 AGT transversions by DNA sequencing.

**AS-PCR**

All genomic DNA samples were satisfactorily amplified when universal primers were used in the first step of nested PCR. Ideal bands were obtained in the second amplification when either primer S2 or primer S3 was used. Typical results are shown in Figure 2. The results of codon 249 mutation detection in DNA are summarized in Table 3. The corresponding rate of the detection of codon 249 mutation between pericancerous tissue and cancerous tissue was 95% (19/20). All the 9 cases of HCCs with positive SSCP were positive for AS-PCR both in cancerous tissue and pericancerous tissue.

**Table 2 Codon 249 AGT transversion detected in cancerous and non-neoplastic liver tissues detected by PCR/SSCP**

Tissue types	Case number	SSCP positive cases	Positive rates (%)
Chronic hepatitis	10	0	0
Cirrhosis	5	0	0
Pericancerous tissues	20	0	0
Cancerous tissues	20	9	45

**Table 3 Detection of codon 249 AGT transversion of p53 gene in cancerous and pericancerous tissues**

Tissues types	Cases	Detective rates of codon 249 mutation (%)
Chronic hepatitis	10	70
Cirrhosis	5	100
Pericancerous tissues	20	70
Cancerous tissues	20	65

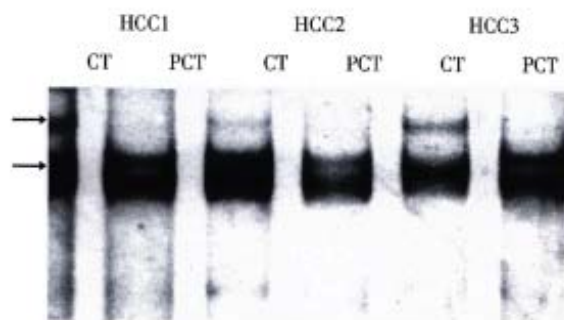


**Figure 1** PCR/SSCP analysis of HCC samples. CT represents cancerous tissue, PCT represents pericancerous tissue, shifted bands were marked by arrows. Silver staining.

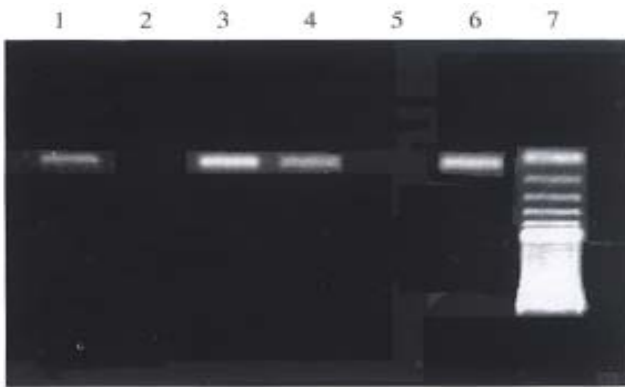


**Figure 1** AS-PCR products were analyzed by running on 2% agarose gel and visualized by staining with ethidium bromide. Lane 1 was 100bp ladder from GIBCO, Gaithersburg, Md, USA; Lane 2, 4, 5, 7 was positive; Lane 3, 6 are negative.

## DISCUSSION

Southern China is one of the endemic areas with a high incidence of HCC in the world. Codon 249 AGT transversion is a major pattern of mutations in HCC from this area, with mutant rate up to 32.9% (23/70). The ratio of codon 249 mutation to all kinds of mutations of *p53* gene was 95.7% (22/23)<sup>[4]</sup>. Therefore, cancerous and non-neoplastic tissue samples from this area is ideal for the study on the effect of codon 249 mutation on hepatocarcinogenesis. Codon 249 mutation may make the mutant-type *p53* protein lose its own functions, or even gain some new functions. Loss of *p53* gene can increase proliferating cells, diploid cells and G1 to G0 ratios, and even made the mutant cells not show apoptosis after exposure to ionizing radiation or therapeutic drugs<sup>[8]</sup>. Codon 249 mutation may gain a new ability to promote G0 to G1 and/or M to G1 transition in hepatocytes of transgenic mice<sup>[9]</sup>. Although the loss of *p53* gene or codon 249 mutation can change the cell proliferating mode, it would only play a minor role in hepatocarcinogenesis, and the researches of this mutation would be of little importance in prevention and treatment of HCC, if the codon 249 mutation only took place in the late stage of HCC.

Some laborious and time-consuming methods, including cloning analysis of RFLP-PCR products were used in detection of codon 249 mutation in non-neoplastic liver tissues of aflatoxin-exposed cultured human hepatocytes and extracted genomic

DNA from individuals exposed to dietary aflatoxin. The results supported the hypothesis that AFB was a causative mutagen in HCC<sup>[10]</sup>. A simple method, AS-PCR, was developed, and used in the detection of codon 249 mutation as well. Codon 249 AGT transversions were detected by AS-PCR in 83.3% (5/6) of non-neoplastic liver tissues from high-incidence regions, while none from low-incidence regions of HCC. Codon 249 mutation was detected in 70% - 100% of 35 subjects of non-neoplastic tissues living in southern China, an endemic areas of HCC using AS-PCR. In comparison of the results between cancerous tissues and pericancerous tissues, the occurrence of mutant codon 249 in cancerous tissues was found not to be an independent event. Thus, codon 249 mutation might take place before or in the initial stage of HCC development.

The cells with mutant *p53* gene extensively existed in non-neoplastic liver tissues though these cells might be in subsection because mutation could not be detected by SSCP analysis. It is still unclear why only a small portion of mutant cells develop into cancer, since about 25% patients with chronic hepatitis or cirrhosis may die from HCC and only 33.7% cases of these HCCs may carry codon 249 mutation.

## REFERENCES

- Hollstein M, Sidransky D, Vogelstein B, Harris CC. *p53* gene mutations in human cancer. *Science*, 1991;253:49-53
- Hsu IC, Metcalf RA, Sun T, Welsh JA, Wang NJ, Harris CC. Mutational hotspot in the *p53* gene in human hepatocellular carcinomas. *Nature*, 1991;350:427-428
- Bressan B, Kew M, Wands J, Ozturk M. Selective G to T mutations of *p53* gene in hepatocellular carcinoma from southern Africa. *Nature*, 1991;350:429-431
- Peng XM, Peng WW, Zhou YP. Studies on mutations of *p53* gene in HCCs. *Zhongshan Yike Daxue Xuebao*, 1997;18:245-248
- Unsal H, Yakicier C, Marçais C. *p53* mutations and hepatitis B virus: cofactor in hepatocellular carcinoma. *Hepatology*, 1995;21:597-599
- Murakami Y, Hayashi K, Hirohashi S, Sekiya T. Aberrations of the tumor suppressor *p53* and retinoblastoma genes in human hepatocellular carcinomas. *Cancer Res*, 1991;51:5520-5525
- Kirby GM, Batist G, Fotouhi-Ardakani N, Nakazawa H, Yamasaki H. Allele-specific PCR analysis of *p53* codon 249 AGT transversion in liver tissues from patients with viral hepatitis. *Int J Cancer*, 1996;68:21-25
- Yin L, Ghebranious N, Chakraborty S, Sheehan CE, Ilic Z, Sell S. Control of mouse hepatocyte proliferation and ploidy by *p53* and *p53* ser246 mutation *in vivo*. *Hepatology*, 1998;27:73-80
- Nishida N, Fukuda Y, Ishizaki K, Nakao K. Alteration of cell cycle-related genes in hepatocarcinogenesis. *Histol Histopathol*, 1997;12:1019-1025
- Aguilar F, Hussain P, Cerutti P. Aflatoxin B1 induces the transversion of G→T in codon 249 of the *p53* tumor suppressor gene in human hepatocytes. *Proc Nat Acad Sci*, 1993;90:8586-8590

# Intestinal flora translocation and overgrowth in upper gastrointestinal tract induced by hepatic failure\*

YI Jian-Hua, NI Ruo-Yu, LUO Duan-De and LI Shu-Li

**Subject headings** hepatic failure; multiple organ dysfunction; bacterial overgrowth; bacterial translocation; intestinal flora

## Abstract

**AIM** To explore the relationship between endoinfection caused by intestinal flora translocation and multiple-organ dysfunction in hepatic failure.

**METHODS** By using the quantitative bacteria culture, bacteria colony was counted in GI tract, bile duct and mesenteric lymphonodus in rat hepatic failure model.

**RESULTS** Intestinal flora migrated up to the upper GI tract and overgrew in stomach and jejunum in rats with hepatic failure. The number of bacteria colonies in the specimens of stomach, jejunum and ileum were  $4.7 \times 10^4/\text{mL}$ ,  $2.1 \times 10^5/\text{mL}$ ,  $5.5 \times 10^6/\text{mL}$  in experiment group and  $4.6 \times 10^2/\text{mL}$ ,  $6.1 \times 10^1/\text{mL}$ ,  $2.4 \times 10^3/\text{mL}$  in control group respectively ( $P < 0.05$ ). Bacteria in bile duct and mesenteric lymphonodus of hepatic failure rats were also cultured. Extensive damages of gastrointestinal mucosa caused by bacterial overgrowth were observed.

**CONCLUSION** Intestinal flora translocation and overgrowth in stomach and jejunum formed an endoinfectious source and caused obvious pathological injury of gastrointestinal mucosa, which play a very important role in developing abdominal distension, toxic intestinal expansion, alimentary tract haemorrhage and endotoxemia in patients with hepatic failure.

## INTRODUCTION

The patients with severe hepatic failure are predisposed to develop toxic intestinal expansion, alimentary tract haemorrhage, endotoxemia, spontaneous bacterial peritonitis, even septicemia<sup>[1-5]</sup>. It is necessary to investigate whether these complications are due to the intestinal bacterial overgrowth and intestinal flora translocation, and the mechanism and consequence of intestinal flora translocation in patients with hepatic failure.

## MATERIALS AND METHODS

### Animal model

Female Wistar rats (weighing 170 g - 220 g, supplied by the Experimental Animal Center of Tongji Medical University) were divided into two groups, five rats in each group. The experimental rats received hypodermic injection of thioacetamide (TAA, 350mg/kg) once a day and 50g/L glucose in NS-10mL three times a day for three days. The experiment was performed in rats that developed II-III phase of hepatic encephalopathy. The control rats received hypodermic injection of 90g/L sodium chloride instead of TAA. After the rats were fasted for 12 hours, the experiments were made under strict sterile condition.

### Bacteria colony counting in different gastrointestinal segment

After being anesthetized with pentobarbital, the stomach, 10cm proximal jejunum and 10cm terminal ileum of rats were cut off, and syringed with 1 mL sterile 90 g/L sodium chloride. The syringing solution was diluted and mixed with nutritive agar. After coagulation, it was turned over on a plate and incubated at 37°C for 24 hours.

### Bacteria culture of biliary tract and mesenteric lymphonodus

Two cm bile duct and mesenteric lymphonodus of the rats were taken and homogenated with 1mL sterile 90g/L sodium chloride. Then the syrup was collected and mixed in a nutritive agar plate. It was cultured in the same manner as described above.

Department of Infectious Diseases, Union Hospital, Tongji Medical University, Wuhan 430022, Hubei Province, China

YI Jian-Hua, male, born on 1963-12-06 in Zhongxiang City, Hubei Province, Han nationality, graduated from Tongji Medical University in 1987, instructor in infectious diseases, majoring in viral hepatitis, having 7 papers published.

\*Supported by the National Natural Science Foundation of China, No. 39370651.

**Correspondence to:** Dr. NI Ruo-Yu, Department of Infectious Diseases, Union Hospital, Tongji Medical University, 1277 Jiefang Avenue, Wuhan 430022, Hubei Province, China

Tel. +86-27-85726132

Received 1999-02-05

### ***Bacteria culture of gastric juice in case of hepatic failure***

Experiment was made in 5 patients with hepatic failure. Two of them had bleeding in alimentary tract. One mL gastric juice was drawn by gastric tube, then was taken to be cultured in the same manner as described above.

### ***The pathological change of the gastrointestinal tract***

At first we observed grossly gastrointestinal specimens in rats with hepatic failure. Then the specimens were fixed with 100mL/L formalin, embedded with paraffin, cut into slices, stained with HE and observed under light microscope.

## **RESULTS**

### ***Bacteria colony counting of stomach, jejunum and ileum in rats***

With bacteria culture of the syringing solution, it was shown that intestinal flora migrated up to the upper GI tract apparently and bacteria overgrew in stomach and jejunum in the rats with hepatic failure while there were few bacteria in the upper GI tract in the control group rats. The number of bacteria colonies in stomach, jejunum and ileum of two groups are shown in Table 1.

**Table 1 Bacteria colonies in different segments of GI tract in rats with hepatic failure (CFU/mL)**

	No	Stomach	Jejunum	Ileum
Experimental group	5	4.7×10 <sup>4a</sup>	2.1×10 <sup>5a</sup>	5.5×10 <sup>6a</sup>
Control group	5	4.6×10 <sup>2</sup>	6.1×10 <sup>1</sup>	2.4×10 <sup>3</sup>

<sup>a</sup>P<0.05 vs control group.

### ***Bacteria culture of biliary tract and mesenteric lymphonodus***

Culture of biliary tract bacteria was positive in all experimental rats. The mean number of bacteria colonies in rats with hepatic failure was 159±116. The culture of mesenteric lymphonodus bacteria was positive in 4 of 5 experimental rats. The mean number of bacteria colonies was 21±19. Bacteria colony number in control rats was 0-11 and 0-4 respectively (P<0.01).

### ***Bacteria culture of gastric juice in patients with hepatic failure***

There was bacterial overgrowth in the gastric juice of patients with hepatic failure. Bacteria colony number was 3.3×10<sup>3</sup>/mL to 7.5×10<sup>5</sup>/mL.

### ***Pathological change of the gastrointestinal tract***

The stomach, jejunum, ileum and colon were

dilated and the smooth muscle was flabby in experimental rats, especially in stomach. The gut lumen was full of fluid and gas. Blood stasis, erosions and bleeding spots in gastrointestinal were easily found. Pathological changes were found under microscope such as thinning of mucosal lamina, degeneration and dropping off of epithelial cells, vascular congestion of submucosa and increasing of lymphocytes in mucosa and submucosa, villus structure change in the distal small intestine, and multiple erosions in stomach mucosa.

## **DISCUSSION**

Bacteria translocation, the phenomena of bacteria migration from the gut lumen into the tissues of intestine and from distal GI tract to proximal, has been identified in the stress status after serious trauma or burn and hepatic failure. In that condition, intestinal flora can pass through the mucosa into the tissues outside bowel such as mesenteric lymphonodus, blood and even other organs in the body, and forms an endogenous infection source.

In normal condition, colon mucosa has an integrated mechanic barrier which can protect the mucosa from harmful irritation and invasion of normal intestinal flora. Though there are plenty of endotoxin and bacterial metabolic outcomes in colon, little can be absorbed into the body<sup>[3]</sup>. The mechanic barrier includes mucus, close junction of epithelial cells and special mucosal structure. In colon mucosa, no villus structure was found to have stuck out to the gut lumen, and the close arrangement of glands minimizes the contacting surface between the mucosa and the content in the gut lumen. Stomach protects itself by secreting gastric acid to kill invading bacteria. In small intestine, villus sticking out to the lumen is helpful for degestion and absorption of food but harmful to the protection of itself from invasion of toxin and destruction of bacteria. Under normal condition, bacteria in chyme has been killed by gastric acid, and bacteria in colon can hardly goup into the upper small intestine mainly as a result of continous propulsive peristalsis of GI tract and scouring of secretary solution by small intestine, liver and pancreas, which contain a large number of antibodies and other bacteria inhibitors. So the exocrine function and GI motility are an important guarantee to maintain its normal flora.

It was confirmed in our experiment that bacteria migrated into the upper GI tract from colon and overgrew in stomach and proximal small intestine of the rats with acute hepatic failure induced by TAA. Bacteria colony number in jejunum of experimental rats was ten thousand times

that of control rats, and bacteria in stomach and ileum also increased distinctly. Bacteria in mesenteric lymphonodus and biliary tract were cultured, while bacteria increased apparently in stomach in hepatic failure patients. These results indicate that there was a bacteria translocation which can damage GI mucosa, and destruct villus structure and mucosal barrier. Both bacteria and gastric acid destroyed the mucosal barrier, resulting in erosions and bleeding of gastric mucosa. Lots of gas produced by migrating bacteria caused gastrointestinal distension.

The above results can explain why many pathological phenomena occurred in hepatic failure. In hepatic failure, the excitability of gastrointestinal nerve, muscle and gland changes, the movement and secretion of gastrointestinal are inhabited. Bacteria in colon migrate rapidly up to the upper GI tract, and proliferate in the upper small intestine and make a great deal of metabolic products and toxins, which result in disruption of gastrointestinal mucosal barrier, damage of mucosal tissues, decrease of villus structure, degeneration and exfoliation of epithelial cells, and change of surface microcircumstance on gastrointestinal mucosa. Bacterial toxin stimulates the glands to secrete mucus and induces dysfunction of absorption which leads to watery stool and diarrhea. Gas resulting from bacterial overgrowth, low blood potassium, intestinal wall edema and ascites can cause abdominal distension, even toxic intestinal expansion. Translocated bacteria can directly injure gastrointestinal mucosa and induce erosion, ulcer and bleeding. In late hepatic failure, many patients develop refractory alimentary tract haemorrhage, which is known as bleeding due to hepatogastrointestinal failure<sup>[4]</sup>. We believe that disruption of mucosal barrier and damage of mucosal tissue caused by bacterial overgrowth in

stomach and proximal small intestine play a very important role in massive damages of gastrointestinal mucosa besides deficiency of blood coagulating factor, DIC and invasion of gastric acid.

In addition, bacterial overgrowth and high concentration toxin in jejunum are not only the direct cause of endotoxemia but also the foci of translocation lesion including bacteremia and infectious peritonitis. This can be confirmed by using oral or venous antibiotics which can partly prevent endogenous infection<sup>[5-7]</sup>.

It is concluded that intestinal flora translocation and overgrowth in stomach and jejunum is an endogenous infectious source and causes obvious pathological damage of gastrointestinal mucosa, which play a very important role in leading to abdominal distension, toxic intestinal expansion, alimentary tract haemorrhage and endotoxemia in patients with hepatic failure.

#### REFERENCES

- 1 Bercoff E, Frebourg T, Senant J, Morcamp D. Epidemiology of infections in cirrhotic patients. *Gastroenterol Clin Biol*, 1985;9(2b):10A
- 2 Kleber G, Braillon A, Gaudin C, Champigneulle B, Cailmail S, Lebrec D. Hemodynamic effects of endotoxin and platelet activating factor in cirrhotic rats. *Gastroenterology*, 1992;103:282-288
- 3 Van Deventer SJH, Ten Cate JW, Tytgat GNJ. Intestinal endotoxemia: clinical significance. *Gastroenterology*, 1988;94:825-831
- 4 Ni RY. Hepatogastrointestinal dysfunction. In: Ni RY. Advanced doctor training course for infectious diseases. *Wuhan: Wuhan University Press*, 1996:33-34
- 5 Kaufhold A, Behrendt W, Krauss T, Van Saene H. Selective decontamination of the digestive tract and methicillin-resistant staphylococcus aureus. *Lancet*, 1992;339:1411-1412
- 6 Blaise M, Pateron D, Trinchet JC, Levacher S, Beaugrand M, Pourriat JL. Systemic antibiotic therapy prevents bacterial infection in cirrhotic patients with gastrointestinal hemorrhage. *Hepatology*, 1994;20:34-38
- 7 Deitch EA, Maejima K, Berg R. Effect of oral antibiotics and bacterial overgrowth on the translocation of the GI tract microflora in burned rats. *J Trauma*, 1985;25:385-392

# Study on liver targeting and hepatocytes permeable valaciclovir polybutylcyanoacrylate nanoparticles \*

ZHANG Zhi-Rong and HE Qin

**Subject headings** valaciclovir; polybutylcyanoacrylate nanoparticles; liver targeting; hepatocytes permeability

## Abstract

**AIM** To prepare valaciclovir polybutylcyanoacrylate nanoparticles (VACV-PBCA-NP) with liver targeting and hepatocyte permeable characteristics.

**METHODS** Emulsion polymerization method was employed to prepare VACV-PBCA-NP. The formula and preparation conditions were optimized by using the uniform design. The organ distribution of the intravenously injected VACV-PBCA-NP and VACV in animal was determined using HPLC. The hepatocytes permeability of VACV-PBCA-NP was demonstrated by cell uptake experiment *in vitro*.

**RESULTS** The drug loading and the drug embedding ratio of VACV-PBCA-NP were 11.20% and 84.85% respectively, with an average diameter of  $10.477\text{nm} \pm 11.78\text{nm}$ . The releasing characteristics *in vitro* fitted the two-phase kinetics. 74.49% of the drug was found to localize in the liver 15min after the administration of VACV-PBCA-NP in the mice. Compared with VACV, VACV-PBCA-NP showed distinct characteristic of sustained-release *in vivo* and the drug entering hepatocytes were also greatly increased.

**CONCLUSION** VACV-PBCA-NP has the characteristic of liver targeting and can increase the permeability of VACV to hepatocytes.

## INTRODUCTION

Valaciclovir (VACV), the L-valyl ester of acyclovir (ACV), is a new antiviral drug which can be hydrolyzed into ACV and L-valyl rapidly in the presence of enzyme *in vivo*. Compared with ACV, VACV has the advantages of better solubility and higher bioavailability<sup>[1,2]</sup>. It has been demonstrated that ACV is effective for hepatitis B<sup>[3-6]</sup>, but not so effective as for herpes virus infection. This is chiefly due to the poor penetration of ACV into the liver cells<sup>[7]</sup>. One approach solving this problem is to use drug carriers capable of enhancing the liver and liver intracellular drug delivery.

Nanoparticles (NP) is a new drug carrier<sup>[8,9]</sup>. We have investigated the action of VACV-loaded NP and demonstrated that the amount of drug increased 2.99 fold in the liver and decreased 5.46 fold in the kidney. Significant increase of intracellular drug was also observed.

## MATERIALS AND METHODS

### Materials

Both VACV obtained from Sichuan Institute for Antibiotics Industry and ACV supplied by Hubei Institute for Medicinal Industry, meet the USP reference standard. Butyl-cyanoacrylate (BCA) monomer was purchased from Shenzhen Nanguang Medicinal Colla Co. Ltd. and collagenase type I from Sigma Co. VACV-PBCA-NP injection was self-made.

Kunming mice, white Japanese rabbits and Wistar rats were all provided by Laboratory Animal Center, West China University of Medical Sciences.

### Methods

**Preparation of VACV-PBCA-NP** VACV-PBCA-NP was prepared by emulsion polymerization method due to the good water solubility of VACV. An optimum procedure was developed based on the uniform design. Briefly, VACV, Dextran 70, pluronic F-68 and NaHSO<sub>3</sub> were weighed and dissolved in water. The pH of the solution was adjusted to 2.2 by adding 0.1N-HCl, and then BCA was added slowly into the solution under electromagnetic stirring, the solution was stirred for additional 2h at room temperature. Then the pH value of this colloidal solution was adjusted to 5-7 with 0.1 N NaOH. The solution was filtered

School of Pharmacy, West China University of Medical Sciences, Chengdu 610041, Sichuan Province, China

Dr. ZHANG Zhi-Rong, male, graduated from West China University of Medical Sciences (WCUMS) as a Ph.D. in 1993, now professor of pharmaceutics, Dean of the School of Pharmacy, WCUMS. Member of Chinese Pharmacopoeia Commission, Council Member of Chinese Pharmaceutical Association (CPA), Member of Society of Pharmaceutics of CPA, specialized in targeted delivery system and has more than 80 papers and 6 books published.

\*Supported by the National Natural Science Foundation of China, No. 39470831

**Correspondence to:** Dr. ZHANG Zhi-Rong, School of Pharmacy, West China University of Medical Sciences, Chengdu 610041, China Tel.+86-28-5501566, Fax.+86-28-5583252

Received 1999-03-10

through a microfilter membrane (0.3mm), filled into ampoules, freeze-dried and stored for later use.

#### Determination of embedding ratio and drug loading

The embedding ratio and the drug loading of VACV were determined by HPLC at 254nm. The HPLC conditions consisted of Shimpack CLC-ODS column (5 $\mu$ m, 150 mm  $\times$  4.6 mm id), mobile phase CH<sub>3</sub>OH-0.02mol·L<sup>-1</sup> KH<sub>2</sub>PO<sub>4</sub> (20:80), and flow rate 1mL·min<sup>-1</sup>. The standard curve equation was  $A = 2704.72 + 26406.30 C$  ( $r = 0.9999$ ). The mean recovery was 97.41%  $\pm$  1.57%. The colloidal solution of VACV-PBCA-NP was freezingly ultracentrifuged, and the content of VACV in the supernatant was assayed. The embedding ratio (ER%) and the drug loading (DL%) were calculated as follows:

$$ER\% = \frac{(\text{VACV added} - \text{VACV in supernatant})}{\text{VACV added}} \times 100\%$$

$$DL\% = \frac{(\text{VACV added} - \text{VACV in supernatant})}{\text{BCA added}} \times 100\%$$

#### Drug release from the VACV-PBCA-NP *in vitro*

Dynamic dialysis bag technique was used to observe the drug release from VACV-PBCA-NP *in vitro*. The freeze-dried powder of VACV-PBCA-NP was dispersed in physiological saline and the dispersion was transferred into a dialysis bag suspended in a conical container containing physiological saline solution. The container was shaken at 37°C  $\pm$  1°C. Samples were withdrawn at predetermined time, adjusted to pH 9-11 with 0.1N-NaOH, boiled for 1 h and determined. The HPLC conditions were the same as mentioned above, the standard curve equation was  $A = 3046.73 + 62647.64 C$  ( $r = 0.9999$ ). The accumulative drug release percentage was calculated to describe the drug release.

#### Measurement of drug in blood and viscera of mice

Thirty Kunming mice were randomly divided into VACV-PBCA-NP group and VACV group, fifteen in each group. Each mouse was intravenously given VACV-PBCA-NP or VACV at a dose of 25mg/kg body weight. The mice were killed and anatomized 15 minutes after the administration, and the heart, liver, lungs, kidneys and blood were taken out. Plasma of 0.5mL or viscera homogenate were piped accurately and 1mL chloroform and 0.5mL 6% perchloric acid were added respectively. The mixture was vortexed and centrifuged, and 20 $\mu$ L supernatant was taken to determine VACV by HPLC.

**Isolation and culture of hepatocytes** The livers of Wistar rats (200 g  $\pm$  20 g in weight, fasted overnight) were taken out under aseptic condition, perfused with Hank's solution until the blood

washed out, cut into tiny pieces, digested with 0.1% collagenase at 37°C for 45min and filtered through a stainless steel mesh (mesh size: 100 $\mu$ m). Hepatocytes were purified after being washed three times with Hank's solution and one more time with RPMI-1640 solution. Cells were seeded at a density of 5 $\times$ 10<sup>5</sup> cells/each culture dish and incubated with 5% CO<sub>2</sub> at 37°C for 18h. Then the medium was replaced with fresh RPMI-1640 solution, VACV-PBCA-NP or VACV was added at various concentrations for further incubation. Six, 12 and 24h after the culture, the hepatocytes were taken out, washed three times with physiological saline and broken, then VACV in the cell was determined by HPLC.

#### Determination of blood concentration in rabbits

Ten white Japanese rabbits were randomly divided into VACV-PBCA-NP group and VACV group, five in each group. Each rabbit was intravenously given VACV-PBCA-NP or VACV at a dose of 15mg/kg body weight, 2mL blood was taken at different time points after the injection and ACV in plasma was detected at 254nm by HPLC method including Shimpack CLC-ODS analytical column (5 $\mu$ m, 150mm $\times$ 4.6mm id) and mobile phase methanol-water-acetic acid (1:99:0.5).

## RESULTS

### Morphology (Figure 1)

The surface of the VACV-PBCA-NP is regular and non-adhesive. The average, the maximum and the minimum diameter of VACV-PBCA-NP is 104.77nm, 141nm and 76nm respectively. Its diameter is not abnormally distributed.

**Drug loading characteristics** Table 1 shows the embedding ratio and drug loading of VACV-PBCA-NP.

**Table 1** Embedding ratio and drug loading of VACV-PBCA-NP

Batch No.	Embedding ratio (%)	Drug loading (%)
961010	85.10	12.15
961012	83.75	10.51
961015	85.70	10.93
Average	84.85	11.20

### Stability

Freeze-dried powder of VACV-PBCA-NP was stored at 3°C - 5°C, 20°C - 25°C and 37°C (RH 75%) respectively for 3 months. There were no noticeable changes in the appearance, morphology, pH and VACV content under the condition of 3°C - 5°C and 20°C - 25°C, but changes were found at 37°C (Table 2).

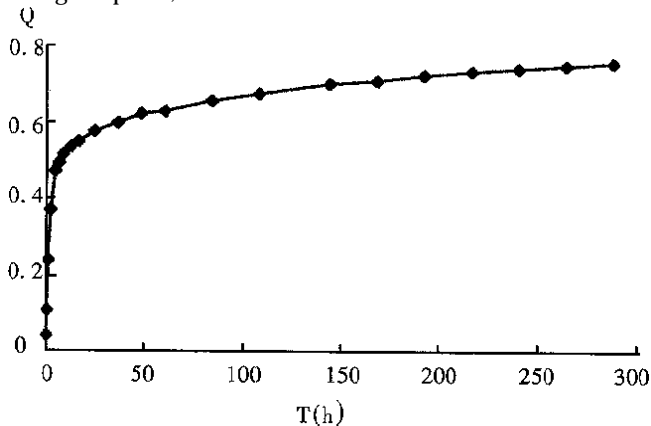
### Drug release characteristics

Figure 2 shows the drug release profile of VACV-PBCA-NP freeze-dried injection. The curve (Figure 2) corresponded to the two-phase kinetics equation:  $1-Q=0.3663e^{-0.0015t}+0.3000e^{-0.0524t}$ .

**Table 2** Stability results of VACV-PBCA-NP

Temperature (°C)	0 month				3 months			
	D/nm	C	pH	Color	Color	D/nm	C	pH
3-5	107.28	0.49	5.34	white	110.42	0.47	5.25	white
15-25	107.28	0.49	5.34	white	109.37	0.48	5.05	white
37(RH75%)	107.28	0.49	5.34	white	105.61	0.43	4.10	white

C: mg/ampoule; D: diameter.



**Figure 1** Transmission electron micrographs of VACV-PBCA-NP.

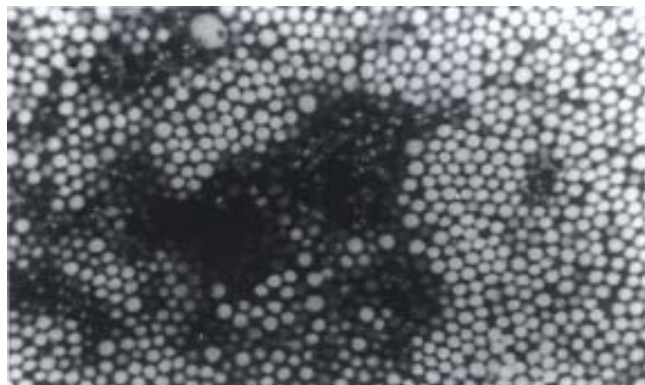


**Figure 2** Release profile of VACV-PBCA-NP freeze-dried injection. Q: Percentage of accumulative drug release.

### Distribution of VACV-PBCA-NP in viscera and blood of mice

The amount of ACV in each organ recorded as  $ACV_i$  and  $ACV_t$  was obtained by adding  $ACV_i$  in all viscera at different time points. The ratio of  $ACV_i/ACV_t \times 100\%$  represented the relative content of VACV-PBCA-NP in viscera and blood (Table 3). Table 3 shows that the relative content of VACV-PBCA-NP in liver was 74.49%, 2.99 times higher than that of VACV, and in kidney was 9.36%, 5.46 times lower than that of VACV.

**Table 3** Relative content in various organs 15min after iv administration of VACV-PBCA-NP and VACV respectively (% ,  $n=3$ )

Sample	Heart	Liver	Spleen	Lung	Kidney	Blood
VACV-PBCA-NP	0.99	74.49	2.46	2.89	9.36	9.82
VACV	2.14	24.92	2.44	3.01	51.15	16.54

### The permeability of VACV-PBCA-NP to hepatocytes

Because of the same amount of the cells added to each culture dish ( $5 \times 10^5$ ), the peak area of ACV was used to represent the effect of the VACV taken in by rat liver cell, the results showed that the drug amount of VACV-PBCA-NP in rat hepatocytes group was 28.77, 21.90 and 5.22 times that of VACV control group at 6 h, 12 h and 24 h, respectively.

### The pharmacokinetic parameters of VACV-PBCA-NP and VACV in rabbit after iv administration

The concentration-time data of the two groups both fitted the two-compartment model, the equation was  $C = 20.88e^{-7.653t} + 0.63e^{-0.0001t}$  and  $C = 10.19e^{-2.67226t} + 0.88e^{-0.3789t}$ . The main pharmacokinetic parameters were analyzed by the single factor variance method. The results are shown in Table 4.

**Table 4** The results of single factor variance analysis of the main pharmacokinetic parameters of VACV-PBCA-NP and VACV

Factors	A	B	DF	F (test)	F (criterion)	P
AUC	223.34	6.40	1.8	35.87	11.30	<0.01
MRT(h)	244.58	0.95	1.8	28.83	11.30	<0.01

A: VACV-PBCA-NP; B: VACV; DF: Degree of freedom.

Table 4 shows that there is a significant difference in the main pharmacokinetic parameters between the two groups.

### DISCUSSION

The VACV-PBCA-NP freeze-dried injection stored at  $37^\circ\text{C}/\text{RH}75\%$  would change in the appearance, pH and the drug content. The results implied that temperature and humidity affect the stability of VACV-PBCA-NP. The reason may be that higher temperature and humidity would speed up the generation of L-valyl and ACV. The refore, VACV-PBCA-NP should be preserved at low temperature and humidity.

VACV will degrade into ACV at  $37^\circ\text{C}$ . The experiment showed that VACV would be completely turned into ACV when heated for 1h at  $100^\circ\text{C}$ , but ACV was stable in this situation. Therefore, in the

*in vitro* experiment of the drug release from nanoparticles, the samples were treated by the method mentioned above. The released amount of VACV could be calculated by measuring ACV.

VACV will turn into ACV rapidly and completely *in vivo* because of the presence of enzyme. Therefore, we determined ACV in blood and viscera of animal after i.v. VACV and VACV-PBCA-NP by a HPLC method of good recovery.

#### REFERENCES

- 1 Beauchamp LM, Orr GF, Mirunda P. Amino and ester prodrugs of acyclovir. *Antiviral Chem Chemother*, 1992;3:157-164
- 2 Stempfen W, Robert BM, Marna D, Thimysta B, Donna MC, Paulo M. Pharmacokinetics of the acyclovir prodrug valaciclovir after escalating single and multiple dose administration to normal volunteer. *Clin Pharmacol Ther*, 1993;54:595-605
- 3 Yang SS, Guan MY, Yang LH. Comparison of acyclovir and interferon in the treatment of chronic hepatitis B. *Hubei Yixueyuan Zazhi*, 1987;8:144-147
- 4 Zhou JL, Xu LZ, Wu H, Min J. The effect of acyclovir to chronic active hepatitis B. *Tianjin Yiyao*, 1989;17:687-689
- 5 Weller IV, Carreno V, Fowler MJ. Acyclovir hepatitis B antigen positive chronic liver disease: inhibition of viral replication and transient renal impairment with iv bolus administration. *J Antimicrob Chemother*, 1983;11:223-225
- 6 Smith CI, Scullard GH, Gregory PB. Preliminary studies of acyclovir in chronic hepatitis B. *Am J Med*, 1982;73(1A):267-269
- 7 Zhang ZR, Liao GT, Hou SX. Study on mitoxantrone polybutyl cyanoacrylate nanoparticles. *Zhongguo Yaoxue Xuebao*, 1994;29:544-549
- 8 Marty JJ, Oppenheim RC, Speiser P. Nanoparticles: a new colloidal drug delivery system. *Pharm Acta Helv*, 1978;53:17-23
- 9 Kreuter J. Nanoparticles and nanocapsules-new dosage forms in the nanometer size range. *Pharm Acta Helv*, 1978;53:33-39

Edited by MA Jing-Yun

Reviews

# Telomere, telomerase and digestive cancer

Javed Yakoob, HU Guo-Ling, FAN Xue-Gong and ZHANG Zheng

**Subject headings** Digestive system neoplasms; telomere; telomerase; antitelomerase therapy

Recent advances suggest that telomerase is associated with cellular immortality which is a hallmark of cancer.

## TELOMERES

Human telomeres contain an array of tandem DNA repeats. We share the telomeric sequence (TTAGGG)<sub>n</sub> with all other vertebrates. Human chromosomes end in several kilobases of telomeric repeat DNA. These are oriented so that the guanine (G)-rich strand runs out to the 3' end of the chromosome. Despite their monotonous sequence, telomeres fulfil important functions. First, they hide natural chromosome end from factors acting on DNA termini unlike broken chromosome ends which either get degraded or fuse to other DNA. Telomeres are resistant to exonucleases and ligases. They also escape detection by the DNA damage checkpoints. The termini of natural chromosome ends are probably concealed by a complex of specialized proteins that bind telomeric DNA. Telomere length is maintained by a balance between the telomeres-lengthening process (e.g., telomerase)<sup>[1]</sup> and the telomeres-shortening process (end replication). The inability of the DNA to completely replicate chromosome termini (telomeres) leads to the progressive shortening of chromosomes upon continuous cell division. The shortening can ultimately lead to loss of telomeric function and chromosomal destabilization. A DNA polymerase called telomerase is required to overcome the end replication.

## TELOMERASE

Human telomerase is a ribonucleoprotein (RNP) composed of an essential RNA and a few proteins. It synthesizes the G-rich tandem repeats that comprise telomeres [(TTAGGG)<sub>150-2000</sub> in humans]

using a template on the RNA that is complementary to the telomeric repeat. By adding hexameric (TTAGGG) repeats to the telomeric ends of the chromosomes, the continued erosion of telomeres is compensated. The enzyme is expressed in embryonic cell and in adult male germ line cells<sup>[2]</sup>, but is undetectable in normal somatic cells except for proliferative cells of renewable tissues (e.g. haemopoietic stem cells and activated lymphocytes, basal cells of the epidermis and intestinal crypt cells). In normal somatic cells, progressive shortening of telomere leads to a limited replicative capacity. Recently more direct evidence has been found in the role of telomere shortening in aging<sup>[3]</sup>.

## TELOMERIC PROTEINS

Telomeres are essential for the maintenance of chromosomes. Another group of important regulators for telomere function is the telomere binding proteins<sup>[4]</sup>. They were originally described as proteins, binding specifically to telomere DNA (for example, to the hexameric repeat). The RAP 1 protein in budding yeasts and the TRF1 protein in mammalian cells are examples of this class of proteins<sup>[5]</sup>. Another type of proteins interacts with the telomere DNA-binding protein/protein-interactions and comprises a large functional chromosome domain called the "telosome"<sup>[6]</sup>. Examples are the SIR 3/SIR 4 proteins and the RIF 1 protein in *Saccharomyces cerevisiae*<sup>[6]</sup>. These proteins associate with the RAP 1 telomere DNA-binding protein and function to establish telomere silencing effect and regulate telomere length respectively. Some of these proteins negatively regulate telomere length, probably by inhibiting telomerase activity<sup>[7]</sup>. Therefore, the length and function of telomere are not determined simply by the balance between the total number of cell divisions and telomerase activity.

## TELOMERASE IN MALIGNANCY

While all of the steps leading to cancer are still unknown, progression to a cancerous state does require the accumulation of a series of genetic alterations similar to those found in the *in vitro* models of carcinogenesis. For instance, hyperproliferation occurs due to the failure to respond to growth inhibitory signals and the functions allowing cells to divide in the absence of

Department of Infectious Diseases, Xiangya Hospital, Hunan Medical University, Changsha 410008, Hunan Province, China

Dr. Javed Yakoob, now a Ph.D. student in the Department of Infectious Diseases, Hunan Medical University, who worked in Dublin, Ireland in the field of medicine for several years.

**Correspondence to:** Prof. FAN Xue-Gong, Department of Infectious Diseases, Xiangya Hospital, Changsha 410008, Hunan Province, China  
Tel. +86-731-4328926

Received 1998-04-20

specific growth stimulatory signals. Additional mutations must take place for cell to progress to invasive and then metastatic states. To the extent that each of these conditions represents a mutational event, a clonal expansion of the cell is required for the occurrence of mutation. Some of these changes involve recessive events where an initial clonal expansion of cell containing the original mutation must be followed by a second clonal expansion with the remaining wild type allele eliminated. If this series of events require a greater number of cell divisions than permitted for normal cells, potential tumor cells must incorporate a mechanism to overcome this limitation. It appears that in many cases, the reactivation of telomerase serves this purpose, yet it may not be the only mechanism. The presence of telomerase activity only indicates that the cell has the ability to inactivate the telomeric "clock" that limits the proliferative capacity of normal somatic cells<sup>[8]</sup>. The presence of telomerase activity in a cell implies very little about malignancy, but only reflects its potentially immortal state. Cell immortality only gives the cells the proliferative capacity to accumulate the necessary mutations to become malignant. As cancer is diverse, some tumors may need only a few mutations in order to become malignant and may not exhaust the normal limits of proliferation before they cause disease. These types of cancer would be expected to be both immortal and negative for telomerase activity. As proliferative limits can be exceeded at any time during cancer progression, the reactivation of telomerase would be expected to occur early in tumors arising from cells near the limits of their proliferative capacity and late in tumors arising from cells with long telomeres. In some cases of tumors arising from telomerase positive stem cells, the initiating cells may already be competent to be immortal.

The fact that almost all cancers have telomerase activity, despite their shortened telomeres<sup>[2,9,10]</sup> indicate that there is an intense selective pressure for telomerase activation with the progression of malignancy. Indirect support for this view comes from the observations that benign or precancerous lesions (e.g. colonic polyps or adenoma; prostate hyperplasia and fibroids) are telomerase silent<sup>[9]</sup>. As telomeres shorten, accumulated mutations in other genes such as the genes encoding p53 and *RB* (retinoblastoma protein) would result in genomic instability, an extended life-span and progressive erosion of telomeres<sup>[11,12]</sup>. At this point, end to end chromosome fusions are frequently observed, concomitantly with critically shortened telomeres. These events could contribute to the loss of heterozygosity and the expression of recessive mutations, which would result in the reactivation of

telomerase and stabilization of telomere length, as well as fixation of the additional mutations required for invasiveness and metastasis.

#### ***Telomerase activity in colorectal cancer***

The colorectal adenoma-carcinoma sequence is one of the best characterized models for multistep tumorigenesis. Progression may be extremely slow due to the high ratio of adenomas to cancers. Telomere shortening is observed in colorectal adenomas and carcinomas<sup>[13]</sup>. Recent studies have demonstrated that although most adenomas lack telomerase activity, the majority of colorectal cancers express this enzyme<sup>[2,9]</sup> and contain detectable telomerase activity regardless of underlying phenotype (77% of hereditary nonpolyposis colorectal cancers; 81% of sporadic tumors, 88% with mutator phenotypes and 75% without mutator phenotypes)<sup>[14]</sup>. Therefore, telomerase expression appears to be commonly acquired in the progression of both mutator phenotype and sporadic colorectal cancers. These findings in colorectal cancer are consistent with the telomere hypothesis. However a minority of colorectal cancers lack detectable telomerase activity<sup>[8]</sup> and other alternatives remain<sup>[10]</sup>.

#### ***Telomerase activity in gastric cancer***

The pattern of multiple gene changes in gastric cancer varies with the histological type, well differentiated or intestinal type and poorly differentiated or diffuse type. However, activation of telomerase, which is responsible for cell immortality is the most common fundamental event in gastrointestinal cancer<sup>[2,9,15]</sup>. Human telomerase RNA (hTR) is expressed in pre-crisis cell lines and non-neoplastic tissues, as well as in immortalized cell lines or tumor specimens and the expression level is not correlated with that of telomerase activity<sup>[16]</sup>. Telomerase activity is detected in 85%-88% of gastric carcinomatous tissues<sup>[16,17]</sup>. Although all tumor specimens and non-cancerous mucosa expressed various levels of hTR, 81% expressed hTR at a higher level in the tumor than that in the corresponding mucosa. All the 8 gastric carcinoma cell lines also expressed hTR at higher levels. Thirty-five percent of non-cancerous mucosa showed telomerase activity and all of them contained intestinal metaplasia. The degree of *Helicobacter pylori*-infection increased in parallel with the level of hTR expression and telomerase positivity<sup>[17]</sup>. These results suggest that *Helicobacter pylori* infection may be a strong trigger for hTR overexpression in intestinal metaplasia, and this may lead to telomerase reactivation. Tumors with telomerase activity were generally large in size with a high frequency of lymph node metastasis. In the

tumors without detectable telomerase activity, 80% were early stage gastric cancer. In gastric cancer, telomerase activation may occur as a late event of cancer progression as demonstrated previously in non-small cell lung cancer<sup>[18]</sup>. Moreover, the patients with telomerase-positive tumors showed poorer prognosis than those with telomerase-negative tumors, indicating that telomerase-positive gastric cancers may have more malignant potential.

### *Telomerase activity and telomere length in HCC and CLD*

It is well known that almost all HCC are preceded by chronic hepatitis (CH) and/or liver cirrhosis (LC). These two conditions are regenerative lesions in response to repeated liver damage induced by hepatitis B or C virus (HBV/HCV) infection or other factors. However, the role of these lesions in HCC carcinogenesis remains unclear, except for the possible involvement of transforming activity of the HBVX protein<sup>[19]</sup>. There was progressive shortening of telomeres during hepatocellular carcinogenesis from normal liver to CH to LC to HCC. The average telomere length of HCC was significantly and consistently shorter than that of adjacent CH or LC<sup>[20]</sup>. The possible role of telomere shortening in regenerative, noncancerous liver lesions (CH and LC) is that it may eventually lead to reactivation of telomerase, which may then contribute to the malignant conversion to HCC. Thus telomere shortening in the regenerative lesions is not merely representative of cellular aging, but may also be a prerequisite for the development of malignancy. A subpopulation of cells in such lesions with telomeres shortened to a critical length, may suffer genetic changes due to chromosome instability<sup>[3]</sup>. These genetic changes would make most cells senescent, but allow a small number of cells to undergo additional mutations, including those activating or upregulating telomerase which then clonally develop into immortal cancer cells. Telomere length was shorter in chronic liver diseases compared with that in normal liver<sup>[21]</sup>. This indicates that senescence of hepatocytes occurs in patients with advanced liver diseases probably as a result of degeneration and the following regeneration of hepatocytes. Although the mechanisms of carcinogenesis in type C chronic liver diseases are not known, the incidence of HCC increases as the stage of the disease advances<sup>[22]</sup>. Telomerase activity was measured in various tissues and cell lines<sup>[2,9,15]</sup> including HCC<sup>[23]</sup> and was shown to be positive in 85%-100% of various malignant tissues and negative in almost all non-malignant tissues, except for reproductive and haemopoietic cells. Telomerase activity was negative in 15% of the HCC specimens<sup>[21]</sup>. One

possible reason for this undetectability might be false negativity due to the possible presence of polymerase chain reaction inhibitor<sup>[24]</sup>. However the presence of such inhibitor was not confirmed. In another previous report the telomerase activity in malignant tissue was not positive<sup>[23]</sup> and a recent report has clearly shown that several tumor cell lines keep their telomere length without telomerase activity<sup>[25]</sup>. Consequently, some unidentified mechanism for restoring the telomere length must exist<sup>[26]</sup>. Thus, it seems that a small number of HCC do not possess telomerase activity.

### **TELOMERASE—A TARGET FOR CANCER TREATMENT**

Telomeres and telomerase play a role in signalling cellular senescence and in the progression of tumorigenesis, anticancer therapies could be targeted at telomerase. The gene encoding the human RNA component of telomerase has been cloned<sup>[27]</sup>. Following strategies are available.

A: Obstructing telomerase RNA activity through an antisense oligonucleotide targeted to the template region. Encouragingly, expression of antisense to hTR in an immortal telomerase-expressing cell line resulted in a gradual reduction of telomere length, leading to death of the cells<sup>[27]</sup>.

B: Generation of mutant telomerase RNA.

C: Protein components of telomerase present another viable target for inhibition.

Telomerase inhibitors may thus provide an effective cancer therapy with no side effects of general cancer therapy in normal somatic cells that lack telomerase expression. A future treatment regimen may include surgical removal of the tumor, followed by combined antitelomerase therapy with conventional radiation and/or chemotherapies. As most cancer cells have much shorter telomeres than the stem cells of renewal tissues, the treatment period could be designed to end prior to stem cell attrition by preserving the replicative abilities to divide stem cells. Thus the effects of inhibiting telomerase activity are likely to eliminate the cancer cells long before telomere lengths in stem cells become limited.

### **CONCLUSION**

Clearly, telomerase regulation is complex and further studies are needed on the multiple mechanisms regulating telomerase activity with respect to the addition of telomeric repeats and its relation to cellular growth. Telomerase fulfills many of the criteria for an ideal cancer target and has a nearly ideal developmental and tissue-expression pattern, what remains is to show that tumors require telomerase for growth and that loss of telomerase function will be clinically useful.

## REFERENCES

- 1 Blackburn EH. Telomeres: no end in sight. *Cell*, 1994;77:621-623
- 2 Kim NW, Piatyszek MA, Prowse KR, Harley CB, West MD, Ho PLC, Coviello GM, Wright WE, Weinrich SL, Shay JW. Specific association of human telomerase activity with immortal cells and cancer. *Science*, 1994;266:2011-2015
- 3 Wright WE, Brasiskyte D, Piatyszek MA, Shay JW. Experimental elongation of telomeres in immortal human cells extends the life span of immortal normal cell x normal cell hybrids. *EMBO J*, 1996;15:1734-1741
- 4 Blackburn EH, Greider CW. (eds). *Telomeres. New York: Cold Spring Harbor Laboratory Press*, 1995:69-105
- 5 Chong L, Van Steensel B, Broccoli D, Erdjument-Bromage H, Hanish J, Tempst P, Lange T. A human telomeric protein. *Science*, 1995;270:1663-1667
- 6 Ishikawa F. Telomere crisis, the driving force in cancer cell evolution. *Biochem Biophys Res Commun*, 1997;230:1-6
- 7 McEachern MJ, Blackburn EH. Run away telomere elongation caused by telomerase RNA gene mutations. *Nature*, 1995;376:403-409
- 8 Counter CM, Avillion AA, Le Feuvre CE, Stewart NG, Greider CW, Harley CB, Bacchetti S. Telomere shortening associated with chromosome instability is arrested in immortal cells which express telomerase activity. *EMBO J*, 1992;11:1921-1929
- 9 Chadeneau C, Hay K, Hirte HW, Gallinger S, Bacchetti S. Telomerase activity associated with acquisition of malignancy in human colorectal cancer. *Cancer Res*, 1995;55:2533-2536
- 10 Rhyu MS. Telomeres, telomerase and immortality. *J Natl Cancer Instit*, 1995;87:884-894
- 11 Shay JW, Tomlinson G, Piatyszek MA, Gollahon LS. Spontaneous *in vitro* immortalisation of breast epithelial cells from a patient with Li-Fraumeni syndrome. *Mol Cell Biol*, 1995;15:425-432
- 12 Klingelhutg AJ, Barber SA, Smith PP, Dyer K, Mc Dougall JK. Restoration of telomerase in human papilloma virus-immortalised human anogenital epithelial cells. *Mol Cell Biol*, 1994;14:961-969
- 13 Hastie ND, Dempster M, Dunlop MG, Thompson AM, Green DK, Allshive RC. Telomere reduction in human colorectal carcinoma and ageing. *Nature*, 1990;346:866-868
- 14 Li ZH, Salovaara R, Aaltoven LA, Shibata D. Telomerase activity is commonly detected in hereditary nonpolyposis colorectal cancers. *Am J Pathol*, 1996;148:1075-1079
- 15 Hiyama E, Yokohama T, Tatsumoto N, Hiyama K, Imamura Y, Marakani Y, Kodama T, Piatyszek MA, Shay JW, Mafura Y. Telomerase activity in gastric cancer. *Cancer Res*, 1995;55:3258-3268
- 16 Avillion AA, Piatyszek MA, Gupta J, Shay JW, Bacchetti S, Greider CW. Human telomerase RNA and telomerase activity in immortal cell lines and tumor tissues. *Cancer Res*, 1996;56:645-650
- 17 Kuniyasu H, Domen T, Hamamoto T, Yokozaki H, Yasui W, Tanara H. Expression of human telomerase RNA is an early event of stomach carcinogenesis. *Jpn J Cancer Res*, 1997;88:103-107
- 18 Hiyama K, Hiyama E, Ishioka S, Yamakido M, Inai K, Gazdar AF, Piatyszek MA, Shay JW. Telomerase activity in small cell and non small cell lung cancers. *J Natl Cancer Inst*, 1995;87:895-902
- 19 Kekule AS, Lauer U, Weiss L, Lubert B, Hofschneider PH. Hepatitis B virus transactivator HBx uses a tumors promoter signalling pathway. *Nature*, 1993;361:742-743
- 20 Miura N, Harikawa I, Nishimoto A, Ohmura H, Ito H, Hirohashi S, Shay JW, Oshimura M. Progressive telomere shortening and telomerase reactivation during hepatocellular carcinogenesis. *Cancer Genet Cytogenet*, 1997;93:56-62
- 21 Kojima H, Yokosuka O, Imazeki F, Saisho H, Omata M. Telomerase activity and telomere length in hepatocellular carcinoma and chronic liver disease. *Gastroenterology*, 1997;112:493-500
- 22 Takano S, Yokosuka O, Imazeki F, Tagawa M, Omata M. Incidence of hepatocellular carcinoma in chronic hepatitis B and C a prospective study of 251 patients. *Hepatology*, 1995;21:650-655
- 23 Tahara H, Nakanishi T, Kitamoto M, Nakashio R, Shay JW, Tahara E, Kajiyama G, Ide T. Telomerase activity in human liver tissues: comparison between chronic liver disease and hepatocellular carcinomas. *Cancer Res*, 1995;55:2734-2736
- 24 Wright WE, Shay JW, Piatyszek MA. Modifications of a telomeric repeat amplification protocol (TRAP) result in increased reliability, linearity and sensitivity. *Nucleic Acid Res*, 1995;23:3794-3795
- 25 Bryan TM, Englezou A, Gupta J, Bacchetti S, Reddel RR. Telomere elongation in immortal human cells with out detectable telomerase activity. *EMBO J*, 1995;14:4240-4248
- 26 Wellinger RJ, Ethier K, Labrecque P, Zakian VA. Evidence for a new step in telomere maintenance. *Cell*, 1996;85:423-433
- 27 Feng J, Funk WD, Wang SS, Weinrich SL, Avillion AA, Chiu CP, Adams RR, Chang E, Allsopp RC, Yu J, Le S, West MD, Harley CB, Andrews WH, Greider CW, Villeponteau B. The RNA component of human telomerase. *Science*, 1995;269:1236-1241

Edited by WANG Xian-Lin

# Liver disease and *Helicobacter*

LUO Yu-Qin<sup>1</sup>, TENG Jin-Bo<sup>2</sup>, PAN Bo-Rong<sup>3</sup> and ZHANG Xue-Yong<sup>3</sup>

**Subject headings** liver diseases; hepatitis; hypertension, portal; *Helicobacter pylori*; hepatic encephalopathy

## INTRODUCTION

The human upper gastrointestinal tract is often infected with *Helicobacter pylori* (*H. pylori*). This urea splitting bacterium is now considered to be a causal agent in some diseases, including antral gastritis and frank duodenal ulceration, in addition to an association with gastric carcinoma and mucosa associated lymphoid tissue (MALT) lymphoma<sup>[1]</sup>. Since the discovery of *H. pylori*, a number of additional *Helicobacter* species have been isolated from the stomachs and intestinal tracts of a variety of mammalian species. At least eighteen separate *Helicobacter* species have been recognized (Table 1)<sup>[2,3]</sup>. The discovery of these *Helicobacter* species, has raised the possibility of a relationship between *Helicobacter* infection and liver diseases<sup>[3]</sup>.

**Table 1 Helicobacter species and their hosts**

Species	Hosts	Primary site	Other sites
<i>H. pylori</i> <sup>*</sup>	Human, macaque, cat	Stomach	
<i>H. mustelae</i>	Ferret, mink	Stomach	
<i>H. felis</i> <sup>*</sup>	Cat, dog	Stomach	
<i>H. bizzozeronii</i> <sup>*</sup>	Dog, human	Stomach	
<i>H. helimannii</i> <sup>△</sup>	Dog, cat, human, monkey	Stomach	
<i>H. nemestrinae</i>	Pig-tailed macaque	Stomach	
<i>H. suis</i> <sup>△</sup>	Swine	Stomach	
<i>H. acinonyx</i>	Cheetah	Stomach	
<i>H. rappini</i> <sup>**</sup>	Sheep, dog, human, mice	Intestine	Liver (sheep), stomach
<i>H. canis</i> <sup>*</sup>	Dog, human	Intestine	Liver (dog)
<i>H. hepaticus</i>	Mice	Intestine	Liver
<i>H. bilis</i>	Mice, dog	Intestine	Liver, stomach (dog)
<i>H. trogontum</i>	Rat	Intestine	
<i>H. muridarum</i>	Mice, rat	Intestine	Stomach (mich)
<i>H. cinaedi</i> <sup>*</sup>	Human, hamster	Intestine	
<i>H. fennelliae</i>	Human	Intestine	
<i>H. pullorum</i> <sup>*</sup>	Chicken, human	Intestine	Liver (chicken)
<i>H. pametensis</i>	Bird, swine	Intestine	
<i>H. cholecystus</i>	Hamsters	Intestine	

<sup>\*</sup>Some data suggest zoonotic potential

<sup>△</sup>Closely related, may be same species

<sup>1</sup>Department of Gastroenterology, Chinese PLA 222 Hospital, Jilin 132011, Jilin Province, China

<sup>2</sup>Department of Gastroenterology, Mianxian Hospital, Mianxian 724200, Shaanxi Province, China

<sup>3</sup>Room 12, 1 Buliding 621, Fourth Military Medical University, Xi'an 710033, Shaanxi Province, China

Dr. LUO Yu-Qin, female, born on 1961-05-12 in Jilin City, Jilin Province, graduated from Jilin Medical College, specialized in the study of digestive diseases, having 18 papers published now studying in Xijing Hospital, Fourth Military Medical University.

**Correspondence to:** Dr. LUO Yu-Qin, Department of Gastroenterology, Chinese PLA 222 Hospital, Jilin 132011, Jilin Province, China

Tel. +86-432-2050789

Received 1998-04-12

## HELICOBACTER PYLORI AND PEPTIC ULCER IN CIRRHOSIS

Historically, it is well recognized that duodenal ulcer disease is more common in patients with cirrhosis as compared with non-cirrhotic patients<sup>[4]</sup>. However, a number of early studies suggested that in cirrhotic patients there was no clear relationship between duodenal ulcers and *H. pylori* infection, suggesting the possibility of other causes<sup>[5]</sup>. Other studies suggested that *H. pylori* infection, as measured by IgG, *H. pylori* serum antibodies, was more common in cirrhotic patients than in non-cirrhotics<sup>[6]</sup>. A study showed that cirrhotic patients were more likely to have a positive *H. pylori* ELISA with a negative histologic examination for *H. pylori* as compared with noncirrhotic patients<sup>[7]</sup>. Whether *H. pylori* is a risk factor for peptic ulcer in cirrhosis remains controversial. In a cross-sectional study by Wang *et al*, 49 cirrhotic patients underwent upper gastrointestinal endoscopy and 75 controls (healthy examinees) without liver disease were also examined by endoscopy. Thirty (61%) of the 49 cirrhotic patients had peptic ulcers as compared with 24 (32%) of the 75 controls. The frequency of *H. pylori* in the antrum in the cirrhotic group was significantly lower than in the control group (39% vs 69%). The presence of *H. pylori* was more frequent in control patients with gastric (75%) and duodenal ulcers (95%) than nonulcerous control patients (59%), the difference between patients with and without peptic ulcer (40% vs 37%) was not significant in cirrhotic patients. *H. pylori* was identified in 40% of the cirrhotic patients with duodenal ulcers as against 95% of controls with duodenal ulcer ( $P < 0.05$ ). Nevertheless, this difference was not significant among patients with a gastric ulcer between the two groups (40% vs 75%). There was no significant difference in the frequency of *H. pylori* infection among nonulcerous patients between the cirrhotic and control groups (37% vs 59%). No evidence was found to substantiate an etiologic role of *H. pylori* in the development of duodenal ulcer in cirrhotic patients<sup>[8]</sup>. In 153 consecutive patients with cirrhosis, Siringo *et al*'s<sup>[9]</sup> assessed the prevalence of IgG to *Helicobacter pylori* and compared it with that in 1010 blood donor-residents in the same area and the relationship of IgG to *H. pylori* with clinical and endoscopic features and with the risk of

peptic ulcer. The prevalence of IgG to *H. pylori* of cirrhosis was significantly higher than in blood donors (76.5% vs 41.8%;  $P < 0.0005$ ) and was not associated with sex, cirrhosis etiology, Child class, gammaglobulins and hypertensive gastropathy. In both groups, the prevalence of IgG to *H. pylori* was significantly higher in subjects aged over 40. Multivariate analysis identified high age and males as risk factors for a positive *H. pylori* serology and no independent risk factors for peptic ulcer. The high prevalence of *H. pylori* positive serology found in this series was related to age and sex and might also be explained by previous hospital admissions and/or upper gastrointestinal endoscopy. Their results did not confirm the role of *H. pylori* as a risk factor for peptic ulcer in patients with liver cirrhosis. *H. pylori* infection is the major pathogenic factor for peptic ulcer disease. Its epidemiology is not fully known; few data are available in patients with chronic liver disease. To investigate the seroprevalence and factors associated with *H. pylori* infection, a series of studies on liver cirrhosis patients is necessary. Two hundred and twenty consecutive patients were prospectively included in a study aimed to evaluate the effect of dietary intervention on cirrhosis complications and survival. An epidemiological and clinical questionnaire was completed. Sera were obtained and stored at  $-70^{\circ}\text{C}$  until analyzed. They were tested for *H. pylori* antibodies using a commercial ELISA kit. Eleven of 220 patients had borderline anti-*H. pylori* -IgG titers. Of the remaining 209 patients, 105 (50.2%) showed positive titers of *H. pylori* IgG. Univariate analysis showed that *H. pylori* infection was more frequent in older patients, those born outside Catalonia, and in patients with a low educational level. Past ethanol consumption and current smoking were correlated negatively with *H. pylori* infection. Selected age (OR 3.1, 95% CI 1.46 - 6.45), educational level (OR 2.2, 95% CI 1.18 - 4.2) and alcohol consumption (OR 0.7, 95% CI 0.45 - 0.99) as the variables were independently related to *H. pylori* infection in multivariate analysis. Their conclusions of *H. pylori* infection in cirrhosis has the same epidemiological pattern as in the general population. Suggestions that the etiology or the severity of the liver disease could be related to *H. pylori* infection were not confirmed by their study<sup>[10]</sup>.

#### **HELICOBACTER PYLORI AND PORTAL HYPERTENSIVE GASTROPATHY**

Yang et al<sup>[11]</sup> have recently investigated the possible relationship between *H. pylori* infection and portal

hypertensive gastropathy (PHG) in cirrhotic patients. Yang's conclusion is that *H. pylori* colonization of the stomach of cirrhotic patients was likely to be contributed to the development of PHG. In other reports, *H. pylori* infection in patients with PHG differed from that in the normal population<sup>[12]</sup>, in contrast with what can be observed in patients with chronic gastritis. Some authors do not agree, however, on Balan's findings that gastric mucus secretion was unaltered in PHG patients. Although there was no difference between *H. pylori*-positive or-negative patients, a previous study showed that both mucus and bicarbonate secretion (so-called mucus-bicarbonate barrier) were impaired in cirrhotic patients with PHG<sup>[13]</sup>, a phenomenon that might account for the high sensitivity of portal hypertensive mucosa to the damaging agents<sup>[14]</sup>. Others have also detected a reduced mucus secretion in PHG patients<sup>[15]</sup>. PHG was also thought to be associated with changes in gastric mucosal blood flow, but, the available data are conflicting<sup>[16]</sup>, although most studies support the concept that gastric perfusion was increased, because *H. pylori* infection had no influence on gastric mucosal blood flow, the state of local microcirculation was unaffected by eradication of the germ<sup>[17]</sup>. Another study suggested that the role of *H. pylori* infection in the pathogenesis of congestive gastropathy seemed to be unlikely and that there was no need for routine eradication in cirrhotic patients<sup>[18]</sup>. Bahnacy et al<sup>[18]</sup> evaluated the prevalence and significance of *H. pylori* infection in patients with portal hypertension. A total of 118 patients were selected, 90 with portal hypertension (66 males, 24 females, mean age  $49.1 \pm 2.1$  years) and 28 noncirrhotic patients with nonulcerative dyspepsia as a control group (12 males, 16 females, mean age  $47.6 \pm 2.8$  years). Endoscopy was performed and gastric biopsies were taken for histological examination and diagnosis of *H. pylori* infection in all the patients. Of the portal hypertensive patients, 42 (47%) had congestive gastropathy, 11 (26%) of whom were positive for *H. pylori* infection and 48 (53%) had no gastropathy, 12 (25%) of whom were positive for *H. pylori* infection. In the control group, 15 (54%) of 28 were positive for *H. pylori* infection. *H. pylori* was found less frequently in congestive gastropathy patients than in the control group.

#### **HELICOBACTER AND BILE DUCT INJURY**

Are there any *Helicobacter* species that can induce bile duct injury and then trigger further autoimmune liver diseases? Recent studies in animals have

provided insight into the possibility. The best model for the *Helicobacter* induced liver disease up to date is the recently isolated and characterized bacterium named *H. hepaticus*<sup>[19-22]</sup>. *H. hepaticus* is a spiral-to-curved bacterium, observed with Steiner's silver stains in livers of barrier-maintained mice suffering from multifocal necrotic hepatitis. *H. hepaticus* persistently colonized in the colon and cecum, and was associated with liver tumors in A/J Cr mice as well as hepatitis in other susceptible inbred mouse strains<sup>[19]</sup>. In A/J Cr mice, *H. hepaticus* can be seen in the liver under electron microscopy, but only infrequently and only in bile canaliculi. *H. hepaticus* is resistant to high levels of bile *in vitro*, which may help explain its ability to colonize in bile canaliculi. Other studies have suggested that *H. pylori* can colonize in the biliary tract. In one study, *H. pylori* DNA was detected by PCR in 3 out of 7 bile samples collected with percutaneous transhepatic cholangiodrainage, suggesting the possibility that this organism can cause asymptomatic cholangitis<sup>[23]</sup>. In another study, a microorganism closely resembling (by PCR and immunohistochemical staining) *H. pylori* was found in the resected gallbladder mucosa of a 41-year-old woman who was admitted to the hospital with fever and upper right quadrant pain<sup>[24]</sup>. However, these studies inferring the presence of *H. pylori* in bile of biliary tissues are not supported by the *in vitro* findings of *H. pylori* being unable to grow in the presence of bile products<sup>[25]</sup>. The author also demonstrated that unconjugated bile salts were more toxic than conjugated bile salts<sup>[25]</sup>. Others have suggested that bile salts *in vivo* can inhibit *H. pylori* colonization. These authors found an association between the absence of *H. pylori* and previous surgery for peptic ulcers, high reflux scores, hypochlorhydria and increased bile acid concentration in the stomach<sup>[26]</sup>. Other reports have also noted that gastric *H. pylori* infection increased following cholecystectomy<sup>[27]</sup>. Nevertheless, *H. pylori* appears in some people to survive in intestinal fluids with bile present as noted by the ability to isolate *H. pylori* from the feces of children and adults<sup>[28,29]</sup>. The sensitivity of *H. pylori* to bile acids is contrasted by the ability of *Helicobacter* colonizing in the liver, i.e. *H. hepaticus*, *H. bilis*, *H. canis*, *H. cholecystus* and *H. pullorum*, to grow in the presence of bile. In addition to *H. hepaticus*, other *Helicobacter* sp can colonize in the hepatobiliary tract. A bacterium was identified in the diseased livers and intestines of aged inbred mice. It has been characterized biochemically by 16s rRNA sequence data, and named *H. bilis*<sup>[30]</sup>.

#### HELICOBACTER AND DIARRHOEA IN CIRRHOSIS

It was observed that *H. hepaticus* can cause inflammatory bowel disease when inoculated into germ free mice. In addition, *H. hepaticus* was associated with colitis and typhlitis in immunocompromised mice<sup>[20,31,32]</sup>. It is well known that *H. cinaedi* and *H. fennelliae* are isolated from the diarrheic feces of immunocompromised patients with proctitis and/or colitis<sup>[33,34]</sup>. *H. canis*, cultured from diarrheic and asymptomatic dog feces as well as feces from humans with diarrhea were isolated from the liver of a dog with acute hepatitis<sup>[35,36]</sup>. Cirrhotic patients often had diarrhea, could it be possible that *H. hepaticus* can cause inflammatory bowel disease in cirrhosis This deserves further studies. As many intestinal *Helicobacters* appeared to cause diarrheal diseases (and perhaps liver disease) in humans, could positive IgG-*H. pylori* antibodies reflect cross-reactivity with other *Helicobacter* species Sera from abattoir workers in direct contact with internal organs of poultry were more frequently positive (ELISA>300) than the sera from other employees<sup>[37,38]</sup>. It is worth noticing that although the prevalence of *H. pylori* infection was not different from controls in the other groups, their *H. pylori* IgG antibody levels were statistically higher<sup>[37,38]</sup>.

#### HELICOBACTER AND HEPATITIS AND LIVER CANCER

Mice infected with *H. hepaticus* developed chronic liver inflammation, with oval cell, Kupffer cell and Ito cell<sup>[20]</sup> hyperplasia, hepatomegaly and bile duct proliferation<sup>[20]</sup>. Eventually, with longstanding infection, A/J Cr mice developed a chronic proliferative hepatitis and hepatocellular carcinoma. There are some similarities of this murine hepatitis to human primary biliary cirrhosis including portal hepatitis, ductular proliferation, and scarring. The murine hepatitis also had features of autoimmune cholangitis<sup>[20]</sup>. The mechanism in which *H. hepaticus* infection caused liver injury is still unclear at present. *H. hepaticus*, like several other *Helicobacter* species, expressed urease enzyme which generated ammonia, the toxic product may damage hepatocytes adjacent to the bacteria. In addition, a soluble cytotoxin has been identified in *H. hepaticus* that produced significant *in vitro* cytopathic effects in a murine hepatic cell line<sup>[39]</sup>. A recently discovered bacterium, *H. hepaticus*, could infect the intrahepatic bile canaliculi of mice, causing a severe chronic hepatitis culminating in liver cancer. Thus, it affords an animal model for study of bacteria-associated tumorigenesis including

*H. pylori* related gastric cancer. Reactive oxygen species are often postulated to contribute to this process. Sipowicz *et al.*<sup>[40]</sup> recently reported that hepatitis of male mice infected with *H. hepaticus* showed significant increases in the oxidatively damaged DNA deoxynucleoside 8-hydroxydeoxyguanosine, with the degree of damage increased with progression of the disease. Perfusion of infected liver with nitro blue tetrazolium revealed that superoxide was produced in the cytoplasm of hepatocytes, especially in association with plasmacytic infiltrates near portal triads. Contrary to expectations, Kupffer cells, macrophages, and neutrophils were rarely involved. However, levels of cytochrome P450 (CYP) isoforms 1A2 and 2A5 in hepatocytes appeared to be greatly increased, as indicated by the number of cells positive in immunohistochemistry and the intensity of staining in many cells, concomitant with severe hepatitis. The CYP2A5 immunohistochemical staining colocalized with formazan deposits resulting from nitro blue tetrazolium reduction and occurred in nuclei as well as cytoplasm. These findings suggest that CYP2A5 contributes to the superoxide production and 8-hydroxydeoxyguanosine formation, although it is possible that reactive oxygen species from an unknown source in the hepatocytes may lead to CYP2A5 induction of coincidental occurrence of these events. Three glutathione S-transferase isoforms, mGSTP1-1 (pi), mGSTA1-1 (YaYa), and mGSTA4-4, also showed striking increases evidencing major oxidative stress in these livers. Luzza *et al.*<sup>[41]</sup> assessed a sample of 705 resident subjects (273 males, aged 1-87 years, median 50) who attended the outpatient medical centre of the rural town of Ciro, Southern Italy (11000 inhabitants) for blood test. All subjects completed a structured questionnaire. A serum sample was drawn from each subject and assayed for *H. pylori* IgG by a validated in-house enzyme linked immunosorbent assay. Antibodies to HAV were determined in 466 subjects (163 males, aged 16-87 years, median 49). The Kappa statistical method was used to measure the agreement between *H. pylori* and HAV seropositivity. Overall, 466 (63%) subjects were seropositive for *H. pylori*. Of the 466 subjects screened for both *H. pylori* and HAV, 291 (62%) were seropositive for *H. pylori*, and 407 (87%) for HAV. Cross-tabulation of these data showed that 275 (59%) were seropositive and 43 (9%) seronegative for both *H. pylori* and HAV; 16 (3%) were seropositive for *H. pylori* and 132 (28%) were seropositive for HAV (OR = 5.6, CI 3-10). There was a parallel, weakly correlated ( $r = 0.278$ ) rise in the seroprevalence of the two

infections with increasing age. However, the agreement between *H. pylori* and HAV seropositivity was a little better than chance (Kappa = 0.21), and in those aged less than 20 years, it was worse than chance (Kappa = -0.064). Furthermore, multiple logistic regression analysis did not show any risk factor shared by both infections. The correlation between *H. pylori* and HAV reflected the age-specific seroprevalence of both infections rather than a true association. This study provided evidence against a common mode of transmission of *H. pylori* and HAV. Chen *et al.*<sup>[42]</sup> examined the seroprevalences of chronic infection with hepatitis B and C viruses and *H. pylori* in Matzu, a group of small islets with 5566 civilian residents who have extremely high mortalities from cancers of the stomach and liver. The standardized mortality ratios (SMR) of all cancer sites combined, liver cancer and stomach cancer in 1984-1993 were calculated using the general population in Taiwan as the reference (SMR = 100). The SMRs (95% CI) for all cancer sites combined, liver cancer and stomach cancer were 160 (131-195), 252 (170-360) and 351 (229-516), respectively, in Matzu. A health survey was carried out with 485 civilian residents aged 30 years or more, giving a response rate of 69% among those who were eligible. Serum samples were tested for antibodies against *H. pylori* (anti-Hp) by enzyme-linked immunosorbent assay and hepatitis B surface antigen (HBsAg) and antibodies against hepatitis C virus (anti-HCV) by enzyme immunoassay. The seroprevalence was 61% for anti-Hp, 24.7% for HBsAg and 1.8% for anti-HCV in Matzu. While mortality rates of liver and stomach cancers were significantly higher in Matzu than in Taiwan, the seroprevalences of anti-Hp, HBsAg and anti-HCV in Matzu were similar to or even lower than those in Taiwan. Their findings suggest the existence of risk factors other than microbial agents involved in the development of stomach and liver cancers. Rudi *et al.*<sup>[43]</sup> examined staff members of an acute care hospital for serum antibodies to *H. pylori* IgG ( $n = 457$ ) and to hepatitis A virus ( $n = 434$ ). The staff members were assigned to three groups: nonmedical staff ( $n = 110$ ); medical and nursing staff ( $n = 272$ ); and medical and nursing staff working in a gastroenterology and endoscopy unit ( $n = 75$ ). Serum antibodies were measured by validated enzyme immunoassays. A questionnaire inquiring about medical and professional history, history of upper GI pain and ulcer, as well as about the use of nonsteroidal anti-inflammatory drugs or medication for GI complaints and smoking habits was completed by each person. The seroprevalence of

*H. pylori* was 35.5% in group I, 34.6% in group II, and 24.0% in group III (not significant). The seroprevalence of *H. pylori* antibodies increased with age ( $P < 0.01$ ), and antibodies were present more frequently in women than in men (36.2% vs 25.4%,  $P < 0.05$ ). After adjustment for age, the duration of experience and the number of years working in the gastroenterology or endoscopy unit did not increase *H. pylori* seropositivity. No significant association was found between *H. pylori* seropositivity and history of upper GI pain, ulcers, use of nonsteroidal anti-inflammatory drugs or medication for GI complaints, or tobacco use. The prevalence of hepatitis A antibodies was similar in the three groups (group I, 26.4%; II 26.5%; III 21.7%; not significant). Cross-tabulation showed that 67 (15.4%) subjects were seropositive for both *H. pylori* and hepatitis A ( $P < 0.01$ ), and that 245 (56.5%) were negative for both. Seventy-seven (17.7%) and 45 (10.4%) were seropositive for only *H. pylori* and for only hepatitis A respectively. Occupational exposure to patients in an acute care hospital as well as to patients and to endoscopic procedures of a gastroenterology and endoscopy unit does not increase the rate of infection with *H. pylori*. The significant correlation between the seroprevalence of *H. pylori* and hepatitis A antibodies suggests the fecal-oral transmission of *H. pylori*.

#### HELICOBACTER AND CHRONIC HEPATIC ENCEPHALOPATHY

Chronic hepatic encephalopathy is a neuropsychiatric disorder with protein manifestations, the pathogenesis of which is poorly understood<sup>[44]</sup>. Ammonia is of key importance in the pathogenesis of hepatic encephalopathy<sup>[45,46]</sup>, and hyperammonemia in patients with cirrhosis is considered to be produced by bacterial urease in the gut flora. The initial study implicating *H. pylori* as a risk factor for hepatic encephalopathy was published in 1993<sup>[47]</sup>. Gastric ammonia production must be evaluated to assess whether the ammonia produced by *H. pylori* can cause hyperammonemia. *H. pylori* has strong urease activity. Ammonia produced by *H. pylori* in the stomach can be a source of systemic ammonia in patients with hepatic dysfunction. The effect of the eradication of *H. pylori* on hyperammonemia was examined in patients with liver cirrhosis. Ammonia concentrations in blood and gastric juice were analysed in 50 patients with liver cirrhosis and hyperammonemia. All patients were first treated with a low protein diet, kanamycin, lactulose, and branched chain enriched amino acid solution.

Hyperammonemia remained in 18 patients. These 18 patients were divided into three groups according to the status of *H. pylori* infection: group I, with a diffuse distribution of *H. pylori* in the stomach; Group II, with a regional distribution; and group III, without *H. pylori*. In group I, ammonia concentrations in blood and gastric juice were significantly reduced after *H. pylori* eradication. The blood ammonia concentration at 12 weeks after the eradication was still significantly lower than that before eradication. In groups II and III, the ammonia concentrations in blood and gastric juice were not significantly reduced after eradication therapy. The authors' conclusion is that diffuse distribution of *H. pylori* in the stomach contributes partly to hyperammonemia in patients with liver cirrhosis, and the eradication of *H. pylori* is effective in patients with liver cirrhosis, and the eradication of *H. pylori* is effective in patients with hyperammonemia with diffuse *H. pylori* infection in the stomach<sup>[48]</sup>. These findings suggest that the contribution of ammonia produced by *H. pylori* to the systemic concentration depends on the number of bacteria and their distribution in the stomach<sup>[48]</sup>. Quero *et al*<sup>[49]</sup> also reported a fall in blood ammonia with the eradication of *H. pylori*, but the blood ammonia rose two months after treatment to baseline values in patients after the eradication of *H. pylori*, suggesting that the effect of the eradication of *H. pylori* on hyperammonemia is a non-specific effect of antibiotics rather than an effect of the eradication of the organism. Plevris *et al*<sup>[50]</sup> found no significant effect of the presence of *H. pylori* on blood ammonia up to two hours after administration of oral urea. They also suggested that the improvement seen in our initial report may be attributed to a non-specific effect of antibiotics rather than to an effect of the eradication of *H. pylori*.

#### CHRONIC ATROPHIC GASTRITIS AND *H. pylori* INFECTION IN PBC

Primary biliary cirrhosis (PBC) is a chronic liver disease characterized by exocrine gland impairment. Up to now there has been no report dealing with gastric mucosa involvement in this autoimmune condition which is frequently associated with Sjogren syndrome. Floreani *et al*<sup>[51]</sup> investigated the morphologic, biochemical and immunological features of the gastric mucosa in PBC. A cross-sectional matching study was performed. Thirty-three PBC patients (30 women, 3 men, mean age 58 years; 17 with stage II - III, and 16 with stage IV disease) and 33 sex- and age-matched dyspeptic controls were included. Six biopsy specimens from

the fundus (2), body (2) and antrum (2) were taken from all patients and controls. A serological assessment was made for each subject, including pepsinogen A (PGA), pepsinogen C (PGC), gastrin (G), and antibodies against *H. pylori* (anti-Hp IgG). Endoscopic gastritis was found in 22 PBC patients (66.6%). There was no difference between PBC patients and controls regarding the percentage of subjects with mild, moderate, severe or atrophic gastritis (AG). There was no difference in gastric mucosal involvement between PBS subjects with or without secondary Sjogren syndrome. A discrepancy was observed in the data obtained with respect to *H. pylori* infection. *H. pylori* colonization was significantly more frequent in controls than in PBC patients (79% vs 49%,  $P < 0.002$ ), but anti-Hp IgG was detected in the same percentage in the two groups (90% vs 83%). There was no difference between the two groups in the PGA, PGC, PGA/PGC ratio, or gastrin. Eight PBC patients had esophageal varices. PBC patients were not characterized by chronic atrophic gastritis. Even though they presented chronic gastritis with the same prevalence as dyspeptic controls, and showed signs of previous *H. pylori* infection as frequently as dyspeptic patients, they are actually much less frequently infected. The reasons for this observation are unclear<sup>[47]</sup>. In summary, many liver diseases in humans though well characterized clinically and pathologically, do not have well defined etiologies. Perhaps like the discovery of *H. pylori* associated gastric disease, the recognition of *Helicobacter SP* induced liver disease in animals, should stimulate studies to ascertain whether these or similar *Helicobacters* play an important role in pathogenesis of idiopathic hepatitis and liver neoplasia in humans.

## REFERENCES

- 1 Helicobacter pylori, ammonia and the brain (commentary). *Gut*, 1997;40:805-806
- 2 Fox JG. The expanding genus of Helicobacter, pathogenic and zoonotic potential. In: Sleisenger, Fordtram, eds: Seminars in gastrointestinal diseases. Philadelphia: W.B. Saunders Co., in press
- 3 Fox JG, Wang TC. Helicobacter and liver disease. *Ital J Gastroenterol Hepatol*, 1997;29:6-12
- 4 Wu CS, Lin CY, Liaw YF. Helicobacter pylori in cirrhotic patients with peptic ulcer disease: a prospective, case controlled study. *Gastrointest Endosc*, 1995;42:424-427
- 5 Chen JJ, Changchien CS, Tai DI, Chiou SS, Lee CM, Kou OH. Role of Helicobacter pylori in cirrhotic patients with peptic ulcer: A serological study. *Dig Dis Sci*, 1994;39:1565-1568
- 6 Flisiak R, Prokopowicz D, Tynecka E. Macroscopic changes in endoscopy of upper digestive tract and Helicobacter pylori infections in patients with liver cirrhosis. *Przegląd Epidemiologiczny*, 1994;48:455-459
- 7 Altman C, Ladouch A, Briantais MJ, Rason T, Martin E, Jacques L. Antral gastritis in chronic alcoholism. Role of cirrhosis and Helicobacter pylori. *Press Med*, 1995;24:708-710
- 8 Wang CH, Ma LR, Lin RC, Kou TY, Chang KK. Helicobacter pylori infection and risk of peptic ulcer among cirrhotic patient. *J Formosa Med Ass*, 1997;96:55-58
- 9 Siringo S, Waira D, Menegatti M, Piscaglia F, Sofia S, Gaetain M. High prevalence of Helicobacter pylori in liver cirrhosis: relationship with clinical and endoscopic features and the risk of peptic ulcer. *Dig Dis Sci*, 1997;42:2024-2030
- 10 Calvet X, Mavarro M, Gil M, Mas P, Rivero E, Sanfeliu I. Seroprevalence and epidemiology of Helicobacter pylori infection in patients with cirrhosis. *J Hepatol*, 1997;26:1249-1254
- 11 Yang DH, Huang CC, Yu JL, Song WS, Mao H, Xu C. The relationship between portal hypertensive gastropathy and Hp infection. *Chin J New Gastroenterol*, 1997;5:27-28
- 12 Teng YN, Yao MY. Clinical observation on gastric H. pylori infection in patients with liver cirrhosis. *Acta Acad Med Xuzhou*, 1998; 18:36-37
- 13 Guslandi M, Foppa L, Sorghi M, Pellegrini A, Fanti L, Tittobello A. Breakdown of mucosal defences in congestive gastropathy in cirrhotics. *Liver*, 1992;12:302-305
- 14 Payen JL, Cales P. Gastric modifications in cirrhosis? *Gastroenterol Clin Biol*, 1991;15:285-295
- 15 Kameyama J, Suzuki Y, Suzuki A, Hoshikawa T, Yasaku Y, Yoshimur N. Gastric mucus secretion in portal hypertension. *J Gastroenterol Hepatol*, 1989;4(Suppl1):126-128
- 16 Guslandi M, Tittobello A. Gastric mucosal haemodynamics in portal hypertensive gastropathy: The debate goes on. *Hepatology*, 1995; 22:1002-1003
- 17 Zhu HH. Prevalence of Helicobacter pylori in cirrhotic patients with portal hypertensive gastropathy. *China Natl J New Gastroenterol*, 1996;2:104-105
- 18 Bahnacy A, Kupcsulik P, Eles ZS, Jaray B, Flautner L. Helicobacter pylori and congestive gastropathy. *Z Gastroenterol*, 1997;35:109-112
- 19 Fox JG, Li X, Yan L, Cahill RJ, Hurley R, Lewis R. Chronic proliferative hepatitis in A/J Cr mice associated with persistent H. hepaticus infection: A model of Helicobacter induced carcinogenesis. *Infect Immun*, 1996;64:1548-1558
- 20 Fox JG, Yan L, Shames B, Campbell J, Murphy JC, Li X. Persistent hepatitis and enterocolitis in germfree mice infected with Helicobacter hepaticus. *Infect Immun*, 1996;64:3673-3681
- 21 Fox JG, Dewhirst FE, Tully JG, Paster BJ, Yan L, Taylor NS. Helicobacter hepaticus sp. nov, a microaerophilic bacterium isolated from livers and intestinal mucosal scrapings from mice. *J Clin Microbiol*, 1994;32:1238-1245
- 22 Ward JM, Fox JG, Anver MR, Haines DC, George CV, Colling MJ Jr. Chronic active hepatitis and associated liver tumors in mice caused by a persistent bacterial infection with a novel Helicobacter species. *J Nat Cancer Inst*, 1994;86:1222-1227
- 23 Lin TT, Yeh CT, Wu CS, Liaw YF. Detection and partial sequence analysis of Helicobacter pylori DNA in the bile samples. *Dig Dis Sci*, 1995;40:2214-2219
- 24 Kawaguchi M, Saito T, Ohno H, Midorikawa S, Sanji T, Handa Y. Bacteria closely resembling Helicobacter pylori detected immunohistologically and genetically in resected gallbladder mucosa. *J Gastroenterol*, 1996;31:294-298
- 25 Hanninen ML. Sensitivity of Helicobacter pylori to different bile salts. *Eur J Clin Microbiol Infect Dis*, 1991;10:515-518
- 26 O'connor HJ, Wyatt JI, Dixon MF, Axon AT. Campylobacter like organisms and reflux gastritis. *J Clin Pathol*, 1986;39:531-534
- 27 Caldwell MT, Mcdermott M, Jazrawi S, Dowd G, Byrne PJ, Walsh TN. Helicobacter pylori infection increases following cholecystectomy. *Irish J Med Sci*, 1995;164:52-55
- 28 Kelly SM, Pitcher MCI, Farmery SM, Gibson GR. Isolation of Helicobacter pylori from feces of patients with dyspepsia in the United Kingdom. *Gastroenterology*, 1994;107:1671-1674
- 29 Fox JG, Yan L, Dewhirst FE, Paster BJ, Shames B, Murphy JG. Helicobacter bilis sp nov, a novel Helicobacter isolated from bile, liver, and intestines of aged, inbred mouse strain. *J Clin Microbiol*, 1995;33:445-454
- 30 Thomas JE, Gibson GR, Parboe MK, Dale A, Weaver LT. Isolation of Helicobacter pylori from human feces. *Lancet*, 1992;340: 1194-1195
- 31 Cahill RJ, Foltz CJ, Fox JG, Danler CA, Powrie F, Schauer DB. Inflammatory bowel disease: an immune mediated condition triggered by bacterial infection. *Infect Immun*, 1996;65:3126-3131
- 32 Ward JM, Anver MR, Haines DC, Melhom JM, Gorelick P, Yan L. Inflammatory large bowel disease in immunodeficient mice naturally infected with Helicobacter hepaticus. *Lab Animal Sci*, 1996; 46:15-20
- 33 Gebhart CJ, Fennell CL, Murtaugh MP, Stamm WE. Campylobacter cinaedi in normal intestinal flora in hamsters. *J Clin Microbiol*, 1989;

- 27:1692-1694
- 34 Stills HF, Hook RR, Kinden DA. Isolation of a campylobacter like organism from healthy Syrian hamsters (*Mesocricetus auratus*). *J Clin Microbiol*, 1989;27:2497-2501
- 35 Fox JG, Drolet R, Higgins R. *Helicobacter canis* isolated from a dog liver with multifocal necrotizing hepatitis. *J Clin Microbiol*, 1996;34:2479-2482
- 36 Stanley J, Linton D, Burens AP, Dewhirst FE, Owen RJ, Porter A. *Helicobacter canis* sp. nov., a new species from dog: an integrated study of phenotype and genotype. *J Gen Microbiol*, 1993;139:2495-2504
- 37 Husson MO, Vincent P, Grabiard MH, Furon D, Leclerc H. Anti-*Helicobacter pylori* IgG levels in abattoir workers. *Gastroenterol Clin Biol*, 1991;15:723-726
- 38 Stanley J, Linton D, Burens AP, Dewhirst FE, On SL, Porter A. *Helicobacter pullorum* sp. nov. genotype and phenotype of a new species isolated from poultry and from human patients with gastroenteritis. *Microbiology*, 1994;140:3441-3449
- 39 Taylor NS, Fox JG, Yan L. In vitro hepatotoxic factor in *Helicobacter hepaticus*, *H. pylori* and other *Helicobacter* species. *J Med Microbiol*, 1995;42:48-52
- 40 Sipowicz MA, Chomarat P, Diwan BA, Anver MA, Awasthi YC, Ward JM. Increased oxidative DNA damage and hepatocyte overexpression of specific cytochrome p450 isoforms in hepatitis of mice infected with *Helicobacter hepaticus*. *Am J Pathol*, 1997;151:933-941
- 41 Luzzza F, Imeneo M, Maletta M, Paluccio G, Giancotti A, Perticone F. Seroepidemiology of *Helicobacter pylori* infection and hepatitis A in a rural area: evidence against a common mode of transmission. *Gut*, 1997;41:164-168
- 42 Chen SY, Liu TY, Chen MJ, Lin JT, Sheu JC, Chen CJ. Seroprevalences of hepatitis B and C viruses and *Helicobacter pylori* infection in a small, isolated population at high risk of gastric and liver cancer. *Int J Cancer*, 1997;71:776-779
- 43 Rudi J, Toppe H, Marx N, Zuna I, Theilmann L, Stremmel W. Risk of infection with *Helicobacter pylori* and hepatitis A virus in different groups of hospital workers. *Am J Gastroenterol*, 1997;92:258-262
- 44 Jalan R, Seery J, Taylor Robinson SD. Pathogenesis and treatment of hepatic encephalopathy. *Aliment Pharmacol Ther*, 1996;10:681-697
- 45 Voorhies TM, Ehrlich ME, Duffy TE, Petito CK, Plum F. Acute hyperammonemia in the young primate: Physiologic and neuropathologic correlates. *Pediatr Res*, 1983;17:970-975
- 46 Blei At, Olafsson S, Therrien G, Butterworth RF. Ammonia induced brain edema and intracranial hypertension in rats after portacaval anastomosis. *Hepatology*, 1994;19:1437-1444
- 47 Gubbins GP, Moritz TE, Marsano LS, Talwalkar R, McClain CJ, Mendenhall CL. *Helicobacter pylori* is a risk factor for hepatic encephalopathy: the ammonia hypothesis revisited. *Am J Gastroenterol*, 1993;88:1906-1910
- 48 Miyaji H, Ito S, Azuma I, Itoy, Yamazaki Y, Ohtaki Y. Effects of *Helicobacter pylori* eradication therapy on hyperammonaemia in patients with liver cirrhosis. *Gut*, 1997;40:726-730
- 49 Quero JC, Hartmann IJ, de Rooij F, Wilson JH, Schalm SW. Hyperammonaemia and *Helicobacter pylori*. *Lancet*, 1995;346:713-714
- 50 Plevris JN, Morgenster R, Hayes PC, Boucher IA. Hyperammonaemia in cirrhosis and *Helicobacter pylori* infection. *Lancet*, 1995;346(8982):1104
- 51 Floreani A, Biagini MR, Zappala F, Farinati F, Flebani M, Rugge M. Chronic atrophic gastritis and *Helicobacter pylori* infection in primary biliary cirrhosis: a cross sectional study with matching. *Ital J Gastroenterol Hepatol*, 1997;29:13-17

# Cloning and expression of HLA-B7 gene

QU Shen, LI Qing-Fen, DENG Yao-Zu, ZHANG Jian-Ming and ZHANG Jie

**Subject headings** HLA-B7; polymerase chain reaction; cDNA; gene expression

## INTRODUCTION

In recent years, it has been found that HLA-B7 plays an important role in the antigen presentation and the research of human tumor therapy. It was reported that if HLA-B7 gene was transfected into target cells, the expression of HLA-B7 gene could stimulate the immune system to recognize the target cells and induce immune response<sup>[1]</sup>. In order to study the HLA-B7 gene vaccine and its feasibility for tumor gene therapy, HLA-B7 cDNA was cloned and an eukaryotic expression vector (pCD-B7) carrying HLA-B7 cDNA was constructed. This construct was transfected into NIH/3T3 cells and injected into the subcutaneous tissue of mice, the expression of HLA-B7 gene could be detected both *in vitro* and *in vivo*.

## MATERIALS AND METHODS

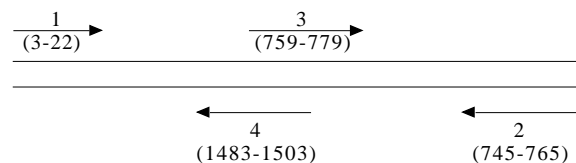
### Materials

**Cells** HLA-B7<sup>+</sup> lymphocytes were isolated from human peripheral blood.

**Reagents** Taq DNA polymerase, Supertranscript kit, and RPMI-1640 are products of GIBCO BRL. Primers were synthesized by Sangon Co. T4 DNA ligase, CIP, X-Gal, IPTG, restriction enzyme, DNA marker, calf serum, medium, PHA and IL-2 are purchased from Promega Company.

### Methods

**Primer designing** The sites of the primers were chosen according to the cDNA sequence of HLA-B7 reported by Sood AK, *et al*<sup>[2]</sup>. Four primers were synthesized as follows:



Primer 1: (cDNA 3 - 22 base) 5-ACGCCGAGATGCTG-GTCATG-3';  
Primer 2: (cDNA 745 - 765 base) 5-TGAGTTTGGTC-CTCGCCATC-3';  
Primer 3: (cDNA 759-779 base) 5-AACTCAGGACACT-GAGCTTG-3';  
Primer 4: (cDNA 1483-1503 base) 5-TTGCTCTCT-CAAATTCAGG-3'.

**Selection and culture of HLA-B7<sup>+</sup> lymphocytes** Five mL peripheral blood was taken from each of 20 healthy persons. The lymphocytes were isolated and then counted. After cytotoxic test<sup>[3]</sup>, the HLA-B7<sup>+</sup> lymphocytes were cultured in medium RPMI-1640 containing 10% calf serum, PHA 50mg/L and IL-2 500U/mL-1000U/mL for 2-3 days.

**Isolation of total RNA** The total RNA was isolated by single step method<sup>[4]</sup>. The quantity and quality of RNA were analyzed by denaturing agarose gel.

**RT-PCR** Reverse transcription was performed according to the method recommended by GIBCO BRL supertranscription kit. Five  $\mu$ L products of reverse transcription was taken as templates for PCR. HLA-B7 target sequence was amplified for 35 cycles using primer 1, 2 and primer 3, 4 as well as primer 1, 4. Fifty  $\mu$ L reaction volume included 0.2mmol/L each of dNTPs, 1.5mmol/L MgCl<sub>2</sub>, 10 $\times$ 5  $\mu$ L buffer, Taq DNA polymerase 2.5 U 0.25mmol/L each of primer and 5 $\mu$ L sample. The reaction volume was denatured at 94 $^{\circ}$ C for 30s, annealed at 53 $^{\circ}$ C for 1 min and extended at 72 $^{\circ}$ C for 2 min. After the last cycle of amplification, 10  $\mu$ L of product was stained with ethidium bromide, and analyzed by agarose gel electrophoresis, and visualized under UV light.

**Recombinant construction** Ligation reaction was performed according to a rapid, easy and effective PCR product cloning method<sup>[5]</sup>. Forty  $\mu$ L PCR product, into which 1 $\mu$ L (2.5U) Klenow enzyme was added, was placed at 37 $^{\circ}$ C for 30min and

Department of Biochemistry, Tongji Medical University, Wuhan 430030, Hubei Province, China

QU Shen, male, born on 1954-08-13 in Wuhan, Hubei Province, China and graduated from Tongji Medical University, professor of biochemistry, specializing in research of gene diagnosis and gene therapy, having 35 papers published.

\*Project supported by the foundation of State Education Commission, No.JW9312.

**Correspondence to:** Prof. QU Shen, Department of Biochemistry, Tongji Medical University, Wuhan 430030, Hubei Province, China  
Tel. +86-27-83692624

Received 1998-11-09

precipitated with ethanol. After drying, it was dissolved into 10 $\mu$ L water. Three  $\mu$ L solution and 0.1 $\mu$ g-pUC19 plasmid digested by Sma I and 15 $\mu$ L-water were added into the tube of T4 DNA ligase, and kept at room temperature for 10 min. The ligated products were subjected to transform competent cells of HB101, and the positive clone was selected by  $\alpha$  complementation detection.

### Construction of eukaryotic expression vector

Construction procedure is shown in Figure 1. Before ligation, digested pcDNA3 was treated with CIP (calf intestinal alkaline phosphatase) for 30 min. The treated linear vector was mixed, and then 2 $\mu$ L 10 $\times$  buffer, 10 unit T<sub>4</sub> DNA ligase, and TE (pH 8.0) were added into HLA-B7 cDNA fragment (ratio 1:5) till the volume was up to 20 $\mu$ L. The mixture was incubated at 16 $^{\circ}$ C for 16h, and then at 70 $^{\circ}$ C for 10min to terminate the reaction.

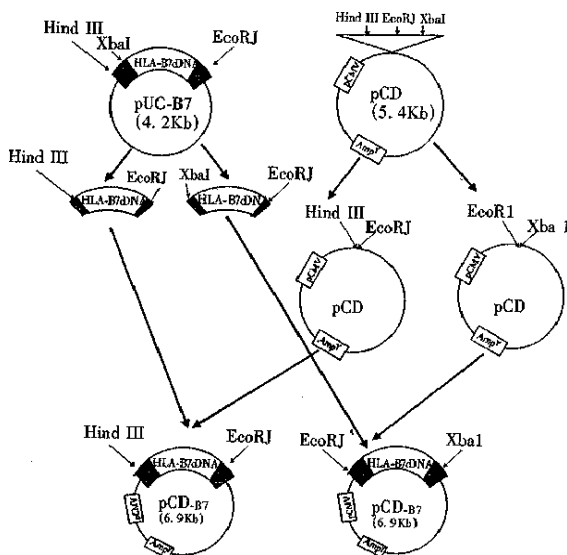


**Figure 1** Construction procedure of eukaryotic expression vector.

### Transfection and expression of pCD-B7 in vitro and in vivo

**Transfection of pCD-B7 in vitro** Lipofectin reagent was used for DNA transfection, logarithmically growing cells were seeded at  $1 \times 10^5$  cells per 35mm plate, and incubated overnight. Ten  $\mu$ g plasmid DNA and 9 $\mu$ L lipofectin were diluted into 100 $\mu$ L serum-free medium respectively, and allowed to stand at room temperature for 30min - 45min. The two solutions were mixed and 0.8mL serum-free medium was added and mixed gently and overlaid the complex onto cells. The cells were incubated for 24h at 37 $^{\circ}$ C in a CO<sub>2</sub> incubator. After the coverslips were taken out of the plate, the cells were fixed with cool acetone, and stored at -20 $^{\circ}$ C.

**Injection of pCD-B7 in vivo** The plasmid was dissolved in PBS (1 $\mu$ g/ $\mu$ L). Forty  $\mu$ L of such plasmid solution was injected into the subcutaneous layer on the back of mice. As a negative control, 40 $\mu$ L- PBS was injected into the same tissue of mice. All injection points were marked. After 15 days, the animals were killed and the skin at the injection points were taken. The sections (10 $\mu$ m) were frozen and fixed with cool acetone and stored at -20 $^{\circ}$ C.

### Detection of the expression

Indirect fluorescent antibody technique was used to detect the expression of HLA-B7. HLA-B7 antibody (dilution 1:10) was added to the coverslip, incubated at 4 $^{\circ}$ C overnight, washed with PBS for 2-3 times. Then FITC-goat antibody against human IgG (dilution 1:20) was added and incubated at 37 $^{\circ}$ C for 30min, washed with PBS 2-3 times and blocked with glycerol buffer. Finally the expression of HLA-B7 was observed under fluorescent microscopy.

## RESULTS

### The electrophoresis results of HLA-B7 cDNA after RT-PCR



**Figure 2** The electrophoresis results of RT-PCR of HLA-B7 cDNA.

1.  $\lambda$ DNA/Hind-III marker
2. The full-length of cDNA (1.5kb)
3. The upstream region of cDNA (750bp)
6. The downstream region of cDNA (750bp)

### Identification of recombinant plasmid pUC-B7

**Identification of recombinant plasmid by restriction enzyme analysis** The white bacterial colony was transferred into LB medium containing ampicillin. Then the plasmid DNA was prepared<sup>[6]</sup>. The pUC-B7 recombinant was digested with Hind-III and EcoR-I. The large fragment was 6.8kb(pUC 19) and the small fragment was 1.5kb (insert fragment). The small fragment was digested with Hinf I again. Four fragments could be seen on the running gel, their length was 976 bp, 230 bp and 200 bp, and

115 bp respectively and was consistent with the restriction sites of HLA-B 7 cDNA(Figure 3).

**Identification of pUC-B7 by PCR** The reaction condition of PCR has been discussed before 0.1 $\mu$ L (0.1  $\mu$ g) pUC-B7 was taken as template. The products of amplification including the full length, the upstream and the downstream region, showed no difference with those of the original products of PCR. So we could conclude that the insert in recombinant is identical to the products of original PCR (Figure 4).

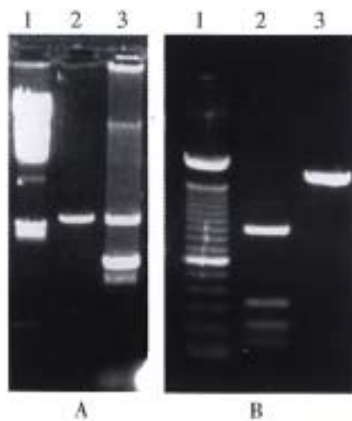


**Figure 3** The results of restriction analysis of pUC-B7.  
A. 1.  $\lambda$ DNA/*Hind* III marker; 2. pUC19/*Hind*-III; 3. pUC - B7/ *Hind* I+ *EcoR* I  
B. 1. pGEM/ *Hinf* I + *Rsa* I + *Sin*I marker; 2. cDNA/*Hinf* I; 3. cDNA (1.5kb)

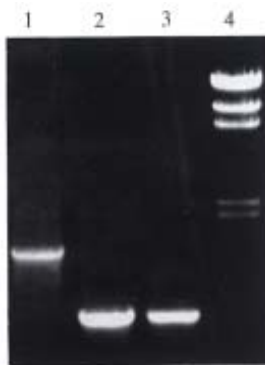


**Figure 4** The results of PCR detection of pUC-B7  
1. Full length of cDNA (1.5kb)  
2. The upstream region of cDNA (750bp)  
3. The downstream region of cDNA (750bp)  
4.  $\lambda$ DNA/*Hind* III marker

#### Identification of pCD-B7

The Amp<sup>+</sup> clone was selected and cultured in LB medium containing ampicillin. Plasmid DNA was prepared with small-scale alkaline lysis, and digested with *Hind* III and *EcoR* I. The length of the two fragments were 1.5kb (HLA-B7 insertor) and 5.4kb (vector) respectively. Four positive clones were obtained.

#### Detection of pCD-B7 expression

Effective expression was achieved in two of the four positive clones, and was consistent with what we anticipated (Figures 5, 6).

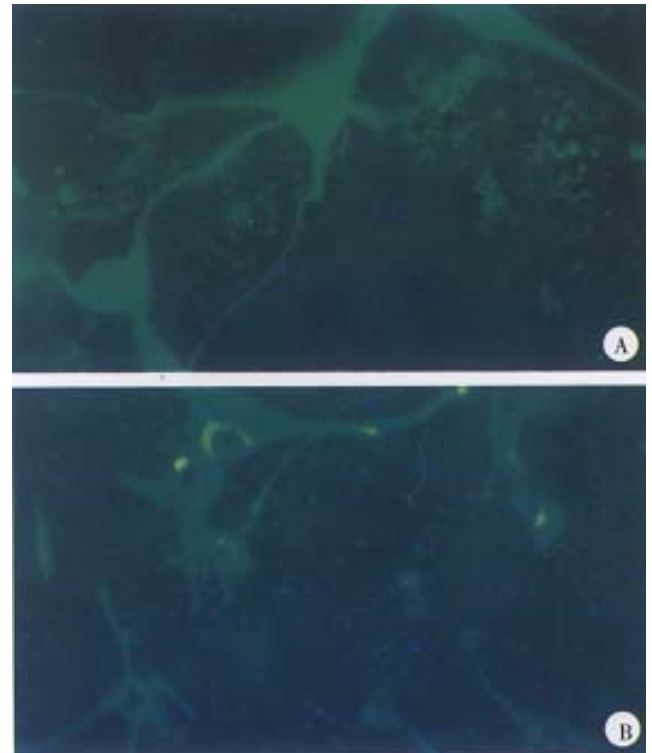


**Figure 5** The expression of pCD-B7 in NIH/3T3 cells.  
A. Negative control; B. Positive cells

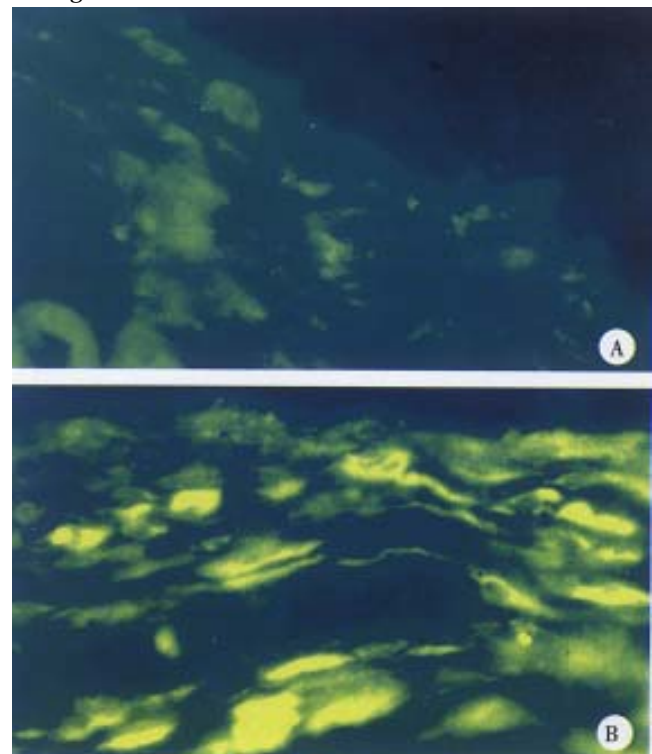


**Figure 6** The results of pCD-B7 expressed in subcutaneous tissue of mice.A. Negative control; B. Positive cells

## DISCUSSION

HLA-B7 cDNA was cloned by RT-PCR from human peripheral blood lymphocytes. The cDNA fragment was inserted into *Sma* I site of pUC19, most of the enzyme sites were kept for further construction. The pUC-B7 clone was identified by restriction enzyme digestion and PCR detection. The results corresponded to the data from Sood AK<sup>[2]</sup>. Furthermore, HLA-B7 cDNA fragment was cloned into pCDNA3. A eukaryotic expression vector was constructed and named pCD-B7. The result of indirect immuno- fluorescence technic demonstrated effective expression of HLA-B7 gene both *in vitro* and *in vivo*. This work provided the basis for further research on anti-tumor effect of HLA-B7 gene.

The study of tumor immune mechanism is deepening with the development of immunological theory. Two signal theory<sup>[7]</sup> accepted publicly laid a foundation for tumor immunotherapy. Activation of T lymphocyte requires two signals, one is the crosslinking of TCR by peptide-MHC complex, the other is the interaction between costimulatory molecule B7 and CD28 on the surface of T lymphocyte. HLA-B7 is one of the powerful signal molecules. There was a foreign report about treatment of HLA-B7 negative patient with melanoma by direct transfer of HLA-B7 gene *in*

*vivo*<sup>[1]</sup>. The efficacy is positive. Tumor cell transfected with HLA-B7 could not grow *in vivo*<sup>[8]</sup>. It acts as a vaccine to induce immune response, so that unmodified tumor cells could be recognized and destroyed by immune system. The study demonstrated that direct transfer of HLA-B7 gene to human *in vivo* is safe, feasible and potent. If HLA-B7 gene can be made into DNA vaccine with corresponding efficacy *in vivo*, it will be a hopeful way for tumor gene therapy.

## REFERENCES

- 1 Nabel GJ, Nabel EG, Yang ZY, Steinman L, Pette M. Direct gene transfer with DNA liposome complexes in melanoma: expression, biologic activity, and lack of toxicity in humans. *Proc Natl Acad Sci USA*, 1993;90:11307-11309
- 2 Sood AK, Pan J, Biro PA, Pereira D, Srivastava R, Reddy V, Duceaman BW, Weissman SM. Structure and polymorphism of class I MHC antigen mRNA. *Immunogenetics*, 1985;22:101-121
- 3 Zhao TM. HLA typing principles. Beijing: People's Health Publishing House, 1988:412-413
- 4 Chomcynski P, Chomczynski P, Sacchi N. Single step method of RNA isolation by acid guanidinium thiocyanate phenol chloro form extraction. *Analytical biochemistry*, 1987;162:156
- 5 Li HW, Tu CC, Jin KS, Zhang JG. A rapid, simple and effective clone method for PCR products. *Biochemistry*, 1995;15(4):28-30
- 6 Lu SD. Laboratory techniques of modern molecular biology. Beijing: Higher Education Publishing House, 1993:412-413
- 7 John Travis. A stimulating new approach to cancer treatment. *Science*, 1993;259:310-311
- 8 Lenog CC, Robinson BWS, Michael J. Generation of an antitumor immune response to a murine mesothelioma cell line by the transfection of allogeneic MHC genes. *Int J Cancer*, 1994;59:210-216

Edited by WANG Xian-Lin

# Preliminary study of a dot immunogold filtration assay for rapid detection of anti-HCV IgG

XIAO Le-Yi<sup>1</sup>, YAN Xiao-Jun<sup>1</sup>, MI Ming-Ren<sup>2</sup>, HAN Feng-Chan<sup>1</sup> and HOU Yu<sup>1</sup>

**Subject headings** hepatitis C virus; IgG/analysis; dot immunogold; filtration assay

## INTRODUCTION

Hepatitis C is a world-wide epidemic disease stemming from the hepatitis C virus (HCV). HCV is not only the pathogenic factor of hepatitis C but also plays an important role in the process of triggering and development of cirrhosis and liver cancer. There are two indicators for detecting HCV infection: one is HCV RNA which is the gene of the virus itself and the other is anti-HCV which is the antibody produced when the HCV antigen stimulates the body. The HCV antibody detection includes the detection of HCV IgG and HCV-IgM antibody. At present, EIA and the recombinant immunoblot assay (RIBA) are mainly used for detecting anti-HCV-IgG. By using the colloidal gold labeling technique to fix the structural and the non-structural domains of HCV recombinant antigen on the millipore membrane, a dot immunogold filtration assay for detecting anti-HCV-IgG was successfully established.

## MATERIALS AND METHODS

### Materials

Nitrocellulose (NC) membrane, 0.6 µm diameter-pore, is the product of the Beijing Chemical School. HCV recombinant antigen (rHcAg) is a gift from Li Yuexi of the Nanjing Military Medical Research Institute. Chloroauric acid is the product of the Chengdu Chemical Reagent Factory (batch number 930821). Anti-HCV antibody EIA kit is produced by the Nanjing Military Medical Research Institute. Serum specimens were provided by the Clinical Lab and the Blood-Transfusion Center of Xijing Hospital. Staphylococcus A protein (SPA) is the product of Shanghai Biological Products Research Institute (batch number 941201).

<sup>1</sup>Institute of Genetic Diagnosis of Chinese People's Liberation Army, Fourth Military Medical University, Xi'an 710033, China

<sup>2</sup>Xi'an Railway Central Hospital, Xi'an 710054, China

Dr. XIAO Le-Yi, male, born on 1955-08-10 in Tianmen City, Hubei Province, graduated from Fourth Military Medical University, majoring molecular biology and biochemistry, having 23 papers published.

**Correspondence to:** Dr. XIAO Le-Yi, Institute of Genetic Diagnosis of Chinese People's Liberation Army, Fourth Military Medical University, Xi'an 710033, China

Tel. +86-29-3374771

Received 1999-01-20

## Methods

**Colloidal gold preparation.** The colloidal gold was prepared by the sodium citrate reduction method<sup>[1-4]</sup>. Fifty mL of the 0.2mL/L chloroauric acid was heated to the boiling point, then added 1.2mL sodium citrate solution under magnetic mixing, kept at boiling point for 5min until the mixture turned dark red.

**SPA labelling.** The pH value of 1mL colloidal gold was adjusted to 5.9 - 6.2 with 0.1 mol/L K<sub>2</sub>CO<sub>3</sub>, and added with 6µg of SPA, stirred for 10min, then added with the bovine serum albumin (BSA) to a final concentration of 1%. The precipitate was discarded after low-speed centrifugation, the supernatant was centrifuged at 12000×g for 20min and discarded, the precipitate was redissolved in 0.01mol/L PBS (pH 7.4) and the working solution of the gold labeled SPA was prepared and stored at 4°C for use.

**Dot immunogold filtration assay (DIGFA).** One µL rHcAg in 0.5mol/L carbonate buffer (pH 9.5) was dotted on NC membrane, dried at room temperature and diluted coated with 5mL/L BSA for 30 min and washed 10min×2 times with 0.01mol/L PBS-T. After that, the membrane was put on filter paper to remove the buffer, dried and placed into a self-made immune filtration device. Before use, a drop of 0.01mol/L PBS-T was applied to activate the membrane surface at first. After fluid-absorbent, 5µL serum, 2-3 drops of PBS-T and 30µL of gold labeled SPA were added sequentially. When the permeation completed, 2-3 drops of PBS-T were added to observe the results, red dots mean positive.

**Blocking test** Ten positive controls were randomly chosen and equal amount of rHcAg with a fixed concentration was added. The samples were kept at 37°C water both for 1h and centrifuged at 800×g for 20s, 10µL of each sample was used for the DIGFA test.

**Detection by EIA** It was performed according to the operation instructions.

## RESULTS

**Comparison of DIGFA and EIA** A total of 131 samples were detected at the same time by DIGFA

and EIA (Table 1). Taking the results of EIA as standard, the sensitivity of DIGFA was 98% and specificity was 98%. The agreement between the two methods was 97%.

**Table 1 Comparison of DIGFA and EIA**

DIGFA	EIA		Total
	Positive	Negative	
Positive	49	3	52
Negative	1	78	79
Total	50	81	131

**Blocking test** To confirm the specificity of DIGFA, a blocking test was conducted in 10 positive control sera, and all turned to negative. To further testify the sensitivity of DIGFA, a dilution test was made in 10 samples of positive controls at random. The highest and the lowest titer were 1:256 and 1:32, respectively. Moreover, identical results were obtained when the 10 samples were tested for 3 times by DIGFA.

## DISCUSSION

It is quite difficult to directly detect the HCV antigen because the virus concentration in the blood of infected person is extremely low. Therefore, it is of great practical importance to establish a specific, sensitive, simple and convenient method for diagnosing HCV-infected persons, screening blood donors and preventing hepatitis C from spreading.

In 1989, Chiron Company developed the first-generation anti-HCV detection kit by applying the gene engineering to express the HCV-encoded 5-1-1 and C100-3 antigen<sup>[5,6]</sup>. Soon after the second generation anti-HCV EIA kit was developed to enhance its specificity and sensitivity<sup>[7,8]</sup>. At present, Ortho Company has produced the third generation EIA kit, the sensitivity and specificity of the anti-HCV were further improved. The difference of the three generation kits was in the varied coated antigens. This means that the difference is caused by the varied antigens<sup>[8]</sup>. At present, the second generation EIA kit is being widely used in detecting anti-HCV around the world. Although better specificity and sensitivity for detecting anti-HCV by EIA can be obtained, the

procedure is comparatively complicated, the process is long, and special instruments are required, it is rather difficult for an ordinary laboratory to carry out the detection. Since SPA can bind human IgG Fc fragment, we used the structural and non-structural domains of recombinant HCV antigens and established a new method for the rapid detection of HCV antibody based on the mechanism of dot immunogold filtration assay. It showed that the specificity and sensitivity of the method are basically equal to EIA. Furthermore, the new method is simple, convenient and rapid. The required amount of sera is less and no special instrument is needed. Using the same antigen coating as EIA, it is easy to get the reagents because anti-human IgG used in EIA is replaced by SPA. Moreover, the easier preparation of SPA do not damage the activity of IgG so that the labeling efficiency is higher. In dot immunogold filtration technique, the reaction is on membrane, the operation is much simple and convenient and the results can be visually read. As a result, the method can be applied for the serological diagnosis and epidemiological investigation of hepatitis C.

## REFERENCES

- 1 Dar VS, Ghosh S, Broor S. Rapid detection of rotavirus by using colloidal gold particles labeled with monoclonal antibody. *J Virol Methods*, 1994;47:51-58
- 2 Spielberg F, Kabeya CM, Ryder RW, Kifuani NK, Harris J, Bender TR, Heyward W, Quinn TC. Field testing and comparative evaluation of rapid, visually read screening assays for antibody to human immunodeficiency virus. *Lancet*, 1989;1:580-584
- 3 Xiao LY, Yan XJ, Chen YX, Su CZ, Xu DZ, Li SQ, Yan YP, Guo YH. Primary study of a dot immunogold filtration assay for rapid detection of HBV anti-HBs, anti-HBe and HBc antibody. *J Fourth Milit Med Univ*, 1995;16:250
- 4 Cai WQ, Wang BY. Practical Immunocytochemistry. First Edition. Chengdu: Sichuan Science and Technology Publishing House, 1988:168-180
- 5 Choo QL, Kuo G, Weiner AJ, Overby LR, Bradley DW, Houghton M. Isolation of a cDNA clone derived from a blood-borne non-A, non-B viral hepatitis genome. *Science*, 1989;244:359-361
- 6 Kuo G, Choo QL, Alter HJ, Gitnick GL, Redeker AG, Purcell RH, Miyamura T, Dienstag JL, Alter MJ, Stevens CE, Tegtmeier GE, Bonino F, Colombo M, Lee WS, Kuo C, Berger K, Shuster JR, Overby LR, Bradley DW, Houghton M. An assay for circulating antibodies to a major etiologic virus of human non A, non B hepatitis. *Science*, 1989;244:362-364
- 7 Kotwal GJ, Baroudy BM, Kuramoto IK, McDonald FF, Schiff GM, Holland PV, Zeldis JB. Detection of acute hepatitis C virus infection by ELISA using a synthetic peptide comprising a structural epitope. *Proc Natl Acad Sci USA*, 1992;89:4486-4489
- 8 Li HM, Wang XT. HCV antibody diagnosis reagent and present situation and prospect of the study of HCV vaccine. *China Microbiol Immunol J*, 1995;15:128-130

# Construction of eukaryotic expression vector of HBV x gene

GUO Shuang-Ping<sup>1</sup>, MA Zhou-Sheng<sup>2</sup> and WANG Wen-Liang<sup>1</sup>

**Subject headings** HBV x gene; carcinoma, hepatocellular; expression vector; liver neoplasms; gene expression

## INTRODUCTION

Chronic infection with hepatitis B virus is closely related to liver diseases, including hepatocellular carcinoma. Hepatitis B virus x gene and its product HBx Ag possibly play an important role in carcinogenesis of hepatocellular carcinoma. HBV x gene can integrate into cellular DNA during chronic infection<sup>[1]</sup>. HBx Ag overexpression may alter signal transduction pathways of hepatocyte<sup>[2]</sup>. HBx Ag can bind to and inactivate negative growth-regulatory molecules such as tumor suppressor p53<sup>[3]</sup>, suggesting its role in hepatocarcinogenesis.

We have constructed the HBV x gene eukaryotic expression vector in order to study its contribution to chronic hepatitis and hepatocellular carcinoma.

## MATERIALS AND METHODS

### Plasmids

Plasmids p<sup>TTHK</sup> containing HBV DNA and p<sup>T7Blue</sup> were provided by Dr. ZHANG Huai-Zhong. PCR primers were synthesized by Shanghai Shengon Biology Corporation. Plasmid p<sup>CDNA3.1</sup> was obtained from our department.

### Enzymes and bacterial cells

All restriction enzymes and T4 DNA ligase were purchased from Hua Mei Corporation. *E. coli* JM109 and DH5 $\alpha$  were obtained from our department.

### Construction of p<sup>T7Blue</sup>-HBX

Polymerase chain reaction (PCR) was used to obtain HBV x gene from the plasmid p<sup>TTHK</sup>. The sequence

of primers was as follows. The restriction enzyme sites of *EcoR* I and *Kpn* I were added at 5' end of upper and lower primer s respectively.

5' ATCGGTACCATGGCTGCTAGGCTG 3'

5' GGAGAATTCATGATTAGGCAGAGGTG 3'

The condition of PCR is 94°C 5min, 59°C 1min, 74°C 1min, 30 cycles and 74°C 10min. The PCR results are shown in Figure 1. The PCR product was recovered from the low melting agarose gel and was digested by endonuclease *EcoR* I and *Kpn* I simultaneously and was ligated to plasmid p<sup>T7Blue</sup> with T4 DNA ligase. After recombinant plasmid p<sup>T7Blue-HBX</sup> was introduced into DH5 $\alpha$ , seven ampicillin resistant clones were selected and the plasmid DNA was extracted. The correct plasmids identified by the restriction analysis were sequenced.

### Construction of eukaryotic expression vector p<sup>CDNA3.1-HBX</sup>

Plasmid p<sup>CDNA3.1</sup> and p<sup>T7Blue-HBX</sup> were digested by endonuclease *EcoR* I and *Kpn* I. 480bp fragment of HBX and 5.4kb fragment of p<sup>CDNA3.1</sup> were recovered from the low melting point agarose gel respectively. They were ligated by T4 DNA and named p<sup>CDNA3.1-HBX</sup>. The recombinant DNA was introduced into DH5 $\alpha$ . Eight clones were selected and correct plasmids were identified by combinative digestion of *EcoR* I and *Kpn* I. One colony exhibited 480bp and 5.4kb was in right junction named p<sup>CDNA3.1-HBX</sup>.

## RESULTS

### Construction of p<sup>T7Blue</sup>-HBX

In order to construct the eukaryotic expression vector of HBV x gene, we first constructed the vector p<sup>T7Blue-HBX</sup>. The PCR result and the gene structure of recombinant plasmid are shown in Figures 1 and 2. The result of the sequence is shown in Figure 3.

### Construction of eukaryotic expression vector p<sup>CDNA3.1-HBX</sup>

On the basis of correct sequence result of p<sup>T7Blue-HBX</sup>, we inserted HBV x gene at the sites of *EcoR* I and *Kpn* I of p<sup>CDNA3.1</sup> to construct the eukaryotic expression vector p<sup>CDNA3.1-HBX</sup>. The recombinant plasmid gene structure is shown in Figure 4.

<sup>1</sup>Department of Pathology, Faculty of Medical Sciences, Fourth Military Medical University, Xi'an 710032, China

<sup>2</sup>Tangdu Hospital, Department of Oncology, Fourth Military Medical University, Xi'an 710038, Shaanxi Province, China

Dr. GUO Shuang-Ping, female, born on December 17, 1967 in Gansu Province, graduated from Department of Medicine in Lanzhou Medical College, engaged in molecular pathology of neoplasm.

**Correspondence to:** Dr. GUO Shuang-Ping, Department of Pathology, Faculty of Medical Sciences, Fourth Military Medical University, Xi'an 710032, China

Tel. +86-29-3221616 Ext. 75272

Received 1998-11-09

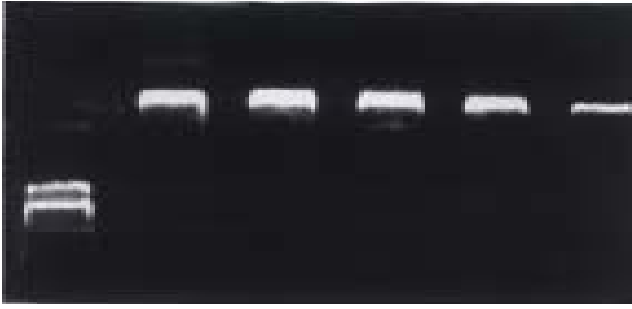


**Figure 1** The PCR product of HBV x gene. Lane 1:  $\lambda$ DNA/*Hind* III marker; Lane 2-6: the PCR product of HBV x gene.



**Figure 2** The structure of recombinant plasmid  $p^{T7Blue-HBX}$ . Lane 1:  $\lambda$ DNA/*Hind* III marker; Lane 2 - 3:  $p^{T7Blue-HBX}$  combinative digested by *Eco*R1 and *Kpn*1; Lane 4:  $p^{T7Blue}$  combinative digested by *Eco*R1 and *Kpn* I; Lane 5:  $p^{T7Blue-HBX}$ .

**DISCUSSION**

Hepatitis B virus (HBV) is a formidable threat to public health. HBV associated HCC is one of the 10 commonly encountered cancers in the world. The relative risk of HBV carriers developing HCC approaches 200:1, which is one of the highest relative risks known for a human cancer<sup>[4]</sup>. HBV x gene and x antigen may play an important role in the development of chronic infections and chronic liver disease. HBV can integrate into cell DNA and the HBV x region is the most frequently integrated sequence<sup>[1]</sup>. These integrated fragments make HBV encode x antigen that is capable of trans-activation both *in vitro* and *in vivo*<sup>[5]</sup>. HBx Ag can stimulate the cell growth directly<sup>[6]</sup>, and inactivate the negative growth regulators, such as tumor suppressor p53<sup>[2]</sup>. Furthermore, HBx Ag can increase the resistance of HBx Ag-positive cells to apoptosis mediated by cytotoxic cytokine through altering signal transduction pathway of

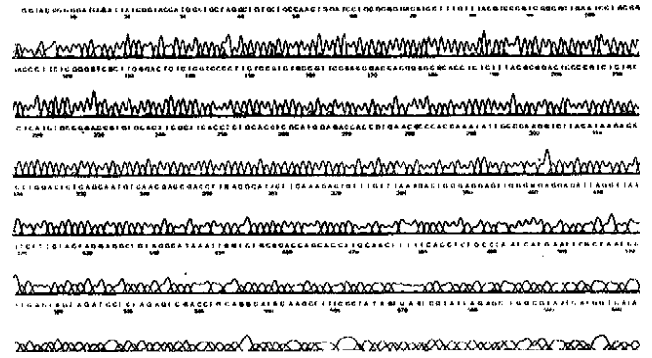


**Figure 3** The sequence result of  $p^{T7Blue-HBX}$ .



**Figure 4** The structure of  $p^{CDNA3.1-HBX}$ . Lane 1-2:  $p^{CDNA3.1-HBX}$  combinative digested by *Eco*R1 and *Kpn* I; Lane 3:  $\lambda$ DNA/*Eco*R1 marker.

hepatocyte<sup>[2]</sup>.

In conclusion, the topic of HBV is an old but important one, and is worthy of further studies. We have constructed the eukaryotic expression vector of HBV x gene for this study.

**REFERENCES**

- 1 Feitelson MA, Duan LX. Hepatitis B virus x antigen in the pathogenesis of chronic infections and development of hepatocellular carcinoma. *Am J of Pathology*, 1997;15:1143-1144
- 2 Wang XW, Forrester K, Yeh H, Feitelson MA, Gu JR, Harris CC. Hepatitis B virus x protein inhibits p53 sequence specific DNA binding, transcription activity, and association with transcription factor ERCC3. *Proc Natl Acad Sci USA*, 1994;91:2230-2232
- 3 Beasley RP. Hepatitis B virus. The major etiology of hepatocellular carcinoma. *Cancer*, 1988;61:1942-1948
- 4 Balsano C, Billet O, Bennoun M, Cavard C, Zider A, Grimber G, Natoli P. Hepatitis B virus x-gene product acts as a transactivator *in vivo*. *J Hepatol*, 1994;21:103-109
- 5 Benn J, Schneider RJ. Hepatitis B virus HBx protein deregulates cell cycle check point controls. *Proc Natl Acad Sci USA*, 1995;92:1215-1219
- 6 Truant R, Antunovic J, Greenblatt J, Prives C, Cromlish JA. Direct interaction of hepatitis B virus HBx protein with p53 response element-directed transactivation. *J Virol*, 1995;69:1851-1859

# Stereotactic conformal radiotherapy of hepatic metastases: clinical analysis of 8 cases

ZHAO Wei-Sheng, ZHI Da-Shi, LIU Bo-Ping, JIANG Wei, CONG Zhen and DONG Cheng

**Subject headings** liver neoplasms/radiotherapy; liver neoplasms/secondary; stereotactic conformal radiotherapy

## INTRODUCTION

It is always a routine to resect lesions of the body by surgery. Scientists have tried to obtain the same results without surgery, but failed. In recent years, with the development of multi-subject and high technology, lesions can be localized precisely with stereotactic technique. And with the help of computer and medical imaging technique, stereotactic conformal radiotherapy (SCR) has become a "no pain, no blood" surgery. At the same time, SCR is recognized globally, its therapeutic range has transferred from intracranial lesions to the lesions of extracranial sites of the body, and is expected to become an important method in conventional surgery. Therefore, it is called "surgery of the 21 century"<sup>[1]</sup>. From May 1997 to April 1998, we treated 8 cases of hepatic metastases with SCR and the results are reported below.

## MATERIALS AND METHODS

### Materials

Eight patients (4 men and 4 women, 1-5 metastases/person) who received stereotactic high-dose radiation therapy for hepatic metastases (21 lesions) using an accelerator were included. Treatments were given from May 1997 to April 1998. The age ranged from 67 to 46 years (mean 55.4). Three cases had one lesion, 5 had more than one lesions (one case had 5 metastases). The maximal clinical target volume (CTV) was 232cm<sup>3</sup>, and the minimal CTV 0.6cm<sup>3</sup>. The majority of the patients had previously received treatment for various types of primary tumors. At the time of treatment most patients had one known lesion increased in size as assessed by repeated CT scanning. Biopsies for histopathological examinations were obtained from some patients

during open surgery. The majority of the irradiated lesions were considered so typical for metastases.

### Methods

**Stereotactic conformal radiotherapy** The stereotactic body-frame was used in treatment. For targets affected by the diaphragmatic motions due to breathing, a device was developed to minimize the motions to 1cm or less<sup>[2]</sup>. The reproducible position of the patient in the frame was obtained by the vacuum pillow and two markers, chest and tibia marker respectively. These markers are set to predefined stereotactic coordinates, at which the markers should correspond to the tattoo-points on the skin over sternum and tibia to ensure a high reproducibility in the cranial-caudal direction.

**Therapeutic technique** Primarily, a positioning and drawing plan was worked out. A stereotactic system (including stereotactic setting and localization) was used for stereotactic radiotherapy (SRT) to improve the accuracy of localization and setting-up. A consecutive CT scan of 2mm slice thickness was outlined manually on the computer screen in every horizontal CT-slice for patients with hepatic metastases. Target point and width of the collimator was calculated with specially designed computer programs. Beam's eye view technique with digitally reconstructed radiographs from the transverse CT scans was adopted to design the 3-D treatment plan. The 3-D treatment planning is a conformal technique, using 6 - 8 non-coplanar stationary beams. On multi-leaf collimator, the shape of beam eye view was similar with the target in all directions. Patients were all treated with a linear accelerator (VARIAN Clinic 600C). The photon energies used were 6Mev.

**Dose distribution** The dose planning was made on a 3-D system (Virtuos 2.8.0). Apart from dose distributions, the clinical target volume (CTV), planning target volume (PTV), and organs at risk volumes were also calculated. Several factors were taken into consideration when the dose/fraction was determined. These included size of the CTV, dose distribution with dose-volume histograms and radiation sensitivity of the surrounding normal tissues. In this series, the CTV of tumors ranged from 0.6cm<sup>3</sup> to 232cm<sup>3</sup> (mean 36.4cm<sup>3</sup>), the prescribed dose (PD) was 4 - 6.5Gy (mean

Huan Hu Hospital, Tianjin 300060, China

Dr. ZHAO Wei-Sheng, male, born on 1946-04-19 in Tianjin City, graduated from Tianjin Medical University in 1970, now professor of surgery, majoring diagnosis and treatment of hepatic, gallbladder, thyroid and pancreatic diseases, having 38 papers published.

**Correspondence to:** Dr. ZHAO Wei-Sheng, Tianjin Huan Hu Hospital, 122 Qixiang Tailu, Hexi District, Tianjin 300060, China  
Tel. +86-22-23354950, Fax. +86-22-23359858

Received 1999-02-05

5.13Gy). Treatments were given in 2-8 fractions. The total dose was 10-45Gy/2-8 fractions.

**RESULTS**

None of the patients died during SRT. Their condition was evaluated by Karnofsky Performance Standard (KPS), 20-90 before treatment (mean 58.75) and 30-100 after treatment. Very few, if any, complications could be ascribed to the SRT. Three (37.5%) patients developed slight fever (< 37.8°C). WBC count and hepatic function had no distinct changes. During a follow-up period of 2-9 months, complete response (CR) was found in two cases (Figures 1,2), partial response (PR) in three cases, no change (NC) in two cases and progressed (PD) in one case. After SCR, 87.5% of tumors were controlled (62.5% of the tumors decreased in size or disappeared). Three patients died during the follow-up period, one died of bone metastases 303 months, one died of MSOF 1.5 months and one died of hepatic failure 2.3 months after treatment (Table 1).

**DISCUSSION**

Most of all patients who receive SCR are advanced patients with tumor who underwent no surgery and conventional radiotherapy. Their prognosis is not well<sup>[3]</sup>. So SCR is a new method for late case of tumor.

**Formation of SCR**

In 1951, the term stereotactic radiosurgery was introduced by Leksell<sup>[4]</sup> who was a neurosurgeon in Karolinska Academy. In 1968, the first  $\gamma$ -knife of the world was developed successfully. It was an epochmaking event to neurosurgery and radiotherapy technique. Since the beginning of 1980, with the improvement of stereotactic system and collimator, stereotactic radiosurgery (X-knife)<sup>[5]</sup> has been performed to intracranial lesions with linear accelerator based radiosurgery, and soon the treatment extended from intracranial to

extracranial tumors. For large and/or irregular lesions, linear accelerator, with circle and multi-leaf collimator was employed. The treatment can be achieved by a combination of several non-coplanar rotational irradiations, each directed at the same point, thus representing a convergent-beam irradiation technique. The 3-D treatment system demonstrates clinical superiority and flexibility to treatment planning.

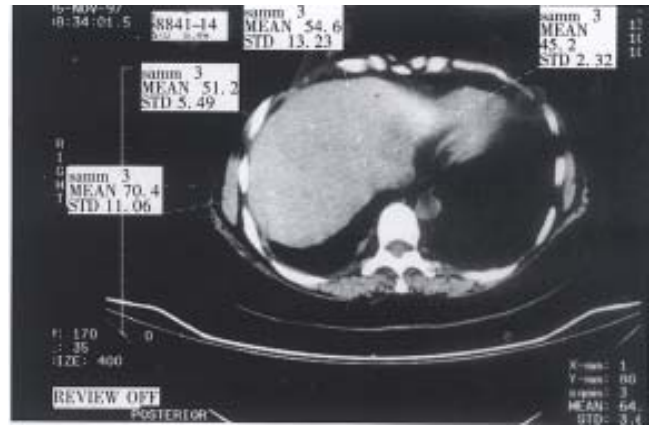


**Figure 1** Preoperative CT image of patient with hepatic metastases of breast tumor.



**Figure 2** Three months postoperative CT image of the same patient.

**Table 1 Clinical data of hepatic metastases with stereotactic conformal radiotherapy**

	Patient No.							
	1	2	3	4	5	6	7	8
Sex (M/F)	M	M	F	F	F	M	F	M
Age (years)	59	46	49	54	67	61	9	58
Primary tumor	Colon	Lung	Breast	Breast	Preventriculus	Stomach	Breast	Cholecyst
Number of irradiated tumor	1	3	1	4	2	5	4	1
Volume of clinical target (cm <sup>3</sup> )	34.5	1.9,1.5	14.8	5.1,0.6	18.4	232,134.1	30.7,11.6	120.3
Prescribed dose (Gy)	5.00	4.50	5.00	5.00	5.00	4.00	6.00	6.50
Number of fractions	3	8	8	5	2	7	7	7
KPS before treatment	80	40	90	90	20	40	40	70
KPS after treatment	80	50	100	100	30	50	70	90
Size of tumor after irradiation	NC	PD	CR	CR	NC	PR	PR	PR
Time period of follow-up	8	4	6	6	2	3	3	2
Time period after irradiation (months)	Unknown	3.3	6	6	1.5	2.3	3	2

### **Facilities and theory of SCR**

Stereotactic radiotherapy is a system of 3-D treatment planning and radiotherapy include hardware and software. X-knife software reconstructs radiograph from image data of CT, MRI and DSA. The 3-D treatment planning was designed by software could be made standard or complex design based on these data from either single or multi-convergent. X-knife software can calculate radiation dose quickly and precisely. Dose-calculate formula is shown by dose-volume histograms (DVHs) on the screening display. Radiation dosage can be calculated by computer. Its important character is to deliver a highly focused radiation distribution to the target volume and to reduce the dose to surrounding normal tissues as much as possible<sup>[6]</sup>.

### **Development of SCR**

Since SCR technique came into being, it has been used to treat intracranial lesions, primarily the AVM and intracranial tumors. In recent years, with the development of stereotactic technique for treatment of intracranial tumors, X-knife technique began to be applied to treat tumors of mediastinum, liver and retroperitoneal metastases in Karolinska Hospital in Sweden in 1993. Lax *et al*<sup>[7]</sup> created a method to treat abdominal malignant tumors with high-dose stereotactic radiotherapy.

### **Evaluation of SCR**

In stereotactic radiotherapy, stereotactic technique (localization and setting-up) is used to improve localization accuracy and setting-up accuracy. The difference between SRT and SRS is, the conception of the former is fractional radiotherapy, the latter is single fraction. When the size of the tumor is large, either from radiobiology and radiophysiology or from clinic, SRT must be adopted instead of SRS<sup>[8]</sup>. Patients treated with SRT all obtained good therapeutic effects. The development of SCR technique will enrich the conventional surgery means. In tumor treatment, SCR will exert an indispensable effect. With the accumulation of clinical experience, SRT will play an important role in treatment of malignancies.

### **REFERENCES**

- 1 Zhang J. Research and clinical practice of X knife. *Shijie Yiliao Qijie*, 1995;25-26
- 2 Blimgren H, Lax I, Naslundb I. Stereotactic high dose fraction radiation therapy of extracranial tumors using an accelerator (clinical experience of the thirty-one patients). *Acta Oncol*, 1995;34:861
- 3 Wu JP, Qiu FZ. Huang Jiasi Surgery. Vol 1, 5th ed. Beijing: Medical Publishing House, 1992:325-326
- 4 Leksell DG. Stereotactic radiosurgery: present status and future trends. *Neurol Res*, 1987;9:60-62
- 5 Zhang KL, Xu T. Treatment of extracranial tumor with stereotactic radiosurgery and the biologic significance of fractional irradiation. *Oncology, Foreign Medicine*, 1996;23:325-326
- 6 Chen BH. Stereotactic radioneurosurgery. Vol 1. Beijing: Beijing Publishing House, 1994:7
- 7 Lax I, Blomgren H, Naslund I, Svanstrom R. Stereotactic radiotherapy of malignancies in the abdomen: methodological aspects. *Acta Oncol*, 1994;33:677-683
- 8 Hu YM, Gu XZ. Conformal radiotherapy: the development of irradiational technique. *Chin J Radiol Tumors*, 1997;6:8-11

Edited by MA Jing-Yun

# Expression and alterations of different molecular form $\gamma$ -glutamyl transferase and total RNA concentration during the carcinogenesis of rat hepatoma \*

TANG Qi-Yun, YAO Deng-Fu, LU Jian-Xin, WU Xin-Hua and MENG Xian-Yong

**Subject headings** liver neoplasms/enzymology;  $\gamma$ -glutamyl transferase/ analysis; disease models, animal; RNA; 2-fluoenylacetamide/analysis

## INTRODUCTION

Carcinogenesis is closely related with DNA synthesis and hypermetabolism of nucleic acid.  $\gamma$ -glutamyl transferase (GGT, EC 2.3.2.2) is a plasma-membrane-combined heterodimeric glycoprotein which initiates the degradation of extracellular glutathione and its conjugates. The cleavage of glutathione by GGT into cysteinylglycine and a  $\gamma$ -glutamyl residue provides a mechanism for the recovery of cysteine by the cell and thus for renewed glutathione synthesis. *In vivo*, GGT is either highly correlated with biotransformation, nucleic acid metabolism and tumorigenesis, or the sensitive enzymatic marker reflecting hepatocyte parenchymatous lesions<sup>[1,2]</sup>. However, the expression and alterations of GGT are not yet clear during the course of hepatocyte damage and canceration. As a consequence, in the present study, the pathological changes, GGT activities and total RNA concentration of rat livers were investigated on experimental rat hepatomas induced with a chemical carcinogenic agent, 2-Fluoenylacetamide (2-FAA), to explore the clinical significance of GGT in showing the extent of hepatocyte damage and in diagnosing hepatoma.

## MATERIALS AND METHODS

### *Animal model*

Forty-eight male Sprague-Dawley (SD) rats

weighing 140 g - 180 g were obtained from the Experimental Animal Centre, Nantong Medical College. The rats were divided into 8 groups at random, 6 in each group. All the rats were housed in controlled surroundings. One of these groups was randomly chosen as a control group. The control group was fed with ordinary natural granular forage, and experimental groups with forage containing 0.05% 2-FAA. One group was killed every two weeks respectively after feeding. Peripheral blood was collected for biochemical assay and a part of the liver tissues was used for liver homogenate preparation and histopathological examination (HE staining).

### *Preparation of hepatic tissue homogenate*

Fresh rat hepatic tissues were washed with 0.9% NaCl solution, and dried with filter paper and cut into pieces. Two portions (part A and part B, 1g each) of the tissues were weighed: to part A was added 5mL homogenate solution (pH 8.6, 0.1mol/L Tris-HCl buffer solution) to extract soluble GGT, to part B was added 5ml homogenate solution containing 0.5% Triton X 100 to extract total GGT. It was porphyrized on ice, then homogenized at 12 000r/min in YQ-3 type homogenizer for 5 times (stopped 5min every 30 second), and followed by centrifugalization at 15 000r/min for 45min at 4°C. In the end, the supernatants of liver homogenates were taken and stored at -20°C for analysis.

### *Total RNA extraction and detection of its concentration*

Fifty mg of hepatic tissue was weighed exactly in analytical balance, and was put in a homogenizer free from RNAase to which 1.0mL of RNazole reagent was added for homogenizing 2 minutes. Total RNA was extracted according to the assay described by Chirgwin, *et al.* RNA absorbance was detected by a ultraviolet spectrophotometer of Shimadzu UV-2201 type and converted to total RNA concentration ( $\mu$ g/mg wet tissue). The GGT activities (U/L) in supernatant of rat hepatic tissue homogenate were detected by a  $\gamma$ -glutamyl p-nitroanilinum directed assay, GGT protein

Department of Gastroenterology and Research Center of Clinical Molecular Biology, Affiliated Hospital, Nantong Medical College, Nantong 226001, Jiangsu Province, China

Dr. TANG Qi-Yun, female, born on 1966-07-16 in Yancheng, Jiangsu Province, Han nationality, graduated from Nantong Medical College as a postgraduate in 1998, now working in Department of Gastroenterology, the First People's Hospital of Yancheng, engaged in the research of early diagnosis of hepatoma, having more than 10 papers published.

\*Project supported by State Education Commission, No.NEM95.

**Correspondence to:** Dr. TANG Qi-Yun, Department of Gastroenterology, the First People's Hospital of Yancheng, Yancheng 224000, Jiangsu Province, China.

Tel. +86-515-8410698

Received 1998-12-22

concentrations were detected by a Follin-phenol reagent assay. GGT specific activities (U/g) were converted according to the ratio of the GGT activity (U/L) to the GGT protein concentration (g/L).

### Statistical analysis

Data were input to the computer, and processed with analysis of variance and analysis of correlation and expressed as  $\bar{x} \pm s$ . Comparison was made between every two groups.  $P < 0.05$  was considered to be statistically significant.

## RESULTS

### Histopathological changes during the induction of rat hepatomas

At the end of the second week, the livers turned to grey-yellow and scabrous, all the hepatocytes manifested granular degeneration. At the end of the fourth week, half of hepatic tissues became precancerous lesions, the histological manifestation was normal liver lobules existing in most part of areas, but hyperplastic small round cells or oval cells or hyperplastic nodules existing in local areas. At the end of the tenth week, most parts of hepatic tissues were already cancerized. At the end of the 12th week, all the hepatic tissues were cancerized, the normal structure of hepatic lobule was completely destroyed and the liver tissues showed diffuse patchy necrosis, a lot of small round cells and overall patchy nodules of cancer nests were the main histological alterations. Histological type of hepatoma was well differentiated hepatocellular cancer. The pathological changes in different stages of rat livers after administration of 2-FAA are shown in Table 1.

**Table 1** The pathological changes of rat livers during different stages of liver cancer induced with 2-FAA

Groups	n	Pathological feature (HE staining)		
		Degeneration	Precancerosis	Cancerization
Control	6	0	0	0
2 <sup>nd</sup> week	6	6	0	0
4 <sup>th</sup> week	6	3	3	0
6 <sup>th</sup> week	6	0	5	1
8 <sup>th</sup> week	6	0	4	2
10 <sup>th</sup> week	6	0	1	5
12 <sup>th</sup> week	5 <sup>a</sup>	0	0	5

<sup>a</sup>One rat died during the experiment.

### Changes of total RNA concentration and GGT specific activities

The total RNA level and GGT activity were observed at the different stages during the induction of rat hepatomas (Table 2). Both total RNA concentration and GGT specific activities increased gradually during the administration of 2-FAA. GGT specific activities were positively correlated with

total RNA concentration ( $r = 0.90$ ,  $P < 0.01$ ). Total RNA concentration of hepatic tissues was also positively correlated with serum GGT specific activities ( $r = 0.79$ ,  $P < 0.01$ ).

**Table 2** Changes of total RNA concentrations and GGT specific activities at different stages of rat hepatomas

Groups	n	Total RNA (μg/mg tissue)	GGT specific activity	
			Liver GGT(U/g)	Serum GGT(U/L)
Control	6	3.67±0.78	1.06±0.24	6.0±4.8
2 <sup>nd</sup> week	6	6.69±6.08	4.77±4.41 <sup>a</sup>	20.2±17.8 <sup>a</sup>
4 <sup>th</sup> week	6	4.81±4.27	9.30±1.81 <sup>b</sup>	31.2±28.1 <sup>b</sup>
6 <sup>th</sup> week	6	5.38±4.84	5.95±1.23 <sup>b</sup>	37.8±32.1 <sup>b</sup>
8 <sup>th</sup> week	6	9.23±6.48 <sup>a</sup>	10.73±4.93 <sup>b</sup>	53.5±43.6 <sup>b</sup>
10 <sup>th</sup> week	6	8.37±6.51 <sup>a</sup>	16.03±5.22 <sup>b</sup>	40.6±23.6 <sup>b</sup>
12 <sup>th</sup> week	5	8.16±8.87 <sup>a</sup>	15.71±3.31 <sup>b</sup>	38.6±8.8 <sup>b</sup>

<sup>a</sup> $P < 0.05$ , <sup>b</sup> $P < 0.01$ , compared with the control group.

### Changes in activities of different molecular forms of GGT

Hepatic soluble and membrane-combined GGT activities increased markedly during the induction of liver cancer, especially in the late phases. There was also significant difference between each experimental group and the control group ( $P < 0.05$  or  $P < 0.01$ ). The activities of two different molecular forms of GGT increased in parallel, the ratio of soluble GGT to total GGT was about 0.7 in all the rats, no significant difference was found between the control group and the experimental groups. The activities of different GGT molecular forms are shown in Table 3.

**Table 3** The changes in specific activities of different GGT forms at different stages of rat hepatomas

Groups	n	Hepatic homogenate GGT (U/g)		
		S(Soluble-type)	T-S(Membrane-type)	S/T-GGT
Control	6	0.74±0.14	0.32±0.14	0.71±0.08
2 <sup>nd</sup> week	6	3.35±2.83 <sup>a</sup>	1.42±0.23	0.72±0.14
4 <sup>th</sup> week	6	7.07±0.92 <sup>b</sup>	2.29±1.28 <sup>b</sup>	0.76±0.10
6 <sup>th</sup> week	6	3.50±0.70 <sup>b</sup>	2.45±1.25 <sup>b</sup>	0.60±0.15
8 <sup>th</sup> week	6	8.68±5.24 <sup>b</sup>	2.39±1.52 <sup>b</sup>	0.74±0.18
10 <sup>th</sup> week	6	12.21±5.49 <sup>b</sup>	3.82±1.32 <sup>b</sup>	0.73±0.13
12 <sup>th</sup> week	5	9.56±2.27 <sup>b</sup>	6.15±4.36 <sup>b</sup>	0.64±0.24

<sup>a</sup> $P < 0.05$ , <sup>b</sup> $P < 0.01$ , compared with the control group.

## DISCUSSION

The activities of GGT are rather low in normal liver tissues, expressed mainly on the border of epithelial cell membrane of biliary duct and intrahepatic cholangioles with strong secretory and absorptive functions. To explore the laws of the production and alterations of hepatoma-specific GGT in the canceration of normal hepatocytes, the diazo chemical carcinogens such as 2-FAA, DEAA, MDA, O-AT, 3'-MC-4DAB are usually

administered to establish hepatoma model in male SD rats or Wistar rats. With the feature of carcino-embryonic protein, hepatoma-related GGT is produced and secreted when the genes controlling GGT synthesis were expressed abnormally. Hence GGT is usually considered as the early enzyme marker of hepatocarcinogenesis.

Hepatocarcinogenesis is closely related with DNA synthesis and nucleic acid metabolism. Hepatic GGT plays an important role in biotransformation and nucleic acid metabolism. In addition, its abnormal expression is a sensitive enzyme marker for hepatocellular paranchymal lesions. Chemical induction of cancer is a multistage course, its fundamental causes are the activation of protooncogenes or the inactivation of tumor-suppressor genes initiated by carcinogens. Thus, the abnormal regulation of genes coordinated to lead cancerization<sup>[3]</sup>. Most chemical carcinogens were turned into strong electrophilic agents by enzymes *in vivo* with high affinity with and response to membrane-combined GGT. In the course of canceration, liver tissues can synthesize and secrete various kinds of hepatocarcinoma-related proteins, polynucleotides, isoenzymes such as AFP, GGT-II<sup>[4,5]</sup>. When the abnormal expression of GGT synthesized genes is controlled, hepatocarcinoma-related GGT is secreted with the characteristics of embryonic liver, which are regarded as the early enzyme marker of hepatocarcinogenesis<sup>[6]</sup>.

In the present study it was observed that in the early phases of hepatoma induced with the chemical carcinogen 2-FAA, the oval cells with the features of undifferentiated type were found to have the function to resist the cytotoxicity of the carcinogen, and could express tumor-related enzymes or proteins. In the precancerous and cancerous phases of hepatic tissues, significant changes occurred in total RNA concentration and GGT specific activities. As a result of the damage of hepatocytes, GGTs were released into blood to bring about the rise of their activities in the serum, suggesting that a lot of GGT were expressed and secreted into blood by hepatocytes in the early phases of cancerization. Moreover, the features of GGT electrochroma-

tography were different from those of normal ones. The results showed that GGT plays an important role in resisting mutagenesis and carcinogenesis. Hepatic functions in detoxification and biotransformation could be strengthened by enzymatic action which relieves toxic effect of chemical mutagens, carcinogens and other substances, and protects normal hepatocytes from the effect of cancer initiating and promoting factors<sup>[7]</sup>.

During the course of canceration, different GGT molecular forms were also overexpressed. As shown in Table 3, the hepatic specific activities of both soluble and membrane-combined GGTs in the experimental groups were higher than those in the control group ( $P < 0.05$  or  $P < 0.01$ ). The ratio of soluble GGT to membrane-combined GGT was 0.7 in all groups. The specific activities of two GGT molecular forms increased three to five times in the early stage, ten to twenty times in the late stage, indicating that the two kinds of hepatic GGT had the parallel tendency to increase not only in the early stage but also in the late stage. Furthermore, hepatic GGT was released into the blood with high level in sera. It is concluded that hepatoma-specific GGT can be used as a tumor marker for the early diagnosis of hepatic cancer<sup>[8]</sup>.

## REFERENCES

- 1 Xu KC, Meng XY, Wu JW, Wei Q, Shen B, Shi YC. Diagnostic value of serum  $\gamma$ -glutamyl transferase isoenzyme for hepatocellular carcinoma. *Am J Gastroent*, 1992;87:991
- 2 Wu JW, Meng XY, Xu KC, Wei Q, Shi YZ, Yi L. Simultaneous determination of multiple markers of primary liver cancer: Diagnostic significance. *J Gastroent Hepatol*, 1988;3:29
- 3 Wang B, Ke Y. Chemical carcinogens and protooncogenes and tumor suppressor genes. *Tumor*, 1995;15:107
- 4 Fishman WH. Clinical and biological significance of an isoenzyme tumor marker pALP. *Clin Biochem*, 1987;20:387
- 5 Smith A. Multiple marker screening in primary liver cancer (PLC). *J Hepatol*, 1986;3(suppl):19
- 6 Yao DF, Meng XY. The advanced on serum hepatoma specific GGT for diagnosis of hepatocellular carcinoma. *Foreign Med Sci*, 1997;24:59
- 7 Zhang H, Yao DF, Wei Q, Huang JF, Meng XY. The relations between serum HBV-DNA, HBV markers and hepatic enzyme in patients with chronic hepatitis B. *Jiangsu J Med*, 1997;23:389
- 8 Huang JF, Yao DF, Meng XY, Wei Q, Zhang H. The value of the rocket electrophoresis of hepatoma specific GGT in the diagnosis of primary hepatic cancer. *Chin J Dig*, 1995;15:269

Edited by WANG Xian-Lin

# Detection of HBV DNA and its existence status in liver tissues and peripheral blood lymphocytes from chronic hepatitis B patients \*

TANG Ren-Xian, GAO Feng-Guang, ZENG Ling-Yu, WANG Ying-Wei and WANG Yu-Long

**Subject headings** hepatitis B; hepatitis B virus; DNA, viral; lymphocytes

## INTRODUCTION

Cumulative clinical and experimental evidence indicates that host immune responses to hepatitis B virus (HBV) are responsible for liver damage in chronic hepatitis B, which leads to cirrhosis and hepatocarcinogenesis. The results of *in vitro* experiments by use of B cell lines expressing HBV antigens as effector cells have demonstrated the presence of cytotoxic T cells recognizing viral antigen epitopes in conjunction with MHC class I molecules<sup>[1]</sup>. Extrahepatic tropism of HBV has been increasingly recognized in recent years. Detection of HBV DNA in peripheral blood leukocytes (PBL) was reported recently<sup>[2]</sup>, but no further study was made on HBV DNA existence status in these cells. In this study, the positive PBL DNA specimens were selected by dot blot hybridization, and HBV DNA existence status was analyzed by Southern blot hybridization in order to provide experimental bases for the treatment of hepatitis B and some fundamental data for the research of hepatocarcinogenesis.

## MATERIALS AND METHODS

### Materials

**Subjects** Liver tissues of 37 cases were obtained from Shandong Provincial Hospital. Their diagnosis was confirmed by histopathological examination ( $n = 37$ , 26 males and 11 females, mean age 33.4 years). At the same time, PBL were separated and stored at  $-20^{\circ}\text{C}$  immediately for use.

**Reagents** Recombinant plasmid pBR<sup>322</sup>-2HBV was provided by Professor CB, and DIG High Prime Labeling and Detection Starter Kit was the product of Boehringer Mannheim Company, Germany. Restriction Endonucleases *EcoR* I, Leukocyte lysis buffer and Proteinase K were purchased from Huamei Company.

### Methods

**HBV DNA labeling** Isolation of recombinant plasmid pBR<sup>322</sup>-2HBV and preparation of HBV DNA probe were carried out as described by Sambrook<sup>[3]</sup>, HBV labeling procedures were described before<sup>[4]</sup>. Template DNA (1.0 $\mu\text{g}$ ) and sterile redist water were added into a reaction vial. The DNA was denatured and DIG high prime was added and incubated for 20 hours at  $37^{\circ}\text{C}$ . Reaction was stopped by adding EDTA. Quantification of labeling efficiency was performed according to the instructions of the manufacturer.

**DNA extraction** Genomic DNA from the liver tissues was isolated according to the standard methods<sup>[3]</sup>. Genomic DNA from PBL was extracted according to WANG *et al*<sup>[5]</sup>. The PBL aliquots were mixed with leukocyte lysis buffer, and proteinase K was added to a final concentration of 100  $\mu\text{g}/\text{L}$ . After being incubated at  $37^{\circ}\text{C}$  for 12h - 16h, the digested preparation was extracted twice with buffer-equilibrated phenol and once with a phenol-chloroform mixture. DNA was precipitated by adding sodium acetate and followed by ice-cold absolute ethanol and stored overnight at  $-20^{\circ}\text{C}$ . After being centrifuged and washed with ice-cold ethanol, the DNA was dried under vacuum at room temperature. It was redissolved in TE buffer and stored at  $-20^{\circ}\text{C}$ .

**HBV DNA dot blot hybridization** Genomic DNA 5 $\mu\text{L}$ ,  $\lambda\text{DNA}$  10ng, HBV DNA 10pg, and 1.0pg were heated in a boiling water bath for 5min - 10min, and cooled quickly in an ice/ethanol bath for 5min. They were mixed with  $20 \times \text{SSC}$  and tipped to nitrocellulose filters. The filters were prehybridized for 8h - 12h, hybridized for 24h - 36h at  $42^{\circ}\text{C}$ , washed and subjected to immunodetection according to the standard dot blot

Department of Microbiology and Immunology, Xuzhou Medical College, Xuzhou 221002, Jiangsu Province, China

Dr. TANG Ren-Xian, female, born on 1968-08-13 in Danyang, Jiangsu Province, graduated from Xuzhou Medical College in 1993, majoring in microbiology, having 3 papers published.

\*Project supported by the Natural Science Foundation of Health Bureau, Jiangsu Province, No. H9724, partly supported by the Natural Science Foundation of Educational Committee, Jiangsu Province, No. JW970044.

**Correspondence to:** TANG Ren-Xian, Department of Microbiology and Immunology, Xuzhou Medical College, Xuzhou 221002, Jiangsu Province, China

Tel. +86-516-5748477, Fax. +86-516-5748429

Received 1999-01-19

hybridization procedures.

**Southern blot hybridization** Positive DNA of liver tissues and PBL containing HBV DNA verified by dot blot hybridization were then digested completely with specific restriction endonucleases according to the proportion of 5U *EcoR* I to 1.0 $\mu$ g DNA electrophoresed in agarose gels, denatured, and transferred to nitrocellulose filters. The filters were performed with standard Southern blot procedures<sup>[6]</sup>.

**Statistical analysis**  $\mu$  test and  $\chi^2$  test of paired data were employed to determine the significance between groups. *P* values <0.05 were considered to be significant.

## RESULTS

### *Probes sensitivity and specificity*

The high sensitivity and specificity of HBV DNA probe were confirmed to be 1.0pg by dot blot hybridization which also confirmed its high specificity.

### *Results of HBV DNA detection in liver tissues and PBL*

The positive rates of liver tissues and PBL are shown in Table 1.

**Table 1 HBV detection in liver tissues and PBL**

Specimens	<i>n</i>	Positive rate	
		<i>n</i>	%
PBL	31	27	87.1
Liver tissues	37	31	83.8

### *HBV DNA detection in liver tissues and PBL*

The results of HBV DNA in liver tissues and PBL are shown in Table 2.

**Table 2 HBV correlation between PBL and liver tissues**

Specimens	<i>n</i>	Positive rate	
		<i>n</i>	%
PBL	31	27	87.1
Liver tissues	31	28	90.3

$r = 0.81, P < 0.05$ .

### *Analysis of HBV DNA existence status*

The existence status of HBV DNA is shown in Table 3.

**Table 3 HBV DNA existence status**

Specimens	<i>n</i>	Integrated type		Mixed type	
		<i>n</i>	%	<i>n</i>	%
PBL	9	5	55.6	4	44.4
Liver tissues	9	5	55.6	4	44.4

## DISCUSSION

In traditional sense, hepatitis B virus (HBV) has

strict hepatic tropism, but in recent years, extrahepatic tropism of HBV has been increasingly recognized. HBV antigen or HBV DNA has been demonstrated in the spleen, kidney, skin, pancreatic tissues and bone marrow cells. Lymphocytes are immunoreactive cells. Cytotoxic lymphocyte recognizes viral antigen epitopes expressed in the surface of target cell<sup>[7]</sup>, and subsequently induced-cytotoxic function which may contribute to the elimination and clearance of HBV<sup>[8]</sup>. In the process of HBV clearance, virus may infect lymphocytes by way of infecting stem cells, phagocytic function of lymphocytes, or the cytotoxic effect mediated by hepatic surface-receptors. In our study, the positive rate of HBV DNA in PBL isolated from chronic hepatitis B (CHB) was 87.1%. The HBV existence in lymphocytes may affect the secretory function of tumor necrosis factor alpha (TNF $\alpha$ ) and prostaglandin E<sub>2</sub> (PGE<sub>2</sub>), which will influence the prognosis of hepatitis<sup>[9]</sup>. So, attention should be paid to the regulation of the function of lymphocytes after HBV infection.

In our study, no statistical significance was found between the HBV DNA positive rates in Liver tissues and PBL. Six specimens of liver tissues which did not acquire PBL because of some reasons were removed from the study, and the data of the 31 paired cases were studied. To our astonishment, a statistical correlation of HBV DNA was found between liver tissues and PBL ( $r=0.81, P<0.05$ ), indicating that HBV DNA of PBL is almost equal to that of liver tissues and HBV DNA of PBL can reflect the viral status in liver tissues. Clinically, HBV DNA of PBL should be detected at first in order to reduce the occurrence of complications in liverbiopsy.

On the basis of HBV DNA integration into chromosome or free existing in plasma, HBV DNA positive specimens can be divided into three types: integrated type which has integrated HBV DNA only, free type which has free HBV DNA in plasma, and mixed type which has HBV DNA both in chromosome and in plasma. As a usual carcinogen, integrated HBV DNA can mediate secondary rearrangements of chromosome and lead to chromosome instability. Also, as a transactivator, integrated HBx DNA can cause cell overproliferation and contain p53-mediated apoptosis, which may be the possible reason of hepatocarcinogenesis. In order to detect HBV existence status in PBL, 9 PBL specimens were selected and analyzed by Southern blot hybridization. The results showed 55.6% was integrated type and 44.4% was mixed type. HBV DNA integration was found in each case of specimens. This result raised the question that can

not be answered by “how PBL function after HBV DNA integration has changed”. The further study on HBV DNA integration may answer it in the future.

The research of HBV status in PBL is of certain significance in the treatment of chronic hepatitis B (CHB). Among the medicines used to treat CHB, interferon  $\alpha$  (IFN $\alpha$ ) is the best one, which contains virus replication by influencing interferon stimulated gene (ISG) protein synthesis and regulating host immune response. HBV DNA in plasma of PBL may be integrated into chromosome with homologous sequence. This integration may lead to repression of ISG expression and make the cell lose its response to IFN $\alpha$ , indicating that HBV existence status should be considered before IFN $\alpha$  is used to treat CHB patients.

#### REFERENCES

- 1 Nancy WY, John ST, Gene TC, Thomas WT, Lau WY, Arthur KC. Hepatitis B virus DNA in peripheral blood leukocytes. *Cancer*, 1994; 73:1143-1148
- 2 Pollicing T, Campo S, Raimondo G. PreS and core gene heterogeneity in hepatitis B virus (HBV) genomes isolated from patients with long-lasting HBV chronic infection. *Virology*, 1995;208:672-677
- 3 Sambrook J. Molecular cloning. 2nd ed. *New York: Cold Spring Harbor Laboratory Press*, 1992
- 4 Gao FG, Sun WS, Cao YL, Zhang LN, Song J. HBx-DNA probe preparation and its application in study of hepatocarcinogenesis. *WJG*, 1998;4:320-322
- 5 Wang SW. Gene diagnosis techniques. *Beijing: Beijing Medical University and Xiehe Medical University Press*, 1993:24-34
- 6 Gao FG, Sun WS, Cao YL, Zhang LN, Song J. HBV DNA detection in liver tissues and peripheral blood leukocytes from chronic hepatitis B patients and its correlation research. *Shandong Yixueyuan Xuebao*, 1996;(2):99-102
- 7 Michalak TI, Lau JYN, Mcfarlane BM, Alexander GJM, Eddleston ALWF, Williams R. Antibody directed complement mediated cytotoxicity to hepatocytes from patients with chronic hepatitis B. *Clin Exp Immunol*, 1995;100:227-232
- 8 Brugger SA, Oesterreicher C, Hofmann H, Kalhs P, Greinix HT, Muller C. Hepatitis B virus clearance by transplantation of bone marrow from hepatitis B immunised donor. *Lancet*, 1997;349:996-997
- 9 Guang LX, Gu CH. The change of TNF $\alpha$  and PGE2 secreted by HBV-infected monocytes and its possible significance in hepatitis patients. *Zhonghua Chuanranbing Zazhi*, 1995;13:204-207

Edited by WANG Xian-Lin

# Hujin Pill's antisteatosis of rat liver: evaluation of histopathology and ultrastructure \*

HUANG Zhao-Sheng, WANG Zong-Wei, HUANG Zhen-Yan, ZHONG Shi-Qing, LI Qiao-Mei and XU Qin

**Subject headings** Hujin pills; fatty liver/ pathology; disease models, animal

## INTRODUCTION

Hujin Pill, is composed of *rhizoma polygoni cuspidati*, *radix curcumae*, *rhizoma alismatis*, *radix notoginseng*, *fructus czataegi* and *ganoderma lucidum*, and has the actions of soothing the liver, removing the blood stasis, promoting the blood circulation and lowering the blood-fat<sup>[1]</sup>. Our clinical practice have revealed that it has a marked effect in treating fatty liver<sup>[1]</sup>. Our pharmacodynamic study also indicated that Hujin Pill could evidently improve the experimental rat fatty liver and markedly decrease the concentration of cholesterol, triglyceride and malondialdehyde in serum and liver, it also could reduce the plasma medium molecular level<sup>[2]</sup>. In order to further testify these effects and investigate its mechanism, the effects of Hujin Pill on the histomorphology of rat fatty liver were observed.

## MATERIALS AND METHODS

### Animals

SD rats, female, 200 g ± 18.5 g, were supplied by the Experimental Animal Center of Guangzhou University of Traditional Chinese Medicine. According to their body weight, the 50 experimental rats were divided randomly into control group A, pathology group B, tabellae jiaogulanosidi treatment group C, low dose Hujin Pill group D (5g/kg body weight) and high dose Hujin Pill group E (4g/kg body weight).

### Diet

Chojkier's method was slightly modified<sup>[3]</sup>. This high fat diet was composed of 79.5% standard diet,

20% lard, 0.4% cholesterol and 0.1% bile salt. The control group was fed with standard diet and others with high fat diet.

### Drugs

According to the ratio of the formula, the herbs were decocted and filtered for three times, then merged and condensed to a concentration of 1g/mL. Before reuse, it was diluted to 0.5g/mL or concentrated to 1.4g/mL. Tabellae jiaogulanosidi (No. 960738), provided by Shaanxi Ankang Chinese Pharmaceutical Factory, was administered at a dose of 0.5g/kg body weight (BW).

### Animal model duplication

The animals were given 30% ethanol at a dose of 1.0mL/100g BW per day except the control group, 40% CCl<sub>4</sub> vegetableoil solution was given to posterior limb by subcutaneous injection of each rat on the 1st, 5th, 10th and 15th day. On the first day, the dose was 0.5 mL/100 g BW, and was 0.3mL/100g BW on the other three days. The rats were treated with different drugs at a dose of 1mL/100g BW each day 2 hours before ethanol was given. At the same time, the control group was given (*i.g. s.c*) the same dose of physiological saline solution.

### Sample preparation

The rats were killed after 15 days of treatment and their livers were taken out and weighed. The left liver lobe was cut into 4mm<sup>3</sup> - 5mm<sup>3</sup> masses and fixed in 200mL/L formaldehyde solution, the paraffin masses were embedded routinely, HE stained, frozen and sectioned. The samples were stained with Sudan III and observed under light microscope. On the other hand, the central part of another liver lobe was cut into 1mm<sup>3</sup> masses and fixed in 25mL/L glutaraldehyde and 10mL/L OsO<sub>4</sub>. After they were rinsed and dehydrated step by step, osmosis and embedding were conducted. The Ultracut-E microtome was used to cut these liver masses into sections, which were stained in uranium acetate and lead citrate and observed under JEM-1200EX electron microscope.

## RESULTS

### Macroscopy

The livers of control group had no abnormal

Guangzhou University of Traditional Chinese Medicine (TCM), College of Chinese Herbal Drugs, Guangzhou 510407, China

Professor HUANG Zhao-Sheng, male, born on 1953-09-02 in Jieyang City, Guangdong Province, and graduated from Guangzhou University of TCM as a postgraduate in 1984, master of Chinese Herbal Drugs, now head of the College of Chinese Herbal Drugs, Guangzhou University of TCM, having more than 30 papers and 10 books published.

\*Supported by the State Administration Bureau of TCM, No. 97A06.

Correspondence to: HUANG Zhao-Sheng, College of Chinese Herbal Drugs, Guangzhou University of TCM, 12 Jichang Road, Guangzhou 510407, Guangdong Province, China

Tel. +86-20-86591233 Ext. 2425

Received 1999-01-09

manifestation. However, the pathological model of livers changed evidently. It could be seen that both their volume and weight increased remarkably (Table 1), their capsules were tense, their edges were obtuse, their sections were greasy and milk-yellow. These were the typical features of hepatocyte steatosis. On the other hand, different doses of Hujin Pill and *tabelae jiaogulosidi* could markedly improve the color, quality, volume and weight of rat livers.

**Table 1** The comparison of liver weight of rats after experiment ( $\bar{x}\pm s$ )

Group	Number of rats	Liver weight (g)
A	10	6.34±0.77 <sup>b</sup>
B	8	10.01±1.03
C	9	8.12±0.90 <sup>a</sup>
D	10	7.93±0.91 <sup>a</sup>
E	10	7.46±1.28 <sup>b</sup>

Compared with group B, <sup>a</sup> $P<0.01$ , <sup>b</sup> $P<0.001$ .

#### Light microscopy

No abnormal change was found in the livers of control rats, but diffuse steatosis was found in the pathological model of rat livers and some severe cases became involved with inflammatory infiltration, fat necrosis and fibrosis. These fatty hepatocytes were mainly located in the peripheral zone and middle zone of hepatic lobules. They extremely swelled and were round in shape. Their volume was 2 to 3 times larger than normal one. A large amount of little fat vacuoles, which are very like foam cells, were found in cytoplasm and some of them became bullous or locally necrosed. The degree of liver steatosis was significantly alleviated with the number of fat drops decreased and the volume of livers reduced. Other changes such as inflammatory infiltration and fat necrosis were also largely decreased with almost no proliferation of fibrous tissue.

#### Statistical analysis of pathology

According to the range and extent of pathological changes in liver and hepatic lobules, liver steatosis could be divided into five grades. Meanwhile, by using rank test, a statistical analysis was made for the number of rat liver steatosis in each group. The results showed that, compared with control group, significant difference was found in the degree of steatosis in the other four groups. The rate of steatosis was 100%, the serious steatosis rate was 80% in group B, while it was much lower in groups C, D and E. Administration of Hujin Pill at a dose of 5g/kg had the best effect, and no significant difference was found between the two groups. These results suggested that there was no dose-effect relationship for Hujin Pill (Table 2).

**Table 2** The results of liver steatosis in rats of each group

Group	The degree of liver steatosis					Number of liver steatosis	Rate of liver steatosis
	-	+	++	+++	++++		
A	9	1	0	0	0	1	10
B	0	1	1	4	4	10	100
C	4	4	1	0	1	6	60
D	5	2	1	2	0	5	50
E	4	2	0	3	1	6	60

The standard of assessing the degree of hepatocytes steatosis: -, no steatosis; +, the steatosis in hepatic lobules  $<1/3$ ; ++, the steatosis in hepatic lobules was between  $1/3-2/3$ ; +++, the steatosis in hepatic lobules was between  $1/2-2/3$ ; +++++, the steatosis in hepatic lobules  $>2/3$ .

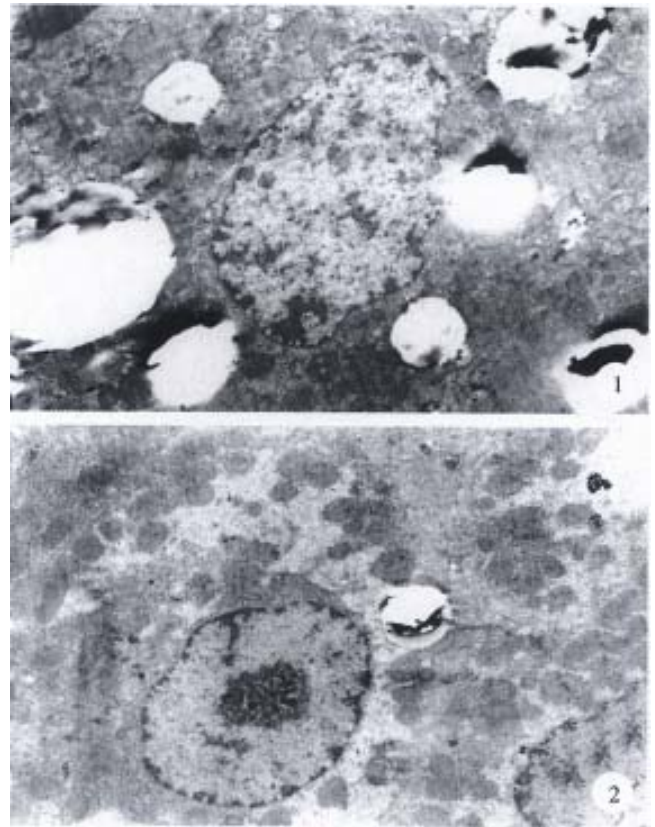


**Figure 1** The ultrastructure of rat hepatocytes in pathology group. The hepatocyte nuclei were crushed by lots of fat drops and became distorted and shrunken. A lot of fat drops were densely accumulated in cytoplasm and the diameter of some single fat drops could reach 4 $\mu$ m. The roughly surfaced endoplasm was broken with distortion, concentration or desalination around mitochondria. HE $\times$ 5000

**Figure 2** The ultrastructure of hepatocytes of rats that administered Hujin Pill at a dose of 5g/kg BW. The fat drops in cytoplasm were largely lessened with insignificantly dilated endoplasm and enlarged mitochondria. Most of the nuclei were regular in shape. The perinuclear space became normal, some of them were slightly shrunken and the chromatin was evenly distributed.

#### Ultrastructural observation

The volume of normal rat hepatocytes was relatively great. These hepatocytes were closely arranged with some desmosomes near the cholangiole. Most of these cells were circular or oval in shape and had monokaryons with reticular or angular 1-3 nucleoli.

There was abundant roughly surfaced endoplasmic reticulum in cytoplasm that was usually distributed near the mitochondrion. However, there was only a small number of smoothly surfaced endoplasmic reticula and ample mitochondria in the cytoplasm, most of which had clear cristae. Meanwhile, a small part of them had high electron densities and indistinct cristae. Occasionally, in cytoplasm, there were a few round or elliptic fat drops which were irregular in tint and their diameter was less than 1 $\mu$ m.

In pathological group, obvious ultrastructure change of hepatocytes was found (Figure 1). A lot of fat drops were densely accumulated in cytoplasm. Most of them were circular in shape and the diameter of some single fat drops could reach 4 $\mu$ m. The roughly surfaced endoplasm was broken, degranulated and dilated into vesicular with distortion, concentration, desalination, swelling and adventitia destruction around mitochondria. Mitochondrial crista was unclear and accompanied by more lysosomes. The nuclei were crushed by lots of fat drops and became distorted and shrunken. The diameter of nucleus was decreased obviously and perinuclear space was large. The sinusoidal endothelial cells obviously swelled with the sinusoid and Diss space became wide, and microvilli were found in some of them. Fat-storing cell and Kupffer cell were obviously hyperplastic. The perinuclear space of Kupffer cell near the sinusoid was obviously broadened. Masses could be found occasionally in the space.

The structure of hepatocytes of rats administered with 5g/kg BW (Figure 2), 14g/kg BW Hujin Pill or tabelle jiaogulosidi, was markedly improved. The best effect was achieved in those that administered Hujin Pill at the dose of 5g/kg BW and the cell ultrastructure almost returned to normal. It also could be observed that the fat drops in cytoplasm were largely lessened with insignificantly dilated endoplasm and enlarged mitochondria. The deletion of mitochondria crista was mild and most of the nuclei were regular in shape. The perinuclear space became normal and some of them were slightly shrunken and the chromatin was

evenly distributed. Now and then, some fat-storing cells could be found.

## DISCUSSION

Generally, it was considered that CCl<sub>4</sub> in hepatocytes could be activated by liver microsome cytochrome P<sub>450</sub> and turned into CCl<sub>3</sub> which could induce microsome lipid peroxide and cause liver steatosis. In this research, we duplicated rat models of fatty liver with comprehensive pathologic factors. The results confirmed that this method not only is reliable and consistent with that reported in literature<sup>[4]</sup>, but also need shorter time than other methods. On the other hand, the effect of Hujin Pill on steatosis hepatocytes also suggested that this drug could be used in treating fatty liver. Our conclusion was coincided with that of pharmacodynamic study. It provides a further basis for the treatment of fatty liver with Hujin Pill.

The pathogenesis of fatty liver is so far unclear. Some researchers hold that the phospholipid of hepatocyte membrane is involved in its formation. Lu *et al*<sup>[5]</sup> showed that the relative percentage of phosphatidyl choline and sphingomyelin in total phospholipid would change when liver was damaged by CCl<sub>4</sub>. From this point of view, we believe that improvement of steatosis hepatocytes by Hujin Pill can be achieved by means of protecting membrane structure and cell organ stabilizing the content of phospholipid. Its exact mechanism needs to be further studied.

## REFERENCES

- 1 Huang ZS, Xu ZH, Zhong SQ, Xiao XH. Clinic observation of Hujin Pill in treating fatty liver. *Shiyong Zhongxiyi Jiehe Zazhi*, 1997;10: 21-28
- 2 Huang ZS, Wang ZW, Liu MP, Zhou L. Pharmacodynamic study on Hujin Pill in treating fatty liver. *Zhongcheng Yao*, 1998;20:27-28
- 3 Chojkier M, Lyche KD, Filip M. Increased production of collagen *in vivo* by hepatocytes and nonparenchymal cells in rats with CCl<sub>4</sub> induced hepatic fibrosis. *Hepatology*, 1988;8:808-814
- 4 Huang ZP, Liang KH, Wang HJ, Ruan YB. Influence of radix *angelica sinensis* on liver ultrastructure in the rat with chronic CCl<sub>4</sub>-induced liver injury. *Zhongxiyi Jiehe Ganbing Zazhi*, 1996;6:16-17
- 5 Lu LG, Wang ZM, Zhang YX, Zhu QS, You YZ. A study on mechanism of liver lesion induced by carbon tetrachloride in rats. *Zhongxiyi Jiehe Ganbing Zazhi*, 1996;6:24-25

# Micronuclei and cell survival in human liver cancer cells irradiated by 25MeV/u $^{40}\text{Ar}^{14+}$ \*

LI Wen-Jian<sup>1</sup>, GAO Qing-Xiang<sup>2</sup>, ZHOU Guang-Ming<sup>1</sup> and WEI Zeng-Quan<sup>1</sup>

**Subject headings** liver neoplasms; heavy ions; micronucleus; cell survival; tumor cell, cultured

## INTRODUCTION

Heavy ions with high linear energy transfer (LET) have the following advantages as compared with the conventional X-rays and  $\gamma$ -rays therapy: a better physical selectivity, a higher relative biological effectiveness (RBE), a greater therapeutic gain factor (TGF), a smaller oxygen enhancement ratio (OER) for LET > 200KeV/ $\mu\text{m}$ , positrons emitted from nuclear reaction products offering the condition of monitoring heavy ion position in tissue, and so on.

During the mid 1970s, 450 patients were treated with heavy ions, mostly neon, at the Bevalac of Lawrence Berkeley Laboratory (LBL), United States<sup>[1]</sup>. Promising results with neon ions were reported when compared with the conventional radiotherapy for soft tissue sarcoma, bone sarcoma and prostate cancer<sup>[2,3]</sup>. In 1994, the Heavy Ion Medical Accelerator in Chiba (HIMAC) of Japan was designed to deliver beams of ions, helium to argon, to energies in the range of 100MeV/u-800MeV/u. Carbon ions were used for clinical treatment. By August 1997, a total of 301 patients had been treated with carbon ions<sup>[4]</sup>. The treatment was started at GSI, Darmstadt, Germany in December 1997. Two patients suffering from tumors at the base of skull were treated with five and four fractions of carbon ions respectively<sup>[5]</sup>. In 1995, HIRFL (Heavy Ion Research Facility in Lanzhou, China) began the basic researches of cancer therapy with heavy ions such as carbon, oxygen and argon.

<sup>1</sup>Institute of Modern Physics, Chinese Academy of Sciences, Lanzhou 730000, Gansu Province, China

<sup>2</sup>Department of Biology, Lanzhou University, Lanzhou 730000, Gansu Province, China

LI Wen-Jian, male, born on 1959-02-22 in Hebei Province, Associate Professor and Deputy Director of the Second Division of Heavy Ion Application. Graduated and obtained a bachelor degree from Hebei University of Technology in 1982, and a master degree from Institute of Modern Physics, Chinese Academy of Sciences in 1992, specialized in the basic study of radiation biological effects and cancer therapy with heavy ions; having 33 papers published.

\*Supported by National Climbing Plan Subject of B Category, No. 85-45-01-3

**Correspondence to:** LI Wen-Jian, Institute of Modern Physics, Chinese Academy of Sciences, Lanzhou 730000, Gansu Province, China

Tel. +86-0931-8854897

Received 1999-01-20

In order to collect basic data for clinical therapy, we studied and discussed the dynamic changes of micronuclei and cell survival in human liver cancer cells SMMC-7721 irradiated by 25MeV/u $^{40}\text{Ar}^{14+}$ .

## MATERIALS AND METHODS

### *Cells and cell culture*

Human liver cancer cells SMMC-7721, purchased from Second Military Medical University in Shanghai, were cultivated in RPMI-1640 medium (Gibco product) supplemented with 10% calf serum in standard incubator at 37°C in air with 5% CO<sub>2</sub>. One passage (subculture) of cells every 6-7 days was performed. The cells were shifted to  $\Phi$ 35mm petri-dishes 2 days before irradiation, each petri-dish had 2mL cell suspension, and density of the cells was  $5 \times 10^4$  cells/mL. Each dose had 6 petri-dishes. Before irradiation, cells in each petri-dish were examined under reverse light microscope so as to select materials good in growth and even in density.

### *Selection of ion beams*

Irradiation was performed using  $^{40}\text{Ar}^{14+}$  ion beam with energy of 25MeV/u and intensity of 0.005nA ( $2.1 \times 10^6$ p/s). The doses of cells were measured by air ionization chamber. Single (0.68, 6.8 and 68Gy) and fractionated (twice and thrice, at an interval of 2h, total dose of 68Gy) irradiations were done.

### *Preparation of samples before irradiation*

Four petri-dishes were taken arbitrarily before irradiation, culture suspension, in which adhesive cells were not included, was harvested, and adhesive cells were fixed with Carnoy's fluid. At the same time, two other petri-dishes were taken and cells were harvested by trypsinization. Cells were stained with typan blue, and number of dead and living cells were counted, respectively. Covers of petri-dishes were removed under condition of asepsis, and irradiation of samples was started after culture medium in petri-dishes was drawn out and the mouths of petri-dishes were sealed using 4 $\mu\text{m}$  sterilized mylar films.

### *Treatment after irradiation*

As soon as irradiation ended, sealed films were taken out from petri-dishes, 2mL fresh 1640 culture

medium was then added into each petri-dish, petri-dishes with cells were then placed in CO<sub>2</sub> incubator and kept on cultivating. Twenty-four, 48, 72, 96 and 120h after cell culture, cells in 2 or 3 petri-dishes from each time point were treated by trypsinization and stained with typan blue to identify the number of dead and living cells. Medium 1640 in other 2 or 3 petri-dishes from each time point was removed, cells were fixed for 4 hours with Carnoy's fluid, and stained for 10 minutes with acridine orange (0.01%, pH 6.8), rinsed three times with PBS buffer at pH 6.8, for 30min each time. Micronuclei were observed under fluorescence microscope. Materials in which micronuclei had been observed were rinsed with PBS and stained for 8min with Giemsa (1:20, pH6.8). Each petri-dish was observed under light microscope. Cells in 9 mesh eye piece micro-ruler were counted, and converted into cell numbers per area.

## RESULTS AND DISCUSSION

### *The dependence of micronucleus frequencies on culture time for SMMC-7721*

From Figure 1, it can be seen that micronucleus frequencies induced by single radiation of 0.68Gy and 6.8Gy and thrice radiation of 68Gy showed a tendency to rise between 24h and 96h culture after radiation. The reasons for this phenomenon might be that: ① micronuclei are delayed to appear following mitoses, as proposed by Mitchell and Norman<sup>[5]</sup>; ② mitoses take place later in cells with severe chromosomal damage expressed as micronuclei<sup>[6]</sup>. As compared with single radiation of 6.8Gy and thrice radiation of 68Gy, the micronucleus frequency of single radiation of 0.68Gy increased over 48h culture after slight irradiation (the micronucleus frequencies at 48h and 96h were 12.86% and 13.45%, respectively). This is because that cells irradiated with single dose of 0.68Gy are damaged to a less degree and easy to recover to normal through 48h culture, thereby the damaged cells inducing micronuclei became so low in number even reaching the number of normal cells. At about 96h, the micronucleus frequencies of cells irradiated with single of 6.8Gy and thrice of 68Gy tended to fall (Figure 1). The reasons might be that: in these cells with less damage, DNA is repaired fast and easily recovered to normal; after culture for a certain duration, normal cells without micronuclei reproduce faster than the damaged cells with micronuclei, ratio (micronucleus frequencies) between the two was lowered.

Micronucleus frequencies are lowest at 48h for single and twice radiation of 68Gy, because the severely damaged cells have not recovered mitoses and only the less-damaged or non-damaged cells

have had mitoses. After 48h culture, the severely damaged cells started mitoses, and the micronucleus frequencies rose significantly (Figure 1).

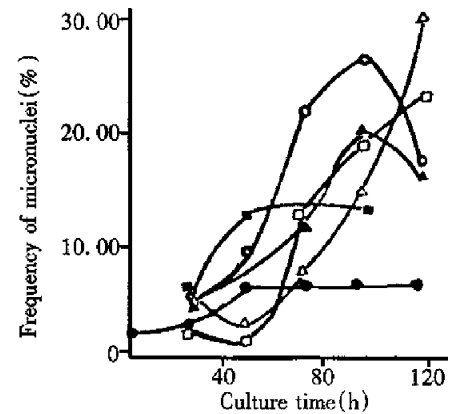


**Figure 1** The dependence of micronucleus frequency on culture time for SMMC-7721.

(●) Control; (□) 0.68Gy; (●) 6.8Gy; (△) 68Gy; (□) Twice, 68Gy; (▲) Thrice, 68Gy

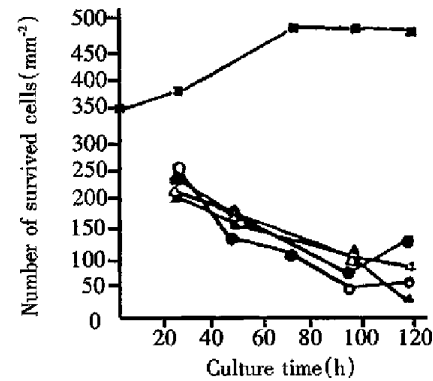


**Figure 2** The dependence of number of living cells on culture time for SMMC-7721.

(□) Control; (●) 6.8Gy; (▲) 68Gy; (△) Twice, 68Gy; (●) Thrice, 68Gy

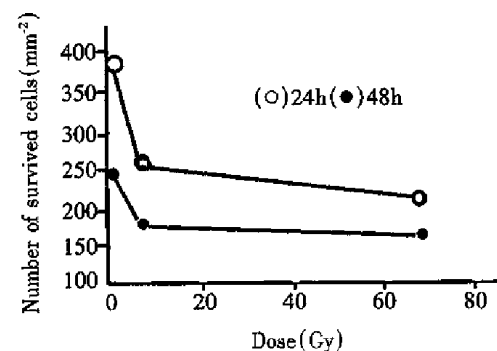


**Figure 3** Dose response to living cells after different culture time for SMMC-7721.

### *Relationship between number of survived cells and culture time for SMMC-7721*

Figure 2 shows the relationship between the number of live cells and culture time for liver cancer cells. It can be seen that irradiated (single or fractionated)

liver cancer cells cultured for 24, 96 and 120 hours grew much slower than control. This showed that growth of liver cancer cells irradiated with heavy ions was obviously inhibited and some of liver cancer cells with different length of culture either exfoliated or died. As culture time was prolonged, survived control cells showed a rising tendency, whereas those of cells irradiated with heavy ions showed attenuating tendency. The latter resulted from radiation with high LET heavy ions which made the cell potentially lethal damage (PLD) enhance obviously. This appearance was also found in typan blue staining. In harvested cell suspension, some of the suspension cells were not deeply stained but stayed in anabiotic state which was a large proportion in irradiated materials. Comparison of single radiation of 6.8Gy, single, twice, and thrice of 68Gy found that the number of survived cells for single and twice radiation of 68Gy lowered gradually during the whole culture period. The difference is that after 96h culture, the number of survived cells for single radiation of 68 Gy decayed faster than those for twice radiation, as there was no interval in the single radiation of 68Gy, i.e., without chance of cell repair, and the number of induced reproductive dead cells increased more obviously than those for twice radiation. The number of survived cells with single radiation of 6.8Gy and thrice radiation of 68Gy increased after 96h culture, which indicates that cell damage by these two kinds of irradiation is slight, with lots of sublethal damage (SLD) cells. These SLD cells reactivated through certain time of culture, therefore, the survived cells increased after 96h culture.

#### *Dynamic analysis of relationship between number of survived cells and micronucleus frequencies*

The results in Tables 1 and 2 illustrate that micronucleus frequencies and survived cells increase or decrease with culture time with single and twice radiation of 68Gy (relative coefficient  $r = -0.97$  and  $r = -0.99$ , respectively). Micronucleus frequencies were negatively related to the number of survived cells. For single dose of 6.8Gy and 3 fraction doses of 68Gy, the micronucleus frequencies both reduced while the number of survived cells increased 96 hours after culture. It is indicated again that there was a negative relationship between micronucleus frequencies and the number of survived cells. Therefore micronucleus frequency is an important parameter describing the degree of the damaged cells.

#### *Dose response to cell micronucleus frequencies after different culture time*

Micronucleus frequencies of cancer cells after 96h culture were significantly higher than those of 24h culture with single radiation of 6.8Gy, single, twice and thrice radiation of 68Gy. Some researchers obtained a similar rule when studying irradiated lymphocytes<sup>[5]</sup>. The reasons are that induced micronucleus cells depend on mitosis while mitotic delay of the damaged cells (chromosome lesion) results in delayed production of large amounts of micronuclei. The changing rule of 24h culture was in agreement with the results by Shibamoto in his studies on lymphocytes<sup>[6]</sup>. After 96h culture, micronucleus frequencies of cells irradiated at a dose of 68Gy fell. This may be because that this kind of cancer cells were damaged more severely and inhibited cell mitotic procedure (mitosis is a prerequisite for micronuclei), therefore damaged cancer cells died before micronuclei were expressed. As compared with cells irradiated with 6.8Gy following 96h culture the micronucleus frequencies of cells irradiated with 68Gy decreased significantly.

**Table 1 Relationship between micronuclei and cell survival in irradiated liver cancer with single irradiation**

Cultural time (h)	Dose (Gy)	No. of scored cells	Frequency of micronuclei (%)	No. of Survived cells (mm <sup>-2</sup> )
24	6.8	2008	4.83	235
48	6.8	2047	9.19	175
72	6.8	2150	21.72	
96	6.8	1924	26.55	79
120	6.8	2096	17.45	129
24	68	1960	5.62	207
48	68	2150	3.00	158
72	68	2070	7.93	
96	68	1975	14.69	107
120	68	2040	30.39	36

**Table 2 Relationship between micronuclei and cell survival in irradiated liver cancer with fractionated irradiation**

Cultural time (h)	Dose (Gy)	Time of irradiation	No. of scored cells	Frequency of micronuclei (%)	No. of Survived cells (mm <sup>-2</sup> )
24	68	2	971	5.13	213
48	68	2	1024	1.56	
72	68	2	964	12.79	
96	68	2	1152	19.01	101
120	68	2	1060	23.02	90
24	68	3	974	2.47	250
48	68	3	1050		136
72	68	3	1000	12.00	109
96	68	3	1000	20.00	50
120	68	3	1116	16.13	59

#### *Dose response to survived cells after different culture time*

Figure 3 shows the dose response to cell survival in human liver cancer cells. It can be seen that survival of liver cancer cells following 24h and 96h culture decreased with increase of radiation dose, i.e. cell

survival was negatively related to doses ( $r_{24h} = -0.68$ ,  $r_{48h} = -0.70$ ). When radiation dose was the same, the number of survived cells in human liver cancer cells for 48h culture was lower than that for 24h culture. The results showed that the number of survived cells of the irradiated liver cancer cells decreased gradually with culture time (survived number of control cells increased with culture time), which results from reproductive death of lots of potentially lethal cells in irradiated cancer cells through several division cycles.

## REFERENCES

- 1 Kraft G. Heavy ion therapy at GSI. *GSI Nachrichten*, 1993;11:3-5
- 2 Castro JR. Future research strategy for heavy ion radiotherapy. *Progress Radiooncol*, 1995;5:643-648
- 3 Linstadt DE, Castro JR, Phillips TL. Neon ion radiotherapy: results of the phase I/II clinical trial. *Int J Radiat Oncol Biol Phys*, 1991; 20:761-769
- 4 Sisterson J. Particles. *News Letter*, 1998;21:1-11
- 5 Mitchell JC, Norman A. The induction of micronuclei in human lymphocytes by low doses of radiation. *Int J Radiat Biol*, 1987; 52:527-535
- 6 Shibamoto Y, Streffer C, Fuhrmann C. Tumor radiosensitivity prediction by the cytokinesis block micronucleus assay. *Rediat Res*, 1991;128:293-300

Edited by MA Jing-Yun

# Molecular mechanisms of *H. pylori* associated gastric carcinogenesis

ZHANG Zun-Wu and Michael J.G. Farthing

**Subject headings** *H. pylori*; carcinogenesis, molecular biology; p53, stomach neoplasms

*H. pylori* infects half of the world population and the prevalence varies widely in different parts of the world with average rates of 40%-50% in western countries, rising to more than 90% in the developing world<sup>[1,2]</sup>. Compelling evidence from epidemiological and histopathological studies has linked *H. pylori* infection to the subsequent development of gastric carcinogenesis<sup>[3]</sup>. Furthermore, Watanabe and colleagues recently induced gastric adenocarcinoma in 37% of orally infected Mongolian gerbils, which were preceded with a series of premalignant changes in gastric mucosa of these gerbils<sup>[4]</sup>. However, in spite of the established causal relationship between *H. pylori* infection and gastric carcinogenesis, the underlying mechanisms remain unknown.

Disturbances in cell turnover in the gastrointestinal tract are believed to predispose to cancer development, and until recently, these changes were considered to be a marker of increased cancer risk<sup>[5]</sup>. It is clear that this organism is the main cause of chronic gastritis and capable of modifying epithelial cell turnover within gastric glands and in culture gastric epithelial cells, by influencing the balance between cell proliferation and apoptosis<sup>[6-9]</sup>. We and others have studied the effect of *H. pylori* infection on gastric epithelial cell turnover and found that patients infected with *H. pylori* had significantly higher proliferation rates as compared with uninfected controls<sup>[6,8-12]</sup>. The density of *H. pylori* may be one of the important determinants as we found that *H. pylori* at low inocula, stimulates cell proliferation, but at higher inocula (bacterium to cell ratio >100), it causes a time- and concentration-dependent reduction of cell number and a marked increase in apoptosis and cell cycle arrest at G1 phase<sup>[8]</sup>.

Antioxidant vitamins C, E and  $\beta$ -carotene affect cell growth in various human cells directly or through their antioxidant properties<sup>[13,14]</sup>. Our *in vitro* studies showed that the above vitamins can also significantly inhibit gastric cancer cell proliferation and induce apoptosis<sup>[15]</sup>. Investigations on gastric vitamins in patients with and without *H. pylori* infection suggest that *H. pylori* infection affects the concentrations of vitamin C, E and  $\beta$ -carotene in the stomach and the CagA<sup>+</sup> strains have an even greater ability to reduce gastric juice vitamin C levels<sup>[16,17]</sup>.

Although many factors may be related to *H. pylori* associated gastric carcinogenesis, the underlying molecular mechanisms are still unknown. However, many mediators and signal transduction pathways are involved in the regulation of gastric epithelial cell homeostasis, some of which may determine the final outcome of *H. pylori* infection. Understanding the molecular basis of *H. pylori* associated gastric carcinogenesis is important for determining prognosis, prevention and treatment of *H. pylori* infection. This review examines the possible molecular mechanisms responsible for *H. pylori* associated gastric carcinogenesis.

## BACTERIAL VIRULENCE FACTORS

Although many factors contribute to *H. pylori* virulence, few have been directly related to gastric carcinogenesis<sup>[18]</sup>. Most strains of *H. pylori* from patients with intestinal-type gastric cancer or with atrophic gastritis are type I and secrete vacuolating cytotoxin (VacA) and carry CagA, a gene that encodes an immunodominant protein of unknown function, whereas many of the strains from asymptotically infected persons lack this gene<sup>[19-21]</sup>. It has been shown that patients harbouring CagA<sup>+</sup> strains have significantly higher gastric epithelial proliferation rates than patients infected with CagA<sup>-</sup> strains, but the apoptotic index in patients infected with CagA<sup>+</sup> strains are lower than in patients infected with CagA<sup>-</sup> strains. Increased cell proliferation in the absence of a corresponding increase in apoptosis may explain the increased gastric cancer risk associated with infection by CagA<sup>+</sup> strains<sup>[10]</sup>. Although there is no direct evidence suggesting that the CagA or VacA

Digestive Diseases Research Centre, St Bartholomew's & the Royal London School of Medicine & Dentistry, London E1 2AT, UK

**Correspondence to:** Dr. ZHANG Zun-Wu, Digestive Diseases Research Centre, St Bartholomew's & the Royal London School of Medicine & Dentistry, London E1 2AT, UK

Tel. +44-(0) 171 295 7203, Fax. +44(0) 171 295 7192

Email: zwzhang@mds.qmw.ac.uk

Received 1999-08-10

protein is carcinogenic, the enhanced inflammation and marked reduction of gastric juice vitamin C levels in CagA<sup>+</sup> strain infected patients may play a role in *H. pylori* associated carcinogenesis<sup>[16]</sup>.

*H. pylori* expresses a powerful urease enzyme, which catalyses the conversion of urea to ammonia. Individuals with *H. pylori* infection have higher ammonia concentrations in gastric juice than uninfected controls<sup>[22]</sup>. A series of studies have demonstrated that concentrations of ammonia comparable to those found in gastric juice of infected individuals can cause gastric atrophy in rats, increase epithelial cell proliferation, and act as a promoter in the methyl- *N*' nitro-*N*-nitrosoguanidine (MNNG) rat model of gastric cancer<sup>[23-28]</sup>.

Furthermore, *H. pylori* phospholipases, proteases and oxidases have been shown to cause degradation of many molecules, such as phospholipids in bio-membranes, transforming growth factor- $\beta$  (TGF- $\beta$ ) and vitamin C, which are important in preventing carcinogenesis<sup>[16,29-31]</sup>.

#### OXIDATIVE DNA DAMAGE AND p53

Mutation of the p53 tumor suppressor gene is the most common alteration found in a variety of human tumor cells and is considered to be one of the steps leading to the neoplastic state. The importance of p53 protein may be due to its effect on cell cycle progression, including cell proliferation and apoptosis, in response to cell DNA damage<sup>[32]</sup>. The activated p53 protein can affect the expression of a number of genes, including the cyclin-dependent kinase inhibitor (CKI) p21, which regulates G1 cell cycle check point and bax, a gene involved in apoptosis. Therefore, the protein can either prevent the cell from entering the S phase until the DNA damage is repaired and/or can turn on the apoptotic pathways to destroy an abnormal cell<sup>[33]</sup>.

The p53 gene abnormalities in gastric cancer are usually point mutations or allelic deletions leading to over-expression of the protein, loss of p53 function and with resulting defects in the protective pathways of cell cycle arrest and apoptosis. Furthermore, the increased p53 expression and gene mutations have also been reported in gastric premalignant mucosa, such as dysplasia, atrophy or even the mucosa without obvious abnormality, suggesting that p53 function is affected from the early stage of gastric carcinogenesis<sup>[34]</sup>.

The role of p53 in *H. pylori* associated carcinogenesis is still unclear, but some evidence suggests that it may be protective in this process. In p53 knockout mice, atrophic gastritis developed in 2 of 4 animals infected with *H. felis* within 3 months including one which developed moderate dysplasia.

In contrast, these changes were not seen in any of the control animals, suggesting that lack of functional p53 accelerated carcinogenesis in experimental *Helicobacter* infection<sup>[35]</sup>. Data from Fox and colleagues further support the protective role of p53. They examined the effect of infection with *H. felis* in heterozygous mice deficient in one p53 allele<sup>[36]</sup>. One year after infection, the wild-type and p53 heterozygous mice both showed severe adenomatous and cystic hyperplasia of the surface foveolar epithelium. However, infected p53 heterozygous mice had a higher proliferative index than the infected wild-type mice.

Whether *H. pylori* and its associated inflammation induces p53 mutations or affects the activity of the protein is not clear, but p53 function may be defective at an early stage in *H. pylori* associated gastric carcinogenesis. Some studies have reported increased expression of p53 protein in gastric mucosa infected with *H. pylori*. However, the enhanced p53 expression failed to have any effect on gastric epithelial cell proliferation or apoptosis, and there appeared to be a positive relationship between the accelerated cell turnover and p53 over-expression. The accumulation of p53 was also not associated with expression of the CDI p21, a down-stream effector of p53<sup>[37,38]</sup>. We have recently initiated a study investigating the role of p53 in *H. pylori* infected gastric cell lines and found that *H. pylori* associated apoptosis is independent to p53 status of gastric cells<sup>[39]</sup>. These findings suggest that p53 function is defective in *H. pylori* infected mucosa. There are several mechanisms which may lead to the loss of p53 function. Firstly, recent studies suggest that p53 mediated apoptosis is suppressed by signals from growth factors, such as interleukin-6 (IL-6), interferon- $\gamma$  (IFN- $\gamma$ ) and protein kinase C, which are shown to be up-regulated by *H. pylori* infection<sup>[40-42]</sup>. Secondly, it is likely that *H. pylori* and its associated inflammatory responses cause p53 gene mutation. *H. pylori* infection induces increased production of reactive oxygen metabolites (ROMs) by persistent inflammatory cell infiltration in gastric mucosa<sup>[43-45]</sup>. Many studies have indicated that ROMs can directly interact with genomic DNA and cause damage in specific genes that control cell growth and differentiation<sup>[46-48]</sup>. Furthermore, it has been reported that intact *H. pylori*, as well as isolated cellular components, stimulate nitric oxide (NO) synthesis<sup>[49-51]</sup>. High concentrations of NO induce wild-type p53 protein accumulation<sup>[52,53]</sup>, and the NO-related deamination of DNA has been reported to cause GC-AT transitions, which are frequently found in p53 mutations in gastric cancer<sup>[23,54]</sup>. In addition, *H. pylori* possesses several proteases which may

directly affect p53 activity though there is no direct experimental evidence of a relationship between these proteases and p53 protein<sup>[55]</sup>.

#### BCL-2 AND OTHER APOPTOSIS RELATED MOLECULES

Bcl-2 protein is a part of a large group of proteins encoded by specific genes belonging to the bcl-2 family, which are known to play an important role in regulation of apoptosis. Some of these proteins (bcl-2 and bcl-xL) support survival, whereas others (bax, bad, bcl-x5) are apoptosis inducers<sup>[56]</sup>. Over-expression of bax and bak proteins encoded by the two pro-apoptotic members of the *bcl-2* gene family has been associated with *H. pylori* infection and to induce apoptosis in the AGS gastric epithelial cell line and in gastric mucosal biopsies from patients colonized by *H. pylori*<sup>[57]</sup>. In contrast, the expression of bcl-2 protein was not affected or even suppressed by this organism<sup>[37]</sup>. However, over-expression of bcl-2 with abnormal distribution of apoptotic cells along the glands, which are usually found at the extremities of normal gastric glands, has been described in both intestinal metaplasia and gastric dysplasia, which occur as a result of long-term *H. pylori* infection<sup>[58,59]</sup>.

Several other molecules may also play a role in *H. pylori* associated apoptosis. Treatment of gastric cells with TNF- $\alpha$  and IFN- $\gamma$  markedly potentiate *H. pylori* induced apoptosis<sup>[60]</sup>. Rudi *et al* have recently reported that *H. pylori* up-regulates the expression of the CD95 (APO-1/FAS) and CD95 ligand (CD95L), which are involved in initiating apoptosis. In fact, the enhanced CD95 expression observed in this study was associated with increased rates of apoptosis in gastric epithelial cell lines and in gastric mucosa<sup>[61]</sup>. The importance of this study is not only the demonstration of the involvement of CD95 mediated apoptotic pathway in *H. pylori* associated apoptosis, but also the expression of CD95L mRNA on surface epithelium and pyloric gland cells of *H. pylori* infected mucosa at levels comparable to those found on lamina propria lymphocytes. CD95L is normally expressed by activated T cells and recently it has been found that many tumors, including gastric adenocarcinomas express CD95L<sup>[62]</sup>. CD95L can induce apoptosis of activated immunocytes and is thought to contribute to tumor immune escape<sup>[62]</sup>. The enhanced expression of CD95L mRNA in *H. pylori* infected gastric mucosa may suppress normal immune responses by inducing immunocyte apoptosis, which may further potentiate genetic instability due to the defect in the DNA damage-p53 mediated protective pathway.

#### TELOMERASE ACTIVITY

Activity of telomerase, which synthesizes the

telomeric DNA to replace the loss that occurs at each cell division, is suppressed in most normal human somatic cells but induced in most human cancers. Normal human cells progressively lose telomere sequences due to the lack of telomerase activity. In contrast, most immortalized cell lines and malignant human tumors appear to maintain constant telomere length via the activation of telomerase<sup>[63,64]</sup>. Reactivation of telomerase is thought to be an important step in carcinogenesis.

Expression of human telomerase RNA (hTR) and telomerase activity have been studied in gastric cancer and corresponding non-cancerous mucosa<sup>[65]</sup>. Telomerase activity was detected in 23 of 26 carcinoma tissues. Although all tumor specimens and non-cancerous mucosa expressed various levels of hTR, 21 cases expressed hTR at a higher level in the tumor than that in the adjacent normal mucosa. Nine of 26 non-cancerous mucosa showed telomerase activity and all of them contained intestinal metaplasia. The incidence of telomerase-positive mucosa in grade II intestinal metaplasia was significantly higher than that in mucosa with grade I intestinal metaplasia or without intestinal metaplasia, whereas hTR over-expression was found both in mucosa with and without intestinal metaplasia regardless to their grades. The level of hTR expression and telomerase positivity was shown to increase in parallel with the degree of *H. pylori* infection. These results suggest that *H. pylori* infection may be a strong trigger for hTR over-expression in intestinal metaplasia, and this may lead to telomerase reactivation<sup>[65,66]</sup>.

Recently, Chin and colleagues examined the interaction between telomere dysfunction and p53 in cells and organs of telomerase-deficient mice. Coincident with severe telomere shortening and associated genomic instability, p53 is activated, leading to growth arrest and/or apoptosis. Deletion of p53 significantly attenuated the adverse effects of telomere dysfunction, but only during the earliest stages of genetic crisis. Correspondingly, the loss of telomere function and p53 deficiency cooperated to initiate the transformation process<sup>[67]</sup>. These findings suggest that p53 deficiency and telomerase reactivation in *H. pylori* infected mucosa may play an important role in *H. pylori* associated gastric carcinogenesis.

#### HOST GENETIC FACTORS

Beales *et al* reported that the frequency of DQ 5, one of the D-related human leukocyte antigen (HLA) molecules, was significantly higher in individuals with gastric atrophy or metaplasia than in those without gastric atrophy or intestinal

metaplasia and in uninfected individuals<sup>[68]</sup>. Azuma and colleagues have studied the relationship between *H. pylori* infection and the genotyping of another D-type HLA molecule, DQA1 in 82 gastric adenocarcinoma patients and 167 unrelated controls. They found that the allele frequency of DQA1 was significantly lower in *H. pylori* positive atrophic gastritis group than in *H. pylori* positive superficial gastritis and normal control groups. In addition, the a1 lele frequency of DQA1 also was significantly lower in *H. pylori* positive intestinal type gastric adenocarcinoma group than in normal control, *H. pylori* positive superficial gastritis, and diffuse type gastric adenocarcinoma groups<sup>[69]</sup>.

The importance of host genetic factors in determining the outcome of *H. pylori* infection was further demonstrated by Sakagami and colleagues. They assessed *H. pylori* infection in different strains of mice and found that the level of bacterial colonisation, the severity of gastritis and the development of gastric atrophy varied within these mice. For example, in infected SJL, C3H/He, DBA/2, and C57BL/6 mice, moderate to severe chronic active gastritis was observed only in the body of the stomach, which increased in severity over time with specialised cells in the body glands being replaced. As the severity of this damage in the body increased and atrophic changes were seen, the level of bacterial colonisation of the antrum decreased. In contrast, in BALB/c and CBA mice, there was only mild gastritis in the antrum, no remarkable changes were detected in the gastric body mucosa, and no atrophy was seen over time. In both these strains of mice, heavy bacterial colonisation was seen, which tended to increase over the period of the experiment<sup>[70]</sup>. These findings suggest that the host genetic factors are important in *H. pylori* associated gastric

carcinogenesis.

#### SUMMARY

Many molecules are involved in *H. pylori* associated gastric carcinogenesis. However, how the organism and its associated inflammation, interact with these molecules in gastric mucosa to induce carcinogenesis is still unknown. Over many years, *H. pylori* infected mucosa may experience sequential exposure to "damage-regeneration" (Figure 1). Following the long-standing repeated damage-regeneration cycle, gastric atrophy and intestinal metaplasia gradually develop, which finally results in adenocarcinoma. During this process, the loss of p53 function may play an important role. As mentioned above, *H. pylori* infection may cause deficiency of p53 function and subsequently, this may not only lead to defects in the DNA damage-p53 mediated protective pathway, but the mutated p53 protein may also provide a possible selective advantage for tumor cell proliferation by attenuating apoptosis<sup>[71]</sup>. Furthermore, *H. pylori* infection has been shown to induce the reactivation of telomerase and to cause telomere dysfunction, which may cooperate with p53 deficiency to accelerate carcinogenesis<sup>[67]</sup>. In early stages of *H. pylori* infection, CD95 and bax mediated apoptosis may play an important role in eliminating damaged DNA or gene mutated cells, thereby maintaining genetic stability. However, *H. pylori* infection induces CD95L expression, which may suppress host immune responses by causing immunocyte apoptosis. Therefore, as shown in Figure 2, the loss of p53 function, reactivation of telomerase activity, inhibition of host immune responses, together with host genetic factors, may play important roles in the development of *H. pylori* associated carcinogenesis.

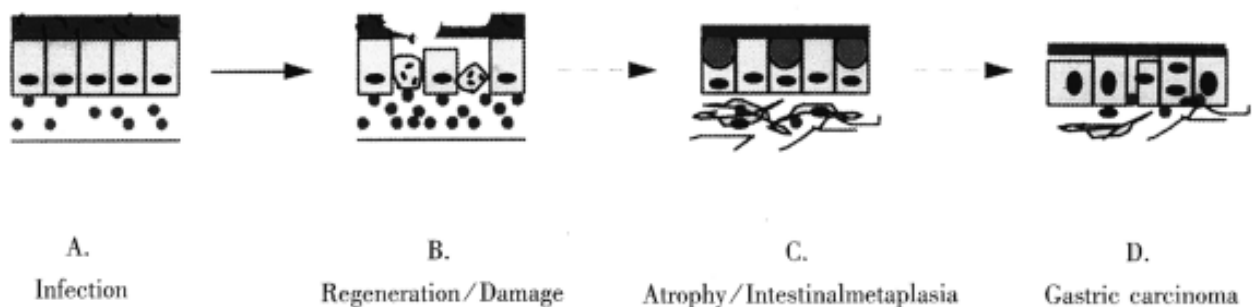


**Figure 1** Long-term *H. pylori* infection may induce a repeated "damage-regeneration" process which gradually leads to gastric atrophy, intestinal metaplasia and finally carcinoma. A. *H. pylori* infected gastric mucosa with inflammatory cell infiltration. B. Gastric epithelial cells are damaged, become apoptotic and then are regenerated, with enhanced inflammatory cell infiltration and disturbance of mucus layer. C. Atrophy and intestinal metaplasia develop; fibrosis and thinning of the lamina propria; finally *H. pylori* is lost due to inhospitable mucosa. D. Gastric carcinoma is induced.

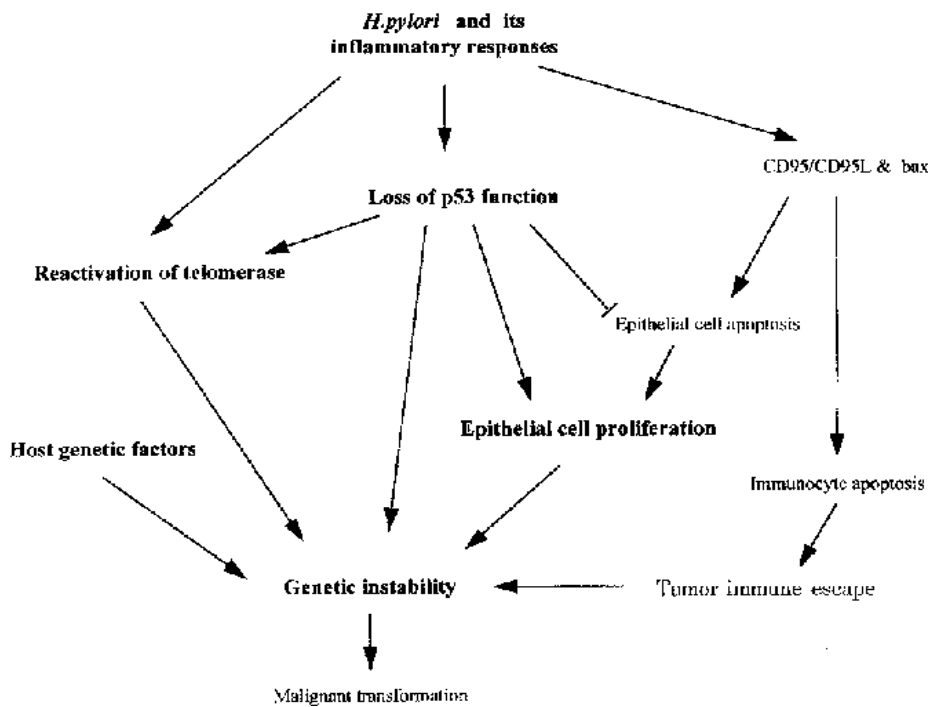


**Figure 2** Possible molecular mechanisms of *H. pylori* associated carcinogenesis. *H. pylori* and its associated inflammatory responses cause reactivation of telomerase, the loss of p53 function and also induce CD95 and bax mediated apoptosis. CD95L produced by gastric epithelial cells may also cause intra-mucosal immunocyte apoptosis, which could facilitate tumor immune escape. However, mutated p53 may attenuate epithelial cell apoptosis, providing a possible selective advantage for tumor cell proliferation. Furthermore, p53 deficiency may cooperate with telomerase dysfunction to accelerate carcinogenesis. All of these changes, together with host genetic factors may play important roles in the development of *H. pylori* associated carcinogenesis.

## REFERENCES

- Farthing MJG. *Helicobacter pylori* infection: an overview. *Br Med Bull*, 1998;54:1-6
- Zhang ZW, Xing YY, Li SQ, Huang ZH. Seroepidemiological investigation of *Helicobacter pylori* infection in a Beijing population (in Chinese). *Beijing Yixue*, 1992;23:250-252
- IARC Working Group on the Evaluation of Carcinogenic Risks to Humans. Schistosomes, liver flukes and *Helicobacter pylori*. Lyon, 7-14 June 1994. *IARC Monogr Eval Carcinog Risks Hum*, 1994; 61:1-241
- Watanabe T, Tada M, Nagai H, Sasaki S, Nakao M. *Helicobacter pylori* infection induces gastric cancer in Mongolian gerbils. *Gastroenterology*, 1998;115:642-648
- Fearon ER, Vogelstein B. A genetic model for colorectal tumorigenesis. *Cell*, 1990;61:759-767
- Zhang ZW, Patchett SE, Farthing MJG. *H. pylori* associated reduction in gastric cell number is associated with increased apoptosis rate, but not cell DNA synthesis rate (abstract). *Gastroenterology*, 1999;116:G1759
- Correa P, Miller MJ. Carcinogenesis, apoptosis and cell proliferation. *Br Med Bull*, 1998;54:151-162
- Zhang ZW, Patchett SE, Farthing MJG. Effect of *H. pylori* on gastric epithelial cell cycle progression (abstract). *Gut*, 1999 in press
- Patchett SE, Katelaris PH, Zhang ZW, Alstead EM, Domizio P, Farthing MJG. Ornithine decarboxylase activity is a marker of premalignancy in long-standing *Helicobacter pylori* infection. *Gut*, 1996;39:807-810
- Peek RM Jr., Moss SF, Tham KT, Perez<sup>2</sup>Perez GI, Wang S, Miller GG, Atherton JC, Holt PR, Blaser MJ. *Helicobacter pylori* cagA+ strains and dissociation of gastric epithelial cell proliferation from apoptosis. *J Natl Cancer Inst*, 1997;89:863-868
- Cahill RJ, Xia H, Kilgallen C, Beattie S, Hamilton H, O'Morain C. Effect of eradication of *Helicobacter pylori* infection on gastric epithelial cell proliferation. *Dig Dis Sci*, 1995;44:1627-1631
- Lynch DA, Mapstone NP, Clarke AM, Sobala GM, Jackson P, Morrison L, Dix MF, Quirke P, Axon ATR. Cell proliferation in *Helicobacter pylori* associated gastritis and the effect of eradication therapy. *Gut*, 1995;36:346-350
- van Poppel G, van den Berg H. Vitamins and cancer. *Cancer Lett*, 1997;114:195-202
- Brigelius-Flohe R, Flohe L. Ascorbic acid, cell proliferation, and cell differentiation in culture. *Subcell Biochem*, 1996;25:83-107
- Zhang ZW, Wilks S, Davies D, Carnaby S, Allen P, Poschet JF, Patchett SE, Farthing MJG. Comparative effects of Antioxidant vitamins C, E and  $\beta$ -carotene on cell proliferation and apoptosis in a gastric epithelial cell line (abstract). *Gastroenterology*, 1998, 114:A709
- Zhang ZW, Patchett SE, Perrett D, Katelaris PH, Domizio P, Farthing MJ. The relation between gastric vitamin C concentrations, mucosal histology, and CagA seropositivity in the human stomach. *Gut*, 1998;43:322-326
- Zhang ZW, Patchett SE, Perrett D, Domizio P, Farthing MJG. The influence of chronic *Helicobacter pylori* infection on gastric mucosal and luminal  $\beta$ -carotene concentrations (abstract). *Gastroenterology*, 1996;110:A619
- Covacci A, Telford JL, Giudice GD, Parsonnet J, Rappuoli R. *Helicobacter pylori* virulence and genetic geography. *Science*, 1999; 284:1328-1333
- Basso D, Navaglia F, Brigato L, Piva MG, Toma A, Greco E, Di Mari F, Galeotti F, Roveroni G, Corsini A, Plebani M. Analysis of *Helicobacter pylori* vacA and cagA genotypes and serum antibody profile in benign and malign gastroduodenal diseases. *Gut*, 1998; 43:182-186
- Parsonnet J, Friedman GD, Orentreich N, Vogelstein H. Risk for gastric cancer in people with CagA positive or CagA negative *Helicobacter pylori* infection. *Gut*, 1997;40:297-301
- Rudi J, Kolb C, Maiwald M, Zuna I, von Herbay A, Galle PR, Stremmel W. Serum antibodies against *Helicobacter pylori* proteins VacA and CagA are associated with increased risk for gastric adenocarcinoma. *Dig Dis Sci*, 1997;42:1652-1659
- Marshall BJ, Langton SR. Urea hydrolysis in patients with *Campylobacter pyloridis* infection. *Lancet*, 1986;1:965-966
- Tsuji S, Tsujii M, Sun WH, Gunawan ES, Murata H, Kawano S, Hori M. *Helicobacter pylori* and gastric carcinogenesis. *J Clin Gastroenterol*, 1997; 25(Suppl 1):S186-197
- Tsuji M, Kawano S, Tsuji S, Ito T, Nagano K, Sasaki Y, Hayashi

- NF, H, Kamada T. Cell kinetics of mucosal atrophy in rat stomach induced by long-term administration of ammonia. *Gastroenterology*, 1993;104:796-801
- 25 Tsujii M, Kawano S, Tsuji S, Takei Y, Tamura K, Fusamoto H, Kamada T. Mechanism for ammonia-induced promotion of gastric carcinogenesis in rats. *Carcinogenesis*, 1995;16:563-566
- 26 Tsujii M, Kawano S, Tsuji S, Nagano K, Ito T, Hayashi N, Fusamoto H, Kamada T, Tamura K. Ammonia: a possible promoter in *Helicobacter pylori*-related gastric carcinogenesis. *Cancer Lett*, 1992;65:15-18
- 27 Suzuki H, Seto K, Mori M, Suzuki M, Miura S, Ishii H. Monochloramine induced DNA fragmentation in gastric cell line MKN45. *Am J Physiol*, 1998;275: G712-716
- 28 Matsui T, Matsukawa Y, Sakai T, Nakamura K, Aoike A, Kawai K. Ammonia inhibits proliferation and cell cycle progression at S-phase in human gastric cells. *Dig Dis Sci*, 1997;42:1394-1399
- 29 Dorrell N, Martino MC, Stabler RA, Ward SJ, Zhang ZW, McColm AA, Farthing MJG, Wren B. Characterisation of the *Helicobacter pylori* PldA, a phospholipase with a role in colonisation of the gastric mucosa. *Gastroenterology*, 1999: in press
- 30 Piotrowski J, Slomiany A, Slomiany BL. Suppression of *Helicobacter pylori* protease activity towards growth factors by sulglycotide. *J Physiol Pharmacol*, 1997;48:345-351
- 31 Odum L, Andersen LP. Investigation of *Helicobacter pylori* ascorbic acid oxidizing activity. *FEMS Immunol Med Microbiol*, 1995;10: 289-294
- 32 Oren M. The involvement of oncogenes and tumour suppressor genes in the control of apoptosis. *Cancer Metastasis Rev*, 1992;11:141-148
- 33 Kastan MB, Kuerbitz SJ. Control of G1 arrest after DNA damage. *Envir on Health Perspect*, 1993;101(Suppl 5):55-58
- 34 Moss SF. Review article: Cellular markers in the gastric precancerous process. *Aliment Pharmacol Ther*, 1998;12(Suppl 1):91-109
- 35 Dunn BE, Phadnis SH, Henderson J, Choi H. Induction of gastric dysplasia by *H. felis* in p53 deficient mice (abstract). *Gut*, 1995; 37:A40
- 36 Fox JG, Li X, Cahill RJ, Andrutis K, Rustgi AK, Odze R, Wang TC. Hypertrophic gastropathy in *Helicobacter felis*-infected wild-type C57BL/6 mice and p53 hemizygous transgenic mice. *Gastroenterology*, 1996;110:155-166
- 37 Hibi K, Mitomi H, Koizumi W, Tanabe S, Saigenji K, Okayasu I. Enhanced cellular proliferation and p53 accumulation in gastric mucosa chronically infected with *Helicobacter pylori*. *Am J Clin Pathol*, 1997;108:26-34
- 38 Jones NL, Shannon PT, Cutz E, Yeager H, Sherman PM. Increase in proliferation and apoptosis of gastric epithelial cells early in the natural history of *Helicobacter pylori* infection. *Am J Pathol*, 1997;151:1695-1703
- 39 Zhang ZW, Patchett SE, Farthing MJG. P53 signal transduction pathway is not essential for *H. pylori* associated apoptosis and cell growth inhibition in gastric cells (abstract). *Gastroenterology*, 1999; 116:G0688
- 40 Hong M, Lai MD, Lin YS, Lai MZ. Antagonism of p53-dependent apoptosis by mitogen signals. *Cancer Res*, 1999;59:2847-2852
- 41 Lindholm C, Quiding-Jarbrink M, Lonroth H, Hamlet A, Svennerholm AM. Local cytokine response in *Helicobacter pylori*-infected subjects. *Infect Immun*, 1998;66:5964-5971
- 42 Terres AM, Pajares JM, Hopkins AM, Murphy A, Moran A, Baird AW, Keller D. *Helicobacter pylori* disrupts epithelial barrier function in a process inhibited by protein kinase C activators. *Infect Immun*, 1998;66:2943-2950
- 43 Hahn KB, Lee KJ, Kim JH, Cho SW, Chung MH. *Helicobacter pylori* infection, oxidative DNA damage, gastric carcinogenesis, and reversibility by Rebamipide. *Dig Dis Sci*, 1998;43:72S-77S
- 44 Farinati F, Cardin R, Degan P, Rugge M, Mario FD, Bonvicini P, Naccarato R. Oxidative DNA damage accumulation in gastric carcinogenesis. *Gut*, 1998 ;42:351-356
- 45 Bagchi D, Bhattacharya G, Stohs SJ. Production of reactive oxygen species by gastric cells in association with *Helicobacter pylori*. *Free Radic Res*, 1996;24:439-450
- 46 Wei YH, Lu CY, Lee HC, Pang CY, Ma YS. Oxidative damage and mutation to mitochondrial DNA and age-dependent decline of mitochondrial respiratory function. *Ann N Y Acad Sci*, 1998;854:155-170
- 47 Barnett YA, Barnett CR. DNA damage and mutation: contributors to the age-related alterations in T cell-mediated immune responses. *Mech Ageing Dev*, 1998;102:165-175
- 48 Olinski R, Jaruga P, Zastawny TH. Oxidative DNA base modifications as factors in carcinogenesis. *Acta Biochim Pol*, 1998;45:561-572
- 49 Brzozowski T, Konturek PC, Sliwowski Z, Drozdowicz D, Pajdo R, Stachura J, Hahn EG, Konturek SJ. Lipopolysaccharide of *Helicobacter pylori* protects gastric mucosa via generation of nitric oxide. *J Physiol Pharmacol*, 1997;48:699-717
- 50 Nagata K, Yu H, Nishikawa M, Kashiba M, Nakamura A, Sato EF, Tamura T, Inoue M. *Helicobacter pylori* generates superoxide radicals and modulates nitric oxide metabolism. *J Biol Chem*, 1998; 273:14071-14073
- 51 Shapiro KB, Hotchkiss JH. Induction of nitric oxide synthesis in murin e macrophages by *Helicobacter pylori*. *Cancer Lett*, 1996; 102:49-56
- 52 Ambs S, Hussain SP, Harris CC. Interactive effects of nitric oxide and the p53 tumour suppressor gene in carcinogenesis and tumour progression. *FASEB J*, 1997;11:443-448
- 53 Forrester K, Ambs S, Lupold SE, Kapust RB, Spillare EA, Weinberg WC, Felley-Bosco E, Wang XW, Geller DA, Tzeng E, Billiar TR, Harris CC. Nitric oxide-induced p53 accumulation and regulation of inducible nitric oxide synthase expression by wild-type p53. *Proc Natl Acad Sci USA*, 1996;93:2442-2447
- 54 Tsuji S, Kawano S, Tsujii M, Takei Y, Tanaka M, Sawaoka H, Nagano K, Fusamoto H, Kamada T. *Helicobacter pylori* extract stimulates inflammatory nitric oxide production. *Cancer Lett*, 1996;108:195-200
- 55 Nilius M, Malfertheiner P. *Helicobacter pylori* enzymes. *Aliment Pharmacol Ther*, 1996;10(Suppl 1):65-71
- 56 O'Connor L, Strasser A. The Bcl-2 protein family. *Results Probl Cell Differ*, 1999;23:173-207
- 57 Chen G, Sordillo EM, Ramey WG, Reidy J, Holt PR, Krajewski S, Reed JC, Blaser MJ, Moss SF. Apoptosis in gastric epithelial cells is induced by *Helicobacter pylori* and accompanied by increased expression of BAK. *Biochem Biophys Res Commun*, 1997;239: 626-632
- 58 Clarke MR, Safatle-Ribeiro AV, Ribeiro U, Sakai P, Reynolds JC. bcl-2 protein expression in gastric remnant mucosa and gastric cancer 15 or more years after partial gastrectomy. *Mod Pathol*, 1997;10:1021-1027
- 59 Lauwers GY, Scott GV, Hendricks J. Immunohistochemical evidence of aberrant bcl-2 protein expression in gastric epithelial dysplasia. *Cancer*, 1994;73:2900-2904
- 60 Wagner S, Beil W, Westermann J, Logan RP, Bock CT, Trautwein C, Bleck JS, Manns MP. Regulation of gastric epithelial cell growth by *Helicobacter pylori*: evidence for a major role of apoptosis. *Gastroenterology*, 1997;113:1836-1847
- 61 Rudi J, Kuck D, Strand S, von Herbay A, Mariani SM, Krammer PH, Galle PR, Stremmel W. Involvement of the CD95 (APO-1/Fas) receptor and ligand system in *Helicobacter pylori*-induced gastric epithelial apoptosis. *J Clin Invest*, 1998;102:1506-1514
- 62 Bennett MW, O'Connell J, O'Sullivan GC, Roche D, Brady C, Kelly J, Collins JK, Shanahan F. Expression of Fas ligand by human gastric adenocarcinomas: a potential mechanism of immune escape in stomach cancer. *Gut*, 1999;44:156-162
- 63 Reddel RR. Genes involved in the control of cellular proliferative potential. *Ann NY Acad Sci*, 1998;854:8-19
- 64 Meyerson M. Telomerase enzyme activation and human cell immortalization. *Toxicol Lett*, 1998;102-103:41-45
- 65 Kuniyasu H, Domen T, Hamamoto T, Yokozaki H, Yasui W, Tahara H, Tahara E. Expression of human telomerase RNA is an early event of stomach carcinogenesis. *Jpn J Cancer Res*, 1997;88:103-107
- 66 Kameshima H, Yagihashi A, Yajima T, Watanabe N, Ikeda Y. *Helicobacter pylori* infection induces telomerase activity in premalignant lesions. *Am J Gastroenterol*, 1999;94:547-548
- 67 Chin L, Artandi SE, Shen Q, Tam A, Lee SL, Gottlieb GJ, Greider CW, De Pinho RA, Alderuccio F. p53 deficiency rescues the adverse effects of telomere loss and co-operates with telomere dysfunction to accelerate carcinogenesis. *Cell*, 1999;97:527-538
- 68 Beales IL, Davey NJ, Pusey CD, Lechler RI, Calam J. Long-term sequelae of *Helicobacter pylori* gastritis. *Lancet*, 1995;346:381-382
- 69 Azuma T, Ito S, Sato F, Yamazaki Y, Miyaji H, Ito Y, Suto H, Kuriyama M, Kato T, Kohli Y. The role of the HLA-DQA1 gene in resistance to atrophic gastritis and gastric adenocarcinoma induced by *Helicobacter pylori* infection. *Cancer*, 1998;82:1013-1018
- 70 Sakagami T, Dixon M, O'Rourke J, Howlett R, Alderuccio F, Vella J, Shimoyama T, Lee A. Atrophic gastric changes in both *Helicobacter felis* and *Helicobacter pylori* infected mice are host dependent and separate from antral gastritis. *Gut*, 1996;39:639-648
- 71 Ishida M, Gomyo Y, Ohfuji S, Ikeda M, Kawasaki H, Ito H. Evidence that expression of a mutated p53 gene attenuates apoptotic cell death in human gastric intestinal-type carcinomas *in vivo*. *Jpn J Cancer Res*, 1997;88:468-475

Search Article Keyword :

 PubMed  Submission  Abstract  PDF  Cited Click Count: **2544** Download Count: **421**

ISSN 1007-9327 CN 14-1219/R World J Gastroenterol 1999; October 5(5):375-382

## Diagnosis and treatment of gastroesophageal reflux disease in infants and children

Vandenplas Yvan

**Vandenplas Yvan**, Academisch Ziekenhuis Kinderen, Vrije Universiteit Brussel, Brussels, Belgium

Professor Yvan Vandenplas, male born on 1956-02-21 in Brussels, Belgium, graduated from the Free University of Brussels in 1981, and is now Head of the Department of Pediatrics, having more than 100 papers published.

**Correspondence to:** Vandenplas Yvan, MD, PhD., Academic Children's Hospital, Free University of Brussels, Laarbeeklaan 101, 1090 Brussels, Belgium

**Telephone:** 00-32-2-477-57-80/81, Fax. 00-32-2-477-57-83

**Received:** 1999-06-23

**Subject headings:** acid suppression; cisapride, endoscopy; esophagitis; gastroesophageal reflux; H<sup>2</sup>-receptor antagonist, pH monitoring; proton pump inhibitor

Vandenplas Y. Diagnosis and treatment of gastroesophageal reflux disease in infants and children.

World J Gastroenterol, 1999;5(5):375-382

Gastroesophageal reflux (GER) is a physiologic phenomenon occurring occasionally in every human being, especially during the postprandial period. Regurgitation occurs daily in almost 70% of 4-month-old infants and about 25% of their parents do consider regurgitation as "a problem" [1,2]. Indeed, it seems against logic that the normal function of the stomach would reflux ingested material back into the esophagus. Whether all infants presenting with regurgitation need drug treatment is a controversial question.

### DEFINITION

GER is best defined as the involuntary passage of gastric contents into the esophagus. The origin of the gastric contents can vary from saliva, ingested food and drinks, gastric, pancreatic to biliary secretions. Vomiting is used as a synonym for emesis, and means that the refluxed material comes out of the mouth "with a certain degree of strength" or "more or less vigorously", usually involuntary and with sensation of nausea. Regurgitation is used if the reflux dribbles effortlessly into or out of the mouth, and is mostly restricted to infancy (from birth to 12 months) [2,3]. Vomiting can be regarded as the top of the iceberg in its relation to the incidence of GER-episodes.

### CLINICAL PRESENTATION

Symptoms of reflux may be observed in normal individuals, but in those cases they are only found incidentally, and they occur more often and are more severe in pathological situations. The usual manifestations and unusual presentations of GER(-

disease) are listed in Table 1 [ 3 ]. Infants with a Roviralta Astoul syndrome have pyloric stenosis associated with hiatal hernia.

Emesis and regurgitation are the most common symptoms of "primary" GER-disease but they are also a manifestation of many other diseases [ 2,3 ]. Such "secondary" GER-disease can be caused by infections (e.g. urinary tract infection, gastroenteritis, etc.), metabolic disorders and especially food allergy [ 2,4 ]. On clinical grounds, "secondary" reflux may be difficult to separate from "primary" reflux. "Secondary" reflux is the result of a stimulation of the vomiting center in the dorsolateral reticular formation by all kinds of efferent and afferent impulses (visual stimuli, the olfactory epithelium, labyrinths, pharynx, gastrointestinal and urinary tracts, testes, etc.). "Secondary" GER is not further discussed in this paper. It is obvious that treatment of "primary" GER-disease should focus on motility and/or acid suppression, and that therapeutic management of "secondary" GER should focus on the etiologic phenomenon.

## PATIENT GROUPS

The following approach is a generalization that, like all generalizations, may need to be modified for an individual patient [ 3 ]. First, interest is focused on uncomplicated GER, mostly restricted to regurgitating infants. In a second paragraph, a proposal is made for optimal management in patients with complicated GER disease (symptoms suggestive of esophagitis). There is a continuum between normal infants with regurgitation and GER and those with severe GER which leads to disability, discomfort or impairment of function. An approach is proposed for the management of patients with atypical presentations of GER.

### **Group 1. Uncomplicated reflux: regurgitation**

Regurgitation may occur in children who are normal and do not have complaints of GER-disease such as nutritional deficits, esophagitis, blood loss, strabismus, apnea or airway manifestations. There is no difference in the incidence of regurgitation in breast-fed and formula-fed infants [ 5 ]. But, infants with uncomplicated regurgitation are frequently perceived by their parents as having a problem, and their parents often seek medical attention. The approach of the infants presenting with "excessive" regurgitation and of their parents has to be well balanced, and cannot be subject to overconcern or disregard. This group of patients are mostly restricted to infants younger than 6 months, or at the most 12 months [ 1,3,5 ]. A careful history, observation of feeding, and physical examination of the infant are mandatory. Although the following statement has not been thoroughly validated because randomization is not possible (only anxious parents seek medical help), it is rather unlikely that regurgitation will result in severe GER-disease. The effect of parental reassurance is suggested by many placebo-controlled studies showing a similar efficacy of placebo and the tested intervention [ 6,7 ]. If simple reassurance fails, dietary intervention is recommended, including restriction of the volume in clearly overfed babies, and change to a thickened "anti-regurgitation" formula [ 5-7 ]. Larger food volumes and high osmolality increase the number of transient lower esophageal sphincter (LES) relaxations and drifts to almost undetectable levels of LES-pressure [ 8 ]. Both are well known pathophysiologic mechanisms provoking GER in infants, which might also explain why feed thickeners sometimes aggravate their symptoms. The thickening of the formula, with starch (e.g. from rice, potato, etc.) or non-nutritive thickeners (bean gum), decreases the frequency and volume of regurgitation [ 5-7,9 ] (Table 2). Some of these "anti-regurgitation" formulae are casein-predominant (casein/whey 80/20%) to optimize the curd formation, while others contain 100% whey (hydrolysate) enhancing gastric emptying. However, the effect of these formulae on GER-parameters, when measured with pH monitoring

or scintigraphy are not convincing: most studies show that reflux parameters can improve, remain unchanged or worsen in approximately one third of infants for each possibility [6,7,10]. In other words, "anti regurgitation" formulae do what they claim to do: they reduce regurgitation [5-7] but they do not influence (acid) GER. Thickened formula also increases the duration of sleep [5,6]. Therefore, anti-regurgitation formula should be considered as the first step in medical treatment, and should only be available on prescription [3,5-7]. Anti-regurgitation formula and/or dietary intervention in general should be nutritionally safe [34]. However, regurgitation may be part of the spectrum of symptom(s) of GER-disease, necessitating an effective intervention to decrease the number and intensity of the GER-episodes. In this situation, an intervention that is limited to alleviate the presenting manifestation (regurgitation) will not suffice. Differentiation between regurgitation and (pathologic) vomiting can be difficult on clinical grounds, since there is a continuum between both conditions [5]. It is not always obvious in this patient group whether the parental complaints relate to physiological regurgitation or whether they suggest GER-disease. In practice, feed thickeners or special formula can not be given to breast-fed infants. Therefore, if the infant is breast-fed and/or in case of GER-disease, drug treatment with prokinetics should be considered prior to diagnostic procedures.

It seems reasonable to add medication such as prokinetics to the treatment of cases that are refractory to dietary intervention. They reduce regurgitation via their effects on the LES pressure and motility, esophageal peristalsis and gastric emptying [11]. For this reason, they interact with the pathophysiologic mechanisms of regurgitations in infants, which are related to immaturity of the gastroesophageal motor function [12]. A link between cisapride and increased salivary secretion has been demonstrated [13]. This indicates that, in combination with increased peristalsis and hence esophageal clearance, cisapride therapy may protect the esophagus via salivary components, such as bicarbonate and non-bicarbonate buffers, thus facilitating symptomatic relief and healing of the esophagus. Metoclopramide and domperidone have anti-emetic properties due to their dopamine-receptor blocking activity, whereas cisapride is a prokinetic acting through indirect release of acetylcholine in the myenteric plexus [11]. Although all three agents have been shown to reduce regurgitation in infants [6,7], data for cisapride are more convincing (Tables 3, 4). When compared to metoclopramide, cisapride appears to be more effective in reducing pH-metric [14], has a faster onset of action [15], and is better tolerated [15]. Cisapride has also been shown to heal oesophagitis [16]. Domperidone has been reported to be as effective as metoclopramide [17] (less effective than cisapride). Extrapyramidal reactions and increased prolactin levels are effects related to the dopamine-receptor blocking activity of these drugs. In case of cisapride, which is devoid of dopamine-blocking properties at therapeutic doses, the most common adverse effects are transient diarrhea and colic (in about 2%) [11,18]. The isolated reports of more serious adverse reactions, i.e., side-effects on the central nervous system, including extrapyramidal reactions and seizures (in epileptic patients), cholestasis (in extreme prematures) and cardiac interactions. Indeed, cisapride, which is metabolized by the cytochrome P450 3A4, has the potential to prolong the QT-interval [18]. However, an extensive review of the literature resulted in reassuring safety consensus statements [18]. To date, serious cardiac adverse reactions have not been reported in patients treated with a dosage within the recommended regimen (0.8mg/kg daily, max. 40mg/day) and in the absence of additional risk factors (Table 4). The association of cisapride with systemic or oral azole antifungals and

with macrolides is contraindicated. Bothazole-antifungals and macrolides interact with the cytochrome P450 3A4, resulting in elevated cisapride plasma levels. In view of its mode of action, efficacy and safety, as well as its lower or equal cost when compared to other therapeutic agents for GER, cisapride is recommended when dietary treatment fails or in regurgitating breast-fed infants, if therapy is indicated. It merits consideration that prokinetics stimulate a physiologic activity (peristalsis), while acid-suppressive medication inhibits a physiologic secretion.

**Table 1** Symptoms of GER(-disease)

Usual manifestations Specific manifestations	Symptoms possibly related to complications of GER*
Regurgitation Nausea Vomiting	Symptoms related to anaemia (iron deficiency anaemia) Haematemesis and melaena Dysphagia (as a symptom of oesophagitis or due to stricture formation) Weight loss and/or failure to thrive Epigastric or retrosternal pain "Non-cardiac angina-like" chest pain Pyrosis or heartburn, pharyngeal burning Belching, postprandial fullness Irritable oesophagus General irritability (infants)
Unusual presentations GER related to chronic respiratory disease (bronchitis, asthma, laryngitis, pharyngitis, etc.) Sandifer Sutcliffe syndrome Rumination Apnea, apparent life threatening event and sudden infant death syndrome	
Associated to congenital and/or central nervous system abnormalities Intracranial tumors, cerebral palsy, psychomotor retardation	

A number of these symptoms may also be caused by other mechanisms.

**Table 2**(PDF) Effect of special formula and milk-thickening products on GOR, gastric emptying (GE) and clinical parameters in infants with GOR disease (= : unchanged, < : worse, > : better)

<sup>a</sup>means of age in groups, <sup>b</sup>O: open, SB: single blind, XO: crossover, PA: parallel, <sup>c</sup>thickened meal (FT) vs unthickened meal (noFT) or vs baseline (B) or comparison of special formula, cn.d.: no data, N.S.: not significant.

**Table 3**(PDF) Effects of cisapride (CIS) on GOR disease in infants

<sup>a</sup>Age: mean(s) of age in group(s); <sup>b</sup>O: open; DB: double blind; PA: parallel; XO: cross-over with wash-out period; <sup>c</sup>CIS: cisapride; PLA: placebo; MCL: metoclopramide; DO: domperidone; CIM: cimetidine; GAV: Gaviscon; AA: antacid; FT: feed

thickener; B: baseline; CO: controls; bm: before meals/each feeding; afm: after meals; DM: dietary measures; SD: standard diet; dex: dextrose; glu: glucose; CF: customary formula; SF: solid food started if not yet done so; PN: parenteral nutrition; \*prior therapeutic measures continued (positional and/or dietary); e,f-Outcome: GOR, reflux parameters on pH monitoring; GE, gastric emptying; >, better than; <, worse than; =, unchanged, referring to the main/all parameters evaluated in paper; exceptions for single parameters are mentioned separately. Symptoms: if not specified, clinical assessment including regurgitation and/or vomiting. PLES: pressure lower esophageal sphincter. n.d.: no data.

**Table 4** Contraindications and risk factors for use of cisapride

<p>Contraindications to cisapride administration in pediatric patients</p> <ul style="list-style-type: none"> <li>-Combination with medication also known to prolong the QT interval or potent CYP3A4 inhibitors, such as astemizole, fluconazole, itraconazole, ketoconazole, miconazole, erythromycin, clarithromycin, troleandomycin, nefazodone, indinavir, ritonavir, josamycin, diphemanil, terfaridine.</li> <li>-Use of the above medications by a breast-feeding mother, as secretion in mother's milk of most of these drugs is unknown.</li> <li>-Known hypersensitivity to cisapride.</li> <li>-Known congenital long QT syndrome or known idiopathic QT prolongation.</li> </ul>
<p>Precautions for cisapride administration in pediatric patients</p> <ul style="list-style-type: none"> <li>-Prematurity (a starting dose of 0.1mg/kg, 4 times daily may be used, although 0.2mg/kg is also for pretermatures the normal dose)</li> <li>-Hepatic or renal failure (particularly when on chronic dialysis). In these cases, it is recommended to start with 50% of the recommended dose.</li> <li>-Uncorrected electrolyte disturbances (hypokalemia, hypomagnesemia, hypocalcemia), as may occur in pretermatures, in severe diarrhea, in treatment with potassium-wasting diuretics such as furosemide or acetazolamide.</li> <li>-History of significant cardiac disease including serious ventricular arrhythmia, second or third degree atrioventricular block, congestive heart failure or ischaemic heart disease, QT prolongation associated with diabetes mellitus.</li> <li>-History of sudden infant death in a sibling, and/or history of a "serious" apparent life threatening event in the infant or a sibling.</li> <li>-Intracranial abnormalities, such as encephalitis or haemorrhage, grape fruit juice.</li> </ul>

In the non-breast-fed infant, a change to a (thickened) hydrolysate or amino-acid formula should be considered, if regurgitation is resistant to a thickened formula with normal proteins and to prokinetics, since protein allergy may present as therapy-resistant GER-disease.

Non-drug treatment (positional therapy, dietary advice) can help convince the parents of the physiologic nature of the regurgitations [3]. The influence of position on the incidence and duration of GER episodes has been demonstrated in adults, children and infants both in asymptomatic healthy controls and symptomatic individuals. The 30° prone reversed Trendelenburg position is nowadays generally recommended and accepted as an essential element of treatment [3,6,7]. However, positional treatment is in practice very difficult to apply correctly in infants and rather unfriendly to the babies, since they have to be tied up in their beds or cot to prevent them from sliding down under the blankets, since an angle of 30° has to be achieved and maintained. The ample evidence that the prone sleeping position is a risk factor in sudden infant death,

independent of overheating, smoking or way of feeding [ 6 ] . Positional treatment remains, in view of its efficacy, a valid “adjuvant” treatment in patients not responding to other therapeutic approaches or beyond the age of sudden infant death [ 6 ] .

### **Group 2. Overt GER-disease**

Patients in this group did not either respond to the previous approach (parental reassurance, dietary treatment and prokinetics) or present with symptoms suggesting esophagitis (hematemesis, retrosternal, epigastric pain, etc.) (Table 1).

Therefore, an underlying anatomic malformation should be excluded, and endoscopy is the investigation of choice [ 3,19 ] . Upper gastrointestinal endoscopy in infants and children should only be performed by experienced and qualified physicians [ 19 ] .

If the question being asked is restricted to underlying anatomic malformations, upper gastrointestinal series can be considered [ 19 ] . If symptoms and/or the esophagitis do not improve despite adequate medical treatment and controlled compliance, upper gastrointestinal series should be performed to exclude anatomical problems such as gastric volvulus, intestinal malrotation, annular pancreas, etc.

Antacids are reported to be effective in the treatment of GER [ 6 ] , although experience is limited in infants. Their capacity to buffer gastric acid is strongly influenced by the time of administration [ 20 ] , and requires multiple doses. Gaviscon (a combination of an antacid and sodium salt of alginic acid) is as effective as antacids and appears to be relatively safe, since only a limited number of side effects have been reported. Occasional formation of large bezoar-like masses of agglutinated intragastric material has been reported with the use of Gaviscon, and it can increase the sodium content of the feeds to an undesirable degree especially in preterm infants (1g Gaviscon-powder contains 46mg sodium, and the suspension contains twice this amount of sodium) [ 6 ] .

H<sup>2</sup>-receptor antagonists, of which ranitidine is by far the mostly used, are effective in healing reflux esophagitis in infants and children [ 6 ] . Many new drugs have been developed (misoprostil, sucralfate, omeprazole, etc.). Of these, the proton pump inhibitors (PPIs) have been studied best, although experience in infants and children is limited [ 21,57 ] . PPIs are effective in suppressing the acidity in patients with gastric stress ulcer(s) and also in neurologically impaired children. Even in patients with circular esophageal ulcerations , recent experience suggests that PPIs should be given a chance prior to surgery [ 21 ] . Omeprazole is known to be effective in patients with severe esophagitis refractory to H<sup>2</sup> blockers [ 21 ] . Sucralfate was shown to be as effective as cimetidine for esophagitis in children [ 22 ] .

Immediate or early surgery is rarely indicated in life threatening conditions where medical management will be of no benefit. Surgery can be life-saving in severely affected patients (notably the neurologically impaired children with recurrent and life-threatening aspiration, etc.). Prior to surgery, a full diagnostic work-up including upper gastrointestinal series, endoscopy, pH monitoring, eventually completed with manometry and gastric emptying studies is recommended.

### **Group 3. Patients with unusual presentations of GER**

The most obvious difference between this patient group and groups 1 and 2, is that this patient group does not present with emesis and regurgitation (Table 1). Since these patients do not vomit, GER-disease is “occult”. Before considering GER as a cause of the symptoms, classic causes of the manifestations need to be excluded, such as allergy in a wheezing patient, tuberculosis in a patient with chronic cough, etc.

If GER-disease is suspected, pH monitoring of long duration (18-24 hours) is the investigation of choice. In this group of patients, pH monitoring may need to be performed in simultaneous combination with other investigations in order to relate pH changes to events (e.g. polysomnography in the infants presenting with an apparent life threatening event). In patients suspected of pulmonary aspiration, a scintigraphy might prove the association (although a negative scintigraphy does not exclude reflux related aspiration, and the therapeutic approach will be identical).

If pH monitoring is abnormal or if events are clearly related to pH changes, prokinetics, eventually in combination with H<sup>2</sup> receptor antagonists or PPIs, are indicated [ 19,21 ]. In this group, repeat pH monitoring under treatment conditions in combination with a clinical follow-up is mandatory. Depending on the unusual presentation, treatment can be stopped after 6 to 12 months, since a possible mechanism for GER in association with unusual manifestations may be self-perpetuating GER [ 23 ]. Once reflux occurs, acid gastric contents containing pepsin and sometimes bile comes into contact with the esophageal mucosa, which increases the esophageal permeability to acid and makes the esophageal mucosa much more susceptible to inflammatory changes. Esophageal inflammation, even restricted to the lower esophagus, impairs LES pressure and function, and favors GER [ 23 ].

### ***Severely neurologically impaired children***

The vast majority of neurologically impaired children suffer from severe GER-disease. Most of these children are under specialized follow-up, and only brief recommendations will be given here. The pathophysiological mechanism of GER-disease in these children is particularly multifactorial: the neurological disease itself (which might cause delayed esophageal clearance and delayed gastric emptying), the fact that most of these children are bedridden (gravity improves esophageal clearance), many are constipated (which increases abdominal pressure and favors GER), etc.

### **CONCLUSIONS**

The diagnostic approach of GER(-disease) in infants and children principally depends on its presenting features. Infants with typical symptoms of uncomplicated GER (the majority of regurgitating babies) should be treated without prior investigations. Endoscopy, in specialized centers, is recommended if esophagitis is suspected. Long-term esophageal pH monitoring is the investigation of choice and occupies a central position in the diagnostic approach of the patient suspected of unusual or atypical presentations of GER-disease ("occult" GER-disease). Non-drug treatment (the importance of parental reassurance cannot be stressed enough) and dietary treatment are an effective and safe approach in infant regurgitation, but does not treat GER-disease. If the symptoms are refractory to this approach, or in reflux-disease, cisapride is the drug of choice. PPIs or H<sup>2</sup>-receptor antagonists, in combination with prokinetics, are recommended in (ulcerative) esophagitis. There is no excuse to persist with an ineffective management of a disease which might result in stunting, chronic illness, persistent pain, esophageal scarring or even death. Management of GER(-disease) in infants and children should therefore be well overthought, avoiding overinvestigations and overtreatment of a self-limiting condition, but also avoiding underestimation of potential severe disease, accompanied by serious morbidity.

### **REFERENCES**

- 1 Nelson SP, Chen EH, Syniar GM, Christoffel KK. Prevalence of symptoms of gastroesophageal reflux in infancy. *Arch Pediatr Adolesc Med*, 1997;151:569-572
- 2 Orenstein S. Gastroesophageal reflux. In: Hyman PE, ed. *Pediatric gastrointestinal motility disorders*. New York: Academy Professional Information Services, 1994:55-88
- 3 Vandenplas Y, Ashkenazi A, Belli D, Boige N, Bouquet J, Cadranel S, Cezard JP, Cucchiara S, Dupont C, Geboes K, Gottrand F, Heymans HSA, Jasinski C, Kneepkens CMF, Koletzko S, Milla P, Mougenot JF, Nussle D, Navarro J, Newell SJ, Olafsdottir E, Peeters S, Ravelli A, Polanco I, Sandhu BK, Tolboom J. A proposition for the diagnosis and treatment of

- gastroesophageal reflux disease in children: a report from a working group on gastroesophageal reflux disease. *Eur J Pediatr*, 1993;152:704-711
- 4 Carvariao F, Iacono G, Montalto G, Soresi M, Tumminello M, Carroccio A. Clinical and pH metric characteristics of gastroesophageal reflux secondary to cow's milk protein allergy. *Arch Dis Child*, 1996;75:51-56
  - 5 Vandenplas Y, Lifshitz JZ, Orenstein S, Lifshitz CH, Shepherd RW, Casaubon PR, Muinos WI, Fagundes-Neto U, Aranda JAC, Gentles M, Santiago JD, Vanderhoof J, Yeung CY, Moran R, Lifshitz F. Nutritional management of regurgitation in infants. *J Am Col Nutr*, 1998;17:308-316
  - 6 Vandenplas Y, Belli D, Benhamou P, Cadranel S, Cezard JP, Cucchiara S, Dupont C, Faure C, Gottrand F, Hassall E, Heymans H, Kneepkens CMF, Sandhu B. A critical appraisal of current management practices for infant regurgitation-recommendations of a working party. *Eur J Pediatr*, 1997;156:343-357
  - 7 Vandenplas Y, Belli D, Cadranel S, Cucchiara S, Dupont C, Heymans H, Polanco I. Dietary treatment for regurgitation-recommendations from a working party. *Acta Paediatr*, 1998;87:462-468
  - 8 Cucchiara S, De Vizia B, Minella R, Calabrese R, Scoppa A, Emiliano M, Iervolino C. Intragastric volume and osmolality affect mechanisms of gastroesophageal reflux in children with GOR disease. *J Pediatr Gastroenterol Nutr*, 1995;20:468 (abstract)
  - 9 Borelli O, Salvia G, Ampanozzi A, Franco MT, Moreira FL, Emiliano M, Campa nozzi F, Cucchiara S. Use of a new thickened formula for treatment of symptomatic gastroesophageal reflux in infants. *Ital J Gastroenterol Hepatol*, 1997;29: 237-242
  - 10 Vandenplas Y. Clinical use of cisapride and its risk-benefit in paediatric patients. *Eur J Gastroenterol Hepatol*, 1998;10:871-881
  - 11 Verlinden M, Welburn P. The use of prokinetic agents in the treatment of gastro-intestinal motility disorders in childhood. In: Milla PJ, ed. *Disorders of gastrointestinal motility in childhood*. John Wiley & Sons Ltd, 1988:125-140
  - 12 Boix-Ochoa J. The physiologic approach to the management of gastric esophageal reflux. *J Pediatr Surg*, 1986;21:1032-1039
  - 13 Heading RC, Baldi F, Holloway RH, Janssens J, Jian R, McCallum RW, Richter JE, Scarpiagnato C, Sontag S, Wienbeck M. Prokinetics in the treatment of gastro-oesophageal reflux disease. *Eur J Gastroenterol Hepatol*, 1998;10:1-7
  - 14 Rode H, Stunden RJ, Millar AJW, Cywes S. Esophageal assessment of gastroesophageal reflux in 18 patients and the effect of two prokinetic agents: cisapride and metoclopramide. *Pediatr Surg*, 1987;22:931-934
  - 15 Mundo F, Feregrino H, Fernandez J, Teramoto O, Abord P. Clinical evaluation of gastroesophageal reflux in children: double-blind study of cisapride vs metoclopramide. *Am J Gastroenterol*, 1990;85:A29
  - 16 Cucchiara S, Staiano A, Capozzi C, Di Lorenzo C, Bocchieri A, Auricchio S. Cisapride for gastroesophageal reflux and peptic oesophagitis. *Arch Dis Child*, 1987;62:454-457
  - 17 De Loore I, Van Ravensteyn H, Ameryckx L. Domperidone drops in the symptomatic treatment of chronic paediatric vomiting and regurgitation. A comparison with metoclopramide. *Postgrad Med J*, 1979;55(S1):40-42
  - 18 Vandenplas Y, Belli DC, Benatar A, Cadranel S, Cucchiara S, Dupont C, Gottrand F, Hassall E, Heymans HSA, Kearns G, Kneepkens CMF, Koletzko S, Milla P, Polanco I, Staiano AM. The role of cisapride in the treatment of paediatric gastro-oesophageal reflux. *J Pediatr Gastroenterol Nutr*, 1999;28:518-528
  - 19 Vandenplas Y, Ashkenazi A, Belli D, Blecker U, Boige N, Bouquet J, Cadranel S, Cezard JP, Cucchiara S, Devreker T, Dupont C, Geboes K, Gottrand F, Heymans HSA, Jasinski C, Kneepkens CMF, Koletzko S, Milla P, Mougnot JF, Nussle D, Navarro J, Newell SJ, Olafsdottir E, Ravelli A, Polanco I, Sandhu BK, Tolboom J. Reflux oesophagitis in infants and children. *J Pediatr Gastroenterol Nutr*, 1994;18:413-422
  - 20 Sutphen JL, Dilalrd VL, Pipan ME. Antacid and formula effects on gastric acidity in infants with gastroesophageal reflux. *Pediatrics*, 1986;78:55-57

- 21 Israel DM, Hassall E. Omeprazole and other proton pump inhibitors: pharmacology, efficacy and safety with special reference to use in children. *J Pediatr Gastroenterol Pediatr*, 1998;27:568-579
- 22 Arguelles-Martin F, Gonzalez-Fernandes F, Gentles MG, Navarro-Merino M. Sucralfate in the treatment of reflux esophagitis in children: preliminary results. *Scand J Gastroenterol*, 1989;156:S43-S47
- 23 Vandeplass Y. Physiopathological mechanisms of gastroesophageal reflux: is motility the clue? *Rev Med Brux*, 1994;15:7-9
- 24 Sutphen JL, Dillard VL. Dietary caloric density and osmolarity influence gastroesophageal reflux in infants. *Gastroenterology*, 1989;97:601-604
- 25 Tolia V, Lin S, Kuhns LR. Gastric emptying using three different formulas in infants with gastroesophageal reflux. *J Pediatr Gastroenterol Nutr*, 1992;15:297-301
- 26 Vandeplass Y, Sacre L, Loeb H. Effects of formula feeding on gastric acidity time and oesophageal pH monitoring data. *Eur J Pediatr*, 1988;148:152-154
- 27 Bailey DJ, Andres JM, Danek GD. Lack of efficacy of thickened feeding as treatment for gastroesophageal reflux. *J Pediatr*, 1987;110:187-190
- 28 Orenstein SR, Magill HL, Brooks P. Thickening of infant feedings for therapy of gastroesophageal reflux. *J Pediatr*, 1987;110:181-186
- 29 Orenstein SR, Shalaby TM, Putman PE. Thickened feedings as a cause of increased coughing when used as therapy for gastroesophageal reflux in infants. *J Pediatr*, 1992;913-915
- 30 Ramenofsky ML, Leape LL. Continuous upper esophageal pH monitoring in infants and children with gastroesophageal reflux, pneumonia and apneic spells. *J Pediatr Surg*, 1981;16:374-378
- 31 Vandeplass Y, Sacre L. Gastro-oesophageal reflux in infants: evaluation of treatment by pH monitoring. *Eur J Pediatr*, 1987;146:504-507
- 32 Vandeplass Y, Sacre L. Milk-thickening agents as a treatment for gastroesophageal reflux. *Clin Pediatr*, 1987;26:66-68
- 33 Vandeplass Y, Hachimi-Idrissi S, Casteels A, Mahler T, Loeb H. A clinical trial with an anti-regurgitation formula. *Eur J Pediatr*, 1994;153:419-423
- 34 Brueton MJ, Clarke GS, Sandhu BK. The effects of cisapride on gastro-oesophageal reflux in children with and without neurological disorders. *Dev Med Child Neurol*, 1990;32:629-632
- 35 Carrasco S, Lama R, Prieto G, Polanco I. Treatment of gastroesophageal reflux and peptic oesophagitis with cisapride. In: Heading RC, Wood JD (eds) *Gastrointestinal dysmotility: focus on cisapride*. New York: Raven Press, 1992:326-327
- 36 Carrocio A, Iacono G, Voti L. Gastric emptying in infants with gastroesophageal reflux. Ultrasound evaluation before and after cisapride administration. *Scand J Gastroenterol*, 1992;27:799-804
- 37 Castro HE, Ferrero GB, Cortina LS, Salces C, Lima M. Efectividad del cisapride en el tratamiento del reflujo gastroesofagico (RGE) en niños. Valoración de un estudio a doble ciego. *An Espagnol Pediatr*, 1994;40:5-8
- 38 Cucchiara S, Staiano A, Capozzi C, Di Lorenzo C, Bocchieri A, Auricchio S. Cisapride for gastroesophageal reflux and peptic oesophagitis. *Arch Dis Child*, 1987;62:454-457
- 39 Cucchiara S, Staiano A, Bocchieri A, Manzi G, Camerlingo F, Paone FM. Effects of cisapride on parameters of oesophageal motility and on the prolonged intra-oesophageal pH test in children with gastroesophageal reflux disease. *Gut*, 1990;31:21-25
- 40 Daoud G, Gonzalez L, Medina M, Stanzione C, Abraham A, Puig M, Daoud N, Martinez M. Efficacy of cisapride in infants with apnea and gastroesophageal reflux evaluated by prolonged intraesophageal pH monitoring. 2nd UEGW, Barcelona, Spain, 19-23/07/1993, A107
- 41 Daoud G, Stanzione C, Abraham A, Lopez C, Henriquez S, Dahdah J, Puig M, Daoud N. Response to cisapride in children with respiratory symptoms and gastroesophageal reflux evaluated by prolonged intraesophageal pH monitoring.

- 2nd UE GW, Barcelon, Spain, 19-23/07/1993, A108
- 42 Evans DF, Ledingham SJ, Kapila L. The effect of medical therapy on gastroesophageal reflux disease in children. World Congresses of Gastroenterology, Sydney, Australia, 26-31/08/1990, A53
- 43 Greally P, Hampton FJ, MacFadyen UM, Simpson H. Gaviscon and carobel with cisapride in gastroesophageal reflux. Arch Dis Child, 1992;67:618-621
- 44 Iacono G, Carrocio A, Montalto G. Valutazione dell' efficacia della cisapride nel trattamento del reflusso gastroesofageo. Minerva Pediatr, 1992 ;44:613-616
- 45 Malfoot A, Vandenplas Y, Verlinden M, Piepsz A, Dab I. Gastroesophageal reflux and unexplained chronic respiratory disease in infants and children. Pediatr Pulm, 1987;3:208-213
- 46 Mundo F, Feregrino H, Fernandez J. Clinical evaluation of gastroesophageal reflux in children: double-blind study of cisapride vs metoclopramide. Am J Gastroenterol, 1990;85:A29
- 47 Rode H, Stunden RJ, Milar AJW, Cywes S. Pharmacologic control of gastroesophageal reflux in infants with cisapride. Pediatr Surg, 1987;22:931-934
- 48 Rode H, Millar AJW, Melis J, Cewis S. Pharmacological control of gastroesophageal reflux with cisapride in infants: long-term evaluation. In: Heading RC, Wood JD, eds. Gastrointestinal dysmotility: focus on cisapride. New York: Raven Press, 1992:325
- 49 Saye Z, Forget PP. Effect of cisapride on esophageal pH monitoring in children with reflux-associated bronchopulmonary disease. J Pediatr Gastroenterol Nutr, 1989;9:28-33
- 50 Saye Z, Forget PP, Geubelle F. Effect of cisapride on gastroesophageal reflux in children with bronchopulmonary disease: a double-blind crossover pH monitoring study. Pediatr Pulm, 1987;3:8-12
- 51 Vandenplas Y, Deneyer M, Verlinden M, Aerts T, Sacre L. Gastroesophageal reflux incidence and respiratory dysfunction during sleep in infants: treatment with cisapride. J Pediatr Gastroenterol Nutr, 1989;8:31-36
- 52 Vandenplas Y, de Roy C, Sacre L. Cisapride decreases prolonged episodes of reflux in infants. J Pediatr Gastroenterol Nutr, 1991;12:44-47
- 53 Van Eygen M, Van Ravenstein H. Effect of cisapride on excessive regurgitation in infants. Clin Ther, 1989;11:669-677
- 54 Scott RB, Ferreira C, Smith L, Jones AB, Machida H, Lohoues MJ, Roy CC. Cisapride in pediatric gastroesophageal reflux. J Pediatr Gastroenterol Nutr, 1997;25:499-506
- 55 Cohen RC, O'Loughlin EV, Davidson GP, Moore DJ, Lawrence DM. Cisapride in the control of symptoms in infants with gastroesophageal reflux: a randomized, double-blind, placebo-controlled trial. J Pediatr, 1999;134:287-292

[Reviews](#)[Add](#)[more>>](#)[Related Articles:](#)[more>>](#)

# Reassessment of barium radiographic examination in diagnosing gastrointestinal diseases

CHEN Jiu-Ru

**Subject headings** gastrointestinal radiography; gastrointestinal diseases/radiography; barium radiographic examination

Gastrointestinal radiography (GIR) has been a major and first-choice method for diagnosing gastrointestinal diseases with barium as contrast media since its emergence in 1910, even in diagnosing the mass lesions of the organs outside gastrointestinal tract (e.g., liver, pancreas, etc) indirectly. The fiber endoscopy invented in the late 1960s can directly observe the changes on mucosal surface intraluminally and obtain biopsies as well, thus greatly improving the detection and sensitivity of small, shallow or tiny lesions originated from mucosa. This discovery is a big challenge to GIR, which has not only profoundly modified the dominant role of GIR in diagnosing gastrointestinal diseases, but also aroused different viewpoints and evaluations even more radically<sup>[1]</sup>. According to the data collected from 69 radiologic units during the 12 years by the American Society of Gastrointestinal Radiography, the number of upper GIR decreased by 24%, colon examinations decreased by 29%, averaging 25%<sup>[2]</sup>. The situation is similar domestically. Some GI radiologists even gave up their experienced studies in GIR. Young radiologists are just eager to study the new inventions such as CT and MR, and neglect GI. All those interfered with and even lowered the quality and quantity of GIR. This is one aspect of the problem.

On the other hand, the invention of endoscopy has positive influence on GIR. It has made many GI radiologists realize that lots of diseases can not be detected with the single contrast GIR, which can not meet the demand of therapy and must be improved. In the 1960s, Japanese scholars developed and created the brand new double-

contrast GI technique on the basis of the traditional single-contrast GIR<sup>[3]</sup>, meanwhile, through studies on barium contrast media, assistant agents (mucus detergent, gas agent)<sup>[4,5]</sup>, radiologic technique, the methods and the principles of imaging<sup>[6,7]</sup>, great achievements in practice and theory have been made (Figure 1)<sup>[8]</sup>. The double-contrast GIR became the universal method in the 1980s, the sensitivity of double-contrast GIR in diagnosing early cancer<sup>[9,10]</sup>, superficial erosion and linear ulcer become higher and higher<sup>[11]</sup>. It made it possible to observe the locations such as cardia which can be hardly shown by single-contrast GIR much easier for diagnosis<sup>[12,13]</sup>, thus re-establishing the status of GIR with high prestige. But it is a regret that this achievement could not be popularized nationwide.

The multiphase gastrointestinal radiography (MPGIR) can not only diagnose shallow mucosal lesions as endoscopy, but also has its own special effects that other approaches can not possess in diagnosing gastrointestinal diseases<sup>[14]</sup>.

## AN IDEAL FIRST-CHOICE DIAGNOSTIC MODALITY FOR GI TRACT

It has been well known that the different diseases of gastrointestinal tract usually present the similar symptoms, which are atypical. Clinical doctors can hardly ascertain the exact location of the lesions when making the diagnoses, and the physical diagnostic approaches are usually necessary. The symptoms caused by these lesions include the following aspects: most of them originated from the mucosa of the gastrointestinal tract, such as inflammation, erosion, ulcer and cancer, etc. (Figure 2); some originated from the submucosa, such as nonepithelial (e.g. smooth muscle, fat and nerve) benign or malignant tumors<sup>[15]</sup>; some are functional disorders<sup>[16]</sup>, such as reflux disorder, achalasia etc.; some are of organic deformation, such as various kinds of organ volvulus, diverticulum and hernia; and some originated from outside gastrointestinal tract (e.g., pancreas, gall bladder, ovarium and uterus). It is doubtless that the first choice for physical diagnosis is to judge several aspects of these lesions mentioned above simultaneously. MPGIR which possesses the advantage of both single-contrast and double-contrast GIR, can not only examine organ morphologic changes caused by the diseases

Department of Radiology, Zha Bei Central Hospital, Shanghai 200070, China

Dr. CHEN Jiu-Ru, male, born on 1932-12-11 in Shanghai, graduated from Shanghai Medical University in 1959, now chief radiologist, Shanghai Zha Bei Central Hospital, professor and tutor of the Shanghai Railway University Medical College, Deputy Editor-in-Chief of the "Chinese Journal of Medical Computed Imaging", specialized in gastrointestinal radiology, having more than 40 papers published as the first author and 4 books (one book as coeditor-in-chief).

**Correspondence to:** Dr. CHEN Jiu-Ru, Zha Bei Central Hospital, 619 Zhong Hua Xin Road, Shanghai 200070, China  
Tel. +86-21-56628584 Ext.2831, Fax.+86-21-63177683

**Received** 1999-01-20 **Revised** 1999-05-10

themselves or adjacent organs, but also identify organic functional changes. It can satisfactorily perform various examinations for the whole gastrointestinal tract, including multiphasic hypotonic upper gastrointestinal radiography, small bowel enema SBE, GI series, and double contrast enema DCE. That can meet the demand of clinical doctors as the first choice examination.

#### AN OVERALL DIAGNOSTIC MODALITY FOR GI TRACT

For the needs of planning the therapy and predicting prognosis correctly, four targets must be considered: site, sickness (qualitative determination), structure (quantitative determination), staging. That is the so called four "S" diagnosis. The basis of four "S" diagnosis is pathomorphologic and pathophysiologic changes<sup>[17]</sup>. All of the physical examination approaches (endoscopy, radiography, ultrasonography and endoscopic ultrasonography, MR, etc.) are all expected to reflect the pathologic changes objectively, and all kinds of examination methods must be based on these criteria.

Refined MPGIR, which can obtain a complete view of the motion, the adoption, the ejection of organs and the pathophysiologic situation of the diseases, especially the location, shape, pathologic changes (different size, degree and extent) caused by mucosal or submucosal lesions, is superior to other techniques<sup>[18]</sup>.

##### *To detect the lesion-site*

With full use of filling phase and double-contrast phase, MPGIR can easily obtain a complete view of the organ. Based on this, it can detect the abnormality of organ location, size and shape, making it easy to diagnose organ volvulus, diverticulum, hernia and so on<sup>[14]</sup>. According to the different organic changes caused by the lesions and the correlation between lesions and organs, MPGIR can clearly establish the origination (such as from the organ itself, the intramural or the extramural) of lesions for most of the patients. It can also show the pattern of lesions, whether protruding or depressing or both.

##### *To determine the nature of the lesion-sickness*

The nature of the lesion of gastrointestinal tract can be determined by its specific signs which appears in MPGIR under different contrast conditions (filling, mucosal, double-contrast, compressed phase) (Figure 3). Many these effective signs have been found by the radiologists, such as "bull eyes sign" indicating submucosal leiomyoma, "target sign" meaning erosion, "dimness, coarse, rigid sign" hinting malignant tumor, "step-like mucosal pattern" suggesting early gastric cancer, etc<sup>[8]</sup>. The

better technical quality the more truthful image and the more specific appearance the more accurate diagnosis<sup>[15,19,20]</sup>.

##### *To identify the degree of the lesion-structure*

Inflated by gas, the lesion outlined by barium is very clear and complete in MPGIR. It is very valuable for judging the size, extent and structure of lesions<sup>[14]</sup>. For example, in Borrmann's type I cancer, it can clearly provide the overview of the size and the shape of the tumor protruded into the lumen, and can also obviously survey the gastric wall involved by the tumor, which is beneficial for surgery (Figure 4). Multiple primary carcinoma (MPC) of gastrointestinal tract is not rare, it can occur at either the same organ, such as multiple esophageal carcinomas, multiple gastric carcinomas or different organs, such as multiple esophagogastric carcinomas and multiple esophagogastric carcinomas<sup>[21]</sup>. Preoperative discovery and diagnosis of all these lesions are especially important. It is less difficult to make diagnosis for MPGIR if more attention is paid to it. Nevertheless, other physical diagnostic approaches can hardly detect all the lesions, which might cause fatal results. For diagnosing gastrointestinal benign or functional disorders, the concept of "structure" still exists, such as evaluating the number and the size of ulcers, the type and the volume of reflux by using MPGIR.

##### *To ascertain the stage of the lesion-staging*

MPGIR can sometimes ascertain the stage of the lesion in diagnosis. A niche suggests "active period" of the ulcer, a linear barium shadow means "healing period", and a scar formation indicates "healed period" of the ulcer (Figure 5)<sup>[11]</sup>. To stage of carcinoma, the present signs can be used for initial judgement, for example, the special changes of mucosal folds imply early cancer, the "stiff gastric wall" sign suggests advanced cancer (Figure 6)<sup>[8]</sup>. However, the preoperational staging of cancers should be combined with CT examination<sup>[17,22]</sup>.

#### THE INNOVATION OF GASTROINTESTINAL (GI) RADIOGRAPHY TECHNIQUE

The traditional GI radiography has experienced the following periods: local-controlled fluoroscopic radiography, remote-controlled image intensifier, TV display, spot film<sup>[1]</sup>, etc. In recent years, with the development of high-speed and high-efficiency computer, radiologic diagnosis has gradually become a new filmless technique using digital and postprocessing imaging systems. Digital GI imaging set on the basis of satisfactory double contrast GI technique possesses many advantages as follows which routine spot-film and fluororadiography do not have<sup>[23,24]</sup>.

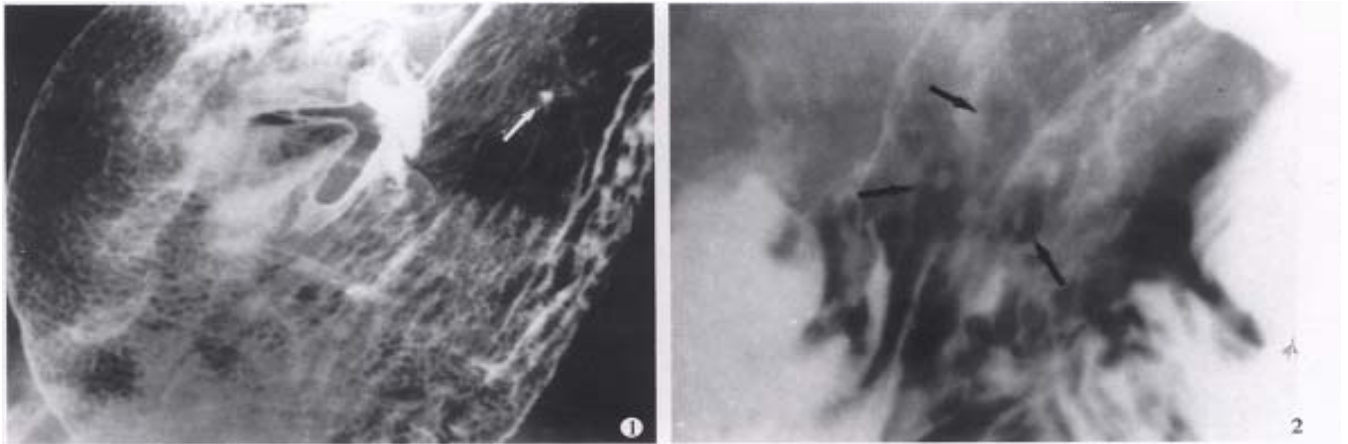


**Figure1** Areae gastricae. Well-circumscribed polygonal radiolucencies surrounded by barium-filled shallow grooves are clearly seen on the mucosal surface. A small benign ulcer is also displayed (arrowhead).

**Figure2** Erosive gastritis. Multiple varioliform erosions (arrows) in the posterior wall of gastric body are seen as tiny barium collections with surrounding halos of edematous mucosa-“target” sign.

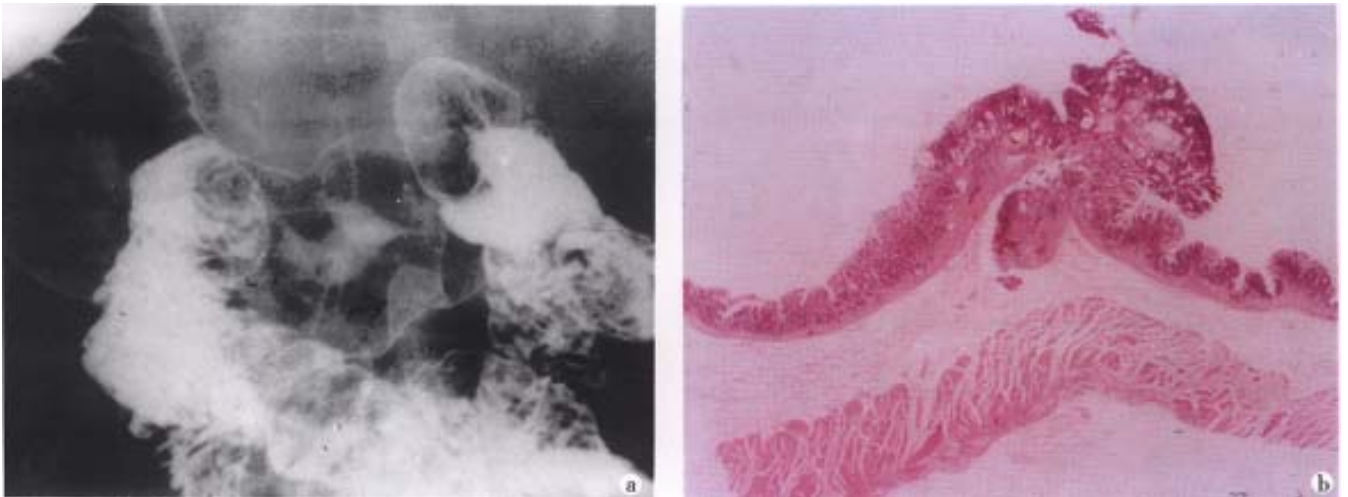


**Figure3** Small early gastric cancer (type I). A sessile protruded lesion (5mm in size) with its base puckered into the lumen is seen on the greater curvature of antrum. B. Micrograph shows the lesion originates from mucosa and infiltrates to the submucosal layer.

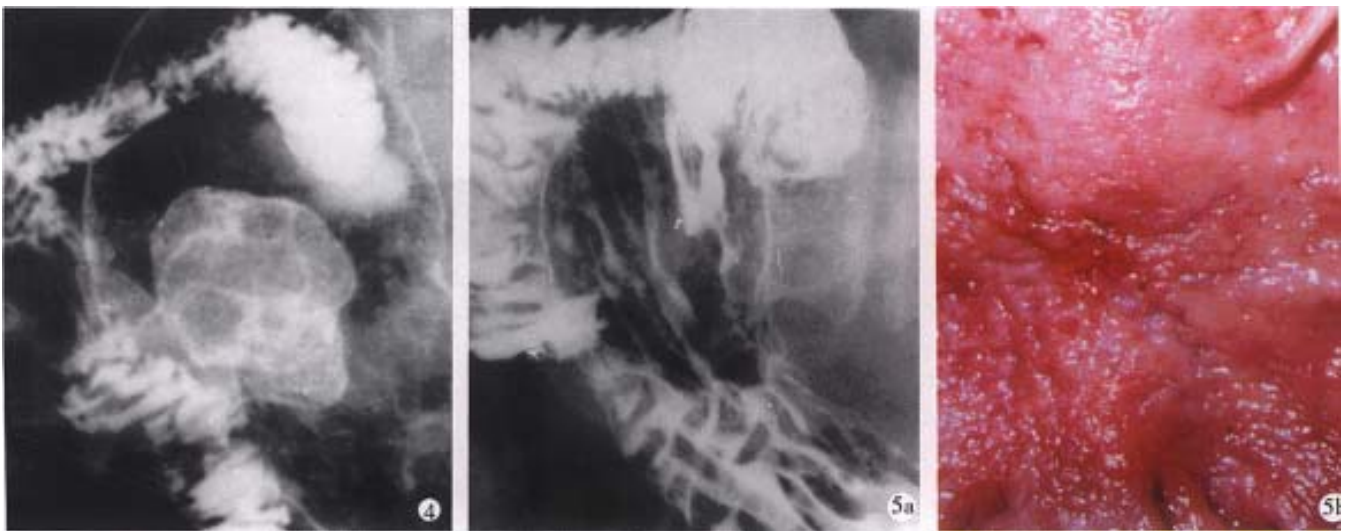


**Figure4** Gastric carcinoma (Borrmann’s type I). A bulky cauliflower-like mass etched in white by a thin layer of barium is seen on the greater curvature of the stomach.

**Figure5** Linear ulcer. A long linear ulcer paralleled to the lesser curvature (arrowhead) shown on the gastric posterior wall, representing the healing and healed stage of ulcer. B. Macrograph shows that the fine curve linear ulcer is composed of re-epithelialized (healed) and granulating part (healing).

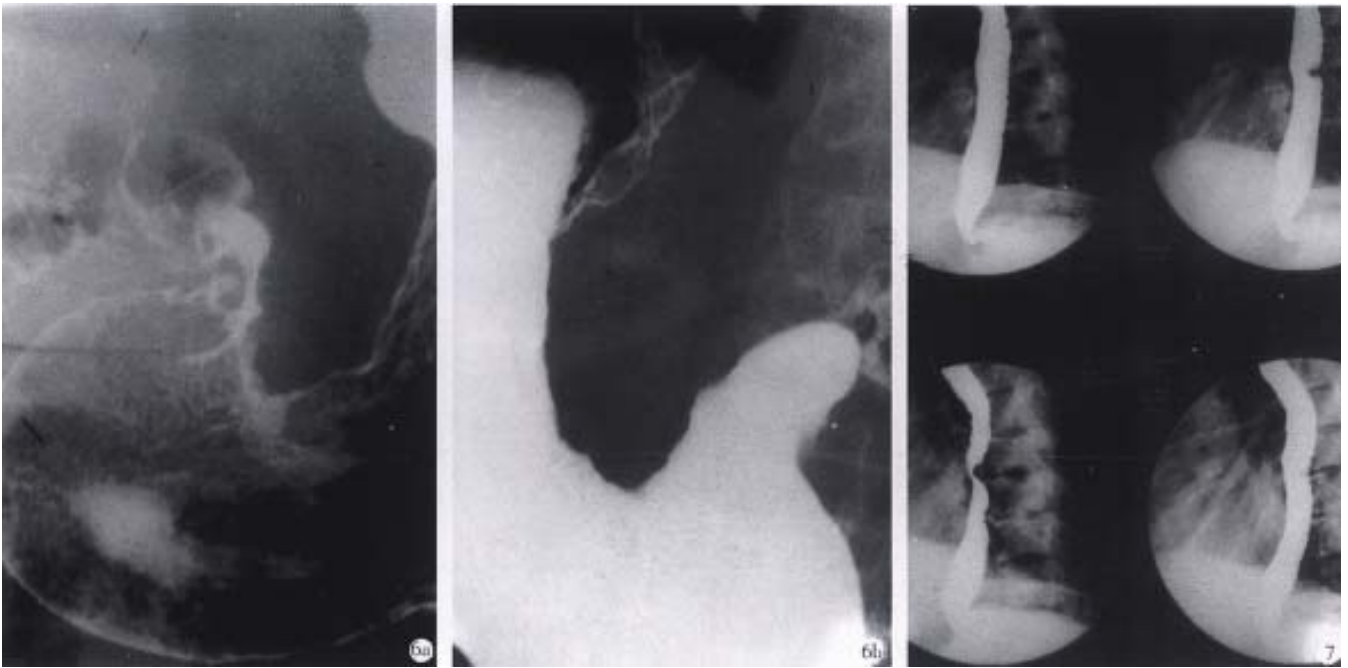


**Figure 6** Advanced gastric carcinoma. A. Double-contrast phase. B. Filling phase reveal marked "rigid" and "coarse" contour of the lesser curvature and lumen narrowing caused by infiltrative carcinoma.

**Figure 7** Digital esophageal barium radiography. The defect on posterior aspect of middle esophagus caused by the proliferation of thoracic vertebrae is easily displayed by rapid sequence images (0.5 picture s/sec) and results in dysphagia clinically.

### **Rapid sequence (0.5-15 pictures/sec) images**

Rapid sequence images is very helpful for surveying the moving gastrointestinal tract, especially in the oral pharynx and the upper esophagus. As sufficient esophageal dilatation and mucosa coating can only keep on comparatively a short time, with the pulsation of heart, the high-quality D.C. films are not easy to acquire. Digital sequence exposure (0.5-2 pictures/sec) which can overcome these deficiencies, is obviously better than traditional imaging technique, for obtaining multiphase images of esophagus (Figure 7)<sup>[25]</sup>.

### **Quality control for the study**

Every continuous picture can be accommodated on the monitor as a "frozen image", until the next fluoroscopy begins. It can give the operator a clue whether the lesion is displayed satisfactorily<sup>[24]</sup>. If not, the doctor can adopt their apt procedure: changing projective position, mucosa recoating, and some more digital images in order to avoid the lesions missed due to slipshod examinational technique. Therefore, it can guarantee the quality of MPGIR, and increase the detectability of lesions.

### **Postprocessing**

Digital imaging is not the same as the routing radiography, which can change the parameters in

workstation, regulate the brightness and contrast of the picture, magnify the interesting area, adjust the edge enhancement, and annotate and print findings, and enter the picture archiving and communication system (PACS). All of these are making MPGIR enter into a brand new information era.

In summary a high-quality MPGIR can not only diagnose gastrointestinal diseases or disorders, but also make more complete judgement at the aspects of "site", "sickness", "structure" and "stage" provided by MPGIR<sup>[14,18,22]</sup>. It is characterized by its own speciality and advantages: the convenient operation, and less sufferings caused to patients. So, it is still an important and the first choice examination. Both MPGIR and endoscopy must be adopted in a complementary manner to make up each other's deficiencies, but not to be replaced one another. Of course, it is essential to maintain and improve the quality of MPGIR constantly. It is gratifying that the use of MPGIR examinations is increasing by 9.8% after 1996 in spite of its decline in the earlier 1990s according to the data from three big comprehensive hospitals in Shanghai. The current gastrointestinal radiology is one of the valuable medical treasures accumulated by many generations of scientists<sup>[8]</sup>. We should practise it continuously and explore, develop and improve it constantly, and do our best to contribute to gastrointestinal radiology.

## REFERENCES

- 1 Amberg JR. Radiology (stomach and duodenum). *Curr Opin Gastroenterol*, 1989;5:813-816
- 2 Gelfand DW, Ott DJ, Chen YM. Decreasing numbers of gastrointestinal studies: report of data from 69 radiologic practices. *AJR*, 1987;148:1133-1136
- 3 Chen JR. Single and double contrast gastric barium studies. *J Clin Radiol*, 1989;8:253-255
- 4 Chen JR, Zhang GL. Clinical investigation on the application of "654-2" and its adverse reactions during double contrast gastrointestinal studies. *Chin J Radiol*, 1992;26:692-695
- 5 Fan J, Shen TZ, Wang HT, Zhou ML. Experimental researches on flocculation and antiflocculation of double contrast barium sulfate preparation. *J Clin Radiol*, 1984;3:125-127
- 6 Shang KZ, Chen JR, Jio TD, Ji BQ, Huang JH, Tan YM, Guo MJ. Investigation on characteristic appearances of lesions located in ab gravitational wall (AW) of stomach and colon in double contrast barium examination. *Chin J Radiol*, 1993;27:462-466
- 7 Shang KZ, Yu X, Guo MJ. An experimental study on the mechanism of gastrointestinal double contrast image formation and its clinical application. *Chin J Radiol*, 1985;19:197-200
- 8 Shang KZ, Chen JR (ed). Principle and diagnosis of gastrointestinal radiography. Shanghai: Shanghai Scientific and Technical Publisher, 1995:23-88
- 9 Chen JR, Jiang H, Zhang GW, Shen MJ, Zhang TQ. Radiological diagnosis of early gastric carcinoma (protruded lesion-type I). *J Clin Radiol*, 1994;13(Suppl2):197-200
- 10 Chen JR, Zu MH, Ling Y, Zhang GL, Shi KX, Tu JT, Hu JQ. Mass survey of gastric carcinoma by X-ray screening. *Chin J Radiol*, 1989;23(Suppl):1-5
- 11 Chen JR, Zhan GL. The radiological investigation of gastrointestinal linear ulcer and its pathological process. *Chin J Radiol*, 1994;28:704-706
- 12 Chen JR, Lu J, Yang QK. Double contrast X-ray examination of esophagogastric junction. *J Clin Radiol*, 1988;7:125-128
- 13 Chen JR, Shang KZ, Zhang FX, Sun CL, Song J. X-ray diagnosis of varices in gastric fundus. *J Clin Radiol*, 1987;6:119-122
- 14 Chen JR, Chen XR. The evaluation of four-phasic gastric radiographic examination. *Shanghai Med J*, 1985;8:406-409
- 15 Chen JR, Lu J, Yang CR, Xu BY, Wang Y, Diao WK, Shen JG. The X-ray diagnosis and signs of gastric benign tumors. *J Clin Radiol*, 1984;3:61-64
- 16 Chen JR. Gastroesophageal reflux. *Chin J Radiol*, 1989;23:118-121
- 17 Chen JR, Chen MQ, Huang JB. The judgement of resectability of gastric cancer by using radiography. *Chin J Radiol*, 1995;29:627-629
- 18 Chen XR, Chen JR, Shen TZ. Making a complete medical imaging diagnosis in localization, quality, quantity and regularity. *Chin Comput Med Imaging*, 1996;2:217-218
- 19 Chen JR, Zhong BY, Zhang HX, Zhang TQ. The differentiation diagnosis of benign and malignant gastric ulcer in double contrast radiography. *Chin J Radiol*, 1989;23:55-56
- 20 Chen JR, Wang Y, Chen XR. The diagnosis and value of benign gastric ulcer by double contrast radiography. In: Double contrast radiography of gastrointestinal tract. Shanghai: Shanghai Branch, CMA, 1984:87-92
- 21 Chen JR, Xu MH, Yi ZR, Shen MJ, Zhang TQ. Multiple primary carcinoma (MPC) in gastrointestinal tract. *Chin J Radiol*, 1990;24:371-374
- 22 Chen JR, Cui KD, Zhang YQ. Application of CT in diagnosis and treatment of gastric carcinoma. *Chin Comput Med Imaging*, 1997;3:97-101
- 23 Barkhof F, David E, de Geest F. Comparison of film-screen combinations and digital fluorography in gastrointestinal barium examinations in a clinical setting. *Eur J Radiol*, 1996;22:232-235
- 24 Levine MS, Laufer I. The gastrointestinal tract: Dos and Don'ts of digital imaging. *Radiology*, 1998;207:311-316
- 25 Takahasi M, Ueno S, Yoshimatsu S. Gastrointestinal examinations with digital radiography. *Radio Graphics*, 1992;12:969-978

Edited by MA Jing-Yun

# Fibrodynamics-elucidation of the mechanisms and sites of liver fibrogenesis

Catherine H. Wu, Ph.D.

See article on page 397

**Subject headings** liver cirrhosis/pathology; liver cirrhosis/etiology; liver cirrhosis/physiopathology; fibrodynamics; hepatic stellate cells

## ORIGINAL ARTICLE

Dynamic changes of type I, III and IV collagen synthesis and distribution of collagen-producing cells in carbon tetrachloride- induced rat liver fibrosis.

## MAJOR POINTS OF THE COMMENTED ARTICLE

In their article that appears in this issue, Du and colleagues used a combination of immunohistochemistry and *in situ* hybridization to demonstrate increased levels of collagen types I, III and IV in CCl<sub>4</sub>/choline deficient rat model of hepatic fibrosis. Over the course of 20 weeks of treatment mRNA levels for all three types of collagen were increased, but there was a preferential increase of type III collagen mRNA over the other two types. This is consistent with the results of previous investigators<sup>[1,2]</sup> where increases in protein levels of collagen types I, III and IV were found in CCl<sub>4</sub> induced liver fibrosis. The authors clearly demonstrated that collagen type I, III and IV mRNAs were localized on sinusoidal cells using *in situ* hybridization. This result is also consistent with previous work of Maher and co-workers<sup>[3,4]</sup> who used the same technique to demonstrate the localization of both interstitial and basement collagen mRNAs in hepatic stellate cells in normal rat and human livers. The authors have utilized state-of-the-art technology to examine an important question in liver fibrosis-the cells responsible for overproduction of liver biomatrix components. Their results are consistent with the results of other investigators in the field. However, caution should be taken not to overinterpret results.

Additional controls in which the *in situ* localization of collagen mRNAs in untreated normal liver as compared to that seen in fibrotic liver could have given a clearer picture of changes in the fibrotic liver. Nevertheless, the results add strong confirmation to the temporal course of fibrogenesis, and localization of the products in an important model.

## COMMENTARY

Liver fibrosis is the common result of chronic hepatic injury of diverse origins such as chronic viral infections (HBV, HCV), metabolic/storage diseases (hemochromatosis), helminthic infections (schistosomiasis), chronic toxin exposure (alcohol and environmental poisons) and biliary obstruction (biliary cirrhosis). In end stage liver fibrosis or cirrhosis, the liver biomatrix may contain up to six to ten times more collagen and proteoglycans than in the normal state<sup>[5,6]</sup>. Because the connective tissue support of the liver parenchyma is particularly critical to its function, research that emphasizes the nature of liver biomatrix, the molecular regulation of the turnover of components of the biomatrix, and identification of liver cells responsible for the synthesis of biomatrix proteins are especially crucial for the ultimate design of effective therapies for liver fibrosis.

In the late 50's, Hans Popper, the eminent hepatologist, observed a correlation between the histomorphology and biochemistry of liver collagens in chronic liver diseases<sup>[7]</sup>. In the four decades following Dr. Popper's original observation, a great deal of research on liver biomatrix has resulted in our current knowledge of the pathogenesis of liver fibrosis. Progress has been made in three areas of liver fibrosis: characterization and quantitation of matrix components in normal and fibrotic liver; identification of hepatic cells responsible for the increased synthesis of matrix proteins; and the role of cellular mediators of fibrogenesis.

## Quantitation of matrix proteins in normal and fibrotic livers

The use of animal models of liver fibrosis such as the administration of liver toxins CCl<sub>4</sub><sup>[8]</sup>, dimethylnitrosamine<sup>[9]</sup>, alcohol<sup>[10]</sup>, helminthic

Department of Medicine, Division of Gastroenterology-Hepatology, University of Connecticut Health Center, Farmington, CT, USA

**Correspondence to:** Catherine H. Wu, Department of Medicine, Division of Gastroenterology-Hepatology, University of Connecticut Health Center, 263 Farmington Avenue, Farmington, Connecticut 06030, USA

Fax: (860) 679-3159

Received 1999-07-01

infections<sup>[11,12]</sup> have greatly helped in the characterization of the temporal expression of various components of the biomatrix during fibrogenesis. There is increase in the amounts of collagens types I, III, IV, V and VI<sup>[1]</sup>. In early fibrosis, the amounts of types III and IV collagens increase relative to other collagens. In late fibrosis, type I collagen predominates<sup>[13]</sup>. Other components of liver biomatrix such as laminin, fibronectin and proteoglycans are also increased in fibrosis<sup>[14,15]</sup>. Although most investigations have shown changes at the protein and mRNA levels of various biomatrix components, the significance of the changes in the fibrogenic process remain hotly debated<sup>[16]</sup>. The biomatrix in the normal liver changes from being rich in basement membrane collagens to interstitial collagens during fibrogenesis.

#### ***Hepatic stellate cells is the major effector cell type in hepatic fibrosis***

The search for effector cells in the liver responsible for collagen synthesis became feasible with the development of molecular probes<sup>[17]</sup> and antibodies<sup>[14,18]</sup> to components of liver biomatrix. Stellate cells are responsible for the increased synthesis in liver biomatrix proteins such as basement membrane collagens, interstitial collagens, fibronectin, laminin and proteoglycans<sup>[3,4]</sup>. Activation of hepatic stellate cells is the earliest response to liver injury. Upon activation, stellate cells lose stored lipids and retinoids<sup>[19]</sup> and rapidly undergo morphological changes to myofibroblast-like phenotype<sup>[20]</sup>. Other phenotypic changes of activated stellate cells include stimulation of  $\alpha$ -actin gene expression<sup>[21,22]</sup> and increased synthesis of hepatic biomatrix components<sup>[3]</sup>. Activation also results in loss of an important feedback regulation of collagen synthesis by its terminal propeptides. In the normal liver, stellate cells are capable of controlling the amount of collagen needed for normal biomatrix formation by a feedback inhibition of collagen synthesis by its terminal propeptides<sup>[23,24]</sup>. Following activation, stellate cells lose their normal feedback regulation of collagen synthesis leading to increased accumulation of collagen<sup>[25]</sup>. In particular, there is an increased synthesis of types I and III collagen resulting in a biomatrix rich in interstitial collagens. There is increasing evidence that accumulation of fibers in the sinusoids is not only due to increased synthesis of collagens, but also is a result of decreased synthesis of tissue collagenases and increased synthesis of inhibitors of collagenase (TIMP-1: tissue inhibitors of metalloprotein-

ase)<sup>[26]</sup>. Thus fibrogenesis is a net result of increased synthesis and decreased degradation of interstitial collagens of activated stellate cells.

#### ***Cellular mediators of hepatic fibrosis***

Understanding the underlying molecular mechanisms responsible for hepatic fibrosis became feasible with the availability of molecular probes to cytokines. It is now accepted that the initial liver injury results in a host of cytokine responses from liver cells. Specifically, TGF $\beta$ <sup>[27]</sup>, TNF $\alpha$ <sup>[28]</sup>, PDGF<sup>[29]</sup> and Kupffer cell soluble factors<sup>[30]</sup> have been implicated in stellate cell activation and proliferation. TGF $\beta$  mRNA and protein levels are increased in activated stellate cells<sup>[27]</sup>. Over-expression of TGF $\beta$  gene in cultured fibroblasts<sup>[27]</sup> and in stellate cells<sup>[31]</sup> results in increased synthesis of collagens. Inhibitors of TGF $\beta$  decrease collagen synthesis *in vivo*<sup>[32,33]</sup> while transgenic mice over expressing TGF $\beta$  have kidney and liver fibrosis<sup>[34]</sup>. Both PDGF<sup>[29]</sup> and TNF $\alpha$ <sup>[35]</sup> are stellate cell mitogens. PDGF-induced stellate cell proliferation and matrix protein synthesis is mediated by factors secreted by Kupffer cells<sup>[30]</sup>. TNF $\alpha$  acts via transcription regulation of tissue collagenase and TIMP-1 genes in activated stellate cells<sup>[28]</sup>.

#### ***Current research***

The elucidation of the molecular mechanisms of cytokine regulation of liver biomatrix protein synthesis continue to be a focus of current research efforts. There is increasing evidence that cytokines may act via interactions with DNA binding proteins to affect matrix proteins synthesis. Both TGF $\beta$  and TNF $\alpha$  interact with known transcription factors such as C/EBP<sup>[36]</sup> and NF $\kappa$ B<sup>[37,38]</sup>. Transcription factors are DNA binding proteins which act as regulators of gene transcriptions<sup>[39,40]</sup>. There is continued interest in the search for regulatory elements within genes of matrix proteins<sup>[41]</sup>. Research on interactions of DNA binding proteins to regulatory elements on matrix protein genes are underway and may provide a link between cytokines and regulation of liver biomatrix.

#### ***Future directions***

Effective therapy for chronic hepatic fibrosis can be designed only with complete understanding of the molecular mechanisms that regulate matrix protein gene expression. Future research may be centered on the application of gene therapy to control hepatic fibrosis<sup>[42]</sup>. Over-expression of tissue collagenase gene, inhibition of TGF $\beta$  gene expression are potential approach in controlling and regulating hepatic fibrosis<sup>[43]</sup>.

## REFERENCES

- 1 Schuppan D. Structure of the extracellular matrix in normal and fibrotic livers: collagens and glycoproteins. *Sem Liver Dis*, 1990; 10:1-10
- 2 Greenwel P, Rojkind M. Accelerated development of liver fibrosis in CCl<sub>4</sub> treated rats by the introduction of acute phase response episodes: upregulation of alpha (I) procollagen and tissue inhibitor of metalloproteinase-1 mRNAs. *Biochim et Biophys Acta*, 1997;1361:177-184
- 3 Maher JJ, McGurie RF. Extracellular matrix gene expression increases preferentially in rat lipocytes and sinusoidal endothelial cells during hepatic fibrosis *in vivo*. *J Clin Invest*, 1980;86:1641-1648
- 4 Friedman SL, Roll FJ, Boyles J, Bissell DM. Hepatic lipocytes: the principal collagen producing cells of normal rat liver. *Proc Natl Acad Sci USA*, 1985;82:8681-8685
- 5 Rojkind M, Kershenovich D. Hepatic fibrosis. *Progress in Liver Diseases*, 1976;5:294-310
- 6 Schuppan D. Structure of the extracellular matrix in normal and fibrotic livers: collagens and glycoproteins. *Sem Liver Dis*, 1990; 10:1-10
- 7 Kent G, Fels IG, Dubin A, Popper H. Collagen content based on hydroxyproline determinations in human and rat livers: its relation to morphologically demonstrable reticulum and collagen fibers. *Lab Invest*, 1959;8:48
- 8 Rojkind M, Giambrone MA, Ehrenpreise M. Proline oxidase activity and the availability of proline for collagen biosynthesis in Livers of CCl<sub>4</sub> treated rats. *Gastroenterology*, 1977;73:1243
- 9 Risteli J, Tuderman L, Kivirikko KI. Intracellular enzymes of collagen biosynthesis in rat liver as a function of age and in hepatic injury produced by dimethylnitrosamine. *Biochem J*, 1976;158:369-376
- 10 Mezey E, Potter JJ, Maddrey WC. Hepatic collagen proline hydroxylase activity in alcoholic liver disease. *Clin Chem Acta*, 1976; 68:313-320
- 11 Dunn MA, Rojkind M, Warren KS, Hait PK, Rifas L, Seifter S. Gene therapy by skeletal muscle expression of decorin prevents fibrotic disease in rat kidney. *Nature Med*, 1996;2:418-423
- 12 Wu CH, Giambrone MA, Howard DJ, Rojkind M, Wu GY. The nature of collagen of hepatic fibrosis in advanced murine schistosomiasis. *Hepatology*, 1982;2:366-371
- 13 Rojkind M, Giambrone MA, Biempica L. Collagen types in normal and cirrhotic liver. *Gastroenterology*, 1979;76:710-719
- 14 Geerts A, Geutz HJ, Slot JW. Immunogold localization of procollagen III, fibronectin and heparan sulfate proteoglycan on ultrathin frozen sections of the normal rat liver. *Histochemistry*, 1986;84:355-362
- 15 Reid LM, Fiorino AS, Sigal SH, Brill, Holst PA. Extracellular matrix gradients in the space of Disse: relevance to liver biology. *Hepatology*, 1992;15:1198-1203
- 16 Jarnagin WR, Roche DC, Kotliansky VE, Wang SS, Bissell DM. Expression of variant fibronectins in wound healing: cellular sources and biological activity of EIIIA segment in rat fibrogenesis. *J Cell Biol*, 1994;127:2037-2048
- 17 Adams SI. Regulation of collagen gene expression. in *Extracellular Matrix: Chemistry, Biology, and Pathobiology with emphasis on the liver*. Zern MA and Reid LM (eds). Marcell Dekker, Inc. New York, 1993:p91-119
- 18 Becker J, Schuppan D, Benzan H. Immunohistochemical distribution of collagen types IV, V, VI and procollagen types I and III in human alveolar bone and dentine. *J Histochem Cytochem*, 1987; 34:1417-1429
- 19 Mak KM, Leo AM, Lieber CS. Alcoholic liver injury in baboons: transformation of lipocytes to transitional cells. *Gastroenterology*, 1984;87:188-200
- 20 Mak KM, Leo AM, Lieber CS. Alcoholic liver injury in baboons: transformation of lipocytes to transitional cells. *Gastroenterology*, 1984;87:188-200
- 21 Tanaka Y, Nouchi T, Yamane M, Irie T, Miyakawa H, Sato C, Marumo F. Phenotypic modulation in lipocytes in experimental liver fibrosis. *J Pathol*, 1991;164:273-278
- 22 Rockey DC, Boyles JK, Gabbiani G, Friedman SL. Rat hepatic lipocytes express smooth muscle actin upon activation *in vivo* and in culture. *J Submicrosc Cytol Pathol*, 1992;24:193-203
- 23 Wu CH, Donovan CB, Wu GY. Evidence for pre translational regulation of collagen synthesis by procollagen propeptides. *J Biol Chem*, 1986;261:10482-10484
- 24 Wu CH, Walton CM, Wu GY. Propeptide-mediated regulation of procollagen synthesis in IMR-90 human lung fibroblast cell cultures. *J Biol Chem*, 1991;266:2983-2987
- 25 Ikeda H, Wu GY, Wu CH. Lipocytes from fibrotic rat liver have an impaired feedback response to procollagen propeptides. *Am J Physiol*, 1993;27:G157-162
- 26 Iredale JP, Murhy G, Hembry RM, Friedman SL, Arther MJP. Human hepatic lipocytes synthesize tissue inhibitor of metalloproteinases-1 (TIMP-1): implications for regulation of matrix degradation in liver. *J Clin Invest*, 1992;90:282-287
- 27 Roberts AB, Sporn MB, Assoian RK, Smith JM, Roche NS, Wakefield LM, Heine UI, Liotta LA, Falanga V, Kehrl JH, Fauci AS. Transforming growth factor type $\beta$ : Rapid induction of fibrosis and angiogenesis *in vivo* and stimulation of collagen formation *in vitro*. *Proc Natl Acad Sci USA*, 1986;83:4167-4171
- 28 Iredale JP. Matrix turnover in fibrogenesis. *Hepato-Gastroenterology*, 1996;43:56-71
- 29 Pinzani M, Gesukado L, Aabbah GM and Abboud HE. Effects of platelet derived growth factor and other polypeptide mitogens on DNA synthesis and growth of cultured rat liver fat storing cells. *J Clin Invest*, 1989;84:1786-1793
- 30 Friedman SL, Arthur MJP. Activation of cultured rat hepatic lipocytes by Kupffer cell conditioned medium. Direct enhancement of matrix synthesis and stimulation of cell proliferation via induction of platelet derived growth factor receptors. *J Clin Invest*, 1989;84:1780-1785
- 31 Milani S, Schuppan D, Herbst H, Surrenti C. Expression of transforming-growth factor beta, in normal and fibrotic human liver. In: Gressner A, Ramadori G, eds. *Molecular and cell biology of liver fibrogenesis*. Dordrecht, The Netherlands: Kluwer Academic Publishers, 1992:254-263
- 32 Border WA, Noble NA, Yamamoto T. Natural inhibitor of transforming growth factor beta protects against scarring in experimental kidney disease. *Nature (London)*, 1990;360:361-364
- 33 Shah M, Foreman DM, Ferguson MWJ. Control of scarring in adult wounds by neutralizing antibody to transforming growth factor beta. *Lancet*, 1992;339:213-214
- 34 Sanderson N, Factor V, Nagy P. Hepatic expression of mature transforming growth factor beta 1 in transgenic mice results in multiple tissue lesions. *Proc Natl Acad Sci USA*, 1995;92:2572-2576
- 35 Camussi G, Albano E, Tetta C and Bussolino F. The molecular action of tumor necrosis factor- $\alpha$ . *Eur J Biochem*, 1991;202:3-14
- 36 Garcia-Trevijano ER, Iraburu MJ, Fontana L, Dominguez-Rosales JA, Auster A, Covarrubias-Pinedo A, Rojkind M. Transforming growth factor beta<sub>1</sub> induces the expression of alpha (I) procollagen mRNA by a hydrogen peroxide-C/EBPbeta-dependent mechanism in rat hepatic stellate cells. *Hepatology*, 1999;29:960-970
- 37 Zeldin G, Yang SQ, Yin M, Lin HZ, Rai R, Diehl AM. Alcohol and cytokine-inducible transcription factors. *Alcoholism, Clinical & Experimental Research*, 1996;20:1639-1645
- 38 Yang SQ, Lin HZ, Yin M, Albrecht JH, Diehl AM. Effects of chronic ethanol consumption on cytokine regulation of liver regeneration. *Am J Physiol*, 1998;275:G696-704
- 39 Hellerbrand C, Stefanovic B, Giordano F, Burchardt ER, Brenner DA. The role of TGFbeta 1 in initiating hepatic stellate cell activation *in vivo*. *J Hepatology*, 1999;30:77-87
- 40 Hellerbrand C, Jobin C, Licato LL, Sartor RB, Brenner DA. Cytokines induce NF-kappa B in activated but no in quiescent rat hepatic stellate cells. *Am J Physiol*, 1998;275:G269-278
- 41 Stefanovic B, Hellerbrand C, Holcik M, Briendl M, Aliehaber S and Brenner DA. Post transcriptional regulation of collagen alpha 1(I) mRNA in hepatic stellate cells. *Mole Cell Biol*, 1997;17:5201-5209
- 42 Hellerbrand C, Jobin C, Iimuro Y, Licato L, Sartor RB, Brenner DA. Inhibition of NFkappaB in activated rat hepatic stellate cells by proteasome inhibitors and an IkappaB super repressor. *Hepatology*, 1998;27:1285-1295
- 43 Isaka Y, Brees DK, Ikegaya K, Kaneda Y, Imai E, Noble NA, Border WA. Gene therapy by skeletal muscle expression of decorin prevents fibrotic disease in rat kidney. *Nature Med*, 1996;2:418-423

# Increased prevalence of intestinal inflammation in patients with liver cirrhosis

Osamu Saitoh<sup>1</sup>, Kazunori Sugi<sup>1</sup>, Keishi Kojima<sup>1</sup>, Hisashi Matsumoto<sup>2</sup>, Ken Nakagawa<sup>1</sup>, Masanobu Kayazawa<sup>1</sup>, Seigou Tanaka<sup>1</sup>, Tsutomu Teranishi<sup>1</sup>, Ichiro Hirata<sup>1</sup> and Ken-ichi Katsu<sup>1</sup>

**Subject headings** liver cirrhosis; intestinal; inflammation; secretory IgA; fecal proteins

## Abstract

**AIM** To investigate the pathophysiology of the digestive tract in patients with liver cirrhosis.

**METHODS** In 42 cirrhotic patients and 20 control subjects, the following fecal proteins were measured by enzyme-linked immunosorbent assay: albumin (Alb), transferrin (Tf), and  $\alpha_1$ -antitrypsin ( $\alpha_1$ -AT) as a marker for intestinal protein loss, hemoglobin (Hb) for bleeding, PMN-elastase for intestinal inflammation, and secretory IgA for intestinal immunity.

**RESULTS** The fecal concentrations of Hb, Alb, Tf,  $\alpha_1$ -AT, and PMN-elastase were increased in 13 (31%), 8(19%), 10(24%), 6(14%), and 11 (26%) cases among 42 patients, respectively. Fecal concentration of secretory IgA was decreased in 7 (17%) of 42 patients. However, these fecal concentrations were not related to the severity or etiology of liver cirrhosis. The serum Alb level was significantly decreased in patients with intestinal protein loss compared to that in patients without intestinal protein loss.

**CONCLUSION** These findings suggest that: ① besides the well-known pathological conditions, such as bleeding and protein loss, intestinal inflammation and decreased intestinal immunity are found in cirrhotic patients; ② intestinal protein loss contributes to hypoalbuminemia in cirrhotic patients, and ③ intestinal inflammation should not be overlooked in cirrhotic patients, since it may contribute to or cause intestinal protein loss and other various pathological conditions.

## INTRODUCTION

Gastrointestinal symptoms are common in patients with liver cirrhosis and portal hypertension. Their pathophysiology remains, for the most part, obscure. It is well known that esophageal varices and portal hypertensive gastropathy<sup>[1,2]</sup> are common causes of upper gastrointestinal (GI) bleeding in patients with liver cirrhosis. Recently, portal hypertensive colopathy, such as colonic vascular ectasia and rectal varices, were recognized as causes of lower gastrointestinal bleeding in cirrhotic patients<sup>[3,4]</sup>. Other than bleeding, various pathological conditions such as malabsorption<sup>[5,6]</sup> and intestinal protein loss<sup>[7,8]</sup> have been reported in cirrhotic patients. We developed fecal tests that are useful for evaluating the various pathophysiologies of the digestive tract<sup>[9-12]</sup>. Fecal hemoglobin (Hb) is a useful marker of bleeding. Fecal albumin, transferrin (Tf), and  $\alpha_1$ -antitrypsin ( $\alpha_1$ -AT) are useful markers of intestinal protein loss. Fecal secretory IgA (sIgA) level reflects the condition of local immunity in the intestine and an increase in fecal neutrophil granule-derived proteins, such as PMN-elastase, indicates the presence of intestinal inflammation. In the present study, we examined the fecal protein profile to investigate the pathophysiology of the digestive tract in cirrhotic patients.

## MATERIALS AND METHODS

### Subjects

Forty-two patients with liver cirrhosis aged 59.0±8.7 years (mean ± SD) were evaluated. The diagnosis of liver cirrhosis in each case was confirmed by a combination of clinical, biochemical, radiological, and pathological methods. The clinical severity of the liver disease in each case was determined using the Pugh modification of Child's original classification<sup>[13]</sup>. These cases consisted of thirty-one males and eleven females. The number of patients with Child A, Child B, and Child C were 27, 6, and 9, respectively. The etiology of the liver cirrhosis was as follows: 33 patients with hepatitis C, 3 with hepatitis B, and 6 with alcoholism. All patients had

<sup>1</sup>Second Department of Internal Medicine, Osaka Medical College, Takatsuki, Japan

<sup>2</sup>Department of Gastroenterology, Ijinkai Takeda General Hospital, Kyoto, Japan

This work was supported in part by Grant-in aid Nos.07670630 and 10670518 (to O. Saitoh) for Scientific Research from the Ministry of Education, Science, Sports, and Culture, Japan

**Correspondence to:** Osamu Saitoh, Second Department of internal Medicine, Osaka Medical College, 2.7 Daigakumachi, Takatsuki, Osaka 569-8686, Japan

Tel.(0726)83-1221, Fax.(0726)84-6532

Received 1999-07-14

no obvious gastrointestinal bleeding. The control group consisted of 20 subjects aged  $41.0 \pm 18.1$  years with no demonstrated abnormality in the upper or lower digestive tract. Informed consent was obtained from each subject in accordance with the Helsinki Declaration.

### ***Stool collection and measurement of fecal proteins***

Patients were instructed to defecate into a polystyrene container (diameter 15 cm, depth 12 cm). The stool samples, collected at 4 °C over a period of 48 h - 72 h, were homogenized with a small amount of water, then stored at -80 °C until the time of measurement. The concentrations of fecal Hb, Alb, Tf,  $\alpha_1$ -AT, PMN-elastase, and sIgA were measured by enzyme-linked immunosorbent assay (ELISA) as described previously<sup>[9-11]</sup>. Briefly, anti-human Hb antibody (Institute of Immunology, Japan), anti-human albumin antibody (Dakopatts, Glostrup, Denmark), anti-human Tf antibody (Dakopatts), anti-human  $\alpha_1$ -AT antibody (Dakopatts), anti-human PMN-elastase antibody (Serotec, Oxford, England), or anti-human secretory component antibody (Dakopatts) was coated in the wells of a 96-well microplate. The diluted fecal samples (100 to 10000 fold) were added to each well. After reaction at 37 °C for 1 h, the wells were washed with water. The samples were then reacted with the respective alkaline phosphatase-labeled antibody except alkaline phosphatase labeled anti-human IgA antibody (Dakopatts) for ELISA of sIgA. The enzyme reaction was then carried out, and color development was measured with a microplate colorimeter at 510/630 nm.

### ***Statistical analysis***

Values were expressed as medians (25%, 75%). The Mann-Whitney U tests and/or  $\chi^2$  tests were used to compare groups. All *P* values were two-tailed; *P* values less than 0.05 were considered statistically significant.

## **RESULTS**

### ***Fecal protein concentrations in control subjects***

Results are shown in Figure 1. Daily stool weight (g/day) was 140 (100, 230) in control subjects. The concentrations of fecal Hb, Alb, Tf,  $\alpha_1$ -AT, sIgA, and PMN-elastase were 1.5 (0.1, 4.0), 0.1 (0.1, 1.8), 0.1 (0.1, 0.4), 327.4 (201.1, 421.3), 214.9 (56.6, 244.1), and 0.6 (0.3, 1.2), respectively. The 95th percentile of the control

subjects was used as the cut-off value (10.6, 5.3, 1.0, 771, and 2.2  $\mu\text{g/g}$  for Hb, Alb, Tf,  $\alpha_1$ -AT, and PMN elastase, respectively). sIgA was important when not only increasing, but also decreasing. Therefore, the lower limit of the normal range was defined as the 5th percentile (26.8  $\mu\text{g/g}$ ) of the control subjects for sIgA.

### ***Fecal protein concentrations in cirrhotic patients***

Daily stool weight (g/day) was 140 (100, 180). In terms of daily stool weight, there was no significant difference between the cirrhotic patients and control subjects. As shown in Figure 1, the fecal concentrations of Hb, Alb, Tf,  $\alpha_1$ -AT, and PMN-elastase were increased in 13 (31%), 8 (19%), 10 (24%), 6 (14%), and 11 (26%) among 42 patients, respectively. Conversely, the fecal concentration of sIgA was decreased in 7 (17%) of 42 patients. There were significant differences in fecal Hb, Alb, sIgA, and PMN-elastase concentrations between the cirrhotic patients and the controls.

### ***Relationship between fecal protein concentrations and the severity of liver cirrhosis***

As shown in Figure 2, there was no relationship between the concentrations of these fecal proteins and the severity of the disease.

### ***Relationship between fecal protein concentrations and the presence of esophageal varices***

As shown in Figure 3, fecal Hb concentration demonstrated a significant difference between the cirrhotic patients and the controls.

### ***Relationship between fecal protein concentrations and the etiology of liver cirrhosis***

There was no association between fecal protein concentrations and the etiology of the liver disease (data not shown).

### ***Intestinal protein loss and nutritional status in cirrhotic patients***

Results are shown in Figure 4. The patient was defined as having intestinal protein loss, when a patient had increased concentrations of at least one of Alb, Tf, and  $\alpha_1$ -AT. The serum Alb level was significantly decreased in patients with intestinal protein loss compared to that in patients without intestinal protein loss. The findings suggest that intestinal protein loss contribute to the development of hypoalbuminemia in cirrhotic patients.

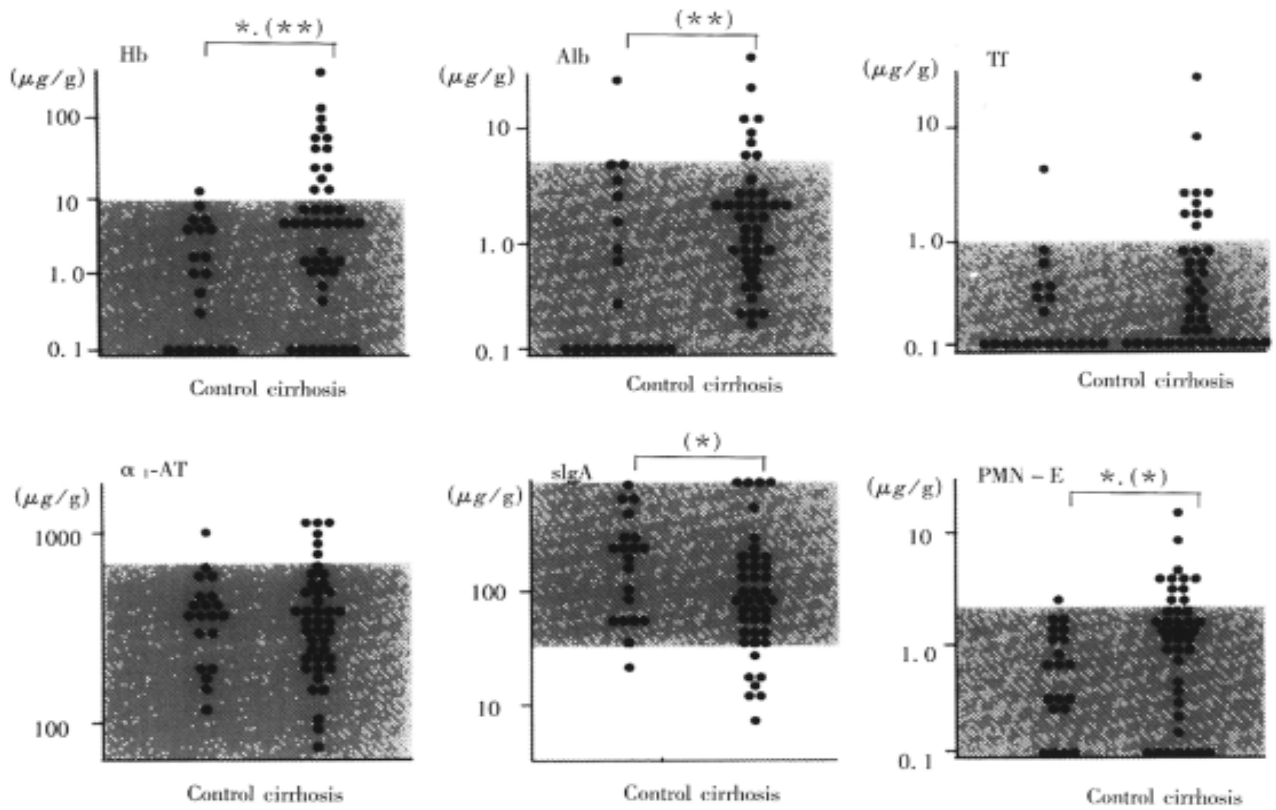


**Figure 1** Fecal protein concentrations in cirrhotic patients and control subjects. The dotted area shows the 95 percentile of the control subjects.  $^a$ :  $P < 0.05$  by  $\chi^2$  test;  $^b$ :  $P < 0.05$ ;  $^c$ :  $P < 0.01$  by Mann-Whitney U test.

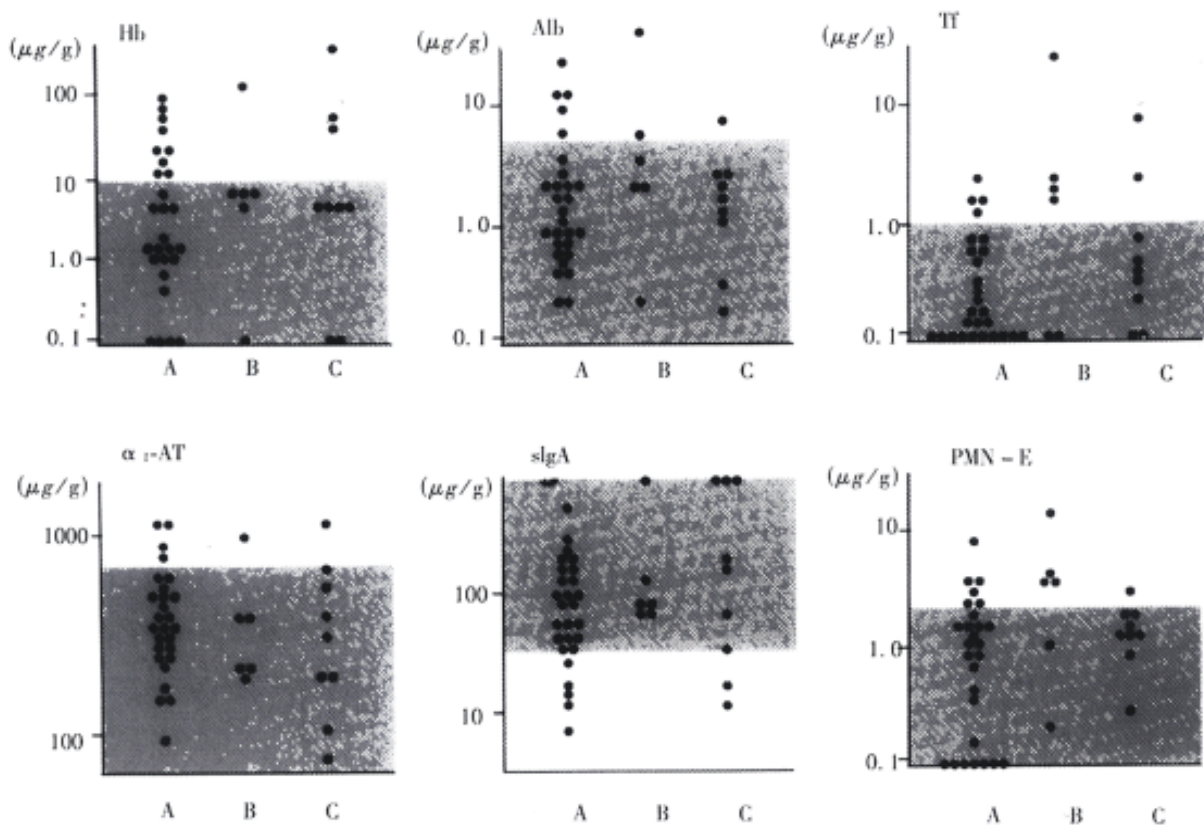


**Figure 2** Relationship between fecal protein concentrations and the severity of the liver cirrhosis. A: Child A, B: Child B, C: Child C. The dotted area shows the 95 percentile of the control subjects.

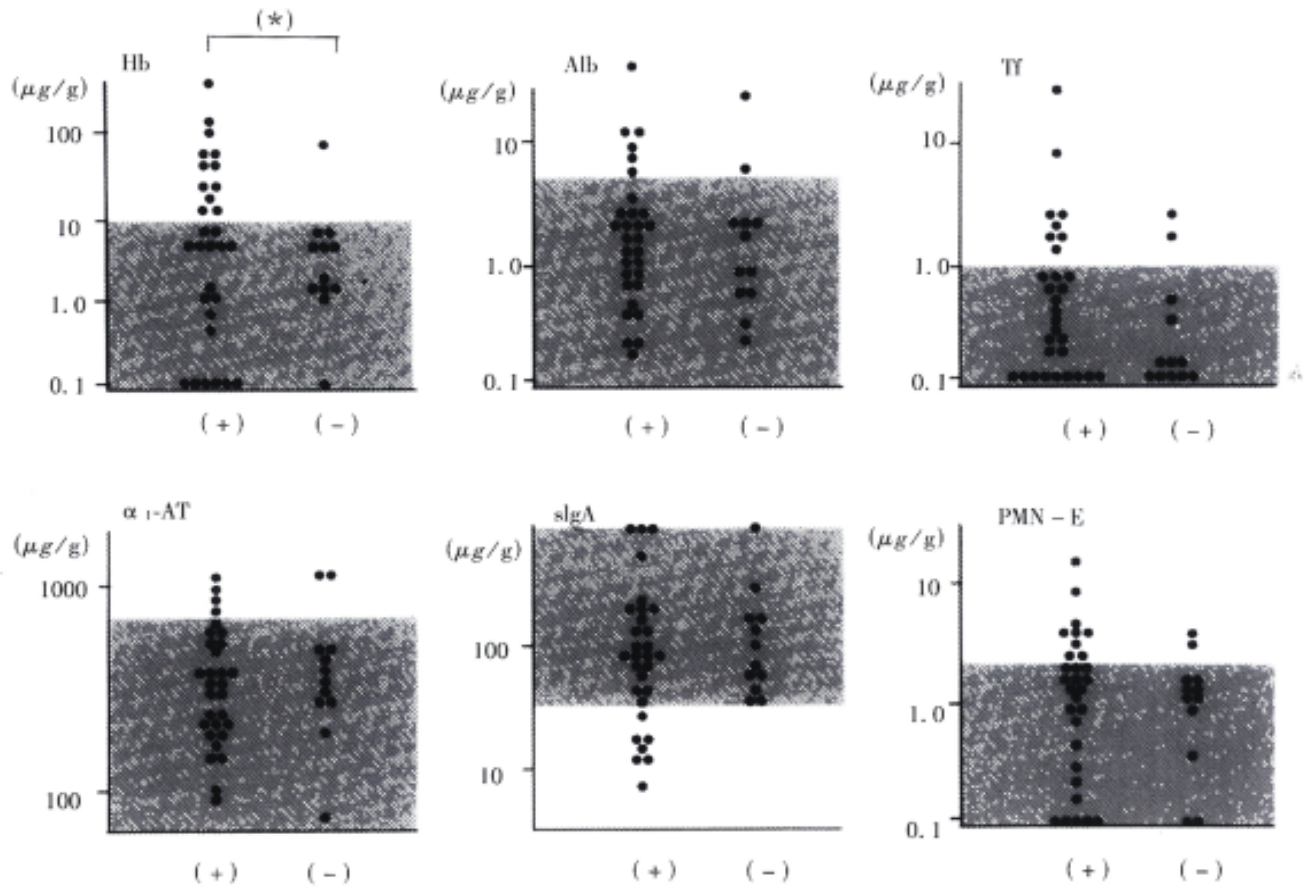


**Figure3** Relationship between fecal protein concentrations and the presence of esophageal varices. (+): cirrhotic patients associated with esophageal varices; (-): cirrhotic patients not associated with esophageal varices; \*:  $P < 0.05$  by  $\chi^2$  test.

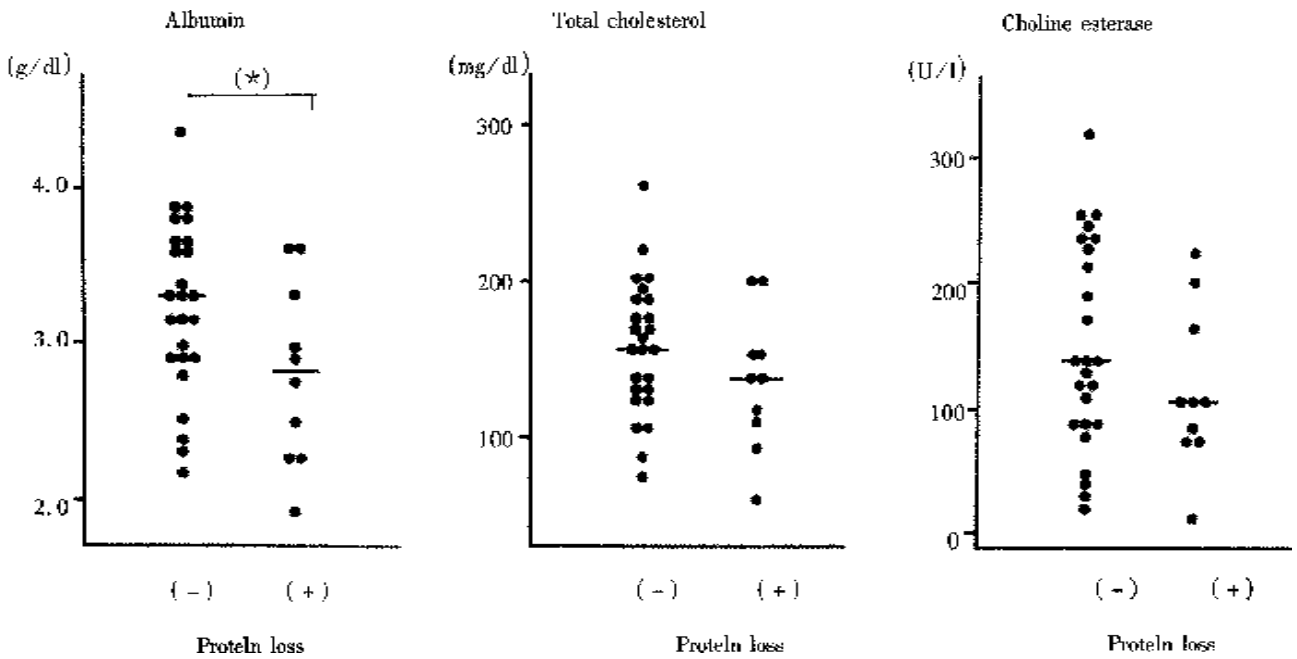


**Figure4** Serum concentrations of albumin, total cholesterol, and choline esterase in cirrhotic patients. Comparison between groups with or without intestinal protein loss. \*:  $P < 0.05$ , NS; not significant by Mann-Whitney U test.

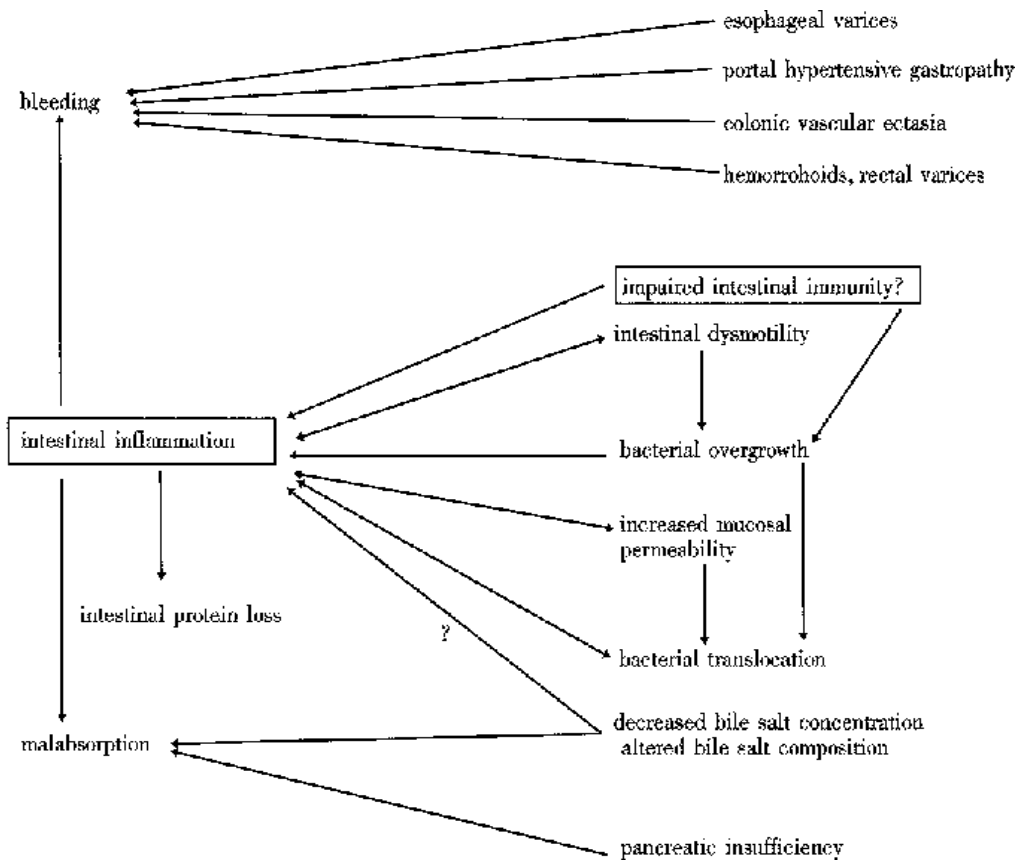


**Figure 5** Proposed pathophysiology of digestive tract in cirrhotic patients.

## DISCUSSION

The present study showed that 26% of the cirrhotic patients had elevated fecal PMN-elastase concentrations and suggested an increased prevalence of intestinal inflammation in cirrhotic patients. Furthermore, occult GI bleeding and intestinal protein loss were observed commonly even in cirrhotic patients who had no massive GI bleeding. The conditions such as bleeding, intestinal protein loss, impaired intestinal immunity, and intestinal inflammation can be considered to be included in portal hypertensive enteropathy, because these seemed to be related not to the severity of the liver disease, but to portal hypertension. Recently, Stanley *et al*<sup>[14]</sup> first demonstrated that many of the manifestations of portal hypertensive enteropathy can be corrected by a transjugular intrahepatic portosystemic stent-shunt (TIPS) procedure. They described a cirrhotic patient with diarrhea and hypoalbuminemia. Protein losing enteropathy was confirmed by analysis of whole gut lavage fluid. They then performed a TIPS procedure, which eliminated the portal hypertension. Both the patient's diarrhea and elevated whole gut lavage fluid protein concentrations were reduced.

It is well known that the mechanism of

hypoalbuminemia observed in cirrhotic patients is multifactorial. Decreased albumin production in the liver is one of the causes. In the present study, the serum Alb level was decreased significantly in patients with intestinal protein loss compared to that in patients without intestinal protein loss. The findings suggest that intestinal protein loss contributes to the development of hypoalbuminemia in cirrhotic patients.

Little attention has been paid to the relation between liver cirrhosis and intestinal inflammation. The prevalence of colitis diagnosed by colonoscopy in cirrhotic patients is not well established in the literature, and ranges from 10% to 57.9%<sup>[3,15-18]</sup>. Such a wide distribution is considered to be due to differences in the definition of inflammation and wide variation between observers in describing the mucosal appearance. The highest value, 57.9%, was reported by Scandalis N *et al*<sup>[16]</sup>. In their study, inflammatory changes included mucosal edema as well as erythema, granularity, and fragility of the mucosa. In contrast to colonoscopy, stool test is presumably a relatively objective test for assessment of inflammation. The value obtained in the present study (26%) was highest among the reported prevalence except for 57.9% reported by Scandalis N *et al*. The following possible reasons

should be taken into consideration. ① Fecal PMN-elastase, a marker of intestinal inflammation in the present study, reflects mucosal inflammation of the small intestine as well as the colon. The prevalence of inflammation of the small intestine has not been studied so far. ② Difference in sensitivity between the stool test and colonoscopy: the stool test seems to be more sensitive than colonoscopy, since colonoscopy does not always detect inflammation if the inflammation is minimal or localized.

Our proposed pathology of the digestive tract in cirrhotic patients is shown in Figure 5. The present study suggested that impaired intestinal immunity might be one of the predisposing factors to intestinal inflammation. In the present study, 17% of the cirrhotic patients showed decreased fecal sIgA concentrations. This is the first report concerning fecal sIgA in cirrhotic patients, although serum sIgA in cirrhotic patients was shown previously to be elevated<sup>[19]</sup>. Besides impaired intestinal immunity, predisposing factors for intestinal inflammation include intestinal dysmotility, bacterial overgrowth, bacterial translocation, and increased mucosal permeability<sup>[20]</sup>. Recently, we reported that bile acids inhibit tumor necrosis factor- $\alpha$ -induced interleukin-8 production in human intestinal cells<sup>[21]</sup>. A decreased level or an altered composition of the intraluminal bile acids may make cirrhotic patients susceptible to intestinal inflammation<sup>[22,23]</sup>.

It is well known that GI bleeding, intestinal protein loss, malabsorption, and bacterial translocation develop in patients with inflammatory bowel diseases<sup>[10,24,25]</sup>. In cirrhotic patients with intestinal inflammation, therefore, such serious pathological conditions may easily occur. Therefore, it is important to evaluate whether a cirrhotic patient has intestinal inflammation or not in order to manage the patient. Measurement of fecal PMN-elastase is preferable to colonoscopy as a screening test for intestinal inflammation in cirrhotic patients, since the former is a sensitive and non-invasive test.

**ACKNOWLEDGMENTS** We thank Drs. Ryoichi Matsuse, Kazuo Uchida, and Kazue Tabata of the Kyoto Medical Science Laboratory for their helpful discussion, and are also grateful to other doctors in the Second Department of Internal Medicine, Osaka Medical College, who have contributed to this work.

## REFERENCES

- McCormack TT, Sims J, Eyre-Brook I, Kennedy H, Goepel J, Johnson AG, Triger DR. Gastric lesions in portal hypertension: inflammatory gastritis or congestive gastropathy? *Gut*,1985;26:1226-1232
- Iwao T, Toyonaga A, Sumino M, Takagi K, Oho K, Nishizono M, Ohkubo K, Inoue R, Sasaki E, Tanikawa K. Portal hypertensive

- gastropathy in patients with cirrhosis. *Gastroenterology*,1992;102:2060-2065
- Kozarek RA, Botoman VA, Bredfeldt JE, Roach JM, Patterson DJ, Ball TJ. Portal colopathy: prospective study of colonoscopy in patients with portal hypertension. *Gastroenterology*, 1991;101:1192-1197
- Naveau S, Bedossa P, Poynard T, Mory B, Chaput JC. Portal hypertensive colopathy. A new entity. *Dig Dis Sci*,1991;36:1774-1781
- Losowsky MS, Walker BE. Liver disease and malabsorption. *Gastroenterology*,1969;56:589-600
- Romiti A, Merli M, Martorano M, Parrilli G, Martino F, Riggio O, Trusscelli A, Capocaccia L, Budillon G. Malabsorption and nutritional abnormalities in patients with liver cirrhosis. *Ital J Gastroenterol*, 1990;22:118-123
- Iber FL. Protein loss into the gastrointestinal tract in cirrhosis of the liver. *Am J Clin Nutr*,1966;19:219-222
- Conn HO. Is protein-losing enteropathy a significant complication of portal hypertension. *Am J Gastroenterol*,1998;93:127-128
- Sugi K, Saitoh O, Nakagawa K, Sugimori K, Takada K, Yoshizumi M, Miyoshi H, Hirata I, Ohshiba S, Matsumoto H, Matsuse R, Uchida K. Fecal secretory IgA levels in patients with colorectal diseases. *Digestion and Absorption*,1993;16:28-33
- Saitoh O, Matsumoto H, Sugimori K, Sugi K, Nakagawa K, Miyoshi H, Hirata I, Matsuse R, Uchida K, Ohshiba S. Intestinal protein loss and bleeding assessed by fecal hemoglobin, transferrin, albumin, and alpha-1-antitrypsin levels in patients with colorectal diseases. *Digestion*,1995;56:67-75
- Saitoh O, Sugi K, Matsuse R, Uchida K, Matsumoto H, Nakagawa K, Takada K, Yoshizumi M, Hirata I, Katsu K. The forms and the levels of fecal PMN elastase in patients with colorectal diseases. *Am J Gastroenterol*,1995;90:388-393
- Sugi K, Saitoh, Hirata I, Katsu K. Fecal lactoferrin as a marker for disease activity in inflammatory bowel disease: comparison with other neutrophil-derived proteins. *Am J Gastroenterol*,1996;91:927-934
- Pugh RNH, Murray Lyon IM, Dawson JL, Pietroni MC, Williams R. Transection of the esophagus for bleeding esophageal varices. *Br J Surg*,1973;60:646-649
- Stanley AJ, Gilmour HM, Ghosh S, Ferguson A, McGilchrist AJ. Transjugular intrahepatic portosystemic shunt as a treatment for protein-losing enteropathy caused by portal hypertension. *Gastroenterology*,1996;111:1679-1682
- Rabinovitz M, Schade RR, Dindzans VJ, Belle SH, van Thiel DH, Gavaler JS. Colonic disease in cirrhosis. An endoscopic evaluation in 412 patients. *Gastroenterology*,1990;99:195-199
- Scandalis N, Archimandritis A, Kastanas K, Spliadias C, Delis B, Manika Z. Colonic findings in cirrhotics with portal hypertension. A prospective colonoscopic and histological study. *J Clin Gastroenterol*, 1994;18:325-329
- Tam TN, Ng WW, Lee SD. Colonic mucosal changes in patients with liver cirrhosis. *Gastrointest Endosc*,1995;42:408-412
- Bresci G, Gambardella L, Parisi G, Federici G, Bertini M, Rindi G, Metrangola S, Tumino E, Bertoni M, Cagno MC, Capria A. Colonic disease in cirrhotic patients with portal hypertension. An endoscopic and clinical evaluation. *J Clin Gastroenterol*,1998;26:222-227
- Pelletier G, Briantais MJ, Buffet C, Pillot J, Etienne JP. Serum and intestinal secretory IgA in alcoholic cirrhosis of the liver. *Gut*,1982;23:475-480
- Quigley EMM. Gastrointestinal dysfunction in liver disease and portal hypertension. Gut liver interactions revisited. *Dig Dis Sci*, 1996;41:557-563
- Saitoh O, Nakagawa K, Sugi K, Matsuse R, Uchida K, Kojima K, Tanaka S, Teranishi T, Hirata I, Katsu K. Bile acids inhibit tumor necrosis factor- $\alpha$ -induced interleukin-8 production in human colon epithelial cells. *J Gastroenterol Hepatol*, 1998;13:1212-1217
- Vlahcevic R, Juttijudata P, Bell CCJr, Swell L. Bile acid metabolism in patients with cirrhosis. II. Cholic and chenodeoxycholic acid metabolism. *Gastroenterology*,1972;62:1174-1181
- J-nsson G, Hedenborg G, Wisen O, Norman A. Presence of bile acid metabolites in serum, urine, and feces in cirrhosis. *Scand J Clin Invest*, 1992;52:555-564
- Laffineur G, Lescut D, Vincent P, Quandalle P, Wurtz A, Colombel JF. Bacterial translocation in Crohn disease. *Gastroenterol Clin Biol*, 1992;16:777-781
- Saitoh O, Nakagawa K, Sugi K, Kojima K, Teranishi T, Tanaka S, Kayazawa M, Maemura K, Hirata I, Katsu K. Plasma endotoxin level as a marker of disrupted intestinal mucosal barrier in inflammatory bowel disease. *Bull Osaka Med Coll*, 1997;43:95-101

# Dynamic changes of type I, III and IV collagen synthesis and distribution of collagen-producing cells in carbon tetrachloride-induced rat liver fibrosis

DU Wei-Dong<sup>1</sup>, ZHANG Yue-E<sup>1</sup>, ZHAI Wei-Rong<sup>1</sup>, ZHOU Xiao-Mei<sup>2</sup>

See invited commentary on page 388

**Subject headings** Procollagen mRNA; immunohistochemistry; Northern blot analysis; *in situ* hybridization; liver fibrosis

## Abstract

**AIM** To find out the relationship between the gene transcripti on of different types of procollagen and the deposition of the relevant collagens in the liver tissue and to confirm the types of collagen producing cells in liver fibrogenesis.

**METHODS** Dynamic changes of the expression of  $\alpha 1(I)$ ,  $\alpha 1(III)$  and  $\alpha 1(IV)$  procollagen mRNA and relevant collagens and the distribution of collagen producing cells during liver fibrogenesis of rat induced by  $CCl_4$  (20 weeks) were investigated with Northern blot analysis, *in situ* hybridization and immunohistochemical techniques.

**RESULTS** The increased expression of  $\alpha_1(III)$  procollagen mRNA by Northern blot analysis was the most predominant one among the three mRNAs during fibrogenesis. However, the enhanced expression of  $\alpha_1(IV)$  procollagen mRNA occurred very early while the expression of  $\alpha 1(I)$  mRNA was not enhanced much until the middle stage of the experiment. Desmin (Dm) positive hepatic stellate cells (HSCs) and few myofibroblasts (MFs) in and around the necrotic

areas expressed  $\alpha 1(I)$ ,  $\alpha 1(III)$  and  $\alpha 1(IV)$  procollagen mRNA signals detected by *in situ* hybridization at the early stage of the experiment. All the three procollagen mRNA signals thereafter mainly localized in fibroblasts (Fbs) and MFs in fibrotic septa during the middle and late stages of fibrosis, which distributed parallel to the corresponding collagens detected by immunohistochemical study. In addition, the endothelial cells of sinusoids and the small blood vessels within the septa also showed  $\alpha 1(IV)$  procollagen mRNA and type IV collagen expression

**CONCLUSION** It is considered that "HSC-MF-Fb" effect cell system is the major cellular source of collagen production in liver fibrosis, in which HSCs are collagen producing precursor cells in the early liver fibrogenesis, thereafter the synthesis of type I, III and IV collagens (Col I, Col III and Col IV) mainly derives from MFs and Fbs, which play a very important role in the progress of liver fibrosis. The endothelial cells along sinusoids, as another source of Col IV production, might participate in the capillization of liver sinusoids.

## INTRODUCTION

The synthesis and the amount of collagen deposited in fibrotic liver have been studied by many investigators. The biochemical data revealed that the content of collagen proteins in liver fibrosis increased. Pierce *et al*<sup>[1]</sup> found that the increased total hydroxyproline was associated with collagen synthesis in early liver fibrosis of the rat induced by carbon tetrachloride ( $CCl_4$ ). Oga wa *et al*<sup>[2]</sup> and Clement *et al*<sup>[3]</sup> investigated the localization and the semiquantitative analysis of the increased collagens in rat liver fibrosis immunohistochemically. The amount of  $\alpha 1(I)$ ,  $\alpha 1(III)$  and  $\alpha 1(IV)$  procollagen mRNA in liver fibrosis was found to be increased by either slot blot or Northern blot<sup>[4-6]</sup>. Many kinds of cells in liver fibrosis, such as hepatic stellate cells (HSCs), myofibroblasts (MFs), fibroblasts (Fbs), parenchyma cells and endothelial cells were

<sup>1</sup>Department of Pathology, Shanghai Medical University, Shanghai 200032, China

<sup>2</sup>National Laboratory for Oncogenes and Related Genes, Shanghai Cancer Institute

DU Wei-Dong, male, born on 1958-11-11, got a doctorate degree in 1996 in Shanghai Medical University and now is working as a postdoctorate in Department of Molecular Biology of Max-Planck-Institute for Biochemistry, Germany, having 35 papers published. Project supported by National Natural Science Foundation of China (No.39 33140) and Shanghai Municipal Education Commission (No. 980802).

**Correspondence to:** Professor ZHANG Yue-E M.D., Department of Pathology, Shanghai Medical University, 138 Yixueyuan Road, Shanghai 200032, China

Tel. +86-21-6404 1900 Ext. 2540, Fax. +86-21-6403 9987

Email. zdxu@shmu.edu.cn

Received 1999-04-28 Revised 1999-04-28

reported to be involved in producing collagens in liver fibrosis *in vivo* and/or *in vitro*, but the results still remain controversial<sup>[1,4,6-12]</sup>. The application of immunohistochemical method provides a useful way for identifying the content and the components of the extracellular matrix in the liver. However, it could not reliably identify the cell types which were responsible for synthesizing collagens during fibrogenesis. The *in situ* hybridization method provides a benefit to identifying the cell types expressing the extracellular matrix gene. Some studies demonstrated the  $\alpha 1(I)$ ,  $\alpha 1(III)$  and  $\alpha 1(IV)$  procollagen mRNA expressing cells with *in situ* hybridization using procollagen cRNA probes labeled with isotope  $^{35}S$  *in vivo* and *in vitro*<sup>[7,8]</sup>. Because of the diffuse localization of  $^{35}S$ -hybridization signals, it is also difficult to identify accurately the cellular composition signals which are exactly responsible for the synthesis of collagen in fibrotic liver. The purpose of this study is to observe the dynamic changes of the expression of  $\alpha 1(I)$ ,  $\alpha 1(III)$  and  $\alpha 1(IV)$  procollagen mRNA by Northern blot analysis and the distribution and content (semiquantitatively) of type I, III and IV collagen (Col I, Col III, Col IV) by immunohistochemistry in different stages of liver fibrogenesis and to clarify the types of collagen producing cells in liver fibrogenesis by immunohistochemical staining of desmin (Dm) and  $\alpha$ -smooth muscle actin ( $\alpha$ -SMA) and *in situ*-hybridization of  $\alpha 1(I)$ ,  $\alpha 1(III)$  and  $\alpha 1(IV)$  procollagen mRNA with the procollagen cDNA probes labeled by digoxigenin in serial tissue sections.

## MATERIALS AND METHODS

### *Animal model*

Male Sprague-Dawley (SD) rats ( $n = 40$ , provided by Shanghai Division of the Animal Center of Chinese Academy of Sciences), weighing 180 g - 220 g, were subcutaneously injected with  $CCl_4$  at a dose of 0.33 mL/100 g of body weight, and an equal mixture of olive oil twice a week with low-choline diet to induce liver fibrosis model<sup>[12]</sup>. The control rats ( $n = 24$ ) were injected with an equal amount of olive oil only and fed with standard diet. Every five experimental rats were killed after 2-, 4-, 6-, 8-, 10-, 12-, 16-, and 20-week treatment and with 3 age-matched ones as control. After removal, small pieces of liver samples (5 mm<sup>3</sup>-10 mm<sup>3</sup>) were immediately frozen in liquid nitrogen and stored at -80 °C for Northern blot analysis, and other pieces of the liver tissues were cut into serial frozen sections with 5  $\mu$ m in thickness and placed on poly-L-lysine coated slides. The sections were fixed in 4 mL/L paraformaldehyde in PBS (0.1 mol/L, pH 7.4, containing 5 mmol/L  $MgCl_2$ ) for 10 minutes, rinsed in PBS, then in 2 $\times$ SSC

three times for 10 minutes each and dehydrated in ethanol and stored at -80 °C for *in situ* hybridization and immunohistochemistry.

### *Northern blot analysis*

Rat  $\alpha 1(I)$ , human  $\alpha 1(III)$  and  $\alpha 1(IV)$  procollagen cDNA plasmids were generously provided by Dr. Chu ML (Jefferson Medical College, USA). The sizes of the inserts contained in the pBR<sub>322</sub> plasmid vectors are 1.3 kb for  $\alpha 1(I)$ , 0.7 kb for  $\alpha 1(III)$  and 2.6 kb for  $\alpha 1(IV)$  in size respectively. The cDNA probes were labeled with  $^{32}P$ -deoxycytidine triphosphate (Amersham) to a specific activity of  $(2.5) \times 10^8$  cpm/ $\mu$ g of DNA using a primer extension kit (Pharmacia) for  $\alpha 1(I)$  and  $\alpha 1(IV)$  procollagen cDNA probes labeling and nick translation kit (Gibco BRL) for  $\alpha 1(III)$  procollagen cDNA probe labeling. Total RNA was isolated from the liver tissue by extraction in guanidine isothiocyanate<sup>[13]</sup>. Twenty  $\mu$ g total RNA from each sample was separated on a 10 g/L agarose gel containing 2.2 mol/L-formaldehyde and then transferred onto nitrocellulose filters (Stratagene), and baked at 80 °C for 2 hours to bind the RNA to the filters. The filters were prehybridized in 500 g/L formamide, 50 mol/L sodium phosphate, 0.8 mol/L NaCl, 1 mmol/L EDTA, and 2 g/L SDS in 4 $\times$ Denhardt's solution with 250  $\mu$ g/L denatured herring sperm DNA (Sigma) for 4 hours at 45 °C and then hybridized in the same fresh solution as above containing the  $^{32}P$ -labeled  $\alpha 1(I)$ ,  $\alpha 1(III)$  and  $\alpha 1(IV)$  procollagen cDNA probes respectively overnight at 45 °C. After high stringency washing in 2 $\times$ SSC, 1 $\times$ SSC, 0.5 $\times$ SSC and 0.1 $\times$ SSC with 1g/L SDS sequentially at 45 °C for 15 minutes each, the nitrocellulose filters were exposed to Kodak film at -80 °C for one week. After autoradiography, the filters were boiled in distilled water for 10 minutes to strip off the radioactive probes and rehybridized again with  $^{32}P$ -labeled-glyceraldehyde-3-phosphate dehydrogenase (GAPDH) cDNA probe ( $1 \times 10^6$  cpm/ $\mu$ g DNA) at 42 °C overnight for internal control. Autoradiographic signals of mRNA bands were quantified by scanning densitometry. The integrated optical density (IOD) of the hybridization bands were analyzed with TSTY-300 software (Sun Company of Tongji University). The IOD of  $\alpha 1(I)$ ,  $\alpha 1(III)$  and  $\alpha 1(IV)$  procollagen mRNA was corrected by the IOD of GAPDH mRNA. The data were analyzed by *t* test.

### *In situ hybridization*

*In situ* hybridization was performed on poly-L-lysine-coated frozen tissue sections with slight modification of our previous report<sup>[14]</sup>. Briefly, frozen liver tissue sections (5  $\mu$ m) were fixed in

40 mL/L paraformaldehyde before rehydrated with 0.1 mol/L PBS (pH 7.4), treated with 4 g/L Triton X-100 in PBS at RT for 10 minutes and incubated with proteinase K (20 mg/L, Merck Co.) in 0.1 mmol/L Tris at 37 °C for 30 minutes. Then the frozen tissue sections were postfixed with 40 mL/L paraformaldehyde in PBS (containing 5 mmol/L MgCl<sub>2</sub>) again at RT for 10 minutes and quenched with glycine (2 mL) in PBS for 5 minutes and acetylated in a freshly prepared solution of 2.5 mL/L acetic anhydride in 0.1 mol/L triethanolamine (pH 8.0, Sigma) for 10 minutes. After rinsing with PBS, the tissue sections were dehydrated in graded ethanols and air dried prior to hybridization.

For *in situ* hybridization, the sections were prehybridized at 37 °C for 1 hour. Twenty µL of hybridization buffer was added to each section, followed by incubation in a sealed humid chamber at 42 °C for 16-18 hours. The hybridization buffer contained 500 mL/L deionized formamide, 100 g/L dextran sulfate (Sigma), 4×Denhardt's solution, 0.3 mol/L NaCl, 1 mmol/L EDTA (pH 8.0), 20 mmol/L Tris Cl (pH 8.0), 200 mg/L denatured herring sperm DNA (Sigma), 200 mg/L yeast tRNA (Sigma) and 500 µg/L denatured procollagen cDNA probes which were labeled with digoxigenin-dUTP by the random priming method using a DNA labeling and detection kit (Boehringer Mannheim). After hybridization the excess of the probes was removed by rinsing in 2×SSC, 1×SSC and 0.5×SSC at 42 °C for 15 minutes each. The same kit as that used for DNA labeling was employed for immunological detection. The sections were washed briefly with buffer I solution (100 mmol/L Tris Cl, 150 mmol/L NaCl, pH 7.6), and incubated with buffer II solution which was prepared by buffer I solution with 10 g/L blocking reagent of the kit at RT for 30 minutes. After washing again briefly with buffer I solution, the sections were incubated with a 1:500-dilution of sheep anti-digoxigenin Fab fragment conjugated with alkaline phosphatase in buffer II solution with 1 mmol/L levamisole (Sigma) at 37°C for 2 hours. The sections were washed twice with buffer I solution at RT for 15 minutes, and equilibrated with the buffer III solution (100 mmol/L TrisCl, 100 mmol/L NaCl, and 50 mmol/L MgCl<sub>2</sub>, pH 9.5) for 10 minutes. Then the sections were incubated with the solution containing 4-nitroblue tetrazoliumchloride and 5-Bromo-4-chloro-3-indolyl-phosphate in buffer III to develop the color in a dark box for 2 hours. After stopping the color reaction with buffer IV solution (10 mmol/L TrisCl, 1 mmol/L EDTA, pH8.0), the sections were mounted with glycerin and observed under light

microscope.

### Immunohistochemistry

The monoclonal antibodies against Col IV, α-SMA and Dm were purchased from DAKO. The rabbit anti-Col I, Col III and mouse and rabbit PAP kits were prepared by our department<sup>[15]</sup>. Col I, Col III, Col IV, α-SMA and Dm in normal and fibrotic livers were detected with PAP method as described previously<sup>[15]</sup>. Briefly, serial cryostat sections (5 µm) were treated with pure methanol (containing 0.2 mL/L H<sub>2</sub>O<sub>2</sub>) at 37 °C for 30 minutes and washed in PBS, and then incubated in PBS with 100 mL/L bovine albumin at 37 °C for 1 hour. The sections were incubated with mouse anti-type IV collagen (1:100 dilution), α SMA (1:40 dilution) and Dm (1:100 dilution), and rabbit anti-type I collagen (1:100 dilution) and type III collagen (1:1 000 dilution) respectively at 37 °C for 1 hour and then at 4 °C overnight. The sections were washed in PBS and incubated with rabbit anti-mouse (1:200 dilution) or goat anti-rabbit IgG (1:200 dilution) at 37 °C for 1 hour. After washing in PBS, the sections were incubated with mouse or rabbit PAP complex (1:200 dilution) at 37 °C for 1 hour. The color was developed with 0.5 g/L 3,3'-diaminobenzidine/0.5 mL/L H<sub>2</sub>O<sub>2</sub>/0.05 mol/L TBS (pH 7.6) for 10 minutes. Normal mouse or rabbit serum instead of the specific primary antibodies were used as negative control.

## RESULTS

### Morphologic changes

Liver fibrosis model of the rats was successfully induced by CCl<sub>4</sub> subcutaneous injection with low-choline diet. At the 2nd week of the experiment, the hepatocytes of pericentral areas of lobules showed steatosis and necrosis. Likewise, HSCs proliferated and enlarged with enhanced Dm expression and some of them began to express α-SMA. At 4th-6th weeks of the experiment, fine cytofibrotic cords derived and extended from the periphery of the central veins. The cells in the cords were mainly composed of Dm and/or α-SMA positive MFs and the negative ones (Fbs) with long oval or spindle nuclei. There were also many activated Dm and α-SMA positive HSCs near the cords. In the middle stage of the experiment (8-12 weeks), the extended cytofibrotic septa connected the neighboring central areas or portal areas gradually. More Dm and/or α-SMA positive MFs or negative Fbs appeared within the septa also with Dm and α-SMA positive HSCs nearby (Figure 1). The proliferated oval cells in portal areas and septa expressed α-SMA and a few scattered hepatocytes might also express α-SMA. Newly formed capillaries could be found in the septa, and the long axes of which were parallel with the septa. In the late stage

(16-20 weeks), fibrotic septa was generally broadened. There were still many cells with long oval or spindle-shaped nuclei within the septa, however, most of them were both Dm and  $\alpha$ -SMA negative. Only the cells located at the margin of the septa still kept positive staining. Daughter septa extended from the widened fibrotic septa might occur and cut the liver parenchyma further. The proliferated HSCs in the daughter septa continued to be  $\alpha$ -SMA and Dm positive.

#### **Procollagen mRNA Northern analysis**

The expression of  $\alpha$ 1(I),  $\alpha$ 1(III) and  $\alpha$ 1(IV) procollagen mRNA was generally enhanced during the experiment, but the sequence and degree of the changes were not synchronous. At the 2nd week of the experiment, the content of  $\alpha$ 1(IV)-procollagen mRNA was obviously increased compared with that of the normal. Then it decreased after the 4th week, but still kept a comparatively higher level during the whole period of the experiment. Although the enhancement of the expression of  $\alpha$ 1(III) procollagen mRNA occurred later than that of  $\alpha$ 1(IV) procollagen mRNA, the increase of the expression of  $\alpha$ 1(III) procollagen mRNA was the most predominant one among the three in the whole experiment. The content of  $\alpha$ 1(III) procollagen mRNA reached its peak at the 10<sup>th</sup> week, then decreased gradually. The expression of  $\alpha$ 1(I) procollagen mRNA was enhanced later than that of  $\alpha$ 1(III) mRNA and reached its first peak at the 12th week, then it decreased a little and increased again after the 16th week. Finally the content of  $\alpha$ 1(I) procollagen mRNA reached the level as high as that of  $\alpha$ 1(III) procollagen mRNA at the 20th week (Figures 2, 3).

#### **Procollagen mRNA in situ hybridization**

The distribution of  $\alpha$ 1(I),  $\alpha$ 1(III),  $\alpha$ 1(IV) procollagen mRNA was similar in the normal rat liver, which mainly localized in mesothelial cells of the liver capsule, smooth muscle cells of blood vessels and periductal mesenchymal cells in portal areas, endothelial cells of central veins and a few HSCs in perisinusoids. In addition,  $\alpha$ 1(IV) procollagen mRNA transcription was also detected in sinusoid endothelial cells. In the early stage of the liver fibrogenesis there were a lot of stellate and spindle cells in the pericentral areas of the lobules expressed strong signals of  $\alpha$ 1(III),  $\alpha$ 1(IV) procollagen mRNA and only some of them expressed  $\alpha$ 1(I) procollagen mRNA signals simultaneously. These cells were mainly regarded as the proliferated HSCs and MFs and proved to express Dm and/or  $\alpha$ -SMA in the adjacent tissue sections. The cytofibrotic septa composed of HSCs, MFs and Fbs with positive hybridization signals connected the neighboring central areas and portal areas gradually (Figures 4, 5). The sinusoid

endothelial cells were also found to express strong signals of  $\alpha$ 1(IV) procollagen mRNA. In the middle stage of the experiment the MFs and Fbs in fibrotic septa further enhanced in expression of  $\alpha$ 1(III) procollagen mRNA, with some positive signals of  $\alpha$ 1(I) and  $\alpha$ 1(IV) procollagen mRNA expression as well. In the late stage of the experiment the spindle-shaped cells within the septa often with negative staining of Dm and  $\alpha$ -SMA expressed strong signals of  $\alpha$ 1(I) and  $\alpha$ 1(III) procollagen mRNA and weak signals of  $\alpha$ 1(IV) procollagen mRNA. In addition, the capillary endothelial cells of small blood vessels in the septa, some sinusoid endothelial cells and HSCs in perisinusoids also expressed strong  $\alpha$ 1(IV) procollagen mRNA (Figure 6). Hepatocytes, oval cells and the epithelia of bile ducts did not express any identifiable procollagen mRNA by *in situ* hybridization.

#### **Immunohistochemical detection of collagens**

Col I, Col III and Col IV of normal rat liver were mainly localized in liver capsule, portal areas and the walls of blood vessels. Liver sinusoids showed interruptedly positive staining with Col III and Col IV, but negative with Col I. In addition, Col IV was also localized at the basement membrane of capillaries and bile ducts. A few HSCs expressed type I and III procollagen with positive staining in cytoplasm. The change of the content of collagens in tissue sections of the experimental groups showed immunohistochemically the similar bias as that of procollagen mRNA by Northern analysis. In the early stage of the experiment, the content of Col III and Col IV was increased, which was mainly distributed in the necrotic areas or in fine cytofibrotic cords and was parallel to the distribution of the increased HSCs. The matrix of these areas was also stained with Col IV diffusely but weakly. However, the increase of Col I deposition was mild. In the middle stage, Col IV and Col III were further increased in the fibrotic septa. The decrease of  $\alpha$ 1(III) procollagen mRNA after the 10th week detected by Northern blot analysis did not seem to affect the content of Col III detected by immunohistochemistry, which was still steadily increased with fine fibers and diffusely distributed in and around the septa. Col I was also increased in the septa with thick fibers. Hyperplastic oval cells and cholangioli in the septa and hepatocytes did not express any procollagens. In the late stage, Col IV and Col III were decreased a little and the deposition of Col I was further increased in the broadened septa. The proliferated small blood vessels with positive staining of Col IV in basement membrane within the septa communicated with each other. The sinusoids were squeezed by the proliferated hepatocytes cords, most of which were Col IV and Col III positive continuously along the sinusoids.

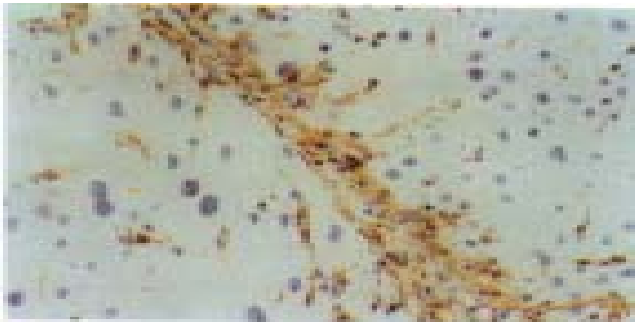


**Figure1** The cells in the cytofibrotic septa we re mainly composed of desmin (Dm) positive hepatic stellate cells (HSCs) and myo fibroblasts (MFs) and some Dm negative fibroblasts (Fbs) (8 weeks of CCl<sub>4</sub> administration). Immunohistochemical staining for Dm, ×200

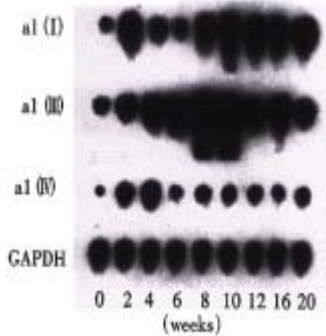


**Figure2** Dynamic changes of α1 (I), α1 (III) and α1 (IV) procollagen mRNA expression in different stages of the experiment (Northern blot analysis).

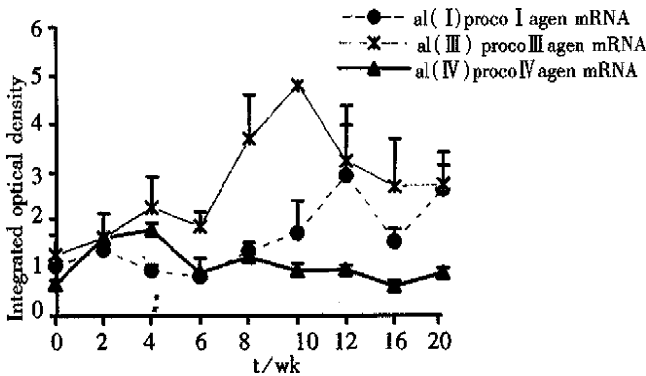


**Figure3** The changes of α1 (I), α1 (III) and α1 (IV) procollagen mRNA expression in different stages of the experiment (Northern blot analysis).



**Figure4** Most of the cells in the cytofibrotic septa expressed α1(III)- procollagen mRNA (6 weeks of CCl<sub>4</sub> administration). *In situ*- hibridization, ×400



**Figure5** The serial tissue section of Figure 4, only a few of the cells in the cytofibrotic septa expressed α1(I) procollagen mRNA. *In situ* hybridization, ×400

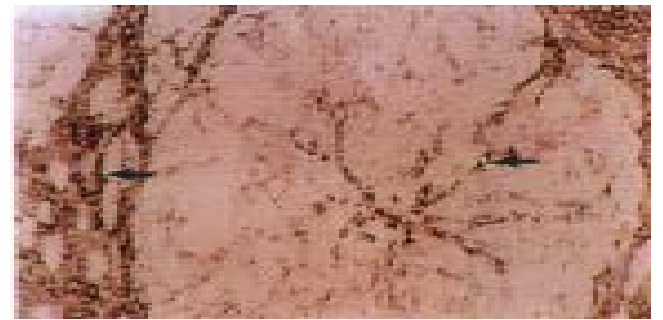


**Figure6** Some spindle cells and the endothelial cells of small blood (arrow) vessels in the fibrotic septa and the endothelial cells of the capillized sinusoids (arrow) expressed strong signals of α1 (IV) procollagen mRNA in the late stage of the experiment (16 weeks of CCl<sub>4</sub> administration). *In situ* hybridization, ×200

**DISCUSSION**

The fibrogenic factors known to contribute to liver fibrosis included CCl<sub>4</sub> administration, alcohol intake, dimethylnitrosamine administration, bile duct obstruction, iron or cholesterol overload, low-nutrient diet, schistosomiasis, immune complex induction, hepatitis virus, etc<sup>[1,4-6,16-18]</sup>. The gene expression of procollagen in liver fibrosis was predominant. The increased procollagen mRNA levels in liver fibrosis might result from both the increased gene transcription and increased mRNA stabilization. In fact, both of the mechanisms have been demonstrated to increase procollagen mRNA levels *in vivo* and *in vitro*<sup>[1,6-8]</sup>. Furthermore, some of cytokines might also be involved in the enhancement of expression of procollagen mRNA<sup>[5,19-21]</sup>. In the present study, the content of α1(I), α1(III) and α1(IV) procollagen mRNA expression in the liver detected by Northern blot analysis are all changed dramatically, but not synchronously during fibrogenesis. In the early stage of the experiment, the expression of α1(IV) procollagen mRNA was increased first, then that of α1(III) mRNA, which always kept the predominant expression over the other two. The expression of the α1(I) procollagen gene increased slowly during

the early stage, not as high as the content of  $\alpha 1(\text{III})$  mRNA until the 20th week. It suggests that there is some difference in the regulation of transcription and stabilization of these procollagen genes. The data from early liver fibrosis in this study were similar to those of Nakatsukasa *et al*<sup>[8]</sup> and our previous investigation<sup>[14]</sup>, but a bit different from that of Pierce *et al*<sup>[11]</sup>, in which slot blot analysis showed the expression of  $\alpha 1(\text{I})$  procollagen mRNA was enhanced at a slightly earlier point in the liver fibrogenesis than those of  $\alpha 1(\text{III})$ , and  $\alpha 1(\text{IV})$  procollagen mRNA. The reason for the discrepancy between the studies is not clear. It might attribute to different ways of  $\text{CCl}_4$  administration; involvement of other fibrogenic factors; and different methods, probes or animals used, etc.

Gene expression control is a very precise and complex mechanism, which is involved at transcription and post-transcription levels. It was reported that the polypeptide fragment of type I collagen could inhibit the transcription and translation of  $\alpha 1(\text{I})$  procollagen gene, and result in a feedback inhibition on procollagen polypeptide synthesis<sup>[22-24]</sup>. Perhaps it is because either the activation of procollagen gene or the feedback inhibition exerted by collagen polypeptides acted alternately so that the enhancement of the procollagen gene transcription during fibrogenesis revealed a ladder-shaped curve rather than a straight-line one. Moreover, the changes of collagen protein contents (average grade detected immunohistochemically) in liver during fibrogenesis were not consistent with the expression contents of their relevant procollagen mRNA completely, possibly because the content of procollagen mRNA was closely related to the real production of procollagen at the certain moment of the experiment, whereas the content of collagen protein in fibrotic liver revealed by immunohistochemistry in fact depended on all the finally accumulated content of collagen production, deposition, and degradation in liver tissue<sup>[14,25-27]</sup>. For this reason, the procollagen gene detection by nucleic hybridization can more sensitively and objectively reflect the trend of collagen synthesis in liver fibrogenesis.

Much more researches have focused on the study of the source of collagen-producing cells in liver fibrosis<sup>[4-8,10,14,16]</sup>. Besides HSCs and the related MFs, Fbs, whether any other cells, i.e. hepatocytes, endothelial cells and bile duct epithelial cell involved in the collagen production, is under active investigation. Some authors indicated that the collagens *in vivo* produced by hepatocytes both in normal and fibrotic liver was responsible for the principal amount of collagen content in liver<sup>[3,28]</sup>. However, the data from other

investigators demonstrated that hepatocytes had no collagen-synthesizing ability<sup>[7]</sup>. *In vitro*, several authors reported that the cultured hepatocytes could synthesize collagens spontaneously. But from the other investigators' point of view, the reason why the collagens appeared in cultured hepatocytes and endothelial cells was because of HSCs contamination<sup>[29,30]</sup>. Recent studies showed that HSCs, when stimulated by fibrogenic factors, were activated and enhanced in expression of Dm and  $\alpha$ -SMA, and underwent a phenotypic transformation to MFs and Fbs, around which there was the deposition of collagens. The increase of the number of these cells was parallel to the increase of the content of collagen deposition and to the changes of their distribution in the liver. Therefore, we suggested that there might be a "HSC-MF-Fb" effect cell system in liver fibrosis, which was responsible for collagen synthesis<sup>[12]</sup>. However, the conclusion described above was mainly derived from the results of our previous immunohistochemical and ultrastructural studies. Up to now, there are still controversies regarding which cell population offers the major contribution to liver fibrosis. In this study, the content and the distribution of  $\alpha 1(\text{I})$ ,  $\alpha 1(\text{III})$ , and  $\alpha 1(\text{IV})$  procollagen mRNA and the relevant collagens of rat liver fibrosis and cirrhosis were observed in detail by both immunohistochemistry and *in situ* hybridization with the procollagen cDNA probes labeled with digoxigenin. The role of "HSC-MF-Fb" effect cell system of collagen synthesis during liver fibrogenesis was further explored. In the early stage of the experiment, a variety of Dm and/or  $\alpha$ -SMA positive HSCs and MFs appeared in necrotic areas around central veins enhanced in the expression of  $\alpha 1(\text{III})$ ,  $\alpha 1(\text{IV})$  and  $\alpha 1(\text{I})$  procollagen mRNA.

Endothelial cells of sinusoids also increased in the expression of  $\alpha 1(\text{IV})$  procollagen mRNA. The distribution of  $\alpha 1(\text{I})$ ,  $\alpha 1(\text{III})$  and  $\alpha 1(\text{IV})$  procollagen mRNA expression cells was similar to those of the deposition of the corresponding collagens. At the middle stage of the experiment, the hybridization signals of these procollagen mRNA were mainly localized in the Dm and/or  $\alpha$ -SMA positive MFs within fibrotic septa and the HSCs around the septa. During the late stage of liver fibrogenesis, except for newly formed daughter septa, the number of Dm and/or  $\alpha$ -SMA positive cells in the fibrotic septa decreased gradually. However, the hybridization signals of these procollagen mRNA were still numerous in the cells with long oval or spindle-shaped nuclei within the septa. Therefore, the hybridization signals of the procollagen mRNA in well developed fibrotic septa was mainly derived from Fbs. Our results are consistent with those of several investigators who

demonstrated that HSCs, as well as MFs and Fbs, contributed to the major source of collagen synthesis during liver fibrogenesis by either *in situ* hybridization or immunohistochemically<sup>[7,8]</sup>. In contrast, no evidence of collagen synthesis by hyperplastic hepatocytes and cholangioli-like tubules, which embedded in the increased extracellular matrix of fibrotic septa and often with large amount of Fbs nearby, could be observed both *in situ* hybridization and immunohistochemically in the present study.

On the basis of our findings described above, it is confirmed that "HSC-MF-Fb" effect cell system is the major cell source of collagen synthesis during liver fibrogenesis, in which HSCs are the collagen-producing precursor cells in the liver. In and after the middle stage of liver fibrosis, the production of Col I, Col III, and Col IV in the fibrotic septa are mainly derived from both MFs and Fbs. The expression of procollagen mRNA in these cells plays a very important role in the process of liver fibrosis. Furthermore, sinusoid endothelial cells, as another source of Col IV production, might also participate in the capillarization of liver sinusoids.

**ACKNOWLEDGMENT** The authors would like to thank Ms. DAI Yue-Zhen for improving the English language in this paper.

## REFERENCES

- Pierce RA, Glaug MR, Greco RS, Mackenzie JW, Boyd CD, Beak SB. Increased procollagen mRNA levels in carbon tetrachloride-induced liver fibrosis in rats. *J Biol Chem*, 1987;262:1652-1658
- Ogawa K, Suzuki JI, Mukai H, Mori M. Sequential changes of extracellular matrix and proliferation of Ito cells with enhanced expression of desmin and actin in focal hepatic injury. *Am J Pathol*, 1986;125:611-619
- Clement B, Grimaud JA, Champion JP, Deugnier Y, Guillouzo A. Cell types involved in collagen and fibronectin production in normal and fibrotic human liver. *Hepatology*, 1986;6:225-234
- Maher JJ, McGuire RF. Extracellular matrix gene expression increases preferentially in rat lipocytes and sinusoidal endothelial cells during hepatic fibrosis *in vivo*. *J Clin Invest*, 1990;86:1641-1648
- Knittel T, Schuppan D, Meyer zum Büschenfelde KH, Ramadori G. Differential expression of collagen types I, III and IV by fat storing (Ito) cells *in vitro*. *Gastroenterology*, 1992;102:1724-1735
- Weiner FR, Shah A, Biempica L, Zern MA, Czaja MJ. The effects of hepatic fibrosis on Ito cell gene expression. *Matrix*, 1992;12:36-43
- Milani S, Herbst H, Schuppan D, Surrenti C, Riecken EO, Stain H. Cellular localization of type I, III, IV procollagen gene transcripts in normal and fibrotic human liver. *Am J Pathol*, 1990;137:59-70
- Nakatsukasa H, Nagy P, Everts RP, Hsia CC, Marsden E, Thorgeirsson SS. Cellular distribution of transforming growth factor  $\beta$ 1 and procollagen types I, III and IV transcripts in carbon tetrachloride induced rat liver fibrosis. *J Clin Invest*, 1990;85:1833-1843
- Ramadori G, Veit T, Schwogler S, Dienes HP, Knittel T, Rieder H, Meyer zum Büschenfelde KH. Expression of the gene of the  $\alpha$ -smooth muscle-actin isoform in rat liver and in rat fat storing (ITO) cells. *Virchows Archiv B Cell Pathol*, 1990;59:349-357
- Tanaka Y, Nouchi T, Yamane M, Irie T, Miyakawa H, Sato C, Marumo F. Phenotypic modulation in lipocytes in experimental liver fibrosis. *J Pathol*, 1991;164:273-278
- Pinheiro-Margis M, Margis R, Borojevic R. Collagen synthesis in an established liver connective tissue cell line (GRX) during induction of the fat-storing phenotype. *Exp Mol Pathol*, 1992;56:108-118
- Zhang YE, Xu ZD, Wang XH, Zao JM, Zhai WR, Zhang XR, Zhu TF. Dynamic changes in extracellular matrix and related interstitial cells in experimental organ sclerosis. *Zhonghua Binglixue Zazhi*, 1994;23:111-114
- Chomczynski P, Sacchi N. Single-step method of RNA isolation by acid guanidinium thiocyanate-phenol-chloroform extraction. *Anal Biochem*, 1987;162:156-159
- Du WD, Zhang YE, Ji XH, Zhai WR, Zhou XM. Synthesis and degradation of type IV collagen in rat experimental liver fibrosis. *Zhonghua Yixue Zazhi*, 1997;77:513-515
- Wang XH, Zhang YE, Zhang JS, Xu ZD, Zhang XR. Purification of human type I and type III collagen and preparation of their antisera. *Shanghai Yike Daxue Xuebao*, 1994;21:405-408
- Annoni G, Weiner FR, Colombo M, Czaja MJ, Zern MA. Albumin and collagen gene regulation in alcohol and virus induced human liver disease. *Gastroenterology*, 1990;98:197-202
- Arthur MJ. Iron overload and liver fibrosis. *J Gastroenterol Hepatol*, 1996;11:1124-1129
- Buysens N, Kockx MM, Herman AG, Lazou JM, Van den Berg K, Wisse E, Geerts A. Centrolobular liver fibrosis in the hypercholesterolemic rabbit. *Hepatology*, 1996;24:939-946
- De Bleser PJ, Niki T, Rogiers V, Geerts A. Transforming growth factor-beta gene expression in normal and fibrotic rat liver. *J Hepatol*, 1997;26:886-893
- Moshage H. Cytokines and the hepatic acute phase response. *J Pathol*, 1997;181:257-266
- Brenzel A, Gressner AM. Characterization of insulin-like growth factor (IGF) I receptor binding sites during *in vitro* transformation of rat hepatic stellate cells to myofibroblasts. *Eur J Clin Chem Clin Biochem*, 1996;34:401-409
- Ikeda H, Wu GY, Wu CH. Lipocytes from fibrotic rat liver have an impaired feedback response to procollagen propeptides. *Am J Physiol*, 1993;264(pt1):G157-G162
- Aycock RS, Raghov R, Stricklin GP, Seyer JM, Kang AH. Post-transcriptional inhibition of collagen and fibronectin synthesis by a synthetic homology of a portion of the carboxyl terminal propeptide of human type I collagen. *J Biol Chem*, 1986;261:14355-14360
- Goldenberg R, Fine RE. Generalized inhibition of cell-free translation by the amino terminal propeptide of chick type I procollagen. *Biochim Biophys Acta*, 1985;826:101-107
- Alcolado R, Arthur MJ, Iredale JP. Pathogenesis of liver fibrosis. *Clin Sci*, 1997;92:103-112
- Herbst H, Wege T, Milani S, Pellegrini G, Orzechowski HD, Bechstein WO, Neuhaus P, Gressner AM, Schuppan D. Tissue inhibitor of metalloproteinase-1 and -2 RNA expression in rat and human liver fibrosis. *Am J Pathol*, 1997;150:1647-1659
- Iredale JP. Matrix turnover in fibrogenesis. *Hepatogastroenterology*, 1996;43:56-71
- Chojkier M. Hepatocyte collagen production *in vivo* in normal rats. *J Clin Invest*, 1986;78:333-339
- Maher JJ, Bissell DM, Friedman SL, Roll FJ. Collagen measured in primary cultures of normal rat hepatocytes derives from lipocytes within the monolayer. *J Clin Invest*, 1988;82:450-459
- Guzelian PS, Qureshi GD, Diegelmann RF. Collagen synthesis by hepatocytes: studies in primary cultures of parenchymal cells from adult rat liver. *Coll Relat Res*, 1981;1:83-93

# Inhibitory activity of polysaccharide extracts from three kinds of edible fungi on proliferation of human hepatoma SMMC-7721 cell and mouse implanted S180 tumor

JIANG Shi-Ming, XIAO Zheng-Ming and XU Zhao-Hui

**Subject headings** polysaccharide, edible fungi; liver neoplasm; carcinoma, hepatocellular; SMMC-7721, tumor cell, cultured; implanted tumor, S-180; cell proliferation

## Abstract

**AIM** To determine the activities of polysaccharide extracts from *Flammulina velutipes* (Curt. ex Fr.) Sing (FV), *Lentinus edodes* (LE) and *Agaricus bisporus*-Sing (AB) on the proliferation of human hepatoma SMMC-7721 cells *in vitro* and on mouse implanted S-180 tumors *in vivo*.

**METHODS** The polysaccharide extracts were isolated from the fruit bodies of FV, LE and AB by the methods of hot-water extraction, Sevag's removal of proteins, ethanol precipitation, trypsin digestion and ethanol fractional precipitation. Human hepatoma SMMC-7721 cells were treated with 50mg/L polysaccharide extracts, and the mitosis index, mitochondria activity and cell proliferation were detected at different times in both control and experimental groups. The mice with S-180 implanted tumors were injected with the polysaccharide extracts at 24mg/kg body weight for 9d and the tumor weight was measured on the 15<sup>th</sup> day.

**RESULTS** The mitosis index of hepatoma cells *in vitro* could be significantly decreased by treatment with the polysaccharide extracts from the three kinds of edible fungi ( $P < 0.005$ ). The cell numbers and mitochondria activity of SMMC-7721 cells treated with polysaccharide extracts

were lower than those in control groups ( $P < 0.005$ ). The inhibition rates of polysaccharide extracts against implanted S-180 tumors in mice were 52.8%, 56.6% and 51.9% respectively compared with that in control groups.

**CONCLUSION** The polysaccharide extracts from the three kinds of edible fungi could inhibit not only the cultured malignant cells *in vitro* but also implanted S-180 tumor *in vivo*.

## INTRODUCTION

The polysaccharides from edible fungi (e.g. LE<sup>[1]</sup>, FV<sup>[2,3]</sup>) were macromolecular substances with strong antigenicity and were also verified to have antitumor activity against S-180 implanted tumor in mice *in vivo* and that from AB were shown to have anti-infection of virus and anticanceration *in vivo*. The references about the effects of polysaccharide extracts from edible fungi on cancer cells *in vitro* were very limited. In this report human hepatoma SMMC-7721 cells were used as a model to detect the anticancer activity of polysaccharide extracts from the three kinds of edible fungi (FV, LE and AB). The mitosis index, cell proliferation and mitochondria metabolism activity of SMMC-7721 cells were compared between the control group and polysaccharide extracts treatment groups. The antitumor activity of polysaccharide extracts from these three kinds of edible fungi against implanted S-180 tumor in mice *in vivo* was also observed.

## MATERIALS AND METHODS

RPMI 1640 medium is product of GIBCO; trypsin and MTT were from Sigma; the fruit bodies of FV, LE and AB were from cultivated products in Jinan. Mice with S-180 and Kunming male mice (22 g - 25 g) were from Shandong Experimental Animal Center; 24 and 96-well plates were from Costar.

## Cell lines and culturing

Human hepatoma SMMC-7721 cells were obtained from the Shanghai Cell Bank of Chinese Academy of Sciences and maintained in our laboratory. The cells were grown as monolayers in RPMI 1640

Biology Department, the Provincial Key Laboratory of Animal Stress, Shandong Normal University, Jinan 250014, Shandong Province, China  
JIANG Shi-Ming, male, born on 1961-11-26 in Zhaoyuan City, Shandong Province, graduated from Shandong Normal University as a postgraduate in 1985, now associate professor of cell biology, an M.Ph.D. candidate of the Heidelberg University, Germany, having more than 30 papers and one book published.

Supported by a grant from the Science and Technology Committee of Shandong Province, No.95071910.

**Correspondence to:** Dr. JIANG Shi-Ming, Biology Department, Shandong Normal University, Jinan 250014, Shandong Province, China

Email: S.Jiang@DKFZ-Heidelberg.de

Received 1999-04-08

medium supplemented with 10% fetal calf serum (FCS) and incubated at 37 °C in the humidified incubator with 5% CO<sub>2</sub>/95% air.

#### **Extraction and purification of polysaccharide extracts from the edible fungi**

The extraction and purification of polysaccharide extracts were modified according to the methods of Cao<sup>[3]</sup>. The fresh fruit bodies of the edible fungi were homogenized for three times, heated at 98 °C-100 °C for 5 h, centrifuged for 15 min with 4500 rpm. The supernatants were collected and the precipitation was extracted for another two times. All the supernatants were concentrated to proper volume and precipitated with 3 times 95% ethanol and stayed overnight at 4 °C. The precipitation was gathered by centrifugation, dissolved in distilled water, dialyzed in 4 °C distilled water for 2 d, digested with trypsin and precipitated protein with Sevag's method. The polysaccharide extracts were dialyzed in 4 °C distilled water for another 2 d, precipitated with 3 times 95% ethanol, stayed overnight and collected with centrifuge. The white precipitation of polysaccharide extracts from the three edible fungi was rinsed with 100% ethanol and acetone and dried at room temperature.

#### **Determination of polysaccharide extracts on the metabolism of mitochondria**

The exponent growing SMMC-7721 cells in culture flasks were harvested by trypsinization with 0.25% trypsin, suspended in RPMI 1640 medium with 10% FCS, adjusted to the concentration of 1×10<sup>5</sup> cells/mL, plated into 96-well plates (200 μL cells/well) and incubated at 37 °C in 5% CO<sub>2</sub>/95% air for 24 h. The medium was aspirated and the cells were washed with RPMI 1640 medium. The medium was replaced with RPMI 1640 containing 50 mg/L polysaccharide extracts from different fungi as treatment groups respectively and medium with 10% FCS and Non-FCS as controls (each group having 8 repeated wells). The cells were incubated in different treatments for 20 h, 44 h and 68 h respectively. The metabolism of mitochondria<sup>[4]</sup> were detected by adding 20 μL- MTT (final concentration 10 mg/L) to media, incubating for 4 h, sucking out the media, adding 100 μL dimethylsulfoxide (DMSO) to dissolve the violet-crystal and measuring the absorption at 570 nm.

#### **Measurement of mitosis index**

The exponent growing SMMC-7721 cells were suspended in RPMI 1640 medium plus 10 % FCS, adjusted to 1×10<sup>5</sup> cells/mL, plated 2 mL cells/well into 24-well plates (with cover glass, 4 repeated wells in each group) and incubated at 37 °C for 24 h. After incubated in medium containing different

polysaccharide extracts (experiment groups) and 10% FCS or non-FCS (as control groups) for 24 h, the cells were fixed with Carnoy solution and stained with Feulgen reaction. The mitosis indexes were detected randomly by counting 1000 cells<sup>[5]</sup>.

#### **Proliferation of SMMC-7721 cells in medium containing polysaccharide extracts**

The SMMC-7721 cells were treated with different polysaccharide extracts for 7 d as above (6 repeated wells in each group) and the proliferation of SMMC-7721 cells were observed by counting the cell number every day.

#### **In vivo experiments with implanted S-180 tumor**

The S-180 tumor cells were washed with normal physiological saline for three times, adjusted to 1×10<sup>7</sup> cells/mL and implanted by subcutaneous injection 200 μL to each mouse. Twenty-four hours late, the mice were injected ip with 24 mg polysaccharide extracts/kg body weight in experimental groups and physiological saline in control group for 9 d. On the 15<sup>th</sup> day after the treatment, the mice were killed and the tumors were isolated and weighed. The inhibition rate of tumor was calculated as follows:

$$\frac{(\text{Mean tumor weight in controls} - \text{mean tumor weight in experiments})}{\text{Mean tumor weight in control group}} \times 100\%$$

## **RESULTS**

#### **The production of polysaccharide extracts**

The production of the polysaccharide extracts extracted from the three kinds of edible fungi were 1.53 mg/g ± 0.11 mg/g fresh fruit bodies of *LE*; 4mg/g ± 0.15 mg/g fresh fruit bodies of *FV* and 1.3 mg/g ± 0.11 mg/g fresh fruit bodies of *AB*, respectively. None of the polysaccharide extracts showed obvious absorption in the range of 220 nm-780 nm.

#### **The effects of polysaccharide extracts on the metabolism of mitochondria**

Within 24 h, the mitochondria metabolism of hepatoma SMMC-7721 cells showed no obvious differences in each group. At 48 h and 72 h, the metabolism activities in experimental groups were much lower than those in both FCS and non-FCS control groups, but in different experimental groups they were similar (Figure 1).

#### **The effects of polysaccharide extracts on mitosis index (MI)**

The MI in all the groups treated with polysaccharide extracts was lower than that in both control groups ( $P < 0.005$ ) (Table 1).

### The effects of polysaccharide extracts on the proliferation of SM MC-7721 cells

The cell number after treatment with polysaccharide extracts for 48 h were obviously lower as compared with both FCS and non-FCS controls (Figure 2). On the 7<sup>th</sup> day the number of the cells covered 55.5% (LE), 59.5% (FV) and 61.6% (AB) of that in the FCS control and 63% (LE), 67.6% (FV) and 70.3% (AB) of that in non-FCS control.

### The inhibition of polysaccharide extracts on the proliferation of S-1 80 implanted tumor

The inhibitions of the three polysaccharide extracts on the proliferation of the S-180 tumor *in vivo* were 52.8% (LE), 56.6% (FV) and 51.9% (AB), respectively (Table 2).

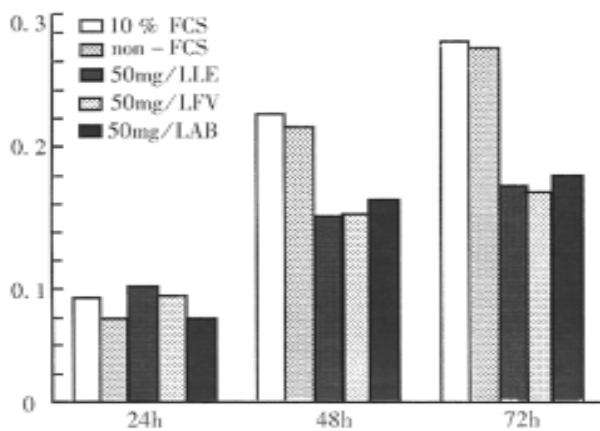


**Figure 1** Effects of polysaccharide extracts on the mitochondria metabolism of SMMC-7721 cells.

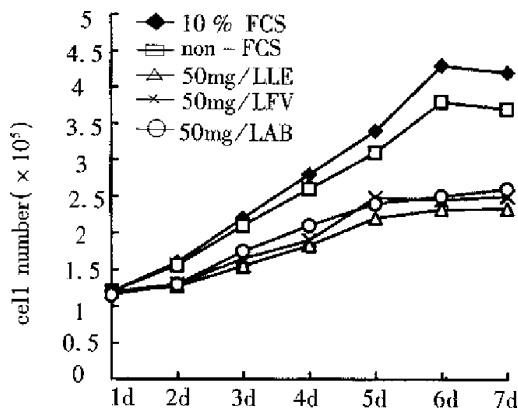


**Figure 2** The effects of polysaccharide extracts on the proliferation of SMMC-7721 cells.

**Table 1** The effects of polysaccharide extracts on the MI of SMMC-7721 cells

Groups	MI(%)	P value
C1	18.2±1.1	
C2	13.4±1.2	
E1	5.8±0.7	<0.005
E2	8.5±0.9	<0.005
E3	8.4±0.8	<0.005

C1: 10% FCS; C2: non-FCS; E1: 50 mg/L polysaccharide extracts from LE; E2: 50 mg/L polysaccharide extracts from FV; E3: 50 mg/L polysaccharide extracts from AB.

**Table 2** The inhibitions of polysaccharide extracts on the proliferation of S-180 implanted tumor *in vivo*

Groups	n	Dose (mg/kg)	Tumor weight (g)	Inhibition (%)	P value	Mean inhibition (%)
LE 1	10	24	0.369±0.058	55.5	<0.005	52.8
LE 2	10	24	0.387±0.069	53.3	<0.005	
LE 3	10	24	0.417±0.085	49.7	<0.005	
FV 1	10	24	0.371±0.034	55.3	<0.005	56.6
FV 2	10	24	0.348±0.039	58.1	<0.005	
FV 3	10	24	0.376±0.044	54.7	<0.005	
AB 1	10	24	0.379±0.049	54.3	<0.005	51.9
AB 2	10	24	0.39±0.067	53	<0.005	
AB 3	10	24	0.427±0.087	48.5	<0.005	
Control 20			0.83±0.17			

## DISCUSSION

### The efficiency of polysaccharide extracts

Following the same processes, the products of polysaccharide extracts in the three kinds of edible fungi were obviously different. The product of polysaccharide extracts in FV was 4 mg/g fresh fruit body, which was 4 times higher than that in AB and 2.6 times than in LE. These differences should be induced by the contents of polysaccharide in different kinds of edible fungi. Although the polysaccharide extracts were a mixture of polysaccharides, they had no obvious absorption peak in the range of 220 nm-780 nm.

### The effects of polysaccharide extracts on the hepatoma cell *in vitro* and S-180 *in vivo*

The polysaccharide from LE was the first extracts which verified the anti-tumor activity in 1969<sup>[1]</sup>, which initiated the study of extraction, purification, structure analysis and anti-tumor activity of polysaccharides from LE. The best result of anti-tumor activity of polysaccharides from LE could reach 90%-100% *in vivo*. So polysaccharides from LE were believed to be one of the best effective substances for antitumor treatment. On the other hand the polysaccharide from LE was also verified to have anti-mutant activity<sup>[6]</sup>. Both pure and mixed polysaccharides from FV were shown to have strong anti-tumor activity against implanted S-180 tumor in mice<sup>[3,7]</sup>. *In vivo* the anti-tumor activities of polysaccharides from edible fungi were mainly induced by activating the immune system, although the detailed mechanism was not clear. In this study, the cultured hepatoma SMMC-7721 cells were used as a model to detect the activity of polysaccharide extracts *in vitro*. The results of MI, mitochondria activity and cell proliferation showed that the extracts from the edible fungi could inhibit the division of the cells and induce the decrease of cell proliferation, which

was similar to that from fruit bodies of *Ganoderma lucidum*<sup>[8]</sup>. The inhibition of the extracts from the three kinds of edible fungi on the growth of implanted S-180 tumor *in vivo* could reach 52.8%, 56.6% and 51.9% respectively, which agreed with the previous reports<sup>[3]</sup>.

These results suggested that the polysaccharide extracts from *LE*, *FV* and *AB* could not only inhibit the growth of implanted S-180 tumor *in vivo* but interfere with the proliferation of human hepatoma SMMC-7721 cells *in vitro* .

#### REFERENCES

1 Du YY. The advantage in the study of polysaccharide from

- Lentinus edodes. *China Edible Fungi*,1995;14:9-11
- 2 Guo JM, Shangguan ZJ, Chen JC. The study and usage of medicinal fungi. *China Edible Fungi*,1994;13:8-10
- 3 Chao PY, Wu ZD, Wang RC. The extraction, purification and analysis of polysaccharide PA3DE from the fruit body of *Flammulina velutipes*(Curt. ex Fr.) Sing.*Acta Biochemica and Biophysica Sinica*,1989;21:152-156
- 4 Huang WD, Wang YF. The colorimetry method for fast detection of cell proliferation and senescence. *Chemist Life*,1994;14:44-45
- 5 Jiang SM, Xu ZH, Shi XM, Zhang Y. The survival and malignant phenotype changes of human hepatoma SMMC-7721 cells induced by -50°C cryopreservation. *China Natl J New Gastroenterol*,1997;3:3
- 6 Zheng JX. The anti-mutant activity of polysaccharide from fruit body. *Lentinus Edodes.China Edible Fungi*,1994;13:5-7
- 7 Yoshioka T. Studies on anti tumor polysaccharide of *Flammulina velutipes* (Curt. ex Fr.) Sing I. *Chem Phar Bull*, 1973;21:1772
- 8 Xu ZH, Jiang SM. The extracts of *Ganoderma Lucidum* on DNA synthesis of hepatoma SMMC-7721 cells. *China Edible Fungi*, 1996;15:34-35

Edited by MA Jing-Yun

# Regulatory effect and mechanism of gastrin and its antagonists on colorectal carcinoma

HE Shuang-Wu, SHEN Kang-Qiang, HE Yu-Jun, XIE Bin and ZHAO Yan-Ming

**Subject headings** colorectal neoplasms; gastrin; proglumide; somatostatin; IP<sub>3</sub>, Ca<sup>2+</sup>; protein kinase C; oncogene; AgNORs

## Abstract

**AIM** To explore the effect and mechanism of gastrin and its antagonists proglumide and somatostatin on colorectal carcinoma and their clinical significance.

**METHODS** A model of transplanted human colonic carcinoma was established from SW480 cell line in gymmouse body. The volume and weight of transplanted carcinoma was observed under the effect of pentagastrin (PG), proglumide (PGL) and octapeptide somatostatin (SMS201-995, SMS). The cAMP content of carcinoma cell was determined by radioimmunoassay and the DNA, protein content and cell cycle were determined by flow-cytometry. The amount of viable cells was determined by MTT colorimetric analysis, IP<sub>3</sub> content was determined by radioimmuno assay, Ca<sup>2+</sup> concentration in cell by fluorometry and PKC activity by isotopic enzymolysis. The expression of gastrin, c-myc, c-fos and rasP21 in 48 cases of colorectal carcinoma tissue was detected by the immunocytochemistry SP method. Argyrophilia nucleolar organizer regions was determined with argyrophilia stain.

**RESULTS** The volume, weight, cAMP, DNA and protein content in carcinoma cell, cell amount and proliferation index of S and G<sub>2</sub>M phase in PG group were all significantly higher than those of control group. When PG was at the

concentration of 25 mg/L, the amount of viable cells, IP<sub>3</sub> content and Ca<sup>2+</sup> concentration in cell and membrane PKC activity in PG group were significantly higher than those in control group; when PGL was at a concentration of 32 mg/L, they dropped to the lowest level in PG (25 mg/L) +PGL group, but without significant difference from the control group. The positive expression rate of gastrin, c-myc, c-fos and rasP21 in carcinoma tissue was 39.6%, 54.2%, 47.9% and 54.2% respectively and significantly higher than that in mucosa 3 cm and 6cm adjacent to carcinoma tissue and normal colorectal mucosa. The positive expression rate of gastrin of highly-differentiated adenocarcinoma group was significantly higher than that of poorly-differentiated and mucinous adenocarcinoma groups. The AgNORs count of carcinoma tissue was significantly higher than that in mucosa 3 cm and 6 cm adjacent to carcinoma tissue and normal colorectal mucosa; and the positive expression of c-myc and c-fos and the AgNORs count in gastrin-positive group was significantly higher than those in gastrin-negative group.

**CONCLUSION** Pentagastrin has a promoting effect on the growth of transplanted human colonic carcinoma from SW480 cell line. PGL has no obvious effect on the growth of human colonic carcinoma SW480 cell line, but could inhibit the growth promoting effect of PG on transplanted carcinoma. Somatostatin can not only inhibit the growth of transplanted human colonic carcinoma from SW480 cell line directly but also depress the growth-promoting effect of gastrin on the transplanted carcinoma. Some colorectal carcinoma cells can produce and secrete gastrin through autocrine, highly-differentiated adenocarcinoma express the highest level gastrin. Endogenous gastrin can stimulate the cell division and proliferation of carcinoma cell and promote the growth of colorectal carcinoma regulating the expression of oncogene c-myc, c-fos. Our study has provided experimental basis for the adjuvant treatment using gastrin antagonist such as PGL, so matostatin of patients with colorectal carcinoma.

Department of General Surgery, Daping Hospital and Research Institute of Surgery, the Third Military Medicine University, Chongqing 400042, China

Dr. HE Shuang-Wu, female, born on 1936-10-11 in Chenzhou City, Hunan Province, graduated from Department of Medicine in Hunan Medical University in 1960, now professor, chief physician, tutor of postgraduate, engaged in the diagnosis and treatment of gastrointestinal carcinoma, focusing on the relation between sex hormone, gastrointestinal hormone and gastrointestinal carcinoma, having 54 papers published.

**Correspondence to:** Dr. HE Shuang-Wu, Department of General Surgery, Daping Hospital and Research Institute of Surgery, the Third Military Medicine University, Chongqing 400042, China

Tel. +86-23-68757268

Received 1999-04-08

## INTRODUCTION

In recent years, some studies indicated that gastrin could promote the growth of some colorectal carcinomas, but gastrin antagonist such as PGL, somatostatin (SS) could inhibit the growth of those colorectal carcinomas. In order to explore the mechanism of the effect and the clinical significance of gastrin and its antagonists on colorectal carcinoma, we established the model of transplanted colonic carcinoma from SW480 cell line in gymnomouse body, and observed the volume and weight of transplanted carcinoma, content of cAMP, DNA, protein and cell cycle of carcinoma cell under the effect of pentagastrin (PG), proglumide (PGL) and octapeptide somatostatin (SMS 201-995, SMS). We also observed the effect of PG and PGL on the amount of viable cells, inositol 1, 4, 5-trisphosphate (IP<sub>3</sub>) content and Ca<sup>2+</sup> concentration in cell and protein kinase C (PKC) activity of colonic carcinoma SW480 cell line cultured *in vitro*, and detected the expression of gastrin, cancer genes c-myc, c-fos and rasP21 in 48 cases of colorectal carcinoma tissue by the immunocytochemical SP method and determined the argyrophilia nucleolar organizer regions count with argyrophilia stain.

## MATERIALS AND METHODS

### Materials

Human colonic carcinoma SW480 cell line (Sloan Kettering Memorial Cancer Center, US A), BALB/C gymnomouse (Experimental Animal Center of Third Military Medical University), pentagastrin (PG, Shanghai Lizhu Chemical Reagent Co.), octapeptide somatostatin (SMS 201-995, SMS, PHARMA, Swiss); proglumide (PGL, No.11 Pharmaceutic al Factory, Shanghai), RPMI1640 culture solution (GIBCO, USA), 3H-myo-inositol (Institute of Atomic Energy, Chinese Academy of Sciences), T-<sup>32</sup>P-ATP (Ya Hui Biology Engineer Co.), Fura-2/AM (Sigma, USA), cAMP radioimmunoassay reagent kit (Department of Nuclear Medicine of Shanghai Second Medical University), monoclonal antibody to gastrin and SP kit (ZYMED Co., USA), monoclonal antibody for c-myc and rasP21, monoclonal antibody for c-fos (Santa Cruz Co., USA).

### Experiment methods

**Establishment of transplanted carcinoma model** The human colonic carcinoma SW480 cell line was resuscitated conventionally. Cell lines with exuberant vitality were selected to form primary transplanted carcinoma, digested with 0.25% trypsin, centrifugated to wipe off the digestive solution, and adjusted the cell concentration with RPMI1640 cultural solution to  $5 \times 10^6$ /mL. The

living cell amount exceeded 99% by trypan-blue stain. Twelve gymnomice were randomized into six groups. The cell line went through six passages, each time two gymnomice were inoculated. After 0.2 mL of carcinoma cell solution was inoculated to the back of the neck of gymnomouse, the gymnomice were raised in clean room. When the diameter of the carcinoma reached 1.5 cm to 2.2 cm, the gymnomice were killed by severing the cervical vertebra, and the carcinoma mass was stripped bacteria-freely. After preserving specimen for histological and electron microscopical examination, the mass was smashed, ground into cell suspension with RPMI1640 cultural solution, adjusted the cell concentration to  $5 \times 10^6$ /mL, the next passage was started with 0.2 mL of the cell suspension.

**Experimental animal grouping** After undergoing passages stably-growing human colonic transplanted carcinoma cells were inoculated into thirty gymnomice. They were randomized into six groups and injected with the experimental drugs subcutaneously the next day, two times per day, for 35 days. The gymnomice were killed 24 hours after the last injection. Control group: 0.4 mL normal saline/mouse. PG group: 4 μg PG/mouse. PGL group: 10 mg PGL/mouse. SMS group: 6 μg SMS/mouse. PG+PGL group: 4 μg PG and 10 mg PGL/mouse. PG+SMS group: 4 μg PG and 6 μg SMS/mouse.

**Volume and weight of transplanted carcinoma** The long diameter and short diameter were measured at the same time every sixth days after the inoculation, and the measurement lasted six weeks. The volume was calculated by the formula:  $V = 1/2a^2b$ . The weight of the mass was then determined after decontamination of the non tumor tissue such as blood and fat tissue.

**Flow-cytometry** Fifteen g transplanted carcinoma tissue was cut and made into single-cell suspension<sup>[1]</sup>, adjusted to a cell concentration of  $1 \times 10^8$ /L, and fixed with 700 g/L alcohol at 4 °C. The DNA was stained with propidium iodide to redish fluorescence and the protein stained with fluorescein isothiocyanate to green fluorescence. Thirty minutes later, the suspension was analyzed on instrument at room temperature. According to Barlogie cell cycle analysis method, the cells were divided into three parts: G<sub>0</sub>/G<sub>1</sub> phase, S phase and G<sub>2</sub>M phase. Proliferation index (PI) of the cell was calculated as:  $PI = (S + G_2M) / (G_0/G_1 + S + G_2M) \times 100\%$ .

**MTT colorimetric analysis**<sup>[2]</sup> Suspend the large intestine carcinoma SW480 cells in logarithmic

growth stage in 100g/L bovine serum culture solution to a concentration of  $5 \times 10^8$ /L. The suspension was inoculated in to a 96-well plate (100  $\mu$ L/well) and cultivated for 24 h. After the supernatant was wiped off, 100  $\mu$ L of 5 g/L bovine serum culture solution was added to each well and the first well as zero control, the second one as cell control, which were added with 100  $\mu$ L of 5 g/L bovine serum culture solution respectively. From the third one on, 100  $\mu$ L different drugs with different concentration were added to each well as follows and repeated 8 times: PG group: the concentration was 6.25, 12.50, 25.00, 50.00 and 100.00 mg/L, respectively. PG (25 mg/L)+PGL group: the concentration of PGL was 8.00, 16.00, 32.00, 64.00 and 128.00 mg/L. They were cultivated in 37 °C, 50 g/L CO<sub>2</sub> incubator for 72h, each well added with 10  $\mu$ L of 5 g/L MTT solution 6 hours before terminating the culture and 100  $\mu$ L of 200 g/LSDS solution was added at the termination, kept overnight in the incubator, and the absorptivity (A value) at the 570 nm wavelength was determined on the instrument the next day.

**Determination of IP<sub>3</sub> content in carcinoma cell** Add 15 mCi/L of [<sup>3</sup>H]-inosito into the suspension of SW480 cell line, cultivate them in 37 °C, 50 g/L CO<sub>2</sub> incubator for 18 hours, then add LiCl solution, 2 hours later, add 100 $\mu$ L different drugs with different concentration to each well and cultivate 1 minute as follows: PG group: the concentration was 6.25, 12.50, 25.00, 50.00 and 100.00 mg/L, respectively; PG (25 mg/L)+PGL group: the concentration of PGL is 16.00, 32.00 and 64.00 mg/L. Separate IP<sub>3</sub> from the suspension with anion change separation column according to the method described in reference<sup>[3,4]</sup>, then determine its CPM value with hydroflicker.

**Determination of PKC activity** Determine the PKC activity in human colonic carcinoma SW480 cell line under the effect of PG and PGL according to the method described in reference<sup>[5]</sup> with isotopic enzymolysis. The grouping and concentration of PG and PGL were the same with IP<sub>3</sub> determination.

**Determination of Ca<sup>2+</sup> concentration** Determine the Ca<sup>2+</sup> concentration in human colonic carcinoma SW480 cell line under the effect of PG and PGL according to the method described in reference<sup>[6]</sup> with fluorometry. The grouping and concentration of PG and PGL were the same with IP<sub>3</sub> determination.

**Specimen** Forty-eight cases of radical resection of colorectal carcinomas collected from August 1996 to April 1997 in our department were chosen as

experimental materials. Ten cases of normal colorectal mucosa served as control group, including 3 cases of inner prolapse of rectum, 2 of volvulus of sigmoid and 5 of sudden death. All the specimens were confirmed by pathological examination. Fresh colorectal carcinoma tissue (3 g) and mucosae 3 cm and 6 cm adjacent to carcinoma were cut respectively, fixed with 40 g/L paraformaldehyde, dehydrated and embedded with paraffin.

**Immunohistochemistry method** Immunohistochemistry staining of gastrin, c-myc, c-fos and rasP21 was carried out by SP method, referring to the illustration of reagent kit. The first antibody dilution of gastrin was 1:50, while the dilution of c-myc, c-fos and rasP21 was all 1:100. Microwave was used to repair the protein of c-myc, c-fos and rasP21. Normal mucosa of antrum was taken as positive control for gastrin, positively stained tissue of hepatic carcinoma served as positive control for c-myc, c-fos and rasP21. PBS solution replacing the first antibody was taken as negative control. Cells containing brown-yellow pellets were considered as positive cells.

**Argyrophilia nucleolar organizer regions count (AgNORs)** Argyrophilia staining was carried out according to Hu PH's modified method<sup>[7]</sup> and observed under  $\times 100$  oil microscope. The nucleus background appeared light yellow while the AgNORs granule appeared palm-black. The amount of AgNORs granule of 50-200 cells and the mean value were calculated.

**Statistics** All the data was expressed as mean  $\pm$  standard deviation ( $\bar{x} \pm s$ ), and analysed with *t* test or one-way analysis of variance; the differences between the rates of different groups were analysed by  $\chi^2$  test.

## RESULTS

### *Model of transplanted human colonic carcinoma in gymnomouse*

The inoculation of transplanted carcinoma was 100% successful, no gymnomouse died. The inoculation period was 6-8 days, the speed of growth became stable till the sixth generation. At the end of the 5th week, the long diameter of the mass reached 1.6 cm-2.0 cm. It was elliptical in shape and smooth on surface in the early stage; while in the advanced stage, the shape became irregular and the surface became nodal. The histological *H.E.* stain and ultrastructure of the transplanted carcinoma had the same pathological feature of human colonic carcinoma.

### *Effect of PG, PGL and SMS on the transplanted*

**human colonic carcinoma in gymnomouse**

All the gymnomice bearing the transplanted carcinoma survived at the end of the experiment. The volume, weight, cAMP, DNA and protein content in carcinoma cell, cell amount and proliferation index of S and G<sub>2</sub>M phase in PG group were significantly higher than those of control group ( $P < 0.05-0.01$ ), markedly lower in PGL and PG+PGL group in PG group ( $P < 0.05-0.01$ ), yet there was no statistical difference between PGL, PG+PGL groups and control group ( $P > 0.05$ ); and markedly lower in SMS and SMS+PG group than in PG group and control group ( $P < 0.01$ ). The cell amount of G<sub>0</sub>/G<sub>1</sub> phase in PG group was obviously lower than in control group ( $P < 0.01$ ), markedly higher in PGL and PG+PGL group than in PG group ( $P < 0.01$ ), without statistical difference between PGL, PG+PGL groups and control group ( $P > 0.05$ ); markedly higher in SMS and SMS+PG group than in PG group and control group ( $P < 0.01$ , Tables 1-3).

**Table 1 Effect of PG, PGL and SMS on the volume and weight of transplanted carcinoma ( $\bar{x} \pm s$ ,  $n = 5$ )**

Group	Volume (mm <sup>3</sup> )	Weight (g)
Control	1766±36	3.04±0.13
PG	1926±98 <sup>a</sup>	3.37±0.21 <sup>a</sup>
PGL	1750±53 <sup>d</sup>	2.98±0.16 <sup>c</sup>
SMS	210±13 <sup>bd</sup>	0.90±0.14 <sup>bdaa</sup>
PG+PGL	1708±59 <sup>d</sup>	2.91±0.23 <sup>c</sup>
PG+SMS	224±19 <sup>bd</sup>	0.95±0.12 <sup>bd</sup>

<sup>a</sup> $P < 0.05$ , <sup>b</sup> $P < 0.01$  vs control group; <sup>c</sup> $P < 0.05$ , <sup>d</sup> $P < 0.01$  vs PG group.

**Table 2 Effect of PG, PGL and SMS on cAMP, DNA and protein content ( $\bar{x} \pm s$ ,  $n = 5$ )**

Group	CAMP(pmol/mL)	DNA(dalton)	Protein(dalton)
Control	2.74±0.14	947±16	364±12
PG	3.18±0.23 <sup>b</sup>	1004±17 <sup>b</sup>	675±18 <sup>b</sup>
PGL	2.72±0.15 <sup>d</sup>	940±21 <sup>d</sup>	356±9 <sup>d</sup>
SMS	1.87±0.14 <sup>bd</sup>	684±13 <sup>bd</sup>	272±11 <sup>bd</sup>
PG+PGL	2.82±0.17 <sup>c</sup>	940±25 <sup>d</sup>	369±14 <sup>d</sup>
PG+SMS	1.86±0.17 <sup>bd</sup>	687±21 <sup>bd</sup>	274±13 <sup>bd</sup>

<sup>b</sup> $P < 0.01$  vs control group; <sup>c</sup> $P < 0.05$ , <sup>d</sup> $P < 0.01$  vs PG group.

**Table 3 Effect of PG, PGL and SMS on cell cycle and proliferation index (PI)**

Group	G <sub>0</sub> /G <sub>1</sub> (%)	S (%)	G <sub>2</sub> M (%)	PI (%)
Control	64.92±1.72	18.24±1.20	16.84±2.35	35.08±1.72
PG	59.22±1.18 <sup>b</sup>	20.16±1.06 <sup>a</sup>	20.62±2.05 <sup>a</sup>	40.78±1.81 <sup>b</sup>
PGL	67.18±2.23 <sup>d</sup>	18.04±1.43 <sup>c</sup>	14.78±1.09 <sup>d</sup>	32.82±2.27 <sup>d</sup>
SMS	80.04±2.29 <sup>bd</sup>	14.90±1.46 <sup>bd</sup>	5.06±1.61 <sup>bd</sup>	19.96±2.39 <sup>bd</sup>
PG+PGL	67.76±2.41 <sup>d</sup>	18.10±1.40 <sup>c</sup>	14.34±0.66 <sup>d</sup>	32.24±2.41 <sup>d</sup>
PG+SMS	80.26±2.73 <sup>bd</sup>	15.22±1.78 <sup>bd</sup>	4.54±1.25 <sup>bd</sup>	19.22±2.73 <sup>bd</sup>

<sup>a</sup> $P < 0.05$ , <sup>b</sup> $P < 0.01$  vs control group; <sup>c</sup> $P < 0.05$ , <sup>d</sup> $P < 0.01$  vs PG group.

**Effect of PG on the amount of viable cells (A value), IP<sub>3</sub> content (CPM) and Ca<sup>2+</sup> concentration in cell and membrane PKC**

**activity of SW480 cell line**

When PG was at the concentration of 12.5 mg/L, the amount of viable cells, IP<sub>3</sub> content and Ca<sup>2+</sup> concentration in the cells of PG group were markedly higher than those in control group ( $P < 0.05$ ) while it was at the concentration of 25 mg/L, they all reached the highest value, but plasma PKC activity decreased, and all had statistical difference from those of control group ( $P < 0.05-0.01$ ). When PG concentration exceeded 50mg/L, these items did not continue to increase and plasma PKC activity did not continue to decrease, but they were all statistically different from those of control group ( $P < 0.05-0.01$ , Table 4).

**Effect of PG+PGL on the amount of viable cells (A value), IP<sub>3</sub> content (CPM) and Ca<sup>2+</sup> concentration in cell and membrane PKC activity of SW480 cell line**

When PGL was at the concentration of 8 mg/L, the amount of viable cells (A value) of PG (25 mg/L)+PGL group was markedly smaller than that of PG group ( $P < 0.01$ ), when at the concentration of 16 mg/L, the amount of viable cells, IP<sub>3</sub> content and Ca<sup>2+</sup> concentration in cell and membrane PKC activity of PG+PGL group decreased and plasma PKC activity increased, all being statistically different from those of control group ( $P < 0.05-0.01$ ). At the concentration of 32mg/L, they decreased to the lowest value and were markedly lower than those in PG group ( $P < 0.05-0.01$ ), and did not differ significantly from those of the control group ( $P > 0.05$ ). At the concentration of 64mg/L, these items in PG+PGL group did not continue to decrease, but they all had statistical difference from those of PG group ( $P < 0.05-0.01$ , Table 5).

**Expression of gastric, c-myc, c-fos and rasP21 and AgNORs count in carcinoma tissue**

The positive expression rate of gastrin, c-myc, c-fos and rasP21 in 48 cases of carcinoma tissue was 39.6%, 54.2%, 47.9% and 54.2% respectively and significantly higher than that in mucosa 3cm and 6cm adjacent to carcinoma tissue and normal colorectal mucosa ( $P < 0.01$ ). The positive expression rate of gastrin of highly-differentiated adenocarcinoma was significantly higher than that of poorly-differentiated and mucinous adenocarcinoma ( $P < 0.05$ ), there was no statistical difference in the positive expression rate of c-myc, c-fos and rasP21 between groups of different pathological types ( $P > 0.05$ ). The AgNORs count of carcinoma tissue was significantly higher than that in mucosa 3 cm and 6 cm adjacent to carcinoma tissue and normal colorectal mucosa ( $P < 0.01$ ); and the count of mucosa 3 cm adjacent to carcinoma

tissue was significantly higher than that in mucosa 6cm adjacent to carcinoma tissue and normal colorectal mucosa ( $P < 0.05$ , Tables 6-7).

**Relationship between gastrin and the expression of c-myc, c-fos, rasP21 and AgNORs count in carcinoma tissue**

The positive expression rate of c-myc and c-fos and the AgNORs count in gastrin-positive group was significantly higher than those in gastrin-negative group ( $P < 0.05 - 0.01$ ), while the positive expression rate of rasP21 in gastrin-positive group was not different from that in gastrin-negative group ( $P > 0.05$ , Table 8).

**Table 4 Effect of PG on VCC, IP<sub>3</sub>, [Ca<sup>2+</sup>] and PKC activity (pmol/min per mg protein) ( $\bar{x} \pm s$ ,  $n = 5$ )**

Group(mg/L)	VCC(A)	IP <sub>3</sub> (CPM)	[Ca <sup>2+</sup> ]i(nM)	Plasma PKC	Membrane PKC
Control	1.554±0.009	8.83±1.33	26.36±2.91	2.39±1.30	1.07±0.28
PG6.25	1.555±0.005	10.16±1.33	30.16±2.16	2.36±0.84	1.09±0.16
12.50	1.563±0.010 <sup>a</sup>	11.18±0.75 <sup>a</sup>	50.69±2.30 <sup>a</sup>	2.30±0.45	1.15±0.15
25.00	1.580±0.011 <sup>b</sup>	16.17±0.75 <sup>b</sup>	101.44±2.49 <sup>b</sup>	0.91±0.34 <sup>a</sup>	2.65±1.21 <sup>a</sup>
50.00	1.579±0.008 <sup>b</sup>	14.10±1.60 <sup>b</sup>	70.63±4.17 <sup>b</sup>	0.92±0.26 <sup>a</sup>	2.65±0.60 <sup>a</sup>
100.00	1.578±0.010 <sup>b</sup>	13.00±2.53 <sup>b</sup>	62.59±2.59 <sup>b</sup>	0.91±0.14 <sup>a</sup>	2.66±0.68 <sup>a</sup>

<sup>a</sup> $P < 0.05$ , <sup>b</sup> $P < 0.01$  vs control group.

**Table 5 Effect of PG+PGL on VCC, IP<sub>3</sub>, [Ca<sup>2+</sup>]i and PKC activity (pmol/min per mg protein) ( $\bar{x} \pm s$ ,  $n = 5$ )**

Group	PG(mg/L)	PGL(mg/L)	VCC(A)	IP <sub>3</sub> (CPM)	[Ca <sup>2+</sup> ]i(nM)	Plasma PKC	Membrane PKC
Control	0.00	0.00	1.554±0.009	8.83±1.33	26.36±2.91	2.39±1.30	1.07±0.28
PG	25.00	0.00	1.580±0.011 <sup>b</sup>	16.17±0.75 <sup>b</sup>	101.44±2.49 <sup>b</sup>	0.91±0.34 <sup>a</sup>	2.65±0.21 <sup>a</sup>
PG+PGL	25.00	8.00	1.553±0.016 <sup>d</sup>				
	25.00	16.00	1.551±0.008 <sup>d</sup>	9.17±1.47 <sup>d</sup>	32.63±2.86 <sup>d</sup>	2.33±0.29 <sup>c</sup>	1.05±0.09 <sup>c</sup>
	25.00	32.00	1.546±0.011 <sup>d</sup>	9.00±1.58 <sup>d</sup>	31.79±4.41 <sup>d</sup>	2.30±0.61 <sup>c</sup>	1.05±0.20 <sup>c</sup>
	25.00	64.00	1.549±0.011 <sup>d</sup>	9.33±1.97 <sup>d</sup>	32.45±2.46 <sup>d</sup>	2.32±0.17 <sup>c</sup>	1.09±0.12 <sup>c</sup>
	25.00	128.00	1.549±0.014 <sup>d</sup>				

<sup>a</sup> $P < 0.05$ , <sup>b</sup> $P < 0.01$  vs control group; <sup>c</sup> $P < 0.05$ , <sup>d</sup> $P < 0.01$  vs PG group.

**Table 6 Expression of gastrin, c-myc, c-fos, rasp21 and AgNORs**

Group	<i>n</i>	gastrin positive (%)	c-myc positive (%)	c-fos positive (%)	rasp21 positive (%)	AgNORs
Carcinoma tissue	48	19(39.6) <sup>b</sup>	26(54.2) <sup>b</sup>	23(47.9) <sup>b</sup>	26(54.2) <sup>b</sup>	7.10±1.48 <sup>b</sup>
3cm mucosa	48	2(4.2)	12(25.0)	9(18.8)	10(20.8)	3.65±1.04 <sup>c</sup>
6cm mucosa	48	0(0)	7(14.6)	4(8.0)	6(12.5)	2.88±0.73
Normal	10	0(0)	1(10.0)	1(10.0)	2(20.0)	2.85±0.60

<sup>b</sup> $P < 0.01$  vs 3cm, 6cm and normal mucosa group. <sup>c</sup> $P < 0.05$  vs 6cm and normal mucosa group.

**Table 7 Expression of gastrin, c-myc, c-fos, rasp21 and AgNORs in different pathological carcinoma tissue**

Group	<i>n</i>	Gastrin positive (%)	c-myc positive (%)	c-fos positive (%)	rasp21 positive (%)	AgNORs
Highly-differentiated	26	14(53.9) <sup>a</sup>	15(57.7)	13(50.0)	15(57.7)	7.12±1.80
Moderately-differentiated	12	4(33.3)	5(41.7)	7(58.3)	6(50.0)	7.25±0.86
Poorly- and mucinous	10	1(10.0)	6(60.0)	3(30.0)	5(50.0)	7.11±1.20

<sup>a</sup> $P < 0.05$  vs poorly-differentiated and mucinous group.

**Table 8 Relation between gastrin and c-myc, c-fos, rasp21 and AgNORs**

Group	<i>n</i>	c-myc positive(%)	c-fos positive(%)	rasp21 positive(%)	AgNORs
Gastrin-positive	19	15(78.9) <sup>a</sup>	14(73.7) <sup>b</sup>	11(57.9)	7.84±1.30 <sup>b</sup>
Gastrin-negative	29	11(37.9)	9(31.0)	15(51.7)	6.22±1.40

<sup>a</sup> $P < 0.05$ , <sup>b</sup> $P < 0.01$  vs gastrin-negative group.

## DISCUSSION

The main physiological function of gastrin is to stimulate the secretion of gastric acid and nourish the gastrointestinal mucosa. In recent years, it has been found that some gastrointestinal carcinomas could express gastrin gene<sup>[8,9]</sup> and there existed gastrin receptor on the carcinoma cell membrane, and gastrin could stimulate the growth of gastrin carcinoma. So, more and more researchers focus their interest on the relationship between gastrin and colonic carcinoma.

The transplanted human colonic carcinoma model from SW480 cell line in gymnomouse established by us remained the biological characteristics of colonic carcinoma. After subcutaneous injection of 8 $\mu$ g pentagastrin per day for 35 days, the volume and weight of transplanted carcinoma, the cAMP content in carcinoma cell were significantly higher than those of control group, indicating that gastrin promoted the proliferation of transplanted colonic carcinoma. Ishizuka<sup>[10]</sup> reported that the combination of gastrin and receptor could increase the content of cAMP in carcinoma cell, then transduce external information into cell through the cAMP or protein kinase C pathway to regulate the cell growth and differentiation. Mauss<sup>[11]</sup> found that the promoting effect of gastrin on colonic carcinoma cell was selective, margarapeptide gastrin stimulated the growth of HT29, LoVo, CoLo32 cell line, but inhibited the growth of T84, HCT116 cell lines. The difference depended on the quality and quantity of cAMP-dependent protein kinase. The increased expression of Type I cAMP protein kinase could promote the differentiation and growth of carcinoma cells, while the decreased expression of Type I cAMP protein kinase or the increased expression of Type II cAMP protein kinase could inhibit the differentiation and growth of carcinoma cells<sup>[12]</sup>. Baldwin<sup>[13]</sup> reported that gastrin could promote the growth of 50 percent of the transplanted colonic carcinoma *in vivo*. We also determined the DNA, protein content and cell cycle by flow-cytometry, and found that DNA and protein content in carcinoma cell and the cell amount and proliferation index of S and G<sub>2</sub>M phase of PG group were significantly higher than those of control group, while the cell amount of G<sub>0</sub>/G<sub>1</sub> phase of PG group was significantly lower than that of control group. It indicated that the mechanism for the promoting effect of gastrin on the cell division and proliferation of the human colonic carcinoma SW480 cell line might be that gastrin could promote the synthesis of cAMP, DNA and protein in carcinoma cells, the cell growth from G<sub>0</sub>/G<sub>1</sub> phase to S and G<sub>2</sub>M phase, and regulate the cell cycle of colonic carcinoma cells after receptor.

Venter<sup>[14]</sup> firstly found that there existed high affinity gastrin receptor on the membrane of human colonic carcinoma cell line LoVo and MC-26, both the nutritive effect of gastrin on the mucosa of normal large intestine and the growth-promoting effect of gastrin on large intestine carcinoma were realized through the combination of gastrin and its receptor on the membrane. We found by MTT colorimetric analysis that pentagastrin could promote the increase of viable cell count of colonic carcinoma SW480 cell line and the effect had a dose-effect dependent relationship with the concentration to some extent, along with the increase of dosage of pentagastrin, its growth-promoting effect did not continue to increase, but inclined to a stable level. This finding was consistent with the receptor theory, i.e., the receptor had saturation and indirectly proved that the growth promoting effect of gastrin on large intestine carcinoma was intermediated by gastrin receptor.

Some researches indicate that gastrin is a kind of autocrine growth-promoting factor. Hoosein *et al.*<sup>[15]</sup> found that after the colonic carcinoma HCT116 and CBS cell line were cultured for 72 hours, the concentration of gastrin was 10.15pg/10<sup>6</sup> cell. Finley *et al.*<sup>[16]</sup> found by the immunocytochemical method that at least 50% of the colorectal carcinoma cells expressed gastrin. In our experiment, 19 of 48 cases of colorectal carcinoma expressed gastrin, with a positive rate of 39.6%, which was significantly higher than that in mucosa adjacent to carcinoma and normal mucosa, the expression rate of gastrin in highly-differentiated group was the highest (53.9%), all these indicated that some colorectal carcinomas could produce gastrin in an autocrine manner. Translational processing of gastrin mRNA to precursor forms of gastrin needs the participation of multiple enzymes and cofactors to produce mature gastrin finally. Therefore, the sound processing enzymes such as peptidylglycine  $\alpha$ -amidating monooxygenase and cofactors in well differentiated carcinoma cells may contribute to the production of mature gastrin, while the lack of other cofactors or enzymes in poorly-differentiated carcinoma cells may contribute to incomplete processing of precursor forms of gastrin and the deficiency of mature gastrin<sup>[17]</sup>. So, the gastrin expression of highly-differentiated adenocarcinoma was obviously higher than that of poorly-differentiated one.

We firstly applied the AgNORs technique to the clinical study of the growth-promoting effect of gastrin on large intestine carcinoma. The AgNORs count could mirror the structure and function of nucleolus, the transcription activity of rRNA and the cell proliferation. The AgNORs count of

colorectal carcinoma in our study was significantly higher than that of mucosa adjacent to carcinoma and normal mucosa, while the count of mucosa 3cm adjacent to carcinoma was higher than that of mucosa 6cm adjacent to carcinoma and normal mucosa. It indicated that the DNA in carcinoma cell and mucosa 3cm adjacent to carcinoma was in a disorder state, the regulation of cell proliferation was uncontrollable. We also found that the AgNORs count of gastrin-positive group was significantly higher than that in gastrin-negative group, indicating that endogenous gastrin had growth-promoting effect on some kinds of colorectal carcinomas.

Oncogene *c-myc* and *c-fos* is a kind of effect protein of the karyomitosis signal, which can trigger and regulate the transcription of the genes related with proliferation, besides, *c-fos* can also regulate its own gene expression with a positive feedback and promote the mitosis and proliferation of the cells<sup>[18]</sup>. Oncogene *ras*, a kind of GPT protein located at cell plasma and membrane, participates in the signal transduction regulation of various growth factor receptors. Once being mutant, *ras* oncogene will be continuously activated and obviously promote the mitosis of the cells<sup>[19]</sup>. Our results revealed that the positive expression rate of gastrin, *c-myc*, *c-fos* and *rasP21* in carcinoma tissue was significantly higher than that in mucosa adjacent to carcinoma tissue and normal colorectal mucosa, the positive expression rate of *c-myc* and *c-fos* in gastrin-positive group was significantly higher than that in gastrin-negative group. It indicated that the growth-promoting effect of gastrin on colorectal carcinoma may be correlated with the activation of oncogenes. Wang *et al.*<sup>[20]</sup> found that administration of gastrin resulted in the rapid appearance of *c-myc* mRNA in IEC-6 cells, the maximum increase in *c-myc* mRNA levels was 7.5-fold that of the normal value. Andrea *et al.*<sup>[21,22]</sup> reported that gastrin had a promoting effect on the growth of AR4-2J cell line, and could induce the increase of *c-fos* mRNA content; after having combined with its receptor, gastrin triggered a series of phosphorylation in PKC signal pathway and induced the activation of extracellular signal regulatory kinase ERK 2, the kinase increased the transcription activity of EIK-1, then enlarged the expression of *c-fos* gene and stimulated the cell proliferation. Seva *et al.*<sup>[23]</sup> reported that gastrin stimulated MAP kinase activation in a dose- and time dependent manner, *rasP21* may link the MAP kinase pathway to gastrin receptors to trigger the activation.

Phosphatidylinositol signal pathway played an important role in the biological transmembrane transduction, which was intimately correlated with cell proliferation and tumorigenesis<sup>[24]</sup>.

Phosphatidylinositol-4, 5-bisphosphate (PIP-2) was the direct precursor of second messengers IP<sub>3</sub> and PG, and it functioned through IP<sub>3</sub>-Ca<sup>2+</sup> pathway and DG-PKC pathway. The ascendance of dissociate Ca<sup>2+</sup> concentration was an important mitosis promoting signal and Ca<sup>2+</sup> correlated with the genesis and growth of many kinds of carcinomas. Protein kinase C was a kind of important kinase in the phosphatidylinositol signal pathway, it existed in plasma of static cells by a non activation form, and once it was activated, it moved to cell membrane. The changes of activity were intimately correlated with cell proliferation. In our study, after we applied pentagastrin to colonic carcinoma SW480 cell line, the VCC, intracellular IP<sub>3</sub> content and Ca<sup>2+</sup> concentration and membrane PKC activity all ascended and were dose-dependent obviously. But when pentagastrin and antagonist of gastrin were taken together, they remained changed, demonstrating that the growth-promoting effect of pentagastrin on human colonic carcinoma SW480 cell line was correlated with phosphatidylinositol signal pathway and it was through its receptor intermediate function in phosphatidylinositol signal pathway that proglumide antagonized the growth-promoting effect of gastrin on carcinoma cell. Ishizuka *et al.*<sup>[10]</sup> suggested that the combination of gastrin and its receptor activated the membrane phospholipase and then hydrolyzed phosphatide to PI and DG, the latter then activated PKC, and finally Ca<sup>2+</sup> was released and functioned.

All the findings above and our results indicated that some carcinoma cells produced gastrin by autocrine, after being intermediated by the second messenger in the cells, the expression of oncogene *c-myc* and *c-fos* was enlarged, thus promoting the proliferation of the carcinoma cells.

To block any link in the function procedure of gastrin could weaken or inhibit the growth-promoting effect of gastrin on large intestine carcinoma. There were three kinds of gastrin receptor antagonists: proglumide, somatostatin and prostaglandin (PG). Most of the interests were focused on proglumide, amide, the functional group of proglumide could particularly compete gastrin receptor with gastrin. In our research, 10mg proglumide was injected subcutaneously into transplanted carcinoma in gymnomice, 35 days later, compared with control group, there was no statistical difference in the volume, weight, intracellular cAMP, DNA, protein content and cell cycle of transplanted carcinoma in the PG group, but all the value above including cell amount of S and G<sub>2</sub>M phase, proliferation index of PG and proglumide group were significantly lower than those of PG group, while the cell amount of G<sub>0</sub>/G<sub>1</sub> phase was higher than that of PG group. All these

showed that proglumide had no effect on the growth of human colonic carcinoma SW480 cell line but could inhibit the growth-promoting effect of gastrin on transplanted carcinoma. Proglumide has been applied to the clinical practice. Kameyama *et al.*<sup>[25]</sup> reported that seven large intestine carcinoma patients with hepatic metastasis were treated with proglumide (three times daily, each time 400mg) and 5'DFUR (800mg) for 2 years after the resection of the hepatic metastatic mass, at the same time, patients received chemotherapy by hepatic artery encephalosis and followed up for an average of 39 months. The relapse rate of the proglumide+chemotherapy group was 14% (1/7), while the rate of the chemotherapy alone group was 52% (14/26), so they drew a conclusion that the hormone therapy could effectively prevent the relapse after the resection of the hepatic metastatic mass. We used proglumide as an adjuvant drug to treat 25 colorectal patients having radical resection, besides administration of 400mg proglumide three times a day, MFA chemotherapy program was undertaken at the same time, while 25 patients as control group undertook MFA chemotherapy program alone. Follow-up results indicated that the 3-year survival rate of proglumide group (80%) was higher than that in control group (64%), the relapse or metastasis rate of proglumide group (12%) was lower than that in control group (20%), but without statistical differences ( $P>0.05$ ). The 3-year survival rate of Duke's C and D patients in proglumide group (73.3%) was obviously higher than that in control group (42.8%) ( $P<0.05$ ). It indicated that administration of proglumide as adjuvant therapy for patients with colorectal carcinomas, particularly the middle and late stage ones, could decrease the relapse or metastasis rate and prolong the survival period. But being a kind of weak gastrin receptor antagonist, only when the gastrin receptor level was high, could proglumide have an inhibitory effect. Therefore, its curable effect on large intestinal carcinoma awaits further evaluation more clinical observations.

Somatostatin is a kind of annular peptide hormone secreting by D cell. The main effect of somatostatin is to inhibit the growth, secretion and absorption of the mucosa of the gastrointestinal tract and to inhibit the release of gastrin, secretin, glucagon and growth hormone. Itzeu *et al.*<sup>[26]</sup> found with immunohistochemistry that there existed D cell in the mucosa of colorectal carcinoma, and suggested that D cell in mucosa of large intestine might have local regulatory effect on the secretion of other hormones. Dy *et al.*<sup>[27]</sup> reported that SMS 20.995 could significantly and concentration-dependently inhibit the growth of transplanted human colonic carcinoma from LIM2405 and

LIM2412 cell line. We found that the volume, weight, DNA and protein content in carcinoma cell, cell amount and proliferation index of S and G<sub>2</sub>M phase in SMS group and SMS+PG group were markedly lower than those in PG group and control group, and markedly higher in PG group than those in control group. The cell amount of G<sub>0</sub>/G<sub>1</sub> phase in SMS group and SMS+PG group was significantly higher than that in PG group and control group. This demonstrated that octapeptide somatostatin had a negative regulatory effect on the transplanted carcinoma, and it could not only inhibit the growth of transplanted human colonic carcinoma from SW480 cell line directly but also inhibit the growth-promoting effect of gastrin on the transplanted carcinoma. The half-life period of somatostatin is shorter than two minutes, so it can not be used pharmaceutically, but its analog manually synthesized such as SMS 201-995 and RC-160 have been used in clinical practice. Having treated 55 patients with advanced digestive tract carcinomas who could not endure chemotherapy with SMS201-995, Cascinu *et al.*<sup>[28]</sup> found that SMS201-995 could relieve symptom and improve the quality of life and prolong the survival.

Colorectal carcinoma is a common kind of malignant carcinoma. The carcinoma was mostly in middle or advanced stage when patients first came to see a doctor. Treatment of gastrin-sensitive patients with colonic carcinoma with gastrin receptor or antagonists such as proglumide and somatostatin as adjuvant therapy is expected to prolong the survival of the patients and to raise the curative effect and to create new approaches for non-cytotoxic therapy such as hormone therapy of patients with colorectal carcinoma.

## REFERENCES

- 1 Zuo LF. Techniques of the preparation of the flow-cytometry sample. Ed 1. Beijing: *Hua Xia Press*, 1989:51-53
- 2 Wu JG. Practical Clinical immunology test. Edition 1. *Nanjing: Jiangsu Kexue Jishu Press*, 1989:39-41
- 3 Olivier M, Baimbridge KG, Reiner NE. Stimulus-response coupling in monocytes infected with leishmania. *J Immunol*, 1992; 148:1188-1196
- 4 Huang JQ, Gong FL, Xiong P. The effect of heparin, trifluoperazine on the regulatory effect of noradrenalin on the expression of Ia antigen in rat abdominal giant phagocyte. *Zhongguo Mianyixue Zazhi*, 1994; 10:35-36
- 5 Yassin RR, Murthy SNS. Possible involvement of protein kinase C in mediating gastrin induced response in rat colonic epithelium. *Peptides*, 1991; 12:925-927
- 6 Ishizuka J, Martinez J, Townsend CM. The effect of gastrin on growth of human stomach cancer cells. *Am Surg*, 1992; 215:528-535
- 7 Hu PH, Hu DY, Zhuang YH, Zhao ML, Wang RN. The implication of AgNORs in pathological diagnosis of stomach mucosa. *Shanghai Sec Med Uni Transaction*, 1989; 9:318-320
- 8 Mongas G, Biagini P, Cantaloube JF. Detection of gastrin mRNA in fresh human colonic carcinomas by reverse transcription polymerase chain reaction. *J Mol Endocrinol*, 1993; 11:223-229
- 9 Xu Z, Dai B, Dhurra B. Gastrin gene expression in human colon cancer cells measured by a simple competitive PCR method. *Life Sci*, 1994; 54:671-678
- 10 Ishizuka J, Townsend JR, Richard J. Effects of gastrin on 3', 5'-

- cyclic adenosine monophosphate, intracellular calcium and phosphatidylinositol hydrolysis in human colon cancer cells. *Cancer Res*, 1994;54:2129-2235
- 11 Mauss S, Niederau C, Hengels K. Effects of gastrin, proglumide, loxiglumide and L-365, 260 on growth of human colon carcinoma cells. *Anticancer Res*, 1994;14(1A):215-220
  - 12 Chochung YS, Clair T, Tortora G, Yokozaki H, Pepe S. Suppression of malignancy targeting the intracellular signal transducing proteins of cAMP: the use of site-selective cAMP analogs antisense strategy and gene transfer. *Life Sci*, 1991;48:1123-1132
  - 13 Baldwin GS, Whitehead RH. Gut hormone growth and malignancy. *Baillieres Clin Endocrinol Metab*, 1994;8:185-214
  - 14 Rae-Venter. Gastrin receptor in cultured human cell derived from carcinoma of colon. *Endocrinology*, 1981;108:153
  - 15 Hoosein NM, Kiener PA, Curry RC. Evidence for autocrine growth stimulation of cultured colon tumor cells by a gastrin/cholecystokinin-like peptide. *Exp Cell Res*, 1990;189:1165-1169
  - 16 Finley GG, Koski RA, Melhem MF, Pipas JM, Meisler AL. Expression of the gastrin gene in the normal human colon and colorectal adenocarcinoma. *Cancer Res*, 1993;53:2919-2926
  - 17 Singh P, Xu Z, Dai B, Rajaraman S, Rubin N, Dhruva B. Incomplete processing of progastrin expressed by human colon cancer cells: role of noncarboxyamidate gastrin. *Am J Physiol*, 1994;266:G459-468
  - 18 Williams GT, Smith CA. Molecular regulation of apoptosis: genetic controls on cell death. *Cell*, 1993;74:777-779
  - 19 Khosravi-Far R, Der CJ. The ras signal transduction pathway. *Cancer Metastasis Rev*, 1994;13:67-89
  - 20 Wang JY, Wang HL, Johnson LR. Gastrin stimulates expression of protooncogene c-myc through a process involving polyamines in IEC-6 cells. *Am J Physiol*, 1995;269(cell physiol. 38):c1474-1481
  - 21 Andrea T, Yoshiaki T, Catherine S, Dickinson CJ, Tadutaka Y. Gastrin and Glycine extended progastrin processing intermediates induce different programs of early gene activation. *J Biol Chem*, 1995;270:28337-28341
  - 22 Todisco A, Takeuchi Y, Urumov A, Yamada J, Stepan VM, Yamada T. Molecular mechanisms for the growth factor action of gastrin. *Am J Physiol*, 1997;273(Gastrointest Liver Physiol, 36):G891-898
  - 23 Seva C, Chauvel AK, Blanchet JS, Vaysse N, Pradayrol L. Gastrin induces tyrosine phosphorylation of shc proteins and their association with the Grb2/Sos complex. *FEBS Letters*, 1996;378:74-78
  - 24 Hill CS, Yreisman R. Transcriptional regulation by extracellular signals: mechanisms and specificity. *Cell*, 1995;80:199-211
  - 25 Kameyama M, Nakamori S, Imaoka S, Yasuda T, Nakano H, Ohigashi H. Adjuvant chemoendocrine chemotherapy with gastrin antagonist after resection of liver metastasis in colorectal cancer. *Gan To Kagaku Ryoho*, 1994;21:2169-2171
  - 26 Itzeu BD, Lolova I, Davidoff M. Immunocytochemical and electromicroscopical data on the differentiation of somatostatin-containing cells in human large intestine. *Anat Anz Jena*, 1988;166:77
  - 27 Dy DY, Whitehead RH, Morris DL. SMS201.995 inhibits in vitro and in vivo growth of human colon cancer. *Cancer Res*, 1992;52:917-923
  - 28 Cascinu S, Ferro ED, Catalano G. A randomised trial of octreotide vs best supportive care only in advanced gastrointestinal cancer patients refractory to chemotherapy. *Br J Cancer*, 1995;71:97-101

Edited by MA Jing-Yun

# Effect of retinoic acid on the changes of nuclear matrix in intermediate filament system in gastric carcinoma cells

LI Qi-Fu

**Subject headings** stomach neoplasms; tumor cell, cultured; retinoic acid; nuclear matrix-intermediate filament system

## Abstract

**AIM** To explore the relationship between the configuration changes of the nuclear matrix-intermediate filament system in cancer cell induced by retinoic acid and the malignant phenotypic reversion of cancer cells.

**METHODS** The human gastric adenocarcinoma cell line MGc80-3 cells were induced with  $10^{-6}$  mol/L retinoic acid and subcultured at cover slip strip and gold grids. The cells were treated by selective extraction method and prepared for whole mount electron microscopy observation. The samples were examined respectively with scanning and transmission electron microscope.

**RESULTS** The nuclear matrix filaments and intermediate filaments in MGc80-3 cells were relatively few and scattered, not well-distributed and arranged irregularly. The nuclear lamina was ununiformly thick and compact, connected to the nuclear matrix filaments and intermediate filaments relaxedly. However, the two kinds of filaments were abundant and well-distributed, different in slender and thick form and interweaved into a regular network in the cells induced by  $10^{-6}$  mol/L RA. The nuclear matrix filaments and intermediate filaments were connected closely by the thin and compact fiber-like lamina, and interlaced into a regular network throughout the whole cell region.

**CONCLUSION** The NM-IF system in MGc80-3 cells had undergone a restorational change similar to those of normal cells after RA

**inducement. This alternation is an important morphological and functional expression to the malignant phenotypic reversion of cancer cells.**

## INTRODUCTION

The nuclear matrix is a fine network in the eukaryotic nucleus and plays an important role in maintaining nuclear morphology, DNA organization, DNA replication and gene expression. The morphological and functional alternations of the nuclear matrix have an important effect on cell proliferation and differentiation<sup>[1,2]</sup>. It has been shown in previous studies that there were dramatic differences in the configuration and protein composition of the nuclear matrix between cancer and normal cells<sup>[3,4]</sup>. Moreover, it has been demonstrated that some carcinogens or anti-cancer agents perform their function by affecting the nuclear matrix<sup>[5]</sup>. These results suggest that abnormal nuclear matrix is closely relevant to cell canceration. However, the alternations of nuclear matrix during the differentiation induced by cancer cells and its relation to the malignant phenotypic reversion of cancer cells are still poorly understood. To explore the correlation between the configurational changes of the nuclear matrix and the malignant phenotypic reversion of cancer cells, a study was made on the alternations of the nuclear matrix-intermediate filament (NM-IF) system in human gastric adenocarcinoma cell line MGc80-3 induced by retinoic acid (RA).

## MATERIALS AND METHODS

### *Cell culture and induced treatment*

MGc80-3 cells were cultured in RPMI-1640 medium supplemented with 20% heat-inactivated fetal calf serum, and an appropriate amount of penicillin, streptomycin and kanamycin. The MGc80-3 cells were induced by the medium containing  $10^{-6}$  mol/L all-*trans*-retinoic acid (RA) (purchased from Sigma Chemical Co.). Then, MGc80-3 cells and the cells treated with RA were seeded in small penicillin bottles with cover slip strip on which some gold grids covered with formvar and coated with carbon were stucked with polylysine, and grown in the

Laboratory of Cell Biology, Xiamen University, Xiamen 361005, Fujian Province, China

Dr. LI Qi-Fu, male, born on 1950-07-30 in Xiamen City, Fujian Province, Han nationality, graduated from Xiamen University as a Ph. D in 1987, associate professor of cell biology, majoring in cancer cell biology, having 26 papers published.

Supported by Scientific Research Foundation for Doctorate Education, State Education Commission.

**Correspondence to:** Dr. LI Qi-Fu, Laboratory of Cell Biology, Xiamen University, Xiamen 361005, Fujian Province, China  
Tel. +86-592-2183619, Fax. +86-592-2186630

Received 1999-01-03

normal medium or the medium containing  $10^{-6}$  mol/L RA respectively. Cells were incubated at  $37^{\circ}\text{C}$  in 5%  $\text{CO}_2$  atmosphere for 72 hours.

#### **Cell selective extraction**

The cells were selectively extracted as described by Capco<sup>[6]</sup>. MGc80-3 cells and the cells treated with RA were rinsed with D-Hank's solution twice at  $37^{\circ}\text{C}$ , and extracted by high ionic strength extraction solution (10 mmol/L PIPES, pH 6.8, 250 mmol/L  $(\text{NH}_4)_2\text{SO}_4$ , 300 mmol/L sucrose, 3 mmol/L  $\text{MgCl}_2$ , 1.2 mmol/L PMSF, 0.5% Triton X-100) at  $4^{\circ}\text{C}$  for 3 min. The extracted cells were rinsed in non-enzyme digestion solution (10 mmol/L PIPES, pH 6.8, 50 mmol/L NaCl, 300 mmol/L sucrose, 3 mmol/L  $\text{MgCl}_2$ , 1.2 mmol/L PMSF, 0.5% Triton X-100), and digested in digestion solution containing DNase I (400mg/L) and RNase A (400 mg/L) for 20 min at  $23^{\circ}\text{C}$ . The samples were placed in high ionic strength extraction solution at  $23^{\circ}\text{C}$  for 5 min. So far only the nuclear matrix- intermediate filament structure remained intact.

#### **Sample preparation for the whole mount electron microscopy**

The NM-IF samples produced by selective extraction were prefixed in 2% glutaraldehyde (made in non-enzyme digestion solution) at  $4^{\circ}\text{C}$  for 30 min. The samples were then rinsed with 0.1 mol/L sodium cacodylate buffer (pH 7.4), postfixed in 1%  $\text{OsO}_4$  (made in 0.1 mol/L sodium cacodylate) at  $4^{\circ}\text{C}$  for 5 min, dehydrated in ethanol series, replaced in isoamyl acetate, dried through the  $\text{CO}_2$  critical point. The cell samples attached to grids were examined with a JEM-100CX II transmission electron microscope (TEM), and the cell samples grown on cover slip strip were gilded in vacuum and examined with a HITACHI S-520 scanning electron microscope (SEM).

### **RESULTS**

It was revealed by TEM and SEM that MGc80-3 cells and the cells induced by RA after selective extraction remained a filament network spreading all over the original cell region and structurally interlinked. In addition, the original nucleus region was maintained by the nuclear lamina and formed an interlinking and integrated NM-IF system (Figures 1-3). After induced treatment with RA, the changes of NM-IF system in MGc80-3 cells were observed.

#### **Nuclear matrix**

The nuclear matrix filaments in MGc80-3 cells were relatively few and scattered, not well-distributed and arranged irregularly within the nucleus region. The

nuclear matrix filaments were short, and there were few single filaments while most of the nuclear matrix filaments were quite thick in bundle-like form and interweaved into an irregular network or in a flocculent structure. One or more residual nucleoli were usually observed within the nucleus region and maintained by a few of nuclear matrix filament bundles (Figures 1, 2). However, in the MGc80-3 cells induced by RA, the nuclear matrix filaments were abundant and well-distributed, different in slender and thick form in the nucleus region. The nuclear matrix filaments were slender, in which the single filaments increased, and interweaved into a regular network. The nuclear matrix filaments or filament bundles were arranged radiately and connected to the residual nucleoli (Figures 3-5).

#### **Nuclear lamina**

The nuclear lamina in MGc80-3 cells was ununiformly thick and compact. The inner nuclear lamina was nonected with some thick nuclear matrix filament bundles or thin and short filaments. It could always be seen that the intermediate filament bundle and the thin or thick filament of its branches were connected to and terminated on the outer nuclear lamina. Nevertheless, the nuclear matrix filaments and the intermediate filaments connected to the nuclear lamina were relatively few and scattered (Figures 1, 2). The nuclear lamina in MGc80-3 cells induced by RA turned into a thin and compact fibroid structure. The inner nuclear lamina was connected closely with the nuclear matrix filaments, and many long and slender intermediate filament bundles were terminated directly on the outer nuclear lamina. Both the nuclear matrix filaments and the intermediate filaments connected to the nuclear lamina increased and appeared quite densely. It impelled the three parts to link up with each other more closely (Figures 3, 5).

#### **Intermediate filament**

The amount of intermediate filaments in MGc80-3 cells was rather small. They were present mainly in the cytoplasm region around the nucleus and only a few in the peripheral region within cytomembrane, and were not well-distributed. The intermediate filaments in which single filaments were few, were chiefly in thick bundles or in strip-rope-like structure, and arranged irregularly (Figures 1, 2). But they were abundant and well-distributed in the cytoplasm in MGc80-3 cells induced by RA. They spread from the region around nucleus and to the cellular edge. Quite a few single filaments were found in intermediate filaments which interweaved with the slender intermediate filament bundles into a well-distributed and regular network throughout the cytoplasm region (Figures 3, 5, 6).

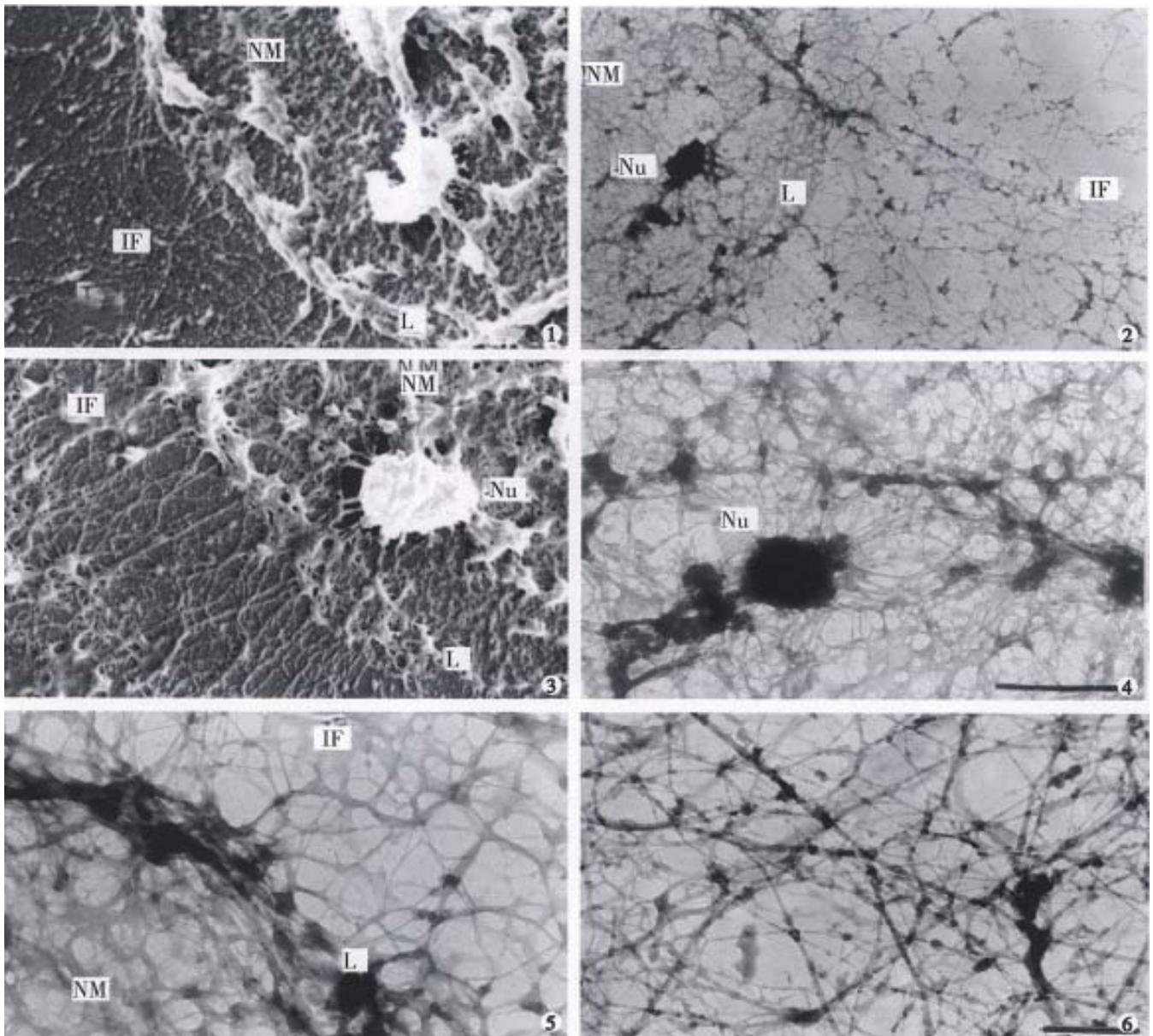


**Figure 1** SEM observation of NM-IF system in MGc80-3 cells (L lamina). Bar=1 $\mu$ m  
**Figure 2** TEM observation of NM-IF system in MGc80-3 cells (Nu residual nucleolus). Bar=1 $\mu$ m  
**Figure 3** SEM observation of NM-IF system in RA-treated cells. Bar=1 $\mu$ m  
**Figure 4** TEM observation of NM filament network in RA-treated cells. Bar=1 $\mu$ m  
**Figure 5** NM filament connects closely with intermediate filament by thin and regular lamina in RA-treated cells. Bar=0.5 $\mu$ m  
**Figure 6** The network of plentiful intermediate filaments in RA-treated cells. Bar=0.5 $\mu$ m

## DISCUSSION

The abnormality of nuclear matrix is largely associated with the canceration of cell. Previous studies demonstrated that the nuclear matrix in cancer cells has undergone an irregular and abnormal configuration distinguished from that of normal cells<sup>[1,3]</sup>, indicating that the nuclear matrix in cancer cells has some distinctive configuration characteristics which differed significantly from those of normal cells. The observation in this study displayed that the nuclear matrix filaments and intermediate filaments in MGc80-3 cells were

relatively few, not well distributed, arranged irregularly, and the single filaments were few while filament bundles were plentiful. The thick nuclear lamina was not largely associated with the nuclear matrix filaments and intermediate filaments. It showed the typical configuration characteristics of nuclear matrix in malignant tumor cells. The NM-IF system in MGc80-3 cells induced with RA had undergone a significant change. The nuclear matrix filaments and intermediate filaments were abundant, well-distributed with the single filaments increased and differed in slender and thick form and

intertwined into a regular network. Meanwhile, the nuclear matrix and intermediate filaments were connected closely by the thin and compact fiber-like nuclear lamina and organized into an integrated network throughout the cell. The characteristics of this organized and integrated configuration of NM-IF system were significantly different from those of MGc80-3 cells but similar to those of normal cells of epithelial origin<sup>[6-7]</sup>. It demonstrated that RA could impel the NM-IF system in MGc80-3 cells to exert a reversional configuration alteration. In this regard, the restoration of the normal configuration of nuclear matrix is obviously an important morphological and functional expression to the malignant phenotypic reversion of gastric carcinoma cells.

The nuclear matrix plays a role not only in maintaining nuclear morphology as a framework within the nucleus, but in DNA replication and chromosomal construction. Consequently, the nuclear matrix can directly affect the cell division and proliferation<sup>[1,2,8]</sup>. It is obvious that the changes of nuclear morphology and the inhibition of DNA synthesis and cell proliferation in MGc80-3 cells induced by RA are associated closely with the configuration and functional alternation of the nuclear matrix. It can be concluded that these effects are resulted from the restoration of normal configuration of nuclear matrix in MGc80-3 cells induced by RA. In addition, the nuclear matrix plays an important influence upon regulating gene expression by acting on gene transcription, RNA processing and modifying, and directional transport<sup>[2,9]</sup>. Previous studies suggested that oncogene of cancer cells mainly existed in DNA

sequences connecting to the nuclear matrix, and the transcription of oncogene couldn't be underway until the oncogene was connected to the nuclear matrix<sup>[3,10]</sup>. It indicates that the nuclear matrix plays an important role in oncogene expression. Therefore, the restoration of normal configuration and function of nuclear matrix in gastric carcinoma cells induced with RA must have an important effect on regulating the expression of oncogene and tumor suppressor gene which are related to gastric carcinoma cells. For this reason, how to investigate the functional alternations of nuclear matrix in cancer cells during the induced differentiation will have a momentous significance in revealing the mechanism of cell canceration and reversion.

## REFERENCES

- 1 Chen F, Zhai ZH. The nuclear matrix. *Chin J Cell Biol*, 1989;11:49-53
- 2 Vemuri MC, Raju NN, Malhotra SK. Recent advances in nuclear matrix function. *Cytobios*, 1993;76:117-128
- 3 Jiang DL. Functions of nuclear matrix and tumorigenesis. *Foreign Med Sci: Mol Bio*, 1989;11:18-21
- 4 Getzenberg RH, Pienta KJ, Huang EY, Coffey DS. Identification of nuclear matrix proteins in the cancer and normal rat prostate. *Cancer Res*, 1991;51:6514-6520-140
- 5 Fernandes DT, Catapano CV. Nuclear matrix targets for anti-cancer agents. *Cancer Cells*, 1991;3:134-140
- 6 Capco DG, Wan KM, Penman S. The nuclear matrix: three-dimensional architecture and protein composition. *Cell*, 1982;29:847-858
- 7 Fey EG, Wan KM, Penman S. Epithelial cytoskeletal framework and nuclear matrix-intermediate filament scaffold: three-dimensional organization and protein composition. *J Cell Biol*, 1984;98:1973-1984
- 8 Tsuchiya E, Miyakawa T. Nuclear structure dynamics during the cell division cycle. *Protein Nucleic Acid Enzyme*, 1994;39:1575-1578
- 9 Getzenberg RH. Nuclear matrix and the regulation of gene expression: tissue specificity. *J Cell Biochem*, 1994;55:22-31
- 10 Chou RH, Churchill JR, Mapstone DE, Flubacher MM. Sequence-specific binding of a c-myc nuclear matrix-associated region shows increased nuclear retention after leukemic cell (HL-60) differentiation. *Am J Anat*, 1991;191:312-320

Edited by WANG Xian-Lin

# Gastroesophageal reflux: the features in elderly patients

HUANG Xun<sup>1</sup>, ZHU Hui-Ming<sup>1</sup>, DENG Chuan-Zhen<sup>1</sup>, G. Bianchi Porro<sup>2</sup>, O. Sangaletti<sup>2</sup> and F. Pace<sup>2</sup>

**Subject headings** gastroesophageal reflux; esophagitis; hiatal hernia

## Abstract

**AIM** To compare the features of gastroesophageal reflux disease between elderly and younger patients.

**METHODS** Twenty-four hour pH-monitoring and endoscopy were performed for the 66 elderly patients with typical gastroesophageal reflux symptoms, and the results were compared with 112 symptomatic younger patients.

**RESULTS** The results of 24-h pH-monitoring and endoscopy showed that the elderly patients had pathological reflux and reflux esophagitis more frequently than the younger patients. Percentage time with pH<4 in elderly patients with reflux esophagitis was 32.5% in 24 hours, as compared with 12.9% in the younger patients with reflux esophagitis ( $P<0.05$ ). The elderly patients with reflux esophagitis have longer periods of acid reflux in both upright and supine positions than the younger patients. Endoscopy showed that 20.8% of elderly patients had grade III/IV esophagitis, whereas only 3.4% of younger patients had grade III/IV esophagitis ( $P<0.002$ ). Percentages of grades I/II esophagitis in the two groups were 12.5% and 26.5%, respectively ( $P<0.002$ ).

**CONCLUSION** Elderly patients, as compared with younger patients, have more severe gastroesophageal reflux and esophageal lesions. The incompetence of lower esophageal sphincter and the presence of hiatal hernia may be important factors leading to the difference in incidence and severity of reflux esophagitis between elderly and younger patients.

## INTRODUCTION

With the introduction of intraesophageal 24-h pH-monitoring in clinical practice, it is now possible to identify patterns of gastroesophageal reflux (GER) in the healthy people and patients and to assess the effect of H<sub>2</sub> blockers and H<sup>+</sup>/K<sup>+</sup> adenosine triphosphatase (ATPase) inhibitors on GER diseases<sup>[1-7]</sup>. It is increasingly recognized that symptomatic GER may occur in the patients of all ages. However, little information is available on symptomatic GER patterns in the elderly. Recently, Mold et al, investigated GER disease (GERD) in patients aged over 62 years in a primary care setting<sup>[8]</sup>. However, the focus of this study was not on patterns of GER, but on prevalence of GER in the elderly. Therefore, the aim of the present study was to identify patterns and features of symptomatic GER in the elderly patients.

## PATIENTS AND METHODS

### Patients

One hundred and seventy-eight consecutive patients who had experienced heartburn, regurgitation and chest pain for at least 6 months were studied. These included 66 elderly patients (36 men, 30 women) ranging in age from 65 to 76 years (mean age 67 years), and 112 younger patients (64 men, 48 women) aged from 21 to 64 years (mean age 41 years). None had undergone upper gastrointestinal surgery such as gastric resection and selective proximal vagotomy. None had taken H<sub>2</sub>-blockers or H<sup>+</sup>/K<sup>+</sup>-ATPase inhibitors in the 2-week period before 24-h pH-monitoring.

### Endoscopy

All patients underwent upper gastrointestinal endoscopy. Esophagitis grade was assessed endoscopically by using the Savary & Miller Criteria<sup>[9]</sup>, that is, from grade I to IV. Of these patients, very few presented with grades II and III esophagitis, and therefore grade I and II, and III and IV were grouped together.

### Twenty-four hour intraesophageal pH-monitoring

Twenty-four hour intraesophageal pH-monitoring was carried out by a routine method used in our laboratory<sup>[10]</sup>. Patients were advised to take a standard 2200 kilocalories meal during 24-h

<sup>1</sup>Department of Gastroenterology, Shenzhen People's Hospital, Shenzhen 518020, Guangdong Province, China

<sup>2</sup>Gastrointestinal Unit, L. Sacco, Milan University, Milan, Italy  
HUANG Xun, female, born on 1960-05-19 in Shanghai, graduated from Shanghai Medical University, now associate professor of gastroenterology, having 5 papers published.

**Correspondence to:** HUANG Xun, Department of Gastroenterology, Shenzhen People's Hospital, Shenzhen 518001, Guangdong Province, China

Tel.+86-755-5533018, Fax.+86-755-5533497

Received 1999-03-06

intraesophageal pH-monitoring. A glass pH-electrode with an incorporated potassium chloride reference electrode (Ingol electrode, No 440) was introduced via the naso-esophageal route and positioned with the tip 5 cm above the gastroesophageal junction identified by the pH-metry<sup>[11,12]</sup>. The output from the pH probe was recorded on a solid-state recorder (Autronicord CM 18), which could be carried on a belt by the patients. Data were analyzed on a computer by means of a dedicated computer program. The parameters recorded included the frequency and duration of GER in 24 hours, upright and supine positions, and frequency of GER longer than 5 minutes. Pathological reflux was diagnosed if 1) the pH value in the regurgitated contents was <4.0, and 2) the complete reflux duration was more than 7% in 24 hours<sup>[10-12]</sup>. Reflux esophagitis was diagnosed if the patient with pathological GER had inflammatory esophageal lesions.

#### Statistical methods

Anamnestic data and endoscopic findings were analysed by means of the Chi-square test. The Mann-Whitney test and Fisher exact test were used to evaluate GER parameters.

## RESULTS

Endoscopic findings showed that elderly patients had more severe esophageal lesions and a higher incidence of hiatal hernia than younger patients (Table 1) ( $P < 0.002$ ).

On the basis of the results of the endoscopy and intraesophageal 24-h pH-monitoring, patients can be divided into three subgroups: physiologic reflux, pathologic reflux and reflux esophagitis. Table 2 lists the percentages of the three groups in elderly and younger patients. The incidence of pathologic reflux and reflux esophagitis in elderly patients was higher than that in younger patients ( $P < 0.05$ ).

Figure 1 shows the percentage time of GER episodes in 24 hours. In the reflux esophagitis group, percentage time of GER episodes in the elderly and younger patients during the entire 24-h period was 36.2% and 17.8%, respectively ( $P < 0.05$ ). No statistically significant differences in the percentage time with GER episodes were found between the elderly and younger patients in either the physiologic or pathologic reflux subgroups.

Figures 2 and 3 show the percentage time of GER episodes in upright and supine positions. Elderly patients with reflux esophagitis had significantly greater percentage time of GER episodes than younger patients with reflux esophagitis (upright position, 32.4% versus 13.6% supine position, 30.7% versus 11.7%;  $P < 0.05$ ).

**Table 1 Endoscopic findings in elderly and younger patients**

	Non-esophagitis (%)	Esophagitis		Hiatal hernia(%)
		I/II(%)	III/IV(%)	
Elderly patients	44(66.7)	8(12.1) <sup>b</sup>	14(21.2) <sup>b</sup>	16(24.2) <sup>b</sup>
Younger patients	78(69.6)	29(25.8)	4(3.6)	17(15.1)

<sup>b</sup> $P < 0.001$ , elderly patients vs younger patients.

**Table 2 Percentages of physiological reflux (PhR), pathological reflux and reflux esophagitis (RE) in elderly and younger patients**

	PhR(%)	PR(%)	RE(%)
Elderly patients	24(36.4) <sup>a</sup>	20(30.3) <sup>a</sup>	22(33.3) <sup>a</sup>
Younger patients	59(52.7)	19(17.0)	34(30.3)

<sup>a</sup> $P < 0.05$ , elderly patients vs younger patients; PhR = physiological reflux; PR = pathological reflux; RE = reflux esophagitis.

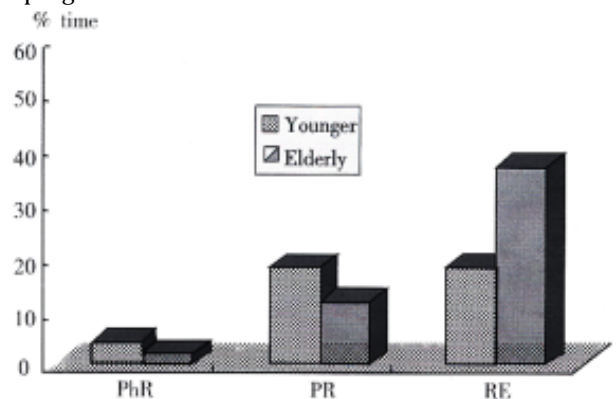


**Figure 1** Percentage time of GER episodes in 24 hours. PhR: physiological reflux; PR: pathological reflux; RE: reflux esophagitis.

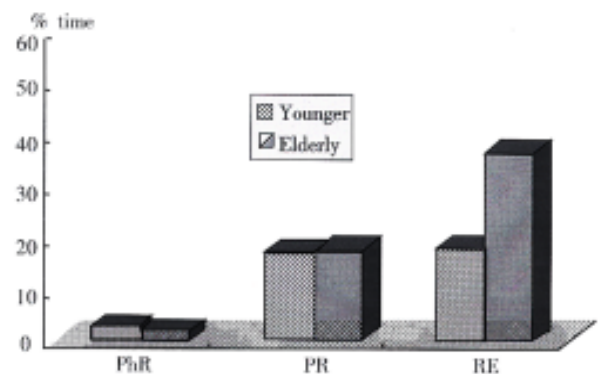


**Figure 2** Percentage time of GER episodes in upright position.

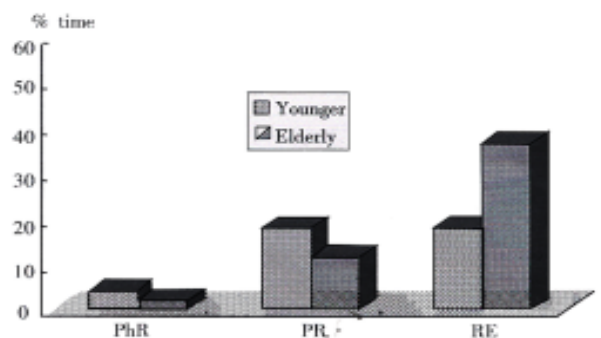


**Figure 3** Percentage time of GER episodes in supine positions.

Elderly patients with reflux esophagitis had a higher frequency of GER episodes than younger patients with reflux esophagitis, the difference being statistically significant (Table 3). There was no significant difference between elderly and younger patients in frequency of GER episodes lasting more than 5 minutes (Table 4).

**Table 3** Frequency of GER episodes in elderly and younger patients ( $\bar{x}\pm s$ )

	Elderly patients		Younger patients	
Upright position				
PhR	10	10 <sup>a</sup>	24	20 <sup>a</sup>
PR	45	21 <sup>b</sup>	55	21 <sup>b</sup>
RE	85	64 <sup>c</sup>	53	32 <sup>c</sup>
Supine position				
PhR	3	4	3	9
PR	17	9 <sup>d</sup>	8	7 <sup>d</sup>
RE	18	3 <sup>e</sup>	7	7 <sup>e</sup>

<sup>a</sup> $P < 0.01$ , elderly vs younger; <sup>c</sup> $P < 0.05$ , elderly vs younger;  
<sup>d</sup> $P < 0.01$ , elderly vs younger; <sup>e</sup> $P < 0.05$ , elderly vs younger.

**Table 4** Frequency of GER episodes lasting more than 5 minutes in elderly and younger patients ( $\bar{x}\pm s$ )

	Elderly patients		Younger patients	
Upright position				
PR	3	2	5	3
RE	9	6	5	6
Supine position				
PR	3	2	5	3
RE	3	2	2	2

$P > 0.05$ , elderly patients vs younger patients; PR=pathological reflux; RE=reflux esophagitis.

## DISCUSSION

Although several studies of GER patterns have been carried out in healthy subjects and patients, the GER profile in the elderly has not been investigated. Many older people, as a result of physiological change or disease, have decreased salivary flow, gastric acid production, esophageal motility, gastric emptying, and/or lower esophageal sphincter tone. These changes may affect the features of symptomatic GER in the elderly patients.

The present study demonstrated that patterns of GER and esophageal lesions in elderly patients with GER symptoms showed different features from those presented by the younger patients. Firstly, the incidence of pathological reflux and reflux esophagitis in the elderly patients with GER symptoms was significantly higher than in the younger patients (66.7% vs 46.9%). Secondly, the elderly patients with GER symptoms have more severe esophageal lesions than younger patients. In the elderly patients, 20.8% of patients had grades III/IV esophagitis, as against only 3.4% of patients in the younger group. In addition, elderly patients had a higher incidence of hiatal hernia than their

younger counterparts. Thirdly, 24-h intraesophageal pH-monitoring showed that elderly patients with reflux esophagitis had a more severe acid reflux than younger patients with reflux esophagitis. This is due to prolonged periods of acid reflux in both upright and supine positions. Similarly, in elderly patients with reflux esophagitis, the frequency of GER episodes in both upright and supine positions is higher than that in younger patients with reflux esophagitis. It is generally agreed that esophagitis may be the result of abnormal acid GER in most patients. Our results suggest that more severe patterns of GER in elderly patients leads to more severe esophageal lesions.

The present results showed that there was no statistically significant difference between the elderly and younger patients regarding frequency of GER episodes lasting more than 5 minutes (Table 4). This suggests that an impaired esophageal clearing function is not responsible for the difference in incidence and severity of reflux esophagitis observed between elderly and younger patients. Therefore, different pathogenetic mechanism such as the incompetence of lower esophageal sphincter and the presence of hiatal hernia may be important factors leading to the difference in incidence and severity of reflux esophagitis between elderly and younger patients.

## REFERENCES

- Smout AJPM, Breedijk M, Vanderzouw C, Akkermans LMA. Physiological gastroesophageal reflux and esophageal motor activity studied with a new system for 24-hour recording and automated analysis. *Dig Dis Sci*, 1989;34:372-378
- Duroux Ph, Emde C, Bauerfeind P, Francis C, Grisel A, Thybaud L, Armstrong D, Depeursinge C, Blum AL. The ion sensitive field effect transistor pH electrode: a new sensor for long term ambulatory pH monitoring. *Gut*, 1991;32:240-245
- Champion G, Richter JE, Vaezi MF, Singh S. Duodenogastro esophageal reflux: relationship to pH and importance in Barrett's esophagus. *Gastroenterology*, 1994;107:747-754
- Breumelhof R, Smout AJPM. The symptom sensitivity index: a valuable additional parameter in 24-hour esophageal pH recording. *Am J Gastroenterol*, 1991;86:160-164
- Hewson EG, Sinclair JW, Dalton CB. Twenty-four-hour esophageal pH monitoring: the most useful test for evaluating noncardiac chest pain. *Am J Med*, 1991;90:576-583
- Richter JE, Bradley LA, DeMeester TR, Wu WC. Normal 24-hr ambulatory esophageal pH values. *Dig Dis Sci*, 1992;37:849-856
- Kahrilas PJ, Quigley EMM. Clinical esophageal pH recording: a technical review for practice guideline development. *Gastroenterology*, 1996;110:1982-1996
- Mold JW, Reed LE, Davis AB, Allen ML, Decktor DL, Robinson M. Prevalence of gastroesophageal reflux in elderly patients in a primary care setting. *Am J Gastroenterol*, 1991;86:965-970
- Savary M, Miller G. The esophagus. Handbook and atlas of endoscopy. *Switzerland: Gassmann*, 1987:1-250
- Zhu HM, Bianchi Porro G, Sangaletti O, Pace F. Thresholds of gastroesophageal reflux in the diagnosis of esophageal reflux diseases. *China Natl J New Gastroenterol*, 1996;2:9-12
- Zhu HM. Study of influence of hiatal hernia on gastroesophageal reflux. *China Natl J New Gastroenterol*, 1997;3:27-30
- Zhu HM, Huang X, Deng CZ, Pianchi Porro G, Pace F, Sangaletti O. Pathogenetic factors affecting gastroesophageal reflux in patients with esophagitis and concomitant duodenal ulcer: a multivariate analysis. *WJG*, 1998;4:153-157

Review

# Human intestinal and biliary cryptosporidiosis

CHEN Xian-Ming and Nicholas F. LaRusso

**Subject headings** *Cryptosporidium parvum*; cryptosporidiosis/epidemiology; cryptosporidiosis/immunology; cryptosporidiosis/diagnosis; cryptosporidiosis/therapy

*Cryptosporidium parvum* (*C. parvum*) is a coccidian parasite of the phylum *Apicomplexa* that infects the gastrointestinal, biliary and respiratory epithelium of humans and animals<sup>[1]</sup>. Early reports described a disease in humans characterized by protracted, watery diarrhea occurring in immunosuppressed patients, many with acquired immunodeficiency syndrome (AIDS). Recent epidemiologic studies indicate that cryptosporidiosis may also present as an acute, self-limited diarrheal disease in immunocompetent individuals and may account for 1%-10% of diarrheal disease worldwide<sup>[2,3]</sup>. Despite the magnitude and severity of cryptosporidial infection, the pathogenesis is poorly understood, and there is currently no effective therapy<sup>[3]</sup>. In this review, we provide a concise summary of what is known about cryptosporidial infection of the intestinal and biliary tract.

## THE PARASITE

*Cryptosporidium* is a coccidian parasite and one of many genera of the protozoan phylum, *Apicomplexa* (class Sporozoa, subclass Coccidia). Six species are currently recognized on the basis of differences in host specificity, oocyst morphology and site of infection (*C. parvum*, *C. muris*, *C. meleagridis*, *C. baileyi*, *C. serpentis* and *C. nesorum*); only *C. parvum* causes diseases in humans<sup>[1,4]</sup>.

*C. parvum* has a monoxenous life cycle, all stages of development (asexual and sexual) occurring in one host. The entire life cycle may be completed in as few as 2 days in many hosts, and infections may be short-lived or may persist for

months. Once ingested, oocysts excyst in the gastrointestinal tract releasing infective sporozoites. The freed sporozoites attach to epithelial cells and become enclosed within parasitophorous vacuoles, developing attachment organelles (stages referred as trophozoites). The trophozoites then undergo asexual proliferation by merogony and form two types of meronts. Type I meronts form 8 merozoites that are liberated from the parasitophorous vacuole when mature; the merozoites then invade other epithelial cells where they undergo another cycle of type I merogony or develop into type II meronts. Type II meronts form 4 merozoites which do not undergo further merogony but produce sexual reproductive stages (called gamonts). Sexual reproduction occurs by gametogony and both microgametes (male) and macrogametocytes (female) are formed. Macrogametocytes are then fertilized by mature microgametes, and the resultant zygotes undergo further asexual development (sporogony) and form sporulated oocysts containing 4 sporozoites. Most oocysts are thick-walled and are excreted from the host in faecal material; some oocysts, however, are thin walled and have been reported to excyst within the same host leading to a new cycle of development<sup>[1]</sup>. The presence of these auto-infective oocysts and recycling type I meronts are believed to be the means by which persistent chronic infections may develop in hosts without further exposure to exogenous oocysts<sup>[1]</sup>.

## EPIDEMIOLOGY

Infection of *C. parvum* in both immunocompetent and immunocompromised humans occurs worldwide. From prevalence studies, oocyst excretion rates are known to vary between 1%-3% in industrialized countries and 10% in less industrialized nations. Seroprevalence rates are much higher. In developed countries, they vary between 25%-35%, while in the developing world these rates are as high as 60%-90% (Figure 1)<sup>[3,5,6]</sup>. *C. parvum* infection was reported in 10%-15% of the children with diarrhea in the developing world. It has been reported that 10%-16% of AIDS patients with chronic diarrhea in North America and 30%-50% in the developing world are infected with *C. parvum*<sup>[7,8]</sup> while the infection mainly occurs in the intestine in both immunocompetent and immunocompromised

The Center for Basic Research in Digestive Diseases, Division of Gastroenterology and Hepatology, Mayo Medical School, Clinic and Foundation, Rochester, MN 55905, USA  
NIH grant. DK24031.

**Correspondence to:** Nicholas F. LaRusso, M.D., Center for Basic Research in Digestive Diseases, Mayo Clinic, 200 First Street, SW, Rochester, MN 55905, USA  
Tel.(507)284-1006, Fax.(507)284-0762  
Email. larusso.nicholas@mayo.edu

Received 1999-07-11

individuals, biliary cryptosporidiosis has only been reported in HIV-infected patients, being found in 20%-65% of the patients with so-called AIDS-cholangiopathy<sup>[9]</sup>.

It has been reported that as low as 10 oocysts of *C. parvum* can cause human diseases. Many instances of human-to-human transmission have been recorded between household and family members, sexual partners (both heterosexual and homo sexual), hospital patients and staff, and children attending day care centers. While most cases of transmission involve oocysts derived from faecal samples, contaminated water is a source of infection among international travelers, and outbreaks have been associated with contamination of well water, surface water, swimming pools and public water supplies. *C. parvum* oocysts have been recovered from untreated surface waters, filtered swimming pool water, and most importantly, from treated drinking water. Homosexuals practicing oral-anal and/or anal-genital sex, veterinary personnel and animal handlers are particularly at risk<sup>[1]</sup>. Immunocompromised individuals with hypogammaglobulinaemia, organ transplanted recipients, patients undergoing bone marrow transplantation and patients on immunosuppressive drugs are also at high-risk<sup>[10]</sup>.

## IMMUNOLOGY AND PATHOGENESIS

### Immunology

Immunocompetent individuals who become infected generally experience a self-limited syndrome and become immune to reinfection. In contrast, severe chronic infections may develop in immunocompromised individuals with either congenital or acquired lymphocyte or  $\gamma$ -globulin deficiencies, suggesting both cell-mediated and humoral immune responses are involved in the resolution of infections and the development of immunity<sup>[1]</sup>.

Immunoserological tests have detected specific IgG, IgM, IgA and even IgE antibodies in acute or convalescent sera from infected patients. Local and secretory antibodies have been detected in association with infections, including IgA antibodies in duodenal fluid<sup>[11]</sup>. Passively acquired antibodies have also been implicated in the prevention or control of infections. Several epidemiological studies recorded a lower prevalence of infections in breast-fed children than in bottle-fed children. However, the role of serum or secretory antibodies in the resolution of infections is unclear. Neutralizing antibodies against surface membrane determinants of free sporozoites and merozoites reduce infectivity, suggesting that some antibodies may neutralize intraluminal stages of the parasite. Whether these antibodies would be effective against

intracellular developmental stages in which the parasite is covered by host membranes is unknown<sup>[1]</sup>.

Experimental studies using immunocompromised SCID mice and nude mice have shown that resolution of a *C. parvum* infection requires B and/or *T lymphocytes*<sup>[12]</sup>. The identification of cryptosporidiosis as one of the opportunistic infections affecting individuals with AIDS also suggests that immunity to this parasite requires CD4<sup>+</sup> T cells. CD4<sup>+</sup> T cells of patients with AIDS infected with *C. parvum* show that fulminant and persistent disease only occurs in individuals with CD4<sup>+</sup> counts < 50 cells/mm<sup>3</sup>. Individuals with CD4<sup>+</sup> T counts > 200 cells/mm<sup>3</sup> display only transient disease. Individuals with CD4<sup>+</sup> T counts < 50 cells/mm<sup>3</sup> have an increased incidence of biliary disease, an indicator of chronic cryptosporidiosis, and a decreased survival when compared to those individuals with higher CD4<sup>+</sup> T cell counts<sup>[9]</sup>. IFN $\gamma$  is important for resistance to *C. parvum*; the absence of this cytokine in mice with a targeted disruption of the IFN $\gamma$  gene (gene knockout) results in uncontrolled *C. parvum* infection<sup>[13]</sup>.

### Pathogenesis

Histological changes associated with intestinal cryptosporidiosis are relatively non-specific and include blunting of villi, hyperplasia of intestinal crypt cells, and infiltration of inflammatory cells into the luminal propria. Neutrophilic infiltrate, villus blunting, cryptitis, epithelial apoptosis and reactive epithelial changes in the intestine in AIDS patients with cryptosporidiosis correlate with the intensity of *C. parvum* infection<sup>[14]</sup>. Biliary cryptosporidiosis is also associated with a non-specific inflammatory response. Histologically, there is a periductal inflammatory response with interstitial edema, mixed inflammatory cell infiltrates, and hyperplasia and dilatation of the periductal glands. The fibrosis that develops around the portal tracts of AIDS patients with chronic cryptosporidial infection can mimic the histologic changes seen in primary sclerosing cholangitis. Autopsy reports and prospective studies have supported an etiologic role for the organism in biliary syndromes like sclerosing cholangitis and acalculous cholecystitis<sup>[15,16]</sup>. However, the pathophysiological mechanisms underlying *C. parvum* infection of intestinal and biliary epithelia are not well understood, and at present our understanding of the pathogenesis is still limited to data from animal experimental studies.

The process by which *C. parvum* sporozoites infect epithelial cells consists of two sequential

steps: ① attachment of sporozoites to the plasma membrane of epithelial cells, a primary event in the initial host-parasite interaction and a prerequisite for the pathophysiological consequences; and ② invasion of sporozoites into host cells by invagination of the host cell plasma membrane, which engulfs and eventually completely surrounds the sporozoite to form a parasitophorous vacuole in which the organism remains intracellular but extracytoplasmic<sup>[17-19]</sup>. Electron microscopy has confirmed the intracellular but extracytoplasmic location of the organism within a parasitophorous vacuole formed by a continuous covering of microvillous membranes, and nearly all endogenous developmental stages of *C. parvum* are confined to the apical surface of epithelial cells. The parasite contains a unique "attachment" or "feeder" organelle which is prominent at the base of each parasitophorous vacuole. Originally, this feeder organelle was thought to be formed by repeated folding of parasite and host epithelial cell membranes. However, recent electron microscopic studies showed that the dense band of feeder organelle underlying the parasite attachment site represents modified host cell cytoskeleton. This organelle is thought to facilitate the uptake of nutrients by the parasite from the host cell.

*C. parvum* displays a clear predilection to infect only certain sites within the host. The parasite usually infects epithelia in the intestine, respiratory tract and bile ducts. In the human intestine, the stomach is rarely infected, and the upper small bowel, colon, and rectum are less affected than the mid small bowel<sup>[1]</sup>. Several cell lines from human or animal intestine are sensitive to *C. parvum*-infection *in vitro*, but the susceptibilities of those cells to infection differ<sup>[20]</sup>. Sporozoites attach to the cultured host cells by their anterior pole and attachment is dose, time, ion, pH and host cell-cycle dependent, and is inhibitable by antibodies against antigens on the sporozoite surface membrane<sup>[21,22]</sup>. Recently, we developed an *in vitro* system of biliary cryptosporidiosis, and demonstrated that the infection is both apical plasma membrane and liver cell specific (i.e., *C. parvum* can infect bile duct cells but not hepatocytes *in vitro*)<sup>[19]</sup>. These characteristics suggested specific molecules on the surface of both epithelial cells and *C. parvum* sporozoites are involved in the infection process. Previous studies did demonstrate the presence of a galactose-N-acetylgalactosamine (Gal-GalNAc) specific *C. parvum* sporozoite surface lectin which may mediate attachment of sporozoites to host cells<sup>[22,23]</sup>. Moreover, recent reports have shown that *C. parvum* sporozoite motility depends on the parasite cytoskeleton, and host cell cytoskeleton

rearrangement might be involved in the biogenesis of parasitophorous vacuoles<sup>[19]</sup>. Nevertheless, the molecular mechanisms and specific molecules involved in the initial interaction between *C. parvum* sporozoites and epithelial cells remain obscure. Moreover, essentially nothing is known about how the organism actually invades cells and forms a parasitophorous vacuole, a complex organelle on which the life cycle and possibly the cytotoxicity of the organism is dependent. Based on our observations on the interaction of *C. parvum* with intestinal and biliary epithelial cells *in vitro*, we propose a molecular model for *C. parvum* infection of epithelial cells shown in Figure 2.

When microbes interact with host cells, the result is generally host cell dysfunction. Recent data in a variety of tissues infected with either parasite (such as *Entamoeba histolytica*, *Schistosoma mansoni*, *Trypanosoma cruzi* and *Toxoplasma gondii*), bacteria or viruses are consistent with the concept that microbial pathogens can kill host cells by an apoptotic mechanism. Experimentally, it has been shown that *C. parvum* infection of intestinal and biliary epithelial cell monolayers results in a functional disruption of the monolayers and release of LDH from the cell surface. Epithelial apoptosis and reactive epithelial changes in the intestine in AIDS patients with cryptosporidiosis have recently been shown to be associated with *C. parvum* infection<sup>[14]</sup>. We found that apoptosis occurs in the epithelial cells adjacent to *C. parvum*-infected biliary epithelia *in vivo* in the gallbladder of a patient with AIDS and biliary cryptosporidiosis<sup>[19]</sup>. More recently, we found that *C. parvum* can induce apoptosis in the cultured human biliary epithelia<sup>[19,24]</sup>. These results suggest that *C. parvum*, like some other parasites, is directly cytopathic for epithelia via an apoptotic mechanism, a mechanism which is believed critical in liver diseases like primary biliary cirrhosis, primary sclerosing cholangitis, and hepatitis<sup>[25]</sup>.

Release of cytokines and chemokine plays a critical role in the inflammation associated with microbial infection. Rapid upregulation of the C-X-C chemokine family was found in human intestinal epithelial cells infected with gram-negative or gram-positive bacteria. In an *in vitro* model of intestinal cryptosporidiosis, *C. parvum* induces IL-8 release from infected intestinal epithelial cell monolayers<sup>[26]</sup>. Release of cytokines and chemokines like IL-8 could be involved in the pathogenesis of inflammation in cryptosporidiosis. However, little is known about the early events following host-parasite interactions that influence the course of cytokine and chemokine upregulation and release.

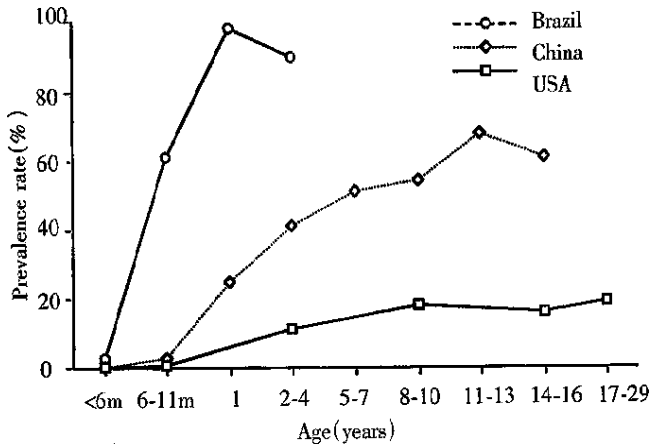


**Figure 1** Prevalence of IgG antibodies to *C. parvum* in different populations from Brazil, China and the United States. M = month. Data reproduced from reference 3 with permission.

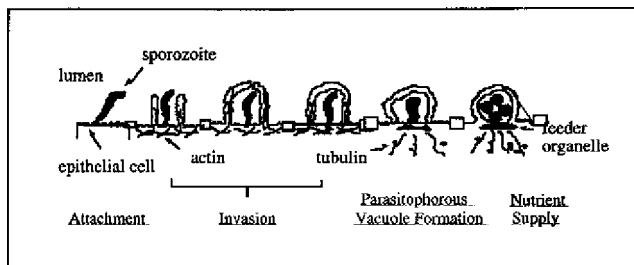


**Figure 2** Molecular model for *C. parvum* infection of epithelial cells. *C. parvum* sporozoite attaches specifically to the apical membrane surface of epithelial cells. The attachment induces rearrangement of the host cell cytoskeleton and facilitates the parasite's invasion and parasitophorous vacuole formation. Host cell cytoskeleton rearrangement forms the feeder organelle underlying the parasite attachment site and facilitates the uptake of nutrients by the parasite from the host cell cytoplasm.

## CLINICAL MANIFESTATIONS AND DIAGNOSIS

### Clinical manifestations

The most common clinical manifestation of cryptosporidiosis is diarrhea, characteristically profuse and watery and often containing mucus but rarely blood or leucocytes. Other clinical signs observed include abdominal cramps, low grade fever, nausea and vomiting<sup>[10]</sup>. The duration and severity of clinical symptoms depend largely on the immune status of the infected individual. In immunocompetent individuals, the disease is usually self-limited. After an incubation period of 7-10 days, >90% of infected cases present with watery diarrhea lasting approximately 2 weeks, 50% present with nausea, vomiting and cramp-like abdominal pain and 36% present with a febrile illness. In immunocompromised individuals, the disease is much more severe. In HIV-infected patients, the disease severity is related to the site of

*C. parvum* infection and CD4<sup>+</sup> cell count<sup>[27]</sup>. The diarrhea is watery and stool frequency can be up to 10 times a day with a mean volume of one liter. Individuals with AIDS infected with *C. parvum* can experience a 10% drop in body weight, and usually develop severe malabsorption. Most of them never clear the infection, and ultimately have a shorter survival than AIDS patients without cryptosporidiosis<sup>[28]</sup>.

AIDS patients infected with *C. parvum* also develop extraintestinal disease, most frequently of the biliary tract<sup>[29]</sup>. Biliary cryptosporidiosis has only recently been recognized as a clinical entity, and is even less understood than the intestinal form of the disease. Although a number of pathogens account for opportunistic biliary tract infections in AIDS patients, *C. parvum* is the single most common identifiable pathogen and is found in 20%-65% of the patients with so-called AIDS-cholangiopathy<sup>[9]</sup>. These patients often have right upper quadrant pain, nausea, vomiting, fever and biochemical evidence of cholestasis. Strictures, narrowing and irregularities of the intrahepatic bile ducts, with dilatation of the common hepatic and common bile ducts and the thickening of the ductal walls, are often found by noninvasive and invasive imaging studies<sup>[30]</sup>.

### Diagnosis

Indirect methods of diagnosing cryptosporidiosis (by comparative symptomatology or clinical parameters) have proven unsatisfactory. Serological studies also have no place in diagnosis as many healthy individuals already have antibodies. At present, most cryptosporidial infections are diagnosed by the microscopic examination of host faecal material for the presence of *C. parvum* oocysts. Experimental studies have shown that oocyst excretion coincides well with the onset and duration of most clinical signs of disease. Most asymptomatic individuals can be screened to detect subclinical infections and even water samples can be examined for contamination by oocysts. *C. parvum* oocysts are much smaller than those of other coccidian parasites, and they differ in many of their staining and buoyancy characteristics. Thus, most conventional coprological techniques used in parasitology and microbiology laboratories are not entirely suitable for their detection. Many specialized staining procedures have been described to stain the oocysts and differential staining techniques are more desirable to avoid confusion. The technique of choice for many diagnostic laboratories has been acid-fast staining. Oocysts stain bright red whereas yeast, bacteria and other faecal debris only take up the counterstain. Several immunolabelling techniques have also been

developed to detect oocysts. Both polyclonal rabbit antisera and monoclonal antibodies have been used to detect *C. parvum* oocysts in faecal and water samples by immunofluorescence and several diagnostic test kits are now commercially available<sup>[19,31,32]</sup>.

When biliary disease is suspected, ultrasonography is the best initial diagnostic method. It will be suggestive in most cases by identifying biliary ductal wall thickening and/or gallbladder dilation or both. Computerized tomography might also be helpful. However, the most sensitive method to diagnose biliary tract disease in HIV-infected patients is endoscopic retrograde cholangiopancreatography (ERCP)<sup>[30]</sup>. If biliary disease is highly suspected and the patient has normal ultrasonography, ERCP should be performed. However, ERCP is not recommended to work-up suspected asymptomatic AIDS-cholangiopathy. The cholangiographic appearance of AIDS cholangiopathy is quite variable and has been described in different ways. Characteristically, the biliary tree appears irregular and distorted with focal dilation and narrowing in the intrahepatic and/or extrahepatic biliary tree. The most common cholangiographic pattern is papillary stenosis associated with intrahepatic sclerosing cholangitis, which occurs in approximately 50% - 60% of patients<sup>[30,33,34]</sup>. Although occasionally diagnostic, percutaneous liver biopsy is rarely helpful and thus plays no role in the diagnosis of AIDS-cholangiopathy. Serum alkaline phosphatase is the most commonly elevated liver biochemical test with mean values in most series of 700 IU/L-800 IU/L. Mild increases in aminotransferases are common with values ranging from 65 to 123 IU/L, whereas hyperbilirubinemia is distinctly uncommon<sup>[30]</sup>.

## THERAPY AND PREVENTION

### Therapy

At present, there is no effective antimicrobial treatment available for cryptosporidiosis in man or animals. Generally, immunocompetent individuals need no specific therapy. Supportive care with oral or intravenous fluids and electrolyte replacement is beneficial in alleviating the dehydration accompanying acute diarrhea while awaiting spontaneous recovery. In children, however, spiramycin may shorten the duration of oocyst excretion and diarrhea, although conflicting results have been obtained<sup>[35,36]</sup>. In AIDS patients without antiretroviral therapy, AZT therapy should be started. In these patients, a relationship between disease severity and CD4<sup>+</sup> count has been documented. Paromomycin is the only agent so far

that has been found to have efficacy in animals and humans in the treatment of intestinal cryptosporidiosis<sup>[37-39]</sup>. It is an aminoglycoside anti biotic that is not significantly absorbed when given orally and is used for intestinal amoebiasis. In most studies, including a double blind trial, there was a good clinical and parasitological response<sup>[37-40]</sup>. However, after discontinuation of treatment, many patients relapse. In a well-documented study, paromomycin, 500 mg 4 times daily for 4 weeks and maintenance therapy of 500mg twice daily, was used<sup>[41]</sup>.

Therapy of biliary cryptosporidiosis in AIDS-cholangiopathy is primarily endoscopic<sup>[30]</sup>. For those patients with abdominal pain or cholangitis associated with papillary stenosis, endoscopic sphincterotomy may provide striking symptomatic relief as it facilitates drainage and decompression of the biliary system. Although survival is not prolonged, sphincterotomy may help improve the quality of life for those with papillary stenosis and pain. There is no evidence that sphincterotomy is beneficial for sclerosing cholangitis in the absence of papillary stenosis and CBD dilation, or in asymptomatic patients and it may be associated with a higher complication rate. Patients with diffuse intra- and extrahepatic sclerosing cholangitis alone have few specific treatment options. Paromomycin is not effective in biliary cryptosporidiosis in AIDS-cholangiopathy<sup>[40]</sup>.

### Prevention

Since therapy remains difficult, prevention of the disease is critical. *C. parvum* infections are contracted by the ingestion or inhalation of oocysts, and therefore effective control measures must aim to reduce or prevent oocyst transmission. *C. parvum* have been proven remarkably resistant to chemical disinfection. Many commercial disinfectants (based on aldehyde, ammonia, alcohol, chlorine or alkaline compounds) are ineffective when used according to the manufacturers' instructions and most conventional methods of water treatment do not effectively remove or kill all the oocysts from contaminated water<sup>[1]</sup>. Many recommendations have been made for the prevention and control of infections in specific locations; such as hospitals, laboratories, and day care centers. These recommendations have basically involved managerial practices designed to minimize further host contact with sources of infection. Isolation of infected individuals, careful handling and disposal of biohazardous waste, and heat treatment (boiling) of suspect contaminated water before consumption are helpful.

## REFERENCES

- 1 O'donoghue PJ. Cryptosporidium and cryptosporidiosis in man and animals. *Int J Parasitol*, 1995;25:139-195
- 2 Newman RD, Sears CL, Moore SR, Nataro JP, Wuhib T, Agnew DA, Guerrant RL, Lima AA. Longitudinal study of cryptosporidium infection in children in Northeastern Brazil. *J Infect Dis*, 1999; 180:167-175
- 3 Guerrant RL. Cryptosporidiosis: an emerging, highly infectious threat. *Emerg Infect Dis*, 1997;3:51-57
- 4 Hoepelman IM. Human cryptosporidiosis. *Int J STD & AIDS*, 1996; 7:28-33
- 5 Ungar BL, Gilman RH, Lanata CF, Perez SI. Seroepidemiology of Cryptosporidium infection in two Latin American populations. *J Infect Dis*, 1988;157:551-556
- 6 Huhls TL, Mosier DA, Crawford DL, Griffis J. Seroprevalence of cryptosporidial antibodies during infancy, childhood and adolescence. *Clin Infect Dis*, 1994;18:731-735
- 7 Colford JM Jr, Tager IB, Hirozawa AM, Lemp GF, Aragon T, Petersen C. Cryptosporidiosis among patients infected with human immunodeficiency virus. Factors related to symptomatic infection and survival. *Am J Epidemiol*, 1996;144:807-816
- 8 Sanchez-Mejorada G, Ponce-de-Leon S. Clinical patterns of diarrhea in AIDS: etiology and prognosis. *Rev Invest Clin*, 1994;46:187-196
- 9 Vakil NB, Schwartz SM, Buggy BP, Brummitt CF, Kherallah M, Letzer DM, Gilson IH, Jones PG. Biliary cryptosporidiosis in HIV-Infected people after the waterborne outbreak of cryptosporidiosis in Milwaukee. *New Engl J Med*, 1996;334:19-23
- 10 Fayer R, Ungar BL. Cryptosporidium spp. and cryptosporidiosis. *Microbiol Rev*, 1986;50:458-483
- 11 Laxer MA, Alcantara AK, Javato-Laxer M, Menorca DM, Fernando MT, Ranoa CP. Immune response to cryptosporidiosis in Philippine children. *Am J Trop Med Hyg*, 1990;42:131-139
- 12 Theodos CM. Innate and cell-mediated immune responses to Cryptosporidium parvum. *Adv Parasitol*, 1998;40:87-119
- 13 Griffiths JK, Theodos C, Paris M, Tzipori S. The gamma interferon gene knockout mouse: a highly sensitive model for evaluation of therapeutic agents against Cryptosporidium parvum. *J Clin Microbiol*, 1998;36:2503-2508
- 14 Lumadue JA, Manabe YC, Moore RD, Belitsos PC, Sears CL, Clark DP. A clinico pathologic analysis of AIDS-related cryptosporidiosis. *AIDS*, 1998;12:2459-2466
- 15 Teare JP, Daly CA, Rodgers C, Padley SP, Coker RJ, Main J, Harris JR, Scullion D, Bray GP, Summerfield JA. Pancreatic abnormalities and AIDS related sclerosing cholangitis. *Genitourin Med*, 1997;73:271-273
- 16 French AL, Beaudet LM, Benator DA, Levy CS, Kass M, Orenstein JM. Cholecystectomy in patients with AIDS: clinicopathologic correlations in 107 cases. *Clin Infect Dis*, 1995;21:852-858
- 17 Rosales MJ, Mascaro C, Osuna A. Ultrastructural study of Cryptosporidium development in Madin-Darby canine kidney cells. *Vet Parasitol*, 1993;45:267-273
- 18 Marcial MA, Madara JL. Cryptosporidium: cellular localization, structural analysis of absorptive cell-parasite membrane-membrane interactions in guinea pigs, and suggestion of protozoan transport by M cells. *Gastroenterology*, 1986;90:583-594
- 19 Chen XM, Levine SA, Tietz P, Krueger E, McNiven MA, Jefferson DM, Mahle M, LaRusso NF. Cryptosporidium parvum is cytopathic for cultured human biliary epithelia via an apoptotic mechanism. *Hepatology*, 1998;28:906-913
- 20 Upton SJ, Tilley M, Brillhart DB. Comparative development of Cryptosporidium parvum (Apicomplexa) in 11 continuous host cell lines. *FEMS Microbiol Lett*, 1994;118:233-236
- 21 Hamer DH, Ward H, Tzipori S, Pereira MEA, Alroy JP, Keusch GT. Attachment of Cryptosporidium parvum sporozoites to MDCK cells *in vitro*. *Infect Immun*, 1994;62:2208-2213
- 22 Joe A, Verdon R, Tzipori S, Keusch GT, Ward HD. Attachment of Cryptosporidium parvum sporozoites to human intestinal epithelial cells. *Infect Immun*, 1998;66:3429-3432
- 23 Thea DM, Pareira MEA, Kotler D, Sterling CR, Keusch GT. Identification and partial purification of a lectin on the surface of the sporozoite of Cryptosporidium parvum. *J Parasitol*, 1992;78:886-893
- 24 Chen XM, Gores GJ, Paya CV, LaRusso NF. Cryptosporidium parvum induces apoptosis in biliary epithelia by a Fas/Fas ligand-dependent mechanism. *Am J Physiol*, 1999 (in press)
- 25 Patel T, Roberts LR, Jones BA, Gores GJ. Dysregulation of apoptosis as a mechanism of liver disease: an overview. *Semin Liver Dis*, 1998;18:105-114
- 26 Laurent F, Eckmann L, Savidge TC, Morgan G, Theodos C, Naciri M, Kagnoff MF. Cryptosporidium parvum infection of human intestinal epithelial cells induces the polarized secretion of C-X-C chemokines. *Infect Immun*, 1997;65:5067-5073
- 27 Flanigan T, Whalen C, Turner J, Soave R, Toerner J, Havlir D, Kotler D. Cryptosporidium infection and CD4 counts. *Ann Intern Med*, 1992;116:840-842
- 28 Manabe YC, Clark DP, Moore RD, Lumadue JA, Dahlman HR, Belitsos PC, Chaisson RE, Sears CL. Cryptosporidiosis in patients with AIDS: correlates of disease and survival. *Clin Infect Dis*, 1998; 27:536-542
- 29 Cello JP. Human immunodeficiency virus-associated biliary tract disease. *Semin Liver Dis*, 1992;12:213-218
- 30 Wilcox CM, Monkemuller KE. Hepatobiliary diseases in patients with AIDS: focus on AIDS cholangiopathy and gallbladder disease. *Dig Dis*, 1998;16:205-213
- 31 MacPherson DW, McQueen R. Cryptosporidiosis: multiattribute evaluation of six diagnostic methods. *J Clin Microbiol*, 1993;31: 198-202
- 32 Aldras AM, Orenstein JM, Kotler DP, Shaddock JA, Didier ES. Detection of microsporidia by indirect immunofluorescence antibody test using polyclonal and monoclonal antibodies. *J Clin Microbiol*, 1994;32:608-612
- 33 Ducreux M, Buffet C, Lamy P, Beaugerie L, Fritsch J, Choury A, Liguory C, Longuet P, Gendre JP, Vachon F. Diagnosis and prognosis of AIDS-related cholangitis. *AIDS*, 1995;9:875-880
- 34 Farman J, Brunetti J, Baer JW, Freiman H, Comer GM, Scholz FJ, Koehler RE, Laffey K, Green P, Clemett AR. AIDS related cholangiopancreatographic changes. *Abdom Imag*, 1994;19:417-422
- 35 Saez-Llorens X, Odio CM, Umana MA, Morales MV. Spiramycin vs. placebo for treatment of acute diarrhea caused by Cryptosporidium. *Pediatr Infect Dis J*, 1989;8:136-140
- 36 Wittenberg DF, Miller NM, van den Ende J. Spiramycin is not effective in treating cryptosporidium diarrhea in infants: results of a double-blind randomized trial. *J Infect Dis*, 1989;159:131-132
- 37 Armitage K, Flanigan T, Carey J, Frank I, MacGregor RR, Ross P, Goodgame R, Turner J. Treatment of cryptosporidiosis with paromomycin. A report of five cases. *Arch Intern Med*, 1992;152: 2497-2499
- 38 Fichtenbaum CJ, Ritchie DJ, Powderly WG. Use of paromomycin for treatment of cryptosporidiosis in patients with AIDS. *Clin Infect Dis*, 1993;16:298-300
- 39 Scaglia M, Atzori C, Marchetti G, Orso M, Maserati R, Orani A, Novati S, Olliaro P. Effectiveness of aminosalicylate (paromomycin) sulfate in chronic Cryptosporidium diarrhea in AIDS patients: an open, uncontrolled, prospective clinical trial. *J Infect Dis*, 1994; 170:1349-1350
- 40 White AC Jr, Chappell CL, Hayat CS, Kimball KT, Flanigan TP, Goodgame RW. Paromomycin for cryptosporidiosis in AIDS: a prospective, double-blind trial. *Infect Dis*, 1994;170:419-424
- 41 Bissuel F, Cotte L, Rabodonirina M, Rougier P, Piens MA, Trepo C. Paromomycin: an effective treatment for cryptosporidial diarrhea in patients with AIDS. *Clin Infect Dis*, 1994;18:447-449

# Expression of inducible nitric oxide synthase in human gastric cancer

Jun Yu, Fei Guo, Matthias P.A. Ebert and Peter Malfertheiner

**Subject headings** stomach neoplasms; nitric oxide synthase; nitric oxide

## INTRODUCTION

Inducible nitric oxide synthase (iNOS) is an enzyme that catalyzes the formation of nitric oxide (NO) from L-arginine. iNOS expression and activity results in the production of high levels of NO<sup>[1]</sup>. The generation of physiological levels of NO is important for mucosal function and it also exerts a cytoprotective effect on the gastrointestinal mucosa. However, increased iNOS expression has been observed in patients with chronic inflammatory diseases of the gastrointestinal tract, such as ulcerative colitis<sup>[2,3]</sup>, and gastritis<sup>[4]</sup> and it has been speculated that increased NO may induce DNA damage<sup>[5,6]</sup> and angiogenesis<sup>[7]</sup>. Nonetheless, the role of iNOS in human GI neoplasia is largely unknown. Previous studies have demonstrated increased iNOS expression in breast cancer<sup>[8,9]</sup>, and increased iNOS activity and protein levels have been demonstrated in colorectal cancer<sup>[10]</sup> and adenocarcinoma of the esophagus<sup>[11]</sup>. However, to date, the role of iNOS in gastric carcinogenesis has not been elucidated.

## MATERIALS AND METHODS

Gastric biopsies were obtained from individuals undergoing gastric endoscopy. Two or three mucosal biopsies were endoscopically obtained for histological study. One or two additional biopsies were obtained for mRNA isolation. The biopsies were snap frozen in liquid nitrogen and stored at -80 °C. The samples used in this study were collected from tumor and a tumor free location in 6 gastric cancer patients, and 7 biopsies were obtained from the histologically normal gastric mucosa in corpus and/or antrum from healthy subjects. RNA was extracted using the RNA-zol B procedure. After completion of this extraction, RNA was separated on

a 1.5% agarose gel and RNA was visualized by ethidium bromide staining. cDNAs were generated from one microgram of total RNA; it was denatured at 65 °C for 10 min and cooled on ice for 2 min. The RNA was reversely transcribed in a 20 µL final volume of 5x AMV RT buffer, MgCl<sub>2</sub>, dNTPs, random primers, 16 U of Rnasin and 1.5 U AMV Reverse Transcriptase. The reaction mixture was incubated for 1 hour at 37 °C, and for 5 min at 96 °C. For confirmation of cDNA integrity, a RT-PCR analysis using β-actin primers was also performed. The sequence of the primers were as follows: sense primer (s-iNOS), 5' TAGAGGAACATCTG-GCCAGG-3'; antisense primer (as iNOS), 5'-TG-GCAGGGTCCCCTCTGATG-3'; generating a 372 bp fragment of the iNOS transcript. PCR was performed under the following conditions: 94 °C for 5 min, 60 °C for 45 sec, 72 °C for 1min; which was repeated for 35 cycles. Ten mL of the PCR reaction was separated on a 1.5% agarose gel and cDNA was visualized by ethidium bromide staining.

## RESULTS

RT-PCR analysis using primers specific for human iNOS mRNA generated a 372 bp fragment of the predicted size. Using this RT-PCR analysis iNOS mRNA was detected in 3 of 6 tumor tissues, and in one of the adjacent tumor free gastric tissues obtained from gastric cancer patients (Table 1). In addition, a fragment of iNOS mRNA was amplified in one of 7 normal gastric tissues obtained from four healthy individuals undergoing endoscopy (Table 2). *H. pylori* infection was detected histologically in 5 of 6 cancer patients and in the stomach of two of the four healthy individuals. In two of the *H. pylori* infected individuals iNOS mRNA was detected in the non-cancerous mucosa, whereas all individuals without *H. pylori* infection did not exhibit iNOS mRNA.

**Table 1** iNOS expression in gastric cancer patients

Patient	Age	Sex	Cancer type	Hp status	iNOS expression	
					Tumor	Tumor-free
1	37	m	Intestinal	+	-	-
2	55	m	Diffuse	+	-	+
3	69	f	Diffuse	+	+	-
4	71	m	Intestinal	+	+	-
5	73	m	Unknown	+	+	-
6	63	m	Intestinal	-	-	-

Department of Gastroenterology, Hepatology and Infectious Diseases, University Hospital of Magdeburg, Germany

**Correspondence to:** P. Malfertheiner, MD, Professor and Head of the Department of Gastroenterology, Hepatology and Infectious Diseases, University Hospital of Magdeburg, Leipziger Str. 44, D-39120 Magdeburg, Germany

Tel.+49-391-6713100, Fax.+49-391-6713105

**Received** 1999-08-10

**Table 2** iNOS expression in healthy individuals

Patient	Age	Hp	Gastritis	iNOS expression	
				Antrum	Corpus
1	24	-	+	-	-
2	37	+	+	-	+
3	60	+	++	-	nd
4	49	-	-	-	-

## DISCUSSION

*H. pylori* infection of the gastric mucosa may lead to chronic gastritis<sup>[12]</sup> and to the development of gastric or duodenal ulcers<sup>[13]</sup>. Furthermore, *H. pylori* infection is considered a risk factor for gastric cancer<sup>[14-16]</sup>. The molecular alterations underlying the pathogenesis of gastric cancer, however, remain largely unknown. In addition, the molecular alterations induced by *H. pylori* infection of the gastric mucosa which may contribute to gastric carcinogenesis are not well established. Recently several studies have identified high levels of iNOS expression in *H. pylori* associated gastritis<sup>[17,18]</sup>. Furthermore, it has been shown that both whole *H. pylori* bacteria and lysates may induce iNOS mRNA levels and iNOS release<sup>[11]</sup>. Interestingly, after eradication of *H. pylori* infection iNOS expression reverts as determined by immunohistochemistry<sup>[18]</sup>. In our present study we found that iNOS expression was present only in individuals infected with *H. pylori* infection, whereas individuals without *H. pylori* infection did not exhibit iNOS mRNA in the gastric biopsies.

The chronic inflammation caused by *H. pylori* may induce molecular and cellular pathways contributing to the malignant transformation of the gastric mucosa. In our study 4 of the 6 cancers exhibited iNOS mRNA. While the increased formation of NO may lead to DNA damage, may stimulate angiogenesis, and may inhibit DNA repair mechanisms, the increased expression of iNOS in gastric cancers raises the hypothesis that the chronic inflammation caused by *H. pylori* infection may lead to molecular alterations of the gastric mucosa which activate molecular pathways that could lead to the transformation of the gastric mucosa and the development of gastric cancer<sup>[19]</sup>.

In summary, our study supports the hypothesis that molecular alterations induced by *H. pylori* infection of the gastric mucosa may precede the development of gastric cancer and provide a further link between chronic inflammation and malignant transformation in the gastrointestinal tract.

**ACKNOWLEDGMENTS** This study was supported by a grant

from the Land Sachsen-Anhalt (2775A/0087H) awarded to M.P.A. Ebert.

## REFERENCES

- Xie Q, Nathan C. The high-output nitric oxide pathway: role and regulation. *J Leukoc Biol*, 1994;56:576-582
- Godkin AJ, De Belder AJ, Villa L, Wong A, Beesley JE, Kane SP, Martin JF. Expression of nitric oxide synthase in ulcerative colitis. *Eur J Clin Invest*, 1996;26:867-872
- Gupta SK, Fitzgerald JF, Chong SK, Croffie JM, Garcia JG. Expression of inducible nitric oxide synthase (iNOS) mRNA in inflamed esophageal and colonic mucosa in a pediatric population. *Am J Gastroenterol*, 1998;93:795-798
- Rachmilewitz D, Karmeli F, Eliakim R, Stalnikowicz R, Ackerman Z, Amir G, Stamler JS. Enhanced gastric nitric oxide synthase activity in duodenal ulcer patients. *Gut*, 1994;35:1394-1397
- Wink DA, Kasprzak KS, Maragos CM, Elespuru RK, Misra M, Dunams TM, Cebula TA, Koch WH, Andrews AW, Allen JS. DNA deaminating ability and genotoxicity of nitric oxide and its progenitors. *Science*, 1991;254:1001-1003
- Nguyen T, Brunson D, Crespi CL, Penman BW, Wishnok JS, Tannenbaum SR. DNA damage and mutation in human cells exposed to nitric oxide *in vitro*. *Proc Natl Acad Sci USA*, 1992;89:3030-3034
- Penkins DC, Charles IG, Thomsen LL, Moss DW, Holmes LS, Baylis SA, Rhodes P, Westmore K, Emson PC, Moncada S. Roles of nitric oxide in tumor growth. *Proc Natl Acad Sci USA*, 1995;92:4392-4396
- Thomsen LL, Lawton FG, Knowles RG, Beesley JE, Riveros-Moreno V, Moncada S. Nitric oxide synthase activity in human gynecological cancer. *Cancer Res*, 1994;54:1352-1354
- Thomsen LL, Miles DW, Happerfield L, Bobrow LG, Knowles RG, Moncada S. Nitric oxide synthase activity in human breast cancer. *Br J Cancer*, 1995;72:41-44
- Amb S, Merriam WG, Bennett WP, Felley-Bosco E, Ogunfusika MO, Oser SM, Klein S, Shields PG, Billiar TR, Harris CC. Frequent nitric oxide synthase-2 expression in human colon adenomas: implication for tumor angiogenesis and colon cancer progression. *Cancer Res*, 1998;58:334-341
- Wilson KT, Fu S, Ramanujam KS, Mettler SJ. Increased expression of inducible nitric oxide synthase and cyclooxygenase-2 in Barrett's esophagus and associated adenocarcinomas. *Cancer Res*, 1998;58:2929-2934
- Miller MJ, Thompson JH, Zhang XJ, Sadowska-Krowicka H, Kakkis JL, Munshi UK, Sandoval M, Rossi JL, Eloby-Childress S, Beckman JS. Role of inducible nitric oxide synthase expression and peroxynitrite formation in guinea pig ileitis. *Gastroenterology*, 1995;109:1475-1483
- Chang AD, Ramanujam KS, Wilson KT. Co-expression of inducible nitric oxide synthase (iNOS), cyclooxygenase (COX-2), and TGF- $\beta$  in rat models of colitis. *Gastroenterology*, 1996;109:1475-1478
- Lin JT, Wang LY, Wang JT, Wang TH, Yang CS, Chen CJ. A nested case-control study on the association between *Helicobacter pylori* infection and gastric cancer risk in a cohort of 9775 men in Taiwan. *Anticancer Res*, 1995;15:603-606
- Forman D, Newell DG, Fullerton F, Yarnell JW, Stacey AR, Wald N, Sitas F. Association between infection with *Helicobacter pylori* and risk of gastric cancer: evidence from a prospective investigation. *BMJ*, 1991;302:1302-1305
- Parsonnet J, Friedman GD, Vandersteen DP, Chang Y, Vogelstein JH, Orentreich N, Sibley RK. *Helicobacter pylori* infection and the risk of gastric carcinoma. *N Engl J Med*, 1991;325:1127-1131
- Wong A, Fu S, Varanasi RV, Ramanujam KS, Fantry GT, Wilkson KT. Expression of inducible nitric oxide synthase and cyclooxygenase-2 and modulation by omeprazole in *Helicobacter pylori* gastritis. *Gastroenterology*, 1997;112:A332
- Mannick EE, Bravo LE, Zarama G, Realpe JL, Zhang XJ, Ruiz B, Fonham ET, Mera R, Miller MJ, Correa P. Inducible nitric oxide synthase, nitrotyrosine, and apoptosis in *Helicobacter pylori* gastritis: effect of antibiotics and antioxidants. *Cancer Res*, 1996;56:3238-3243
- Williamson WA, Ellis FH Jr, Gibb SP, Shahian DM, Aretz HT, Heatley GJ, Watkins E Jr. Barrett's esophagus. Prevalence and incidence of adenocarcinoma. *Arch Intern Med*, 1991;151:2212-2216

# Partial sequencing of 5' non-coding region of 7 HGV strains isolated from different areas of China

WANG Xing-Tai<sup>1</sup>, ZHUANG Hui<sup>2</sup>, SONG Hai-Bo<sup>3</sup>, LI He-Min<sup>1</sup>, ZHANG Hua-Yuan<sup>1</sup> and YU Yang<sup>1</sup>

**Subject headings** hepatitis G virus; polymerase chain reaction; nucleotide sequence; RNA, viral

## INTRODUCTION

Although sensitive tests for detection of known hepatitis viruses are available, the etiology of 10%-15% post-transfusion and community-acquired hepatitis cases has remained undefined. It suggests the existence of unknown causative agents associated with the disease. GBV-C and HGV were newly discovered as putative non-A to E hepatitis viruses reported by Simons<sup>[1]</sup> and Linnen<sup>[2]</sup> independently. However, the sequence homology analysis of the two strains revealed that they are different isolates of the same virus. HGV is a positive-strand RNA virus with an entire genome of 10kb which contains a continuous open reading frame (ORF) encoding a viral polyprotein. The structural region (C, E1 and E2) is located at the N-terminal, while the non-structural region (NS2, NS3, NS4A/B, NS5A/5B) is situated at the C-terminal. The long ORF is preceded by a 5' untranslated sequence and followed by a 3' untranslated sequence. Our previous report has confirmed the existence of HGV infection in China<sup>[3]</sup>. There is evidence that the gene of hepatitis C virus (HCV) is hypervariable in different areas<sup>[4-8]</sup>. The variability of HCV is also found in the same strain of the virus. HGV and HCV are classified in the same genus of the flaviviridae family. So it is of great significance to clarify the geographical distribution of HGV genotypes in the world<sup>[9]</sup>. In this study, the partial sequences of 5' non-coding region of 7 HGV strains isolated from different areas of China were analyzed

and compared with GBV-C (U36380) and HGV (U44402) reported from the United States.

## MATERIALS AND METHODS

### Subjects

Seven HGV RNA positive sera tested by RT-PCR were collected from blood donors of Beijing, Jiangsu, Anhui, Liaoning, Hebei Provinces, and Guangxi Zhuang and Xinjiang Uighur Autonomous Regions.

### Primers

According to the nucleotide sequence of 5' non-coding region of a Chinese HGV strain, the primers for RT nPCR were designed using the software of OLIGO 5.0. They were as follows: S1 5' GGT GGT GGA TGG GTG ATGAC 3'; A1 5' CCG AAG GAT TCT TGG GCT AC 3'; S2 5' GCT GGT AGG TCG TAA ATC 3'; A2 5' ACT GGT CCT TGT CAA CTC 3'.

### Detection of HGV RNA and nucleotide sequencing

HGV RNA extraction, HGV cDNA synthesis and PCR procedure were performed by the methods described previously<sup>[3]</sup>. All the PCR products were cloned into the pGEMT vector (Promega, Madison, WI), and positive clones were identified. The PCR products were purified and sequenced bidirectionally using the dideoxynucleotide chain termination method. The HGV cDNA sequences were analyzed with a DNA sequencer (ABI PRISM 377 DNA Sequencer, Perkin-Elmer Cetus).

## RESULTS

### Detection of HGV RNA

The positive rates of anti-HGV varied from 1.2% (35/2916) to 5.4% (49/907) in blood donors and 42.9% (15/35) 75.5% (37/49) of anti-HGV positive sera were also HGV RNA positive.

### Partial sequencing of 7 Chinese HGV strains

The partial nucleotide sequences of the 5' non-coding region of 7 HGV strains isolated from blood donors of Beijing, Jiangsu, Anhui, Liaoning, Hebei Provinces, and Guangxi Zhuang and Xinjiang Uighur Autonomous Regions, China were analyzed and compared with GBV-C (U36380) and HGV (U44401) (Figure 1).

<sup>1</sup>National Institute for the Control of Pharmaceutical and Biological Products, Beijing 100050, China

<sup>2</sup>Department of Microbiology, Beijing Medical University, Beijing 100083, China

<sup>3</sup>Laboratory for Clinical Diagnosis, Hefei 230000, Anhui Province, China

WANG Xing-Tai, male, born on 1966-03-25 in Lujiang County, Anhui Province, graduated from Anhui Medical University in 1990, earned Ph.D. degree in 1997, now associate professor of virology, having 20 papers published.

Supported by the Research Fund for the Doctoral Program of Higher Education, China, No.96024027 and won the Second-Class Prize of Science and Technology Progress, the Ministry of Education, China.

**Correspondence to:** Prof. ZHUANG Hui, Department of Microbiology, Beijing Medical University, Beijing 100083, China

Tel. +86-10-62091617, Fax. +86-10-62092221

Email.Zhuanghu@publica.bj.cninfo.net

Received 1999-02-05

```

U44402 GGT AGG TCG TAA ATC CCG GTC ACC TTG GTA GCC ACT ATA GGT GGG
U36380 GGT AGG TCG TAA ATC CCG GTC ACC TTG GTA GCC ACT ATA GGT GGG
Ch2 GGT AGG TCG TAA ATC CCG GTC ACC TTG GTA GCC ACT ATA GGT GGG
Ch3 GGT AGG TCG TAA ATC CCG GTC ACC TTG GTA GCC ACT ATA GGT GGG
Ch4 GGT AGG TCG TAA ATC CCG GTC ACC TTG GTA GCC ACT ATA GGT GGG
Ch5 GGT AGG TCG TAA ATC CCG GTC ACC TTG GTA GCC ACT ATA GGT GGG
Ch6 GGT AGG TCG TAA ATC CCG GTC ACC TTG GTA GCC ACT ATA GGT GGG
Ch7 GGT AGG TCG TAA ATC CCG GTC ACC TTG GTA GCC ACT ATA GGT GGG
Ch8 GGT AGG TCG TAA ATC CCG GTC ACC TTG GTA GCC ACT ATA GGT GGG

U44402 TCT TAA GAG AAG GTT AAG ATT CCT CTT CTG CCT CCG GCG AGA CCG
U36380 TCT TAA GAG AAG GTT AAG ATT CCT CTT GCG CAT ATG GAG GAA AAG
Ch2 ACT TAA GGG ATG GTC AAG CTC CCT CTG GCG CTT CTG GCG GAA AAG
Ch3 TCT TAA GGG AAG GTC AAG GTC CCT CTG GCG CTT CTG GAG AGA AAG
Ch4 TCT TAA GGG TTG GTC AAG GTC CCT CTG GCG CTT GTG GAG AAG AAG
Ch5 TCT TAA GGG CTG GTC AAG GTC CCT CTG GCG CTT GTG GCG AGA AAG
Ch6 TCT TAA GGG TTG GTC AAG GTC CCT CTG GCG CTT CTG GAG AAG AAG
Ch7 CCT TAA GGG CTG GCT AAG GTC CCT CTG GCG CTT GTG GCG AGA AAG
Ch8 TCT TAA GGG ATG GGT AAG GTC CCT CTG GCG CTT GTG GCG AAG AAG

U44402 CGC ACC GTC CAC AGG TGT TGG CCC TAC CCG TGG GAA TAA GGG CCC
U36380 CGC ACC GTC CAC AGG TGT TGG TCC TAC CCG TGG TAA TAA GGA CCC
Ch2 CGC ACC GTC CAC AGG AGA TGG CCC TAC CCG TGA GGG TAA GGG CCC
Ch3 CGC ACC GTC CAC AGG TGT TGG CCC TAC CCG TGG GAA TAA GGG CCC
Ch4 CGC ACC GTC CAC AGG TGT TGG CCC TAC CCG TGT GAA TAA GGG CCC
Ch5 CGC ACC GTC CAC AGG TGT TGG CCC TAC CCG TGT GGA TAA GGG CCC
Ch6 CGC ACC GTC CAC AGG TGA TGG CCC TAC CCG TGT GAA TAA GGG CCC
Ch7 CGC ACC GTC CAC AGG TGT TGG CCC TAC CCG TGT GGA TAA GGG CCC
Ch8 CGC ACC GTC CAC AGG TGT TGG CCC TAC CCG TGG GAA TAA GGG CCC

U44402 GAC GTC AGG CTC GTC GTT AAA CCG AGC CCG TTA CCC ACC TGG GCA
U36380 GGC GTC AGG CTC GTC GTT AAA CCG AGC CCG TTA CTC CCC TGG GCA
Ch2 GGC GTC AGG CTC GTC GTT AAA CCG GGC CCA TTA CCC ACC TGG GCA
Ch3 GGC GTC AGG CTC GTC GTT AAA CCG AGC CCA TTA CCC ACC TGG GCA
Ch4 GAC GTC AGG CTC GTC GTT AAA CCG AGC CCA TTA CCC ACC TGG GCA
Ch5 GGC GTC AGG CTC GTC GTT AAA CCG GGC CCA TTA CCC ACC TGG GCA
Ch6 GAC GTC AGG CTC GTC GTT AAA CCG AGC CCA TTA CCC ACC TGG GCA
Ch7 GGC GTC AGG CTC GTC GTT AAA CCG GGC CCA TTA CCC ACC TGG GCA
Ch8 GGC GTC AGG CTC GTC GTT AAA CCG AGC CCA TTA CCC ACC TGG GCA

U44402 AAC GAC GCC CAC GTA CCG TCC ACC TCG CCC TTC AAT GTC TCT CTT
U36380 AAC GAC GCC CAC GTA CCG TCC ACC TCG CCC TTC AAT GTC TCT CTT
Ch2 AAC AAC GCC CAC GTA CCG TCC ACC TCG CCC TTC AAT GGA TCT CTT
Ch3 AAC AAC GCC CAC GTA CCG TCC ACC TCG CCC TTC AAT GAA TCT CTT
Ch4 AAC AAC GCC CAC GTA CCG TCC ACC TCG CCC TTC AAT GAA TCT CTT
Ch5 AAC AAC ACC CAC GTA CCG TCC ACC TCG CCC TTC AAT GTC TCT ATG
Ch6 AAC AAC GCC CAC GTA CCG TCC ACC TCG CCC TTC AAT GAA TCT CTT
Ch7 AAC AAC GCC CAC GTA CCG TCC ACC TCG CCC TTC AAT GGA TCT CTT
Ch8 AAC AAC GCC CAC GTA CCG TCC ACC TCG CCC TTC AAT GTC TCT CTT

U44402 GAC CAA TAG GCG TAG CCG GCG AGT TGA CAA GGA CCA GT
U36380 GAC CAA TAG GCG TAG CCG GCG AGT TGA CAA GGA CCA GT
Ch2 GAC CAA TAG GCG TAG CCG GCG AGT TGA CAA GGA CCA GT
Ch3 GAC CAA TAG GCG TAG CCG GCG AGT TGA CAA GGA CCA GT
Ch4 GAC CAA TAG GCG TAG CCG GCG AGT TGA CAA GGA CCA GT
Ch5 GAC CAA TAG GCG TAG CCG GCG AGT TGA CAA GGA CCA GT
Ch6 GAC CAA TAG GCG TAG CCG GCG AGT TGA CAA GGA CCA GT
Ch7 GAC CAA TAG GCG TAG CCG GCG AGT TGA CAA GGA CCA GT
Ch8 AAC CAA TAG GCG TAG CCG GCG AGT TGA CAA GGA CCA GT

```

**Figure 1** Comparison of partial nucleotide sequences of the 5' non-coding region of 7 HGV strains isolated from different regions of China. Ch2: Beijing; Ch3: Jiangsu; Ch4: Anhui; Ch5: Liaoning; Ch6: Guangxi; Ch7: Xinjiang; Ch8: Hebei

**Table 1 Comparison of the partial nucleotides of 7 Chinese strains of HGV with reported strains**

HGV strains	Homology of the nucleotides (%)								
	U36380	U44402	Ch2	Ch3	Ch4	Ch5	Ch6	Ch7	Ch8
U36380	100.0								
U44402	87.23	100.0							
Ch2	85.92	86.85	100.0						
Ch3	88.26	92.02	93.42	100.0					
Ch4	88.26	86.67	92.96	96.24	100.0				
Ch5	85.54	89.20	92.96	93.90	94.37	100.0			
Ch6	86.85	89.67	92.96	96.24	99.06	93.43	100.0		
Ch7	85.92	89.67	94.84	97.18	95.31	96.71	95.31	100.0	
Ch8	88.26	91.55	92.02	95.30	95.31	93.70	95.31	94.37	100.0

### Homology of 7 Chinese HGV strains

The nucleotide homology of the 5' non-coding region of 7 Chinese HGV strains was 85.92%, 88.26%, 88.26%, 85.45%, 86.85%, 85.92% and 88.26%, respectively, as compared with the African strain GBV-C (U36380). It was 86.85%, 92.02%, 86.67%, 89.02%, 89.67% and 91.55%, respectively, as compared with the American strain HGV (U44402). The homology of nucleotide sequences was 92.02% - 97.18% among the 7 Chinese HGV strains (Table 1).

### DISCUSSION

HGV is transmitted parenterally, and the infection seems not to cause significant hepatic damage as hepatitis viruses A-E do. Although transmission through blood or parenteral exposure is well documented for HGV, little is known about its prevalence in blood donors of China. This study shows that the prevalence rate of anti-HGV ranged from 1.2% to 5.4% in the population of different areas of China. The data indicate that the HGV infection is widely spread in the different areas of China. The nucleotide homology of the 5' non-coding region among the 7 Chinese HGV strains was 92.0%-97.2%. However, the identity of these 7-Chinese strains was 85.9% - 92.0% at the nucleotide level as compared with the African strain of GBV-C (U36380) and the American HGV strain (U44402). The data suggest that the Chinese HGV isolates belong to a new group which is different from the African and American strains reported by Simons<sup>[1]</sup> and Linnen<sup>[2]</sup>. The divergence of nucleotide sequences among Chinese HGV strains shows the correlation between HGV variation and the geographical locations.

The homology of NS3 nucleotide sequences of the 3 Chinese HGV strains reported previously by our group<sup>[3]</sup> was 92.48%, 89.09% and 85.34%, respectively with GBV-C (U36380), and 89.09%,

85.34% and 85.34% with HGV (U44402). It is very close to the homology of the 5' non-coding region of 7 Chinese HGV strains with GBV-C (U36380) and HGV (U44402), indicating that the NS3 region may not be the site of immune selection.

**ACKNOWLEDGEMENTS** We are grateful to FAN Jin-Shui, LI Kui and ZHU Yong-Hong for their helpful advices.

### REFERENCES

- 1 Simons JN, Leary TP, Dawson GJ, Pilot Matias TJ, Muerhoff AS, Schlauder GG, Desai SM, Mushahwar IK. Isolation of novel virus-like sequences associated with human hepatitis. *Nature Med*, 1995; 1:564-569
- 2 Linnen J, Jr JW, Zhang-keck ZY, Fry KE, Krawczynski KZ, Alter H, Koonin E, Gallagher M, Alter M, Hadziyannis S, Karayiannis P, Fung K, Nakatsuji Y, Shih JWK, Young L, Jr MP, Hoover C, Fernandez J, Chen S, Zou JC, Morris T, Hyams KC, Ismay S, Lifson JD, Hess G, Fong SKH, Thomas H, Bradley D, Margolis H, Kim JP. Molecular cloning and disease association of hepatitis G virus: a transfusion-transmissible agent. *Science*, 1996; 271:505-509
- 3 Wang XT, Zhuang H, Li HM, Fan JS, Qi ZB, Liu G. Detection of GBV-C: infection and sequencing of partial gene of a Chinese strain of GBV-C. *Zhonghua Weishengwuxue He Mianyixue Zazhi*, 1996; 16:263-265
- 4 Lesniewski RR, Boardway KM, Casey JM, Desai SM, Devare SG, Leung TK, Mushahwar IK. Hypervariable 5'-terminus of hepatitis C virus E2/NS1 encodes antigenically distinct variants. *J Med Virol*, 1993; 40:150-156
- 5 Choo QL, Richman KH, Han JH, Berger K, Lee C, Dong C, Gallegos C, Coit D, Medina\_Selby A, Barr PJ, Weiner AJ, Bradley DW, Kuo G, Houghton M. Genetic organization and diversity of the hepatitis C virus. *Proc Natl Acad Sci USA*, 1991; 88:2451-2455
- 6 Kato N, Ootsuyama Y, Tanaka T, Nakagawa M, Nakazawa T, Muraiso K, Ohkoshi S, Hijikata M, Shimotohno K. Marked sequence diversity in the putative envelope proteins of hepatitis C viruses. *Virus Res*, 1992; 22:107-123
- 7 Kato N, Hijikata M, Ootsuyama Y, Nakagawa M, Ohkoshi S, Shimotohno K. Sequence diversity of hepatitis C viral genomes. *Mol Biol Med*, 1990; 7:495-501
- 8 Okamoto H, Kojima M, Okada SI, Yoshizawa H, Iizuka H, Tanaka T, Muchmore EE, Peterson DA, Ito Y, Mishiro S. Genetic drift of hepatitis C virus during an 8.2-year infection in a chimpanzee: variability and stability. *Virology*, 1992; 190:894-899
- 9 Schlauder GG, Dawson GJ, Simons JN, Pilot-Matias TJ, Gutierrez RA, Heynen CA, Knigge MF, Kurpiewski GS, Buijk SL, Leary TP, Muerhoff AS, Desai SM, Mushahwar IK. Molecular and serologic analysis in the transmission of the GB hepatitis agents. *J Med Virol*, 1995; 46:81-90

# Apoptosis of neoplasm cell lines induced by hepatic peptides extracted from sucking porcine hepatocytes

KONG Xiang-Ping<sup>1</sup>, ZOU Qing-Yan<sup>1</sup>, LI Ru-Bing<sup>1</sup>, ZHENG Ping-Lu<sup>1</sup>, YANG Lian-Ping<sup>1</sup>, JIN Shan-Wen<sup>2</sup>

**Subject headings** neoplasm cell lines; apoptosis; hepatic peptides; hepatic extracts; liver neoplasms; hepatocytes

## INTRODUCTION

Promoting hepatocyte growth factor (pHGF) extracted from the sucking pig liver is a series of polypeptides with molecular weight less than  $M_r$  10 000 and has specific biological activities to stimulate the rat hepatocyte DNA synthesis after 1/3 partial hepatectomy and promote recovery of rat hepatic injuries induced by endotoxin and D-aminogalactose. These properties are similar to the results reported by Labrecque<sup>[1]</sup>. pHGF can effectively cure clinical acute fulminant hepatitis, chronic hepatitis and other hepatic injuries by significantly reducing serum alanine aminotransferase (sALT), eliminating jaundice and increasing the survival rate of fulminant hepatitis<sup>[2,3]</sup>.

It was reported that three of the six fractions of pHGF purified by HPLC, can promote the DNA synthesis of rat primarily cultured hepatocytes<sup>[4,5]</sup>. Two of the fractions can inhibit the proliferation of BEL-7402 hepatoma cell line, their activities were not cross-affected, indicating that there exist at least two different active components in pHGF. To investigate the inhibitory mechanism of pHGF, we purified these inhibitory components and studied their physico-chemical properties and apoptosis inducing effects.

## MATERIALS AND METHODS

### Primarily cultured hepatocytes

Male Sprague Dowley rats of 250g±30g in weight were purchased from the Experimental Animal Center, Sun Yatsen University of Medical Sciences, Guangzhou, China. The animals were

anaesthetized with ether, and their livers were removed, decapsulated, cut into small pieces, rinsed with PBS (pH 7.4) to wash away the blood. The liver pieces were incubated with 0.25% trypsin (Gibco) for 30min and gently homogenized. The hepatocytes were collected after centrifugation at 1000×g for 10min. Pellet parenchyma cells were washed three times with PBS (pH 7.4) by centrifugation, resuspended in RPMI-1640 medium containing 10 % FCS, 100 IU/mL penicillin and 100 µg/mL streptomycin and placed to Costar (3596) 96 well culture plate at a density of 10.6 cells/cm<sup>3</sup>, 0.1mL each well. The cells were cultured at 37 °C, 5% CO<sub>2</sub> until use.

### Neoplasm cell lines

BEL-7402 human hepatoma cell, Hep2 murine hepatoma cell and CNE-2 human nasopharyngeal carcinoma cell lines were gifts of Experimental Animal Center, Sun Yat-sen University of Medical Sciences. SMMC-7721, QGY-7703 human hepatoma cell lines, HCT<sub>8</sub> human colic adenocarcinoma cell and GLC-82 human lung adenocarcinoma cell lines were purchased from the Cellular Institute of Chinese Academy of Sciences. SGC-7901 human gastric carcinoma cell line was purchased from the Biochemistry Department of the Fourth Military Medical University. The cultured cells were grown to confluence, digested with 2.5 g/L trypsin containing 0.2 g/L EDTA, washed with PBS (pH 7.4) and resuspended in DME/F12 or RPMI-1640 medium, added into Costar (3596) well culture plates at a density of 2.5-5.0×10<sup>4</sup> cells/mL in 0.05 mL each well, then incubated at 37 °C, 5% CO<sub>2</sub> for 24h. After remained at 4 °C for 1 h, the cells were immediately recovered at 37 °C for further use.

### Proliferation inhibitory experiments

Various concentrations of HP (S4) in DME/F12 or RPMI-1640 medium containing 10% FCS were added to the cultures, incubated for another 12, 24, 48 and 72 h, MTT solution (1.5 g/L in PBS) was then added to all wells (10 µL per 100 µL medium) in the last 4 h-6 h, rinsed with PBS, DMSO was added and vibrated to dissolve the dark blue crystals. After placed at room temperature for a few minutes until all crystals were dissolved, the optic-metric density (OD) was read on  $\Sigma$  960 ELISA

<sup>1</sup>Infectious Disease Center, Chinese PLA 458 Hospital, Guangzhou 510602, Guangdong Province, China

<sup>2</sup>Shanghai Institute of Organic Chemistry, Chinese Academy of Sciences, Shanghai 200032, China

Dr. KONG Xiang-Ping, male, born on 1952-10-01 in Hebei Province, graduated from Bethune University of Medical Sciences in 1977, chief physician of infectious disease, having 37 papers published, won 15 national and military awards, engaged in molecular biological research in hepatitis and hepatic cancer.

Tel. +86-20-87378532

Received 1999-04-20

reader at test wavelength of 570 nm and referent wavelength of 630 nm.

### **Apoptosis inducing experiments**

In situ cell death detection kits (POD) were purchased from Oncor Co., USA. The cells were adjusted to a density of  $2.5 - 5.0 \times 10^4$  cells/cm<sup>3</sup>, added to 24-well plates with cover glass-slides in 0.5 mL each well. Incubated at 37 °C 5% CO<sub>2</sub> for 24 h, the cells were remained at 4 °C for 1h, the temperature was then promptly recovered to 37 °C. Various concentrations of S4 were added and incubated for different periods. The glass slides were taken out, rinsed, fixed and immunohistochemically stained. The negative control with omission of Tunel enzyme was designed according to the manufacturer's manual. The cells stained with dark yellow brown nucleus were considered as positive cells. Ten optical fields, about 500-1 000 cells were counted in each glass-slide under the high magnification ( $\times 400$ ) microscope. Results presented as  $\pm$  indicated 5% slightly positively stained cells; +, >5 <10% positive cells; ++, >10 <20% positive cells; and +++, >20 <30% positive cells.

### **Effects of S4 on the expressions of 4 oncogenes in 8 neoplasm cell lines**

The antibodies used in this study including p53, a murine monoclonal antibody IgG2b against human p53, and Bcl-2, a murine monoclonal antibody against human Bcl-2 -p25 oncoprotein were purchased from DAKO Co Inc. Fas, a rabbit polyclonal antibody against human Fas oncoprotein, and c-myc, a murine monoclonal antibody IgG2a against p67 oncoprotein purchased from Santa Cruz Biotechnology Inc, UK. Secondary antibody (DAKO products) was a rabbit antibody against murine immunoglobulin conjugated with horseradish peroxidase.

The neoplasm cells were adjusted to  $2.5-5.0 \times 10^4$  cells/cm<sup>3</sup>, added into 24 -well culture plates with cover glass-slides in 0.5 mL each well, incubated at 37 °C 5% CO<sub>2</sub> for 24 h, then remained at 4 °C for 1 h for cell growth at the same step. Immediately after the temperature was recovered to 37 °C, S4 was added and continued to inoculate for 48 h, then the cells were fixed and immunohistochemically stained following the instruction of the manufacturer. The negative control with primary antibody was replaced by PBS, and observed under light microscope. The results were presented as “+ +” to “+ + +” which indicated the slight positive staining to the strongest positive staining.

### **Northern blot**

The quantity of cells was adjusted to  $1 \times 10^7$  per

dish, and RNA in the cells was extracted rapidly with Guanidinium isothiocyanate. According to the method of random primer (Promega), the cDNA probe of human Bcl-2 gene was labeled with  $\alpha$ -<sup>32</sup>P-dCTP, and hybridized for 24 h at 68 °C in 6 $\times$ SSC, 2 $\times$ Denhart's reagent and 0.5% SDS. After the filters were washed, autoradiography was performed by exposing the filter to X-ray film at -70 °C for 48 h. The results were determined with an intensifying screen.

### **Apoptosis of BEL-7402 hepatoma cells transplanted in BALB/C nude mice induced by S4**

Male BALB/C nude mice, weighing 18 g-22 g were provided by the Experimental Animal Center of Sun Yat sen University of Medical Sciences. BEL-7402 hepatoma cells were injected s.c. into the right neck ( $1.46 \times 10^7$  cells/mL) of BALB/C male nude mice. When growing to about 0.8 cm<sup>3</sup>, tumors were cut into small pieces of about 1 mm<sup>3</sup> and transplanted into the renal capsulae of BALB/C nude mice, and their width and lengths were measured with micrographer. Twenty-six mice were divided into four groups. In the high-dose group, the six mice were injected ip with 1.0 mg S4/kg-per day and in the low-dose group, with 0.5 mg of S4/kg per day. In the positive control group, the six mice were injected ip with 1 mg Doxorubicin (Huaming Pharmaceutical Co, LTD)/kg per day, while in the negative control group, the eight mice were injected ip with 0.4 mL physical saline daily for 16 days. The nude mice were killed 2 days after the end of treatment. The width and lengths of the tumors were measured with a micrographer. All the data including body weight of mice were input to computer to calculate the growth inhibitory rate of tumors and T value.

### **Statistical analysis**

Statistical significance was determined by using  $\chi^2$  test or Student's *t* test.

## **RESULTS**

### **Homogeneous peak of hepatocyte extracts**

DEAE-Sephadex A25 purified hepatocyte extract was desalted and lyophilized, the proliferation inhibitory activities were tested. The active fraction was further purified by Superdex 75 and C<sub>18</sub> reversed-phase chromatography and lyophilized. The last purified fraction was called Subfraction 4 (S4). A combination of the above procedures produced an almost pure peak with 95.8% relative area, and molecular weight of  $M_r$  4020.6 determined by HPLC and MALDI-TOF-MS mass spectrometer.

### **Proliferation inhibitory effect of pHGF and its**

### *fractions on normal hep atocytes and 7402 hepatoma cells*

After the hepatocytes were removed from the livers of the SD rats, 7402 hepatoma cells were incubated for 24 h, 500, 1 000 and 2 000 mg/L of pHGF and 20 mg/L S4 purified by DEAE-Sephadex A25 were added into each well with 0.1mL medium. After incubation at 37 °C, 5% CO<sub>2</sub> for 48 h, MTT was added and reincubated for 4 h-6 h, then DMSO was added and mixed thoroughly to dissolve the dark blue crystals. OD value was read on  $\Sigma$ 960 ELISA reader. The inhibitory rate (%)=(100 test group OD value/control group OD value  $\times$ 100%). pHGF apparently inhibited the proliferation of BEL-7402 hepatoma cells at concentrations of 500 mg/L-2 000 mg/L, and promoted the activities of primarily cultured hepatocytes. Of six fractions of pHGF purified by DEAE- Sephadex A25, fractions 3 and 4 significantly inhibited the growth of 7402 hepatoma cells while fractions 1, 2 and 5 promoted the activities of primarily cultured hepatocyte dehydrogenase (Table 1).

The results showed that the fractions of pHGF both promoted the activities of normal hepatocyte dehydrogenase and inhibited the activities of hepatoma cell dehydrogenase. There were no cross effects between the two actions.

### *Inhibition of S4 on the proliferation of 8 neoplasm cell lines*

S4 at concentrations of 1, 5, 10 mg/L were added into the culture plates (96 wells), each well containing 0.1 mL medium, and incubated at 37 °C, 5% CO<sub>2</sub> for 12, 24, 48 and 72h. MTT solution (1.5 g/L in PBS) was added to all the wells (10  $\mu$ L per 100  $\mu$ L medium), and incubation was continued for h - 6 h, then 100  $\mu$ L DMSO was added and mixed to dissolve MTT dark blue crystals. After vibrated at room temperature for 15min, the plates were read on  $\Sigma$ 960 ELISA reader at test wavelength of 570 nm and referent wavelength of 630 nm. The results showed that S4 can significantly inhibit the proliferation of the 8 neoplasm cells with a clear dose and time dependent manner (Table 2).

### *Apoptosis of 8 neoplasm cells induced by S4*

Based on the above results that S4 can induce tumor

cells to die at concentrations of 1 mg/L-10 mg/L from 24 to 72 h, we selected the 5 mg/L of S4 and 48 h affecting period as experimental conditions so as to better compare the results of S4 on 8 neoplasm cell lines. The apoptosis inducing effect of pHGF and S4 on BEL-7402 hepatoma cells showed that the apoptosis inducing effect of S4 is 100 times as strong as that of pHGF calculated by their activities in weight. S4 induced apoptosis of 8 neoplasm cell lines with different activities, and apparently induced all the hepatoma cells to die, the effect on non-hepatoma cell lines being smaller than that of hepatoma cell lines. S4 had no apparent apoptotic effect on HCT-8 cell line, and even stagnated the apoptosis of CNE-2 cell line (Table 3). All these may be related to the histocellular sources and the signal differences tran smitted in the cells.

### *Effect of S4 on the 4 oncoprotein expressions of 8 neoplasm cell lines*

Confluent cells digested by trypsin, adjusted to 2.5-5.0 $\times$ 10<sup>4</sup> cells/cm<sup>3</sup>, added into 24 - well Costar plates with cover glass-slides in each well with 0.1mL medium and cultured in DME/F12 medium containing 10% FCS, at 37 °C, 5% CO<sub>2</sub> for 24 h. To grow at the same step, the cells were placed at 4 °C for 1h before use. Temperature was quickly recovered to 37 °C, 5 mg/L S4 was added and incubated for an other 48 h. Immunohistochemistry staining was performed following the manufacturer's manual and positive and negative controls were designed. The results ( Table 4 ) showed that S4 significantly up -regulated the expression of P53, Fas and depressed Bcl-2, but had no apparent effect on the expression of c-myc in 4 hepatoma cell lines, and the most prominent effect fell upon the BEL-7402 cell line. Effects of S4 on regulating oncogene expressions of 4 nonhepatoma neoplasm cell lines differed. S4 slightly promoted the expression of Fas and depressed Bcl-2 and c-myc in 7901 cell line; slightly down-regulated Bcl-2 and c-myc in GLC-82 cell line; but promoted the expression of Bcl-2 in CNE-2 cell line. Based on the results in 8 neoplasm cells, the apoptotic induction of S4 on the cells was considered to be exerted via affecting the Bcl-2 oncogene expression.

**Table 1 Effect of pHGF and its fractions on normal hepatocytes and hepatoma cells ( $\bar{x}\pm s$ , n = 8)**

	pHGF (OD, mg/L)			Fractions (OD, 20mg/L)						Control
	500	1000	2000	1	2	3	4	5	6	
7402 cells	0.422 $\pm$ 0.11 <sup>b</sup>	0.410 $\pm$ 0.09 <sup>b</sup>	0.401 $\pm$ 0.07 <sup>b</sup>	0.545 $\pm$ 0.03	0.601 $\pm$ 0.11	0.427 $\pm$ 0.067 <sup>b</sup>	0.411 $\pm$ 0.09 <sup>b</sup>	0.580 $\pm$ 0.08	0.649 $\pm$ 0.21	631 $\pm$ 0.12
Primary hepatocytes	0.390 $\pm$ 0.07 <sup>b</sup>	0.398 $\pm$ 0.09 <sup>b</sup>	0.388 $\pm$ 0.06 <sup>b</sup>	0.293 $\pm$ 0.06 <sup>b</sup>	0.308 $\pm$ 0.06 <sup>b</sup>	0.223 $\pm$ 0.07	0.236 $\pm$ 0.06	0.280 $\pm$ 0.10 <sup>b</sup>	0.219 $\pm$ 0.11	0.218 $\pm$ 0.07

<sup>b</sup>P<0.01, vs control.

**Table 2 Effects of S4 on 8 neoplasm cell lines at different time points**

Cells	IC50 (mg/L)		
	24h	48h	72h
BEL-7402	8.2	5.0	3.9
SMMC-7721		8.4	4.2
QGY-7703		24.2	9.5
Hepe	15.2	8.9	6.5
SGC-7901	30.2	19.7	14.3
GLC-821	2.4	9.9	5.4
CNE-2			8.9
HCT-8			9.9

IC<sub>50</sub>: the half inhibitory concentration.

**Table 3 Apoptosis of 8 neoplasm cell line induced by S4 (5mg/L, 48h)**

	Control	S4 Treatment
BEL-7402	+	++
SMMC-7721	+	++
QGY-7703	±	++
Hepe	+	++
HCT-8	±	±
GLC-82	±	+
SGC-7901	±	+
CNE-2	++	+

**Table 4 Effects of S4 on the 4 oncogene expressions of 8 neoplasm cell lines (S4, 5µg/well, 48h)**

	P53		Fas		Bcl-2		c-myc	
	C	T	C	T	C	T	C	T
BEL-7402	+	++	+	++	+	±	+	+
SMMC-7721	+	++	+++	+++	+	±	++	++
QGY-7703	±	+	+	+++	±	±	+	++
Hepe	+	++	++	++	++	±	++	+
HCT-8	+	+	++	++	±	±	++	+
GLC-82	++	+	+++	+++	+	±	++	+
SGC-7901	+	+	±	+	+	±	++	+
CNE-2	+	++	+++	++	±	+	++	+

C: control group; T: test group.

### Northern blot

The changes of Bcl-2 mRNA in BEL-7402 cell line after incubation with 5 mg/L S4 were observed by blot hybridization. The results showed that S4 can apparently inhibit the Bcl-2 mRNA transcription determined by the quantity measurement of intensifying screen. Relative value of the test group was related to the dose of S4. This result was concordant with the oncoprotein expression and demonstrated that S4 can inhibit the Bcl-2 oncogene expression at mRNA transcript level.

### Experiments of BALB/C nude mice transplanted with BEL-7402 hepatoma cells

The mice transplanted with BEL-7402 hepatoma cells were injected ip with S4 at d3 after tumor transplantation, once daily for 16 days. The results showed that S4 can apparently inhibit the growth of BEL-7402 hepatoma cells in nude mice. This inhibitory effect was also induced by apoptosis (Tables 5 and 6). S4 had no apparent effect on the

mitosis and differentiation of BEL-7402 hepatoma cells observed under the optical microscope. Cell shrinkage and condensation, microvillus disappearance, condensed chromatin margination and apoptotic body formation were found under electronic microscope.

**Table 5 Inhibition of S4 on hepatoma cells in nude mice ( $\bar{x}\pm s$ , n=6)**

	Dose (mg/kg)	Do (mm <sup>3</sup> )	Dn (mm <sup>3</sup> )	Dn-Do (mm <sup>3</sup> )	Inhibitory rate (%)
High dose of S4	2.0	2.19±0.24	2.81±0.49	0.61±0.38	59 <sup>b</sup>
Low dose of S4	1.0	2.00±0.12	2.55±0.22	0.56±0.26	63 <sup>b</sup>
Doxorubicin	1.0	2.26±0.12	2.16±0.32	0.10±0.29	107 <sup>b</sup>
Control	0.0	2.17±0.23	3.67±0.52	1.50±0.55	

Do: Dimension of tumors at onset; Dn: Dimension of tumors at necropsy. <sup>b</sup>P<0.01, vs control.

**Table 6 Apoptosis of hepatoma cells in nude mice induced by S4 (LI,  $\bar{x}\pm s$ , n=6)**

	Dose (mg/kg)	LI (%)
High dose of S4	2.0	18.70±4.92 <sup>b</sup>
Low dose of S4	1.0	13.22±1.74 <sup>b</sup>
Doxorubicin	1.0	14.18±2.46 <sup>b</sup>
Control	0.0	8.40±2.81

<sup>b</sup>P<0.01, vs control. LI: lable index.

## DISCUSSION

There are lots of substances in the human body which can stimulate the proliferation and regeneration of liver, e.g. insulin, platelet derived growth factor (PDGF), transfer growth factor  $\beta$  (TGF- $\beta$ ), epithelial growth factor (EGF), etc, but their effects are not specific. It has been shown that the hepatocytes of young animal livers might produce network self-regulators to modulate their growth, differentiation and apoptosis. Because of the differences in extracting and preparing the liver derived growth stimulating factors and inhibitors, it is difficult to enunciate whether these stimulating or inhibitory effects are caused by the double or poly-functional effects of one factor or by the specific effects of two factors with different functions.

It was reported by Labrecque<sup>[1]</sup> that a series of substances extracted from the regenerating livers of young rats, dogs and rabbits with  $M_r$ 12 000-21 000 are called hepatic stimulating substance (HSS) that can stimulate the DNA synthesis of the primarily cultured hepatocytes and the hepatocytes after partial hepatectomy (2/3)<sup>[1]</sup>. HSS can raise the survival rate of rats with fulminant hepatic failure and inhibit the growth of some neoplasm cell lines.

A series of polypeptides which can raise the survival rate of human fulminant hepatitis, reduce sALT, eliminate jaundice and ameliorate liver functions are called promoting hepatocyte growth factors (pHGF). The monoclonal

immunohistochemical study showed that pHGF is located in the hepatocytes, not in mesenchymal cells such as Kupffer cells, endotheliocytes and fibroblasts<sup>[6]</sup>.

In our previous papers<sup>[4]</sup>, we found that pHGF contained not only hepatic regeneration stimulating substances, but also growth inhibitory factors which can inhibit the growth of hepatoma cell lines. These inhibitory factors can not inhibit the growth of normal primarily cultured hepatocytes. Homogeneous fraction S4 extracted from sucking pig liver by HPLC and FPLC in this report is a small peptide with *M*<sub>r</sub>4020. Its inhibitory activities are 100 times as that of pHGF and can be destroyed by pronase K, but resist to acids, alkalis, RNAase and DNAase.

We selected 8 neoplasm cell lines to study the biological activities of S4 in the growth inhibition, apoptotic induction and oncogene expression related with apoptosis of these cell lines *in vitro*, and studied the effects of S4 in the hepatoma cells transplanted in nude mice *in vivo*. The results showed that S4 inhibit the proliferation of neoplasm cell lines *in vitro* by inducing apoptosis in a clear dose and time dependent manner. The apoptotic effect of S4 on the se cells is exerted via regulating the expression of oncogenes related to apoptosis, especially by affecting Bcl-2 gene expression. It was testified by *in vitro* and *in vivo* tests that S4 is an effective apoptotic inducer of neoplasm cell lines.

Modern molecular biology investigations have indicated that proliferation inhibition of some neoplasm cells is related to apoptosis induction regulated by the oncogene expression of these cells. The different growth inhibitions of S4 were found in 8 neoplasm cell lines with the different expressions of p53, Fas, Bcl-2 and c-myc oncogenes. S4 can apparently promote the oncoprotein expression of p53, Fas and depress the Bcl-2 and c-myc oncogenes while inducing hepatoma cells to die. It was reported that p53 induced apoptosis via stimulating apoptosis inducing genes, and inhibiting the survival

necessitating genes, or participating in the enzyme cleavage of DNA. The apoptotic induction of Fas is caused by its ligands and receptor reaction, and the apoptotic induction of c-myc is related to the apoptotic mechanism controlled by Bcl-2 gene, which depends on the circumstantial factors, leading to either death or proliferation<sup>[7,8]</sup>.

It is generally considered that Bcl-2 is an important gene for cells to survive, we have further confirmed that the Bcl-2 gene expression of BEL-7402 hepatoma cells is inhibited by S4 at m-RNA transcript level by using the techniques of blot hybridization. This may be the initial factor for the cell apoptotic induction, because Bcl-2 gene can inhibit the apoptosis by blocking the last tunnel of apoptotic signal transmitted system.

S4 inhibited the growth of hepatoma *in vivo* by inducing apoptosis, and had no apparent effect on the mitosis and differentiation of hepatoma cells. The results showed that the apoptotic induction of S4 is directly working against the target cells.

## REFERENCES

- 1 LaBrecque DR, Steele G, Fogerty S, Wilson M, Barton J. Purification and physical chemical characterization of hepatic stimulator substance. *Hepatology*, 1987;7:100-106
- 2 Zhang YJ, Kong XP, Zhen GC, Chen GM, Yang FQ. Investigation in clinical treatment of 1668 cases of virus hepatitis with hepatocyte growth factor promoting. *Linchuang Gandanbing Zazhi*, 1995;11:137-140
- 3 Zhang YJ, Kong XP, Zheng GC, Chen GM, Yang FQ. Evaluation of hepatocyte growthpromoting factors in treating 1687 cases of fulminant hepatitis. *Chin Med J*, 1995;108:928-929
- 4 Kong XP, Zou QY, Yang LP, Zhang YJ, Zheng PL, Li ZL. Experimental studies on apoptosis of neoplasm cells induced by pHGF. *Linchuang Gandanbing Zazhi*, 1995;11(Suppl 1):31-33
- 5 Kong XP, Zou QY, Yang LP, Zhang YJ, Zheng PL, Li ZL, Li RB, Yi XS. Experimental study of the effect of hepatocyte extracts (HE) on normal liver and hepatoma cells. *Shanghai Mianyixue Zazhi*, 1997;17:108-111
- 6 Kong XP, Zhang YJ, Zou QY, Zheng GC, Yang LP, Zhang CQ, Xiao XB. Establishment of monoclonal antibody against hepatocyte growth promoting factors (pHGF) and its immun histochemical study. *Zhongguo Bingli Shengli Zazhi*, 1994;10:165-169
- 7 Evan J, Littlewood T. A matter of life and cell death. *Science*, 1998; 281:1317-1321
- 8 Adams JM, Cory S. The Bcl-2 protein family: arbiters of cell survival. *Science*, 1998;281:1322-1326

Edited by MA Jing-Yun

# The possible relationship between hepatomegaly and release of HGF into plasma induced by clofibrate in rats

XU Wei and WU Shu-Guang

**Subject headings** clofibrate; hepatocyte growth factors; hepa tomegaly; rat

## INTRODUCTION

Hepatocyte growth factor (HGF) is a newly discovered multifunctional growth factor, and the most potent mitogen known for hepatocyte<sup>[1]</sup>. It has been shown that recombinant human HGF can protect animal liver against the damaging action of carbon tetrachloride<sup>[2]</sup>. However, the generation of HGF is also associated with certain liver diseases and several extra-hepatic diseases<sup>[3-5]</sup>. For example, after partial hepatectomy or carbon tetrachloride poisoning, HGF level in rat plasma increases markedly<sup>[3,4]</sup>. Therefore, it is believed that HGF plays an important role in the restoration and regeneration of liver after injury.

As hypolipidemic drugs, such as clofibrate, may cause experimental hepatomegaly, proliferation of hepatic peroxisomes and hepatic carcinoma, they are taken as a unique class of carcinogens<sup>[6-8]</sup>. How the HGF level changes after liver damage due to clofibrate or the like has not been reported. This study was designed for examination of the relation between hepatomegaly and the changes of plasma HGF levels in rats caused by clofibrate.

## MATERIALS AND METHODS

### *Animals*

Male Wistar and Sprague-Dawley rats were supplied by the Laboratory Animal Center of the First Military Medical University.

### *Clofibrate administration*

Clofibrate (bought from Shanghai 19th Pharmaceutical Factory) was given at doses of 500,

400, 300, 200 or 100mg·kg<sup>-1</sup>·d<sup>-1</sup> by adding it into food.

### *Measurement of liver weight*

At different time intervals after clofibrate administration, the rats were killed with their livers weighed, and the weight was expressed as the percentage of body weight.

### *Serum preparation*

At different time intervals after clofibrate administration, the tail of the rat was severed with a knife and the whole blood was collected. After centrifuge, the serum was stored at -20 °C in a freezer.

### *Measurement of the biological activity of HGF in the primary culture of rat hepatocytes[9]*

**Isolation of rat hepatocytes** Male Sprague-Dawley rats were supplied by the Laboratory Animal Center of the First Military Medical University. The rats were 6-7 weeks old, weighing about 200 g. They were fasted for 8 h-10 h before operation, then were anesthetized with ether. Anesthesia was discontinued when the respiration turned from rapid and shallow to slow and deep. The rats were fixed on a wooden plate, and the whole abdomen was sterilized with 750 mL/L (V/V) alcohol. The peritoneal cavity was cut open along the midline, and the portal vein and the inferior vena cava were exposed accordingly. The distal part of the portal vein was ligated, and a cannula was inserted into the proximal portal vein. D-Hank's solution (preheated to 37 °C) was used for the infusion of liver, and at the same time, the inferior vena cava was cut open for blood-letting. The rate of infusion was about 30 mL·min<sup>-1</sup>-40 mL·min<sup>-1</sup> from slow to rapid to wash out any stagnant blood from the liver. After infusion, the surface of liver became smooth and wet, and light-yellow in color. The infusion fluid was then changed to 0.3 g·L<sup>-1</sup> collagenase solution. Small vacuoles formed slowly on the connective tissue membrane of the liver surface with gaps in the liver tissue under the vacuoles. Eye-forceps were used to press lightly on the surface, and when the pressure was relieved, the infusion was stopped. The capsule of the liver was then torn open very carefully, and the liver tissue was put into Ham-F12

Institute of Pharmaceutical Sciences, The First Military Medical University, Guangzhou 510515, China  
Supported by the Fund for Key Scientific Research of Military Medicine, No.962025

**Correspondence to:** Prof. WU Shu-Guang, Institute of Pharmaceutical Sciences, The First Military Medical University, Guangzhou 510515, China

Tel. +86-20-85148178, Fax. +86-20-87644781

Email.gzwsqxw@public.guangzhou.gd.cn

Received 1999-04-08 Revised 1999-06-16

hepatocyte culture medium (preheated to 37 °C), and was blown mildly with a pipette into dispersed free liver cells, which were then filtered through nylon nets of 200 and 400 mesh size, and were centrifuged with 50 ×g three times at 4 °C. Thus, the hepatocytes with more than 90% viability could be obtained. The cell density was adjusted to  $1.5 \times 10^5/\text{mL}$ , and the cells were plated in a 96-well culture plate at 200  $\mu\text{L}$  per well. These liver cells were incubated in 50 mL/L  $\text{CO}_2$  for 24 h. After the cells adhere to the vessel wall, the culture media were replaced by serum-free ones and incubated for another 24 h. Afterwards,  $^3\text{H-TdR}$  ( $185 \text{ MBq} \cdot \text{L}^{-1}$ ) and the animal serum to be tested (which was diluted to different concentrations) were added and incubation continued for 24 h. Standard recombinant human HGF (to replace the animal serum) was used as the positive control. After incubation, the cells were harvested with a multi-channel cell collector and cpm values were measured with a liquid scintillation counter (Beckman Co., USA, Model LS9800).

## RESULTS

### *The variation of HGF level in rat serum 4 days after clofibrate administration*

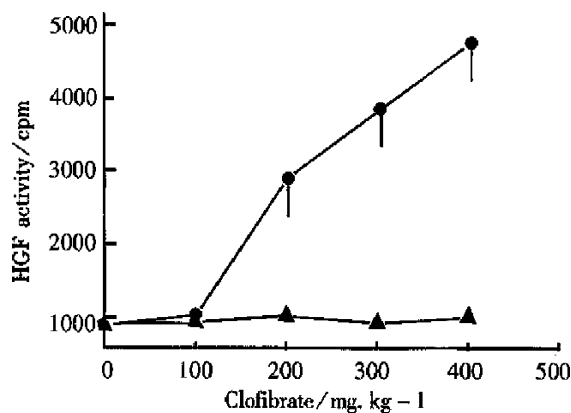


**Figure 1** Dose-effect curve of the effect of clofibrate on the HGF level in rat serum 4 days after clofibrate administration. ▲-▲: Normal control group. ●-●: Clofibrate administration group.

As shown in Figure 1, in the normal control group, the cpm value caused by the incorporation of  $^3\text{H-TdR}$  in the primary liver cells was  $800 \pm 150$ , as it was promoted by the serum of the normal rats. However, in the clofibrate ( $100 \text{ mg} \cdot \text{kg}^{-1} \cdot \text{d}^{-1}$ ) group, the undiluted rat serum caused significant increase of the cpm value to  $1010 \pm 180$ . Moreover, in pace with the increasing dosage of clofibrate, the cpm value increased also. When the dose of clofibrate increased to  $500 \text{ mg} \cdot \text{kg}^{-1} \cdot \text{d}^{-1}$ , the cpm value reached as much as  $4800 \pm 810$ , so the dose-effect relationship was eminent.

Rats were given  $500 \text{ mg} \cdot \text{kg}^{-1} \cdot \text{d}^{-1}$  of clofibrate

with their serum collected 4 days after. We could see that when the serum was diluted sequentially, the increased cpm value would fall down gradually, showing good dose-effect relationship. After the serum was diluted five-fold, the cpm value was still higher than that of the normal control group (Figure 2).

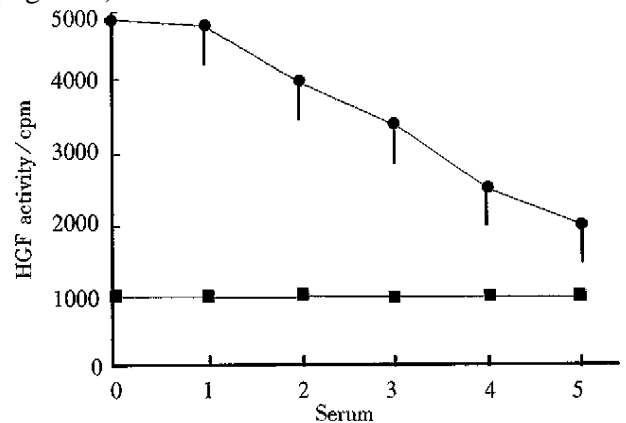


**Figure 2** Variation of HGF level in rat serum 4 days after clofibrate administration. ■-■: Normal control group, ●-●: Clofibrate administration group.

### *Variation of the weight of rat liver and the HGF level in rat serum at different time intervals after clofibrate administration*

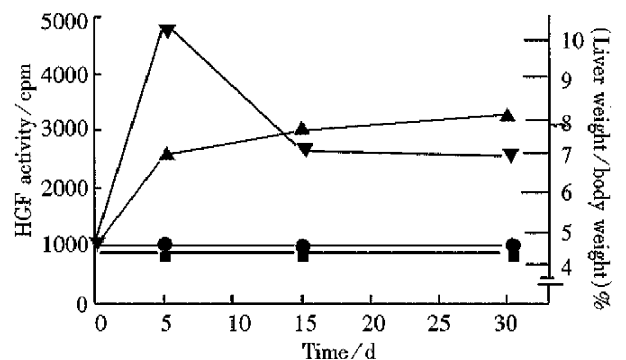


**Figure 3** Variation of liver weight and serum HGF level in rats after clofibrate administration.

■-■: HGF level in normal control group, ▼-▼: HGF level in clofibrate administration group, ●-●: Liver weight of normal control group, ▲-▲: Liver weight of clofibrate administration group.

As shown in Figure 3, 4 days after clofibrate administration, HGF level in serum reached its peak, and then fell gradually. Two weeks after taking clofibrate, HGF level still remained high, about 2-fold of the normal level while hepatomegaly also reached its highest level 2 weeks after intake of drug, and remained at this high level (1.8-fold above the normal level).

## DISCUSSION

It was discovered in our study that after administration of clofibrate which can induce hepatomegaly, the HGF activity in rat serum increased significantly.

Previous studies by other investigators indicated that 24 h after carbon tetrachloride (a hepatotoxin) administration, the HGF level in rat plasma increased by over 20-fold of the normal level<sup>[3]</sup>. In patients with partial hepatectomy or with severe fulminating hepatitis, the releasing of HGF into plasma was closely related to liver injury<sup>[4]</sup>. Many experiments indicate that clofibrate-related compounds can induce hepatomegaly, proliferation of hepatic peroxisomes, and hepatic carcinoma<sup>[6]</sup>. It is shown in our experiments that the release of HGF induced by clofibrate reached a high level 4 days after the drug administration, and could maintain for a long time, while hepatomegaly reached its peak 2 weeks after drug administration and remained at a relatively steady level. So the HGF level is somewhat related to hepatomegaly, suggesting that hepatomegaly induced by clofibrate may depend partly upon the promoting action of HGF on liver regeneration. Although the mechanism of liver injury by clofibrate and carbon tetrachloride is different, both of them can induce liver injury, which is a signal leading to the generation of HGF. Via the action of HGF, DNA synthesis in liver is promoted, which ultimately results in repair and regeneration of the injured

liver. Therefore, HGF plays an important role in the repair and regeneration of liver. However, the mechanism through which the release of HGF is promoted by these two compounds (clofibrate and carbon tetrachloride) is still unclear and needs further studies.

## REFERENCES

- 1 Strain AJ, Ismail T, Tsubouchi H, Arakaki N, Hishida T, Kitamura N, Daikuhara Y, McMaster P. Native and recombinant human hepatocyte growth factors are highly potent promoters of DNA synthesis in both human and rat hepatocytes. *J Clin Invest*, 1991; 87:1853-1857
- 2 Takehara T, Nakamura T. Protective effect of hepatocyte growth factor on in vitro hepatitis in primary cultured hepatocytes. *Biomed Res*, 1991; 12:354-358
- 3 Asami O, Ihara I, Shimidzu N, Shimizu S, Tomita Y, Ichihara A, Nakamura T. Purification and characterization of hepatocyte growth factor from injured liver of carbon tetrachloride treated rats. *J Biochem*, 1991; 109:8-13
- 4 Lindroos PM, Zarnegar R, Michalopoulos GK. Hepatocyte growth factor (Hepatopoietin A) rapidly increases in plasma before DNA synthesis and liver regeneration stimulated by partial hepatectomy and carbon tetrachloride administration. *Hepatology*, 1991; 13:743-749
- 5 Yamashita JI, Ogawa M, Yamashita SI, Nomura K, Kuramoto M, Saishoji T, Shin S. Immunoreactive hepatocyte growth factor is a strong and independent predictor of recurrence and survival in human breast cancer. *Cancer Res*, 1994; 54:1630-1633
- 6 Reddy JK. Hepatic peroxisome proliferative and carcinogenic effects of hypolipidemic drugs. In: Remo Fumagalli, eds. *Drugs affecting lipid metabolism*, Paolett. *New York:Remo Fumagalli, David Kritchevsky and Rodolfo*, 1980:301-309
- 7 Wu SG, Shen YA, Zheng Z, Long K. Effects of clofibrate, silybin, safflower oil and lamindran on liver peroxisome proliferation and enzyme activities in rats. *Zhongguo Yaoli Xuebao*, 1986; 7:283-284
- 8 Wu SG, Long K. Hypolipidemic drug and oncogenesis. *Guowai Yixue Zhongliuxue Fence*, 1985; 12:76-78
- 9 McGowan JA, Strain AJ, Bucher NR. DNA synthesis in primary cultures of adult rat hepatocytes in a defined medium: effects of epidermal growth factor, insulin glucagon, and cyclic AMP. *J Cell Physiol*, 1981; 108:353-363

Edited by WANG Xian-Lin

# The effect of retinoic acid on Ito cell proliferation and content of DNA and RNA

GAO Ze-Li<sup>1</sup>, LI Ding-Guo<sup>2</sup>, LU Han-Ming<sup>2</sup> and GU Xiao-Hong<sup>1</sup>

**Subject headings** liver fibrosis; retinoic acid; Ito cell; cell culture; microspectrophotometer; DNA; RNA

## INTRODUCTION

The development of liver fibrosis is due to an imbalance between synthesis and degradation of extracellular matrix. Recent studies have shown that Ito cells which are located along the sinuses of liver, can store and metabolize Vit A, and are the main cells that produce collagen, among which type I, III and IV and laminin, account for 80%-95% of the total hepatic collagen<sup>[1]</sup>. Ito cells in the course of proliferation and synthesis of collagen showed a reduction of Vit A contents and retinoic acid receptors<sup>[2]</sup>. This study was designed to investigate the effect of retinoic acid on Ito cell proliferation and the contents of DNA/RNA and to analyse further its mechanism or pathways.

## MATERIALS AND METHODS

### Reagents

DMEM medium (Gibco Company); all trans-retinoic acid (RA), retinol palmitate (RP) (Sigma Company); <sup>3</sup>H-TdR (Shanghai Nuclear Energy Research Institute); Solution A: 0.1% Triton X-100, 0.08N HCl, 0.15N NaCl; solution B: 120μM acridine orange (AO), 1mM EDTA, 0.15N NaCl; vidas microspectrophotometer analysis system.

### <sup>3</sup>H-TdR incorporation test

The isolation and culture of Ito cells were done by the method as published before<sup>[3]</sup>. Rat Ito cells of 5-day primary culture were suspended on DMEM medium containing 20% bovine serum. The number of the cells was adjusted to 1×10<sup>5</sup>/mL. One mL of

the cell suspension was put into each well of the 24-well culture plate, which contained serial concentrations of RA/RP. The control wells contained no RA/RP. After incubating for 24 h, 8μCi-<sup>3</sup>H-TdR was added to each well and incubated for another 48h. The cells were collected on the F49 filter paper, fixed with 4mL 10% trichloroacetic acid and dehydrated with 4mL alcohol. The dried filter papers were put on the bottom of the scinti bottle which contained 5 mL scintillating solution for counting the pulse per minute (CPM). The degree of DNA replication was indicated by CPM/well. We set three wells for each sample.

### DNA/RNA content analysis

Ito cell culture and treatment were handled with the same procedure as above and the difference was as follows: drug treatment with RA/RP at 10<sup>-4</sup>mol/L, small cover glass was put into each well of the plate to bear the growing cells. After the culture medium was discarded, the Ito cells on the small cover glass were fixed for 30min with 70% alcohol and washed with PBS solution. Solution A (0.4mL) was added into each well, the preparation was set on ice bath for reacting 15 seconds, 1.2mL solution B was then used for 8min staining. The small cover glass was put on a glass slide, fluorescent microscopic examination was made immediately with the exciting light wave of 488 nm. DNA was examined with a screened filter at a wave-length of 530 nm, with green in stain, whereas RNA examined with a filter at 610 nm showed a red fluorescence. Fifty cells were examined in each group with fluorescent microspectrophotometer-30 (FMSP-30); the fluorescence intensity was converted into grey scale value, corresponding to the relative average DNA/RNA contents of Ito cells.

## RESULTS

### <sup>3</sup>H-TdR incorporation test

Lower densities of RA/RP (10<sup>-6</sup>mol/L) had no effect on the <sup>3</sup>H-TdR incorporation of Ito cell. With higher densities <sup>3</sup>H-TdR incorporation of Ito cell was inhibited as compared with the control ( $P<0.05$ )(Table 1).

### DNA/RNA content analysis

The results showed that RA/RP at 10<sup>-4</sup>mol/L

<sup>1</sup>Department of Gastroenterology, Yangpu Central Hospital, Shanghai 200092, China

<sup>2</sup>Department of Gastroenterology, Xin Hua Hospital, Shanghai Second Medical University, Shanghai 200090, China

Dr. GAO Ze-Li, male, born on 1961-05-30 in Huanren County, Liaoning Province, graduated from the Harbin Medical University in 1983, got the doctor de gree in Shanghai Second Medical University in 1997, now working in the Department of Gastroenterology, Yangpu Central Hospital, Shanghai, having 11 papers published.

**Correspondence to:** Dr. GAO Ze-Li, Department of Gastroenterology, Yangpu Central Hospital, 130 Boyang Road, Shanghai 200090, China

Tel. +86-21-58615242

Email. yanhang@online.sh.cn

Received 1999-04-15

could reduce DNA/RN A- contents of Ito cells as compared control ( $P<0.01$ ) (Table 2).

**Table 1  $^3\text{H-TdR}$  incorporation test**

Group	Dosage (mol/L)	(CPM $\pm$ s)/well
Control		2866.4 $\pm$ 253.2
Test groups		
	RA	
	10 <sup>-6</sup>	2657.6 $\pm$ 104.8
	10 <sup>-5</sup>	1279.4 $\pm$ 236.4 <sup>a</sup>
	10 <sup>-4</sup>	182.2 $\pm$ 67.6 <sup>a</sup>
RP		
	10 <sup>-6</sup>	2598.4 $\pm$ 76.4
	10 <sup>-5</sup>	1182.6 $\pm$ 154.4 <sup>a</sup>
	10 <sup>-4</sup>	897.2 $\pm$ 82.6 <sup>a</sup>

<sup>a</sup> $P<0.05$  vs control group (Student's *t* test).

**Table 2 DNA, RNA content analysis**

Group	Dosage (mol/L)	DNA	RNA
Control		101.98 $\pm$ 21.58	89.38 $\pm$ 22.03
RA	10 <sup>-4</sup>	61.79 $\pm$ 18.31 <sup>a</sup>	56.31 $\pm$ 14.72 <sup>a</sup>
RP	10 <sup>-4</sup>	46.85 $\pm$ 11.52 <sup>a</sup>	49.20 $\pm$ 10.12 <sup>a</sup>

<sup>a</sup> $P<0.05$  vs control group (Student's *t* test).

## DISCUSSION

Ito cells which have the characteristics of fibroblasts cell and myofibroblasts are the main collagen-producing cells in the liver. Bamard H<sup>[4]</sup> and Seifert WF<sup>[5]</sup> reported that RA could reduce the deposition of types I and III collagen in the CCl<sub>4</sub>-induced liver fibrosis of the rat through its inhibitory effect on the transformation of Ito cell to myofibroblasts.

Our study showed that RA/RP could inhibit <sup>3</sup>H-TdR incorporation of rat Ito cells and reduced the DNA/RNA contents of rat Ito cells. Our previous study indicated that RA could restore retinoic acid receptor content and increase cAMP content in the primary culture of rat Ito cells<sup>[6]</sup>. The form of biologic effect of RA was similar to that of thyroxin<sup>[7]</sup>, i.e. they both act on nuclear receptor resulting in a change of the second messenger and regulating the gene expression of RAR and collagen in the Ito cells. RA may be expected to be an effective antihepatofibrotic agent.

## REFERENCES

- 1 Ramadori G. The stellate cell of the liver. *Virchows Archiv B Cell Pathol*, 1991;61:147-158
- 2 Gao ZL, Li DG, Lu HM. The retinoic aci content of Ito cell, the expression of retinoic acid receptor and liver fibrosis. *Zhonghua Xiaohua Zazhi*, 1993;13:295-296
- 3 Gao ZL, Liu SR, Li DG, Lu HM. The isolation and culture of rat ito cell and the effect of retinoic acid on the proliferation of Ito cell. *Shanghai Dier Yikedaxue Xuebao*, 1995;15(Supp 1):93-95
- 4 Davis BH, Kramer RT, Davidson NO. Retinoic acid modulates rat Ito cell proliferation, collagen, and transforming growth factor  $\beta$  production. *J Clin Invest*, 1990;86:2062-2070
- 5 Seifert WF, Hendriks HFJ, van Leeuwen REW, van Thiel-de Ruitter GCF, Seifert Bock I, Knook DL, Brouwer A. Beta-carotene (provitamin A) decreases the severity of CCl<sub>4</sub>-induced hepatic inflammation and fibrosis in rats. *Liver*, 1995;15:1-8
- 6 Gao ZL, Li DG, Lu HM. The effect of retinoic acid on Ito cell retinoic acid receptor and cAMP content. *Weichangbingxue He Ganbingxue Zazhi*, 1995;4:20
- 7 Weiner FR, Blaner WS, Czaja MJ, Shah A, Geerts A. Ito cell expression of a nuclear retinoic acid receptor. *Hepatology*, 1990; 11:336-342

Edited by MA Jing-Yun

# The mutation induced by space conditions in *Escherichia coli*

WENG Man-Li, LI Jin-Guo, GAO Fei, ZHANG Xiu-Yuan, WANG Pei-Sheng and JIANG Xing-Cun

**Subject headings** *Escherichia coli*; mutation; space conditions; microorganism breeding

## INTRODUCTION

Progress has been made in microorganism breeding under space conditions by boarding on recoverable satellite and high altitude balloon in China. To further study the mutagenesis in space, three strains of *E. coli* were put on board the recoverable satellite (JB1-B9611020) launched in October, 1996. After the satellite returned to the earth, the survival and mutation frequencies were determined and the results were discussed as well.

## MATERIALS AND METHODS

### Bacterial strains

CSH108<sup>[1]</sup>, an arginine autotrophic (Arg) strain, was provided by the *E. coli* Genetic Stock Center, USA (CGSC) and was used to study Arg<sup>+</sup> reversion mutation. Both Arg<sup>-</sup> and LacZ<sup>-</sup> in CSH108 were caused by amber mutation. The strain A2 and A3 were constructed for lacI<sup>-</sup> mutation in this study (the detailed procedure was not described here). A3 was a lacI-q strain used for the selection of LacI<sup>-</sup> mutation after boarding, while A2 is a lacI<sup>-</sup> strain serving as a control strain. The properties of flight *E. coli* strains are listed in Table 1.

**Table 1 Properties of the boarded *E. coli* strains**

Strain	Genotype
A2	<i>ara(lac proB)strA/F<sup>+</sup>lacI<sup>-</sup> proA<sup>+</sup>B<sup>+</sup></i>
A3	<i>ara(lac proB)strA/F<sup>+</sup>lacI<sup>q</sup> pro<sup>+</sup></i>
CSH108	<i>ara(gpt-lac)gyrA argE<sub>am</sub> proB/F<sup>+</sup>lacI<sup>-</sup> ZproA<sup>+</sup>B<sup>+</sup></i>

### Boarding methods and space conditions

Since *E. coli* strains usually are hard to survive

from space board, soft agar culture of *E. coli* cells was made in this boarding. It was prepared as below: the cells grown on plate were suspended in a small amount of LB liquid medium, and then added melted sterile agar to get soft agar culture (the final concentration of agar was 3.5 µg/L).

In order to study the mutagenesis induced by different factors in space conditions, the boarding samples were divided into three groups and each group included the three strains. When boarding on the satellite Group I was held in small polymethyl methacrylate tubes, Group II was placed in a centrifuge inside DM-11 small biocabin, where oxygen was supplied<sup>[2]</sup> and the gravity was adjusted to 1g, and Group III was placed in a lead chamber (usually used to store radioisotope) which had 3.5 mm-8.0 mm thick wall and coated with 5 mm layer of hard plastics outside. The lead chamber could block part of the radiation, but the exact amount of block efficiency was not determined in this study. Part of the ground control bacteria was placed in a dark vessel at room temperature (13 °C-20 °C), the other was stored in a freezer (-60 °C).

The satellite flew for 15 days. The angle of satellite orbit was 63°, apogee was 354 km, perigee was 175 km, microgravity was 5×10<sup>-5</sup>g, density of high energy particle was 136 counts/cm<sup>2</sup> [it was (35.6±6) counts/cm<sup>2</sup> on the earth]. The records show that the biocabin worked regularly in flight, in which the temperature was 17 °C-26 °C and the mean dosage of ionizing radiation was 0.177 mGy/d.

### Mutation frequency of the bacteria

The mutation frequency was measured soon after the flight. The procedure was as follows: 0.5 mL of the boarded and control samples were inoculated in 5 mL of LB medium respectively. After 4 h at 37 °C, 2.5 mL of 50% sterile glycerol was added, and all samples were divided into 1 mL of aliquot, and stored at -20 °C. During the measurement, an aliquot of the sample was used for bacterial cell counting, and then concentrated sample was spread on screening plates to select mutants. The number of mutants was scored in 48 h-72 h incubation at 37 °C. The mutation frequency of bacteria was calculated according to the formula: The mutation frequency=mutant cells per mL/total bacterial cells per mL.

Institute of Genetics, Chinese Academy of Sciences, Beijing 100101, China

Professor WENG Man-Li, female, born on 1944-12-05 in Shanghai, Han nationality, graduated from Beijing Agricultural University in 1967. Professor of genetics, majoring in microbiological genetics, having more than 20 papers published.

Supported by the State High Technology Program of Space Science, Project No.863-2-7-2-7

**Correspondence to:** Professor WENG Man-Li, Institute of Genetics, Chinese Academy of Sciences, Beijing 100101, China

Tel. +86-10-64889353, Fax.+86-10-64854896

Email. bwwang@mimi.cnc.ac.cn

Received 1999-04-15

### Media

The LB medium, minimal medium, MacConkey medium and Pgal medium were used in experiment as described<sup>[1]</sup>.

### Selection of Arg<sup>+</sup> reversion mutants and test of Arg<sup>+</sup> Lac<sup>+</sup> mutants

The concentrated CSH108 sample was spread on minimal plate without arginine. The Arg<sup>+</sup> revertants could grow after incubation. Then the Arg<sup>+</sup> revertants were streaked on minimal plate with lactose as the only carbon source. If some of the revertants could grow up on the medium, they were Arg<sup>+</sup> Lac<sup>+</sup> revertants. These were determined by the method of Miller<sup>[1]</sup>.

### Selection of LacI<sup>-</sup> mutant

Phenyl-β-D-galactoside (Pgal) is a noninducing sugar that serves as a substrate for β-galactosidase and can provide a carbon source for growth, but only the constitutive mutants of LacI, which produce enough β-galactosidase, can form colonies on Pgal<sup>[1]</sup>. To prove to be LacI<sup>-</sup> mutants, the colonies grown on the Pgal plate were streaked on MacConkey plate to compare with A2 strain as the LacI<sup>-</sup> control.

## RESULTS

### The survival of the boarded strains

Before boarding, the cell counting of samples was up to 2×10<sup>9</sup>/mL and after flight the survival of each sample was about 3×10<sup>8</sup>/mL counted on LB plate, suggesting that the survival of the strains was accomplished as expected in this study.

### The Arg<sup>+</sup> reversion frequency of strain CSH 108

After flight the Arg<sup>+</sup> reversion frequencies of CSH108 in the three groups and the ground control were determined. The results are shown in Table 2 (the reversion frequency of each was the mean of seven tests). In fact the Arg<sup>+</sup> reversion frequency of the ground control was the spontaneous reversion frequency. It was worth mentioning that the Arg<sup>+</sup> reversion frequency of Group III was 10 times that of the ground control.

**Table 2 The Arg<sup>+</sup> reversion frequency of strain CSH108 in different boarding ways**

Sample	Group	Arg <sup>+</sup> reversion frequency(×10 <sup>-8</sup> )
Boarding sample	Group I	2.9
	Group II	1.8
	Group III	26.3
Ground control	A <sup>(1)</sup>	1.2
	B <sup>(2)</sup>	2.8

(1) Ground control: strain was kept at room temperature; (2) Ground control: strain was stored in freezer (-60°C).

### The Lac mutation frequency among Arg<sup>+</sup> revertant

The Lac<sup>+</sup> mutation frequency of CSH108 varied with the groups. As shown in Tables 2 and 3, Group III had not only a high Arg<sup>+</sup> reversion frequency, but also a high Arg<sup>+</sup> Lac<sup>+</sup> frequency. It is suggested that most of the Arg<sup>+</sup> revertants were suppresser mutations, which resulted from mutations located in tRNA genes.

**Table 3 The occurrence of Lac<sup>+</sup> phenotype among Arg<sup>+</sup> revertants**

Sample	Group	Total No. of Arg <sup>+</sup> reversion	No. of Lac <sup>+</sup>	Lac <sup>+</sup> /Arg <sup>+</sup> (%)
Boarding sample	Group I	60	25	41.7
	Group II	139	52	37.4
	Group III	384	376	97.9
Ground control	A <sup>(1)</sup>	36	14	38.9
	B <sup>(2)</sup>	39	27	69.2

A<sup>(1)</sup> and B<sup>(2)</sup> are the same with that in Table 2.

### The LacI<sup>-</sup> mutation in A3 strain

In A3 strain, the survival and LacI<sup>-</sup> frequencies are shown in Table 4. The LacI<sup>-</sup> frequency in Group II was remarkably higher than that in other groups and it was 67 times that of the ground control. In addition, we also observed that when the boarded strains were plated on Pgalagar at 37°C, Group II formed colonies in 48h, while other groups formed colonies in 72h. From Table 4, it also can be seen that the LacI<sup>-</sup> mutation frequency in Group III was 4.4 times that in the ground control. A further test showed that most of the LacI<sup>-</sup> mutation in A3 strain could not be suppressed in suppresser strains, therefore they were not amber mutations (The detailed result was not described here).

**Table 4 The survival and frequency of LacI<sup>-</sup> mutant from A3 strain**

Sample	Group	Survival (×10 <sup>8</sup> )	LacI <sup>-</sup> frequency (×10 <sup>-8</sup> )
Boarding sample	Group I	3.6	0.4
	Group II	5.5	240.0
	Group III	3.0	15.8
Ground control	A <sup>(1)</sup>		3.6

All figures were means of four tests. (1) Ground control: strain was kept at room temperature.

## DISCUSSION

### Arg<sup>+</sup> revertant

Reversion mutation is a simple and accurate method used to determine the mutation frequency of bacteria<sup>[5]</sup>. At least two kinds of mutations can reverse the Arg<sup>-</sup> (arginine synthesis defective)

phenotype in CSH108: the mutation at ArgE<sub>am</sub> position and the suppresser mutation. They are both point mutations, but occur in different places. In the revertants with only Arg<sup>+</sup> phenotype, the mutation results from a base substitution at ArgE<sub>am</sub> position to restore Arg<sup>+</sup> by a sense triplet; in the revertants with Arg<sup>+</sup> Lac<sup>+</sup> phenotype, the mutation occurs in tRNA gene and gets the intergenic repressor by suppresser mutation<sup>[1,3]</sup>. According to the results shown in Table 3, the revertants of suppresser mutation in Group III covered 97%, while the frequencies of such mutation were below 70% in other groups, usually about 50% (Table 3).

### **LacI mutant**

*lacI* gene encoded repressor for *lacZ* gene. LacI<sup>+</sup> bacteria could not grow in Pgal plate unless they were mutated to LacI<sup>-</sup> strain. According to the results in Table 4, the LacI<sup>-</sup> mutation frequency in Group II was 67 times that of the ground control, and was 4.4 times in Group III that in the ground control. Both mutation and reversion are often used in microorganism genetic experiment<sup>[1]</sup>. It is convincing to use the markers in this study to investigate the mutagenesis of microorganism in space conditions.

### **Boarding methods**

Three boarding methods were used, and the reversion mutation frequency of Arg<sup>+</sup> and the mutation frequency of LacI<sup>-</sup> were measured in this study. The samples of Group II were placed in DM-11 small biocabin, therefore the microgravity had little effect. The main factor affecting the samples was space radiation. In addition, oxygen was supplied in biocabin. It had been reported that in mammalian cell the break incidence of single-stranded DNA in O<sub>2</sub> environment was four times higher than that in no O<sub>2</sub> environment<sup>[4]</sup>, and the occurrence of mutation was closely related with the repair of DNA damage<sup>[3,5]</sup>. These are probably the reasons why the LacI<sup>-</sup> mutation frequency of A3 strain in biocabin was 67 times that of the ground control.

The small lead chamber could block part of the space radiation in flight. The results showed that in lead chamber the Arg<sup>+</sup> reversion frequency of CSH108 was 10 times that of the ground control,

and that the LacI<sup>-</sup> mutation frequency of A3 strain was 4 times that of the ground control. In this test, the effect of space radiation was decreased by the chamber, the main effective factor should be the microgravity.

The boarded Group I was influenced by microgravity and strong space radiation, but no significant effect on mutation in *E. coli* strains was found. It may be due the interference of the samples located in the satellite, or the antagonism between different space factors, or some unknown reasons.

It was shown that after flight some *E. coli* strains had high mutation frequencies which varied with boarding conditions. That is to say, in different boarding conditions, there were different space factors that influenced the bacteria mutagenesis, therefore different types and frequencies of mutations were induced. The effects of spaceflight have been increasingly understood<sup>[1]</sup>. This research indicated that the spaceflight may greatly enhance the mutation frequency of certain genes in microorganism and may provide an effective way for microorganism breeding. But space factors, such as strong radiation, microgravity and so on, which influence the mutation of *E. coli* are complicated. The mutation effect would vary with strain, gene, and even the nucleotide location in DNA. Therefore much work is to be done in understanding the mechanism of space induced breeding. In addition, it is meaningful to take the advantages of quick growth and clear selective markers in *E. coli* strains to develop a high-speed routine method for predicting the space induced efficiency. The method can serve all the purposes of biological investigation.

**ACKNOWLEDGMENTS** We would like to thank Professor LI Xiang-Gao for kindly providing the boarding of biocabin. We also thank Professor TONG Ke-Zhong for his support and advice to our work.

### **REFERENCES**

- 1 Miller JH. A Short Course in Bacterial Genetics. Plainview, New York: Cold Spring Harbor Laboratory Press, 1992;57-72, 131-185
- 2 Li XG, Chen M. A new method of oxygen generation inside a small biocabin. *Hangtian Yixue yu Yixue Gongcheng*, 1996;9:377-380
- 3 Sun NE, Sun DX, Zhu DX. Molecular genetics. Nanjing: Nanjing University Press, 1996:159-183
- 4 Yang CX, Mei MT. Space radiological biology. *Guangzhou: Zhongshan University Press*, 1995;25:126-129
- 5 Dutcher FR, Hess LE, Halstead TW. Progress in plant research in space. *Adv Space Res*, 1994;14:159-171

Edited by WANG Xian-Lin

# Treatment of corticosteroid-resistant ulcerative colitis with oral low molecular weight heparin

CHI Hui-Fei<sup>1</sup> and JIANG Xue-Liang<sup>2</sup>

**Subject headings** colitis; ulcerative/drug therapy; heparin/therapeutic use; corticosteroid-resistant

## INTRODUCTION

The etiology and pathogenesis of ulcerative colitis (UC) have remained unclear. Treatment is nonspecific based on the anti-inflammatory agents corticosteroid and sulfasalazine. A significant proportion fail to respond to this therapy<sup>[1]</sup>. As the relapse, refractory or serious UC patients had a hypercoagulable state and an increased incidence of thromboembolic events<sup>[2-4]</sup>, heparin has been used by some authors<sup>[5-7]</sup>. Yet, its half-life period is short, needing long-term injection, which restricts its further clinical application. Our previous studies have demonstrated oral LMWH not only overcomes the shortcomings of common heparin<sup>[8,9]</sup>, but also has anti-inflammatory effects<sup>[10,11]</sup>. The aim of this paper is to study the therapeutic effects and mechanism of oral LMWH in patients with corticosteroid-resistant UC.

## MATERIALS AND METHODS

### Clinical materials

There were eight men and twelve women aged 21 years to 56 years (mean 33 years). All cases were histologically confirmed and met the diagnostic standard of chronic non-infectious intestinal disease of China (Taiyuan meeting, 1993), including seventeen cases of severe, and three moderate UC. Duration of diseases ranged from 8 months to 11 years (mean 4.1 years). Rectal bleeding, diarrhea, mucus stool, abdominal pain were the main symptoms. Four patients were associated with thromboembolic diseases. All patients were treated

with high-dose corticosteroid and sulfasalazine for more than 4 weeks without effect, sulfasalazine was maintained in combination with oral LMWH (366U/kg, twice daily) for more than 4 weeks. Prednisolone was tapered and stopped.

### Monitoring parameters

#### Assessment of platelet activation and aggregability<sup>[2,4]</sup>

We used a sensitive flow cytometric technique designed to minimize sample handling and render fixation unnecessary to quantify platelet activation. Blood samples were incubated by 10 minutes of venesection with fluorescein isothiocyanate (FITC) conjugated antibodies to the platelet surface antigens, P-selectin (CD<sub>62P</sub>) and CD<sub>63</sub> (Immunotech, Marseilles, France). Analysis was made within 15 minutes of venesection using a BD (Becton Dickinson Immunocytometry Systems) FAC Scan. TXA-2 (Suzhou Medical College) was measured using RIA method, samples were taken without tourniquet into chilled tubes containing 1:9 anticoagulant/antiaggregant solution (trisodium citrate 3.8%), centrifuged for 15min-30min, later at 4 °C for 30 minutes to minimize *in vitro* activation, supernatant was decanted off and stored at -20 °C for assay within 3 months. Platelet aggregation rates (PAR) and thrombosis length (TL) *in vitro* were assessed by XSN-R II instrument according to the manufacturer's instruction.

**Measurement of CD<sub>54</sub>.** CD<sub>54</sub> in blood and tissues were measured using flow cytometric technique according to our previous report<sup>[12]</sup>.

#### Assessment of efficacy<sup>[7]</sup>

Pre- and post-treatment scores were calculated for the following disease parameters: ① Stool frequency (average number per day for the past week). ② Rectal bleeding (0: absent, 1: streak of blood on stools occasionally, 2: obvious blood on stool frequently, 3: complete bloody stools). ③ Colonoscopic appearance 0: normal vascular pattern, 1: mild lesion (loss of vascular pattern, mucosa edema, no bleeding), 2: moderate lesion (granularity and friability of the mucosa), 3: severe lesion (discrete ulceration and spontaneous bleeding). ④ Histological grading: serial biopsies of the rectum and the colon were taken. Five histological changes seen in UC (cellular infiltrate in the lamina propria, cryptitis, crypt abscess

<sup>1</sup>Department of Biochemical Pharmaceutics, Shandong Medical University, Jinan 250012, China

<sup>2</sup>Department of Gastroenterology, Chinese PLA General Hospital of Jinan Command, Jinan 250031, China

CUI Hui-Fei, female, born on 1968-01-09 in Shanghai, graduated from Shandong Medical University in 1993 with a master degree, engaged in the research of drug preparation, having 20 papers published.

Project supported by the National Fund for New Drug Research and Development, No.96-901-05-103 and the Committee of Science and Technology, Shandong Province, No.9575.

**Correspondence to:** CUI Hui-Fei, Department of Biochemical Pharmaceutics, Shandong Medical University, Jinan 250012, China. Tel. +86-531-2600132

Email: xiaohuak@jn-public.sd.cninfo.net

Received 1999-04-15 Revised 1999-06-18

formation, goblet cell depletion, and regenerative hyperplasia of the epithelium) each were scored from 0 (absent) to 3 (severe), a total UC score of 5 or less indicated mild disease, a score of 5-10, moderate, and a score of 10-15 severe disease. ⑤ General health status (0: excellent, 1: good, 2: poor, 3: poorer, 4: very poor, 5: poorest).

### Statistical analysis

Student's *t* test and Friedman test were used to assess the significance of differences between mean pre- and post-treatment parameters.

## RESULTS

### Therapeutic effects

Nineteen patients (95.0%) achieved clinical remission (normal stool frequency and no rectal bleeding) on a combination of oral LMWH and sulfasalazine. One patient had reduced rectal bleeding only. The average period of marked improvement was 2.9 weeks (range 1 week-4 weeks), and of remission was 5 weeks (range 1 week-12 weeks). Rectal bleeding ceased in 19 patients (5 patients within 5 days -8 days, the others within 2 weeks-7 weeks). Nineteen patients had general health condition improved earlier on oral LMWH, than bowel symptoms. There were highly significant improvement in mean scores for all disease parameters (Table 1).

**Table 1 Therapeutic effects of oral LMWH in corticosteroid-resistant UC patients**

Group	Stool frequency (times/day)	Rectal bleeding (score)	Colonoscopy (score)	Histology (score)	Well-being (score)
Pre-treatment	8.6	2.6	2.7	12.0	4.0
Post-treatment	1.5 <sup>b</sup>	0.2 <sup>b</sup>	1.0 <sup>b</sup>	4.0 <sup>b</sup>	0.6 <sup>b</sup>

<sup>b</sup>*P*<0.01 vs pretreatment.

### Blood contents of CD<sub>62P</sub>, CD<sub>63</sub>, TXA<sub>2</sub>, platelet aggregation rate (PAR) and thrombosis length (TL) *in vitro*

All the indexes in corticosteroid-resistant UC patients increased significantly as compared with the normal controls (*P*<0.01). After treatment with oral LMWH, all the parameters of UC patients decreased (*P*<0.01), but CD<sub>62P</sub> and CD<sub>63</sub> remained higher than normal (*P*<0.01), (Table 2).

**Table 2 Effects of oral LMWH on CD<sub>62P</sub> and CD<sub>63</sub>, TXA<sub>2</sub>, platelet aggregation rate (PAR) and thrombosis length (TL) *in vitro* in UC patients ( $\bar{x}\pm s$ )**

Group	CD <sub>62P</sub> (%)	CD <sub>63</sub> (%)	TXA <sub>2</sub> (ng/L)	PAR(%)	TL(cm)
UC patients					
Pre-treatment	8.1±3.2 <sup>b</sup>	6.2±2.2 <sup>b</sup>	541.7±82.4 <sup>b</sup>	44.5±10.1 <sup>b</sup>	2.4±0.5 <sup>b</sup>
Post-treatment	4.2±1.9 <sup>a,d</sup>	3.1±1.7 <sup>ab</sup>	396.4±75.8 <sup>d</sup>	35.2±8.7 <sup>d</sup>	1.9±0.4 <sup>d</sup>
Normal controls	1.9±0.4	1.6±0.8	340.2±40.4	34.1±9.1	

<sup>a</sup>*P*<0.05, <sup>b</sup>*P*<0.01 vs normal person; <sup>d</sup>*P*<0.01 vs pretreatment.

### CD<sub>54</sub> in blood and tissues

CD<sub>54</sub> elevated in both blood and tissues in corticosteroid-resistant UC patients (*P*<0.01), CD<sub>54</sub> in tissues being higher than in blood. After oral LMWH, CD<sub>54</sub> lowered significantly in both blood and tissues (*P*<0.01), but still higher than that of normal controls (*P*<0.05), (Table 3).

**Table 3 Effects of oral LMWH on CD<sub>54</sub> in UC patients**

Group	Blood CD <sub>54</sub>	Tissue CD <sub>54</sub>
UC patients		
Pre-treatment	28.7±6.1 <sup>b</sup>	50.7±6.8 <sup>b</sup>
Post-treatment	14.6±5.2 <sup>a,d</sup>	22.8±4.7 <sup>a,d</sup>
Normal controls	6.2±3.7	8.8±3.2

<sup>a</sup>*P*<0.05, <sup>b</sup>*P*<0.01 vs normal; <sup>d</sup>*P*<0.01 vs post-treatment.

### Complications

No serious complications were associated with the use of oral LMWH.

## DISCUSSION

Heparin, a group of sulphated glycosaminoglycans, in addition to its physiological effects and anticoagulant, antithromboembolic, antiallergic, antiviral, antiendotoxic and immunoregulative biological activities, has a wide range of potentially anti-inflammatory effects, including inhibition of neutrophil elastase and inactivation of chemokines<sup>[5,13]</sup>. Compared with heparin, LMWH has an enhanced antithromboembolic effect, longer half life period, less bleeding tendency, higher bioavailability, easier absorption by oral administration<sup>[8,9]</sup>, and has the anti-inflammatory effects as well<sup>[10,11]</sup>. Previous reports<sup>[5-7]</sup> on improvement in UC patients treated with heparin prompted us to perform a pilot study of oral LMWH to find a more convenient and effective drug for patients with corticosteroid-resistant UC. The observed response to oral LMWH is paradoxical. Nineteen of 20 patients with corticosteroid-resistant UC achieved clinical remission and became asymptomatic on oral LMWH combined with sulfasalazine. Opposite to the traditional idea that heparin can enhance bleeding, rectal bleeding was the first symptom to be improved by oral LMWH. The results are similar to other reports of heparin treatment<sup>[5-7]</sup>.

If oral LMWH has a therapeutic effect in UC, its mechanism of action should shed some light on the elusive pathogenesis of this disease. There are several thrombophilic features of UC that suggest the effect of oral LMWH on colitic symptoms may be attributable to its anticoagulant and antithrombotic properties. Evidence of a

thrombotic process in UC includes: reports of a hypercoagulable state<sup>[2-4]</sup>, an increased incidence of thromboembolic event<sup>[14]</sup>, and ischemic complications such as toxic megacolon and pyoderma gangrenosum. In this study, the membrane marks of platelet activity CD<sub>62P</sub> and CD<sub>63</sub> increased significantly, and the derivative of active platelet TXA-2 also elevated, suggesting that the blood platelet was in an active state, which not only led to a hypercoagulable state and an increased incidence of thromboembolic events, but also enhanced inflammatory reaction<sup>[24]</sup>. Activated hyperaggregable platelets in the mesenteric circulation could amplify the inflammatory cascade by promoting neutrophil recruitment and chemotaxis. P-selectin has an established action as the adhesion molecule for neutrophils, and circulating platelet aggregates may contribute to ischemic damage and infarction by occluding the intestinal microvasculature. Platelet derived thromboxane A<sub>2</sub> may also contribute to the ischemia by inducing local vasoconstriction. After treatment with oral LMWH, all these parameters dropped markedly, suggesting that the therapeutic effect of LMWH is partly related to inhibition of platelet activity<sup>[9]</sup>. CD<sub>54</sub> antigen reacts with the 85 kD-110 kD integral membrane glycoprotein, is also known as an intercellular adhesion molecule-1 (ICAM-1) expressed on endothelial cells and both resting (weak) and activated (moderate) lymphocytes and monocytes. CD<sub>54</sub> is ligand for the leukocyte function antigen-1 (CD<sub>11a</sub>). Its expression is up-regulated upon stimulation by inflammatory mediators such as cytokines and LPS, and it is involved in B cell-T cell co-stimulatory interactions. In this study, CD<sub>54</sub> elevated significantly in blood and tissues of UC patients, being in tissues higher than in blood<sup>[12]</sup>. Therefore, it could reflect the inflammation of intestinal mucosa. After oral LMWH, CD<sub>54</sub> dropped significantly in both blood and tissues, indicating that oral LMWH could relieve the inflammatory activity in these patients who received prednisolone for a long period (more than 4 weeks) and had no significant improvement and were regarded as corticosteroid-resistant refractory cases of UC. In other reports<sup>[5]</sup>, heparin

can also inhibit c-reactive protein (CRP), tumor necrosis factor (TNF) and L-selectin of UC patients. The detailed mechanisms by which the anti-inflammatory properties of oral LMWH are mediated in UC remain to be elucidated further.

From these results, we conclude that oral LMWH may play a role in treating corticosteroid-resistant UC, the mechanism is partly related to inhibition of platelet activity, hypercoagulable state and anti-inflammatory effects. No serious complications were found associated with the use of oral LMWH.

## REFERENCES

- Jiang XL, Quan QZ, Sun ZQ, Wang YJ, Qi F. Effect of glucorticoid on lymphocyte adhesion molecule phenotype expression in patients with ulcerative colitis. *Zhongguo Weizhongbing Jijiu Yixue*, 1998;10:366-368
- Collins CE, Cahill MR, Newland AC, Rampton DS. Platelets circulate in an activated state in inflammatory bowel disease. *Gastroenterology*, 1994;106:840-845
- Jiang XL, Quan QZ, Liu TT, Wang YJ, Sun ZQ, Qi F, Ren HB, Zhang WL, Zhang L. Detection of platelet activity in ulcerative colitis patients. *Xin Xiaohuabingxue Zazhi*, 1997;11:736
- Jiang XL, Quan QZ, Sun ZQ, Wang YJ, Qi F. Relationship between syndrome-typing of ulcerative colitis and activation of platelet. *Zhongyi Zazhi*, 1997;38:730-731
- Folwaczny C, Frike H, Endres S, Hartmann G, Jochum M, Loeschke K. Anti-inflammatory properties of unfractionated heparin in patients with highly active ulcerative colitis: a pilot study. *Am J Gastroenterol*, 1997;92:911-912
- Evans RC, Wong VS, Morris AI, Rhodes JM. Treatment of corticosteroid-resistant ulcerative colitis with heparin: a report of 16 cases. *Aliment Pharmacol Ther*, 1997;11:1037-1040
- Gaffney PR, Doyle CT, Gaffney A, Hogen J, Hayes DP, Annis P. Paradoxical response to heparin in 10 patients with ulcerative colitis. *Am J Gastroenterol*, 1995;90:220-223
- Cui HF, Zhang TM. Studies of oral preparation of low molecular weight heparin. *Zhongguo Yaoxue Zazhi*, 1995;4:51-52
- Cui HF, Zhang TM. Studies of oral preparation of low molecular weight heparin from low anticoagulant activity heparin. *Zhongguo ShenghuaYaowu Zazhi*, 1993;4:10-15
- Jiang XL, Cui HF, Wang YJ, Quan QZ, Sun ZQ. Effects of oral low molecular weight heparin on hemorrheology of rabbit liver damaged by D-galactosamine. *Xin Xiaohuabingxue Zazhi*, 1997;5:355-356
- Jiang XL, Zhang JZ, Cui HF, Dong ZL, Wang JY. Treatment on acute hepatitis with oral low molecular weight heparin. *Xin Xiaohuabingxue Zazhi*, 1997;5:296
- Jiang XL, Quan QZ, Chen GY, Yin GP, Sun ZQ, Wang YJ. Expression of adhesion molecules on tissues and peripheral lymphocytes in patients with ulcerative colitis. *Zhonghua Xiaohua Neijing Zazhi*, 1998;15:292-294
- Tyrrell DJ, Kilfeather S, Page CP. Therapeutic uses of heparin beyond its traditional role as an anticoagulant. *Tips*, 1995;16:198-204
- Koenigs KP, Mcphedran P, Spiro HM. Thrombosis in inflammatory bowel disease. *J Clin Gastroenterol*, 1987;9:627-631

Edited by MA Jing-Yun

# Methylation status of *p16* gene in colorectal carcinoma and normal colonic mucosa

ZHANG Jing<sup>1</sup>, LAI Mao-De<sup>2</sup> and Chen Jian<sup>2</sup>

**Subject headings** Colonic mucosa; colorectal neoplasms; *p16* gene; methylation

## INTRODUCTION

*p16* gene (also known as MTS-1, INK4a, CDKN2A), located on chromosome 9p21, is a G1-specific cell-cycle regulatory gene. It is composed of three exons, which encode 156 amino acids<sup>[1]</sup>. The gene is frequently inactivated in many human cancers. Unlike other tumor-suppressor genes that are commonly inactivated by point mutations, small homozygous deletions and methylation of the promoter represent the major mechanism of *p16* gene inactivation<sup>[2,3]</sup>. In the Western countries, colorectal carcinoma ranks first among malignant tumors. The mortality from colorectal carcinoma has been rapidly growing in China in the last two to three decades. The genetic alterations involved in this tumor are still unclear. Rare mutation and infrequent deletion of *p16* gene in primary colorectal carcinoma has been widely reported<sup>[4]</sup>. There were a few papers on *p16* gene methylation in colorectal carcinoma, but the results were contradictory<sup>[5,6]</sup>. In this study, we have examined a total of 60 samples of colorectal carcinoma and paired 60 samples of the normal colonic mucosa for methylation by means of PCR-based methylation assay. There is infrequent methylation in the promoter of *p16* gene both in colorectal carcinoma and normal colonic mucosa. The methylation status in 5' CpG island of *p16* gene in colorectal carcinoma is not related to the clinical pathologic parameters of these tumors.

## MATERIALS AND METHODS

### *Patients and specimens*

The samples were provided by the First and Second Affiliated Hospitals of Zhejiang Medical University and Hangzhou Railway Central Hospital from 1996 to 1998. Colorectal carcinoma specimens ( $n = 60$ ) and matched normal colorectal mucosa ( $n = 60$ ) were obtained from 60 patients (38 men and 22 women) with colorectal carcinoma. Their ages ranged from 20 to 78 years with a mean age of 57. The size of the tumors ranged from 1.5 cm to 7.8 cm in diameter.

### *Template preparation*

DNA was isolated by proteinase K digestion and phenol chloroform extraction. The DNA concentration and purity were determined on the ultraviolet ray spectrometer (Pharmacia Bioth Ultraspec 2000). All DNA templates were diluted to 1  $\mu\text{g}/\mu\text{L}$  with TE.

### *PCR-based methylation assay*

Genomic DNA (1  $\mu\text{g}$ ) was either overdigested with 20 U three methylation-sensitive restriction enzymes (*Hpa* II, *Sac* II and *Sma* I) or placed in the appropriate buffer without enzyme (control) overnight. Aliquots of 120 ng of the digested and non-digested DNA were PCR amplified using primers 5'-GAAGAAAGAGGAGGGGGTG-3' (sense) and 5'-GCGCTACCTGATTCCAATTC-3' (antisense), which corresponded to a part of 5' noncoding region and a part of the 3' end of exon 1 of the *p16* gene. The undigested DNA of the correspondent samples was also amplified and used as control. A total of 25  $\mu\text{L}$  volume of PCR mixture contained 2  $\mu\text{L}$  of 10 $\times$ buffer, 0.8  $\mu\text{L}$  of  $\text{MgCl}_2$  (25 mM), 2  $\mu\text{L}$  of dNTP (0.2 mM), 2  $\mu\text{L}$  of primer (20 pM), 15 U of Taq polymerase and 2.5  $\mu\text{L}$  of digested DNA. Amplifications were performed in a temperature cycler (MJ Research, Inc., USA) for 1 cycle at 95  $^\circ\text{C}$  (5 min), 30 cycles at 95  $^\circ\text{C}$  (30 s), 55  $^\circ\text{C}$  (30 s) and 72  $^\circ\text{C}$  (30 s), and 1 cycle at 72  $^\circ\text{C}$  (5 min). After PCR, the reaction mixture was electrophoresed in 1.5% agarose gel and examined to find out whether a 340 bp long product was generated. The sample which is unmethylated and cut by restriction enzyme, has no amplified product while the sample which is methylated and not cut by

<sup>1</sup>Department of Clinical Pathology, Hangzhou Railway Central Hospital, Hangzhou 310009, Zhejiang Province, China

<sup>2</sup>Department of Pathology, Zhejiang University, Hangzhou 310006, Zhejiang Province, China

ZHANG Jing, female, graduated from Nanjing Railway Medical College in 1986, M.D. candidate majoring tumor pathology in Department of Pathology, Zhejiang University, having 4 papers published.

Supported by Scientific Foundation of Ministry of Health (No.96-1-349) and Scientific Fund of Hangzhou Railway Branch.

**Correspondence to:** Dr. LAI Mao-De, Department of Pathology, School of Medicine, Zhejiang University, Hangzhou 310006, Zhejiang Province, China.

Tel.+86-571-7217134, Fax.+86-571-7217044

Received 1999-04-08

restriction enzyme, has amplified product.

### Statistical analysis

Statistical analysis was made by Chi-square test. The difference was regarded significant when *P* value is less than 0.05.

## RESULTS

Methylation of the *p16* gene in colorectal carcinoma and normal colonic mucosa. We have investigated the biopsies of 60 cases of primary colorectal carcinoma and paired 60 cases of normal colonic mucosa for methylation of the *p16* gene in *Hpa*-II, *Sac*-II and *Sma*-I sites. All of the undigested control of 60 cases of colorectal carcinoma and 60 cases with normal colonic mucosa got the same PCR products of 340 bp, while the digested samples achieved the different results (Figure 1). In the normal colonic mucosa, at the *Hpa*-II site in 5' CpG island of *p16* gene, 13 (21.6%) of 60 samples showed full methylation and 7 (11.6%) samples partial methylation, at the *Sac*-II site 28 (46.6%) of 60 showed full methylation and 8 (13.3%) partial methylation and at the *Sma*-I site, 5 (8.3%) showed full methylation and 4 (6.7%) partial methylation. In the colorectal carcinoma, at the *Hpa*-II site, 11 (18.3%) samples showed full methylation and 10 (16.7%) partial methylation, at the *Sac*-II site, 22 (33.3%) full methylation and 6 (10%) partial methylation, and at the *Sma*-I site, 9 (15%) full methylation and 3 (5%) partial methylation. In comparison of the methylation status of colorectal carcinoma and that of normal colonic mucosa, there was no significant difference ( $P > 0.05$ ).

Statistical analysis revealed a marked significant difference in the methylation status of *Hpa*-II, *Sac*-II and *Sma*-I sites of *p16* gene in normal colonic mucosa ( $\chi^2 = 28.6, P < 0.01$ ), and the methylation of promoter in *p16* gene tended to be associated with aging ( $\chi^2 = 5.64, 0.1 > P > 0.05$ ) (Table 1).

**Table 1 Correlation between methylation of *p16* gene and age, enzyme cutting site of normal colonic mucosa**

	Number of site	Full methylation	Partial methylation	Un-methylation
Age (yrs)				
≤40	33	4	3	26 <sup>a</sup>
41-60	60	19	8	33
>60	87	23	8	56
Site				
<i>Hpa</i> -II	60	13	7	40 <sup>b</sup>
<i>Sac</i> -II	60	28	8	24
<i>Sma</i> -I	60	5	4	51

<sup>a</sup>0.1 > P > 0.05, <sup>b</sup>P < 0.005.

The 60 cases of colorectal carcinoma were divided into groups according to the pathological types and size of cancer and the lymph node metastasis. It was found that the methylation of 5' CpG island of the *p16* gene was not related to the clinicopathologic parameters (Table 2).

**Table 2 Correlation between methylation of *p16* gene and clinicopathologic parameters of colorectal carcinoma**

	Numbers of site	Full methylation	Partial methylation	Un-methylation
Histological type (adenocarcinoma)				
Well-differentiated	18	6	3	9 <sup>a</sup>
Moderately-differentiated	117	26	14	77
Poorly-differentiated	15	3	2	10
Mucinous	21	6	0	15
Size (cm)				
≤2.5	27	5	4	18 <sup>a</sup>
2.6-4	54	15	5	34
>4	87	21	10	56
Lymph node metastases				
With LN metastases	78	20	5	53 <sup>a</sup>
Without LN metastases	102	26	14	62

<sup>a</sup>P > 0.05.

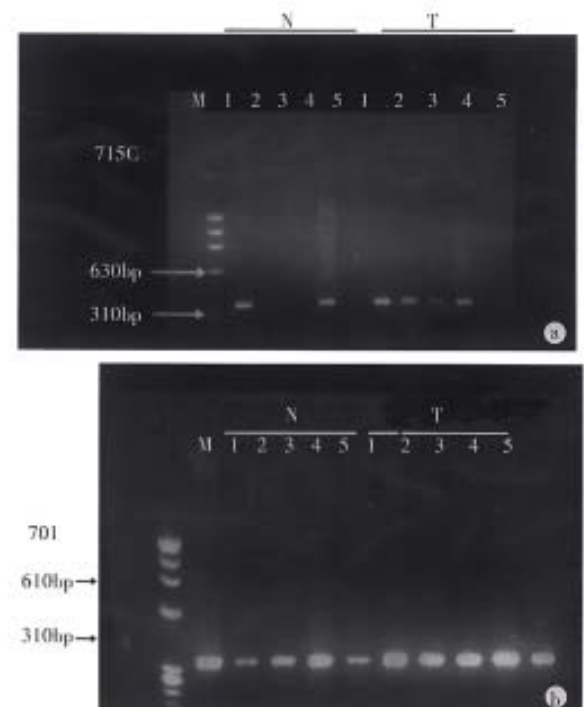


**Figure 1** PCR-based detection of 5' CpG island methylation. N: normal colonic mucosa; T: colorectal carcinoma. A 5' CpG island sequence (340 bp) of the *p16* gene was PCR amplified after sufficient digestion with a methylation sensitive enzyme *Hpa*-II (2), *Sac*-II(3) and *Sma*-I(5) and undigested control (1, 4). A: case 715c, in the normal colonic mucosa, *Hpa*-II and *Sma*-I sites unmethylation (N2, N5) and *Sac*-II sites partial methylation (N3); in the colorectal carcinoma, *Hpa*-II and *Sac*-II sites partial methylation (T2, T3) and *Sma*-I site unmethylation (T5). B: case 701, in the normal colonic mucosa, *Sac*-II site full methylation (N3) and *Sma*-I and *Hpa*-II sites partial methylation (N5, N2); in the colorectal carcinoma, *Hpa*-II, *Sac*-II and *Sma*-I sites full methylation (T2, T3, T5).

## DISCUSSION

There are two major mechanisms of gene inactivation. One is the genetic mechanism, i.e. the aberration of DNA structure such as homozygous deletion or intragenic mutation resulting in the gene inactivation. The other is the epigenetic mechanism, i.e., the methylation of the position 5 of cytosine (C) leading to the lack of gene expression, while the structure and the product of the gene remained unchanged. In higher order eukaryotes, DNA is methylated only at cytosines located 5' to guanosine in the CpG dinucleotide. This modification has important regulatory effects on gene expression, especially when involving CpG-rich areas known as CpG islands, located in the promoter region of many genes. While almost all gene-associated islands are protected from methylation on autosomal chromosomes, extensive methylation of CpG islands has been associated with transcriptional inactivation of selected imprinted genes and the genes on inactivated X-chromosome of females. Aberrant methylation of normally unmethylated CpG islands has been associated with transcription inactivation of gene<sup>[7]</sup>.

The exon 1 coding sequences of the *p16* gene resides within 5' CpG islands. This area is not methylated in most normal tissues but methylated in many human cancers. The rates of homozygous deletion and intragenic mutation of *p16* gene in colorectal carcinoma are very low, but how about the methylation of 5' CpG islands of *p16* gene in this tumor? We examined the methylation status of 3 40bp sequence within 5' CpG islands of *p16* gene in colorectal carcinoma and normal colonic mucosa using the PCR-based methylation assay. Our data suggest that there was no significant difference in the methylation status of *p16* gene 5' CpG islands between the colorectal carcinoma and normal colonic mucosa. We further studied the correlation between methylation of *p16* gene and clinicopathologic parameters of colorectal carcinoma, which also showed that the methylation of *p16* gene did not play an important role in the progress of colorectal carcinoma. Recently, some scholars suggest that the cell proliferation in colorectal carcinoma, unlike in most other tumor types, could bypass *p16*ink4a-mediated growth arrest<sup>[8]</sup>. Our experiment, which combined with the reports of low rates of homozygous deletion and intragenic mutation of *p16* gene in colorectal carcinoma, supports this opinion.

There are contradictory results on the methylation of the 5' CpG island of *p16* in colorectal carcinoma and normal colonic mucosa reported by Herman *et al* and Gonzalez-Zulueta *et*

*al*<sup>[5,6]</sup>. We found the methylation of the 5' CpG island of *p16* gene in colonic mucosa was very complicated. The full methylation rates of *Hpa*-II and *Sma*-I sites in 5' CpG island of *p16* gene were low (21.6% and 8.3%), while that of *Sac*-II site was high (46.6%). There were significant differences in methylation status of three different sites ( $P < 0.01$ ). It suggested that using different methylation-sensitive restriction enzymes in different experiments without self control might lead to contradictory results.

The existence of partial methylation status has also been verified. We could see the weak bands (1/2-1/8 of control) after the samples were digested by methylation-sensitive restriction enzymes in some cases. It was confirmed by repeated digestion. This could be explained by the presence of distinct cell subpopulation. The other explanation is the methylation of one allele. As PCR-based technique facilitates the detection of low numbers of methylated alleles, the DNA of stroma may influence the results.

DNA methylation plays an important role in the development, imprinting and aging. It has been reported that the methylation of estrogen receptor gene CpG island links with aging in human colon<sup>[9]</sup>. In this experiment, the rates of the methylation of promoter in *p16* gene increased with aging in colonic mucosa.

Southern hybridization is a classical method for detecting methylation status of specific sequence in specific genes, it needs not only more DNA but also radioactive element. PCR-based methylation assay has provided significant advantages of being markedly more sensitive and highly efficient, and need no radioactive element and expensive instruments.

To avoid false positive results, the key problem of this method is the sufficient digestion of DNA templates with restriction enzymes. In this experiment, we diluted all the DNA sample to 1μg/μL, and selected the smallest numbers of template which could find clear PCR product by ladder diluted method. We digested the DNA with the largest amount of enzyme, prolonged the digestion time (overnight) and repeated digestion to some partial methylation cases to confirm results. We used the digested products without ethanol precipitation as template of PCR to avoid the loss of DNA and adjusted the reaction mixture in accordance with different buffers (*Hpa*-II, *Sac*-II with buffer A, *Sma*-I with buffer J) used in different restriction enzyme digestion. For each case, we amplified the digested template and the undigested one simultaneously with the same

digestion buffers as control.

## REFERENCES

- 1 Kamb A, Gruis NA, Weaver-Feldhaus J, Liu QY, Harshman K, Tavitgian SV, Stockert E, Day RS 3rd, Johnson BE, Skolnick MH. A cell cycle regulator potentially involved in genesis of many tumor types. *Science*, 1994;264:436-440
- 2 Nobori T, Miura K, Wu DJ, Lois A, Takabayashi K, Carson DA. Deletions of the cyclin dependent kinase-4 inhibitor gene in multiple human cancers. *Nature*, 1994;368:753-756
- 3 Lo KW, Cheung ST, Leung SF, van Hasselt A, Tsang YS, Mak KF, Chung YF, Woo JK, Lee JC, Huang DP. Hypermethylation of the *p16* gene in nasopharyngeal carcinoma. *Cancer Res*, 1996;56:2721-2725
- 4 Okamoto A, Demetrick DJ, Spillare EA, Hagiwara K, Hussain SP, Bennett WP, Forrester K, Gerwin B, Serrano M, Beach DH, Harris CC. Mutations and altered expression of *p16INK4* in human cancer. *Proc Natl Acad Sci USA*, 1994;91:11045-11049
- 5 Herman JG, Merlo A, Mao L, Lapidus RG, Issa JP, Davidson NE, Sidransky D, Baylin SB. Inactivation of the *CDKN2/p16/MTS1* gene is frequently associated with aberrant DNA methylation in all common human cancers. *Cancer Res*, 1995;55:4525-4530
- 6 Gonzalez-Zulueta M, Bender CM, Yang AS, Nguyen T, Beart RW, Van Tornout JM, Jones PA. Methylation of the 5'CpG island of the *p16/CDKN2* tumor suppressor gene in normal and transformed human tissues correlates with gene silencing. *Cancer Res*, 1995;55:4531-4535
- 7 Zingg JM, Jones PA. Genetic and epigenetic aspects of DNA methylation on genome expression, evolution, mutation and carcinogenesis. *Carcinogenesis*, 1997;18:869-882
- 8 He TC, Sparks AB, Rago C, Hermeking H, Zawel L, da Costa LT, Morin PJ, Vogelstein B, Kinzler KW. Identification of c-MYC as a target of the APC pathway. *Science*, 1998;281:1509-1512
- 9 Issa JP, Ottaviano YL, Celano P, Hamilton SR, Davidson NE, Baylin SB. Methylation of the oestrogen receptor CpG island links ageing and neoplasia in human colon. *Nat Genet*, 1994;7:536-540

Edited by MA Jing-Yun

# Study on the expression of matrix metalloproteinase-2 mRNA in human gastric cancer

Ji Feng, WANG Wei-Lin, YANG Zi-Li, LI You-Ming, HUANG Huai-Di and CHEN Wei-Dong

**Subject headings** matrix metalloproteinase-2 mRNA; stomach neoplasms; polymerase chain reaction

## INTRODUCTION

During tumor invasion and metastasis, malignant cells in primary site acquire the ability to degrade extracellular matrix (ECM) and penetrate tissue barriers. Among the proteolytic enzymes which degrade ECM, matrix metalloproteinase (MMP) is one of the important ones. MMP<sub>2</sub> (72kDa type IV collagenase) is a member of the MMPs gene family which degrades the macromolecules of connective tissue and ECM, such as collagen, proteoglycans, laminin and fibronectin. Thus MMP<sub>2</sub> is believed to play an important role in tumor invasion and metastasis. Several immunohistochemical studies have shown that MMP<sub>2</sub> mRNA is overexpressed in gastric cancer and related to the clinical stage of cancer<sup>[1,2]</sup>. However, samples were not enough and lack completeness in these studies. Reverse transcriptase-polymerase chain reaction (RT-PCR) was used in our study to examine the expression of MMP<sub>2</sub> mRNA in tumor and normal tissues adjacent to human gastric cancer.

## MATERIALS AND METHODS

### Samples

The samples, including tumour tissue and tumour-adjacent normal tissue (2 cm and 5 cm or over 5 cm distance from the tumour) came from twenty gastric cancer patients at the surgery department of our hospital and People's Hospital of Yun-He County, Zhejiang. Gastric tissues from five benign ulcer patients after partial gastrectomy were used as controls. The histological diagnosis was made by the

pathologists of these two hospitals. Patients' clinical features are shown in Table 1. Among these cancer patients, five and fifteen were cases of early and advanced cancer respectively. All samples were quenched in liquid nitrogen immediately after operation and were then stored at -70°C until used for the study.

### Reagents and primer synthesis

The dNTP, RNasin and MMLV reverse transcriptase and Taq DNA were provided by Stratagene, La Jolla, CA, U.S.A. MMP<sub>2</sub> primer pair was synthesized by Shanghai Cell Research Institute, Chinese Academy of Sciences<sup>[2]</sup> and its sense and anti-sense were 5'-ACAAAGAGTGGCAGTGCAA-3' and 5'-CACGAGCAAAGGCATCATCC-3' respectively. The expected size of MMP-2 product was 302bp.

### RT-PCR analysis

Total RNA was extracted from frozen tissues by cesium chloride purifying method. A total amount of 20 µL reaction solution contained 5 µg RNA sample tissue, 1 mmol/L dNTP, 10 U RNasin, 100 mmol/L Tris-HCl pH 8.4, 50 mmol/L KCl, 2.5 mmol/L MgCl<sub>2</sub>, 100 mg/mL BSA, 100 pmol random six-polyoligo-nucleotide and 100 U MMLV reverse transcriptase. The reverse transcription condition was 37 °C for 1 h, and 95 °C for 5 min. Twenty µL cDNA reverse transcriptase product was put in PCR reaction solution containing 100 mmol/L Tris-HCl, pH 8.4, 50 mmol/L KCl, 2.5 mmol/L MgCl<sub>2</sub>, 100 mg/mL BSA, 30 pmol sense and anti-sense primers, and then 2 U Taq DNA polymerase was added in the solution. The PCR amplification condition was: denatured at 95 °C for 1 min, annealed at 65 °C for 1 min and extended at 72 °C for 1 min. The number of cycles was 35. 10 µL DNA, amplifying product was subjected to electrophoresis in 4% agarose gel, stained with ethidium bromide and observed under ultraviolet light. The photographs of PCR results were used to measure the level of optical density (OD) of MMP-2 cDNA bands with densitometry (Backman CD 2000).

### Statistical analysis

The significance of differences in expression rates and OD levels among groups was determined by  $\chi^2$  test and Student's *t* test respectively.

First Affiliated Hospital of Zhejiang University, Hangzhou 310003, Zhejiang Province, China

Department of Gastroenterology, First Affiliated Hospital, Medical College of Zhejiang University, No.261, Qing Chun Road, Hangzhou 310003, Zhejiang, China

Dr. Ji Feng, male, born on 1962-11-26 in Lingbo City, Zhejiang, graduated from Zhejiang Medical University as a M.D. in 1989, associate professor of internal medicine and director of master student, having 25 papers published.

Project supported by the Zhejiang Natural Science Foundation, No. 925006.

**Correspondence to:** Dr. Ji Feng, Department of Gastroenterology, First Affiliated Hospital, Medical College of Zhejiang University, No.261, Qing Chun Road, Hangzhou 310003, Zhejiang, China  
Tel. +86-571-7072524 Ext.4402, Fax. +86-571-7072577

Received 1999-03-05

## RESULTS

**Expression of MMP-2 mRNA in tumor and tumor-adjacent tissues (Figure 1)**

In 20 cases of gastric cancer, MMP<sub>2</sub> mRNA was expressed in 13 tumor tissues, 11 in 2 cm and 6 in  $\geq 5$  cm adjacent tissues respectively (Table 1). The positive rate of MMP<sub>2</sub> mRNA expression in tumor tissues was significantly higher than that in  $\geq 5$  cm adjacent tissues ( $P < 0.05$ ). There was no positive expression of MMP<sub>2</sub> mRNA in the 5 samples of the control group.

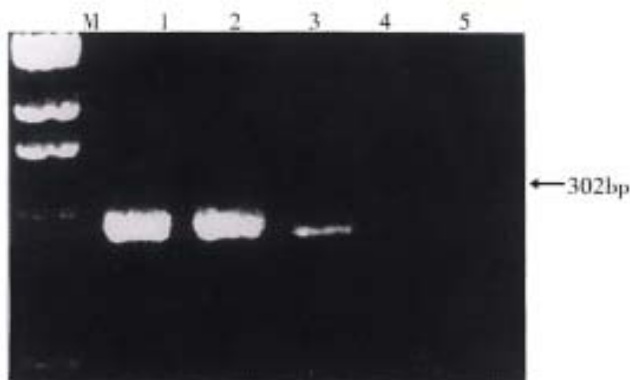


**Figure 1** Expression of MMP-2 mRNA in case No.3  
Lane M: Marker; Lane 1, 2: tumor tissues; Lane 3-5: 2cm,  $\geq 5$ cm adjacent tissues and normal gastric tissue of one control.

**Table 1** Clinical features of cases and expression of MMP-2 mRNA

No.	Age/sex	Location	Histology	Clinical stage <sup>b</sup>	MMP2 mRNA expression		
					T	2cm	$\geq 5$ cm
1 <sup>a</sup>	64/M	Pylorus	Poor	T1N0M0(I)	-	-	-
2	48/M	Body	Poor	T4N0M0(IV)	+	+	-
3	72/F	Lesser curve	Poor	T4N2M1(IV)	+	+	-
4	75/F	Lesser curve	Poor	T3N0M0(II)	+	+	-
5	71/M	Body	Poor	T2N1M0(IVA)	+	+	-
6	63/M	Lesser curve	Well	T4N2M0(IV)	-	-	+
7 <sup>a</sup>	73/F	Lesser curve	Poor	T1N1M0(IIIA)	+	-	-
8 <sup>a</sup>	46/M	Lesser curve	Poor	T1N0M0(I)	-	-	-
9	60/F	Body	Poor	T3N0M0(II)	+	-	-
10	57/M	Pylorus	Poor	T3N1M1(IV)	+	+	+
11	53/M	Body	Poor	T4N1M0(IV)	+	+	-
12 <sup>a</sup>	72/F	Antrum	Poor	T1N0M0(I)	-	-	-
13	59/M	Body	Poor	T3N2M0(IIIB)	+	-	-
14 <sup>a</sup>	38/M	Antrum	Well	T1N0M0(I)	-	-	-
15	66/F	Cardia	Poor	T3N1M0(IIIA)	+	+	+
16	55/M	Antrum	Well	T2N0M0(II)	-	-	-
17	74/M	Body	Poor	T4N2M1(IV)	+	+	+
18	67/M	Cardia	Well	T3N2M0(IVB)	-	-	-
19	67/F	Body	Poor	T4N2M1(IV)	+	+	+
20	56/M	Body	Poor	T4N2M1(IV)	+	+	+

T: Tumor tissues; 2cm: 2cm adjacent tissue from tumor;  $\geq 5$ cm: 5cm or over 5cm adjacent tissue from tumor. <sup>a</sup>: early gastric cancer. Poor: poorly differentiated adenocarcinoma; Well: well differentiated adenocarcinoma. <sup>b</sup>: According to the American Joint Commission Staging of Gastric Cancer.

**The OD levels of MMP-2 mRNA in tumor and tumor-adjacent tissues (Figure 2)**

The OD of MMP-2 detected cDNA signals ranged

from 1.10 to 19.23 (mean  $5.38 \pm 0.98$ ) in tumor tissues, 0.86 to 4.17 (mean  $2.41 \pm 0.30$ ) in 2 cm and 0.78 to 3.80 (mean  $1.88 \pm 0.22$ ) in  $\geq 5$  cm adjacent tissues respectively. There was significant difference in OD levels between tumor tissues group and 2 cm or  $\geq 5$  cm tumoradjacent tissues one ( $P < 0.01$ ), and no significant difference in OD levels between the two adjacent tissues groups.

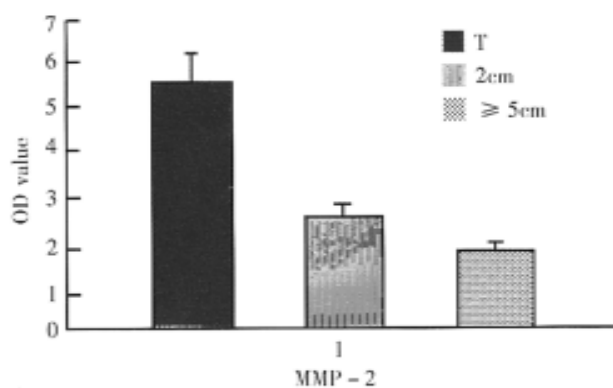


**Figure 2** OD of MMP-2 cDNA signals in tumor tissues and tumor-adjacent tissues (2cm and  $\geq 5$ cm). As compared with tumor tissues: 2cm:  $P < 0.01$ ;  $\geq 5$ cm:  $P < 0.01$ .

**The OD levels of MMP-2 mRNA in early and advanced cancer (Table 2)**

The MMP-2 cDNA signals in tumour and 2cm adjacent tissues of 15 advanced cancer were significantly higher than those in the two corresponding tissues of 5 early cancer respectively ( $P < 0.05$ ). In the  $\geq 5$  cm adjacent tissues, there was no-significant difference in the signals between the advanced and early cancer.

**Table 2** OD of MMP-2 cDNA signals in early and advanced cancer ( $\bar{x} \pm s_x$ )

	T	2cm	$\geq 5$ cm
Early cancer (n=5)	$1.63 \pm 0.42$	$1.07 \pm 0.29$	$1.50 \pm 0.22$
Advanced cancer (n=15)	$6.63 \pm 1.12^a$	$2.80 \pm 0.34^a$	$1.94 \pm 0.29$

<sup>a</sup> $P < 0.05$ , vs early cancer.

## DISCUSSION

In 20 gastric cancer cases, 13, 11 and 6 cases positively expressed MMP-2mRNA in tumor, 2cm adjacent and  $\geq 5$  cm adjacent tissues respectively. The cases with MMP-2 mRNA expression in tumor tissues and their corresponding tumor adjacent normal tissues (2 cm and/or  $\geq 5$  cm) were almost poorly differentiated adenocarcinoma and in higher clinical stage. MMP-2 mRNA was seldom expressed in tumor and tumor adjacent tissues of well differentiated or early carcinoma. These results

showed that proliferative and invasive gastric cancer cells had higher MMP-2 secretion. In ultrastructural study, MMP-2 mRNA was expressed markedly in cancer cells with rich false feet and rapid movement in culture, but insignificantly or with few false feet in cancer cells from unmetastatic and uninvase gastric cancerous tissues, indicating that MMP-2 secretion was correlated with the invasion and metastasis of gastric cancer<sup>[3]</sup>. In addition, some immunohistochemistry studies have shown that the positive rate of staining cells for MMP-2 protein was consistently higher in poorly differentiated and diffuse gastric carcinoma than that in well differentiated and early gastric carcinoma<sup>[1,4]</sup>. The results of these studies were very similar to those of MMP-2 mRNA expression in our study, indicating that the increased MMP-2 positive staining was related to the overexpression of MMP-2 mRNA. This is probably due to increase in MMP-2 transcriptional activity and MMP-2 protein products in the cell proliferative process of gastric cancer which is often accompanied with the acceleration of cancer invasion and metastasis.

In the current study, although the levels of MMP-2 cDNA signals in tumor-adjacent tissues (2 cm and/or  $\geq 5$  cm) were lower than those in tumor tissues, MMP-2 mRNA was overexpressed in the tumor adjacent tissues in certain extent, suggesting that both gastric cancer cells and adjacent mesenchymal cells, including fibrocyte, endothelium cell, macrophage and lymphocyte have the ability to secrete MMP-2. There may be information exchange between the cancer cells and these mesenchymal cells through the dissolvable intercellular substance and membrane cement factor, and such information exchange may regulate the production of MMP-2. This may be very

important in elucidating the mechanism of invasion and metastasis of cancer cells<sup>[5,6]</sup>. In our case No. 6, MMP-2 mRNA was detected only in tumor-adjacent tissues, but not in tumor tissue. The reason for this is unclear. The discrepancy may be due to the necrotic tumor tissue. Overexpression of MMP-2 mRNA only in tumour adjacent tissues also indicates the malignant degree of cancer is rather high.

The prognosis of early gastric cancer is better than that of advanced cancer. Our study showed that the levels of MMP-2 cDNA signal in advanced cancer tissues (tumor and 2 cm tumor-adjacent tissues) were significantly higher. This suggests MMP-2 may play a role in gastric cancer invasion and metastatic progression, and the overexpression may be associated with poor prognosis. Further study on relationship between the expression of MMP-2 mRNA and the survival rate of gastric cancer is being carried out.

## REFERENCES

- 1 Grigioni WF, D'Errico A, Fortunato C, Liotta LA, Rogers L. Prognosis of gastric carcinoma revealed by interactions between tumor cells and basement membrane. *Mod Pathol*, 1994;7:220-225
- 2 Huang Y, Ti TK, Mochhala SM. Expression of matrix metalloproteinases (MMP-2 and MMP-7) mRNA in human gastric cancer. *Med Sci Res*, 1997;25:405-407
- 3 Schwartz GK, Wang H, Lampen N, Altorki N, Kelsen D, Albino AP. Defining the invasive phenotype of proximal gastric cancer cells. *Cancer*, 1994;73:22-27
- 4 D'Errico A, Garbisa S, Liotta L, Jeffery RE. Augmentation of type IV collagenase, laminin receptor and Ki67 proliferation antigen associated with human colon, gastric, and breast carcinoma progression. *Mod Pathol*, 1991;4:239-246
- 5 Poulson R, Pignatelli M, William G, Liotta LA, Wright PA, Jeffery RE, Longcroft JM, Rogers L, Stamp GWH. Stromal expression of 72kDa type IV collagenase and TIMP-2 mRNAs in colorectal neoplasia. *Am J Pathol*, 1992;141:389-396
- 6 Grigioni WF, D'Errico A, Fiorentino M, Baccarini P, Onisto M, Caccanzo C, Stetler Stevenson WG, Garbisa S, Mancini AM. Gelatinase A (MMP-2) and its mRNA detected in both neoplastic and stromal cells of tumors with different invasive and metastatic properties. *Diagn Mol Pathol*, 1994;3:163-169

# Islet separation and islet cell culture *in vitro* from human embryo pancreas

YUAN Zhu<sup>1</sup>, WU Guang-Ying<sup>2</sup>, HE Yong-Shu<sup>3</sup>, SHAO Chen-Ming<sup>2</sup> and ZHAN Ya<sup>1</sup>

**Subject heading** cell culture; islet cell; islets of langerhans; transplantation; pancreas/embryology

## INTRODUCTION

Diabetes mellitus is the most common disease and its death rate ranks the 8th in the world. Up to now, its incidence has a tendency to increase<sup>[1]</sup>. Since disorder of sugar metabolism might result in microvascular degeneration and injury of important human organs, it will endanger human health seriously. In 1969, Younszai first reported the method that could decrease diabetes symptoms by islet tissue transplantation. In 1981, our country began to treat diabetes type I by transplanting cultured islet tissues. In our study, we digested the pieces of pancreas with collagenase and made morphological observation on islet cells cultured for 3 d, 5 d, 7 d, 9 d and 13 d respectively, and the contents of insulin and C-peptide in the supernatant were detected by radioimmunoassay. The experimental model of rabbit diabetes was established, and certain curative effect was achieved in the treatment of experimental diabetes in rats.

## MATERIALS AND METHODS

### *Islet isolation*

Four cases of 18wk-28wk human embryo induced by hydrostatic bag were sterilized with 75% alcohol, and their pancreas were removed with the surrounding connective tissues eliminated. After the pancreas were washed with cold Hank's balanced

salt solution, they were cut into 1 mm fragments digested three times with 0.5 g/L collagenase (Sigma Type V 663 U/mg) and shaken thoroughly. Then the islets were carefully isolated under stereoscope (islets are white with different dimensions), and washed two times with Hank's balanced salt solution and put into glass bottles to be cultured.

### *Islet cells culture*

Islet cells were cultured with RPMI-1640 medium containing 20% bovine serum, 10 mmol/L glutamine, 80 U penicillin and 0.5 g streptomycin. Approximately 30 islets were inoculated in the 5mL bottles, and were cultured in CO<sub>2</sub> incubator (95% atmosphere, 5% CO<sub>2</sub>, 37 °C). The cells were digested by 0.25% sodium citrate and their fibroblast was cleaned<sup>[2]</sup>. The medium solution was replaced every 2 d after the 3 days. One mL-2 mL culture solution was put into clean bottles which were placed into refrigerator (4 °C) to detect the contents of insulin and C-peptide.

### *Observation of islet cell morphology*

In the process of culture, growth of islet cells was observed under invert microscope, and the islet cells cultured for 3 d, 5 d, 7 d, 9 d and 13 d respectively were observed under transmission electron microscope. The samples were fixed with 1.25% glutaraldehyde, and embedded with epoxy 618, sectioned with LKB-V ultramicrotome, and observed under JEM-100CX electron microscope.

### *Measurement of content insulin and C-peptide by radioimmunoassay*

FT-630G computer with multiprobe  $\gamma$  counter and kit of De Pu Company were used to collect the supernatant fluid of islet cells cultured for 3 d, 5 d, 7 d, 9 d and 13 d respectively by strict standard operation, and contents of insulin and C-peptide in the culture suspension were measured by radioimmunoassay (RIA) with antigen labeled by radionuclide <sup>125</sup>I.

### *Establishment of experimental model of rabbit diabetes and evaluation of experimental cure*

<sup>1</sup>Department of Histology and Embryology, Kunming Medical College, Kunming 650031, Yunnan Province, China

<sup>2</sup>Department of Nuclear Medicine, First Affiliated Hospital of Kunming Medical College, Kunming 650032, Yunnan Province, China

<sup>3</sup>Department of Biology, Kunming Medical College, Kunming 650031, Yunnan Province, China

<sup>4</sup>Department of Radiology, First Affiliated Hospital of Kunming Medical College, Kunming 650032, Yunnan Province, China

Dr. YUAN Zhu, male, born on 1942-11-15 in Kunming City of Yunnan Province, graduated from Kunming Medical College in 1966, specialized in research and teaching of histology and embryology, professor of Kunming Medical College, having 20 papers and one book published.

Supported by Basic Scientific Research Foundation of the Science Committee of Yunnan Province.

**Correspondence to:** Dr. YUAN Zhu, Department of Histology, Kunming Medical College, Kunming 650031, Yunnan Province, China  
Tel. +86-871-5339284

Received 1999-04-22

**effect**

Fasting blood sugar, insulin and C peptide were detected in 18 adult rabbits (9 male and 9 female weighing 1.5 kg - 2.0 kg). All rabbits were given injection of alloxan of 150 mg/kg into the posterior auricular vein to establish the model of rabbit experimental diabetes. Their biological behavior was observed after 48 h, and the contents of blood sugar, insulin and C- peptide were measured<sup>[3]</sup>. The cultured rabbit embryo islet cells were injected ( $1.1 \times 10^7$  cells/each) into their pancreatic artery after 72 h and the experimental treatment was evaluated.

**RESULTS****Morphology of the cultured islet cells**

After the islets were cultured for 24 h, fibroblast growth was found on the wall of glass bottle, but no islet cell mass was found. After the fibroblasts were eliminated with citrate sodium, islet cells began to grow and form a single layer of cells with typical morphology. Under invert microscope, the cells were found growing quite well, most of them were of epithelioid type with plenty of cytoplasm. The cell number was counted directly after stained with trypan blue and their survival rate reached up to 90%. Many cells were observed under transmission electron microscope and most of them were found to be beta cells with many  $\beta$ -granules, alpha cells, and a few extracrinous cells and macrophages. These beta cells after cultured for 5 d-9 d with a high density cytoplasm and cytoplasmic  $\beta$ -granule developed well. But eleven days later, the number of cytoplasmic granules decreased with karyopyknosis and degeneration in them.

**Contents of insulin and C-peptide in human embryo islet cell culture solution (Table 1)****Table 1 Contents of insulin and C-peptide in human embryo islet cell culture solution**

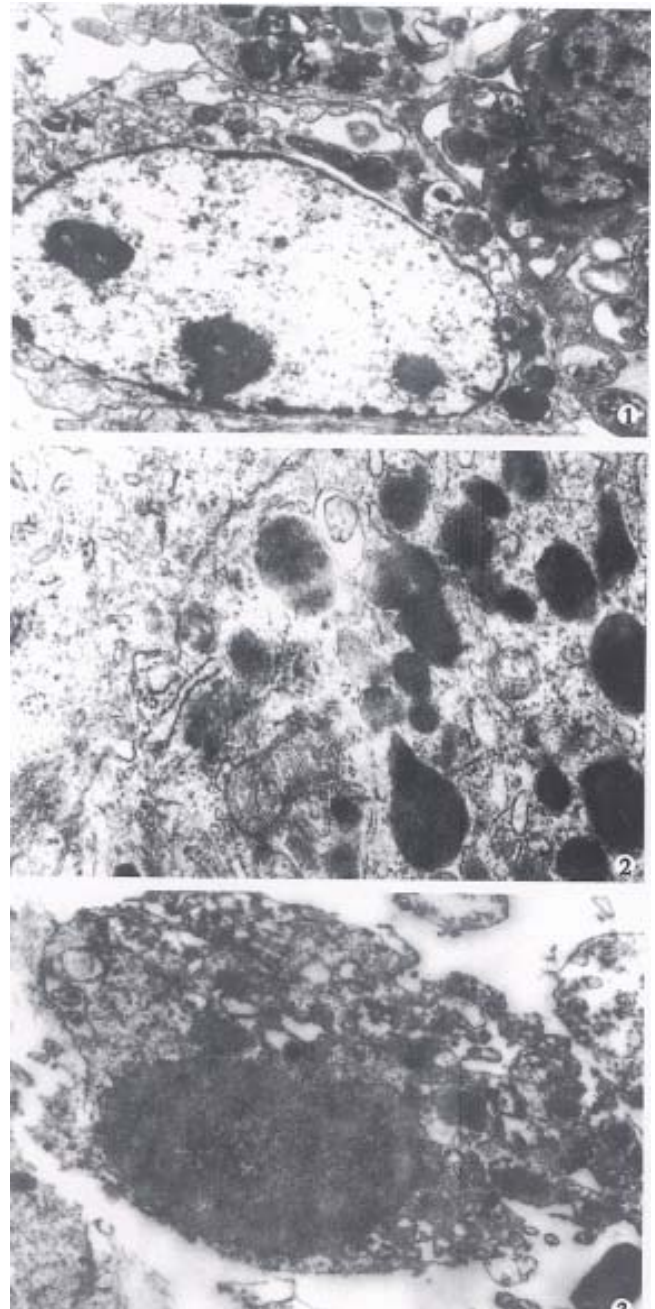
Islet cells (culture days)	Contents of insulin (IU/L)	Contents of C-peptide (mg/L)
3	47.30	3.05
5	64.75	6.05
7	72.30	6.20
9	72.70	>6.00
11	68.75	5.15
13	72.20	>6.00

\*Insulin antibody is negative in all tubes.

**Contents of blood sugar, insulin and C-peptide in normal rabbits and diabetes rabbits after experimental treatment (Table 2)****Table 2 Changes of blood sugar, insulin, C-peptide after experimental treatment in normal and diabetes rabbits ( $\bar{x} \pm s$ )**

Experimental rabbits	Blood sugar (g/L)	Contents of insulin(IU/L)	Contents of C-peptide (mg/L)
Normal controls	1.0524 $\pm$ 0.0510	6.27 $\pm$ 4.6	13.23 $\pm$ 4.77
Diabetes rabbits	4.7979 $\pm$ 0.9233	2.65 $\pm$ 1.4	Not detected
Experimentally treated rabbits	3.3193 $\pm$ 0.4110 <sup>a</sup>	13.88 $\pm$ 1.5 <sup>a</sup>	Not detected
<i>P</i>	<0.01	<0.05	

<sup>a</sup>After transplanted with rabbit islet cells, diabetes rabbits showed good spirit, less drinking and urine excretion.

**Figure 1** Islet cells developed well after cultured for 5d. TEM  $\times 10\ 000$ **Figure 2** Cytoplasmical APUD granules were observed after cultured for 9d. TEM $\times 20\ 000$ **Figure 3** Islet cells were aging after cultured for 13d with karyopyknosis and cytoplasmic lysis. TEM $\times 30\ 000$

## DISCUSSION

The quality and quantity of islet cells play a crucial role in the effectiveness of transplantation. An ideal preparative method can provide sufficient pure, viable and functional islet cells. We have achieved good digestive effect by digesting pancreas with collagenase at optimum pH and temperature<sup>[4]</sup>. In order to obtain good islets, it is necessary to control digestive time and mix the pieces of pancreas with collagenase thoroughly. The islet cells obtained were growing and their structure was not mature before they were cultured for 5 d. But after 5 d-9 d, they grew well with their structure fully matured. The survival rate was 90% according to the trypan blue staining. However, eleven days later, most cells became ageing with karyopyknosis and cytoplasmic lysis.

Activity and function are the important indexes in assessing the effect of islet cells. The contents of insulin and C-peptide in the culture suspension measured by radioimmunoassay were two times higher than those in normal control serum, indicating that our method is rather good. The highest amount of contents of insulin and C-peptide was found after they were cultured for 13 d, but was not in accordance with the morphological data. The reason why their contents increased in insulin culture solution was aging and released the remaining insulin that made insulin contents of the degeneration of most cells and release of the remaining insulin from cells from the 11th day.

We have used the same method to culture rabbit islet cells and made experimental treatment of rabbit diabetes model after rabbit islet cells were

cultured for 7 d. Blood sugar was  $1.052 \text{ g/L} \pm 0.5012 \text{ g/L}$  and  $4.7979 \text{ g/L} \pm 0.9233 \text{ g/L}$  in normal and experimental rabbits. Three days after the rabbits were given an injection via pancreatic artery at a density of  $1.1 \times 10^7$  cells/each islet cell, their blood sugar decreased to  $3.3193 \text{ g/L} \pm 0.4110 \text{ g/L}$ . Compared with diabetes rabbit ( $P < 0.01$ ), the difference was significant. Serum insulin contents increased from  $2.65 \text{ IU/L} \pm 1.4 \text{ IU/L}$  to  $13.88 \text{ IU/L} \pm 1.5 \text{ IU/L}$  ( $P < 0.05$ ), the difference was also significant. All these indicated that experimental treatment was effective.

In the past ten years, most tissue transplantation focused on subcutaneous and intramuscular transplantation of cultured islets. Present method is to treat diabetes type I with cultured islet cells which were planted by portal vein<sup>[5]</sup>.

Therefore, we believe that the culture of the islet cells by this method can be used to treat diabetes type I, and the optimum time of transplantation is 5-9 days after the islet cells were cultured.

## REFERENCES

- 1 Fu YF, Gu BF, Zhang HD, Ye RS. The present clinical situation of islet transplantation in our country-analysis of clinical material in 416 cases diabetes patients. *Zhonghua Qiguanyizhi Zazhi*, 1988;9: 102-104 (in Chinese with English abstract)
- 2 Burghen GA, Murrell LR. Factors influencing isolation of islets of Langerhans. *Diabetes*, 1989;38(Suppl 1):129-130
- 3 Li SG. Animal models of diabetes. In: Xi SY, Bian RL, Chen X, eds. The experimental methodology of pharmacology. *Beijing, People's Health Publishing House*, 1982:987-989 (in Chinese)
- 4 Maitland JE. Purification and culture of human fetal pancreas. *Diabetes*, 1980;29(Suppl 1):57
- 5 Lacy PE. Treating diabetes with transplanted cells. *Scientific American*, 1995;273:40-46

Edited by WANG Xian-Lin

# Update of preclinical and human studies of calcium and colon cancer prevention

Martin Lipkin

**Subject headings** calcium/metabolism; colonic neoplasms/prevention and control; vitamin D

Many articles on the subject of colon cancer begin by noting that the disease continues to be a major cause of tumor mortality in the United States and other countries. Despite attempts at reduction, the incidence of this disease is still high in Western populations and is increasing in some Eastern countries. Chemoprevention of this disease therefore continues to be an important public health objective. Among recent chemopreventive approaches, an increased intake of calcium and vitamin D continues to be evaluated in both preclinical and clinical studies. Many experimental findings, as described below, have indicated real associations between high calcium and vitamin D intake and decreased risk for colorectal cancer.

## BASIC STUDIES OF CALCIUM METABOLISM

Calcium is both an essential structural body component and a critical functional element in living cells. It is a key component for maintaining cell structure, membrane viscosity or rigidity, and the related membrane permeability is partly dependent on local calcium concentration. Calcium is also a pivotal regulator of a wide variety of cell functions in its role as a major second messenger<sup>[1]</sup>.

Among the numerous cell properties modulated by calcium, its participation in cell division and the regulation of cell proliferation and differentiation are particularly important<sup>[2]</sup>. Low levels of intracellular ionized calcium contribute to cell proliferation, and increasing calcium concentration in cell and organ culture media decreased cell proliferation; and induced cell differentiation in rat esophageal epithelial cells<sup>[3]</sup>, murine epidermal cells<sup>[4]</sup>, mammary cells<sup>[5,6]</sup>, and colon cells<sup>[7]</sup>.

The absorption and metabolism of calcium are

carefully regulated, 1, 25-dihydroxyvitamin D<sub>3</sub> is an important calcium modulator that can become deficient as a consequence of inappropriate diet or inadequate exposure to sunlight. Therefore vitamin D<sub>3</sub> also may have a role in the regulation of cell proliferation and differentiation while modulating calcium metabolism. It has also been shown to directly inhibit the proliferation of several malignant cell lines *in vitro*<sup>[8-10]</sup>, and to induce the differentiation of human colonic cells<sup>[11]</sup>, human myeloid leukemia cells<sup>[12]</sup>, and other cell lines *in vitro*<sup>[13,14]</sup>. A role of vitamin D as a chemopreventive agent has also been studied in rodent models<sup>[15-19]</sup>, and the tumor growth and promotional stage of chemical carcinogenesis have been inhibited by vitamin D. On the other hand, vitamin D<sub>3</sub> enhanced chemically-induced transformation of cultured cells *in vitro*<sup>[20,21]</sup> and promoted skin tumor formation in mice<sup>[22]</sup>.

## PRECLINICAL AND EARLY HUMAN INTERVENTION STUDIES OF EFFECTS OF INCREASED DIETARY CALCIUM

### *Preclinical studies*

The results of direct experimental studies of calcium intake and colon cancer development are summarized in Table 1. The results of many individual studies are further described in Tables 2-5. In many preclinical experimental models, calcium effects on colon cancer development and on cellular processes associated with colon cancer have been remarkably consistent: ① decreasing and normalizing excessive proliferation of colonic epithelial cells, reducing the susceptibility of proliferating epithelial cells to accumulate abnormalities in their DNA; ② reducing the cytotoxicity of fecal water; ③ increasing the differentiation and maturation of colonic epithelial cells; and ④ decreasing the end-stage development of colon cancer itself.

In animal models (Tables 2,3), oral calcium supplementation decreased epithelial cell hyperproliferation when it was induced by several factors that stimulate tumor promotion: the administration of bile acids and fatty acids, dietary fat, a Western-style diet, and partial enteric resection. Of further importance colonic

Strang Cancer Research Laboratory at the Rockefeller University and Weill Medical College of Cornell University, New York, NY 10021, USA

**Correspondence to:** Martin Lipkin, Strang Cancer Research Laboratory at the Rockefeller University and Weill Medical College of Cornell University, New York, NY 10021, USA

Tel. +1-212-5342024, Fax. +1-212-8799371

Email.lipkin@rockvax.rockefeller.edu

Received 1999-09-28

carcinogenesis itself, when induced by chemical carcinogens, decreased with increasing dietary calcium intake, with almost all studies showing a decrease in the number of tumors induced, the percent of invasive carcinomas, or the number of animals with multiple tumors.

Thus, a wide variety of rodent studies (Tables 1-3 with references) demonstrated that increasing dietary calcium intake reduced colonic tumor formation: mechanisms involved included decreased epithelial cell hyperproliferation; decreased or nilthine decarboxylase activity; decreased ras mutations in colonic epithelial cells; and calcium-binding of bile acids, fatty acids and phosphate into insoluble complexes, reducing their direct irritant and hyperproliferative effects on colonic epithelial cells and reducing the cytotoxicity of fecal water.

Two recent series of studies also have evaluated the effects of calcium and vitamin D on colonic tumor development when these nutrients were fed to rodents on Western-style diets. The first group of studies utilized preclinical models of normal mice. In the colonic crypts of these normal mice hyperproliferation, hyperplasia, abnormal differentiation and maturation of colonic crypt epithelial cells, and the late-stage preneoplastic lesion of whole-colonic-crypt dysplasia developed when the mice were fed Western-style diets containing low calcium and vitamin D<sup>[26,33,34]</sup>.

The second series of studies utilized mice having targeted mutations that are relevant to human colon cancer, the targeted mutation causing adenomas and carcinomas to develop in the mice<sup>[35,36]</sup>. Recent studies demonstrated the Western-style diets increased the development of the neoplastic colonic lesions that were initiated by those mutations; and the neoplasms together with carcinomas were decreased by: increasing calcium and vitamin D together with lowering fat content of diet<sup>[37]</sup>, or increasing dietary calcium and vitamin D alone (Yang *et al.*, unpublished data).

In other organs, Western-style diets also have induced epithelial cell hyperproliferation and hyperplasia in mammary gland<sup>[38,39]</sup>, and hyperproliferation in pancreas<sup>[40]</sup> and prostate gland<sup>[41]</sup> in short-term studies; increasing dietary

calcium and vitamin D alone also inhibited the development of those lesions<sup>[25]</sup>.

## EARLY HUMAN CLINICAL TRIALS OF CALCIUM AND COLON CANCER CHEMOPREVENTION

Prior to most of the preclinical studies noted above, a first human study was carried out<sup>[28]</sup> which began to evaluate calcium's chemopreventive effects on the human colon. That first study, and a majority of the human studies that followed demonstrated that increased dietary calcium could decrease hyperproliferation of colonic epithelial cells in human subjects; and several studies further demonstrated calcium's binding of bile acids and fatty acids into insoluble complexes in the colon, decreasing the cytotoxicity of fecal water, the latter contributing to the decreased colonic epithelial cell hyperproliferation observed in human subjects (Tables 4,5).

The first pilot study in this human series noted above, and several other that followed, demonstrated significant reduction of excessive colonic epithelial cell proliferation, or reduced size of the proliferative compartment in colonic crypts. However, other human studies of supplemental calcium administration did not show this effect<sup>[42]</sup>. Several of those studies were accompanied by experimental techniques that included extremely low initial baseline levels of colonic cell proliferation measured before calcium administration, very high amounts of calcium intake by subjects before calcium was given, and enemas given prior to colonic biopsies that likely perturbed the mucosa<sup>[42]</sup>. Because early positive results were found in humans where calcium reduced colonic epithelial cell proliferation<sup>[28]</sup>, a further large randomized adenoma-recurrence clinical trial was developed and carried out, recently verifying that increased calcium intake caused a significant reduction in the development of actual tumors (recurrent adenomas) in the human colon<sup>[32]</sup>. A further human study was recently carried out increasing dietary calcium intake through low fat dairy foods: this caused increased maturation and decreased proliferation of colonic epithelial cells following the increased dietary calcium intake<sup>[43]</sup>.

**Table 1 Summary of studies on calcium and colon cancer**

---

·Majority of epidemiologic studies suggest protective effect
· <i>In vitro</i> studies: decreased proliferation and increased differentiation and maturation of many types of epithelial cells
· <i>In vivo</i> rodent studies: numerous studies demonstrated inhibition of colonic tumor development preceded by decreased hyperproliferation, ODC and ras mutations, binding of bile and fatty acids into insoluble complexes reducing irritant and hyperproliferative effects, reduced cytotoxicity of fecal water
·Human studies: decreased hyperproliferation in most studies, increased differentiation and maturation of colonic epithelial cells, binding of bile and fatty acids into insoluble complexes, decreased cytotoxicity of fecal water
·Decreased recurrence of human adenomas

---

**Table 2 Dietary calcium effects on epithelial cells in the colon and other organs of rodents**

Cell proliferation	References*
Calcium decreased hyperproliferation	Gover <i>et al</i> , 1994
Calcium: decreased hyperproliferation when induced by doxycholic acid	Wargovich <i>et al</i> , 1983
Decreased hyperproliferation when induced by fatty acids	Wargovich <i>et al</i> , 1984
Decreased hyperproliferation when induced by cholic acid	Bird <i>et al</i> , 1986
Decreased hyperproliferation induced by partial enteric resection	Appleton <i>et al</i> , 1986
Decreased deoxycholic acid-induced hyperproliferation	Hu <i>et al</i> , 1989
Decreased MNNG-induced hyperproliferation on diet low in fat and calcium	Reshef <i>et al</i> , 1990
Decreased hyperproliferation induced by Western-style diet	Newmark <i>et al</i> , 1991
Decreased AOM-induced ODC and Tyr K	Arlow <i>et al</i> , 1989
Decreased ODC induced by bile acids	Baer <i>et al</i> , 1989
Decreased hyperproliferation when induced by Western-style diet	Richter <i>et al</i> , 1995 <sup>[24]</sup>
Decreased hyperproliferation in other organs when induced by Western-style diet	Xue <i>et al</i> , 1999 <sup>[25]</sup>

\*Studies without reference numbers are found in<sup>[23]</sup>.

**Table 3 Dietary calcium effects on colonic epithelial cells of rodents**

Tumor development	References*
Calcium: decreased tumors induced by partial enteric resection and carcinogen	Appleton <i>et al</i> , 1987
Decreased proliferation and tumor formation induced by dietary fat and carcinogen	Pence <i>et al</i> , 1988
Decreased intestinal tumors after AMO	Skrypec <i>et al</i> , 1988
Decreased colonic tumors induced by AMO	Wargovich <i>et al</i> , 1990
Decreased the number of invasive carcinomas after MNU and cholic acid	McSherry <i>et al</i> , 1989
Decreased the number of rats with multiple tumors after DMH	Sitrin <i>et al</i> , 1991
Decreased K-ras mutations	Llor <i>et al</i> , 1990
Unchanged tumor incidence after DMH	Karkara <i>et al</i> , 1989
Unchanged tumor incidence after DMH	Kaup <i>et al</i> , 1989
Decreased late-stage precancerous lesion of whole colonic crypt dysplasia	Risio <i>et al</i> , 1996 <sup>[26]</sup>

\*Studies without reference numbers are found in [23].

**Table 4 Calcium effects on colonic cell proliferation, differentiation and cytotoxicity in human subjects**

<i>In vitro</i>	References*
Decreased proliferation (2mM)	Buset <i>et al</i> , 1986
Decreased proliferation (2.4mM)	Appleton <i>et al</i> , 1988
Decreased proliferation (2mM)	Arlow <i>et al</i> , 1988
Decreased proliferation (2mM)	Buset <i>et al</i> , 1987
Decreased proliferation (2mM)	Friedman <i>et al</i> , 1989
Protected colonic cells against toxicity of bile acids and fatty acids (5mM)	Buset <i>et al</i> , 1989
Decreased growth of human colon cancer cell lines	Guo <i>et al</i> , 1990 <sup>[27]</sup>
Increased histone acetylation: cell differentiation (1-2mM)	Boffa <i>et al</i> , 1989

\*Studies without reference numbers are found in<sup>[23]</sup>.

**Table 5 Calcium effects on colonic cell proliferation, differentiation and cytotoxicity of fecal water in human subjects**

<i>In vivo</i>	References*
Decreased hyperproliferation	Lipkin <i>et al</i> , 1985 <sup>[28]</sup>
Decreased hyperproliferation	Lipkin <i>et al</i> , 1989
Decreased hyperproliferation	Rozen <i>et al</i> , 1989
Decreased proliferation	Lynch <i>et al</i> , 1991
Decreased proliferation	Berger <i>et al</i> , 1991
Decreased proliferation	Wargovich <i>et al</i> , 1992
Decreased proliferation	Barsoum <i>et al</i> , 1992
Decreased proliferation	O'Sullivan <i>et al</i> , 1993
Decreased proliferation	Bostick <i>et al</i> , 1995
Unchanged proliferation	Gregoire <i>et al</i> , 1989
Unchanged proliferation	Cats <i>et al</i> , 1995
Decreased ODC	Lans <i>et al</i> , 1991 <sup>[29]</sup>
Normalized differentiation-associated lectin binding	Yang <i>et al</i> , 1991 <sup>[30]</sup>
Decreased cytotoxicity of fecal water	Govers <i>et al</i> , 1996 <sup>[31]</sup>
Increased maturation of colonic epithelial cells	Holt <i>et al</i> , 1998 <sup>[43]</sup>
Decreased adenoma recurrence	Baron <i>et al</i> , 1999 <sup>[32]</sup>

\*Studies without reference numbers are found in<sup>[23]</sup>.

## REFERENCES

- 1 Rasmussen H. The calcium messenger system (in 2 parts). *N Engl J Med*, 1986;314:1094,1164
- 2 Whitfield JF, Boynton AL, MacManus JP, Sikorsaka M, Tsang BK. The regulation of cell proliferation by calcium and cyclic AMP. *Mol Cell Biochem*, 1979;27:155-179
- 3 Bakcock MS, Marino MR, Gunning WT III, Stoner GD. Clonal growth and serial propagation of rat esophageal epithelial cells. *In Vitro*, 1983;19:403-415
- 4 Hennings H, Michael D, Chang C, Steinhart P, Holbrook K, Yuspa SH. Calcium regulation of growth and differentiation of mouse epidermal cells in culture. *Cell*, 1980;19:245-254
- 5 McGrath MC, Soule HD. Calcium regulation of normal mammary epithelial cell growth in culture. *In Vitro*, 1984;20:652-662
- 6 Soule HD, McGrath CM. A simplified method for passage and long term growth of human mammary epithelial cell. *In Vitro*, 1985; 22:6-12
- 7 Boffa LC, Mariani MR, Newmark H, Lipkin M. Calcium as modulator of nucleosomal histones acetylation in cultured cells. *Proc Am Assoc Cancer Res*, 1989;30:8
- 8 Niendorf A, Arps H, Dietel M. Effect of 1,25 dihydroxyvitamin D3 on human colon cancer *in vitro*. *J Steroid Biochem*, 1987;27:825-828
- 9 Colston K, Colston MJ, Feldman D. 1,25 Dihydroxyvitamin D3 and malignant melanoma: the presence of receptors and inhibition of cell growth in culture. *Endocrinology*, 1981;108:1083-1086
- 10 Lointier P, Wargovich MJ, Saez S, Levin B, Wildrick DM, Boman BM. The role of vitamin D3 in the proliferation of a human colon cancer cell line *in vitro*. *Anticancer Res*, 1987;7:817-822
- 11 Higgins PJ, Tanaka Y. Cytoarchitectural response and expression of c-fos/p52 genes during enhancement of butyrate initiated differentiation of human colon carcinoma cells by 1,25 Dihydroxyvitamin D3 and its analogs. In: Lipkin M, Newmark HL, Kelloff G, eds. Calcium, vitamin D, and prevention of colon cancer. *Boca Raton: CRC Press*, 1991:305-326
- 12 Miyaura C, Abe E, Kuribayashi T, Tanaka H, Konno K, Nishii Y, Suda T. 1 $\alpha$ ,25 Dihydroxyvitamin D3 induced differentiation of human myeloid leukemia cells. *Biochem Biophys Res Comm*, 1981; 102:937-943
- 13 Kuroki T, Chida K, Hashiba H, Hosoi J, Hosomi J, Sasaki K, Abe E, Suda T. Regulation of cell differentiation and tumor promotion by 1 $\alpha$ ,25 Dihydroxyvitamin D3. In: Humberman E, Barr SH, eds. *Carcinogenesis a comprehensive survey*. New York: Raven Press, 1985:275-286
- 14 Suda T, Miyaura C, Abe E, Kuroki T. Modulation of cell differentiation, immune responses and tumor promotion by vitamin D compounds. *Bone Min Res*, 1986;4:1-48
- 15 Eisman JA, Barkla DH, Tutton PJM. Suppression of *in vivo* growth of human cancer solid tumor xenografts by 1,25 dihydroxyvitamin D-3. *Cancer Res*, 1987;47:21-25
- 16 Honma Y, Hozumi M, Abe E, Konna K, Fukushima M, Hata S, Nishiji Y, Deluca HF, Suda T. 1 $\alpha$ ,25-Dihydroxyvitamin D-3 and 1 $\alpha$ -hydroxyvitamin D-3 prolong survival time of mice inoculated with myeloid leukemia cells. *Proc Natl Acad Sci USA*, 1983;80:201-204
- 17 Chida K, Hashiba H, Fukushima M, Suda T, Kuroki T. Inhibition of tumor promotion in mouse skin by 1 $\alpha$ ,25-dihydroxyvitamin D-3. *Cancer Res*, 1985;45:5426-5430
- 18 Kawaura A, Tanida N, Sawada K, Oda M, Shimoyama T. Supplemental administration of 1 $\alpha$  hydroxyvitamin D-3 inhibits promotion by intrarectal instillation of lithocholic acid in N methyl N-nitrosourea induced colonic tumorigenesis in rats. *Carcinogenesis*, 1989;10:647-649
- 19 Hashiba H, Fukushima M, Chida K, Kuroki T. Systemic inhibition of tumor promoter induced ornithine decarboxylase in 1 $\alpha$ -hydroxyvitamin D-3 treated animals. *Cancer Res*, 1987;47:5031-5035
- 20 Kuroki T, Sasaki K, Chida K, Abe E, Suda T. 1 $\alpha$ ,25 Dihydroxyvitamin D-3 markedly enhances chemically induced transformation in BALB 3T3 cells. *Gann*, 1983;4:611-614
- 21 Jones CA, Callahan MF, Huberman E. Enhancement of chemical carcinogen induced cell transformation in hamster embryo cells by 1,25 dihydroxycholecalciferol, the biologically active metabolite of vitamin D-3. *Carcinogenesis*, 1984;5:1155-1159
- 22 Wood AW, Chang RL, Huang M T, Baggiolini E, Partridge JJ, Uskokovic M, Conney AH. Stimulatory effect of 1 $\alpha$ ,25-dihydroxyvitamin D3 on the formation of skin tumors in mice treated chronically with 7,12 dimethylbenz[ $\alpha$ ]ant hracene. *Biochem Biophys Res Comm*, 1985;130:924-931
- 23 Lipkin M, Newmark H. Calcium and the prevention of colon cancer. *J Cell Biochem*, 1995;22(Suppl):65-73
- 24 Richter F, Newmark H, Richter A, Leung D, Lipkin M. Inhibition of Western diet induced hyperproliferation and hyperplasia in mouse colon by two sources of calcium. *Carcinogenesis*, 1995;16: 2685-2689
- 25 Xue L, Lipkin M, Newmark H, Wang J. Influence of dietary calcium and vitamin D on diet induced epithelial cell hyperproliferation in mice. *J Natl Can Inst*, 1999;91:176-181
- 26 Risio M, Lipkin M, Newmark H, Yang K, Rossini F, Steele V, Boone C, Kelloff G. poptosis, cell replication, and Western style diet induced tumorigenesis in mouse colon. *Cancer Res*, 1996;56: 4910-4916
- 27 Guo YS, Draviam E, Townsend, CM Jr, Singh P. Differential effects of Ca<sup>2+</sup> on proliferation of stomach, colonic, and pancreatic cancer lines *in vitro*. *Nutr Cancer*, 1990;14:149
- 28 Lipkin M, Newmark H. Effect of added dietary calcium on colonic epithelial cell proliferation in subjects at high risk for familial colonic cancer. *N Engl J Med*, 1985;313:1381-1384
- 29 Lans JJ, Jaszewski R, Arlow FL, Tureaud J, Luk GD, Majumdar AP. Supplemental calcium suppresses colonic mucosal ornithine decarboxylase activity in elderly patients with adenomatous polyps. *Cancer Res*, 1991;51:3416-3419
- 30 Yang K, Cohen L, Lipkin M. Lectin soybean agglutinin: measurements in colonic epithelial cells of human subjects following supplemental dietary calcium. *Cancer Lett*, 1991;56:65-69
- 31 Govers MJ, Tremont DS, Lapre JA, Kleibeuker JH, Vonk RJ, Van der Meer R. Calcium in milk products precipitates intestinal fatty acids and secondary bile acids and thus inhibits colonic cytotoxicity in humans. *Cancer Res*, 1996;56:3270-3275
- 32 Baron JA, Beach M, Mandel JS. Calcium supplements for the prevention of colorectal adenomas. *N Engl J Med*, 1999;340: 101-107
- 33 Newmark H, Lipkin M, Maheshwari N. Colonic hyperplasia and hyperproliferation induced by a nutritional stress diet with four components of Western style diet. *J Natl Cancer Inst*, 1990;82: 491-496
- 34 Newmark H, Lipkin M, Maheshwari N. Colonic hyperproliferation induced in rats and mice by nutritional stress diets containing four components of human Western style diet (Series 2). *Am J Clin Nutr*, 1991;54:209-214s
- 35 Fodde R, Edelmann W, Yang K, van Leeuwen C, Carlson C, Renault B, Breukel C, Alt E, Lipkin M, Khan P. A targeted chain termination mutation in the mouse Apc gene results in multiple intestinal tumors. *Proc Natl Acad Sci USA*, 1994;91:8969-8973
- 36 Yang K, Edelmann W, Fan K, Lau K, Kolli VR, Fodde R, Khan M, Kucherlapti R, Lipkin M. A mouse model of human familial adenomatous polyposis. *J Exp Zool*, 1997;277:245-254
- 37 Yang K, Edelmann W, Fan KH, Lau K, Leung D, Newmark H, Kucherlapati R, Lipkin M. Dietary influences on neoplasms in a mouse model for human familial adenomatous polyposis. *Cancer Res*, 1998;58:5713-5717
- 38 Khan N, Yang K, Newmark H, Wong G, Telang N, Rivlin R, Lipkin M. Mammary duct epithelial cell hyperproliferation and hyperplasia induced by a nutritional stress diet containing four components of a Western style diet. *Carcinogenesis*, 1994;15: 2645-2648
- 39 Xue L, Newmark H, Yang K, Lipkin M. Model of mouse mammary gland hyper proliferation and hyperplasia induced by a Western style diet. *Nutr Cancer*, 1996;26:281-287
- 40 Xue L, Yang K, Newmark H, Leung D, Lipkin M. Epithelial cell hyperproliferation induced in the exocrine pancreas of mice by a Western style diet. *J Natl Can Inst*, 1996;88:1586-1590
- 41 Xue L, Yang K, Newmark H, Lipkin M. Induced hyperproliferation in epithelial cells of mouse prostate by a Western style diet. *Carcinogenesis*, 1997;18:995-999
- 42 Lipkin M, Newmark H. Chemoprevention studies: controlling effects of initial nutrient levels. *J Natl Can Inst*, 1993;85:1870-1871
- 43 Holt P, Atallosoy E, Gelman J, Guss J, Moss S, Newmark H, Fan K, Yang K, Lipkin M. Modulation of abnormal colonic epithelial cell proliferation and differentiation by low fat dairy foods. *JAMA*, 1998;280:1074-1079

# A DNA delivery system containing listeriolysin O results in enhanced hepatocyte-directed gene expression

Cherie M. Walton, Catherine H. Wu and George Y. Wu

**Subject headings** DNA; gene expression; listeriolysin O; hepatocytes

## Abstract

**AIM** To determine whether incorporation of the pH-dependent bacterial toxin listeriolysin O (LLO) into the DNA carrier system could increase the endosomal escape of internalized DNA and result gene expression.

**METHODS** A multi-component delivery system was prepared consisting of asialoglycoprotein (ASG), poly L-lysine (PL), and LLO. Two marker genes, luciferase and  $\beta$ -galactosidase in plasmids were complexed and administered *in vitro* to Huh7[ASG receptor (+)] and SK Hep1 [ASG receptor (-)] cells. Purity, hemolytic activity, gene expression, specificity, and toxicity were evaluated.

**RESULTS** An LLO-containing conjugate retained cell-targeting specificity and membranolytic activity. In ASG receptor (+) cells, luciferase gene expression was enhanced by more than 7-fold over that of conjugates without the incorporation of listeriolysin O. No significant expression occurred in ASG receptor (-) cells. Enhancement of  $\beta$ -galactosidase gene expression was less, but still significantly increased over controls. There was no detectable toxicity at concentrations shown to be effective in transfection studies.

**CONCLUSIONS** ASOR-PL can be coupled to LLO using disulfide bonds, and successfully target and increase the gene expression of foreign DNA.

## INTRODUCTION

We have previously demonstrated targeted delivery of DNA to the liver via the recognition of asialoglycoprotein-polylysine (PL) containing conjugates by the hepatic asialoglycoprotein (ASG) receptors<sup>[1,2]</sup>. Binding of the ASG-PL-DNA complexes to the ASG receptors resulted in internalization of the ligand-receptor complex into the cells via receptor-mediated endocytosis. However, a problem with using receptor-mediated endocytosis as a gene delivery system is that once the specific ligand-DNA complex is internalized, it must escape the endosome before delivery to the lysosome in order to avoid intracellular degradation. The endocytosis pathway is somewhat "leaky", which allows for the escape of some DNA without additional membrane disruption. However, most of the delivered genetic material remains trapped in the endosome and is degraded by lysosomal proteases. This may account for low transfection efficiency and transient expression<sup>[3]</sup>.

To address this problem we sought to use the natural properties of a bacterial toxin to enable targeted DNA to escape from endosomal vesicles. Listeriolysin O (LLO) is a pH dependent, thiol-activated, membranolytic protein secreted by the bacteria *Listeria monocytogenes*. LLO is necessary for the pathogenicity of *L. monocytogenes*. Ingested bacteria are taken up by host cells, primarily by macrophages, into phagolysosomes. However, the organism secretes LLO in the phagolysosome, where upon acidification, the LLO undergoes a conformational change, resulting in rupture of the vesicle. Escape of the bacteria from the vesicle occurs before contact with lysosomal enzymes allowing for further replication in the cytosol<sup>[4,5]</sup>.

In the following report, we demonstrate that the incorporation of LLO into the ASG-PL carrier system results in increased gene expression while retaining cell type specificity.

## MATERIALS AND METHODS

### *Synthesis of asialoorosomucoid (ASOR)-PL-LLO conjugates*

ASOR and polylysine were chemically conjugated

Department of Medicine, Division of Gastroenterology-Hepatology, University of Connecticut Health Center, Farmington, CT

**Correspondence to:** George Y. Wu, M.D., Ph.D., Department of Medicine, Division of Gastroenterology-Hepatology, University of Connecticut Health Center, Farmington, CT 06030, USA

Tel.(860)679-3878, Fax.(860)679-3159

Email.Wu@nso.uhc.edu

Received 1999-08-17

using a water soluble carbodiimide as described previously<sup>16,71</sup>. In brief, ASOR, prepared by desialylation of orosomucoid from pooled human serum<sup>61</sup>, was mixed with PL, MW=38500 (Sigma Chemical Co.), in a 1:1 weight ratio. The reactants were coupled by addition of 1-ethyl-3-(3-dimethylaminopropyl)-carbodiimide (Pierce Chemical Co.) and purified by cation exchange chromatography. LLO was purified using a CH<sub>2</sub> spiral concentrator (Amicon) and DEAE Sephacel column (Pharmacia Fine Chemicals)<sup>1181</sup>. The cleavable cross linker N-succinimidyl 3-(2-pyridylidithio) propionate, SPDP, (Pierce Chemical Co.) was added to both ASOR-PL and LLO proteins according to the Pierce protocol. One milligram of both proteins was incubated with 25mM SPDP in dimethylsulfoxide for 30 minutes at room temperature. Free SPDP was separated from linked by application to a PD-10 desalting column (Pharmacia Fine Chemicals) and elution with water. The concentration of SPDP linked to the proteins was determined by measuring the release of 2-thione after reduction with 100 mM DTT and reading the absorbance at 343 nm. The LLO-SPDP was activated for coupling by reduction with 12mg DTT in 100 mM NaCl, 100 mM Na acetate pH 4.5. Free DTT was removed by application to a PD-10 desalting column and elution with water.

#### **Preparation of ASOR-PL-DNA complexes**

The reporter genes used in these experiments were either CMV luciferase (CMV luc) or  $\beta$ -galactosidase ( $\beta$ -gal) plasmid DNA. The ratio of conjugate needed to bind a specific amount of DNA was determined by adding increasing amount of ASOR-PL-SPDP to 1 mg of CMV luc or  $\beta$ -gal plasmid DNA in 0.15 M saline. These samples were run on 1% agarose gels, and the point of DNA retardation was visualized by staining with ethidium bromide and observation with UV. This ratio was used in subsequent experiments. One milligram of the SPDP linked ASOR-PL and CMV luc or  $\beta$ -gal plasmid DNA in the proper proportion were incubated for 30min at room temperature in 0.15M saline. The ASOR-PL-SPDP-DNA complex was added to DTT reduced LLO-SPDP in a 2:1 molar ratio. The conjugate was incubated overnight at 4°C and filtered through a 0.2  $\mu$ m Nalgene syringe filter.

#### **Characterization of protein-DNA complexes**

The conjugate was characterized by Western blotting with polyclonal antibodies to LLO (Immune Response Corporation). One milligram of LLO and the final conjugate either with or without DTT (100 mM) reduction were run on a 7.5% SDS-PAGE gel. The proteins were transferred to a nylon membrane (Amersham), quenched for one hour in 5% dry milk dissolved in 10 mM Tris, 150 mM NaCl

and 0.5% Tween-20, and probed in the same buffer with a polyclonal antibody to LLO. Detection of the antigen-antibody complex was determined by exposure to anti-rabbit IgG horseradish peroxidase (Sigma) and developed with 3',3'-diaminobenzidine and hydrogen peroxide (Sigma)<sup>91</sup>.

To determine if the DNA remained bound conjugates under experimental conditions, agarose gels were run. One microgram of DNA bound to conjugate was run in a 1% agarose gel and visualized with ethidium bromide and UV.

#### **Hemolytic activity**

Hemolytic activity was determined by the adding the conjugate to one milliliter of PBS, pH 5.5, and 5 mM DTT plus  $6 \times 10^8$  human red blood cells. Samples were incubated for 30 minutes at 37 °C and quantified by absorbance at 541 nm on a spectrophotometer. One hemolytic unit (HU) is the amount of LLO needed to release hemoglobin from 50% of the red blood cells<sup>110</sup>.

#### **Targeted gene expression**

Conjugates containing 1  $\mu$ g of CMV luc or  $\beta$ -gal DNA were added to Huh7 (ASG receptor positive) or SK Hep1 (ASG receptor negative) cells in 1 mL of DMEM containing 2 mM CaCl<sub>2</sub> and incubated for 4 h at 37 °C. Then FBS was added to a final concentration of 10% and cells were further incubated for 48 h. ASOR-PL-DNA, ASOR-PL-DNA plus free LLO, and ASOR-PL-LLO-DNA plus a 200-fold excess ASOR were used as controls. Gene expression was measured by luciferase detection using the luciferin substrate (Promega), and detection of activity using a luminometer. Luciferase expression results were standardized by measuring protein concentrations according to the Bradford assay<sup>91</sup>.

Cells incubated with  $\beta$ -gal were washed with PBS pH 7.4, fixed with 4% paraformaldehyde, and stained with X-gal (20  $\mu$ g/L in dimethylformamide) for 30 minutes at 37 °C. Cells were observed with light microscopy and positive (blue stained) cells were counted.

#### **Toxicity studies**

Huh7 and SK Hep1 cells were incubated with ASOR-PL-DNA, free LLO, ASOR-PL-LLO-DNA or ASOR-PL-LLO-DNA in the presence of a 200-fold excess of ASOR in Du lbecco's minimal essential media (DMEM)+2 mM CaCl<sub>2</sub> for 4 h at 37 °C. Fetal bovine serum (FBS) in a final concentration of 10% was added, and the cells were further incubated for 24 and 48 hrs at 37 °C. Cell viability was determined by trypan blue exclusion<sup>111</sup>.

## **RESULTS**

The molar ratio of SPDP linked to ASOR-PL and

LLO, determined by the release of 2-thione after reduction, was found to be 1:1. The ratio of ASOR-PL-SPD P needed to retard migration of DNA in agarose gels was 114:1 moles. ASOR- PL-LLO-DNA complexes were analyzed on a Western blot with a polyclonal antibody to LLO. As shown in Figure 1, purified LLO migrated at a position expected for  $M_r$ 58000, lane 2. Molecular weight markers are shown in lane 1. ASOR-PL alone, as expected, did not bind to the antibody indicating that the ASOR-PL conjugate itself was not capable of non-specific binding with the anti-LLO antibody, lane 3. However, after coupling to LLO, the conjugate did react with anti-LLO antibody, and this conjugate was found not to migrate into the gel, lane 4. No contaminating bands were visualized. Chemical reduction of the complex with DTT resulted in a free band migrating at the position of LLO, lane 5. An agarose gel of the conjugate revealed no migrating bands, indicating that DNA remained bound (data not shown).

The results of hemolytic assays are shown in Table 1. LLO alone, as expected, was highly hemolytic at pH 5.5, but only minimally active at pH 7.4 when concentrations were low. However, at high concentrations, greater than 0.5  $\mu\text{g}/\text{mL}$ , the pH had little effect. Hemolytic assays demonstrated that hemolytic activity of the conjugate was concentration dependent. Similar to LLO alone, the highest activity occurred at pH 5.5. At pH 7.4, the conjugate did not cause appreciable hemolysis. This suggested the conjugation procedure does not appreciably alter the hemolytic characteristics of the LLO, and that at physiological pH, the conjugate has no active LLO.

Figure 2, panel A, shows that prototype ASOR-PL-DNA complexes introduced into Huh7 [ASG receptor positive] cells produced approximately 5000 light units, lane 1. However, compared to the prototype, ASOR-PL-LLO-DNA complexes produced luciferase activity 7 times higher, lane 2. This enhancement was decreased by 60% with the addition of free ASOR to compete with the complex for ASG receptors, lane 3. The addition of free (not conjugated) LLO to ASOR-PL complexes in exactly the same molar concentration as provided by the ASOR-PL-LLO conjugate did not enhance luciferase gene expression, lane 4. This indicates that the observed enhancement of transfection could not be due to the effects of any free LLO. DNA alone had no significant gene expression, lane 5. In SK Hep1 [ASG receptor negative] cells there was no significant gene expression with prototype, lane 1, or ASOR-PL-LLO-DNA complexes, lane 2. Of course, controls consisting of addition of LLO to prototype ASOR-PL complexes, and DNA alone in this cell line alone had no detectable levels of luciferase expression, lanes 3 and 4, respectively.

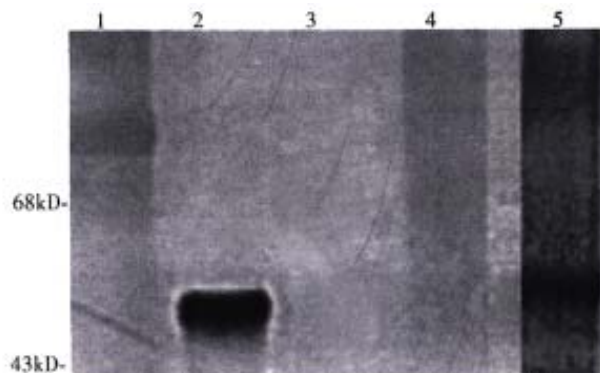


**Figure 1** A Western blot of purified conjugates. One milligram of LLO and the final conjugate either with or without DDT (100mM) reduction were run on a 7.5% SDS-PAGE gel. The proteins were transferred to anylon membrane, quenched, and probed with a polyclonal antibody to LLO. Detection of the antigen-antibody complex was determined by exposure to anti-rabbit IgG horseradish peroxidase and developed with 3',3'-diaminobenzidine and hydrogen peroxide as described in Materials and Methods. Molecular weight markers, lane 1; LLO alone, lane 2; ASOR-PL, lane 3; ASOR-PL-LLO-DNA, lane 4; ASOR-PL-LLO-DNA+100mM DTT, lane 5.

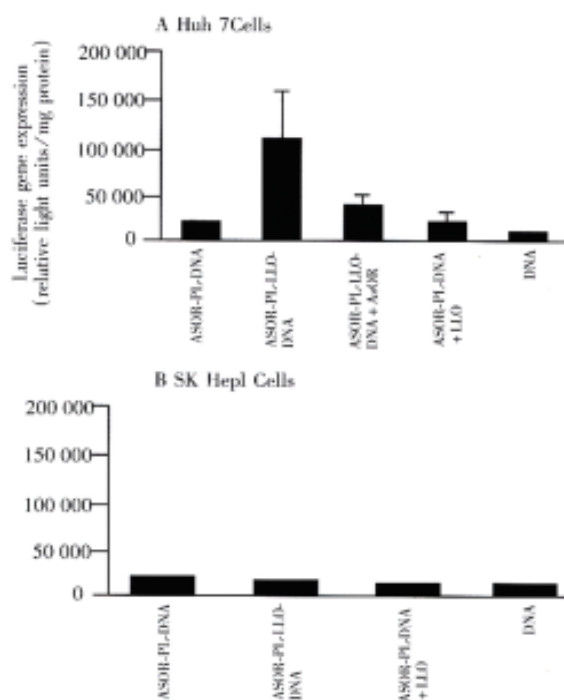


**Figure 2** Targeted luciferase gene expression. Conjugates containing 1  $\mu\text{g}$  of CMV luc were added to Huh7 (ASG receptor positive) or SK Hep1 cells (ASG receptor negative) and incubated for 48h as described in Materials and Methods. Gene expression was measured by luciferase detection using the luciferin substrate, and detection of activity using a luminometer. Luciferase expression results were standardized by measuring protein concentrations according to the Bradford assay. Panel A, Huh7 cells: ASOR-PL-DNA, lane 1; ASOR-PL-LLO-DNA, lane 2; ASOR-PL-LLO-DNA+200-fold molar excess of ASOR, lane 3; ASOR-PL-DNA+LLO, lane 4; DNA alone, lane 5. Panel B, SK Hep1 cells: ASOR-PL-DNA, lane 1; ASOR-PL-LLO-DNA, lane 2; ASOR-PL-DNA+LLO, lane 3; DNA alone, lane 4.

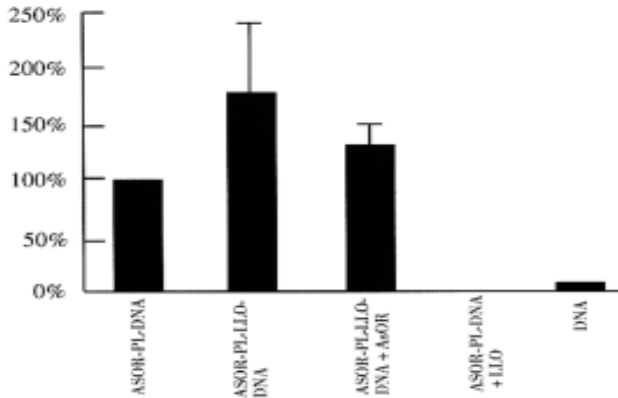


**Figure 3** Targeted  $\beta$ -galactosidase gene expression. Conjugates containing  $1\mu\text{g}$  of  $\beta$ -gal DNA were added to Huh7 (ASG receptor positive) or SK Hep1 cells (ASG receptor negative) and incubated for 48h. Cells incubated with  $\beta$ -gal were washed with PBS pH 7.4, fixed with 4% paraformaldehyde and stained with X-gal as described in Materials and Methods. Cells were observed with light microscopy and positive (blue stained) cells were counted. ASOR-PL-DNA, lane 1; ASOR-PL-LLO-DNA, lane 2; ASOR-PL-LLO-DNA+ASOR, lane 3; ASOR-PL-DNA+LLO, lane 4; DNA alone, lane 5.

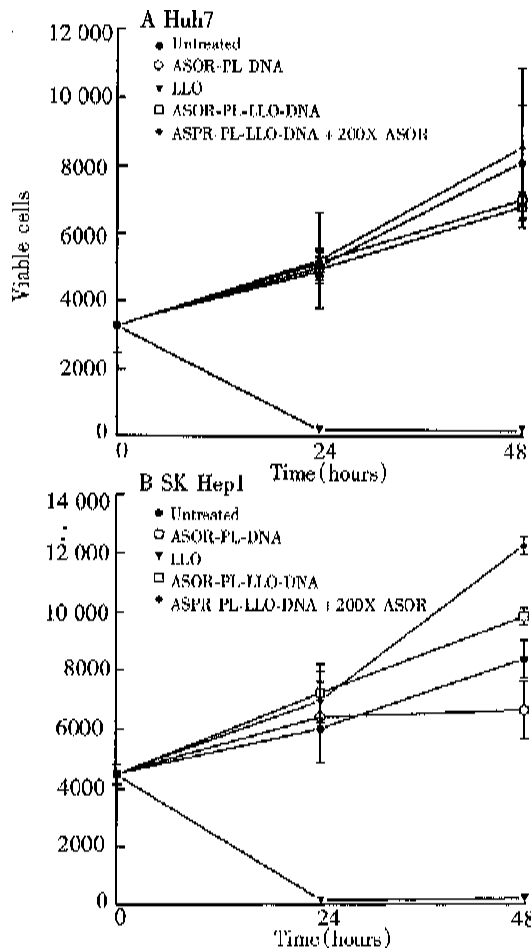


**Figure 4** Toxicity of complexes. Huh7 (ASG receptor positive) and SK Hep1 (ASG receptor negative) cells were incubated with ASOR-PL-DNA, free LLO, ASOR-PL-LLO-DNA or ASOR-PL-LLO-DNA in the presence of a 200-fold excess of ASOR as described in Materials and Methods. Cell viability was determined by trypan blue exclusion. Panel A, Huh7 cells; Panel B SK Hep1 cells.

**Table 1** Hemolytic activity\* of ASOR-PL-LLO and LLO alone

LLO ( $\mu\text{g}$ )	LLO		ASOR-PL-LLO-DNA	
	pH 5.5	pH 7.4	pH 5.5	pH 7.4
0.005	1.000	0.024	0	0
0.010	1.380	0.051	0	0
0.050	1.680	0.074	0.010	0
0.100	1.900	1.280	0.021	0
0.500	1.900	1.730	0.349	0
1.000	2.100	1.900	0.947	0.013
2.000	2.100	2.100	1.900	0.020

\*A<sup>541</sup> where 100% hemolysis a value of 2.100.

Figure 3 shows the results of studies of Huh7 cells transfected with a gene for  $\beta$ -galactosidase. The ASOR-PL-LLO-DNA complex containing  $\beta$ -gal DNA increased gene expression 185% over prototype ASOR-PL complexes (complex lacking LLO), lane 2. The enhancement was inhibited by 30% with addition of a 200-fold excess ASOR, lane 3. ASOR-PL-DNA plus free LLO, and DNA alone had no significant gene expression, lanes 4 and 5, respectively.

In order to determine whether the LLO-containing conjugate was toxic, cell viability studies were performed and the results are shown in Figure 4. Huh7 and SK Hep1 cells, panels A and B respectively, treated with ASOR-PL-DNA, ASOR-PL-LLO-DNA with or without an excess of ASOR proliferated at the same rate as control (untreated) cells. However, LLO alone in the same concentration as present in the ASOR-PL-LLO-DNA rapidly decreased viable cell numbers. Thus, the concentration of complexes used for expression studies were found not to be toxic to either Huh7 or SK Hep1 cells.

**DISCUSSION**

Many approaches have been developed to solve the problem of low transfection efficiency and transient expression of gene delivery systems. Partial hepatectomy, chloroquine administration, and viruses or viral peptides have shown to be useful in increasing in the duration of expression<sup>[6,12-16]</sup>. The current report is the first demonstration that the natural escape strategies of the bacterial toxin LLO can be useful as a potential component of a targetable DNA delivery system to increase efficiency<sup>[4,5]</sup>.

LLO is a thiol-containing protein<sup>[5]</sup>. Experiments on direct bonding to ASOR-PL-SPDP resulted in low efficiency (data not shown). In subsequent experiments LLO was also treated with SPDP to increase the number of potential cross linking residues. Subsequent reduction with DTT resulted in successful conjugation.

The conjugated LLO had lower hemolytic activity compared to equal amounts of free LLO.

This was in spite of the fact that DTT is added to samples to activate the thiol groups. This reduction would also cleave coupled LLO from the conjugate. The lower molar activity of the released LLO may have been due to the addition of SPDP, or to interference from ASOR or DNA that was independent of thiol reduction. Nevertheless, the hemolytic activity of the conjugate was pH dependent as seen with native LLO. This is important as one of the theoretical advantages for the use of LLO was the lack of activity at physiological pH, and restored activity in the acidic environment of the endosome. Toxicity due to extracellular activity would be minimized.

In summary, the above experiments show that ASOR-PL can be coupled to LLO using disulfide bonds, and successfully target and increase the gene expression of foreign DNA. The increase in expression was blocked with the addition of a large molar excess of ASOR, and was present only in ASG receptor positive cells, indicating retention of hepatocyte specificity.

**ACKNOWLEDGMENTS** The technical assistance of Ying Zhang, and the secretarial assistance of Martha Schwartz are gratefully acknowledged. This work was supported in part by a grant from the National Institutes of Health, DK -42182 (GYW), the Immune Response Corporation (GHW), and the Herman Lopata Chair for Hepatitis Research.

## REFERENCES

- 1 Wu GY, Wu CH. Receptor mediated *in vitro* gene transformation by a soluble DNA carrier system. *J Biol Chem*, 1987;262:4429-4432
- 2 Wu GY, Wu CH. Receptor mediated gene delivery and expression *in vivo*. *J Biol Chem*, 1988;263:14621-14624
- 3 Cotten M, Baker A, Saltik M, Lehmann H, Panzenbock B, Chiocca S. Receptor mediated gene delivery. In: Blum HE, ed. *Molecular diagnosis and gene therapy*. Boston MA: Kluwer Academic Publishers, 1996:80-91
- 4 Geoffrey C, Gaillard JL, Alouf FE, Berche P. Purification, characterization and toxicity of the sulfhydryl activated hemolysin listeriolysin O from *Listeria monocytogenes*. *Infect Immun*, 1987; 55:1641-1646
- 5 Vasquez Boland JA, Dominguez L, Rodriguez-Ferri EF, Suarez G. Purification and characterization of two *Listeria ivanovii* cytolytins, a sphingomyelinase C and a thiol activated toxin (ivanolysin O). *Infect Immun*, 1989;57:3928-3935
- 6 Wu GY, Zhan P, Sze LL, Rosenberg AR, Wu CH. Incorporation of adenovirus into a ligand based DNA carrier system results in retention of original receptor specificity and enhances targeted gene expression. *J Biol Chem*, 1994;269:11542-11546
- 7 McKee TD, DeRome ME, Wu GY, Findeis MA. Preparation of asialoorosomucoid polylysine conjugates. *Bioconj Chem*, 1994;5: 306-311
- 8 Walton CM, Wu CH, Wu GY. A method for purification of listeriolysin O from a hypersecretor strain of *Listeria monocytogenes*. *Prot Express Purif*, 1999;15:243-245
- 9 Harlowe E, Lane D (eds). *Antibodies, a laboratory manual*. Cold Spring Harbor Laboratories, 1988
- 10 Cossart P, Vicente MF, Mengaud J, Baquero F, Perez Diaz JC, Berche P. Listeriolysin O is essential for virulence of *Listeria monocytogenes*: direct evidence obtained by gene complementation. *Infect Immun*, 1989;57:3629-3636
- 11 Garvey JS, Cremer NE, Sussendorf DN (eds). *Methods in immunology*. 3rd ed. Reading MA: WA Benjamin, Inc, 1997:449
- 12 Wu CH, Wilson JM, Wu GY. Targeted genes: delivery and persistent expression of a foreign gene driven by mammalian regulatory elements *in vivo*. *J Biol Chem*, 1989;264:16985-16987
- 13 Roy Chowdhury N, Hays RM, Bommineni VR, Franki N, Roy Chowdhury J, Wu CH, Wu GY. Microtubular disruption prolongs the expression of human bilirubinuridinediphosphoglucuronate glucuronyl transferase1 gene transferred into Gunn rats livers. *J Biol Chem*, 1996;271:2341-2346
- 14 Feng M, Jackson WH Jr, Goldman CK, Rancourt C, Wang M, Dusing SK, Siegal G, Curiel DT. Stable *in vivo* gene transduction via a novel adenoviral/retroviral chimeric vector. *Nat Biotech*, 1997;15:866-870
- 15 Schlegel R, Wade M. Biologically active peptides of the vesiculo stomatitis virus glycoprotein. *J Virol*, 1985;53:319-323
- 16 Wagner E, Plank C, Zatloukal K, Cotton M, Birmstiel ML. Influenza virus hemagglutinin HA 2 N terminal fusogenic peptides augment gene transfer by transferring polylysine DNA complexes: toward a synthetic virus like gene transfer vehicle. *Proc Natl Acad Sci USA*, 1992;89:7934-7938

Edited by MA Jing-Yun  
Proofread by MIAO Qi-Hong

# Characterization of six tumor suppressor genes and microsatellite instability in hepatocellular carcinoma in southern African blacks

C. Martins, M.A. Kedda, M.C. Kew\*

**Subject headings** carcinoma, hepatocellular; southern African blacks; cumulative LOH; tumor suppressor genes; microsatellite genomic instability; liver neoplasms

## Abstract

**AIM** To analyse cumulative loss of heterozygosity (LOH) of chromosomal regions and tumor suppressor genes in hepatocellular carcinomas (HCCs) from 20 southern African blacks.

**METHODS** *p53*, *RB1*, *BRCA1*, *BRCA2*, *WT1* and *E-cadherin* genes were analysed for LOH, and *p53* gene was also analysed for the codon 249 mutation, in tumor and adjacent non-tumorous liver tissues using molecular techniques and 10 polymorphic microsatellite markers.

**RESULTS** *p53* codon 249 mutation was found in 25% of the subjects, as was expected, because many patients were from Mozambique, a country with high aflatoxin B<sub>1</sub> exposure. LOH was found at the *RB1*, *BRCA2* and *WT1* loci in 20%(4/20) of the HCCs, supporting a possible role of these genes in HCC. No LOH was evident in any of the remaining genes. Reports of mutations of *p53* and *RB1* genes in combination, described in other populations, were not confirmed in this study. Change in microsatellite repeat number was noted at 9 / 10 microsatellite loci in different HCCs, and changes at two or more loci were detected in 15%(3/20) of subjects.

**CONCLUSION** We propose that microsatellite/genomic instability may play a role in the pathogenesis of a subset of HCCs in black Africans.

## INTRODUCTION

The evolution of cancer is thought to occur from the stepwise accumulation of genetic aberrations in the same cell. These include loss of function of tumor suppressor genes, activation of proto-oncogenes, faulty DNA mismatch repair, and the integration of viral DNA<sup>[1,2]</sup>. Hepatocellular carcinoma (HCC) is a leading cause of death in both Africa and the Far East, resulting in at least 310000 deaths worldwide each year<sup>[3]</sup>. HCC is multifactorial in aetiology and its pathogenesis is complex. The major risk factors involved in the development of the tumor are chronic HBV and HCV infections, cirrhosis and aflatoxin B<sub>1</sub> (AFB) exposure<sup>[4,5]</sup>.

Heavy dietary AFB intake is thought to cause a guanine (G) to thymine (T) transversion at the third base of codon 249 of the *p53* gene, and for this reason clustering of this point mutation occurs in HCCs from Africa and China<sup>[6-8]</sup>. In addition, other mutations in, or deletions of, the *p53* gene (on chromosome 17p13.1) are found with relatively high frequency in human HCCs in other countries. The functional loss of this tumor suppressor gene, as well as its abnormal expression, have been proposed to play a significant role in HCC development<sup>[9]</sup> or at least in the development of a subset of HCCs. The majority of *p53* alterations reported to date have loss of one allele accompanied by mutations of the second allele<sup>[10]</sup>. Abnormalities of the *p53* gene, such as gene mutation, deletion, or the nuclear accumulation of mutant *p53* protein have also been found to correlate with increased allelic loss at the Breast Cancer Susceptibility Gene 1 (*BRCA1*) locus (17q21). This gene is thought to encode a transcription factor which acts as a tumor suppressor<sup>[11]</sup>. LOH of the *BRCA1* gene in HCC was reported in a Korean study<sup>[12]</sup>. The Breast Cancer Susceptibility Gene 2 (*BRCA2*) (13q12-13) product is thought to be a tumor suppressor<sup>[13]</sup> involved in cellular proliferation and differentiation<sup>[14]</sup>, and may be involved in the development of HCC<sup>[15]</sup>. LOH at the *BRCA2* locus has been reported in HCC<sup>[15,16]</sup> and it has been suggested that mutations of the *BRCA2* gene may be involved in hepatocarcinogenesis<sup>[15]</sup>. The retinoblastoma (*RB1*) gene (13q14.2) product (*pRB*) functions as a cell cycle regulator<sup>[17]</sup>, and its

MRC/CANSA/University Molecular Hepatology Research Unit, Department of Medicine, University of the Witwatersrand Medical School, 7 York Road, Parktown 2193, Johannesburg, South Africa. Supported in part by grants/bursaries from the University of the Witwatersrand, and the Foundation for Research Development, Pretoria, South Africa.

**Correspondence to:** Professor M.C. Kew, Department of Medicine, Medical School, 7 York Road, Parktown, 2193, Johannesburg, South Africa.

Tel. +27(0)11 488 3626, Fax. +27(0)11 643 4318

Email:014anna@chiron.wits.ac.za

Received 1999-08-10

absence leads to unrestricted cell growth. Although there is no definite evidence that mutations of the RB gene are involved in HCC, LOH of the RB1 gene has been documented in human HCCs<sup>[18,12]</sup>. LOH of WT1 and 11p13 have been reported in human HCCs<sup>[12,16]</sup>. WT1 appears to be involved in proliferation, differentiation and apoptosis<sup>[19,20]</sup>. The product of the E-cadherin (Uvomorulin) gene (16q221) is the primary adhesion molecule in epithelium<sup>[21]</sup>. Loss of function of E-cadherin may lead to decreased cell-cell adhesion<sup>[22]</sup>, cellular phenotypic changes, and the development of invasive properties<sup>[23]</sup>. In HCC, multicentric development and the formation of intrahepatic metastases is common<sup>[24]</sup>. LOH on chromosome 16q has been previously reported to be important in the initiation or progression of HCC<sup>[25,26]</sup>.

Polymerase chain reaction (PCR) amplification of microsatellites (sequences uniformly distributed throughout the human genome) provides a simple and effective method of rapidly detecting loss of heterozygosity/microsatellite instability (LOH/MI)<sup>[27]</sup>. Microsatellite instability is defined as the loss or gain of microsatellite repeats at 2 or more loci and is detected by the presence of extra bands or band shifts between tumor and non-tumorous tissue DNA.

In this study, we examined the G-T transversion at codon 249 of the *p53* gene, LOH of the *p53*, RB1, BRCA1, BRCA2, WT1 and E-cadherin genes, and microsatellite instability at 10 loci flanking these genes, in HCC and adjacent non-tumorous liver, from 20 southern African blacks.

## MATERIALS AND METHODS

### Subjects

The subjects included 20 southern African black men, aged between 20 and 40 years. HCC tissue and matched non-tumorous liver were obtained at necropsy or during surgical resection. DNA was extracted from the tissues using a modified "salting-out" procedure<sup>[28]</sup>.

### HBV markers

The HBV status of the subjects was determined previously using commercially available kits to detect HBV markers in serum (Abbott Labs, Chicago, IL, USA).

### LOH and microsatellite instability

Microsatellite instability (MI) and loss of heterozygosity (LOH) studies were carried out by PCR and gel electrophoresis using polymorphic repeat markers (Table 1).

PCR products of the polymorphic loci *p53*, D17S846 and RB1.20 were resolved on 4%

composite agarose gels, while radioactively labeled PCR products of the remaining loci were resolved on polyacrylamide gels, and viewed by autoradiography. Band mobility shifts between tumor and matched non-tumorous liver DNA were scored as a change in allele repeat number. LOH was characterized by the disappearance of one band or a considerable (≥80%) decrease in band intensity in heterozygotes, whilst microsatellite instability was determined by expansion and/or contraction of microsatellite sequences.

### PCR for LOH and MI

A standard PCR protocol (primers, Table 1) was followed for the *p53*, WT1, D13S137, RB(1.20), D13S120, D13S127, D17S855, and D17S846 loci. Each PCR reaction consisted, at final volume, of 100ng DNA, 1U *Taq* DNA polymerase (Promega, Madison, USA), 1×buffer, 1 mM each dATP, dTTP, dGTP, 0.1 mM dCTP, 0.025 μCi α<sup>32</sup>P dCTP, and 50 pmol of each primer; in a total volume of 50 μL, amplification for 30 cycles of denaturation at 94 °C for 30 s, annealing 55 °C for 30 s, extension at 72 °C for 1min, and a final cycle of 72 °C for 10 minutes.

The PCR reaction for the D16S301 and D16S260 loci (primers, Table 1) consisted, at final volume, of 100 ng DNA, 1U *Taq*-DNA Polymerase, 1×buffer, 0.1 % gelatin, 1 mM each dGTP, dATP, dTTP, 0.1 mM dCTP, and 0.025 μCi α<sup>32</sup>P dCTP, 50 pmol of each primer; in a total volume of 25 μL, amplification for 25 cycles of denaturation at 94 °C for 1 min, annealing at 55 °C for 2 min, extension at 72 °C for 2.5 min, and a final cycle of 72 °C for 10 minutes.

### *p53* codon 249 mutation

The *p53* codon 249 mutation was detected by PCR-RFLP using primer sequences F3 and R3 (Table 1), and confirmed by sequence analysis. The PCR reaction consisted of, at final volume<sup>[6]</sup>, 100 ng DNA, 2.5U of *Taq*-DNA polymerase (Promega), 1×buffer, 1mM MgCl<sub>2</sub>, 0.8 mM each of dCTP, dATP, dGTP, dTTP, and 50 pmol of each primer; in a total volume of 50 μL, amplification for 30 cycles of denaturation at 94 °C for 15 s, annealing at 56 °C for 15 s, and extension at 72 °C for 30 s. The 110 bp PCR product was sized on ethidium bromide stained agarose gels against a 100 bp DNA ladder (Promega). AG to T transversion at the third base of codon 249 was detected by the presence or absence of a *Hae*III restriction site<sup>[6]</sup>. All samples shown by digestion to have the codon 249 mutation were sequenced in both directions both upstream and downstream in separate reactions, to confirm the presence of the mutation.

**Table 1 PCR primers**

Gene/Locus	Primer	Primer sequence	Amplicon	Amplicon length
<i>p53</i>	<i>p53F3</i> <i>p53R3</i>	5'GTTGGCTCTGACTGT-ACCAC 5'CTGGAGTCTTCCAGT-GTGAT	exon 7 spanning codon 249 <sup>[6]</sup>	110bp
<i>p53</i>	<i>p53ivs1a</i> <i>p53ivs1b</i>	5'GCACTTTCCTCAACTCTACA 5'AACAGCTCCTTTAATGGCAG	ALU sequence within intron 1 of <i>p53</i> gene <sup>[43]</sup>	200bp-300bp
D13S120 (BRCA2)	1353L 1353R	5'ATGACCTAGAAATGATACTGGC 5'CAGACACCACAACACACATT	(AC) <sub>73</sub> repeat at D13S120 <sup>[44]</sup>	112bp-136bp
D17S846 (BRCA1)	FF RF	5'TGCATACCTGTACTACTTCAG 5'TCCTTTGTTGCAGATTCTTC	(GGAA) <sub>25</sub> repeat at D17S846 <sup>[45]</sup>	250bp-300bp
D17S855 (BRCA1)	FS RS	5'GGATGGCCTTTTAGAAAGTGG 5'ACACAGACTTGTCTACTGCC	AC repeat at D17S855 <sup>[46]</sup>	145bp
WT1	400 401	5'AATGAGACTTACTGGGTGAGG 5'TTACACAGTAATTTCAAGCAACGG	AC repeat within 3' untranslated sequence of WT33 <sup>[47]</sup>	100bp-200bp
RB1	B57 B103	5'TGTATCGGCTAGCCTATCTC 5'AATTAACAAGGTGTGGTGGT	[CTTT(T)] <sub>n</sub> (n=14-26) repeat within intron 20 of RB gene <sup>[48,49]</sup>	400bp-600bp
D13S127 (BRCA2/RB1)	1341L 1341R	5'CAGATATGTACTCATGCACATG 5'AAACAAATGAGTTGGCTGT	(AC) <sub>35</sub> repeat at D13S127 <sup>[44]</sup>	130bp-142bp
D13S137 (RB1)	F R	5'TTTCCTCATCTTTCCCAATTG 5'CAGGAGGGATGGACTCACTTC	(GT) <sub>22</sub> repeat at D13S137 <sup>[50]</sup>	±135bp
E-cadherin	E-cadF1 E-cadF1	5'GATCCTAAGGACAAATGTAGATGCTCT 5'AGCCACTTCCCAGAAGTTGGCTTCC	D16S301 locus polymorphic AC region <sup>[51]</sup>	146bp
E-cadherin	E-cadF2 E-cadR2	5'GGTTGAGATGCTGACATGC 5'CAGGGTGGCTGTTATAATG	D16S260 locus polymorphic AC repeat region <sup>[52]</sup>	±234bp

Note: WT1: Wilm's tumor gene; RB1: Retinoblastoma gene; BRCA1: Breast cancer susceptibility gene 1; BRCA2: Breast cancer susceptibility gene 2; bp: base pairs.

### Sequencing

All sequencing was carried out using the Sequenase PCR Product Sequencing Kit (United States Biochemical Corp., Cleveland, Ohio), according to the manufacturer's instructions.

## RESULTS

### HBV status

Seven patients were currently infected with HBV (5 of these were HBsAg-positive; HBeAg-negative; the HBeAg status of the remaining 2 was unknown), and 6 were previously infected (anti-HBc and anti-HBs-positive). The HBV status of the remaining patients was not known (Table 2).

### LOH/MI analyses

LOH was noted for the WT1 (1/13 subjects), RB (1.20) (1/10 subjects), D13S120 (1/20 subjects) and D13S127 (2/14 subjects) loci (Table 2).

The D13S137 and D13S127 loci flank the RB1 gene, while the RB (1.20) repeat sequence is within intron 20 of the same gene. LOH at the D13S127 locus suggests loss of at least a portion of the RB1 gene as shown in 2/14 informative subjects. LOH at RB (1.20) indicated loss of the RB1 gene in a

further 1/10 informative subjects. The RB1 gene was thus lost in 3/18 informative subjects (Table 2). LOH at the D13S120 and D13S127 loci flanking the BRCA2 gene was shown in 2/20 informative subjects (Table 2). No LOH was found for any of the remaining loci (Table 2).

Microsatellite/genomic instability (or a gain/loss of microsatellite repeats) was found in 15% (3/20) of subjects.

### *p53* gene codon 249 analysis

The *p53* codon 249 mutation was detected in 25% of the subjects using PCR-RFLP analysis, and confirmed by sequencing. The *p53* codon 249 mutation was detected in the tumor tissue of 3 subjects, in the non-tumorous liver of 1 subject, and in both the tumor and non-tumorous liver tissue of 1 subject (Table 2).

Sequencing gel electrophoresis of the *p53* gene product revealed a gel artifact, in all subjects with wild-type chromosomes, previously described by Kapelner *et al* (1994).

All tumors were at an advanced stage. No attempt was made to correlate the presence of LOH or microsatellite instability with clinical or other features.

Table 2 LOH, SSCP and sequence analysis

Subject number	VNTRs											p53 codon 249		HBV status
	p53	WT1	RB1		BRCA2		BRCA1		E-cadherin		T	NT		
	(ALU)	(AC)	D13S137 (GT) <sub>22</sub>	RB1.20 [CTTT(T)] <sub>n</sub>	D13S120 (AC) <sub>73</sub>	D13S127 (AC) <sub>35</sub>	D17S855 (AC)	D17S846 (GGAA) <sub>25</sub>	D16S301 (AC)	D16S260 (AC)				
1	NI	NI	-	-	-	NI	-	-	-	NI	-/-	-/-	HBsAg+; HBeAg-	
2	-	-	-	-	-	NI	-	-	-	NI	-/-	-/-	HBsAg+	
3	-	-	-	-	-	-	-	-	NI	-	+/-	-/-	HBsAg+; HBeAg-	
4	-	-	-	NI	-	-	?	NI	-	-	-/-	-/-	anti-HBc+; anti-HBs+	
6	-	?	?	?	-	NI	?	-	?	-	+/-	-/-	HBsAg+; HBeAg-	
7	?	?	?	?	-	-	?	?	-	-	-/-	-/-	anti-HBs+; anti-HBc+	
8	↑	△	NI	+	↓	↓	△	△	↑	-	+/-	-/-	anti-HBs+; anti-HBc+	
14	-	NI	?	NI	-	+	-	?	?	NI	-/-	-/-	anti-HBs+; anti-HBc+	
16	?	?	△	?	+	+	?	?	△	↑	-/-	-/-	HBsAg+	
18	↑	+	?	?	↑	-	?	?	?	↑	-/-	-/-	HBsAg+; HBeAg-	
24	NI	-	NI	-	-	-	-	-	NI	-	-/-	+/-	anti-HBs+; anti-HBc+	
39	-	NI	-	?	-	-	-	NI	?	-	-/-	-/-	HBsAg+; HBeAg-	
40	NI	-	?	-	-	NI	-	-	?	-	-/-	-/-	anti-HBs+; anti-HBc+	
48	NI	-	-	-	-	-	-	-	?	?	-/-	-/-	?	
50	NI	-	-	NI	-	-	-	NI	-	NI	-/-	-/-	?	
51	NI	-	?	NI	-	NI	-	-	-	-	-/-	-/-	?	
52	NI	-	NI	-	-	NI	-	-	-	-	+/-	-/-	?	
53	-	-	-	-	-	-	-	-	NI	-	-/-	-/-	?	
54	-	?	-	-	-	-	-	-	-	NI	-/-	-/-	?	
56	NI	-	-	NI	-	-	-	NI	NI	NI	-/-	-/-	?	

Note: LOH: loss of heterozygosity; -: HBV status-negative for particular antigen/antibody, mutation studies-mutation absent; LOH studies: no LOH; →p53 codon 249 mutation analysis: G→T transversion absent; +: HBV status-positive for particular antigen/ antibody, mutation studies-mutation present, →LOH studies: LOH, →p53 codon 249 mutation analysis: G→T transversion present;

?: results not obtained because of unsuccessful PCR or HBV status unknown; △: a change in repeat number between tumor (T) and non-tumorous liver (NT) in both chromosomes; ↑ / ↓ : an increase/decrease in repeat number between tumor (T) and non-tumorous liver (NT) in one chromosome; NI: not informative; VNTRs: Variable number of tandem repeat sequences; HBV: Hepatitis B virus; WT1: Wilm's tumor gene; RB1: Retinoblastoma gene; BRCA1: Breast cancer susceptibility gene 1; BRCA2: Breast cancer susceptibility gene 2; HBsAg: hepatitis B virus S antigen; HBeAg: hepatitis B virus E antigen; anti-HBs: antibody to hepatitis B virus S antigen; anti-HBc: antibody to hepatitis B virus C antigen

## DISCUSSION

LOH of the *p53* gene has been reported with relatively high frequency in HCCs from Japan (29%-69%)<sup>[29,30]</sup>, and also from southern Africa (60%), and Taiwan (39.3%)<sup>[6,31]</sup>. No LOH was detected for *p53* in this study, although inactivation/reduction of *p53* gene expression or of its product by means other than LOH may have occurred in our population. In a study by Walker *et al* (1991), *p53* allele loss occurred only in HBV-negative tumors. It thus appeared as if a mechanism other than loss of one *p53* allele and mutation of the second allele was operating in HBV-positive tumors, thereby eliminating fully functional *p53* protein. The obvious mechanism would be the formation of complexes between wild-type *p53* protein and viral protein/s leading to the loss of function of wild-type *p53* protein. Such associations have been well documented in the literature<sup>[32]</sup>. In our study most samples were HBV positive and a mechanism such as that mentioned above, rather than *p53* gene inactivation by physical mutation and LOH, may have been operating in our tumors to eliminate the function of the *p53* protein. Alternatively, should

both alleles of the *p53* gene be mutated in ways other than LOH in our samples, such as point mutations and small deletions (<50bp)<sup>[18]</sup>, these would not have been detected by the techniques employed in this study.

The *p53* codon 249 mutation was detected in 25% (5/20) subjects. This was expected as the subjects were southern African blacks, some of whom came from Mozambique and other areas where aflatoxin exposure is prevalent. The *p53* codon 249 mutation was found in both tumor and non-tumorous liver tissues of one subject. This could have been caused by contamination of the non-tumorous liver with tumor tissue. In another subject the mutation was detected in the non-tumorous liver only. The presence of this mutation has been documented in non-tumorous liver and not in the corresponding tumor tissues<sup>[33]</sup>, where it was proposed that normal liver subjected to prolonged aflatoxin exposure could gradually accumulate high levels of AGT mutations, whereas the mutation would not necessarily arise in neoplastic populations that were cloned from single progenitor cells resistant to aflatoxin. Unfortunately, insufficient

tissue was available in these two patients for histopathological examination, so we cannot exclude microscopic contamination as a cause of this finding in the two subjects. Two patients with a codon 249 G $\rightarrow$ T transversion were HBsAg positive, 2 subjects were anti-HBs/anti-HBc positive and the HBV status of 1 subject was unknown. This concur red with previous studies where mutations at codon 249 were not found in non-HB V-related HCCs<sup>[34]</sup>, and is in agreement with previous work which suggests that both aflatoxin exposure and HBV infection are required for this mutation to occur<sup>[29,33]</sup>.

A gel artefact generated by formation of a mini hairpin secondary structure in the codon 249 region of the *p53* gene in 34 wild type chromosomes, lead to a "missing" G at the third base of codon 249 in the sequence of the sense strand<sup>[35]</sup>. In a study by Kapelner *et al* (1994), as with our samples, Hae-III digest confirmed the presence of the recognition sequence GGCC. However, since there has been no other report of this "G deletion" in such a commonly sequenced region, Kapelner *et al* (1994) suggested that this artifact may not occur often.

LOH appears to have occurred in 4 subjects at the RB1 (3/18 or 17%), BRCA2 (2/20 or 10%) and WT1 (1/13 or 8%) loci (2 of these subjects had LOH at both the RB1 and BRCA2 genes). Although reduction to homozygosity has been apparent in certain individuals, and has consistently been scored as LOH, 'band disappearance' may also be caused by a gain/loss in microsatellite repeats. We think, however, that this is unlikely to be the case in so many individuals.

LOH of the retinoblastoma gene has been documented in 33% of HCCs from Korea<sup>[12]</sup>, 16%-73% of HCCs from Japan<sup>[18,30]</sup> and 27% of HCCs from Australia<sup>[36]</sup>. One copy of the RB1 gene was lost in 17% (3/18) of HCCs in this study. Although our sample is small, this frequency differs from the higher percentages found thus far. This may reflect population differences, LOH of the RB1 gene may play a role in a small subset of southern African HCCs. Coincident mutation of the *p53* and RB1 genes has been observed in 25%<sup>[18]</sup>, and 12.9%<sup>[37]</sup> of advanced HCCs in Japan and Australia respectively<sup>[36]</sup>. Mutations and LOH in these genes is most frequently observed in advanced stage HCCs, like those investigated here. However, no coincident mutation of these genes was detected in this study.

LOH of the BRCA2 gene has been reported in 3% of Japanese HCCs<sup>[15]</sup>, and in 40% of HCCs from the USA<sup>[16]</sup>. In this study one copy of the BRCA2 gene was lost in 10% (2/20) HCCs. This

finding supports the notion that BRCA2 may function as a tumor suppressor gene in the liver<sup>[15]</sup>, and that it may in some way be involved in the progression of a small number of HCCs. To our knowledge, LOH of the BRCA1 gene has been reported only once, in a study in which 11.5% (3/6) of HCCs showed LOH at this locus<sup>[12]</sup>. No LOH was found for this gene in our sample population. LOH at 11p13, the region containing the WT1 gene, as well as LOH of the gene itself has been reported in 4%-7% HCCs<sup>[12,16]</sup>. Our result of 8% (1/13) LOH agrees with these findings. LOH of the region where the E-cadherin gene is located (16q22) has been reported in 64%-91% of Chinese and Japanese HCCs<sup>[25,26]</sup>. No LOH was found for this gene in our study. Although all the HCCs used in this study were in advanced stages, it was not established whether they were highly undifferentiated. There may be retention of *E-cadherin* expression in these samples and no loss of intercellular adhesiveness.

We cannot say whether HBV played any role in the chromosome losses reported here<sup>[37]</sup>. Cumulative LOH is thought to reflect the sequential development of HCC progression.

LOH of a number of tumor suppressor genes may be important in the advancement of HCC<sup>[37]</sup>. Frequent loss of tumor suppressor genes has been reported in Korean HCCs, where 86% HCCs had LOH of 1 gene, and 59% had LOH of 2-4 genes<sup>[12]</sup>. Piao *et al* (1997), investigated 10 tumor suppressor genes (-VHL, APC, EXT1, WT1, RB1, *p53*, BRCA1, nm23, DPC4, DCC). The genes most often lost were *p53* (66%), RB1 (33%), EXT1 (33%), and APC (20%). The genes found to be lost most often in our study were RB1 (17%) and BRCA2 (10%). However, as the total LOH of the *p53*, RB1, BRCA1, BRCA2, WT1 and *E-cadherin* genes in this study was 20% (4/20), we conclude that LOH of tumor suppressor genes is infrequent in our HCCs.

Microsatellite/genomic instability is reflected in the expansion/contraction of microsatellite sequences, and is thought to be a product of replication errors<sup>[38]</sup>. Microsatellite instability has been considered to be insignificant in HCC development by some authors, while others believe that it may be significant<sup>[39]</sup>. To our knowledge, this is the first time microsatellite instability has been looked at in HCCs from a southern African black population. It is important to note that there are differences in allele frequency between our southern African Negroid population and the Asian, European and Australian populations, characterized previously at the WT1, D13S137, D13S120,

D13S127, D17S855, D16S301, and D16S260 loci (paper in preparation). Microsatellite instability has been documented in 40% of HCCs from the USA<sup>[39]</sup>, and in 41% of HCCs at two or more loci in a French study<sup>[40]</sup>. In a Korean study microsatellite instability was detected in 4/10 (40%) HCCs, where each subject showed instability at two or more loci<sup>[39]</sup>. Of the 9 markers used in their study, 3 showed genetic instability in one or more subjects. In our study 3/20 (15%) HCCs showed instability at two or more loci. Of the 10 loci investigated, 9 showed genetic instability in one or more subjects. Cumulative microsatellite instability indicates advanced HCC. One of these subjects also had the codon 249 mutation in the *p53* gene. We were not able to determine whether joint changes at the loci were necessary for tumor development, or whether they represented independent events in tumor initiation and/or progression. Microsatellite/genomic instability is believed to occur at random and may reflect alteration of the entire genome of the cancer cell<sup>[41]</sup>. The order of these changes is most likely insignificant. Their cumulative effect however, may be important<sup>[42]</sup>. We propose that microsatellite/genomic instability may play a role only in a small subset of HCC in our population.

In conclusion, our observations support a possible role of *p53*, WT1 and BRCA2 genes in the pathogenesis of HCC, and that microsatellite instability appears to be an important factor contributing to HCC development in a subset of our HCCs.

## REFERENCES

- 1 Yee CJ, Roodi N, Verrier CS, Parl FF. Microsatellite instability and loss of heterozygosity in breast cancer. *Cancer Res*, 1994;54:1641-1644
- 2 Fujimoto Y, Kohgo Y. Alteration of genomic structure and/or expression of cancer associated genes in hepatocellular carcinoma. Abstract in English, article in Japanese. *Rinsho Byori*, 1998;46:9-14
- 3 Parkin DM, Stjernsward J, Muir C. Estimates of the worldwide frequency of twelve major cancers. *Bull WHO*, 1984;62:163-182
- 4 Harris CC. Hepatocellular carcinogenesis: recent advances and speculations. *Cancer Cells*, 1990;2:146-148
- 5 Saito I, Miyamura T, Ohbayashi A, Harada H, Katayama T, Kikuchi S, Watanabe Y, Koi S, Onji M, Ohta Y, Choo QL, Houghton M, Kuo G. Hepatitis C virus infection is associated with the development of hepatocellular carcinoma. *Proc Natl Acad Sci USA*, 1990;87:6547-6549
- 6 Bressan B, Kew M, Wands J, Ozturk M. Selective G to T mutations of *p53* gene in hepatocellular carcinoma from southern Africa. *Nature*, 1991;350:429-431
- 7 Hsu IC, Metcalf RA, Sun T, Welsh JA, Wang NJ, Harris CC. Mutational hotspot in the *p53* gene in human hepatocellular carcinomas. *Nature*, 1991;350:427-428
- 8 Scorsone KA, Zhou YZ, Butel JS, Slagle BL. *p53* mutations cluster at codon 249 in hepatitis B virus-positive hepatocellular carcinomas from China. *Cancer Res*, 1992;52:1635-1638
- 9 Bressan B, Galvin KM, Liang TJ, Isselbacher KJ, Wands JR, Ozturk M. Abnormal structure and expression of *p53* gene in human hepatocellular carcinoma. *Proc Natl Acad Sci USA*, 1990;87:1973-1977
- 10 Nigro JM, Baker SJ, Preisinger AC, Jessup JM, Hostetter R, Cleary K, Bigner S, Davidson N, Baylin S, Devilee P, Glover T, Collins F, Weston A, Modali R, Harris C, Vogelstein B. Mutations in the *p53* gene occur in diverse human tumor types. *Nature*, 1989;342:705-708
- 11 Smith SA, Easton DF, Evans DGR, Ponder BAJ. Allele losses in the region 17q12-21 in familial breast and ovarian cancer involve the wild-type chromosome. *Nature Genet*, 1992;2:128-131
- 12 Piao Z, Kim H, Jeon B, Lee WJ, Park C. Relationships between loss of heterozygosity of tumor suppressor genes and histologic differentiation in hepatocellular carcinoma. *Cancer*, 1997;80:865-872
- 13 Gudmundsson J, Johannesdottir G, Bergthorsson JT, Arason A, Ingvarsson S, Egilsson V. Different tumor types from BRCA2 carriers show wild-type chromosome deletions on 13q12-13. *Cancer Res*, 1995;55:4830-4832
- 14 Rajan JV, Marquis ST, Gardner HP, Chodosh LA. Developmental expression of BRCA2 colocalizes with BRCA1 and is associated with proliferation and differentiation in multiple tissues. *Dev Biol*, 1997;184:385-401
- 15 Katagiri T, Nakamura Y, Miki Y. Mutations in the BRCA2 gene in hepatocellular carcinomas. *Cancer Res*, 1996;56:4575-4577
- 16 Wang HP, Rogler CE. Deletion in human chromosome arms 11p and 13q in primary hepatocellular carcinomas. *Cytogenet Cell Genet*, 1988;48:72-78
- 17 Hsia CC, Di Bisceglie AM, Kleiner DE Jr., Farshid M, Tabor E. RB tumor suppressor gene expression in hepatocellular carcinomas from patients infected with the hepatitis B virus. *J Med Virol*, 1994;44:67-73
- 18 Murakami Y, Hayashi K, Hirohashi S, Sekiya T. Aberrations of the tumor suppressor *p53* and retinoblastoma genes in human hepatocellular carcinomas. *Cancer Res*, 1991;51:5520-5525
- 19 Evans RM, Hollenberg SM. Zinc fingers: guilt by association. *Cell*, 1988;52:1-3
- 20 Menke AL, Shvarts A, Riteco N, Van Ham RCA, Van Der Eb AJ, Jochemsen AG. Wilms' tumor 1-Kts isoforms induce *p53* independent apoptosis that can be partially rescued by expression of the epidermal growth factor receptor or the insulin receptor. *Cancer Res*, 1997;57:1353-1363
- 21 Shimoyama Y, Hirohashi S, Hirano S, Noguchi M, Shimosato Y, Takeichi M, Abe O. Cadherin cell adhesion molecules in human epithelial tissues and carcinomas. *Cancer Res*, 1989;49:2128-2133
- 22 Takeichi M. Cadherins: a molecular family important in selective cell cell adhesion. *Ann Rev Biochem*, 1990;59:237-252
- 23 Behrens J, Mareel MM, Van Roy FM, Birchmeier B. Dissecting tumor cell invasion: epithelial cells acquire invasive properties after the loss of uvomorulin-mediated cell-cell adhesion. *J Cell Biol*, 1989;108:2434-2447
- 24 Nagao T, Inoue S, Yoshimi F, Sodeyama M, Omori Y, Mizuta T, Kawano N, Morioka Y. Postoperative recurrence of hepatocellular carcinoma. *Ann Surg*, 1990;211:28-33
- 25 Slagle BL, Zhou YZ, Birchmeier W, Scorsone KA. Deletion of the E-cadherin gene in hepatitis B virus-positive Chinese hepatocellular carcinomas. *Hepatology*, 1993;18:757-762
- 26 Tsuda H, Zhang W, Shimosato Y, Yokota J, Terada M, Sugimura T, Miyamura T, Hirohashi S. Allele loss on chromosome 16 associated with progression of human hepatocellular carcinoma. *Proc Natl Acad Sci USA*, 1990;87:6791-6794
- 27 Weissbach J, Gyapay G, Dib C, Vignal A, Morissette J, Millasseau P, Vaysseix G, Lathrop M. A second-generation linkage map of the human genome. *Nature*, 1992;359:794-801
- 28 Miller S, Dykes D, Polesky H. A simple salting out procedure for extracting DNA from human nucleated cells. *Nuc Acids Res*, 1988;16:1215
- 29 Oda T, Tsuda H, Scarpa A, Sakamoto M, Hirohashi S. *p53* gene mutation spectrum in hepatocellular carcinoma. *Cancer Res*, 1992;52:6358-6364
- 30 Fujimoto Y, Hampton LL, Wirth PJ, Wang NJ, Xie JP, Thorgeisson SS. Alterations of tumor suppressor genes and allelic losses in human hepatocellular carcinomas in China. *Cancer Res*, 1994;54:281-285
- 31 Slagle BL, Zhou YZ, Butel JS. Hepatitis B virus integration event in human chromosome 17p near the *p53* gene identifies the region of the chromosome commonly deleted in virus positive hepatocellular carcinomas. *Cancer Res*, 1991;51:49-54
- 32 Wang XW, Forrester K, Yeh H, Feitelson MA, Gu JR, Harris CC. Hepatitis B virus X protein inhibits *p53* sequence-specific DNA binding, transcriptional activity, and association with transcription factor ERCC3. *Proc Natl Acad Sci USA*, 1994;91:2230-2234
- 33 Kirby GM, Batist G, Fotouhi Ardakani N, Nakazawa H, Yamasaki H, Kew M, Cameron RG, Alaoui-Jamali MA. Allele-specific PCR analysis of *p53* codon 249 AGT transversion in liver tissues from patients with viral hepatitis. *Int J Cancer*, 1996;68:21-25

- 34 Hollstein M, Sidransky D, Vogelstein B, Harris CC. *p53* mutations in human cancers. *Science*, 1991;253:49-53
- 35 Kapelner SN, Turner RT, Sarkar G, Bolander ME. Deletion mutation can be an unsuspected gel artifact. *Biotechniques*, 1994;17:64-66
- 36 Walker GJ, Hayward NK, Falvey S, Graham W, Cooksley WGE. Loss of somatic heterozygosity in hepatocellular carcinoma. *Cancer Res*, 1991;51:4367-4370
- 37 Yumoto Y, Hanafusa T, Hada H, Morita T, Ooguchi S, Shinji N, Mitani T, Hamaya K, Koide N, Tsuji T. Loss of heterozygosity and analysis of mutation of *p53* in hepatocellular carcinoma. *J Gastroenterol Hepatol*, 1995;10:179-185
- 38 Gao X, Zacharek A, Salkowski A, Grignon DJ, Sakr W, Porter AT, Honn KV. Loss of heterozygosity of the BRCA1 and other loci on chromosome 17q in human prostate cancer. *Cancer Res*, 1995;55:1002-1005
- 39 Kazachkov Y, Yoffe B, Khaoustov VI, Solomon H, Klintmalm GB, Tabor E. Microsatellite instability in human hepatocellular carcinoma: relationship to *p53* abnormalities. *Liver*, 1998;18:156-161
- 40 Salvucci M, Lemoine A, Azoulay D, Sebah M, Bismuth H, Reyns M, May E, Debuire B. Frequent microsatellite instability in post hepatitis B viral cirrhosis. *Oncogene*, 1999;13:2681-2685
- 41 Li C, Larsson C, Futreal A, Lancaster J, Phelan C, Aspenblad U, Sundelin B, Liu Y, Ekman P, Auer G, Bergerheim USR. Identification of two distinct deleted regions on chromosome 13 in prostate cancer. *Oncogene*, 1998;16:481-487
- 42 Butel JS, Lee TH, Slagle BL. Is the DNA repair system involved in hepatitis B-virus mediated hepatocellular carcinogenesis. *Trends Microbiol*, 1996;4:119-124
- 43 Futreal PA, Barrett JC, Wiseman RW. An ALU polymorphism intragenic to the TP53 gene. *Nuc Acids Res*, 1991;19:6977
- 44 Bowcock A, Osborne Lawrence S, Barnes R, Chakravarti A, Washinton S, Dunn C. Microsatellite polymorphism linkage map of human chromosome 13q. *Genomics*, 1993;15:376-386
- 45 Fletjer WL, Kukowska-latallo JF, Kiouisis S, Chandrasakharappa SC, King SE, Chamberlain JS. Tetranucleotide repeat polymorphism at D17S846 maps within 40kb of GAS at 17q12.22. *Hum Molec Genet*, 1993;2:1
- 46 Anderson LA, Friedman L, Osborne Lawrence S, Lynch E, Weissenbach J, Bowcock A, King MC. High density genetic map of the BRCA1 region of chromosome 17q12 q21. *Genomics*, 1993;17:618-623
- 47 Haber DA, Buckler AJ, Glaser T, Call KM, Pelletier J, Sohn RL, Douglass EC, Housman DE. An internal deletion within an 11p13 Zinc finger gene contributes to the development of Wilm's tumor. *Cell*, 1990;61:1257-1269
- 48 Henson JW, Schnitker BL, Correa KM, von Deimling A, Fassbender F, Xu HJ, Benedict WF, Yandell DW, Louis DN. The retinoblastoma gene is involved in malignant progression of astrocytomas. *Ann Neurol*, 1994;36:714-721
- 49 Yandell DW, Dryja TP. Detection of DNA sequence polymorphisms by enzymatic amplification and direct genomic sequencing. *Am J Hum Genet*, 1989;45:547-555
- 50 Petrukhin KE, Speer MC, Cayanis E, Bonaldo MF, Tantravahi U, Soares MB, Fischer SG, Warburton D, Gilliam C, Ott J.A microsatellite genetic linkage map of human chromosome 13. *Genomics*, 1993;15:76-85
- 51 Thompson AD, Shen Y, Holman K, Sutherland GR, Callen DF, Richards RI. Isolation and characterization of (AC)<sub>n</sub> microsatellite genetic markers from human chromosome 16. *Genomics*, 1992;13:402-408
- 52 Weber JL, Kwitek AE, May PE. Dinucleotide repeat polymorphisms at the D16S260, D16S261, D16S265, D16S266, and D16S267 loci. *Nuc Acids Res*, 1990;18:4034

# Protective effect of Irsogladine on monochloramine induced gastric mucosal lesions in rats: a comparative study with rebamipide

H Yamamoto, M Umeda, H Mizoguchi, S Kato and K Takeuchi

**Subject headings** irsogladine; rebamipide; monochloramine; gastric mucosal lesions; rats; comparative study

## Abstract

**AIM** To examine the effect of irsogladine, a novel antiulcer drug, on the mucosal ulcerogenic response to monochloramine (  $\text{NH}_2\text{Cl}$  ) in rat stomach, in comparison with rebamipide, another antiulcer drug with cytoprotective activity.

**METHODS AND RESULTS** Oral administration of  $\text{NH}_2\text{Cl}$  (120 mM) produced severe hemorrhagic lesions in unanesthetized rat stomachs. Both irsogladine (1 mg/kg-10 mg/kg, po) and rebamipide (30 mg/kg -100 mg/kg, po) dose-dependently prevented the development of these lesions in response to  $\text{NH}_2\text{Cl}$ , the effect of irsogladine was significant at 3 mg/kg or greater, and that of rebamipide only at 100 mg/kg. The protective effect of irsogladine on  $\text{NH}_2\text{Cl}$ -induced gastric lesions was significantly reduced by  $\text{N}^G$ -nitro-L-arginine methyl ester (L-NAME) but not by indomethacin, while that of rebamipide was significantly mitigated by indomethacin but not by L-NAME. Topical application of  $\text{NH}_2\text{Cl}$  (20mM) caused a marked reduction of potential difference (PD) in *ex-vivo* stomachs. This PD reduction was not affected by mucosal application of irsogladine, but significantly prevented by rebamipide. The mucosal exposure to  $\text{NH}_4\text{OH}$  (120 mM) also caused a marked PD reduction in the ischemic stomach (bleeding from the carotid artery),

resulting in gastric lesions. These ulcerogenic and PD responses caused by  $\text{NH}_4\text{OH}$  plus ischemia were also significantly mitigated by rebamipide, in an indomethacin-sensitive manner, while irsogladine potently prevented such lesions without affecting the PD response, in a L-NAME-sensitive manner.

**CONCLUSION** These results suggest that ①  $\text{NH}_2\text{Cl}$  generated either exogenously or endogenously damages the gastric mucosa, ② both irsogladine and rebamipide protect the stomach against injury caused by  $\text{NH}_2\text{Cl}$ , and ③ the mechanism underlying the protective action of irsogladine is partly mediated by endogenous nitric oxide, while that of rebamipide is in part mediated by endogenous prostaglandins.

## INTRODUCTION

*Helicobacter pylori*, recognized as the major cause of gastritis and peptic ulcer diseases<sup>[1-3]</sup> has a high activity of urease, resulting in a high concentration of ammonia ( $\text{NH}_4\text{OH}$ ) in the stomach of infected patients<sup>[3]</sup>. Since *H. pylori* associated chronic active gastritis is characterized by an invasion of neutrophils in the gastric mucosa<sup>[1,2,4]</sup> and since neutrophils utilize the  $\text{H}_2\text{O}_2$ -myeloperoxidase-halide system to generate an oxidant capable of destroying a variety of mammalian cell targets as well as microorganisms<sup>[5,6]</sup>, it is assumed that neutrophil-derived hypochlorous acid (HClO) interacts with  $\text{NH}_4\text{OH}$  to generate cytotoxic monochloramine ( $\text{NH}_2\text{Cl}$ )<sup>[7,8]</sup>. Indeed, it has been shown that  $\text{NH}_2\text{Cl}$  plays a role in the pathogenesis of  $\text{NH}_4\text{OH}$ -induced gastric lesions in rats<sup>[9,10]</sup>. We have also reported previously that both endogenous and exogenous  $\text{NH}_2\text{Cl}$  damaged the gastric mucosa at much lower concentrations than  $\text{NH}_4\text{OH}$ <sup>[11,12]</sup>.

Irsogladine, a novel antiulcer drug [2,4-diamino-6-(2,5-dichlorophenyl)-s-triazine maleate], has been shown to not only prevent gastric mucosal lesions in a wide variety of experimental models but show the healing promoting action of gastric ulcers as well, without any suppression of gastric secretion<sup>[13-15]</sup>. These

Department of Pharmacology and Experimental Therapeutics, Kyoto Pharmaceutical University, Misasagi, Yamashina, Kyoto 607-8414, Japan

Hedeichiro Yamamoto, male born on 1975-07-10 in Osaka City, Japan, graduated from Kyoto Pharmaceutical University in 1998, now a graduated student of Kyoto Pharmaceutical University, majoring in gastrointestinal pharmacology and physiology and having 6 papers published.

This work was supported in part by a grant from Nippon Shinyaku Co. Ltd.

**Correspondence to:** Shinichi Kato, Ph.D., Department of Pharmacology and Experimental Therapeutics, Kyoto Pharmaceutical University, Misasagi, Yamashina, Kyoto 607-8414, Japan  
Tel. +81-75-595-4680, Fax. +81-75-595-4774  
Email.skato@mb.kyoto-phu.ac.jp

Received 1999-08-31

effects of irsogladine may be accounted for by cytoprotective activity, yet the detailed mechanism is not fully understood. Thus, it is of interest to test whether this agent has any prophylactic action against  $\text{NH}_2\text{Cl}$ -induced gastric lesions.

In the present study, we examined the effects of irsogladine on the mucosal ulcerogenic response induced by  $\text{NH}_2\text{Cl}$ , either administered exogenously or occurring endogenously, and compared those with the effects of another cytoprotective drug, rebamipide. We also investigated the underlying mechanism of their protection, especially in relation to endogenous prostaglandins (PGs) and nitric oxide (NO).

## MATERIALS AND METHODS

### Animals

Male Sprague-Dawley rats (200 g-240 g in weight, Nippon Charles River, Shizuoka, Japan) were used in all experiments. The animals, kept in separate cages with raised mesh bottoms, were deprived of food but allowed free access to tap water for 18 hours prior to the experiments. Studies were carried out using four to eight rats under either conscious or anesthetized conditions induced by urethane (1.25 g/kg, ip). All experimental procedures described here were approved by the Experimental Animal Research Committee of the Kyoto Pharmaceutical University.

### General procedures

The experiments were classified into roughly two studies: one was to investigate the effects of irsogladine and rebamipide on gastric ulcerogenic response to exogenously administered  $\text{NH}_2\text{Cl}$  in unanesthetized rats, and the other was to investigate their effects on gastric ulcerogenic response to  $\text{NH}_4\text{OH}$  in anesthetized rats subjected to ischemia. In the latter situation, it is assumed that  $\text{NH}_2\text{Cl}$  is generated endogenously from interaction of  $\text{NH}_4\text{OH}$  with neutrophil-derived  $\text{HClO}^{[10]}$ .

### Induction of gastric lesions induced by $\text{NH}_2\text{Cl}$

The effects of irsogladine and rebamipide on gastric mucosal ulcerogenic response induced by exogenous  $\text{NH}_2\text{Cl}$ . The animals were administered 1 ml of  $\text{NH}_2\text{Cl}$  (120 mM)-po by esophageal intubation. The solution of  $\text{NH}_2\text{Cl}$  was prepared by mixing  $\text{NH}_4\text{OH}$  (240 mM) and  $\text{HClO}$  (240 mM) in a test tube, immediately before the administration. The animals were sacrificed 1 hour after the administration of  $\text{NH}_2\text{Cl}$ , and the stomachs were removed, inflated by injecting 8 mL of 2% formalin and immersed in 2% formalin for 10 min to fix the gastric wall, and opened along the greater curvature. The area ( $\text{mm}^2$ ) of hemorrhagic lesions was measured under a dissecting microscope with a square grid ( $\times 10$ ).

The person measuring the lesions did not know the treatment given to the animals. These procedures were used in all the subsequent studies for evaluating macroscopical lesions. Irsogladine (1, 3 and 10 mg/kg) and rebamipide (30 and 100 mg/kg) were administered po 30 min before  $\text{NH}_2\text{Cl}$  treatment. In some cases, indomethacin (10 mg/kg, sc) or L-NAME (10 mg/kg, iv) was given 60 min or 40 min before  $\text{NH}_2\text{Cl}$  treatment.

### Measurement of transmucosal potential difference

Transmucosal potential difference (PD) was measured in chambered stomachs of anesthetized rats as previously described<sup>[15]</sup>. Briefly, a rat stomach was mounted on an *ex-vivo* chamber (area exposed 3.14  $\text{cm}^2$ ) and perfused at a flow rate of 1 mL/min with saline (154 mM-NaCl). PD was determined using two agar bridges, one positioned in the chamber and the other in the abdominal cavity, and monitored continuously on a recorder (U-228, Tokai-Irika, Tokyo, Japan). Approximately 1 h after PD was stabilized, the perfusion system was interrupted and the solution in the chamber was withdrawn, and the mucosa was exposed to 1 mL carboxymethyl cellulose (CMC) solution (control group), 20 min later followed by 1 mL  $\text{NH}_2\text{Cl}$  (20 mM, the final concentration is 10 mM) for 10 min. After application of  $\text{NH}_2\text{Cl}$ , the mucosa was rinsed with saline, another 2 mL saline was instilled, and the perfusion system was resumed. Irsogladine (3 mg/kg) or rebamipide (100 mg/kg) was applied to the chamber for 30 min in place of CMC solution, starting 20 min before  $\text{NH}_2\text{Cl}$  treatment. In a separate experiment, the animals were subjected to ischemia by bleeding from the carotid artery (1 mL/100 g body weight), then the mucosa was exposed to 1 mL of CMC, 20 min later followed by 1 mL of  $\text{NH}_4\text{OH}$  (120 mM, the final concentration is 60 mM) for 1 hour. At the end of the experiment, the mucosa was excised, and the area ( $\text{mm}^2$ ) of hemorrhagic lesions was measured as described as above. Irsogladine (3 mg/kg) or rebamipide (100 mg/kg) was applied to the chamber 10 min before the onset of ischemia plus  $\text{NH}_4\text{OH}$  treatment. Control animals received CMC as the vehicle. In some cases, indomethacin (10 mg/kg) was given sc 30 min before rebamipide, while L-NAME (10 mg/kg) was given iv 10 min before irsogladine treatment.

### Preparation of drugs

Drugs used in this study were urethane (Tokyo Kasei, Tokyo, Japan), irsogladine (Nihon-Shinyaku Co., Kyoto, Japan), rebamipide (Otsuka Pharmaceutical Co., Tokushima, Japan), indomethacin and L-NAME (Sigma Chemicals, St. Louis, MO, USA). Indomethacin was suspended in

saline with a drop of Tween 80 (Wako, Osaka, Japan), while L-NAME was dissolved in saline. Other drugs were suspended with 0.5% CMC solution. Each drug was prepared immediately before use and administered *po* in a volume of 0.5 mL/100 g body weight or *iv* in a volume of 0.1 mL/100 g body weight or applied topically to the chamber in a volume of 1 mL/stomach.

### Statistics

Data are presented as the means $\pm$ SE from 4 to 8 rats per group. Statistically analyses were performed using two-tailed Student's *t* test or Dunnett's multiple comparison test, and  $P < 0.05$  values were regarded as significant.

## RESULTS

### *Effects of irsogladine on gastric ulcerogenic response to NH<sub>2</sub>Cl*

Intragastric administration of NH<sub>2</sub>Cl caused severe band-like hemorrhagic lesions in the gastric mucosa, the lesion score being 138.0 mm<sup>2</sup>  $\pm$  19.0 mm<sup>2</sup>. Pretreatment of the animals with irsogladine (1, 3 and 10 mg/kg, *po*) significantly reduced the severity of gastric lesions in response to NH<sub>2</sub>Cl in a dose-dependent manner. The degree of inhibition was 35.1%, 86.3% and 83.3%, respectively (Figure 1). Rebamipide (30 and 100 mg/kg, *po*) also lowered the severity of gastric lesions induced by NH<sub>2</sub>Cl, but the degree of inhibition at 100 mg/kg was 59.3%, which was less than that observed by irsogladine at 3 mg/kg.

### *Effects of L-NAME and indomethacin on protective action of irsogladine against NH<sub>2</sub>Cl-induced gastric lesions*

The severity of gastric lesions induced by NH<sub>2</sub>Cl was not affected by prior administration of either indomethacin (5 mg/kg, *sc*) or L-NAME (10 mg/kg, *iv*), the lesion score being 146.8 mm<sup>2</sup>  $\pm$  9.8 mm<sup>2</sup> or 135.6 mm<sup>2</sup>  $\pm$  7.0 mm<sup>2</sup>, respectively (Figure 2). However, the protective action of irsogladine (3 mg/kg, *po*) against NH<sub>2</sub>Cl-induced gastric lesions was significantly mitigated by prior administration of L-NAME but not indomethacin; the lesion score in the presence of L-NAME was 72.8 mm<sup>2</sup>  $\pm$  9.1 mm<sup>2</sup>, which was significantly greater than that observed in the absence of L-NAME (19.8 mm<sup>2</sup>  $\pm$  3.1 mm<sup>2</sup>). By contrast, indomethacin but not L-NAME significantly antagonized the protective action of rebamipide (100 mg/kg, *po*) against these lesions.

### *Effects of irsogladine on mucosal PD response induced by NH<sub>2</sub>Cl*

Normal stomachs mounted on the chamber and perfused with saline generated a stable PD of -30 to -38 mV (mucosa negative), and the values

remained relatively unchanged during a 2-hour test period. Mucosal exposure to NH<sub>2</sub>Cl (10 mM) caused a marked reduction of PD to 60.0%  $\pm$  6.2% of basal values within 10 min, and the PD remained low for 1 hour thereafter (Figure 3). The PD reduction in response to NH<sub>2</sub>Cl was not affected by prior exposure of the mucosa to irsogladine (3 mg/kg). However, the reduced PD response to NH<sub>2</sub>Cl was significantly mitigated when the mucosa was pre-exposed to rebamipide (100 mg/kg) for 30 min; the PD reduced to 57.7%  $\pm$  3.1% of basal values 10 min later, which was significantly less as compared with that (60.0%  $\pm$  6.2% of basal values) in control rats.

### *Effects of irsogladine on mucosal ulcerogenic and PD responses induced by NH<sub>4</sub>OH under ischemic conditions*

To confirm the protective action of irsogladine and rebamipide on NH<sub>2</sub>Cl-induced gastric toxicity, we tested the effects of these drugs on the mucosal ulcerogenic and PD responses induced by endogenously generated NH<sub>2</sub>Cl by application of a low concentration of NH<sub>4</sub>OH (60 mM) in the ischemic stomach<sup>[9]</sup>. As shown in Figure 4, topical application of NH<sub>4</sub>OH at 60 mM produced a persistent reduction of PD in the stomach made ischemic by bleeding; the PD was reduced to 42.6%  $\pm$  6.2% of basal values within 10 min and remained low thereafter. This concentration of NH<sub>4</sub>OH did not have any effect on PD in normal stomachs without subjecting to ischemia (not shown). The reduced PD response to NH<sub>4</sub>OH plus ischemia was not affected by prior exposure of the mucosa to irsogladine (3 mg/kg), in the absence or presence of L-NAME. By contrast, rebamipide (100 mg/kg)-pre-exposed to the mucosa significantly attenuated the PD reduction in response to NH<sub>4</sub>OH plus ischemia. In these animals the recovery of PD was also significantly expedited, and the PD almost completely normalized within 60 min after NH<sub>4</sub>OH plus ischemia. In addition, the preventive effect of rebamipide on the PD response to NH<sub>4</sub>OH plus ischemia was also significantly antagonized in the presence of indomethacin.

On the other hand, the mucosal exposure to NH<sub>4</sub>OH in the ischemic stomachs resulted in severe hemorrhagic lesions within 1 hour, the lesion score being 53.6 mm<sup>2</sup>  $\pm$  12.2 mm<sup>2</sup> (Figure 5). The development of gastric lesions induced by NH<sub>4</sub>OH plus ischemia was significantly prevented by irsogladine (3 mg/kg) as well as rebamipide (100 mg/kg), the inhibition being 79.5% and 82.3%, respectively. The protective effect of irsogladine or rebamipide against NH<sub>4</sub>OH plus ischemia-induced gastric lesions was significantly antagonized by L-NAME or indomethacin, respectively.

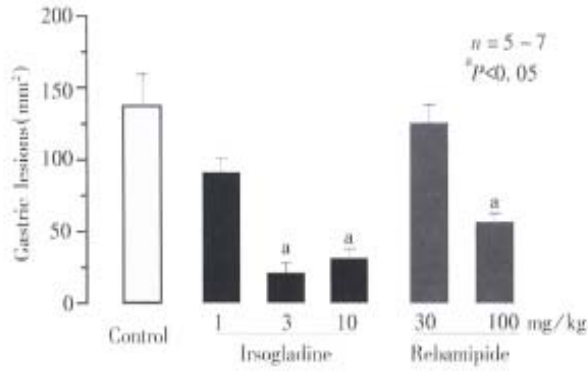


**Figure1** Effects of irsogladine and rebamipide on gastric lesions induced by NH<sub>2</sub>Cl in rats. The animals were given NH<sub>2</sub>Cl (120 mM;5mL/kg) po, and sacrificed 1 hour later. Irsogladine (1mg/kg-10 mg/kg) or rebamipide (30, 100 mg/kg) was given po 30 min before administration of NH<sub>2</sub>Cl. Data are presented as the mean±SE from 5-7 rats. \*Statistically significant difference from control (P<0.05).

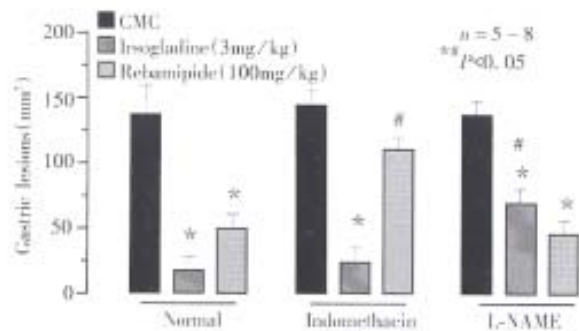


**Figure2** Effects of indomethacin and L-NAME on the mucosal protective action of irsogladine and rebamipide against NH<sub>2</sub>Cl-induced gastric lesions in rats. The animals were administered po with 1mL of NH<sub>2</sub>Cl (120 mM), and sacrificed 1 hour later. Irsogladine (3 mg/kg) or rebamipide (100 mg/kg) was given po 30 min before NH<sub>2</sub>Cl treatment. Indomethacin (5 mg/kg, sc) or L-NAME (10 mg/kg, iv) was given 30 or 10 min before the above agents. Data are presented as the mean±SE from 5-8 rats. Statistically significant difference at P<0.05; \*from the corresponding control (CMC);#from the corresponding value in normal group.

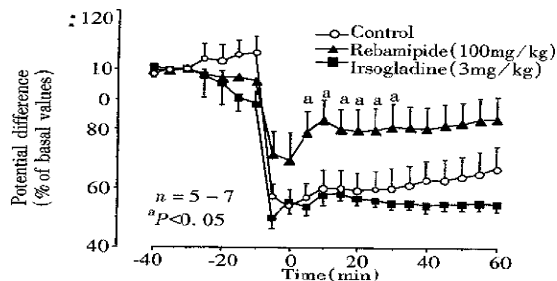


**Figure3** Effects of irsogladine and rebamipide on changes in transmucosal PD in response to NH<sub>2</sub>Cl in anesthetized rat stomachs. The stomach was mounted on an ex-vivo chamber, and NH<sub>2</sub>Cl (20 mM; 1 mL) was applied topically to the stomach for 10min. Irsogladine (3 mg/kg) or rebamipide (100 mg/kg) was applied to the chamber for 30 min, starting 20 min before exposure to NH<sub>2</sub>Cl. Data are presented as the mean ± SE of value determined every 5min from 5-7 rats. \*Statistically significant difference from control, P<0.05.

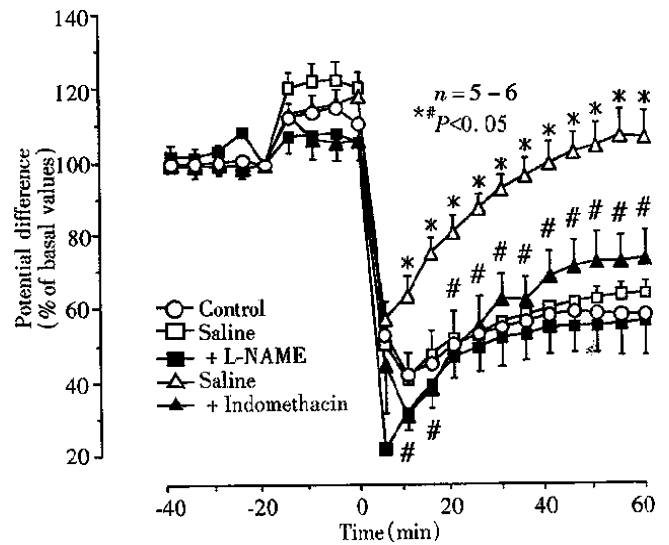


**Figure4** Effects of irsogladine and rebamipide on changes in transmucosal PD in response to NH<sub>4</sub>OH in rat stomachs under ischemic conditions. The stomach mounted on a ex-vivo chamber was subjected to ischemia by bleeding from the carotid artery (1 mL/100 g body wt), and then exposed to NH<sub>4</sub>OH (120 mM; 1 mL) for 1h thereafter. Irsogladine (3 mg/kg) or rebamipide (100 mg/kg) was applied to the chamber 20 min before the onset of ischemia and NH<sub>4</sub>OH treatment. Indomethacin (5 mg/kg, sc) or L-NAME (10 mg/kg, iv) was given 30 or 10 min before the above agents. Data are presented as the mean±SE of values determined every 5 min from 5-6 rats. Statistically significant difference at P<0.05; \*from control; #from vehicle.

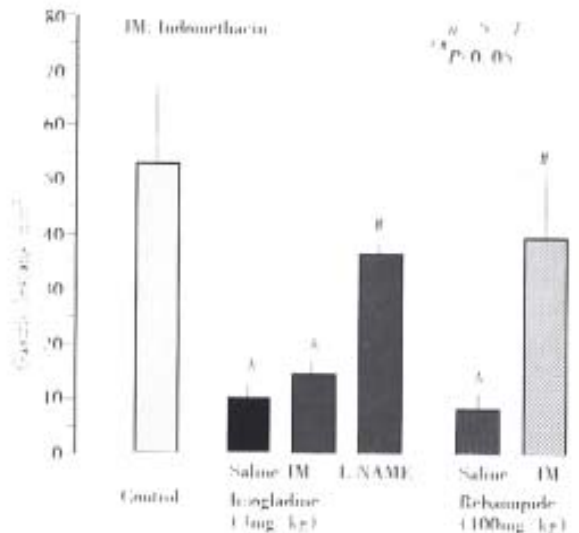


**Figure5** Effects of irsogladine and rebamipide on gastric mucosal lesions induced by NH<sub>4</sub>OH in anesthetized rat stomachs under ischemic conditions. The stomach mounted on an ex-vivo chamber was subjected to ischemia by bleeding from the carotid artery (1 mL/100 g body weight), and then exposed to NH<sub>4</sub>OH (120 mM) for 1 h thereafter. Irsogladine (3 mg/kg) or rebamipide (100 mg/kg) was applied to the chamber 20 min before the onset of ischemia and NH<sub>4</sub>OH treatment. Indomethacin (5 mg/kg, sc) or L-NAME (10 mg/kg, iv) was given 30 or 10 min before the above agents. Data are presented as the mean±SE from 4-6 rats. Statistically significant difference at P<0.05; \*from control; #from vehicle.

## DISCUSSION

The present study demonstrated that irsogladine, a novel antiulcer drug, conferred a protection against gastric damage induced in rat stomachs by  $\text{NH}_2\text{Cl}$ , either given exogenously or occurred endogenously. We also found that rebamipide, another antiulcer drug, showed similar protection against such damage, although the effect was less potent than that of irsogladine. In addition, the present results suggest that the mechanisms underlying their protection are different; the protective action of irsogladine is partly mediated by endogenous NO, while that of rebamipide is accounted for by endogenous PGs as well as a radical scavenging action.

*H. pylori* has a high urease enzyme activity, resulting in an abnormally high concentration of ammonia ( $\text{NH}_4\text{OH}$ ) in the stomach of infected patients<sup>[3]</sup>. It is also known that  $\text{NH}_4\text{OH}$  interacts with neutrophil-derived HClO to generate cytotoxic  $\text{NH}_2\text{Cl}$ , a powerful oxidant capable of destroying a variety of micro-organisms as well as mammalian cell targets<sup>[4,7]</sup>. Murakami *et al.*<sup>[17]</sup> demonstrated in rats that  $\text{NH}_4\text{OH}$ -induced gastric mucosal lesions were significantly inhibited by taurine, a scavenger of HClO, suggesting a pathogenic role of  $\text{NH}_2\text{Cl}$  in the development of such lesions. We also found previously that the mixture of low concentration of  $\text{NH}_4\text{OH}$  and HClO, which did not have any gastric mucosal toxicity by each alone, caused severe lesions in the rat gastric mucosa under unanesthetized conditions<sup>[11,12]</sup>. In addition, we reported that the gastric lesions induced by endogenously generated  $\text{NH}_2\text{Cl}$  by a low concentration of  $\text{NH}_4\text{OH}$  plus ischemia were totally prevented by taurine in anesthetized *ex-vivo* stomachs<sup>[11,12]</sup>. It is known that ischemia activates xanthine oxidase, which is responsible for the production of reactive oxygen metabolites such as  $\text{H}_2\text{O}_2$ , and that the generation of HClO by neutrophils is dependent on the quantity of  $\text{H}_2\text{O}_2$  produced<sup>[4,5]</sup>. It may therefore be assumed that  $\text{NH}_4\text{OH}$  even at low concentrations produces  $\text{NH}_2\text{Cl}$  by interaction with HClO in the ischemic stomach, resulting in damage to the mucosa.

The gastric lesions induced by oral administration of  $\text{NH}_2\text{Cl}$  were significantly prevented by irsogladine as well as rebamipide in a dose-dependent manner, although the effect of irsogladine was more potent than that of rebamipide. Similar results were obtained by these drugs against gastric lesions induced by  $\text{NH}_4\text{OH}$  plus ischemia, where  $\text{NH}_2\text{Cl}$  is assumed to be generated endogenously from interaction of  $\text{NH}_4\text{OH}$  with neutrophil-derived HClO<sup>[10]</sup>. These results clearly showed that both irsogladine and rebamipide conferred a protection against damage induced by

$\text{NH}_2\text{Cl}$ , either administered exogenously or occurring endogenously. However, the mechanisms underlying gastric protection seemed to be different between these two drugs. The protective action of irsogladine was significantly attenuated by pretreatment with L-NAME but not indomethacin, while that of rebamipide was attenuated by indomethacin but not L-NAME. These results suggest that the protective action of irsogladine and rebamipide may be mediated by endogenous NO and PGs, respectively. Moreover, these drugs caused different effects on the PD response induced by  $\text{NH}_2\text{Cl}$  or  $\text{NH}_4\text{OH}$  plus ischemia. Rebamipide significantly prevented the PD reduction in response to these treatments while irsogladine had no effect on such PD responses. It is considered that gastric PD is one of the indicators for the integrity of the gastric mucosa, including the development of mucosal injury as well as the recovery from injury<sup>[18,19]</sup>. From the present results, it is suggested that irsogladine does not inhibit the onset of injury caused by  $\text{NH}_2\text{Cl}$  but prevents the ultimate generation of gastric damage, probably by preventing the later extension of injury, while rebamipide reduced the gastric ulcerogenic response by inhibiting the initial irritating action of  $\text{NH}_2\text{Cl}$  on the mucosa.

The local release of NO regulates the gastric mucosal microcirculation and maintains the mucosal integrity in collaboration with PGs and sensory neurons<sup>[20,21]</sup>. At present, the mechanism by which irsogladine stimulates the release of NO in the gastric mucosa remains unknown. We previously reported that mucosal application of NO donor prevented the development of gastric lesions induced by  $\text{NH}_2\text{Cl}$  without any influence on the PD responses<sup>[11,12]</sup>. These data are in agreement with the present findings that irsogladine reduced the severity of  $\text{NH}_2\text{Cl}$ -induced gastric lesions but had no effect on the reduced PD response. On the other hand, it has been shown that rebamipide protects the gastric mucosa from various necrotizing agents by increasing PG biosynthesis in the mucosa and scavenging free radicals<sup>[22-24]</sup>. Exogenous  $\text{PGE}_2$  has also been shown to inhibit gastric lesions in response to  $\text{NH}_2\text{Cl}$  or  $\text{NH}_4\text{OH}$  plus ischemia<sup>[11]</sup>. These data support the present observation that rebamipide protected the stomach against  $\text{NH}_2\text{Cl}$ -induced damage, in an indomethacin-sensitive manner. It should also be noted in the present study that rebamipide prevented the PD reduction in response to  $\text{NH}_2\text{Cl}$  or  $\text{NH}_4\text{OH}$  plus ischemia. Since taurine, a scavenger of HClO, markedly suppressed the PD reduction caused by  $\text{NH}_2\text{Cl}$ <sup>[11,12]</sup>, it is likely that rebamipide may prevent gastric ulcerogenic and PD responses to  $\text{NH}_2\text{Cl}$  through a radical scavenging

action, in addition to mediation by endogenous PGs.

In conclusion, the present results taken together suggest that  $\text{NH}_2\text{Cl}$  generated either endogenously or exogenously, damages the gastric mucosa at a low concentration. Gastric mucosal lesions caused by  $\text{NH}_2\text{Cl}$  was prevented by both irsogladine and rebamipide, although the former action was more potent than the latter. Although the exact mechanisms underlying gastroprotection afforded by irsogladine and rebamipide remain unknown, it is assumed that their mechanisms are different; the effect of irsogladine is mediated at least partly by endogenous NO, while that of rebamipide is attributable to endogenous PGs as well as its radical scavenging action. Since an important feature of *H. pylori* infection is neutrophil infiltration in the gastric mucosa<sup>[1,2]</sup>, it is possible that  $\text{NH}_2\text{Cl}$  is formed in the inflamed gastric mucosa, where neutrophil and *H. pylori* are located in juxtaposition. Thus, the present study also suggests that irsogladine may have therapeutic potential in the prevention and/or treatment of gastric mucosal damage related to *H. pylori*.

## REFERENCES

- 1 Marshall BJ, Warren JR. Unidentified curved bacilli on gastric epithelium in active chronic gastritis. *Lancet*, 1983;1:1273-1275
- 2 Graham DY. Campylobacter pylori and peptic ulcer disease. *Gastroenterology*, 1989;96(Suppl):615-625
- 3 Marshall BJ, Langton SR. Urea hydrolysis of patients with Campylobacter pyloridis infection. *Lancet*, 1983;1:965-966
- 4 Whitehead R, Truelove SC, Gear MWL. The histological diagnosis of chronic gastritis in fibrotic gastroscopy biopsy specimens. *J Clin Pathol*, 1972;25:1-11
- 5 Badwey JA, Karnovsky ML. Active oxygen species and the functions of phagocytic leukocytes. *Ann Rev Biochem*, 1980;46:695-726
- 6 Klevanoff SJ. Oxygen metabolism and the toxic properties of phagocytes. *Ann Intern Med*, 1980;93:480-489
- 7 Grisham MB, Jefferson MM, Thomas EL. Chlorination of endogenous amines by isolated neutrophil. Ammonia-dependent bactericidal, cytotoxic, and cytolytic activities of the chloramines. *J Biol Chem*, 1984;259:10404-10413
- 8 Grisham MB, Hernandez LA, Granger DN. Xanthine oxidase and neutrophil infiltration in intestinal ischemia. *Am J Physiol*, 1986; 251:G567-G574
- 9 Murakami M, Asagoe K, Dekigai H, Kusaka S, Saita H, Kita T. Products of neutrophil metabolism increase ammonia induced gastric mucosal damage. *Dig Dis Sci*, 1995;40:268-273
- 10 Dekigai H, Murakami M, Kita T. Mechanism of *Helicobacter pylori* associated gastric mucosal injury. *Dig Dis Sci*, 1995;40:1332-1339
- 11 Nishiwaki H, Kato S, Takeuchi K. Irritant action of monochloramine in rat gastric mucosa. *Gen Pharmacol*, 1997;29:713-718
- 12 Kato S, Nishiwaki H, Kanaka A, Takeuchi K. Mucosal ulcerogenic action of monochloramine in rat stomachs. *Dig Dis Sci*, 1977;42: 2156-2161
- 13 Ueda F, Aratani S, Mimura K, Kimura K, Nomura A, Enomoto H. Effect of 2,4 diamino 6 (2,5-dichlorophenyl) s triazine maleate (MN-1695) on gastric ulcers and gastric secretion in experimental animals. *Arzneimittelforschung*, 1984;34P:474-477
- 14 Ueda F, Aratani S, Mimura K, Kimura K, Nomura A Enomoto H. Effect of 2,4<sup>2</sup>diamino 6 (2,5-dichlorophenyl) s triazine maleate (MN-1695) on gastric mucosal damage induced by various necrotizing agents in rats. *Arzneimittelforschung*, 1984;34:478-484
- 15 Okabe S, Takeuchi K, Ishihara Y, Kunimi H. Effect of 2,4 diamino 6 (2,5 dichlorophenyl) s triazine maleate (MN-1695) on gastric secretion and on experimental gastric ulcers in rats. *Pharmacometrics*, 1984;24:683-689
- 16 Takeuchi K, Ishihara Y, Okada M, Niida H, Okabe S. A continuous monitoring of mucosal integrity and secretory activity in rat stomach. A preparation using a lucite chamber. *Jpn J Pharmacol*, 1989;49:235-244
- 17 Murakami M, Saita H, Teramoto S, Dekigai H, Asagoe K, Kusaka S, Kita T. Gastric ammonia has a potent ulcerogenic action on the rat stomach. *Gastroenterology*, 1993;105:1710-1715
- 18 Ivy KJ, Den Besteubm L, Glifton JA. Effect of bile salts on ionic movement across the human gastric mucosa. *Gastroenterology*, 1970;59:683-690
- 19 Svanes K, Ito S, Takeuchi K, Silen W. Restitution of the surface epithelium of the in vitro frog gastric mucosa after damage with hyperosmolar sodium chloride; morphologic and physiologic characteristic. *Gastroenterology*, 1982;82:1409-1426
- 20 Whittle BJR, Lopez Belmonte J, Moncada S. Regulation of gastric mucosal integrity by endogenous nitric oxide; interactions with prostanoids and sensory neuropeptides in the rat. *Br J Pharmacol*, 1990;99:607-611
- 21 Tepperman BL, Whittle BJR. Endogenous nitric oxide and sensory neuropeptides interact in the modulation of the rat gastric microcirculation. *Br J Pharmacol*, 1992;105:171-175
- 22 Ishihara K, Komuro Y, Nishiyama N, Yamasaki K, Hotta K. Effect of rebamipide on mucus secretion by endogenous prostaglandin-independent mechanism in rat gastric mucosa. *Arzneimittelforschung*, 1992;42:1462-1466
- 23 Yamasaki K, Kanbe T, Chijiwa T, Ishihara H, Morita S. Gastric mucosal protection by OPC-12759, a novel antiulcer compound in the rat. *Eur J Pharmacol*, 1987;142:23-29
- 24 Yoshikawa T, Naito Y, Tanigawa T Kondo M. Free radical scavenging activity of the novel anti ulcer agent rebamipide studied by electron spin resonance. *Arzneimittelforschung*, 1993;43:363-366

Edited by MA Jing-Yun

Proofread by MIAO Qi-Hong

# Hepatocellular carcinoma in central Sydney: a 10 year review of patients seen in a medical oncology department

Desmond Yip<sup>1</sup>, Michael Findlay<sup>2</sup>, Michael Boyer<sup>1</sup> and Martin H. Tattersall<sup>3</sup>

**Subject headings** carcinoma, hepatocellular; liver neoplasms; survival/rate; Australia

## Abstract

**AIM** To report a single Australian oncology unit's experience with the management of patients with hepatocellular carcinoma (HCC), in the context of a literature review of the current management issues.

**METHODS** Retrospective case record review of 76 patients with diagnosis of HCC referred to the unit between 1984 and 1995.

**RESULTS** Sixty-three patients had adequate records for analysis. Thirty-six (56%) were migrants with half from Southeast Asia. Twenty-four patients had a documented viral aetiology. Nine (14%) of 51 patients with pathological confirmation of HCC had normal alpha-fetoprotein levels. Median survival of the 20 patients managed palliatively was 5 weeks compared to 16 weeks for the cohort overall. Surgery in 16 patients rendered all initially disease free with a median survival of 88 weeks. Chemoembolisation induced tumor responses in 5 of the 11 patients so treated. Systemic chemotherapy and tamoxifen treatment caused tumor response in two of 12 and one of 25 respectively.

**CONCLUSION** Prolonged survival of patients with HCC depends on early detection of small tumors suitable for surgical resection. Other active treatments are palliative in intent and have limited success. In addition to tumor response and survival duration, the toxicities of

therapies and the overall quality of life of patients need to be considered as important outcomes. Viral hepatitis prevention and screening of individuals at risk are strategies that are important for HCC management in communities where the disease is endemic.

## INTRODUCTION

Hepatocellular carcinoma (HCC) is the fourth most common cause of death from malignancy in the world and the third most common in men<sup>[1]</sup>. High risk areas such as Asia and Africa are associated with endemic hepatitis B and C infections. In Australia HCC is still a relatively uncommon cancer as it is in most developed nations. In the state of New South Wales the incidence was 2.6 per 100 000 for males and 1.1 per 100 000 for females from 1985 to 1989. The incidence is significantly higher in male and female migrants from China, Taiwan and Vietnam<sup>[2]</sup>.

We reviewed all cases of HCC that were seen in the Department of Medical Oncology at Royal Prince Alfred Hospital a tertiary centre situated in central Sydney between January 1984 to December 1995. Patient demographics, presenting symptoms, disease stage, prognostic indicators as well as treatment and outcomes were determined.

## METHOD

Using the Clinical Reporting System (CRS) database in the Department of Medical Oncology, the names of 76 patients with the diagnosis of HCC were obtained. The departmental files and the medical records were then examined and information collected using a proforma. Parameters collected included sex, age, nationality, clinical and pathological status, presenting symptoms, ECOG (Eastern Cooperative Oncology Group) performance status at time of initial contact, presence or absence of cirrhosis, documentation of possible etiological factors and alpha-fetoprotein (AFP) levels. Tumor response to therapy was recorded using WHO response criteria. Partial response was defined as a greater than 50% reduction in the sum of the products of the longest tumor dimension and its widest perpendicular, in

<sup>1</sup>Department of Medical Oncology, Royal Prince Alfred Hospital, Camperdown, NSW, Australia

<sup>2</sup>Wellington Cancer Centre Private Bag 7902, Wellington, New Zealand  
Email. michael.findlay@wnhealth.co.nz

<sup>3</sup>University of Sydney, Camperdown NSW, Australia  
Dr. Desmond Yip, male, born on 1966-01-28 in Sydney, Australia. Graduated from Sydney University in 1989, trained in medical oncology, now working in clinical research with an interest in gastrointestinal malignancies and novel therapies. Currently a clinical research fellow, Department of Medical Oncology, Guy's Hospital, London, United Kingdom.

**Correspondence to:** Dr. Michael Findlay, Wellington Regional Oncology Unit, Wellington Hospital, Private Bag 7902, Wellington, New Zealand

Tel. +64-4 385 5999, Fax. +64-4 385 5984

Email. woncmf@wnhealth.co.nz

Received 1998-08-10

the absence of new lesions. Where disease was not measurable, changes in AFP level were monitored. Complete response was defined as no tumor evident on imaging plus normalisation of AFP if this was measured. Progressive disease was defined as 25% increase in measurable tumor size or sustained increase in AFP.

Survival time was measured from the date of diagnosis to the date of death determined where possible from the hospital records, contact with local doctors and computer search of the New South Wales Cancer Registry databases.

## RESULTS

Seventy-six patients with a diagnosis of HCC were seen in the Department during this period. Of these, sixty-three patients had records that contained sufficient information for analysis.

### *Demographics*

The mean age of the patients was 50 years (range 27-77) with 43 males and 20 females. Fifty-six percent of the patients were born overseas with over half of these born in Southeast Asia (Table 1).

### *Clinical characteristics*

Of 57 patients where data on symptoms were available, thirteen (23%) patients were asymptomatic at the time of diagnosis. Three had an ECOG performance status of 4 (totally bedbound) and six a score of 3 (spending more than 50% of waking hours in bed). The most common presenting symptom was pain in 33 (58%) followed by weight loss in 27 (47%) and abdominal distension in 17 (30%). Sixteen (28%) patients presented with jaundice. The median duration of symptoms before presentation was two months, ranging from immediately prior to presentation up to 50 weeks.

The most common documented aetiological factor for hepatocellular carcinoma in this series was hepatitis B infection in 21 (33%) patients. Five patients had hepatitis C infection, and three of these were co-infected with both hepatitis B and C. Routine testing for hepatitis C at Royal Prince Alfred Hospital only became available from mid 1989 and retrospective testing was not done in the cohort, which may explain the relatively low infection rate in this series. Five (22%) of the 23 patients with viral hepatitis were Australian born. Of the three patients who had cirrhosis secondary to hemochromatosis all had alcohol as a cofactor. Alcohol was a cofactor in 5 (19%) of the 26 Australian born patients and five (14%) of the overseas born patients. Twenty-three patients had no apparent causative factor. One patient had a past history of low grade lymphoma and another hydatid liver disease. These causative factors are listed in Table 2.

Pathological confirmation of diagnosis was

obtained in 51 patients (81%) mainly by fine needle aspiration biopsy. In the remainder, a clinical diagnosis was based on radiological appearance on CT scan or hepatic angiogram and a raised serum AFP level. There were nine patients (14%) with pathological confirmation of HCC who had normal AFP levels at presentation. The initial levels ranged from 0 to 36000 IU. Thirty-five (69%) of the 51 patients where information was available had clinical, pathological or radiological evidence of cirrhosis at initial presentation. Thirty-four patients (of 56 evaluable) had multifocal tumors on imaging or pathology and six had regional node enlargement. Ten of 61 patients (16%) had distant metastases with the sites being lung in (7) and bone (4).

### *Treatment*

Twenty (30%) patients received no anti-tumor treatment and were managed with supportive care. Six of these patients presented with ECOG performance status 3 or 4. The median survival of this group was five weeks from the time of diagnosis.

The remaining 43 patients received some form of anti-tumor therapy. The median time from diagnosis to initiation of treatment was 15 days (range 0 days to 5.2 years). Seventeen patients received two types of therapy and four patients received three or four different treatments.

Surgery was performed in 16 (25%) patients, either in the form of a lobectomy or hemihepatectomy. Three of these patients had surgery after chemoembolization. Two patients had repeat resections for relapse 5 and 39 months after curative resection. No patients in the series received allograft transplantation as their first therapeutic intervention. All patients who underwent surgery were rendered clinically disease free afterwards. Their median survival was 88 weeks (range 5-354 weeks) from diagnosis or surgery with the median time to relapse being 43 weeks (range 4-182). Two patients are still alive at one year and two years after surgery.

Chemoembolization of the HCC by the selective injection of cisplatin and Lipiodol into the hepatic artery was carried out in 11 (17%) patients. In three patients this was done prior to surgery in an attempt to reduce the vascularity and size of the tumor. One of these patients received alcohol injection into the tumor as well and proceeded to an orthotopic liver transplantation. The other two patients had initial marked falls in the AFP to almost within normal range but these had risen to beyond pretreatment levels prior to surgery. Six patients (55%) had a 50% reduction in AFP with the median time to progression being 25 weeks (excluding the transplanted patient from the calculation of the duration of response). Median

survival from chemoembolization was 48.5 weeks.

Twelve (19%) patients were treated with systemic chemotherapy. Three were given anthracycline treatment alone (2 adriamycin, 1 epirubicin), while others received various combinations of cisplatin, adriamycin, 5-fluorouracil (5FU), etoposide and mitomycin C. Two patients received more than one regimen of chemotherapy. Only two patients had objective tumor responses to chemotherapy. Another two had stable disease. The median time to tumor progression was 26 weeks.

Tamoxifen was administered to 25 (40%) patients, with only one showing evidence of AFP response. The time to progression was 44 weeks. Two other patients had stable disease.

Table 3 summarises the response rates, response duration and overall survival of the groups of patients according to the treatments received. The median survival of the group as a whole was 16 weeks with the mean being 50 weeks.

**Table 1 Countries of birth of cohort**

Country of Birth	No.
Australia	26
Egypt	3
Europe	11
India	1
Pacific Islands	1
Southeast Asia	20
Unknown	1
Total	63

**Table 2 Breakdown of established aetiological factors in cohort**

Alcohol	10
Chronic autoimmune hepatitis	3
Hepatitis B	21
Hepatitis C	5
Hepatitis B+C	3
Haemochromatosis	3
Unknown	23
Total	63

**Table 3 Summary of treatments received for hepatocellular carcinoma**

Treatment	Number of patients (%)	Number responding (%)	Median time to progression (weeks)
Observation	20 (30)		
Surgery	16 (25)	16 (100)	43
Chemoembolization	11 (17)	6 (54)	25
Systemic chemotherapy	12 (19)	2 (27)	26
Tamoxifen	25 (40)	1 (4)	44

## DISCUSSION

Despite a variety of therapeutic strategies HCC remains a significant cause of cancer death worldwide. The mainstay of treatment is resection of the disease. This is facilitated by early detection of tumors and by liver transplantation when poor hepatic function would otherwise prevent resection.

Other treatments, largely directed at palliation such as chemotherapy ( $\pm$ embolization), percutaneous ethanol injection, radiation and hormone therapy are modest in their effects however they may play a role in conjunction with surgery. Equally or more important strategies are prevention of predisposing illnesses (e.g., hepatitis B) or modification of the cirrhotic pre-malignant field defect.

Hepatic resection is generally only feasible in patients with focal lesions and with adequate underlying hepatic function<sup>[3]</sup>. Because of tumor stage at presentation and the presence of cirrhosis, the proportion of patients suitable for surgery is generally small. The role of orthotopic hepatic transplantation is still controversial. There have been concerns about the perioperative mortality and the frequency of tumor recurrence in the transplanted liver, but transplantation offers some chance of cure of both the tumor and the cirrhosis. A recent series<sup>[4]</sup> of 48 patients with small tumors (single <5 cm or no more than three <3 cm) and cirrhosis undergoing transplantation, reported overall survival and disease free survival at four years to be 75% and 83% respectively. Ninety-four percent of these patients had underlying viral hepatitis.

Percutaneous ethanol injection of these tumors has usually been restricted to non-surgical candidates and one series from Italy has shown encouraging survival figures where ethanol injection was used instead of surgery<sup>[5]</sup>. This approach may provide a treatment for patients with no access to resection services or those with poor liver reserve, who are not otherwise able to have a liver transplant. Other forms of imaging-directed destruction such as cryotherapy, laser and thermotherapy may have similar potential.

As is the published experience, we found the response rate with systemic chemotherapy low and of short duration. Doxorubicin, remains the most widely used agent but being liver metabolized it may result in unpredictable toxicity in those with hepatic disease. When used as a single agent it generally has a response rate below 20%<sup>[6]</sup>. Epirubicin, idarubicin and mitoxantrone all have activity comparable to doxorubicin. Single agent activities of other intravenously administered cytotoxics such as cisplatin, 5-fluorouracil, etoposide and mitomycin C are all in the range of 0%-15%<sup>[6]</sup>. The Eastern Cooperative Oncology Group<sup>[7]</sup> has evaluated 432 patients in four sequential trials of varying combinations of 5-FU, streptozotocin, semustine, doxorubicin, zinostatin, amsa crine and cisplatin. The median survival of the group as a whole with systemic chemotherapy was 14 weeks with a one-year survival of only 15%. The best median survival of 24 weeks was obtained with the combination of 5-FU and semustine. Although any

of these agents may cause greater response rates if given intra-arterially with or without embolization, most reports of trials of chemotherapy, both single agent and combinations have small patient numbers and none shows a convincing superiority to be considered standard treatment<sup>[7,8]</sup>.

Chemoembolization consists of a relatively selective embolization of the tumor blood supply with agents such as cisplatin and Lipiodol. While theoretically attractive, the technique may result in hepatic decompensation because the cirrhotic liver is more dependent on blood from the hepatic artery than the portal vein. For this reason embolization techniques are suitable for a small group of patients. In the Group D'Etude de Traitement du Carcinome Hepatocellulaire<sup>[9]</sup> randomised trial of chemoembolisation versus conservative management in 96 selected patients from 24 centres, there was no significant survival difference detected after accounting for differences in baseline and prognostic characteristics. Small survival differences however would not be detected by a study of this size. Half of the patients in the treatment group had reduction in AFP levels. These observations are in keeping with the findings in our study. Hepatic decompensation however was seen in 70% of patients having chemoembolization. Another multicentre randomised study<sup>[10]</sup> of Lipiodol/cisplatin chemoembolization in 73 patients also reported no survival difference. Transarterial embolization without chemotherapy in a single institutional study has also demonstrated no survival advantage versus supportive care<sup>[11]</sup>. In these circumstances, a more appropriate endpoint may be symptom control, analgesic requirements and quality of life rather than survival. Symptomatic rather than asymptomatic patients may be more appropriate candidates for chemotherapy.

Oestrogen receptors have been detected in normal liver tissue and in HCC with the levels tending to be higher in the neoplastic tissue. This provides the rationale of using the anti-oestrogen tamoxifen. Seven randomized trials of tamoxifen versus placebo in advanced HCC have been reported<sup>[12-18]</sup>. Three<sup>[12-14]</sup> which had under 38 patients each reported improved survival in the tamoxifen treated arms. An additional two randomized trials investigating chemotherapy and tamoxifen found no improvement in response or survival when tamoxifen was added to doxorubicin<sup>[19]</sup> or intra-arterial cisplatin and 5FU<sup>[15]</sup>. An overview of the published randomised trials of tamoxifen versus active or no active treatment in HCC between 1978 and 1995 suggested a moderate benefit with a 2.2 odds ratio for 1 year survival<sup>[20]</sup>. However the largest randomized study so far involving 496 patients has recently been presented and showed no survival benefit of

tamoxifen compared to supportive care<sup>[19]</sup>.

Antiandrogen therapy has also been tried in HCC on the basis that it is a male predominant disease, it can be induced by androgen therapy and that the receptors are expressed in high levels in the tumors. A European Organisation for Research and Treatment of Cancer (EORTC) multicentre trial<sup>[21]</sup> compared antiandrogen therapy with a luteinising hormone-releasing hormone (LHRH) agonist either goserelin or triptoreline, with a pure antiandrogen nilutamide alone or in combination against placebo in 244 patients with advanced HCC. No significant difference however was found in any of the groups.

A recent study reports an apparent reduction in the incidence of new primary HCCs in patients administered polyphenolic acid, an acyclic retinoid, after resection for HCC. This strategy targets the pre-malignant field defect that leads to HCC<sup>[22]</sup>.

Radiation therapy has been more usually applied in the form of radioactive ligands injected into the hepatic artery than as external radiation. A preliminary report of a randomized trial from Hong Kong has shown that <sup>131</sup>I labelled lipiodol injected post-resection improves the time to tumor recurrence<sup>[23]</sup>. Similarly data from pilot studies suggest post-transplant/resection - chemotherapy may improve outcome, although randomized trials are still underway<sup>[24]</sup>.

Viral hepatitis is a significant causative factor for HCC in our cohort especially in those born overseas, being present in over one-third. In the migrant population high hepatitis B endemicity accounts for the high prevalence rate. In hepatitis B associated cirrhosis the cumulative incidence of hepatocellular carcinoma has been found to be 59% over a six-year period<sup>[25]</sup>. With hepatitis C associated cirrhosis, a Japanese prospective study<sup>[26]</sup> has reported that 75% of patients will develop HCC by 15 years. Preventative measures such as hepatitis B vaccination in endemic disease populations is obviously an important and effective strategy. A recent study from Taiwan has reported that a national hepatitis B vaccination program has reduced the annual HCC incidence in children of aged 6-14 years from 0.7 to 0.36 per 100 000 ( $P < 0.01$ ), with a similar effect on population mortality<sup>[27]</sup>. Treatment of viral related chronic active hepatitis with interferon alpha may not only prevent development of cirrhosis but also reduce the frequency of subsequent HCC<sup>[28]</sup>.

Alcohol was also an important risk factor in the Australian born patients in our series. In a larger published series of HCC<sup>[29]</sup> from western Sydney it was found to be an association in 46% of the Australian patients and only 13% of those born overseas.

Screening of high risk populations for HCC by a combination of serum AFP determination and

imaging with high resolution real time ultrasound can detect HCC at an early stage which might be amenable to curative resection. AFP however can be normal in patients with asymptomatic small tumors. The reliability of ultrasound is operator dependent and many studies have been in Japanese patients who have generally a thinner body habitus which may make imaging easier than in Westerners. Studies suggest that treatment of these early lesions may produce a true survival benefit although there have been no randomized trials reporting mortality reduction from screening<sup>[30]</sup>. This strategy can only be considered an option in high risk populations, rather than on a general population basis.

## CONCLUSION

Hepatocellular carcinoma is becoming a greater problem in developed countries such as Australia with the wave of immigration from countries affected by endemic viral hepatitis. Treatment modalities are unsatisfactory once the tumor has spread and become inoperable. Public health measures need to focus on the targeting of risk factors and surveillance of at risk subgroups.

## REFERENCES

- Pisani P, Parkin DM, Bray FI, Ferlay J. Estimates of the worldwide mortality from twenty five major cancers in 1990. *Int J Cancer*, 1999;83:18-29
- McCredie M, Coates M, Duque-Portugal. Common cancers in migrants to New South Wales 1972-1990. Cancer Epidemiology Research Unit. NSW Central Cancer Registry, 1993
- Farmer DG, Rosove MH, Shaked A, Busuttill RW. Current treatment modalities for hepatocellular carcinoma. *Ann Surg*, 1993; 219:236-247
- Mazzaferro V, Regalia E, Doci R, Andreola S, Pulvirenti A, Bozzetti A, Montalto F, Ammatuna M, Morabito A, Gennari L. Liver transplantation for the treatment of small hepatocellular carcinomas in patients with cirrhosis. *N Engl J Med*, 1996;334:693-699
- Livraghi T, Giorgio A, Marin G, Salmi A, de Sio I, Bolondi L, Pompili M, Brunelo F, Lazzaroni S, Torzilli G. Hepatocellular carcinoma and cirrhosis in 746 patients: long term results of percutaneous ethanol injection. *Radiology*, 1995;197:101-108
- Ahlgren J, Wanebo H, Hill M. Hepatocellular carcinoma. In: Gastroenterological oncology. Philadelphia: J B Lippincott, 1992: 428-430
- Falkson G, Cnaan A, Schutt AJ, Ryan LM, Falkson HC. Prognostic factors for survival in hepatocellular carcinoma. *Cancer Res*, 1988; 48:7314-7318
- Farmer DG, Rosove MH, Shaked A, Busuttill RW. Current treatment modalities for hepatocellular carcinoma. *Ann Surg*, 1994; 219:236-247
- Groupe D'Etude et de Traitement du Carcinome Hepatocellulaire. A comparison of lipiodol chemoembolisation and conservative treatment for unresectable hepatocellular carcinoma. *New Eng J Med*, 1995;332:1256-1261
- Rougier P, Pelletier G, Ducreux M, Gay F, Luboinski M, Hagege H, Dao T, Van Steenberghe V, Buffet C, Adler M, Pignon JP, Roche A et le groupe CHC2. Unresectable hepatocellular carcinoma: lack of efficacy of lipiodol chemoembolization. Final results of a multicentre randomized trial (Abstract). *Proc Am Soc Clin Oncol*, 1997;16:279
- Bruix J, Llovet J, Castells A, Montana X, Bru C, Ayuso MC, Vilana R, Rodes J. Transarterial embolization versus symptomatic treatment in patients with advanced hepatocellular carcinoma: results of a randomized, controlled trial in a single institution. *Hepatology*, 1998; 27:1578-1583
- Farinati F, Salvagnini M, de Maria N, Fornasiero A, Chiaramonte M, Rossaro L, Naccarato R. Unresectable hepatocellular carcinoma: a prospective controlled trial with tamoxifen. *J Hepatol*, 1990;11:297-301
- Martinez Cerezo FJ, Tomas A, Donosi L, Enriquez J, Guarner C, Balanzo J, Martinez Noguera A, Vilardell F. Controlled trial of tamoxifen in patients with advanced hepatocellular carcinoma. *J Hepatol*, 1994;20:702-706
- Elba S, Giannuzzi V, Misciagna G, Manghisi O. Randomised controlled trial of tamoxifen versus placebo in inoperable hepatocellular carcinoma. *Ital J Gastroenterol*, 1994;26:66-68
- Uchino J, Une Y, Sato Y, Gondo H, Nakajima Y, Sato N. Chemohormonal therapy of unresectable hepatocellular carcinoma. *Am J Clin Oncol*, 1993;16:206-209
- Castells A, Bruix J, Bru C, Ayuso C, Roca M, Boix L, Vilana R, Rodes J. Treatment of hepatocellular carcinoma with tamoxifen: a double blind placebo-controlled trial in 120 patients. *Gastroenterology*, 1995;109:917-922
- Riestra S, Rodriguez M, Delgado M, Suarez A, Gonzalez N, de la Mata M, Diaz G, Mino Fugarolas G, Rodrigo L. Tamoxifen does not improve survival of patients with advanced hepatocellular carcinoma. *J Clin Gastroenterol*, 1998;26:200-203
- Pignata S, Izzo F, Farinati F, Palmieri G, Belli M, Manzione L, Pedicini T, D'Aprile M, Giorgio A, Russo M, Calandra M, Monfardini S, Galo C, Perrone F. Role of Tamoxifen (TM) in the treatment of hepatocellular carcinoma (HCC). Results from the CLIP-01 randomised trial (Abstract). *Proc Am Soc Clin Oncol*, 1998;17:257a
- Melia P, Johnson P, Williams R. Controlled clinical trial of doxorubicin and tamoxifen versus doxorubicin alone in hepatocellular carcinoma. *Cancer Treat Rep*, 1987;71:1213-1216
- Simonetti R, Liberati A, Angiolini C, Pagliaro L. Treatment of hepatocellular carcinoma: a systematic review of randomized controlled trials. *Ann Oncol*, 1997;8:117-136
- Grimaldi C, Bleiberg H, Gay F, Messner M, Rougier P, Kok L, Cirera L, Cervantes A, De Greve J, Paillot B, Buset M, Nitti D, Sahmoud T, Duez N, Wils J. Evaluation of antiandrogen therapy in unresectable hepatocellular carcinoma: results of a European Organization for Research and Treatment of Cancer multicentric double blind trial.
- Muto Y, Moriwaki H, Ninomiya M, Adachi S, Saito A, Takasaki KT, Tanaka T, Tsurumi K, Okuno M, Tomita E, Nakamura T, Kojima T. Prevention of second primary tumours by an acyclic retinoid, polypropionic acid, in patients with hepatocellular carcinoma. *N Eng J Med*, 1996;334:1561-1567
- Leung WT, Lau WY, Ho S, Chan M, Lee WY, Leung N, Chan A, Yeo W, Johnson PJ. Reduction of local recurrence after adjuvant intra arterial lipiodol-iodine 131 for hepatocellular carcinoma-a planned interim analysis of a prospective randomized study. *Proc Am Soc Clin Oncol*, 1997;19:279a (abstract 988)
- Olthoff KM, Rosove MH, Shackleton CR, Imagawa DK, Farmer DG, Northcross P, Pakrasi AL, Martin P, Goldstein LI, Shaked A. Adjuvant chemotherapy improves survival after liver transplantation for hepatocellular carcinoma. *Ann Surg*, 1995;221:734-743
- Oka H, Kurioka N, Kim K, Kanno T, Kuroki T, Mizoguchi Y, Kobayashi K. Prospective study of early detection of hepatocellular carcinoma in patients with cirrhosis. *Hepatology*, 1990;12: 680-687
- Ikeda K, Saitoh S, Koida I, Arase Y, Tsubota A, Chayama K, Kumada H, Kawanishi M. A multivariate analysis of risk factors for hepatocellular carcinoma carcinogenesis: a prospective observation of 795 patients with viral and alcoholic cirrhosis. *Hepatology*, 1993;18:47-53
- Chang MH, Chen CJ, Lai MS, Hsu HM, Wu TC, Kong MS, Liang DC, Shau WY, Chen DS. Universal hepatitis B vaccination in Taiwan and the incidence of hepatocellular carcinoma in children. *N Engl J Med*, 1997;336:1855-1859
- Nishiguchi S, Kuroki T, Nakatani S, Morimoto H, Takeda T, Nakajima S, Shiomi S, Seki S, Kobayashi K, Otani S. Randomised trial of effects of interferon alpha on incidence of hepatocellular carcinoma in chronic active hepatitis C with cirrhosis. *Lancet*, 1995;346:1051-1055
- Brotodihardjo AE, Tait N, Weltman MD, Liddle C, Little JM, Farrell GC. Hepatocellular carcinoma in western Sydney. Aetiology, changes in incidence, and opportunities for better outcomes. *Med J Aust*, 1994;161:433-435
- Dusheiko GM, Hobbs KE, Dick R, Burroughs AK. Treatment of small hepatocellular carcinomas. *Lancet*, 1992;340:285-288

# The expression of c-src gene in the carcinogenesis process of human cardia adenocarcinoma

WANG Xiu-Jia, YUAN Shu-Lan, XIAO Lin, WANG Xu-Hua and WANG Chao-Jun

**Subject headings** c-src gene; expression product; PP60<sup>c-src</sup>; cardia adenocarcinoma; carcinogenesis; neoplasm metastasis; immunohistochemistry

## Abstract

**AIM** To investigate the activation, expression of c-src gene and its role in the carcinogenic process of human cardia adenocarcinoma (CA). **METHODS** Fifty-six cases of CA, 34 cases of normal, 36 cases of proliferative epithelia adjacent to carcinoma, and 20 cases of lymph node metastases of CA were studied for PP60<sup>c-src</sup>, the expression product of c-src gene immunohistochemically by using the specific monoclonal antibody, Mab327.

**RESULTS** The positive rates of PP60<sup>c-src</sup> in the normal epithelia, proliferative epithelia, CA and lymph node metastases were 29.4% (10/34), 94.4% (34/36), 71.4% (40/56) and 60.0% (12/20), respectively, among them, the differences of the positive rates were statistically significant ( $P < 0.01$ ). The expression levels of PP60<sup>c-src</sup> in CA and proliferative epithelia were significantly higher than that in the normal epithelia ( $P < 0.01$ ). The PP60<sup>c-src</sup> positive rates in the papillary, tubular, poorly differentiated and mucous adenocarcinoma were 75.0% (6/8), 81.8% (18/22), 50.0% (10/20) and 100.0% (6/6), respectively, whereas those of tubular and mucous adenocarcinomas were significantly higher than those of papillary and poorly differentiated adenocarcinomas ( $P < 0.05$ ), and the PP60<sup>c-src</sup> expression levels of tubular and

mucous adenocarcinomas were also significantly higher than those of papillary and poorly differentiated adenocarcinomas ( $P < 0.01$ ).

**CONCLUSION** The activation and expression of c-src gene are associated with the initiation and development of human CA; the protein amount of PP60<sup>c-src</sup> increased during the process of carcinogenesis; and PP60<sup>c-src</sup> expression is also related to lymph node metastases.

## INTRODUCTION

There is a general tendency in gastric cancer that the incidence rate of cardia adenocarcinoma (CA) is increasing steadily, and cancer of the distal stomach is decreasing proportionately. The biological and epidemiological features of CA are distinct from those of the distal stomach, and the underlying cause remained unelucidated<sup>[1-3]</sup>. PP60<sup>c-src</sup> is the product of c-src gene possessing the activity of tyrosine kinase. Increased expression of c-src gene had been reported in some human sarcoma and cancers of breast<sup>[4]</sup>, esophagus<sup>[5]</sup>, stomach<sup>[6]</sup> and colon<sup>[7]</sup>, and the activation and expression of c-src gene might be associated with the initiation and development of some cancers. Our previous study showed the activation and expression of c-src gene was associated with the development and differentiation of esophageal squamous cell carcinomas<sup>[8]</sup>, we believed that similar changes might occur in cancer of cardia, therefore, the following study was carried out.

## MATERIALS AND METHODS

### Sample collection and processing

All 56 cases of CA samples were collected from the CA patients surgically treated in Yanting Institute of Cancer Prevention of Sichuan Province. All tissue specimens were routinely processed, formalin-fixed and paraffin-embedded, at least 2 serial paraffin sections of 4  $\mu$ m - 6  $\mu$ m thickness were made, one was stained with hematoxylin and eosin (HE) and the other was used for PP60<sup>c-src</sup> protein detection by immunohistochemical staining.

### Reagents

The monoclonal antibody Mab327 (mouse IgG) was kindly given by the Molecular Pathology

Institute of Cancer Research, Cancer Center, The First University Hospital of West China University of Medical Sciences, Chengdu 610041, Sichuan Province, China

WANG Xiu-Jie, male, born on 1957-02-15 in Ziyang, Sichuan Province and graduated from West China University of Medical Sciences in 1982, now Associate Professor of Oncology, engaged in the researches of etiology and mechanisms of carcinogenesis of cancers, screening and developing anti-cancer drugs, having 20 papers published.

Project supported by the grant of West China University of Medical Sciences, No.L293015

Correspondence to: WANG Xiu-Jie, Institute of Cancer Research, Cancer Center, The First University Hospital of West China University of Medical Sciences, Chengdu 610041, Sichuan Province, China.

Tel. +86-28-5501218, Fax. +86-28-5583252

Received 1999-07-21 Accepted 1999-09-22

Department of Nagoya University, Japan; Streptavidin-Peroxidase Immunohistochemical Staining Kit (Zymed USA) was purchased from Fuzhou Maxim Biotech, Inc.

#### **Immunohistochemical analysis of PP60<sup>c-src</sup> protein**

PP60<sup>c-src</sup> protein was detected immunohistochemically with LSAB method according to the manufacturer's instructions with slight modification. Briefly, the tissue sections were deparaffinized and rehydrated through graded alcohols, and digested with trypsin. Then, endogenous peroxidase activity was blocked with 3% H<sub>2</sub>O<sub>2</sub>, and after treatment with normal serum, the sections were incubated with Mab 327 at a dilution of 1:100 overnight at 4 °C, with biotinylated second antibody 20 min, and with streptavidin peroxidase 30 min at room temperature. Subsequently, the sections were subjected to color reaction with 0.02% 3,3-diaminobenzidine tetrahydrochloride containing 0.005% H<sub>2</sub>O<sub>2</sub> in PBS (pH 7.4), and were counterstained with hematoxylin lightly. In each staining run, a known PP60<sup>c-src</sup> positive sample was added as positive control, and a section of the same sample was incubated with PBS instead of Mab327 as negative control.

#### **Histopathological examination**

Histopathological diagnosis for CA and related lesions were made, and the histological types of CA were examined by 2 experienced pathologists according to the given criteria<sup>[8]</sup>.

#### **Qualitative and quantitative analysis of immunohistochemical staining of PP60<sup>c-src</sup>**

The immunostaining results of PP60<sup>c-src</sup> were analyzed according to the known criteria<sup>[5]</sup>. The percentages of positive PP60<sup>c-src</sup> cell in CA and related lesions were assessed and scored as follows: negative (-), <25% (+), 25%-50% (++) , >50% (+++); The intensity of staining in PP60<sup>c-src</sup> positive cytoplasm and/or cell membrane were compared with the negative control and scored as follows: negative (-), weak (+), moderate (++) and strong (+++).

## **RESULTS**

#### **Histopathologic examination**

Among the 56 cases of CA samples, there were 34 normal epithelia adjacent to cancer, 36 proliferative epithelia adjacent to cancer, 56 adenocarcinomas including papillary (8/56), tubular (22/56), poorly differentiated (20/56), mucous adenocarcinomas (6/56), and 20 CA with lymph node metastases.

#### **Localization and distribution of PP60<sup>c-src</sup>**

Positive PP60<sup>c-src</sup> protein cells showed brown staining in their cytoplasm s and cell membranes, no positive staining was found in the negative controls. The intensity of staining varied with different lesions and different histologic types. Positive staining of PP60<sup>c-src</sup> was localized in apex of glandular epithelial cells (Figure 1); in papillary and tubular adenocarcinomas, positive staining was distributed along the papillary margin or glandular lining, both the cytoplasm s and cell membranes were positively stained but that of cell membranes were stronger than those in cytoplasm s (Figure 2); the positive staining in poorly differentiated adenocarcinomas were evenly distributed in cytoplasm s and cell membranes (Figure 3); and in the mucous adenocarcinomas, the positive PP60<sup>c-src</sup> staining was unevenly distributed as micromasses.

#### **PP60<sup>c-src</sup> expression in CA and in the related lesions**

The positive rates of PP60<sup>c-src</sup> expression in CA, proliferative and normal epithelia adjacent to cancer were 71.4% (40/56), 94.4% (34/36) and 29.4% (10/34), respectively (Table 1). The positive rates of the former two were higher than that in the latter ( $P<0.01$ ), and the positive staining in intensities in CA and proliferative epithelia were also stronger than that in the normal epithelia ( $P<0.01$ ).

#### **PP60<sup>c-src</sup> expression in different histological types**

The positive rates of PP60<sup>c-src</sup> in papillary, tubular, poorly differentiated and mucous adenocarcinoma were 75.0% (6/8), 81.8% (18/22), 50.0% (10/20), and 100.0% (6/6), respectively (Table 2) and the positive rates in tubular and mucous adenocarcinomas were higher than those in poorly differentiated or papillary adenocarcinomas ( $P<0.05$ ); the percentages of high PP60<sup>c-src</sup> expression (+ + - + + +) in tubular and mucous adenocarcinoma were 63.6% (14/24) and 100.0% (6/6), respectively; while that in papillary and poorly differentiated ones were all low (+), there were significant differences between them ( $P<0.01$ ).

#### **PP60<sup>c-src</sup> expression in CA with lymph node metastases**

The positive rate of PP60<sup>c-src</sup> expression was 60.0% (12/20) in 20 cases of metastatic lymph node (Table 1), among them, the positive ones in papillary, tubular, poorly differentiated and mucous adenocarcinomas were 2/2, 2/4, 6/12 and 2/2, respectively; the expression intensity of PP60<sup>c-src</sup> in CA with lymph node metastases was the same as those without (Figure 4).

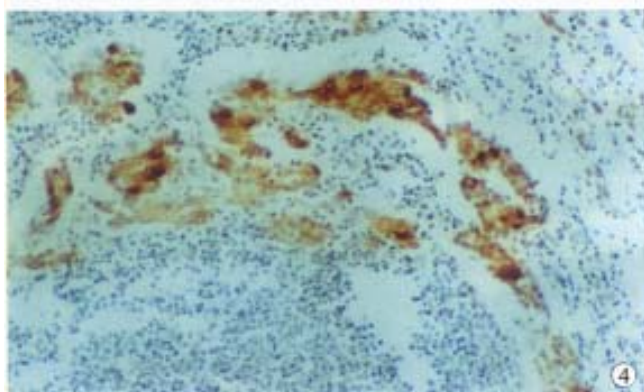
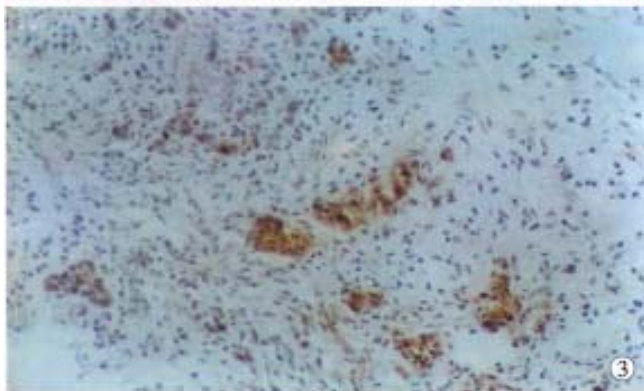
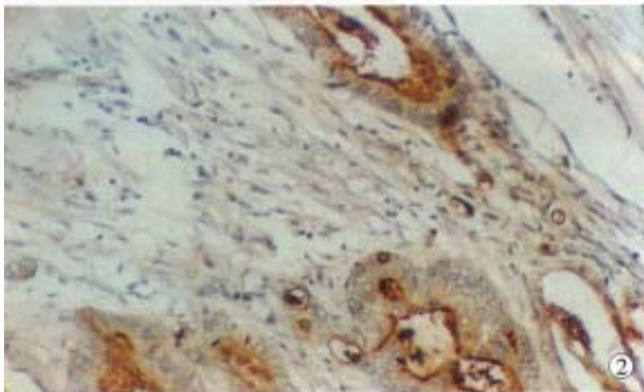
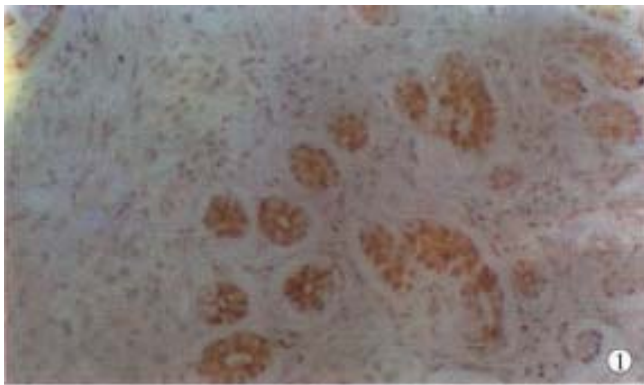


**Figure 1** The expression of PP60<sup>c-src</sup> in the proliferative epithelia adjacent to carcinoma. LSAB×200

**Figure 2** The expression of PP60<sup>c-src</sup> in tubular adenocarcinoma. LSAB×200

**Figure 3** The expression of PP60<sup>c-src</sup> in the poorly differentiated adenocarcinoma. LSAB×200

**Figure 4** The expression of PP60<sup>c-src</sup> in the lymph node metastasis of CA. LSAB×200

**Table 1** The expression of PP60<sup>c-src</sup> in CA and related lesions

Lesion	Case	Staining intensity			Positive rate (%)
		- (%)	+ (%)	+++ + (%)	
Normal epithelia	34	24(70.5)	10(29.4)	0(0)	10(29.4)
Proliferative epithelia	36	2 (5.6)	6(16.7)	28(77.8) <sup>d</sup>	34(94.4) <sup>b</sup>
Cardia adenocarcinoma	56	16(28.6)	20(35.7)	20(35.7) <sup>d</sup>	40(71.4) <sup>b</sup>
Lymph node metastases	20	8(40.0)	8(40.0)	4(20.0)	12(60.0)

<sup>b</sup> $P < 0.01$ , in comparison of the positive rates in different lesions ( $\chi^2 = 34.19$ ) vs normal epithelia; <sup>d</sup> $P < 0.01$ , in comparison of the positive intensity in different lesions ( $\chi^2 = 25.08$ ) vs normal epithelia.

**Table 2** The expression of PP60<sup>c-src</sup> in CA of different histological types

Lesion	Case	Staining intensity			Positive rate (%)
		-(0/10)	+ (%)	++++ + (%)	
Papillary	8	2(25.0)	6(75.0)	0(0)	6(75.0)
Tubular	22	4(18.2)	4(18.2)	14(63.6) <sup>b</sup>	18(81.8) <sup>a</sup>
Poorly differentiated	20	10(50.0)	10(50.0)	0(0)	10(50.0)
Mucous	6	0(0)	0(0)	6(100.0) <sup>b</sup>	6(100.0) <sup>a</sup>
Total	56	16(28.6)	20(35.7)	20(35.7)	40(71.4)

<sup>a</sup> $P < 0.05$ , in comparison of the positive rates of tubular and mucous adenocarcinomas vs those of papillary and poorly differentiated adenocarcinomas ( $\chi^2 = 8.11$ ); <sup>b</sup> $P < 0.01$ , in comparison of the positive rates of tubular and mucous adenocarcinomas vs those of papillary and poorly differentiated adenocarcinomas ( $\chi^2 = 27.56$ ).

## DISCUSSION

PP60<sup>c-src</sup> is a phosphorylated cytoplasmic protein encoded by c-src gene, having the activity of tyrosine kinase. The expression of PP60<sup>c-src</sup> can be found in many normal cells, which plays important roles in the regulation of cell proliferation, differentiation and transformation<sup>[4]</sup>. Recent studies indicated that the increase in the amount of PP60<sup>c-src</sup> protein and kinase activity was associated with initiation and development of some human neoplasms, and the activation and increase of expression were one of the factors for cancer initiation<sup>[4-8]</sup>. In this study, the expressions of PP60<sup>c-src</sup> in CA, proliferative epithelia and normal epithelia were 71.4% (40/56), 94.4% (34/36) and 29.4% (10/34), respectively and the positive rates of PP60<sup>c-src</sup> in CA and proliferative epithelia were much higher than that in the normal epithelia ( $P < 0.01$ ). Jankowski *et al* analyzed the expression product of c-src gene in 15 cases of esophageal adenocarcinoma and 15 cases of Barrett's esophageal epithelia immunohistochemically, the positive rates were 20% (3/15), suggesting that the expression of c-src gene is related to the development of esophageal adenocarcinoma. Therefore, the results of this study indicated that the activation and expression of c-src gene might be associated with the initiation and development of CA. However, the high expression of PP60<sup>c-src</sup> in the proliferative epithelia might be associated with the proliferation of glandular epithelial cells, occurring in the aged rats<sup>[9]</sup>. The low PP60<sup>c-src</sup> expression in some normal epithelia adjacent to cancer might be explained by the fact that there had

been PP60<sup>c-src</sup> expression in the normal epithelia related to the initiation of cancer<sup>[5-8]</sup>. On the other hand, it indicated that the activation and expression of *c-src* gene might be an early event in the carcinogenesis of CA.

Although it was well known that the activation and expression of *c-src* gene were associated with the initiation of some human neoplasms. The results obtained mainly from biochemical assay by measuring the protein amount and kinase activity of PP60<sup>c-src</sup> varied with the methodology. Most of the studies reported that PP60<sup>c-src</sup> protein kinase activity increased in the cancer cell lines and cancer tissues from cancers of stomach, colon, lung and kidney, etc., but compared with those of normal tissues related to cancer, no difference of PP60<sup>c-src</sup> protein amount was found, the increase in PP60<sup>c-src</sup> protein kinase activity could not be explained by the increase of protein expression encoded by *c-src* gene<sup>[6,10]</sup>. In the present study, PP60<sup>c-src</sup> protein was detected by using the specific monoclonal antibody Mab 327, immunohistochemically, the high level of PP60<sup>c-src</sup> expressions ( + + - + + ) in CA and proliferative epithelia were 35.7% and 77.8%, respectively, a low PP60<sup>c-src</sup> expression (+) was found in some normal epithelia adjacent to cancer, the difference of expression intensity was significant statistically ( $P < 0.01$ ). The results of this study suggested that the protein amount of PP60<sup>c-src</sup> expression was increased in carcinogenesis of CA.

With regard to the relationship between expression product of *c-src* gene, PP60<sup>c-src</sup> and the differentiation of cancer cells, there was no consensus in this aspect<sup>[6,8,9,11]</sup>. Fanning *et al*<sup>[1]</sup> reported a high level of *c-src* expression in well differentiated bladder cancers, and proposed that PP60<sup>c-src</sup> protein and kinase activity were associated with the differentiation of epithelial cells of urinary tract and grade I-II bladder carcinomas. However, Takekura *et al*<sup>[6]</sup> could not find the difference of PP60<sup>c-src</sup> kinase activity between well and poorly differentiated gastric carcinomas. In this study, PP60<sup>c-src</sup> positive rates varied in different histological types of CA; the positive rates in mucous adenocarcinomas (100.0%, 6/6) and tubular adenocarcinomas (81.8%, 18/22) were higher than those in papillary (75.0%, 6/8) and poorly differentiated types (50.0%, 10/20), the difference being significant statistically ( $P < 0.05$ ). And the high level of expressions (++ - +++) in mucous and tubular adenocarcinomas were 100.0% (6/6) and 63.6% (14/18), respectively, only low expression (+) was found in papillary and poorly differentiated adenocarcinomas, the differences of expression level were also significant statistically

( $P < 0.01$ ). These results suggested that the expression level of PP60<sup>c-src</sup> was associated with the differentiation and histological types of CA, high PP60<sup>c-src</sup> expressions in mucous and tubular adenocarcinomas might be related to their well differentiation and other biologic behaviors.

The relationship between the PP60<sup>c-src</sup> expression with increase in kinase activity and metastatic colon carcinomas had been reported already<sup>[12,13]</sup>, but there was no report of detection of PP60<sup>c-src</sup> protein in lymph node metastases by immunohistochemical staining. Talamonti *et al*<sup>[12]</sup> discovered increase in PP60<sup>c-src</sup> kinase activity, in the stages of polyps and primary carcinomas. Termuhlen *et al*<sup>[13]</sup> reported that PP60<sup>c-src</sup> kinase activity in hepatic metastases of colorectal carcinoma increased by 2.2 folds, and in extrahepatic metastases increased by 12.7 folds, while compared with that in normal mucosa, PP60<sup>c-src</sup> kinase activity in the hepatic metastases of non-colorectal carcinomas increased only slightly. In this study, PP60<sup>c-src</sup> protein was detected in the lymph node metastases of CA, the positive rate was 60.0% (12/20), the expression level of PP60<sup>c-src</sup> was equal to that of the same primary adenocarcinoma. The results of this study suggested that PP60<sup>c-src</sup> expression is associated with the lymph node metastases of CA, which deserved further investigation.

## REFERENCES

- Powell J, McConkey CC. Increasing incidence of adenocarcinoma of the gastric cardia and adjacent sites. *Br J Cancer*, 1990;62:440-443
- Blot WJ, Devesa SS, Kneller RW, Fraumeni JF. Rising incidence of adenocarcinoma of the esophagus and gastric cardia. *JAMA*, 1991;265:1287-1289
- Sampliner RE. Adenocarcinoma of the esophagus and gastric cardia: is there progress in the face of increasing cancer incidence. *Ann Intern Med*, 1999;130:67-69
- Jacobs C, Rübsamen H. Expression of PP60 *c-src* protein kinase in adult and fetal human tissue: high activities in some sarcomas and mammary carcinomas. *Cancer Res*, 1983;43:1696-1702
- Jankowski J, Coghill G, Hopwood D, Wormley KG. Oncogenes and onco suppressor genes in adenocarcinoma of the esophagus. *Gut*, 1992;33:1033-1038
- Takekura N, Yasui W, Yoshida K, Tsujino T, Nakayama H, Kameda T, Yokozaki H, Nishimura Y, Ito H, Tahara E. PP60 *c-src* protein kinase activity in human gastric carcinomas. *Int J Cancer*, 1990;45:847-851
- Cartwright CA, Kamps MP, Meisler AI, Pipas JM, Eckert W. PP60<sup>c-src</sup> activation in human colon carcinoma. *J Clin Invest*, 1989;83:2025-2033
- Wang XJ, Wang CJ, Huang GQ, Xiao HY. A study of *c-src* gene expression product PP60<sup>c-src</sup> in esophageal carcinoma. *J WCUIMS*, 1995;26:197-201
- Majumdar APN, Tureaud J, Relan NK, Kessel A, Dutta S, Hatfield JS, Fligel SEG. Increased expression of PP60<sup>c-src</sup> in gastric mucosa of aged rats. *J Gerontol*, 1994;49:B110-116
- Cartwright CA, Meisler AI, Eckhart W. Activation of the PP60<sup>c-src</sup> protein kinase is an early event in colonic carcinogenesis. *Proc Natl Acad Sci USA*, 1990;87:558-562
- Fanning P, Bulovas K, Saini KS, Libertino JA, Joyce AD, Summerhayes IC. Elevated expression of PP60 *c-src* in low grade human bladder carcinomas. *Cancer Res*, 1992;52:1457-1462
- Talamonti MS, Roh MS, Curley SA, Gallick GE. Increase in activity and level of PP60<sup>c-src</sup> in progressive stages of human colorectal cancer. *J Clin Invest*, 1993;91:53-60
- Termuhlen PM, Curley SA, Talamonti MS, Saboorian MH, Gallick GE. Site specific differences in PP60<sup>c-src</sup> activity in human colorectal metastases. *J Surg Res*, 1993;54:293-298

# Clinical and experimental study on regional administration of phosphorus 32 glass microspheres in treating hepatic carcinoma

LIU Lu, JIANG Zao, TENG Gao-Jun, SONG Ji-Zhi, ZHANG Dong-Sheng, GUO Qing-Ming, FANG Wen, HE Shi-Cheng, GUO Jin-He

**Subject headings** liver neoplasms/therapy; phosphorus-32 glass microspheres ( $^{32}\text{P-GMS}$ );  $^{31}\text{P-GMS}$ ; interventional therapy

## Abstract

**AIM** To study the therapeutical effectiveness, dosage range and toxic adverse effects of domestic phosphorus 32 glass microsphere and evaluate its clinical significance.

**METHODS** I. Fifty-two BALB/c tumor bearing male nude mice were allocated into treatment group ( $n = 38$ ) and control group ( $n = 14$ ). In the former group different doses of  $^{32}\text{P-GMS}$  were injected into the tumor mass, while in the latter  $^{31}\text{P-GMS}$  or no treatment was given. The experimental animals were sacrificed in batches, and then the tumors and their nearby tissues were examined by light and electron microscopy. II. Through selective catheterization of hepatic artery,  $^{32}\text{P-GMS}$  was infused to 5 healthy domestic pigs in a dosage equivalent to the therapeutic dose for human being, and  $^{31}\text{P-GMS}$  was infused to another 5 healthy domestic pigs. Two pigs infused with contrast medium served as whole course blank controls. One pig from each group was surrendered to euthanasia at week 1, 4, 8 and 16 respectively. The ultrastructural histopathological changes in liver tissues taken from different sites were evaluated *semiquantitatively*. III. One hundred and twenty-seven times of  $^{32}\text{P-GMS}$  intrahepatic artery interventional therapies were performed on 93

patients with hepatic carcinoma, including 79 cases of primary hepatic carcinoma and 14 cases of secondary hepatic carcinoma.  $^{32}\text{P-GMS}$  ( $n = 30$ ), and group B,  $^{32}\text{P-GMS}$  and half-dose of trans-hepatic artery embolization (TAE) ( $n = 49$ ), and 18 patients with HCC by TAE only as control group C. Fourteen patients with secondary hepatic carcinoma were treated in the same way as group B or C.

**RESULTS** I. Comparing with the control group, the treatment group of tumor bearing nude mice attained the tumor inhibition rates of 59.7%-93.7% ( $F = 579.62, P < 0.01$ ) at 14d. At an absorbed dose of 7320Gy, the tumor cells were completely destroyed. When the absorbed doses ranged from 1830Gy to 3660Gy, most of the tumor cells showed the evidences of injury or necrosis, but there appeared some well-differentiated tumor cells and enhanced effect of the autoimmunocytes. At an absorbed dose of 366Gy or less, some tumor cells still remained active proliferative ability. The definite anticancer effect appeared as early as 3d after intratumoral injection of  $^{32}\text{P-GMS}$ . II. The cumulative amount of  $^{32}\text{P-GMS}$  in the target tissue after trans-hepatic artery instillation attained more than 90% of the total dose administered. Semiquantitative analysis of ultrastructural morphology in the experimental group showed no statistical difference between the nuclear abnormality ( $n_{\text{abn}}$ ) and mitochondrial variability ( $M_{\text{var}}$ ) at week 1 or 2, but revealed prominent difference ( $\chi^2 = 6.70-9.68, P < 0.01, \chi^2 = 65.09-115.09, P < 0.001$ ) as compared with those in the other groups. In the experimental group the  $n_{\text{abn}}$  in tissues showed no significant difference between week 8 and week 16. no apparent changes were found in the stomach, spleen, kidney and lung tissues of the experimental pigs. III. The therapeutical results of HCC patients in group A were closely approximated to those of group C, no hematological toxic side effects were noted, and the systemic reaction was mild. In some patients 2 mos-3 mos after treatment some secondary

Experimental Center of Modern Medical Sciences, Nanjing Railway Medical College, Nanjing 210009, Jiangsu Province, China  
LIU Lu, M.D. female, born in 1946-10-17 in Jinan, Shandong Province, Han nationality, graduated from Nanjing Railway Medical College in 1970 and is now an Associate Professor, majoring in nuclear medicine and having more than 50 papers published at home and abroad.

Supported by the Science and Technology Commission of Jiangsu Province, No. BJ93077. Sponsored by Project No. 863 of National High-Tech Research and Development Program, No. 715-002-0200.  
**Correspondence to:** LIU Lu, Experimental Center of Modern Medical Sciences, Nanjing Railway Medical College, Nanjing 210009, China  
Tel. +86-25-3301508 Ext. 2708, Fax +86-25-3426368  
Email.xue-c@263.net  
Received 1999-07-14

**foci appeared around the periphery of the primary lesion. In general better effectiveness was obtained in patients with small lesion. After analyzing by RIDIT method, the therapeutic result in group B was significantly better than that in group C, and secondary foci around the original lesion were rarely seen at 3mos after treatment. In group C the collateral circulation was reestablished along the periphery of primary foci and the secondary foci appeared more frequently, and were required to undergo several courses of treatment. In group B, 4 cases of HCC were treated surgically as their mass decreased in size after <sup>32</sup>P-GMS treatment. Resected specimens showed that the tumor was encapsulated by fibrotic tissue and most of the tumor cells necrosed. The 3-year survival rates were 43.3%-51.0% after A and B regimen treatment. In 14 cases of secondary HCC, the foci were well controled within one year after-treatment.**

**CONCLUSION When the experimental model of implanted human liver cancer cells received <sup>32</sup>P-GMS of 1830Gy-3660Gy, it produced excellent anticancer effect without any injury to the normal neighboring tissues and the prominent anticancer effect was shown within 3d after intratumoral injection. Intrahepatic arterial administration of <sup>32</sup>P-GMS at the macrocosmic absorbed dosage less than 190 Gy/dose exerted reversible sub-lethal injury to domestic pig liver tissues. It took more than 8 weeks to repair the injured liver tissue and restore its function. <sup>32</sup>P-GMS trans-hepatic artery embolization is an effective and safe regimen in treating hepatic carcinoma.**

## INTRODUCTION

Trans-hepatic artery embolization (TAE)<sup>[1]</sup> is the main regimen for treating unresectable hepatic carcinoma (HCC). The experimental investigation using microsphere carriers such as colloidal microsphere, artificial cell membrane-liposome etc, in treating malignant tumors had been carried out for more than a decade with advanced development<sup>[2]</sup>. The microspheres mainly conjugated with anticancer drugs released slowly into the cancer tissue. Up to now, a novel anticancer microsphere preparation has been evolved, i.e. incorporation of radionuclide (<sup>32</sup>P or <sup>90</sup>Y) to the glass microspheres forming a nontoxic, undegradable radioactive radiation source through

regional medication, which aroused the interest and notice of investigators in this field<sup>[3-5]</sup>.

We report the results of evaluating the pharmacology, toxicology and clinical effect of <sup>32</sup>P-phosphorus-glass microspheres (<sup>32</sup>P-GMS) in three parts. I. By using human liver cancer cell bearing nude mouse model to explore the experimental anti cancer effect of intratumoral injection of <sup>32</sup>P-GMS and investigate the appropriate dose range, time course and the influence on the neighboring tissues. II. By administrating <sup>32</sup>P-GMS to the whole liver or certain liver lobes of domestic pig model and observing the local irradiative reaction and systemic toxic effect on the normal liver tissue to provide the experimental basis for determining the appropriate tolerable dosage and treatment course of <sup>32</sup>P-GMS internal irradiation in normal human liver tissues. III. From 1996 to 1998, 93 patients with liver cancer received 127 times of interventional <sup>32</sup>P-GMS internal irradiation.

## MATERIALS AND METHODS

### *Medicaments*

By activation of standardized glass microspheres with nonradioactive <sup>31</sup>P (<sup>31</sup>P-GMS, cold sphere) through nuclear-chemical reaction [<sup>31</sup>P (n,γ)<sup>32</sup>P] transformed into radioactive <sup>32</sup>P glass microsphere (provided by nuclear Power Research Institute of China, nPIC)<sup>[6]</sup>, having the properties as follows: diameter of glass sphere 46 μm-76 μm, radioactive nuclide purity >99%, radioactivity per unit 550 MBq·g<sup>-1</sup> 3700 MBq·g<sup>-1</sup> (15 mCi·g<sup>-1</sup>-100 mCi·g<sup>-1</sup>), <sup>32</sup>P elution rate <0.1% within 30 days; <sup>32</sup>P physical half-life 1428 days, average β ray energy per disintegration: 0.695 MeV (maximum energy 1.711 MeV); and soft tissue penetration distance, max. 8.0 mm, averaging 3.2 mm. <sup>32</sup>P-GMS suspension was prepared by mixing <sup>32</sup>P-GMS with super-liquidized iodized oil or 50% glucose solution to the concentration of 100 mg·mL<sup>-1</sup> on oscillator.

### *Dosimetry*

Loevinger's formula<sup>[7]</sup> for calculating the absorbed dose of β emitter radionuclide:

$$D_{\beta\infty} = 73.8E_{\beta}C_0T_{\text{eff}}$$

where  $D_{\beta\infty}$  the total absorbed beta particle dose (cGy),  $E_{\beta}$ , the average beta ray energy per disintegration (MeV),  $C_0$ , the initial tissue concentration of radioactivity (mCi/kg) and  $T_{\text{eff}}$ , the effective half-life (days).

Based on the pharmacokinetic characteristics of regional administration of <sup>32</sup>P-GMS and the related parameters, the following formulae were established<sup>[8]</sup>:

$$D \text{ (cGy)} = 20A \text{ (MBq)} \cdot m \text{ (kg)}^{-1}$$

$$D \text{ (cGy)} = 732A \text{ (mCi)} \cdot m \text{ (kg)}^{-1}$$

where A: the cumulative activity of radioactive nuclide, D: the total dose of absorbed  $\beta$  particles in tissue, m: the tissue weight.

### Animal experiment

**Human liver cancer cell-bearing nude mouse model and anti-cancer effect of  $^{32}\text{P}$ -GMS** Human liver cancer cell line subset (H-CS)<sup>[9]</sup> with higher oncogenicity and liability of metastasis was implanted into the dorsal subcutaneous tissue of 52BALB/c nu/nu nude mice (male, body weight 16.8 g-21.3 g, mean 19.2 g, aged 4 weeks, derived from Shanghai Experimental Animal Center, Chinese Academy of Sciences) at the dosage of 0.1 mL-0.2 mL ( $1 \times 10^7$  tumor cells for each animal).

Experiment 1. Forty tumor-bearing nude mice with the tumor mass diameter of 0.7 cm-1.0 cm, different doses of  $^{32}\text{P}$ -GMS were injected to the mass center of 32 nude mice (subgroup 1-V) in the treatment group and non-radioactive  $^{31}\text{P}$ -GMS to mass center of 8 nude mice as the control subgroup. The animals were sacrificed on the 14th day.

Experiment 2. Twelve tumor-bearing nude mice with matched tumor size were equally allocated into treatment and control group, and  $^{32}\text{P}$ -GMS 3.7 MBq were injected to the tumor mass at points with 0.8 cm apart from each other, the total dosage being 7.4 MBq-14.8 MBq, varied with the size of tumor. no treatment was given to the control animals. The mice in the treatment group were sacrificed in batches on day 3, 6, 13, 20, and 28 after medication and the same was done for those in control group. The tumor masses were disposed similar to Experiment 1. One mouse in both treatment and control groups died on day 19 and 22 spontaneously without any difference from the survivals in appearance. All of the tumor specimens were submitted to gross inspection, light and electron microscopy to observe the morphological and ultrastructural changes and then calculate the tumor inhibition rate. Tumor inhibition rate (at the time of execution) = (tumor weight of control-tumor weight of treatment group) / tumor weight of control group  $\times 100\%$ .

### Experimental study on the toxicology of $^{32}\text{P}$ -GMS

Twelve domestic pigs (6 males, 6 females) with average body weight of 23.4 kg, were randomly divided into 3 groups: warm sphere group,  $^{32}\text{P}$ -GMS ( $n = 5$ ), cold sphere group  $^{31}\text{P}$ -GMS ( $n = 5$ ) and whole course blank control group ( $n = 2$ ). Under generalized anesthesia the catheter was inserted through femoral artery to the hepatic artery of the experimental animal. To the warm sphere group  $^{32}\text{P}$ -GMS was administered at a dose equivalent to that of man,  $^{31}\text{P}$ -GMS administered to the cold

sphere group and roentgenographic contrast medium to the blank control group. For the pigs with  $^{32}\text{P}$ -GMS, the distribution of nuclide radioactivity was studied by SPECT. The radioactivity count rate was recorded on the body surface of hepatic, pulmonary and splenic regions of pigs for 14 consecutive days. One pig a time was surrendered to euthanasia on week 1, 2, 4, 8 and 16. The animal liver was dissected and weighed as soon as possible. From different sites of liver 8 tissue specimens were taken for light and electron microscopy. And at the same time, the major organs suspected to be involved such as lung, spleen, stomach and kidney were sampled for light microscopy. At the corresponding time point, liver biopsies were performed on the rest surviving animals for light and electron microscopy.

Venous blood specimens were taken for routine blood count, estimation of liver and renal function and for dynamic study of liver fibrosis markers, such as hyaluronic acid (HA), human procollagen III (hPCIII), collagen IV(C-IV), laminin (LN) and glycocholate (CG) by radioimmunoassay. The specimens prepared routinely were studied under H-600 electron microscopy at 8 000 folds magnification, to observe the ultrastructure and analyze morphometrically. A total of 100 hepatocyte nuclei and 100 mitochondria were observed in each sample group, and the nuclear abnormality ( $N_{\text{abn}}$ ) and mitochondrial variability ( $M_{\text{var}}$ ) were calculated respectively. The characteristics of abnormal nuclei were: nuclei irregular and deformed in shape; abnormal nuclear membrane, distension of the perinuclear gap; abnormal chromatin with peripheral condensation, and increase in intranuclear inclusion bodies with giant nucleolus. The abnormal mitochondria were characterized by swelling with disrupted external membrane and decrease in cristae; shrunken mitochondria, deep staining of ground matrix with decreased granules but with some vacuoles. The rates of abnormal nucleus and mitochondria variation were the percentage calculated from the number of abnormal or variation per total number of nuclei observed.

### Preliminary clinical application of $^{32}\text{P}$ -GMS in treating hepatic carcinoma

**Clinical materials** Seventy-nine cases of primary hepatocellular carcinoma, male 67 and female 12 with average age of 52 years (32 years-77 years). The diagnosis was based on the evidence afforded from the results of B-mode sonography, computed tomography or angiogram and blood AFP  $> 400 \mu\text{g/L}$ . In some cases with negative AFP, their pathological and cytological evidence settled the diagnostic problem. The clinical types in 79 cases of HCC were single massive types (52 cases, left lobe 3, right lobe 49); multi-nodular type (24 cases); and

diffuse type (3 cases). According to Child's classification of liver function, 25 were of grade A, 40 grade B and 14 grade C. The average diameter of tumor mass was 8 cm (3 cm-15 cm), 62 cases (78.5%) showed positive hepatitis B antigen, 52 cases (65.8%) were complicated with cirrhosis, 4 cases (5.1%) portal vein embolization, 6 (7.6%) pulmonary metastasis, 7 (8.9%) peritoneal lymph node metastasis and 8 (10.1%) had family histories of gastrointestinal tumors. In 14 cases of secondary hepatic carcinoma, 6 were primary colonic tumors, 5 gastric, 1 pulmonary and 2 esophageal cancers.

**Treatment regimen and grouping** Superselective catheterization was performed by Seldinger's procedure to the distal end of hepatic artery proper for 127 times in 93 cases of hepatic carcinoma. No hepatic A-V fistula was found in all of the cases as confirmed by DSA, then the <sup>32</sup>P-GMS suspension prepared by occlusion of super-liquidized iodized oil 4 mL-10 mL and <sup>32</sup>P-GMS with calculated tumor tissue absorbed dose of 50Gy -100Gy and activity range from 370 MBq-470 MBq was instilled. HCC patients were allocated randomly into 3 groups. Group A: <sup>32</sup>P-GMS internal irradiation embolization therapy (30 cases); Group B: <sup>32</sup>P-GMS and half dose TAE [Adriamycin (Adr) 30 mg/m<sup>2</sup>+cis-diammine dichloroplatinum (CDDP) 50 mg/m<sup>2</sup>+iodized oil] combined therapy (49 cases); Group C: TAE (18 cases). Fourteen cases of secondary hepatic carcinoma were treated by B and C regimen. After embolization the vasculature and tumors staining disappeared on DSA.

**Follow-up** Before treatment the average life quantity score was 65.5 (Karnofsky score)<sup>[10]</sup>. The results in liver and renal function, ECG, routine blood counts, blood AFP and CEA on day 10-14 after treatment were compared with the corresponding basal data. SPECT liver images were conducted in 20 cases before treatment. Distribution of nuclide radioactivity in chest and abdomen within 80 h after treatment was studied using bremsstrahlung lung conducted by SPECT. Plain film of liver region showed the foci of condensed iodized oil shadow within 5 days after treatment. B-mode sonogram, or computed tomogram or plain film of abdomen was taken at the scheduled time of follow-up.

**Evaluation of therapeutical results** According to the modified WHO<sup>[10]</sup> criteria for tumor therapy, the effectiveness of grades A, B and C was the product of two perpendicular diameters which were decreased >50%, 50%-25% and 25%-10%, respectively, while the product decreased <10% was defined as stable. When the product was increased, it meant ineffective.

### Statistical method

Chi-square test and RIDIT method were used for analyzing categorical data, *t* test and ANOVA were used for analyzing numerical data and survival rate was calculated by life-table method.

## RESULTS

### Changes in implanted human hepatic carcinoma

**Gross inspection (Figure 1)** The similar manifestation in Experiments I, II and controls was the rapid progressive growth of tumor mass, beginning from the dorsal injection points extended to the contralateral side, eventually distributed to the whole dorsa and buttocks. At the time of execution, the tumor mass presented nodular or lobular in shape with axial diameter of 2.3 cm - 4.0 cm, hard and firm in consistency on palpitation with thin intact reddish covering epiderma without ulceration. After the covered epiderma was incised, there was plenty of blood vessels on the mass surface, bleeding readily, and the section showed light reddish in color, dense in consistency, rich in vessels, and sometimes with central necrosis and focal liquification. In the treatment group the growth of tumor mass was evidently inhibited, and the inhibiting rate was directly proportional to the dosage administered and time elapsed (Tables 1, 2). About 5 days after medication, the tumor mass began with ulceration, bleeding or petechia, liquification and cystic degeneration. These changes might result in increase in tumor size, but that was qualitatively different from the growth of tumor in control group. The tumor of subgroups I and II shrank with scars or cystic degeneration. The section of tumor showed grayish white color with poor vascularity. In subgroups III-IV, most of the implanted tumors presented with ulceration, bleeding, liquification and cystic degeneration, the section of tumor showed grayish white in color with poor vascularity, too. These changes had already appeared on 3 day after medication.

**Table 1** Nude mice in different absorbed dosage group the tumor weight (g) variance, SNK analysis and tumor inhibiting rate (14d)

Group	No. of Cases (n)	Tumor weight <sup>①</sup> ( $\bar{x}\pm s$ )	SNK <sup>②</sup>	Absorbed dose mean value (Gy)	Tumor inhibiting rate (%)	Necrosed tumor cell (%)
Control	8	6.25±0.39	A	-	-	4
I	6	0.40±0.10 <sup>a</sup>	B	7320	93.6	82
II	6	0.46±0.08 <sup>a</sup>	B	3660	92.5	78
III	8	0.94±0.10 <sup>a</sup>	C	1830	84.8	70
IV	6	2.17±0.26 <sup>a</sup>	D	366	65.3	47
V	6	2.43±0.33 <sup>a</sup>	E	183	59.7	40

①Variance analysis of the mean tumor weight of different doses and control group after square root correction,  $F = 579.62$ ,  $^aP < 0.01$ . ②Different or same alphabets denote with or without statistical significance of mean deviations between groups respectively.

**Table 2 Relationship between tumor inhibiting rate and execution time in tumor-bearing nude mice accepted <sup>32</sup>P-GMS in absorbed dose of 366Gy**

Time of execution (d)	Weight of tumor (g) treatment group/control group	Tumor inhibiting rate (%)
3	1.5/2.3	34.8
6	1.7/3.2	46.9
13	2.1/5.9	64.4
20	1.6/6.7	76.1
28	1.0/6.8	85.3

**Light microscopy (Figure 2)** The tumor cells of control group were closely arranged in the form of trabeculae with large nuclei and prominent nucleoli. Some cells showed binuclei or giant nucleus and mitosis were readily found. Plenty of blood sinusoids and concentrated bile could be found between the intercellular space of tumor cells. Some of the tumor tissues showed fatty change or scattered focal necrosis. In the treatment group the microscopic manifestation varied with the different activities of the <sup>32</sup>P-GMS administered. In the I and II subgroups the tumor cells were loosely arranged with widely distributed coagulation necrosis. Some nuclei showed prominent shrinking degeneration. In subgroup III the tumor cells were loosely arranged and separated by thick or thin bundles of vesiculo-fibro-connective tissue forming pseudoacini, and in the nest some nuclei were broken with deeply stained scant cytoplasm. The histological characters in subgroups IV and V were that the arrangement of tumor cells transformed from dense to loose with scattered spot necrosis, blood sinuses being not found. In loosely arranged tumor cells desmosomes were fewer than those in the closely arranged tumor cells, but the degenerated necrotic cells increased. The necrosis was mainly located at the center of tumor mass and scattered among the dispersed tumor cells. In this experiment, a tumor mass with largest dose of radiation showed metaplasia in the neighboring epidermal tissues.

**Electron microscopy (Figure 3)** In the control group, most of the tumor cells were poorly differentiated and rapidly multiplied, with the characteristics of irregular large nuclei with deep indentation, pseudo-inclusion body formation, large and prominent nucleoli, several peripherally aggregated, nucleoli with plenty of chromatin in it. In cytoplasm mainly free polyribosome presented, while mitochondria, glycogen and rough endoplasmic reticulum were scant. In the nearby interstitial tissue infiltrated tumor cells, degenerated lymphocytes, damaged fibroblasts,

loose collagen fiber, and many vesicular inclusion bodies in the nuclei were found. The tumor cells of subgroup I revealed necrotic injury, and in the severely injured cells the nuclei lysed, cell membrane disrupted and numerous debris were found. The injured tumor cells showed condensation of nuclear chromatin, peripheral aggregation of heterochromatin in pieces, damaged organelles in cytoplasm, disappearance of mitochondrial cristae and ribosomes, appearance of many vacuoles and lipid particles. In subgroup II, many tumor cells presented histological structures similar to those in subgroup I, but with many lysosomes and mimetic secretory granules. Some were differentiated tumor cells with the characters of round nucleus with small nucleolus, evenly distributed chromatin, mainly euchromatin, mitochondria and rough endoplasmic reticula in the cytoplasm, formation of microvilli at the interface of tumor cells. The capillaries between the moderately differentiated tumor cells had thickened or loosened basal membrane with local defects, and abundant fibroblast and collagen fibers could be found in the matrix. And there was a tendency of bile canal iculi formation somewhere in the matrix. The tumor cells in subgroup III showed different morphologic appearance, some damaged mildly and others severely, but some were moderately differentiated with plenty of cytoplasmic free polyribosomes. Plasma cells scattered among the tumor cells, and some lymphocytes protruded pseudopodia when contacted with the tumor cells, no abnormality was found in the dermal cells of adjacent skin. There were residual tumor cells showing active proliferation in subgroup IV, and some normal or degenerated lymphocytes, fibroblasts and collagen fibers presented in the interstitial tissue near the tumor. In subgroup V, the histological structure was manifested in various complicated forms, and the active multiplication of tumor cells were readily seen.

#### *Toxicological manifestation of liver tissue in domestic pigs*

**Absorbed dose of <sup>32</sup>P-GMS** Liver tissue histological parameter of domestic pigs with intrahepatic arterial administration of <sup>32</sup>P-GMS and the absorbed dose of internal radiation in liver lobe at the time of euthanasia were estimated (Table 3). By scanning the different body surface regions of experimental pigs, the macrocosmic radioactivity counts in the target organ might attain more than 90% of total dose of <sup>32</sup>P-GMS given through the hepatic arterial catheterization. The effect of the dispersed radiation was also included in this rate.



**Figure 1** ①After intratumoral injection of  $^{32}\text{P}$ -GMS, SPECT revealed radioactive image condensed in the tumor but not in the non- target tissue. ②On the 14th day tumor in treatment group shrank prominently. ③Increased in size and plenty of blood supply in control group.

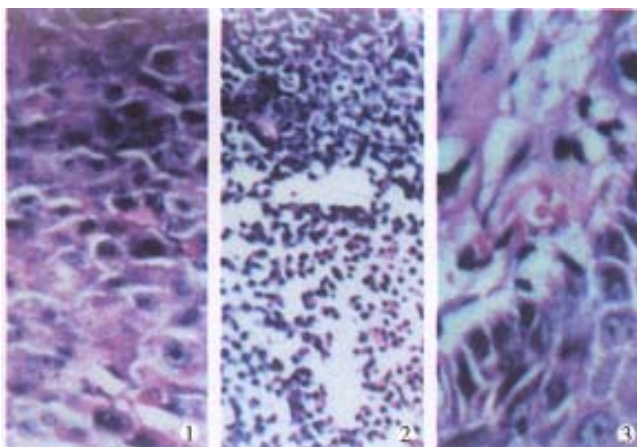


**Figure2** On the 14th day, ①Control group tumor cell s densely arranged and actively growing (HE $\times$ 100). ②Treatment group, tumor cells in coagulation necrosis (HE $\times$ 100). ③ Treatment group, radiation injury in neighboring epidermal tissue (HE $\times$ 200).

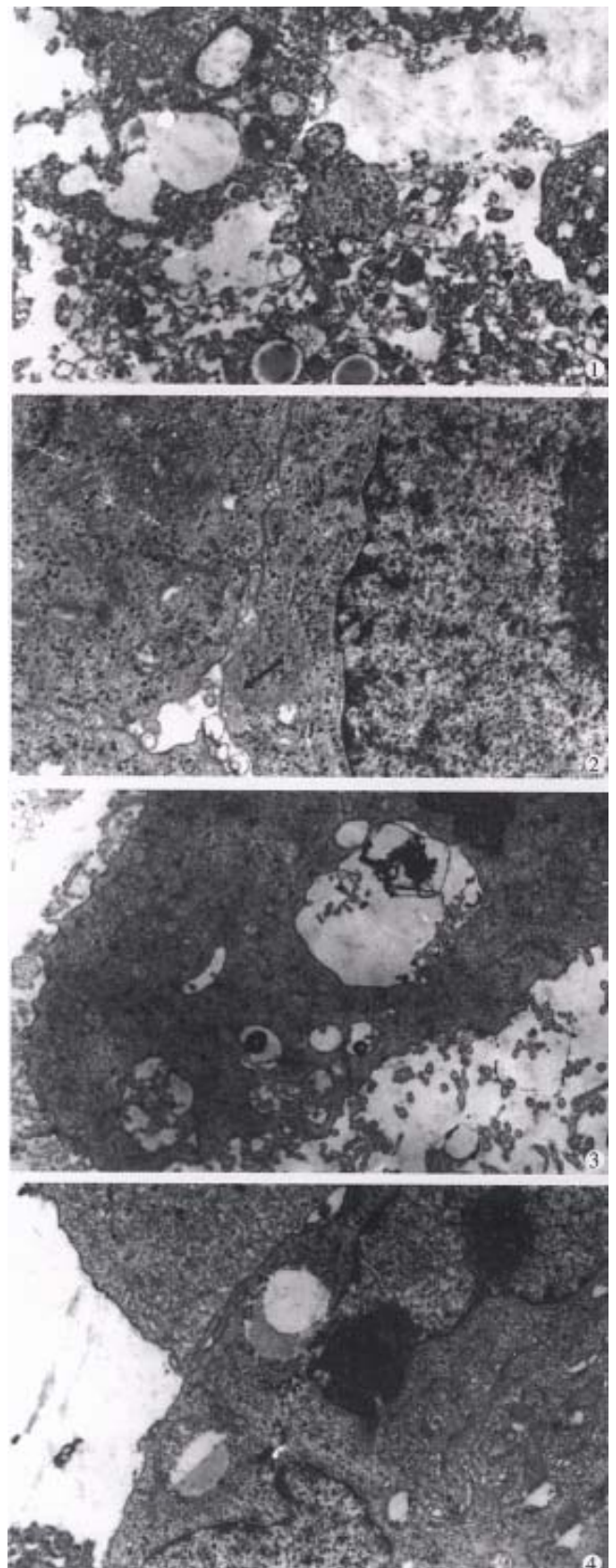


**Figure3** Results of intratumoral injection of  $^{32}\text{P}$ -GMS demonstrated by electron microscopy: ①Necrosed tumor cells ( $\times$ 5000 ). ②Formation of bile duct-like structure among tumor cells (solid arrow) ( $\times$ 8 000). ③Plenty of microvilli on the surface of tumor cell ( $\times$ 7000). ④In control group, intratumoral injection of  $^{32}\text{P}$ -GMS showing heteromorphic tumor cell with cleavage of nucleus and scanty microvilli on surface ( $\times$ 7000).

**Table 3** Histological liver tissue parameter and estimated value of a absorbed dose in domestic pigs with hepatic arterial administration of <sup>32</sup>P-GMS

Animal serial No.	Sex	Route of medication	Time of death (wk)	<sup>32</sup> P-GMS (MPq·mg <sup>-1</sup> )		Weight (mg)	Tissue macrocosmic mean absorbed dose (Gy)
				Administered activity (MBq)	Cumulated activity (MBq)		
1	F	Right hepatic artery	1	0	0	300	
2	M	Left hepatic artery	2	0	0	260	
3	F	Hepatic artery proper	4	0	0	1353	
4	M	Hepatic artery proper	8	0	0	374	
5	F	Right hepatic artery	16	0	0	1000	
6	M	Right hepatic artery	1	925	266	313	48
7	F	Left hepatic artery	2	944	465	705	190
8	M	Hepatic artery proper	4	1070	825	375	104
9	F	Left hepatic artery	8	459	529	343	136
10	M	Right hepatic artery	16	461	459	349	61 <sup>△</sup>
11	F	Hepatic artery proper	16	0		0	
12	M	Hepatic artery proper	16	0		0	

<sup>△</sup>Calculated from the estimated liver weight of 1.5kg before medication.

**Serological manifestation** In warm sphere group, the lactic acid dehydrogenase level attained 2 folds to the upper limit of normal in human being at the beginning, and one week later it rose to 4-6 folds. It did not decline significantly to 3-4 folds until week 4, and then it continuously declined to the initial level at week 8. As for aspartate aminotransferase (AST) or  $\gamma$ -glutamyl transpeptidase ( $\gamma$ -GT) there was an elevation in different degree, but for total protein (TP) and total bilirubin (TB) no changes were observed. These items were neither found abnormal in the cold sphere group nor in blank control one. As for the markers of pig liver fibrosis, the basal level of HA was within normal human range (2 $\mu$ g/L-100 $\mu$ g/L), in the warm sphere group and rose to the peak and then declined to normal. While in the cold sphere one, it rose slightly at week 1, then restored gradually to normal. The initial level of hPCIII was 2 folds to the upper limit of normal (<120 $\mu$ g/L). Within two weeks of warm sphere administration it increased to 3 folds of the normal value and recovered to initial level within 8 weeks; for the cold sphere group, hPCIII value increased slightly at week 2, then returned to the initial level at week 4. There was no abnormality of above markers in the blank control group. In the dynamic studies of G-IV, C G and LN, no apparent alterations were found in any animal group.

**Light microscopy** In the portal area the debris of <sup>32</sup>P-GMS (Figure 4) was found. In the warm sphere group, some hepatocytes showed granulation and eosinophil granulocytes infiltration at week 2 and week 4; slight granulation of hepatocytes and some with fatty change were found at week 8; no apparent abnormalities were found at the week 16

and during the whole course in cold sphere and blank control groups. No apparent changes were seen in the lung, spleen, stomach and kidney of all the experimental animals.

**Electron microscopy (Figure 5)** By electron microscopic morphometric analysis, the  $N_{abn}$  and  $M_{var}$  of the hepatocytes are shown in Table 4. One to two weeks after internal irradiation, in the warm sphere group there were alterations in nuclei and mitochondria, dilatation of rough endoplasmic reticulum, local lytic injury in endothelial lining of sinusoid, and pale faint halo at the periphery of erythrocyte. No liver tissue abnormality was found in the cold sphere group. In warm sphere one at week 4 of internal irradiation, the hepatocytes still showed some abnormal features including decreased mitochondria, distended rough endoplasmic reticulum, detached ribosome, greatly increased lysosomes and myeloid bodies, bile canaliculi disrupted showing cholestasis, and vascular endothelium was prominently damaged. Eight weeks after irradiation, the injured hepatocytes decreased. There were plenty of organelles and glycogen particles in cytoplasm, intercellular junction among the hepatocytes showed normal configuration with regularly arranged microvilli, the matrix of mitochondria condensed, rough endoplasmic reticulum distended, and fat-storing cells of collagen fibers were prominently presented in the Disse's spaces; and endothelium of blood sinus was integrated and accompanied with neutrophil granulocytes infiltration. In the liver tissue of whole liver embolization with cold spheres the nuclei of hepatocytes remained normal, but the cytoplasm revealed the changes similar to those found 4 weeks-8 weeks after internal irradiation.

The liver tissue specimens taken at 16 week of internal irradiation demonstrated that most of the hepatocytes recovered almost to normal with abundant collagen fibers in the Disse's space, while those from cold sphere group were essentially normal. The liver tissue was morphologically normal in the whole course of blank control group.

**Table 4**  $N_{abn}$  and  $M_{var}$  of nucleated hepatocytes and their standard error ( $P \pm SE$ )

No. of week	Warm sphere group		Cold sphere group		Bland control	
	$N_{abn}$	$M_{var}$	$N_{abn}$	$M_{var}$	$N_{abn}$	$M_{var}$
1	60±4.09 <sup>a</sup>	80±4.00 <sup>a</sup>	9±2.86 <sup>c</sup>	5±2.18 <sup>c</sup>		
2	58±4.94 <sup>a</sup>	77±4.21 <sup>a</sup>	8±2.71 <sup>c</sup>	4±1.96 <sup>c</sup>		
4	38±4.85 <sup>b</sup>	60±4.90 <sup>b</sup>	5±2.18 <sup>c</sup>	6±2.37 <sup>c</sup>		
8	8±2.71 <sup>cd</sup>	12±3.25 <sup>ce</sup>	3±1.71 <sup>c</sup>	5±2.18 <sup>c</sup>		
16	4±1.96 <sup>cd</sup>	4±1.40 <sup>ce</sup>	2±1.40 <sup>c</sup>	2±1.96 <sup>c</sup>	2±1.40	2±1.40

Warm sphere group no statistical significance between week 1 and week 2,  $\chi^2=0.27$ , <sup>a</sup> $P<0.50$ . In warm sphere group comparison of week 1 and week 2 with week 4,  $\chi^2=6.70-9.68$ , <sup>b</sup> $P<0.01$  and with other groups,  $\chi^2=65.09-115.09$ , <sup>c</sup> $P<0.001$ .  $N_{abn}$  of week 8 compared with that of week 16,  $\chi^2=1.42$ , <sup>d</sup> $P<0.20$ .  $M_{var}$  of week 8 compared with that of week 16,  $\chi^2=7.68$ , <sup>e</sup> $P<0.01$ .

### Clinical application

**Therapeutic effectiveness (Table 5)** In groups A and B, most of the HCC patients with <sup>32</sup>P-GMS treatment revealed prominent symptomatic improvement, relief of pain in liver region, improvement of appetite, gain of body weight, decreased tumor-size and iodized oil condensed in the form of fragments or encapsulated cumulation on the film or CT (Figure 6). No collateral circulation around the tumor body was found after <sup>32</sup>P-GMS treatment, but in 5 cases of group A some secondary foci neighboring the primary foci which had been controlled, appeared within 2-3 months after therapy. no such problem was found in group B. In three cases of diffused type of HCC, the foci were not controlled effectively. Of the 79 cases of HCC, the post-treated tumor size as compared with their original sizes, was decreased more than 50%, 50%-25%, 25%-10% and less than 10% in 24 (30.37%) cases, 25 (31.64%), 22 (27.84%) and 8 (10.1%), respectively. After <sup>32</sup>P-GMS and TAE treatment in group B, 4 received surgical resections of tumor with fair results but the other 6 with decreased tumor size refused to be operated on. Twelve of 14 cases of metastatic hepatic carcinoma after regimen B and C treatment showed decrease in size of foci, giving an effective rate of 85.71%.

**Toxic or adverse effects** About 2-3 days after TAE treatment in group C, some patients experienced fever of 38.5 °C and had grade IV leukocytopenia, almost all patients had nausea, vomiting and upset

or pain in liver region. Serum ALT, ALP and bilirubin were slightly elevated, the markers of liver fibrosis HA and hPCIII revealed transient elevation, restored to the pretreatment level about half month later, C-IV, LN and CG did not show any fluctuation. no abnormalities were found in renal function and ECG. As compared with group C, the above features in group A patients were rare and mild, among them 7 cases had pre treatment WBC  $<2.0 \times 10^9/L$  and one patient with uremia under regimen A treatment did not present significant side effects or complications. In group B patients no grade III-IV gastrointestinal reaction and no grade IV leukocytopenia occurred after treatment (Table 6).

**Living quality and survival period** The median survival period of HCC patients in groups A and B was 585 days, in group C, 455 days. The 0.5, 1, 2 and 3 year survival rates in group A, B and C were 100%, 96.7%, 56.7%, 43.3%; 97.7%, 91.8%, 61.2%, 51.0% and 96.4%, 81.8%, 41.2%, 31.0%, respectively. The living quality of patients in groups A and B has improved prominently as evaluated by Karnofsky score, which rose from the basal level of 65.5 to 75.5, eventually to 80 in the recovery stage of some individual patients. A patient complicated with uremia maintained by hemodialysis survived up to 26 months after treatment, another patient committed suicide due to the cause unrelated to his illness. Two cases complicated with cancer cell embolism of portal vein survived merely 3.5 and 6.5 months and died from upper digestive tract bleeding and hepatorenal syndrome respectively.

### Prognostic factors affecting the survival rate

Multifactorial analysis revealed that the following prognostic factors may affect the survival rate: accumulation of <sup>32</sup>P-GMS in the tumor mass, parameters of hepatic fibrosis, the clinical types, size and its magnitude of decrease after treatment and whether intrahepatic or remote metastasis was present. The therapeutic effectiveness was not fully dependent upon the different histocytological types.

**Table 5** Comparison of effectiveness in different therapeutic groups

Grade of effectiveness	Group A	Group B (n)	Group C
>50%	9	15	4
50%-25%	7	18	5
25%-10%	9	13	5
<10%	5	3	4
Effective rate %	83.33	93.87	77.77

RIDIT analysis: A/C:  $\alpha \neq 0.05$ , no statistical difference between two groups. B/C:  $\alpha=0.05$ , significant difference between two groups.

**Table 6 Comparison of toxic hematological reaction in different groups**

Grading	Group A (n)			Group B (n)			Group C (n)		
	Hb	WBC	Plt	Hb	WBC	Plt	Hb	WBC	Plt
0	10	12	12	18	15	16	2	4	2
I	12	16	10	22	24	23	5	2	4
II	8	2	8	7	8	9	6	6	6
III				2	2	1	3	4	3
IV							2	2	3



**Figure 4** Pig no.10 by intrahepatic artery instillation of  $^{32}\text{P}$ -GMS after 16wk, showing the glass fragments (solid arrow) in the portal area, the distorted venule in the lower part of the picture is the artifact due to compression of interlobular venule by the glass microsphere during preparing slide. HE stain  $\times 400$

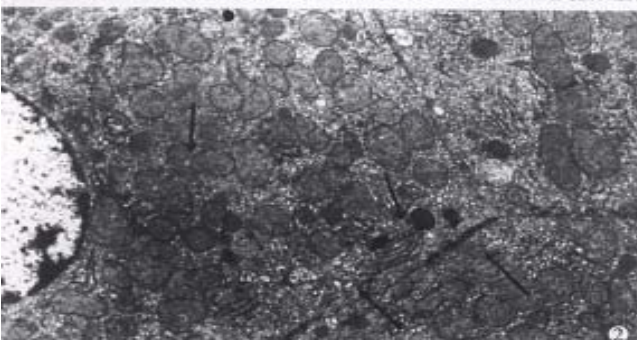
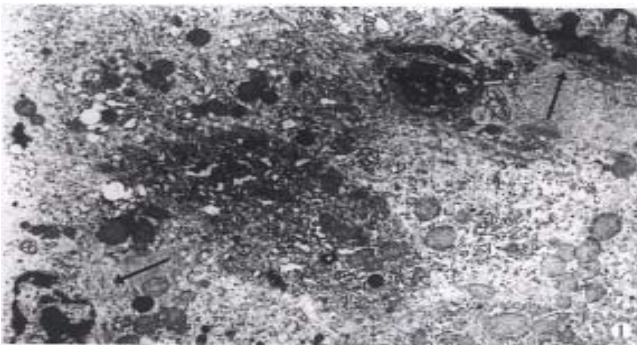


**Figure 5** ①First week of internal irradiation irregularly distorted nuclei of hepatocytes, aggregation of heterochromatin at the periphery of nuclei, distension of perinuclear gap (solid arrow); decreased number of mitochondria in cytoplasm with heavy or light stained substance; dilatation of rough endoplasmic reticulum, depleted glycogen, and increased lysosomes and vacuoles.  $\times 10000$  ②16wk of internal irradiation: normal configuration of hepatocytes, plenty of plasma mitochondria with normal cristae (curved arrow), no distention of the rough endoplasmic reticulum pool (small arrow), nor mal cellular junction (solid arrow).  $\times 6000$

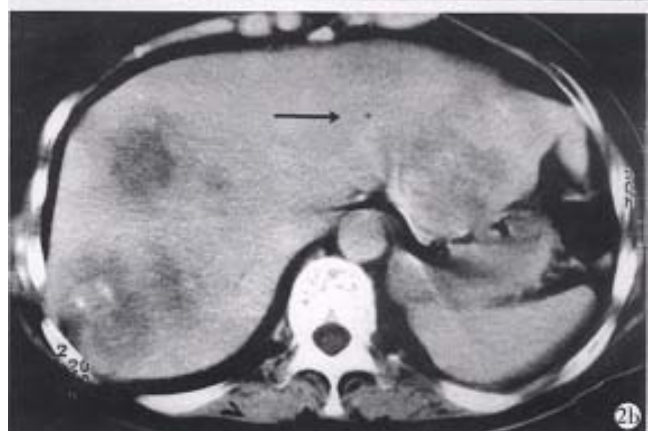
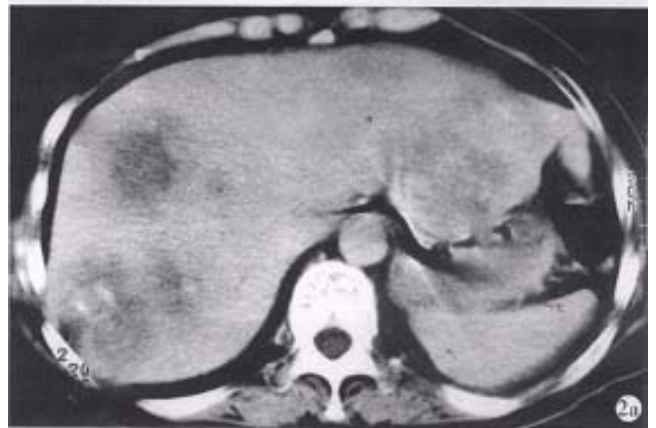
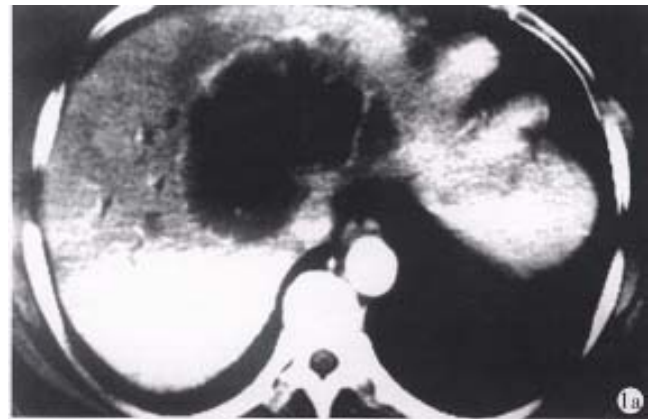


**Figure 6** ①Case 1. Hepatic carcinoma, massive type, apparently decreased in size two months after  $^{32}\text{P}$ -GMS treatment (solid arrow). ②Case 2. Multiple metastatic hepatic tumor apparently decreased in size of left lobe focus after  $^{32}\text{P}$ -GMS treatment (solid arrow).

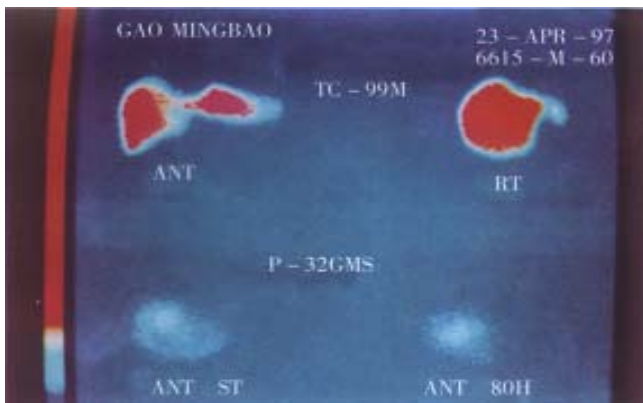


**Figure 7** SPECT imaging before and after  $^{32}\text{P}$ -GMS internal irradiation in patients with relapsed HCC (interlobular) after operation. Upper picture demonstrates interlobular colloidal image (anterio-posterior and light lateral position). Lower picture shows 80h after  $^{32}\text{P}$ -GMS treatment, most of  $^{32}\text{P}$ -GMS cumulated in the foci, no extrahepatic organ imaging was found.

## DISCUSSION

As the experiment demonstrated that the local internal irradiation of  $^{32}\text{P}$ -GMS surely had the cytotoxic effect on tumor cells and exerted a potent inhibitive effect on the growth of tumor even at the third day of medication. The  $\beta$ -ray generated from  $^{32}\text{P}$ -GMS exerted injurious effect on tumor tissue with very complicated mechanism: ①After the tumor cells absorbed the  $\alpha$ -ray energy, it directly affected the ionization and excitation of biological active macromolecules or broke its chemical bonds and destroyed the molecular structure. Since the active biological macromolecules were the main component of cell membrane, organelle and nucleus, defects in these structures apparently would reflect the impairment of their function. ②The indirect effect of  $\alpha$ -ray irradiation was to conduct ionization and irradiation of the water molecule in intracellular environment and to generate many kinds of free radicals and superoxides such as  $\text{O}_2$ ,  $\text{H}_2\text{O}_2$  etc. having very active chemical property with high oxidative toxicity. These irradiative products injured or destroyed the biological macromolecules<sup>[12]</sup>. ③ $\beta$ -ray acted on the cell DNA to induce the cell-death related gene expression, hence to accelerate the apoptosis of cancer cells<sup>[13]</sup>. When the cancer cells received massive dose of irradiation, the metabolic activity ceased immediately, the cell structure disrupted and lysed, resulting in cell death at metaphase; when the cancer cells received irradiation at a certain dosage, and fulfilled several times of multiplication, they would lose the ability of proliferation leading to proliferative death<sup>[14]</sup>. In addition,  $\beta$ -ray irradiation had the effect on occluding capillary vessels and inducing the hyperplasia of connective

tissue in tumor resulting in structural derangement and promotion of the injury and necrosis of tumor cells.

On the 14th day of local injection of  $^{32}\text{P}$ -GMS to the tumor, the tumor cell death rate was 43%-82% in different treatment groups, but 4% in control group. The anticancer effect of  $^{32}\text{P}$ -GMS was directly proportional to the dose administered. In a particular time period, the rate of tumor cell death exceeded its rate of proliferation, then the tumor decreased in size; on the contrary, the death rate of tumor cell did not exceed their rate of growth, the tumor growth might be somewhat inhibited in a certain extent too. In the specimens of different treatment groups, the tumor cells might exhibit as survived, denatured or necrosed (in early or typical changes). This reflected essentially the whole course of tumor cell progression from denaturing to cell death after irradiation. The ultrastructural changes demonstrated that under the effect of high-dose irradiation, the tumor tissues received a lethal radiation energy in a short period, resulting in nonexistence of tumor cells which had a high ability to synthesize endogenous protein. In subgroup I, two tumor masses ne crossed thoroughly the skin neighboring to one of them showing metaplasia. Whether this was the result of radiation injury evolving to malignant change and degeneration or not should be further investigated. Under the appropriate dose of irradiation (subgroup II and III), besides most of the tumor cells necrosed, the tendency of deriving to nearly normal histological picture evolved, such as plenty of microvilli on the cell surface, genesis of bile canaliculi-like structure, etc. These demonstrated that the  $^{32}\text{P}$ -GMS has the ability of killing the actively proliferative tumor cells and promoted the normalization of regenerative cells. These were similar to the effect of irradiation in trace amount which might stimulate and enhance the local metabolism of inflammatory tissues, accelerate the death of injured cells and promote the growth of normal tissue, but this was not found in control group. It is also observed that the synergistic effect of immunocytes, cytolytic phenomena and its inhibition on the dispersion of tumor cells were enhanced in the tumor cells or nearby tissues. It denoted that the anticancer effect of  $^{32}\text{P}$ -GMS was directly proportional to the time course of medication, based on the principle of after effect and cumulative effect of radioactive nuclide therapy. After intratumoral injection of  $^{32}\text{P}$ -GMS, it was not dispersed or displayed to the non-targeting tissue as confirmed by SPECT imaging. In comparison with intratumoral injection of ethyl alcohol<sup>[15]</sup> or acetic acid<sup>[16,17]</sup>,  $^{32}\text{P}$ -GMS needs no repeated injection, with minimal side reaction<sup>[18]</sup>.

Intratumoral injection of  $^{32}\text{P}$ -GMS was the best choice in treating the unresectable tumor or some metastasized lesion as well as those unsuitable for intra-arterial interventional therapy, it was also suitable for solid malignant tumors which could be reached anywhere on the human body.

We have got sufficient data from the dynamic study on the ultrastructural morphometric analysis of liver tissues taken from warm sphere, cold sphere and control groups. According to the injury of normal liver after internal irradiation and its repairing process, it was allocated into 4 periods: ① acute reactive period (within 2 weeks), ② subacute reactive period (2-4 weeks), ③ prerecovery period (4-8 weeks), ④ recovery period (8-16 weeks). In the acute period of warm sphere group, there was decreased proteosynthetic function and alteration of energy metabolism, decreased synthetic ability of ATP. The faint halo around the erythrocytes in the blood sinus as shown under electron microscopy probably was the super liquidized iodized oil. The disruption of sinusoidal endothelium was closely related to the route of medication. No apparent injury of hepatic tissue was found in the control group. This suggested that the serial changes in ultrastructure which was seen in the warm sphere group might be the result of radiation injury. The sinusoidal endothelium was most prominently disrupted. All these changes represented the synergistic action of internal irradiation and embolization. At the prerecovery period, the abnormal nuclei of hepatocytes were scarcely seen, but the cytoplasmic organelles recovered more slowly than the nuclei. Cell injury was resulting in increase in myeloid bodies in the cytoplasm, which indicated the liver tissue evolved into self-repairing stage. The hepatocytes appeared essentially normal in the recovery period. Electron microscopy revealed prominent collagen fibers in the Disse's space in some of the liver specimens, whether it indicated the tendency of early liver fibrosis or not should be further studied.

Recent evidences<sup>[19]</sup> showed the C-IV increases prominently in the early stage of liver fibrosis, LN is closely related to the genesis of liver fibrosis, and CG is the important marker for estimating the severity of biliary cirrhosis, but the serum C-IV, LN and CG all fell into the human normal range in the whole course of the experimental animals. Therefore, the presence of collagen fibers in the Disse's space was probably of transient local changes. The transient changes in HA value were similar to those of hPCIII, and the liver injury induced serum HA elevation was positively proportional to the severity of illness, and the serum hPCIII level was closely related to the extent of fibrosis. When the function of hepatocyte was

damaged, hPCIII might be released to circulation and often used as the guidance for selection of therapeutic medicine<sup>[20]</sup>. Therefore, the transient changes in domestic pig serum HA and hPCIII values were the impairment of liver function resulted from  $^{32}\text{P}$ -GMS administration. It was reported<sup>[21]</sup> that intra-hepatic arterial administration of cold spheres to the dosage equivalent to 12 folds of the human tolerable dose merely induced the clinically permissible intrahepatic changes and did not follow with portal fibrosis or hepatic cirrhosis after 90 days observation. The experiment demonstrated that the cold sphere slightly injured the hepatocytes, probably being the embolization of the nutritional artery rather than irradiation. In this experiment, through hepatic artery medication, no non-target organs developed in all of the domestic pigs. No prominent ultrastructural changes were found in the hepatic lobe during the whole course in the control animals. The experiment demonstrates that intrahepatic change of clinically permissible extent might be induced in the liver tissue of domestic pigs that received  $^{32}\text{P}$ -GMS in the macrocosmic average absorbed dosage of 48Gy-190Gy. These changes were reversible sublethal injury<sup>[14]</sup> and essentially recovered within 8 weeks. In the observation of 120 days there was no evidence of portal fibrosis. This is the evidence that superselective intrahepatic medication may yield a high energy region and without serious injury to the nearby non-medicated tissues or organs.

Hepatic artery embolization is the important measure in treating hepatic carcinoma<sup>[22,23]</sup>. Investigating an ideal embolizing agent is the substantial project in interventional therapy of tumor. The ideal internal radioactive nuclide should serve as a spotted source of radiation with high energy reserve and the carrier having high orientating rate, lasting longer in the target tissue, and the loaded nuclide was not easy in detaching or leaking to circulation.  $^{32}\text{P}$ -GMS, administrated through the hepatic artery, wedged in the terminals of this artery with its mixed iodized oil which was not absorbable could occlude the arterial capillary. In addition to the radiation obliteration of blood vessels induced by internal irradiation, the collateral circulation was not readily generated in the foci. All of the above mentioned advantages will benefit to boosting therapeutic efficiency. Therefore  $^{32}\text{P}$ -GMS is an appropriate internal radioactive embolizing agent with medium or long duration. It has been confirmed in the clinical investigation, the tumor in liver showed angiogenesis at the microcirculatory level and might trap microspheres 3-4 folds to that of normal liver tissue<sup>[24-26]</sup>. Instillation of therapeutic dose of radionuclide to the nutritional arteries of tumor, particularly condensed in the tumor tissue, may exert potent cytotoxic effect to

fulfill the purpose of therapy. It has been reported<sup>[27-29]</sup> that Yttrium-90-GMS ( $^{90}\text{Y}$ -GMS) used in intrahepatic arterial embolization got fair result, and the absorbed dosage attained 50Gy-100Gy in the tumor may have radical effectiveness<sup>[29]</sup>. Nevertheless  $^{90}\text{Y}$ -has the disadvantages of short half-life, inconvenienced in clinical application, and  $^{90}\text{Y}$ -GMS having smaller diameter, and higher hepato-pulmonary shunting index than that of  $^{32}\text{P}$ -GMS<sup>[30]</sup>. As reported that intratumoral injection of  $^{90}\text{Y}$ -GMS in 33 cases of hepatic carcinoma, the bremsstrahlung radiation conducted by SPECT showed 21.4% had development in lung, and 14.3% in intestine. In our study  $^{32}\text{P}$ -GMS in therapeutic dosage through superselective hepatic arterial regional instillation, particularly condensed in the tumor tissue including the central and peripheral portions, forming a high energy region and it is worth noting that extrahepatic development was not found (Figure 7). Therefore transhepatic artery administration of anticancer agent is the first choice in regional medication to treat hepatic tumor. If the hepatic artery is severely distorted or fails in catheterization, intraparenchymal injection of  $^{32}\text{P}$ -GMS should be considered instead.

The therapeutical results of TAE were inconsistent in different histocytological type of HCC<sup>[31]</sup>. The clear cell type was most sensitive, the small cell and poorly or undifferentiated type was moderately sensitive. Based on the radio-biology, cell sensitivity to nuclide beam depended upon the functional status of the cell proper. The cytotoxic effect and durability of  $^{32}\text{P}$ -GMS was superior to the other anticancer chemicals. The therapeutic results depended upon the clinical classification rather than histocytological types.

The results of clinical observation revealed that the clinical classification and the specific features of angiogram might be the basis for evaluating the therapeutical effectiveness and predicting the prognosis. The clinical materials suggested that the regimen B is superior to regimen A and C in the respect of decreasing tumor size and prolonging the survival period. The follow-up results demonstrated that the excellent effect was evolved in the cases with small tumors, plenty of blood supply, intact capsule and heavily aggregated  $^{32}\text{P}$ -GMS in the tumor as revealed by SPECT. Analysis of the clinical classification showed that in average survival time of the 3 clinical types of HCC solitary mass type was longer than the multiple and diffuse type. The patients with apparent decrease in AFP level were consistently accompanied with decrease in tumor size and necrosis in the tumor. In case of these features relapsed and elevation of AFP or complicated with intrahepatic or remote metastasis, all these would result in poor prognosis.

Strategy of therapy: for those hepatic

carcinoma with intact capsule and diameter below 6cm treated by the regimen A for 1 or 2 courses could get satisfactory result, and for those with occult metastatic foci, the secondary foci would be present besides the controlled original lesion several months later. It is of significance to use  $^{32}\text{P}$ -GMS and TAE in combination resulting in apparent synergetic effect (regimen B), which not only enhanced the anticancer and embolic effects but also lessened the side effects, and could completely cure the small liver cancer, eliminated the need of operation (Figure 8), diminished the number of medication with mild liver injury and low relapse rate. After undergoing regimen B treatment, some cases of unresectable tumor acquired the possibility of being resected (Figures 9, 10). The dosage of  $^{32}\text{P}$ -GMS should be decided by the specialists majoring in nuclear medicine and interventional therapy. The optimal schedule was to give two courses of medicine at an interval of 2 months, and as the tumor size decreased, the residual lesion should be resected as soon as possible in order to improve the survivability. There were few viable cancer cells in the 4 resected specimens on pathological examination after the regimen B treatment. Hepatic carcinoma readily invaded the portal vein with cancer cell emboli. It is apparent in such case that intrahepatic artery medication should be complemented with other measures as minimal invasive embolotherapy which will be an intelligent choice. For the metastatic abdominal lymph nodes intratumoral injection of  $^{32}\text{P}$ -colloids under the guidance of CT is also a helpful measure. It is emphasized that we should choose reasonable regimen, strict manipulation, superselective catheterization, well controlled speed in medication to avoid regurgitation of nuclide to the non-target blood vessel, and lessen the complication, particularly depending on the individualized situation. The hepatic arterio-venous fistula should be considered as the contraindication for medication via catheterization.

In conclusion,  $^{32}\text{P}$ -GMS which possesses the anticancer effect through interventional medication may block the blood supply to tumor and evenly distribute the highly concentrated anticancer medicines in the tumor to exert the radioactive cytotoxic effect with the advantage of low local radiation reaction and no apparent systemic toxic effect.  $^{32}\text{P}$ -GMS is an effective measure for the comprehensive treatment of hepatic cancer. Owing to the moderate half-life of  $^{32}\text{P}$ , the dosage of  $^{32}\text{P}$ -GMS required to attain the same absorbed radioactivity is approximately one-fourth or one-third of  $^{90}\text{Y}$ -GMS dosage<sup>[8]</sup>. Therefore it will satisfy the clinical requirement in reducing the risk of radiation to the handlers, simplifying the medical care and lowering the expenses. Thus, a hopeful prospective therapeutic weapon will be developed and popularized in the near future.

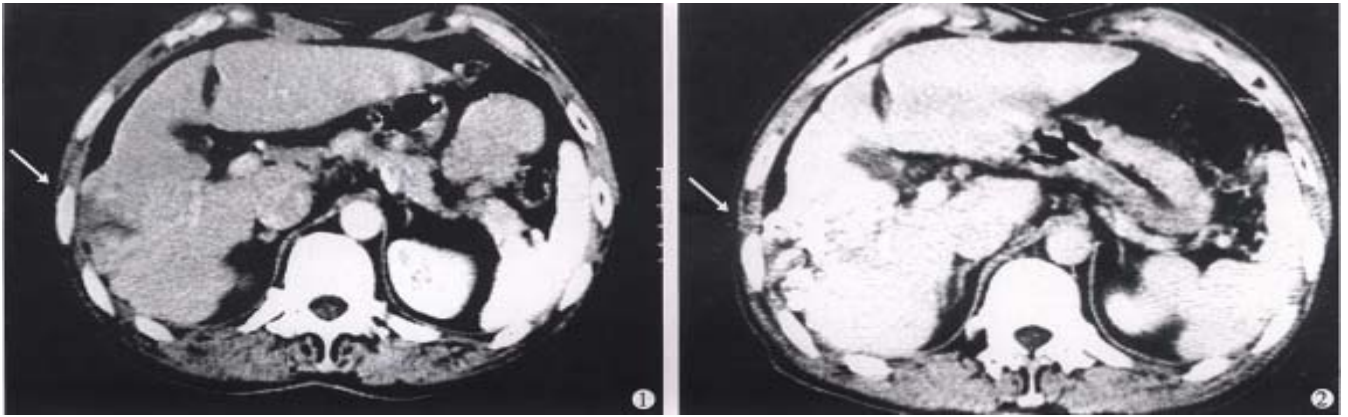


**Figure 8** Male, aged 60, hospital no.202929, clinical diagnosis: right lobe medium sized hepatic carcinoma (4cm×5cm), treated by regimen A and B with an interval of 2 months. AFP from 103 $\mu$ g/L restored to normal range, tumor size decreased >50%, CT: 1, on pre-treatment showing a low density region in right lobe (arrow), 2, on post-treatment iodized oil distributed in fragments or encapsulated forms (arrow). Body weight gained more than 5kg and no subjective symptoms on 36 months follow-up.

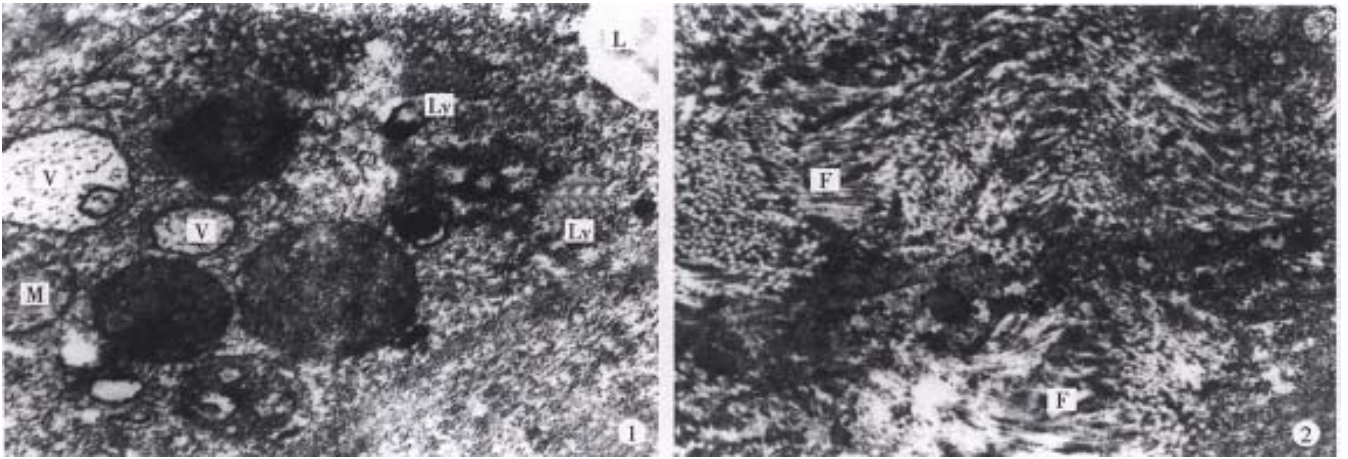


**Figure 9** Male, aged 55, hospital no.202295, clinical diagnosis: left lobe medium sized hepatic carcinoma (5cm×6cm) near the hepatic hilus, treated by TAE and regimen B, with interval of 2 months, and left hepatic lobectomy was performed 6 months later. The tumor (4cm×4cm) was with hard consistency, and encapsulated fibrotic degeneration. Most of the cancer cells showed necrosis under light microscopy. Some cancer cells in the cholecystic wall were alive (may be due to the blood supply from cholecystic artery). The electron microscopy showed: 1, cancer cells degenerated and necrotic; in cytoplasm some vacuolized mitochondria (M), irregular sized vacuoles (V) and lysosome (Ly) and lipid droplet (L) were seen. The rest structures were not clear ( $\times 30000$ ). 2, Prominent fibro-connective tissue hyperplasia (F) in the tumor tissue ( $\times 10000$ ) was found. Patient gained body weight and no subjective upset on follow up until 12 months after operation.

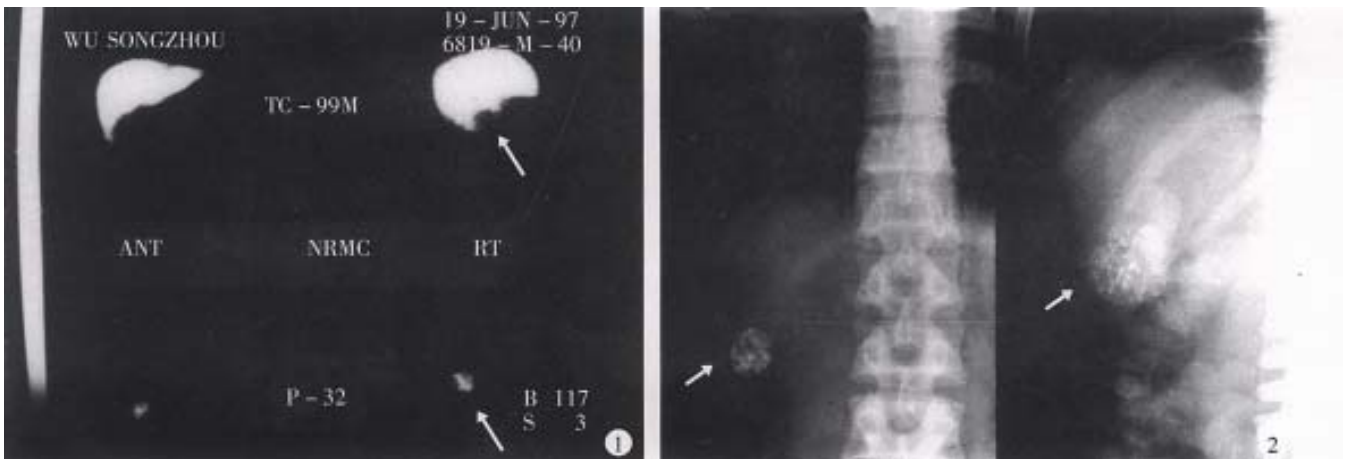


**Figure 10** Male, aged 41, hospital no.207089, clinical diagnosis: uremia, right hepatic small carcinoma (4cm×3cm), with AFP >400 $\mu$ g/L treated by regimen A for 2 courses with interval of 3 months, resulted in AFP restored to normal level and decreased tumor size over 50%. 1, Colloidal SPECT imaging showed the space occupying lesion in the right liver lobe (as shown by arrow). 2, Comparing the tumor size before and after treatment of plain film (as arrow shown), the patient died from renal failure 26 months after operation.

## REFERENCES

- 1 Tang YX, Jiang YD, Zhang Y, Li YJ, Nie Y, Zang H, Zhang XZ, Qiao WA, Lan FS. Observation on the therapeutic results of interventional irradiation in mid and late stage hepatic carcinoma. *Linchuang Yixue Yingxiang Zazhi*, 1997;8:224-225
- 2 Zhang YH, Wu YB. Advances of anticancer target preparation. *Zhongguo Yaoxue Zazhi*, 1992;27:389-393
- 3 Kobayashi H, Hidaka H, Kajiya Y, Tanoue P, Inoue H, Ikeda K, Nakajo M, Shinohara S. Treatment of hepatocellular carcinoma by transarterial injection of anticancer agents in iodized oil suspension or of radioactive iodized oil solution. *Acta Radiol Diag*, 1986;27:139-147
- 4 Herba MJ, Illescas FF, Thirlwell MP, Boos GJ, Rosenthal L, Atri M, Bret PM. Hepatic malignancies: improved treatment with intraarterial Y90. *Radiology*, 1988;169:311-314
- 5 Houle S, Yip TCK, Shepherd FA, Rotstein LE, Sniderman KW, Theis E, Cawthorn RH, Richmond Cox K. Hepatocellular carcinoma: pilot trial of treatment with Y 90 microspheres. *Radiology*, 1989;172:857-860
- 6 Sun WH, Zhang LZ, Li ML. Research on radiotherapy of 32 P glass microsphere. *Hedongli Gongcheng*, 1990;11:75-78
- 7 Loveinger R, Holt JG, Hine GJ. Internally administered radio isotopes. In: Hine GJ, Brownell GL, eds. Radiation Dosimetry. *New York: Academic Press*, 1956:801-873
- 8 Liu L, Sun WH, Wu FP, Han DQ, Teng GJ, Fan J. An experimental study of treatment of liver cancer by locally administration with phosphate 32 glass microspheres & estimation of tissue absorbed dose. *Nanjing Tiedao Yixueyuan Xuebao*, 1997;16:223-226
- 9 Bao JZ, Wang Y, Zhan RZ, Wu MC. Clonal analysis of a hepatocarcinoma cell line: an experimental model of tumor heterogeneity. *Zhongliu Fangzhi Yanjiu*, 1995;22:65-67
- 10 Common statistic form and method in the diagnosis and treatment of tumor. In standards for diagnosis and treatment of common malignant tumor in China, Section 9, edited by Dept Medical Administration, Ministry of Public Health, PRC. Beijing: Beijing Med Univ & China Union Med College Joint Press, 1991:10-15
- 11 Yang SQ, eds. Health statistics. 3rd edition. Beijing: The Public Health Press, 1993:43-181
- 12 Editorial board of practical oncology. Practical Oncology. Vol. 1. Beijing: People's Medical Press, 1997:406-413
- 13 Zheng DX. Advance in apoptosis research. *Zhonghua Binglixue Zazhi*, 1996;25:50-53
- 14 Liu XC, Han KC. Hygienic protection and safety transportation of radioactive materials. Beijing: *Zhongguo Tiedao Chubanshe*, 1990:55-66
- 15 Ohto M, Karasawa E, Tsuchiya Y, Kimura K, Saisho H, Ono T, Okuda K. Ultrasonically guided percutaneous contrast medium injection and aspiration biopsy using a real time puncture transducer. *Radiology*, 1980;136:171-176
- 16 Ohnishi K, Ohyama N, Ito S, Fujiwara K. Small hepatocellular carcinoma: treatment with US guided intratumoral injection of acetic acid. *Radiology*, 1994;193:747-752
- 17 Zhao YF, Wen QS, Jia ZS. Local acetic acid injection in the treatment of transplanted tumor in mice. *Shijie Huaren Xiaohua Zazhi*, 1999;7:43-45
- 18 Liu L, Fan J, Zhang J, Du MH, Wu FP, Teng GJ. Experimental treatment carcinoma in a mouse model by local injection of phosphorus 32 glass microspheres. *J Vasc Interv Rad*, 1998;9:166
- 19 Ueno T, Inuzuka S, Torimura T, Oohira H, Ko H, Obata K, Sata M, Yoshida H, Tanikawa K. Significance of serum type IV collagen levels in various liver diseases. *Scand J Gastroenterol*, 1992;27:513-520
- 20 Axel MG, Wolfgang T, Anne N, Karl Heinz PK. Serum concentrations of laminin and aminoterminal propeptide of type III procollagen in relation to the portal venous pressure of fibrotic liver diseases. *Clin Chim*, 1986;161:249-258
- 21 Wollner I, Knutsen C, Smith P, Prieskorn D, Chrisp C, Andrews J, Juni J, Warber S, Klevering J, Crudup J, Ensminger W. Effects of hepatic arterial yttrium-90 glass microspheres in dogs. *Cancer*, 1988;61:1336-1344
- 22 Wang DZ, Sun WH, Zheng GY, Li ML, Wen YM. A study about the anticancer effect and the clinical application of the phosphate 32 glass microspheres (P32 GMS) by local arterial infusion. I. The ultrastructural study after internal radiation of P 32GMS in cancer cells. *Huaxi Kouqiang Yixue Zazhi*, 1991;9:7-10
- 23 Chen XL, Wu YT, Yan LN, Li L, Tan TZ, Sun WH, Li ML, Jia QB, Du JP, Shen WL. Treatment of liver cancer with 32P glass microsphere-an experimental study. *Puwai Jichuyulinchuang Zazhi*, 1996;3:68-70
- 24 Blanchard RJ, Grotenhuis I, Lafave JW, Perry JF. Blood supply to hepatic V2 carcinoma implants as measured by radioactive microspheres. *Proc Soc Exp Biol Med*, 1965;118:465-468
- 25 Sundqvist K, Hafstrom I, Perrson B. Measurements of total and regional blood flow and organ blood flow using Tc-99m labeled microspheres. *Eur Surg Res*, 1978;10:433-443
- 26 Gyves JW, Ziessman HA, Ensminger WD, Thrall JH, Niederhuber JE, Keyes JW, Walker S. Definition of hepatic tumor microcirculation by single photon emission computerized tomography (SPECT). *J Nuc Med*, 1984;25:972-977
- 27 Yan ZP, Lin G, Zhao HY, Dong YH. An experimental study and clinical pilot trials on yttrium 90 glass microspheres through the hepatic artery for treatment of primary liver cancer. *Cancer*, 1993;72:3210-3215
- 28 Andrews JC, Walker SC, Ackermann RJ, Cotton LA, Ensminger WD, Shapiro B. Hepatic radioembolization with yttrium-90 containing glass microspheres: preliminary results and clinical follow-up. *J Nucl Med*, 1994;35:1637-1644
- 29 Shepherd FA, Rotstein LE, Houle S, Yip TCK, Paul K, Sniderman KW. A phase I dose escalation trial of yttrium-90 microspheres in the treatment of primary hepatocellular carcinoma. *Cancer*, 1992;70:2250-2254
- 30 Tian JH, Xu BX, Zhang JM, Dong BW, Liang P, Wang XD. Ultrasound guided internal radiotherapy using yttrium 90 glass microspheres for liver malignancies. *J Nucl Med*, 1996;37:958-963
- 31 Wang YP, Zhang JS, Gao YA. Therapeutic efficacy of transcatheter arterial embolization of primary hepatocellular carcinoma: discrepancy in different histopathological types of HCC. *Zhonghua Fangshexue Zazhi*, 1997;31:586-588

Edited by WU Xie-Ning and MA Jing-Yun  
Proofread by MIAO Qi-Hong

# Portal vein embolization by fine needle ethanol injection: experimental and clinical studies

LU Ming-De, CHEN Jun-Wei, XIE Xiao-Yan, LIANG Li-Jian, HUANG Jie-Fu

**Subject headings** liver neoplasms/therapy; portal vein embolization; ethanol injection; carcinoma, hepatocellular/therapy

## Abstract

**AIM** To improve the technique of intraportal embolization (PVE) therapy, a new embolic method, was devised and the safety, effectiveness and feasibility were evaluated.

**METHODS** PVE with intraportal ethanol injection via a fine needle was performed in 28 normal dogs, 22 SD rats, and 24 cirrhotic SD rats. After PVE, portography, histological and functional alteration of the liver were evaluated in dogs and rats, and the changes in portal hemodynamics as well as hepatic anatomy were observed in rats. In the clinical study, PVE by ethanol injection was performed in 61 patients with hepatocellular carcinoma under the guidance of portochography with intraportal injection of CO<sub>2</sub>. The effect of PVE was evaluated by ultrasonography and laparotomy. **RESULTS** The effectiveness and toxicity were dependent on the dose of ethanol. In the dogs, 0.25mg/kg of ethanol caused incomplete embolization with least liver damage, while 1.0mg/kg induced complete embolization with a high mortality of 57.1% (4/7) due to respiratory arrest. The dose of 0.5mg/kg resulted in complete embolization with slight toxicity to the liver. In the rats, the survival rate was 100% in normal group but 40.9% in cirrhotic models after ethanol injection by dose of 0.05mg/100g. PVE for cirrhotic rats with 0.03mg/100g of ethanol induced satisfactory embolization with

significant hypertrophy in nonembolized lobes, and only slight damage to the hepatic parenchyma, and transient alteration in liver function, portal pressure and portal flow. In the clinical study, 12 cases with reverse portal flow were excluded judged by portochography. Satisfactory embolization was gained in 90.2% (55/61) of the remaining patients determined by ultrasonography and surgery. All cases ran an uneventful postembolization course with no aberrant embolization.

**CONCLUSION** PVE with intraportal ethanol injection of appropriate dosage via a fine needle is safe and effective and has several advantages comparing with transcatheter method. Portochography is a mandatory approach for the prevention of aberrant embolization.

## INTRODUCTION

Hepatocellular carcinoma (HCC) is one of the most common malignancies in China. The resection rate is less than 30% since most patients are associated with cirrhosis and poor liver function. Furthermore, there are tumor emboli in the portal vein which limits surgical resection. Portal vein embolization (PVE) has been performed to increase the safety and resectability of hepatectomy by improving the functional reserve of the liver<sup>[1-3]</sup>, and prevent cancerous dissemination via portal vein<sup>[4]</sup> and enhance the therapeutic efficacy of transcatheter arterial chemoembolization (TACE)<sup>[5]</sup>. However, conventional PVE requires catheterization under both sonographic and fluoroscopic guidance, and selective embolization is not easy. To improve the technique, we developed a method of intraportal ethanol injection via a fine needle under the guidance of portochography. This study is mainly to investigate the safety, effectiveness and feasibility of this technique and a series of experimental and clinical studies were carried out.

## MATERIALS AND METHODS

### *PVE in dogs with normal liver*

Twenty-eight mongrel dogs of both sexes weighing 7.5kg-15.0kg were provided from the Laboratory Animal Center of our university. Under

Department of Hepatobiliary Surgery, the First Affiliated Hospital, Sun Yat-Sen University of Medical Sciences, Guangzhou 510080, Guangdong Province, China

Dr LU Ming-De, male, born on 1951-03-25 in Hunan Province, graduated from Sun Yat-Sen University and earned Doctoral Degree (DMSc) from Kyushu University (Japan), Professor and Director of Department of Surgery, majoring in hepatobiliary surgery, having 95 papers published.

Supported by grants from the National Science Foundation of China, No.393706697 and Science and Technology Commission, Guangdong Province, China, No.970066.

**Correspondence to:** Dr Lu Ming-De, Department of Hepatobiliary Surgery, the First Affiliated Hospital, Sun Yat-Sen University of Medical Sciences, Guangzhou 510080, China

Tel. +86-20-87755766 Ext. 8599, Fax. +86-20-87765183

Received 1999-07-11 Accepted 1999-09-22

intraperitoneal anesthesia with sodium pentobarbital 30 mg/kg, laparotomy was performed and the left portal branches were exposed. Puncture of the origin of the portal branches supplying the left central and lateral lobes was done with a 22-gauge needle. Then 95% ethanol was injected at a dose of 0.25 mL/kg (group A,  $n=7$ ), 0.5 mL/kg (group B,  $n=11$ ) and 1.0 mL/kg (group C,  $n=7$ ) at a rate of 3 mL/min.

One or two dogs in each group underwent relaparotomy 30 or 60 min after injection and a 6 Fr catheter was placed in the portal trunk. The liver together with the portal trunk was taken out. Portography with the mixture of Urografin (Schering AG, Germany) and Lipiodol (Guerbet, France) via the catheter was performed. Then the intrahepatic portal system was dissected to confirm the site of the thrombus. The same procedures were carried out at day 1 and 3, as well as of week 1, 2 or 4 in groups A and B and week 2 or 4 in group C after ethanol embolization. Tissue samples from embolic and nonembolic liver lobes were examined histologically at the same time.

#### *PVE in rats with normal and cirrhotic liver*

Sprague-Dawley (SD) rats with a body weight between 200 g-250 g were used in this experiment. Initially, twenty normal rats had liver resected under anesthesia, and the right, middle, left lobes and the whole liver of each rat were weighed. The mean weight ratios of right, middle and left lobes to the whole liver were 40.5%, 36.5% and 23.0%, respectively.

The cirrhotic model of rat was reproduced by subcutaneously injection of 60% CCl<sub>4</sub> with a dose of 0.3 mL/100 g once every 4 days. Throughout the period, the rats were fed with ordinary food and 5% ethanol drinking water. Histological examination confirmed the development of cirrhosis at 60 days after initial administration of CCl<sub>4</sub>.

In order to test ethanol tolerance of the normal and cirrhotic rats, laparotomy was performed in both normal ( $n=10$ ) and cirrhotic rats ( $n=22$ ) under intraperitoneal anesthesia with pentobarbital. After exposure of the hepatic hilum, portal vein was punctured with a 3-gauge needle and inject a dose of 0.05 mL/100 g of absolute ethanol. All rats in the normal group were alive but only 9 of 22 (40.9%) in the cirrhotic group survived 4 days after the injection.

Based on the technique and the results described above, embolization of the portal branches of left and central lobes (the embolized tissue accounted for 77% of the whole liver) was employed for 22 normal rats (NE group) with a dose of 0.05 mL/100 g of absolute ethanol. The portal branch of middle lobe (accounted for 36.5% of the

liver) was embolized in 24 cirrhotic rats (ME group) with a dose of 0.03 mL/100 g. The same amount of normal saline was injected into portal vein in 10 normal rats (NC group) and 10 cirrhotic rats (MC group).

At day 1, 3, 7 and 14 after PVE, the following examinations were carried out: X-ray portography, the weight ratio of hepatic lobes, liver function tests (ALT, TBIL, ALP, ALB, A/G), liver histology, portal blood flow and portal pressure measured by MRF-1200 electromagnetic flowmetry (Nikon, Japan).

#### *PVE in patients with HCC under the guidance of portoechoigraphy*

PVE was undertaken under local anesthesia. A portal branch supplied the tumor bearing segment was punctured percutaneously under the guidance of Aloka SSD 650 or 1200 ultrasound system and 3.5 MHz linear puncture probe. In order to identify the precision of the puncture and whether or not a retrograde blood flow was present, portoechoigraphy was initially introduced with injection of 5 mL carbondioxide (CO<sub>2</sub>). If the diffusion of CO<sub>2</sub> was beyond the ipsilateral lobe of the liver, PVE was abandoned in case of aberrant embolization; otherwise PVE was performed with intraportal injection of 95% ethanol. The dose of ethanol ranged from 4mL to 10mL depending on the level the portal branch to be blocked.

From February 1993 to February 1993, portoechoigraphy was performed in 73 patients with HCC. But was quit in 12 cases due to CO<sub>2</sub> diffusing into both lobes of the liver. Sixty-one patients (55 males and 6 females) with an average age of 52.5 years received PVE. Forty-nine patients had cirrhosis without jaundice, ascites or serious liver function had damage<sup>[6]</sup>. The tumors ranged from 3 cm to 12 cm in diameter, located at right lobe in 58 and left lobe in 15. All 61 patients underwent surgery 3-5 days after PVE including hepatectomy in 37 patients.

## RESULTS

### *Canine experiment*

One dog in group B died of wound infection on day 5. Four of 7 dogs in group C died of respiratory arrest on the day of the injection.

Intrahepatic portography and dissection of the portal system showed the injected portal branches were patent at 30min and 60min after embolization. Thrombosis was developed on day 1. In group A, portal vein embolization occurred at one segment of the liver in six dogs and failure of embolization in one dog. In groups B and C, embolization occurred at both left and central lobes in most dogs. In one dog of group B, the orifice of the branch of the

quadrate lobes was approximate to the branch of left lobe, and overembolization involving the quadrate lobes occurred. No thrombus was detected at the non-injected branches in any other dogs.

Macroscopically, the embolized lobes were swollen and congested but without any evidence of necrosis. Dark red thrombus had developed within the ethanol-injected portal branches on day 1 or 3, which were organized one week after PVE. Microscopically, focal inflammation of the intima was found in the affected portal branches. Small foci of coagulation necrosis prominently surrounding Glisson cap sule were detected at the embolized lobes and the normal structure of the lobules was preserved. The necrotic area was less than 10% of the effected lobes. Transient elevation of white blood cell and alanine aminotransferase (ALT) occurred at day 1 but returned to the baseline values within one week. The level of total bilirubin, albumin and  $\gamma$ -globulin did not significantly change after PVE.

#### Rat experiment

The survival rate after PVE was 95.8% in both NE and ME group. Postoperative portography demonstrated filling defects at injection sites and dissection of the portal system indicated the corresponding portal branches were embolized. The weight of the embolized hepatic lobes decreased gradually as the weight of non-embolized lobes increased with the time after PVE (Figure 1). On day 14, the weight of nonembolized lobes was significantly greater than the baseline value in both NE group ( $5.25 \text{ g} \pm 0.38 \text{ g}$  vs  $1.86 \text{ g} \pm 0.42 \text{ g}$ ,  $P < 0.01$ ) and ME group ( $9.58 \text{ g} \pm 1.10 \text{ g}$  vs  $5.13 \text{ g} \pm 0.53 \text{ g}$ ,  $P < 0.01$ ) and ratio of the nonembolized lobes to the whole liver significantly increased from 23% to 68.8% in NE group and from 63.5% to 86.8% in ME group.

Histological findings on day 1 or 2 were similar to that in the experiment of normal dogs. With respect to the ratio of total necrosis area to embolized area, ME group (30%-40%) was more severe than NE group (10%-20%). One week after PVE, organization or calcification of thrombi with partial recanalization as well as hyperplasia of fibrotic tissue in the embolized lobes was noted. Hepatocytes of the non-embolized lobes became hypertrophied and proliferative, which were more remarkable in ME group than in NE group.

The hemodynamic study demonstrated that ME group had significantly higher portal blood flow and portal pressure than NE group before PVE. On day 1 after PVE, portal blood flow and portal pressure declined slightly in both groups, then increased to a limited degree and returned to the baseline values at week 1 after PVE (Figures 2 and 3).

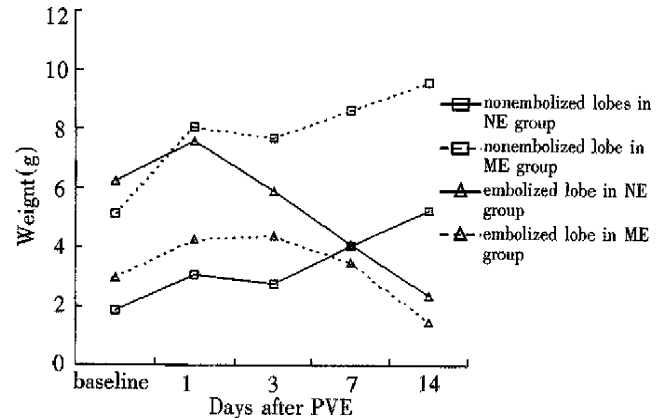


Figure 1 Changes in weight of hepatic lobes after PVE with fine needle technique.

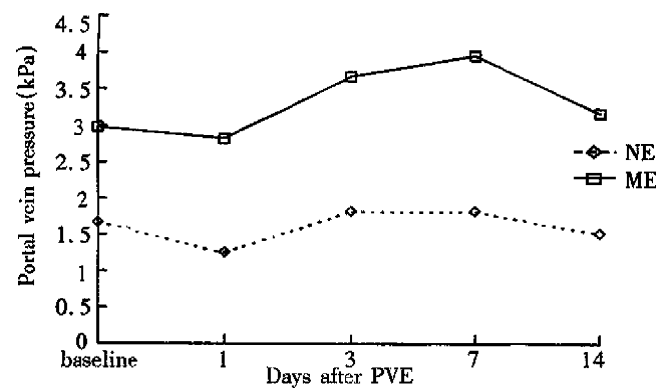


Figure 2 Changes in portal vein pressure after PVE.

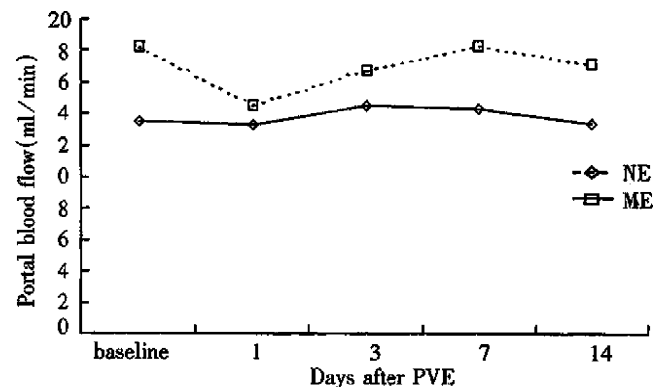


Figure 3 Changes in portal blood flow after PVE.

The serum ALT, TBIL and ALP were elevated. After PVE, they began to fall on day 3 and returned to the pre-PVE level. The albumin and A/G ratio did not significantly change in both groups after PVE.

#### Clinical study

The punctures were confirmed to be proper by portocography in all cases. By  $\text{CO}_2$  injection, a regional liver parenchyma was enhanced as high-echo pattern and developed a hyperechoic ring surrounding the tumors as our previous observation<sup>[7]</sup>. The echo within the tumors

remained unchanged in 64 patients, but enhanced in 9 patients which represented portal blood stream within the tumors.

Enhancement of the hepatic parenchyma was localized to the area supplied by the injected branches or confined in the same lobe in 61 patients and subsequent PVE was performed. PVE was abandoned in 12 cases due to CO<sub>2</sub> diffusing into both lobes of the liver.

Ultrasonography did not reveal any abnormality in the injected portal branches on the day of PVE. Forty-eight hours after PVE, embolization was found in 55/61 patients (90.2%), exhibiting substantial hypoechoes within the lumen of portal vein. Of 37 patients who underwent hepatectomy afterwards the specimen inspection confirmed the injected portal veins were occluded by thrombosis. Embolization failed to develop in six patients, who were the initial cases of PVE, due to inadequate amount of ethanol (4 mL - 5 mL) injected.

Forty-five patients (73.8%) complained of abdominal pain at the right upper quadrant, sweating, transient low-grade fever or decreased pulse rate during ethanol injection. Acute ischemic cholecystitis was encountered in one patient, for which the needle may be displaced accidentally during the injection, resulting in vascular occlusion of the gallbladder. Accidental embolization by reflux ethanol was not found in all patients and the liver function tests did not show significant change following PVE.

## DISCUSSION

Comparing with transcatheter PVE, the advantages of PVE with fine needle are obvious: easy to achieve selective embolization, simple in manipulation, inexpensive and radiation free. However, at least two questions have to be answered which are prerequisite for conducting this procedure. The first question is about the safety of this procedure and the second is how to avoid a possible reflux of the ethanol to other portal branches. Furthermore, the feasibility of this technique should be convinced clinically.

Absolute ethanol is an effective embolizer in PVE. However, its toxic effect should not be neglected. In the present study, the dose of 0.25 mg/kg had little toxic effect but failed to induce complete embolization. While the dose of 1.0 mg/kg caused complete embolization but resulted in severe liver dysfunction and even respiratory arrest. Satisfactory embolization could be obtained at a dose of 0.5 mg/kg in normal dogs with mild toxicity to the liver parenchyma and only transient changes in the liver function. In transcatheter PVE with ethanol injection while the

portal was occluded to blood flow, a rapid vascular obliteration and immediate embolization with entire necrosis at the affected region occurred<sup>[8]</sup>. On the contrary, since the portal vein was not occluded during ethanol injection in our technique, most of the ethanol might be diluted by the slow blood stream rather than flushed up to the liver parenchyma. The thrombosis was resulted from agglutinations, coagulation of plasma proteins and local pylephlebitis, and the thrombosis development was relatively slow. Thus, the damage to the liver tissue was relatively mild. Such a mechanism may be more favorable for the patients with HCC and underlying cirrhosis. The local overembolization in one dog in our study was probably due to an extension of the thrombus after the injection. This complication could be prevented by carefully selecting a point for puncture that is not too close to the confluence of the portal branches.

Since 80% of the patients with HCC are associated with cirrhosis, it is necessary to investigate the effect of PVE on cirrhotic liver for a better orientation on its clinical application. The present study indicated the cirrhotic rats were less tolerant to ethanol than the normal rats, so the dose of ethanol used for PVE should be strictly controlled. On the other hand, once PVE was undertaken with a tolerant dose, the changes in histology, liver function and portal hemodynamics in cirrhotic rats were not more severe and persistent than those of normal rats. It indicated that an uneventful postoperative course could also be achieved in cirrhotic rats with an appropriate dose of ethanol.

In both normal and cirrhotic liver, the weight of nonembolic lobe was increased with hypertrophy and proliferation in the nonembolized lobe in the current study. Increase in mitotic index, DNA synthesis and the number and function of mitochondrial in these lobes has been reported<sup>[9,10]</sup>. The hypertrophy may be contributed to the increase of nourishing factors carried by portal blood flow to the nonembolized lobes. This mechanism may play an important role in the surgery for cirrhotic patients as the improvement of functional reserve on the nonembolized lobe, hence the resectibility of HCC increased and the risk of postoperative liver failure reduced.

The features of portal circulation in the liver with HCC and cirrhosis were considered when our approach was planned for clinical use. Portal flow reflux may occur due to the circulatory disturbances within the tumor, portal branch compressed by huge mass, serious cirrhosis, portal hypertension and arteriovenous shunts. According to our previous portoecography and color Doppler study on patients with HCC, the incidence of portal vein

reflux was about 10%-30%<sup>[11]</sup>. Since the injected portal branches were not be occluded during ethanol injection, accidental embolization could occur as the embolic agent might be carried to other branches by the reverse flow. In order to avoid the accidental embolization, it is important to obtain the information of portal hemodynamics individually prior to the procedure. Matsuda and Yabuuchi first reported a method of contrast-enhanced ultrasonography with arterial infusion of CO<sub>2</sub> microbubbles for assessment of the nature of liver tumor<sup>[12]</sup>. Because the ultrasonic impedance of CO<sub>2</sub> gas is much different from that of the liver and the gas can be rapidly washed out off the liver. It possesses excellent contrast effect without hepatic injury. This technique has been demonstrated as high sensitivity and specificity in clinical use<sup>[13,14]</sup>. Furthermore, the CO<sub>2</sub> was directly injected into the destined portal branches, such portoechography could truly reveal the hemodynamics status of the portal branch<sup>[7]</sup>. In addition, it can be conveniently applied during the procedure of PVE. In the present study, reflux of portal stream was detected by portoechography in 12/73 patients and subsequent embolization was ceased for those patients. No accidental aberrant embolization occurred in the patients with CO<sub>2</sub> confined at ipsilateral half of the liver, substantiating the usefulness of portoechography in our procedure.

The present study demonstrated that intraportal ethanol injection via fine needle was able to produce complete portal vein embolization with mild liver injury in both normal and cirrhotic liver in animal and patients with HCC. Portoechography was a mandatory approach for the prevention of aberrant embolization in patients with HCC.

## REFERENCES

- 1 Shimamura T, Nakajima Y, Une Y, Namieno T, Ogasawara K, Yamashita K, Haneda T, Nakanishi K, Kimura J, Matsushita M, Sato N, Uchino J. Efficacy and safety of preoperative percutaneous transhepatic portal embolization with absolute ethanol: a clinical study. *Surgery*, 1997;12:135-141
- 2 Nagino M, Nimura Y, Kamiya J, Kondo S, Uesaka K, Kin Y, Kutsuna Y, Hayakawa N, Yamamoto H. Right or left trisegment portal vein embolization before hepatic trisegmentectomy for hilar bile duct carcinoma. *Surgery*, 1995;117:677-681
- 3 Kawasaki S, Makuuchi M, Kakazu T, Miyagawa S, Takayama T, Kosuge T, Sugihara K, Moriya Y. Resection for multiple metastatic liver tumors after portal embolization. *Surgery*, 1994;115:674-677
- 4 Kinoshita H, Sakai K, Hirohashi K, Igawa S, Yamasaki O, Kubo S. Preoperative portal vein embolization for hepatocellular carcinoma. *World J Surg*, 1986;10:803-808
- 5 Fujio N, Sakai K, Kinoshita H, Hirohashi K, Kubo S, Iwasa R, Lee KC. Results of treatment of patients with hepatocellular carcinoma with severe cirrhosis of the liver. *World J Surg*, 1989;13:211-218
- 6 Liang LJ, Lu MD, Ye WJ, Huang YF. Two stage resection for advanced hepatocellular carcinoma. *Zhonghua Zhongliu Zazhi*, 1992;14:449-451
- 7 Lu MD, Liang LJ, Xie XY, Li DM, Li MD, Xie YY, Peng BG. Hepatic angio echography and its clinical application. *Zhonghua Chaosheng Yingxiangxue Zazhi*, 1993;2:154-156
- 8 Ogasawara K, Uchino J, Une Y, Fujioka Y. Selective portal vein embolization with absolute ethanol induces hepatic hypertrophy and makes more extensive hepatectomy possible. *Hepatology*, 1996;23:338-345
- 9 Lee KC, Kinoshita H, Hirohashi K, Kubo S, Iwasa R. Extension of surgical indications for hepatocellular carcinoma by portal vein embolization. *World J Surg*, 1993;17:109-115
- 10 Harada H, Imamura H, Miyagawa S, Kawasaki S. Fate of the human liver after hemihepatic portal vein embolization cell kinetic and morphometric study. *Hepatology*, 1997;1162-1170
- 11 Lu MD, Xie YY, Liang LJ, Huang JF, Cao XH. Portal hemodynamics in hepatocellular carcinoma: observation by angioechography and color Doppler. *Zhonghua Chaosheng Yixue Zazhi*, 1994;10(6):24-27
- 12 Matsuda Y, Yabuuchi I. Hepatic tumors: US contrast enhancement with CO<sub>2</sub> microbubbles. *Radiology*, 1986;161:701-705
- 13 Kudo M, Tomita S, Tochio H, Kashida H, Hirasawa M, Todo A. Hepatic focal nodular hyperplasia: specific findings at dynamic contrast enhanced US with carbon dioxide microbubbles. *Radiology*, 1991;179:377-382
- 14 Takasaki K, Saito A, Nakagawa M. Significance of angioechography for diagnosis of small intrahepatic metastasis. *Kanzuo*, 1988;29:917-920

Edited by WU Xie-Ning

Proofread by MIAO Qi-Hong

# Study on the anticarcinogenic effect and acute toxicity of liver-targeting mitoxantrone nanoparticles

ZHANG Zhi-Rong, HE Qin, LIAO Gong-Tie and BAI Shao-Huai

**Subject headings** mitoxantrone-nanospheres toxicity; neoplasm transplantation; nude mice

## Abstract

**AIM** To study the anticarcinogenic effect and acute toxicity of liver targeting mitoxantrone-nanospheres.

**METHODS** The anticarcinogenic effect of mitoxantrone-polybutyl cyanoacrylate-nanoparticles (DHAQ-PBCA-NP) was investigated by using heterotopic and orthotopic transplantation models of human hepatocellular carcinoma (HCC) in nude mice and was compared with mitoxantrone (DHAQ) and doxorubicin (ADR). The acute toxicity of DHAQ-PBCA-NP lyophilized injection in mice was also studied.

**RESULTS** The tumor inhibition rates of ADR, DHAQ, DHAQ-PBCA-NP to orthotopically transplanted HCC were 60.07%, 67.49% and 99.44%, respectively, but regard to heterotopically transplanted HCC, these were 80.03%, 86.18% and 92.90%, which were concordant with the results acquired by mitosis counting and proliferating cell nuclear antigen (PCNA). After iv administration to mice with DHAQ-PBCA-NP, the LD<sub>50</sub> was 16.9mg/kg±3.9mg/kg, no obvious local irritation was observed and there was no significant damage to the structure of liver cells, and that of the heart, spleen and kidneys.

**CONCLUSION** The effect of DHAQ-PBCA-NP was significantly higher than that of DHAQ and ADR in the anti-orthotopically transplanted HCC and the acute toxicity was relatively low.

School of Pharmacy, West China University of Medical Sciences, Chengdu 610041, Sichuan Province, P.R. China

Dr. ZHANG Zhi-Rong, male, 43 years old, graduated from West China University of Medical Sciences (WCUMS) as a Ph.D. in 1993. Professor of pharmaceuticals, Dean of the School of Pharmacy of WCUMS, member of Chinese Pharmacopoeia Commission, council member of Chinese Pharmaceutical Association (CPA), member of Society of Pharmaceutics of CPA, specializes in targeted delivery system and has more than 80 papers and 6 books published. Supported by the National Natural Sciences Foundation of China, No.39270786.

**Correspondence to:** Dr. ZHANG Zhi-Rong, School of Pharmacy, West China University of Medical Sciences, Chengdu, 610041, China. Tel.+86-28-5501566, Fax.+86-28-5583252

Received 1999-08-10

## INTRODUCTION

DHAQ is a new synthetic antitumor agent, effective in many cancers, especially in hepatic cancer, a principal cancer of high incidence and mortality<sup>[1]</sup>. Nanoparticles (NP) is a new drug carrier<sup>[3]</sup> showing a distinguished liver targeting ability, therefore, NP loading with antihepatic cancer drug could improve the effect of original drug. The DHAQ-PBCA-NP used in this study has been proved to have remarkable liver-targeting effect. In this paper, the anticarcinogenic effect, acute toxicity and local irritation of DHAQ-PBCA-NP were studied and compared with those of ADR and DHAQ injection.

## MATERIALS AND METHODS

### Materials

DHAQ was obtained from Organic Chemistry Department, School of Pharmacy, West China University of Medical Sciences. DHAQ-PBCA-NP was self-made with a content of DHAQ 0.15 mg/mL diameter 55.82 nm ± 12.46 nm (n = 505) and drug loading 51.03%. The lyophilized ADR injection was provided by TuoBin Pharmaceutical Factory and DHAQ injection provided by Hua Da Pharmaceutical Factory with a content of DHAQ 2 mg/2 mL.

BALB/C-nu/nude mice, Kunming mice and the heterotopic and orthotopic transplantation models of HCC in nude mice were all supplied by our Laboratory Animal Center. Animal tumor cells LTNM<sub>4</sub> (86 generation) was obtained from Liver Cancer Laboratory, Zhongshan Hospital, Shanghai Medical University.

### Methods

**Tumor inhibition test of DHAQ-PBCA-NP** Twenty nude mice were randomly divided into physiological saline group (0.1 mL/10 g), ADR group (20 µg/10 g), DHAQ group (20 µg/10 g) and DHAQ-PBCA-NP (15 µg/10 g) group. The drug was given intravenously to each mouse 36 h after the transplantation of HCC, then given continuously once every three days for four times. On the 14th day after the last injection, the diameter of the armpit tumors of nude mice in the physiological saline group was found over 10 mm, and one mouse died. The mice were killed, and the livers as well as the tumors were taken out, weighed and the rate of

tumor inhibition (TRI) was calculated by the following formula:

$$RTI\% = \frac{\text{The average tumor weight of control group} - \text{average tumor weight of experimental group}}{\text{The average tumor weight of control group}} \times 100\%$$

**Microscopic observations and nuclear division count of tumor** The hepatic cancer of nude mice taken from control group and experimental group was sectioned into ultra-slices and observed under microscope.

**Calculation of positive rate of the tumor PCNA** The tumor of each groups was sampled, fixed in formalin and embedded in paraffin wax, then anti-proliferating cell nuclear antigen (PCNA) monoclonal antibody PC10 was used to show the proliferating cells by highly sensitive method of ABPAP, the number of tumor cells were counted and positive rate was calculated<sup>[4]</sup>.

**Acute toxicity** One hundred and eight Kunming mice were randomly divided into DHAQ-PBCA-NP group, PBCA-NP group and DHAQ group. Each group was given 6 different dosages with the maximum dose 75.0 mg/kg, 1150 mg/kg and 25.2 mg/kg, respectively. The mice were observed for 21 d and the death rate of each group was recorded.

**Pathologic examination** Nine of 10 Kunming mice were given DHAQ -PBCA-NP intravenously in the dosage of 15 mg/kg and were killed after 5 min, 10 min, 15 min, 20 min, 30 min, 1 h, 24 h, 38 h and 72 h, respectively, another one was injected normal saline at the dosage of 0.1 mL/10 g. Tissue samples of the heart, liver, spleen, lung and kidney were fixed in formalin and embedded with paraffin wax for routine section, HE stain and observed under microscope. The liver tissue was fixed by glutaraldehyde, dehydrated with acetone gradually, embedded with 618 to make ultrathin section, then stained by uranium acetate and lead citrate and examined under transmission electron microscope.

**Local irritation testing** Ten Kunming mice were given DHAQ-PBCA -NP intravenously at a dosage of 0.1 mL/kg and the changes at the tail were observed for 1-7 days.

## RESULTS

### Tumor inhibition rate

The tumors obtained from the liver and armpit in each group were photographed (Figures 1-3). The tumor and tumor inhibition rate are listed in Tables 1 and 2, respectively. No significant difference was noted among the anti-HCC effect of DHAQ-PBCA-NP, DHAQ and ADR, but in the anti-orthotopically transplanted HCC, the effect by DHAQ-PBCA-NP was much higher than that by DHAQ or ADR.



**Figure 1** The liver in nude mice taken from armpit.

**Figure 2** Tumor taken from liver.

**Figure 3** Tumor taken from armpit.

### Microscope observations of the tumor

The tumor cell proliferation in control group was very active. The tumor cell karyokinesis in DHAQ-PBCA-NP, DHAQ and ADR groups was less than that of control group (508/HP), especially in the DHAQ-PBCA-NP group, only 0-3/PH, and most were in the metaphase.

**Tumor cell proliferative activity analysis** The PCNA positive percentage of nude mice tumor in each

group was shown in Table 3, the killing activity of DHAQ-PBCA-NP was significantly stronger than that of DHAQ and ADR ( $P<0.05$ ) on nude mice transplanted with HCC, and the activity of DHAQ was almost equal to the of ADR ( $P>0.05$ ).

**Table 1 Weight (g) of tumor taken from four different groups**

Group	Liver tumor	Armpit tumor
DHAQ-PBCA-NP		
1	0.000	0.215
2	0.000	0.060
3	0.000	0.005
4	0.000	0.015
5	0.030	0.015
ADR		
1	0.820	0.100
2	0.000	0.050
3	0.675	0.137
4	0.210	0.410
DHAQ		
1	0.585	0.270
2	0.650	0.120
3	0.000	0.065
4	0.000	0.082
5	0.500	0.066
0.9% NS		
1	1.320	1.160
2	1.530	1.026
3	1.000	0.635
4	0.420	0.670

**Table 2 Rate of tumor inhibition (RTI, %) of each group of nude mice**

Drug	RTI (orthotopic)	RTI (heterotopic)
DHAQ	67.49 <sup>a</sup>	86.18 <sup>d</sup>
ADR	60.07 <sup>b</sup>	80.03 <sup>e</sup>
DHAQ-PBCA-0.9%NS	99.44 <sup>c</sup>	92.90 <sup>f</sup>

c vs b, a  $P<0.05$ ; f vs d, e  $P>0.05$ ; b vs a  $P>0.05$ .

**Table 3 The cell proliferative activity of tumor of each nude mice**

	DHAQ-PBCA-NP					DHAQ					ADR					0.9%NS				
	1	2	3	4	5	1	2	3	4	5	1	2	3	4	5	1	2	3	4	5
PCNA(%)	7	2	1	3	2	7	9	7	6	9	7	9	10	82	10	95	10	90	0	0
$\bar{x}\pm s$ (%)	31.0±23.0 <sup>a</sup>					76±13.4 <sup>b</sup>					85.5±12.7 <sup>c</sup>					96.3±4.8				

a vs b, c  $P<0.05$ ; b vs c  $P<0.05$ .

**LD<sub>50</sub> and toxicity parameters** The LD<sub>50</sub> was calculated by Karber method based on the mice death rate of each dosage group (Table 4).

The absolute lethal dose of DHAQ-PBCA-NP and DHAQ in mice was 75.0 mg/kg and 25.2 mg/kg, respectively whereas the minimal lethal dose was 6.5 and 4.8 mg/kg, respectively, the maximum tolerance dose was 4.5 mg/kg and 3.0 mg/kg, the earliest time of death was 7 d and 4 d, the latest time of death was 21 d and 16 d and the average time of death was 9.7 d ± 8.8 d and 7.5 d ± 4.2 d, respectively.

**Table 4 The LD<sub>50</sub> of DHAQ-PBCA-NP, DHAQ and PBCA-NP i.v. in mice**

Group	n	LD <sub>50</sub> (mg/kg, $P=0.95$ )*		
		7d	14d	21d
DHAQ	60	12.8±1.9	8.2±1.7	6.1±1.0
DHAQ-NP	60	309.9±26.2	301.0±28.3	299.0±24.2
DHAQ-PBCA-NP	60	16.9±3.9	12.3±2.7	10.1±1.9

\*Dosage calculated as DHAQ.

**Results of pathologic examination**

There were no apparent pathological changes in the heart, liver, spleen, lung and kidney. Under the transmission electron microscope, the liver cells were structurally intact and arranged normally, only part of the mitochondria criste were sparse and swollen (Figure 4A), but the cells returned to normal in 24 h (Figure 4B).

**Local irritation**

The tail veins of the mice were stained blue 1-7 days after i.v. DHAQ-PBCA-NP. Except one which appeared red and swollen slightly, the stained blue disappeared completely 4 days later, which demonstrated no irritation by DHAQ-PBCA-NP injection.

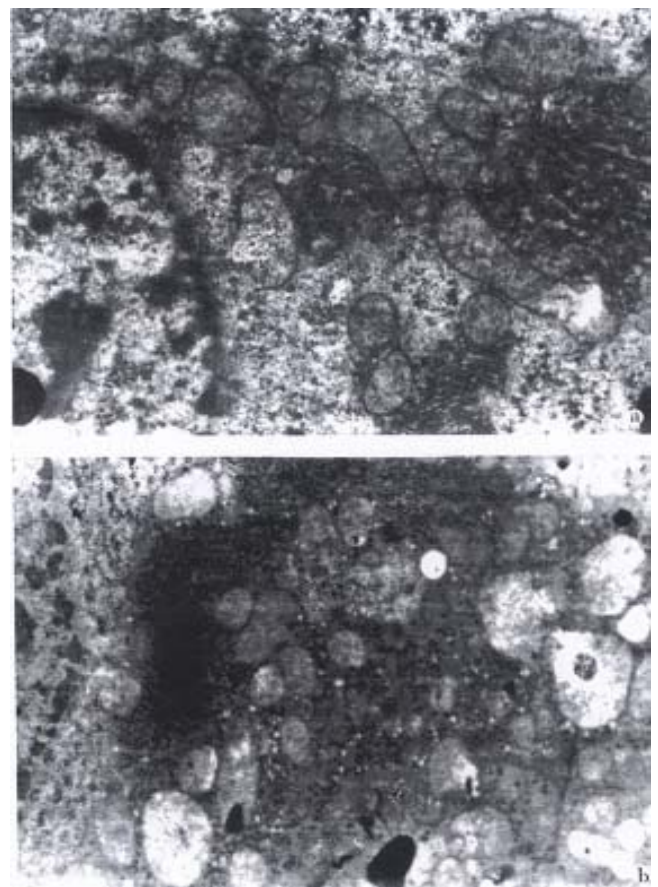


**Figure 4** The mouse liver cell at 20 min (A) and 24 h (B) after i.v.15mg/kg DHAQ-PBCA-NP. TEM×800

## DISCUSSION

The effect of DHAQ-PBCA-NP on the anti-heterotopically transplanted HCC was almost the same as that of DHAQ and ADR, which implied that it was more eligible to use the model of orthotopic transplantation than to use the heterotopic one.

The cell proliferative activity could be used for assessing the efficacy of chemotherapy. PCNA was an antigen existed largely at the junction of G<sub>1</sub> phase and S phase in the process of tumor cell proliferation, PC10 was the monoclonal antibody of PCNA. In order to investigate inhibiting effect of various drugs on tumor cell proliferation, a highly sensitive method of ABPAP was used for expression of PCNA by PC10 in this study, and the results were satisfactory. Furthermore, the DHAQ-PBCA-NP

injection had no adverse effect on the structure of heart, spleen, lung and kidney only some mild and reversible changes on the mitochondria of the hepatocytes implicating preparation of DHAQ-PBCA-NP was more effective and much less toxic than DHAQ.

## REFERENCES

- 1 Gu GW, Lu SZ. Hepatocarcinoma pathological epidemiology. *Foreign Med Sci-Physiol, Pathol Clin Fascicle*, 1991;11:91-93
- 2 Ma YP, Zheng S. The anticancer drug mitoxantrone. *World Pharm-Synthet Drug, Biochem Drug Pharmac Fascicle*, 1986;7:324-327
- 3 Couvreur P, Kante B, Roland M, Guito P, Bauduin P, Speiser P. Polycyanoacrylate nanocapsules as potential lysosomotropic carriers: preparation, morphological and sorptive properties. *J Pharm Pharmacol*, 1979;31:331-336
- 4 Garcia RL, Coltrera MD, Gown AM. Analysis of proliferative grade using antiPCNA/cyclin monoclonal antibodies in fixed embedded tissues. *Am J Pathol*, 1989;134:733-739

Edited by WU Xie-Ning

Proofread by MIAO Qi-Hong

# Study of the mechanisms of acupuncture and moxibustion treatment for ulcerative colitis rats in view of the gene expression of cytokines

WU Huan-Gan, ZHOU Li-Bin, PAN Ying-Ying, HUANG Cheng, CHEN Han-Ping, SHI Zheng and HUA Xue-Gui

**Subject headings** colitis, ulcerative/therapy; acupuncture and moxibustion therapy; gene expression; cytokines; interleukin-1 $\beta$ ; interleukin-6

## Abstract

**AIM** To observe the effect of acupuncture and moxibustion on the expression of IL-1 $\beta$  and IL-6 mRNA in ulcerative colitis rats.

**METHODS** The SD rat ulcerative colitis model was created by immunological method associated with local stimulation. Colonic mucosa was prepared from human fresh surgical colonic specimens, homogenized by adding appropriate amount of normal saline and centrifuged at 3000r/min. The supernatant was collected for measurement of protein concentration and then mixed with Freund adjuvant. This antigen fluid was first injected into the plantae of the model group rats, and then into their plantae, dorsa, inguina and abdominal cavities (no Freund adjuvant for the last injection) again on the 10th, 17th, 24th and 31st day. When a certain titer of serum anti-colonic anti body was reached, 2% formalin and antigen fluid ( no Freund adjuvant ) were administered separately by enema. The ulcerative colitis rat model was thus set up. The animals were randomly divided into four groups: model control group ( MC,  $n = 8$  ), electro-acupuncture group (EA,  $n = 8$ ), herbs-partition moxibustion group (HPM 8), normal control group ( NC,  $n = 8$  ). HPM: Moxa cones made of refined mugwort floss were placed on the

medicinal pad (medicinal pad dispensing: Radix Aconiti praeparata, cortex Cinnamomi, etc) for Qihai (RN 6) and Tianshu (S T 25, bilateral) and ignited. Two moxa cones were used for each acupoint once a day and 14 times in all. EA: Tianshu (bilateral) and Qihai were stimulated by the intermittent pulse with 2Hz frequency, 4mA intensity for 20 minutes once a day and 14 times in all. After treatment, rats of all four groups were killed simultaneously. The spleen was separated and the distal colon was dissected. Total tissue RNA was isolated by the guanidinium thiocyanate phenol-chloroform extraction method. RT-PCR technique was used to study the expression of IL-1 $\beta$  and IL-6 mRNA. **RESULTS** IL-1 $\beta$  and IL-6 mRNAs were not detected in the spleen and colonic mucosa of the NC rats, whereas they were significantly expressed in that of the MC rats. IL-1 $\beta$  and IL-6 mRNAs were markedly lower in the EA and HPM rats than that in MC rats. There was no significant difference between the levels of IL-1 $\beta$  and IL-6 mRNAs in the EA and HPM rats. The expressions of IL-1 $\beta$  and IL-6 mRNAs were nearly the same in the spleen and colon of all groups. **CONCLUSION** Acupuncture and moxibustion greatly inhibited the expression of IL-1 $\beta$  and IL-6 mRNA in the experimental ulcerative colitis rats.

## INTRODUCTION

Ulcerative colitis (UC) is a nonspecific inflammatory bowel disorder of unknown etiology but associated with immunological abnormalities<sup>[1]</sup>. The cytokines, involved in the regulation of the immune response, play important roles in the pathogenesis of UC. Especially the interleukin-1 $\beta$  (IL-1 $\beta$ ) and interleukin -6 (IL-6), inflammatory mediators released by lymphocytes, monocytes and macro phages, are intricately linked with the initiation and propagation of the inflammatory reaction in UC<sup>[2]</sup>. Both clinical and experimental researches indicated that acupuncture and moxibustion had good therapeutic effects on UC.

Shanghai Institute of Acupuncture-Moxibustion and Meridians, Shanghai 200030, China

Dr. WU Huan-Gan, male, born on 1956-11-21 in Xianju County, Zhejiang Province, graduated from Zhejiang College of Traditional Chinese Medicine, with Master Degree in 1990, and from Shanghai University of Traditional Chinese Medicine with Doctoral Degree in 1993; now professor, director, majoring the research of acupuncture-moxibustion immunity, having 26 papers published.

Supported by the National Natural Science Foundation of China, No.39670899.

**Correspondence to:** Prof. WU Huan-Gan, Shanghai Institute of Acupuncture-Moxibustion and Meridians, 650 South Wan Ping Road, Shanghai 200030, China

Tel.+86-21-64395972

Received 1999-05-23

The mechanism of such effects may be related to its immunoregulation, but the role of cytokines in it has not been reported. In this study, a UC rat model was established by immunological method to observe the effect of acupuncture and moxibustion on the expression of IL-1 $\beta$  and IL-6 mRNA in spleen and colonic mucosa of model rats, in order to clarify the possible mechanism of acupuncture and moxibustion on UC.

## MATERIALS AND METHODS

### Material

Male SD rats weighing, 140g $\pm$ 20g, were provided by The Experimental Animal Center of Shanghai University of TCM. The rats were randomly divided into the model group ( $n=24$ ) and normal control group (NC,  $n=8$ ). We consulted the Methodology of Pharmacy and created the rat model by immunological method associated with local stimulation (refer to the Abstract). These models were randomly subdivided into three groups after being created: model control group (MC,  $n=8$ ), electro-acupuncture group (EA,  $n=8$ ) and herbs-partition moxibustion group (HPM,  $n=8$ ). The points Qihai (CV6) and bilateral Tianshu (ST25) were located on analogy of person's points. HPM: Moxa cones made of refined mugwort floss were placed on the medicinal pad (medicinal pad dispensing: *Radix Aconiti praeparata*, *cortex Cinnamomi*, etc) for Qihai (RN 6) and Tianshu (ST 25, bilateral) and ignited. Two moxa cones were used for each acupoint once a day and 14 times in all. EA: Tianshu (bilateral) and Qihai were stimulated by the intermittent pulse with 2Hz frequency, 4mA intensity for 20 minutes once a day and 14 times in all. After treatment, all rats of the four groups were killed simultaneously. The spleen was separated and the distal colon 6cm long was dissected and reserved in liquid nitrogen.

### Method

According to the reference<sup>[3]</sup>, total tissue RNA was isolated by the guanidinium thiocyanate phenol chloroform extraction method. The concentration of sample RNA was measured with ultraviolet spectrophotometer OD260; the integrity of RNA was identified by agarose (sepharose) gel (10g/L) electrophoresis.

Two  $\mu$ g total RNA was reverse transcribed to cDNA, 20 $\mu$ L reverse transcription reaction system (Promega), which comprised 10 $\times$  reverse transcription buffer solution 2  $\mu$ L, 25 mmol/L MgCl<sub>2</sub> 4 $\mu$ L, 4 $\times$ dNTPs (10mmol/L for each) 2 $\mu$ L, RNAase inhibitor 0.5  $\mu$ L (20U), AMV reverse transcriptase 0.65  $\mu$ L (15U), oligomer (dT)<sub>15</sub> and primer 1  $\mu$ L (0.5  $\mu$ g); added DEPC up to 20  $\mu$ L, well mixed, placed in 42 $^{\circ}$ C water for 40 minutes,

heated in 95 $^{\circ}$ C water for 5 minutes to deactivate reverse transcriptase, and then preserved at -20 $^{\circ}$ C.

According to the reference<sup>[4]</sup>, the primer was synthesized in the oncogene laboratory of the Cell Institute of the Chinese Academy of Sciences. The sequence of IL-1 $\beta$  was ATAGCAGCTTTCGACAGTGAG (sense chain), GTCAACT ATGTCCC-GACCATT (antisense chain) 748bp; IL-6, TTCCCTACTTCACAAGTC (sense chain), CTAGGTTTGCCGAGTAGA (antisense chain) 567bp; glyceraldehyde dehydrogenase (GAPDH) triphosphate, TGAAGGTCGGTGTCAACGGATTTGTC (sense chain), CAGTAGGCCATGAGGTCCACCAC (antisense chain) 983bp. GAPDH as house keeping gene monitors the consumption of RNA and eliminates the errors among samples.

The total 50 $\mu$ L PCR reaction system consisted of 10 $\times$  amplification buffer solution 5  $\mu$ L, 4 $\times$  dNTPs (2.5 mmol/L for each) 4  $\mu$ L, primers of sense chain and antisense chain 50 pmol for each, 2 $\mu$ L reverse transcriptase product, Taq-DNA polymerase 2.5U, and added ddH<sub>2</sub>O up to 50  $\mu$ L, to mix them together. After 10 second centrifugation, 50 $\mu$ L liquid paraffin was added and placed in PCR Gene Amp Machine (Pharmacia). The amplification condition: IL-1 $\beta$ :94 $^{\circ}$ C pre-denature 4min, 94 $^{\circ}$ C 30s, 50 $^{\circ}$ C 45s, 72 $^{\circ}$ C 90s for 30 cycles; IL-6 and GAPDH: 94 $^{\circ}$ C pre-denature 4min, 94 $^{\circ}$ C 1min, 52 $^{\circ}$ C 1min, 72 $^{\circ}$ C 1min for 30 cycles.

Ten  $\mu$ L PCR product was added to 6 $\times$  electrophoresis buffer solution 2 $\mu$ L, and underwent agarose gel (1.5 g/L, containing Ethidium bromide 0.5mg/L) electrophoresis at 100V for 1 hour and photographed under ultraviolet lamp.

## RESULTS

### Total RNA extraction

The ratios of OD260/OD280 of the total RNA samples were between 1.70-2.00 and two bands, 18s and 28s, were shown in electrophoresis, indicating that the total RNA was not polluted and degraded.

### IL-1 $\beta$ and IL-6 mRNA in spleen and colon mucosa (Figure 1)

IL-1 $\beta$  and IL-6 mRNA expressions of spleen and colon mucosa were observed in model control group, electro-acupuncture group and herbs-partition moxibustion group, but the degrees of expression in EA or HPM were lower than that in MC. There was no significant difference between EA and HPM, but the degree of expression in HPM as a whole tended to be less. The expressions of spleen and colon mucosa in all groups were nearly the same. Neither IL-1 $\beta$  nor IL-6 mRNA expression of spleen and colon mucosa could be observed in the normal control group.

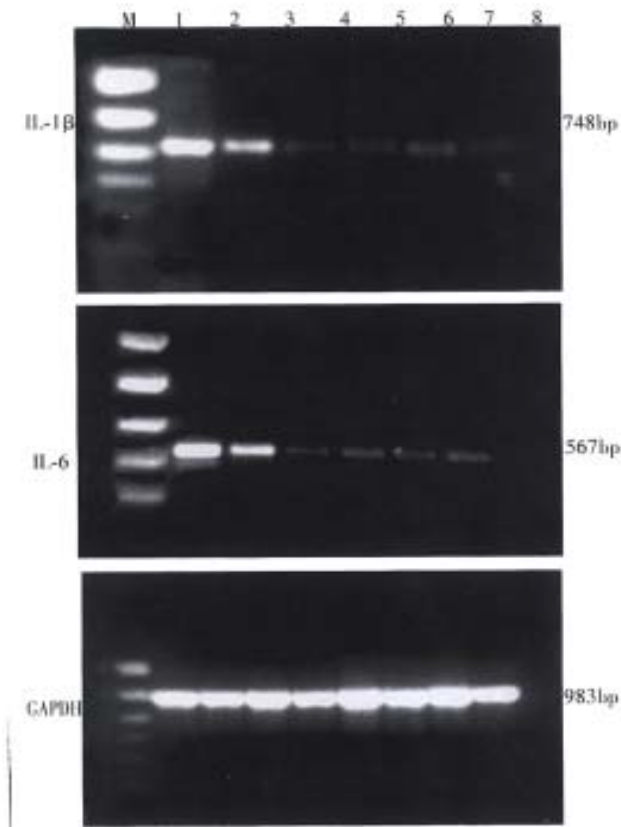


**Figure 1** The effect of acupuncture and moxibustion on IL-1 $\beta$  and IL-6 mRNA expression in spleen and colonic mucosa of ulcerative colitis rats.

M: Sign of PCR (Hua Mei), 1543, 994, 694, 515, 377 and 237bp from up to down respectively. 1, 3, 5 and 7 are mRNA of colonic mucosa in MC, EA, HPM and NC groups respectively; 2, 4, 6 and 8 are mRNA of spleen in MC, EA, HPM and NC groups respectively.

## DISCUSSION

The pathogenesis of UC may involve in both local and systemic immunological abnormalities. Cytokines now have attracted special attention by virtue of their participation in the intestinal inflammation and immune reactions. IL-1 $\beta$  and IL-6, as important inflammatory factors and immune regulators, play a fundamental role in the pathogenesis of UC. Many studies showed increased IL-1 $\beta$  and IL-6 levels in the colonic mucosa and peripheral blood of patients with UC, and indicated that IL-6 was possibly correlated with the severity of the manifestations in UC patients<sup>[5,6]</sup>. IL-1 $\beta$  and IL-6, produced mainly by activated phagocytes and lymphocytes, show a wide variety of biological functions. They can influence secretion of other cytokines and inflammatory mediators in an autocrine or paracrine fashion, induce expression of surface immune molecules of antigen-presenting cells to serve as an activation factor and differentiate on factor on T cells and B cells, mediate

immunoglobulin secretion, activate the complements, killer cells and phagocytes, and enhance tissue injury mediated by cellular and humoral immune reactions. In addition, IL-1 $\beta$  and IL-6 can promote the expression of adhesion molecules on endothelial-leukocyte and are regarded as a chemoattractant of circulating neutrophils to migrate in to the inflamed site, thus causing a series of long lasting intestinal inflammatory reaction and tissue injury<sup>[7-9]</sup>.

This study demonstrated that IL-1 $\beta$  and IL-6 were undetectable in the spleen and colonic mucosa of the normal control rats, whereas they were significantly expressed in that of the model control rats. Lymphocytes and monocytes/macrophages in the rats were activated by persistent stimulation of exogenous antigens which might contribute to the expression of cytokines. The amount of IL-1 $\beta$  and IL-6 mRNA was nearly the same between the spleen and colon in different groups, suggesting that immunocytes in the spleen and colon responded to the antigen in a similar way and interacted through the pathway of cytokines. In our study the markedly decreased expressions of IL-1 $\beta$  and IL-6 mRNA in EA and HPM suggested that acupuncture and moxibustion could inhibit the expression of inflammatory cytokines in UC model rats, regulate the immunological abnormalities, reduce immunocyte response to inflammation, and then contribute to the elimination of inflammation and repair of tissue.

The pathogenesis of UC may be due to an imbalance between inflammatory cytokines on one hand and anti-inflammatory immune factors such as IL-4, IL-1ra, IL-10, etc on the other. Our results suggest that in addition to inhibit the expression of inflammatory cytokines, acupuncture and moxibustion can activate the anti-inflammatory factors, but further studies are needed.

## REFERENCES

- 1 Kusugami K, Fukatsu A, Tanimoto M, Shinoda M, Haruta J, Kuroiwa A. Elevation of interleukin 6 in inflammatory bowel disease in macrophage and epithelial cell dependent. *Dig Dis Sci*, 1995;40:949-959
- 2 Hyams JS, Fitzgerld JE, Treem WR, Wyzga N, Kreutzer DL. Relationship of functional and antigenic interleukin 6 to disease activity in inflammatory bowel disease. *Gastroenterology*, 1993;104:1285-1292
- 3 Chomczynski P, Sacchi N. Single step method of RNA isolation by acid guanidinium thiocyanate phenol chloroform extraction. *Anal Biochem*, 1987;162:156-159
- 4 Murphy PG, Grondin J, Altares M, Richardson PM. Induction of interleukin 6 in axotomized sensory neurons. *J Neurosci*, 1995;15:5130-5138
- 5 Mitsuyama K, Toyonaga A, Sasaki E, Ishida O, Ikeda H, Tsuruta O. Soluble interleukin 6 receptors in inflammatory bowel disease: relation to circulating interleukin 6. *Gut*, 1995;36:45-49
- 6 Stevens C, Walz G, Singaram C, Lipman ML, Zanker B, Muggia A. Tumor necrosis factor- $\alpha$ , interleukin 1 $\beta$ , and interleukin 6, expression in inflammatory bowel disease. *Dig Dis Sci*, 1992;37:818-826
- 7 Hogaboam CM, Snider DP, Collins SM. Cytokine modulation of T lymphocyte activation by intestinal smooth muscle cells. *Gastroenterology*, 1997;112:1986-1997
- 8 Nassif A, Longo WE, Mazuski JE, Vemava AM, Kaminski DL. Role of cytokines and platelet activating factor in inflammatory bowel disease. *Dis Colon Rectum*, 1996;39:217-223
- 9 Schreiber S, Raedler A, Stenson WF, MacDermott RP. The role of the mucosal immune system in inflammatory bowel disease. *Gastroenterol Clin North Am*, 1992;21:451-502

Edited by LU Han-Ming

Proofread by MA Jing-Yun

Review

# Intestinal stasis associated bowel inflammation

Shunichiro Komatsu<sup>1</sup>, Yuji Nimura<sup>1</sup> and D. Neil Granger<sup>2</sup>

**Subject headings** intestinal stasis; bowel inflammation; endothelial cell intercellular adhesion molecule-1

## INTRODUCTION

Anatomical structures that create reservoirs for stagnant intestinal contents are a characteristic feature of common inflammatory disorders such as diverticulitis and appendicitis. Intestinal diverticula, surgically constructed blind loops and pouches, obstructing carcinomas of the colon, and Hirschsprung's disease are accompanied by chronic inflammatory changes in the intestine, and are occasionally associated with mucosal ulceration followed by massive bleeding. These diseases are etiologically associated with disorders characterized by intestinal stasis and/or an altered fecal stream, resulting from "cul de sac" structures (blind loop or pouch) in the intestinal tract, bowel obstruction or impaired motility. Furthermore, some of these chronic inflammatory conditions appear to exhibit similar pathological features, such as ischemic colitis. Although these inflammatory changes have been described individually, often as case reports, relatively little attention has been devoted to the overall clinical impact of these diseases and to understanding the pathophysiology of disease initiation and progression. Studies in our laboratory and by others have provided novel insights into the molecular and cellular basis for the intense inflammatory responses that are associated with intestinal stasis. This review summarizes the findings of these studies and provides a unifying theory to explain the inflammatory responses that result from intestinal stasis.

## CLINICOPATHOLOGICAL FEATURES

Whereas most intestinal (duodenal, jejunal, Meckel's, and colonic) diverticula remain asymptomatic, gastrointestinal bleeding is the most common complication, associated with mucosal ulceration<sup>[1-4]</sup>. Meckel's diverticulum, located on the antimesenteric border of the ileum, is the most common congenital anomaly of the gastrointestinal tract. Although ulcer formation in Meckel's diverticulum is generally thought to result from ectopic gastric tissue, all of the cases cannot be explained by acid production from the functioning gastric mucosa<sup>[2]</sup>. The diagnosis of gastrointestinal bleeding due to diverticula of the small bowel is difficult, because neither the symptoms nor physical findings are specific and endoscopic observation is hampered by the length of the intestine. Surgical resection of the involved segment of the intestine is the treatment of choice for the diverticula identified as a source of gastrointestinal hemorrhage<sup>[1]</sup>.

The terms "blind pouch" or "blind loop syndrome" represent the complications resulting from a stagnant intestine that are usually created by a side-to-side anastomosis with or without bowel resection, respectively. In cases of this syndrome, diarrhea and occult intestinal bleeding are usually found as well as symptoms resulting from malabsorption<sup>[5-9]</sup>. Shallow and longitudinal ulcerations are occasionally observed in the resected blind intestine, similar to those of ischemic enteritis<sup>[5,6]</sup>. Bacterial overgrowth in the blind loop has been presented in experimental models of animals<sup>[8,9]</sup>. While this syndrome is now rare because the safety of an end-to-end anastomosis has been established, the pathological features of this condition may provide important insights concerning the linkage between intestinal stasis and the resulting inflammatory response.

Restorative proctocolectomy with ileal pouch anal anastomosis has become the surgical treatment of choice for both ulcerative colitis and familial adenomatous polyposis. In spite of the excellent functional results and improved quality of life with this procedure, major concerns persist regarding the risks for and consequences of ileal pouchitis, a long term complication that is recognized with increasing frequency. Pouchitis is a nonspecific inflammation of an ileal reservoir that typically results in

<sup>1</sup>First Department of Surgery, Nagoya University School of Medicine, Nagoya, Japan

<sup>2</sup>Department of Molecular & Cellular Physiology, Louisiana State University Health Sciences Center, Shreveport, LA, USA

Supported by Grant-in Aid for Scientific Research (C), 11671230, by the Ministry of Education, Science, Sports and Culture of Japan.

**Correspondence to:** Shunichiro Komatsu, MD, First Department of Surgery, Nagoya University School of Medicine, 65 Tsurumai-cho, Showa-ku, Nagoya City 466-8550, Japan

Tel. +81-52-744-2220, Fax. +81-52-744-2230

Email. skomat@atnet.ne.jp

Received 1999-09-22

increased bowel frequency, decreased stool consistency, diminished continence, low-grade fever, malaise, and arthralgias. Oral treatment with antibiotics, such as metronidazole, is an effective therapy for active pouchitis<sup>[10-12]</sup>.

The term "obstructive colitis" was originally used to define the ulcerative inflammatory lesions that occur proximal to the colonic lesion and which is partially or potentially obstructive rather than completely obstructed<sup>[13-16]</sup>. Complications include peritonitis, perforation, and breakdown of anastomoses made through involved segments of the colon that may appear externally normal at surgery<sup>[13,15]</sup>. The inflammatory response associated with colonic obstruction exhibits a variety of pathological features, including ischemic<sup>[13-16]</sup>, acute necrotizing<sup>[17]</sup>, or pseudomembranous colitis<sup>[18]</sup>, resulting in confusion about the definition of this disease<sup>[14]</sup>. The area of colitis is usually mildly dilated with moderate thickening of the wall. Thus, it is characteristically distinguished from marked distension of the bowel that is associated with thinning of the wall and transmural necrosis caused by an increased intraluminal pressure, followed by acutely developing arrest of the intramural circulation<sup>[13]</sup>.

Enterocolitis associated with Hirschsprung's disease, which can induce perforation and/or systemic sepsis, remains a major source of morbidity and mortality, both before and after definitive surgical treatment<sup>[19-22]</sup>. The risk of postoperative enterocolitis is significantly increased by mechanical factors related to anastomotic stricture and intestinal obstruction<sup>[21,22]</sup>, possibly eliciting a delayed intestinal transit. Crypt abscess, intraluminal fibrinopurulent debris, or mucosal ulceration are histologically observed<sup>[19,20]</sup>. The etiology of enterocolitis is uncertain; ischemic and bacterial causes and recently, rotavirus infections, have been suggested<sup>[23,24]</sup>.

While much attention has been devoted to defining the relationship between enteric bacteria and the pathogenesis of inflammatory bowel disease (IBD), it remains unclear whether intestinal stasis, resulting in overgrowth of enteric bacteria, contributes to the development of IBD. However, there are several interesting published observations that suggest the linkage between intestinal stasis and the pathogenesis of IBD. A previous study showed evidence that the recurrence of Crohn's disease in the neoterminal ileum after curative ileal resection is dependent on intestinal transit<sup>[25]</sup>. Although ulcerative colitis (UC) has been described as a continuous inflammatory process starting from the rectum, isolated inflammatory changes can be

observed in the periappendicial area of a number of patients with left-sided UC<sup>[26,27]</sup>. In recent epidemiology-based studies, the risk of progression of UC was significantly lower after previous appendectomy<sup>[28,29]</sup>.

Although peptic ulcers (gastric or duodenal) have been extensively studied, the mechanisms underlying the ulcerative inflammatory changes in the stagnant intestine, where acid from the stomach has already been neutralized, remains poorly characterized. Many of the features of the disease suggest an ischemic origin, which cannot be explained by atherosclerotic obstruction of the feeding arteries. Microvascular dysfunction, due to hypoperfusion following raised intraluminal pressure, has been assumed to account for the mucosal ischemia<sup>[13]</sup>. Contribution of enteric bacteria has also been suggested, based on the observation that treatment with oral antibiotics can often relieve clinical symptoms induced by these diseases<sup>[10-12,30,31]</sup>.

#### INTESTINAL STASIS AND ENDOTHELIAL CELL ADHESION MOLECULES

Leukocyte-endothelial cell adhesion is now recognized to represent an early and rate-limiting step in the leukocyte infiltration and accompanying tissue injury associated with acute or chronic inflammation. There is also evidence that adherent and activated leukocytes produce microvascular dysfunction by occluding microvessels, damaging endothelial cells and increasing vascular protein leakage<sup>[32,33]</sup>. Leukocyte-endothelial cell adhesive interactions, such as rolling, firm adhesion, and transendothelial migration, represent a highly coordinated process that is governed by a number of factors, including the expression of specific adhesion glycoproteins, physical forces generated within the microcirculation, and inflammatory mediators released by a variety of activated cells<sup>[32-37]</sup>. The pivotal role of endothelial cell adhesion molecules (CAMs) in regulating leukocyte recruitment has been demonstrated in different models of gastrointestinal and liver inflammation using either blocking monoclonal antibodies directed against specific CAMs or mice that is genetically deficient in one or more endothelial CAMs<sup>[34,35]</sup>. The  $\alpha 2$  subfamily of integrins (CD18) are expressed on leukocytes and these integrins firmly bind to glycoproteins of the immunoglobulin superfamily, such as intercellular adhesion molecule-1 (ICAM-1) and ICAM<sub>2</sub>, which are expressed on vascular endothelium. ICAM-1 is constitutively expressed on the surface of endothelial cells and this expression can be enhanced by endotoxin or cytokines<sup>[36,37]</sup>.

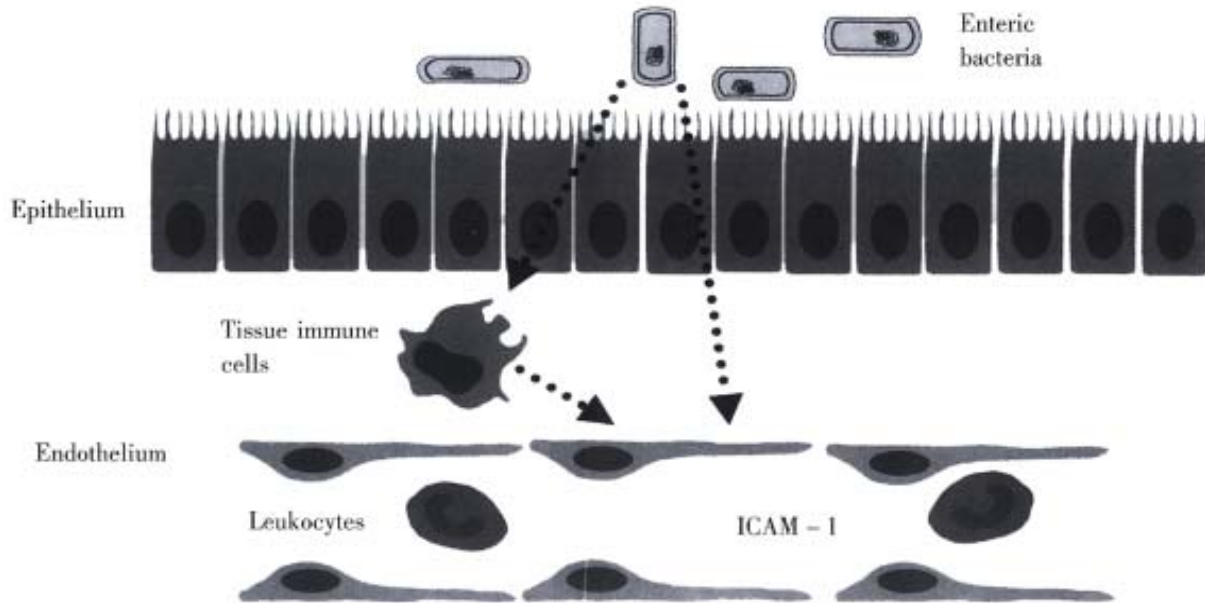


**Figure 1** Mechanism underlying the influence of enteric bacteria on ICAM-1 expression on endothelial cells of the intestinal vasculature. Intestinal stasis likely causes an increased production bacterial factors that promote ICAM-1 expression and consequently enhances the recruitment and activation of leukocytes in the intestine.

Our previous study, which employed surgical procedures to improve cecal stool flow in the rats<sup>[38]</sup>, represented the first attempt to address the issue of how intestinal stasis results in an inflammatory response. The findings of this study indicate that intestinal stasis is associated with an increased expression of ICAM-1 on endothelial cells and granulocyte infiltration. This study also suggested that it be the bacterial load of a stagnant intestine that determines the activation of mechanisms leading to infiltration of inflammatory cells, based on the responses noted in animals receiving oral antibiotics. This view is supported by a previous study, in which pretreatment with metronidazole inhibited the leukocyte-endothelial cell adhesion in rat mesenteric venules elicited by indomethacin or leukotriene B<sub>4</sub><sup>[39]</sup>.

A definitive explanation concerning how enteric bacteria enhance ICAM-1 expression on endothelial cells in the stagnant intestine is not readily available. However, our recent work on germfree mice demonstrated that the expression of ICAM-1, but not other endothelial CAMs such as ICAM-2, vascular cell adhesion molecule-1 (VCAM-1), or E-selectin, is altered by germfree conditions<sup>[40]</sup>. The ICAM-1 specificity of this response argues against a role for systemic levels of bacterial endotoxin or tumor necrosis factor- $\alpha$  released from macrophages, which are powerful stimuli for VCAM-1 and E-selectin as well as ICAM-1<sup>[34]</sup>, as mediators of the response. There is a growing body of evidence, derived from germ free

animals, that enteric microflora contribute to the basal level of activation of the immune system, such as antibody-forming potential, phagocytosis, T-cell population and responsiveness to cytokines<sup>[41-47]</sup>. As illustrated in Figure 1, some unique factor that is normally released from enteric bacteria promotes the increased constitutive expression of ICAM-1 in the intestinal microvasculature. Events associated with an altered enteric microflora, such as intestinal stasis or an altered fecal stream, are likely to affect the amount of this bacteria-derived factor that regulates ICAM-1 expression. In doing so, the enteric bacteria can exert a profound influence on the trafficking of leukocytes in the intestinal microcirculation. As intestinal stasis and overgrowth of enteric bacteria are associated with increased ICAM-1 expression, subsequently affecting leukocyte-endothelial cell adhesion, it is tempting to speculate that the ischemic and inflammatory changes observed in the several disorders associated with intestinal stasis may have share a common underlying mechanism that largely explains the ulcerative inflammatory lesions.

## REFERENCES

- 1 Miller LS, Friedman LS. Less frequent causes of lower gastrointestinal bleeding. *Gastroenterol Clin North Am*, 1994;23:21-52
- 2 Kusumoto H, Yoshida M, Takahashi I, Anai H, Maehara Y, Sugimachi K. Complications and diagnosis of Meckel's diverticulum in 776 patients. *Am J Surg*, 1992;164:382-383
- 3 Donald JW. Major complications of small bowel diverticula. *Ann Surg*, 1979;190:183-188
- 4 de Bree E, Grammatikakis J, Christodoulakis M, Tsiftsis D. The clinical significance of acquired jejunoileal diverticula. *Am J*

- Gastroenterol*, 1998;93:2523-2528
- 5 Clawson DK. Side to side intestinal anastomosis complicated by ulceration, dilatation and anemia. *Surgery*, 1953;34:254-257
  - 6 Adachi Y, Matsushima T, Mori M, Sugimachi K, Oiwa T. Blind loop syndrome: multiple ileal ulcers following side to side anastomosis. *Pathology*, 1993;25:402-404
  - 7 Woelfel GF, Campbell DN, Penn I, Reichen J, Warren GH. Inflammatory polyposis in an ileal blind loop. *Gastroenterology*, 1983;84(5 Pt 1):1020-1024
  - 8 Justus PG, Fernandez A, Martin JL, King CE, Toskes PP, Mathias JR. Altered myoelectric activity in the experimental blind loop syndrome. *J Clin Invest*, 1983;72:1064-1071
  - 9 Welkos SL, Toskes PP, Baer H. Importance of anaerobic bacteria in the cobalamin malabsorption of the experimental rat blind loop syndrome. *Gastroenterology*, 1981;80:313-320
  - 10 Hurst RD, Molinari M, Chung TP, Rubin M, Michelassi F. Prospective study of the incidence, timing and treatment of pouchitis in 104 consecutive patients after restorative proctocolectomy. *Arch Surg*, 1996;131:497-502
  - 11 Sandborn WJ, McLeod R, Jewell DP. Medical therapy for induction and maintenance of remission in pouchitis: a systematic review. *Inflamm Bowel Dis*, 1999;5:33-39
  - 12 Kubbacher T, Schreiber S, Runkel N. Pouchitis: pathophysiology and treatment. *Int J Col Dis*, 1998;13:196-207
  - 13 Toner M, Condell D, O'Briain DS. Obstructive colitis: ulceroinflammatory lesions occurring proximal to colonic obstruction. *Am J Surg Pathol*, 1990;14:719-728
  - 14 Levine TS, Price AB. Obstructive enterocolitis: a clinico pathological discussion. *Histopathology*, 1994;25:57-64
  - 15 Reeders JW, Rosenbusch G, Tytgat GN. Ischaemic colitis associated with carcinoma of the colon. *Eur J Radiol*, 1982;2:41-47
  - 16 Feldman PS. Ulcerative disease of the colon proximal to partially obstructive lesions: report of two cases and review of the literature. *Dis Col Rec*, 1975;18:601-612
  - 17 Hurwitz A, Khafif A. Acute necrotizing colitis associated with colonic carcinoma. *Surg Gynecol Obstet*, 1960;111:749-753
  - 18 Goulston SJ, McGovern VJ. Pseudomembranous colitis. *Gut*, 1965;6:207-212
  - 19 Elhalaby EA, Teitelbaum DH, Coran AG, Heidelberger KP. Enterocolitis associated with Hirschsprung's disease: a clinical histopathological correlative study. *J Pediatr Surg*, 1995;30:1023-1026
  - 20 Teitelbaum DH, Caniano DA, Qualman SJ. The pathophysiology of Hirschsprung's associated enterocolitis: importance of histologic correlates. *J Pediatr Surg*, 1989;24:1271-1277
  - 21 Hackam DJ, Filler RM, Pearl RH. Enterocolitis after the surgical treatment of Hirschsprung's disease: risk factors and financial impact. *J Pediatr Surg*, 1998;33:830-833
  - 22 Teitelbaum DH, Qualman SJ, Caniano DA. Hirschsprung's disease. Identification of risk factors for enterocolitis. *Ann Surg*, 1988;207:240-244
  - 23 Imamura A, Puri P, O'Briain DS, Reen DJ. Mucosal immune defence mechanisms in enterocolitis complicating Hirschsprung's disease. *Gut*, 1992;33:801-806
  - 24 Wilson-Storey D, Scobie WG, McGenity KG. Microbiological studies of the enterocolitis of Hirschsprung's disease. *Arch Dis Child*, 1990;65:1338-1339
  - 25 Rutgeerts P, Geboes K, Peeters M, Hiele M, Penninckx F, Aerts R. Effect of faecal stream diversion on recurrence of Crohn's disease in the neoterminal ileum. *Lancet*, 1991;338:771-774
  - 26 D'Haens G, Geboes K, Peeters M, Baert F, Ectors N, Rutgeerts P. Patchy cecal inflammation associated with distal ulcerative colitis: a prospective endoscopic study. *Am J Gastroenterol*, 1997;92:1275-1279
  - 27 Cohen T, Pfeffer RB, Valensi Q. "Ulcerative appendicitis" occurring as a skip lesion in chronic ulcerative colitis; report of a case. *Am J Gastroenterol*, 1974;62:151-155
  - 28 Russel MG, Dorant E, Brummer RJ, van de Kruijs MA, Muris JW, Bergers JM. Appendectomy and the risk of developing ulcerative colitis or Crohn's disease: results of a large case control study. *Gastroenterology*, 1997;113:377-382
  - 29 Rutgeerts P, D'Haens G, Hiele M, Geboes K, Vantrappen G. Appendectomy protects against ulcerative colitis. *Gastroenterology*, 1994;106:1251-1253
  - 30 Breatly S, Armstrong GR, Nairn R, Gornall P, Currie ABM, Buick RG. Pseudomembranous colitis: a lethal complication of Hirschsprung's disease unrelated to antibiotic usage. *J Pediatr Surg*, 1987;22:257-259
  - 31 Leung FW, Drenick EJ, Stanley TM. Intestinal bypass complications involving the excluded small bowel segment. *Am J Gastroenterol*, 1982;77:67-72
  - 32 Granger DN, Kubes P. The microcirculation and inflammation: modulation of leukocyte-endothelial cell adhesion. *J Leuko Biol*, 1994;55:662-675
  - 33 Granger DN, Grisham MB, Kvietys PR. Mechanisms of microvascular injury. In: Physiology of the gastrointestinal tract, edited by Johnson LR. Third edition. New York: Raven Press, 1994:1693-1722
  - 34 Panes J, Granger DN. Leukocyte endothelial cell interactions: molecular mechanisms and implications in gastrointestinal disease. *Gastroenterology*, 1998;114:1066-1090
  - 35 Granger DN. Cell adhesion and migration. II. Leukocyte endothelial cell adhesion in the digestive system. *Am J Physiol*, 1997;273(5 Pt 1):G982-986
  - 36 Anderson DC. The role of  $\beta 2$  integrins and intercellular adhesion molecule type 1 in inflammation. In: Physiology and pathophysiology of leukocyte adhesion, edited by D.N. Granger and G.W. Schmid-Sch-bein. New York: Oxford University Press, 1995:3-42
  - 37 Springer TA. Traffic signals for lymphocyte recirculation and leukocyte emigration: the multistep paradigm. *Cell*, 1994;76:301-314
  - 38 Komatsu S, Panes J, Grisham MB, Russell JM, Mori N, Granger DN. Effects of intestinal stasis on intercellular adhesion molecule 1 expression in the rat: role of enteric bacteria. *Gastroenterology*, 1997;112:1971-1978
  - 39 Arndt H, Palitzsch KD, Grisham MB, Granger DN. Metronidazole inhibits leukocyte endothelial cell adhesion in rat mesenteric venules. *Gastroenterology*, 1994;106:1271-1276
  - 40 Komatsu S, Berg RD, Russell JM, Nimura Y, Granger DN. Enteric microflora contribute to constitutive ICAM-1 expression: studies on germfree mice. *Gastroenterology*, 1999;116:A897
  - 41 Granholm T, Froysa B, Lundstorm C, Wahab A, Midtvedt T, Soder O. Cytokine responsiveness in germfree and conventional NMRI mice. *Cytokine*, 1992;4:545-550
  - 42 Morland B, Midtvedt T. Phagocytosis, peritoneal influx, and enzyme activities in peritoneal macrophages from germfree, conventional and ex germfree mice. *Infect Immun*, 1984;44:750-752
  - 43 Starling JR, Balish E. Lysosomal enzyme activity in pulmonary alveolar macrophages from conventional, germfree, monoassociated and conventionalized rats. *J Reticuloendothel Soc*, 1981;30:497-505
  - 44 Sellon RK, Tonkonogy S, Schultz M, Dieleman LA, Grenther W, Balish E. Resident enteric bacteria are necessary for development of spontaneous colitis and immune system activation in interleukin 10 deficient mice. *Infect Immun*, 1998;66:5224-5231
  - 45 Gautreaux MD, Deitch EA, Berg RD. T lymphocytes in host defense against bacterial translocation from the gastrointestinal tract. *Infect Immun*, 1994;62:2874-2884
  - 46 Shroff KE, Meslin K, Cebra JJ. Commensal enteric bacteria engender a self-limiting humoral mucosal immune response while permanently colonizing the gut. *Infect Immun*, 1995;63:3904-3913
  - 47 Umesaki Y, Setoyama H, Matsumoto S, Okada Y. Expansion of alpha beta T cell receptor bearing intestinal intraepithelial lymphocytes after microbial colonization in germ free mice and its independence from thymus. *Immunology*, 1993;79:32-37

Edited by WU Xie-Ning

Proofread by MIAO Qi-Hong

Brief Reports

# Preparation and purification of F(ab')<sub>2</sub> fragment from anti hepatoma mouse IgG<sub>1</sub> mAb

LIU Cheng-Gang<sup>1</sup>, ZHU Mei-Cai<sup>1</sup> and CHEN Zhi-Nan<sup>2</sup>

**Subject headings** antibody, monoclonal; F(ab')<sub>2</sub> fragment; papain digestion; liver neoplasms; ion-exchange chromatography

## INTRODUCTION

Since the advent of hybridoma technology<sup>[1]</sup>, monoclonal antibodies have been widely used in basic studies and clinical application. F(ab')<sub>2</sub> is a bivalent antibody fragment which is currently used for both diagnosis and treatment<sup>[2]</sup>, and better than the original mAbs, because it does not retain complement binding function due to lack of Fc regions and reduced interaction with non-specific proteins and the smaller molecular weight than the mAbs, furthermore, it can be digested by pepsin or papain and purified by size exclusion chromatography<sup>[4]</sup>, ion-exchange chromatography<sup>[6]</sup> or hydrophobic interaction<sup>[7]</sup>. However, these methods are time-consuming, and cannot attain sufficient purity and recovery of F(ab')<sub>2</sub> fragment. Development of efficient procedures for F(ab')<sub>2</sub> preparation is an urgent necessity.

In the present paper, we described a method for preparation of F(ab')<sub>2</sub> fragment from papain digest of mouse IgG<sub>1</sub> mAb Hab18 and then purified by FPLC using DEAE-Sepharose-FF gel. The results showed this method was suitable for large-scale preparation and purification of F(ab')<sub>2</sub> fragments.

## MATERIALS AND METHODS

### Materials

Mouse mAb Hab18 belonged to the IgG<sub>1</sub> subclass

was used, and the specific antigen was human hepatoma. It was produced by our laboratory; papain was purchased from Sigma.

### Methods

**Papain digestion** MAb HAB18 was purified from the ascitic fluid which was centrifuged at 1000 r/min for 20 min to remove cells, and the supernatant was dialyzed against 10 mmol/L phosphate buffer (PB), pH 5.5, and then placed at column of SP-cellulose FPLC, the fraction containing IgG<sub>1</sub> HAB18 was precipitated by adding ammonium sulfate to give 50% saturation, followed by centrifugation at 5000 r/min for 10 min after standing for 2 h. The precipitate was dissolved in PBS (10 mmol/L sodium phosphate, pH 7.4, 150 mmol/L NaCl) to 20 g/L, and dialyzed overnight against 0.1 mol/L sodium acetate, pH 5.5.

MAb digestion was carried out by the method of Parham *et al*<sup>[8]</sup> with some modification. Briefly, papain was dissolved in 0.1 mol/L sodium acetate, pH 5.5 with 3 mmol/L EDTA, 1 mmol/L DTT (Sigma) and then incubated for 30 min at 37 °C. Activated papain was freed from excess DTT by gel filtration of the Sephadex G-25 (Pharmacia). The papain was determined by measuring absorbance at 280 nm and adjusted to 2 g/L. Preactivated papain was added to mAb HAB18 at a ratio of 1:20 (w/w) and the mixture was incubated at 37 °C for 2h. The reaction ceased by addition of 30 mmol/L iodoacetamide (Fluca) and the products analyzed by SDS-PAGE in the absence of β-mercaptoethanol.

**Chromatographic purification** The papain digest was dialyzed against 10 mmol/L Tris-HCl, pH 8.0 and applied to a column of DEAE-Sepharose-FF (2 cm×18 cm, Pharmacia) connected to FPLC which was equilibrated and then washed in the same buffer until the absorbance at 280 nm reached a background value of 0.01. The column was then eluted with a linear gradient from 0 mmol/L - 100 mmol/L NaCl in the same buffer. Fractions were collected and assayed for absorbance at 280 nm and analyzed by SDS-PAGE.

<sup>1</sup>Center of Clinical Molecular Biology, General Hospital of Air Force, Beijing 100036, China

<sup>2</sup>Department of Pathology, the Fourth Military Medical University, Xi'an 710032, Shaanxi Province, China

LIU Cheng-Gang, female, born in 1971-06-09 in Weichang, Hebei Province, graduated from the Fourth Military Medical University in 1989, now technologist of molecular biology, majoring hepatoma targeting drug and molecular biology, having 4 papers published. Project supported by the National "863" Fund of China, No.863-102-12(01).

**Correspondence to:** LIU Cheng-Gang, Center of Clinical Molecular Biology, General Hospital of Air Force, Fu Cheng Road 30, Beijing 100036, China

Tel. +86-10-66928154

Received 1999-07-11

**Analytical studies** The purity of F(ab')<sub>2</sub> fraction was detected by SDS-PAGE which was performed in a 10% gel under reduction or non-reduction conditions according to the method of Laemmli<sup>[9]</sup>. Proteins were treated with loading buffer in the absence or presence of  $\beta$ -mercaptoethanol at 100°C for 5min and stained with Coomassie Brilliant Blue R-250.

Antigen binding activities of F(ab')<sub>2</sub> were measured by indirect immunofluorescence. Viable hepatoma cells were fixed on the plates. F(ab')<sub>2</sub> fraction was diluted with PBS to 1 mg/L, and series of two-fold dilutions were prepared and added to plates which were incubated for 60 min at 37 °C, washed with BPS, and added fluorochrome-conjugated rabbit anti-mouse F(ab')<sub>2</sub> antibody (Sigma) then incubated for 30 min at 37 °C and examined under an immunofluorescence microscope.

Concentrations of F(ab')<sub>2</sub> and mAb were estimated using an extinction coefficient at 280nm and at 260 nm, protein concentration (g/L) = 1.45 × OD<sub>280</sub> - 0.74 × OK<sub>260</sub>.

## RESULTS

### Papain digestion

The ascitic fluid from which the mAb was purified by SP-FPLC, the product of the papain digestion for 2 h and the purified F(ab')<sub>2</sub> were applied to SDS-PAGE under non-reduction and reduction conditions, the results indicated about 95% of the antibody were degraded to F(ab')<sub>2</sub> fragment after 2 h incubation. The digest contained F(ab')<sub>2</sub>, F(ab'), and Fc fragments as well as intact IgG and other contaminating proteins. A band with  $M_r$  160000 was corresponding to IgG under non-reduction condition before the reaction, and a band of  $M_r$  160 000 was considered to be F(ab')<sub>2</sub> after digestion. Under reduction condition, IgG showed two bands of  $M_r$  50 000 and  $M_r$  28 000, which corresponded to heavy (H) and light (L) chains, respectively. In contrast, the H and L chains of F(ab')<sub>2</sub> were about  $M_r$  30 000 and  $M_r$  28 000 (Figure 1).

### Chromatographic purification

The papain digest was separated by FPLC using DEAE-Sepharose-FF column. As shown in Figure 2, the strength of interaction with DEAE was papain < F(ab')<sub>2</sub> < IgG < Fc. Papain flow through the column, F(ab')<sub>2</sub>, F(ab'), IgG, Fc and other protein bound to the column and purified F(ab')<sub>2</sub> fragment was obtained after elution with 50mmol/L NaCl. According to the SDS-PAGE result, the fragment was separated entirely with intact IgG, Fc, papain and other proteins.

### Analytical studies

The collected F(ab')<sub>2</sub> pool from the DEAE column was applied to SDS-PAGE and then examined by thin-layer chromatography scanning. The results showed that the purity of F(ab')<sub>2</sub> fragment was more than 95%.

The immunoactivity of initial mAb and the F(ab')<sub>2</sub> obtained after digestion were determined using indirect immunofluorescence. After proteolytic digestion and chromatographic purification, the minimal detective concentration F(ab')<sub>2</sub> was 0.125 μg/mL, corresponding to 90% of their initial mAb activity.

The total protein digested by papain was 100mg. The quantity of the F(ab')<sub>2</sub> obtained from the DEAE-FPLC was 53mg, and the purity greater than 95 %, due to the molecular size of F(ab')<sub>2</sub> fragment is 68% of the intact IgG, thus, the actual yield of F(ab')<sub>2</sub> was about 78% of theoretical yield.

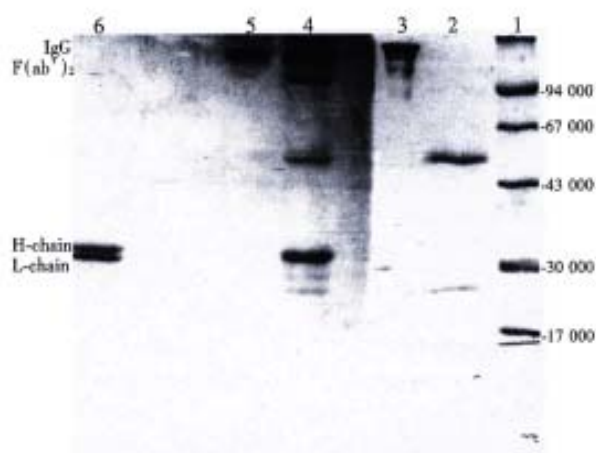


**Figure 1** Photograph of SDS-PAGE gel of anti-hepatoma IgG<sub>1</sub> mAb HAB18 before and after digestion and purification. Lane 1, molecular weight standards; lane 2-3, reduced and non-reduced mAb HAB18; lane 4, papain digest of HAB18; lane 5-6, purified F(ab')<sub>2</sub> fragment under non-reduction and reduction conditions.

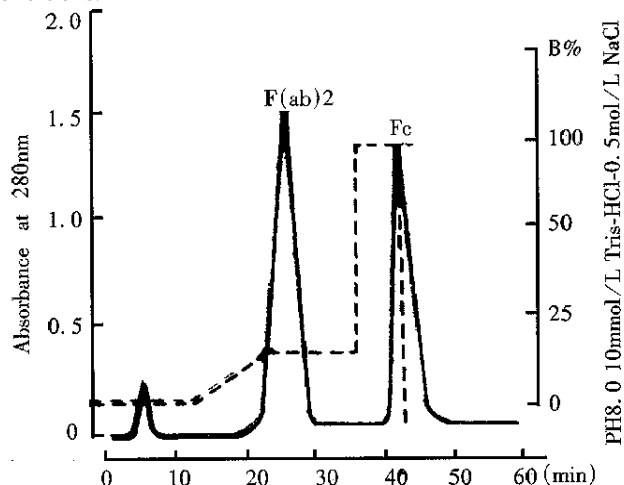


**Figure 2** Purification of F(ab')<sub>2</sub> fragment from papain digest of mAb HAB18 by FPLC using DEAE-Sepharose-FF column.

## DISCUSSION

Classical preparation of F(ab')<sub>2</sub> fragments from mouse IgG mAbs used to be digested by pepsin, however, Lamoyi *et al*<sup>[3,4]</sup> reported that the sensitivity to pepsin varied in different mouse IgG subclass, it was IgG<sub>3</sub>>IgG<sub>2a</sub>>IgG<sub>2b</sub>>IgG<sub>1</sub>, pepsin had little effect on most mouse IgG<sub>1</sub> proteins. Parham *et al*<sup>[6,8]</sup> used preactivatedthiol-free papain to cleave IgG<sub>1</sub> mAbs to F(ab')<sub>2</sub> and Fc fragments efficiently, but it needed 18h- 25h for digestion. The method described here was modified according to the reference<sup>[8]</sup>, the study showed that 2h was sufficient, more than 95 % of mAb was cleaved successfully to F(ab')<sub>2</sub> fragment using papain digest ion. Under the conditions described above, 3 anti-hepatoma IgG<sub>1</sub> mAbs had been so far tried and the same results obtained. The relative amounts of F(ab')<sub>2</sub> produced might vary with changes in the conditions of digestion, duration and concentration<sup>[8]</sup>, so we suggested that the conditions of digestion for each monoclonal antibody preparation be assessed by experience. In addition, it was critical to inactivate the papain, for we observed in our experiment that it might retain activity and led to degradation of F(ab')<sub>2</sub> to Fab and smaller fragments.

There have been some papers reporting the purification of F(ab')<sub>2</sub> fragments by gel filtration<sup>[2]</sup> or ion-exchange chromatography<sup>[3,6]</sup>. However, F(ab')<sub>2</sub> cannot be purified to homogeneity by single-step chromatography. Koichi<sup>[7]</sup> reported a purification scheme for F(ab')<sub>2</sub> fragment, using hydrophobic interaction, and ammonium sulfate was used in protein precipitation and purification. However, this technique might reduce significantly the antibody activity<sup>[10]</sup>. In the present paper, we described the use of FPLC using DEAE-Sepharose-FF to the purification of F(ab')<sub>2</sub> fragment of mouse IgG<sub>1</sub> MA b. The advantage of the method described here was not only could be completed within on

single-step, but also the fraction containing F(ab')<sub>2</sub> fragment was homogeneous (Figure 1), which had been separated entirely from papain, intact IgG and Fc fragment, though F(ab')<sub>2</sub> sometimes contain a little of F(ab'), for many purposes it was no need for further purification. To be more important, the recovered F(ab')<sub>2</sub> retained 90% of their initial mAb activity.

By using the procedures above a purification cycle was only 60 min, and F(ab')<sub>2</sub> fragment obtained from each cycle could reach the level of preparation scale. Because of these advantages, they could be a simple and rapid process. This method was quite useful in immunological diagnosis and therapy with antibody fragment.

## REFERENCES

- 1 Kohler G, Milstein C. Continuous cultures of fused cells secreting antibody of predefined specificity. *Nature*, 1975;256:495-497
- 2 Goding JW. Monoclonal antibodies: principles and practice. 2nd Edn. London: Academic Press, 1986:125-133
- 3 Lamoyi E, Nisonoff A. Preparation of F(ab')<sub>2</sub> fragments from mouse IgG of various subclasses. *J Immunol Methods*, 1983;56:235-243
- 4 Parham P. On the fragmentation of monoclonal IgG1, Ig G2 a and IgG 2b from BALB/c mice. *J Immunol*, 1983;131:2895-2902
- 5 Yurov GK, Neugodova GL, Verkhovsky OA, Naroditsky BS. Thiophilic adsorption: rapid purification of F(ab')<sub>2</sub> and Fc fragments of IgG1 antibodies from murine ascitic fluid. *J Immunol Methods*, 1994;177:29-33
- 6 Clezardin P, McGregor JL, Manach M, Boukerche H, Dochavanne M. One step procedure for the rapid isolation of mouse monoclonal antibodies and their antigen binding fragments by fast protein liquid chromatography on a Mono Q anion exchange column. *J Chromatography*, 1985;319:67-77
- 7 Morimoto K, Inouye K. Single step purification of F(ab')<sub>2</sub> fragments of mouse monoclonal antibodies (immunoglobulins G 1) by hydrophobic interaction high performance liquid chromatography using TSK gel phenyl 5PW. *J Biochem Biophys Methods*, 1992;24:107-117
- 8 Parham P, Androlewicz MJ, Brodsky FM, Holmes NJ, Ways JP. Monoclonal antibodies: purification, fragmentation and application to structural and functional studies of Class I MHC antigens. *J Immunol Methods*, 1982;53:133-173
- 9 Laemmli UK. Cleavage of structural proteins during the assembly of the head of bacteriophage T4. *Nature*, 1970;227:680-685
- 10 Bruck C, Portetelle D, Glineur C, Bollen A. One step purification of mouse monoclonal antibodies from ascitic fluid by DEAE affinity blue chromatography. *J Immunol Methods*, 1982;53:313-319

Edited by WU Xie-Ning

Proofread by MIAO Qi-Hong

# Measurement of liver volume and its clinical significance in cirrhotic portal hypertensive patients

ZHU Ji-Ye, LENG Xi-Sheng, DONG Nan, QI Gui-Ying and DU Ru-Yu

**Subject headings** liver volume; hypertension, portal; liver cirrhosis; prognosis

## INTRODUCTION

Accurate assessment of hepatic reserve function in cirrhotic portal hypertensive patients is important for selection of surgical procedure and evaluation of prognosis. The measurement of liver volume has been applied in clinic as widely as Child's class<sup>[1,2]</sup>. Limited by technical condition, measurement of liver volume *in vivo* has seldom been reported in China. Using double helix-spiral CT (Elscent CT Twin), the liver volume of 25 cirrhotic patients and 30 patients in controls was assessed, and a correlation analysis was made between the liver volume and preoperative natural shunting rate, portal vein flow, portal pressure and prognosis of cirrhotic patients.

## MATERIALS AND METHODS

### Patients

Twenty-five patients with post-hepatitis cirrhotic portal hypertension were included in this study (16 males and 9 females, aged 24-66 years, averaging 44.2 years  $\pm$  10.7 years, 1.58 m-1.76 m in height and 47.5kg-70.5kg in weight). All patients were HBsAg or HCV-antigen positive with no cardiac disease and hepatic space-occupying lesion.

Thirty patients with chronic cholelithiasis with no hepatic disease served as controls (13 males and 17 females, averaging 45.1 years  $\pm$  14.0 years, 1.58 m-1.82 m in height and 48 kg - 85 kg in weight). All patients were HBsAg negative with no cardiac disease.

### Methods

**Measurement of liver volume** The upper abdomen was scanned by double helix-spiral CT (Elscent CT Twin). The liver volume was measured by 3-dimensional shaded surface display software<sup>[3]</sup>.

### Measurement of natural portal-systemic shunting rate

<sup>99m</sup>Tc-MIBI750mBq (20mci) was given intrarectally to cirrhotic portal hypertensive patients who lied supine under the detector of Techneca 438H/560 $\gamma$  camera to image heart, liver and spleen. The region of interest (ROI) with equal area was set up over the surface of heart and liver, portal-systemic shunting index (SI) = ROI (heart)/ROI (heart) +ROI (liver).

### Measurement of portal flow and portal pressure

During breath holding after inspiration, the bore and average/maximal blood flow rate of portal vein were measured from 2-dimensional real-time ultrasonographic image with AC USON 128P/10 color Doppler ultrasound system. The portal flow was measured according to the formula (flow volume = sectional area  $\times$  flow rate). Portal pressure was measured by gastroepiploic venous centesis.

## RESULTS

According to double helix-spiral CT, the average liver volume in the control group was 1070.68cm<sup>3</sup> $\pm$  227.52cm<sup>3</sup>, and was positively correlated with height, the correlation coefficient ( $\gamma$  = 0.42,  $P$  < 0.05) was not correlated with that ( $\gamma$  = 0.17,  $P$  > 0.05) of body weight.

According to double helix-spiral CT, the average liver volume of portal hypertensive patients was 797.02cm<sup>3</sup> $\pm$  135.11cm<sup>3</sup>, which was significantly smaller than that in the controls ( $P$  < 0.05).

The liver volume of cirrhotic portal hypertensive patients was correlative with Child's class, the liver volume and liver volume/height of patients who were Child B were significantly greater than that of patients who were Child C ( $P$  < 0.05). There was no significant correlation between liver volume and natural portal-systemic shunting index (SI) (correlation coefficient  $\gamma$  = -0.27,  $P$  > 0.05) and portal flow (correlation coefficient  $\gamma$  = 0.17,  $P$  > 0.05)(Table 1).

Among the 24 cirrhotic portal hypertensive patients who received H-graft portal-caval shunt (the bore of the artificial vessel was 8 mm), the morbidity of postoperative encephalopathy and the one-year mortality in patients with their liver volume lower than 750 cm<sup>3</sup> were found to be higher than those in patients with their liver volume higher than 750 cm<sup>3</sup>. Significant difference was found in the morbidity of postoperative encephalopathy (Table 2).

Department of Surgery, People's Hospital of Beijing Medical University, Beijing 100044, China

Dr. ZHU Ji-Ye, associate professor of surgery, male, born on July 30, 1963 and graduated from Beijing Medical University, being engaged in study on the therapy of portal hypertension.

Tel. +86-10-68314422 Ext.3500

Received 1999-04-08

**Table 1 Comparison of liver volume in different hepatic function class ( $\bar{x}\pm s$ )**

Hepatic function class	Case(n)	Liver volume (cm <sup>3</sup> )	Liver volume/height (cm <sup>3</sup> /m)
Child A class	2	1133.0	645.6
Child B class	13	888.2±92.6 <sup>a</sup>	533.1±50.1 <sup>a</sup>
Child C class	10	672.4±91.1	393.8±48.2

<sup>a</sup>Compared with Child C class,  $P<0.05$ .

**Table 2 Morbidity of post-shunting encephalopathy and post-shunting mortality in patients with different liver volume**

	Case (n)	Encephalopathy (n)	Morbidity of encephalopathy	One-year death	Mortality
Liver volume>750cm <sup>3</sup>	13	1	7.7% <sup>a</sup>	1	7.7%
Liver volume<750cm <sup>3</sup>	11	4	36.4%	1	9.1%

<sup>a</sup>Compared with liver volume<750 cm<sup>3</sup> group,  $P<0.05$ .

## DISCUSSION

Liver cirrhotic portal hypertension is a disease with considerable individual difference. The complicated liver function and other factors will influence portal pressure and the operational results. How to evaluate patients' tolerance to operation, how to select optimal operation for patients and how to predict the prognosis are challenges to surgeons. Age, nutritional condition and hepatic function class (Child's class) have often been regarded as the criteria. Liver volume and amount of liver cells, which is an important index of the hepatic function, were overlooked, while the volume and weight of liver have been regarded as the factors as important as Child's class<sup>[3,4]</sup>.

Liver is an irregular wedge-shaped organ, critical deformity is present during the course of cirrhosis, which has brought certain difficulty to the measurement of liver volume and its weight *in vivo*. With the help of double helix-spiral CT (Elscent CT Twin), scanning could be completed during the course of breath holding, thus reduced the error. Liver volume was measured by 3-dimensional integral software accurately. The result showed that liver volume in adult had a positive and linear correlation with height, but no close correlation with body weight, this will guide the selection of donor and receptor for liver transplantation. The liver volume of cirrhotic portal hypertensive patients decreased by 25.6% as against controls. The liver volume of patients in Child C class decreased obviously in contrast with patients in Child B class, indicating that hepatic reserve function was correlative with liver volume. If patients were divided into two groups according to liver volume of 750 cm<sup>3</sup>, the morbidity of postoperative encephalopathy in patients who received portal-caval shunt with their liver volume

less than 750 cm<sup>3</sup>, was 4.5 times that of patients with their liver volume higher than 750 cm<sup>3</sup>. Owing to the poor hepatic reserve function, patients with lower liver volume were prone to encephalopathy, therefore it was not adequate to perform shunt operation on patients whose liver volume was too low. It played a role in objective evaluation of patients' tolerance to operation and selection of operational procedure<sup>[5,6]</sup>. Our study showed that although the extent of liver atrophy was negatively correlated with portal pressure, correlation coefficient was small. Statistical analysis showed no significant difference, and portal flow was not closely correlated with liver volume. These suggest that there are many factors that influence portal pressure, natural portal-systemic shunting index and portal flow. Liver volume is probably just one of them. At the same time, the relationship between liver volume and portal pressure, portal flow and portal-systemic shunting rate needs to be further studied.

## REFERENCES

- Galambos JT. Evaluation of patients with portal hypertension. *Am J Surg*, 1990;160:14-18
- Zoli M, Cordiani MR, Marchesini G, Iervese T, Bonazzi C, Bianchi G, Pisi E. Prognostic indicators in compensated cirrhosis. *Am J Gastroenterol*, 1991;86:1508-1513
- Ogasawara K, Une Y, Nakajima Y, Fukumoto T, Sane S. The significance of measuring liver volume using computed tomographic images before and after hepatectomy. *Surg Today*, 1995;25:43-48
- Ros PR, Eirahman MM, Barrda R, Somers G. Three dimensional imaging of liver masses: preliminary experience. *Appl Radiol*, 1990;19:28
- Adler M, Van Laethem J, Gilbert A, Gelin M, Bourgeois N, Vereerstraeeten P, Cremer M. Factors influencing survival at one year in patients with nonbiliary hepatic parenchymal cirrhosis. *Dig Dis Sci*, 1990;35:1-5
- Albers, Hartmann H, Bircher J, Creutzfeldt W. Superiority of the Child Pugh classification to quantitative liver function tests for assessing prognosis of liver cirrhosis. *Scand J Gastroenterol*, 1989; 24:269-276

# Localization of keratin mRNA and collagen I mRNA in gastric cancer by in situ hybridization and hybridization electron microscopy

SU Chang-Qing<sup>1</sup>, QIU Hong<sup>1</sup> and Zhang Yan<sup>2</sup>

**Subject headings** keratin; collagen; *in situ* hybridization; nucleic acid; stomach neoplasms; mRNA

## INTRODUCTION

Immunohistochemistry and immune electron microscopy were used to determine the keratin and collagen I polypeptides expressed in gastric mucosa and gastric cancer. We found that the canceration of gastric epithelia and the infiltration and metastasis of gastric cancer are closely related with cellular skeleton and extracellular matrix<sup>[1]</sup>. The *in situ* hybridization (ISH) technique, developed by Gall and Pardue in 1969<sup>[2,3]</sup>, has become an essential tool for detecting the localization of synthesis and abundance of RNA transcripts on tissue sections. With a K<sub>6</sub> (M<sub>r</sub> 56000) keratin cDNA probe and a collagen I  $\alpha_1$ -chain cDNA probe, the cDNA-mRNA ISH technique was used to study changes of keratin mRNA and collagen I mRNA expression in gastric mucosa and gastric cancer.

## MATERIALS AND METHODS

### Tissue preparation

Tissue samples of 58 cases of gastric cancer and 40 cases of gastric mucosa were obtained from fresh surgical specimens at the Cancer Center of PLA, Nanjing 81 Hospital, Nanjing, China. The samples for light microscopic ISH were immediately fixed in 100mL/L buffered formalin. The samples for ultrastructural ISH were fixed in PG fixative solution.

### Probe preparation

Biotinylated probes of K<sub>6</sub> keratin cDNA and collagen I  $\alpha_1$ -chain cDNA were prepared from the Pst I fragments cloned at plasmid PBR322 (Amersham). The probe preparation was essentially carried out according to the methods of Obara *et al*<sup>[4,5]</sup> by randomly primed *in vitro* transcription, with the use of biotin-11-dUTP (BRL).

### Light microscopic ISH

Formalin-fixed, paraffin-embedded tissue sections were cut and mounted on glass slides that had been treated to inactivate RNase and coated with 0.05% polylysine (Sigma). All hybridization procedures were tested according to Plummer *et al*<sup>[3]</sup> and Mandry *et al*<sup>[6]</sup>.

The sections were deparaffinized in xylene, washed in alcohol, and then air-dried. After washed in PBS, the sections were treated with 3 mg/L proteinase K (Sigma) in 10 mmol/L Tris-HCl, pH 7.4, 2mmol/L CaCl<sub>2</sub> for 10 min at 37 °C, and washed in PBS containing 0.2% glycine followed by fixation in 4% paraformaldehyde for 5min at 37 °C, and then dehydrated and air-dried. All sections were covered with prehybridization buffer (50% formamide, 2×SSC, 2×Denhardt's solution, 10% dextran sulfate, 500mg/L herring sperm DNA, 500mg/L yeast tRNA) for 60min at room temperature. The labeled probes were diluted to the concentration of 0.5 mg/L in the same buffer, heat-denatured at 100 °C for 5min. Each section was overlaid with this hybridization solution, covered with a coverslip, and then incubated overnight for 24 hours at 44 °C in moist chamber. Posthybridization washing was either with 50% formamide in 2×SSC or with 1mmol/L-EDTA in PBS. Blocking solution containing 3% BSA and 1mmol/L EDTA in 0.1mol/L, pH 7.4, TBS was used to reduce background staining, 10min at room temperature, followed by a brief washing in distilled water. Tissues were reacted with 1:20 streptavidin-peroxidase (Maxim) in the blocking solution for 60min at 37 °C, washed thoroughly with 2×SSC and 0.1mol/L, pH 7.4, TBS, and revealed by the addition of hydrogen peroxide and AEC, finally counterstained with hematoxylin.

The positive staining was classified into four grades: (-) no positive grains, (+/-) a few tiny

<sup>1</sup>Central Laboratory of Nanjing 81 Hospital, Nanjing 210002, Jiangsu Province, China

<sup>2</sup>Department of Radiation Oncology, Nanjing Second Hospital, Nanjing 210003, Jiangsu Province, China

SU Chang-Qing, male, born on 1964-01-27 in Tonghua, Jilin Province, graduated from Anhui Medical University as a postgraduate in 1990, Ph.D. of molecular biology, majoring in mechanism of tumor infiltration and metastasis, having more than 50 papers published.

Project supported by the Military Youth Science Fund of China, No. 94008

**Correspondence to:** Dr. SU Chang-Qing, Central Laboratory of Nanjing 81 Hospital, Nanjing 210002, China

Tel. +86-25-6648090 Ext.241

Email.sucq@jlonline.com

Received 1999-04-28

grains in the cells, (+) many positive grains gathered to coarse grains, (+ +) thick grains in the cells gathered to slices.

### Ultrastructural ISH

The positive cases demonstrated by light microscopic ISH on paraffin sections were chosen to be used for ultrastructural ISH, including 22 cases of gastric mucosa and 49 cases of gastric cancer. The prepared samples fixed in PG fixative solution were washed in PBS containing 5% sucrose, cut into 30 $\mu$ m-50 $\mu$ m thick oscillating sections and mounted on slides. The ultrastructural ISH steps, including enzymatic digestion, denaturation, hybridization, and detection probe, were carried out the same as in light microscopic ISH, with the exceptions of probe concentration of 0.1mg/L and streptavidin-peroxidase working titer of 1:100.

After the hybridization signals had been revealed, the sections were gently separated from slides and carefully folded to tissue blocks, followed by postfixation in 1% osmium tetroxide. The following procedures, including dehydration, embedded in Epon-812, ultrathin section making and staining with lead citrate and uranyl acetate, were executed according to the conventional steps of diagnostic electron microscopy. Finally, the hybridization signals were observed under H-300 transmission electron microscope.

### Negative controls

Negative controls included the sections digested previously with RNase A (Sigma) and the sections incubated in prehybridization solution without probes, all of which had undergone the simultaneous ISH processes.

## RESULTS

### Distribution of keratin mRNA

Under light microscopy, different extent of hybridization signals was found in 22 of 40 cases of gastric mucosa, and positive grains were found in 49 of 58 cases of gastric cancer. The gastric epithelial cells positive for keratin mRNA were scattered in mucosal glands, especially in the bases of glands. The hybridization grains were tiny and dense in cytoplasm. Keratin mRNA in cancer cells increased, the quantity and distribution of positive grains were related to the histological type and differentiation of cancer cells. In well-differentiated cancer, the grains in cancer cells were thick and coarse, while in poorly-differentiated cancer, the positive grains distributed in all cytoplasm matrix and always gathered to form slices (Figure 1).

Ultrastructurally, 8 cases showed positive reaction in 22 cases of gastric mucosa, and 21 cases

positive signals were found in 21 of 49 cases of gastric cancer. The positive grains in the epithelia were tiny and distributed in cytoplasm, especially more around nuclei (Figure 2). In cancer cells, keratin mRNA positive grains increased and appeared in two forms, one was tiny grains gathered in certain sites of cytoplasm and distributed irregularly, most of which came out in poorly-differentiated cancer cells; the other was coarse grains scattered evenly in cytoplasm, which mostly emerged in well differentiated cancer cells (Figure 3). The sections of cancer tissue, through the treatment of RNase A before ISH, had few tiny grains in cytoplasm of cancer cells.

### Expression of collagen I mRNA

Collagen I mRNA positive reaction was localized in the cytoplasm of mesenchymal cells, like fibroblasts in mucosal and cancer stroma. The reaction in mucosal mesenchymal cells showed dense black staining. In the stroma of well-differentiated cancer, the positive cells distributed around or in the cancer nests dispersively, most cells had coarse and thick grains and some cells only had a few tiny grains (Figure 4). In poorly-differentiated cancer, collagen I mRNA reaction distributed irregularly in fibroblasts was dense and looked like the form of dust.

Comparison of mRNA expression in gastric mucosa and gastric cancer is shown in Table 1.

**Table 1 Comparison of keratin mRNA and collagen I mRNA expression**

Staining grade	Keratin mRNA		Collagen I mRNA	
	Mucosa	Cancer <sup>a</sup>	Mucosa	Cancer
-	18	9	19	25
+/-	10	23	12	18
+	7	12	5	9
++	5	14	4	6
Total	40	58	40	58

<sup>a</sup>P<0.05 vs mucosa group.

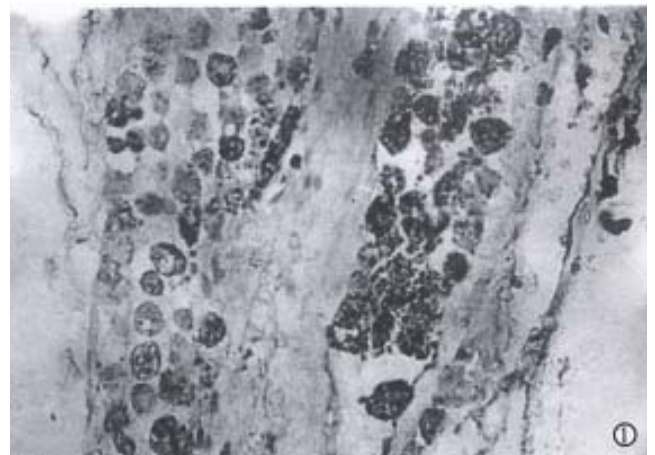


**Figure 1** Poorly-differentiated carcinoma, keratin mRNA positive grains increased and distributed in cytoplasm.  $\times 400$

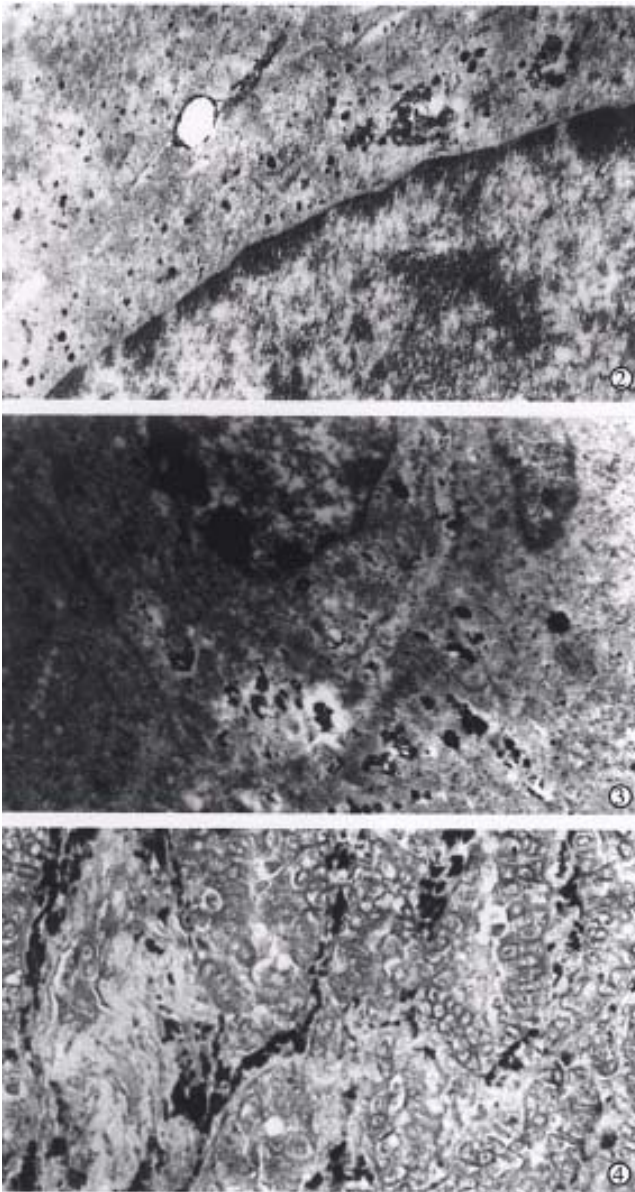


**Figure 2** Normal gastric mucosa: the positive grains for keratin mRNA in the epithelial cell were tiny and distributed around nucleus.  $\times 15000$

**Figure 3** Well-differentiated adenocarcinoma: coarse grains for keratin mRNA increased and scattered evenly in cancer cell cytoplasm.  $\times 1500$

**Figure 4** Well-differentiated adenocarcinoma: collagen I mRNA positive grains appeared in mesenchymal cells.  $\times 200$

## DISCUSSION

In the past experiments, immunohistochemistry was used to localize cellular skeleton and extracellular matrix at gene product levels. But it is unable to differentiate active production of proteins on site from proteins stored in passive cells<sup>[4]</sup>. A valuable alternative is the detection of mRNAs by ISH which can identify specific cell types actively transcribing specific genes. With the use of K<sub>6</sub> keratin cDNA probe and collagen I  $\alpha_1$ -chain cDNA probe, the detection of specific mRNAs by ISH was applied to

the study of their changes in gastric mucosa and gastric cancer. On paraffin sections, the expression of keratin mRNA and collagen I mRNA in target cells was directly observed, and on ultrathin sections, keratin mRNA positive reaction was observed under electron microscope. But on sections that had been treated with RNase A before ISH and hybridized without probes, no obviously positive reaction grains were found. The results demonstrated that the hybridization signals originated from RNA. The technique of pre-embedding hybridization and tissue section posthybridization treatment, is a new pre-embedding method for ultrastructural ISH. Although pre-embedding technique has the disadvantages of loss of ultrastructural membrane detail and potential loss of label during the embedding procedure, it is sufficient to localize mRNA ultrastructurally and to study the transcription and expression of genes.

The keratin, characteristic of epithelial cells, represents a complex family of 19 different components with molecular weights varying from  $M_r 4000$  to  $M_r 67000$ . Because individual keratin is synthesized from different mRNA, the transcript level of specific keratin reflects changes in the expression of the genes, cDNA probes for various keratin mRNAs from various species have been produced. With K<sub>6</sub> keratin cDNA probe, which has been shown to be complementary to the mRNA for the  $M_r 56000$  keratin and to share significant homology with the mRNA for  $M_r 58000$  keratin<sup>[4]</sup>, the positive hybridization signals appeared clear in gastric mucosa and gastric cancer. The hybridization grains in epithelia were tiny and distributed around nuclei, and the grains in cancer cells increased ( $P < 0.05$ ), often gathered to coarse grains or slices, and distributed heterogeneously, especially in poorly-differentiated cancer cells. The results, unanimous with that of immunohistochemistry<sup>[1]</sup>, demonstrated further that the increase of keratin in cancer cells is due to its active synthesis in cancer cells. This ability to synthesize cellular skeleton protein is related to the active reproduction and strong motility. The positive rate of keratin mRNA by ISH in gastric mucosa and cancer was lower than that of keratin by immunohistochemistry<sup>[1]</sup>, due to loss of hybridization information during the sample treatment and weakness of gene expression in some cells.

Collagen I, one of extracellular matrix components, mainly arises from mesenchymal cells. A few investigators, with immunohistochemistry and ISH, described that epithelial tissue and cancer cells, such as hepatocytes and hepatocarcinoma cells, can produce collagen I<sup>[7]</sup>. With the use of

collagen I cDNA probe, we found that collagen I mRNA was expressed only in mesenchymal cells. Further study will prove whether this is related to the difference of probes or not. In gastric cancer stroma, the hybridization grains were thick and dense in mesenchymal cells which were distributed around or in the cancer nests. The active synthesis of collagen I plays an important role in the formation of fibrous capsule around cancer nests and in the inhibition of cancer cell infiltration and metastasis. During the process of cell canceration and cancer infiltration and metastasis, some changes will occur in extracellular matrix including collagen I, possibly due to the changes of synthesis and degradation of these components [1,8]. In our current study, the expression of collagen I in cancer stroma had no obvious changes compared with that in gastric mucosa ( $P>0.05$ ), so that we believe that the degradation yielded by cancer cells is an essential factor in the changes of extracellular matrix. This degradation is of great importance to the infiltration and metastasis of cancer cells.

Finally, the changes in the biological characteristics of gastric cancer are due to the effect of cellular skeleton and extracellular matrix. The increase of keratin synthesis and the ability of extracellular matrix degradation in cancer cells are the key mechanism of cancer infiltration and

metastasis. The ISH technique has been proven to be a powerful tool *in situ* gene expression in individual cell. Further study of other cellular skeleton and extracellular matrix components is in progress.

## REFERENCES

- 1 Su CQ, Xu SF. Relationship between cytoskeleton and extracellular matrix and gastric cancer infiltration and metastasis. *Zhonghua Yixue Zazhi*, 1994;74:432-433
- 2 Capodiceci P, Magi Galluzzi C, Moreira G, Zeheb R, Loda M. Automated *in situ* hybridization: diagnostic and research applications. *Diagn Mol Pathol*, 1998;7:69-75
- 3 Plummer TB, Sperry AC, Xu HS, Lloyd RV. *In situ* hybridization detection of low copy nucleic acid sequences using catalyzed reporter deposition and its usefulness in clinical human papillomavirus typing. *Diagn Mol Pathol*, 1998;7:76-84
- 4 Obara T, Baba M, Yamaguchi Y, Fuchs E, Resau JH, Trump BF, Klein Szanto AJP. Localization of keratin mRNA in human tracheobronchial epithelium and bronchogenic carcinomas by *in situ* hybridization. *Am J Pathol*, 1988;131:519-529
- 5 Shi QH, Shan XN, Zhang JX, Zhang XR, Chen YF, Deng XZ, Huang HJ, Yu L, Zhao SY, Zheng QP, Adler ID. A DNA probe suitable for the detection of chromosome 21 copy number in human interphase nuclei by fluorescence *in situ* hybridization. *Zhonghua Yixue Yichuanxue Zazhi*, 1999;16:36-40
- 6 Mandry P, Murray AB, Rieke L, Becke H, Hfler H. Postembedding ultrastructural *in situ* hybridization on ultrathin cryosections and LR white resin sections. *Ultrastruct Pathol*, 1993;17:185-194
- 7 Wang YJ, Yang LS, Dai YM. Expression of collagen  $\alpha 1$  gene in human primary carcinoma. *Linchuang & Shiyan Binglixue Zazhi*, 1993;9:167-169
- 8 Bu W, Tang ZY, Ye SL, Liu KD, Huang XW, Gao DM. Relationship between type IV collagenase and the invasion and metastasis of hepatocellular carcinoma. *Zhonghua Xiaohua Zazhi*, 1999;19:13-15

Edited by WANG Xian-Lin  
Proofread by MA Jing-Yun

# ***In situ* detection of Epstein Barr virus in gastric carcinoma tissue in China highrisk area**

WAN Rong, GAO Mei-Qin, GAO Ling-Yun, CHEN Bi-Feng and CAI Qian-Kun

**Subject headings** stomach neoplasms; Epstein-Barr virus; *In situ* hybridization; LMP-1 protein

## **INTRODUCTION**

Epstein-Barr virus (EBV), a gammaherpesvirus, has been strongly associated with African Burkitt's lymphoma and nasopharyngeal carcinoma. Recently it has been identified in lymphoepithelioma-like carcinoma of thymus, tonsil, lung and in some gastric carcinoma<sup>[1-4]</sup>. The development of very sensitive methods for detection of EBV infection in archival pathologic tumor sections has allowed us to study the association of EBV with gastric adenocarcinomas by using *In situ* hybridization with EBER-1 oligoprobes and immunohistochemistry with anti-LMP1 antibodies.

## **MATERIALS AND METHODS**

### **Materials**

Cases were selected from a series of primary gastric carcinomas collected at the Department of Pathology, Fujian Medical University, Fuzhou, Fujian. The specimens included 58 primary gastric carcinomas, 5 chronic peptic ulcer and 10 additional specimens of normal gastric mucosa obtained from postmortem patients without gastrointestinal disease. Formalin-fixed, paraffin-embedded tissues were prepared for light microscopic examination.

### **Method**

***In situ* hybridization** The EBV sequence, EBER-1, was detected with a complementary digoxigeninlabeled 30 -base oligomer using a procedure previously described<sup>[5]</sup>. A blue-brown or brown color within

the nucleus over background levels was considered positive. In each case, hybridization was applied to section that contained both neoplastic and adjacent non-neoplastic mucosa.

A known EBV-positive nasopharyngeal carcinoma served as positive control and *In situ* hybridization without EBER probe was taken as negative control.

### **Immunohistology**

Paraffin-embedded sections were stained with monoclonal antibodies (CS1-4, DAKO) to evaluate the expression of LMP-1. Immunostaining was performed with the avidin-biotin complex (ABC) method as previously described. For these antibodies, the method of antigen retrieval was used by microwave oven pretreatment in place of proteolytic digestion before immunostaining. LMP-1 positive nasopharyngeal carcinomas were used as positive controls.

## **RESULTS**

### ***Clinical data and histological subtype***

The age range of patients was 37-74 years, with a median age of 54.5 years. Fifty patients were males and 8 were females, the ratio of males to females being 6.3:1. Among the 58 gastric adenocarcinomas, 22 were poorly-differentiated, 18 tubular, 10 mucinous, 7 signet-ring cell carcinoma, 1 papillary adenocarcinoma.

### ***EBV gene expression***

**EBER-1 expression** *In situ* hybridization, signals were strong and limited to the nucleus of carcinoma cell (Figure 1). A blue-brown or brown color was considered a positive signal. Six cases (10.3%) showed EBER-1 expression, including 5-poorly-differentiated and 1 papillary adenocarcinoma. In positive cases, virtually all malignant cells were strongly labeled with EBER probes, while the infiltrating lymphocytes, blood vessels and smooth muscle were EBER-1 negative. No EBER-1 signals were observed in adjacent non-neoplastic epithelial cells, dysplastic epithelial cells and normal gastric mucosa.

**LMP-1 expression** No expression of LMP-1 was seen in both EBER-1 positive and negative cases.

Department of Pathology, Fujian Medical University, Fuzhou 350004, Fujian Province, China

WAN Rong, female, born in 1965-03-23 in Fuzhou, Fujian Province, Han nationality, graduated from Fujian Medical University as a postgraduate in 1993, specialized in research of gastroenteric tumors, having 5 papers published.

**Correspondence to:** WAN Rong, Department of Pathology, Fujian Medical University, 88 Jiaotong Road, Fuzhou 350004, Fujian Province, China

Tel. +86-591-3314484, Fax. +86-591-3351345

Email: guhuang@pub3Fz.fj.cn

Received 1999-06-30 Accepted 1999-09-15

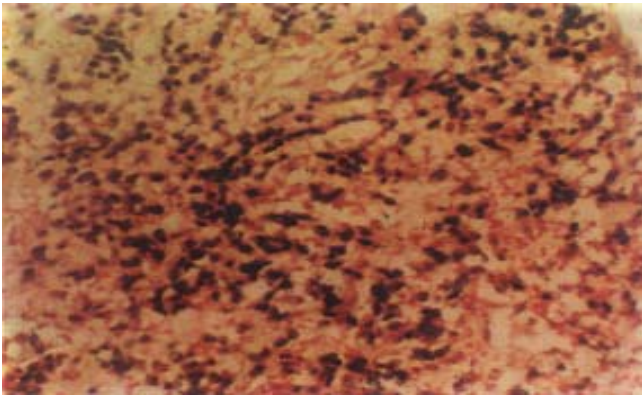


**Figure 1** EBER-1 expression in nuclei of essentially all gastric malignant cells.  $\times 200$

## DISCUSSION

EBER-1 is EBV encoded small RNA, of which high levels expression can be up to  $10^6$ - $10^7$  copies per cell exceeding DNA in EBV-infected cell. EBER oligoprobe may combine with EBER-1 enabling for detecting EBV on paraffin-embedded tissues using non-isotopic labeling and *In situ* hybridization technique which are now considered the most sensitive methods.

EBV is an oncogenic virus which has neoplastic transforming properties. The incidence of EBV infection is high in Chinese population especially in east and south China. In the current study, we had demonstrated the presence of viral RNA in 10.3% of our cases of gastric carcinomas by this method. The frequency of EBV gene expression in gastric malignant epithelium in Fuzhou was higher than that (1.6% to 6.1%) reported in Changsha and Shenyang<sup>[6]</sup>. Our study suggested that the frequency of EBV infection was different in different regions of China.

The presence of EBV in neoplasms seemed to be related to the histological subtype of neoplasms. Raab-Traub *et al*<sup>[7]</sup>, found EBV in undifferentiated and poorly differentiated nasopharyngeal carcinomas, which generally contained a relatively large number of EBV genome equivalents. In Hodgkin's disease, presence of EBV was often in mixed cellularity (HD-MC, 91%) and nodular sclerosis (HD-NS, 43%) subtypes<sup>[8]</sup>. In our study, most of the EBV-positive cases were poorly

differentiated gastric carcinomas. The relation between EBV infection and poorly differentiated carcinomas is unknown. Many believed that EBV virus might multiply easier in the poorly differentiated carcinoma, EBV genome amplification favored growth of malignant cells, promote infiltration and metastasis<sup>[7]</sup>. We failed to detect LMP-1 expression in this tumor due to the methylation of coding and regulatory regions of this protein<sup>[9]</sup>.

Shibata *et al*<sup>[10]</sup> and Gulley *et al*<sup>[11]</sup>, found that the EBER-1 was present in dysplastic epithelium of gastric mucosa before malignancy transformation. But our result showed no EBER-1 expression in the adjacent non-neoplastic epithelium, dysplastic cells and normal gastric mucosa. Finally low frequency of Epstein-Barr virus in gastric carcinoma suggests that EBV does not play any important role in the pathogenesis of gastric carcinoma.

## REFERENCES

- 1 Dimery IW, Lee JS, Blick M, Pearson G, Spitzer G, Hong WK. Association of the Epstein Barr virus with lymphoepithelioma of the thymus. *Cancer*, 1988;61:2475-2480
- 2 Brich ek B, Hirsch I, "bl O, Viikusov E, Vonka V. Presence of Epstein Barr virus DNA in carcinomas of the palatine tonsil. *JNCI*, 1984;72:809-815
- 3 Kasai K, Sato Y, Kameya T, Inoue H, Yoshimura H, Kon S, Kikuchi K. Incidence of latent infection of Epstein-Barr virus in lung cancers: an analysis of EBER-1 expression in lung cancers by *in situ* hybridization. *J Pathol*, 1994;174:257-265
- 4 Shibata D, Tokunaga M, Uemura Y, Sato E, Tanaka S, Weiss LM. Association of Epstein Barr virus with undifferentiated gastric carcinomas with intense lymphoid infiltration (lymphoepithelioma-like carcinoma). *Am J Pathol*, 1991;139:469-474
- 5 Hamilton Dutoit SJ, Raphael M, Audouin J, Diebold J, Lisse I, Pedersen C, Oksenhendler E, Marelle L, Pallesen G. *In situ* demonstration of Epstein-Barr virus small RNAs (EBER-1) in acquired immunodeficiency syndrome-related lymphomas: correlation with tumor morphology and primary site. *Blood*, 1993;82:619-624
- 6 Wang M, Tokunaga M, Jia XS, Ding JY, Hou ZJ. Observations on the relation of gastric carcinoma to Epstein Barr virus. *Zhonghua Binglixue Zazhi*, 1994;23:285-287
- 7 Raab Traub N, Flynn K, Pearson G, Huang A, Levine P, Lanier A, Pagano J. The differentiation form of nasopharyngeal carcinoma contains Epstein Barr virus DNA. *Int J Cancer*, 1987;39:25-29
- 8 Zhou XG, Hamilton Dutoit SJ, Yan QH, Pallesen G. High frequency of Epstein Barr virus in Chinese peripheral T-cell lymphoma. *Histopathology*, 1994;24:115-122
- 9 Imai S, Koizumi S, Sugiura M, Tokunaga M, Uemura Y, Yamamoto N, Tanaka S, Sato E, Osato T. Gastric carcinoma: monoclonal epithelia malignant cells expression Epstein Barr virus latent infection protein. *Proc Natl Acad Sci USA*, 1994;91:9131-9135
- 10 Shibata D, Weiss LM. Epstein Barr virus associated gastric adenocarcinoma. *Am J Pathol*, 1992;140:769-774
- 11 Gulley ML, Pulitzer DR, Eagan PA, Schneider BG. Epstein-Barr virus infection is an early event in gastric carcinogenesis and is independent of bcl-2 expression and p53 accumulation. *Hum Pathol*, 1996;27:20-27

Edited by WU Xie-Ning

Proofread by MIAO Qi-Hong

# Comparison of gene expression between normal colon mucosa and colon carcinoma by means of messenger RNA differential display

WANG Li<sup>1</sup>, LU Wei<sup>1</sup>, CHEN Yuan-Gen<sup>1</sup>, ZHOU Xiao-Mei<sup>2</sup> and GU Jian-Ren<sup>2</sup>

**Subject headings** colonic mucosa; colonic neoplasms; RNA, messenger; gene expression

## INTRODUCTION

Messenger RNA differential display technique, developed by Dr. Liang in 1992<sup>[1]</sup>, is a powerful new tool for identifying and cloning differentially expressed genes in a certain type of cell line, tissue or a special developing stage. Using this method, large amounts of molecular biological information can be obtained easily and quickly. In our study, this technique was used to compare genes expressed differentially between normal colon mucosa and colon carcinomas, in order to understand the molecular biological basis of colon cancer.

## MATERIALS AND METHODS

### Samples

Fifteen samples of colon carcinoma were obtained from radical colectomy, samples of normal colon mucosa were obtained 8 cm - 10 cm apart from colon carcinoma.

### Reagents

Guanidine thiocyanate and  $\beta$ -mercaptoethanol were purchased from BRL (America); T<sub>12</sub>MN primer and AP primer were presented by the National Laboratory for Oncogene and Related Genes, Shanghai Cancer Institute.

### Experimental procedures

**RNA preparation** Total RNA was isolated from

normal colon mucosa and colon carcinoma using single-step method of guanidine thiocyanate described by Chomczynski<sup>[2,3]</sup>, some steps had been modified.

**Reverse transcription** DNA-free RNA was reversely transcribed using the oligo-dT primer T<sub>12</sub>MN in the presence of [ $\gamma$ -<sup>32</sup>P]dATP.

**PCR amplification** Using cDNA products as templates, PCR reactions were performed in the presence of [ $\gamma$ -<sup>35</sup>S] dATP, the primer combination was T<sub>12</sub>MN and AP. Following denaturation for 30 seconds at 94 °C, the PCR steps consisted of 30 seconds at 94 °C, 2 minutes at 40 °C, 30 seconds at 72 °C for 40 cycles, followed by 5 minutes at 72 °C. Amplified PCR products from normal colon mucosa and colon carcinomas were separated side by side on a 7.5 M urea/6% polyacrylamide gel.

**Recovery of differentially expressed bands** After autoradiography, the cDNA bands representing differentially expressed mRNAs were excised from the gel. For each band, extracted cDNA was reamplified for 30 cycles with the same primers and the same PCR conditions used in the initial PCR, except that no radioactive dNTP was included. After PCR, the product was run on 1.5% low melt agarose gel and stained with ethidium bromide.

**Northern blot analysis** PCR bands of the expected size were cut from the gel, purified and used as probes. DNA probes were radio-labeled by the random prime labeling method, hybridized with RNA from pre samples and other RNA samples respectively.

## RESULTS

Total RNAs from normal colon mucosa and colon carcinomas were isolated using single-step method of guanidine thiocyanate, then reversely transcribed into first string of cDNA, T<sub>12</sub>MA, T<sub>12</sub>MC, T<sub>12</sub>MT and T<sub>12</sub>MG were used as oligo-dT primer individually. The result of alkaline denatured electrophoresis indicated that cDNA molecules were in the range of 0.5kb-5kb. cDNAs were amplified

<sup>1</sup>Department of Gastroenterology, Huashan Hospital, Shanghai Medical University, Shanghai 200040, China

<sup>2</sup>National Laboratory for Oncogene and Related Genes, Shanghai Cancer Institute, Shanghai 200032, China

Dr. WANG Li, female, born on 1996-11-24 in Jingjiang, Jiangsu Province, Han nationality, graduated from Shanghai Medical University as a Ph.D. fellow in 1999, attending doctor of gastroenterology, majoring in molecular biology research of gastroenterology, having 12 papers published.

Supported by the National Natural Science Foundation of China, No. 39470329.

**Correspondence to:** Dr. WANG Li, Department of Gastroenterology, Huashan Hospital, 12 Wu Lu Mu Qi Zhong Road, Shanghai 200040, China

Tel. +86-21-62489999 Ext.274

Email: Wangli@shtel.net.cn

Received 1999-04-08

by PCR reaction using the primer combination. T<sub>12</sub> MN and AP<sub>2</sub>, AP<sub>4</sub>, PCR products were separated by 6% polyacrylamide gel electrophoresis. Fourteen bands were obtained which were differentially displayed between normal colon mucosa and colon carcinoma. Eight bands (T<sub>1</sub>-T<sub>8</sub>) were highly expressed in carcinomas, and the other 6 bands were expressed only in normal tissues. T<sub>1</sub> band was verified to be highly expressed in tumor, but had no expression in normal tissues by Northern blot. This cDNA band would be used for cloning and sequencing.

#### DISCUSSION

The technique of mRNA differential display, by means of combining T<sub>12</sub>MN and arbitrary primer AP, can detect all expressed genes in mammalian cells and recover their molecular biological information. These cDNA fragments can be used as probes to isolate target genes from genomic DNA or cDNA library for intensive molecular biological identification. The technique has several advantages over other methods, such as simplicity, sensitivity, reproducibility, versatility and speed, so that it has been used in researches of many diseases, especially

in molecular biological study of malignant tumors. We screened 14 cDNA fragments by means of mRNA DD, one of these bands (T<sub>1</sub>) was highly expressed in the colon carcinoma which was used for differential display. Using T<sub>1</sub> band as probe, we found that it was also highly expressed in many other colon carcinomas (12/15). In the further study, this DNA fragment can be used for cloning and sequencing. Checking the database of Genbank, if the sequence of this cDNA band has no homology to the sequences of other nucleic acids, it can be considered as partial cDNA fragment of a new colon carcinoma-related gene. By screening the genomic DNA or a certain cDNA library, the full-length cDNA can be cloned, which may be helpful in the study of the molecular biology of colon carcinoma.

#### REFERENCES

- 1 Liang P, Pardee AB. Differential display of eukaryotic mRNAs by means of the polymerase chain reaction. *Science*, 1992;257:967-971
- 2 Chomczynski P, Sacchi N. Single-step method of RNA isolation by acid guanidinium thiocyanate phenol chloroform extraction. *Anal Biochem*, 1987;162:156-159
- 3 Sibert PD, Chenchik A. Modified and guanidinium thiocyanate phenol chloroform RNA extraction method which greatly reduced DNA contamination. *Nucleic Acid Res*, 1993;21:2019-2020

Edited by WANG Xian-Lin  
Proofread by MA Jing-Yun

# An improvement method for the detection of *in situ* telomerase activity: *in situ* telomerase activity labeling

FENG De-Yun, ZHENG Hui, FU Chun-Yan and CHENG Rui-Xue

**Subject headings** methodology; telomerase; *in situ* labeling ; polymerase chain reaction

## INTRODUCTION

Telomerase is a special reverse transcriptase which consists of a template RNA and protein, and uses the RNA template to catalyze the addition of telomeric DNA to chromosome ends<sup>[1-5]</sup>. The enzyme is active in adult male germ-line cells, embryonic cells and hemopoietic stems, but is undetectable in normal somatic cells except for proliferative cells of renewal tissue, e.g., activated lymphocytes, basal cells of the epidermis and intestinal crypt cells, whereas in almost all malignant tumor cells and immortal cell lines, telomerase activity has been measured. Thus, it is believed that activation of telomerase is closely associated with genesis and development of malignant tumors. Most studies to date have measured telomerase activity by telomeric repeat amplification protocol (TRAP) in heterogeneous tissue extracts<sup>[1,3-5]</sup>. With the introduction of sensitive TRAP, telomerase has been reported to be detectable in small tissue samples from almost all tumors and tumors-derived cell lines. It is not known if all cells within a tumor have telomerase activity or if only a subset does. It is necessary to develop an *in situ* assay for detecting telomerase activity levels in cytological and tissue samples. Ohyashiki<sup>[2]</sup> reported an *in situ* assay for telomerase activity by *in situ* PCR with fluorescence TS and CX telomerase primers to detect telomerase activity of cultured cells and free cells, but the attempts to use *in situ* PCR telomerase assay on frozen sections of pathological materials were unsuccessful. Now we report an improved *in situ* telomerase activity

assay on the basis of TRAP, which is very easy to be performed. A stable result can be gained on frozen sections of tumor tissue.

## MATERIALS AND METHODS

### *Samples and reagents*

Twenty-four hepatocellular carcinoma (HCC), 20 colorectal carcinoma (CRC) and 18 nasopharyngeal carcinoma (NPC) tissues were obtained from patients in Xiangya Hospital and the Second Affiliated Hospital of Hunan Medical University, Changsha, People's Republic of China. Each tissue was divided into 2 pieces. One piece was fixed in 100 mL/L formalin and embedded in paraffin for pathological diagnosis, the other was soaked in liquid nitrogen, and preserved at -76 °C.

*In situ* TRAP kit was purchased from Department of Pathology, Beijing Medical University (P.R.China). SP detection kit and development kit were from Maixing Comp (Fuzhou, P.R.China). RNase was the product of Sino-American Ltd (Shanghai, P.R.China).

### *Methods-In situ telomerase activity labeling*

Six frozen tissue sections were cut by freezing microtome (Leica, Germany) and the slides treated by poly-lysine were mounted, and detected for *in situ* telomerase activity. Briefly, each section was added 20 µL telomerase reaction mixture containing up-stream primer TS (5' AATCCGTCGAGCAGAGTT-3') 0.5 µL, down-stream primer CX (5'-CCCTTACCCTT ACCCTTACCCTTA-3') 0.5 µL, 2 mM biotin-dNTP 2 µL, 2×buffer A 5 µL, 10×buffer B µL and H<sub>2</sub>O 11 µL, coverslips were sealed. They were then incubated at 30 °C for 60 min, rinsed with 0.01 M PBS for 3 min, fixed by 40 g/L paraformaldehyde for 15 min, rinsed with 0.01 M PBS for 2×3 min, submerged into 800 mL/L ethanol for 2 min and dried, dealt with 2% H<sub>2</sub>O<sub>2</sub> for 20 min to block endoperoxidase, rinsed with 0.01 M PBS for 2×3 min, blocked by normal goat serum for 60 min, incubated by peroxidase-streptavidin at 37 °C for 60 min, rinsed with 0.01 M PBS for 3×5 min, developed with DAB, and then counterstained with hematoxylin.

Department of Pathology, Hunan Medical University, Changsha, 410078, Hunan Province, China

Dr. FENG De-Yun, male, born in 1964 in Hunan Province, graduated from Hunan Medical University in 1991, Master degree of Pathology.

Project supported by the Health Ministry Science Fund of China, No. 98-1-110

**Correspondence to:** Dr. FENG De-Yun, Department of Pathology, Hunan Medical University, Changsha 410078, Hunan Province, China  
Tel. +86-731-4475356

Email: fdyh@public.cs.hn.cn

**Received** 1999-04-08

### *In situ* TRAP

*In situ* telomerase activity was also detected by *in situ* TRAP. The procedure was as follows: 6  $\mu$ m frozen sections were dripped with 20  $\mu$ L mixture (primer TS 0.5  $\mu$ L, 2 $\times$ buffer A 5 $\mu$ L, H<sub>2</sub>O 14.5  $\mu$ L), incubated at 30  $^{\circ}$ C for 60 min, rinsed with 0.01 M PBS for 3 min, fixed by 40 g/L paraformaldehyde for 10 min, rinsed with 0.01 M PBS for 3 min, digested with 25 mg/L proteinase K at 37  $^{\circ}$ C for 10 min, washed with 0.01 M PBS for 2 $\times$ 3 min, soaked in 800 mL/L ethanol for 2 min and dried, dripped with PCR mixture (primer TS and CX 0.5  $\mu$ L respectively, 2 mM biotin-dNTPs 2  $\mu$ L, 10 $\times$ buffer B 1  $\mu$ L, Taq polymerase 2 U and H<sub>2</sub>O 15  $\mu$ L), added coverglasses and sealed with liquid paraffin, and amplified by PCR (PCR conditions were 35 cycles at 95  $^{\circ}$ C for 1min, at 50  $^{\circ}$ C for 1min, at 72  $^{\circ}$ C for 1 min) on Ericomp Thermocycler (Ericomp Ltd Comp. America), washed by chloroform and absolute ethanol for 5min respectively to scavenge the liquid paraffin and the coverglasses, washed with 0.01 M PBS for 4 $\times$ 5 min, blocked by normal goat serum at 37  $^{\circ}$ C for 60 min, dripped with ABC reagent and incubated at 37  $^{\circ}$ C for 1h, rinsed with 0.01 M PBS for 3 $\times$ 5 min, developed by DAB, and counterstained with hematoxylin.

### Negative control

Distilled water replaced primer TS and CX in reaction mixture or biotin-dNTPs in PCR mixture. The sections were digested by RNase at 37  $^{\circ}$ C for 60 min to remove telomerase RNA templates. The sections were heated at 95  $^{\circ}$ C for 10min to inactivate telomerase.

### Positive control

Positive sections in the kit were used for positive control.

## RESULTS

### Detection of telomerase activity in HCC, CRC and NPC tissues

We first tested *in situ* labeling to detect telomerase activity in HCC, CRC and NPC tissues. Cancer cells contained detectable levels of telomerase activity. Positive signals of telomerase activity in HCC were almost in nuclei (Figure 1), a few in cytoplasm. Distributions of the positive cells were clustered or diffused in HCC. Weaker telomerase activity was also detected in cytoplasm and nuclei in liver tissues surrounding HCC, and mainly localized in nuclei of hepatocytes near cancer tissues, and positive cells were small patchy or clustered (Figure 2). In CRC, positive signals of telomerase activity were principally localized in nuclei, and much weaker in cytoplasm. In NPC, the telomerase activity was detected in nuclei (Figure 3). Distributions of

positive cells were small nested or patchy in shape.

Positive results for telomerase activity were obtained from positive control group, and negative results from negative control groups.

### Comparison of results obtained by two methods

When our improved method was used to detect *in situ* telomerase activity, its positive signal localization, intensity and character, and distribution of positive cells were very similar to the results by *in situ* PCR-TRAP with much better morphology preservation and background of tissues.

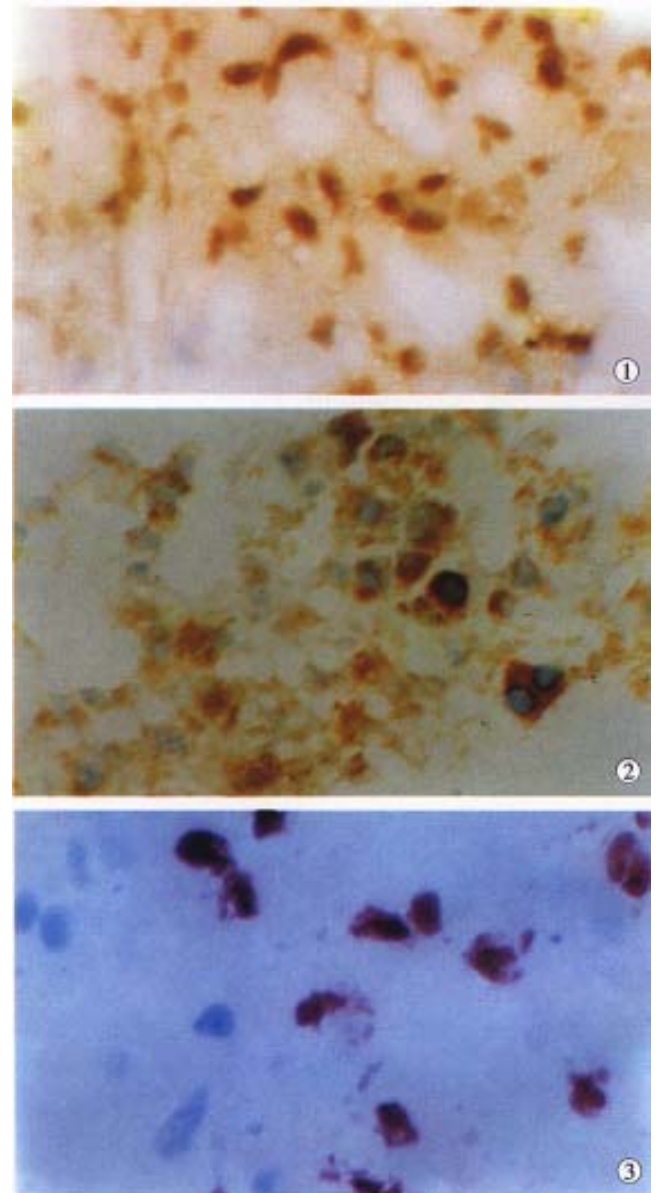


**Figure 1** Positive signal of telomerase activity localized in nuclei of HCC. *In situ* labeling,  $\times 400$

**Figure 2** Weak positive signal of telomerase activity in liver tissue surrounding HCC in nuclei and cytoplasm of hepatocytes. *In situ* labeling,  $\times 400$

**Figure 3** Nuclear positive signal of telomerase activity in NPC. *In situ* labeling,  $\times 400$

## DISCUSSION

Telomerase is a specific reverse transcriptase which utilizes its own RNA as a template to catalyze synthesis of telomere<sup>[1-5]</sup>. According to molecular biological theory, if the telomerase is active, it can synthesize cDNA by adding the primers and dNTPs under suitable condition. Because dNTPs used to synthesize cDNA are labeled with biotin which has an affinity for streptavidin-peroxidase, and when developed by DAB, the telomerase activity can be detected. Affinity reaction of streptavidin with biotin can amplify positive signals, therefore PCR amplification procedure may be omitted for *in situ* detection of telomerase activity. Thus, the method for *in situ* detection of telomerase activity is very simple and particularly successful on frozen sections of pathological materials. Morphological preservation and background of tissue sections are much better.

According to the data, in order to achieve satisfactory results during experiment. The following points are worth notice: ① Coverglasses, tips, forceps and distilled water must be sterilized by high temperature; ② After sections were

incubated with reaction mixture, the sections should not be rinsed too long, and intensity should not be too strong, otherwise, synthetic cDNA by reverse transcription is easy to be washed away, resulting in false negative, because cDNA is not fixed and fast adhered to the sections; ③ The slides must be treated with poly-lysine to avoid separation of the sections from slides.

## REFERENCES

- 1 Nakayama J, Tahara H, Tahara E, Toyama K, Ebihara Y, Kato H, Wright WE, Shay JW. Telomerase activation by hTERT in human normal fibroblast and hepatocellular carcinomas. *Nat Genet*, 1998; 18:65-68
- 2 Ohyashiki K, Ohyashiki JH, Nishimaki J, Toyama K, Ebihara Y, Kato H, Wright WE, Shay JW. Cytological detection of telomerase activity using an *in situ* telomeric repeat amplification protocol assay. *Cancer Res*, 1997;57:2100-2103
- 3 Nouse K, Urabe Y, Higashi T, Nakatsukasa H, Hino N, Ashida K, Kinugasa N, Yoshida K, Uematsu S, Tsuji T. Telomerase as a tool for the differential diagnosis of human hepatocellular carcinoma. *Cancer*, 1996;78:232-236
- 4 Miura N, Horikawa I, Nishimoto A, Ohmura H, Ito H, Hirohashi S, Shay JW, Oshimura M. Progressive telomere shortening and telomerase reactivity during hepatocellular carcinogenesis. *Cancer Genet Cytogenet*, 1997;93:56-62
- 5 Wu S, Liew CT, Li XM, Lau WY, Leow CK, Wu BQ, Li CJ. Study on telomerase activity in hepatocellular carcinoma and chronic hepatic disease. *Zhonghua Binglixue Zazhi*, 1998;27:91-93

Edited by WANG Xian-Lin  
Proofread by MA Jing-Yun

# Clinicopathologic study of primary intestinal B cell malignant lymphoma

ZHOU Qin, XU Tian-Rong, FAN Qin-He and ZHEN Zou-Xung

**Subject headings** lymphoma/pathology; intestinal neoplasms/pathology; intestinal neoplasms/diagnosis

## INTRODUCTION

Primary intestinal B cell lymphoma is one of the most common extra-nodal lymphomas, which includes two types: intestinal mucosa-associated lymphoid tissue lymphoma (IMALToma) and lymphomatous polyposis (LP). Both have characteristic pathologic features, immunophenotypes and biological behaviors. In this article, twenty-five cases were retrospectively analyzed with regard to criteria of diagnosis and clinicopathologic characteristics.

## MATERIALS AND METHODS

### Methods

All 25 tissue specimens obtained from surgical operation, were embedded in paraffin, sectioned and stained by haematoxylin-eosin and immunohistochemical stains (ABC method). The first antibody (CD<sub>20</sub>, CD<sub>45</sub>, CD<sub>45RO</sub>, CD<sub>68</sub>, CD<sub>30</sub>, K, λ, IgG, IgM, IgA, IgD and bcl-2), second antibody and ABC Kit were produced by Dako and Vector Co. PBS buffer solution was substituted for the first antibodies as the negative control, whereas the lymphoma cases were used for positive control.

### Clinical data

There were 21 cases of IMALToma, in which 16 were males and 5 females, age ranged 9-70 years, mean age 39.6 years. Location of tumors, 10 were situated in ileum, 2 at jejunum, 6 in colon, 1 at rectum and 2 in both ileum and colon; there were 4-cases of LP, 3 men and 1 woman, age 30-47

(average 38.8) years, all were located at the terminal ileum. Clinical manifestations of IMALToma were similar to LP with abdominal pain and mass, melena and mucous stool, intestinal intussusception and intestinal obstruction, fever, loose bowel movement.

### Pathological data

Macroscopically, the IMALToma could be categorized into mushroom, constrictive and ulcerative types; the size of tumor varied from 2 cm × 1 cm × 1 cm to 20 cm × 10 cm × 3.5 cm. Sixteen cases had single nodule, five were multiple. The lymphomatous cells infiltrated in the mucosa, submucosa and muscular layer diffusely or focally. Lymphoid follicles were seen in 7 cases. In 9 cases, the germinal centers were partly or entirely replaced by lymphoma cells. Dendritic cells and macrophages with chromophilic bodies disappeared. This phenomenon is called follicular colonization (FC). 9 cases showed lymphoepithelial lesion (LEL) in which there were clusters of lymphomatous cells infiltrated focally at the surface epithelium and/or glands (Figure 1). The glandular epithelia were destroyed. The neoplastic cells presented a serial cell lineage of small lymphocyte, centrocyte-like cell (CCL), monocyte-like B cell (MCB) and lymphoplasmal cell (LPC), and also centroblast like cells (CBL). All these cells, several kinds were in a mixed distribution, but usually one kind was predominant. IMALToma was divided into following subtypes:

① CCL subtype seen in 11 cases. The tumor cells were medium and small in size, with less cytoplasm, irregular and angular nuclei of dark staining, which looked like centrocytes.

② MCB subtype seen in 4 cases. The tumor cells were of medium size, their cytoplasm was abundant, lightly stained and clear. The nuclei were round, with visible nuclear membrane, fine chromatin and small nucleoli.

③ LPC subtype seen in 2 cases. The cytoplasm tumor cells looked like plasma cells and nuclei like small lymphocytes. The cytoplasm was abundant and stained red, in some, the cytoplasm contained immunoglobulin inclusions. The nuclei of tumor cells were round, dark stained, similar to small lymphocyte.

④ CBL subtype: CBL cells were more than 50% in four cases, medium size with light stained

Department of Pathology, the First Affiliated Hospital of Nanjing Medical University, Nanjing 210029, Jiangsu Province, China  
Dr. ZHOU Qin, female, born in 1960-07-29 in Xuzhou, Jiangsu Province, graduated from the Shanghai Second Medical University with Master degree in 1990, associate chief, Department of Pathology, with twenty-three papers published.

Supported by the Natural Science Foundation of Jiangsu Province Education Commission, No.(Educ.)94051.

**Correspondence to:** ZHOU Qin, Department of Pathology, the First Affiliated Hospital of Nanjing Medical University, 300 Kwangzhou Road, Nanjing, 210029, China

Tel. +86-25-3718836 Ext. 6445, Fax. +86-25-3724440

Email.Pathojph@jlonline.com

Received 1999-05-25 Accepted 1999-09-13

cytoplasm and round vacuolated nuclei, and 1-3 basophilic nucleoli nearby the nuclear membrane. CBL cells were focally distributed with a few CCL cells scattering or clustering around the CBL cells. Transition could be shown between CBL and CCL cells. Mitoses were easily found, especially the pathologic mitoses.

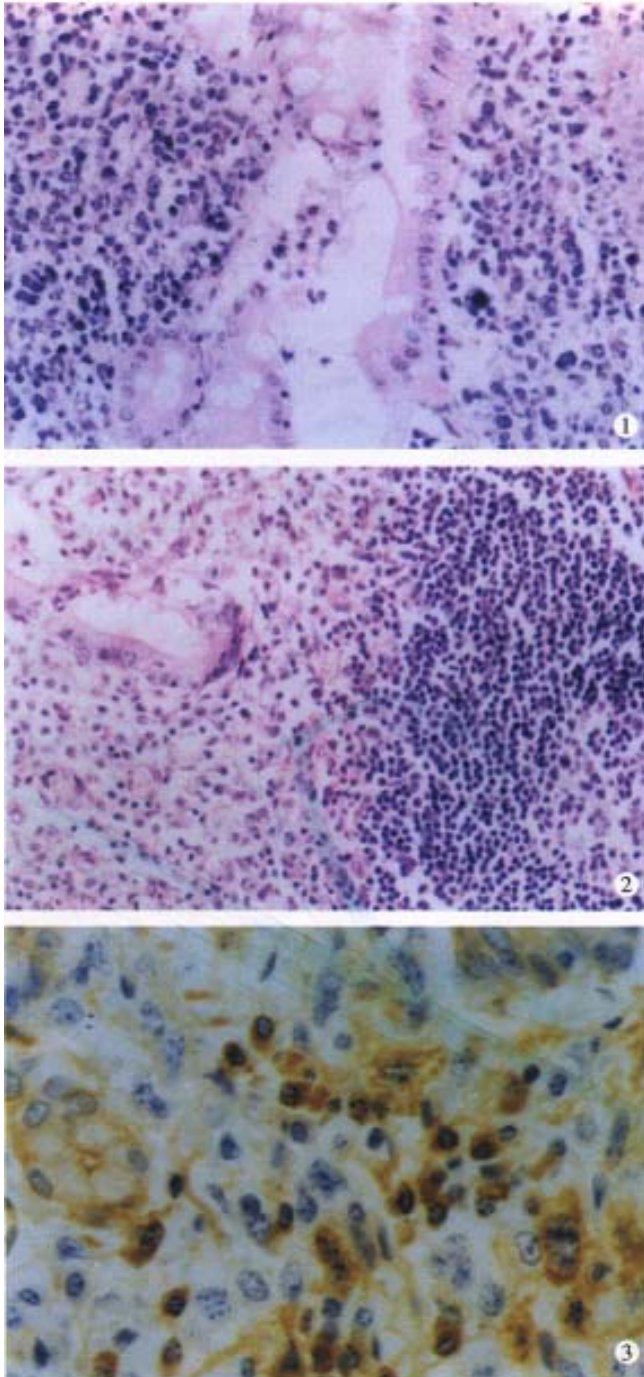


**Figure 1** In IMALToma CCL cell infiltrated and destroyed glands forming the lymphoepithelial lesion, HE stains.  $\times 100$

**Figure 2** In LP, mantle cells increased in layers and infiltrated into germinal centers, dendritic cells and the macrophages with chromophilic bodies were replaced entirely.

**Figure 3** In IMALToma, lymphoplasmatic cells infiltrated mucosa membrane, in which the CD<sub>20</sub> was positive, ABC method.  $\times 100$

In the above 3 subtypes, 14 with few or none of CBL cells were low-grade malignant. Another 2 of CCL type and 1 MCB type was low-grade malignant but with high-grade malignant component, of which the proportion of CBL cells was more than 25%. Four CBL types having more than 50% CBL cells were highly malignant. Lymph node metastases were seen in 3 of 14 cases of low grade malignancy, 2 low grade malignancy with high-grade malignant component and 4 high grade malignant IMALToma.

Four cases of LP were located at terminal ileum within the range of 20cm-40cm. They were hundreds stalkless polyps, varied from millet to broad bean. Three-fourth were mushroom-like or narrow masses, which were 1 cm  $\times$  1 cm  $\times$  1 cm-6 cm  $\times$  4 cm  $\times$  2.5 cm in size; with ulceration on the surface. Histologically, the lymph follicles were surrounded by numerous layers of lymphomatous lymphocytes, infiltrating into the germinal centers. The dendritic cells and macrophages with chromophilic bodies decreased and even disappeared. Neoplastic cells infiltrated diffusely, forming nodular and mantle-like growth pattern. The nuclei of the lymphomatous cells were round or irregularly angular with thick nuclear membrane and condensed chromatin (Figure 2). One case showed blast cell transformation.

## RESULT

Immunohistochemically, twenty one cases of IMALToma and four cases of LP were CD<sub>45</sub> and CD<sub>20</sub> positive (Figure 3). The reactive lymph follicles were polyclonal, while LEL and FC were monoclonal; one case of CBL lymphoma was negative for bcl-2. Ten cases and 5 cases were positive in CD<sub>68</sub> and CD<sub>45RO</sub>, in reactive histocytes and small lymphocytes, respectively.

## DISCUSSION

The significance of the LEL and FC pathological diagnosis of IMALToma.

LEL is considered a characteristic feature of IMALToma<sup>[1]</sup>. In our data, less than 50% (9/21) had LEL. The nest formation could also be found in the inflammatory and reactive status, it might be difficult to distinguish them from the real LEL, in such case, immunohistochemistry may be helpful. The former is several leukocytes with poly-clone and the latter is the lymphocytes with mono-clone. FC, appeared in 9 cases, is easy to misjudge as reactive follicles. The following morphological characteristics and immuno-phenotype may be helpful for the differentiation: ① FC has no dendritic cells or macrophages with chromophilic bodies. ② CCL cell is the immunophenotype of B

cells in the marginal area, rather than at the germinal center<sup>[2]</sup>.

Both LEL and FC were characteristic features for diagnosis<sup>[3]</sup>, but they could only be seen in some of the cases, then, immunohistochemistry and molecular biology technique should be done.

#### ***The diagnostic criteria and correlations of clinico-pathologic features of low and high-grade malignant IMALToma***

Fourteen were of low-grade malignancy, including CCL, MCB and LPC subtypes. The proportion of CBL cells was more than 25% in two CCL lymphoma and one MCB lymphoma, one should pay attention to transformation from low-to high-grade malignancy. Four CBL lymphomas were of high-grade malignancy, in which the CBL cells were > 50%, distributing around the FC in fused clusters or trabeculae, and Igmight be positive and *bcl-2* negative<sup>[4,5]</sup>. The rates of metastasis of the above three types of lymphoma were 28.5%, 66.7% and 100%, respectively, which proved that histological grading and the clinical staging were intimately related to prognosis.

#### ***The origination of LP***

The lymphomatous polyps were first described, and named LP by Corn in 1961. The origination of LP was argued for a long time. Only recently, LP could be defined as originating from both mantle cells and the centrocytes, which were similar in morphology<sup>[6]</sup>. The former was positive in IgD,

CD<sub>5</sub> and cyclin D<sub>1</sub> without blastocyte transformation, while the latter was positive in IgM and CD<sub>10</sub> with blastocyte transformation<sup>[7,8]</sup>. In our group, three cases had the morphologic feature of mantle cells, one was originated from germinal center, which was transformed from centrocytes to centroblastocytes. Thus the term LP could not reflect the origination and the nature. LP has two patterns, showing similar macroscopic and histologic features here we suggest a better terms for LP: mucosal mantle cell lymphoma and mucosal follicular lymphoma.

#### **REFERENCES**

- 1 Isaacson PG, Frcpath D. Gastrointestinal lymphoma. *HumPathol*, 1994;25:1020-1029
- 2 Isaacson PG. Malignant lymphomas with a follicular growth pattern. *Histopathology*, 1996;28:487-495
- 3 Montalban C, Manzanal A, Castrillo JM, Escribano L, Bellas C. Low grade B cell MALT lymphoma progressing into high grade lymphoma. Clonal identity of the two stages of the tumour, unusual bone involvement and leukaemic dissemination. *Histopathology*, 1995;27:89-91
- 4 Navratil E, Gaulard P, Kanavaros P, Audouin J, Bougaran J, Martin N, Diebold J, Mason DY. Expression of the bcl-2 protein B cell lymphomas arising from mucosa associated lymphoid tissue. *J Clin Pathol*, 1995;48:18-21
- 5 Ashton Key M, Biddolph SC, Stein H, Gatter KC, Mason DY. Heterogeneity of bcl-2 expression in MALT lymphoma. *Histopathology*, 1995;26:75-78
- 6 Moynihan MJ, Bast MA, Chan WC, Delabie J, Wickert RS, Wu GQ, Weisenburger MD. Lymphomatous polyposis: a neoplasm of either follicular mantle or germinal center cell origin. *Am J Surg Pathol*, 1996;20:442-452
- 7 Fraga M, Lloret E, Sanchez-Verde L, Orradre JL, Campo E, Bosch F, Piris MA. Mucosal mantle cell (centrocytic) lymphomas. *Histopathology*, 1995;26:413-422
- 8 Robert ME, Kuo FC, Longtine JA, Sklar JL, Schrock T, Weidner N. Diffuse colonic mantle cell lymphoma in a patient with presumed ulcerative colitis. *Am J Surg Pathol*, 1996;20:1024-1031

Edited by WU Xie-Ning  
Proofread by MIAO Qi-Hong

# VIP immunoreactive nerves and somatostatin and serotonin containing cells in Crohn's disease

LU Shi-Jun<sup>1</sup>, LIU Yu-Qing<sup>1</sup>, LIN Jian-Shao<sup>2</sup>, WU Hong-Juan<sup>1</sup>, SUN Yong-Hong<sup>1</sup> and TAN Yu-Bin<sup>2</sup>

**Subject headings** vasoactive intestinal peptide; somatostatin; serotonin; Crohn's disease; immunohistochemistry; histomorphometry

## INTRODUCTION

With the progress of the studies on neuroendocrine and immunology in the gastrointestinal tract, it has been recognized that the intestinal neuroendocrine system and the immune system can influence and modulate each other and a neuroendocrine immunomodulation network in the intestine has been established<sup>[1]</sup>. Neuropeptides, such as vasoactive intestinal peptide (VIP), substance P (SP), somatostatin (SS) etc. are widely distributed in the gastrointestinal tract and they play an important role in the immunomodulation of the intestinal mucosa.

## MATERIALS AND METHODS

### Tissue specimens

Surgical specimens were obtained from ileum of 25 cases of CD (25 ileum) and 10 normal subjects (from sudden death and who received surgery for intestinal neoplasm). The specimens were fixed in 10% formalin and embedded in paraffin. Sections with thickness of 4 $\mu$ m were made continuously.

### Staining method

Immunohistochemical staining was carried out by ABC method. Antibodies included rabbit polyclonal antibodies to VIP (1:400), NSE (1:200), S-100 protein (1:400), SS (1:200), serotonin (1:600) (Dako Co.) and ABC Kit.

### Histomorphometric analysis

Olympus CH light microscopy with ocular linear micrometer and double quadrantal grid test system C64 (from the Academy of Military Medical Sciences) were used to measure immunoreactive neurons and nerve fibers in 10 $\times$ 40 high power field. The point count method was used<sup>[2]</sup>. Fifteen neuron cells (with nucleus) were examined at random, the maximal diameter of each was measured and the values were averaged. The total length of all immunoreactive nerve fibers was measured separately in the mucosa and the length was estimated per unit area ( $\mu\text{m}/\mu\text{m}^2$ ) which was expressed as linear density ( $L_v\%$ ). In the submucosa and the muscle layers, the total volume of the immunoreactive neurons together with the nerve fibers was measured and the volume was estimated per unit which was expressed as volume density ( $V_v\%$ ). The numbers of SS, serotonin immunoreactive cells and argyrophil cells in the mucosa were counted at random in 10 high power fields of each case. The results averaged.

### Statistical analysis

Results were analysed by *t* and *t'* test.

## RESULTS

### Immunohistochemistry of neurons and nerve fibers

In CD, the VIP-IR and NSE-IR nerve fibers in the mucosa of ileum were markedly increased. They were deeply stained, coarse, irregular (Figure 1) and the linear densities were significantly raised ( $P < 0.01$ ,  $P < 0.01$ , respectively, Table 1). In the submucosa, the VIP-IR neurons were hypertrophial ( $P < 0.01$ , Figure 2). VIP-IR, S-100 protein IR and NSE-IR nerve fibers were all remarkably increased. They were coarse, thickened and irregular (Figure 3). The neuron and nerve fiber volume density of each immunoreactive type stated above was significantly increased ( $P < 0.01$ , respectively). In the muscle layers the volume density of neurons and nerve fibers containing NSE or S-100 protein was also significantly increased ( $P < 0.01$ , respectively, Figure 4), but the changes in VIP-IR neurons and nerve fibers were unremarkable.

<sup>1</sup>Department of Pathology, Weifang Medical College, Weifang 261042, Shandong Province, China

<sup>2</sup>Department of Pathology, Tianjin Medical University, Tianjin 300070, Tianjin, China

Dr. LU Shi-Jun, male, born in 1961-11-03, in Linqu, Shandong Province, graduated from Tianjin Medical University with Master degree in 1991, now associate professor in pathology, majoring gastroenterologic neuroendocrine immunopathology and having more than 20 papers published.

Supported by the National Natural Science Foundation of China No. 39170334

**Correspondence to:** Dr. LU Shi-Jun, Department of Pathology, Weifang Medical College, Weifang 261042, China  
Tel. +86-536-8210220

**Received** 1999-07-11 **Accepted** 1999-09-22

### Immunoreactive cells of somatostatin and serotonin

In CD, argyrophil and serotonin-IR cells in the ileal mucosa around the lesions were significantly reduced ( $P<0.01$ , respectively, Figure 5). SS- IR cells were decreased ( $P<0.01$ , Figure 6), Table 2

### DISCUSSION

In CD, there had been several reports about the morphological alterations in the enteric nervous system. Dvorak *et al*<sup>[3]</sup> described the changes in enteric nervous system in the surgical specimens from patients with CD including proliferation and focal necrosis of nerve fibers and hypertrophy of neurons in the myenteric plexus. Bishop *et al*<sup>[4]</sup> and Sj-lund *et al*<sup>[5]</sup> assessed the alterations of VIP-IR enteric nerve fibers in CD observation and counting. In the study, we used the histomorphometric analysis to obtain objective information about the changes in the immunoreactive enteric nervous system in CD. We found that in the submucosal plexus the VIP containing neurons were markedly hypertrophied, the linear density of VIP-IR nerve fibers in the mucosa and the VIP-IR neuron nerve fiber volume density in submucosa were significantly increased. The results were consistent with that of Bishop *et al* and O'Morain *et al*<sup>[6]</sup> who measured by

immunohistochemistry and radioimmuno assay, but different from that by Sj-lund *et al* and Koch. By immunohistochemistry, Sj-lund *et al* found that in unaffected muscle layer of the ileum and the affected muscle layer of colon, the VIP-IR nerve fibers were reduced. The coarse VIP-IR nerve fibers were more frequently observed in the affected mucosa of ileum and in the affected muscle layers of the colon than those in the control. El-Sathy *et al*<sup>[7]</sup> reported that the areas of the argyrophil cells as well as those immunoreactive to chromogranin A and serotonin were significantly increased in both patients with UC and CD, compared with those in the controls. In patients with CD, the areas of polypeptide YY (PYY) and pancreatic polypeptide (PP) immunoreactive cells were significantly reduced. In this study, we also found that SS and serotonin containing cells and argyrophil ones were reduced in CD. These diversities among different investigators may be due to the various locations selected the difference in degree of activity and the methods used.

This paper shows that VIP immunoreactive neurons and nerve fibers are increased whereas the immunoreactive cells containing somatostatin and serotonin are reduced, suggesting that there be abnormalities in neuroendocrine system in CD which may play an important role in the pathogenesis of CD.

**Table 1 Lv and Vv of immunoreactive nerve fibers and neurons for VIP, S-100 protein and NSE in Crohn's disease**

Item	CD		Control		P
	n	$\bar{x}\pm s$	n	$\bar{x}\pm s$	
VIP					
Mucosa Lv	25	3.6±1.2	10	2.0±0.8	<0.01
Submucosa Vv	25	2.0±1.1	10	0.9±0.8	<0.01
Submucosal neuron (diameter, $\mu\text{m}$ )	25	21.1±5.6	10	13.1±2.0	<0.01
Myenteric plexus Vv	25	3.2±1.8	10	2.6±1.4	<0.01
NSE					
Mucosa Lv	25	3.4±0.7	10	1.9±1.4	<0.01
Submucosa Vv	25	5.1±2.2	10	1.3±0.5	<0.01
Myenteric plexus Vv	25	11.1±2.6	10	5.1±1.2	<0.01
S-100 protein					
Submucosa Vv	25	3.9±1.0	10	2.3±0.4	<0.01
Myenteric plexus Vv	25	9.4±2.3	10	5.7±1.0	<0.01

**Table 2 Density of serotonin, SS containing cells and argyrophil cells in Crohn's disease**

Group	Serotonin containing cell		SS containing cell		Argyrophil cell	
	n	$\bar{x}\pm s$	n	$\bar{x}\pm s$	n	$\bar{x}\pm s$
CD	25	4.2±1.7 <sup>b</sup>	25	1.0±0.6 <sup>b</sup>	25	3.2±1.5 <sup>b</sup>
Control	10	8.9±2.9	10	2.0±1.2	10	7.7±2.5

<sup>b</sup> $P<0.01$ , vs normal control.

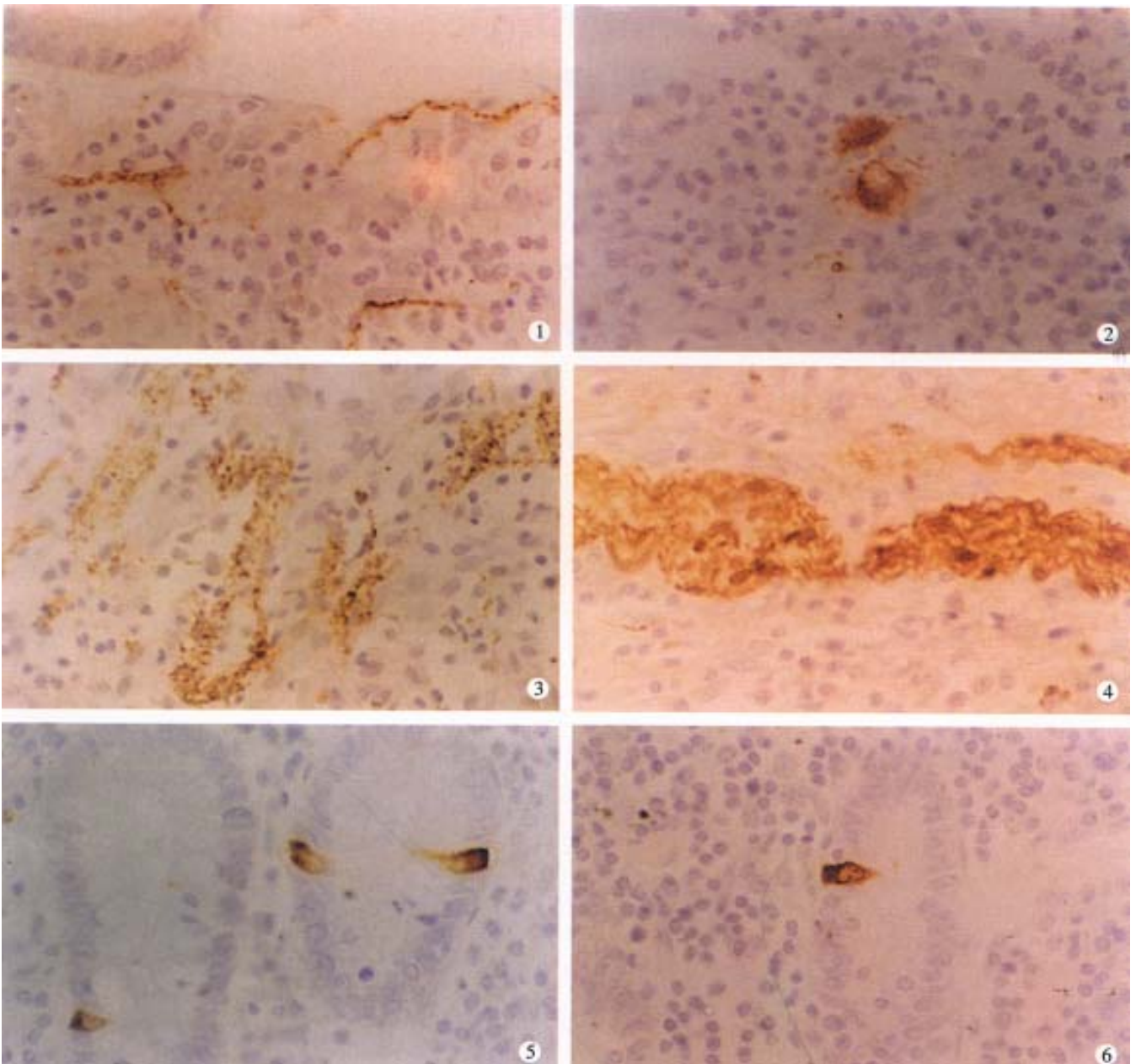


**Figure 1** VIP immunoreactive nerve fibers were coarse in mucosa of CD. ABC method  $\times 400$

**Figure 2** VIP immunoreactive neurons were hypertrophied in submucosa of CD. ABC method  $\times 400$

**Figure 3** VIP immunoreactive nerve fibers were irregularly thickened in submucosa of CD. ABC method  $\times 400$

**Figure 4** S-100 protein immunoreactive nerve fibers were increased in myenteric plexus of CD. ABC method  $\times 400$

**Figure 5** Serotonin immunoreactive cells in mucosa of CD. ABC method  $\times 400$

**Figure 6** Somatostatin immunoreactive cells in mucosa of CD. ABC method  $\times 400$

## REFERENCES

- 1 Shanahan F, Anton P. Neuroendocrine modulation of the immune system. Possible implications for inflammatory bowel disease. *Dig Dis Sci*, 1988;33:41s-49s
- 2 Zheng F. Stereocytomorphometry. 1st Ed. Beijing: Beijing Medical University and Union Medical College United Press, 1990:18-20,146-147
- 3 Dvorak AM, Osage JE, Monahan RA, Dickersin GR. Crohn's disease: transmission electron microscopic studies. III. Target tissues. Proliferation of and injury to smooth muscle and the autonomic nervous system. *Human Pathol*, 1980;11:620-634
- 4 Bishop AE, Polak JM, Bryant MG, Bloom SR, Hamilton S. Abnormalities of vasoactive intestinal polypeptide-containing nerves in Crohn's disease. *Gastroenterology*, 1980;79:853-860
- 5 Sjlund K, Muckadell OBSD, Fahrenkrug J, H-kanson R, Peterson BG, Sundler F. Peptide containing nerve fibres in the gut wall in Crohn's disease. *Gut*, 1983;24:724-733
- 6 O'Morain C, Bishop AE, McGregor GP, Levi AJ, Bloom SR, Polak JM, Peters TJ. Vasoactive intestinal peptide concentrations and immunohistochemical studies in rectal biopsies from patients with inflammatory bowel disease. *Gut*, 1984;25:57-61
- 7 El-Sathy M, Danielsson A, Stenling R, Grimelius L. Colonic endocrine cells in inflammatory bowel disease. *J Intern Med*, 1997;242:413-419

# Study on incisional implantation of tumor cells by carbon dioxide pneumoperitoneum in gastric cancer of a murine model

WANG Hao, ZHENG Min-Hua, ZHANG Hao-Bo, ZHU Jian, HE Jian-Rong, LU Ai-Guo, JI Yu-Bao, ZHANG Min-Jun, JIANG Yu, YU Bao-Ming and LI Hong-Wei

**Subject headings** stomach neoplasms; colonic neoplasms; cell movement; carbon dioxide pneumoperitoneum; murine model

## INTRODUCTION

Port-site recurrence after laparoscopic tumor surgery is a frequent complication in cancer operations, such as gallbladder, stomach, ovary and colon<sup>[1-5]</sup>. The incidence of port-site recurrence after laparoscopic colectomy ranged from 1.1% to 6.3%, in contrast to a 0.68% tumor wound recurrence rate in patients undergoing curative open colectomy<sup>[6-8]</sup>. The possible mechanisms proposed were: ① contaminated laparoscopic instruments passing in and out of the port frequently; ② increased exfoliated cancer cells from laparoscopic manipulation; ③ adhered tumor cells by pneumoperitoneum<sup>[9-12]</sup>. Some experiment reported that desufflation related to seeding of port wounds via a stable suspension of tumor cells in CO<sub>2</sub> gas was an unlikely cause of port tumors, some supported a direct intraperitoneal seeding of exfoliated tumor cells as its etiology and the instruments passing in and out of the port may play an important role in local recurrence<sup>[13-15]</sup>. The colon tumor cells were more common since laparoscopic colectomy was widely performed.

The purpose of this study was to determine whether CO<sub>2</sub> pneumoperitoneum could increase tumor implants in the port site.

## MATERIALS AND METHODS

### Materials

A 5mm laparoscopic port (5 mm trocar) was inserted in the left iliac fossa and Veress needle was placed in the right iliac fossa, below which was the injection site of malignant cells. Then the right iliac fossa port was used for insufflation, and another was used for desufflation, through the same collection device. Laparoflator was made in Germany (laparoflator electronic 3509 WEST GmbH).

Colon cancer cell line LoVo and gastric cancer cell line SGC-7901 (from Shanghai Institute of Digestive Surgery) were suspended in liquid culture media and divided into 2 groups: ① the liquid tumor cell suspension contained 1 million cells in 1mL volume (10<sup>9</sup> cells/L); ② the liquid tumor cell suspension contained 10 thousand cells in 1mL volume (10<sup>7</sup> cells/L). The concentration of cells was calculated with a hemocytometer (Fischer Scientific, Pittsburg, PA) and then appropriately diluted to achieve the final concentration. Liquid culture media were RPMI 1640 containing 10 percent fetal bovine serum. Cell viability control culture and cell viability of each tumor cell preparation were determined to be greater than 95 percent by trypan blue exclusion. Continuous flow of CO<sub>2</sub> was allowed by leaving the outflow port opened during insufflation, intraperitoneal pressure was maintained at the desired level *via* constant insufflation during continuous flow studies.

### Methods

Male Sprague-Dawley rats (250 g-350 g, from Shanghai Experimental Animal Center) were anesthetized with 25 g/L sodium barbitone (1 μL/g). Abdomens were shaved and prepared with bromo-geramine. Animals then received a right lower quadrant intraperitoneal injection of 1 mL of a suspension of SGC-7901 gastric cancer cells or LoVo colon cancer cells (10<sup>7</sup>/L, 10<sup>9</sup>/L), respectively. Veress needle and 5mm trocar were placed in the abdomen and served as port sites. There were 4 pairs of groups for LoVo or SGC-7901 (4 rats for each group): ① continuous pneumo of

Department of Surgery, Ruijin Hospital of Shanghai Second Medical University, Shanghai 200025, China Shanghai Institute of Digestive Surgery, Shanghai 200025, China

Dr. WANG Hao, male, born in 1972-09 in Nanyan, Henan Province, Han nationality, graduated from Shanghai Second Medical University as a postgraduate in 1998, majoring in colorectal oncology and laparoscopy, having 20 papers published.

Supported by the Shanghai Technological Development Funds, No. 98QMB1405

**Correspondence to:** Dr. WANG Hao, Department of Surgery, Ruijin Hospital of Shanghai Second Medical University, 197 Ruijin Er Road, Shanghai 200025, China

Tel. +86-21-64370045, Fax. +86-21-64333548

Email: wanghaosh@hotmail.com

**Received** 1999-07-18 **Accepted** 1999-09-18

2 kPa (5 min) at gas flow of 5 L/min for 5 min with ( $10^7/L$ ,  $10^9/L$ ) cells injected; ② continuous flow (5 L/min) of CO<sub>2</sub> with ( $10^7/L$ ,  $10^9/L$ ) cells injected, maintaining a pressure of 4 kPa for 5 min inside the peritoneal cavity; ③ continuous flow (5 L/min) of CO<sub>2</sub> with ( $10^7/L$ ,  $10^9/L$ ) cells injected, maintaining a pressure of 2 kPa inside the peritoneal cavity for 60 min; and ④ continuous flow (5 L/min) of CO<sub>2</sub> with ( $10^7/L$ ,  $10^9/L$ ) cells injected, maintaining a pressure of 4 kPa for 60 min inside the peritoneal cavity. At the end of the experiments, a peritoneal washing sample was cultured as a cell viability control. All collection dishes were incubated at 37 °C and 50 mL/L CO<sub>2</sub> concentration for one week, then detected under microscopy to demonstrate whether tumor cells existed or not.

## RESULTS

Continuous CO<sub>2</sub> pneumoperitoneum with different number of cell injection in LoVo & SGC-7901 cell line were shown in Table 1 and Table 2, respectively. After one week of incubation, in the group of 5 L/min, continuous CO<sub>2</sub> flow of 4 kPa for 60 min with  $10^9/L$  SGC-7901 cell injected, it demonstrated tumor growth in 3 of 4 dishes when compared with the same experimental condition in LoVo cell. All 4 peritoneal washing samples also showed tumor growth, whereas other dishes showed none.

**Table 1 Results in continuous flow pneumo with LoVo cell injection**

Cell number	No. of rats	Pressure (kPa)	Duration (min)	Tumor growth
$10^9/L$	4	2	5	0/4
$10^7/L$	4	2	5	0/4
$10^9/L$	4	4	5	0/4
$10^7/L$	4	4	5	0/4
$10^9/L$	4	2	60	0/4
$10^7/L$	4	2	60	0/4
$10^9/L$	4	4	60	0/4
$10^7/L$	4	4	60	0/4
Control	2			2/2

**Table 2 Results in continuous flow pneumo with SGC7901 cell injection**

Cell number	No. of rats	Pressure (kPa)	Duration (min)	Tumor growth
$10^9/L$	4	2	5	0/4
$10^7/L$	4	2	5	0/4
$10^9/L$	4	4	5	0/4
$10^7/L$	4	4	5	0/4
$10^9/L$	4	2	60	0/4
$10^7/L$	4	2	60	0/4
$10^9/L$	4	4	60	3/4
$10^7/L$	4	4	60	0/4
Control	2			2/2

## DISCUSSION

Laparoscopic surgery has been carried out nationwide in patients with cancer of the gastrointestinal tract despite relatively high incidence of port site recurrence after curative resection<sup>[1,7]</sup>. Several clinical reports have proposed that recurrence may be caused by direct implantation of the tumor cells, whereas the proof is still uncertain. Many experimental studies of colon carried out more than those in gastric cancer<sup>[16]</sup>.

Our design was to evaluate and compare the incidence of port site recurrence by direct seeding of either colon or gastric cancer cells. We injected LoVo cells into the mice and found none of the 32 mice had tumor growth in the dishes, but when injected SGC-7901 cells into the mice with  $10^9/L$  SGC901 cells and pneumoperitoneum pressure 4 kPa for 60 min, 3 out of 4 dishes showed tumor cells growth. The gastric cancer cell line SGC-7901 was more likely to cause port-site recurrence than colon cancer LoVo cell line. This may partly be due to the difference of tumor metastatic behavior. It had been reported that the capacity of gastric cancer cell implantation in the peritoneum was much easier than that of the colon cancer cells<sup>[18,19]</sup>. Our finding corroborated the above conclusion. The pneumoperitoneum pressure in the abdominal cavity and its duration played an important role in the development of port-site recurrence of gastric cancer cells.

The mechanism for tumor cell port-site implantation may be explained as follow: ① tumor cell exfoliation by surgical manipulation of the tumor; ② contaminated laparoscopic instruments frequently passing in and out of the ports; ③ tumor cell viability, number of cells, duration, pneumoperitoneum pressure and the metastatic nature of tumor cells; ④ surgery induced immunosuppression facilitating tumor growth at the port-site wounds<sup>[13,20]</sup>. Thus significant effort should be strived for to prevent tumor growth in the port wound. It has been suggested that all instruments should be routinely wiped on withdrawal from a port with a cytotoxic agent (povidone-iodine) and a similar agent flushing the laparoscopic port before withdrawal. The external aspect of the port should be sprayed and wound liberally irrigated with a cytotoxic agent<sup>[17]</sup>.

## REFERENCES

- Alexander RJ, Jaques BC, Mitchell KG. Laparoscopically assisted colectomy and wound recurrence. *Lancet*, 1993;341:249-250
- Drouard F, Delamarre J, Capron JP. Cutaneous seeding of gallbladder cancer after laparoscopic cholecystectomy. *N Engl J Med*, 1991;325:1316

- 3 Cava A, Roman J, Gonzalez QA, Quintela A, Martin F, Aramburo P. Subcutaneous metastasis following laparoscopy in gastric adenocarcinoma. *Eur J Surg Oncol*, 1990;16:63-67
- 4 Clair DG, Lautz DB, Brooks DC. Rapid development of umbilical metastases after laparoscopic cholecystectomy for unsuspected gallbladder carcinoma. *Surgery*, 1993;113:355-358
- 5 Gleeson NC, Nicosia SV, Mark JE, Hoffman MS, Cavanagh D. Abdominal wall metastases from ovarian cancer after laparoscopy. *Am J Obstet Gynecol*, 1993;169:522-523
- 6 Ramos JM, Gupta S, Anthone GJ, Ortega AE, Simons AJ, Beart RW Jr. Laparoscopy and colon cancer. Is the port site at risk. A preliminary report. *Arch Surg*, 1994;129:897-900
- 7 Vukasin P, Ortega AE, Greene FL, Steele GD, Simons AJ, Anthone GJ, Weston LA, Beart RW Jr. Wound recurrence following laparoscopic colon cancer resection. *Dis Colon Rectum*, 1996;39: S20-S23
- 8 Hughes ES, McDermott FT, Polglase AL, Johnson WR. Tumor recurrence in the abdominal wall scar tissue after large bowel cancer surgery. *Dis Colon Rectum*, 1983;26:571-572
- 9 Nduka CC, Monson JR, Menzies Gow N, Darzi A. Abdominal wall metastases following laparoscopy. *Br J Surg*, 1994;81:648-652
- 10 Fusco MA, Paluzzi MW. Abdominal wall recurrence after laparoscopic assisted colectomy for adenocarcinoma of the colon: report of a case. *Dis Colon Rectum*, 1993;36:858-861
- 11 Cirocco WC, Schwartzman A, Golub RW. Abdominal wall recurrence after laparoscopic colectomy for colon cancer. *Surgery*, 1994;116:842-846
- 12 Umpleby HC, Fermor B, Symes MD, Williamson RC. Viability of exfoliated colorectal carcinoma cells. *Br J Surg*, 1982;71:659-663
- 13 Iwanaka T, Arya G, Ziegler MM. Mechanism and prevention of port site tumor recurrence after laparoscopy in a murine model. *J Pediatr Surg*, 1998;33:457-461
- 14 Whelan RL, Sellers GJ, Allendorf JD, Laird D, Bessler MD, Nowygrod R, Treat MR. Trocar site recurrence is unlikely to result from aerosolization of tumor cells. *Dis Colon Rectum*, 1996;39: S7-S15
- 15 Allardyce R, Morreau P, Bagshaw P. Tumor cell distribution following laparoscopic colectomy in a porcine model. *Dis Colon Rectum*, 1996;39:S47-S52
- 16 Hubens G, Pauwels M, Hubens A, Vermeulen P, Van-Marck E, Eyskens E. The influence of a pneumoperitoneum on the peritoneal implantation of free intraperitoneal colon cancer cells. *Surg Endosc*, 1996;10:809-812
- 17 Hewett PJ, Thomas WM, King G, Eaton M. Intraperitoneal cell movement during abdominal carbon dioxide insufflation and laparoscopy. *Dis Colon Rectum*, 1996;39:S62-S66
- 18 Asao T, Nagamachi Y, Morinaga N, Shitara Y, Takenoshita S, Yazawa S. Fucosyltransferase of the peritoneum contributed to the adhesion of cancer cells to the mesothelium. *Cancer*, 1995;75 (6 Suppl):1539-1544
- 19 Asao T, Yazawa S, Kudo S, Takenoshita S, Nagamachi Y. A novel ex vivo method for assaying adhesion of cancer cells to the peritoneum. *Cancer Lett*, 1994;78:57-62
- 20 Murthy SM, Goldschmidt RA, Rao LN, Ammirati M, Buchmann T, Scanlon EF. The influence of surgical trauma on experimental metastasis. *Cancer*, 1989;64:2035-2044

Edited by WU Xie-Ning  
Proofread by MIAO Qi-Hong

# HCV genotypes in hepatitis C patients and their clinical significances

HUANG Fen, ZHAO Gui-Zhen and LI Yeng

**Subject headings** hepatitis C; hepatitis C virus; genotyping

## INTRODUCTION

It has been discovered that hepatitis C virus (HCV) presents considerable nucleotide variation and has many genotypes. At least twelve, 5 of which prevalent, i.e.: I/1a, II/1b, III/2a, IV/2b, and V/3a types. The different genotypes of HCV may possess some relationship with regional distribution, clinical manifestation, response to treatment and prognosis of HCV infection, thus to study the genotypes of HCV further in different areas is of practical value. We detected HCV genotypes in 94 patients with hepatitis C and in 6 patients with primary hepatocarcinoma by PCR assay with four kinds of type-specific primers with a view to study the distribution of HCV genotypes in hepatitis C in Shenyang area and their clinical significances.

## MATERIALS AND METHODS

### Patients

One hundred serum samples with positive anti-HCV and HCV RNA were received from patients who were in clinic or in ward of our department from July 1993- June 1 1996. Among the 94 patients with hepatitis C, there were 9 acute hepatitis, 73 chronic hepatitis (50 mild degree, 14 moderate and 9 severe ones), 12 active posthepatitic cirrhosis. Mean age 38.8 years  $\pm$  15.6 years, male 77 and female 17. Forty-nine of them (52.1%) had history of blood or blood product transfusion. Superinfection or coinfection with B hepatitis was excluded, 2 cirrhosis were confirmed pathologically after operation. Six patients with primary hepatocarcinoma were diagnosed by serum AFP, B-ultrasound, CT and MRI. One had surgical biopsy.

The Department of Infectious Diseases, The Second Affiliated Hospital of China Medical University, Shenyang 110003, Liaoning Province, China

Dr HUANG Fen, female, born in 1962-10-06 in Shenyang, Liaoning Province, Han nationality, graduated from China Medical University in 1985 and got master degree from CMU in 1991, now Associated Professor, majoring in pathogenesis and therapy of viral hepatitis, having 20 papers published.

**Correspondence to:** Dr. HUANG Fen, Department of Infectious Diseases, The Second Affiliated Hospital of China Medical University, 36 block 1, San Hao Street, He-Ping District, Shenyang, Liaoning, 110003, China

Tel. +86-24-23893501-961, Fax. +86-24-23892617

Received 1999-07-03 Accepted 1999-09-18

## HCV genotyping primers

HCV genotyping primers in core region were synthesized by the Bioengineering Research Center in Shanghai of Chinese Academy of Sciences. The nucleotide sequences of primers were as follows: universal primers: P<sub>1</sub> sense 5' CGCGCGACTAG-GAAGACTTC 3' (nt 139-158); P<sub>2</sub> antisense 5' ATGTACCCCATGAGGTCGCT 3' (nt 391-410), type specific primers: P<sub>3</sub> sense 5' AGGAA-GACTTCCGAGCGGTC 3' (nt 148-167); P<sub>4</sub> antisense 5'TGCCTTGGGGATAGGCTGAC 3' (nt 185-204) (HCV-I); P<sub>5</sub> antisense 5' GAGCCATCCT-GCCCACCCCA 3' (nt 272-291) (HCV-II); P<sub>6</sub> antisense 5' CCAAGAGGGACGGGAACCTC 3' (nt 302-321) (HCV-III); P<sub>7</sub> antisense 5' ACC-CTCGTTTCCGTACAGAG 3' (nt 251 - 270) (HCV-IV).

## Methods

Serum HCV RNA was extracted using one-step method of guanidinium thiocyanate. For detecting HCV genotypes, Okamoto's<sup>[1]</sup> method was used but modified. Major procedures were: ① reverse transcription and first PCR amplification: in extracted RNA, we added 5 units of avian myeloblastosis virus reverse transcriptase (AMV-RT) (Promega), 20 units of inhibitor of RNAase (RNasin) (Promega), 2 U *Taq* enzyme (Promega), 2 mM dNTP 3  $\mu$ L, 10 $\times$ AMV- RT buffer 3  $\mu$ L and universal primers (P<sub>1</sub>, P<sub>2</sub>) 0.8  $\mu$ mol/L. Total volume was 30  $\mu$ L. After reverse transcription at 42  $^{\circ}$ C for 20 min, first PCR was performed for 35 cycles. Each cycle included denaturation at 94  $^{\circ}$ C for 1 min, annealing at 55  $^{\circ}$ C for 1.5 min and extension at 72  $^{\circ}$ C for 2min. ② The second PCR amplification: in 5  $\mu$ L products of the first PCR, we added 3  $\mu$ L 10 $\times$ AMV-RT buffer, 2 mM dNTP 3  $\mu$ L, 2 U *Taq* enzyme and 0.8  $\mu$ mol/L of type-specific primers (P<sub>3</sub>, P<sub>4,5,6,7</sub>). Total volume was 30  $\mu$ L. PCR conditions were: denaturation at 94  $^{\circ}$ C for 1 min, annealing at 60  $^{\circ}$ C for 1 min, extension at 72  $^{\circ}$ C 1.5 min, for 30 cycles, then another extension at 72  $^{\circ}$ C for 5 min. In every amplification, positive control of HCV RNA serum and negative control of normal blood sample were provided. ③ Ten microliters products of the second PCR were subjected to electrophoresis on 6% polyacrylamide gel, stained with ethidium bromide, and observed under ultraviolet ray. Each HCV genotype was characterized by different nucleotide lengths: 57 bp

for type I, 144 bp for type II, 174 bp for type III and 1.23 bp for type IV.

## RESULTS

One hundred serum samples were genetically classified into 3 types: type II in 58 samples (58%), type III in 27 (27%) and mixed type (II/III) in 14 (14%), only 1 sample (1%) remained unclassified (Figure 1).

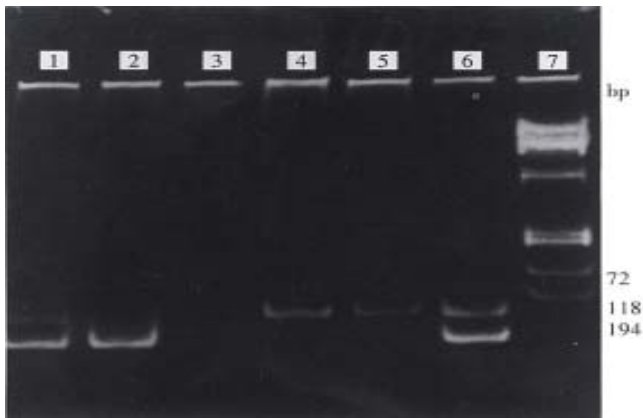


**Figure 1** The results in HCV genotyping.

1, 6: II/III mixed type. 2: HCV-II genotype. 3: Negative control. 4, 5: HCV-III genotype. 7:  $\Phi$ x 174 DNA / Hae III marker.

In 94 patients with hepatitis C, the distribution of HCV genotypes in patients with hepatitis C was not identical. The data were analyzed with R×C Table test,  $\chi^2=28.9$ ,  $P<0.01$ . In acute hepatitis, in mild, moderate and severe chronic hepatitis, cirrhosis, the infectious rates of type II were 55.6%, 36.0%, 71.4%, 88.9% and 91.7%, respectively, but those of type III were 22.2%, 46.0%, 7.14%, 0% and 8.3%, respectively. In moderate and severe chronic hepatitis and cirrhosis, the proportion of type II was significantly elevated in comparison with that in mild chronic hepatitis

( $P<0.05$  or  $P<0.01$ ), but the proportion of type III was significantly lower than that in mild ones ( $P<0.05$ ). Six patients with hepatocarcinoma were all infected by genotype II HCV (Table 1). The genotype distribution of HCV in post-transfusional and sporadic hepatitis C was identical. The results were analyzed with R×C Table  $\chi^2$  test,  $\chi^2=3.74$ ,  $P>0.05$  (Table 2).

## DISCUSSION

There are some differences in distribution of HCV genotypes in different regions. In America, infection of HCV-I genotype is predominated, but in China and Japan, HCV-II genotype is dominant over HCV-III genotype. Du *et al*<sup>[2]</sup> reported that infection by type II was predominant in Beijing, Wuhan, Guangzhou, Xi'an, Chongqing, Guangxi areas. Among these areas the highest infection rate of type III was in Beijing (19%), the infection rates of mixed type II/III were the highest in Guangzhou (9%). Our study showed in Shenyang that the infection rate of type II (58%) > type III (27%) and mixed type II/III (14%), the latter two were higher in Shenyang than those in other parts of China. Therefore, future prevention and treatment strategy should be directed towards type II HCV mainly, but not neglecting type III and type II/III. In our study, no HCV-I and HCV-IV were found. One serum sample was positive for HCV RNA by repeated PCR assay, but it could not be classified after the two tests, indicating there might be other HCV genotype in our area.

Clinical manifestations of hepatitis C infected by HCV type II are usually more severe, those of HCV type III are milder. The HCV genotypes seem to be closely related to the clinical condition and degree of severity of hepatitis C. All our 6 patients with hepatocarcinoma were found to carry HCV type II which indicated that infection of type II may be related to occurrence of hepatocarcinoma<sup>[3]</sup>.

**Table 1** HCV genotypes of hepatitis C and hepatocarcinoma

Clinical status	Cases	HCV II		HCV III		Mixed (II/III)		Unknown	
		Cases	(%)	Cases	(%)	Cases	(%)	Cases	(%)
Acute hepatitis	9	5	(55.6)	2	(22.2)	2	(22.2)		
Chronic hepatitis									
Mild degree	50	18	(36.0)	23	(46.0)	9	(18.0)		
Moderate degree	14	10	(71.4) <sup>a</sup>	1	(7.14) <sup>a</sup>	2	(14.3)	1	(7.14)
Severe degree	9	8	(88.9) <sup>b</sup>			1	(11.1)		
Cirrhosis of liver	12	11	(91.7) <sup>b</sup>	1	(8.3)				
Hepatocarcinoma	6	6	(100.0) <sup>a</sup>						
Total	100	58	(58)	27	(27)	14	(14)	1	(1)

<sup>a</sup> $P<0.05$ , <sup>b</sup> $P<0.01$ , compared with mild chronic hepatitis, by  $\chi^2$  test.

**Table 2 HCV genotypes of post-transfusional and sporadic hepatitis C**

Groups	Cases	HCV II		HCV III		Mixed (II/III)		Unknown	
		Cases	(%)	Cases	(%)	Cases	(%)	Cases	(%)
Post-transfusional hepatitis	49	26	(53.1)	12	(24.5)	10	(20.4)	1	(2.0)
Sporadic hepatitis	45	26	(57.8)	15	(33.3)	4	(8.9)		

No significant difference was found in the distribution of HCV genotypes in post-transfusional and sporadic hepatitis C, showing HCV genotypes may be not related to routes of infection. The infection rate (20.9%) of mixed type (II/III) in post-transfusional hepatitis was higher than that in sporadic hepatitis (9.8%), indicating repeated blood or blood product transfusion may be contributory.

#### REFERENCES

- 1 Okamoto H, Sugiyama Y, Okada S, Kurai K, Akahane Y, Sugai Y, Tanaka T, Sato K, Tsuda F, Miyakawa Y, Mayumi M. Typing hepatitis C virus by polymerase chain reaction with type specific primers: application to clinical surveys and tracing infectious sources. *J Gen Virol*, 1992;73:673-679
- 2 Du SC, Tao QM, Zhu L, Liu JX, Wang H, Sun Y. Genotyping study of hepatitis C virus by restriction fragment length polymorphism in its 5'NC region. *Zhonghua Yixue Zazhi*, 1993;1:7-9
- 3 Yang JM, Liu WW, Luo YH. Genotypic investigation of hepatitis C virus in patient with primary hepatic carcinoma, liver cirrhosis and hepatitis. *Zhonghua Chuanranbing Zazhi*, 1995;1:1-3

Edited by WU Xie-Ning  
Proofread by MIAO Qi-Hong

# Establishment and preliminary use of hepatitis B virus preS1/2 antigen assay

CHEN Kun, HAN Bao-Guang, MA Xian-Kai, ZHANG He-Qiu, MENG Li, WANG Guo-Hua, XIA Fang, SONG Xiao-Guo and LING Shi-Gan

**Subject headings** hepatitis B virus; PreS1/S2 antigen; ELISA; hepatitis B; E antigen/analysis

## INTRODUCTION

Hepatitis B virus (HBV) is a DNA virus with an envelope, its membrane protein gene preS/S have three parts-preS1, preS2 and S, there is a translation initiation codon ATG in each of them. By different ATG, the membrane protein gene can be translated into three kinds of products, i.e. the large protein (preS1 + preS 2 + S), medium (preS2 + S) and small (S) (also called primary protein). In patients with acute hepatitis B, PreS antigen occurred together with other HBV markers and parallels the level of HBV DNA. Disappearance of PreS antigen predicts a benign outcome<sup>[1]</sup>. Its presence in chronic hepatitis B is somewhat correlated with HBsAg, the ratio of PreS1/HBsAg antigen titers can reflect the level of DNA replication<sup>[2]</sup>. Meanwhile, the PreS domain in the membrane protein include the binding sites for hepatocyte receptor and a number of epitopes of B cells and T cells. The PreS domain possesses very strong immunogenicity in mouse and man. In mice with consanguinity, the PreS domain can induce broad-spectrum protective antibodies and overcome their nonresponsiveness to protein S. In human body, it has been proved the PreS domain is an effective immunogen at both B and T cell levels. The antibodies directing against synthetic peptides (PreS: 21 - 47) mimicking receptor-binding sites can protect chimpanzee from HBV infection<sup>[3]</sup>. During the disease course appearance of antibody against PreS1 is considered an early marker for elimination of HBV infection<sup>[4,5]</sup>. Therefore PreS antigen/ antibody is a pair of important indexes for diagnosis of hepatitis B. As one part of a research project granted by the EC Foundation, we have

prepared a recombinant PreS protein with high purity, a polyclonal anti -PreS antibody and established the ELISA method for detection of PreS antigen, preliminary clinical studies had been carried out.

## MATERIALS AND METHODS

### *Immunologic reagents*

HRP-conjugated murine anti-human IgG was provided by Department of Molecular Immunology, Institute of Basic Medical Sciences, Academy of Military Medical Sciences; HRP-conjugated murine anti-human HBs were provided by the Department of Immunology, No.302 Hospital of PLA; and HRP-conjugated sheep anti-rabbit IgG was provided by the Department of Molecular Biology, No.307 Hospital of PLA.

### *Blood specimens*

They were provided by the Central Blood Bank of PLA units under Beijing Command and No.301, 302 Hospitals of PLA.

### *Preparation of PreS antigen*

The engineered *E. coli* for hepatitis B viral PreS/2 recombinant antigen was provided by Department of Virology, Max-Planck Institute of Biochemistry, Germany. The PreS1/2 recombinant antigen containing PreS1:10-108PreS2: 1-55/S1-22 (ayw subtype) was expressed by using pQe8 (Quiagen) expression vector and six histidin residuals were fused to the N-terminal of the product, which was purified by affinity chromatography using Ni-NTA agarose column (Quiagen) to a purity above 95%. The purified protein was stored at -20°C for use.

### *Preparation of recombinant antigen-directed immune sera*

New Zealand large-ear white rabbits were immunized by four injections of renatured PreS recombinant antigen, once each on the wk 0, wk 2, wk 7 and wk 11. One hundred micrograms of the antigen were injected subcutaneously on multiple sites at one time. In the first injection, Freund's complete adjuvant was used, while Freund's incomplete adjuvant was used in the latter three injections. Blood samples were obtained before each booster injection for determination of serum antibody titer. Serum was separated from blood

Institute of Basic Medical Sciences, Academy of Military Medical Sciences, Beijing 100850, China

CHEN Kun, female, born in 1964-02-28 in Beijing, graduated from Department of Medical Laboratory Science, High Medical College, in 1992, Technician, majoring in molecular biology of viral hepatitis, having 6 papers published.

Supported by joint research with EC (CI1-CT94-0023).

**Correspondence to:** Institute of Basic Medical Sciences, Academy of Military Medical Sciences, Beijing 100850, China  
Tel. +86-10-68285463, Fax. +86-10-68285463  
Email.lingsg@nic.bmi.ac.cn

Received 1999-07-11 Accepted 1999-09-05

samples. The anti-PreS sera were purified using Protein A Sepharose 4B Fast Flow affinity adsorption column and was stored at -20 °C for later use.

#### Preparation of ELISA plate for detection of PreS antigen

The ELISA plate was coated with purified rabbit anti-PreS polyclonal antibody at a concentration of 10 mg/L at 4 °C stored overnight. After blockage with 1% BSA and dilution, the plate was vacuum-dried. then it was stored at 4 °C for later use. When it is used, test blood sample (50 µL) was added and incubated at 37 °C for 30min. After washing, the enzyme-labelled anti-HBs monoclonal antibody was added and incubated at 37 °C for 30 min after washing, OPD color developer was added to develop the color by protecting from light at 37 °C for 10 min, then 2 mol/L H<sub>2</sub>SO<sub>4</sub> was added to terminate the reaction. The OD value was determined using DG3022 Enzyme Labelling Instrument. When the D value of the test sample was  $\geq$  the average positive value  $\times 0.08$ , it was taken as positive, otherwise, as negative.

#### Competitive inhibition test

The PreS-positive sera were diluted with serum-diluting solution containing purified rabbit anti-PreS antigen polyclonal antibody (20 mg/L). After incubation at 37 °C for 1 h, the diluted sera were placed at 4 °C overnight. The 100 µL of the sera were taken out and were added to the ELISA plate coated with rabbit anti-PreS1 antibody. After that the plate was incubated at 37 °C for 30 min. The rest steps were carried out by following the routine. The neutralizing inhibition rate  $\geq 50\%$  was taken as positive.

$$\text{Competitive inhibition rate} = \frac{\text{Average non-competitive D value} - \text{Average competitive D value}}{\text{Average non-competitive D value}} \times 100\%$$

## RESULTS

#### Purification of recombinant antigen

Using pQe8 expression vector, the vector pQePreS1/2 expressing HBV ayw subtype including PreS1 and PreS2 gene fragments was constructed. After incubation, PreS1/2 protein with the relative molecular mass of 22000 (including three parts-PreS1:10-108/preS2:1-55/S1-22) was expressed. There were six histidine residues binding to the N-terminal of the product, the quantity of the recombinant protein expressed amounted to about 10% of the whole *bacteria*. The PreS1/2 existed mainly in inclusion bodies. The inclusion bodies were dissolved by denaturant and were purified on Ni-NTA agarose column. A purity over 95% was achieved. From 1 L cultured bacteria, 10 mg

purified protein could be obtained. Then the denaturant was removed from the purified protein in the course of renaturation.

#### Results

Using routine methods, rabbits were immunized with renatured recombinant PreS1/2 antigen and the titers of their immune sera against the recombinant protein were determined by ELISA. Rabbit sera of blood samples taken before immunization served as the negative control (D value  $< 0.01$ ). The titer of antibody directing against PreS1/2 antigen in rabbit sera reached 1:128 000, 1:512000, respectively on 40 d, 60 d after first immunization. In order to identify the immunogenicity of different components of the recombinant PreS1/2 antigen, recombinant PreS2 (PreS2: 1-55/S:1-9) and PreS121-47 synthetic polypeptides were also used in determination of the serum titer on d40 (Figure 1), and the result indicated in the immune sera the titers of antibodies directing against PreS1 polypeptide and PreS2 antigen were similar.

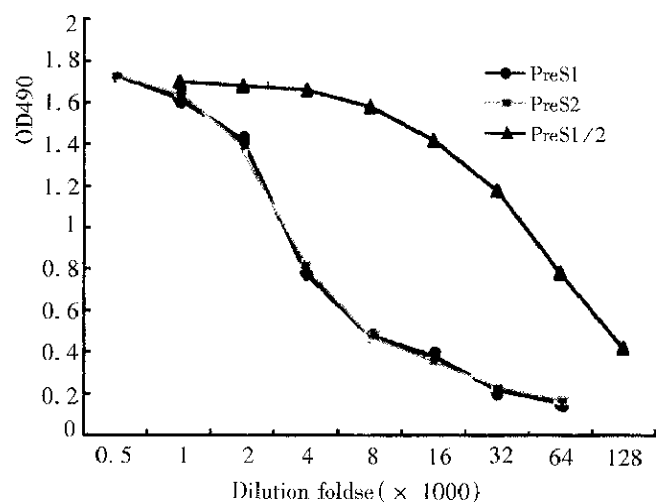


**Figure 1** The immunogenicity of different components of the recombinant PreS1/2 antigen

#### Establishment of a detection method for PreS antigen and determination of its sensitivity, specificity and preciseness

Using purified anti-PreS1/2 polyclonal antibody a double antibody sandwich ELISA method for detecting PreS1/2 antigen was established. The anti-sera of rabbits immunized with PreS1/2 were purified by using Protein A Sepharose 4B Fast Flow affinity adsorption gel column. Then 10 mg/L of the purified antibody was used to coat ELISA plate to adsorb HBV viral particles present in the sera and PreS1/2 antigen on the subunit particles. The specifically absorbed particles were detected with enzyme labeled anti-HBs antibody. This method was used in determination of purified Dane particle

sera. Along with multiple proportional dilution, the D values of reaction wells decreased successively and the dilution titer of the sera could be up to 1:2048, corresponding to detection of 5000 HBV viral particles per mL. Purified Dane particle sera and 99 hepatitis C patients' positive sera were detected and the result of the former was positive, whereas that of the latter was negative. Neutralization of PreS antigen-positive patients' sera with purified rabbit anti-PreS antibody resulted in competitive inhibition all rates reached over 80%.

Judged by intra-and inter-assay coefficients of variation, the precision of the detection method for PreS/2 antigen was evaluated. The intra-assay coefficient of variation was revealed by choosing PreS antigen-positive sera with high, medium and low values one each and by paralleled determination of 10 wells simultaneously each. The inter-assay coefficient of variation was demonstrated by determination of the above three sera for 10 times each at different time. The intra-assay coefficients of variation of the high, medium, low PreS antigen-positive sera were 3.8%, 4.5% and 13.3%, respectively; while the inter-assay coefficients of variation were 2.56%, 3.17% and 10.5%, respectively. These results indicate that precision has reached the requirement of Ministry of Public Health of China for intra and inter-assay coefficients of variation for diagnostic reagents (the national standard is  $\leq 15\%$ ). Detection rates of PreS1/2 antigen in various populations of people, in sera of 200 normal blood donors, PreS1/2 was not positively detected. The detection rates of PreS1/2 antigen in sera of patients at different phases of HBV infection were listed in Table 1.

**Table 1 Positive rates in sera at different phases of HBV infection**

Phase of infection	Number of cases			Positive rate(%)
	Negative PreS1/2	Positive PreS1/2	Total	
HBsAg(+)HBeAg(+)Anti-HBc(+)	40	260	300	87
HBsAg(+)Anti-HBe(+)Anti-HBc(+)	50	142	192	74
Anti-HBs(+)	24	0	24	0

## DISCUSSION

The PreS domain of HBV protein locates on the

surface of HBV particle and can induce protective antibody in human body and in mouse. In the literature it is reported that the elimination of PreS antigen from serum patients with acute hepatitis B can foresee the disappearance of clinical symptoms. For patients with chronic hepatitis B, persistent existence of PreS in serum indicates progression of the disease course. In the meantime, monitoring PreS1/2 antigen has also important significance for evaluation of curative effect of antiviral therapy in the se patients.

Most investigators have established detection methods for PreS antigen by using anti-PreS monoclonal antibody. This study used highly expressed in *Escherichia coli* and purified HBV PreS antigens, which cover the whole PreS2 domain and the most parts of PreS1 domain. Three experimental results indicate that the re comb inant PreS antigen is also a good immunogen in rabbit. In rabbit anti-PreS sera, the titer of antibody directing against PreS1:21-47 basically equal to the o f antibody directing against PreS2: 1 - 55. A method of detecting PreS antigen established by using purified rabbit polyclonal antibody is predicted to be able to determine simultaneously PreS1 and PreS2 antigens in serum of patient. By using this method, we have detected preliminarily PreS antigen in HBeAg positive and anti-HBeAg positive and the results show that the detection frequency of PreS antigen is relatively high in both situations. Statistical analysis indicates that the presence of PreS antigen in serum is independent of the existence of HBeAg ( $\chi^2 = 12.59, P < 0.01$ ).

## REFERENCES

- 1 Delfini C, Colloca S, Taliani G, Mazzotta F, D'Agata A, Buonamici C, Stroffolini T, Carloni G. Clearance of hepatitis B virus DNA and pre S surface antigen in patients with markers of acute viral replication. *J Med Virol*, 1989;28:169-175
- 2 Petit MA, Zoulim F, Capel F, Dubanchet S, Daugute C, Trepo C. Variable expression of preS1 antigen in serum during chronic hepatitis B virus infection: an accurate marker for the level of hepatitis B virus replication. *Hepatology*, 1990;11:809-814
- 3 Neurath AR, Seto B, Strick N. Antibodies to synthetic peptides from the preS1 region of the hepatitis B virus (HBV) envelope (env) protein are virus-neutralizing and protective. *Vaccine*, 1989;7:234-236
- 4 Galn MI, Toms J, Bernal MC, Salmeron FJ, Maroto MC. Evaluation of the pre-S (preS(1)Ag/preS(2)Ab) system in hepatitis B virus infection. *J Clin Pathol*, 1991;44:25-28
- 5 Coursaget P, Buisson Y, Bourdil C, Yvonne B, Molinie C, Diop MT, Chiron JP, Bao O, Diop Mar I. Hepatitis B virus induced liver disease and after immunization. *Res Virol*, 1990;141:563-570

Edited by WU Xie-Ning  
Proofread by MIAO Qi-Hong